



UiT The Arctic University of Norway

Faculty of Science and Technology

Department of Chemistry

Method development towards synthesis of carbapenemase inhibitors

Aya Ismael

A dissertation for the degree of Philosophiae Doctor [September 2020]

Abstract

Carbapenemases are enzymes able to hydrolyze the last resort β -lactam antibiotics (carbapenems), which are used for the treatment of infections caused by resistant bacteria. Carbapenemases are structurally and mechanistically classified into serine- β -lactamases (SBLs) and metallo- β -lactamases (MBLs). In order to combat the hydrolytic activity of these enzymes, combination therapy of β -lactam with β -lactamase inhibitor have been clinically successful. Nevertheless, clinically approved inhibitors for a number of important carbapenemases are still missing and resistance against some of the clinically successful combinations have been already reported.¹ Therefore, there is an urgent need to find new effective inhibitors that could potentially reach clinical use. The approach targeted in this thesis is to design new inhibitors against carbapenemases that could be used in the combination therapy with a carbapenem antibiotic to restore its effect.

The goal of my work was to develop synthetic methods for the synthesis of inhibitors targeting two clinically relevant carbapenemases - the serine- β -lactamase oxacillinase 48 (OXA-48) and the metallo- β -lactamase Verona integron-encoded metallo- β -lactamase (VIM-2). For the design and development of inhibitors, a fragment-based approach based on previously discovered inhibitory fragments and structural data of the fragments in complex with the target enzymes was chosen.

In this thesis I discuss the developed synthetic strategy towards unsymmetrical 3,5-disubstituted benzoic acids using selective Suzuki-Miyaura cross-coupling. Applying the developed method, I synthesized a small extended fragment library of both symmetrical and unsymmetrical 3,5-disubstituted benzoic acids targeting OXA-48. The aim of synthesizing these extended fragments was to target two directions in the binding pocket as suggested by overlaying structural data of smaller fragments in complex with OXA-48.

I also developed a synthetic strategy towards 2-aryloxybenzoic acid analogues via carbonylative Suzuki coupling using CO in a safe fashion. 2-Aryloxybenzoic acids were known to inhibit the carbapenemase VIM-2. Through my investigations about a general synthetic strategy towards 2-aryloxybenzoic acid, I found some limitations about substrates with ionizable functional groups and sterically hindered substrates. I then extended my investigation to find

better reaction conditions for carbonylative coupling reactions. I also introduced sustainability to the project by using renewable solvents aiming for better reactivity in palladium-catalyzed C-C, C-O, C-N bond forming carbonylative couplings.

In summary, through the presented work a range of carbapenemase (OXA-48 and VIM-2) inhibitors have been synthesized. Additionally, the developed synthetic strategies are considered to be a starting point to build a general approach to synthesize a wide range of potent inhibitors against carbapenemases. The work resulted in three publications (Paper I, II, III).

Abbreviations

| | |
|------------|--|
| Ampc | Class C β -lactamase |
| aq | Aqueous |
| Arg | Arginine |
| Asn | Asparagine |
| Asp | Aspartic acid |
| BL | β -lactamase |
| Bp | Boiling point |
| CataCXiumA | Di(1-adamantyl)- <i>n</i> -butylphosphine |
| CC | Column chromatography |
| COgen | 9- methylfluorene-9-carbonyl chloride |
| CphA | <i>Aeromonas</i> carbapenem-hydrolyzing β -lactamase |
| CTX-M | Ceftoximase-Munich |
| Cym | <i>p</i> -Cymene |
| Cyr | Cyrene |
| Da | Dalton |
| DBO | diazabicyclooctanone analogue |
| DCM | Dichloromethane |
| DEC | Diethylcarbonate |
| DIPEA | N,N-Diisopropylethylamine |
| DMAc | N,N-Dimethylacetamide |
| DMAP | 4-Dimethylaminopyridine |
| DMC | Dimethylcarbonate |
| DME | Dimethyl ether |
| DMF | Dimethylformamide |
| DMSO | Dimethyl sulfoxide |
| DPEPhos | Bis[(2-diphenylphosphino)phenyl] ether |
| EC | Ethylenecarbonate |
| EDTA | Ethylemediaminetetraacetic acid |
| Equiv | Equivalent |

| | |
|------------------|--|
| ESBL | Extended spectrum β -lactamase |
| FBDD | Fragment based drug design |
| FDA | Food and drug administration |
| GIM | German imipenemase metallo- β -lactamase |
| Gly | Glycerol |
| GVL | γ -valerolactone |
| His | Histidine |
| HPLC | High-performance liquid chromatography |
| HRMS | High resolution mass spectrometry |
| HTS | High throughput screening |
| IC ₅₀ | Half maximal inhibitory concentration |
| Ile | Isoleucine |
| IMP | Imipenemase |
| K _d | Dissociation constant |
| K _i | Inhibitory constant |
| KPC | <i>Klebsiella pneumoniae</i> carbapenemase |
| L.E. | Ligand efficiency |
| L1 | <i>Stenotrophomonas maltophilia</i> L1 (β -lactamase 1) |
| LBDD | Ligand based drug design |
| Leu | Leucine |
| Lim | Limonene |
| MBL | Metallo- β -lactamase |
| MS | Mass spectrometry |
| MW | Micro waves |
| NDM | New Delhi metallo- β -lactamase |
| NHC | N-Heterocyclic carbene |
| Ni(COD) | Bis(cyclooctadiene)nickel(0) |
| NMP | N-Methyl-2-pyrrolidine |
| NMR | Nuclear magnetic resonance |
| Nu | Nucleophile |
| OTf | triflate |
| OXA | Oxacillinase |
| PAINS | Pan assay interference compounds |

| | |
|--|---|
| PBP | Penicillin binding protein |
| PC | Propylenecarbonate |
| PCy ₃ | Tricyclohexylphosphine |
| Pd(acac) ₂ | Palladium(II) bis(acetylacetonate) |
| Pd(TFA) ₂ | Palladium(II) trifluoroacetate |
| Pd(tmhd) ₂ | Bis(2,2,6,6-tetramethyl-3,5-heptanedionato)palladium(II) |
| Pd ₂ (dba) ₃ | Tris(dibenzylideneacetone)dipalladium(0) |
| Pd ₂ (dppf)Cl ₂ | [1,1'-Bis(diphenylphosphino)ferrocene]dichloropalladium(II) |
| PdCl(C ₃ H ₅)(dppb) | Dichloro-1,4-bis(diphenylphosphino)butane-palladium(II) |
| PdCl ₂ (dppp) | Dichloro[1,3-bis(diphenylphosphino)propane]palladium(II) |
| Phe | Phenylalanine |
| R.T | Room temperature |
| RuPhos-Pd G ₃ | (2-Dicyclohexylphosphino-2',6'-diisopropoxy-1,1'-biphenyl)[2-(2'-amino-1,1'-biphenyl)]palladium(II) |
| SAR | Structure activity relationship |
| SBDD | Structure based drug design |
| SBL | Serine-β-lactamase |
| Ser | Serine |
| SilaCOgen | Methyldiphenylsilacarboxylic acid |
| SMC | Suzuki-Miyaura coupling |
| SPhos | [2-Dicyclohexylphosphino-2',6'-dimethoxybiphenyl] |
| SPR | surface plasmon resonance |
| TEA | Triethylamine |
| THF | Tetrahydrofuran |
| Thr | Threonine |
| TLC | Thin layer chromatography |
| Trp | Tryptophan |
| Tyr | Tyrosine |
| UV | Ultraviolet |
| Val | Valine |
| VIM | Verona integron-encoded metallo-β-lactamase |
| X-Phos | [2-Dicyclohexylphosphino-2',4',6'-triisopropylbiphenyl] |
| Xantphos | 4,5-Bis(diphenylphosphino)-9,9-dimethylxanthene |

Acknowledgements

I would like to express my gratitude to my main supervisor Dr. Annette Bayer for giving me the opportunity to work under her supervision. I am very thankful for her guidance, knowledge, support and care through the journey of my PhD. I would like to thank her for all the opportunities and encouragement that were given to me to visit other research groups and widen my knowledge and research experience. I also would like to thank my co-supervisor Dr. Hanna-Kristi S. Leiros for all the support, knowledge and the nice collaboration at the Norwegian Structural Biology Centre (NorStruct). I always found our meetings very helpful and I really appreciate her valuable and friendly feedback and discussions.

Thanks to Dr. Troels Skrydstrup for having me as part of his research group at the INANO center in Aarhus, Denmark and for the valuable and productive research visit. Thank you for the great discussions and guidance you gave me. Thank you for the nice experience and collaboration, I learned a lot working in his group. I also would like to thank Dr. Kathrin Hopmann for the great opportunity to be part of the CHOCO group and for the nice discussions in the CO₂ workshops and the CHOCO group meetings.

My gratitude and appreciation go to my friends and colleagues at the Department of chemistry for the good work environment and the nice discussions. My thanks go to the engineers who make our work easy, Truls Ingebrigtsen, Jostein Johansen, Frederic Alan Leeson and Arnfinn Kvarsnes. I am also thankful to all my former and present group members. Thanks to Marc Boomgaren, Manuel Langer, Marianne Paulsen. Thanks to Sasha for the good company and help with reading through the thesis. Thanks to Yngve Guttormsen for reading through my thesis and the positive attitude through the years.

A special thanks to Dr. Tamer Abu-Alam for helping me with reading through the thesis and giving me helpful advices. Thanks to Susann Skagseth for the productive discussions, encouragement and the nice collaboration at the NorStruct.

I would also like to thank Dr. Ashot Gevorgyan for the valuable advice and the productive collaboration.

I would also like to thank my dear friend Ljiljana Pavlovic for our friendship and the help she provided me with while writing and delivering this thesis.

I thank my co-authors Sundus Ahkter, Bjarte Aarmo Lund, Johan Isaksson, Tony Christopheit, Zeeshan Muhammad, Christopher Fröhlich.

I would like to express my love and gratitude to people who are very special to me, they have shown me nothing but love, care and support. Thanks to Uranbaatar Erdenebileg, Fatemeh Shouli Pour, and Harald Magnussen.

Last, I want to express my deep gratitude to my beloved dad and sisters Ola and Hala who always loved me unconditionally, supported me and encouraged me to finish the thesis. I also would like to praise my mom's soul who was my biggest fan and supporter forever and ever, may her soul rest in peace.

Aya Hashim Ismael

September 2020, Tromsø, Norway

Table of Contents

| | |
|--|------|
| Abstract..... | i |
| Abbreviations..... | iii |
| Acknowledgements..... | vii |
| Summary of publications and author contributions..... | xiii |
| 1. Introduction..... | 1 |
| 1.1 Aim of the study..... | 2 |
| 1.2 Outline..... | 3 |
| 2. Relevant background for the thesis..... | 5 |
| 2.1 Antibiotics & antibiotic resistance..... | 5 |
| 2.2 β -lactam antibiotics..... | 5 |
| 2.3 Antibiotic resistance: bacterial resistance modes against β -lactam antibiotics..... | 8 |
| 2.4 β -Lactamases, carbapenemases and their classification..... | 9 |
| 2.4.1 Serine β -lactamases..... | 10 |
| 2.4.2 Metallo β -lactamases..... | 11 |
| 2.5 Carbapenemase inhibitors..... | 12 |
| 2.5.1 Metallo- β -lactamase inhibitors..... | 13 |
| 2.5.2 Inhibitors of serine- β -lactamases with carbapenemase activity..... | 15 |
| 2.5.3 Summary of MBL and SBL inhibitors in different development stages..... | 17 |
| 2.6 Fragment based drug discovery (FBDD)..... | 18 |
| 3. Relevant reactions..... | 23 |
| 3.1 Palladium catalyzed C-C couplings - Suzuki-Miyaura reaction (SMC)..... | 23 |
| 3.2 Palladium catalyzed carbonylative transformation of aryl halides..... | 28 |
| 3.2.1 Carbonylative Suzuki-Miyaura coupling..... | 33 |
| 3.2.2 Aminocarbonylation..... | 36 |
| 3.2.3 Alkoxy carbonylation..... | 38 |

| | | |
|-------|--|----|
| 3.3 | Reactions for the preparation of 2-arylbenzoic acid derivatives | 40 |
| 3.4 | Solvent effect and sustainability..... | 41 |
| 3.4.1 | Biomass and CO ₂ derived solvents and their application in Pd catalyzed C-C couplings..... | 42 |
| | General discussion of results from the thesis | 47 |
| 4. | Design, synthesis and evaluation of <i>meta</i> -substituted benzoic acid derivatives as OXA-48 inhibitors (Paper I) | 47 |
| 4.1 | Background for the work in paper I..... | 47 |
| 4.2 | Research hypothesis of paper II..... | 49 |
| 4.3 | Evaluation of 3-substituted benzoic acid derivatives | 49 |
| 4.4 | Synthesis and evaluation of symmetrically and unsymmetrically 3,5-disubstituted benzoic acid derivatives..... | 51 |
| 4.5 | Additional results not included in Paper I..... | 55 |
| 4.6 | Conclusion from paper I..... | 56 |
| 5. | Development of carbonylative C-C couplings for the synthesis of VIM-2 inhibiting fragments (Paper II) | 57 |
| 5.1 | Paper II background..... | 57 |
| 5.2 | Initial work and research focus of paper II | 58 |
| 5.3 | Discussion of the results of Paper II | 60 |
| 5.4 | Conclusion from paper II | 65 |
| 5.5 | Additional results not included in Paper II..... | 65 |
| 6. | Development of carbonylative C-C, C-N, C-O couplings using renewable solvents | 69 |
| 6.1 | Paper III background..... | 69 |
| 6.2 | Paper III results and discussion | 69 |
| 6.3 | Additional results not included in Paper III | 76 |
| 6.4 | Conclusion from Paper III..... | 77 |
| 7. | Conclusion | 79 |
| 8. | Future direction | 81 |

| | |
|---------------------------------|----|
| 9. Appendix..... | 83 |
| 9.1 Experimental..... | 83 |
| 9.1.1 General methods | 83 |
| 9.1.2 Experimental details..... | 83 |
| 9.1.3 Spectral data..... | 88 |
| References..... | 99 |

Summary of publications and author contributions

Paper I A focused fragment library targeting the antibiotic resistance enzyme - Oxacillinase-48: Synthesis, structural evaluation and inhibitor design

Sundus Ahkter, Bjarte Aarmo Lund, **Aya Ismael**, Manuel Langer, Johan Isaksson, Tony Christopeit, Hanna-Kirsti Schröder Leiros, Annette Bayer. *European Journal of Medicinal Chemistry*, 2018, 145, 634–648. DOI: [10.1016/j.ejmech.2017.12.085](https://doi.org/10.1016/j.ejmech.2017.12.085).

I contributed with the development of a synthetic strategy towards unsymmetrically disubstituted benzoic acids. Synthesis of fragment 36, 37, 38, in-40, 40. I also contributed to data analysis and writing the experimental section of the mentioned fragments.

Paper II Carbonylative Suzuki–Miyaura couplings of sterically hindered aryl halides: synthesis of 2-arylbenzoate derivatives

Aya Ismael, Troels Skrydstrup, and Annette Bayer.

Org. Biomol. Chem., 2020, 18, 175. DOI: [10.1039/d0ob00044b](https://doi.org/10.1039/d0ob00044b).

I contributed to the planning and developing of the synthetic methodology. I performed all the experiments and data analysis. I also contributed to the manuscript writing.

Paper III Renewable Solvents for Pd-Catalyzed Carbonylations

Aya Ismael, Ashot Gevorgyan, Troels Skrydstrup, and Annette Bayer

Manuscript submitted to Organic Process Research & Development

I contributed to the planning and developing of the synthetic methodology. I performed all the experiments, data analysis and contributed to the manuscript writing.

Related publication not included in this thesis: **Structural studies of triazole inhibitors with promising inhibitor effects against antibiotic resistance metallo- β -lactamases**

Zeeshan Muhammad, Susann Skagseth, Marc Boomgaren, SundusAkhter, Christopher Fröhlich, **Aya Ismael**, Tony Christopeit, Annette Bayer, Hanna-Kirsti S. Leiros.

Bioorganic & Medicinal Chemistry 28 (2020) 1155983 DOI: [10.1016/j.bmc.2020.115598](https://doi.org/10.1016/j.bmc.2020.115598)

1. Introduction

Antibiotic resistance is among the most challenging threats to the global health in the 21st century and soon will be one of the top public health challenges unless urgent actions are taken. Infections such as pneumonia, tuberculosis, gonorrhoea and salmonellosis are becoming more challenging to treat as the bacteria are becoming more resistant to the current antibiotics.² Antibiotic resistance is mainly caused by their misuse in humans, animals and accelerating agricultural processes. The world needs urgent actions to find solutions for the spread of resistant bacteria not only by developing new medicines but also by changing the public behavior towards antibiotic consumption.²

β -Lactam antibiotics are one of the most widely used antibiotics and they include penicillins, cephalosporins, monobactams and carbapenems. All members of β -lactam antibiotics share the β -lactam ring as the common feature in their chemical structure.^{3,4} The continuous evolution of bacteria containing β -lactam antibiotic-hydrolyzing enzymes is one of the main reasons behind the rise of antibiotic resistance. The enzymes hydrolyzing β -lactam antibiotics are called β -lactamases and they are divided into two main groups based on their hydrolyzing mechanism: serine- β -lactamases (SBLs) and metallo- β -lactamases (MBLs). The β -lactamases (BLs) with activity towards carbapenems are called carbapenemases and they are of high importance as they are threatening the most important groups of β -lactams, carbapenems, used for the treatment of serious bacterial infections. Carbapenemases can be serine- β -lactamases (SBLs) or metallo- β -lactamases (MBLs) that are active against the last resort antibiotics- carbapenems. In addition, carbapenemases not only can hydrolyze carbapenems but also nearly all groups of β -lactams.⁵⁻⁹

There are several approaches to combat the threat of the antibiotic resistance such as the continuous development of new antibiotic lines against the resistant bacteria or the development of inhibitors that could suppress or disturb the resistance mechanism of the bacteria. A very successful approach to overcome bacterial resistance caused by β -lactamases is the combination therapy using an antibiotic and a β -lactamase inhibitor. The role of the β -lactamase inhibitor is to block the hydrolyzing enzyme from reaching the antibiotic and thus preserving the antibiotic's activity against the bacterial infection.¹

The combination therapy approach has proven to be a successful strategy regarding β -lactamases. Combination therapy using β -lactamase inhibitors such as tazobactam, clavulanic acid, sulbactam, etc. targeting SBLs that are not active against carbapenems have been available for clinical use.¹ There are several inhibitors against serine- β -lactamases, which are active against carbapenems that have recently been approved for clinical use or are in a late stage of the drug development process.¹ However, there are no MBL inhibitors that have reached clinical use so far. In addition, MBL carrying bacteria are spread globally. Therefore, the lack of MBL inhibitors can eventually lead to the world standing helpless against common bacterial infections that are caused by bacteria carrying MBLs. Thus, the global need for carbapenemase inhibitors restoring the potency of the last-line antibiotics is outstanding.^{4,10,11}

1.1 Aim of the study

The long-term goal of our work is to develop carbapenemase inhibitors that could potentially block the resistance enzymes and restore the activity of the carbapenem. Our research group is especially interested in carbapenemases (e.g., VIM-2, NDM-1, GIM-1, TMB-1, KPC and OXA-48).¹²⁻¹⁵ Over time, the group has obtained structural data from crystal structures of these enzymes in complex with a range of inhibitory fragments (small-sized compounds MW < 300) and inhibitors. The structural data gives us insight into the binding site and assists us with generating ideas for further development of active inhibitors by structure-based drug design (SBDD).

The overarching aim of my PhD work was to develop active inhibitors of two carbapenemases to restore the carbapenem antibiotic activity. I have mainly focused on two carbapenemases- the verona integron-encoded metallo- β -lactamase (VIM-2) and the serine- β -lactamase oxacillinase-48 (OXA-48).

In order to achieve the overall aim, the work in the thesis had several subgoals:

- Use the structural data from two carbapenemases (VIM-2 & OXA-48) in complex with inhibitory fragment complexes to develop fragment libraries (Figure 1). The crystal structures gave us insight into the binding site and helped identify possible interactions that we could target while designing the fragment library.

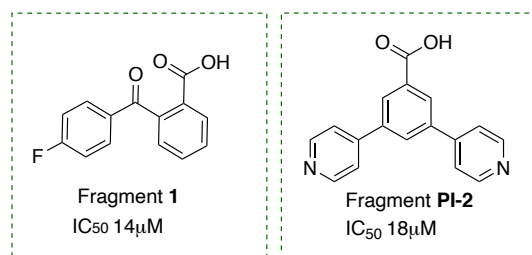


Figure 1. (left) Fragment 1 targeting VIM-2, (right) Fragment PI-2 targeting OXA-48.

- Develop efficient synthetic methods for the synthesis of fragment libraries.
- Synthesize analogues of the initial fragment and evaluate their inhibitory activity.

1.2 Outline

The thesis consists of 9 chapters. The first three chapters introduce the research question, the background and the existing knowledge. Chapter 4, 5 and 6 present the three papers resulting from the research described in the thesis. Chapter 7 presents the concluding remarks, while chapter 8 highlights open research question for future studies. A more detailed presentation of the content of the chapters follows:

- Chapter 1** Introduces the aim of the study and places the study in a wider context.
- Chapter 2** Discusses β -lactamase antibiotics including carbapenems and the antibiotic resistance assembled in carbapenemases. It also addresses the different carbapenemase enzymes and their mode of action. Furthermore, it discusses the combination therapy approach and the evolution of inhibitors used against carbapenemases. The chapter also includes a short introduction to fragment-based drug design.
- Chapter 3** Provides the chemical background for the reactions applied in this thesis. For each reaction an overview of the reaction mechanism is provided. In addition, some examples from literature are discussed to provide some knowledge about the reaction applications. Green solvents.
- Chapter 4** Introduces the background for the research described in **paper I**. In addition, it illustrates the fragment design and important features that should be included in the structure to target both binding sites R^1 & R^2 . The chapter also discusses a developed general synthetic strategy to synthesize a number of extended fragments against OXA-48 via the selective Suzuki-Miyaura coupling. Finally, the chapter addresses results presented in paper I.

Chapter 5 Introduces the background for the research described in **paper II**. The chapter illustrates the different possible synthetic routes to synthesize active fragments containing the 2-arylbenzoic acid moiety against VIM-2. I highlight the best synthetic route in my hands towards the targeted VIM-2 fragments. The chapter also discusses reaction optimization for carbonylative Suzuki-Miyaura coupling and our efforts to suppress the competing normal Suzuki-Miyaura coupling required to synthesize a number of developed fragments against VIM-2. Finally, it addresses results presented in the paper together with some findings about the reaction limitations.

Chapter 6 Is a continuation of the work conducted in paper II. It discusses the extended optimization of carbonylative Suzuki-Miyaura coupling to find a better system and cover the reaction limitation addressed in paper II. In this chapter I introduce sustainability character to my research by using new renewable solvents and test them for better reactivity within Pd-catalyzed carbonylation reactions such as carbonylative Suzuki-Miyaura coupling (C-C), alkoxy carbonylation (C-O), aminocarbonylation (C-N). The chapter highlights that changing the common organic solvents to greener alternatives is a positive step towards sustainability without losing activity in the chemical reactions. A number of applications is mentioned to address the importance of the studied solvents in both academia and industry. Finally, it addresses some results presented in the paper.

Chapter 7 Conclusion.

Chapter 8 Future direction

Chapter 9 Appendix: this chapter includes experimental details and spectral data of fragments presented in Chapter 5.5, Table 8 (entry 1-7).

2. Relevant background for the thesis

2.1 Antibiotics & antibiotic resistance

An antibiotic is a substance that can kill or cause inhibition of the microbial growth. The name “antibiotic” was first introduced by Selman Waksman in 1942. Since their discovery, antibiotics have saved many lives and improved life quality.^{16,17}

There are several classes of antibiotics such as β -lactams, macrolides, sulfonamides, aminoglycosides, quinolones etc. Each class of antibiotics affect the bacteria in different ways. For instance, β -lactams interfere with the cell-wall synthesis of the bacteria, thus killing it. While quinolones inhibit topoisomerases preventing the DNA replication and cause death of the bacteria.¹⁸

Due to the overuse of antibiotics and the resulting evolutionary pressure, bacteria have learnt to resist antibiotics. Bacteria identify antibiotics, and thus adapt and build immunity against them. Furthermore, the rapid generation time of bacteria makes it even quicker for the bacteria to evolve and build resistance against antibiotics in a short time.¹⁹ The uncontrolled growth of bacterial resistance leads to the suppression of the antibiotics effect. Bacterial infection and associated diseases that could be treated by antibiotics earlier are becoming harder to treat.² This is a growing concern threatening the health and welfare of the population worldwide and thus needs an urgent resolution.

2.2 β -lactam antibiotics

β -Lactams are considered to be among the most used antibiotics, more than 65% of the antibacterial prescriptions include β -lactam antibiotics.²⁰ There are several β -lactam antibiotics on the market. The class of β -lactam antibiotics shares a common core structure, which is a four membered ring known as the β -lactam ring. The importance of this class of antibiotics lies in their broad-spectrum antibacterial activity as they are active against both gram-negative and gram-positive bacteria.³ β -lactams are structurally classified into penicillins, cephalosporins, carbapenems and monobactams (Figure 2).^{3,4}

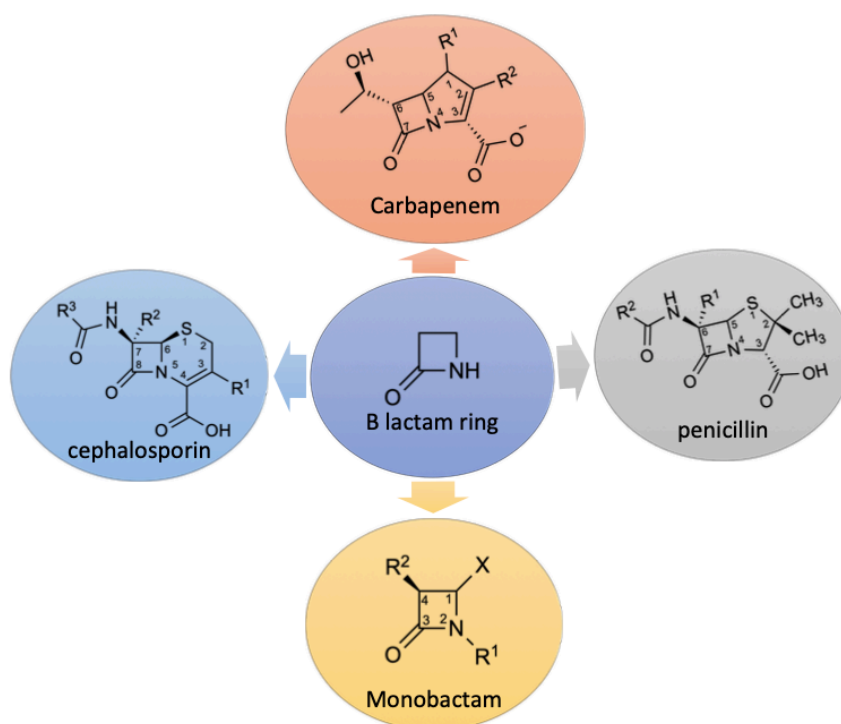


Figure 2. Chemical structure of β -lactam antibiotics with a common β -lactam ring. The R groups differs in various antibiotics. The X in the monobactam chemical structure represents α -methyl.

Penicillins: were the first developed β -lactam antibiotics and were used to treat a wide range of infections caused by bacteria such as *streptococcus*, *staphylococcus*. Penicillins have a five membered ring fused to the β -lactam ring and an amide moiety attached to the β -lactam ring. There are several penicillins available on market, all of which are β -lactam antibiotics and only differ in the side chain of the penicillin. Ampicillins, oxacillin and amoxicillin are examples of penicillins.^{21,22}

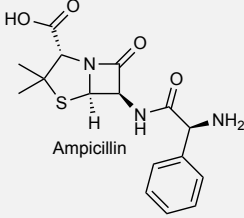
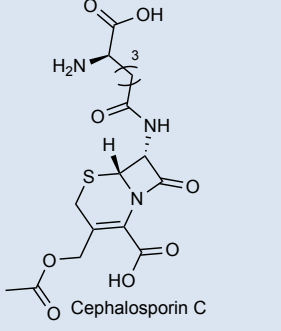
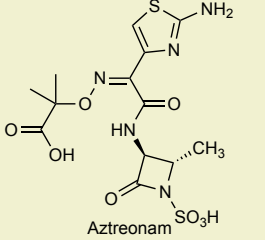
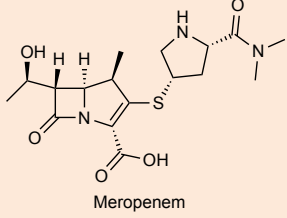
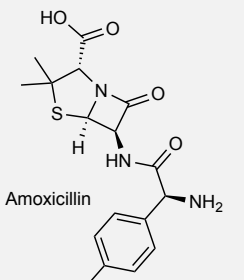
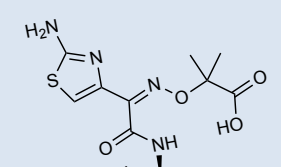
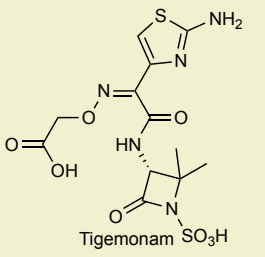
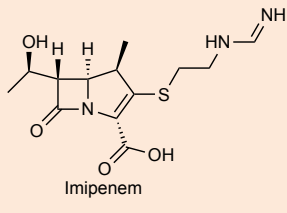
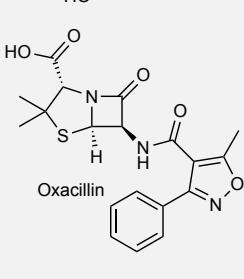
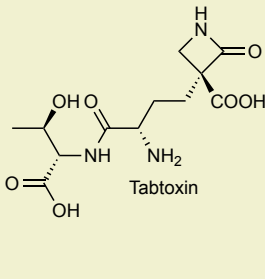
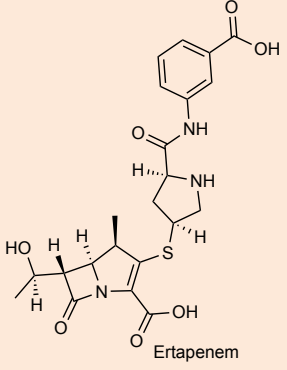
Cephalosporins: have a six membered ring fused to the β -lactam ring and an amide moiety attached to the β -lactam ring as in penicillins. Cephalosporins cover a broader spectrum of both gram-negative and gram-positive bacteria than penicillins.^{23–25} Cephalosporins are grouped into different generations based on the modified structure and the activity spectrum. For instance, the first generation was similar to the cephalosporine C, which was introduced in 1940s. Structural modification of the cephalosporine C by adding a methoxy group on the β -lactam ring resulted in the second generation of cephalosporines e.g. cefoxitin. The methoxy group added some steric hindrance to the β -lactam ring, which made it harder to hydrolyze by the BLs. Ceftazidime is an example of the third generation cephalosporines, they are characterized by the aminothiazole ring added to the side chain of the cephalosporine structure.^{22,24} The new features of the aminothiazole ring made the antibiotics of this generation more active against

gram-negative bacteria and increased the potency against penicillin-binding proteins (PBPs). Cefepime belongs to the fourth generation, while ceftobiprole²⁶ and ceftaroline²⁷ belong to the fifth generation.²² Cefiderocol is a recently US FDA-approved cephalosporin, which is used for the treatment of urinary tract infections. Moreover, cefiderocol is currently being tested in phase III against nosocomial pneumonia and infections resulted from carbapenem-resistant gram-negative bacteria.²⁸

Monobactams: are the only β -lactam antibiotics that have no ring fused to the β -lactam ring. Monobactams are only active against gram-negative bacteria such as *Neisseria* and *pseudomonas*.²⁹ Tigemonam, nocardicin³⁰, taboxin and aztreonam are examples of monobactams.²²

Carbapenems: have an unsaturated five membered ring fused to the β -lactam ring, they also have a chiral center with a hydroxyethyl side chain on the β -lactam ring. An example of a carbapenem is thienamycin, which has potency against both gram-positive and gram-negative bacteria but it is unstable for clinical applications.³¹ Imipenem is also a carbapenem but it is hydrolyzed by dehydropeptidase (human enzyme). However, a dehydropeptidase inhibitor (cilastatin) could be used to prevent the human enzyme from hydrolyzing the imipenem and thus could be used as an antibiotic.²² Meropenem, doripenem and ertapenem are more stable carbapenems than thienamycin and imipenem due to the bulkier substituents on the five membered ring. Carbapenems are known for their broad-spectrum activity against gram-negative bacteria, gram-positive bacteria and anaerobes.³¹ Carbapenems are also used recently as last resort antibiotics against antibiotic-resistant bacteria. Tebipenem is one of the latest approved carbapenems for clinical use, but it is only available in Japan.^{31,22}

Table 1. Examples of available β -lactam antibiotics.

| penicillin | cephalosporine | monobactam | carbapenem |
|--|--|---|---|
|  <p>Ampicillin</p> |  <p>Cephalosporin C</p> |  <p>Aztreonam</p> |  <p>Meropenem</p> |
|  <p>Amoxicillin</p> |  <p>Tigemonam</p> |  <p>Tigemonam</p> |  <p>Imipenem</p> |
|  <p>Oxacillin</p> |  <p>Ceftazidime</p> |  <p>Tabtoxin</p> |  <p>Ertapenem</p> |

2.3 Antibiotic resistance: bacterial resistance modes against β -lactam antibiotics

Bacteria adapt to the known antibiotics by developing several mechanisms to gain resistance against antibiotics (Figure 3).³² Bacteria can as well combine the different mechanisms and become multidrug resistant, which increases the severity of the problem.^{17,33} Bacteria can obtain resistance to the antibiotic by reducing the permeability of the drug into its cell wall. Bacteria with no cell walls e.g. *mycoplasma-genus* are not affected by antibiotics targeting the cell wall and tend to express their resistance in another way. For instance, some other bacteria contain efflux pumps that transfer the antibiotics out of the cell directly after their entry before they reach the target.³⁴ Another resistance mechanism is based on structurally mutating the targeted enzyme so that the antibiotic is not be able to bind to its target.³⁵ An example of the mutating bacteria is *Staphylococcus aureus*, which rapidly gains resistance to linezolid (antibiotic targets

23S rRNA ribosomal subunit of gram-positive bacteria) via selection of mutated copies of the gene encoding the targeted subunit.¹⁸ Bacteria can use other enzymes to modify the binding site itself and thus prevent the drug from recognizing it so that the drug would not bind to the active site and lose its activity. Macrolide erythromycin functions by binding to the bacterial ribosome. In this case, the bacteria produce an enzyme called erythromycin ribosome methylase, the enzyme methylates the binding site and prevents the antibiotic from binding. In addition, some gram-positive and gram-negative bacteria tend to produce specific enzymes to modify or inactivate the antibiotic itself and make it lose its activity. For instance, BLs enzymatically hydrolyze β -lactam antibiotics leaving them inactive.^{36,37,18,32}

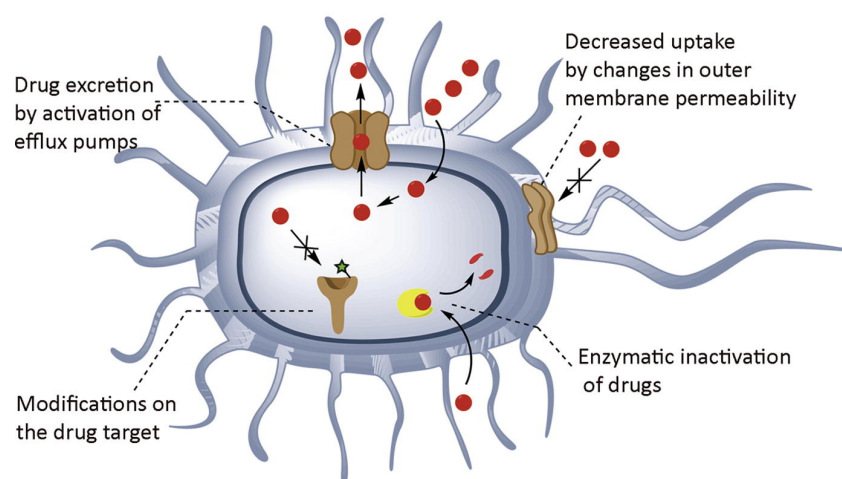


Figure 3. General presentation of the main bacterial resistance mechanism. Red represents the antibiotic, yellow represents the different bacterial resistance actions. The picture acquired from Gonzalez-Bello.³²

2.4 β -Lactamases, carbapenemases and their classification

The biological effect of β -lactams depends on their availability to their target and the ability to inhibit these targets. As mentioned before, bacteria have several resistance mechanisms. The most common mechanism of resistance towards β -lactam antibiotics in gram-negative bacteria is to produce specific hydrolytic enzymes that inactivate β -lactam antibiotics by hydrolyzing the drug core of the β -lactam ring, these hydrolyzing enzymes are known as β -lactamases.^{38,39} They were first reported even before the clinical release of penicillin in *Escherichia coli* (*E. coli*) in 1940. So far 4944 β -lactamases have been reported in gram-positive, gram-negative bacteria and mycobacteria.^{8,40-42} β -lactamases are of great diversity, they are classified based on their amino acid sequence and biochemical properties into four classes A, B, C, D; known as the Ambler classes.^{5,43,44} Nevertheless, the 4 Ambler classes (Figure 4) can be structurally grouped into two super families: SBLs, which consist of class A, C and D, all the three classes

having a serine residue in their active site in a sequence of Ser-X-X-Lys motif, and MBLs, which consist of class B, they contain Zn atom(s) in the active site, which is very important for the catalytic activity of MBLs.⁴⁵ Both groups are β -lactam hydrolytic enzymes that use different hydrolysis mechanisms to inactivate the antibiotic. Among the most important BLs are those who are active against the last resort antibiotics - carbapenems (e.g. meropenem). These BLs are called carbapenemases and they belong to both class A and D SBLs (e.g. KPC, OXA-48, AmpC) and MBLs (e.g. VIM, NDM, GIM) as shown in Figure 4.

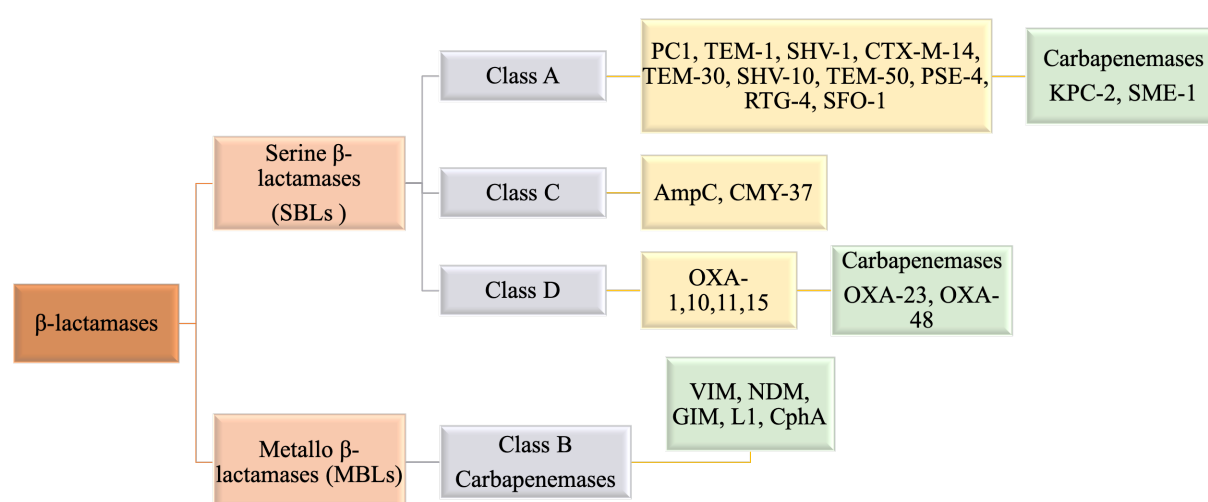


Figure 4. Ambler classification of lactamases and examples of BLs. Both metallo and serine carbapenemases are shown in green.

2.4.1 Serine β -lactamases

Generally, most β -lactamases are serine- β -lactamases; they constitute Ambler classes A, C, D, which share common active site features including the serine residue (Ser70). Only KPC-2 and SME-1 of class A and OXA-23 and OXA-48 of class D are described as carbapenemases with catalytic efficiencies for carbapenem hydrolysis. Among the most common serine carbapenemases are OXA-48 and KPC-2.⁴⁶ OXA-48 is the most efficient SBL in class D as it rapidly transfers high-level antibiotic-resistance genes to human pathogens such as *E. coli* and *Acinetobacter baumannii* (*A. baumannii*).⁴⁷ OXA-48 has a broad activity spectrum not only against carbapenems but also against penicillins and some cephalosporins (e.g. cefepime, ceftazidime or cefotaxime). OXA-48 was first reported in *Klebsiella pneumoniae* isolate in 2008, but it has been recently identified in range of *Enterobacteriaceae*.⁴⁶⁻⁴⁹ Serine carbapenemases including OXA-48 exhibit resistance through a mechanism of action that relies

on the active serine residue (Ser 70 according to DBL numbering). The carboxylated Lys73 residue is believed to activate the catalytic Ser70 residue.⁴⁹

The Ser 70 residue acts as a nucleophile and attacks the carbonyl group in the β -lactam ring forming a covalent acyl-enzyme intermediate (Figure 5, Inter I), which then forms an acyl-enzyme complex by breaking the C-N bond. Lys208 stabilizes the hydroxyl group that attacks the carbonyl group of the acyl-enzyme complex to form the second tetrahedral intermediate (Figure 5, Inter II) leaving the antibiotic inactive.⁵⁰

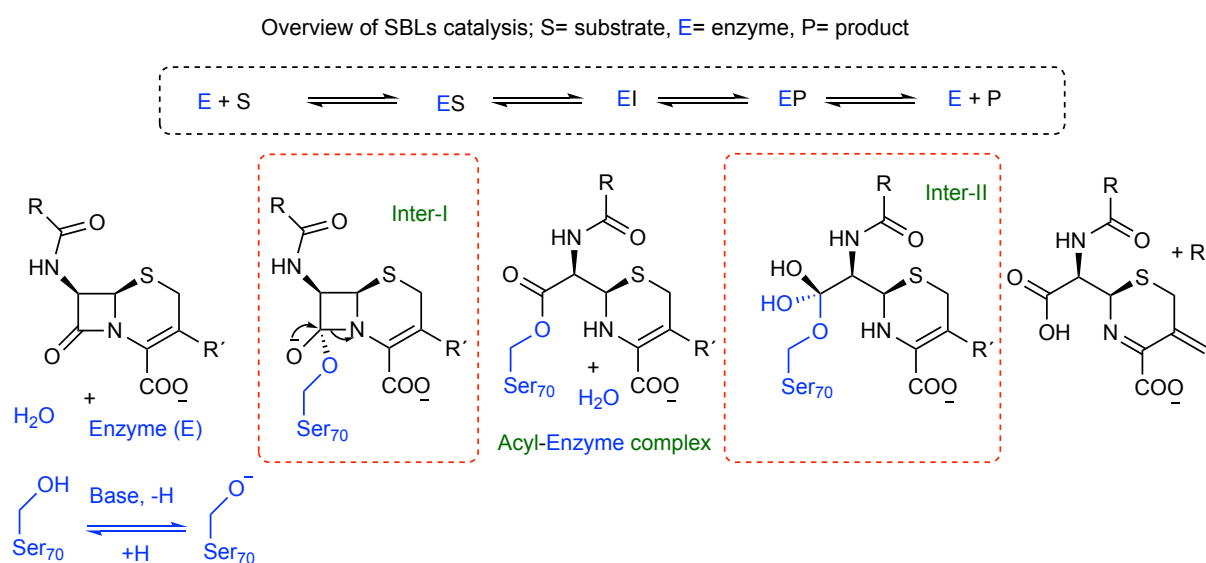


Figure 5. Mechanism of action of SBLs against an example of cephalosporin antibiotics. The picture modified from Brem et al.⁵⁰

2.4.2 Metallo β -lactamases

MBLs belong to the metallo-hydrolase superfamily.⁵¹ All MBLs are described as carbapenemases (metallo carbapenemases) as they exhibit enzyme activities against carbapenems. Metallo carbapenemases constitute Ambler class B, which shares common active site features including either one Zn^{2+} ion or two Zn^{2+} ions coordinated by different ligands and a hydroxyl ion, all of which are essential for the hydrolysis of the β -lactam ring.^{52,44} MBLs are divided into three subclasses (B1, B2, B3) based on the structure and if they contain one or two zinc ions. All three classes contain a common four-layer “ $\alpha\beta/\beta\alpha$ ” motif, with the active site centered in the groove. The active site is in between the “ $\beta\beta$ ”- sandwich with Zn^{2+} ion(s), and two α -helices on either side.^{53,54,171}

The mechanism of meropenem hydrolysis by NDM-1 was previously described and supported by X-ray structure in a published study on NDM-1.^{55,56} The hydrolysis mechanism

includes the activation of the hydroxyl groups of the hydroxyl group bridging the Zn^{2+} ions to attack the carbonyl group of the β -lactam ring cleaving the C-N bond.^{57,58} After ring cleavage, the second Zn^{2+} ion coordinates to the negative charge on the nitrogen atom and stabilizes it. A proton transfer from the bridging hydroxyl group to Asp120, followed by insertion of a water molecule into the active site forms complex **2'**. Water molecules serve as a proton source throughout the catalytic cycle. The nitrogen will then abstract a proton from the water molecule in the binding site (Figure 6, complex **3** and **4'**), which would eventually lead to the detachment of the inactive meropenem and restoration of the active site **1** (Figure 6).⁵⁶

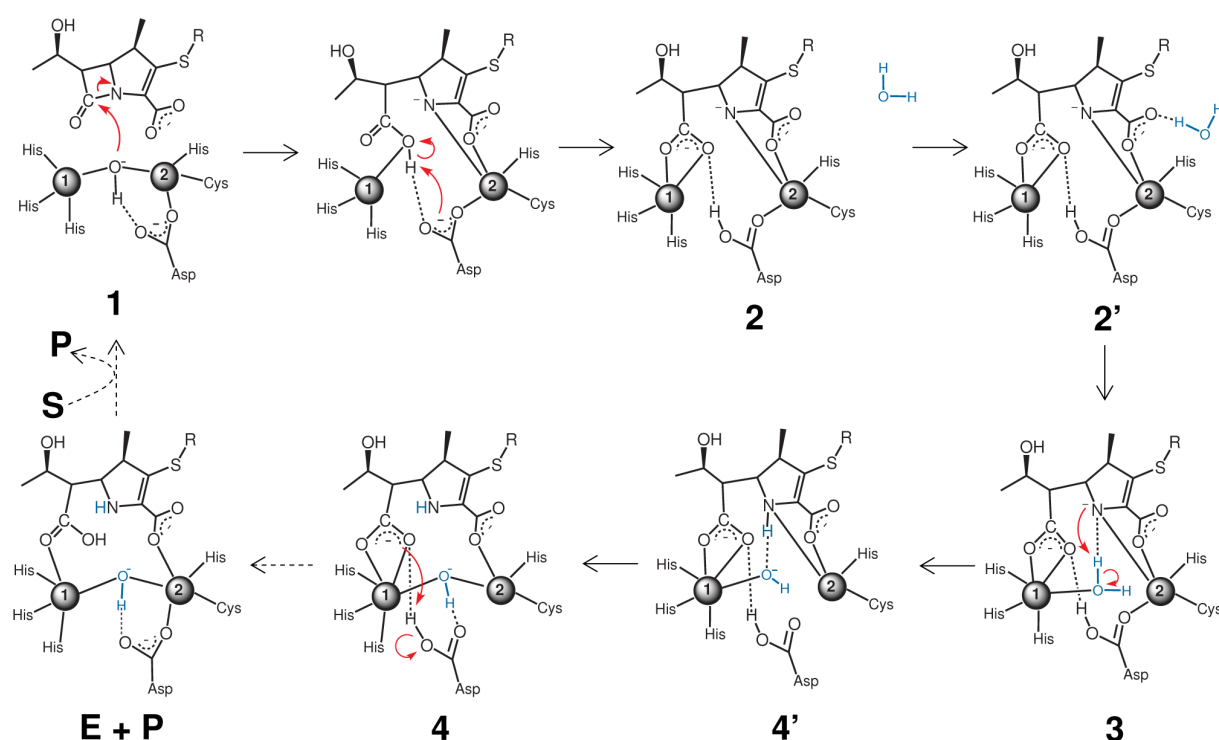


Figure 6. NDM-1 hydrolysis mechanism of meropenem. 1 and 2 grey spheres represent Zn^{2+} ions. Figure acquired with permission from Triphati et al.⁵⁶

2.5 Carbapenemase inhibitors

One of the most successful therapy approaches against BLs is combination therapy. The inhibitors combined with the β -lactam antibiotic inactivate the β -lactamase, thus preventing the hydrolysis of the antibiotic, making it possible for the antibiotic to reach its target. This method of using β -lactam/ β -lactamase inhibitors has proven to be an effective approach to restore the efficacy of the β -lactam antibiotic against pathogens producing BLs (e.g. ceftolozan/tazobactam, ceftazidime/avibactam, relebactam/imipenem, nacubactam/meropenem, vaborbactam/meropenem, ETX2514/sulbactam, VNRX-5133/cefepime, ANT431/meropenem).¹ Inhibitors such as clavulanic acid, sulbactam,

vaborbactam and tazobactam have reached clinical use but they are only active against SBLs and inactive against MBLs. Despite the efforts of finding new synthetic or natural compounds that show *in vitro* inhibition against MBLs, none of them have reached clinical use.^{59,1}

The focus of this work was to develop inhibitors targeting various BL inhibitors including MBL and SBL inhibitors that especially show activity against carbapenemases VIM-2 (paper II, III), OXA-48(paper I).

2.5.1 Metallo- β -lactamase inhibitors

There are several compounds that have showed potency against MBLs (Figure 7).^{160,61,1} However, there is still no MBL inhibitor that has reached clinical use until now.

However, recently, a boronic acid-based inhibitor called taniborbactam (Figure 7) has been reported as a “pan-spectrum β -lactamase inhibitor”⁶² against gram-negative bacteria.^{63,64} It showed a wider scope of activity than the clinically approved vaborbactam (Figure 8). Taniborbactam is considered a highly potent inhibitor of all four Ambler classes of β -lactamase enzymes. It exhibits inhibition activity against both MBLs (e.g. VIM-2) and SBLs (e.g. OXA-48, KPC-2) in a wide range of gram-negative bacteria. Structurally, taniborbactam is closely related to vaporbactam as they both possess a cyclic boronate, while taniborbactam is a bicyclic boronate with N-(2-aminoethyl) cyclohexylamine as the side chain (Figure 8). *In vitro*, cefepime/taniborbactam and meropenem/taniborbactam combinations are active against all six of the NDM-1-producing clinical isolates from *E. coli* and *K. pneumoniae*. Cefepime/taniborbactam also passed phase I of the clinical trials.⁶³

ANT431 is in preclinical trials as MBL inhibitor in combination with meropenem.¹ As mentioned before, MBLs express resistance by a different hydrolysis mechanism than SBLs. MBLs rely on the Zn^{2+} in their active site to activate the hydroxyl group to initiate the hydrolysis mechanism. Therefore, enzyme activity is affected by the availability of the Zn^{2+} ions to deactivate the antibiotic. As a result, blocking the Zn^{2+} ions by using metal chelators would disturb the hydrolysis mechanism and prevent the antibiotic degradation. EDTA is an example of a metal chelator inhibitor (Figure 7) that inactivates the active site of MBLs by coordinating to the Zn^{2+} ions and hinders its hydrolysis ability of the β -lactam.⁶⁵ EDTA has not reached clinical use due to its toxicity. Recently, Samuelsen *et al.* reported a metal chelator ZN148 that has a great potential as a MBL inhibitor. *In vitro* analysis demonstrated that ZN148 was able to

restore the effect of meropenem against NDM-1.⁶⁶ Metal chelator inhibitors show activity against MBLs including VIM-1, VIM-2, NDM-1, IMP-1, IMP-8, IMP-7, NDM-4.^{10,67,66}

Thiol-based mercaptocarboxylates (Figure 7) exhibit high potency and broad-spectrum inhibitory activity against MBLs (e.g. IMP-1, VIM-4, VIM-2, NDM-1, CphA, etc). For instance, 3-(3-mercaptopropionyl-sulfanyl)-propionic acid derivatives were reported as covalent and irreversible inhibitors of IMP-1 that restore the activity of meropenem.⁶⁸ Captopril is a thiol derivative that has been studied as broad-spectrum inhibitor against MBLs, it has shown better potency against NDM-1, VIM-2 and IMP-1 rather than other MBL inhibitors.⁶⁹ It is also used as a standard to compare the inhibition potency of new inhibitors.^{70,71} In addition, bithiazolidine possessing inhibitors especially those containing a free thiol, a carboxylate group or a tetrahedral nitrogen were found to be effective against most MBLs. ME1071 is a maleic acid derivative; it showed in vitro activity against carbapenemases with less toxicity to animals compared to other MBL inhibitors. ME1071 potentiates carbapenems e.g. biapenem against NDM-1, VIM-2 and IMP-1.⁷² Natural products and fungus extracts have also shown activity against MBLs. Aspergillomarasmine A is a fungal natural product that shows inhibition potency against VIM-2 and NDM-1.^{73,74} Biphenyl tetrazoles were described as potent inhibitors of CcrA and IMP-1. Triazoles such as triazolethioacetamide and arylsulfonyl-NH-1,2,3-triazole were described to have inhibition potentiality against VIM-2. There are several other inhibitors (e.g. thioesters, trifluoromethyl alcohols and ketones, pyridine carboxylates, benzohydroxamic acid etc.) that showed inhibition activity against MBLs. Phthalic acid/derivatives have shown to express inhibition activity against the MBL IMP-1.⁷⁵ *The group of Prof. Leiros reported phthalic acid derivatives to have potential inhibition activity in vitro against VIM-2 (chapter 5).*⁷⁶

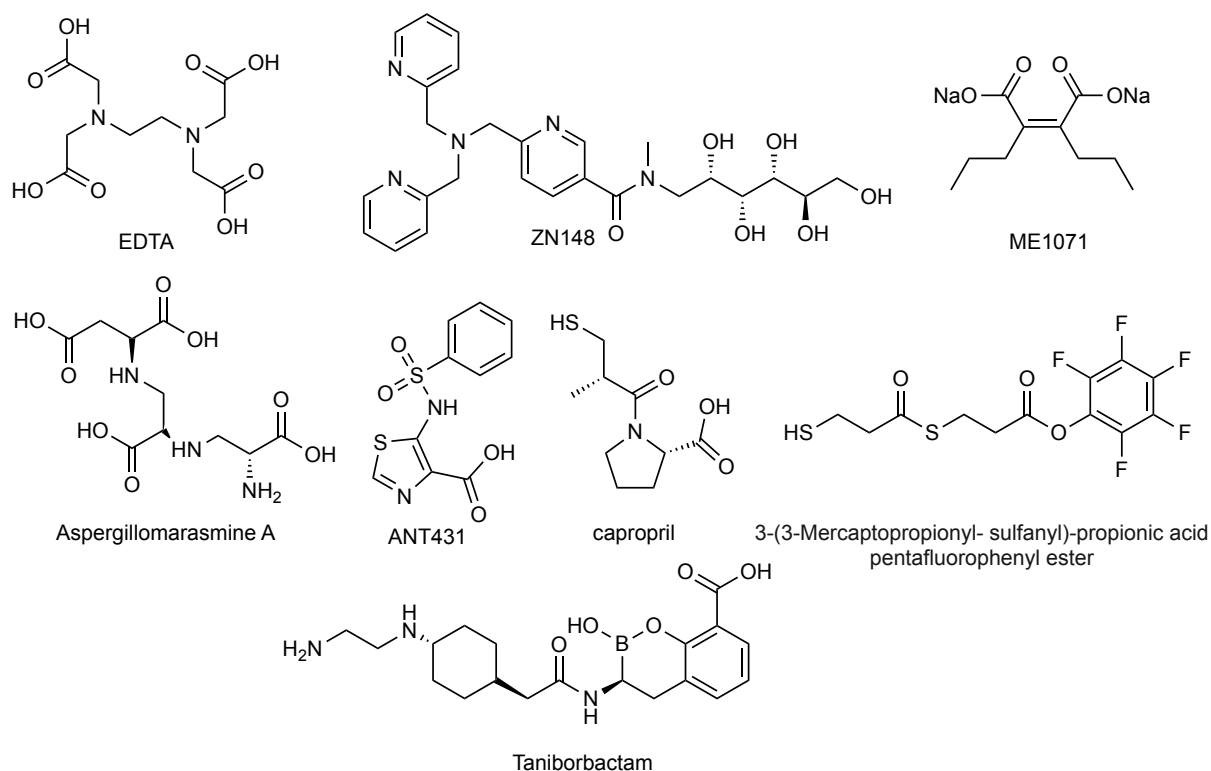


Figure 7. Examples of inhibitors against MBLs.

2.5.2 Inhibitors of serine- β -lactamases with carbapenemase activity

SBLs rely on the active serine residue (Ser70) to initiate the hydrolysis mechanism of the β -lactams. In principle, blocking the active serine residue would inactivate the enzyme and prevent it from hydrolyzing the drug. Inhibitors accompanied with the β -lactam antibiotic such as clavulanic acid and derivatives, tazobactam, sulbactam, avibactam, vaborbactam, relebactam, are shown to be efficient in suppressing the resistance mechanism in many examples for some SBLs. However, of the aforementioned inhibitors only avibactam, vaborbactam, relebactam have inhibition activity against carbapenemases.^{1,77-78}

The combination between ceftazidime/avibactam was approved by the Food and Drug Administration (FDA) in February 2015 for the combination therapy.⁷⁷ Ceftazidime/avibactam combination is active against serine carbapenemases OXA-48 and KPC. However, resistance towards ceftazidime/avibactam has already been identified in clinical multi-resistant OXA-48.⁷⁹

Avibactam is a reversible β -lactamase inhibitor that binds covalently to the active serine residue and inactivates the enzyme, it poses a broader spectrum of inhibitory activity compared

to tazobactam, sulbactam, and clavulanic acid. Avibactam exhibits activity against most BLs of class A and C such as TEM-1, KPC-2 and extended spectrum β -lactamases (ESBLs) such as CTX-M-15.^{32,80} In addition, avibactam inhibits some of class D enzymes such as OXA-48.⁸⁰ Moreover, combinations of avibactam with aztreonam (monobactam) or ceftaroline (cephalosporine) were found to show inhibition activity against OXA-48 and OXA-24.²⁷ The avibactam/aztreonam combination has reached phase III of the clinical trials, while avibactam/ceftaroline has reached phase II of clinical trials.⁷⁸

Relebactam (MK-7655) is structurally similar to avibactam (Figure 8), it also shares the same spectrum of activity as in the case of avibactam. Imipenem/cilastatin+ relebactam combination shows great activity against KPC-2 and restores the efficiency of imipenem. Moreover, the combination was approved in July 2019 by the FDA and it is used for the treatment of complicated urinary tract infections and intra-abdominal infections.^{31,67,79,81}

Vaborbactam (RPX7009) is a novel boronic acid-based inhibitor that shows activity against SBLs.⁸² The meropenem/vaborbactam combination was approved by the FDA in August 2017 for the inhibition of pathogens producing serine carbapenemases KPC-2, KPC-3, KPC-4.⁸³

Taniborbactam (see also chapter 2.5.1) is a promising inhibitor of all four Ambler classes of β -lactamase enzyme including the carbapenemases OXA-48 and KPC-2 in a wide range of gram-negative bacteria.

Recently, Taylor *et al.* described the high potentiality of CDD-97 and its derivatives (Figure 8) against OXA-48.⁸⁴

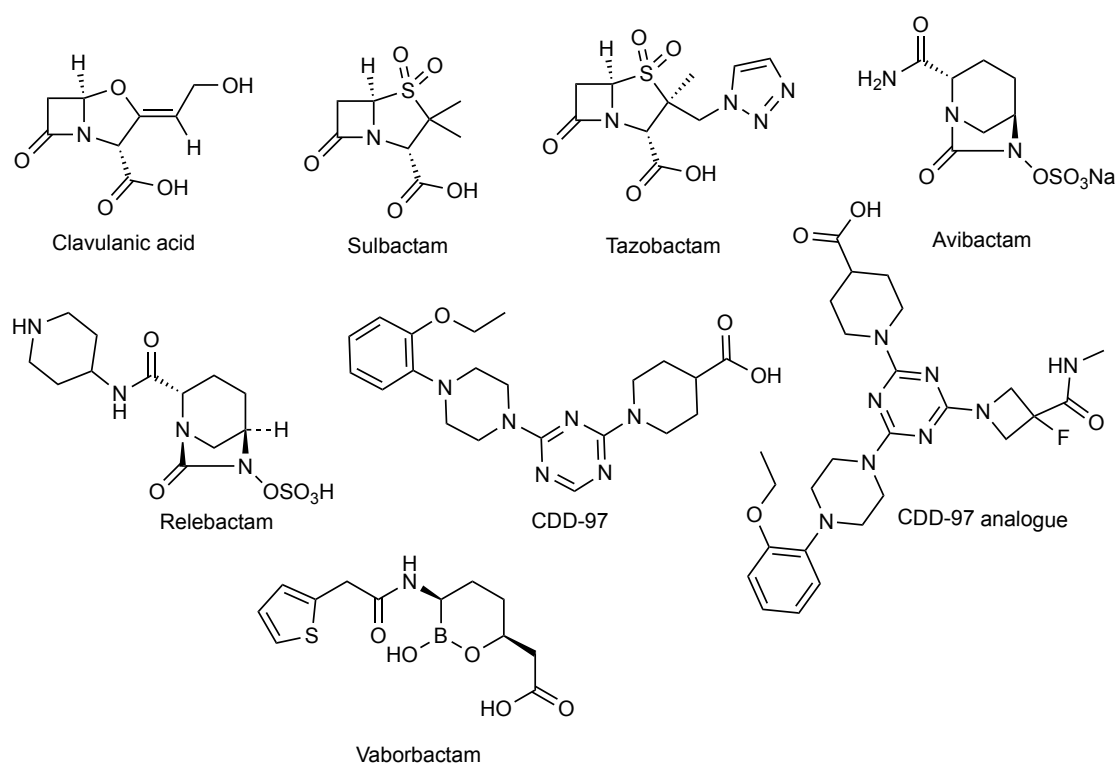


Figure 8. Examples of SBL inhibitors.

2.5.3 Summary of MBL and SBL inhibitors in different development stages

As mentioned before using combinations of β -lactam/ β -lactamase inhibitors has proven to be an effective approach to restore the efficacy of the β -lactam antibiotic against pathogens producing BLs.¹ Inhibitors such as clavulanic acid, sulbactam, avibactam, vaborbactam and tazobactam have reached clinical use but they are only active against SBLs and inactive against MBLs. However, the avibactam/aztreonam combination has reached phase III of clinical trials against MBLs.^{59,1} Combinations such as VNRX-5133/Cefepime (phase I) and ANT431/Meropenem (preclinical stage) are also active against MBLs (Table 2).¹

Table 2. Summary of BL inhibitors.¹

| Inhibitor | β -lactam | Stage | ESBL | AmpC | KPC | OXA-48 | MBL |
|-----------------|-----------------|-------------|------|------|-----|--------|-----|
| Clavulanic acid | Amoxicillin | approved | yes | - | - | - | - |
| | Ticarcillin | approved | yes | - | - | - | - |
| Sulbactam | Ampicillin | approved | yes | - | - | - | - |
| Tazobactam | Piperacillin | approved | yes | - | - | - | - |
| | Cefepime | approved | | | | | |
| | Ceftolozane | approved | | | | | |
| Enmetazobactam | Cefipeme | Phase II | yes | - | - | - | - |
| Avibactam | Ceftazidime | approved | yes | yes | yes | yes | |
| | Aztreonam | Phase III | yes | yes | yes | yes | yes |
| Relebactam | Imipenem | Phase III | yes | yes | yes | | |
| Nacubactam | Meropenem | Phase I | yes | yes | yes | | |
| Zidebactam | Cefepime | Phase I | yes | yes | yes | | |
| ETX2514 | Sulbactam | Phase II | yes | yes | yes | yes | |
| Vaborbactam | Meropenem | approved | yes | yes | yes | yes | |
| VNRX-5133 | Cefepime | Phase I | yes | yes | yes | yes | yes |
| ANT431 | Meropenem | preclinical | - | - | - | - | yes |

– no useful inhibitory activity shown; DBO, diazabicyclooctanone analogue; ESBL, extended-spectrum β -lactamase; MBL, metallo- β -lactamase, carbapenemases (green).

2.6 Fragment based drug discovery (FBDD)

In drug discovery campaigns, the identification of lead compounds can be achieved through one of the two major approaches: high-throughput screening (HTS) or fragment-based drug discovery (FBDD).⁸⁵

HTS is based on screening a large collection of drug-like compounds that follow the Lipinski's rule of five,^{86,87} (i.e. the compounds should have ≤ 5 hydrogen bond donors (N-H and O-H bonds), ≤ 10 hydrogen bond acceptors (N, O atoms), molecular weight of ≤ 500 Da and an octanol-water partition coefficient ($\log P$) ≤ 5) against a predefined drug target with the goal to find potent hits with activity in the low millimolar to nanomolar range. HTS has been successfully used in identifying novel inhibitors against MBLs.⁸⁸⁻⁹⁰ One disadvantage of the HTS approach is that it can result in misleading information concerning inhibition and binding. In the case of large-sized compounds as the space in the binding site is restricted, they are prevented from binding efficiently to several different residues. In this way the inhibition might be acceptable not because of the good binding but rather by occupying the active site.

In contrast, FBDD⁹¹ is based on the screening of a library of smaller compounds - fragments- that follow the rule of three (i.e. they have molecular weight < 300 Da, ≤ 3 hydrogen bond donors/acceptors, and CLogP below 3) in order to find efficient binders with a high possible binding efficiency.⁹² Using smaller compounds increases the chance to detect binding possibilities as the smaller size makes the compound more flexible to the binding pocket when compared to larger compounds (Figure 9). A well-established value to evaluate the binding efficiency of fragments is their ligand efficiency (LE), which is a measure of the binding energy per heavy atom in the fragment. The higher the LE-values the better as it is recommended that good hits should have LE in the range of 0.3-0.4 kcal/(mol atom).⁹³ The LE can be obtained from half maximal inhibitory concentrations (IC₅₀) (or the dissociation constant (K_d)) according to the following formula(s):

$$\Delta G = -RT \ln(K_d)$$

$$LE = \Delta G / N, \text{ where } N = \# \text{ of non-hydrogen atoms } ^{93}$$

$$LE = 1.4 (-\log (IC_{50}))/N ^{94}$$

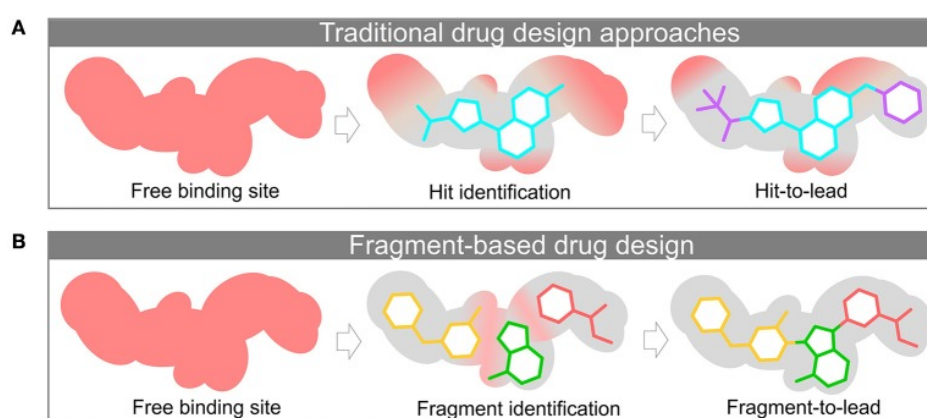


Figure 9. HTS hit (A) versus FBDD hit (B). Adapted from *frontiers in chemistry, in silico strategies to support fragment to Lead optimization in Drug Discovery*, Neto et al. Copyright (2020), open access.⁹⁵

A challenge in FBDD is that the fragments bind only weakly to the enzymes (IC₅₀ in the micro- or millimolar range), thus each atom of the fragment has to contribute to the overall binding of the fragment to be detected. Another challenge with fragments is the unspecific binding of fragments and pan assay interference compounds (PAINS), which can be solved by using orthogonal assays, such as the combination of surface plasmon resonance (SPR) and a biochemical assays to identify false positive results.^{76,96}

Fragments most likely do not have the required potency to be considered as a lead compound and would need further improvement. To guide the fragment evolution, structural

information of the fragment in complex with the targeted enzyme are needed to give insight into possible interactions in the binding site. This process is called structure-based drug design (SBDD) and it relies on the available information about the 3D structure of the drug target.^{85,92,97} The 3D structure of the drug target can be mainly obtained through experimental approaches such as X-ray crystallography or nuclear magnetic resonance spectroscopy (NMR).^{98,99} With the structural information in hand, it would be possible to predict the necessary characteristics for binding and use this information to evolve the fragments to drug candidates of high potentiality to bind to the drug target with higher affinity.⁸⁵ Fragments evolution can be achieved by several approaches:⁹⁷

Fragment-growing: It employs modification of the fragments by adding more groups in order to increase the size of the fragments without losing binding efficiency (Figure 10. A). This approach was the aim of papers II and III.

Fragment-linking: With the help of the structural information of the inhibitor/enzyme complex, if several fragments that bind in adjacent binding sites can be identified, those fragments can be chemically connected to form a new optimized ligand with better binding and higher potency (Figure 10. B).

Fragment-merging: This approach is very useful if there are two identified binding site and their ligands are competing for the chemical space or if there are two different fragments that partially occupy the same site. In either of the cases, overlaying structures of the two fragments helps bring the dissimilar parts together and design a new potent fragment towards drug like compounds (Figure 10. C). We applied this approach in paper I to optimize fragments against OXA-48.

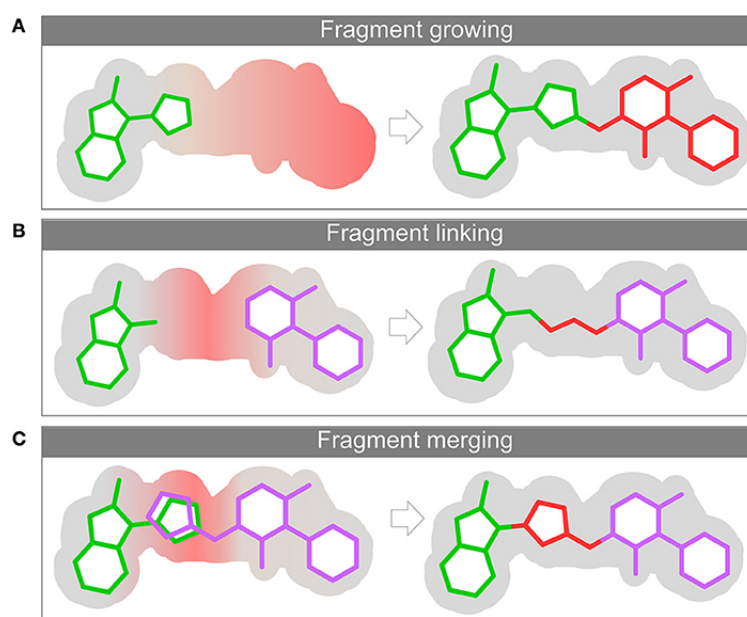


Figure 10. Different approaches towards fragment optimization. Adapted from *frontiers in chemistry, in silico strategies to support fragment to Lead optimization in Drug Discovery*, Neto *et al.* Copyright (2020), open access.⁹⁵

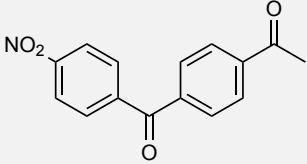
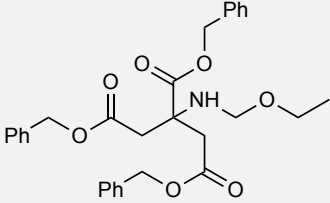
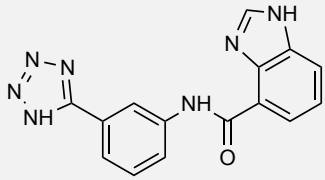
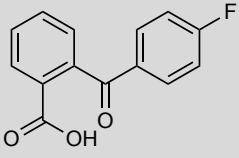
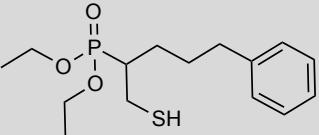
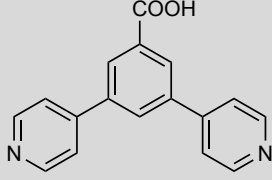
The advantage of the FBDD approach is that it allows for lead optimization to detect the chemical space with compounds of high development potentiality within the rule of 5, required for identifying lead compounds. Moreover, it allows for more hydrophilic hits that can enhance the affinity via the accessible hydrogen bonding. The fragments identified by FBDD can be optimized further to acquire drug-like properties such as solubility properties, high potency, LE and the size of the compound.¹⁰⁰

FBDD was first employed successfully against kinase targets.^{101,102} However, it is now being applied against a diversity of targets. Zelboraf (a drug for the treatment of late-stage melanoma) was the first FDA approved drug developed by FBDD.^{103,104} In addition, FBDD is proven to be a successful approach to develop drugs against both SBLs and MBLs. Chen *et al.* identified micromolar-range noncovalent inhibitors including thiol derivatives and dicarboxylates against class A β -lactamases using FBDD approach.¹⁰⁵ Moreover, Nicholas *et al.* have modified polycarboxylic acids-based fragments that are considered to be a starting point to target SBLs (class A and D) using FBDD (Table 3. entry 1).¹⁰⁶

The group of Prof. Leiros has utilized surface plasmon resonance to identify potent inhibitory fragments against both serine- and metallo-carbapenemases (chapter 4.1 and 5.1). Christopheit *et al.* reported inhibitory fragments targeting the MBLs NDM-1 and VIM-2,^{14,107,76} among them a novel inhibitor scaffolds against VIM-2 based on phthalic acid derivatives

(chapter 5).¹³ Lund *et al* reported 3,5-disubstituted benzoic acid/ derivatives scaffolds against SBLs (OXA-48) using FBDD.¹⁵

Table 3. Examples inhibitors developed from fragments targeting BLs provided by Nicholas *et al.*¹⁰⁶ and by Leiros.^{13-15,76,107}

| | | | |
|---|---|---|--|
| 1 |  <p>$K_i = 11 \mu\text{M}$ fragment against MBLs (IMP-1)</p> |  <p>$K_i = 20 \mu\text{M}$ fragment against SBLs (OXA-10)</p> |  <p>$K_i = 89 \text{ nM}$ fragment against SBLs (CTX-M-9)</p> |
| 2 |  <p>$\text{IC}_{50} = 14 \mu\text{M}$ fragment against MBLs (VIM-2)</p> |  <p>($\text{IC}_{50} = 0.38, 0.31, 1.8 \mu\text{M}$) fragment against MBLs VIM-2, GIM-2, NDM-1 respectively</p> |  <p>$\text{IC}_{50} = 18 \mu\text{M}$ fragment against SBLs (OXA-48)</p> |

3. Relevant reactions

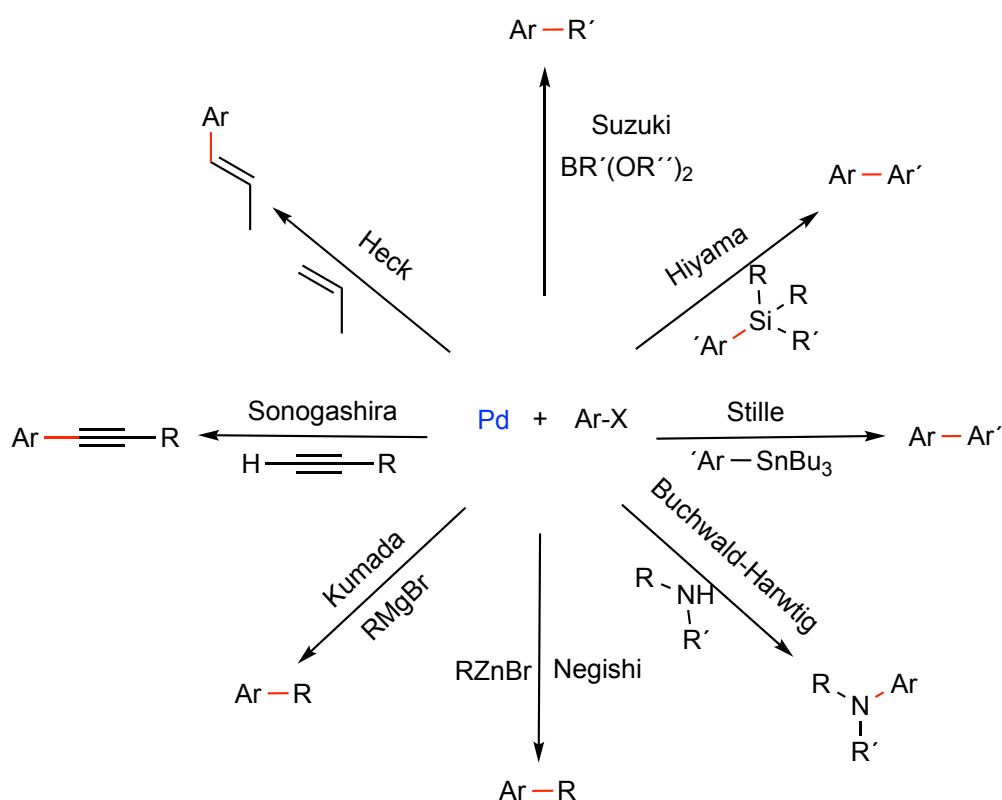
During the course of our research project on the synthesis of fragment libraries towards a new line of carbapenemase inhibitors (OXA-48 and VIM-2), reliable synthetic methods for preparing the designed fragment libraries were required.

Reactions relevant to the work presented in this thesis are:

- Suzuki-Miyaura coupling (SMC): used for the preparation of 3,5-disubstituted benzoic acids and acid derivatives as inhibitor scaffolds against the SBL OXA-48 (chapter 4).
- Carbonylative Suzuki-Miyaura coupling: used for the preparation of 2-arylbenzoic acids and acid derivatives as inhibitor scaffolds against the MBL VIM-2 (chapter 5 & 6).
- Reaction for the preparation of 2-arylbenzoic acids derivative (chapter 5 & 6).
- Aminocarbonylation & Alkoxy carbonylation: used for the preparation of primary and secondary amides and carboxylic esters as inhibitor scaffolds against MBL VIM-2 (chapter 5 & 6).
- The aforementioned reactions have been used as reaction models to test a new series of sustainable solvents aiming to find optimized conditions for the preparation of inhibitor scaffolds against MBL VIM-2 (chapter 6).

3.1 Palladium catalyzed C-C couplings - Suzuki-Miyaura reaction (SMC)

Palladium catalyzed couplings are a powerful tool for advanced chemical synthesis of C-C bonds for both academic and industrial applications. Negishi, Heck and Suzuki-Miyaura couplings are examples of the most commonly used palladium catalyzed reactions.¹⁰⁸ However, Suzuki-Miyaura coupling is extensively studied. The used boronic acids are generally nontoxic and thermally and moisture stable, which is an advantage over other cross-coupling reactions that include toxic additives and metals. Negishi couplings require the use of air and moisture sensitive organozinc compounds as the nucleophile, which makes the reaction relatively intolerant to functional groups in comparison to the Suzuki-Miyaura coupling.^{108,109} The main disadvantage of Stille couplings is that they require the use of toxic organotin compound (Scheme 1).^{108,110}

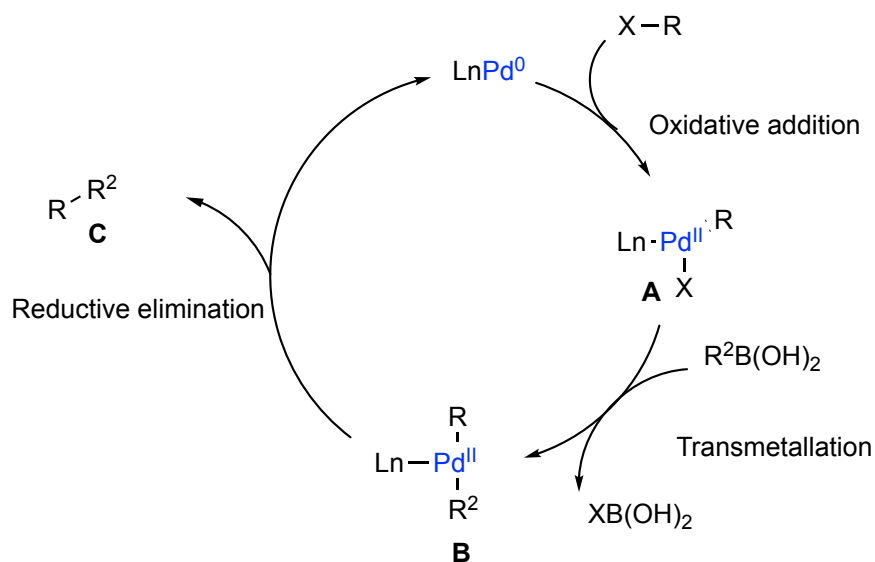


Scheme 1. Common palladium catalyzed cross-coupling reactions.

General mechanism of palladium catalyzed C-C cross-couplings

Palladium activation of Ar-X is commonly used for selective and specific formation of new C-C bonds in Suzuki-Miyaura coupling by coupling with the corresponding nucleophile. The reaction mechanism is similar to most of the cross-coupling reactions. The main difference is the choice of the transition metal. Considering the Suzuki-Miyaura coupling as an example of general palladium cross-coupling, the reaction mechanism proceeds via a three steps catalytic cycle (Scheme 2). The first step is oxidative addition of the organohalide to the active Pd⁰ species forms complex **A** (X-LnPd^{II}-Ar). Electron-rich ligands are favored, as it gives an electron-rich metal center that facilitates the oxidative addition. The reactivity of organohalides/pseudo-halides in C-C couplings varies with respect to the bond dissociation energy of the R-X (I > OTf > Br > Cl > OTs > OAc). The second step in the catalytic cycle is transmetalation with the nucleophile in presence of a base to form complex **B**. Different nucleophiles can be introduced in this step based on the type of couplings e.g; boronic acids and derivatives, organozinc or -tin reagents, etc. After the two organic groups are coordinated to the Pd^{II} complex, they undergo trans-cis isomerization to form the correct geometry needed for the

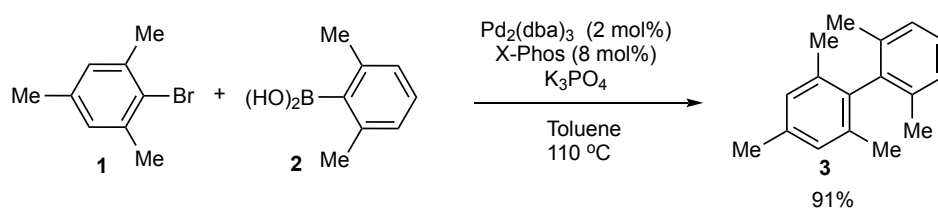
reductive elimination. This could be assisted by bulky ligands to furnish the coupled product **C** and to restore again the active Pd^0 .



Scheme 2. General reaction mechanism for the Suzuki cross-coupling reaction.

The impact of the reaction components on the reaction rate

The nature of the coupling partners has a significant influence on the reactivity. It is known that palladium cross-coupling reactions can be selective in favor of less sterically hindered and electronically more deficient position of the electrophile (Ar-X).^{111–113} Aryl iodides are more active in oxidative addition to Pd^0 center than their corresponding bromides and chlorides. Oxidative addition of iodobenzene with $\text{Pd}(\text{PPh}_3)_4$ could occur at room temperature while heating is required for bromobenzene to undergo oxidative addition. This is the reason for using additives such as NaI in reactions including aryl bromides to facilitate oxidative addition step by forming *in situ* aryl iodides. Electron-rich and bulky ligands such as $\text{P}(t\text{-Bu})_3$, Buchwald phosphine-based ligands, carbene ligands are used for couplings of less reactive aryl bromides and chlorides.^{120,121,116} For instance, coupling of 2,6-di-substituted aryl halides and aryl boronic acid was obtained in 91% yield using $\text{Pd}_2(\text{dba})_3$ and a Buchwald ligand X-Phos^{122} (Scheme 3).



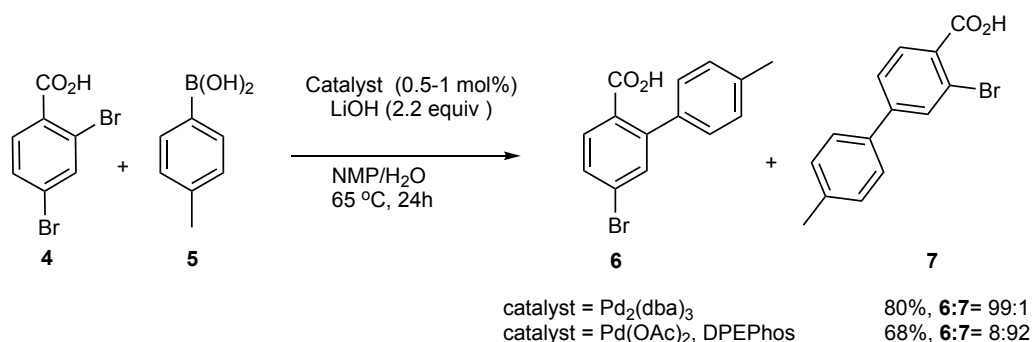
Scheme 3. Suzuki couplings of hindered electron-poor aryl bromides.

The difference in reactivity for example in di-haloaryls can be advantageous as it can lead to chemo- or regioselectivity in cross-coupling reactions. There is also reactivity difference between transmetalating agents. For example, electron deficient boronic acids or protected boronic acids are less reactive than electron rich unprotected boronic acids.

Chemo- and regio-selectivity in Suzuki-Miyaura coupling

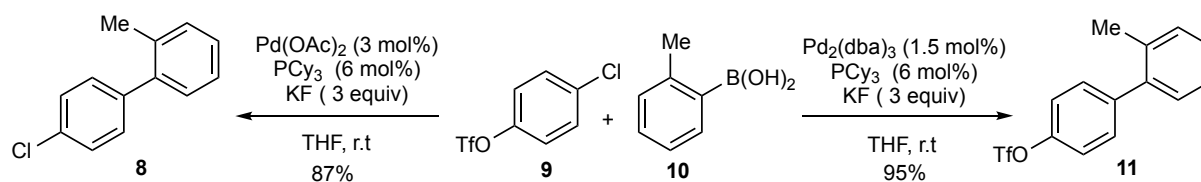
Over the last decades many catalysts and ligands have been designed and tested in several palladium catalyzed cross-couplings. The achievements in this area are related to the design and development of ligands that not only promote the catalytic transformation but also provide both regio-, chemo- and enantioselective control over the reaction.¹¹⁴

Regioselectivity of substrates where two of the same halo group are present for coupling can be achieved by catalyst control.^{117,118} Houpis and coworkers reported the regioselective coupling reaction of 2,4-dibromobenzoic acid with 4-tolylboronic acid, where the reaction gave excellent regioselective coupling at the ortho position in 80% yield when using Pd₂(dba)₃. On the other hand, using the bulky bidentate DPEPhos as a ligand together with Pd(OAc)₂ reversed the selectivity and the 4-tolyl-2-bromobenzoic acid was formed in 68% yield (Scheme 4).¹¹⁹



Scheme 4. Regioselective Suzuki-Miyaura coupling reaction of 2,4-dibromobenzoic acid with 4-tolyl-boronic acid.

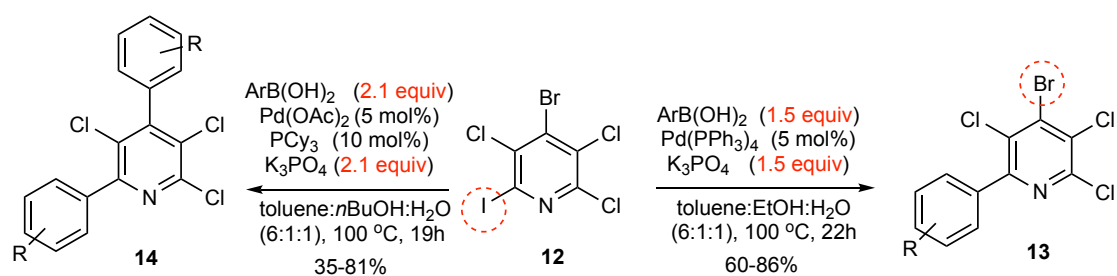
An example showing the chemoselectivity is the reaction of 4-chlorophenyl triflate with 2-methylphenyl boronic acid using two different Pd catalysts, while using the same ligand. Pd(OAc)₂ and PCy₃ gave selective coupling at the triflate position and the product was obtained in 87% yield, while using Pd₂(dba)₃ and PCy₃ gave the selective coupling on the chloride position instead and the product was obtained in 95% yield (Scheme 5).¹¹⁶



Scheme 5. Chemoselective cross-coupling of 4-chlorophenyl triflate with 2-methylphenyl boronic acid.

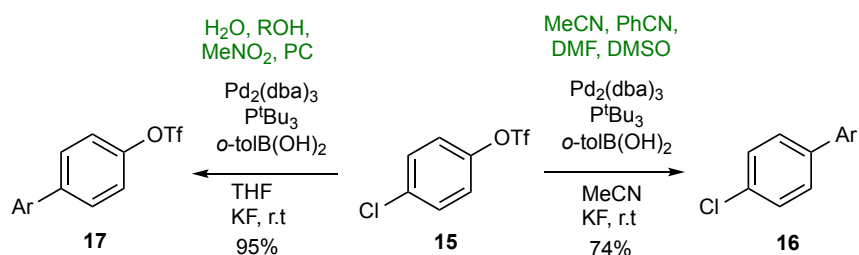
Selective Suzuki-Miyaura coupling on di-haloaryls are also considered challenging due to the high chances of obtaining mixtures of different coupling products in symmetrical or unsymmetrical fashion that might be hard to separate. The key in this process is tuning the reaction condition to allow the coupling of only one of the two halogens and result in monosubstituted product without affecting the other possible coupling position. For instance, using less equivalency of the boronic acid, low temperature, less catalyst loading or by changing the nature of the solvent.

Langer *et al.* reported chemo and site selective Suzuki-Miyaura coupling on 4-bromo-2,3,5-trichloro-6-iodopyridine.¹¹² Selective coupling on the active C-I on the 6-position occurred using only 1.5 equivalents of the boronic acid, K_3PO_4 (1.5 equiv.) and $Pd(PPh_3)_4$ in a solvent mixture of toluene, ethanol and water (6:1:1) (Scheme 6). Although a slight drop in yield in case of electron-poor arylboronic acid, the reaction still showed high degree of chemoselectivity at position 6. It was also shown that switching the catalyst system to a more reactive catalyst $Pd(OAc)_2$ and PCy_3 gave 4,6-biarylated compounds as the main product where the chemoselectivity on iodide was lost and the reaction occurred on both C-I and C-Br. Furthermore, increasing the amount of the base and boronic acid in addition to using more active catalyst (Pd/PCy_3) allows the chemoselective diarylation of pyridine on both C-I and C-Br. Although the less active C-Cl stayed unreacted under these conditions, traces of triarylated pyridine was observed. This indicated that increasing the amount of the boronic acid and the base could lead to highly arylated pyridine. Tuning the reaction conditions could allow for high degree of selectivity, which makes it a very useful tool for the synthesis of unsymmetrically arylated pyridines.



Scheme 6. Chemoselective SMC on 4-Bromo-2,3,5-trichloro-6-iodopyridine.

In some cases, the choice of the solvent can strongly influence the chemoselectivity of the reaction. This is illustrated by the selectivity of Suzuki-Miyaura coupling on chloroaryl triflate with *o*-tolylboronic acid (Scheme 7). The reaction using Pd₂(dba)₃ and P(*tert*-Bu)₃, as catalytic system showed reactivity towards the chloride (95%) when using non-polar solvents such as toluene. In case of polar solvents such as MeCN and DMF the reactivity was opposite and the coupling occurred on the triflate (C-OTf) instead (74%).^{123,116} This observation is explained by the hypothesis that polar solvents stabilizes the charged palladium species. A follow up study by Sharon *et al.* demonstrated that the SMC selectivity on the triflates using Pd/P(*t*-Bu)₃ does not generally follow the claimed trend using polar solvents.¹²⁴ Selectivity on C-OTf is only limited to few coordinating solvents such as NMP, DMF, MeCN, DMSO. On the other hand, reactivity on the C-Cl was observed with other polar solvents (H₂O, MeOH, *i*PrOH, etc.) as with non-polar (toluene, dioxane, etc.) solvents. This observation is related to solvent role where it does not only dissolve the reaction component into a homogenous mixture but also influences the reaction kinetics by stabilizing charged intermediates in the catalytic cycle.

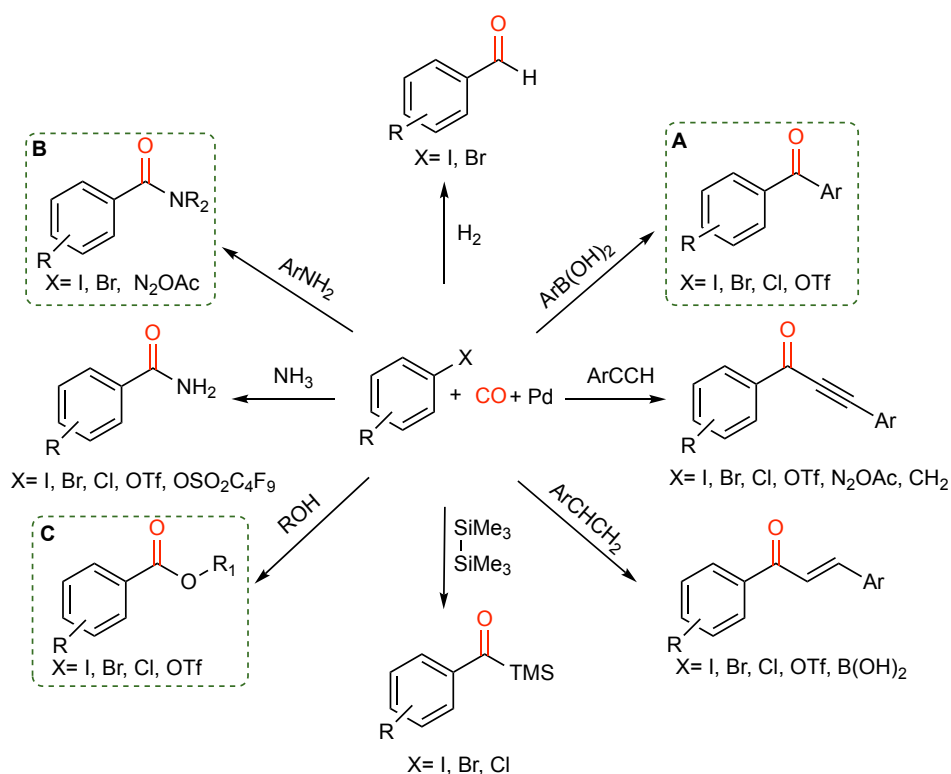


Scheme 7. Solvent effect on the chemoselectivity of arylchloride triflate.

3.2 Palladium catalyzed carbonylative transformation of aryl halides

Palladium carbonylative couplings covers many closely related reactions that incorporate CO into a substrate by adding it into an aryl-, benzyl- or vinylpalladium complex in the presence of various nucleophiles.¹²⁵ It is a very important tool for a wide range of synthetic transformations that allows direct formation of biaryl and hetero-aryl ketones, benzylic aldehydes, benzoic acid

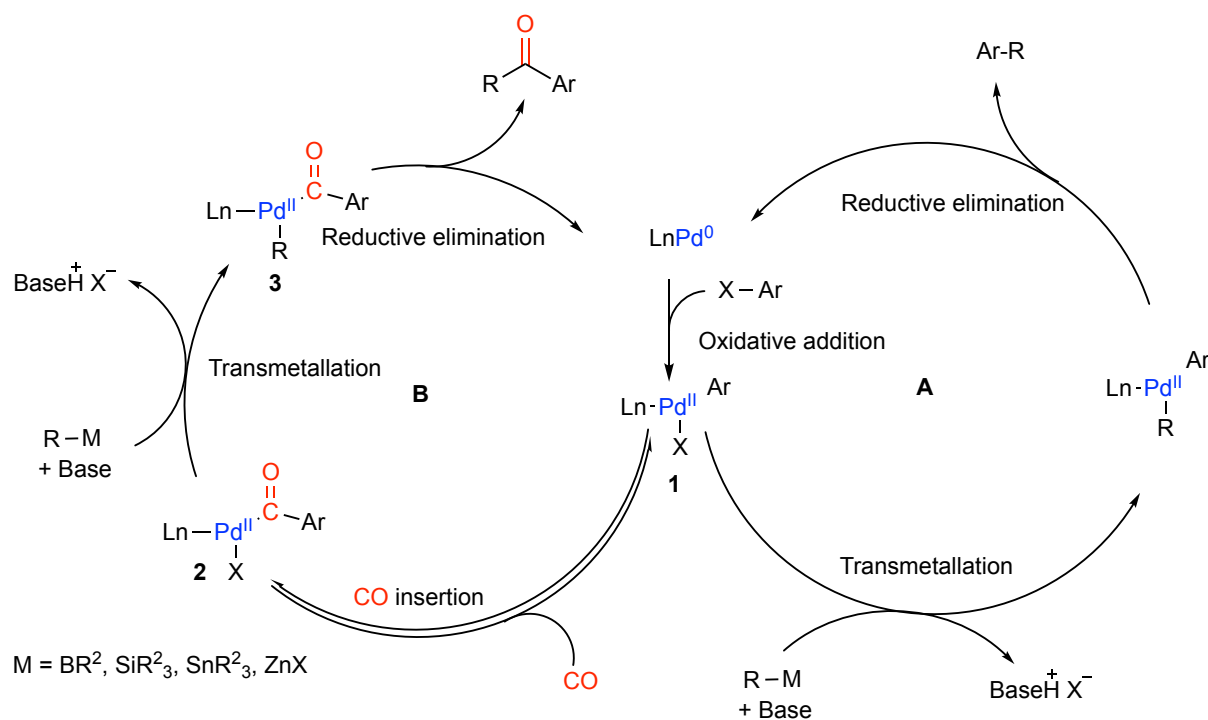
and acid derivatives, amides, etc (Scheme 8).¹²⁶ Based on the type of the nucleophile, the transition metal catalyzed carbonylation can be carbonylative Suzuki-Miyaura cross-coupling, aminocarbonylation and alkoxy carbonylation (Scheme 8. **A**, **B**, **C** respectively). The reaction can occur intermolecularly and/or intramolecularly, which allows a wide application of the reaction. Intramolecular carbonylation enables the synthesis of heterocycles for instance, alkoxy- or aminocarbonylation of hydroxy or amino-substituted aryl/vinyl halides enables the synthesis of lactones, lactams, oxazoles, thiazoles, imidazoles, and other heterocycles.^{127,128,125}



Scheme 8. Examples of palladium catalyzed carbonylation reactions.¹²⁶

Palladium catalyzed carbonylation reaction (Scheme 9. cycle **B**) is mechanistically similar to the non-carbonylative one (Scheme 9. cycle **A**) as it consists of the same basic steps; oxidative addition, transmetalation, and reductive amination. It consists of an extra step, which is the coordination and the insertion of the CO after the oxidative addition forming the acylpalladium intermediate (Scheme 9, complex **2**). In general, the aromatic halides (ArX) react with an appropriate nucleophile in the presence of catalytic amounts of a palladium complex in carbon monoxide atmosphere, where the leaving group X (e.g. I, Br, Cl, OTf, etc.) is replaced by the nucleophile with incorporation of the CO molecule(s) (Scheme 9, cycle **B**).¹²⁹ The reaction often take place at 60–140 °C under 5–60 bar of CO, and may also require a stoichiometric amount of base to regenerate the catalyst.¹²⁵

Several factors make it challenging to find suitable catalytic systems and reaction conditions for carbonylative couplings. For instance, in carbonylative Suzuki-Miyaura coupling, it is very challenging to find a catalytic system and reaction condition to favor the carbonylative reaction over the competing non carbonylative reaction. The oxidative addition can favor electron-rich metal center in carbonylative coupling reactions.^{130,126} However, the CO insertion favors an electron-deficient metal center.¹²⁶ On the other hand, reductive elimination can be assisted with bulky ligands, while CO insertion requires less bulky ligands. In addition, elevated temperatures could be advantageous in favor of oxidative addition, while it could lead to decarbonylation of the acylpalladium after CO insertion.^{128,130-132} Therefore, the success of the optimal catalyst/ligands depends most likely on the individual substrates, CO pressure and reaction conditions.



Scheme 9. General mechanism of non-carbonylative cross-coupling (A) versus carbonylative cross-coupling (B).

The product of the carbonylation reaction is dependent on the rate of the CO insertion, which should be faster than other processes like transmetalation in order to obtain the carbonylated product (Ar-CO-Nu) rather than the non-carbonylated by product (Ar-Nu).¹³³ This could be achieved by altering the other reagents by carefully choosing their functionalities or concentration by slow addition.¹³³ On the other hand, using CO in high pressure might increase the CO insertion rate and thus favor the carbonylative product rather than other by-products such as the non-carbonylative product.¹³³ However, if CO gas is used in excess hoping to

overcome these problems the result might be opposite to the intended one as the palladium atoms could cluster and agglomerate forming the nonactive palladium black.¹³⁴ The Pd⁰ reactivity towards oxidative addition could be negatively influenced by the strong binding ability of the CO. This is because CO is a good π -acceptor and would receive electrons from the metal center to form a π -back bond.¹³⁰

All these factors could interrupt the catalytic transformation in one way or another. However, a possibility to overcome this problem is to use electron-rich ligands. Generally, ligands with strong σ donor ability might prevent the direct coordination between Pd⁰ and the CO.¹³⁰ Wide range of powerful ligands have been developed to accelerate many of the carbonylative reactions.^{135,136,137} The achievement in this area did not only include the most studied phosphine ligands (monodentate and bidentate) but also included NHC and other nitrogen and thiourea ligands (Figure 11).^{130,136,138}

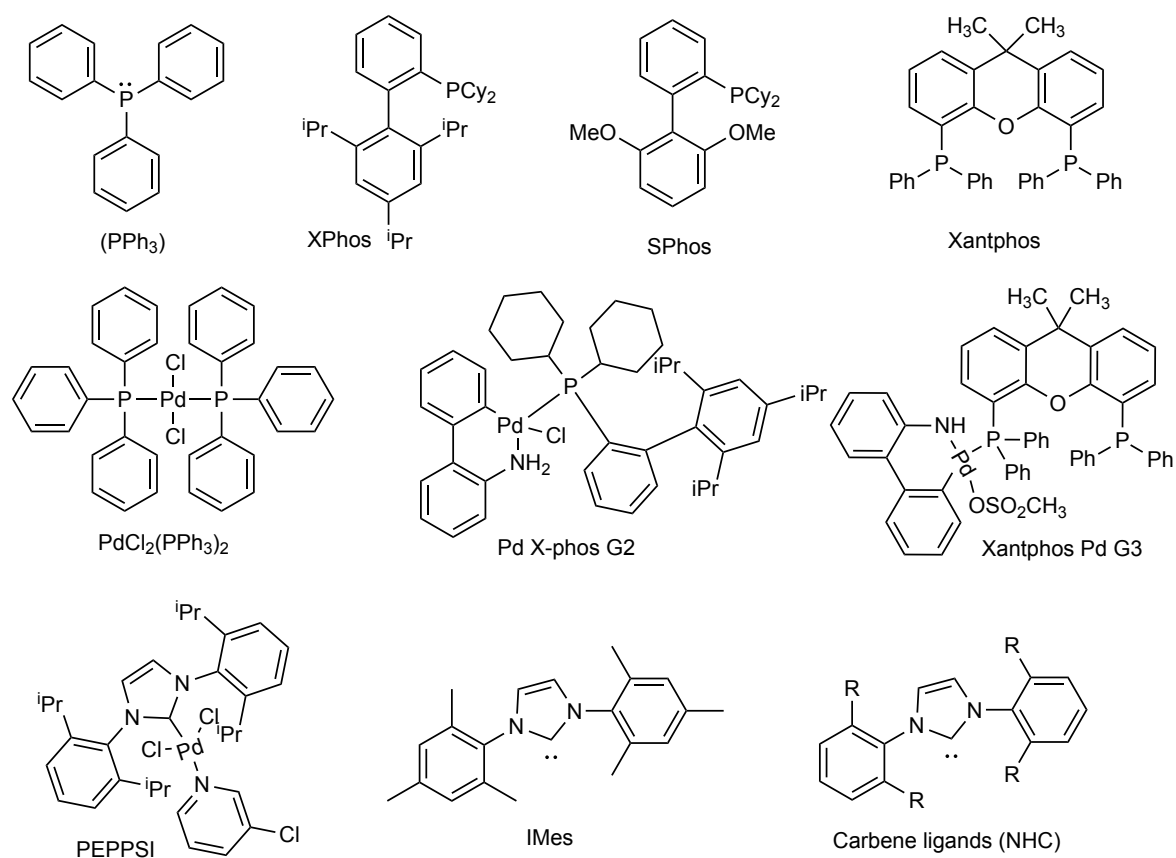


Figure 11. Selected examples of Pd complexes and commonly used ligands.

Use of CO gas and potential CO sources

The installation of the carbonyl group can be achieved by using CO gas. Despite the hazard related to the handling of the toxic, corrosive, and high flammable CO gas, it is widely used as an available and important C1 building block.¹²⁹ Synthetic transformations using gaseous reagents as CO are commonly performed in autoclaves under high pressure or under atmospheric pressure using a balloon. Safety equipment is necessary to reduce safety concerns when handling CO. However, it is commonly used in research and industrial process due to its availability and low cost.

Alternatively, safer sources of CO including transition metal carbonyl complexes (e.g. Cr(CO)₆, W(CO)₆, Co₂(CO)₈, Mo(CO)₆)¹³⁹, carbamoylsilane¹⁴⁰, oxalyl chloride¹⁴¹, formats¹⁴², aldehydes in addition to in situ decarbonylation protocols have been developed.^{143,144} The use of these carbonyl complexes introduces potential byproducts from the CO surrogate, which interrupt or get mixed with the desired product and complicate workup and isolation.¹⁴⁵ Moreover, they could potentially inhibit the possibility of developing novel carbonylative transformations.

Skrydstrup and coworkers have developed a two-chamber system setup for in situ generation of CO from stable solid CO precursors, 9-methylfluorene-9-carbonyl chloride (COgen), which releases CO once activated by Pd catalyst or methyldiphenylsilacarboxylic acid (SilaCOgen), which is activated by adding fluoride (Figure 12).¹⁴⁶ The carbonylation reaction takes place in one chamber, while the other chamber is used for the CO release. CO releases upon treating the stable acid chloride (COgen) with tri-*tert*-butylphosphine ligated Pd catalyst and amine base in an aprotic solvent. The CO gas release is proven to be almost quantitative as illustrated throughout the wide synthetic applications using COgen as the carbonylating agent.¹⁴⁶

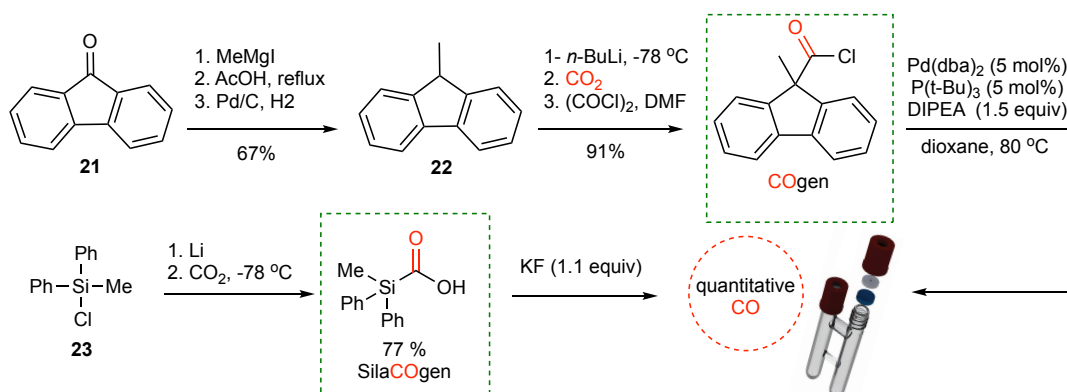
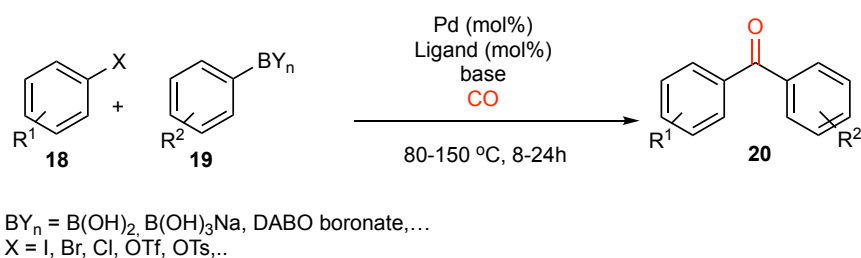


Figure 12. Synthesis and decarbonylation of COgen, SilaCOgen and COware.¹⁴⁶

Despite COgen being an expensive source of CO and requiring the use of two chamber systems, it gives access to stoichiometric amounts of CO for many low pressure carbonylation reactions in a safer fashion than other CO sources. In addition, being a stable solid makes it convenient to handle in the lab. Releasing the CO in another chamber than the carbonylation reaction chamber prevents problems such as formation of undesired by-product, separation problems etc. Moreover, this method allows introducing isotopically labelled CO by using labelled COgen.^{146–148}

3.2.1 Carbonylative Suzuki-Miyaura coupling

The carbonylative version of the SMC reaction has been investigated using different Pd-based complexes/catalysts and reaction conditions. However, most of the literature on this particular cross-coupling requires high CO pressure protocols except few reports applying carbonylation at atmospheric pressure.^{129,149,132}

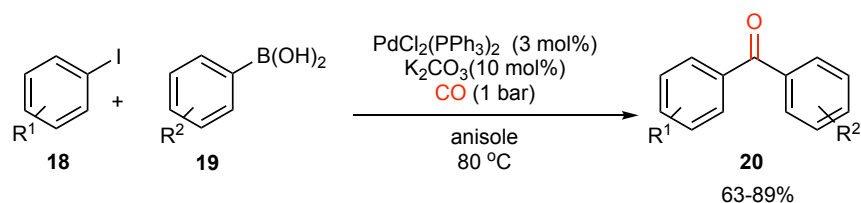


Scheme 10. General presentation of Suzuki-Miyaura coupling.

The common problem with this reaction lies in the formation of biaryl products, which results from the competing direct SMC coupling without carbon monoxide insertion. Nevertheless, the reaction conditions including nature of the palladium catalyst precursor, ligand, base, additive as well as the nature of the substrates (aryl halide and boronic acid), influence the ratio of ketone to direct coupling product.

Suzuki and coworkers described the palladium carbonylative SMC where they synthesized a variety of diaryl ketones from aryl iodides and boronic acids in high yields using PdCl₂(PPh₃)₂ and K₂CO₃ as a base in anisole (Scheme 11).¹²⁹ The choice of both base and solvent played an important role to obtain the desired ketone with minimum formation of biaryls as by-product. A range of bases; K₂CO₃, Cs₂CO₃, Tl₂CO₃, K₃PO₄ were tested in anisole to test reaction selectivity towards carbonylative coupling reaction versus non carbonylative one. Tl₂CO₃ gave the lowest selectivity towards the carbonylated product and resulted in 38% biaryl ketone and

24% biaryl by-product. On the other hand, K_2CO_3 in anisole was very efficient to yield the desired biaryl ketone in 84% yield, while it gave only 11% of the biaryl by-product.



Scheme 11. Carbonylative Suzuki-Miyaura coupling of aryl iodides and boronic acids.

Skrydstrup coworkers tested several carbonylative Suzuki-Miyaura coupling of 1-(4-iodophenyl)ethan-1-one with phenylboronic acid using low CO pressure and a range of Pd sources resulted in different ratios between biaryl ketone and biaryl (Table 4, **23**, **24**, respectively).¹⁴⁹ The phosphine based $Pd(dba)_2$ and $PdCl_2$ were shown to be favoring the carbonylative coupling over the direct coupling (Table 4, entry 2, 4 respectively). It is noteworthy that increasing the catalyst loading to more than 1% increased the chance of obtaining the undesired biaryl product. The best selectivity towards the desired biaryl ketone was obtained using ligand free system based on $PdCl_2$ and K_2CO_3 in anisole under CO (1 atm). A range of substituted biaryl ketones was obtained in moderate to high yield (50-93%).

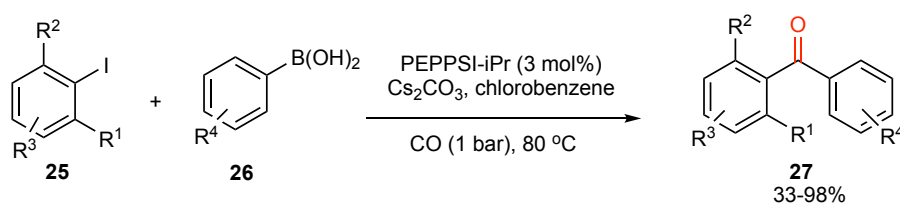
Table 4. Selected examples of different palladium sources used in carbonylative SMC.

| Entry | Pd cat (mol %) | Ratio 23:24 |
|-------|--------------------|----------------|
| 1 | $Pd(OAc)_2$ 1 mol% | 69:31 |
| 2 | $Pd(dba)_2$ 1 mol% | 71:29 |
| 3 | $Pd(TFA)_2$ 1 mol% | 58:42 |
| 4 | $PdCl_2$ 1 mol% | 95:5 |

Bhanage and coworkers reported $Pd(tmhd)_2$ as a catalyst for carbonylative Suzuki-Miyaura coupling of aryl iodides with arylboronic acids in anisole under 8 bars of CO. Although the reaction gave access to a range of biaryl and heteroaryl ketones in moderate to high yields it

still lacks wider scope with respect to *ortho* substituted aryls and electron-withdrawing groups in addition to the required high pressure.¹⁵⁰

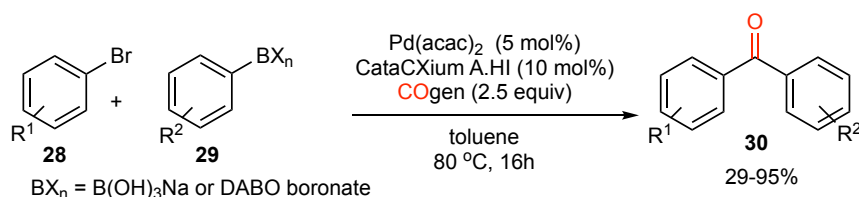
The use of carbene ligands and thiourea based ligands has drawn a keen interest in carbonylative Suzuki-Miyaura coupling especially with sterically hindered substrates.¹⁵¹ Keffe *et al.* reported the use of NHC palladium complex PEPPSI-*i*Pr in the synthesis of sterically hindered biaryl ketones in moderate to high yields (Scheme 12).¹³²



Scheme 12. Suzuki-Miyaura coupling of *ortho*-disubstituted aryl iodide with NHC catalyst.

Despite the achievements in this area, coupling of aryl bromides are still challenging especially in case of *ortho* substituted aryl bromides, which is noticeable in many of the published reports. Only few methods were successful for carbonylative coupling of aryl bromides and chlorides.^{152,153} The carbonylative Suzuki-Miyaura coupling of aryl bromides and chlorides typically requires harsh conditions such as high temperature, high CO pressure and longer reaction time in comparison to their corresponding aryl iodides. Additives such as NaI, KI would enhance the reaction rate as it might involve in situ generation of aryl iodides and thus faster oxidative addition.¹²⁹

Coupling of aryl bromides with aryl trihydroxyborates or DABO boronate using Pd(acac)₂ and the phosphine ligand cataCXium A.HI as a ligand in toluene under CO (1 atm) gave access to a range of substituted biaryl ketones in moderate to high yields (Scheme 13).¹⁵³ Unfortunately, these conditions also showed several limiting factors, as they gave poor yields with electron-withdrawing groups and they did not support *ortho* substituted aryls as they have low conversion. In addition, an additional step is required for the preparation of the boronic acid derivatives.¹⁵³

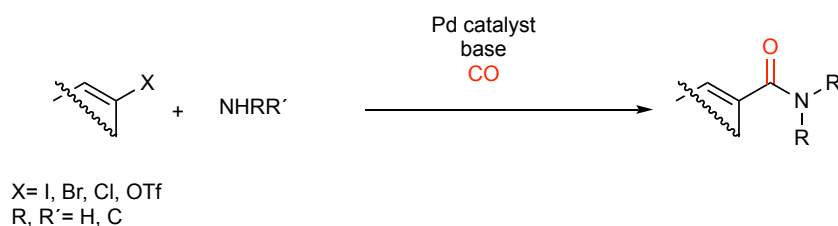


Scheme 13. Suzuki-Miyaura coupling of aryl bromides with organoboron using CataCXium A.HI.

Another catalytic system was reported by Beller and coworkers using CataCXium A as a ligand together with Pd(II)acetate to access a wide range of biaryl and heteroaryl ketones. Although the reaction showed good tolerance of both electron-rich and electron-deficient aryl halides and boronic acids, it required high CO pressure in case of aryl bromides with electron-withdrawing groups (2.5-5 bar).¹⁵²

3.2.2 Aminocarbonylation

Amides are considered to be one of the most important functional groups in chemistry, they are essential in many biological process and chemicals required for sustaining life. Amides are normally found in many natural products, linking amino acids in proteins such as enzymes, they are also found in many medicinal and pharmaceutical products. Different synthetic approaches towards amides require stoichiometric amounts of amide-coupling reagents, which make it an expensive and wasteful procedures. On the other hand, palladium-catalyzed aminocarbonylation of aryl or heteroaryl halides give a direct access to the corresponding carboxamides.^{137,139,157-159}

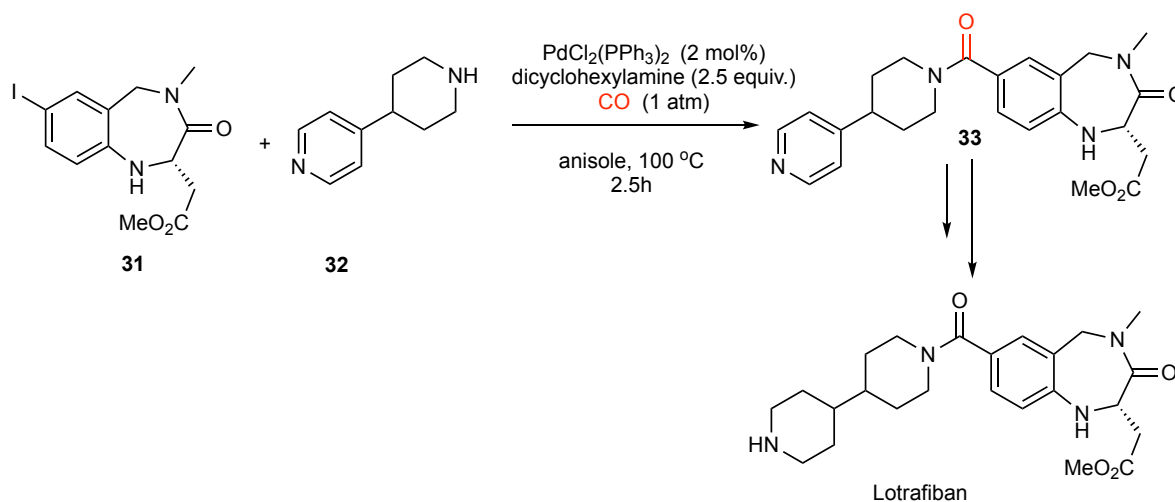


Scheme 14. General aminocarbonylation reaction.

The use of primary or secondary amines as the nucleophile under catalytic conditions will provide the desired amide following a similar catalytic cycle as the carbonylative cross-couplings with differences in the last steps. One possibility for the amine (nucleophile) to approach the catalytic cycle is that it could coordinate to the palladium followed by reductive elimination to obtain the amide. Another possibility, which is believed to be the dominant route, is nucleophilic attack on the acylpalladium carbonyl.¹⁶⁰

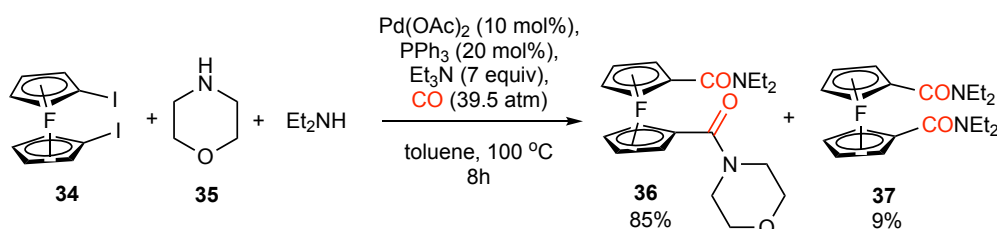
Since common catalytic systems for aminocarbonylation showed good tolerance to a wide range of functional groups, it is considered to be a versatile method in organic synthesis to access amides with a variety of N-substituents. It has been applied for the synthesis of molecules of medicinal interest such as lotrafiban, itopride, bromopride and butoxycaine.¹⁶¹⁻¹⁶⁴ For example, the key step in the synthesis of lotrafiban is the aminocarbonylation step of the

aryl iodide and the amine using $\text{PdCl}_2(\text{PPh}_3)_2$ in anisole for 2.5 h under 1 atm of CO pressure to furnish the desired amide (Scheme 15).¹⁶¹



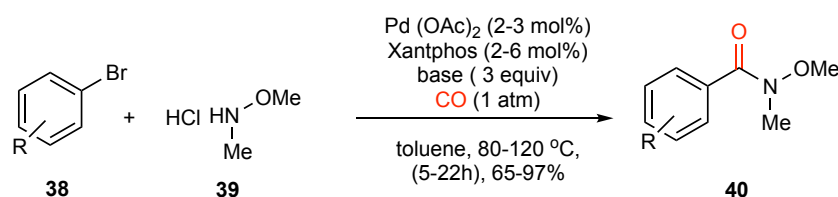
Scheme 15. Aminocarbonylation towards synthesis of lotrafiban.

Moreover, aminocarbonylation can be used for the synthesis of ferrocene based chiral ligands that are used in asymmetric catalysis.¹⁶⁵ For instance, the synthesis of asymmetrically disubstituted ferrocenebiscarboxamide (Scheme 16) was obtained via aminocarbonylation between symmetrical ferrocenyl di-iodide with morpholine and diethylamine under high CO pressure (40 atm) yielding the desired asymmetric ligand in 85%.¹⁶⁶



Scheme 16. Aminocarbonylation for the synthesis of asymmetrically disubstituted ferrocenebiscarboxamide.

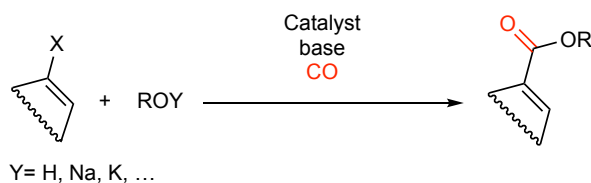
Weinreb amides are also accessible via aminocarbonylation under mild conditions. Buchwald and coworkers reported the synthesis of Weinreb amides from a wide range of electron-rich and electron-deficient aryl and alkenyl halides using $\text{Pd}(\text{OAc})_2$ and Xantphos under 1 atm CO pressure to furnish the desired amide in moderate to excellent yields (Scheme 17).¹⁶⁷



Scheme 17. Synthesis of weinreb amides via aminocarbonylation.

3.2.3 Alkoxy carbonylation

Alkoxy carbonylation is an important method for the synthesis of esters. Different alkyl and aryl halides were converted into their corresponding carboxylic esters in presence of transition metal complexes and the corresponding alcohol under CO pressure (Scheme 18). Installing the carboxylic acid/ester into aryl/alkyl halides is a very attractive tool for late stage functionalization and C-C bond formation.

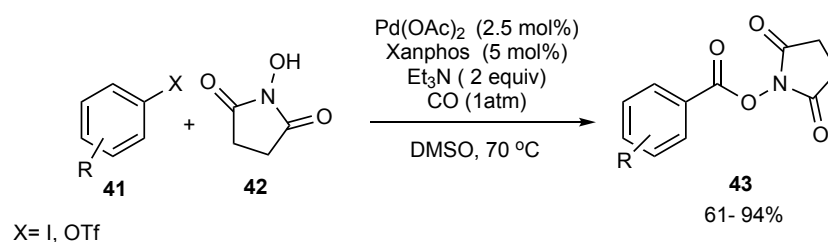


Scheme 18. General transformation of aryl or vinyl halide into their corresponding esters via alkoxy carbonylation.

Alkoxy carbonylation follows a similar mechanism as aminocarbonylation where the nucleophile is the alcohol or metal alkoxides instead of the amine to form esters. Alkoxy carbonylation e.g. methoxycarbonylation are widely described including both inter- and intramolecular reactions.^{168,169,134,170} Intramolecular alkoxy carbonylation of pendant alcohol leads to the formation of five, six, and seven membered ring lactones.¹⁷⁵

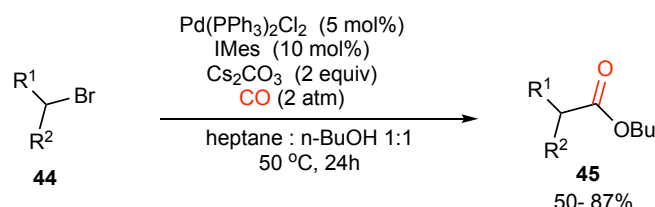
Buchwald and coworkers reported methoxycarbonylation of a range of aryl bromides under low CO pressure (1 atm) using 2 mol% Pd(OAc)₂, 4 mol% Xantphos and 10 equiv MeOH at 70 °C for 24 h. The reaction gave access to a range of methyl esters with various function groups such as aryl nitriles, fluorides, ethyl ether, *tert*-butyl carbamate, in high yields (80-91%). However, scope limitations were described due to low reaction temperature.¹⁷⁶

A variety of methods for the transition metal catalyzed alkoxy carbonylation of aryl halides, tosylates and triflates has been described.^{177,172} Lou *et al.* reported the synthesis of N-hydroxysuccinimido esters from aryl iodide or triflates using Pd(OAc)₂ and Xantphos in DMSO under 1 atm CO (Scheme 19).¹⁷⁷ In addition, Angelina *et al.* reported also the synthesis of N-hydroxysuccinimido esters together with active esters from pentafluorophenol, hexafluoroisopropyl alcohol, p-nitrophenol and N-hydroxyphthalimide from aryl bromide in excellent yields (59-99%) using 3 mol% (Pd(cinnamyl)Cl)₂, HBF₄P(*tert*-Bu)₃ (6 mol%) and Cy₂NMe (1.5 equiv) in toluene at 95 °C for 16 h.¹⁷²



Scheme 19. Synthesis of *N*-hydroxysuccinimido esters via alkoxy carbonylation.

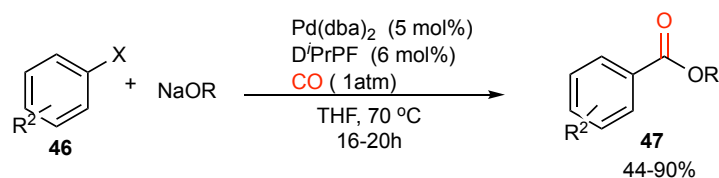
Palladium catalyzed alkoxy carbonylation has been performed with the inactivated alkyl halides such as inactivated secondary alkyl bromides and alkyl chlorides, which are challenging substrates that require harsh conditions, high CO pressure in comparison to more active alkyl iodide. Alexanian and coworkers, reported esterification of less active alkyl bromides to the corresponding *tert*-butyl ester version using $\text{Pd}(\text{PPh}_3)_2\text{Cl}_2$ and IMes as a ligand under CO pressure of only 2 atm at 50 °C in DMSO, which are milder conditions for this type of reactions (Scheme 20). The reaction was tolerant to a variety of function groups such as silyl protecting group, esters, five and six membered carbocycles and heterocycles and gave good results with alkyl possessing both electron-deficient and electron-withdrawing group with yield range of 50-87 %. Using carbene ligand (IMes) in this case shown to facilitate the reaction in combination with $\text{Pd}(\text{PPh}_3)_2\text{Cl}_2$. Being able to perform this reaction on the stable alkyl bromide makes it useful as late stage C-C bond formation.¹⁷⁰



Scheme 20. *tert*-Butyl ester from deactivated alkyl bromides.

Alkoxy carbonylation can be also done using metal alkoxide (e.g. EtONa , *tert*- BuONa , etc) instead of the direct use of the corresponding alcohol. This approach ensures presence of the nucleophile in the reaction medium and prevent volatile alcohols (e.g. MeOH , EtOH , etc) from escaping the reaction mixture.^{171,178} Skrydstrup and coworkers reported alkoxy carbonylation of aryl bromides into their *tert*-butyl ester using $\text{Pd}(\text{dba})_2$ and DiPrPF under 1 atm of CO pressure in THF (Scheme 21). The reaction showed great results with more bulky tertiary alcohols such as the sodium adamantoxide and sodium 9-methyl-9-fluorenoxide, which indicates bulky nucleophiles are more favorable for efficient reductive elimination. While on the other hand

less bulky alcohols such as sodium methoxide were not successfully used as nucleophiles in this reaction.¹⁷¹

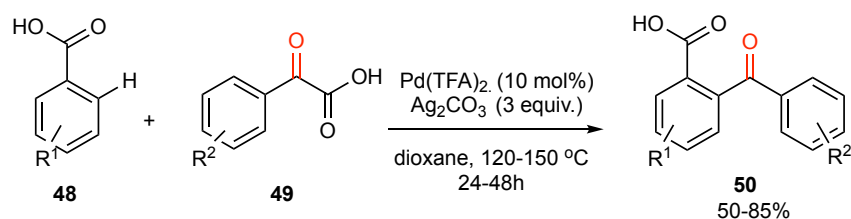


Scheme 21. Alkoxy carbonylation of aryl bromide using bulky sodium alkoxides.

3.3 Reactions for the preparation of 2-arylbenzoic acid derivatives

2-Arylbenzoic acids and derivatives have gained noticeable interest as synthetic intermediates for accessing bioactive compounds, and they were the aim of the work presented in paper II. Only few reported methods towards formation of 2-arylbenzoic acids are found in literature, comprising Friedel-Craft acylation,¹⁵⁴ Pd-catalyzed ortho-C–H activation of aryl amides followed by coupling with aryl aldehydes,¹⁵⁵ Pd-catalyzed ortho-C–H activation of benzoic acids followed by decarboxylative coupling with α -oxocarboxylic acids.¹⁵⁶ The available methods generally show limitation regarding regiocontrol and/or substrate scope especially with regard to electron-deficient aryl groups.

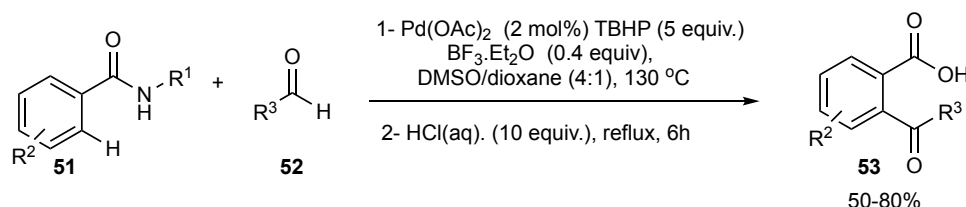
Ge and coworkers reported the synthesis of a range of substituted 2-arylbenzoic acids in moderate yields through chemoselective decarboxylative cross-coupling of benzoic acids via C-H bond functionalization with α -oxocarboxylic acid as the coupling partner. The reaction required the use of harsh conditions including use of an excess of the oxidant (Ag_2CO_3), high catalyst loading (10 mol%), the elevated temperatures (120-150 °C) and extended reaction time up to 48h (Scheme 22). Moreover, the substrate scope suffered from some limitations especially with electron withdrawing groups that were not well tolerated under these conditions.¹⁵⁶



Scheme 22. Chemoselective decarboxylation cross-coupling of benzoic acids via C-H bond functionalization.

Another method to access 2-arylbenzoic acids via C-H activation directed by aryl amides that would undergo ortho acylation followed by ring closing to form amide containing four-member ring and then ring opening to give the ortho imino carboxylic acid (Scheme 23). The reaction

then would be submitted to reflux in concentrated aqueous HCl in order to obtain the 2-arylbenzoic acids. The reaction had a limited substrate scope, where functional groups like esters, nitriles, imines, etc. were not tolerant, due to the harsh acidic conditions required to eventually obtain the ketone form of the imino-aryl.¹⁵⁵



Scheme 23. C-H activation of aryl amides to form 2-arylbenzoic acids.

3.4 Solvent effect and sustainability

The growing awareness of the impact of chemical process, e.g. solvent use on the environment and their contribution to the climate change, has resulted in an increasing interest in both research and industry in finding sustainable alternatives.¹⁸¹ Sustainable alternatives are needed for media to perform reactions as well as for work-up and purification, catalysts and energy sources. Sustainability has been previously described as “resources including energy should be used at a rate at which they can be replaced naturally and the generation of waste cannot be faster than the rate of their remediation.”¹⁸¹ This description coincides with the definition by the world commission on environment and development stating that sustainability is “development that meets the needs of the present without compromising the ability of future generations to meet their own needs”.¹⁸¹ A noticeable success has been achieved in the synthesis of new products since 1990s when the twelve principles of “green chemistry” were formulated.^{182,183} These principles are considered to be the guidelines that chemists in both academia and industry try to follow while carrying out chemical reaction in a sustainable fashion. Despite the difficulties following all the twelve principle for preparative purposes, chemists and industries have already made noticeable moves towards sustainability by considering the key principle of green chemistry.

The solvent may perform a mechanical role in the mechanism, but sometimes it plays also an essential role of bringing the immiscible reactants together rapidly so that the reaction could occur. In addition to dissolving reactants, the solvent can participate in several ways to the reaction itself. The choice of the solvent could influence reactivity, introduce selectivity,

and produce different products.¹⁷⁹⁻¹⁸⁴ It might interact with the reactants individually or get involved in the transition state.^{180,181}

Many of the organic solvents that are commonly used in organic synthesis and post reaction processes are with poisonous and carcinogenic nature such as halogenated hydrocarbons (DCM, CHCl₃, CCl₄, etc.). This type of solvents has created serious harm to the environment and human health in general. However, two of the twelve principles of green chemistry are based on usage of safer solvent and reaction conditions and to prevent waste. One principle is “Safer Solvents and Auxiliaries” where the use of auxiliary substances such as solvent and separation agents are not favorable and should be decreased. The other principle is “use of renewable feedstock” where raw materials or feedstock are attractive renewable alternatives and should be used whenever possible.¹⁸² As a consequence, the direction of using less amount of solvents and finding renewable and less toxic solvent alternatives has recently gained a lot of attention in the area of green chemistry.¹⁸³

One approach is to run reaction in neat conditions without the use of solvent. Unfortunately, solvent free reactions are not necessarily solvent free as claimed. Even if the reaction itself took place in a solvent free medium, it would still need an appreciable amount of solvents for reaction adsorption, elution of products and pre or post handlings of the reaction mixture. In addition, many extractions, purifications, and cleaning processes also depend on solvents, with large excesses necessary to achieve sufficient product purity.¹⁸¹ A brief survey of academic researchers were conducted in 2010 by Jessop, where a question brought up “...what class of solvent will be responsible for the greatest reduction in environmental damage?”.¹⁸⁴ The answers to the raised question were in favor of CO₂ derived solvents, water and careful selection of organic solvents. This turn our focus now towards CO₂ and biomass derived solvents.

3.4.1 Biomass and CO₂ derived solvents and their application in Pd catalyzed C-C couplings

Plant biomass (crops) such as corn, sugar cane, citrus, grasses and agricultural residues are all considered to be the main feedstock for generating renewable fuels and solvents. Recently, biomass derived solvents as well as chemicals derived from the reduction of CO₂ have been increasingly tested as green medium replacing the common nonrenewable solvents utilized in organic synthesis. The most studied solvents available from biomass are polar protic solvents;

ethanol, glycerol and its derivatives, choline chloride based deep eutectic solvents, as polar aprotic solvents; 2-methyltetrahydrofuran (2-MeTHF), cyrene (Cyr) and γ -valerolactone (GVL), as well as non-polar aprotic solvent; limonene (Lim) and *p*-cymene (Cym). In case of CO₂-derived chemicals, particular attention has been paid to the use of carbonates and ethers like methylal (Figure 13). These solvents are shown to be suitable renewable solvent alternatives for different chemical transformations in classical condensation reactions and transition-metal catalyzed cross-couplings.^{181,183,185,186}

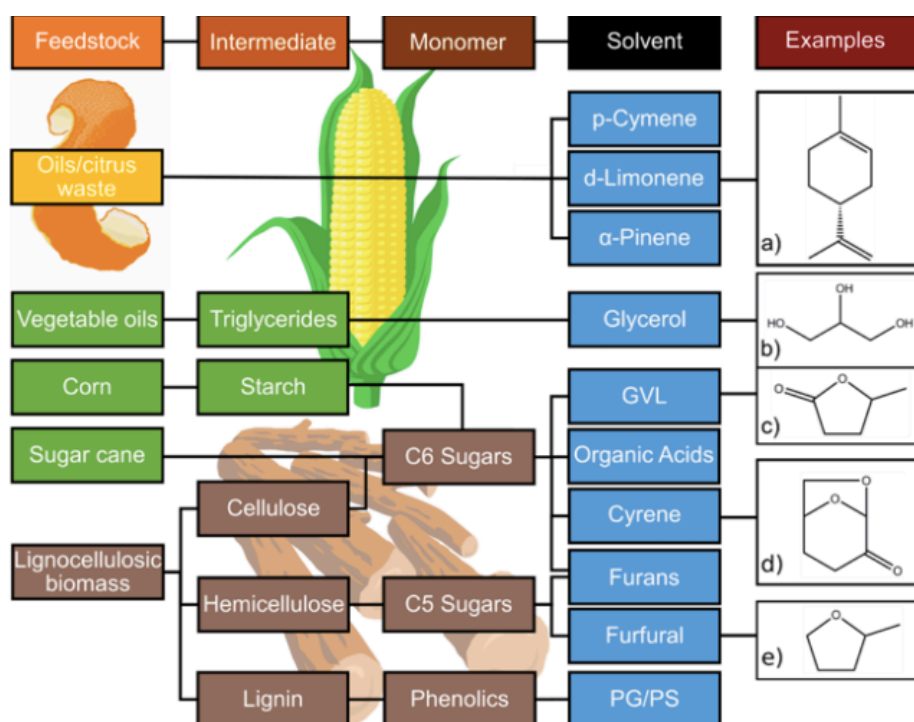
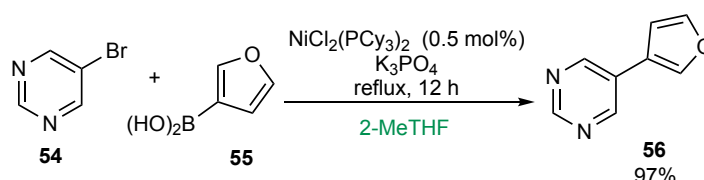


Figure 13. A number of sustainable solvents derived from plant biomass, sugars and oils. lignocellulosic biomass. Adapted with permission from Clarke et al (2018).¹⁸¹

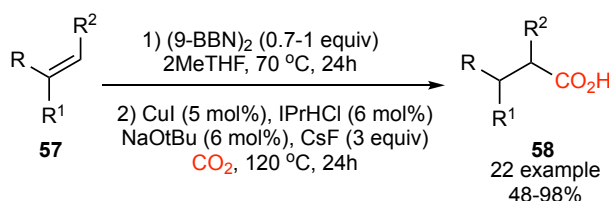
2-MeTHF and GVL are both commercially available solvent obtained from furfural or levulinic acid, which are produced from lignocellulosic biomass.^{181,135} Great attention has been paid to the use of these solvents as an alternative bio-based medium for several reactions including cross-couplings. Solvents, such as THF, toluene and highly regulated chlorinated solvents including dichloromethane and 1,2-dichloroethane can all theoretically be replaced by 2-MeTHF, due to its stability to acid and base in addition to its low miscibility with H₂O. It can also be used as a replacement of DCM in biphasic reactions and in work up process. 2-MeTHF was used as a sustainable media for a variety of organometallic reactions such as Grignard reactions, hydride reduction of carbonyl groups with LiAlH₄, lithiation, cross-coupling

reactions.^{181,187,188} Few examples of SMC coupling in 2-MeTHF have been reported. Nickel-catalyzed SMC coupling between arylboronic acids and aryl halides or phenol derivatives in 2-MeTHF was successfully reported by Garg and coworkers.¹⁸⁹ The reaction shown applicability with a notable substrate scope of 30 coupled products in 33-100% yield using 1-10 mol% of bis(tricyclohexylphosphine) Nickel(II)dichloride $\text{NiCl}_2(\text{PCy}_3)_2$. The reaction is also reproducible on 5-gram scale, coupling of 5-bromopyrimidine with 3-furanylboronic acid using just 0.5 mol% of the nickel catalyst yielded the product in 97% yield (Scheme 24). Nickel catalyzed amination of aromatic chlorides and O-sulfamates in 2-MeTHF was also reported by the same group using $\text{NiCl}_2(\text{DME})_2$ as a pre-catalyst, the reaction showed general applicability in terms of substrate scope as well.¹⁸⁹



Scheme 24. Nickel catalyzed amination of 5-bromopyrimidine and 3-furanylboronic acid.

Recently, our group reported the activity of MeTHF and GVL among other solvents on Cu-catalyzed carboxylation and decarboxylation reactions. Although 2-MeTHF was not universal for all the tested carboxylation reactions, but it was the best alternative in most cases. Cu-catalyzed carboxylation of organoboronates with both electron-rich and electron-poor arylboronic acid pinacol esters showed best results over 16 examples where the yield was 68-98%. In addition, 2-MeTHF has shown to be a good reaction medium for Cu-catalyzed and Cu-free hydrocarboxylation of olefins (Scheme 25).¹⁹⁰



Scheme 25. Cu-Catalyzed and Cu-free hydrocarboxylation of olefins.

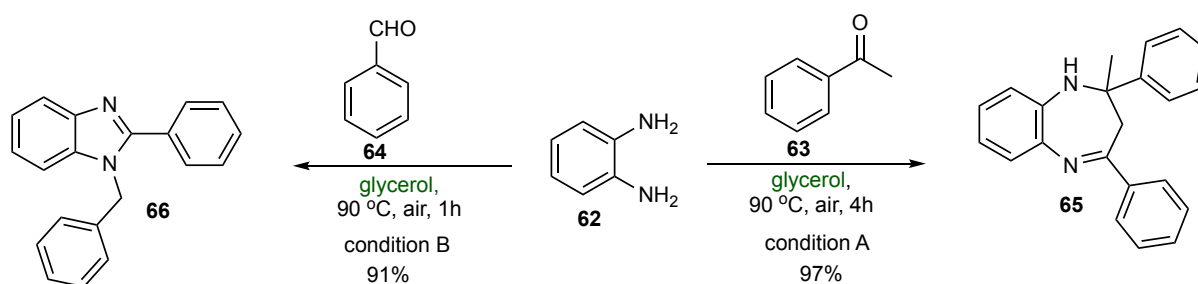
Similarly, GVL has lately drawn great attention to it as a green solvent. It has been frequently used as a food additive and a flavoring agent. It has similar polarity as dipolar aprotic solvents such as DMF and NMP. Therefore, it has been intensively studied on cross-coupling reactions since they often rely on the use of dipolar aprotic media.¹⁸⁸ A couple of examples illustrated the applicability of GVL as suitable bio-based medium for reactions involving C-H activation,

arylation and Hiayama couplings.¹⁸⁷ Mizoroki-Heck reaction between iodoarenes and styrenes or acrylates using 0.1 mol% Pd/C in GVL gave the coupled product after 2.5h (Scheme 26). The reaction showed general applicability through a substrate scope, over 20 examples in 80-90% yields.¹⁹¹



Scheme 26. Mizoroki-Heck reaction catalysed by Pd/C in GVL.

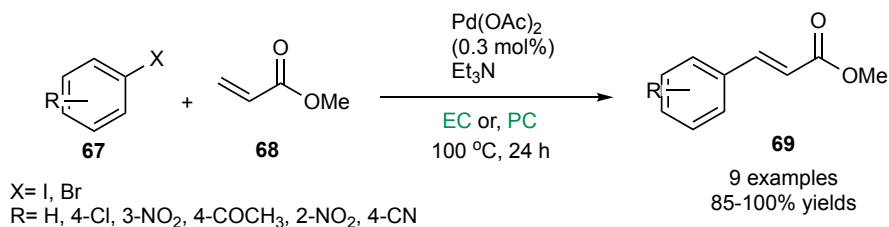
Glycerol is one of the common green solvents that has shown great applicability in many types of reactions such as; catalytic hydrogenation of various unsaturated organic compounds and cross-coupling reactions. In addition, condensation reactions are also compatible in glycerol due to its hydrogen bonding ability, which might stabilize transition states and intermediates. For example, catalyst free (e.g. Lewis acid) condensation of phenylenediamine and acetophenone was performed in glycerol with high yield (Scheme 27. condition A).¹⁹² Condensation of phenylenediamine with benzaldehyde under solvent free conditions or reflux in ethanol was not successful. However, replacing the solvent with glycerol yielded 91% of the benzodiazepine, which support the advantage of using glycerol (Scheme 27. condition B).¹⁹²



Scheme 27. Condensation of *o*-diaminobenzene in glycerol.

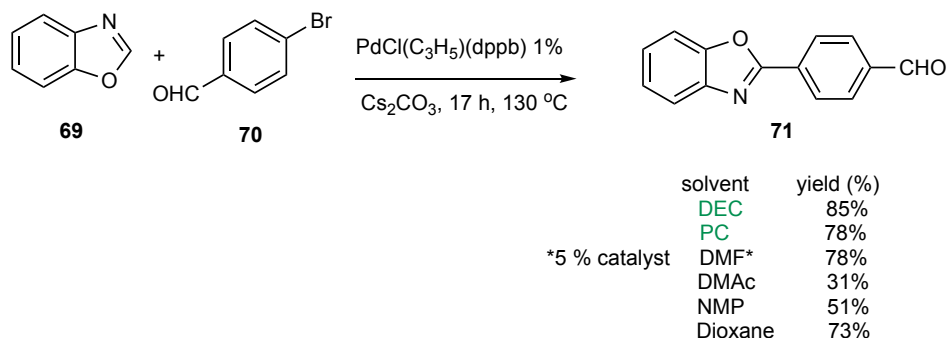
Organic carbonates are considered to be a promising renewable dipolar reaction media, due to their biodegradability and low toxicity.¹⁹³⁻¹⁹⁶ Cyclic carbonates such as propylene carbonate (PC), ethylene carbonate (EC) are derived from CO₂ and bioethene, which make them of a high potential as bio-based solvents.¹⁹⁷ A previous study showed the successful application of PC and EC as the reaction solvent in the Mizoroki-Heck reaction between aryl iodides/bromides and acrylate (Scheme 28). The results in terms of conversion were comparable or even better to the same reaction performed in NMP as solvent or even better (80-100%). It is worth

mentioning that bromobenzene showed no reactivity in NMP, while it gave up to 40% conversion in case of EC of the desired product.¹⁴⁰



Scheme 28. Mizoroki-Heck cross-coupling reaction in ethylene carbonate or propylene carbonate.

Palladium catalyzed direct arylation of (hetero) aromatic derivatives has been carried out successfully in dialkyl carbonate such as dimethoxycarbonate (DMC), diethoxycarbonate (DEC). Direct arylation of benzoxazole with 4-bromoacetophenone using only 1 mol% of $\text{PdCl}(\text{C}_3\text{H}_5)(\text{dppb})$ as the catalyst was reported to provide the coupling product in 85% isolated yield (Scheme 29). The reaction performed in diethyl carbonate gave the best alternative compared to common organic solvents such as DMF, DMAc, NMP or dioxane as it gave only traces of unidentified side-products.¹⁹⁷



Scheme 29. Coupling of benzoxazole with 4-bromoacetophenone.

General discussion of results from the thesis

The numbering system applied in the discussion part is designed to be as follows:

Numbering of compounds introduced in papers is with the name Px-y, where x is the number of the paper (I, II, III) and y is the compound number used in the paper. Other compounds that are not included in the papers are numbered chronologically.

4. Design, synthesis and evaluation of *meta*-substituted benzoic acid derivatives as OXA-48 inhibitors (Paper I)

4.1 Background for the work in paper I

The work presented in paper I is a continuation of previous research conducted by the group of Prof. Leiros in collaboration with our group with focus on screening and development of fragments of the carbapenemase OXA-48.¹⁵ Previously, a library of 490 fragments was screened to identify fragments that showed direct binding to the OXA-48 enzyme using SPR as the primary assay. The identified fragments from the SPR were examined further in a secondary biochemical screen via enzymatic assays in order to measure the binding efficiency of the fragments. Enzyme : inhibitor crystal structures were obtained for 3 fragments.¹⁵

The fragments shared the same core structure of a monosubstituted benzoic acid, and thus, shared some similar interactions such as hydrophobic interactions with Ser70, Ser118, Gly210, Tyr211. The carboxylate group showed an ionic interaction with Arg250 residue in the binding site. The negatively charged carboxylate had a charge induced hydrogen bond with the side-chain oxygen of Thr209. In addition, the π -system of the benzoic acid might allow for π - π stacking depending on the fragment conformation.

The crystal structure identified two different binding conformations of fragment **PI-1**. The first conformation (Figure 14, 1A) shows the fragment facing out of the active site and has hydrophobic interactions with Trp105, Thr209, Gly210, Tyr211, and Leu247 – the fragment is occupying the out-pocket (called R² side in Paper I). In the other conformation (Figure 14, 1B) the fragment is embedded in the active site and has hydrophobic interactions with Val120,

Leu158, and Tyr211 – the fragment is occupying the inn-pocket (called R¹ side in Paper I). The carboxylate group in both conformations forms ionic bonding with Arg250.

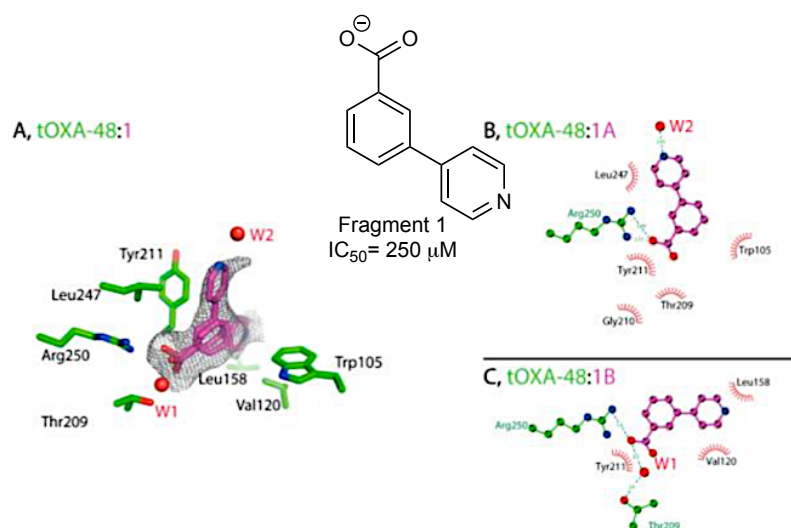


Figure 14. Crystal structures of OXA-48 (green) in complex with fragments (magenta). Two conformations are shown for compound 1 in A–C. Adapted with permission from Lund et al. (2016).¹⁵

As fragment **PI-1** tends to bind in two different conformations, it was suggested that structurally merging both conformations would lead to a better fragment with higher binding affinity occupying both the inn- and out-pocket. The merging resulted in a more potent inhibitor-fragment **PI-2** - with better K_d of 50 μM and lower IC_{50} of 18 μM (Figure 15).

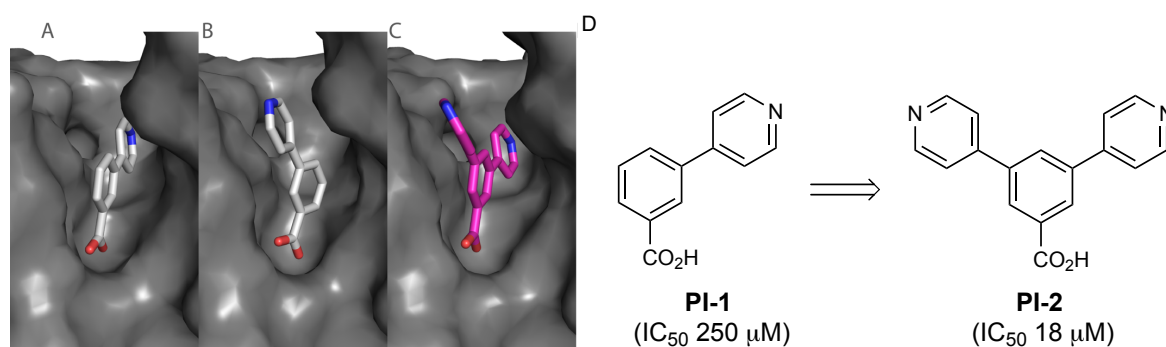


Figure 15. (A and B) Different conformations of fragment PI-1 (light grey) in complex with OXA-48 (dark grey surface), (C) the merged compound PI-2 (pink) in complex with OXA-48 (dark grey surface) and (D) a schematic view of the merging approach described in previous work.¹⁵

4.2 Research hypothesis of paper II

Based on the findings described in the previous section, the fragment hit **PI-1** was envisioned as the starting point for a library of mono-substituted analogues of fragment **PI-1** (Figure 16). The goal was to find good fragments with affinity for either the inn- or the out-pocket (R^1 or R^2 side) or both. The small size of the fragments makes them more flexible and efficient in exploring the binding site, which would allow us to identify better fragments for each pocket with a promising overlap. The best fragments that bind to each pocket would then be optimized further using a merging approach, which would lead to the synthesis of di-substituted fragments based on the suggestions from the overlay structures of the best identified fragments (Figure 16, **PI-2**).

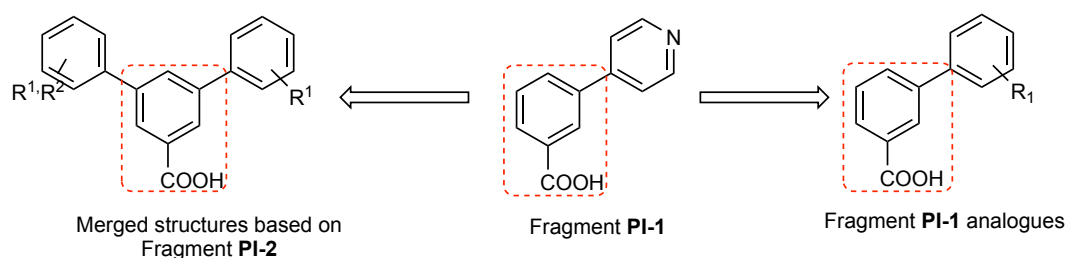
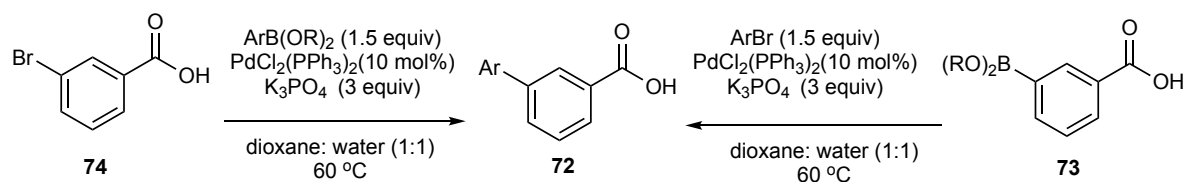


Figure 16. Fragment development approach.

4.3 Evaluation of 3-substituted benzoic acid derivatives

In paper I, co-authors were able to synthesize a fragment library of 49 candidates of 3-aryl benzoic acids and derivatives. The fragments were synthesized via SMC starting from 3-carboxyphenylboronic acid pinacol ester or 3-bromobenzoic acid, resulting in a wide range of 3-substituted aryl benzoic acids. The coupling partners included heterocycles and substituted aryls with polar groups such as amides, phenols, sulphonic acid derivatives, esters and tetrazoles. The benzoic acid moiety was left unaltered due to the main interaction of the carboxylate group with the Arg250. Evaluation using a biochemical assay indicates that most of the tested fragments show a similar inhibition level with IC_{50} values ranging from 200 to 1000 μ M and LE values ranging from 0.2 to 0.42 ($-\log_{10}IC_{50}/\text{heavy atom}$). All fragments share common interactions such as the ionic bond between the carboxylate group and the Arg250. Five fragments (Table 5, **PI-4a**, **PI-21a**, **PI-26a**, **PI-26b**, **PI-35**) show stronger inhibition with LE values of 0.38, 0.33, 0.3, 0.3, 0.42 μ M, respectively.

Table 5. Selected best 6 fragments from the 49-fragment library.



| Entry | ID (Paper I) | Ar | IC ₅₀ (μM) | K _D (μM) | LE | Pocket |
|-------|--------------|----|-----------------------|---------------------|------|----------------|
| 1 | PI-4a | | 50 | 175 | 0.38 | R ² |
| 3 | PI-21a | | 35 | 100 | 0.33 | R ¹ |
| 4 | PI-26a | | 60 | 70 | 0.3 | R ² |
| 5 | PI-26b | | 36 | 70 | 0.3 | R ¹ |
| 6 | PI-35 | | 35 | 159 | 0.42 | both |

Out of the 49 synthesized fragments, 33 fragments were co-crystallized with the enzyme OXA-48 and analyzed by X-ray crystallography in order to evaluate the binding poses of the fragments. All fragments formed an ionic bond between the carboxylate group and the Arg250. Most of the fragments were found to occupy the out-pocket (R²) where they engaged in edge-to-face π - π stacking with Tyr211. Fragment **PI-4a** was shown to be the strongest among the R² binders with IC₅₀ of 50 μ M and LE of 0.38 (Table 5, entry 1). Only fragments **PI-21a** and **PI-26b** were found to bind in the inn-pocket (R¹ side) with IC₅₀ of 35 and 36 μ M, respectively, and LE of 0.33 and 0.30, respectively. Both fragments could form a hydrogen bond with the guanidine group of Arg214, which made them loose the π - π stacking with Tyr211 and direct them to be oriented towards R¹ binding site instead of the common R². Fragment **PI-35** occupied both binding sites so it was not classified as R¹ or R² binder. However, fragment **PI-35** was the best fragment among the tested fragments as it showed the best ligand efficiency with IC₅₀ of 35 μ M and LE of 0.42 ($-\log_{10}IC_{50}/\text{heavy atom}$) (Table 5, entry 6).

In order to optimize the fragments into more potent fragments, a merging approach was initiated by overlaying two crystal structures of the most promising mono-substituted benzoic acids (Table 5). A structural overlay of fragments **PI-21a** and **PI-26b**, which were the only R¹ binders with different R² binders (PI-1, PI-28, PI-35) suggests some promising combination (Figure 17) leading to structures **PI-39**, **PI-40** and **PI-41**. Therefore, we initiated the synthesis of a small library including symmetrical and unsymmetrical 3,5-disubstituted benzoic acids including the suggested combination from the merging approach using SMC.

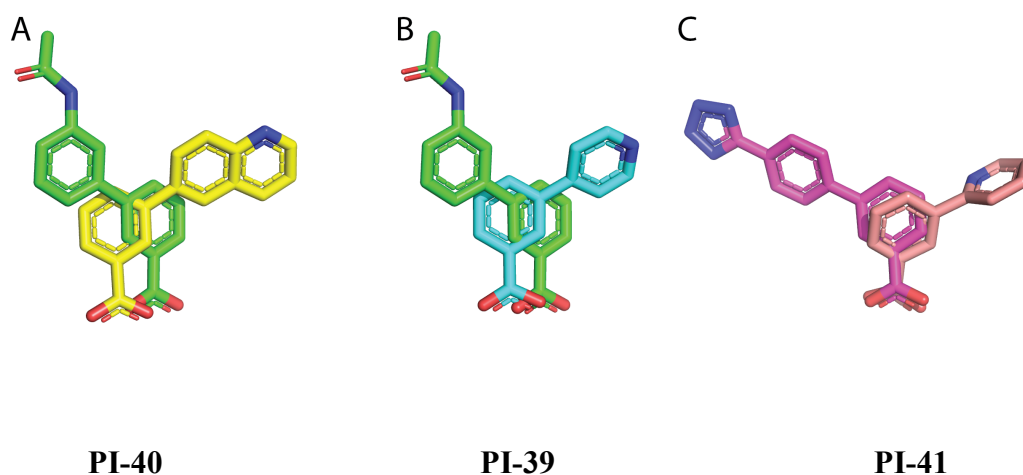
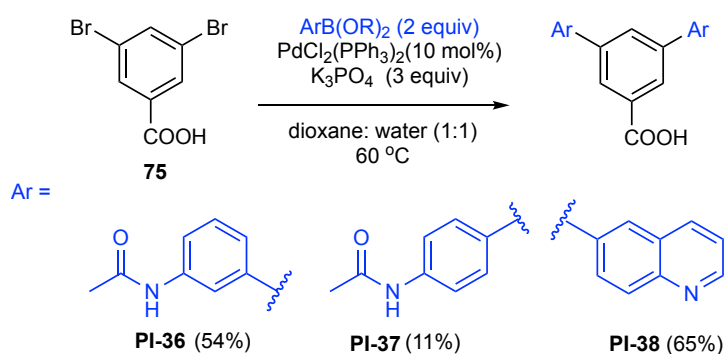


Figure 17. Overlay structure of the binding poses observed for PI-21a/28 (A), PI-21a/1 (B) and PI-26b/35 (C) leading to 3,5-disubstituted benzoic acids **PI-40**, **PI-39** and **PI-41**.

4.4 Synthesis and evaluation of symmetrically and unsymmetrically 3,5-disubstituted benzoic acid derivatives

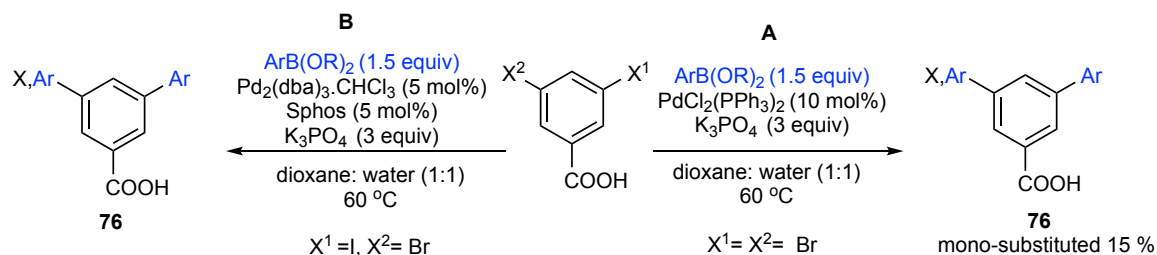
I was responsible for developing a method for the synthesis of unsymmetrically 3,5-disubstituted benzoic acid derivatives. I also contributed to the synthesis of the symmetrically 3,5-disubstituted benzoic acid derivatives.

Choosing 3,5-dibromobenzoic acid as a starting point allowed us to access symmetric 3,5-disubstituted benzoic acid. As 3,5-dibromobenzoic acid **75** contains two coupling positions (*m*-BrAr) of the same activity, so the reaction was not regioselective. Using an excess of the boronic acid and the base would allow the symmetrical substitution. The synthesis of three fragments (Scheme 30, Fragments **PI-36**, **PI-38**, **PI-37**) was achieved under the same reaction conditions as for mono-substituted fragments using Pd₂(dba)₃ (5mol%)/XPhos(5 mol%) or XPhos-Pd G2 (5 mol%) as catalysts, K₃PO₄ (5 equiv) and 2 equiv. of the corresponding boronic acid at 60 °C.



Scheme 30. Synthesis of symmetric 3,5-disubstituted benzoic acid derivatives.

For the synthesis of unsymmetrical 3,5-disubstituted benzoic acids, chemoselectivity was required in order to introduce different boronic acids to the 3- and the 5- position of the dihalobenzoic acid. The first approach was based on using 3,5-dibromobenzoic acid and sequentially adding the two different boronic acids and/or reducing the amount of the boronic acid under the previously established conditions (Scheme 31. **A**). This approach was not successful as it only yielded 15% of the desired product. For example, fragment **PI-39** was obtained from the 3,5-dibromobenzoic acid in a very low yield (11%). In addition, a mixture of mono-substituted 5-bromobenzoic acid, symmetrical and unsymmetrical 3,5-disubstituted benzoic acids was always obtained. Moreover, purification of the reaction mixture was found to be difficult and required several HPLC purifications.

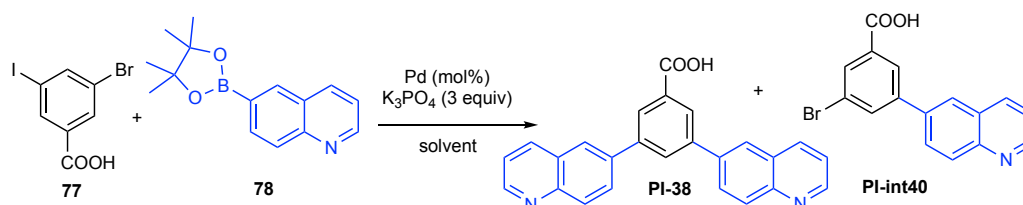


Scheme 31. Initial attempts of the preparation of unsymmetrical 3,5-disubstituted benzoic acids.

To introduce a higher degree of selectivity, we changed the starting material to 3-bromo-5-iodobenzoic acid (Scheme 31. **B**). As mentioned before (Chapter 3.1), Ar-I is more active than Ar-Br in SMC reactions, which could allow a faster reaction on C-I than C-Br and limit the formation of symmetrical compounds. We initiated a chemoselective reaction of 3-iodo-5-bromobenzoic acid with 6-quinolineboronic acid pinacol ester to form a mono-substituted product using $\text{Pd}_2(\text{dba})_3 \cdot \text{CHCl}_3$ (5 mol%) and SPhos (5 mol%) in dioxane/water (1:1) at 60 °C. However, a second coupling on the bromide was always observed.

We then started reaction optimization to find conditions that would suppress the second coupling in favor of obtaining only the mono-substituted product after the first coupling. The model reaction was carried out between 3-bromo-5-iodobenzoic acid with 6-quinolineboronic acid pinacol ester. The reaction optimization included different catalysts (e.g. RuPhos-Pd G3, Sphos/Pd₂(dba)₃, Xphos/Pd₂(dba)₃, SPhos-Pd G3, XPhos-Pd G2, Pd₂(dppf)Cl₂), solvents (toluene/water, anhydrous THF, dioxane/water, *tert*-butanol), reaction temperature (40–80 °C) and time (10–48 h) (Table 6). The crude reaction mixtures were analyzed and the ratios between the mono- and disubstituted products as well as unreacted starting material were determined by mass spectrometry (MS).

Table 6. Reaction optimization for the coupling of 3-bromo-5-iodobenzoic acid.



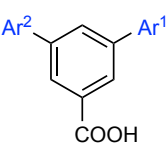
| Entry | Catalyst (Mol%) | T (°C) / T (H) | Solvent | Ratio (PI-int40:38:80) | Isol. yield Int40 (%) |
|-------|---|----------------|---------------------|------------------------|-----------------------|
| 1 | RuPhos-Pd G3 (10) | 60/24 | Dioxane/water (1:1) | 8: 10: 10 | nd |
| 2 | RuPhos-Pd G3 (5) | 60/24 | Dioxane/water (1:1) | 10: 6: 0.3 | nd |
| 3 | XantPhos-Pd G3 (5) | 60/48 | Dioxane/water (1:1) | 10: 1: 0 | nd |
| 4 | XantPhos-Pd G3 (5) | 40/24 | Dioxane/water (1:1) | 10: 1: 3 | 70 ^a |
| 5 | Pd ₂ (dppf)Cl ₂ | 60/24 | Dioxane/water (1:1) | 10: 1: 3 | 80 ^a |
| 6 | Xphos-Pd G2 (1) | 60/24 | Dioxane/water (1:1) | 10: 7: 1 | nd |
| 7 | SPhos-Pd G3 (5) | 60/24 | Dioxane/water (1:1) | 10: 2: 0 | 40 |
| 8 | Pd ₂ (dba) ₃ .CHCl ₃ /SPhos 1:1 (10) | 60/24 | Dioxane/water (1:1) | 10: 1: 0.4 | 55 |
| 9 | Pd ₂ (dba) ₃ .CHCl ₃ /SPhos 1:1 (10) | 40/24 | n-BuOH | 10: 4: 4 | nd |
| 10 | Pd ₂ (dba) ₃ .CHCl ₃ /SPhos 1:1 (10) | 80/24 | Dioxane/water (1:1) | 10: 1: 0.3 | 55 |
| 11 | Pd ₂ (dba) ₃ .CHCl ₃ /SPhos 1:1 (10) | 40/20 | Dioxane/water (1:1) | 10: 1: 3 | 65 |
| 12 | Pd ₂ (dba) ₃ .CHCl ₃ /SPhos 1:1 (10) | 60/10 | Dioxane/water (1:1) | 5: 4: 10 | nd |
| 14 | Pd ₂ (dba) ₃ .CHCl ₃ /SPhos 1:1 (10) | 60/48 | Dioxane/water (1:1) | 10: 4: 1 | nd |
| 15 | Pd ₂ (dba) ₃ .CHCl ₃ /SPhos 1:1 (10) | 60/24 | Dioxane/water (1:1) | 10: 0.7: 0 | 40 |

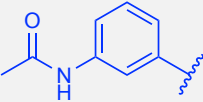
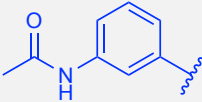
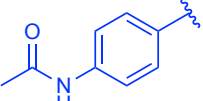
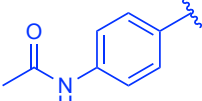
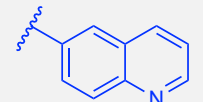
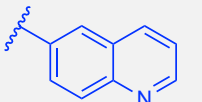
*nd= not determined, a= mixture of PI-int40 and PI-38.

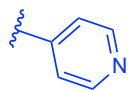
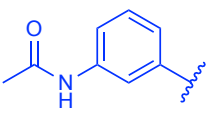
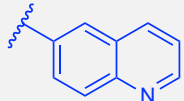
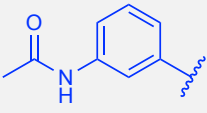
Among the tested catalysts, XantPhos-Pd G3, Pd₂(dppf)Cl₂ and SPhos/Pd₂(dba)₃ showed the best selectivity for the aryl iodide when the reaction was performed with K₃PO₄ as the base in dioxane/water at 60 °C for 24 h (Table 6, entries 3, 8, 15). The mono-substituted intermediate **PI-int40** was obtained as the main product using SPhos/Pd₂(dba)₃, only small amounts of the disubstituted by-product (8–10%) were observed. Careful purification to remove any traces of the disubstituted compound provided **PI-int40** in a moderate yield (45%). The mono-substituted product was then subjected to a second coupling with (3-acetamidophenyl)boronic acid using XPhos-Pd G2 (5 mol%) as a catalyst to provide the unsymmetrical 3,5-disubstituted benzoic acid (Table 7, **PI-40**) in a high yield (90%).

The inhibitory activity of the disubstituted compounds against OXA-48 was evaluated and compounds **PI-36**, **PI-37** and **PI-40** (IC₅₀ (μM)/LE: 2.9/ 0.27, 48/0.21 and 2.9/0.27) showed better inhibition activity in comparison to their corresponding mono-substituted fragments **PI-21a**, **PI-21b** and **PI-28** (IC₅₀ (μM)/LE: 35/0.33, 450/0.26, 240/0.3). The best two fragments were the symmetrical 3,5-disubstituted benzoic acid **PI-36** and the unsymmetrical 3,5-disubstituted benzoic acid **PI-40** with IC₅₀ values of 2.9 μM and LE of 0.27 (Table 7). Crystal structures of fragments **PI-36** and **PI-40** were obtained. They emphasized that the interactions exhibited by the individual fragments were also preserved in the merged structure.

Table 7. Inhibitory activity of 3,5-disubstituted benzoic acid analogues against OXA-48 (IC₅₀, K_d, LE).

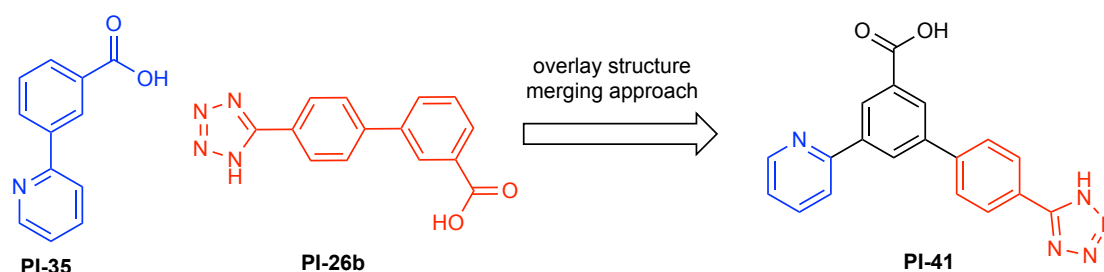


| ID (Paper I) | Ar ¹ | Ar ² | IC ₅₀ (μM) | K _d (μM) | LE |
|--------------|---|---|-----------------------|---------------------|-------------|
| PI-36 |  |  | 2.9 | 20 | 0.27 |
| PI-37 |  |  | 48 | 70 | 0.21 |
| PI-38 |  |  | 110 | 70 | 0.19 |

| | | | | | |
|--------------|---|---|------------|-----------|-------------|
| PI-39 |  |  | 100 | 70 | 0.22 |
| PI-40 |  |  | 2.9 | 49 | 0.27 |

4.5 Additional results not included in Paper I

Attempts to synthesis the third fragment suggested from the merging approach compound **PI-41** (Figure 17). The strategy was based on using 3-(pyridin-2-yl)benzoic acid (Scheme 32, **PI-35**) and 4'-(1H-tetrazol-5-yl)-[1,1'-biphenyl]-3-carboxylic acid (Scheme 32, **PI-26b**). In order to synthesize 3-bromo-5-(pyridin-2-yl)benzoic acid (**PI-41**), two synthetic strategies were considered. The first strategy was SMC of 3-bromo-5-iodobenzoic acid and pyridin-2-ylboronic acid followed by a second SMC with (4-cyanophenyl)boronic acid. The resulting coupled product would then be submitted to a tetrazole formation step (Scheme 33, S1). The other strategy was to conduct the second coupling and install the tetrazole group first then submit the product to SMC with 2-pyridinylboronic acid (Scheme 33, S2).

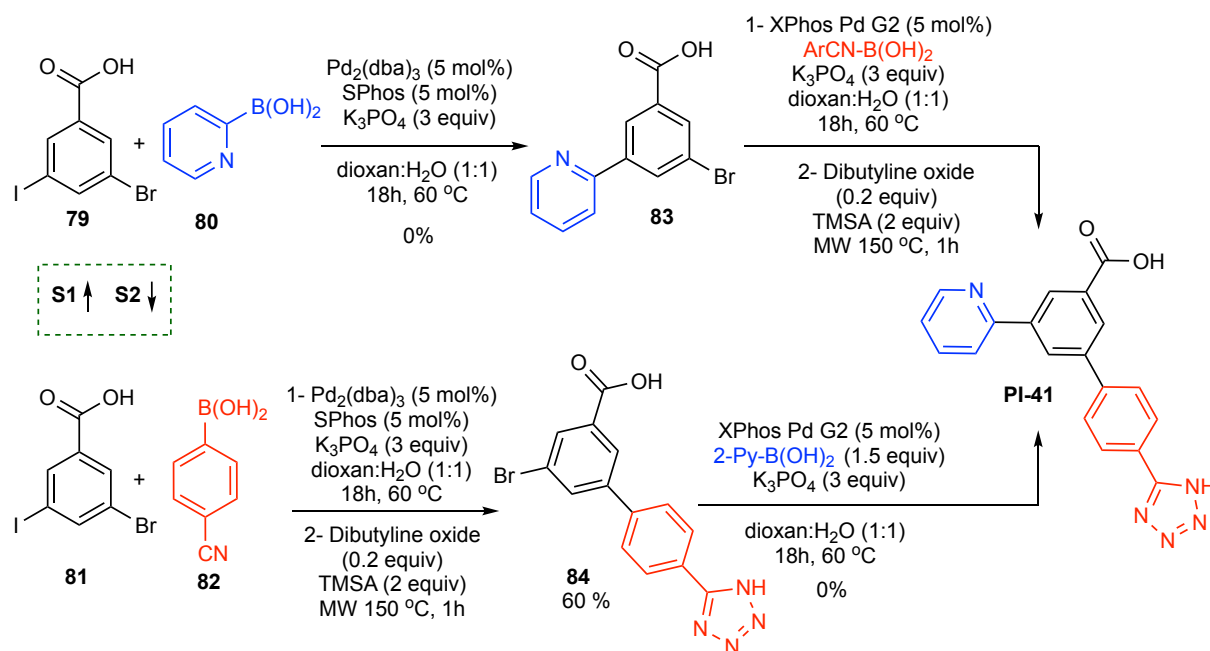


Scheme 32. Promising fragment based on overlay structures from paper I.

In both synthetic strategies coupling with 2-pyridinylboronic acid or ester was not accessible. This might be due to the low reactivity of pyridine boronic acid. It is known that pyridine boronic acids tend to have a slow transmetalation rate due to the electron-deficiency of the pyridine ring. Thus, they require higher temperatures and longer reaction times.¹⁹⁸

The SMC with (4-cyanophenyl)boronic acid resulted in a mixture of mono- and di-substituted benzoic acids in 60% and 25% yield, respectively. The compounds were submitted for the tetrazole formation and the symmetrical 3,5-di-(4-1H-tetrazolyl)phenyl benzoic acid was tested against OXA-48. These compounds were tested in a cell-based assay showing that

the compounds killed the bacteria at 250 and 500 μM concentrations. Therefore, the compounds were not further evaluated as inhibitors.



Scheme 33. Two synthetic strategies to synthesize fragment **PI-41**.

4.6 Conclusion from paper I

In summary, the Suzuki-Miyaura cross-coupling was a successful approach to access a fragment library of 49 candidates of 3-substituted boronic acids. The crystal structures of 33 fragments of the fragment library gave a closer insight into the possible interactions in the binding site R^2 and the preferred binding site R^1 . The most efficient binders were selected to design a small fragment library based on the merging approach. Five fragments of both symmetrical and unsymmetrical 3,5-disubstituted benzoic acids were synthesized and tested for their inhibition activity. Selective Suzuki-Miyaura cross-coupling was applied to obtain the mono-substituted intermediate **PI-int40** in a moderate yield of 45%. The best inhibitors with the lowest IC_{50} values (2.9 μM) are **PI-36** and **PI-40**.

5. Development of carbonylative C-C couplings for the synthesis of VIM-2 inhibiting fragments (Paper II)

5.1 Paper II background

The group of our collaborator Prof. Leiros has previously identified novel fragments inhibiting the metallo- β -lactamase VIM-2.¹³ The study involved an orthogonal screening approach based on a surface plasmon resonance (SPR) assay combined with an enzyme inhibition assay of a library of 490 fragments. The identified fragments were submitted for characterization by determining the K_d , LE, and IC_{50} values. The IC_{50} ranged from 14 to 1500 μ M and the LE ranged from 0.48-0.23 kcal/mol per heavy atom.

Fragment **1** ($IC_{50}/LE= 14/0.38$) shows two important interactions with the residues in the binding site (Figure 18). The carboxyl group displayed two types of interactions, it interacts with Zn2 in the binding site and also forms hydrogen bonds with two water molecules (W1 and W2). The other carbonyl group participated in two interactions, weak chelation with Zn1 and hydrogen bond with Asn233. In addition, the phenyl ring on both sides shows parallel π - π stacking with His263 and a T-shaped π - π stacking with Tyr67. The side chain of Arg228 showed high mobility with different conformations partly forming a hydrogen bond with the carboxyl group in the fragment.

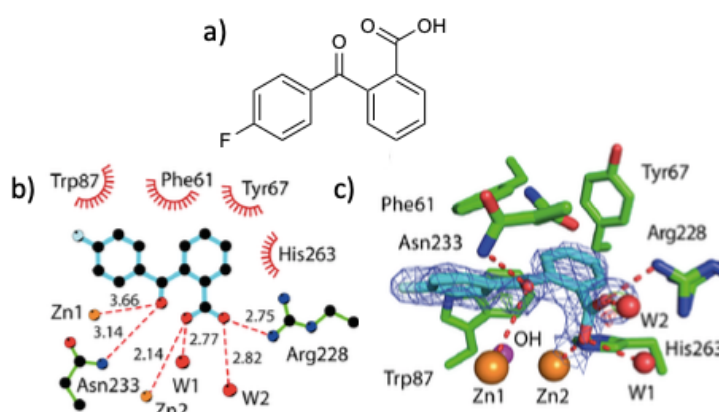


Figure 18. X-ray structure of fragment **1** bound to the active site of VIM-2. Hydrogen bonds are shown as red dashed lines, and hydrophobic interactions are indicated by a red arc. Adapted from Tony et al. (2015).¹³

Additional hydrophobic interaction of the fluorine substituted phenyl group with Phe61 and Trp87 stabilize the fragment binding. Furthermore, the carbonyl group favors the coplanar orientation of the two phenyl groups that enables the hydrophobic interactions with His263, Tyr67, Phe61, and Trp87. Based on the structural information in hand we used fragment **1** as the starting point for paper II.

5.2 Initial work and research focus of paper II

According to the previously reported observation and the information from the crystal structures, we used fragment **1** as a starting point for a fragment library. The 2-benzoylbenzoic acid system (Figure 19, B), where both the carbonyl group and the carboxylic acid are adjacent to each other is necessary for the binding. Phenyl rings could be changed to other heterocycles or substituted phenyl rings in order to keep the possibility of the π - π stacking.

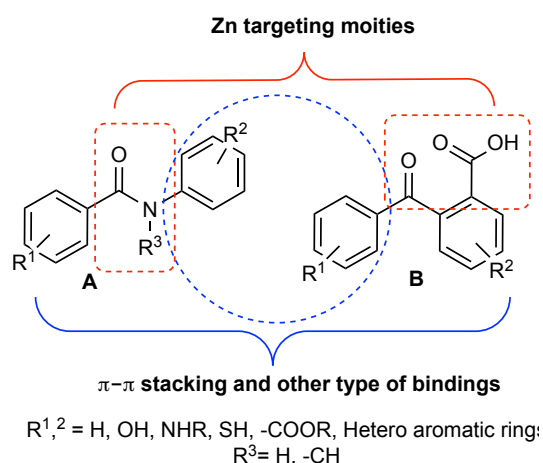
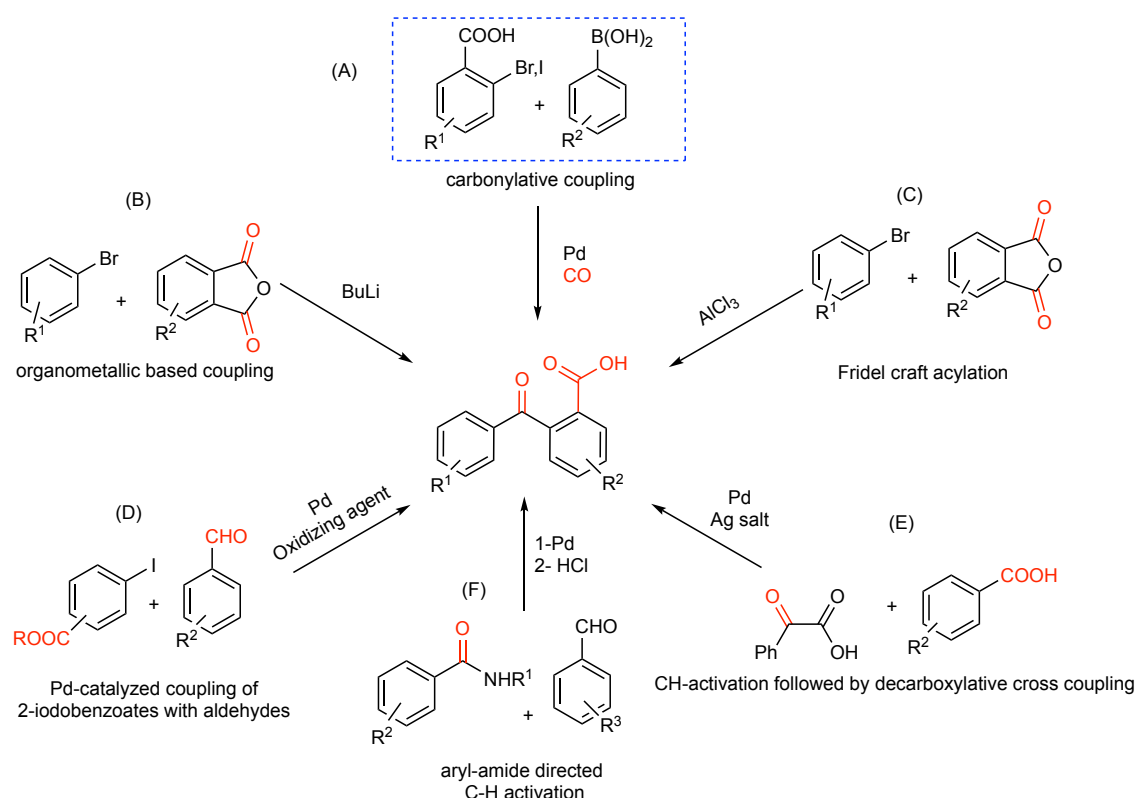


Figure 19. Structure model based on fragment **1** (A) & (B). Red; moieties targeting Zn ions. Blue; substituted aromatic rings for π - π stacking and different ionic and hydrophilic interactions.

In order to synthesize a library of these fragments, several synthetic routes were evaluated to develop a general strategy that would provide a wide range of functionalized 2-arylbenzoic acids without increasing the number of reaction steps. Our initial attempts to synthesize 2-arylbenzoic acids and derivatives were based on the most common methods such as the reaction of phthalic anhydride with organometallic reagents¹⁹⁹ (Scheme 34, B) or Friedel-Craft acylation with aromatic nucleophiles (Scheme 34, C).¹⁵⁴ Although we could obtain a small library of fragments (Chapter 5.5, Table 8, Fragment 1-7) using these methods, we found that they have limitations and are not suitable for obtaining a larger library of the desired

compounds. Many functional groups were not tolerated in these reactions due to the harsh conditions and the use of excess Lewis acids.

Simpler systems such as biaryl ketones have been synthesized by transition metal-catalyzed carbonylative cross-couplings of organometallic reagents and aryl electrophiles¹⁷⁴, or by the non-decarbonylative coupling of acyl electrophiles.^{200–202} Although there are a number of reports describing the synthesis of biaryl ketones in general, only a few methods have proven to be applicable for the formation of 2-aryl benzoic acid derivatives (Scheme 34. D-F).



Scheme 34. Possible approaches towards 2-aryl benzoic acid derivatives.

For instance, Pd-catalyzed *ortho*-C–H activation of benzoic acids followed by decarboxylative coupling with α -oxocarboxylic acids (Scheme 34, E) showed several limitations regarding reaction conditions and substrate scope.¹⁵⁶ This reaction was performed under harsh conditions in DME for 24–48h at 150 °C. In addition, the reaction might provide poor regioselectivity of the desired *ortho* position to the carboxylic group as there are several competing reaction sites. Although the reaction provided the 2-aryl benzoic acid derivatives, it was not compatible with a wide range of functional groups, especially electron-withdrawing functional groups such as nitro groups, nitrile groups, amides, and aldehydes. The scope did not include highly substituted substrates and the yield range was from low to moderate (40–80%). In addition, it excluded

heterocyclic substrates as the coupling partner on both the benzoic acid side and/or the α -oxocarboxylic acids.¹⁵⁶

Pd-catalyzed *ortho*-C–H activation of aryl amides followed by coupling with aryl aldehydes (Scheme 34, F) is another possibility to access 2-aryl benzoic acid derivatives.¹⁵⁵ The reaction includes directed C–H activation, *ortho*-acylation of the aryl amide, then ring closure of the five-membered hydroxyl isoindolone. The five-member ring is then opened to give the biaryl imino carboxylic acid. The imine is then subjected to concentrated HCl in order to hydrolyze it to the keto form and eventually obtain the biaryl imino/keto carboxylic acids.¹⁵⁵ Regarding the substrate scope, the reaction shares the same limitations with the Pd-CH activation and decarboxylative coupling.

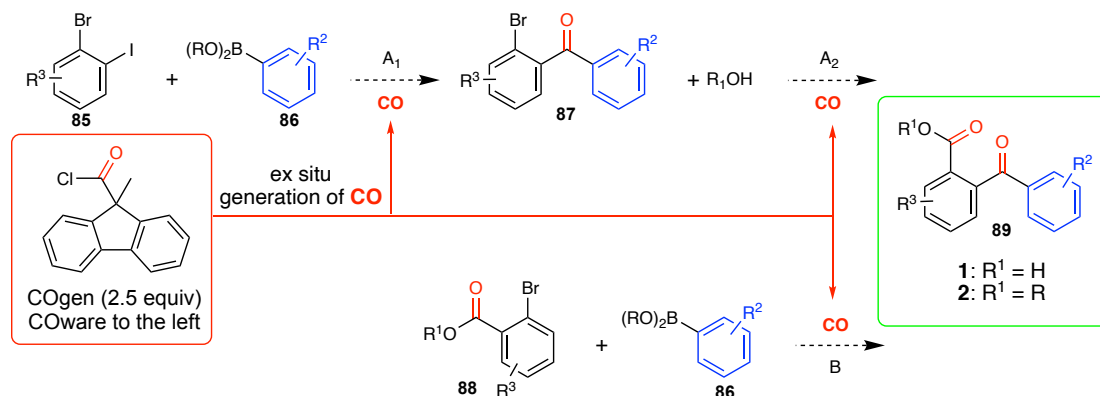
Another possible approach is the Pd-catalyzed coupling of 2-iodobenzoates with aldehydes (Scheme 34, D). The advantages of this method are that it does not require any directing group assistance or *in situ* enamine formation and it prevents the use of CO.²⁰³ However, it showed poor tolerance of substituted benzaldehydes with electron-withdrawing groups such as nitro or nitrile groups. In addition, the yield ranged from low to moderate throughout the whole substrate scope, while it was unsuccessful with amides and heterocyclic aldehydes.²⁰³

5.3 Discussion of the results of Paper II

Based on the analysis above, we decided to develop an alternative route to functionalized 2-arylbenzoic acids using palladium-catalysed carbonylative C–C couplings using CO as the carbonylating agent as key step. In particular we hoped to develop an approach that gave access to functionalized 2-aryl benzoic acid derivatives where $R^2 = \text{OH}$, NHR or other functionalisable handles.

Based on a literature research, carbonylative C–C couplings the reaction showed widespread application in the synthesis of biaryl ketones. The vast majority of the studies reported carbonylative Suzuki-Miyaura couplings using aryl iodides with boronic acids, while few of them addressed the use of less reactive aryl bromides.^{129,153,152,204} Only a few reports discussed the challenging *ortho*-substituted systems, especially the electron-deficient substituted substrates on both coupling partners, the aryl bromide and the boronic acid.^{204,129} Despite the hazard related to the toxic CO gas, we could use it in a safe fashion to avoid the direct handling of the toxic gas by generating it *in situ* using COgen as the CO source.^{146–148}

We addressed two possible routes towards 2-arylbenzoate esters as illustrated in Scheme 35. The aim was to identify a route with a high degree of functional group compatibility that could be used to establish a VIM-2 fragment library of analogues of fragment 1.



Scheme 35. Two possible routes towards 2-arylbenzoate esters.

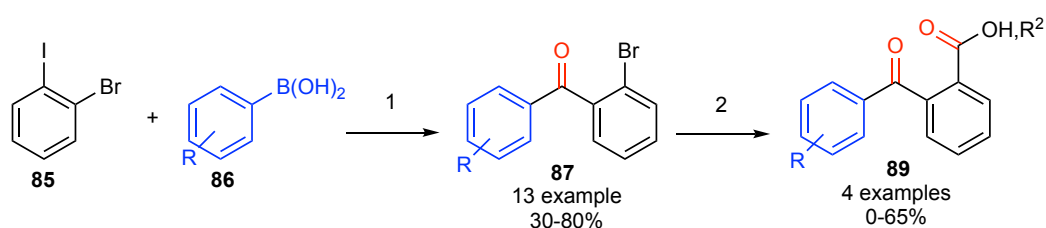
Route A

The first route (Scheme 35, route A) comprises a carbonylative Suzuki-Miyaura coupling of 2-bromoiodobenzene with phenyl/hetero-boronic acids via carbonylative Suzuki-Miyaura, followed by Pd catalyzed hydroxy- or alkoxy-carbonylations of the 2-bromo functionalized biaryl ketones to obtain the 2-arylbenzoic acids derivatives. The initial attempts of step 1 in route A indicated the high impact of the competing non-carbonylative SMC reaction on the results. The product of the competing direct coupling (bi-aryl) was always observed in a considerable amount together with the desired carbonylated product (bi-arylketone). The maximum obtained yield under the optimized conditions was 60 % of the carbonylated product. The competing SMC reaction is a common challenge concerning carbonylative SMC. It is known that in some cases the increase of the CO pressure, temperature and the catalyst loading could enhance the reaction in favor of the desired carbonylative SMC.^{128,130-132,133} However, in our hands increasing the temperature and catalyst loading decreased the yield and favored the direct coupling. High CO pressure would require special equipment and is associated with a risk of faster formation of the inactive palladium black when compared to reactions closer to atmospheric CO pressure.¹³⁴

Thus, we focused on finding conditions that enhanced the carbonylative SMC. First, we thought that making the CO available for the reaction before the transmetalation reagent may provide higher CO pressure before the reaction starts. Thus, the pre-generation of CO was

attempted as it could help to enhance the rate of the CO insertion. However, having the boronic acid readily available for the reaction would not allow the CO insertion to occur faster than the transmetalation and the reductive elimination steps. As already known, the transmetalation and the reductive elimination steps are faster than the CO insertion.¹³³ Accordingly, slowing down the transmetalating agent from reaching the metal center might allow the CO insertion step to occur first. Introducing the boronic acid slowly into the reaction mixture after the complete release of the CO was an attractive approach to the test. Slow addition of the boronic acids was envisioned to enhance the reaction rate in favor of the desired carbonylative SMC. By adding the boronic acid slowly over 2-3h, the yield increased from 60% to 80%. This improvement encouraged us to proceed with the reaction scope, while applying the slow addition. The reaction was compatible with both electron-rich and electron-deficient aryl boronic acids giving moderate to high yields. In addition, electron-rich heterocycles and *ortho*-substituted boronic acids were also tolerated under the reaction conditions. However, some heterocyclic boronic acids (e.g. 2-furanyl boronic acid), hydroxy and N-acyl substituted aryl boronic acids were not tolerated and favored direct coupling instead of the carbonylative alternative.

To emphasize the effect of the slow addition, selected substrates were tested applying slow addition and normal addition. The yield of the carbonylative coupling products were higher, which concludes slow addition can impact the reaction result in favor of the carbonylative coupling. 13 examples of substituted 2-bromobiaryl ketones were synthesized in low to high yields (Scheme 36).



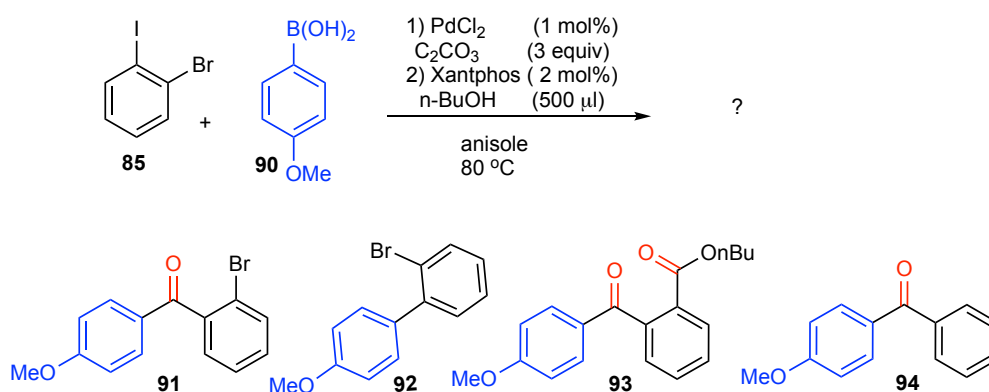
Scheme 36. Route A, 1) PdCl₂ (1 mol%), C₂CO₃ (3 equiv), COgen (2 equiv) in anisole. 2) PdCl₂ (1 mol%), Xantphos (2 mol%), C₂CO₃ (3 equiv), COgen (2 equiv) in anisole: *n*-BuOH (2:1).

The second step of route A (Scheme 36, 2) was hydroxy- or alkoxy-carbonylation of the obtained 2-bromo functionalized biaryl ketones. Our initial attempts to directly obtain carboxylic acids by hydroxycarbonylation using SilaCOgen were unsuccessful. This might be due to steric hindrance at the *ortho* position of the ketone. However, we intended to try alkoxy-carbonylation on 2-bromo-4-methoxybenzophenones as a test substrate. We tested different reaction conditions including a range of Pd catalysts and ligands, nucleophiles, bases,

and solvents. Few reaction conditions gave access to the desired alkyl 2-(4-methoxybenzoyl)benzoate. The best result was obtained with PdCl₂ (1 mol%) and Xantphos (2 mol%), *n*-BuOH, and K₂CO₃ in anisole (Scheme 36, 2). The desired butyl 2-(4-methoxybenzoyl)benzoate was obtained with a 65% yield. Applying these conditions to a number of 2-bromobenzophenone derivatives from step 1, we found that the reaction is substrate-dependent. Thus, we concluded that this approach is limited and not suitable for synthesizing a larger library of 2-aryl benzoic acid derivatives.

One-pot approach to synthesize 2-arylbenzoic ester

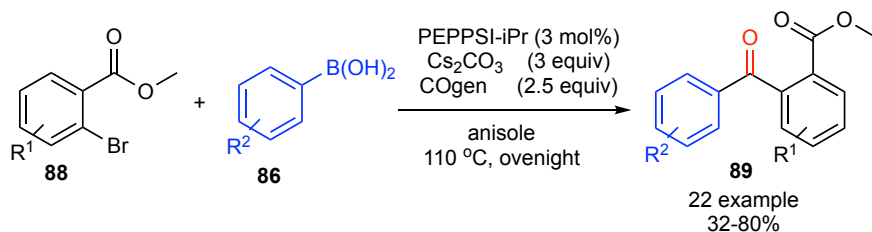
The two steps of route **A** seemed to be feasible in one pot. The reagents required for the alkoxyacylation step such as the ligand and the nucleophile can be added later after 18 hours from the first step. In this case no excess of catalyst or COgen is required (Scheme 37). Unfortunately, our initial attempts of a one-pot synthesis of 2-arylbenzoic ester were not successful. Introducing extra fresh catalyst to the second step did not prove to be beneficial. We obtained several products after the second step including the biaryl ketone **88**, the biphenyl coupled product **93** as a byproduct from the first step, the desired biphenyl keto ester **90** and the biaryl ketone without the bromide **94** (Scheme 37). Palladium black formation was always observed in the first step, which could be a reason that hindered the second step and decreased the activity of the freshly added PdCl₂. Despite the addressed limitations of the one-pot approach, we could still observe some of the biaryl keto esters, which indicated that the reaction could be further developed to obtain the desired activity. We were therefore interested to study the reaction from another direction to learn about the sequence influence on the reaction reactivity, so the second route was evaluated.



Scheme 37. One-pot synthesis of 2-aryl benzoic ester.

Route B

In route B, we started from commercially available 2-bromo substituted benzoate esters as starting material for the carbonylative SMC. 2-Bromobenzoate was submitted to a range of experimental conditions including different palladium and Ni sources and ligands such as $\text{Pd}(\text{acac})_2$ or $\text{Pd}(\text{OAc})_2/\text{CataCXium A}$ or A-HI, $\text{Pd}(\text{OAc})_2$ or $\text{PdCl}_2/\text{Xantphos}$, $\text{Ni}(\text{COD})/\text{dcype}$ and others to find the best conditions for the reaction (Paper II, Table ESI-6). Our observations mainly concluded the dominance of the undesired non-carbonylative coupling pathway. Only the $\text{Pd}(\text{IPr})$ -based catalytic systems showed promising results as it could accomplish the carbonylative SMC. In the carbonylative coupling of methyl 2-bromobenzoate with 4-methoxyboronic acid, PEPPSI-IPr (3 mol%) as catalyst precursor, Cs_2CO_3 as a base in chlorobenzene or anisole as solvent proved to be the best system, providing the desired product in 63% yield (paper II, S 4, 2aa). In order to enhance the yield, we tested the slow addition of the boronic acid to the reaction mixture over 2-3h. This approach showed great influence on the SMC in route A, so it was expected to give relatively similar results in route B. The yield was further increased to 80% by slow addition of the boronic acid. The reaction showed very good compatibility with different functional groups on both coupling partners including electron-withdrawing, electron-donating, and heterocyclic boronic acids (Scheme 38). Boronic acids with electron-donating groups such as -OMe, -SMe, and heterocyclic boronic acids such as thiophene and benzothiophene gave moderate to high yields. Boronic acids with electron-withdrawing groups such as -CN, -F, -COOMe gave low to moderate yields. Sterically hindered *ortho*-substituted boronic acids were also compatible under the reaction conditions and gave acceptable yields. Aryl bromides with both electron-withdrawing and electron-donating groups were tolerated and gave moderate yields (Paper II, Scheme 4, 5).



Scheme 38. Route B, Suzuki-Miyaura coupling of methyl 2-bromobenzoate.

Scope limitations and general findings

The paper aimed to establish a general method to synthesize a wide range of 2-arylbenzoic acid derivatives to test against VIM-2. Initially, we designed the fragments to contain functional

groups on both aryl rings (Scheme 38, R¹ and R²) with a potential binding ability to the VIM-2 binding site. Functional groups such as -OH, -NH₂, -CONHR, NO₂ could act as hydrogen bond donors and/or acceptors in the binding site. In addition, the fragments were also envisioned to contain functional groups that allow for late-stage functionalization of both aryl rings. Unfortunately, substituents such as hydroxy, amines, and amides could not be introduced with the developed method. Moreover, the solubility of the reagents including boronic acids or acid derivatives in the reaction solvent can impact the success of the reaction. As we developed the slow addition method, we introduced the boronic acid/anisole solution to the reaction mixture over 2-3h. Boronic acids with a low solubility in anisole were challenging substrates and thus were incompatible under reaction conditions. However, the strategy has good potential for further optimization. Therefore, an extended study to find a better system to overcome the scope limitations and allow for a wider range of VIM-2 inhibitors is an attractive research point for the future.

5.4 Conclusion from paper II

In conclusion, two routes for accessing 2-arylbenzoate esters have been evaluated. This evaluation suggests that the second route (B), which employed a carbonylative Suzuki-Miyaura coupling of 2-bromobenzoate esters, could be a better strategy than route (A). Although the suggested slow addition of the boronic acids is dependent on the solubility of them in the reaction solvent, it is considered to be a finding of general value as it allowed us to enhance the reaction reactivity to favor carbonylative over non-carbonylative processes in Suzuki-Miyaura couplings. A range of diversely substituted 2-arylbenzoate esters that share the same structure core as our targeted structure model (Figure 18, Fragment **1**) was prepared and sent for biological testing at Nordstruct. The fragments were lacking some promising functional groups such as OH, NO₂, NH₂, etc. These types of substituents on both aryl rings could enhance the binding of the fragments with the active site via hydrogen bonding, ionic or covalent interactions. Due to the lacking of such functional groups, further optimization to find better reaction conditions including the solvent and the catalytic system is suggested in paper III.

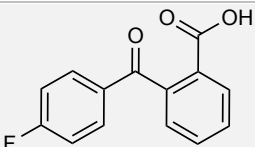
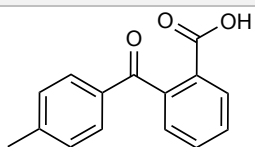
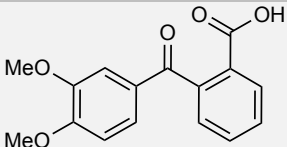
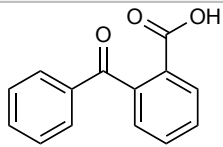
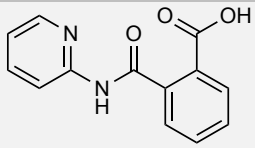
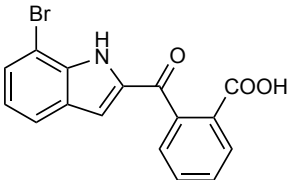
5.5 Additional results not included in Paper II

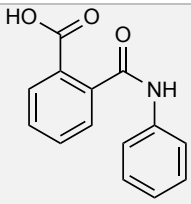
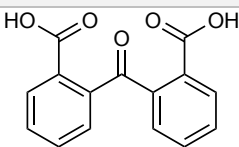
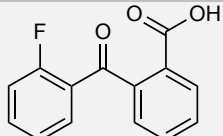
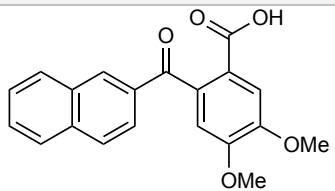
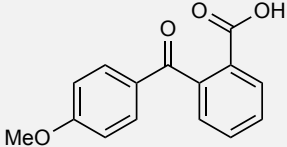
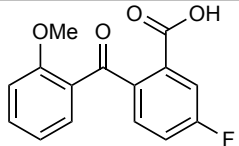
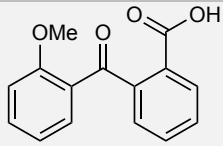
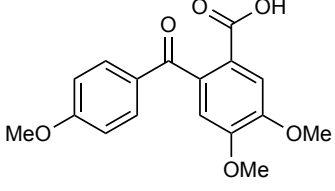
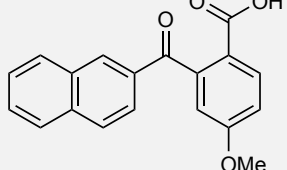
The initial trials of preparing 2-arylbenzoic acids by reacting phthalic anhydride with organometallic reagents or by Friedel-Craft acylation of aromatic nucleophiles resulted in a small library of fragments (Table 8, Fragments **F1a-F7**). The fragments were evaluated against

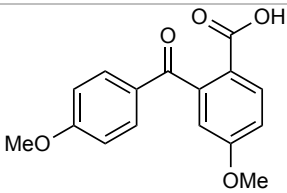
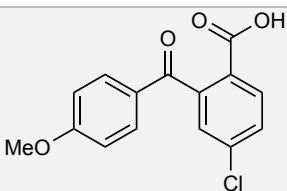
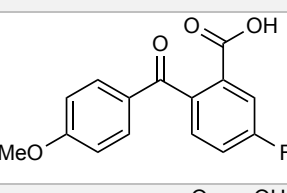
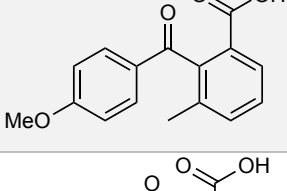
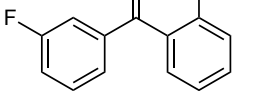
VIM-2 and IC_{50} values were obtained. None of these fragments showed improved inhibition activity when compared to fragment **1** ($IC_{50}/LE= 14/0.38$).

Fragments obtained via carbonylative Suzuki-Miyaura coupling were also tested against VIM-2 and IC_{50} values were obtained (Table 8, Fragments **F8-F20**). All the tested fragments showed inhibition in the μM range. Two fragments (Table 8, Fragments **F9** and **F13**) showed inhibition activity comparable to fragment **1** with LE of 9.96 and 10.77, respectively. Fragment **F20** showed the best ligand efficiency with LE of 0.43. The obtained results can be used as a starting point for further optimization towards better hits against VIM-2.

Table 8. Biological data of tested fragments against VIM-2.

| Fragment no. | Structure | IC_{50} (μM) | LE |
|--------------|---|-----------------------------|------|
| F1-a |  | 12.5 | 0.38 |
| F2 |  | 97.6 | 0.23 |
| F3 |  | 10.7 | 0.33 |
| F4 |  | 8 | 0.35 |
| F5 |  | >1 mM | |
| F6 |  | Precipitated undetected | - |

| | | | |
|------------|---|-------|------|
| F7 |  | 1000 | 0.23 |
| F8 |  | 160.4 | 0.27 |
| F9 |  | 9.964 | 0.39 |
| F10 |  | 111.7 | 0.22 |
| F11 |  | 58.69 | 0.31 |
| F12 |  | 32.59 | 0.31 |
| F13 |  | 10.77 | 0.37 |
| F14 |  | 117.4 | 0.24 |
| F15 |  | 111.7 | 0.24 |

| | | | |
|------------|---|-------|------|
| F16 |  | 176.9 | 0.25 |
| F17 |  | 221.6 | 0.26 |
| F18 |  | 298.9 | 0.25 |
| F19 |  | 564 | 0.23 |
| F20 |  | 2.852 | 0.43 |

6. Development of carbonylative C-C, C-N, C-O couplings using renewable solvents

6.1 Paper III background

As the method developed in paper II still showed limitations with regard to substituents such as -OH, -NH₂, -NHR and -NO₂, we continued our efforts to improve the carbonylative SMC of aryl bromides with aryl boronic acids. In paper III, an alternative method for carbonylative SMC in green solvents is described.

Renewable solvents have been described to be suitable medium for several chemical transformations including classical condensation reactions and transition-metal (TM)-catalyzed cross-couplings.²¹¹⁻²¹³ including biphasic reactions such as metal catalyzed carboxylation reactions using CO₂.¹⁹⁰ However, carbonylative reactions have not been studied in renewable solvents. In addition, we extended the study to investigate the efficiency of green solvents in alkoxy-carbonylation that showed carbonylative couplings of aryl bromides with amines and alcohols, both reactions that were investigated during the work leading to paper II. For the latter two, we focused on catalytic systems that have already proven to be suitable systems for Pd-catalyzed carbonylation reactions.^{153,176,171}

6.2 Paper III results and discussion

Solvent properties

In general, liquids that are available from biomass and CO₂ derived chemicals have a great potential to replace non-renewable solvents that are frequently utilized in organic synthesis.^{188,205,206,187,181} In this study, we examined both known renewable solvents and some recently introduced biomass-derived solvents¹⁹⁰ as shown in Figure 20.

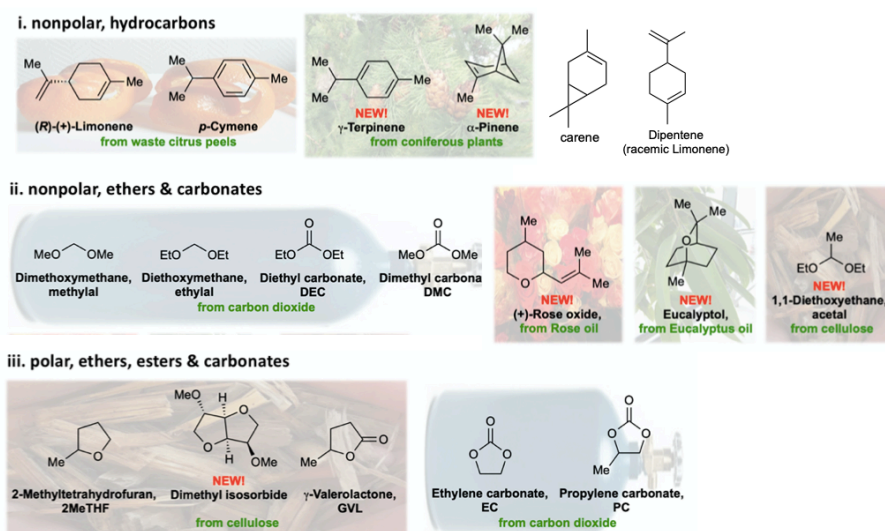


Figure 20. Structure of the renewable solvent used in paper III.

The polarity of the solvents was estimated based on their dielectric constant. Solvents with dielectric constant higher than 5 are considered to be polar, while solvents with dielectric constant below 5 were considered as non-polar (Table 9). Thus, the solvents could roughly be grouped into non-polar hydrocarbons (α -pinene, γ -terpinene, limonene, *p*-cymene), non-polar ethers (diethoxymethane (methylal), dimethoxymethane (ethylal), 1,1-diethoxyethane (acetal), rose oxide, eucalyptol) and carbonates (dimethylcarbonate (DMC), diethylcarbonate (DEC)), and polar ethers (dimethyl isosorbide, 2-methyltetrahydrofuran (2MeTHF)) comparable to e.g. THF and highly polar esters and carbonates (γ -valerolactone (GVL), propylenecarbonate (PC), ethylenecarbonate (EC)) comparable to e.g. DMF.

Table 9. Solvent properties and overview of the solvent performance in the three tested carbonylative reactions.

| Solvent | MW (g/mol) | Bp (°C) | Dielectric constant ¹ | Compound class | C-C yield (%) | C-N yield (%) | C-O yield (%) |
|-------------------------------|------------|-------------|----------------------------------|--------------------|-------------------------|-------------------------|-------------------------|
| non-polar | | | | | | | |
| α -Pinene | 136.24 | 156 | 2.18 | hydrocarbon | 50 | 97 | 93 |
| γ -Terpinene | 136.24 | 174 | 2.27 ²⁰⁷ | hydrocarbon | 50 | 94 | 93 |
| (+)-Limonene | 136.24 | 178 | 2.37 | hydrocarbon | 80 | 99 | 56 |
| <i>p</i> -Cymene | 134.22 | 177 | 2.25 ²⁰⁸ | hydrocarbon | 75 | 97 | |
| Toluene | 92.14 | 111 | 2.38 | hydrocarbon | 90¹⁵³ | 97¹⁷⁶ | |
| Diethoxymethane (ethylal) | 104.15 | 87 | 2.53 ²⁰⁹ | ether | | 62 | 64 |
| Dimethoxymethane (methylal) | 76.10 | 42 | 2.64 | ether | 50 | | 45 |
| Diethoxymethane (ethylal) | 104.15 | 87 | 2.53 ²⁰⁹ | ether | | 62 | 64 |
| Diethylcarbonate (DEC) | 118.13 | 126 | 2.82 | carbonate | | 94 | 45 |
| Dimethylcarbonate (DMC) | 90.08 | 90 | 3.13 ²¹⁰ | carbonate | 16 | 97 | 93 |
| 1,1-Diethoxyethane (acetal) | 118.18 | 102 | 3.80 | ether | | 62 | 55 |
| (+)-Rose oxide | 154.25 | 86/20 mmHg | | ether | 33 | 78 | 36 |
| Eucalyptol | 154.25 | 176 | 4.57 | ether | | 89 | 82 |
| polar aprotic | | | | | | | |
| Dimethyl isosorbide | 174.20 | 94/0.1 mmHg | 6.20 ²¹¹ | ether | | 89 | 30 |
| 2-MeTHF | 86.13 | 79 | 6.97 ²¹² | ether | 30 | 83 | 91 |
| Tetrahydrofuran (THF) | 72.11 | 65 | 7.52²¹³ | ether | | | 88¹⁷¹ |
| γ -Valerolactone (GVL) | 100.12 | 207 | 36.47 | ester | | 74 | 64 |
| Propylenecarbonate (PC) | 102.09 | 242 | 66.14 | carbonate | | 80 | 60 |
| Ethylenecarbonate (EC) | 88.06 | 261 | 92.8 | carbonate | | | 30 |

¹ Values obtained from CRC Handbook of Chemistry and Physics (85th ed.) unless mentioned otherwise. Solvents are organized by increasing dielectric constant.

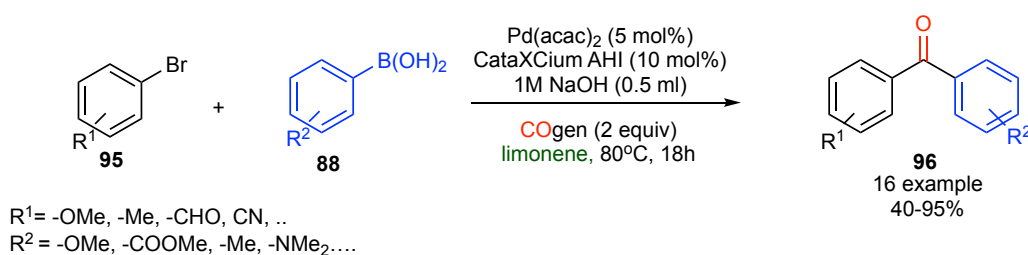
Carbonylative SMC (C-C)

The reaction of 3-bromoanisole with *m*-tolylboronic acid was used as a model reaction for the screen. The reaction conditions were based on a catalytic system, which is originally developed in the group of Skrydstrup.¹⁵³ The catalytic system relied on using Pd(acac)₂ and di(1-adamantyl)-*n*-butylphosphine hydroiodide (cataCXium AHI) as a ligand. The original method relied on using boronic acid derivatives such as diethanolamine-complexed heterocyclic boronic acids (DABO boronates) or aryl trihydroxyborates in toluene/H₂O (10:1) or pure toluene as a solvent.¹⁵³ When repeating the original reaction using aryl trihydroxyborates, we could obtain comparable result and the desired product was achieved in 83% yield (see paper III ESI, Table S1, entry 3). However, we found that the extra step of preparing the aryl trihydroxyborates was not needed. We were able to simplify the method by generating the aryl trihydroxyborates *in situ* by adding 1M NaOH (aq) instead of preparing the organoborates separately.

We tested a range of renewable solvents using the model reaction of 3-bromoanisole with *m*-tolylboronic acid under the developed method. Non-polar ethers, like rose oxide and methylal, carbonate like DMC and polar ethers, like 2-MeTHF, gave the carbonylated product in low to moderate yield (16-50%) and favored direct coupling over the carbonylated product. On the other hand, non-polar hydrocarbons such as limonene, *p*-cymene, γ -terpinene, α -pinene gave better yields (80%, 75%, 50%, 50%, respectively) in correlation with the use of toluene in the original conditions. Limonene favored the carbonylative coupling reaction over the direct coupling and provided the desired biaryl ketone in 80%. Although limonene has a terminal no side product related to the Heck-type arylation of the solvent was observed under reaction conditions neither with rose oxide, γ -terpinene, α -pinene.

We tested the scope of the reaction to check the generality of the carbonylative SMC in limonene. We examined a wide range of boronic acids and aryl bromides, which have shown a good scope. As we are generating the trihydroxyborates *in situ*, this allowed us to use a wide range of boronic acids and avoid the limitations associated with isolation of unstable trihydroxyborate salts. The reaction showed excellent compatibility with electron-rich, electron-deficient and heterocyclic boronic acids and gave high to excellent yields (71-95%). Moreover, electron-rich, electron-deficient and heterocyclic aryl bromides were successfully transformed to the desired products in high to excellent yield (75-91%). It is also noteworthy

that the reaction still shows limitation regarding sterically hindered, electron-withdrawing group aryl bromide such as methyl 2-bromobenzoate, which gave the product in moderate yield (40%). The scope of the reaction allowed for 16 examples of substituted biaryl ketones in moderate to excellent yields (Scheme 39). We can conclude that the obtained yields were in correlation with original reports using non-renewable solvents such as toluene. This emphasizes that limonene is a renewable alternative for carbonylative SMC and can replace the commonly used non-renewable solvents such as toluene, dioxane, chlorobenzene, DMF.^{131,134,137,156,181,155}



Scheme 39. Carbonylative SMC of aryl boronic acids with boronic acid in limonene.

Aminocarbonylation (C-N)

For aminocarbonylation we used the catalytic system developed by Buchwald and coworkers, where they used Pd(OAc)₂, Xantphos and triethylamine as base in toluene. The Pd-catalyzed aminocarbonylation of 4-bromobenzonitrile and N-methylaniline was used as model reaction for the solvent screening.¹⁷⁶ The aminocarbonylation reaction in sustainable solvents gave yields comparable to the result under original conditions in toluene, and even better in some cases.¹⁷⁶ Non-polar hydrocarbons such as limonene, *p*-cymene, γ -terpinene, α -pinene gave excellent yields (99, 97, 94, 97%, respectively), which was not surprising given that these solvents can be expected to have similar properties as toluene.¹⁷⁶ However, the performance of non-polar carbonates (DMC, DEC) was also excellent and the products were obtained in 97% and 94% yield, respectively. The performance of polar carbonates (PC, GVL) and polar/non-polar ethers (2-MeTHF, rose oxide, acetal, etc.) was less good than the other solvents but the product was also here obtained in moderate to high yields (62-89%). Under the reaction conditions, no sign of side reaction such as hydroamination or Mizoroki-Heck coupling for solvents possessing double bonds was observed. As we obtained excellent results in many of the tested solvents, we performed several experiments in the best 3 solvent candidates (limonene, DMC, α -pinene) to check their scope tolerance. We found that limonene, DMC gave comparable results and showed excellent performance in the tested reactions in contrast to α -

pinene, which showed high substrate dependence (Paper III, Scheme 2). Among other renewable solvents DMC is described to be less toxic, cheaper and more viable replacement for toluene.²¹⁶⁻²¹⁹ Thus, we tested the reaction scope to check the generality of the reaction in DMC. The renewable solvent DMC showed excellent performance throughout the tested scope and showed tolerance for many functional groups on both coupling partners. In general, aryl bromides with electron-withdrawing groups provided the product in high to quantitative yields (81-99%). However, electron-rich aryl bromides were obtained from low to moderate yields (16-64%). Different amines were also tested and both electron-rich or electron-deficient primary and secondary amines were well tolerated and the desired products were obtained in high to excellent yields (85-94%). In addition, we could synthesize commercial drugs such as Trimetozine,^{220,221} which is used as a sedative and analogue of Itopride,²²²⁻²²⁴ which is used for treatment of gastrointestinal symptoms in excellent yields (Paper III, Scheme 2). The scope of the reaction allowed for 20 examples of primary and secondary substituted amides (Scheme 40) and the results were in correlation with reports of aminocarbonylation in non-renewable solvents. We therefore conclude that renewable solvents such as limonene and DMC can efficiently replace toluene, THF or dioxane that are usually used in Pd-catalyzed aminocarbonylation reactions.^{139,158,159,163,166,176}



Scheme 40. Aminocarbonylation in dimethyl carbonate.

Alkoxy carbonylation (C-O)

Similarly, in case of alkoxy carbonylation, we preliminary tested the renewable solvents on a model reaction of 2-bromonaphthalene with sodium *tert*-butoxide and CO using the catalytic system based on Pd(dba)₂ as catalyst precursor and 1,1'-bis(diisopropylphosphino)ferrocene (dippf) as ligand in THF that was first developed in the Skrydstrup group.¹⁷¹ As expected, 2-MeTHF gave excellent results (91%). Non-polar ethers like methylal, ethylal, acetal, rose oxide and eucalyptol and carbonates like DEC showed moderate efficiency and the product was obtained in 45, 64, 55, 36, 82 and 45% yield. Polar solvents such as PC, EC, GVL and dimethyl isosorbide were less efficient and the product was obtained in only low to moderate yields (30-

64%). In case of non-polar carbonate DMC, the alkoxy carbonylation worked well, but we obtained methyl ester in 93% isolated yield instead of *tert*-butyl ester. DMC played a dual role in the reaction where it worked as the reaction medium and as a reagent, which allowed for a transesterification step on the *tert*-butyl ester. However, the non-polar hydrocarbons γ -terpinene and α -pinene gave also excellent yields of 93%.

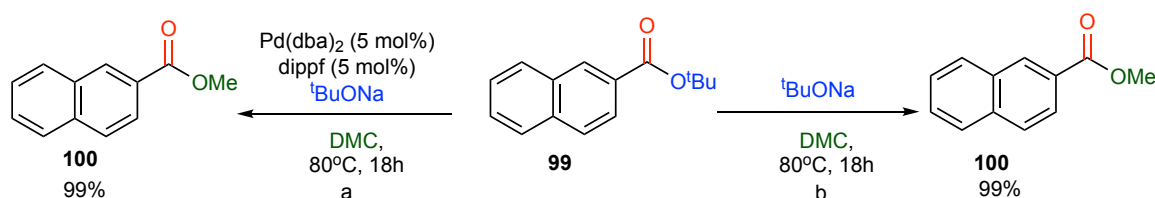
As several solvents showed good performance in *tert*-butoxycarbonylation, we tested the best 3 candidates (2-MeTHF, γ -terpinene, α -pinene) with several substrate to check their scope tolerance. The experiments showed that the performance of the solvent depends on the substrate. However, α -pinene showed good general tolerance with the tested substrates. Then we tested the reaction scope to evaluate the generality of *tert*-butoxycarbonylation in α -pinene. Electron-rich aryl bromides could be transformed to the corresponding *tert*-butyl ester in moderate to excellent yields (80-93%), while electron-deficient aryl bromides were less reactive and the products were obtained in low to moderate yields (25-51%). The scope resulted in 10 examples and the yields are comparable original reported results in THF.¹⁷¹ Therefore, we suggest that renewable solvents such as 2-MeTHF, α -pinene and γ -terpinene can replace non-renewable solvents (DMSO, THF, TEA, etc.) that are usually used for alkoxy carbonylation reactions.¹⁷⁰⁻¹⁷³

Further studies on the renewable solvent DMC

As mentioned before (Chapter 3.3.1) Pd-catalyzed alkoxy carbonylation of aryl bromides are mainly based on using bulky alcohols, phenols or corresponding alkoxides.^{168,169,134,170,171,172,173} Alcohols containing α -hydrogens were found to be challenging due to the side reactions they can undergo, such as β -hydride elimination. Moreover, low boiling point alcohols e.g; methanol could be challenging. Thus, we were encouraged to investigate the scope of the observed methoxy carbonylation in (Paper III, Scheme 4). Electron-rich aryl bromides gave excellent yields, while electron-deficient aryl bromides were less reactive and gave only moderate yields. Traces of *tert*-butoxycarbonylation product were always observed with the main methoxy carbonylation product throughout the whole scope.

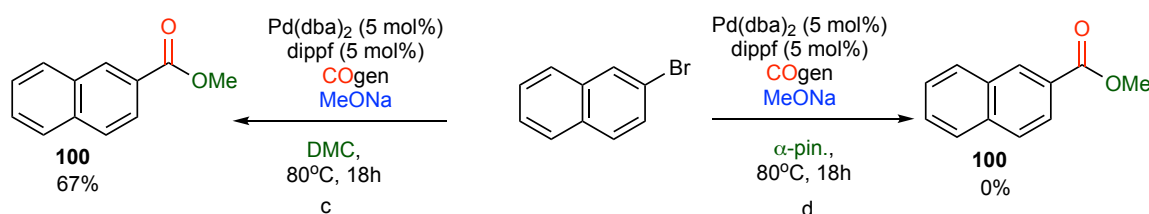
We intended to perform a set of control experiments to gain closer overview of the possible products of the reaction and to confirm that obtaining the methyl ester occurs after the initial installation of the *tert*-butyl ester resulted from the *tert*-butoxycarbonylation mechanism (Paper III, Scheme 5). The *tert*-butyl-2-naphthoate was transformed to methyl-2-naphthoate

when treated with NaOtBu in DMC. According to the experimental results, the transesterification happens both with and without the Pd-catalyst (Scheme 41). However, when testing methoxycarbonylation of 2-bromonaphthalene using MeONa as a nucleophile in DMC, the corresponding methyl ester resulted in 67% yield (Scheme 42, c). While the same reaction in α -pinene resulted in no product and the starting material was recovered (Scheme 42, d).



Scheme 41. Control experiment on *tert*-butyl 2-naphthoate.

These results indicate that the observed methoxycarbonylation can be a result of two simultaneous pathways. In one pathway, the *tert*-butyl ester is installed on the aryl bromide via Pd-catalyzed alkoxylation followed by a transesterification with sodium methoxide generated *in situ* from the reaction of the excess sodium *tert*-butoxide with DMC. In the other pathway, *in-situ* generated sodium methoxide is involved in a Pd-catalyzed methoxycarbonylation.



Scheme 42. MeONa initiated alkoxylation in DMC.

6.3 Additional results not included in Paper III

Column chromatography (C.C) and extraction are important means of purification. Common organic solvents used in these processes are heptane, DCM, MeOH, EtOAc, and many more. The amount of solvent needed for each synthesis until obtaining the pure product could reach couple of liters. Therefore, it is of high importance to find sustainable alternatives for the common solvents used in the purification process. The success of the renewable solvents as sustainable reaction medium in the reactions studied in paper III encouraged us to test them as a purification and isolation medium. Therefore, we attempted to replace the common non-polar hydrocarbon solvent heptane or pentane, commonly used in C.C and TLC systems, with greener alternatives.

Therefore, we tested some non-polar hydrocarbons such as *p*-cymene (bp = 177 °C), carene (bp = 171 °C) and dipentene (bp = 170-180 °C) as the mobile phase in C.C to each model reaction of the three transformation - carbonylative SMC, aminocarbonylation and alkoxy carbonylation. In case of *p*-cymene as eluent, we faced difficulties with visualizing the compounds spots on the TLC plate and thus difficult separation. As *p*-cymene is a UV active solvent with high boiling point (177 °C), evaporating the TLC plate and detecting the spots was not successful. In case of carene and dipentene, we saw good separation on TLC. The product was separated with similar solvent system as for heptane-EtOAc mixtures. However, after evaporation of the pure fractions, we always noticed some remaining solvent together with the pure product. The solvent residues could not be removed using rotavap, high vacuum pump or overnight freeze drying. Thus, with the time available, we were not able to provide a green CC system. However, among the introduced sustainable solvents and other new candidates there might be some solvent that could replace common organic solvent in purification processes. Finding green CC systems is an important goal that should gain research interest. The field of green chemistry is a wide field and the development of greener methods including finding new sustainable solvents and testing them for application is interesting and useful environmental wise.

6.4 Conclusion from Paper III

The goal of this study was to determine green solvents for Pd-catalyzed carbonylative C-C, C-N, and C-O bond forming reactions. A sub-goal was to find conditions that could be used in the synthesis of VIM-2 inhibitory fragments. We have found several renewable solvents, which can successfully substitute traditional non-renewable solvents for three types of palladium catalyzed cross-coupling transformations. Our investigation regarding carbonylative coupling reactions has proven that limonene and its derivatives (γ -Terp, α -Pin, Cym) can replace non-polar petroleum solvents such as toluene, dioxane in both carbonylative SMC, aminocarbonylations and alkoxy carbonylations.

Another stream of sustainable solvents including new candidates such as acetaldehyde diethyl acetal - readily available from ethanol; eucalyptol - from Eucalyptus oil; rose oxide - from rose oil has been introduced. However, they showed weaker performance in comparison to the other solvent candidates. We also reported the behavior of CO₂ derived solvents (DMC, DEC, PC) as the media for Pd-catalyzed cross-coupling reactions. The overall performance of these

solvents was found to be good. Especially DMC was an excellent media for aminocarbonylation and alkoxy carbonylation. In addition, DMC can be used in methoxycarbonylation reaction instead of using the low boiling point methanol to avoid associating problems such as evaporation or side reactions as β -hydride elimination. It also could serve as transesterification agent to obtain methyl ester in late stage optimization.

With regard to the synthesis of VIM-2 inhibitory fragments, more experiments are needed to evaluate if the procedures described in paper III will give excess to a broader substitution pattern compared with the method described in paper II.

7. Conclusion

The aim of the thesis was to develop methods for the synthesis of carbapenemase inhibitors targeting OXA-48 and VIM-2 using a fragment based approach based on previous work in our group^{13-15,107} and to apply the methods to the synthesis of inhibitory fragments or inhibitors.

In chapter 4, a synthesis of a range of symmetrical and unsymmetrical 3,5-disubstituted benzoic acids using selective Suzuki-Miyaura coupling was developed. The synthesis of 3,5-disubstituted benzoic acids was according to the merging approach of the promising mono-substituted benzoic acids targeting OXA-48 reported in paper I. The synthesized di-substituted benzoic acid fragments were evaluated and their inhibition activity was found to be better than the mono-substituted benzoic acids. Crystal structures of the tested fragments were obtained and provided us with further knowledge about the active site of OXA-48 to be used for further development.

In chapter 5, I developed a method for the synthesis of 2-arylbenzoic acids and derivatives via carbonylative SMC using CO gas in a safe fashion. Challenges found upon synthesizing 2-arylbenzoic acids were also discussed together with suggested solutions. In addition, I discovered the importance of slow addition of the boronic acid to suppress the competing SMC and to favor the carbonylative SMC. The developed method resulted in a range of 2-arylbenzoic acids that were tested and evaluated against the carbapenemase VIM-2. The tested fragments gave IC₅₀ values in the μM range. However, we were not able to expand the fragment library to include specific groups such as OH, NH₂, NHR, etc. Accordingly, an expanded study to find a better system to include more challenging substrate was carried out.

In chapter 6, I tried to extend our study to find better reaction conditions to cover the scope limitations in paper II. In addition, I aimed to synthesize a larger fragment library to test against VIM-2. During the study, we found that sustainable solvents are efficient in Pd-catalyzed coupling reactions and a wide range of sustainable solvents was tested to evaluate their impact on Pd-catalyzed couplings. The effect of sustainable solvents in the challenging carbonylative SMC, alkoxycarbonylation and aminocarbonylation was investigated. The tested sustainable solvents showed very good results in all the aforementioned reactions. Due to time limitations the improved conditions were not evaluated in the synthesis of inhibitory fragments.

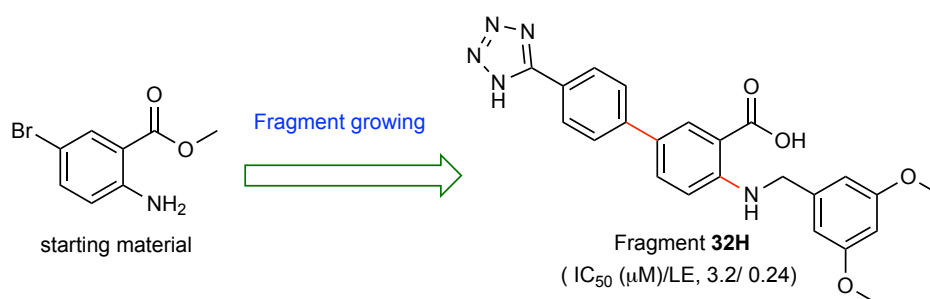
The work presented in the thesis could be a starting point towards the synthesis of inhibitors against VIM-2, OXA-48, and maybe other carbapenemases. The developed synthetic methods could also be applied in many other research projects where selective SMC and Pd-catalyzed carbonylation reactions are employed. The sustainability approach that we addressed in this work is a valuable approach to consider, while running organic chemical reactions. The promising results obtained with Pd-catalyzed carbonylations using sustainable solvents are very encouraging to be taken further and to be tested in many other chemical transformations. Therefore, our research recommends including sustainability considerations as a priority in the future studies. The addressed research points in paper I, II, III are of high interest for further development in order to answer the new research questions raised within this work.

8. Future direction

The ultimate goal of my thesis was to use fragment optimization approaches to improve previously identified fragments into drug like compounds with better binding affinity against carbapenemases VIM-2 & OXA-48. This goal is part of a larger goal to discover new inhibitors that can reach clinical trials and can be used in combination therapy with carbapenem in order to save the last resort antibiotic class carbapenems.

I focused on developing synthetic strategies to prepare 3,5-symmetrical and unsymmetrical disubstituted benzoic acids as extended fragments targeting OXA-48. These types of compounds were designed to reach the two identified binding sites. The future goal of this project is to further investigate the synthesis of the third fragment suggested by the merging approach **PI-41**.

In silico optimization study performed by Sundus Akhter suggested that growing the fragment in the 2-ortho position might favor binding in the inner binding pocket instead of pointing out to the solvent. Therefore, we intended to extend the fragments in the 2-ortho position instead of 3-meta position. I supervised a master student, Harald Magnussen, that was responsible of preparing a library of 2,5-disubstituted benzoic acids from methyl 2-amino-5-bromobenzoate. The synthesized fragment (Scheme 43, Fragment **32H**) was submitted for biological testing. The fragment showed comparable IC_{50} (3.275 μ M) to fragment **PI-40**. However, the LE of fragment **32** (0.24 kcal/(mol atom)) was slightly lower than fragment **PI-40** (0.27 kcal/(mol atom)). In the future a crystal structure of fragment/OXA-48 complex is a logical step in order to identify the binding modes of 2,5-disubstituted fragments assembled in fragment **32**.



Scheme 43. Fragment growing towards a drug like compound. Fragment **32H** was synthesized by Harald Magnussen.

In paper II, I developed a method to synthesize a range of sterically hindered 2-aryloxybenzoic acid derivatives from simple boronic acids via carbonylative SMC. Applying slow addition of boronic acid to the reaction is a promising approach to suppress the undesired direct SMC coupling. This work was continued in Paper III and the choice of the renewable solvents showed great impact on the tested Pd-catalyzed carbonylation reactions. Limonene showed good performance in carbonylative SMC and it favored the carbonylation product over the direct coupling product without applying the slow addition. In future work, it would be interesting to combine the findings of paper II and III - slow addition of boronic acid and the use of renewable solvent. The future goal regarding this project is to test carbonylative coupling to synthesize the challenging substrates, which contain functional groups such as phenols, amides, amines, and strong electron-withdrawing groups such as nitro, nitrile, which can allow for late stage functionalization.

9. Appendix

This chapter includes additional experimental procedures and spectral data for compounds not included in paper II and presented in Table 8, entry 1-7.

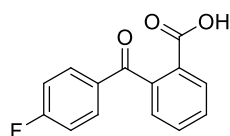
9.1 Experimental

9.1.1 General methods

All purchased chemicals were used as received without further purification. Solvents were dried according to standard procedures. Automated reverse-phase flash chromatography was performed using pre-packed C18-modified silica columns. The chemical shifts are reported in ppm relative to the solvent residual peak. NMR spectra were obtained on a 400 MHz Bruker Avance III HD equipped with a 5 mm SmartProbe BB/1H (BB = 19F, 31P-15N). Data are represented as follows: chemical shift, multiplicity (s = singlet, d = doublet, t = triplet, q = quartet, m = multiplet), coupling constant (J, Hz) and integration. Chemical shifts (δ) are reported in ppm relative to the residual solvent peak (CDCl₃: δ_H 7.26 and δ_C 77.16; Methanol-d₄: δ_H 3.31 and δ_C 49.00; Deuteriumoxide: δ_H 4.79; DMSO-d₆: δ_H 2.51 and δ_C 39.52). The raw data was analysed with MestReNova (Version 10.0.2-15465). Positive ion electrospray ionization mass spectrometry was conducted on a Thermo electron LTQ Orbitrap XL spectrometer. The data was analysed with Thermo Scientific Xcalibur software.

9.1.2 Experimental details

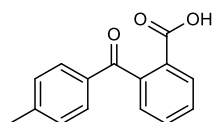
1- 2-(4-fluorobenzoyl)benzoic acid



Anhydrous AlCl₃ (91 mg, 0.68 mmol) was suspended in fluorobenzene (20 ml) before phthalic anhydride (50 mg, 0.34 mmol) was added in portions to the reaction mixture at 0 °C while stirring. Upon complete addition of the phthalic anhydride, the reaction mixture was submitted to reflux for 3h. The reaction was quenched by adding ice-cold HCl (50%, 100 mL). The reaction mixture was concentrated on a rotavapor. The precipitate was dissolved in sodium carbonate solution and then filtered. The resulted filtrate was acidified with aqueous HCl and

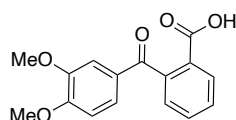
the solid product was filtered and submitted for further purification by reverse phase flash chromatography using 30% acetonitrile: H₂O. The pure product was obtained (50 mg, 60%) as a white powder. ¹H NMR (400 MHz, CDCl₃) δ 10.22 (bs, 1H), 8.09 (d, *J* = 7.6 Hz, 1H), 7.80 – 7.71 (m, 2H), 7.69-7.65 (m, 1H), 7.59-7.55 (m, 1H), 7.36 (d, *J* = 7.6 Hz, 1H), 7.08 (t, *J* = 8.6 Hz, 2H). ¹³C NMR (101 MHz, CDCl₃) δ 195.6, 170.9, 165.9 (d, *J* = 255.3 Hz), 142.4, 133.6 (d, *J* = 2.9 Hz), 133.5, 132.1 (d, *J* = 9.4 Hz), 131.1, 129.8, 127.8, 127.7, 115.9, 115.7, 77.5, 77.4, 77.2, 76.8. HRMS (ESI): Calcd. for C₁₄H₉FNaO₃ [M+H]⁺ 267.0428; found C₁₄H₉FNaO₃ 267.0428.

2- 2-(4-methylbenzoyl)benzoic acid^{226,227}



Anhydrous AlCl₃ (91 mg, 0.68 mmol) was suspended in toluene (20 ml) before phthalic anhydride (50 mg, 0.34 mmol) was added in portions to the reaction mixture at 0 °C while stirring. Upon complete addition of the phthalic anhydride, the reaction mixture was submitted to reflux for 3h-6h. The reaction was quenched by adding ice-cold HCl (50%, 100 mL). The reaction mixture was concentrated on a rotavapor. The precipitate was dissolved in sodium carbonate solution and then filtered. The resulted filtrate was acidified with aqueous HCl and the solid product was filtered and submitted for further purification by reverse phase flash chromatography. The pure product was obtained (71 mg, 87%) as a white powder. ¹H NMR (400 MHz, CDCl₃) δ 8.06 (d, *J* = 7.6 Hz, 1H), 7.66-7.62 (m, 3H), 7.54 (t, *J* = 7.6 Hz, 1H), 7.35 (d, *J* = 7.6 Hz, 1H), 7.20 (d, *J* = 7.8 Hz, 2H), 5.86 (bs, 1H), 2.39 (s, 3H). ¹³C NMR (101 MHz, CDCl₃) δ 170.4, 144.2, 142.9, 134.6, 133.1, 130.9, 129.7, 129.5, 129.3, 128.2, 127.7, 21.8. HRMS (ESI): Calcd. for C₁₅H₁₂NaO₃ [M+H]⁺ 263.0679; found C₁₅H₁₂NaO₃ 263.0680.

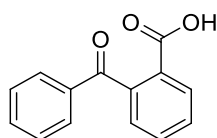
3- 2-(3,4-dimethoxybenzoyl)benzoic acid²²⁸



1,2-dimethoxybenzene (47 mg, 34 mmol) and phthalic anhydride (50 mg, 0.34 mmol) were added to a suspension of AlCl₃ (91 mg, 0.68 mmol) in DCM (20 ml) at 0 °C. The reaction was left stirring for 5h at rt. Upon reaction completion the reaction mixture was poured onto ice.

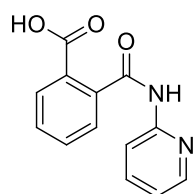
The organic layer was collected and dried over MgSO₄. The organic phase was concentrated on a rotavapor and the residue was triturated with diethyl ether. The product was submitted to reverse phase flash chromatography resulting in pure product (44 mg, 45%) as a yellowish solid. ¹H NMR (400 MHz, DMSO-d₆) δ 13.03 (s, 1H), 7.93 (d, *J* = 7.4 Hz, 1H), 7.72 – 7.54 (m, 2H), 7.35 (d, *J* = 12.3 Hz, 2H), 6.95 (s, 2H), 3.76 (s, 6H). ¹³C NMR (101 MHz, DMSO-d₆) δ 204.40, 176.45, 162.56, 158.23, 150.96, 141.65, 139.53, 139.38, 139.17, 139.02, 136.98, 134.22, 120.21, 119.60, 65.26, 64.95. HRMS (ESI): Calcd. for C₁₆H₁₄NaO₅ [M+H]⁺ 309.0739; found C₁₆H₁₅NaO₅ 309.0737.

4- 2-benzoylbenzoic acid^{226,227}



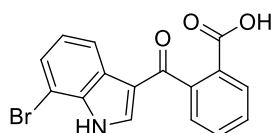
Anhydrous AlCl₃ (91 mg, 0.68 mmol) was suspended in benzene (20 ml) before phthalic anhydride (50 mg, 0.34 mmol) was added in portions to the reaction mixture at 0 °C while stirring. Upon complete addition of the phthalic anhydride, the reaction mixture was submitted to reflux for 5h. The reaction was quenched by adding ice-cold HCl (50%, 100 mL). The reaction mixture was concentrated on a rotavapor. The precipitated product was dissolved in sodium carbonate solution and then filtered. The resulted filtrate was acidified with aqueous HCl and the solid product was filtered. The pure product was collected without further purification (69 mg, 90%) as white powder. ¹H NMR (400 MHz, CDCl₃) δ 8.08 (d, *J* = 7.8 Hz, 1H), 7.72 (d, *J* = 7.6 Hz, 2H), 7.69-7.65 (m, 1H), 7.59-7.52 (m, 2H), 7.45-7.35 (m, 3H), 5.07 (bs, 1H). ¹³C NMR (101 MHz, CDCl₃) δ 197.5, 170.5, 143.0, 137.4, 133.6, 133.6, 131.3, 123.0, 129.9, 128.9, 128.4, 128.2, 77.8, 77.7, 77.5, 77.2. HRMS (ESI): Calcd. for C₁₄H₁₀NaO₃ [M+H]⁺ 249.0522; found C₁₄H₁₀NaO₃ 249.0527.

5- 2-(pyridin-2-ylcarbamoyl)benzoic acid²²⁹



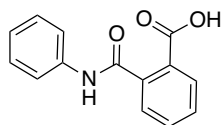
Phthalic anhydride (500 mg, 3.4 mmol) was added to the pyridine-2-amine (390 mg, 4.1 mmol) in DCM (20 mL) and the reaction mixture was left stirring for 18h at room temperature. The product was recrystallized in DCM, the pure product was obtained by vacuum filtration in (710 mg, 85%) yield. ^1H NMR (400 MHz, MeOD) δ 8.24-8.20 (m, 1H), 7.93-7.91 (m, 1H), 7.81-7.78 (m, 1H), 7.69-7.65 (m, 1H), 7.62-7.50 (m, 2H), 7.12-7.09 (m, 1H), 6.78 (d, $J = 8.7$ Hz, 1H), 6.70 (t, $J = 6.5$ Hz, 1H). ^{13}C NMR (101 MHz, MeOD) δ 158.6, 154.2, 147.8, 146.6, 144.7, 137.0, 136.2, 135.9, 133.9, 126.2, 121.2, 118.8, 118.0, 54.9, 54.6, 54.4, 54.2, 54.0, 53.7, 53.5. HRMS (ESI): Calcd. For $\text{C}_{13}\text{H}_{11}\text{O}_3\text{N}_2$ $[\text{M}+\text{H}]^+$ 243.0770; found $\text{C}_{13}\text{H}_{11}\text{O}_3\text{N}_2$ 243.0771.

6- 2-(7-bromo-1*H*-indole-3-carbonyl)benzoic acid



Anhydrous AlCl_3 (91 mg, 0.68 mmol) was suspended in DCM (20 ml) before phthalic anhydride (50 mg, 0.34 mmol) and 7-bromoindole (67 mg, 34 mmol) were added in portions to the reaction mixture at 0 °C while stirring. Upon complete addition of the phthalic anhydride, the reaction mixture was submitted to reflux for 6h. The reaction was quenched by adding ice-cold HCl (50%, 100 mL). The reaction mixture was concentrated on a rotavapor. The precipitated product was dissolved in sodium carbonate solution and then filtered. The resulted filtrate was acidified with aqueous HCl and extracted with EtOAc. The organic phase was collected, dried over Na_2SO_4 and concentrated on a rotavapor. The product was submitted for to reverse phase flash chromatography using 30-50% acetonitrile: H_2O . The pure product was obtained (78 mg, 67%) as a gummy solid. ^1H NMR (400 MHz, MeOD) δ 8.18 (d, $J = 7.9$ Hz, 1H), 8.05 (d, $J = 7.7$ Hz, 1H), 7.69 (t, $J = 7.5$ Hz, 1H), 7.62 (t, $J = 7.5$ Hz, 1H), 7.49 (d, $J = 7.4$ Hz, 1H), 7.44 (d, $J = 7.7$ Hz, 2H), 7.15 (t, $J = 7.8$ Hz, 1H). ^{13}C NMR (101 MHz, MeOD) δ 194.6, 169.5, 144.1, 137.1, 136.9, 133.1, 131.4, 130.6, 128.9, 127.2, 124.5, 122.2, 119.8, 105.9. HRMS (ESI): Calcd. for $\text{C}_{16}\text{H}_{10}\text{BrNNaO}_3$ $[\text{M}+\text{H}]^+$ 365.9742; found $\text{C}_{16}\text{H}_{10}\text{BrNNaO}_3$ 365.9744.

7- 2-(phenylcarbamoyl)benzoic acid²²⁹

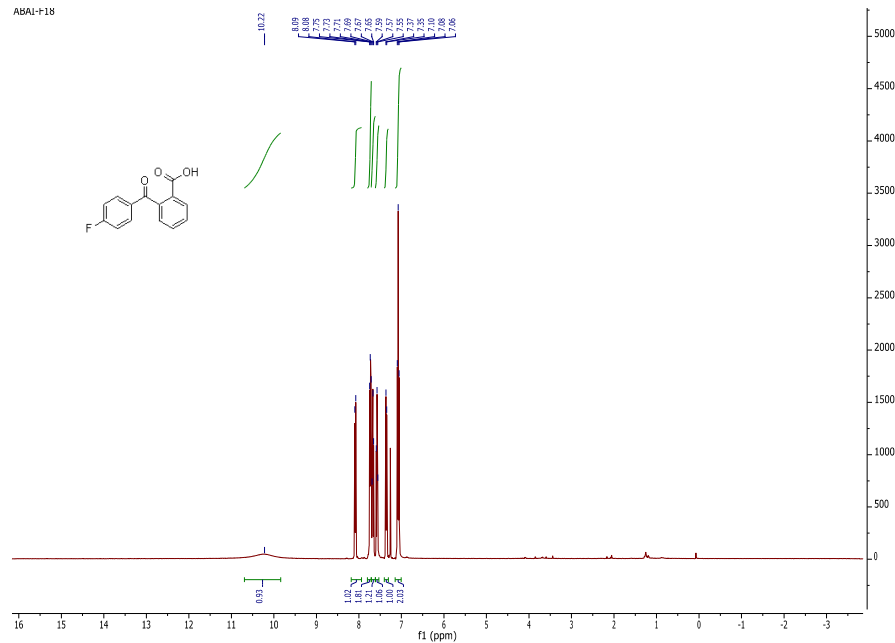


Phthalic anhydride (500 mg, 3.4 mmol) was added to the aniline (380 mg, 4.1 mmol) in DCM (20 mL) and the reaction mixture was left stirring for 6h at room temperature. The product was obtained by vacuum filtration. The precipitate was recrystallized in DCM-heptane mixture. The pure product was obtained (76 mg, 92%) a white solid. ¹H NMR (400 MHz, MeOD) δ 8.02 (d, *J* = 7.5 Hz, 1H), 7.65-7.63 (m, 3H), 7.57-7.55 (m, 2H), 7.33 (t, *J* = 7.7 Hz, 2H), 7.12 (m, 2H), 6.77-6.70 (m, 2H). ¹³C NMR (101 MHz, MeOD) δ 171.1, 169.3, 140.3, 140.1, 133.2, 131.4, 130.6, 130.1, 129.7, 128.8, 125.4, 121.7, 119.9, 117.1, 49.6, 5.4, 49.2, 49.0, 48.8, 48.6, 48.6. HRMS (ESI): Calcd. for C₁₄H₁₁NNaO₃ [M+H]⁺ 264.0628; found C₁₄H₁₁NNaO₃ 264.0637.

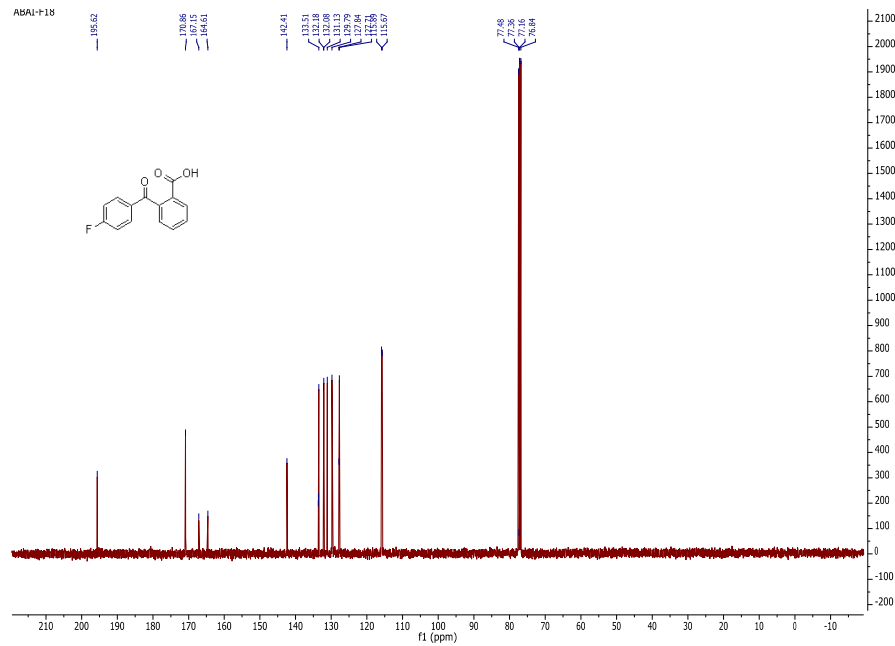
9.1.3 Spectral data

1-

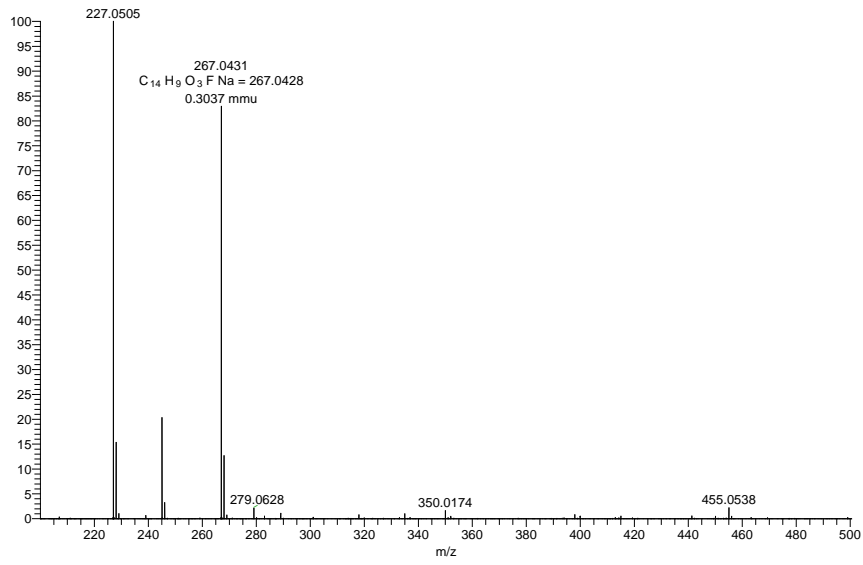
ABAI-F18



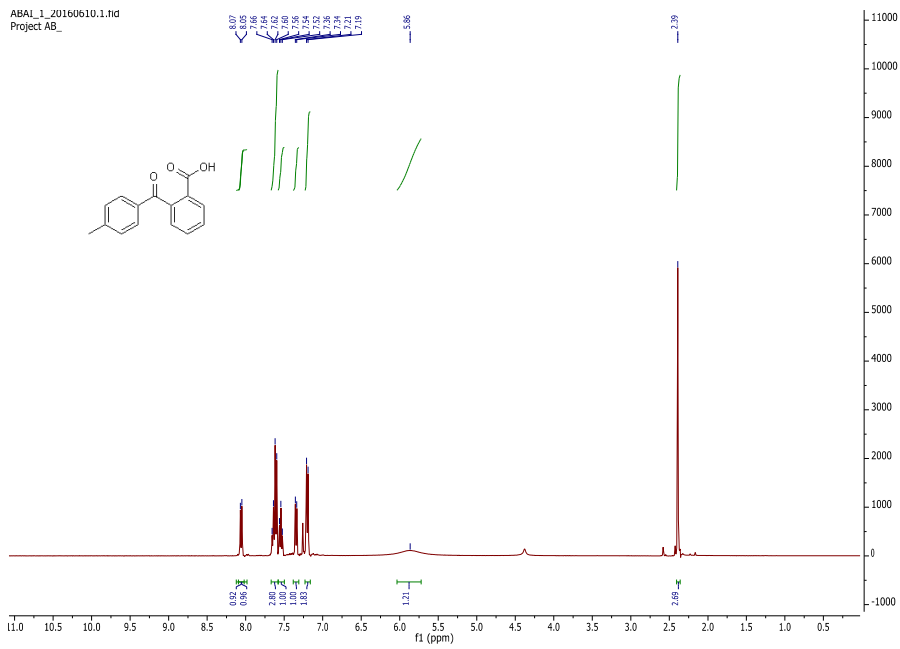
ABAI-F18



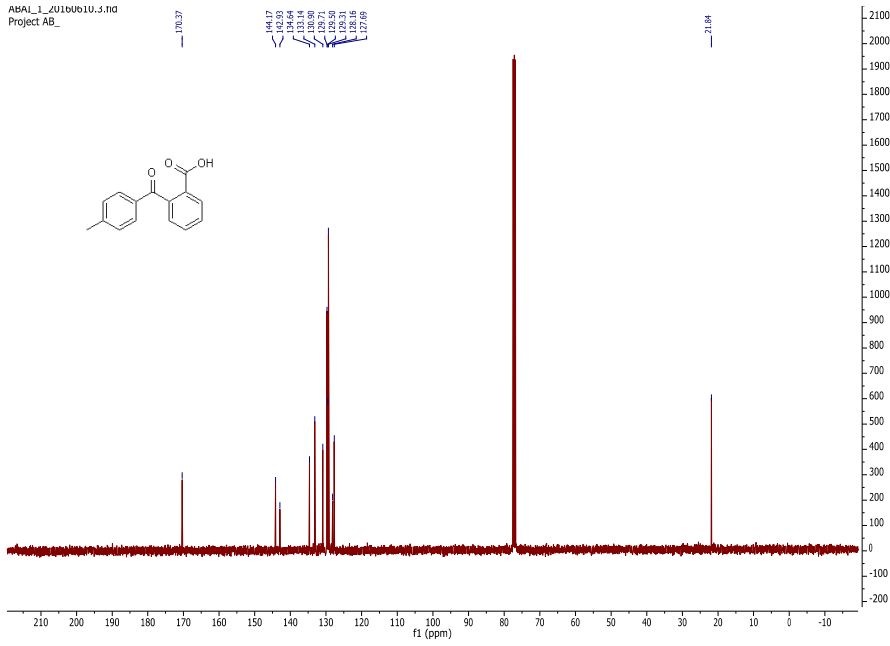
1-6D_180907162546 #1-5 RT: 0.00-0.11 AV: 5 NL: 7.16E
FTMS + p ESI Full ms [200.00-500.00]



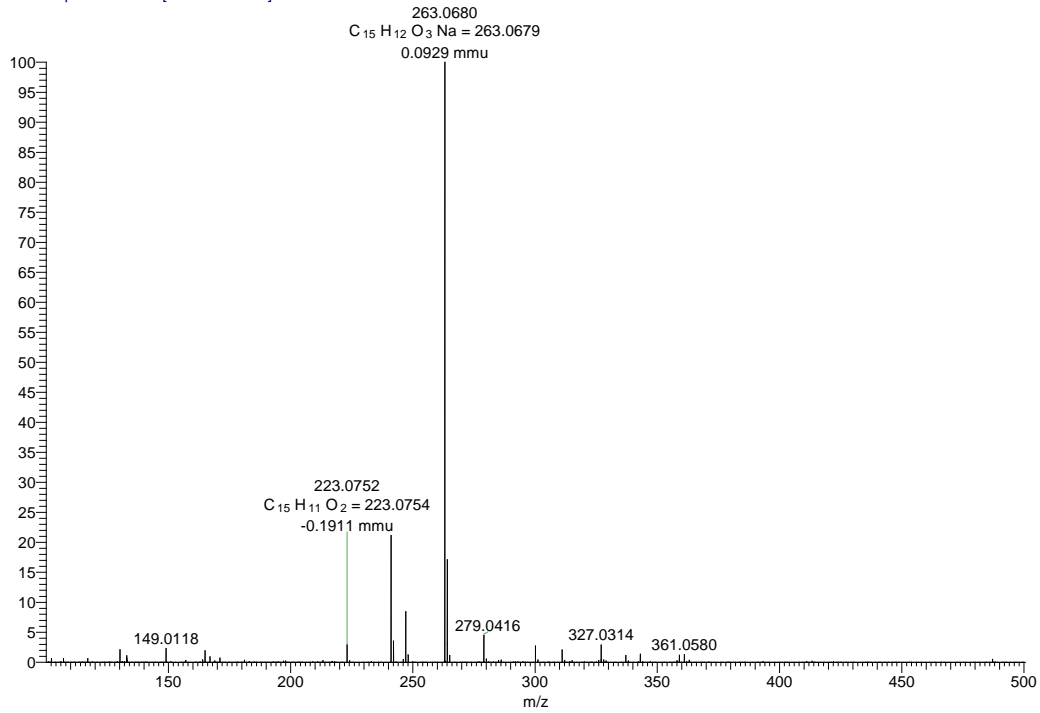
2-



ABAL_1_01180610.5.HD
Project AB_

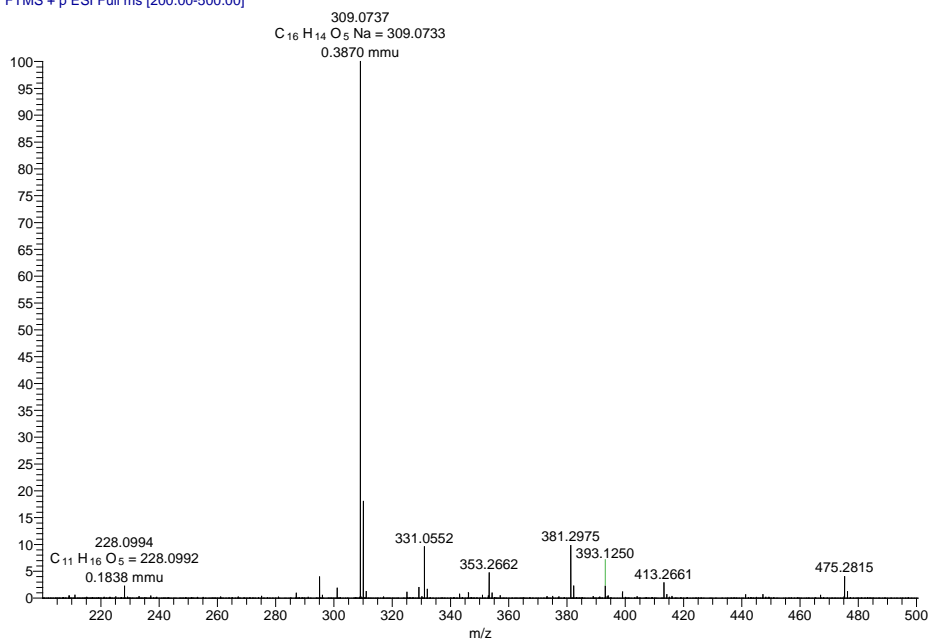


ABAL_1 #1-5 RT: 0.01-0.13 AV: 5 NL: 8.63E6
T: FTMS + p ESI Full ms [100.00-500.00]

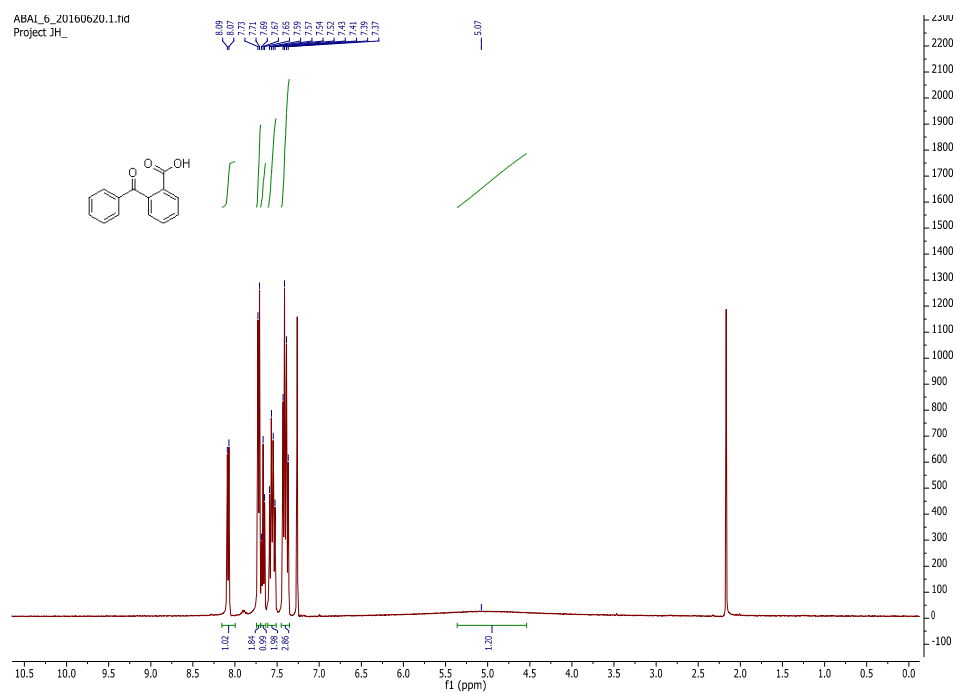


3-

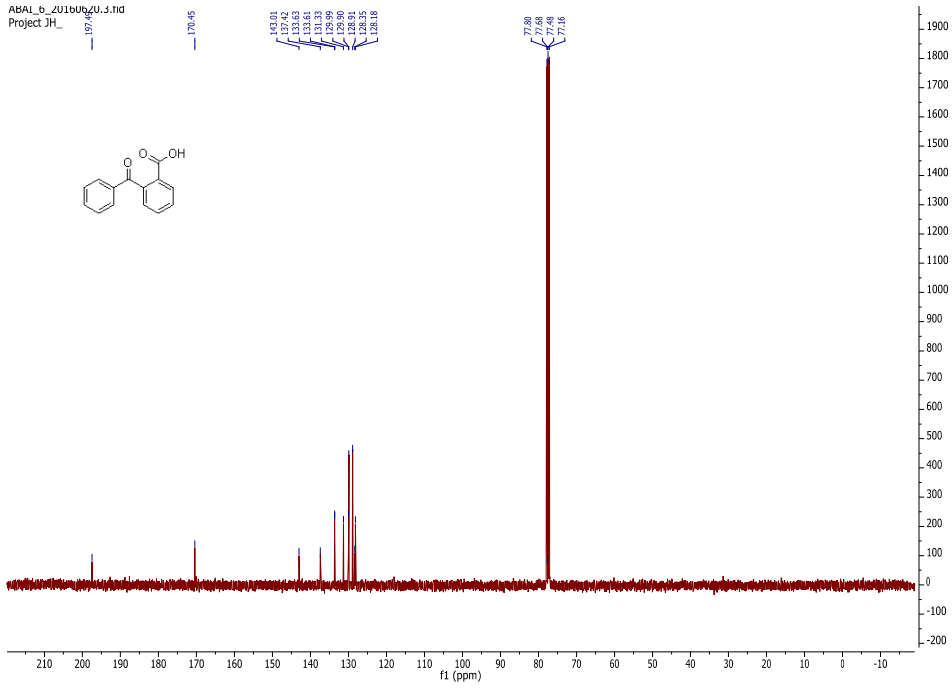
1,2 dimeth biotag 2 #1-5 RT: 0.01-0.12 AV: 5 NL: 5.54E6
T: FTMS + p ESI Full ms [200.00-500.00]



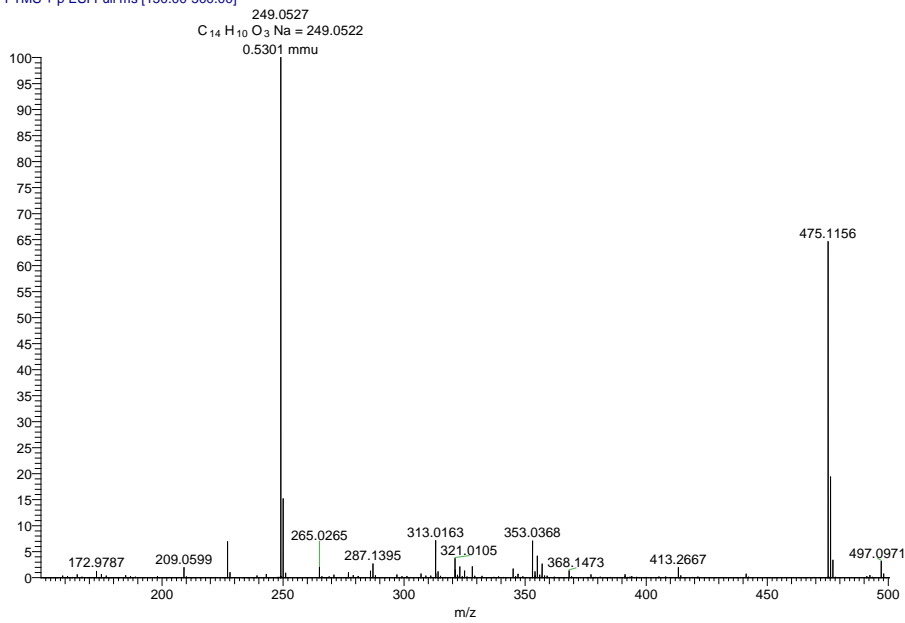
4-



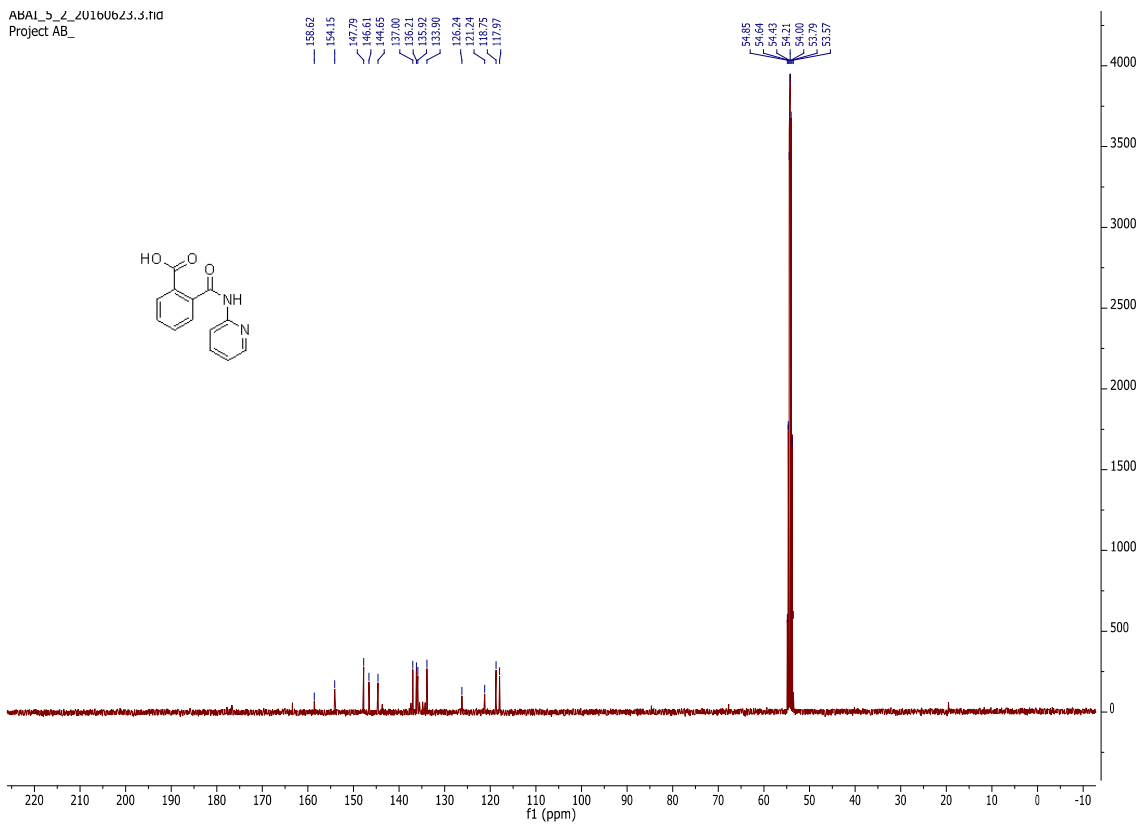
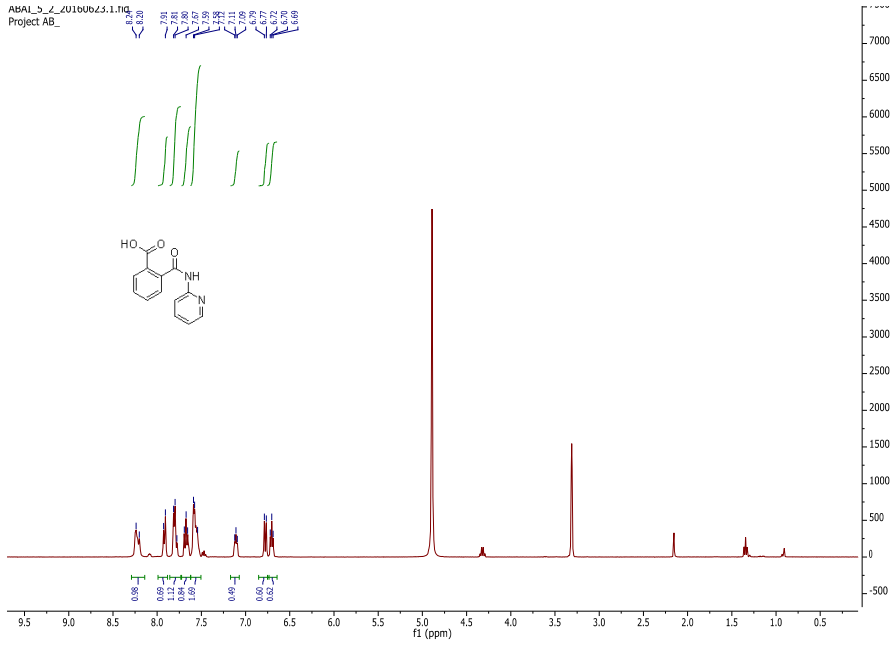
ABAL-6_ZU16UNU.5.HD
Project IH

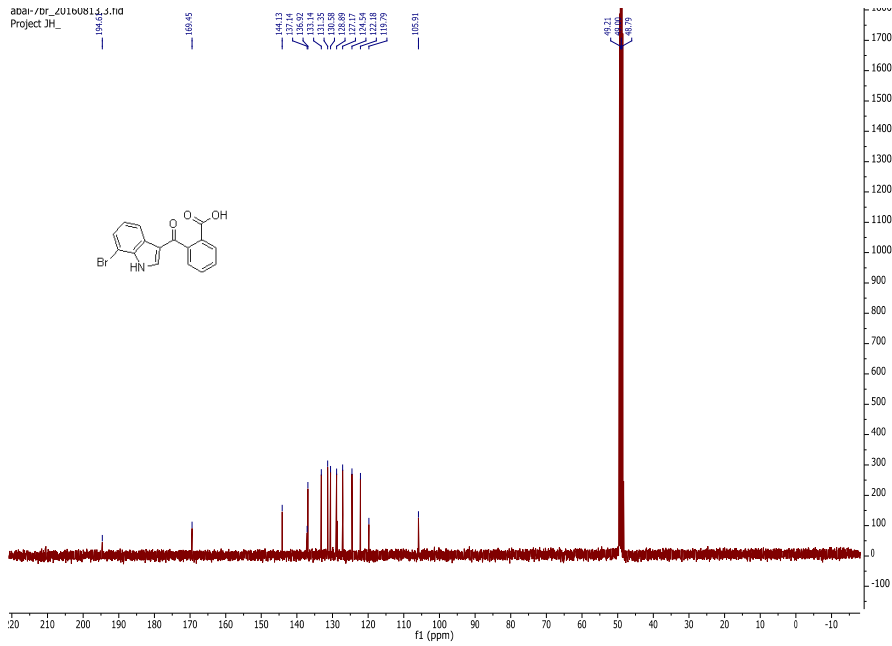


ABAI-1-6 #1-5 RT: 0.00-0.11 AV: 5 NL: 1.08E7
T: FTMS + p ESI Full ms [150.00-500.00]

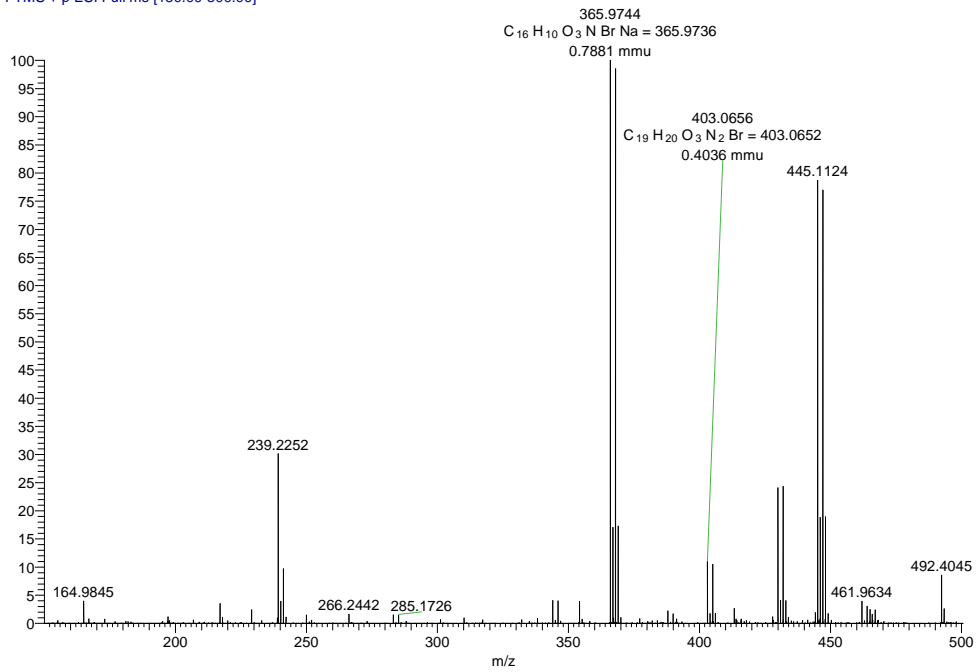


5-

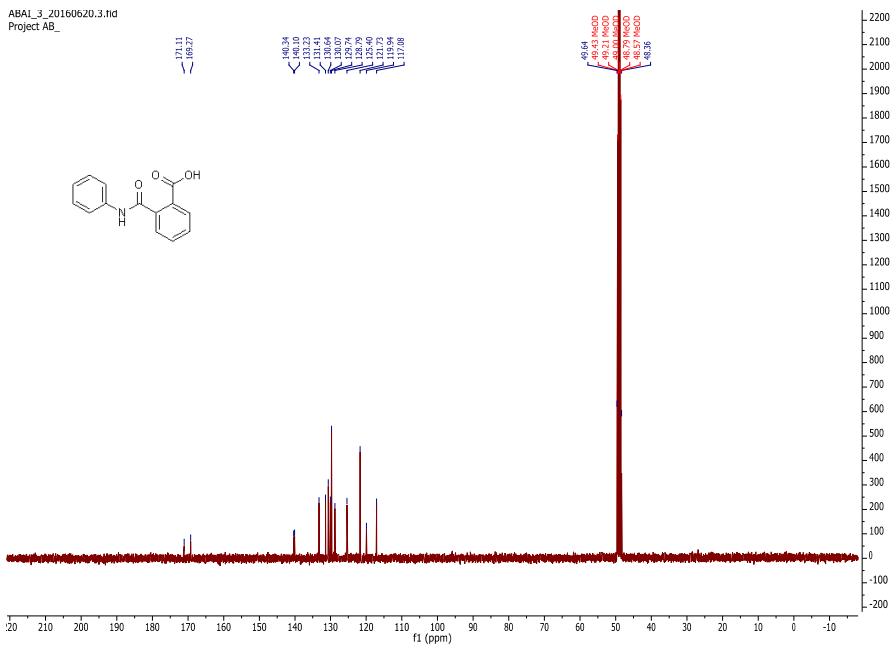
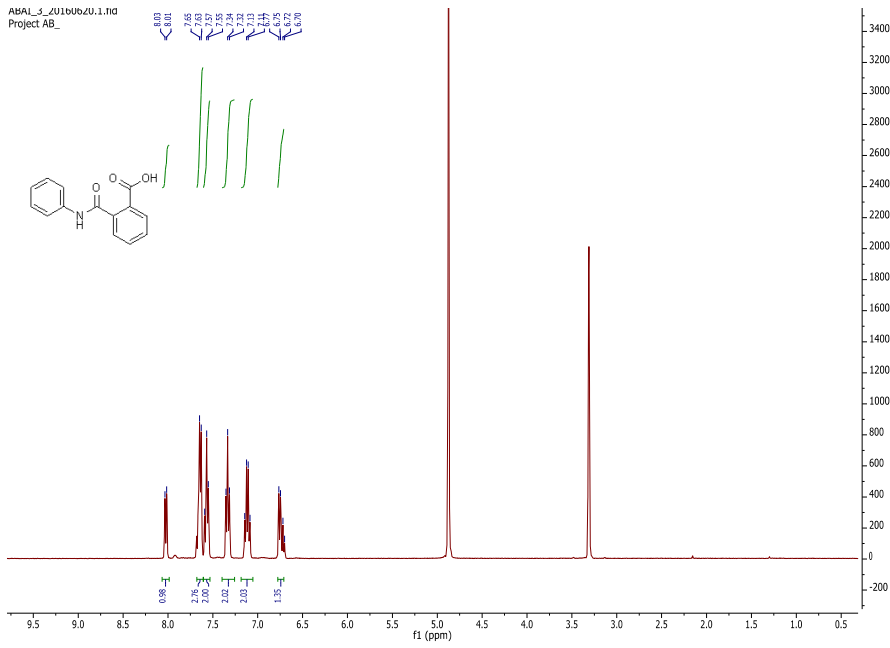




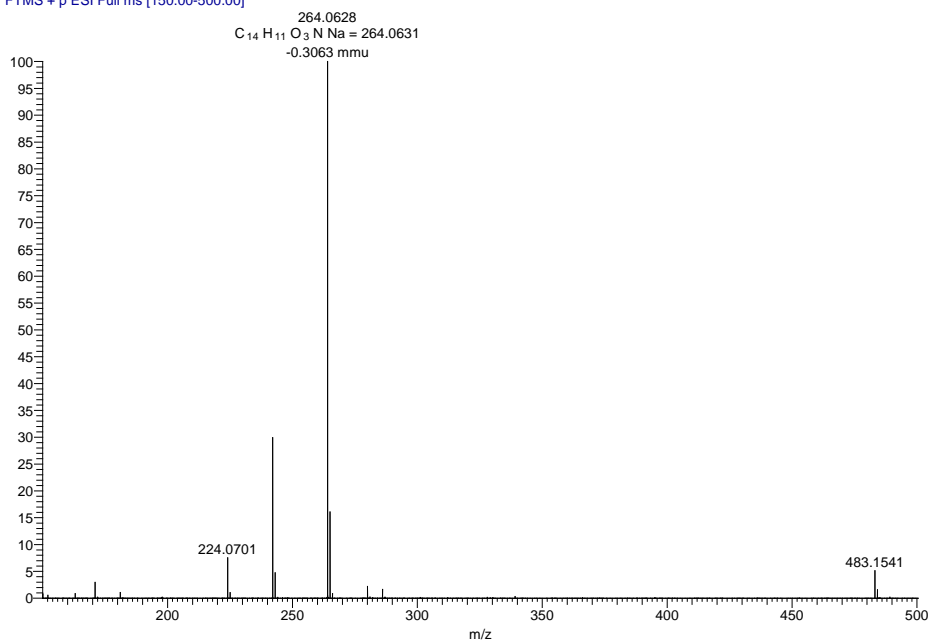
abai_9_7bro #1-5 RT: 0.01-0.12 AV: 5 NL: 3.84E6
T: FTMS + p ESI Full ms [150.00-500.00]



7-



anil test pow #1-5 RT: 0.01-0.16 AV: 5 NL: 1.02E6
T: FTMS + p ESI Full ms [150.00-500.00]



References

- (1) Bush, K.; Bradford, P. A. Interplay between β -Lactamases and New β -Lactamase Inhibitors. *Nat. Rev. Microbiol.* **2019**, 17, 295-306.
<https://doi.org/10.1038/s41579-019-0159-8>
- (2) World Health Organization, (2020). Fact sheet for antibiotic resistance. Available at:
<https://www.who.int/news-room/fact-sheets/detail/antibiotic-resistance>.
[Accessed July 2020]
- (3) Palzkill, T. Metallo- β -Lactamase Structure and Function. *Ann. N. Y. Acad. Sci.* **2013**, 1277 (1), 91-104.
<https://doi.org/10.1111/j.1749-6632.2012.06796.x>
- (4) González, M. M.; Vila, A. J. (2017) An Elusive Task: A Clinically Useful Inhibitor of Metallo- β -Lactamases. In *Topics in Medicinal Chemistry*; Springer Verlag.
https://doi.org/10.1007/7355_2016_6
- (5) Bush, K.; Jacoby, G. A.; Medeiros, A. A. A Functional Classification Scheme for β -Lactamases and Its Correlation with Molecular Structure. *Antimicrob. Agents Chemother.* **1995**, 39 (6) 1211-1233.
<https://doi.org/10.1128/AAC.39.6.1211>
- (6) Drawz, S. M.; Bonomo, R. A. Three Decades of β -Lactamase Inhibitors. *Clin. Microbiol. Rev.* **2010**, 23 (1) 160-201.
<https://doi.org/10.1128/CMR.00037-09>
- (7) Walsh, T. R.; Toleman, M. A.; Poirel, L.; Nordmann, P. Metallo- β -Lactamases: The Quiet before the Storm? *Clin. Microbiol. Rev.* **2005**, 18 (2) 306-325.
<https://doi.org/10.1128/CMR.18.2.306-325.2005>
- (8) Majiduddin, F. K.; Materon, I. C.; Palzkill, T. G. Molecular Analysis of Beta-Lactamase Structure and Function. *Int. J. Med. Microbiol.* **2002**, 292 (2), 127-137.
<https://doi.org/10.1078/1438-4221-00198>
- (9) Levy, S. B.; Bonnie, M. Antibacterial Resistance Worldwide: Causes, Challenges and Responses. *Nat. Med.* **2004**, 10, S122–S129.
<https://doi.org/10.1038/nm1145>
- (10) Somboro, A. M.; Tiwari, D.; Bester, L. A.; Parboosing, R.; Chonco, L.; Kruger, H. G.; Arvidsson, P. I.; Govender, T.; Naicker, T.; Essack, S. Y. NOTA: A Potent Metallo- β -Lactamase Inhibitor. *J. Antimicrob. Chemother.* **2015**, 70 (5), 1594-1596.
<https://doi.org/10.1093/jac/dku538>

- (11) Nukaga, M.; Bethel, C. R.; Thomson, J. M.; Hujer, A. M.; Distler, A.; Anderson, V. E.; Knox, J. R.; Bonomo, R. A. Inhibition of Class a β -Lactamases by Carbapenems: Crystallographic Observation of Two Conformations of Meropenem in SHV-1. *J. Am. Chem. Soc.* **2008**, 130 (38), 12656-12662.
<https://doi.org/10.1021/ja7111146>
- (12) Akhter, S.; Lund, B. A.; Ismael, A.; Langer, M.; Isaksson, J.; Christopeit, T.; Leiros, H.-K. S.; Bayer, A. A Focused Fragment Library Targeting the Antibiotic Resistance Enzyme - Oxacillinase-48: Synthesis, Structural Evaluation and Inhibitor Design. *Eur. J. Med. Chem.* **2017**, 135, 159-173.
<https://doi.org/10.1016/j.ejmech.2017.04.035>
- (13) Christopeit, T.; Carlsen, T. J. O.; Helland, R.; Leiros, H. K. S. Discovery of Novel Inhibitor Scaffolds against the Metallo- β -Lactamase VIM-2 by Surface Plasmon Resonance (SPR) Based Fragment Screening. *J. Med. Chem.* **2015**, 58 (21), 8671-8682.
<https://doi.org/10.1021/acs.jmedchem.5b01289>
- (14) Christopeit, T.; Leiros, H. K. S. Fragment-Based Discovery of Inhibitor Scaffolds Targeting the Metallo- β -Lactamases NDM-1 and VIM-2. *Bioorganic Med. Chem. Lett.* **2016**, 26 (8), 1973-1977. <https://doi.org/10.1016/j.bmcl.2016.03.004>
- (15) Lund, B. A.; Christopeit, T.; Guttormsen, Y.; Bayer, A.; Leiros, H. K. S. Screening and Design of Inhibitor Scaffolds for the Antibiotic Resistance Oxacillinase-48 (OXA-48) through Surface Plasmon Resonance Screening. *J. Med. Chem.* **2016**, 59 (11), 5542–5554. <https://doi.org/10.1021/acs.jmedchem.6b00660>.
- (16) Walsh, C. Molecular Mechanisms That Confer Antibacterial Drug Resistance. *Nature* **2000**, 406, 775-781. <https://doi.org/10.1038/35021219>
- (17) Davies J.; Davies D. Origins and Evolution of Antibiotic Resistance. *Microbiol. Mol. Biol. Rev.* **2010**, 74 (3), 417-433. <https://doi.org/10.1128/membr.00016-10>
- (18) Blair, J. M. A.; Webber, M. A.; Baylay, A. J.; Ogbolu, D. O.; Piddock, L. J. V. Molecular Mechanisms of Antibiotic Resistance. *Nat. Rev. Microbiol.* **2015**, 13, 42-51.
<https://doi.org/10.1038/nrmicro3380>
- (19) Sykes, R. The 2009 Garrod Lecture: The Evolution of Antimicrobial Resistance: A Darwinian Perspective. *J. Antimicro. Chemother.* **2010**, 65 (9), 1842-1852.
<https://doi.org/10.1093/jac/dkq217>
- (20) Bush, K. The Coming of Age of Antibiotics: Discovery and Therapeutic Value. *Ann. N. Y. Acad. Sci.* **2010**, 1213 (1), 1-4. <https://doi.org/10.1111/j.1749-6632.2010.05872.x>

- (21) Kardos, N., Demain, A.L. Penicillin: the medicine with the greatest impact on therapeutic outcomes. *Appl. Microbiol. Biotechnol.* **2011**, 92, 677-687.
<https://doi.org/10.1007/s00253-011-3587-6>
- (22) Patric, G.L. (2013) An Introduction to Medicinal Chemistry, 3rd ed. Oxford: Oxford University Press, 2005. [Accessed July 2020]
- (23) DePestel, D. D.; Benninger, M. S.; Danziger, L.; LaPlante, K. L.; May, C.; Luskin, A.; Pichichero, M.; Hadley, J. A. Cephalosporin Use in Treatment of Patients with Penicillin Allergies. *J. Am. Pharm. Assoc.* **2008**, 48 (4), 530-540.
<https://doi.org/10.1331/JAPhA.2008.07006>
- (24) Chaudhry, S. B.; Veve, M. P.; Wagner, J. L. Cephalosporins: A Focus on Side Chains and β -Lactam Cross-Reactivity. *Pharmacy* **2019**, 7 (3), 103.
<https://doi.org/10.3390/pharmacy7030103>
- (25) Werth, B.J. (2020) Cephalosporins. Available at:
<https://www.merckmanuals.com/professional/infectious-diseases/bacteria-and-antibacterial-drugs/cephalosporins>. [Accessed August 2020]
- (26) Chahine, E. B.; Nornoo, A. O. Ceftobiprole: The First Broad-Spectrum Antimethicillin-Resistant Staphylococcus Aureus Beta-Lactam. *J. Exp. Clin. Med.* **2011**, 3 (1), 9-16.
<https://doi.org/10.1016/j.jecm.2010.12.007>
- (27) Zhanel, G. G.; Sniezek, G.; Schweizer, F.; Zelenitsky, S.; Lagacé-Wiens, P. R. S.; Rubinstein, E.; Gin, A. S.; Hoban, D. J.; Karlowsky, J. A. Ceftaroline: A Novel Broad-Spectrum Cephalosporin with Activity against Methicillin-Resistant Staphylococcus Aureus. *Drugs* **2009**, 69, 809-831. <https://doi.org/10.2165/00003495-200969070-00003>
- (28) Wu, J. Y.; Srinivas, P.; Pogue, J. M. Cefiderocol: A Novel Agent for the Management of Multidrug-Resistant Gram-Negative Organisms. *Infect. Dis. Ther.* **2020**, 9, 17-40.
<https://doi.org/10.1007/s40121-020-00286-6>
- (29) Shlaes, D. M. New β -lactam- β -lactamase inhibitor combinations in clinical development. *Ann. N. Y. Acad. Sci.* **2013**, 1277, 105-114.
<https://doi.org/10.1111/nyas.12010>
- (30) Fuchs, P. C.; Jones, R. N.; Barry, A. L.; Ayers, L. W.; Gerlach, E. H.; Allen, S. D.; Pfaller, M. In Vitro Antimicrobial Activity of Tigemonam, a New Orally Administered Monobactam. *Antimicrob. Agents Chemother.* **1988**, 32 (3), 346-349.
<https://doi.org/10.1128/AAC.32.3.346>
- (31) Krisztina M. Papp-Wallace, Andrea Endimiani, Magdalena A. Taracila, Robert A.

- Bonomo. *Antimicro. Agents Chemother.* **2011**, 55 (11) 4943-4960.
<https://doi.org/10.1128/AAC.00296-11>
- (32) González-Bello, C. Antibiotic Adjuvants - A Strategy to Unlock Bacterial Resistance to Antibiotics. *Bioorg. Med. Chem. Lett.* **2017**, 27 (18), 4221-4228.
<https://doi.org/10.1016/j.bmcl.2017.08.027>
- (33) Stein, G. E. Antimicrobial Resistance in the Hospital Setting: Impact, Trends, and Infection Control Measures. *Pharmacotherapy* **2005**, 25, 44S-54S.
<https://doi.org/10.1592/phco.2005.25.10part2.44S>
- (34) Kumar, A.; Schweizer, H. P. Bacterial Resistance to Antibiotics: Active Efflux and Reduced Uptake. *Adv. Drug Deliv. Rev.* **2005**, 57, 1486-1513.
<https://doi.org/10.1016/j.addr.2005.04.004>
- (35) Spratt, B. G. Resistance to Antibiotics Mediated by Target Alterations. *Science* **1994**, 264 (5157), 388-393. <https://doi.org/10.1126/science.8153626>
- (36) Fisher, J. F.; Meroueh, S. O.; Mobashery, S. Bacterial Resistance to β -Lactam Antibiotics: Compelling Opportunism, Compelling Opportunity. *Chem. Rev.* **2005**, 105, 395-424. <https://doi.org/10.1021/cr030102i>
- (37) Matagne, A.; Lamotte-Brasseur, J.; Frère, J. M. Catalytic Properties of Class A β -Lactamases: Efficiency and Diversity. *Biochem. J.* **1998**, 332 (2), 581-598.
<https://doi.org/10.1042/bj3300581>
- (38) LK, S. Antibiotics: Action and Resistance in Gram-Negative Bacteria. *J. Microbiol. Immunol. Infect.* **2002**, 35 (1), 1-11. <https://pubmed.ncbi.nlm.nih.gov/11950113>
- (39) Essack, S. Y. The Development of β -Lactam Antibiotics in Response to the Evolution of β -Lactamases. *Phar. Res.* **2001**, 18, 1391-1399.
<https://doi.org/10.1023/A:1012272403776>
- (40) Livermore, D. M. β -Lactamases in Laboratory and Clinical Resistance. *Clin. Microbiol. Rev.* **1995**, 8(4), 557-58. <https://www.ncbi.nlm.nih.gov/pmc/articles/PMC172876>
- (41) Naas, T.; Oueslati, S.; Bonnin, R. A.; Dabos, M. L.; Zavala, A.; Dortet, L.; Retailleau, P.; Iorga, B. I. Beta-Lactamase Database (BLDB)–Structure and Function. *J. Enzyme Inhib. Med. Chem.* **2017**, 32 (1), 917-919.
<https://doi.org/10.1080/14756366.2017.1344235>
- (42) bldb. Beta-Lactamase DataBase, (2020) Structure and Function.
Available at: <http://bldb.eu/>. [Accessed August 2020]
- (43) Bush, K.; Jacoby, G. A. Updated Functional Classification of β -Lactamases. *Antimicrob.*

- Agents Chemother.* **2010**, 54 (3), 969-976. <https://doi.org/10.1128/AAC.01009-09>
- (44) Bush, K. The ABCD's of β -Lactamase Nomenclature. *J. Infect. and Chemother.* **2013**, 19 (4), 549-559. <https://doi.org/10.1007/s10156-013-0640-7>
- (45) Ambler, R. P. The Structure of Beta-Lactamases. *Philos. Trans. R. Soc. Lond. B. Biol. Sci.* **1980**, 289 (1036), 321-331. <https://doi.org/10.1098/rstb.1980.0049>
- (46) Mover, E.; Wu, Y.; Lambeau, G.; Kahn, F.; Touqui, L.; Areschoug, T. Using Patient Pathways to Accelerate the Drive to Ending Tuberculosis. *J. Infect. Dis.* **2013**, 208 (12), 2025-2035. <https://doi.org/10.1093/INFDIS>
- (47) Paton, R.; Miles, R. S.; Hood, J.; Amyes, S. G. B.; Miles, R. S.; Amyes, S. G. B. ARI 1: β -Lactamase-Mediated Imipenem Resistance in *Acinetobacter Baumannii*. *Int. J. Antimicrob. Agents* **1993**, 2 (2), 81-87. [https://doi.org/10.1016/0924-8579\(93\)90045-7](https://doi.org/10.1016/0924-8579(93)90045-7)
- (48) Bebrone, C.; Lassaux, P.; Vercheval, L.; Sohier, J. S.; Jehaes, A.; Sauvage, E.; Galleni, M. Current Challenges in Antimicrobial Chemotherapy: Focus on β -Lactamase Inhibition. *Drugs* **2010**, 70, 651-679. <https://doi.org/10.2165/11318430-000000000-00000>
- (49) Vercheval, L.; Bauvois, C.; Di Paolo, A.; Borel, F.; Ferrer, J.-L.; Sauvage, E.; Matagne, A.; Frère, J.-M.; Frère, F.; Charlier, P.; Galleni, M.; Kerff, F. Three Factors That Modulate the Activity of Class D β -Lactamases and Interfere with the Post-Translational Carboxylation of Lys 70. *Biochem. J.* **2010**, 432, 495-504. <https://doi.org/10.1042/BJ20101122>
- (50) Brem, J.; Cain, R.; Cahill, S.; McDonough, M. A.; Clifton, I. J.; Jiménez-Castellanos, J. C.; Avison, M. B.; Spencer, J.; Fishwick, C. W. G.; Schofield, C. J. Structural Basis of Metallo- β -Lactamase, Serine- β -Lactamase and Penicillin-Binding Protein Inhibition by Cyclic Boronates. *Nat. Commun.* **2016**, 7, 12406. <https://doi.org/10.1038/ncomms12406>
- (51) Bebrone, C. Metallo- β -Lactamases (Classification, Activity, Genetic Organization, Structure, Zinc Coordination) and Their Superfamily. *Biochem. Pharmacol.* **2007**, 74 (12), 1686-1701. <https://doi.org/10.1016/j.bcp.2007.05.021>
- (52) Ganta, S. R.; Perumal, S.; Pagadala, S. R. R.; Samuelsen, Ø.; Spencer, J.; Pratt, R. F.; Buynak, J. D. Approaches to the Simultaneous Inactivation of Metallo- and Serine- β -Lactamases. *Bioorganic Med. Chem. Lett.* **2009**, 19 (6), 1618-1622. <https://doi.org/10.1016/j.bmcl.2009.02.018>
- (53) Hinchliffe, P.; González, M. M.; Mojica, M. F.; González, J. M.; Castillo, V.; Saiz, C.; Kosmopoulou, M.; Tooke, C. L.; Llarrull, L. I.; Mahler, G.; Bonomo, R. A.; Vila, A. J.;

- Spencer, J. Cross-Class Metallo- β -Lactamase Inhibition by Bisthiazolidines Reveals Multiple Binding Modes. *Proc. Natl. Acad. Sci. U. S. A.* **2016**, 113 (26), E3745-E3754. <https://doi.org/10.1073/pnas.1601368113>
- (54) Fabiane, S. M.; Sohi, M. K.; Wan, T.; Payne, D. J.; Bateson, J. H.; Mitchell, T.; Sutton, B. J. Crystal Structure of the Zinc-Dependent β -Lactamase from *Bacillus Cereus* at 1.9 Å Resolution: Binuclear Active Site with Features of a Mononuclear Enzyme. *Biochemistry* **1998**, 37 (36), 12404-12411. <https://doi.org/10.1021/bi980506i>
- (55) Das, C. K.; Nair, N. N. Hydrolysis of Cephalexin and Meropenem by New Delhi Metallo- β -Lactamase: The Substrate Protonation Mechanism Is Drug Dependent. *Phys. Chem. Chem. Phys.* **2017**, 19 (20), 13111-13121. <https://doi.org/10.1039/c6cp08769h>
- (56) Tripathi, R.; Nair, N. N. Mechanism of Meropenem Hydrolysis by New Delhi Metallo β -Lactamase. *ACS Catal.* **2015**, 5 (4), 2577-2586. <https://doi.org/10.1021/acscatal.5b00242>
- (57) Zhang, gMin; Hao, Q. Crystal Structure of NDM-1 Reveals a Common β -lactam Hydrolysis Mechanism. *FASEB J.* **2011**, 25 (8), 2574-2582. <https://doi.org/10.1096/fj.11-184036>
- (58) Park, H.; Brothers, E. N.; Merz, K. M. Hybrid QM/MM and DFT Investigations of the Catalytic Mechanism and Inhibition of the Dinuclear Zinc Metallo- β -Lactamase CcrA from *Bacteroides Fragilis*. *J. Am. Chem. Soc.* **2005**, 127 (12), 4232-4241. <https://doi.org/10.1021/ja042607b>
- (59) Aghamali, M.; Zahedi Bialvaei, A.; Aghazadeh, M.; Asgharzadeh, M.; Samadi Kafil, H. Carbapenemase Inhibitors. *Rev. Med. Microbiol.* **2017**, 28 (3), 104-113. <https://doi.org/10.1097/MRM.0000000000000106>
- (60) Tooke, C. L.; Hinchliffe, P.; Bragginton, E. C.; Colenso, C. K.; Hirvonen, V. H. A.; Takebayashi, Y.; Spencer, J. β -Lactamases and β -Lactamase Inhibitors in the 21st Century. *J. Mol. Bio.* **2019**, 431 (18), 3472-3500. <https://doi.org/10.1016/j.jmb.2019.04.002>
- (61) Bush, K.; Bradford, P. A. β -Lactams and β -Lactamase Inhibitors: An Overview. *CSH. Perspect. Med.* **2016**, 6 (8). <https://doi.org/10.1101/cshperspect.a025247>
- (62) MedChemExpress. (2020) Taniborbactam (VNRX-5133). Available at: <https://www.medchemexpress.com/Taniborbactam.html>. [Accessed July 2020]
- (63) Liu B.; Trout R. E. L.; Chu G.-H.; McGarry D.; Jackson R. W.; Hamirick J. C.; Daigle

- D. M.; Cusick S. M.; Pozzi C.; De Luca F.; Benvenuti M.; Mangani S.; Docquier J. D.; Weiss W. J.; Pevear D. C.; Xerri L.; Burns C. J. Discovery of Taniborbactam (VNRX-5133): A Broad-Spectrum Serine- And Metallo- β -Lactamase Inhibitor for Carbapenem-Resistant Bacterial Infections. *J. Med. Chem.* **2020**, 63 (6), 2789-2801.
<https://doi.org/10.1021/ACS.JMEDCHEM.9B01518>
- (64) Krajnc A.; Brem J.; Hinchliffe P.; Calvopiña K.; Panduwawala T. D.; Lang P.A.; Kamps J. J. A. G.; Tyrrell J. M.; Widlake E.; Seward B. S.; Walsh T. R.; Spencer J.; and Schofield C. J.; Bicyclic Boronate VNRX-5133 Inhibits Metallo- And Serine- β -Lactamases. *J. Med. Chem.* **2019**, 62 (18), 8544-8556.
<https://doi.org/10.1021/ACS.JMEDCHEM.9B00911>
- (65) Aoki, N.; Ishii, Y.; Tateda, K.; Saga, T.; Kimura, S.; Kikuchi, Y.; Kobayashi, T.; Tanabe, Y.; Tsukada, H.; Gejyo, F.; Yamaguchi, K. Efficacy of Calcium-EDTA as an Inhibitor for Metallo- β -Lactamase in a Mouse Model of Pseudomonas Aeruginosa Pneumonia. *Antimicrob. Agents Chemother.* **2010**, 54 (11), 4582-4588.
<https://doi.org/10.1128/AAC.00511-10>
- (66) Samuelsen, Ø.; Åstrand, O. A. H.; Fröhlich, C.; Heikal, A.; Skagseth, S.; Carlsen, T. J. O.; Leiros, H. K. S.; Bayer, A.; Schnaars, C.; Kildahl-Andersen, G.; Lauksund, S.; Finke, S.; Huber, S.; Gjøen, T.; Andresen, A. M. S.; Økstad, O. A.; Rongved, P. Zn148 Is a Modular Synthetic Metallo- β -Lactamase Inhibitor That Reverses Carbapenem Resistance in Gram-Negative Pathogens in Vivo. *Antimicrob. Agents Chemother.* **2020**, 64 (6). e02415-19. <https://doi.org/10.1128/AAC.02415-19>
- (67) Bush, K. A Resurgence of β -Lactamase Inhibitor Combinations Effective against Multidrug-Resistant Gram-Negative Pathogens. *Int. J. Antimicrob. Agents* **2015**, 46 (5), 483-493.
<https://doi.org/10.1016/j.ijantimicag.2015.08.011>
- (68) Kurosaki, H.; Yamaguchi, Y.; Higashi, T.; Soga, K.; Matsueda, S.; Yumoto, H.; Misumi, S.; Yamagata, Y.; Arakawa, Y.; Goto, M. Irreversible Inhibition of Metallo- β -Lactamase (IMP-1) by 3-(3-Mercaptopropionylsulfanyl)Propionic Acid Pentafluorophenyl Ester. *Angew. Chemie. Int. Ed.* **2005**, 44 (25), 3861-3864.
<https://doi.org/10.1002/anie.200500835>
- (69) King, D. T.; Worrall, L. J.; Gruninger, R.; Strynadka, N. C. J. New Delhi Metallo- β -Lactamase: Structural Insights into β -Lactam Recognition and Inhibition. *J. Am. Chem. Soc.* **2012**, 134 (28), 11362-11365. <https://doi.org/10.1021/ja303579d>

- (70) Li, N.; Xu, Y.; Xia, Q.; Bai, C.; Wang, T.; Wang, L.; He, D.; Xie, N.; Li, L.; Wang, J.; Zhou, H. G.; Xu, F.; Yang, C.; Zhang, Q.; Yin, Z.; Guo, Y.; Chen, Y. Simplified Captopril Analogues as NDM-1 Inhibitors. *Bioorg. Med. Chem. Lett.* **2014**, 24 (1), 386-389. <https://doi.org/10.1016/j.bmcl.2013.10.068>
- (71) Heinz, U.; Bauer, R.; Wommer, S.; Meyer-Klaucke, W.; Papamichaels, C.; Bateson, J.; Adolph, H. W. Coordination Geometries of Metal Ions in D- or L-Captopril-Inhibited Metallo- β -Lactamases. *J. Biol. Chem.* **2003**, 278 (23), 20659-20666. <https://doi.org/10.1074/jbc.M212581200>
- (72) Livermore, D. M.; Mushtaq, S.; Morinaka, A.; Ida, T.; Maebashi, K.; Hope, R. Activity of Carbapenems with ME1071 (Disodium 2,3-Diethylmaleate) against Enterobacteriaceae and Acinetobacter Spp. with Carbapenemases, Including NDM Enzymes. **2013**, 68 (1), 153-158. <https://doi.org/10.1093/jac/dks350>
- (73) Payne, D. J.; Hueso-Rodríguez, J. A.; Boyd, H.; Concha, N. O.; Janson, C. A.; Gilpin, M.; Bateson, J. H.; Cheever, C.; Niconovich, N. L.; Pearson, S.; Rittenhouse, S.; Tew, D.; Díez, E.; Pérez, P.; De la Fuente, J.; Rees, M.; Rivera-Sagredo, A. Identification of a Series of Tricyclic Natural Products as Potent Broad-Spectrum Inhibitors of Metallo- β -Lactamases. *Antimicrob. Agents Chemother.* **2002**, 46 (6), 1880-1886. <https://doi.org/10.1128/AAC.46.6.1880-1886.2002>
- (74) Fast, W.; Sutton, L. D. Metallo- β -Lactamase: Inhibitors and Reporter Substrates. *BBA - Proteins and Proteom.* **2013**, 1834 (8), 1648-1659. <https://doi.org/10.1016/j.bbapap.2013.04.024>
- (75) Hiraiwa, Y.; Saito, J.; Watanabe, T.; Yamada, M.; Morinaka, A.; Fukushima, T.; Kudo, T. X-Ray Crystallographic Analysis of IMP-1 Metallo- β -Lactamase Complexed with a 3-Aminophthalic Acid Derivative, Structure-Based Drug Design, and Synthesis of 3,6-Disubstituted Phthalic Acid Derivative Inhibitors. *Bioorg. Med. Chem. Lett.* **2014**, 24 (20), 4891-4894. <https://doi.org/10.1016/j.bmcl.2014.08.039>
- (76) Christopheit T.; Yang K.-W.; Yang S.-K. and Leiros H.-K.S. The structure of the metallo- β -lactamase VIM-2 in complex with a triazolylthioacetamide inhibitor Acta Cryst. **2016**, F72, 813-819. <https://doi.org/10.1107/S2053230X16016113>
- (77) Liscio, J. L.; Mahoney, M. V.; Hirsch, E. B. Ceftolozane/Tazobactam and Ceftazidime/Avibactam: Two Novel β -Lactam/ β -Lactamase Inhibitor Combination Agents for the Treatment of Resistant Gram-Negative Bacterial Infections. *Int. J.*

- Antimicrob. Agents.* **2015**, 46 (3), 266-271.
<https://doi.org/10.1016/j.ijantimicag.2015.05.003>
- (78) Ehmann, D. E.; Jahić, H.; Ross, P. L.; Gu, R. F.; Hu, J.; Kern, G.; Walkup, G. K.; Fisher, S. L. Avibactam Is a Covalent, Reversible, Non- β -Lactam β -Lactamase Inhibitor. *Proc. Natl. Acad. Sci. U. S. A.* **2012**, 109 (29), 11663-11668.
<https://doi.org/10.1073/pnas.1205073109>
- (79) Neetu Kumra Taneja; Jaya Sivaswami Tya. Resazurin Reduction Assays for Screening of Anti-Tubercular Compounds against Dormant and Actively Growing Mycobacterium Tuberculosis, Mycobacterium Bovis BCG and Mycobacterium Smegmatis. *J. Antimicrob. Chemother.* **2007**, 43 (1), 1-4. <https://doi.org/10.1093/JAC>
- (80) Watkins, R. R.; Papp-Wallace, K. M.; Drawz, S. M.; Bonomo, R. A. Novel β -Lactamase Inhibitors: A Therapeutic Hope against the Scourge of Multidrug Resistance. *Front. Microbiol.* **2013**, 4, 392. <https://doi.org/10.3389/fmicb.2013.00392>
- (81) FDA. (2020) FDA approves new treatment for complicated urinary tract and complicated intra-abdominal infections. Available at: <https://www.fda.gov/news-events/press-announcements/fda-approves-new-treatment-complicated-urinary-tract-and-complicated-intra-abdominal-infections>. [Accessed August 2020]
- (82) Drawz, S. M.; Papp-Wallace, K. M.; Bonomo, R. A. New β -Lactamase Inhibitors: A Therapeutic Renaissance in an MDR World. *Antimicrob. Agents Chemother.* **2014**, 58 (4), 1835-1846. <https://doi.org/10.1128/AAC.00826-13>
- (83) Castanheira, M.; Rhomberg, P. R.; Flamm, R. K.; Jones, R. N. Effect of the β -Lactamase Inhibitor Vaborbactam Combined with Meropenem against Serine Carbapenemase-Producing Enterobacteriaceae. *Antimicrob. Agents Chemother.* **2016**, 60 (9), 5454-5458. <https://doi.org/10.1128/AAC.00711-16>
- (84) Taylor, D. M.; Anglin, J.; Park, S.; Ucisik, M. N.; Faver, J. C.; Simmons, N.; Jin, Z.; Palaniappan, M.; Nyshadham, P.; Li, F.; Campbell, J.; Hu, L.; Sankaran, B.; Prasad, B. V. V.; Huang, H.; Matzuk, M. M.; Palzkill, T. Identifying Oxacillinase-48 Carbapenemase Inhibitors Using DNA-Encoded Chemical Libraries. *ACS Infect. Dis.* **2020**, 6 (5), 1214-1227.
<https://doi.org/10.1021/acsinfecdis.0c00015>
- (85) Jhoti, H.; Leach, A. R. (2007) *Structure-Based Drug Discovery*; Springer, Dordrecht. <https://doi.org/10.1007/1-4020-4407-0>.
- (86) A Decade of Drug-Likeness. *Nat. Rev. Drug Discov.* **2007**, 6, 853.

- <https://doi.org/10.1038/nrd2460>
- (87) Schneider, G. (2013) *Prediction of Drug-Like Properties*. In: Madame Curie Bioscience Database [Internet]. Austin (TX): Landes Bioscience; 2000-2013. Available from: <https://www.ncbi.nlm.nih.gov/books/NBK6404>
- (88) Hiraiwa, Y.; Morinaka, A.; Fukushima, T.; Kudo, T. Metallo- β -Lactamase Inhibitory Activity of Phthalic Acid Derivatives. *Bioorg. Med. Chem. Lett.* **2009**, 19 (17), 5162-5165. <https://doi.org/10.1016/j.bmcl.2009.07.018>
- (89) Toney, J. H.; Fitzgerald, P. M. D.; Grover-Sharma, N.; Olson, S. H.; May, W. J.; Sundelof, J. G.; Vanderwall, D. E.; Cleary, K. A.; Grant, S. K.; Wu, J. K.; Kozarich, J. W.; Pompliano, D. L.; Hammond, G. G. Antibiotic Sensitization Using Biphenyl Tetrazoles as Potent Inhibitors of *Bacteroides Fragilis* Metallo- β -Lactamase. *Chem. Biol.* **1998**, 5 (4), 185-196. [https://doi.org/10.1016/S1074-5521\(98\)90632-9](https://doi.org/10.1016/S1074-5521(98)90632-9)
- (90) Minond, D.; Saldanha, S.; Spicer, T.; Qin, L.; Mercer, B.; Roush, W.; Hodder, P. (2010) *HTS Assay for Discovery of Novel Metallo- β -Lactamase (MBL) Inhibitors*; National Center for Biotechnology Information (US).
- (91) Scott, D. E.; Coyne, A. G.; Hudson, S. A.; Abell, C. Fragment-Based Approaches in Drug Discovery and Chemical Biology. *Biochemistry* **2012**, 51 (25), 4990-5003. <https://doi.org/10.1021/bi3005126>
- (92) Hubbard, R. E. Fragment Approaches in Structure-Based Drug Discovery. *J. Synchrotron Radiat.* **2008**, 15 (3), 227-230. <https://doi.org/10.1107/S090904950705666X>
- (93) Hopkins, A. L.; Groom, C. R.; Alex, A. Ligand Efficiency: A Useful Metric for Lead Selection. *Drug Discov. Today* **2004**, 9 (10), 430-431. [https://doi.org/10.1016/S1359-6446\(04\)03069-7](https://doi.org/10.1016/S1359-6446(04)03069-7)
- (94) Shultz, M. D. Setting Expectations in Molecular Optimizations: Strengths and Limitations of Commonly Used Composite Parameters. *Bioorganic Med. Chem. Lett.* **2013**, 23 (21), 5980-5991. <https://doi.org/10.1016/j.bmcl.2013.08.029>
- (95) De Souza Neto, L. R.; Moreira-Filho, J. T.; Neves, B. J.; Maidana, R. L. B. R.; Guimarães, A. C. R.; Furnham, N.; Andrade, C. H.; Silva, F. P. In Silico Strategies to Support Fragment-to-Lead Optimization in Drug Discovery. *Front. Chem.* **2020**, 8, 93. <https://doi.org/10.3389/fchem.2020.00093>

- (96) Zartler, E.R. and Shapiro, M.J. (2008) "Designing a Fragment Process to Fit Your Needs". In: *Fragment-Based Drug Discovery*. John Wiley & Sons, Ltd, 2008, pp. 15-37. <https://doi.org/10.1002/9780470721551.ch2>
- (97) Lamoree, B.; Hubbard, R. E. Current Perspectives in Fragment-Based Lead Discovery (FBLD). *Essays Biochem.* 2017, 61 (5), 453-464. <https://doi.org/10.1042/EBC20170028>
- (98) Li, R.; Martin, M. P.; Liu, Y.; Wang, B.; Patel, R. A.; Zhu, J. Y.; Sun, N.; Pireddu, R.; Lawrence, N. J.; Li, J.; Haura, E. B.; Sung, S. S.; Guida, W. C.; Schonbrunn, E.; Sebti, S. M. Fragment-Based and Structure-Guided Discovery and Optimization of Rho Kinase Inhibitors. *J. Med. Chem.* 2012, 55 (5), 2474–2478. <https://doi.org/10.1021/jm201289r>
- (99) Merz, K. M.; Ringe, D.; Reynolds, C. H. (2010) *Drug Design: Structure-and Ligand-Based Approaches*, Cambridge University Press. https://assets.cambridge.org/97805218/87236/frontmatter/9780521887236_frontmatter.
- (100) Erlanson, D. A.; McDowell, R. S.; O'Brien, T. Fragment-Based Drug Discovery. *J. Med. Chem.* 2004, 47 (14), 3463-3482. <https://doi.org/10.1021/jm040031v>
- (101) Mortenson, P. N.; Berdini, V.; O'Reilly, M. (2014) Fragment-Based Approaches to the Discovery of Kinase Inhibitors. In *Methods in Enzymology*; Academic Press Inc.; Chapter Three, Vol. 548, 69-92. <https://doi.org/10.1016/B978-0-12-397918-6.00003-3>
- (102) Murray, C. W.; Rees, D. C. The Rise of Fragment-Based Drug Discovery. *Nat. Chem.* 2009, 1 (3), 187-192. <https://doi.org/10.1038/nchem.217>
- (103) Tsai, J.; Lee, J. T.; Wang, W.; Zhang, J.; Cho, H.; Mamo, S.; Bremer, R.; Gillette, S.; Kong, J.; Haass, N. K.; Sproesser, K.; Li, L.; Smalley, K. S. M.; Fong, D.; Zhu, Y. L.; Marimuthu, A.; Nguyen, H.; Lam, B.; Liu, J.; Cheung, I.; Rice, J.; Suzuki, Y.; Luu, C.; Settachatgul, C.; Shellooe, R.; Cantwell, J.; Kim, S. H.; Schlessinger, J.; Zhang, K. Y. J.; West, B. L.; Powell, B.; Habets, G.; Zhang, C.; Ibrahim, P. N.; Hirth, P.; Artis, D. R.; Herlyn, M.; Bollag, G. Discovery of a Selective Inhibitor of Oncogenic B-Raf Kinase with Potent Antimelanoma Activity. *Proc. Natl. Acad. Sci. U. S. A.* 2008, 105 (8), 3041-3046. <https://doi.org/10.1073/pnas.0711741105>
- (104) Bollag, G.; Hirth, P.; Tsai, J.; Zhang, J.; Ibrahim, P. N.; Cho, H.; Spevak, W.; Zhang, C.; Zhang, Y.; Habets, G.; Burton, E. A.; Wong, B.; Tsang, G.; West, B. L.; Powell, B.; Shellooe, R.; Marimuthu, A.; Nguyen, H.; Zhang, K. Y. J.; Artis, D. R.; Schlessinger, J.; Su, F.; Higgins, B.; Iyer, R.; Dandrea, K.; Koehler, A.; Stumm, M.; Lin, P. S.; Lee, R.

- J.; Grippo, J.; Puzanov, I.; Kim, K. B.; Ribas, A.; McArthur, G. A.; Sosman, J. A.; Chapman, P. B.; Flaherty, K. T.; Xu, X.; Nathanson, K. L.; Nolop, K. Clinical Efficacy of a RAF Inhibitor Needs Broad Target Blockade in BRAF-Mutant Melanoma. *Nature* **2010**, 467 (7315), 596-599. <https://doi.org/10.1038/nature09454>
- (105) Chen, Y.; Shoichet, B. K. Molecular Docking and Ligand Specificity in Fragment-Based Inhibitor Discovery. *Nat. Chem. Biol.* **2009**, 5 (5), 358-364. <https://doi.org/10.1038/nchembio.155>
- (106) Nichols, D. A.; Renslo, A. R.; Chen, Y. Fragment-Based Inhibitor Discovery against β -Lactamase. *Future Med. Chem.* **2014**, 6:4, 413-427. <https://doi.org/10.4155/fmc.14.10>
- (107) Christopeit, T.; Albert, A.; Leiros, H. K. S. Discovery of a Novel Covalent Non- β -Lactam Inhibitor of the Metallo- β -Lactamase NDM-1. *Bioorganic Med. Chem.* **2016**, 24 (13), 2947-2953. <https://doi.org/10.1016/j.bmc.2016.04.064>
- (108) Kürti, L.; Czakó B. (2005) Strategic Applications of Named Reactions in Organic Synthesis. Academic Press, Elsevier (1st Edition).
- (109) Lessene, G. Advances in the Negishi Coupling. *Aust. J. Chem.* **2004**, 57 (1), 107. <https://doi.org/10.1071/CH03225>
- (110) Cordovilla, C.; Bartolomé, C.; Martínez-Ilarduya, J. M.; Espinet, P. The Stille Reaction, 38 Years Later. *ACS Catalysis.* **2015**, 5, 3040-3053. <https://doi.org/10.1021/acscatal.5b00448>
- (111) Schröter, S.; Stock, C.; Bach, T. Regioselective Cross-Coupling Reactions of Multiple Halogenated Nitrogen-, Oxygen-, and Sulfur-Containing Heterocycles. *Tetrahedron*, **2005**, 61 (9), 2245-2267. <https://doi.org/10.1016/j.tet.2004.11.074>
- (112) Perdomo Rivera, R.; Ehlers, P.; Ohlendorf, L.; Torres Rodríguez, E.; Villinger, A.; Langer, P. Chemoselective Synthesis of Arylpyridines through Suzuki-Miyaura Cross-Coupling Reactions. *Eur. J. Org. Chem.* **2018**, 990-1003. <https://doi.org/10.1002/ejoc.201701718>
- (113) Fyfe, J. W. B.; Fazakerley, N. J.; Watson, A. J. B. Chemoselective Suzuki-Miyaura Cross-Coupling via Kinetic Transmetalation. *Angew. Chem. Int. Ed.* **2017**, 56, 1249-1253. <https://doi.org/10.1002/anie.201610797>
- (114) Ashcroft, C. P.; Fussell, S. J.; Wilford, K. Catalyst Controlled Regioselective Suzuki Cross-Coupling of 2-(4-Bromophenyl)-5-Chloropyrazine. *Tetrahedron Lett.* **2013**, 54 (34), 4529-4532. <https://doi.org/10.1016/j.tetlet.2013.06.068>

- (115) Kamikawa, T.; Hayashi, T. Control of Reactive Site in Palladium-Catalyzed Grignard Cross-Coupling of Arenes Containing Both Bromide and Triflate. *Tetrahedron Lett.* **1997**, 38 (40), 7087-7090. [https://doi.org/10.1016/S0040-4039\(97\)01655-9](https://doi.org/10.1016/S0040-4039(97)01655-9)
- (116) Littke, A. F.; Dai, C.; Fu, G. C. Versatile Catalysts for the Suzuki Cross-Coupling of Arylboronic Acids with Aryl and Vinyl Halides and Triflates under Mild Conditions. *J. Am. Chem. Soc.* **2000**, 122 (17), 4020-4028. <https://doi.org/10.1021/ja0002058>
- (117) Manabe, K.; Yamaguchi, M. Catalyst-Controlled Site-Selectivity Switching in Pd-Catalyzed Cross-Coupling of Dihaloarenes. *Catalysts* **2014**, 4 (3), 307-320. <https://doi.org/10.3390/catal4030307>
- (118) Almond-Thynne, J.; Blakemore, D. C.; Pryde, D. C.; Spivey, A. C. Site-Selective Suzuki-Miyaura Coupling of Heteroaryl Halides-Understanding the Trends for Pharmaceutically Important Classes. *Chem. Sci.* **2016**, 8 (1), 40-62. <https://doi.org/10.1039/C6SC02118B>
- (119) Houpis, I. N.; Huang, C.; Nettekoven, U.; Chen, J. G.; Liu, R.; Canters, M. Carboxylate Directed Cross-Coupling Reactions in the Synthesis of Trisubstituted Benzoic Acids. *Org. Lett.* **2008**, 10 (24), 5601-5604. <https://doi.org/10.1021/ol802349u>
- (120) Martin, R.; Buchwald, S. L. Palladium-Catalyzed Suzuki-Miyaura Cross-Coupling Reactions Employing Dialkylbiaryl Phosphine Ligands. *Acc. Chem. Res.* **2008**, 41 (11), 1461-1473. <https://doi.org/10.1021/ar800036s>
- (121) Zhang, Y.; Zhang, R.; Ni, C.; Zhang, X.; Li, Y.; Lu, Q.; Zhao, Y.; Han, F.; Zeng, Y.; Liu, G. NHC-Pd(II)-Azole Complexes Catalyzed Suzuki-Miyaura Cross-Coupling of Sterically Hindered Aryl Chlorides with Arylboronic Acids. *Tetrahedron Lett.* **2020**, 61 (10), 151541. <https://doi.org/10.1016/j.tetlet.2019.151541>
- (122) Yin, J.; Rainka, M. P.; Zhang, X. X.; Buchwald, S. L. A Highly Active Suzuki Catalyst for the Synthesis of Sterically Hindered Biaryls: Novel Ligand Coordination. *J. Am. Chem. Soc.* **2002**, 124 (7), 1162-1163. <https://doi.org/10.1021/ja017082r>
- (123) Proutiere, F.; Schoenebeck, F. Solvent Effect on Palladium-Catalyzed Cross-Coupling Reactions and Implications on the Active Catalytic Species. *Angew. Chem. Int. Ed.* **2011**, 50 (35), 8192-8195. <https://doi.org/10.1002/anie.20110174>
- (124) Reeves, E. K.; Bauman, O. R.; Mitchem, G. B.; Neufeldt, S. R. Solvent Effects on the Selectivity of Palladium-Catalyzed Suzuki-Miyaura Couplings. *Isr. J. Chem.* **2019**, 60, 406-409. <https://doi.org/10.1002/ijch.201900082>
- (125) Brennführer, A.; Neumann, H.; Beller, M. Palladium-Catalyzed Carbonylation Reactions

- of Aryl Halides and Related Compounds. *Angew. Chem. Int. Ed* **2009**, 48, 4114-4133.
<https://doi.org/10.1002/anie.200900013>
- (126) Wu, X. F. Palladium-Catalyzed Carbonylative Transformation of Aryl Chlorides and Aryl Tosylates. *RSC Adv.* **2016**, 6, 83831-83837.
<https://doi.org/10.1039/c6ra18388c>
- (127) Jan, N. W.; Liu, H. J. An Enantioselective Total Synthesis of (+)-Ricciocarpin A. *Org. Lett.* **2006**, 8 (1), 151-153. <https://doi.org/10.1021/ol052638r>
- (128) Yao, T.; Yue, D.; Larock, R. C. An Efficient Synthesis of Coumestrol and Coumestans by Iodocyclization and Pd-Catalyzed Intramolecular Lactonization. *J. Org. Chem.* **2005**, 70 (24), 9985-9989. <https://doi.org/10.1021/jo0517038>
- (129) Ishiyama, T.; Kizaki, H.; Hayashi, T.; Suzuki, A.; Miyaura, N. Palladium-Catalyzed Carbonylative Cross-Coupling Reaction of Arylboronic Acids with Aryl Electrophiles: Synthesis of Biaryl Ketones. *J. Org. Chem.* **1998**, 63, 14, 4726-4731
<https://doi.org/10.1021/jo980417b>
- (130) Fang, W.; Zhu, H.; Deng, Q.; Liu, S.; Liu, X.; Shen, Y.; Tu, T. Design and Development of Ligands for Palladium-Catalyzed Carbonylation Reactions. *Synthesis* **2014**, 46 (13), 1689-1708. <https://doi.org/10.1055/s-0033-1338635>
- (131) Li, H., Yang, M., Qi, Y. and Xue, J. (2011), Ligand-Free Pd-Catalyzed Carbonylative Cross-Coupling Reactions under Atmospheric Pressure of Carbon Monoxide: Synthesis of Aryl Ketones and Heteroaromatic Ketones. *Eur. J. Org. Chem.*, **2011**: 2662-2667. doi:10.1002/ejoc.201001685
- (132) Michael O 'Keefe, B.; Simmons, N.; Martin, S. F. Carbonylative Cross-Coupling of Ortho-Disubstituted Aryl Iodides. Convenient Synthesis of Sterically Hindered Aryl Ketones. *Org. Lett.* **2008**, 10 (22), 5301-5304. <https://doi.org/10.1021/ol802202j>
- (133) Bates, R. (2012) *Organic Synthesis Using Transition Metals*; John Wiley & Sons, Ltd: Chichester, UK. <https://doi.org/10.1002/9781119942863>
- (134) Fairlamb, I. J. S.; Grant, S.; McCormack, P.; Whittall, J. Alkoxy- and Amido-carbonylation of Functionalised Aryl and Heteroaryl Halides Catalysed by a Bedford Palladacycle and Dppf: A Comparison with the Primary Pd(II) Precursors (PhCN)₂PdCl₂ and Pd(OAc)₂. *J. Chem. Soc. Dalt. Trans.* **2007**, 8, 859-865.
<https://doi.org/10.1039/b615874a>
- (135) Wu, X.-F.; Neumann, H.; Beller, M. Palladium-Catalyzed Carbonylative Suzuki Coupling of Benzyl Halides with Potassium Aryltrifluoroborates in Aqueous Media.

- Adv. Synth. Catal.* **2011**, 353 (5), 788–792. <https://doi.org/10.1002/adsc.201000804>.
- (136) Wu, X. F.; Neumann, H.; Beller, M. Palladium-Catalyzed Carbonylative Coupling Reactions between Ar–X and Carbon Nucleophiles. *Chem. Soc. Rev.* **2011**, **40** (10), 4986–5009. <https://doi.org/10.1039/c1cs15109f>.
- (137) Hajipour, A. R.; Tavangar-Rizi, Z.; Iranpoor, N. Palladium-Catalyzed Carbonylation of Aryl Halides: An Efficient, Heterogeneous and Phosphine-Free Catalytic System for Aminocarbonylation and Alkoxy carbonylation Employing Mo(CO)₆ as a Solid Carbon Monoxide Source. *RSC Adv.* **2016**, 6 (82), 78468–78476. <https://doi.org/10.1039/c6ra18679c>
- (138) Buchspies, J.; Szostak, M. Recent Advances in Acyl Suzuki Cross-Coupling. *Catalysts* **2019**, 9 (1), 53. <https://doi.org/10.3390/catal9010053>
- (139) Nordeman, P.; Odell, L. R.; Larhed, M. Aminocarbonylations Employing Mo(CO)₆ and a Bridged Two-Vial System: Allowing the Use of Nitro Group Substituted Aryl Iodides and Aryl Bromides. *J. Org. Chem.* **2012**, 77 (24), 11393–11398. <https://doi.org/10.1021/jo302322w>
- (140) Sharma, P.; Rohilla, S.; Jain, N. Palladium Catalyzed Carbonylative Coupling for Synthesis of Arylketones and Arylestere s Using Chloroform as the Carbon Monoxide Source. *J. Org. Chem.* **2017**, 82 (2), 1105–1113. <https://doi.org/10.1021/acs.joc.6b02711>
- (141) Hansen, S. V. F.; Ulven, T. Oxalyl Chloride as a Practical Carbon Monoxide Source for Carbonylation Reactions. *Org. Lett.* **2015**, 17 (11), 2832–2835. <https://doi.org/10.1021/acs.orglett.5b01252>
- (142) Cacchi, S.; Fabrizi, G.; Goggiamani, A. Palladium-Catalyzed Hydroxycarbonylation of Aryl and Vinyl Halides or Triflates by Acetic Anhydride and Formate Anions. *Org. Lett.* **2003**, 5 (23), 4269–4272. <https://doi.org/10.1021/ol0354371>
- (143) Gautam, P.; Bhanage, B. M. Recent Advances in the Transition Metal Catalyzed Carbonylation of Alkynes, Arenes and Aryl Halides Using CO Surrogates. *Catal. Sci. Technol.* **2015**, 5, 4663–4702. <https://doi.org/10.1039/c5cy00691k>
- (144) Morimoto, T.; Kakiuchi, K. Evolution of Carbonylation Catalysis: No Need for Carbon Monoxide. *Angew. Chem. Int. Ed.* **2004**, 43, 5580–5588. <https://doi.org/10.1002/anie.200301736>
- (145) Roberts, B.; Liptrot, D.; Alcaraz, L.; Luker, T.; Stocks, M. J. Molybdenum-Mediated Carbonylation of Aryl Halides with Nucleophiles Using Microwave Irradiation. *Org.*

- Lett.* **2010**, 12 (19), 4280-4283. <https://doi.org/10.1021/ol1016965>
- (146) Friis, S. D.; Lindhardt, A. T.; Skrydstrup, T. The Development and Application of Two-Chamber Reactors and Carbon Monoxide Precursors for Safe Carbonylation Reactions. *Acc. Chem. Res.* **2016**, 49 (4), 594-605.
<https://doi.org/10.1021/acs.accounts.5b00471>
- (147) Korsager, S.; Taaning, R. H.; Lindhardt, A. T.; Skrydstrup, T. Reductive Carbonylation of Aryl Halides Employing a Two-Chamber Reactor: A Protocol for the Synthesis of Aryl Aldehydes Including ¹³C- and D-Isotope Labeling. *J. Org. Chem.* **2013**, 78 (12), 6112-6120. <https://doi.org/10.1021/jo400741t>
- (148) Yin, H.; Nielsen, D. U.; Johansen, M. K.; Lindhardt, A. T.; Skrydstrup, T. Development of a Palladium-Catalyzed Carbonylative Coupling Strategy to 1,4-Diketones. *ACS Catal.* **2016**, 6 (5), 2982-2987. <https://doi.org/10.1021/acscatal.6b00733>
- (149) Ahlburg, A.; Lindhardt, A. T.; Taaning, R.; Modvig, A. An Air Tolerant Approach to the Carbonylative Suzuki-Miyaura Coupling Applications in Isotope Labelling. *J. Org. Chem.* **2013**, 78, 10310-10318. <https://pubs.acs.org/doi/abs/10.1021/jo401696c>
- (150) Tambade, P. J.; Patil, Y. P.; Panda, A. G.; Bhanage, B. M. Phosphane-Free Palladium-Catalyzed Carbonylative Suzuki Coupling Reaction of Aryl and Heteroaryl Iodides. *Eur. J. Org. Chem.* **2009**, 3022-3025. <https://doi.org/10.1002/ejoc.200900219>
- (151) Mingji, D.; Liang, B.; Wang, C.; You, Z.; Xiang, J.; Dong, G.; Chen, J.; Yang, Z. A Novel Thiourea Ligand Applied in the Pd-Catalyzed Heck, Suzuki and Suzuki Carbonylative Reactions. *Adv. Synth. Catal.* **2004**, 346, 1669-1673.
<https://doi.org/10.1002/adsc.200404165>
- (152) Neumann, H.; Brennführer, A.; Beller, M. A General Synthesis of Diarylketones by Means of a Three-Component Cross-Coupling of Aryl and Heteroaryl Bromides, Carbon Monoxide, and Boronic Acids. *Chem. - A Eur. J.* **2008**, 14 (12), 3645-3652.
<https://doi.org/10.1002/chem.200800001>
- (153) Bjerglund, K. M.; Skrydstrup, T.; Molander, G. a. Carbonylative Suzuki Couplings of Aryl Bromides with Boronic Acid Derivatives under Base-Free Conditions Experimental Procedures and Characterization Data for Novel Compounds in Tables 2 and 3 and Scheme 2. *Org. Lett.* **2014**, 16, 1888-1891.
<https://pubs.acs.org/doi/full/10.1021/ol5003362>
- (154) Calloway, N. O. The Friedel-Crafts Syntheses. *Chem. Rev.* **1935**, 17 (3), 327-392.
<https://doi.org/10.1021/cr60058a002>

- (155) Zhang, N.; Yu, Q.; Chen, R.; Huang, J.; Xia, Y.; Zhao, K. Synthesis of Biaryl Imino/Keto Carboxylic Acids via Aryl Amide Directed C-H Activation Reaction. *Chem. Commun.* **2013**, 49 (82), 9464. <https://doi.org/10.1039/c3cc45449e>
- (156) Miao, J.; Ge, H. Palladium-Catalyzed Chemoselective Decarboxylative Ortho Acylation of Benzoic Acids with α -Oxocarboxylic Acids. *Org. Lett.* **2013**, 15 (12), 2930-2933. <https://doi.org/10.1021/ol400919u>
- (157) Hermange, P.; Lindhardt, A. T.; Taaning, R. H.; Bjerglund, K.; Lupp, D.; Skrydstrup, T. Ex Situ Generation of Stoichiometric and Substoichiometric ^{12}CO and ^{13}CO and Its Efficient Incorporation in Palladium Catalyzed Aminocarbonylations. *J. Am. Chem. Soc.* **2011**, 133, 15, 6061-6071. <https://doi.org/10.1021/ja200818w>
- (158) Mamone, M.; Aziz, J.; Le Bescont, J.; Piguel, S. Aminocarbonylation of N -Containing Heterocycles with Aromatic Amines Using $\text{Mo}(\text{CO})_6$. *Synth.* **2018**, 50 (7), 1521-1526. <https://doi.org/10.1055/s-0037-1609152>
- (159) Friis, D. S.; Skrydstrup, T. Buchwald, S. L. Mild Pd-Catalyzed Aminocarbonylation of (Hetero)Aryl Bromides with a Palladacycle Precatalyst. *Org. Lett.* 2014, 16, 16, 4296-4299 <https://doi.org/10.1021/ol502014b>
- (160) Ojima, I.; Athan, A.; Commandeur, C.; Chiou, W.-H. (2013) Amidocarbonylation, Cyclohydrocarbonylation, and Related Reactions. In *Reference Module in Chemistry, Molecular Sciences and Chemical Engineering*; Elsevier Inc. <https://doi.org/10.1016/B978-0-12-409547-2.03980-9>
- (161) Andrews, I. P.; Atkins, R. J.; Badham, N. F.; Bellingham, R. K.; Breen, G. F.; Carey, J. S.; Etridge, S. K.; Hayes, J. F.; Hussain, N.; Morgan, D. O.; Share, A. C.; Smith, S. A. C.; Walsgrove, T. C.; Wells, A. S. A New Synthesis of the Gpiib/Iiia Receptor Antagonist Sb-214857-A. *Tetrahedron Lett.* **2001**, 42 (29), 4915-4917. [https://doi.org/10.1016/S0040-4039\(01\)00843-7](https://doi.org/10.1016/S0040-4039(01)00843-7)
- (162) Banks, A.; Breen, G. F.; Caine, D.; Carey, J. S.; Drake, C.; Forth, M. A.; Gladwin, A.; Guelfi, S.; Hayes, J. F.; Maragni, P.; Morgan, D. O.; Oxley, P.; Perboni, A.; Popkin, M. E.; Rawlinson, F.; Roux, G. Process Development and Scale up of a Glycine Antagonist. *Org. Process Res. Dev.* **2009**, 13 (6), 1130-1140. <https://doi.org/10.1021/op9001824>
- (163) Sharma, N.; Sekar, G. Stable and Reusable Binaphthyl-Supported Palladium Catalyst for Aminocarbonylation of Aryl Iodides. *Adv. Synth. Catal.* **2016**, 358 (2), 314-320. <https://doi.org/10.1002/adsc.201500642>
- (164) Andrews, I. P.; Atkins, R. J.; Breen, G. F.; Carey, J. S.; Forth, M. A.; Morgan, D. O.;

- Shamji, A.; Share, A. C.; Smith, S. A. C.; Walsgrove, T. C.; Wells, A. S. The Development of a Manufacturing Route for the GPIIb/IIIa Receptor Antagonist SB-214857-A. Part 1: Synthesis of the Key Intermediate 2,3,4,5-Tetrahydro-4-Methyl-3-Oxo-1H-1,4-Benzodiazepine-2-Acetic Acid Methyl Ester, SB-235349. *Org. Process Res. Dev.* **2003**, 7 (5), 655-662.
<https://doi.org/10.1021/op034024c>
- (165) Kagan, H. B. (1982) Asymmetric Synthesis Using Organometallic Catalysts. In *Comprehensive Organometallic Chemistry*; Elsevier Inc., Vol. 8, 463-498.
<https://doi.org/10.1016/B978-008046518-0.00112-4>
- (166) Szarka, Z.; Kuik, Á.; Skoda-Földes, R.; Kollár, L. Aminocarbonylation of 1,1'-Diiodoferrocene, Two-Step Synthesis of Heterodisubstituted Ferrocene Derivatives via Homogeneous Catalytic Carbonylation/Coupling Reactions. *J. Organomet. Chem.* **2004**, 689 (17), 2770-2775. <https://doi.org/10.1016/j.jorganchem.2004.05.046>
- (167) Martinelli, J. R.; Freckmann, D. M. M.; Buchwald, S. L. Convenient Method for the Preparation of Weinreb Amides via Pd-Catalyzed Aminocarbonylation of Aryl Bromides at Atmospheric Pressure. *Org. Lett.* **2006**, 8 (21), 4843-4846.
<https://doi.org/10.1021/ol061902t>
- (168) Soderberg, B. C. (1995) Transition Metal Alkyl Complexes: Oxidative Addition and Insertion. In *Comprehensive Organometallic Chemistry II*; Elsevier Ltd., Vol 12, 241-297. <https://doi.org/10.1016/b978-008046519-7.00112-x>
- (169) Bhat, B. A.; Rashid, S.; Mehta, G. (2019) Advances in the Synthesis of Furo[2,3-b]Furanone-Containing Natural Products. In *Studies in Natural Products Chemistry*; Elsevier B.V., Vol. 63, 461-487. <https://doi.org/10.1016/B978-0-12-817901-7.00014-9>
- (170) Sargent, B. T.; Alexanian, E. J. Palladium-Catalyzed Alkoxy carbonylation of Unactivated Secondary Alkyl Bromides at Low Pressure. *J. Am. Chem. Soc.* **2016**, 138 (24), 7520-7523. <https://doi.org/10.1021/jacs.6b04610>
- (171) Xin, Z.; Gøgsig, T. M.; Lindhardt, A. T.; Skrydstrup, T. An Efficient Method for the Preparation of Tertiary Esters by Palladium-Catalyzed Alkoxy carbonylation of Aryl Bromides. *Org. Lett.* **2012**, 14 (1), 284-287. <https://doi.org/10.1021/ol203057w>
- (172) De Almeida, A. M.; Andersen, T. L.; Lindhardt, A. T.; De Almeida, M. V.; Skrydstrup, T. General Method for the Preparation of Active Esters by Palladium-Catalyzed Alkoxy carbonylation of Aryl Bromides. *J. Org. Chem.* **2015**, 80 (3), 1920-1928.
<https://doi.org/10.1021/jo5025464>

- (173) Koziakov, D.; Wangelin, A. J. von. Metal-Free Radical Aromatic Carbonylations Mediated by Weak Bases. *Org. Biomol. Chem.* **2017**, 15 (32), 6715-6719.
<https://doi.org/10.1039/C7OB01572K>
- (174) (a) Kollár, L. *Modern Carbonylation Methods*, Wiley-VCH, Weinheim, **2008**. (b) Ryu, I.; Ui, T.; Sumino, S. Synthesis of aromatic β -keto esters via a carbonylative Suzuki–Miyaura coupling reaction of α -iodo esters with arylboronic acids. *Org. Chem. Front.*, 2015, 2, 1085-1087. DOI: 10.1039/C5QO00185D
- (175) Cowell, A.; Stille, J. K. Synthesis of Lactones by the Palladium-Catalyzed Carbonylation of Halo Alcohols. *J. Am. Chem. Soc.* **1980**, 102 (12), 4193-4198.
<https://doi.org/10.1021/ja00532a034>
- (176) Bhanage, B. M.; Gadge, S. T. Recent developments in palladium catalysed carbonylation reactions. *RSC Adv.*, **2014**, **4**, 10367-10389. <https://doi.org/10.1039/C3RA46273K>
- (177) Lou, R.; VanAlstine, M.; Sun, X.; Wentland, M. P. Preparation of N-Hydroxysuccinimido Esters via Palladium-Catalyzed Carbonylation of Aryl Triflates and Halides. *Tetrahedron Lett.* **2003**, 44 (12), 2477-2480.
[https://doi.org/10.1016/S0040-4039\(03\)00337-X](https://doi.org/10.1016/S0040-4039(03)00337-X)
- (178) Jensen, M. T.; Rønne, M. H.; Ravn, A. K.; Juhl, R. W.; Nielsen, D. U.; Hu, X.-M.; Pedersen, S. U.; Daasbjerg, K.; Skrydstrup, T. Scalable Carbon Dioxide Electroreduction Coupled to Carbonylation Chemistry. *Nat. Commun.* **2017**, 8 (1), 489.
<https://doi.org/10.1038/s41467-017-00559-8>
- (179) Friedfeld, M. R.; Zhong, H.; Ruck, R. T.; Shevlin, M.; Chirik, P. J. Cobalt-Catalyzed Asymmetric Hydrogenation of Enamides Enabled by Single-Electron Reduction. *Science* **2018**, 360 (6391), 888-893. <https://doi.org/10.1126/science.aar6117>
- (180) Dyson, P. J.; Jessop, P. G. Solvent Effects in Catalysis: Rational Improvements of Catalysts: Via Manipulation of Solvent Interactions. *Catal. Sci. Technol.* **2016**, 6, 3302-3316. <https://doi.org/10.1039/c5cy02197a>
- (181) Clarke, C. J.; Tu, W. C.; Levers, O.; Bröhl, A.; Hallett, J. P. Green and Sustainable Solvents in Chemical Processes. *Chem. Rev.* **2018**, 118 (2), 747-800.
<https://doi.org/10.1021/acs.chemrev.7b00571>
- (182) Anastas, P.; Eghbali, N. Green Chemistry: Principles and Practice. *Chem. Soc. Rev.* **2010**, 39 (1), 301-312. <https://doi.org/10.1039/b918763b>
- (183) Sarkar, A.; Santra, S.; Kundu, S. K.; Hajra, A.; Zyryanov, G. V.; Chupakhin, O. N.; Charushin, V. N.; Majee, A. A Decade Update on Solvent and Catalyst-Free Neat

- Organic Reactions: A Step Forward towards Sustainability. *Green Chem.* **2016**, 18 (16), 4475–4525. <https://doi.org/10.1039/c6gc01279e>
- (184) Jessop, P. G. Searching for Green Solvents. *Green Chem.* **2011**, 13, 1391. <https://doi.org/10.1039/c0gc00797h>
- (185) Cséfalvay, E.; Akién, G. R.; Qi, L.; Horváth, I. T. Definition and Application of Ethanol Equivalent: Sustainability Performance Metrics for Biomass Conversion to Carbon-Based Fuels and Chemicals. *Catal. Today* **2015**, 239, 50-55. <https://doi.org/10.1016/j.cattod.2014.02.006>
- (186) Millar, C.; Hind, P.; Magala, S. Sustainability and the Need for Change: Organisational Change and Transformational Vision. *J. Organ. Chang. Manag.* **2012**, 25 (4), 489-500. <https://doi.org/10.1108/09534811211239272>
- (187) Santoro, S.; Ferlin, F.; Luciani, L.; Ackermann, L.; Vaccaro, L. Biomass-Derived Solvents as Effective Media for Cross-Coupling Reactions and C-H Functionalization Processes. *Green Chem.* **2017**, 19, 1601-1612. <https://doi.org/10.1039/c7gc00067g>
- (188) Gu, Y.; Jérôme, F. Bio-Based Solvents: An Emerging Generation of Fluids for the Design of Eco-Efficient Processes in Catalysis and Organic Chemistry. *Chem. Soc. Rev.* **2013**, 42, 9550-9570. <https://doi.org/10.1039/c3cs60241a>
- (189) Ramgren, S. D.; Hie, L.; Ye, Y.; Garg, N. K. Nickel-Catalyzed Suzuki-Miyaura Couplings in Green Solvents. *Org. Lett.* **2013**, 15 (15), 3950-3953. <https://doi.org/10.1021/ol401727y>
- (190) Gevorgyan, A.; Hopmann, K. H.; Bayer, A. Exploration of New Biomass-Derived Solvents: Application to Carboxylation Reactions. *Chem. Sus. Chem.* **2020**, 13 (8), 2080-2088. <https://doi.org/10.1002/cssc.201903224>
- (191) Strappaveccia, G.; Ismalaj, E.; Petrucci, C.; Lanari, D.; Marrocchi, A.; Drees, M.; Facchetti, A.; Vaccaro, L. A Biomass-Derived Safe Medium to Replace Toxic Dipolar Solvents and Access Cleaner Heck Coupling Reactions. *Green Chem.* **2015**, 17 (1), 365-372. <https://doi.org/10.1039/c4gc01677g>
- (192) Radatz, C. S.; Silva, R. B.; Perin, G.; Lenardão, E. J.; Jacob, R. G.; Alves, D. Catalyst-Free Synthesis of Benzodiazepines and Benzimidazoles Using Glycerol as Recyclable Solvent. *Tetrahedron Lett.* **2011**, 52 (32), 4132-4136. <https://doi.org/10.1016/j.tetlet.2011.05.142>
- (193) Parker, H. L.; Sherwood, J.; Hunt, A. J.; Clark, J. H. Cyclic Carbonates as Green

- Alternative Solvents for the Heck Reaction. *ACS Sustainable Chem. Eng.* **2014**, 2, 1739-1742. <https://doi.org/10.1021/sc5002287>
- (194) Wang, J. L.; He, L. N.; Miao, C. X.; Li, Y. N. Ethylene Carbonate as a Unique Solvent for Palladium-Catalyzed Wacker Oxidation Using Oxygen as the Sole Oxidant. *Green Chem.* **2009**, 11 (9), 1317-1320. <https://doi.org/10.1039/b913779n>
- (195) Schäffner, B.; Schäffner, F.; Verevkin, S. P.; Börner, A. Organic Carbonates as Solvents in Synthesis and Catalysis. *Chem. Rev.* **2010**, 110 (8), 4554-4581. <https://doi.org/10.1021/cr900393d>
- (196) Pereira, F. S.; Pereira, L. J.; Crédito, D. F. A.; Girão, L. H. V.; Idehara, A. H. S.; González, E. R. P. Cycling of Waste Fusel Alcohols from Sugar Cane Industries Using Supercritical Carbon Dioxide. *RSC Adv.* **2015**, 5 (99), 81515-81522. <https://doi.org/10.1039/c5ra16346c>
- (197) Fischmeister, C.; Doucet, H. Greener Solvents for Ruthenium and Palladium-Catalysed Aromatic C-H Bond Functionalisation. *Green Chem.* **2011**, 13, 741-753. <https://doi.org/10.1039/c0gc00885k>
- (198) Billingsley, K.; Buchwald, S. L. Highly Efficient Monophosphine-Based Catalyst for the Palladium-Catalyzed Suzuki-Miyaura Reaction of Heteroaryl Halides and Heteroaryl Boronic Acids and Esters. *J. Am. Chem. Soc.* **2007**, 129 (11), 3358-3366. <https://doi.org/10.1021/ja068577p>
- (199) Aeberli, P.; Eden, P.; Gogerty, J. H.; Houlihan, W. J.; Penberthy, C. 5-Aryl-2,3-Dihydro-5H-Imidazo[2,1-a]Isoindol-5-Ols. A Novel Class of Anorectic Agents. *J. Med. Chem.* **1975**, 18 (2), 177-182. <https://doi.org/10.1021/jm00236a014>
- (200) Si, S.; Wang, C.; Zhang, N.; Zou, G. Palladium-Catalyzed Room-Temperature Acylative Suzuki Coupling of High-Order Aryl Borons with Carboxylic Acids. *J. Org. Chem.* **2016**, 81 (10), 4364-4370. <https://doi.org/10.1021/acs.joc.6b00421>
- (201) Garcia-Barrantes, P.M; McGowan, K; Ingram, S.W; Lindsley, C.W., One pot synthesis of unsymmetrical ketones from carboxylic and boronic acids via PyCIU-mediated acylative Suzuki coupling. *Tetrahedron Lett.*, **2017**, 58 (9), 898-901. <https://doi.org/10.1016/j.tetlet.2017.01.064>
- (202) Panja, S.; Maity, P.; Ranu, B. C. Palladium-Catalyzed Ligand-Free Decarboxylative Coupling of α - Oxocarboxylic Acid with Aryl Diazonium Tetrafluoroborate: An Access to Unsymmetrical Diaryl Ketones. *J. Org. Chem.* **2018**, 83 (20), 12609-12618. <https://doi.org/10.1021/acs.joc.8b01922>

- (203) Suchand, B.; Satyanarayana, G. Palladium-Catalyzed Environmentally Benign Acylation. *J. Org. Chem.* **2016**, 81, 6409-6423.
<https://doi.org/10.1021/acs.joc.6b01064>
- (204) Couve-Bonnaire, S.; Carpentier, J.-F.; Mortreux, A.; Castanet, Y. Palladium-Catalyzed Carbonylative Coupling of Pyridine Halides with Aryl Boronic Acids. *Tetrahedron* **2003**, 59 (16), 2793-2799. [https://doi.org/10.1016/S0040-4020\(03\)00342-9](https://doi.org/10.1016/S0040-4020(03)00342-9)
- (205) Hulsbosch, J.; De Vos, D. E.; Binnemans, K.; Ameloot, R. Biobased Ionic Liquids: Solvents for a Green Processing Industry? *ACS Sustainable Chem. Eng.* **2016**, 4 (6), 2917-2931. <https://doi.org/10.1021/acssuschemeng.6b00553>
- (206) Ashcroft, C. P.; Dunn, P. J.; Hayler, J. D.; Wells, A. S. Survey of Solvent Usage in Papers Published in Organic Process Research & Development 1997-2012. *Org. Process Res. Dev.* **2015**, 19, 7, 740-747. <https://doi.org/10.1021/op500276u>
- (207) Nagakura, S.; Kuboyama, A. Dipole Moments and Absorption Spectra of O-Benzoquinone and Its Related Substances. *J. Am. Chem. Soc.* **1954**, 76 (4), 1003-1005.
<https://doi.org/10.1021/ja01633a017>
- (208) Altshuller, A. P. The Dielectric Constants, Polarizations and Dipole Moments of Some Alkylbenzenes. *J. Phys. Chem.* **1954**, 58 (5), 392-395.
<https://doi.org/10.1021/j150515a003>
- (209) Philippe, R.; Piette, A. M. Recherches de Stoechiométrie VII(1) Contribution à l'étude de La Constante Diélectrique Des Composés Organiques Purs. *Bull. des Sociétés Chim. Belges* **2010**, 64 (9-10), 600-627. <https://doi.org/10.1002/bscb.19550640910>
- (210) Rivas, M. A.; Pereira, S. M.; Banerji, N.; Iglesias, T. P. Permittivity and Density of Binary Systems of {dimethyl or Diethyl Carbonate} + N-Dodecane from T = (288.15 to 328.15) K. *J. Chem. Thermodyn.* **2004**, 36 (3), 183-191.
<https://doi.org/10.1016/j.jct.2003.11.007>
- (211) Zia, H.; Ma, J. K. H.; O'Donnell, J. P.; Luzzi, L. A. Cosolvency of Dimethyl Isosorbide for Steroid Solubility. *Pharm. Res. An Off. J. Am. Assoc. Pharm. Sci.* **1991**, 8 (4), 502-504. <https://doi.org/10.1023/A:1015807413141>
- (212) Aycock, D. F. Solvent Applications of 2-Methyltetrahydrofuran in Organometallic and Biphasic Reactions. *Org. Process Res. Dev.* **2007**, 11 (1), 156-159.
<https://doi.org/10.1021/op060155c>
- (213) Aparicio, S.; Alcalde, R. Characterization of Two Lactones in Liquid Phase: An Experimental and Computational Approach. *Phys. Chem. Chem. Phys.* **2009**, 11 (30),

- 6455-6467. <https://doi.org/10.1039/b823507d>
- (214) Ibrahim, M.; Malik, I.; Mansour, W.; Sharif, M.; Fettouhi, M.; El Ali, B. Efficient N-Heterocyclic Carbene Palladium(II) Catalysts for Carbonylative Suzuki-Miyaura Coupling Reactions Leading to Aryl Ketones and Diketones. *J. Organomet. Chem.* **2018**, 859, 44-51. <https://doi.org/10.1016/J.JORGANCHEM.2018.01.028>
- (215) Beller, M.; Wu, X. F. *Transition Metal Catalyzed Carbonylation Reactions: Carbonylative Activation of C-X Bonds*; Springer-Verlag Berlin Heidelberg, **2013**; Vol. 9783642390. <https://doi.org/10.1007/978-3-642-39016-6>.
- (216) Garcia-Herrero, I.; Cuéllar-Franca, R. M.; Enríquez-Gutiérrez, V. M.; Alvarez-Guerra, M.; Irabien, A.; Azapagic, A. Environmental Assessment of Dimethyl Carbonate Production: Comparison of a Novel Electrosynthesis Route Utilizing CO₂ with a Commercial Oxidative Carbonylation Process. *ACS Sustain. Chem. Eng.* **2016**, 4 (4), 2088-2097. <https://doi.org/10.1021/acssuschemeng.5b01515>
- (217) Fiorani, G.; Perosa, A.; Selva, M. Dimethyl Carbonate: A Versatile Reagent for a Sustainable Valorization of Renewables. *Green Chem.* **2018**, 20, 288-322. <https://doi.org/10.1039/c7gc02118f>
- (218) Liu, H.; Li, Z.; Wang, J.; Lu, S.; Wang, M.; Liu, Y.; Li, C. Carboxylation of Toluene with CO₂-Derived Dimethyl Carbonate over Amorphous Ti-Zr Mixed-Metal Oxide Catalysts. *Chem. Cat. Chem.* **2020**, 12 (1), 95-99. <https://doi.org/10.1002/cctc.201901276>
- (219) Zhou, R.; Niu, Z.; Jia, L.; Liu, J.; Lü, X.; Song, Z. CH₃ONa-Initiated Two-Step Transesterification of DMC (Dimethyl Carbonate) and α,ω -Alkanediol for Poly(Alkylene Carbonate). *Inorg. Chem. Commun.* **2018**, 90, 82-85. <https://doi.org/10.1016/j.inoche.2018.02.017>
- (220) NIH. (2020) TRIMETOZINE. Available at: <https://drugs.ncats.io/drug/31EPT7G9PL>. [Accessed February 2020]
- (221) Hosni Z.; Rajoub N.; Houson I.; Nordon A.; Benyahia B.; Florence A. Autonomous Control and Dynamics Simulation of a 3-Stages Countercurrent Liquid-Liquid Extraction: Trimetozine Purification as a Case Study. *ChemRxiv. Preprint.* **2019**. <https://doi.org/10.26434/chemrxiv.9542378.v1>
- (222) Holtmann, G.; Talley, N. J.; Liebrechts, T.; Adam, B.; Parow, C. A Placebo-Controlled Trial of Itopride in Functional Dyspepsia. *N. Engl. J. Med.* **2006**, 354 (8), 832-840. <https://doi.org/10.1056/NEJMoa052639>

- (223) DrugBank. (2020) Itopride.
Available at: <https://www.drugbank.ca/drugs/DB04924>. [Accessed February 2020]
- (224) Mushiroda, T.; Douya, R.; Takahara, E.; Nagata, O. The Involvement of Flavin-Containing Monooxygenase but Not CYP3A4 in Metabolism of Itopride Hydrochloride, a Gastroprokinetic Agent: Comparison with Cisapride and Mosapride Citrate. *Drug Metab. Dispos.* **2000**, 28 (10), 1231-1237. <https://pubmed.ncbi.nlm.nih.gov/10997945>
- (225) Burhardt, M. N.; Taaning, R.; Nielsen, N. C.; Skrydstrup, T. Isotope-Labeling of the Fibril Binding Compound FSB via a Pd-Catalyzed Double Alkoxyacylation. *J. Org. Chem.* **2012**, 77 (12), 5357-5363. <https://doi.org/10.1021/jo300746x>
- (226) Đud, M.; Briš, A.; Jušinski, I.; Gracin, D.; Margetić, D. Mechanochemical Friedel–Crafts Acylations. *Beilstein J. Org. Chem.* **2019**, 15 (1), 1313–1320.
<https://doi.org/10.3762/bjoc.15.130>
- (227) Chakiri, A. B.; Hodge, P. Synthesis of Isopropyl-Substituted Anthraquinones via Friedel–Crafts Acylations: Migration of Isopropyl Groups. *R. Soc. Open Sci.* **2017**, 4 (8), 170451. <https://doi.org/10.1098/rsos.170451>
- (228) Veerman, J.; Van Den Bergh, T.; Orrling, K. M.; Jansen, C.; Cos, P.; Maes, L.; Chatelain, E.; Ioset, J. R.; Edink, E. E.; Tenor, H.; Seebeck, T.; De Esch, I.; Leurs, R.; Sterk, G. J. Synthesis and Evaluation of Analogs of the Phenylpyridazinone NPD-001 as Potent Trypanosomal TbrPDEB1 Phosphodiesterase Inhibitors and in Vitro Trypanocidals. *Bioorganic Med. Chem.* **2016**, 24 (7), 1573–1581.
<https://doi.org/10.1016/j.bmc.2016.02.032>
- (229) Al-Jaroudi, Z.; Mohapatra, P. P.; Jha, A. Facile Synthesis of 3-Substituted Isoindolinones Dedicated to the Memory of Professor Sharon Roscoe, a Colleague and Mentor Instrumental in Shaping the Careers of Many Chemists. *Tetrahedron Lett.* **2016**, 57 (7), 772–777. <https://doi.org/10.1016/j.tetlet.2016.01.021>

Paper I

**A focused fragment library targeting the antibiotic resistance enzyme -
Oxacillinase-48: Synthesis, structural evaluation and inhibitor design**

Sundus Ahkter, Bjarte Aarmo Lund, **Aya Ismael**, Manuel Langer, Johan Isaksson, Tony Christopeit, Hanna-Kirsti Schrøder Leiros, Annette Bayer.

Eur. J. Med. Chem., **2018**, *145*, 634–648. DOI: [10.1016/j.ejmech.2017.12.085](https://doi.org/10.1016/j.ejmech.2017.12.085).

Only the synthesis supporting information of this paper is included. Biological and structural information can be found on the webpages of the publisher.



Research paper

A focused fragment library targeting the antibiotic resistance enzyme - Oxacillinase-48: Synthesis, structural evaluation and inhibitor design

Sundus Akhter^{a,1}, Bjarte Aarmo Lund^{b,1}, Aya Ismael^a, Manuel Langer^a, Johan Isaksson^a, Tony Christopheit^b, Hanna-Kirsti S. Leiros^{b,**}, Annette Bayer^{a,*}^a Department of Chemistry, Faculty of Science and Technology, UiT-The Arctic University of Norway, N-9037 Tromsø, Norway^b The Norwegian Structural Biology Centre (NorStruct), Department of Chemistry, Faculty of Science and Technology, UiT-The Arctic University of Norway, N-9037 Tromsø, Norway

ARTICLE INFO

Article history:

Received 6 July 2017

Received in revised form

24 December 2017

Accepted 26 December 2017

Available online 30 December 2017

Keywords:

Crystal structure

Inhibition properties

Benzoic acid derivatives

Serine-β-lactamase inhibitors

Fragments

Structure-guided drug design

ABSTRACT

β-Lactam antibiotics are of utmost importance when treating bacterial infections in the medical community. However, currently their utility is threatened by the emergence and spread of β-lactam resistance. The most prevalent resistance mechanism to β-lactam antibiotics is expression of β-lactamase enzymes. One way to overcome resistance caused by β-lactamases, is the development of β-lactamase inhibitors and today several β-lactamase inhibitors e.g. avibactam, are approved in the clinic. Our focus is the oxacillinase-48 (OXA-48), an enzyme reported to spread rapidly across the world and commonly identified in *Escherichia coli* and *Klebsiella pneumoniae*. To guide inhibitor design, we used diversely substituted 3-aryl and 3-heteroaryl benzoic acids to probe the active site of OXA-48 for useful enzyme-inhibitor interactions. In the presented study, a focused fragment library containing 49 3-substituted benzoic acid derivatives were synthesised and biochemically characterized. Based on crystallographic data from 33 fragment-enzyme complexes, the fragments could be classified into R¹ or R² binders by their overall binding conformation in relation to the binding of the R¹ and R² side groups of imipenem. Moreover, binding interactions attractive for future inhibitor design were found and their usefulness explored by the rational design and evaluation of merged inhibitors from orthogonally binding fragments. The best inhibitors among the resulting 3,5-disubstituted benzoic acids showed inhibitory potential in the low micromolar range (IC₅₀ = 2.9 μM). For these inhibitors, the complex X-ray structures revealed non-covalent binding to Arg250, Arg214 and Tyr211 in the active site and the interactions observed with the mono-substituted fragments were also identified in the merged structures.

© 2018 Elsevier Masson SAS. All rights reserved.

1. Introduction

Years of overuse of antibiotics have selected for antibiotic resistant strains [1], and today medical personnel are frequently forced to administer last-resort antibiotics. However, the number of cases where last-resort antibiotics fail in treatment are

increasing [2] and deaths due to antibiotic resistant infections are expected to surpass cancer deaths by 2050 [3]. Bacterial resistance towards clinically important β-lactam antibiotics [4] like penicillins, cephalosporins and carbapenems originates most often from the occurrence of β-lactam-hydrolysing enzymes – the β-lactamases.

The β-lactamase enzymes are of ancient origin [5] and today over 2600 enzymes spanning four classes of β-lactamases are known [6–8]. β-Lactamases are grouped into two super families based on the enzyme mechanism for β-lactam hydrolysis: the serine dependent β-lactamases (SBLs; Amber class A, C, and D) and metallo-β-lactamases (MBLs; Amber class B) [7,9]. SBLs are characterized by a serine residue in the active site, while MBLs require a metal co-factor, usually one or two zinc ions, for enzyme activity. This work focuses on the class D SBLs – also called oxacillinases (OXAs) – and in particular on the oxacillinase-48 (OXA-48).

Abbreviations: DMSO, dimethyl sulfoxide; OXA, oxacillinase; IC₅₀, half maximal inhibitory concentration; LE, ligand efficiency; MBL, metallo-β-lactamase; NMR, nuclear magnetic resonance; SBL, serine-β-lactamase; SPR, surface plasmon resonance.

* Corresponding author.

** Corresponding author.

E-mail addresses: hanna-kirsti.leiros@uit.no (H.-K.S. Leiros), annette.bayer@uit.no (A. Bayer).¹ These authors have contributed equally to this work.

The class D SBLs are characterized by a hydrophobic environment in the active site, that facilitates the carboxylation of a lysine residue. The *N*-carboxylated lysine plays a critical role in the substrate hydrolysis [10]. Originally, the OXAs were believed to have a limited substrate profile only hydrolysing penicillins, but with the emergence of carbapenem-hydrolysing OXA variants, e.g. OXA-23, OXA-24 and OXA-48, their clinical relevance has increased [11]. OXA-48 was reported for the first time in 2001 and has since then spread rapidly across the world [11]. It is commonly identified in *Escherichia coli* and *Klebsiella pneumoniae*.

One strategy to circumvent resistance in β -lactamase producing pathogens is the use of β -lactamase inhibitors [4,12] in combination with the β -lactam antibiotic. Inhibitors of class A SBLs like clavulanic acid, sulbactam and tazobactam became clinically available from the 1980s [13], but only a few class D β -lactamases are inhibited by these β -lactamase inhibitors e.g. OXA-2 and OXA-18 [14]. In 2015, a new SBL inhibitor, avibactam, targeting class A, C and some class D SBLs, including OXA-48, was approved by the FDA for treatment of complicated urinary tract and intra-abdominal infections [15]. However, the inhibition level of different class D β -lactamases by avibactam varies [16,17]. With the first reports of resistance to avibactam published [18], one can speculate that it will only be a matter of time before class D β -lactamases show resistance to avibactam as well.

The development of new OXA inhibitors, either with a different enzyme-inhibition profile compared to existing inhibitors, or as alternative when resistance to existing inhibitors arises, is of importance. We have previously reported a fragment-based screening approach to identify weak inhibitors of OXA-48 [19]. The most interesting hit was 3-(pyridin-4-yl)benzoic acid **1** with an IC_{50} of 250 μ M and a ligand efficiency (LE) of 0.32. Crystallographic data from enzyme-fragment complexes indicated two overlapping binding conformations of the fragment. Merging of the two conformations of **1** into one molecule **2** (Fig. 1) gave a 10-fold increase in binding affinity improving the IC_{50} from 250 μ M to 18 μ M [19].

In this study, we describe the use of small mono-substituted fragments - analogues of fragment **1** - as probes to explore the OXA-48 binding site. The aim was to identify fragment-enzyme interactions in the two alternate binding pockets of the active site of OXA-48, which could be of general interest for the design of OXA-48 inhibitors. We wanted to exploit the ability of small fragments to efficiently explore the binding pocket as they are less restricted by size and more flexible compared to more elaborated inhibitors. Moreover, the smaller fragments generally have the advantage of being more easily prepared making the discovery process more work-efficient. Furthermore, we wanted to translate the knowledge gained into the rational design of di-substituted inhibitors related to compound **2** circumventing the laborious preparation of a large library of elaborated inhibitors.

Towards this goal, we prepared a focused fragment library containing 3-aryl benzoic acids decorated with a wide range of polar groups and a number of 3-heteroaryl benzoic acid derivatives. In total 49 fragments were tested for inhibitory activity against OXA-48 and the binding conformations of 33 fragment-enzyme complexes were analyzed by X-ray crystallography. Based on the structural information, fragments could be classified according to their preferred binding pocket and useful fragment-enzyme interactions e.g. hydrogen bonds were identified. Moreover, several new orthogonally binding fragments were found leading to the design of symmetrically and unsymmetrically di-substituted inhibitors with improved IC_{50} in the low micromolar range. The structural data from enzyme-inhibitor complexes was compared with enzyme-fragment complexes.

2. Results and discussion

2.1. Synthesis

2.1.1. Synthesis of 3-substituted benzoic acids

A fragment library containing 49 3-substituted benzoic acid analogues **3a–35** was prepared (Table 1). The fragments generally fulfilled the demands of libraries for fragment-based ligand design (MW < 300, clogP < 3, hydrogen bond acceptor/donors < 3) [20]. For the synthesis, a strategy based on the Suzuki-Miyaura (SM) cross-coupling reaction to join two sp^2 -hybridized carbons was employed [21]. Two alternate coupling strategies were successful starting with either 3-bromobenzoic acid (Table 1, strategy A) or 3-carboxyphenylboronic acid pinacol ester (Table 1, strategy B) as starting materials allowing for the utilisation of a wide range of aryl boronic acids or aryl bromides to introduce diversity in the library.

Many of the required aryl boronic acids and bromides were commercial available, while the aryl bromides used as starting materials for fragments **17–20**, **24**, **29** and **30** were prepared according to standard acylation and sulphonylation protocols. The NH-tetrazol-5-yl-substituted arylbromides (starting material for fragments **26a** and **26b**) were prepared by a [3 + 2] intermolecular cycloaddition of 3- or 4-bromobenzonitrile with trimethyl silyl azide in the presence of dibutyltin oxide in anhydrous 1,4-dioxane. The reaction mixture was subjected to microwave irradiation in a tightly sealed vessel for 50 min at 150 °C to afford 3- or 4-bromobenzotetrazole in 86% and 82% yield, respectively.

In general, couplings under standard aqueous conditions using $PdCl_2(PPh_3)_2$ as catalyst (5–10 mol%), K_3PO_4 as base (5 equiv.) in dioxane/water gave good yields. The couplings leading to fragments **9**, **17–20** and **22–24** were not successful under these standard conditions. More efficient catalysts (XPhos-Pd G2 or $PdCl_2(dppf)$) and water-free conditions (anhydrous THF instead of dioxane/water) were successfully employed to solve reactivity and solubility problems and to prevent hydrolysis for base sensitive products (**9** and **24**). However, for some products (**19a**, **19b** and **20**) the yields were still low (<20%). Generally, the reactions were easily purified by automated C18 flash chromatography to provide compounds of high purity (>95% as determined by UHPLC). For some compounds (**15**, **16**, **19**, **23**, **24**, **32** and **34**), additional silica flash chromatography was necessary to provide sufficiently pure products.

2.1.2. Synthesis of 3,5-disubstituted benzoic acid derivatives

To study inhibitor properties like activity and enzyme interactions of merged fragments, a small series of symmetrical and unsymmetrical 3,5-disubstituted benzoic acids was designed (*vide infra*) and prepared. The synthesis of symmetrical 3,5-disubstituted compounds **36** and **38** was achieved under the conditions established for the coupling of mono-substituted fragments using $Pd_2(dba)_3/XPhos$ or XPhos-Pd G2 as catalysts (Scheme 1) [19]. The di-substituted coupling products **36** and **38** were obtained from 3,5-dibromobenzoic acid as starting material and an increased amount of the boronic acid derivative (2 equiv.) in 54% and 65% yield, respectively. Compound **37** was isolated in 11% yield as by-product in an attempt to selectively mono-substituted 3,5-dibromobenzoic acid (*vide infra*).

For the synthesis of unsymmetrical 3,5-disubstituted benzoic acids **39**, the sequential addition of two different aryl boronic acids under the previously established conditions gave only 15% isolated yield (Scheme 2). In addition, the procedure involved tedious HPLC purifications as the reaction mixture was difficult to purify due to occurrence of symmetrical by-products with similar properties. To improve the selectivity of the reaction, we changed the starting material from 3,5-dibromobenzoic acid to 3-iodo-5-bromobenzoic

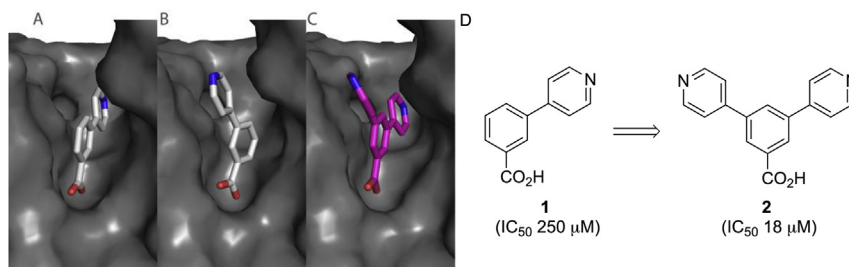


Fig. 1. The two alternate conformations of fragment **1** (light grey) in complex with OXA-48 (dark grey surface) (A and B), the merged compound **2** (pink) in complex with OXA-48 (dark grey surface) (C), and a schematic view of the merging approach described in previous work (D) [19]. (For interpretation of the references to color in this figure legend, the reader is referred to the Web version of this article.)

acid in order to take advantage of the faster coupling reaction of aryl iodides when compared with aryl bromides and thereby to prevent formation of symmetrical disubstituted by-products (Scheme 2). Investigation of the chemoselective coupling of 3-iodo-5-bromobenzoic acid with quinolin-6-ylboronic acid pinacol ester to form mono-substituted **int-40** showed that a second, unwanted coupling was not easily prevented and a careful fine tuning of catalyst (RuPhos-Pd G3, XantPhos-Pd G3, SPhos/Pd₂ (dba)₃, Xphos/Pd₂ (dba)₃, SPhos-Pd G3, XPhos-Pd G2, Pd₂ (dppf)Cl₂), solvent (toluene/water, anhydrous THF, dioxane/water, *tert*-butanol), reaction temperature (40–80 °C) and time (10–48 h) was initiated (Table S11, see Supporting information). The composition of the crude reaction mixtures with respect to mono- and disubstituted products as well as unreacted starting material was determined by mass spectrometry (MS). The most chemoselective catalysts were XantPhos-Pd G3, Pd₂ (dppf)Cl₂ and SPhos/Pd₂ (dba)₃ showing good selectivity for the aryl iodide when the reaction was performed with K₃PO₄ as base in dioxane/water at 60 °C for 24 h (Scheme 2). At this conditions with SPhos/Pd₂ (dba)₃ as catalyst, the mono-substituted intermediate **int-40** was obtained as main product together with small amounts of the disubstituted by-product (8–10%). Careful purification to remove any traces of the disubstituted compound provided **int-40** in moderate yield (45%). The mono-substituted **int-40** was further subjected to a second coupling with XPhos-Pd G2 (5 mol%) as catalyst to provide **40** in good yields (90%).

2.2. Evaluation of 3-substituted benzoic acids

2.2.1. Inhibitor activity of 3-substituted benzoic acids

The mono-substituted fragments **3–35** were initially investigated for their inhibitory activity against OXA-48 in an enzymatic assay and by SPR. Inhibition and binding data are given in Table 1 along with the associated ligand efficiencies (LE). The original hit fragment **1** had an IC₅₀ of 250 μM and an LE of 0.32. Most of the fragments in this study showed inhibition at a similar level with IC₅₀ > 200 μM and LE ≤ 0.30. Fragments **4a** (IC₅₀ (μM)/LE: 50/0.38), **18** (IC₅₀ (μM)/LE: 60/0.24), **21a** (IC₅₀ (μM)/LE: 35/0.33), **26b** (IC₅₀ (μM)/LE: 36/0.30) and **35** (IC₅₀ (μM)/LE: 35/0.42) showed an order of magnitude stronger inhibition and were the most potent fragments. Even though there are some discrepancies between the inhibition and binding data, the same trends are maintained when comparing similar compounds, indicating that the compounds indeed bind specifically to one site of the enzyme.

2.2.2. Structural analysis of 3-substituted benzoic acids

To evaluate the binding poses of our fragments, enzyme-fragment complexes for x-ray crystallographic analysis were prepared. Rewardingly, 33 out of 49 fragments were successfully soaked with OXA-48 and yielded crystal structures with resolution

high enough to warrant placement of the inhibitor in the electron density (Table 1). In addition, a crystal structure of OXA-48 in complex with the substrate imipenem was obtained to better understand substrate binding and to compare substrate and fragment binding interactions.

The crystal structure of the acyl-enzyme complex of OXA-48 with imipenem (Fig. 2A) revealed a conformation close to previously observed conformations with OXA-13 (PDB-ID: 1h5x). In the complex the ring-opened imipenem was bound to OXA-48 covalently with continuous electron density from the hydroxyl group of Ser70. There was an ionic bond from the carboxylate group of imipenem to the guanidine group of Arg250. The carbonyl-group of the now ring-opened β-lactam ring was positioned in the oxyanion-hole forming hydrogen bonds to the main chain amides of Tyr211 and Ser70. The 6α-hydroxyethyl group (R¹) of imipenem was positioned towards the hydrophobic residues Trp105, Val120 and Leu158 and in the following discussion this region will be called the R¹ site. The amidine group (R²) was situated in the cleft defined by Ile102, Tyr211, Leu247 and Thr213 and this region will be called the R² site. The R¹ and R² side chains of imipenem (Fig. 2A) had the same overall directions as the pyridinyl substituents in the two overlapping binding conformations observed with our initial hit 3-pyridin-4-ylbenzoic acid **1** [19].

In all our structures of OXA-48 in complex with fragments, an ionic bond between the carboxylate group of the fragments and the guanidine group of Arg250 was observed, which resembled the interaction of the carboxylate group of imipenem or the sulfamate group of avibactam with Arg250 [17,22]. In some cases, the carboxylate group was oriented in such a way that also Thr209 (fragments **9b**, **28**, **35**), Lys208 (fragment **34**) or both (fragment **26a**) participated in binding.

Another common feature found in almost all crystal structures, except for fragments **21a** and **26b**, was a π-π stacking interaction of the 3-aryl substituents attached to the benzoic acid scaffold with Tyr211. This is consistent with the binding of imipenem, where the R₂ side chain was oriented towards Tyr211 (Fig. 2C). The importance of Tyr211 as a non-polar patch that contributes in binding substrate side-chains has been recognised before [23]. We also observed this interaction with our unsubstituted pyridyl benzoic acids previously [19].

The weaker binding fragments (**3a**, **3b**, **4a–c**, **5**, **6a–c**, **8a–c**, **9b**, **11b**, **12a**, **13**, **14**, **17**, **24**) all bound in nearly the same conformation with the ionic bond of the benzoic acid and Arg250 and the π-π stacking interaction with Tyr211 as major interactions. In these structures, the 3-aryl substituent on the benzoic acid was directed towards the R₂ pocket (Fig. 2C). Only minor conformational differences were observed as described in the following. To help the reader in the following discussion, we will describe the fragments by the identity of the Ar groups (Table 1), as the structural differences of the fragments relate to this group *i.e.* 3-(2-methyl)

Table 1
Preparation strategy and inhibitor activities of a library of 3-substituted benzoic acids analogues against OXA-48 (IC₅₀, K_D and LE).

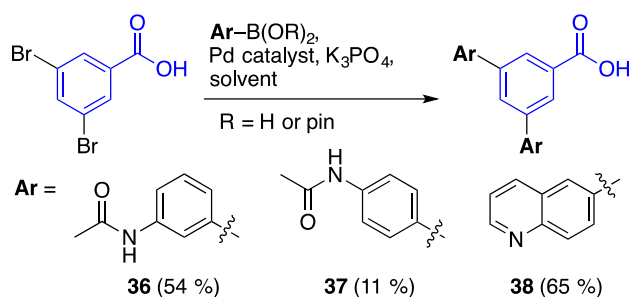
| Comp. ID | Ar = | Strateg. Yield | IC ₅₀ (μM) | K _D (μM) | LE ^d | Comp. ID | Ar = | Strateg. Yield | IC ₅₀ (μM) | K _D (μM) | LE ^d |
|----------|------|-----------------------|-----------------------|---------------------|-----------------|----------|------|-----------------------|-----------------------|---------------------|-----------------|
| 3a* | | B 78% | 90 | 170 | 0.35 | 11b* | | A 97% | 180 | 350 | 0.29 |
| 3b* | | B 67% | 170 | 300 | 0.33 | 12a* | | A 82% | 120 | 150 | 0.29 |
| 4a* | | A 94% | 50 | 175 | 0.38 | 12b | | A 90% | 380 | 361 | 0.25 |
| 4b* | | A 98% | 110 | 110 | 0.35 | 13* | | B 35% | 330 | 330 | 0.29 |
| 4c* | | A 39% | 470 | 170 | 0.29 | 14* | | A 95% | 390 | 220 | 0.27 |
| 5* | | A 84% | 900 | 230 | 0.25 | 15a | | B 36% | 600 | 800 | 0.27 |
| 6a* | | A 98% | 250 | 123 | 0.30 | 15b | | B 86% | 1400 | 550 | 0.23 |
| 6b* | | A 98% | 360 | 226 | 0.28 | 16a | | B 15% | 110 | 300 | 0.31 |
| 6c* | | A 86% | 150 | 250 | 0.31 | 16b | | B 67% | 1000 | 970 | 0.23 |
| 7 | | A 91% | 400 | 1000 | 0.28 | 17* | | B ^{a, c} 41% | 370 | 100 | 0.24 |
| 8a* | | A 68% | 130 | 170 | 0.34 | 18 | | B ^{a, c} 65% | 60 | 210 | 0.24 |
| 8b* | | A 98% | 130 | 240 | 0.34 | 19a | | B ^{a, c} 26% | 110 | 110 | 0.26 |
| 8c* | | A 78% | 360 | 312 | 0.30 | 19b | | B ^{a, c} 10% | 450 | 240 | 0.22 |
| 9a | | A ^{a, c} 57% | 210 | 200 | 0.27 | 20 | | B ^{a, c} 11% | 370 | 200 | 0.22 |
| 9b* | | A 54% | 260 | 144 | 0.26 | 21a* | | A 98% | 35 | 100 | 0.33 |
| 10 | | A 98% | 380 | 280 | 0.27 | 21b* | | A 98% | 450 | 290 | 0.25 |
| 11a | | A 98% | 260 | 220 | 0.28 | 22 | | B ^{a, b} 87% | 130 | 130 | 0.27 |
| 23a | | B ^{a, c} 46% | 230 | 170 | 0.24 | 29 | | B 36% | 170 | 130 | 0.33 |
| 23b | | B ^{a, c} 34% | 520 | 190 | 0.22 | 30 | | B 45% | 800 | 900 | 0.29 |

(continued on next page)

Table 1 (continued)

| Comp. ID | Ar = | Strateg. Yield | IC ₅₀ (μM) | K _D (μM) | LE ^d | Comp. ID | Ar = | Strateg. Yield | IC ₅₀ (μM) | K _D (μM) | LE ^d |
|----------|------|------------------------|-----------------------|---------------------|-----------------|----------|------|----------------|-----------------------|---------------------|-----------------|
| 24* | | A ^a , b 34% | 250 | 140 | 0.25 | 31 | | B 67% | 350 | 113 | 0.28 |
| 25 | | B 15% | 1300 | >1000 | 0.20 | 32 | | A 6% | 500 | 590 | 0.31 |
| 26a* | | B 98% | 60 | 70 | 0.30 | 33 | | B 24% | 800 | 900 | 0.31 |
| 26b | | B 98% | 36 | 70 | 0.30 | 34 | | B 20% | 310 | 400 | 0.27 |
| 27* | | B 67% | 110 | 400 | 0.30 | 35* | | A 98% | 35 | 159 | 0.42 |
| 28* | | B 87% | 240 | 160 | 0.27 | | | | | | |

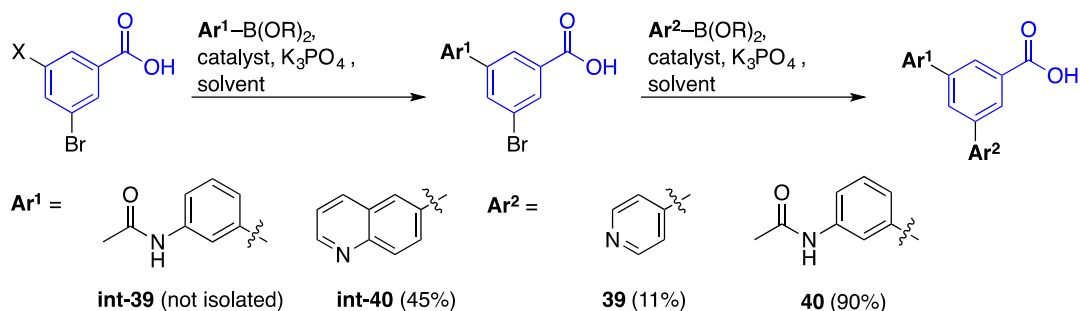
*X-ray structure of fragment-enzyme complex available. ^a Reaction in anhydrous THF instead of dioxane:water as solvent; ^b XPhos-Pd G2 as catalyst instead of PdCl₂(PPh₃)₂; ^c PdCl₂(dppf) as catalyst instead of PdCl₂(PPh₃)₂. ^d LE = (-1.4 * log₁₀IC₅₀)/HeavyAtomCount, with units kcal/(mol per heavy atom).



Scheme 1. Preparation of symmetrical 3,5-disubstituted benzoic acids. Reagents and conditions: **36**: 3-acetamidophenylboronic acid (1.5 equiv.), Pd₂(dba)₃•CHCl₃ (5 mol%), XPhos (5 mol%), dioxane:water (1:1), 60 °C, 54%; **37**: 4-acetamidophenylboronic acid (0.75 equiv.), PdCl₂(PPh₃)₂ (10 mol%), dioxane:water (1:1), 95 °C, 11%; **38**: quinolin-6-ylboronic acid pinacol ester (2.0 equiv.), XPhos-Pd G2 (5 mol%), *tert*-butanol, 60 °C, 65%.

phenylbenzoic acid **3a** will be described as 2-methylphenyl substituted fragment.

The methylphenyl substituted fragments **3a** (IC₅₀ (μM)/LE: 90/0.35) and **3b** (IC₅₀ (μM)/LE: 170/0.33) had similar conformations, however, the 2-methyl group in **3a** was facing towards the hydrophobic C^β of Ser244 explaining the more favourable binding.



Scheme 2. Preparation of unsymmetrical 3,5-disubstituted benzoic acids. Reagents and conditions: **39**: i. X = Br, 3-acetamidophenylboronic acid (0.75 equiv.), PdCl₂(PPh₃)₂ (10 mol%), dioxane:water (1:1), 60 °C; ii. pyridin-4-ylboronic acid (1.2 equiv.), PdCl₂(PPh₃)₂ (10 mol%), dioxane:water (1:1), 60 °C; **int-40**: X = I, quinolin-6-ylboronic acid pinacol ester (2.0 equiv.), Pd₂(dba)₃•CHCl₃ (5 mol%), SPhos (5 mol%), dioxane:water (1:1), 60 °C; **40**: 3-acetamidophenylboronic acid (1.5 equiv.), XPhos-Pd G2 (5 mol%), *tert*-BuOH, 60 °C.

Fragments **4a–c** (IC₅₀ (μM)/LE: 50/0.38, 110/0.35 and 470/0.29, respectively) also had very similar conformations, but again we saw that more favourable van der Waals interactions gave higher affinity for the 2-hydroxyphenyl substituted **4a**. The 4-hydroxy isomer **4c** had an unfavourable solvent exposure of the hydroxyl group. Adding a methylene bridge yielding 3-hydroxymethylphenyl **5** (IC₅₀ (μM)/LE: 900/0.25) did not lead to any favourable interactions. The methoxyphenyl fragments **6a–c** (IC₅₀ (μM)/LE: 250/0.30, 360/0.28 and 150/0.31) shared the canonical R² binding pose. The methoxy group of the 2-substituted **6a** appeared more shielded from solvent exposure than in **6b** and **6c**, yet the methoxy group did not seem to make any strong contacts. The weak inhibition seen with methyl thioether **7** (IC₅₀ (μM)/LE: 400/0.28) corresponded to the results observed with the methoxy ethers **6**. The fluorophenyl substituted **8a–c** (IC₅₀ (μM)/LE: 130/0.34, 130/0.34 and 360/0.30) had nearly identical binding poses. The 4-substituted **8c** gave the highest IC₅₀ value, most likely due to the solvent exposed fluorine. The 2-substituted **8a** seemed more favourable based on the decreased solvent exposure of the fluorine atom, however, the difference to **8b** was negligible only observed by SPR.

The methoxyacetylphenyl esters **9a** and **9b** (IC₅₀ (μM)/LE: 210/0.27 and 260/0.26) showed no clear additional interactions in the complex structures with OXA-48, and the methyl group appeared to be unfavourably exposed to the solvent. The corresponding 4-

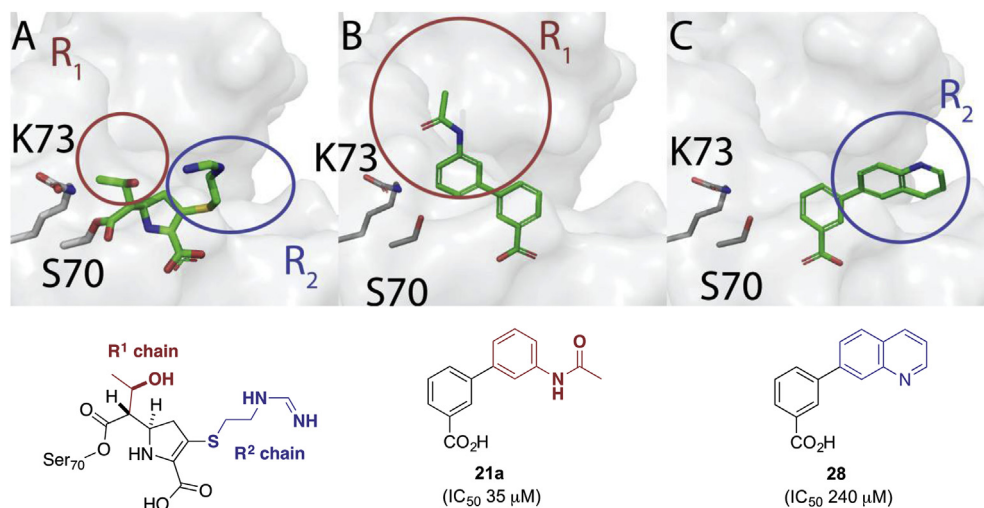


Fig. 2. The crystal structure of imipenem in complex with OXA-48 (A) shows that the two side chains of imipenem extends in separate directions. The carbapenem substrates of OXA-48 have small R¹ side chains. We were however able to fit larger groups in the R¹ site like the N-acetamide substituted phenyl ring in compound **21a** (B). Yet, most of the tested 3-substituted benzoic acids bind towards the larger R² site, like the quinolin-7-yl substituted compound **28** (C).

acetylphenyl substituted **10** (IC₅₀ (μM)/LE: 380/0.27) and carbamoylphenyl substituted **11a** and **11b** (IC₅₀ (μM)/LE: 260/0.28 and 180/0.29) gave generally weak inhibition indicating that a carbonyl group attached to the aromatic ring was not contributing to binding. No complex structures are available for **10** and **11a**, but the complex structure of 4-carbamoylphenyl **11b** was similar in conformation to the esters **9a** and **9b**. Slightly tighter binding was observed with the *meta*-substituted sulfone **12a** (IC₅₀ (μM)/LE: 120/0.29), which also shares the same overall conformation.

The 4-aminophenyl substituent of **13** (IC₅₀ (μM)/LE: 330/0.30) did not appear to make any interaction with the enzyme, and the inhibition was weak. The complex structure of the corresponding *N,N*-dimethyl-4-aminophenyl substituted **14** (IC₅₀ (μM)/LE: 390/0.27) showed that the two methyl groups are solvent exposed, and this is reflected in the poor inhibition by this compound. Similar to the complex structure of **14**, the methyl 4-sulfonamidophenyl group of **17** (IC₅₀ (μM)/LE: 370/0.24) was seemingly pushed out of the active site and appears completely exposed to the solvent. The larger phenyl 4-sulfonamidophenyl substituted fragment **18** (IC₅₀ (μM)/LE: 60/0.24) showed lower IC₅₀ values probably driven by the increase in hydrophobicity, and no complex structure was obtained.

The corresponding 4-acetamidophenyl **21b** (IC₅₀ (μM)/LE: 450/0.25) showed weak inhibition, likely due to the solvent exposure of the hydrophobic methyl group. The 3-acetamidophenyl containing fragment **21a** (Fig. 3), however, showed a 10-fold increased inhibition (IC₅₀ (μM)/LE: 35/0.33). The complex structure of OXA-48 with fragment **21a** revealed that the carbonyl of the acetyl formed a hydrogen bond to the guanidine group of Arg214, which directs the 3-acetamidophenyl substituent to the R¹ site (Fig. 2B) and lead to a T-shaped π-π-stacking interaction of the 3-acetamidophenyl substituent with Trp105. The π-π stacking of the 3-acetamidophenyl substituent to Tyr211 normally observed with these fragments was not observed; instead Tyr211 interacted with the benzoic acid by T-shaped π-π-stacking. The interaction of an acetamide with Arg214 has been described previously for the avibactam analogue FPI-1523 in complex with OXA-48 (PDB-ID: 5fas) [22].

Encouraged by the results for fragment **21a**, we designed a series of fragments incorporating a hydrocarbon linker between the phenyl ring and the amino, sulfonamido or acetamido groups of **13**, **18** and **21**. The amines **15** and **16**, the sulfonamides **19** and **20**, the

amides **22**, **23a**, **23b** and the acetate **24** are more flexible, thus, increasing the potential of hydrogen bonding. However, none of these fragments showed substantially improved binding (IC₅₀: 110–1000; LE: 0.19–0.30). Moreover, the crystal structures of the amides **22**, **23a**, **23b** and the acetate **24** (IC₅₀ (μM)/LE: 230/0.24, 520/0.22 and 250/0.25) did not show any specific interactions for the functional groups.

In fragments **26a** and **26b** NH-tetrazole substituted phenyl rings were investigated as Ar substituents. Introducing the weakly acidic tetrazol-5-ylphenyl substituent in either 3-position **26a** (IC₅₀ (μM)/LE: 60/0.30) or 4-position **26b** (IC₅₀ (μM)/LE: 36/0.30) yielded good binding for both fragments. However, the binding poses for the two compounds were very different. The 3-tetrazol-5-ylphenyl substituted **26a** bound in two alternate positions. The π-π-stacking with Tyr211 was maintained for both conformations, but the tetrazoles appeared completely solvent exposed with no interactions with the enzyme. The 4-tetrazol-5-ylphenyl substituted **26b** formed a hydrogen bond with the guanidine group of Arg214 (Fig. 4), interrupting the π-π-stacking with Tyr211. Fragment **26b** occupied the R¹ site rather than the more common R² site.

A number of heterocyclic aryl substituents were also evaluated (fragments **25**, **28–35**). With some exceptions of the pyridinyls **29** and **35** (IC₅₀ (μM)/LE: 170/0.33 and 35/0.42) most of these fragments showed only weak inhibition. The quinolin-7-yl substituted fragment **28** (IC₅₀ (μM)/LE: 240/0.30) did maintain the overall conformation of the previous R² binding fragments (Fig. 5), and so did the corresponding naphthalen-2-yl substituted fragment **27** (IC₅₀ (μM)/LE: 110/0.29). In the same manner the indol-5-yl substituted fragment **34** (IC₅₀ (μM)/LE: 310/0.27) did show acceptable binding, yet no specific interaction except for the π-stacking with Tyr211. In our previous paper, we investigated pyridin-4-yl and pyridin-3-yl substituted fragments [19], and both inhibited OXA-48 with the same potency (IC₅₀ (μM)/LE: 250/0.32). The pyridin-2-yl substituted fragments **35** (IC₅₀ (μM)/LE: 35/0.41) showed a 10-fold improvement in binding (Fig. 6A and B). In the crystal structure, two alternative conformations were observed (Fig. 6C). One conformation was the canonical with π-stacking of the pyridinyl ring with Tyr211 occupying the R² site (Fig. 6E), but in the other conformation the pyridinyl ring was orientated to the R¹ site. The second conformation showed a hydrogen bond from the protonated N atom in the pyridine ring to the backbone carbonyl of Tyr117,

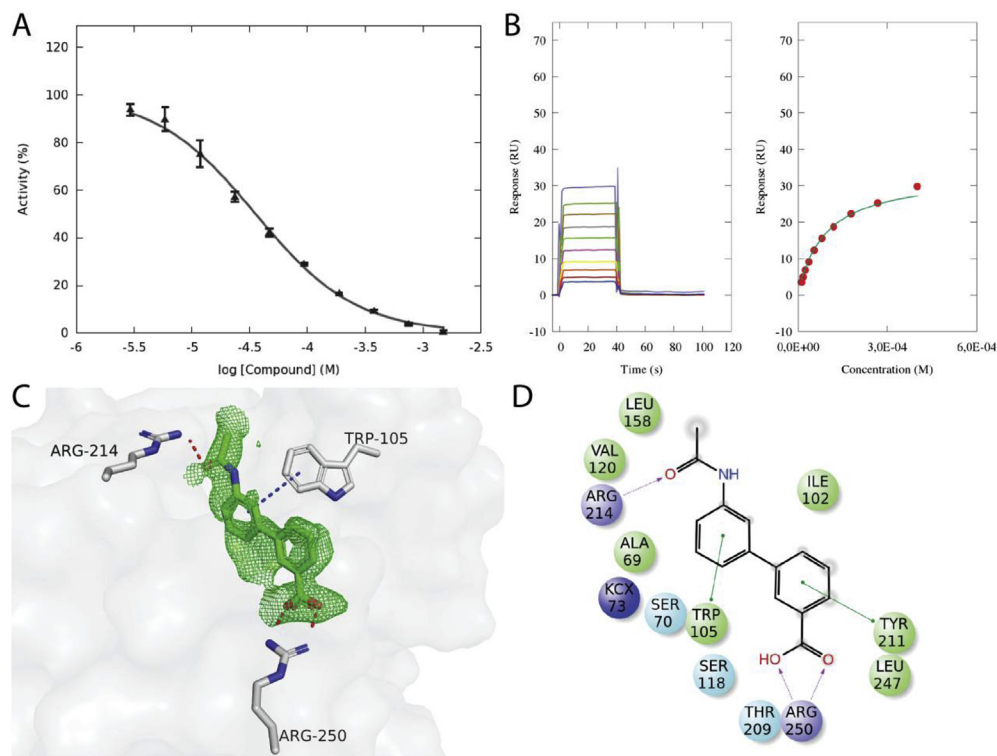


Fig. 3. Compound **21a** was one of the most potent 3-substituted benzoic acid derivatives we found. The IC_{50} -value (A) was determined to be $35 \mu\text{M}$, while the K_d was found to be $100 \mu\text{M}$ (B). The crystal structure of the complex OXA-48:**21a** with an omit-type polder-map (2.5σ) (C) and its 2D-representation (D) shows that the carbonyl of the acetamido-group forms a hydrogen bond with the guanidine of Arg214. The interaction with Arg214 causes the B-ring to move away from Tyr211, introducing a new interaction with Trp105.

which represents a unique interaction for the fragments in the library (Fig. 6D). Only the protonated pyridinyl-nitrogen would be able to form hydrogen bonds to the Tyr117 mainchain, which may explain the slower on/off-rates observed for fragment **35** in the SPR-experiments (Fig. 6B).

In the discussion above most fragments were identified as R^2 binders with fragment **4a** (IC_{50} (μM)/LE: 50/0.38) being the strongest binder among them. For R^2 binders, the edge-to-face π - π -stacking with Tyr211 appears to be an important interaction in accordance with previous analyses [23]. Fragment **35** showed the best ligand efficiency (IC_{50} (μM)/LE: 35/0.42), but could not be classified as a R^1 or R^2 binder as both binding pockets showed useful interactions (Fig. 6C–E). Only two R^1 binders – fragments **21a** and **26b** – were identified, both showing hydrogen bonds with Arg214 as cause for the fragments orientation towards the R^1 site.

2.2.3. NMR studies

In order to evaluate the fragment-enzyme binding in solution, a ^{13}C NMR experiment for OXA-48 was developed based on previous studies [24,25]. OXA enzymes can be selectively carbamylated with bicarbonate at an active site lysine to provide the corresponding carbamic acid [24,26,27]. For OXA-48 the carbamylated residue is Lys73, which is situated in the R^1 site (Fig. 2B). By using ^{13}C -labeled sodium bicarbonate ($\text{NaH}^{13}\text{CO}_3$), a ^{13}C atom was introduced in the R^1 site of OXA-48, which can be used as a reporter probe for fragment binding in ^{13}C NMR studies.

Fragments binding in the R^1 site were expected to change the local environment of the ^{13}C labeled Lys73, which results in a change of the ^{13}C chemical shift of $\text{Lys-NH-}^{13}\text{CO}_2\text{H}$, while ligands binding in the R^2 site are further than $\sim 9 \text{ \AA}$ away from the Lys73 carbamic acid, and are therefore not expected to directly affect the

^{13}C chemical shift.

NMR experiments were performed by equilibrating OXA-48 with ^{13}C -labeled sodium bicarbonate followed by the addition of inhibitor **2** and selected fragments **21a**, **28** and **35** with known binding modes from X-ray analysis. The results are shown in Fig. 7. The ^{13}C NMR spectrum of OXA-48 after equilibration with $\text{NaH}^{13}\text{CO}_3$ showed the carbamate resonance at 163.95 ppm as a broad signal (Fig. 7E), which is in good agreement with the reported chemical shift for carbamylated OXA-48 [28]. In addition, two unassigned signals were observed at 164.04 ppm similar to the results reported for carbamylation of OXA-58 [27]. Here the authors speculated that the unassigned signal may be related to a second carbamylation site [27].

On addition of R^1 binding fragment **21a** and inhibitor **2**, the ^{13}C chemical shifts of the carbamate signal were consistently deshielded in both experiments ($\delta = 164.25$, $\Delta\delta = 0.28$ ppm, Fig. 7E and F). These findings support that the compounds bind competitively in the active site. Moreover, the observed chemical shift perturbation indicates that the compounds occupy the R^1 site as found in the crystal structures. The R^2 binding fragment **28** showed a similar deshielding of the carbamate signal though at a smaller amplitude ($\delta = 164.13$, $\Delta\delta = 0.16$ ppm, Fig. 7D) supporting that the fragment binds in the active site, while fragment **35**, which was identified as R^1 or R^2 binder, only slightly affected the chemical shift ($\delta = 164.00$, $\Delta\delta = 0.04$ ppm, Fig. 7C). The observed chemical shift perturbations for fragments **28** and **35** may indicate that fragment **28** has an effect on carbamylated Lys73, while fragment **35** do not interact with the R^1 site, which is not consistent with the X-ray structures. However, a more detailed study of the NMR conformations would be needed to be conclusive about the binding poses in solution.

The small amplitudes of the observed chemical shift

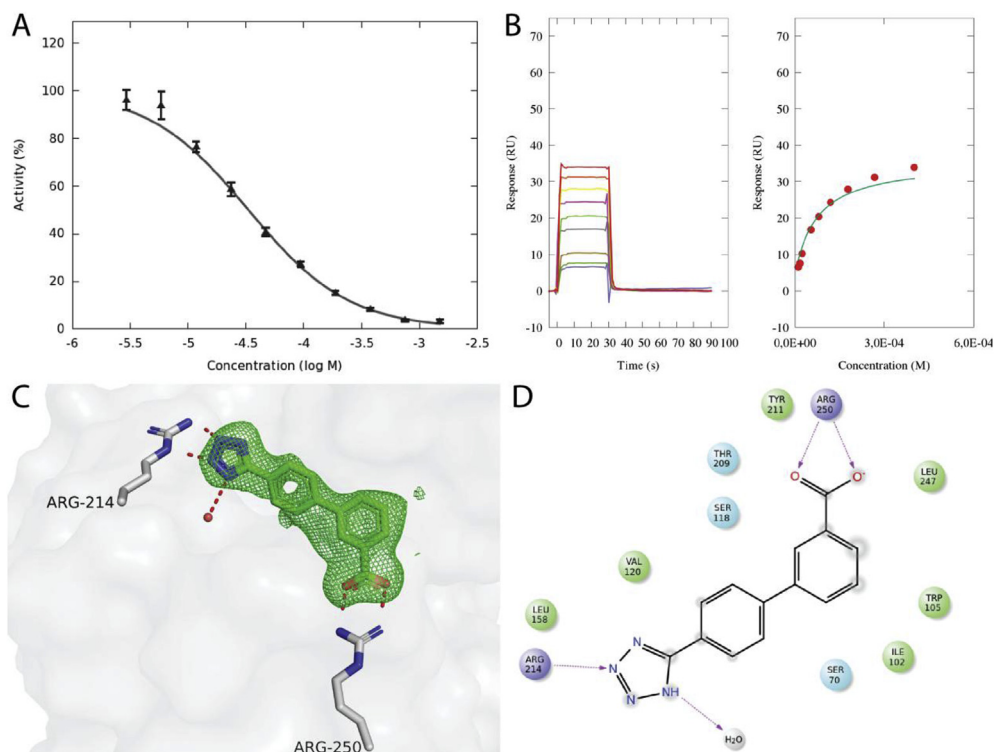


Fig. 4. The IC_{50} -value of compound **26b** (A) was determined to be $36 \mu\text{M}$, while the K_D was found to be $70 \mu\text{M}$ (B). The crystal structure of the complex OXA-48:**26b** with an omit-type polder-map (2.5σ) (C) and a 2D-representation of the protein:compound complex interactions. (D).

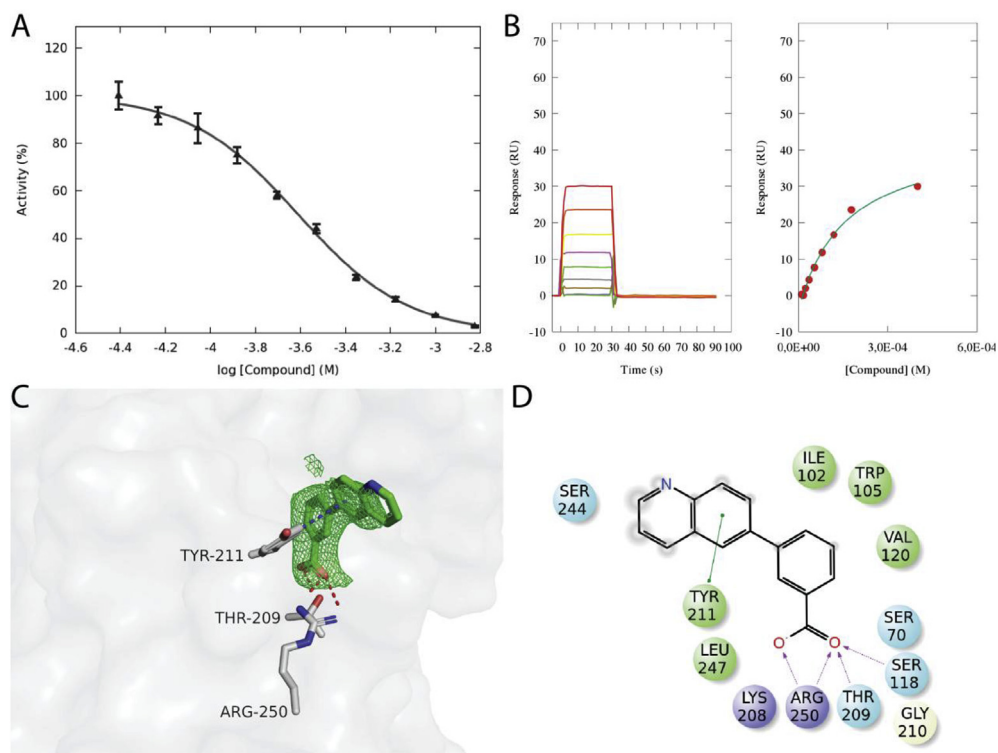


Fig. 5. The IC_{50} -value of compound **28** (A) was determined to be $240 \mu\text{M}$, while the K_D was found to be $160 \mu\text{M}$ (B). The crystal structure of the complex OXA-48:**28** with an omit-type polder-map (2.5σ) (C) and a 2D-representation of the protein:compound complex interactions. (D).

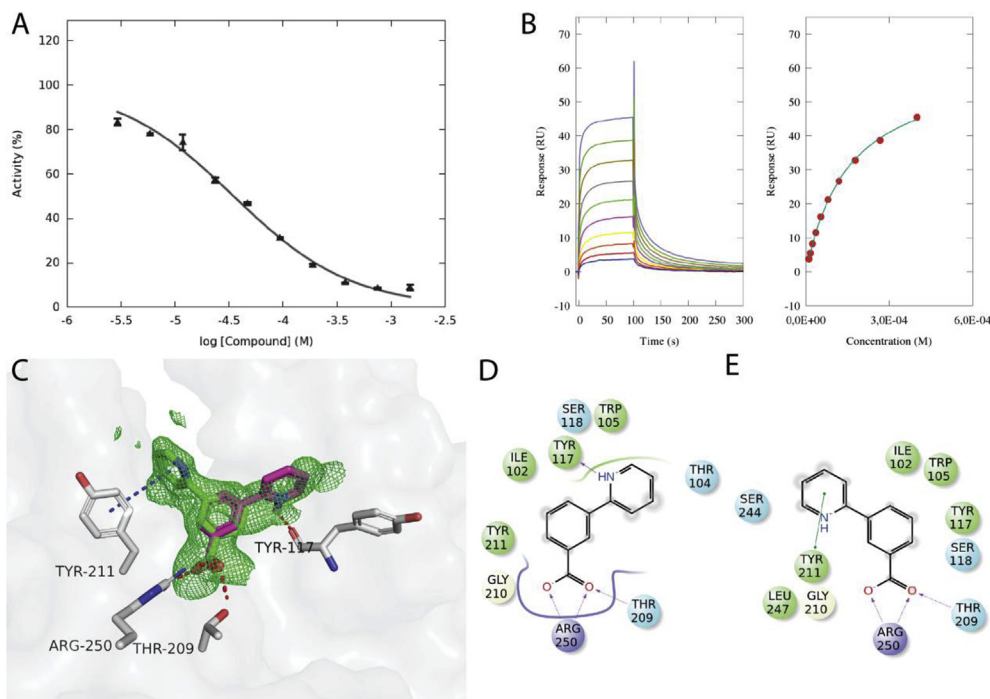


Fig. 6. Compound **35** bound in the two alternate conformations. The IC_{50} -value (A) was determined to be $35 \mu\text{M}$, while the K_D was found to be $159 \mu\text{M}$ (B). The crystal structure of the complex OXA-48:**35** with an omit-type polder-map (2.5σ) (C) and a 2D-representation of the protein:compound complex interactions. (D for green colored conformation, E for magenta colored conformation). (For interpretation of the references to color in this figure legend, the reader is referred to the Web version of this article.)

perturbations indicated that the effect is not caused by direct hydrogen bonding of the carbamic carbonyl, for which a $\Delta\delta$ of several ppm would be expected, even for a μM binder [29]. This was supported by the crystal structures of OXA-48 indicating that the Lys73 carbamic acid was preoccupied in hydrogen bonding to Trp157 and was not affected by ligand binding. The observed consistent, but rather subtle, deshielding of the Lys73 carbamic acid ($\delta = 164.25$, $\Delta\delta = 0.28$ ppm, Fig. 7E and F) for our R^1 binding fragments can possibly be explained by an anisotropic magnetic deshielding by the edge of the aromatic rings of these fragments, which were positioned roughly 5 \AA away from the reporter carbon for R^1 binding fragments. Moreover, amplitude of the chemical shift perturbation observed with R^1 binding fragments **21a** and inhibitor **2** (Fig. 7E and F) were in line with the reported changes observed for OXA enzymes on coordination with inhibitors like β -hydroxyisopropylpenicillanates [24], cyclic boronates [25] and avibactam [28].

2.3. Inhibitor activity and structural analysis of 3,5-disubstituted benzoic acids

In an attempted to design more potent inhibitors from our fragments, the mono-substituted benzoic acids were evaluated for a merging approach (Fig. 8). By overlaying X-ray structures, promising combinations showing orthogonal binding poses were identified and some of the combined structures were prepared and evaluated with good results.

An overlay of fragment **21a** as well as **26b** with several R^2 binders identified the combinations of fragments **21a/28**, **21a/1** and **26b/35** as interesting partners (Fig. 9). The combination **21a/1** and **21a/28** were synthetically feasible and gave compounds **39** and **40** (Scheme 2), respectively. In addition, the symmetrical 3,5-disubstituted benzoic acids **36–38** representing the symmetrical combinations of fragments **21a**, **21b** and **28** were included in this

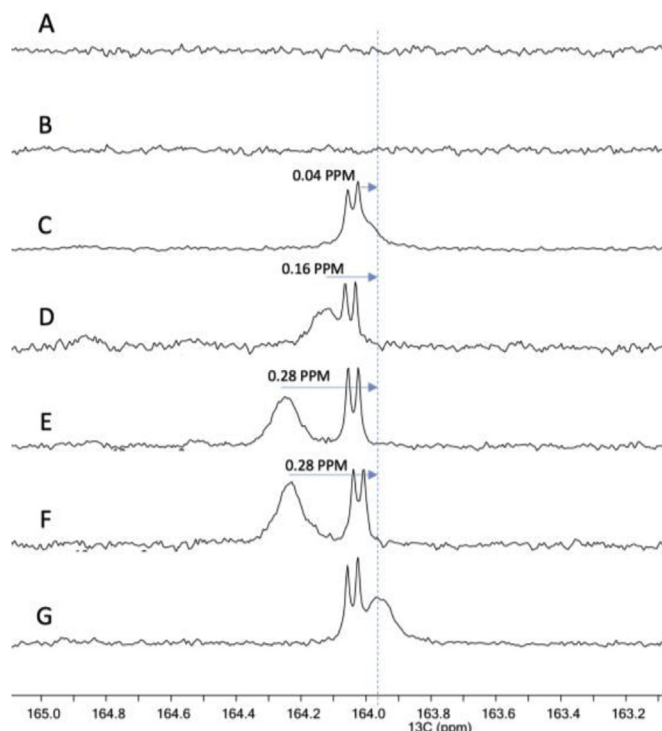


Fig. 7. ^{13}C NMR of the buffer alone including ^{13}C labeled bicarbonate (A); OXA-48 without ^{13}C labeled bicarbonate (B), OXA-48 with ^{13}C labeled bicarbonate and fragment **35** (C); OXA-48 with ^{13}C labeled bicarbonate and fragment **28** (D); OXA-48 with ^{13}C labeled bicarbonate and fragment **21a** (E); OXA-48 with ^{13}C labeled bicarbonate and 3,5-di(4-pyridinyl)benzoic acid **2** (F) and OXA-48 with ^{13}C labeled bicarbonate and no fragment (G). Two unassigned signals were observed at 164.1 ppm, and are believed to originate in a second carboxylated site of OXA-48.

study (Scheme 1).

The 3,5-disubstituted compounds **36–40** were evaluated for their inhibitory activity against OXA-48 as measured by their IC_{50} , K_d and LE and complex structures with OXA-48 and compounds **36**, **38** and **40** were obtained (Table 2). The merged compounds **37**, **38** and **39** (IC_{50} (μM)/LE: 110/0.19, 48/0.21, 100/0.22) failed to adequately maintain the binding interactions as the IC_{50} values were at a similar level as the corresponding mono-substituted fragments **28**, **1** and **21a** (IC_{50} (μM)/LE: 240/0.33, 250/0.32 and 35/0.33). When comparing the IC_{50} values of compounds **36**, **37** and **40** (IC_{50} (μM)/LE: 2.9/0.27, 48/0.21 and 2.9/0.27) with the corresponding fragments **21a**, **21b** and **28** (IC_{50} (μM)/LE: 35/0.33, 450/0.26, 240/0.3), a 10-fold decrease of the IC_{50} value was observed. Nevertheless, the improved binding was associated with a decrease in LE showing that the fragment-enzyme interactions are less efficient with the merged compounds. The reduction in LE probably relates to the rigid structure of the merged compounds allowing for little conformational freedom. Overall, the strongest inhibitors in this study are compounds **36** and **40** with IC_{50} values of 2.9 μM and LE of 0.27.

The structural analysis of the OXA-48 complexes with **36**, **38** and **40** showed that the interaction of the carboxylic acid with Arg214 is maintained. For compound **36**, a near perfect overlay was obtained with the complex structure of fragment **21a** showing that all interactions seen with the fragments were preserved in the larger compound (Fig. 10). The second 3-*N*-acetamidophenyl group forms a not previously observed hydrogen bond with Ser244. In the SPR sensorgrams some concentration dependent aggregation was observed [30].

Interestingly, the conformation of compound **38** in complex with OXA-48 was changed compared with the mono-substituted fragment **28**. In the OXA-48:**38** complex, one quinolinyl group bound in the R^1 site similar to fragment **21a**. The other quinolinyl group positions itself in a conformation similar to the alternative conformation observed with fragment **35** (Fig. 6). No specific interactions were observed, but this conformation shielded the hydrophobic quinoline ring from solvent exposure by burying the compound deep in the hydrophobic cleft.

The complex structure of the unsymmetrical compound **40** (Fig. 11) that was composed of the quinoline ring of fragment **28** and the 3-*N*-acetamidophenyl substituent of fragment **13a** shared the key interactions of both mono-substituted fragments validating our approach, with an IC_{50} of 2.9 μM .

3. Conclusion

A targeted fragment library consisting of 49 diversely 3-substituted benzoic acid derivatives was prepared and biochemically analyzed for their inhibitory activity against OXA-48. Enzyme-fragment complexes for crystallographic studies were obtained for 33 fragments. By systematically changing the substituent-groups of the benzoic acid derivatives we were able to identify inhibitory fragments with $IC_{50} < 40 \mu M$ (**21a**, **26b**, **35**). Based on the structural

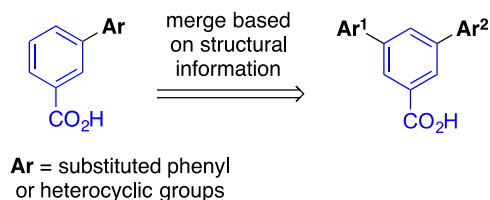


Fig. 8. Strategy for substitution of the Ar^1 and Ar^2 groups in the focused fragment library of 3-substituted benzoic acids analogues.

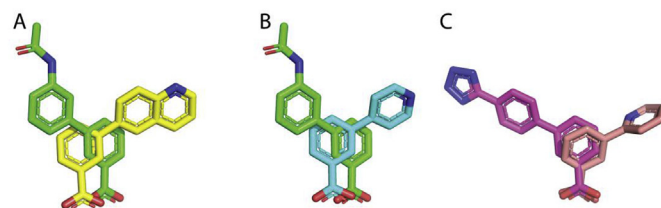


Fig. 9. Superimpositions of the binding poses observed for **21a/28** (A), **21a/1** (B, 1: PDB-ID:5dva) and **26b/35** (C) showing some of the possible combinations for 3,5-disubstituted benzoic acids.

Table 2

Inhibitor activities of 3,5-disubstituted benzoic acids analogues against OXA-48 (IC_{50} , K_D and LE).

| Ar^1 | Ar^2 | ID | IC_{50} (μM) | K_D (μM) | LE ^a |
|--------|--------|------------------------|-----------------------|-------------------|-----------------|
| | | 36 [*] | 2.9 | 20 | 0.27 |
| | | 37 | 48 | 70 | 0.21 |
| | | 38 [*] | 110 | 70 | 0.19 |
| | | 39 | 100 | 70 | 0.22 |
| | | 40 [*] | 2.9 | 49 | 0.27 |

*X-ray structure of fragment-enzyme complex available.

^a LE = $(-1.4 * \log_{10} IC_{50}) / \text{HeavyAtomCount}$, with units kcal/(mol heavy atom).

information, fragments could be classified according to their preferred binding pocket. Most fragments were orientated towards the R^2 site induced by a π - π -stacking with Tyr221. Unfortunately, no further interactions in the R^2 site could be identified from our library. The strongest binding fragments **21a** and **26b** were binding in the R^1 site due to a hydrogen bond to Arg214 and for fragment **35** a hydrogen bond to the carbonyl backbone of Tyr117 was observed. By overlaying the complex crystal structures of fragments **1**, **21a**, **26b**, **28** and **35**, the design of five new 3,5-disubstituted inhibitors evolved. The strongest 3,5-disubstituted inhibitors **36** and **40** showed IC_{50} values as low as 2.9 μM , thus have improved inhibitory potential. The complex crystal structures of **36** and **40** revealed that the interactions of the individual fragments were mainly retained in the merged structures. In addition, for inhibitor **36** a previously not observed hydrogen bond from the 3-*N*-acetamidophenyl group in the R^2 site to Ser244 was found, which is interesting as we otherwise found few interactions in this region. Future work will focus on the evaluation of fragments with increased flexibility e.g. by introducing a CH_2 or heteroatom linker bridging the aromatic ring systems to further explore the active site.

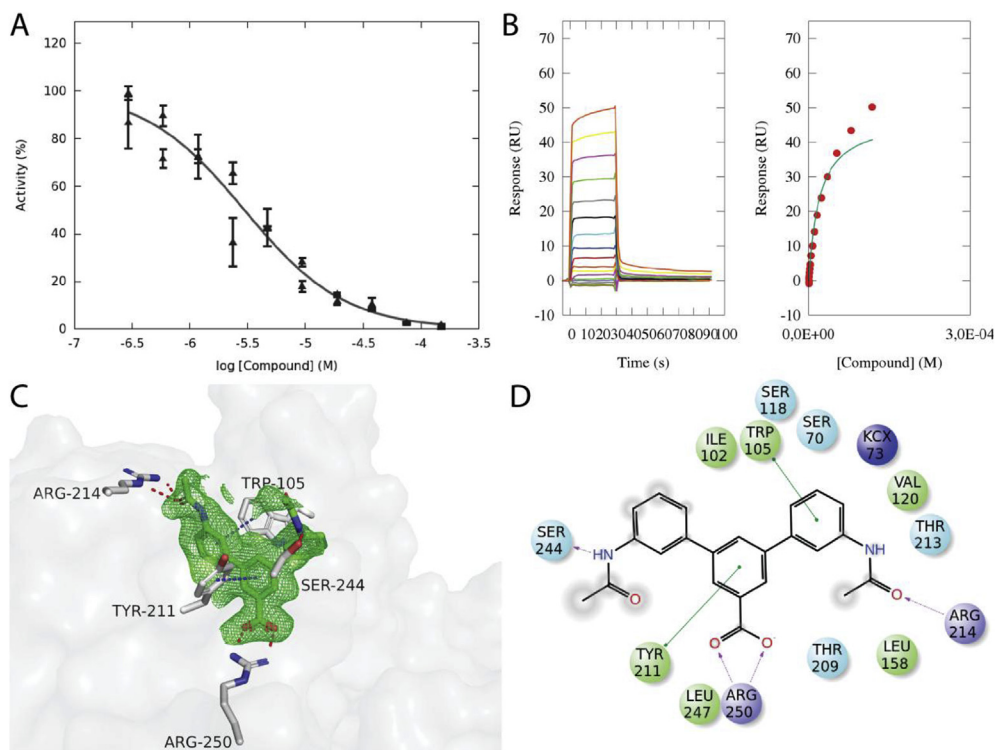


Fig. 10. Compound **36** maintained the interaction with Arg214 as we observed for the 3-substituted benzoic acid derivative. The IC_{50} -value (A) was determined to be $2.9 \mu\text{M}$, while the K_D was found to be $30 \mu\text{M}$ (B). For the higher concentrations of compound **36** some unspecific binding was observed. The crystal structure of the complex OXA-48:**36** with an omit-type polder-map (2.5σ) (C) and its 2D-representation (D) shows one of the acetamide-groups interacted with the guanidine group of Arg214, while the other group was solvent exposed.

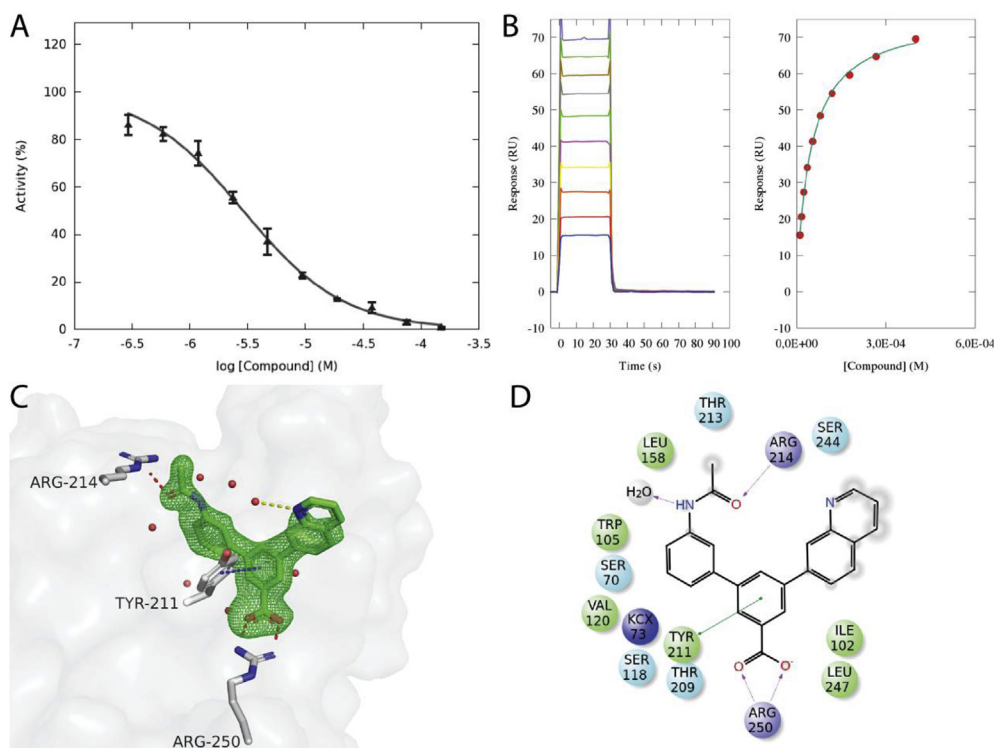


Fig. 11. Compound **40** maintained the interaction with Arg214 as we observed for the 3-substituted benzoic acid derivative. The IC_{50} -value (A) was determined to be $2.9 \mu\text{M}$, while the K_D was found to be $49 \mu\text{M}$ (B). The crystal structure of the complex OXA-48:**40** with an omit-type polder-map (2.5σ) (C) and its 2D-representation (D) shows that the acetamide-group interacted with the guanidine group of Arg214, while the quinoline-ring was partially solvent exposed.

4. Experimental

4.1. Synthesis

4.1.1. *Synthesis of 3-substituted benzoic acids (complete data for all procedures and compounds is found in the Supporting information)*

4.1.1.1. *General procedure A – aqueous conditions.* The halo aryl (1.0 equiv) was dissolved in a mixture of water:dioxane (1:1). The boronic acid or ester (1.5 equiv) and potassium phosphate (5.0 equiv) were added. The solution was degassed by vacuum/Argon cycles (10 times) before addition of PdCl₂(PPh₃)₂ (10 mol%) and further degassed (5 times). The resulting mixture was stirred at 95 °C under argon atmosphere for 16–20 h. The reaction mixture was filtered through Celite and diluted with water (approx. 30 mL) before washing with chloroform (3 × 30 mL). If not stated otherwise, the aqueous phase was concentrated under reduced pressure and applied to a C18 precolumn before purification on a 10 g or 60 g C18 column with a gradient of acetonitrile in water (10–100%) to yield the desired product.

4.1.1.2. *General procedure B – anhydrous conditions.* The halo aryl (1.0 equiv) was dissolved in anhydrous THF. The aryl boronic acid or aryl boronic ester (1.5 equiv) and inorganic base (5.0 equiv) were added. The solution was degassed by vacuum/Argon cycles (10 times), before addition of a palladium catalyst (10 mol%) and further degassed (5 times). The resulting mixture was stirred at 75–90 °C under an inert atmosphere for 16–20 h. The reaction mixture was filtered through Celite and diluted with water (approx. 30 mL) before washing with ethyl acetate (3 × 30 mL). If not stated otherwise, the aqueous phase was concentrated under reduced pressure and applied to a C18 precolumn before purification on a 10 g or 60 g C18 column with a gradient of acetonitrile in water (10–80%) to yield the desired molecule.

4.1.2. *Screening of catalysts (for results see Table S11)*

4.1.2.1. *General procedure.* 3-Bromo-5-iodobenzoic acid (0.03–0.06 mmol, 1.0 equiv.) was dissolved in the indicated solvent (0.5–1 mL/0.01 mmol substrate). The boronic acid or ester (1.5 equiv.) and base (5.0 equiv.) were added. The solution was degassed by vacuum/Ar cycles (10 times) before addition of the palladium catalyst and further degassed (5 times). The resulting mixture was stirred at the indicated temperature under an inert atmosphere for the indicated reaction time. The crude reaction mixture was analyzed by HRMS to determine the ratio of **int-39**: disubstituted **38**: starting material. The reaction mixture was filtered through Celite bed and diluted with water (approx. 30 mL) before washing with chloroform (3 × 30 mL). The aqueous phase was concentrated under reduced pressure and applied to a C18 precolumn before purification on a 60 g C18 column with a gradient of acetonitrile in water (0–5% over 15 min) to yield the product.

4.1.3. *Synthesis of symmetrical 3,5-disubstituted benzoic acid derivatives*

4.1.3.1. *3,5-Di(3-acetamidophenyl)benzoic acid 36.* 3-Bromo-5-iodobenzoic acid (0.30 mmol, 100 mg, 1.0 equiv), 3-acetamidophenylboronic acid (0.45 mmol, 816 mg, 1.5 equiv), potassium phosphate (1.5 mmol, 324 mg, 5.0 equiv) were dissolved in a mixture of water/dioxane (1:1). The solution was degassed by vacuum/Ar cycles (10 times) before addition of Pd₂(dba)₃•CHCl₃ (15 mg, 5 mol%), and XPhos (7.2 mg, 5 mol%) and further degassed (5 times). The resulting mixture was stirred at 60 °C for 20–24 h. The reaction mixture was filtered through Celite bed and diluted with water (approx. 30 mL) before washing with chloroform (3 × 30 mL). The aqueous phase was concentrated under reduced pressure and applied to a C18 precolumn before purification on a

60 g C18 column with a gradient of acetonitrile in water (0–5% over 15 min) to provide **36** (60 mg, 54%) as white powder. ¹H NMR (400 MHz, methanol-*d*₄) δ 8.21 (s, 2H), 7.90 (t, *J* = 1.7 Hz, 1H), 7.81 (t, *J* = 1.7 Hz, 2H), 7.68 (d, *J* = 8 Hz, 2H), 7.43 (s, 1H), 7.49–7.46 (m, 2H), 7.43–7.39 (m, 2H), 2.16 (s, 6H). ¹³C NMR (101 MHz, methanol-*d*₄) δ 175.0, 171.8, 142.9, 142.3, 140.5, 132.2, 130.4, 128.2, 128.1, 123.9, 120.3, 119.7, 24.0. HRMS (ESI): Calcd. for C₂₃H₁₉N₂O₄ [M-H]⁻ 387.1350; found 387.1342. UPLC: purity = 97.5%

4.1.3.2. *3,5-di(4-acetamidophenyl)benzoic acid 37.* 3,5-Dibromobenzoic acid (1.01 mmol, 300 mg, 1.0 equiv), 3-acetamidophenylboronic acid (0.81 mmol, 178 mg, 0.75 equiv), potassium phosphate (3.76 mmol, 0.80 g, 3.5 equiv) and PdCl₂(PPh₃)₂ (0.11 mmol, 77 mg, 10 mol%) were stirred in a mixture of water/dioxane (1:1) for 24 h at 95 °C under argon atmosphere. The crude reaction mixture was filtered through Celite and diluted with water (approx. 30 mL) before washing with chloroform (3 × 30 mL). The aqueous phase was concentrated under reduced pressure and applied to a C18 precolumn before purification on a 60 g C18 column with a gradient of acetonitrile in water (0–100% over 12 min). The fractions were analyzed by MS and fractions containing **37** were combined. The product was purified by reverse-phase automated flash chromatography before being subjected to purification by HPLC, to yield **37** (0.09 mmol, 34 mg, 11%) as a white solid. ¹H NMR (400 MHz, methanol-*d*₄) δ 8.24 (s, 2H), 7.98 (d, *J* = 7.8 Hz, 2H), 7.85 (d, *J* = 7.9 Hz, 2H), 7.68–7.66 (m, 2H), 7.63–7.60 (m, 2H), 7.57–7.53 (m, 1H), 2.16 (s, 6H). ¹³C NMR (101 MHz, methanol-*d*₄) δ 175.2, 171.7, 142.0, 140.2, 139.4, 137.9, 131.7, 128.4, 128.2, 127.6, 127.4, 123.3, 121.4, 116.2, 23.9. HRMS (ESI): Calcd. for C₂₃H₁₉N₂O₄ [M-H]⁻ 387.1350; found 387.1340. UPLC: purity >99.5%

4.1.3.3. *3,5-Diquinolin-6-ylbenzoic acid 38.* 3,5-Dibromobenzoic acid (0.11 mmol, 33 mg, 1.0 equiv), 6-quinolinylboronic acid pinacol ester (0.23 mmol, 60 mg, 2.0 equiv), potassium phosphate (0.58 mmol, 125 mg, 5.0 equiv) were dissolved in tert-butanol. The solution was degassed by vacuum/Ar cycles (10 times) before addition of XPhos-Pd G2 (5 mol%, 5 mg) and further degassed (5 times). The resulting mixture was stirred at 60 °C for 20–24 h. The reaction mixture was filtered through Celite bed and diluted with water (approx. 30 mL) before washing with chloroform (3 × 30 mL). The aqueous phase was concentrated under reduced pressure and applied to a C18 precolumn before purification by C18 RP flash chromatography with a gradient of acetonitrile in water (0–5% over 15 min) to yield **38** (0.08 mmol, 29 mg, 65%) as white powder. ¹H NMR (400 MHz, methanol-*d*₄) δ 8.87–8.86 (m, 2H), 8.52 (s, 1H), 8.50 (s, 1H), 8.46 (m, 2H), 8.38 (m, 2H), 8.29–8.26 (m, 3H), 8.18 (s, 1H), 8.16 (s, 1H), 7.61–7.58 (dd, *J* = 8.3, 4.2 Hz, 2H). ¹³C NMR (101 MHz, methanol-*d*₄) δ 174.4, 151.1, 148.0, 141.5, 140.5, 138.6, 130.6, 130.1, 129.5, 128.7, 126.9, 122.8. HRMS (ESI): Calcd. for C₂₅H₁₅N₂O₂ [M-H]⁻ 375.1139; found 375.1133. UPLC: purity = 99.1%

4.1.4. *Synthesis of unsymmetrical 3,5-disubstituted benzoic acid derivatives*

4.1.4.1. *3-(3'-Acetamidophenyl)-5-pyridin-4-ylbenzoic acid 39: attempted synthesis from 3,5-dibromobenzoic acid.* 3,5-Dibromobenzoic acid (1.01 mmol, 300 mg, 1.0 equiv), 3-acetamidophenylboronic acid (0.81 mmol, 178 mg, 0.75 equiv), potassium phosphate (3.76 mmol, 0.80 g, 3.5 equiv) and PdCl₂(PPh₃)₂ (0.11 mmol, 77 mg, 10 mol%) were stirred in a mixture of water/dioxane (1:1) for 24 h at 95 °C under argon atmosphere. The crude reaction mixture was filtered through Celite and diluted with water (approx. 30 mL) before washing with chloroform (3 × 30 mL). The aqueous phase was concentrated under reduced pressure and applied to a C18 precolumn before purification by C18

RP flash chromatography with a gradient of acetonitrile in water (10–100% over 12 min). The fractions were analyzed by MS and fractions containing **int-39** were combined and reacted with pyridin-4-ylboronic acid (0.97 mmol, 119 mg, 1.2 equiv), potassium phosphate (4.05 mmol, 0.86 g, 5.0 equiv) and PdCl₂(PPh₃)₂ (0.08 mmol, 56 mg, 10 mol%). The product was purified by reverse-phase automated flash chromatography before being subjected to purification by HPLC, to yield **39** (0.12 mmol, 39 mg, 15%) as a white solid. ¹H NMR (400 MHz, methanol-*d*₄) δ 8.22 (s, 1H), 7.92 (d, *J* = 7.6 Hz, 1H), 7.76 (s, 2H), 7.68–7.60 (m, 3H), 7.46–7.33 (m, 4H), 2.14 (s, 3H). ¹³C NMR (101 MHz, methanol-*d*₄) δ 175.3, 171.7, 143.0, 141.5, 140.4, 139.8, 130.3, 129.7, 129.3, 129.3, 128.9, 123.7, 120.1, 119.6, 23.9. UPLC: purity = 97.9%

4.1.4.2. 3-Bromo-5-(quinolin-6-yl) benzoic acid int-40. 3-Bromo-5-iodobenzoic acid (0.15 mmol, 50 mg, 1.0 equiv), 6-quinolinylboronic acid pinacol ester (0.22 mmol, 58 mg, 1.5 equiv) and potassium phosphate (0.76 mmol, 162 mg, 5.0 equiv) were dissolved in a mixture of water/dioxane (1:1). The solution was degassed by vacuum/Ar cycles (10 times) before addition of Pd₂(dba)₃·CHCl₃ (5 mol%, 7.5 mg), and SPhos (5 mol%, 3.1 mg) and further degassed (5 times). The resulting mixture was stirred at 60 °C for 20–24 h. The reaction mixture was filtered through a Celite bed and diluted with water (approx. 30 mL) before washing with chloroform (3 × 30 mL). The aqueous phase was concentrated under reduced pressure and applied to a C18 precolumn before purification on a 60 g C18 column with a gradient of acetonitrile in water (0–5% over 20 min). Product **int-40** (0.07 mmol, 23 mg, 45%) was obtained as a white powder. ¹H NMR (400 MHz, methanol-*d*₄) δ 8.92–8.91 (m, 1H), 8.49–8.46 (m, 1H), 8.35 (s, 1H), 8.28 (s, 2H), 8.10 (s, 2H), 8.02–8.01 (m, 1H), 7.97–7.96 (m, 1H), 7.59–7.56 (dd, *J* = 8.3, 4.2 Hz, 1H). ¹³C NMR (101 MHz, DMSO-*d*₆) δ 166.6, 150.8, 147.2, 143.6, 140.6, 136.8, 136.5, 131.7, 131.1, 129.6, 128.5, 128.2, 127.4, 126.5, 125.8, 121.9, 121.7; HRMS (ESI): Calcd. for C₁₆H₉⁹⁹BrNO₂ [M-H]⁻ 325.9822; found 325.9822.

4.1.4.3. 3-(3'-Acetamidophenyl)-5-quinolin-6-ylbenzoic acid 40. 3-Bromo-5-(quinolin-6-yl) benzoic acid **int-40** (0.039 mmol, 13 mg, 1.0 equiv), 3-acetamidophenylboronic acid (0.55 mmol, 10 mg, 1.5 equiv) and potassium phosphate (0.20 mmol, 0.42 g, 5.0 equiv) were dissolved in *tert*-butanol. The solution was degassed by vacuum/Ar cycles (10 times) before addition of Xphos-Pd G2 (5 mol%, 1.5 mg) and further degassed (5 times). The resulting mixture was stirred at 60 °C for 20–24 h. The reaction mixture was filtered through Celite bed and diluted with water (approx. 30 mL) before washing with chloroform (3 × 30 mL). The aqueous phase was concentrated under reduced pressure and applied to a C18 precolumn before purification on a 60 g C18 column with a gradient of acetonitrile in water (0–5% over 20 min). Product **40** (0.023 mmol, 9 mg, 90%) was obtained as white powder. ¹H NMR (400 MHz, methanol-*d*₄) δ 8.87–8.83 (m, 1H), 8.56–8.45 (m, 1H), 8.41–8.39 (m, 1H), 8.35–8.20 (m, 3H), 8.18–8.11 (m, 1H), 8.08 (t, *J* = 1.8 Hz, 1H), 7.87–7.86 (m, 1H), 7.72–7.68 (m, 1H), 7.62–7.56 (m, 1H), 7.56–7.49 (m, 1H), 7.46–7.42 (m, 1H), 2.17 (s, 3H). ¹³C NMR (101 MHz, DMSO-*d*₆) δ 174.7, 171.8, 151.2, 148.2, 142.8, 142.5, 141.4, 140.8, 140.7, 140.5, 138.8, 130.8, 130.4, 130.3, 129.7, 128.6, 128.5, 128.5, 127.0, 123.9, 123.0, 120.3, 119.7, 23.9. HRMS (ESI): Calcd. for C₂₄H₁₈N₂O₃ [M-H]⁻ 381.1245; found 381.1243. UPLC: purity = 96.4%

4.2. Protein production

For the biochemical assay OXA-48 was expressed with the native signal-peptide and purified from the periplasm as described earlier [31]. For surface plasmon resonance assays, nuclear magnetic resonance and crystallization a His-tagged construct was used

[19].

4.3. Biochemical assay

All experiments were performed using a Spectramax M2e at 25 °C in 100 mM sodium phosphate (pH 7.0) supplemented with 50 mM NaHCO₃ and 0.2 mg/mL bovine serum albumin (BSA). Velocities from the linear range were determined in the SoftMax Pro software (Molecular Devices). All experiments were done with a sample volume of 100 μL. IC₅₀ values were determined for all compounds in competition with 25 μM of the chromogenic substrate nitrocefin. The log₁₀ of the inhibitor concentrations to the response with bottom and top constant based on controls were fitted nonlinearly in GraphPad Prism 6 (GraphPad Software) to determine the IC₅₀ value.

4.4. Surface plasmon resonance

All SPR experiments were performed on a Biacore T200 at 25 °C. The data were analyzed using Biacore T200 Evaluation Software 2.0 (GE Healthcare). The sensorgrams were double reference subtracted using a reference surface and blank injections. The final running buffer included 50 mM HEPES pH 7.0, 50 mM K₂SO₄, 0.5% Tween-20, 50 mM NaHCO₃, and 2.5% DMSO. The enzyme, OXA-48, was diluted to 25 μg/mL in 10 mM MES pH 5.5. The enzyme was immobilized to a level of around 5000 RU on a CM5 chip using standard amine coupling.

Compounds were tested with 10 dilutions from 400 μM to 10.5 μM, with 30 s injection and 60 s dissociation time. Compounds exhibiting kinetic behavior had the dissociation time extended to 300 s. Seven startup cycles with buffer were performed. Solvent correction was performed every 48th cycle and a positive control was included every 24th cycle with 3.5-Di(4-pyridinyl)benzoic acid as the control [19]. Affinities were calculated from the steady-state affinity model with a constant *R*_{max} adjusted by the control and the molecular weight of the compound.

4.5. ¹³C nuclear magnetic resonance

A solution of NaH¹³CO₃ in D₂O (50 mM) was prepared. The NaH¹³CO₃/D₂O-mixture was added to 1 mM OXA-48 in 50 mM sodium phosphate and 50 mM sodium bicarbonate pH 6.5 in a 1: 9 ratio of bicarbonate to enzyme. Compounds were diluted from a 150 mM stock solution in 100% DMSO to a final concentration of 3.75 mM (2.5% DMSO). Sample volumes of 500 μL were used. We performed the experiment at 37 °C with a Bruker Avance III HD with an inverse detected TCI probe with cryogenic enhancement for ¹H, ¹³C and ²H, operating at 599.90 MHz for protons and 150.86 MHz for carbon. 10 000 scans at 30° pulse angle with 2 s relaxation delay were collected using 1D¹³C NMR with power-gated decoupling of protons (zgpg30 using waltz16).

4.6. Crystallization and data processing

Crystals of OXA-48 was grown from hanging drops containing 0.1 M HEPES pH 7.5, 8–11% PEG 8000 and 4–8% 1-butanol as previously described [17]. Compounds were diluted to 3.75 mM in the cryo solution with 0.1 M HEPES pH 7.5, 10% PEG 8000, 5% 1-butanol, and 25% ethanediol, usually overnight. The exception was the crystal soaked in imipenem. Imipenem was added to saturation in the cryosolution, and the crystal was just given a quick soak.

Crystals were flash cooled in liquid nitrogen. X-ray diffraction data were collected at BL 14.1 and BL14.2 at BESSY (Berlin, Germany) [32], and at ID23-1, ID23-2 and ID30B at ESRF (Grenoble, France). In most cases the structures were solved by refining

against the protein-atoms of previous structures (P2₁2₁ PDB ID: 5DVA and P2₁ PDB ID: 5DTK), but in cases where the unit cells were to different PHASER was used with chain A from PDB ID: 5dtk as the search model for molecular replacement. In most cases images were autoprocessed using the tools at the beamlines [33–37], but in some cases we found it useful to reprocess using DIALLS or XDS together with AIMLESS [38–40].

The compounds were built into difference density maps after initial refinement in phenix.refine [41], with waters deleted from the active site. Restraints for the compounds were prepared using the GRADE Web Server [42]. Omit maps were calculated using the phenix.polder-tool which excludes bulk-solvent from the volume surrounding the ligand [43]. Figures were made using PyMOL [44]. Ligand-interaction diagrams were prepared using the Maestro-suite from Schrödinger Release 2016-3 (Schrödinger, LLC, New York).

Author contributions

Designed the experiments: AB, BAL, HKSL, SA, TC. Performed the organic synthesis: SA, AI, ML. Determined IC₅₀ values and K_d-values: BAL. Prepared and solved crystal structures: BAL. Analyzed 3D structures: AB, BAL, SA. NMR studies: BAL, JI. Analyzed data and wrote the paper: AB, BAL, HKSL, JI, SA, TC. All authors have given approval to the final version of the manuscript.

PDB accession codes

Coordinates and structure factors for all OXA-48 complexes are deposited in the Protein Data Bank. Accession numbers are listed with reference to the complexed compound. PDB IDs: imipenem: 5QB4; **3a**: 5QA4; **3b**: 5QA5; **4a**: 5QA6; **4b**: 5QA7; **4c**: 5QA8; **5**: 5QA9; **6a**: 5QAA; **6b**: 5QAB; **6c**: 5QAC; **8a**: 5QAD; **8b**: 5QAE; **8c**: 5QAF; **9a**: 5QAG; **9b**: 5QAH; **12a**: 5QAI; **13**: 5QAJ; **14**: 5QAK; **11b**: 5QAL; **17**: 5QAM; **19a**: 5QAN; **19b**: 5QAO; **21a**: 5QAP; **21b**: 5QAQ; **23a**: 5QAR; **23b**: 5QAS; **24**: 5QAT; **26a**: 5QAU; **26b**: 5QAV; **27**: 5QAW; **28**: 5QAX; **32**: 5QAY; **34**: 5QAZ; **35**: 5QBO; **36**: 5QB1; **38**: 5QB2; **40**: 5QB3.

Acknowledgement

This study was supported by The National Graduate School in Structural Biology (BioStruct) and The Norwegian Research Council (FRIMEDBIO project number 213808 and SYNKNOYT project number 218539). Provision of beam time at BL14.1 and BL14.2, Bessy II, Berlin, Germany, and the MX beamlines ID23-1, ID23-2 and ID30B at the European Synchrotron Radiation Facility (ESRF), Grenoble, France are highly valued.

Appendix A. Supplementary data

Supplementary data related to this article can be found at <https://doi.org/10.1016/j.ejmech.2017.12.085>.

References

- [1] T. Guillard, S. Pons, D. Roux, G.B. Pier, D. Skurnik, Antibiotic resistance and virulence: understanding the link and its consequences for prophylaxis and therapy, *Bioessays* 38 (2016) 682–693.
- [2] L. Chen, R. Todd, J. Kiehlbauch, M. Walters, A. Kallen, Notes from the Field: Pan-Resistant New Delhi Metallo-β-lactamase-producing *Klebsiella pneumoniae* - Washoe County, Nevada, 2016, *MMWR Morb. Mortal. Wkly. Rep.* 66, 2017, p. 33.
- [3] J. O'Neill, Tackling Drug-resistant Infections Globally (final report and recommendations. Review on Antimicrobial Resistance, London, UK), 2016.
- [4] K. Bush, P.A. Bradford, β-lactams and β-lactamase inhibitors: an overview, *CSH Perspect. Med.* 6 (2016).
- [5] B.G. Hall, M. Barlow, Evolution of the serine β-lactamases: past, present and future, *Drug Resist. Update.* 7 (2004) 111–123.
- [6] L. Poirel, T. Naas, P. Nordmann, Diversity, epidemiology, and genetics of class D β-lactamases, *Antimicrob. Agents Chemother.* 54 (2010) 24–38.
- [7] K. Bush, G.A. Jacoby, Updated functional classification of β-lactamases, *Antimicrob. Agents Chemother.* 54 (2010) 969–976.
- [8] T. Naas, S. Oueslati, R.A. Bonnin, M.L. Dabos, A. Zavala, L. Dortet, P. Retailleau, B.I. Iorga, Beta-lactamase database (BLDB) – structure and function, *J. Enzym. Inhib. Med. Chem.* 32 (2017) 917–919.
- [9] R.P. Ambler, The structure of β-lactamases, *Philos. Trans. R. Soc., B* 289 (1980) 321–331.
- [10] D. Golemi, L. Maveyraud, S. Vakulenko, J.-P. Samama, S. Mobashery, Critical involvement of a carbamylated lysine in catalytic function of class D β-lactamases, *Proc. Natl. Acad. Sci. U. S. A.* 98 (2001) 14280–14285.
- [11] L. Poirel, A. Potron, P. Nordmann, OXA-48-like carbapenemases: the phantom menace, *J. Antimicrob. Chemother.* 67 (2012) 1597–1606.
- [12] S.M. Drawz, R. a Bonomo, Three decades of β-lactamase inhibitors, *Clin. Microbiol. Rev.* 23 (2010) 160–201.
- [13] J.D. Buynak, Understanding the longevity of the β-lactam antibiotics and of antibiotic/β-lactamase inhibitor combinations, *Biochem. Pharmacol.* 71 (2006) 930–940.
- [14] N. Antunes, J. Fisher, Acquired class D β-lactamases, *Antibiotics* 3 (2014) 398.
- [15] J.L. Liscio, M.V. Mahoney, E.B. Hirsch, Ceftolozane/tazobactam and ceftazidime/avibactam: two novel β-lactam/β-lactamase inhibitor combination agents for the treatment of resistant Gram-negative bacterial infections, *Int. J. Antimicrob. Agents* 46 (2015) 266–271.
- [16] D.E. Ehmman, H. Jahić, P.L. Ross, R.-F. Gu, J. Hu, T.F. Durand-Réville, S. Lahiri, J. Thresher, S. Livchak, N. Gao, T. Palmer, G.K. Walkup, S.L. Fisher, Kinetics of avibactam inhibition against class a, C, and D β-Lactamases, *J. Bio. Chem.* 288 (2013) 27960–27971.
- [17] S.D. Lahiri, S. Mangani, H. Jahic, M. Benvenuti, T.F. Durand-Reville, F. De Luca, D.E. Ehmman, G.M. Rossolini, R.A. Alm, J.D. Docquier, Molecular basis of selective inhibition and slow reversibility of avibactam against class D carbapenemases: a structure-guided study of OXA-24 and OXA-48, *ACS Chem. Biol.* 10 (2015) 591–600.
- [18] R.K. Shields, L. Chen, S.J. Cheng, K.D. Chavda, E.G. Press, A. Snyder, R. Pandey, Y. Doi, B.N. Kreiswirth, M.H. Nguyen, C.J. Clancy, Emergence of ceftazidime-avibactam resistance due to plasmid-borne bla(KPC-3) mutations during treatment of carbapenem-resistant *Klebsiella pneumoniae* infections, *Antimicrob. Agents Chemother.* 61 (2017).
- [19] B.A. Lund, T. Christopheit, Y. Guttormsen, A. Bayer, H.K.S. Leiros, Screening and design of inhibitor scaffolds for the antibiotic resistance Oxacillinase-48 (OXA-48) through surface plasmon resonance screening, *J. Med. Chem.* 59 (2016) 5542–5554.
- [20] M. Congreve, R. Carr, C. Murray, H. Jhoti, A 'Rule of Three' for fragment-based lead discovery? *Drug Discov. Today* 8 (2003) 876–877.
- [21] S.M. Lukyanov, I.V. Bliznets, S.V. Shorshnev, G.G. Aleksandrov, A.E. Stepanov, A.A. Vasil'ev, Microwave-assisted synthesis and transformations of sterically hindered 3-(5-tetrazolyl)pyridines, *Tetrahedron* 62 (2006) 1849–1863.
- [22] A.M. King, D.T. King, S. French, E. Brouillette, A. Asli, J.A.N. Alexander, M. Vuckovic, S.N. Maiti, T.R. Parr, E.D. Brown, F. Malouin, N.C.J. Strynadka, G.D. Wright, Structural and kinetic characterization of diazabicyclooctanes as dual inhibitors of both serine-β-lactamases and penicillin-binding proteins, *ACS Chem. Biol.* 11 (2016) 864–868.
- [23] D.A. Leonard, R.A. Bonomo, R.A. Powers, Class D β-lactamases: a reappraisal after five decades, *Acc. Chem. Res.* 46 (2013) 2407–2415.
- [24] L. Maveyraud, D. Golemi-Kotra, A. Ishiwata, O. Meroueh, S. Mobashery, J.-P. Samama, High-resolution x-ray structure of an acyl-enzyme species for the class D OXA-10 β-lactamase, *J. Am. Chem. Soc.* 124 (2002) 2461–2465.
- [25] S.T. Cahill, R. Cain, D.Y. Wang, C.T. Lohans, D.W. Wareham, H.P. Oswin, J. Mohammed, J. Spencer, C.W.G. Fishwick, M.A. McDonough, C.J. Schofield, J. Brem, Cyclic boronates inhibit all classes of β-lactamases, *Antimicrob. Agents Chemother.* 61 (2017).
- [26] J. Li, J.B. Cross, T. Vreven, S.O. Meroueh, S. Mobashery, H.B. Schlegel, Lysine carboxylation in proteins: OXA-10 β-lactamase, *Proteins* 61 (2005) 246–257.
- [27] V. Verma, S.A. Testero, K. Amini, W. Wei, J. Liu, N. Balachandran, T. Monoharan, S. Stynes, L.P. Kotra, D. Golemi-Kotra, Hydrolytic mechanism of OXA-58 enzyme, a carbapenem-hydrolyzing class D β-lactamase from acinetobacter baumannii, *J. Bio. Chem.* 286 (2011) 37292–37303.
- [28] C.T. Lohans, D.Y. Wang, C. Jorgensen, S.T. Cahill, I.J. Clifton, M.A. McDonough, H.P. Oswin, J. Spencer, C. Domene, T.D.W. Claridge, J. Brem, C.J. Schofield, ¹³C-Carbamylation as a mechanistic probe for the inhibition of class D β-lactamases by avibactam and halide ions, *Org. Biomol. Chem.* 15 (2017) 6024.
- [29] N. Asakawa, S. Kuroki, H. Kurosu, I. Ando, A. Shoji, T. Ozaki, Hydrogen-bonding effect on carbon-13 NMR chemical shifts of L-alanine residue carbonyl carbons of peptides in the solid state, *J. Am. Chem. Soc.* 114 (1992) 3261–3265.
- [30] A.M. Giannetti, B.D. Koch, M.F. Browner, Surface plasmon resonance based assay for the detection and characterization of promiscuous inhibitors, *J. Med. Chem.* 51 (2008) 574–580.
- [31] B.A. Lund, H.K.S. Leiros, G.E. Bjerga, A high-throughput, restriction-free cloning and screening strategy based on ccdB-gene replacement, *Microb. Cell Fact.* 13 (2014) 38.
- [32] U. Mueller, R. Förster, M. Hellmig, F.U. Huschmann, A. Kastner, P. Malecki, S. Pühringer, M. Röwer, K. Sparta, M. Steffen, M. Ühlein, P. Wilk, M.S. Weiss, The macromolecular crystallography beamlines at BESSY II of the Helmholtz-

- Zentrum Berlin: current status and perspectives, *Eur. Phys. J. Plus* 130 (2015) 141.
- [33] J. Gabadinho, A. Beteva, M. Guijarro, V. Rey-Bakaikoa, D. Spruce, M.W. Bowler, S. Brockhauser, D. Flot, E.J. Gordon, D.R. Hall, B. Lavault, A.A. McCarthy, J. McCarthy, E. Mitchell, S. Monaco, C. Mueller-Dieckmann, D. Nurizzo, R.B.G. Ravelli, X. Thibault, M.A. Walsh, G.A. Leonard, S.M. McSweeney, MxCuBE: a synchrotron beamline control environment customized for macromolecular crystallography experiments, *J. Synchrotron Radiat.* 17 (2010) 700–707.
- [34] M.F. Incardona, G.P. Bourenkov, K. Levik, R.A. Pieritz, A.N. Popov, O. Svensson, EDNA: a framework for plugin-based applications applied to X-ray experiment online data analysis, *J. Synchrotron Radiat.* 16 (2009) 872–879.
- [35] S. Delageniere, P. Brechereau, L. Launer, A.W. Ashton, R. Leal, S. Veyrier, J. Gabadinho, E.J. Gordon, S.D. Jones, K.E. Levik, S.M. McSweeney, S. Monaco, M. Nanao, D. Spruce, O. Svensson, M.A. Walsh, G.A. Leonard, ISPyB: an information management system for synchrotron macromolecular crystallography, *Bioinformatics* 27 (2011) 3186–3192.
- [36] G.P. Bourenkov, A.N. Popov, Optimization of data collection taking radiation damage into account, *Acta Cryst. Section D* 66 (2010) 409–419.
- [37] K.M. Sparta, M. Krug, U. Heinemann, U. Mueller, M.S. Weiss, XDSAPP2. 0, *J. Appl. Cryst.* 49 (2016) 1085–1092.
- [38] D.G. Waterman, G. Winter, R.J. Gildea, J.M. Parkhurst, A.S. Brewster, N.K. Sauter, G. Evans, Diffraction-geometry refinement in the DIALS framework, *Acta Cryst. Section D* 72 (2016) 558–575.
- [39] P.R. Evans, G.N. Murshudov, How good are my data and what is the resolution? *Acta Cryst. Section D* 69 (2013) 1204–1214.
- [40] W. Kabsch, XDS, *Acta Cryst. Section D* 66 (2010) 125–132.
- [41] P.V. Afonine, R.W. Grosse-Kunstleve, N. Echols, J.J. Headd, N.W. Moriarty, M. Mustyakimov, T.C. Terwilliger, A. Urzhumtsev, P.H. Zwart, P.D. Adams, Towards automated crystallographic structure refinement with phenix.refine, *Acta Cryst. Section D* 68 (2012) 352–367.
- [42] O.S. Smart, T.O. Womack, A. Sharff, C. Flensburg, P. Keller, W. Paciorek, C. Vonrhein, G. Bricogne, Grade, version 1.102. Global Phasing, 2014.
- [43] D. Liebschner, *phenix.polder* – a Tool for Calculating Difference Maps Around Atom Selections by Excluding the Bulk Solvent Mask (The Phenix Project, Berkeley, California), 2016.
- [44] L.L.C. Schrodinger, The PyMOL Molecular Graphics System, Version 1.8, 2015.

Supporting information for

A focused fragment library targeting the antibiotic resistance enzyme - oxacillinase-48: synthesis, structural evaluation and inhibitor design

Sundus Akhter^{1,#}, Bjarte Aarmo Lund^{2,#}, Aya Ismael¹, Manuel Langer¹, Johan Isaksson¹, Tony Christopeit², Hanna-Kirsti Schrøder Leiros^{2,*}, Annette Bayer^{1,*}

¹ Department of Chemistry, Faculty of Science and Technology, UiT The Arctic University of Norway, N-9037 Tromsø, Norway. ² The Norwegian Structural Biology Centre (NorStruct), Department of Chemistry, Faculty of Science and Technology, UiT The Arctic University of Norway, N-9037 Tromsø, Norway.

* Corresponding authors: Annette Bayer, E-mail: annette.bayer@uit.no, Phone +47 77 64 40 69; Hanna-Kirsti S. Leiros, E-mail: hanna-kirsti.leiros@uit.no, Phone +47 77 64 57 06;

These authors have contributed equally to this work.

Table of content:

| | |
|---|------------|
| A focused fragment library targeting the antibiotic resistance enzyme - oxacillinase-48: synthesis, structural evaluation and inhibitor design | 1 |
| 1 Synthesis | 2 |
| 1.1 Material and methods | 2 |
| 1.2 Synthesis of 3-substituted benzoic acids | 2 |
| 1.3 Screening of catalysts | 17 |
| 1.4 Synthesis of symmetrical 3,5-disubstituted benzoic acid derivatives..... | 18 |
| 1.5 Synthesis of unsymmetrical 3,5-disubstituted benzoic acid derivatives..... | 19 |
| 2 NMR spectra of compounds 3–40: | 21 |
| 3 Biophysical, biochemical and structural analysis of OXA-48 with compound 3-40..... | 76 |
| 4 Data collection and processing statistics for X-ray crystallographic analysis..... | 103 |
| 5 Inhibition and binding data for compounds 3-40 with standard errors..... | 108 |

1 Synthesis

1.1 Material and methods

All reagents and solvents were purchased from commercial sources and used as supplied, unless otherwise stated. Solvent mixtures are given in (v|v). The water used for reactions, was purified on a Millipore RiOs™ device. The aqueous phase was concentrated under reduced pressure and Purification of compounds was carried out by automated RP flash chromatography with preloading to a C18 Samplet® cartridge (Biotage) before purification on a C18 RP column (Biotage) or by flash chromatography using silica gel from Merck (Silica gel 60, 0.040–0.063 mm). For thin layer chromatography TLC-PET sheets precoated with silica gel (60 F254) were used. Visualization was accomplished with either UV light or by immersion in potassium permanganate, phosphomolybdic acid (PMA) or ninhydrin followed by light heating with a heating gun. Purity analysis was carried out on Waters Acquity UHPLC® BEH C18 (1.7 μm, 2.1 × 100 mm) column on a Waters Acquity I-class UHPLC with a photodiode array detector. NMR spectra were recorded on a 400 MHz Bruker Avance III HD equipped with a 5 mm SmartProbe BB/1H (BB = ¹⁹F, ³¹P, ¹⁵N). Data are represented as follows: chemical shift, multiplicity (s = singlet, d = doublet, t = triplet, q = quartet, dt = double triplet, m = multiplet), coupling constant (*J*, Hz) and integration. Chemical shifts (δ) are reported in ppm relative to the residual solvent peak (CDCl₃ : δ_{H} 7.26 and δ_{C} 77.16; methanol-d₄ : δ_{H} 3.31 and δ_{C} 49.00, deuterium oxide: δ_{H} 4.79 and δ_{C} 49.00; DMSO-*d*₆ δ_{H} 2.51 and δ_{C} 39.52). The raw data was analysed with MestReNova (Version 10.0.2-15465). Electrospray ionization mass spectrometry was conducted on a Thermo electron LTQ Orbitrap XL spectrometer. The data was analyzed with Thermo Scientific Xcalibur software. Melting points were determined on a Büchi 535 device or a ThermoFischer Scientific IA9100 Digital Melting Point apparatus.

1.2 Synthesis of 3-substituted benzoic acids

General procedure A – Aqueous conditions:

The halo aryl (1.0 equiv) was dissolved in a mixture of water:dioxane (1:1). The boronic acid or ester (1.5 equiv) and potassium phosphate (5.0 equiv) were added. The solution was degassed by vacuum/argon cycles (10 times) before addition of PdCl₂(PPh₃)₂ (10 mol%) and further degassed (5 times). The resulting mixture was stirred at 95 °C under argon atmosphere for 16-20 hours. The reaction mixture was filtered through Celite and diluted with water (approx. 30 mL) before washing with chloroform (3 x 30 mL). If not stated otherwise, the aqueous phase was concentrated under reduced pressure and applied to a C18 precolumn before purification on a 10g or 60 g C18 column with a gradient of acetonitrile in water (10-100%) to yield the desired product.

General procedure B – Anhydrous conditions:

The halo aryl (1.0 equiv) was dissolved in anhydrous THF. The aryl boronic acid or aryl boronic ester (1.5 equiv) and inorganic base (5.0 equiv) were added. The solution was degassed by vacuum/Argon cycles (10 times), before addition of a palladium catalyst (10 mol%) and further degassed (5 times). The resulting mixture was stirred at 75–90 °C under an inert atmosphere for 16-20 hours. The reaction mixture was filtered through Celite and diluted with water (approx. 30 mL) before washing with ethyl acetate (3 x 30 mL). If not stated otherwise, the aqueous phase was concentrated under reduced pressure and applied to a C18 precolumn before purification on a 10 g or 60 g C18 column with a gradient of acetonitrile in water (10–80%) to yield the desired molecule.

2'-methylbiphenyl-3-carboxylic acid, **3a**:

According to procedure A, 3-carboxyphenylboronic acid pinacol ester (1.32 mmol, 326 mg, 1.5 equiv), 2-bromotoluene (0.88mmol, 150 mg, 1 equiv), potassium phosphate (4.39 mmol, 929 mg, 5 equiv) and PdCl₂(PPh₃)₂ (0.088 mmol, 62 mg, 10 mol%) gave **3a** (0.64 mmol, 136 mg, 78 %) as white solid. *T*_m =

288-289°C. ¹H NMR (400 MHz, methanol-*d*₄) δ 7.90-7.79 (m, 2H), 7.33-7.29 (m, 1H), 7.24 (dt, *J* = 7.6, 1.6 Hz, 1H), 7.18-7.07 (m, 4H), 2.14 (s, 3H). ¹³C NMR (101 MHz, methanol-*d*₄) δ 175.4, 143.2, 142.9, 139.1, 136.4, 131.9, 131.3, 131.1, 130.7, 128.7, 128.5, 128.3, 126.8, 20.6. HRMS (ESI): Calcd. for C₁₄H₁₀O₂ [M-H]⁻ 211.0765; found 211.0766. UHPLC: purity = 97.5 %

3'-methylbiphenyl-3-carboxylic acid, **3b**:

According to procedure A, 3-carboxyphenylboronic acid pinacol ester (1.32 mmol, 326 mg, 1.5 equiv), 3-bromotoluene (0.88 mmol, 150 mg, 1.0 equiv), potassium phosphate (4.39 mmol, 929 mg, 5.0 equiv) and PdCl₂(PPh₃)₂ (0.088 mmol, 62 mg, 10 mol%) gave **3b** (0.59 mmol, 124 mg, 67 %) as white solid. T_m = 257-258°C. ¹H NMR (400 MHz, methanol-*d*₄) δ 8.12 (s, 1H), 7.81 (d, *J* = 7.7 Hz, 1H), 7.55 (d, *J* = 7.8 Hz, 1H), 7.40-7.28 (m, 3H), 7.21 (t, *J* = 7.6 Hz, 1H), 7.05 (d, *J* = 7.5 Hz, 1H), 2.31 (s, 3H). ¹³C NMR (101 MHz, methanol-*d*₄) δ 175.4, 142.3, 142.1, 139.6, 139.5, 129.7, 129.7, 129.2, 129.1, 128.9, 128.9, 128.7, 125.1, 21.6. HRMS (ESI): Calcd. for C₁₄H₁₀O₂ [M-H]⁻ 211.0765; found 211.0768. UHPLC: purity = 95.5 %

2'-hydroxybiphenyl-3-carboxylic acid, **4a**:

According to procedure A, 3-bromobenzoic acid (1.24 mmol, 250 mg, 1.0 equiv), 3-hydroxyphenylboronic acid (1.86 mmol, 256 mg, 1.5 equiv), potassium phosphate (6.20 mmol, 1.32 g, 5.0 equiv) and PdCl₂(PPh₃)₂ (0.124 mmol, 87 mg, 10 mol%) gave **4a** (1.17 mmol, 250 mg, 94 %) as white solid. T_m = 290-291°C. ¹H NMR (400 MHz, DMSO-*d*₆) δ 8.09 (s, 1H), 7.79 (d, *J* = 7.7 Hz, 1H), 7.47 (d, *J* = 7.7 Hz, 1H), 7.27 (t, *J* = 7.6 Hz, 1H), 7.21 (dd, *J* = 7.6, 1.6 Hz, 1H), 7.14-6.99 (m, 2H), 6.82 (td, *J* = 7.2, 1.6 Hz, 1H). ¹³C NMR (101 MHz, DMSO-*d*₆) δ 169.9, 155.6, 141.0, 138.2, 130.6, 130.4, 129.7, 128.7, 128.5, 127.7, 127.0, 119.2, 116.7. HRMS (ESI): Calcd. for C₁₃H₉O₃ [M-H]⁻ 213.0557 found 213.0561. UHPLC: purity > 99.5%

3'-hydroxybiphenyl-3-carboxylic acid, **4b**:

According to procedure A, 3-bromobenzoic acid (1.24 mmol, 250 mg, 1.0 equiv), 3-hydroxyphenyl boronic acid (1.86 mmol, 256 mg, 1.5 equiv), potassium phosphate (6.20 mmol, 1.32 g, 5.0 equiv) and PdCl₂(PPh₃)₂ (0.124 mmol, 87 mg, 10 mol%) gave **4b** (1.21 mmol, 260 mg, 98 %) as white solid. T_m = 279-280°C. ¹H NMR (400 MHz, DMSO-*d*₆) δ 8.19 (s, 1H), 7.82 (d, *J* = 7.5 Hz, 1H), 7.53 (d, *J* = 7.7 Hz, 1H), 7.32 (t, *J* = 7.6 Hz, 1H), 7.23-7.17 (m, 2H), 7.01 (s, 1H), 6.73 (d, *J* = 7.9 Hz, 1H). ¹³C NMR (101 MHz, DMSO-*d*₆) δ 169.5, 159.4, 142.2, 141.8, 139.7, 130.1, 128.4, 128.0, 127.6, 127.1, 116.8, 114.9, 114.1. HRMS (ESI): Calcd. for C₁₃H₉O₃ [M-H]⁻ 213.0557; found 213.0565. UHPLC: purity = 96.0 %

4'-hydroxybiphenyl-3-carboxylic acid, **4c**:

According to general procedure A, 3-bromobenzoic acid (0.75 mmol, 150 mg, 1.0 equiv), (4-hydroxyphenyl)boronic acid (1.12 mmol, 154 mg, 1.5 equiv), potassium phosphate (3.73 mmol, 792 mg, 5.0 equiv) and PdCl₂(PPh₃)₂ (0.07 mmol, 52 mg, 10 mol%) were stirred at 95°C. The aqueous phase was washed with a mixture of hexane/ethyl acetate (1:1, v/v, 3 x 30 mL) instead of chloroform. After purification the title compound, **4c** (0.29 mmol, 63 mg, 39%) was obtained as a dark brown solid. T_m = 257-259°C. ¹H NMR (400 MHz, methanol-*d*₄) δ 8.13 (t, *J* = 1.8 Hz, 1H), 7.83 (dt, *J* = 7.7, 1.4 Hz, 1H), 7.62 (dt, *J* = 7.8, 1.4 Hz, 1H), 7.55-7.49 (m, 2H), 7.43 (t, *J* = 7.7 Hz, 1H), 6.95-6.88 (m, 2H). ¹³C NMR (101 MHz, methanol-*d*₄) δ 175.7, 157.5, 141.5, 138.8, 133.5, 129.4, 129.3, 129.0, 128.3, 128.0, 116.8. HRMS (ESI): Calcd. for C₁₃H₉O₃ [M-H]⁻ 213.0557; found 213.0577. UHPLC: purity = 97.8 %

3'-(hydroxymethyl)biphenyl-3-carboxylic acid, **5**:

According to procedure A, 3-bromobenzoic acid (1.24 mmol, 250 mg, 1.0 equiv), 3-(Hydroxymethyl)phenylboronic acid (1.86 mmol, 282 mg, 1.5 equiv), potassium phosphate (6.20 mmol, 1.32 g, 5.0 equiv) and PdCl₂(PPh₃)₂ (0.124 mmol, 87 mg, 10 mol%) gave **5**, (1.04 mmol, 239 mg,

84 %) as white solid. $T_m = 241-242^\circ\text{C}$. $^1\text{H NMR}$ (400 MHz, $\text{DMSO-}d_6$) δ 8.14 (s, 1H), 7.87 (d, $J = 7.9$ Hz, 1H), 7.81 (d, $J = 8.0$ Hz, 1H), 7.68 (d, $J = 13.8$ Hz, 2H), 7.58-7.52 (m, 2H), 7.42 (d, $J = 8.0$ Hz, 1H), 4.72 (s, 2H). $^{13}\text{C NMR}$ (101 MHz, $\text{DMSO-}d_6$) δ 169.1, 143.7, 142.6, 141.1, 139.4, 129.1, 128.5, 128.1, 127.8, 126.9, 125.7, 125.3, 125.1, 63.4. HRMS (ESI): Calcd. for $\text{C}_{14}\text{H}_{11}\text{O}_3$ $[\text{M-H}]^-$ 227.0714; found 227.0716. UHPLC: purity = 95.1 %

2'-methoxybiphenyl-3-carboxylic acid, **6a**:

According to procedure A, 3-bromobenzoic acid (1.24 mmol, 250 mg, 1.0 equiv), 3-methoxyphenylboronic acid (1.86 mmol, 282 mg, 1.5 equiv), potassium phosphate (6.20 mmol, 1.32 g, 5.0 equiv) and $\text{PdCl}_2(\text{PPh}_3)_2$ (0.124 mmol, 87 mg, 10 mol%) gave **6a** (0.89 mmol, 205 mg, 73 %) as white solid. $T_m = 88-89^\circ\text{C}$. $^1\text{H NMR}$ (400 MHz, $\text{DMSO-}d_6$) δ 7.93 (s, 1H), 7.79 (d, $J = 7.6$ Hz, 1H), 7.38-7.22 (m, 4H), 7.10 (d, $J = 8.2$ Hz, 1H), 7.02 (t, $J = 7.4$ Hz, 1H), 3.75 (s, 3H). $^{13}\text{C NMR}$ (101 MHz, $\text{DMSO-}d_6$) δ 169.2, 156.7, 141.9, 137.3, 131.1, 130.9, 130.4, 129.5, 128.9, 127.9, 126.9, 121.1, 112.1, 55.9. HRMS (ESI): Calcd. for $\text{C}_{14}\text{H}_{11}\text{O}_3$ $[\text{M-H}]^-$ 227.0714; found 227.0712. UHPLC: purity = 98.0 %

3'-methoxybiphenyl-3-carboxylic acid, **6b**:

According to procedure A, 3-bromobenzoic acid (1.24 mmol, 250 mg, 1.0 equiv), 3-methoxyphenylboronic acid (1.86 mmol, 282 mg, 1.5 equiv), potassium phosphate (6.20 mmol, 1.32 g, 5.0 equiv) and $\text{PdCl}_2(\text{PPh}_3)_2$ (0.124 mmol, 87 mg, 10 mol%) gave **6b** (1.04 mmol, 237 mg, 84 %) as white solid. $T_m = 149-150^\circ\text{C}$. $^1\text{H NMR}$ (400 MHz, $\text{DMSO-}d_6$) δ 8.12 (s, 1H), 7.84 (d, $J = 7.0$ Hz, 1H), 7.55 (d, $J = 7.7$ Hz, 1H), 7.35 (dt, $J = 18.7, 7.7$ Hz, 2H), 7.21 (d, $J = 7.6$ Hz, 1H), 7.15 (s, 1H), 6.92 (dd, $J = 8.2, 2.5$ Hz, 1H), 3.83 (s, 3H). $^{13}\text{C NMR}$ (101 MHz, $\text{DMSO-}d_6$) δ 168.3, 159.7, 142.5, 138.7, 129.9, 128.3, 127.5, 127.3, 126.5, 118.9, 112.7, 111.9, 99.5, 55.1. HRMS (ESI): Calcd. for $\text{C}_{14}\text{H}_{11}\text{O}_3$ $[\text{M-H}]^-$ 227.0714; found 227.0711. UHPLC: purity > 99.5 %

4'-methoxybiphenyl-3-carboxylic acid, **6c**:

According to procedure A, 3-bromobenzoic acid (1.24 mmol, 250 mg, 1.0 equiv), 4-methoxyphenyl boronic acid (1.86 mmol, 282 mg, 1.5 equiv), potassium phosphate (7.44 mmol, 1.58 g, 6.0 equiv) and $\text{PdCl}_2(\text{PPh}_3)_2$ (0.124 mmol, 87 mg, 10 mol%) gave **6c** (1.07 mmol, 244 mg, 86 %) as white solid. $^1\text{H NMR}$ (400 MHz, methanol- d_4) δ 8.19 (s, 1H), 7.87 (d, $J = 7.5$ Hz, 1H), 7.75-7.51 (m, 3H), 7.40 (t, $J = 7.7$ Hz, 1H), 7.00 (d, $J = 8.0$ Hz, 2H), 3.83 (s, 3H). $^{13}\text{C NMR}$ (101 MHz, methanol- d_4) δ 175.3, 160.6, 141.5, 139.4, 134.7, 129.2, 129.1, 128.9, 128.4, 128.3, 115.2, 55.6. HRMS (ESI): Calcd. for $\text{C}_{14}\text{H}_{11}\text{O}_3$ $[\text{M-H}]^-$ 227.0708; found 227.0724. UHPLC: purity = 98.8 %

4'-methylthiobiphenyl-3-carboxylic acid, **7**:

According to general procedure B, 3-bromobenzoic acid (0.75 mmol, 150 mg, 1.0 equiv), 4-(methylthio)phenyl boronic acid (1.12 mmol, 188 mg, 1.5 equiv), Na_2CO_3 (3.73 mmol, 395 mg, 5.0 equiv), $\text{PdCl}_2(\text{dppf})$ (0.07 mmol, 55 mg, 10 mol%) in anhydrous THF (8 mL) was stirred at 75°C for 18h. After purification the title compound, **7** (0.68 mmol, 167 mg, 91%) was obtained as a brownish solid. $T_m = 228^\circ\text{C}$. $^1\text{H NMR}$ (400 MHz, methanol- d_4) δ 7.93-7.85 (m, 1H), 7.69-7.62 (m, 1H), 7.63-7.58 (m, 2H), 7.45 (t, $J = 7.9$ Hz, 1H), 7.37-7.30 (m, 2H). $^{13}\text{C NMR}$ (101 MHz, methanol- d_4) δ 175.4, 141.0, 139.2, 138.9, 138.7, 129.5, 129.5, 129.0, 128.3, 127.8, 15.7. HRMS (ESI): Calcd. for $\text{C}_{14}\text{H}_{11}\text{O}_2\text{S}$ $[\text{M-H}]^-$ 243.0485; found 243.0483. UHPLC: purity = 98.4 %

2'-fluorobiphenyl-3-carboxylic acid, **8a**:

According to procedure A, 3-bromobenzoic acid (1.24 mmol, 250 mg, 1.0 equiv), 2-fluorophenylboronic acid (1.86 mmol, 256 mg, 1.5 equiv), potassium phosphate (6.20 mmol, 1.32 g, 5.0 equiv) and $\text{PdCl}_2(\text{PPh}_3)_2$ (0.124 mmol, 87 mg, 10 mol%) gave **8a** (0.84 mmol, 181 mg, 68 %) as white

solid. $T_m = 260-261^\circ\text{C}$. $^1\text{H NMR}$ (400 MHz, methanol- d_4) δ 8.04 (s, 1H), 7.86 (d, $J = 7.6$ Hz, 1H), 7.49 (d, $J = 7.7$ Hz, 1H), 7.42 (t, $J = 7.8$ Hz, 1H), 7.37-7.20 (m, 1H), 7.15 (t, $J = 7.5$ Hz, 1H), 7.12-7.02 (m, 1H). $^{13}\text{C NMR}$ (101 MHz, methanol- d_4) δ 175.1, 161.1 (d, $J = 246.5$ Hz), 139.5, 136.6, 131.9 (d, $J = 3.4$ Hz), 131.8 (d, $J = 3.5$ Hz), 130.9 (d, $J = 2.4$ Hz), 130.3 (d, $J = 8.4$ Hz), 129.6, 128.8, 125.6 (d, $J = 3.8$ Hz), 116.9 (d, $J = 22.9$ Hz). HRMS (ESI): Calcd. for $\text{C}_{13}\text{H}_8\text{FO}_2$ $[\text{M}-\text{H}]^-$ 215.0514; found 215.0511. UHPLC: purity > 99.5%

3'-fluorobiphenyl-3-carboxylic acid, **8b**:

According to procedure A, 3-bromobenzoic acid (1.24 mmol, 250 mg, 1.0 equiv), 3-fluorophenylboronic acid (1.86 mmol, 256 mg, 1.5 equiv), potassium phosphate (6.20 mmol, 1.32 g, 5.0 equiv) and $\text{PdCl}_2(\text{PPh}_3)_2$ (0.124 mmol, 87 mg, 10 mol%) gave **8b** (1.03 mmol, 222 mg, 83 %) as white solid. $T_m = 239-241^\circ\text{C}$. $^1\text{H NMR}$ (400 MHz, methanol- d_4) δ 8.13 (s, 1H), 7.85 (d, $J = 7.6$ Hz, 1H), 7.58 (d, $J = 7.7$ Hz, 1H), 7.49-7.20 (m, 4H), 6.97 (t, $J = 8.6$ Hz, 1H). $^{13}\text{C NMR}$ (101 MHz, methanol- d_4) δ 175.05, 164.71 (d, $J = 244.0$ Hz), 144.83, 140.56, 139.90, 131.53, 129.78, 129.68, 129.44, 128.89, 123.87, 123.84, 114.74 (dd, $J = 25.9, 21.8$ Hz). HRMS (ESI): Calcd. for $\text{C}_{13}\text{H}_8\text{FO}_2$ $[\text{M}-\text{H}]^-$ 215.0514; found 215.0511. UHPLC: purity = 98.7%

4'-fluorobiphenyl-3-carboxylic acid, **8c**:

According to procedure A, 3-bromobenzoic acid (1.24 mmol, 250 mg, 1.0 equiv), 4-fluorophenylboronic acid (1.86 mmol, 256 mg, 1.5 equiv), potassium phosphate (6.20 mmol, 1.32 g, 5.0 equiv) and $\text{PdCl}_2(\text{PPh}_3)_2$ (0.124 mmol, 87 mg, 10 mol%) gave **8c** (0.97 mmol, 169 mg, 78 %) as white solid. $T_m = 298-299^\circ\text{C}$. $^1\text{H NMR}$ (400 MHz, DMSO- d_6) δ 8.10 (s, 1H), 7.83 (d, $J = 7.5$ Hz, 1H), 7.75-7.58 (m, 2H), 7.52 (d, $J = 7.8$ Hz, 1H), 7.42-7.19 (m, 3H). $^{13}\text{C NMR}$ (101 MHz, DMSO- d_6) δ 168.9, 162.1 (d, $J = 243.6$ Hz), 142.8, 138.27, 137.8, 137.81, 128.9, 128.9, 128.6, 128.1, 127.7, 126.8, 116.1 (d, $J = 21.2$ Hz). HRMS (ESI): Calcd. for $\text{C}_{13}\text{H}_8\text{FO}_2$ $[\text{M}-\text{H}]^-$ 215.0514; found 215.0511. UHPLC: purity > 99.5%

2'-(methoxycarbonyl)biphenyl-3-carboxylic acid, **9a**:

According to general procedure B, 3-bromobenzoic acid (0.75 mmol, 150 mg, 1.0 equiv), (2-(methoxycarbonyl)phenyl)boronic acid (1.12 mmol, 201 mg, 1.5 equiv), Na_2CO_3 (3.73 mmol, 395 mg, 5.0 equiv) and $\text{PdCl}_2(\text{dppf})$ (0.07 mmol, 55 mg, 10 mol%) in anhydrous THF (8 mL) was stirred at 90°C for 20h. After purification the title compound, **9a** (0.43 mmol, 109 mg, 57%) was obtained as a brown solid. $T_m = 206-208^\circ\text{C}$. $^1\text{H NMR}$ (400 MHz, methanol- d_4) δ 7.97-7.92 (m, 2H), 7.77 (dd, $J = 8.0, 1.5$ Hz, 1H), 7.61-7.53 (m, 1H), 7.47-7.36 (m, 3H), 7.31 (dt, $J = 7.7, 1.5$ Hz, 1H), 3.60 (s, 3H). $^{13}\text{C NMR}$ (101 MHz, methanol- d_4) δ 175.1, 171.0, 143.6, 142.1, 139.2, 132.5, 132.4, 131.8, 131.2, 130.6, 130.3, 129.2, 128.5, 128.3, 52.4. HRMS (ESI): Calcd. for $\text{C}_{15}\text{H}_{11}\text{O}_4$ $[\text{M}-\text{H}]^-$ 255.0663; found 255.0660. UHPLC: purity > 99.5%

3'-(methoxycarbonyl)biphenyl-3-carboxylic acid, **9b**:

According to procedure A, 3-bromobenzoic acid (1.24 mmol, 250 mg, 1.0 equiv), 3-Methoxycarbonylphenylboronic acid (1.86 mmol, 335 mg, 1.5 equiv), potassium phosphate (6.20 mmol, 1.32 g, 5.0 equiv) and $\text{PdCl}_2(\text{PPh}_3)_2$ (0.124 mmol, 87 mg, 10 mol%) gave **9b** (0.68 mmol, 174 mg, 54 %) as white solid. $T_m = 163-164^\circ\text{C}$. $^1\text{H NMR}$ (400 MHz, DMSO- d_6) δ 8.21 (s, 1H), 8.18 (s, 1H), 7.97-7.94 (m, 2H), 7.88 (d, $J = 7.6$ Hz, 1H), 7.63 (t, $J = 8.0$ Hz, 2H), 7.38 (t, $J = 7.6$ Hz, 1H), 3.91 (s, 3H). $^{13}\text{C NMR}$ (101 MHz, DMSO- d_6) δ 168.6, 166.7, 142.9, 141.7, 138.1, 131.8, 130.7, 129.9, 129.1, 128.3, 128.2, 127.7, 127.4, 126.9, 52.7. HRMS (ESI): Calcd. for $\text{C}_{15}\text{H}_{11}\text{O}_4$ $[\text{M}-\text{H}]^-$ 255.0663; found 255.0660. UHPLC: purity = 97.8 %

4'-acetylbiiphenyl-3-carboxylic acid, **10**:

According to procedure A, 3-bromobenzoic acid (1.24 mmol, 250 mg, 1.0 equiv), 4-acetylphenylboronic acid (1.86 mmol, 305 mg, 1.5 equiv), potassium phosphate (6.20 mmol, 1.32 g, 5.0 equiv) and

PdCl₂(PPh₃)₂ (0.124 mmol, 87 mg, 10 mol%) gave **10** (0.68 mmol, 174 mg, 54 %) as white solid. T_m = 287-289°C. ¹H NMR (400 MHz, DMSO-*d*₆) δ 8.23 (s, 1H), 8.06 (d, *J* = 8.2 Hz, 2H), 7.91 (d, *J* = 7.6 Hz, 1H), 7.82 (d, *J* = 8.1 Hz, 2H), 7.66 (d, *J* = 7.9 Hz, 1H), 7.40 (t, *J* = 7.6 Hz, 1H), 2.63 (s, 3H). ¹³C NMR (101 MHz, DMSO-*d*₆) δ 197.9, 168.7, 145.7, 142.9, 138.0, 135.8, 129.5, 129.4, 128.3, 127.9, 127.2, 127.2, 27.2. HRMS (ESI): Calcd. for C₁₅H₁₁O₃ [M-H]⁻ 239.0714; found 239.0709. UHPLC: purity = 95.4 %

3'-carbamoylbiphenyl-3-carboxylic acid, **11a**:

According to procedure A, 3-bromobenzoic acid (1.24 mmol, 250 mg, 1.0 equiv), 3-aminocarbonylphenylboronic acid (1.86 mmol, 307 mg, 1.5 equiv), potassium phosphate (6.20 mmol, 1.32 g, 5.0 equiv) and PdCl₂(PPh₃)₂ (0.124 mmol, 87 mg, 10 mol%) gave **11a** (1.59 mmol, 383 mg, 85 %) as white solid. T_m = 235-237°C. ¹H NMR (400 MHz, DMSO-*d*₆) δ 8.25 (s, 1H), 8.23 (s, 2H), 7.93-7.90 (m, 2H), 7.85 (d, *J* = 7.8 Hz, 1H), 7.67 (d, *J* = 7.5 Hz, 1H), 7.59 (t, *J* = 7.7 Hz, 1H), 7.46-7.40 (m, 2H). ¹³C NMR (101 MHz, DMSO-*d*₆) δ 168.8, 168.4, 142.9, 141.3, 138.7, 135.4, 129.8, 129.3, 128.9, 128.1, 127.9, 126.9, 126.7, 126.1. HRMS (ESI): Calcd. for C₁₄H₁₀NO₃ [M-H]⁻ 240.0666; found 240.0662. UHPLC: purity = 96.7 %

4'-carbamoylbiphenyl-3-carboxylic acid, **11b**:

According to procedure A, 3-bromobenzoic acid (1.24 mmol, 250 mg, 1.0 equiv), 4-aminocarbonylphenylboronic acid (1.86 mmol, 307 mg, 1.5 equiv), potassium phosphate (6.20 mmol, 1.32 g, 5.0 equiv) and PdCl₂(PPh₃)₂ (0.124 mmol, 87 mg, 10 mol%) gave **11b** (1.20 mmol, 290 mg, 97 %) as white solid. T_m = 262-263°C. ¹H NMR (400 MHz, methanol-*d*₄) δ 8.19 (s, 1H), 7.92-7.83 (m, 3H), 7.71-7.59 (m, 3H), 7.37 (t, *J* = 7.7 Hz, 1H). ¹³C NMR (101 MHz, methanol-*d*₄) δ 175.0, 172.1, 145.8, 140.7, 139.9, 133.6, 130.7, 129.9, 129.8, 129.5, 129.3, 129.0, 128.0, 116.5. HRMS (ESI): Calcd. for C₁₄H₁₀NO₃ [M-H]⁻ 240.0666; found 240.0671. UHPLC: purity = 97.5 %

3'-(methylsulfonyl)biphenyl-3-carboxylic acid, **12a**:

According to procedure A, 3-bromobenzoic acid (1.24 mmol, 250 mg, 1.0 equiv), 3-methanesulfonylphenyl boronic acid (1.24 mmol, 248 mg, 1 equiv), potassium phosphate (3.72 mmol, 789 mg, 3 equiv) and PdCl₂(PPh₃)₂ (0.124 mmol, 87 mg, 10 mol%) gave **21a** (1.02 mmol, 283 mg, 82 %) as white solid. T_m = 96-98°C. ¹H NMR (400 MHz, methanol-*d*₄) δ 8.20 (s, 1H), 8.15 (s, 1H), 7.95-7.88 (m, 2H), 7.84 (d, *J* = 7.8 Hz, 1H), 7.67-7.61 (m, 2H), 7.40 (t, *J* = 7.7 Hz, 1H), 3.09 (s, 3H). ¹³C NMR (101 MHz, methanol-*d*₄) δ 174.8, 143.9, 142.8, 140.2, 139.9, 133.3, 131.1, 130.2, 129.8, 129.7, 129.0, 126.9, 126.6, 44.4. HRMS (ESI): Calcd. for C₁₄H₁₁O₄S [M-H]⁻ 275.0384; found 275.0389. UHPLC: purity = 95.4 %

4'-(methylsulfonyl)biphenyl-3-carboxylic acid, **12b**:

According to procedure A, 3-bromobenzoic acid (1.24 mmol, 250 mg, 1.0 equiv), 4-methanesulfonylphenyl boronic acid (1.24 mmol, 248 mg, 1.0 equiv), potassium phosphate (3.72 mmol, 789 mg, 3.0 equiv) and PdCl₂(PPh₃)₂ (0.124 mmol, 87 mg, 10 mol%) gave **21b** (1.12 mmol, 309 mg, 90 %) as white solid. T_m = 127-129°C. ¹H NMR (400 MHz, DMSO-*d*₆) δ 8.23 (s, 1H), 8.05-7.86 (m, 5H), 7.66 (d, *J* = 7.6 Hz, 1H), 7.41 (t, *J* = 7.6 Hz, 1H), 3.26 (s, 3H). ¹³C NMR (101 MHz, DMSO-*d*₆) δ 168.7, 146.2, 142.9, 139.7, 137.6, 129.8, 128.4, 128.10, 127.9, 127.4, 44.1. HRMS (ESI): Calcd. for C₁₄H₁₁O₄S [M-H]⁻ 275.0384; found 275.0380. UHPLC: purity = 96.2 %

4'-aminobiphenyl-3-carboxylic acid, **13**:

According to general procedure A, 4-bromoaniline (1.45 mmol, 250 mg, 1.0 equiv), 3-(4,4,5,5-tetramethyl-1,3,2-dioxaborolan-2-yl)benzoic acid (2.18 mmol, 541 mg, 1.5 equiv) potassium phosphate (7.27 mmol, 1.54 g, 5.0 equiv) and PdCl₂(PPh₃)₂ (0.15 mmol, 102 mg, 10 mol%), gave **13** (0.51 mmol, 109 mg, 35%) as a white solid. T_m = 195°C. ¹H NMR (400 MHz, methanol-*d*₄) δ 8.13 (t, *J* =

1.8 Hz, 1H), 7.85-7.77 (m, 1H), 7.65-7.57 (m, 2H), 7.41 (t, $J = 7.7$ Hz, 1H), 6.90-6.84 (m, 2H). ^{13}C NMR (101 MHz, methanol- d_4) δ 169.0, 148.0, 141.9, 139.3, 128.2, 127.3, 127.0, 126.5, 126.1, 125.2, 114.2. HRMS (ESI): Calcd. for $\text{C}_{13}\text{H}_{10}\text{O}_2\text{N}$ [M-H] $^-$ 212.0717; found 212.0712. HPLC, purity = 98.3 %

4'-dimethylaminobiphenyl-3-carboxylic acid, **14**:

According to general procedure A, 3-bromobenzoic acid (0.75 mmol, 150 mg, 1.0 equiv), 3-dimethylaminophenyl boronic acid (1.12 mmol, 185 mg, 1.5 equiv), potassium phosphate (3.73 mmol, 792 mg, 5.0 equiv) and $\text{PdCl}_2(\text{PPh}_3)_2$ (0.07 mmol, 52 mg, 10 mol%) gave **14** (0.71 mmol, 172 mg, 95%) as red solid. $T_m = 192$ - 194°C . ^1H NMR (400 MHz, deuterium oxide) δ 8.09 (t, $J = 1.7$ Hz, 1H), 7.89-7.80 (m, 1H), 7.68-7.60 (m, 1H), 7.47 (t, $J = 7.7$ Hz, 1H), 7.32 (t, $J = 7.9$ Hz, 1H), 7.12 (t, $J = 2.0$ Hz, 1H), 7.11-7.04 (m, 1H), 6.96-6.88 (m, 1H), 2.80 (s, 6H). ^{13}C NMR (101 MHz, deuterium oxide) δ 175.3, 151.8, 141.2, 140.7, 136.8, 129.9, 129.6, 128.8, 127.9, 127.4, 118.1, 114.9, 113.8, 41.1. HRMS (ESI): Calcd. for $\text{C}_{15}\text{H}_{14}\text{NO}_2$ [M-H] $^-$ 240.1030; found 240.1029. HPLC purity = 95.1 %

3'-(aminomethyl)biphenyl-3-carboxylic acid, **15a**:

According to general procedure A, 3-bromobenzylamin hydrochloride (250 mg, 1.12 mmol, 1.0 equiv), 3-(4,4,5,5-tetramethyl-1,3,2-dioxaborolan-2-yl) benzoic acid (1.69 mmol, 418 mg, 1.5 equiv), potassium phosphate (5.62 mmol, 1.19 g, 5.0 equiv), $\text{PdCl}_2(\text{PPh}_3)_2$ (0.11 mmol, 79 mg, 10 mol%), after purification by flash chromatography on silica gel using a mixture of an acidic stock solution (acetic acid/ H_2O /MeOH/ethyl acetate, 3:2:3:3) and ethyl acetate (1:9), then acidic stock solution/ethyl acetate (1:2) as eluent, gave **15a** (0.40 mmol, 91 mg, 36%) as a slightly yellow solid. $T_m = 346^\circ\text{C}$ (decomposes). ^1H NMR (400 MHz, deuterium oxide) δ 8.06 (d, $J = 1.8$ Hz, 1H), 7.80-7.77 (m, 1H), 7.66-7.63 (m, 1H), 7.52-7.42 (m, 3H), 7.38 (t, $J = 7.6$ Hz, 1H), 7.25 (d, $J = 7.5$ Hz, 1H), 3.71 (s, 2H). ^{13}C NMR (101 MHz, deuterium oxide) δ 176.1, 144.2, 141.5, 141.4, 138.1, 130.4, 130.3, 129.8, 128.9, 128.3, 127.6, 126.7, 126.4, 45.8. HRMS (ESI): Calcd. for $\text{C}_{14}\text{H}_{12}\text{NO}_2$ [M-H] $^-$ 226.0874; found 226.0872. UHPLC: purity = 95.2 %

4'-(aminomethyl)biphenyl-3-carboxylic acid, **15b**:

According to general procedure A, 4-bromobenzylamin hydrochloride (250 mg, 1.12 mmol, 1.0 equiv), 3-(4,4,5,5-tetramethyl-1,3,2-dioxaborolan-2-yl) benzoic acid (1.69 mmol, 418 mg, 1.5 equiv), potassium phosphate (5.62 mmol, 1.19 g, 5.0 equiv), $\text{PdCl}_2(\text{PPh}_3)_2$ (0.11 mmol, 79 mg, 10 mol%), after purification by flash chromatography on silica gel using a mixture of an acidic stock solution (acetic acid/ H_2O /MeOH/ethyl acetate, 3:2:3:3) and ethyl acetate (1:9), then acidic stock solution/ethyl acetate (1:2) as eluent, gave **15b** (0.96 mmol, 220 mg, 86%) as a slightly yellow solid. $T_m = 213$ - 215°C . ^1H NMR (400 MHz, deuterium oxide) δ 8.00 (s, 1H), 7.74 (d, $J = 7.7$ Hz, 1H), 7.64 (d, $J = 8.2$ Hz, 1H), 7.54 (d, $J = 8.0$ Hz, 2H), 7.42 (t, $J = 7.7$ Hz, 1H), 7.31 (d, $J = 8.0$ Hz, 1H), 3.67 (s, 2H). ^{13}C NMR (101 MHz, deuterium oxide) δ 175.3, 141.9, 140.1, 138.5, 136.9, 129.4, 128.9, 127.9, 127.8, 127.1, 127.0, 44.3. HRMS (ESI): Calcd. for $\text{C}_{14}\text{H}_{12}\text{NO}_2$ [M-H] $^-$ 226.0874; found 226.0872. UHPLC: purity = 83.2 %

3'-(2-aminoethyl)biphenyl-3-carboxylic acid, **16a**:

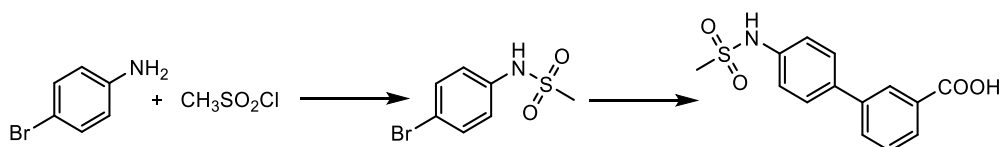
According to general procedure A, 3-bromobenzylamin hydrochloride (250 mg, 1.25 mmol, 1.0 equiv), 3-(4,4,5,5-tetramethyl-1,3,2-dioxaborolan-2-yl) benzoic acid (1.87 mmol, 465 mg, 1.5 equiv), potassium phosphate (1.33 mmol, 1.33 g, 5.0 equiv), $\text{PdCl}_2(\text{PPh}_3)_2$ (0.12 mmol, 88 mg, 10 mol%), after purification by flash chromatography on silica gel using a mixture of an acidic stock solution (acetic acid/ H_2O /MeOH/ethyl acetate, 3:2:3:3) and ethyl acetate (1:9), then acidic stock solution/ethyl acetate (1:2) as eluent, gave **16a** (0.19 mmol, 45 mg, 15%) as a slightly yellow solid. $T_m = 232$ - 235°C . ^1H NMR (400 MHz, methanol- d_4) δ 8.23 (s, 1H), 7.93-7.91 (m, 1H), 7.65-7.63 (m, 1H), 7.52-7.48 (m, 2H), 7.43-7.31 (m, 2H), 7.20-7.18 (m, 1H), 2.97 (t, $J = 7.1$ Hz, 2H), 2.85 (t, $J = 7.1$ Hz, 2H). ^{13}C NMR (101 MHz,

methanol-*d*₄) δ 173.8, 141.1, 140.2, 139.4, 138.0, 128.5, 128.1, 127.7, 127.6, 127.4, 127.2, 127.0, 124.6, 42.3, 38.1. HRMS (ESI): Calcd. for C₁₄H₁₂O₂N [M-H]⁻ 240.1030; found 240.1028. UHPLC: purity = 95.5 %

4'-(2-aminoethyl)biphenyl-3-carboxylic acid, **16b**:

The compound was prepared according to general procedure A. 4-Bromophenethylamine (1.25 mmol, 250 mg, 1.0 equiv), 3-(4,4,5,5-tetramethyl-1,3,2-dioxaborolan-2-yl)benzoic acid (1.87 mmol, 465 mg, 1.5 equiv), potassium phosphate (6.25 mmol, 1.33 g, 5.0 equiv) and PdCl₂(PPh₃)₂ (0.12 mmol, 88 mg, 10 mol%), after purification by flash chromatography on silica gel with a mixture of an acidic stock solution (acetic acid/H₂O/MeOH/ethyl acetate, 3:2:3:3) and ethyl acetate (1:9), then acidic stock solution/ethyl acetate (1:2) as eluent, gave **16b** (0.84 mmol, 201 mg, 67%) as a slightly brownish solid. T_m = 312 °C (decomposes). ¹H NMR (400 MHz, deuterium oxide) δ 8.06 (s, 1H), 7.79 (d, *J* = 7.7 Hz, 1H), 7.67 (d, *J* = 8.2 Hz, 1H), 7.55 (d, *J* = 7.9 Hz, 4H), 7.46 (t, *J* = 7.7 Hz, 2H), 7.27 (d, *J* = 7.9 Hz, 5H), 2.79 (t, *J* = 7.0 Hz, 4H), 2.69 (t, *J* = 6.9 Hz, 4H). ¹³C NMR (101 MHz, methanol-*d*₄) δ 176.2, 141.2, 140.7, 139.0, 138.0, 130.5, 130.3, 129.9, 128.7, 128.0, 127.9, 43.1, 38.8. HRMS (ESI): Calcd. for C₁₅H₁₄NO₂ [M-H]⁻ 240.1030; found 240.1029. UHPLC: purity = 95.8 %

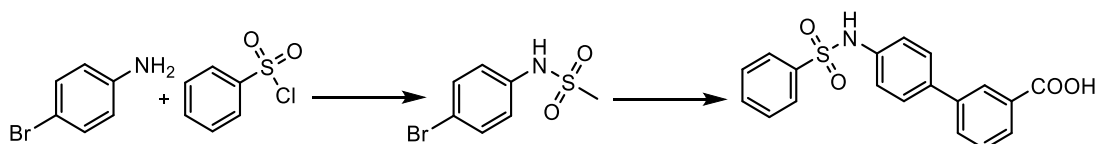
4'-(methylsulfonamido)biphenyl-3-carboxylic acid, **17**:



Synthesis of *N*-(4-bromobenzyl)methanesulfonamide: To a solution of methanesulfonyl chloride (1.60 mmol, 0.12 mL, 1.0 equiv) in ethanol (5 mL) 4-bromoaniline (3.20 mmol, 550 mg, 2.0 equiv) was added and the mixture was stirred at room temperature. The reaction was monitored by TLC until completion. After 2 h, the solvent was removed under reduced pressure and the remaining solid dissolved in a small amount of water. The remaining solid was dissolved in a small amount of water and applied to a C18 precolumn before purification on a 60 g C18 column with a gradient of acetonitrile in water (10-80%) to yield the sulfonamide (0.93 mmol, 232 mg, 93%) as a white solid. ¹H NMR (400 MHz, methanol-*d*₄): δ 7.27 (2H, dd, *J* = 8.8 Hz, *J* = 2.0 Hz), 7.02 (2H, dd, *J* = 9.0 Hz, *J* = 2.1 Hz), 2.84 (3H, s). ¹³C NMR (101 MHz, methanol-*d*₄): δ 146.5, 132.6, 123.8, 113.5, 39.0. HRMS (ESI): Calcd. for C₇H₇O₂NBrS [M+H]⁺ 247.9386; found 247.9389.

Synthesis of 4'-(methylsulfonamido)biphenyl-3-carboxylic acid, **17**: The compound was prepared according to general procedure B. *N*-(4-bromobenzyl)methanesulfonamide (0.72 mmol, 180 mg, 1.5 equiv), 3-(4,4,5,5-tetramethyl-1,3,2-dioxaborolan-2-yl)benzoic acid (0.48 mmol, 119 mg, 1.0 equiv), Na₂CO₃ (2.40 mmol, 254 mg, 5.0 equiv) and PdCl₂(dppf) (0.05 mmol, 35 mg, 10 mol%) in anhydrous THF (6 mL) was stirred at 80 °C for 20h. After purification the title compound, **17** (0.20 mmol, 58 mg, 41%) was obtained as a yellowish solid. T_m = 280 °C. ¹H NMR (400 MHz, methanol-*d*₄) δ 8.20 (t, *J* = 1.8 Hz, 1H), 7.84 (dt, *J* = 7.7, 1.4 Hz, 1H), 7.66-7.58 (m, 1H), 7.55-7.49 (m, 2H), 7.38 (t, *J* = 7.7 Hz, 1H), 7.23-7.16 (m, 2H), 2.88 (s, 3H). ¹³C NMR (101 MHz, methanol-*d*₄) δ 175.7, 147.0, 142.0, 139.5, 134.1, 129.1, 129.0, 128.3, 128.2, 122.5, 39.0, 25.0. HRMS (ESI): Calcd. for C₁₄H₁₂NO₄S [M-H]⁻ 290.0493 found 290.0485. UHPLC: purity > 99.5%

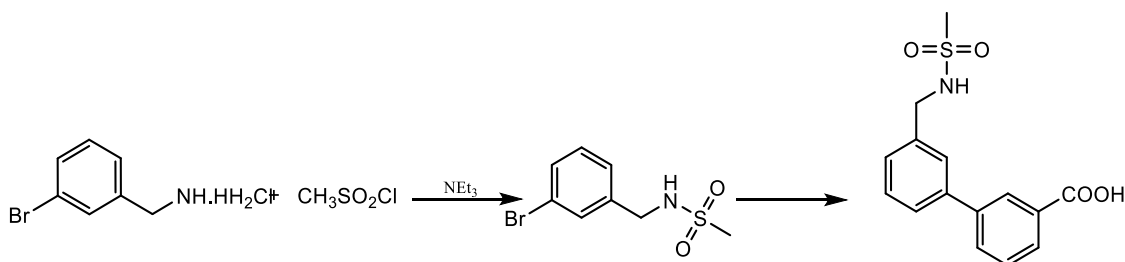
4'-(phenylsulfonamido)biphenyl-3-carboxylic acid, **18**:



Synthesis of *N*-(4-bromophenyl)benzenesulfonamide: To a solution of benzenesulfonyl chloride (1.28 mmol, 0.16 mL, 1.0 equiv) in ethanol (5 mL) 4-bromoaniline (2.56 mmol, 441 mg, 2.0 equiv) was added and the mixture stirred at rt. The reaction was monitored by TLC until completion. After 2 h the solvent was removed and the remaining solid dissolved in ethyl acetate. The solution was submitted to a silica precolumn and purified on a silica column with a gradient of ethyl acetate in heptane (10-35%) and then a constant value of 35% ethyl acetate in heptane. The title compound (300 mg, 75%) was obtained as a yellowish solid. ¹H NMR (400 MHz, CDCl₃): δ 7.78-7.74 (m, 2H), 7.82-7.76 (m, 2H), 7.55 (m, 1H), 7.49-7.43 (m, 2H), 7.37-7.32 (m, 2H), 7.00-6.95 (m, 2H). ¹³C NMR (101 MHz, CDCl₃): δ 138.7, 135.6, 133.4, 132.5, 129.3, 127.3, 123.4, 118.9. HRMS (ESI): Calcd. for C₁₂H₉O₂BrNS [M+H]⁺ 309.9543; found 309.9537.

Synthesis of 4'-(phenylsulfonamido)biphenyl-3-carboxylic acid, **18**: The compound was prepared according to general procedure B. *N*-(4-bromophenyl)benzenesulfonamide (0.48 mmol, 150 mg, 1.0 equiv), 3-(4,4,5,5-tetramethyl-1,3,2-dioxaborolan-2-yl)benzoic acid (0.72 mmol, 180 mg, 1.5 equiv), potassium phosphate (1.92 mmol, 408 mg, 4.0 equiv) and XPhos-Pd G2 (4.8x10⁻³ mmol, 3.8 mg, 1 mol%) in anhydrous THF (4 mL) was stirred at 84 °C for 16 h. The aqueous phase was washed with hexane (3 x 30 mL). After purification **18** (0.31 mmol, 110 mg, 65%) was obtained as beige solid. T_m = 303°C. ¹H NMR (400 MHz, methanol-*d*₄) δ 8.09 (s, 1H), 7.94-7.83 (m, 2H), 7.75 (d, *J* = 9.2 Hz, 1H), 7.51 (d, *J* = 9.5 Hz, 1H), 7.41-7.24 (m, 6H), 6.98 (d, *J* = 8.5 Hz, 2H). ¹³C NMR (101 MHz, methanol-*d*₄) δ 175.8, 148.9, 146.6, 142.2, 139.3, 132.8, 131.3, 129.3, 129.0, 128.9, 128.0, 127.9, 127.9, 127.8, 123.0. HRMS (ESI): Calcd. for C₁₉H₁₄NO₄S [M-H]⁻ 352.0649; found, 352.0642. UHPLC: purity = 95.6 %

3'-(methylsulfonamidomethyl)biphenyl-3-carboxylic acid, **19a**:

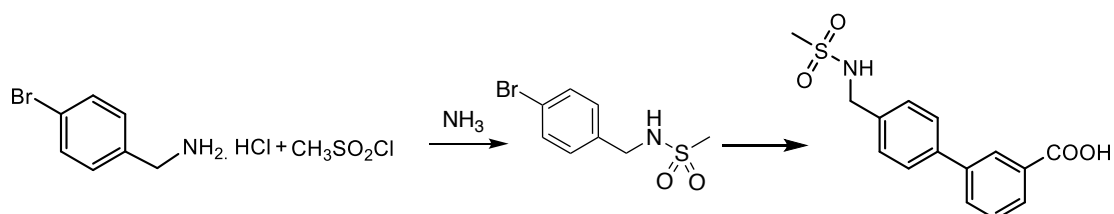


Synthesis of *N*-(3-bromobenzyl)methanesulfonamide: A solution of 3-bromobenzylamine hydrochloride (1.51 mmol, 337 mg, 1.0 equiv) and triethylamine (3.18 mmol, 0.44 mL, 2.1 equiv) in CH₂Cl₂ (5.5 mL) was cooled to 0 °C. Methanesulfonyl chloride (1.52 mmol, 0.12 mL, 1.01 equiv) was added dropwise and the reaction mixture was allowed to warm to room temperature with stirring. The reaction was monitored by TLC until completion. After 1h 45 minutes the reaction was stopped and the mixture was washed with water (3 x 10 mL). The organic layer was dried over MgSO₄, filtrated and the solvent removed under reduced pressure. The title compound (1.34 mmol, 349 mg, 88%) was obtained as a offwhite solid and used in the next step without further purification. ¹H NMR (400 MHz, methanol-*d*₄): δ 7.51 (t, *J* = 1.9 Hz, 1H), 7.45 (dt, *J*₁ = 7.6 Hz, *J*₂ = 1.6 Hz, 1H), 7.29 (m, 1H), 7.24 (t, *J* = 7.6 Hz, 1H), 4.81 (s, 1H), 4.30 (s, 2H), 2.90 (s, 3H). ¹³C NMR (101 MHz, methanol-*d*₄): δ 139.2, 131.3, 131.0, 130.6, 126.6, 123.0, 46.6, 41.3. HRMS (ESI): Calcd. for C₈H₁₀O₂NBrNaS [M+Na]⁺ 285.9508; found 285.9503.

Synthesis of 3'-(methylsulfonamidomethyl)biphenyl-3-carboxylic acid, **19a**: The compound was synthesized according to general procedure B. *N*-(3-bromobenzyl) methanesulfonamide, (0.57 mmol, 150 mg, 1.0 equiv), 3-(4,4,5,5-tetramethyl-1,3,2-dioxaborolan-2-yl) benzoic acid (0.85 mmol, 211 mg, 1.5 equiv), Na₂CO₃ (2.84 mmol, 301 mg, 5.0 equiv) and PdCl₂(dppf) (0.06 mmol, 42 mg, 10 mol%) in anhydrous THF (8 mL), was stirred at 84 °C for 20 h. Additional purification was carried out by flash

chromatography on silica gel with hexane/ethyl acetate/acetic acid (1:1:1%). To the resulting solid was added heptane (10 mL x 3) and removed under reduced pressure to remove residual acetic acid. The title compound, **19a** (0.15 mmol, 45 mg, 26%) was obtained as a slightly yellow solid. $T_m = 175-177^\circ\text{C}$. $^1\text{H NMR}$ (400 MHz, methanol- d_4) δ 8.28 (s, 1H), 8.01 (d, $J = 7.7$ Hz, 1H), 7.86 (d, $J = 7.9$ Hz, 1H), 7.68 (s, 1H), 7.60-7.54 (m, 4H), 7.47 (t, $J = 7.6$ Hz, 2H), 7.41 (d, $J = 7.7$ Hz, 2H). $^{13}\text{C NMR}$ (101 MHz, methanol- d_4) δ 169.9, 142.4, 141.9, 140.2, 132.9, 132.4, 130.4, 130.1, 129.7, 129.1, 128.4, 127.6, 127.3, 47.7, 40.6. HRMS (ESI): Calcd. for $\text{C}_{15}\text{H}_{14}\text{NO}_4\text{S}$ [M-H] $^-$ 304.0649; found 304.0647. UHPLC: purity = 95.0 %

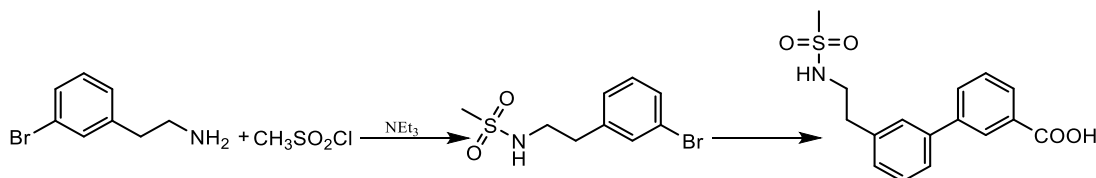
4'-(methylsulfonamidomethyl)biphenyl-3-carboxylic acid, **19b**:



Synthesis of *N*-(4-bromobenzyl)methanesulfonamide: The compound was prepared according to the procedure described for *N*-(3-bromobenzyl)methanesulfonamide. The title compound (1.45 mmol, 380 mg, 95%) was obtained as a beige solid. $^1\text{H NMR}$ (400 MHz, chloroform- d): δ 7.49 (m, 2H), 7.23 (m, 2H), 4.80 (s, 1H), 4.27 (d, $J = 4.5$ Hz, 2H), 2.88 (s, 3H). $^{13}\text{C NMR}$ (101 MHz, CDCl_3): δ 135.9, 132.2 (2C), 129.7 (2C), 122.2, 46.7, 41.4. HRMS (ESI): Calcd. for $\text{C}_8\text{H}_{10}\text{O}_2\text{NBrClS}$ [M+Cl] $^+$ 285.9508; found, 299.2368.

Synthesis of 4'-(methylsulfonamidomethyl)biphenyl-3-carboxylic acid, **19b**. The compound was prepared according to general procedure B. *N*-(4-bromobenzyl)methanesulfonamide (0.57 mmol, 150 mg, 1.0 equiv), 3-(4,4,5,5-tetramethyl-1,3,2-dioxaborolan-2-yl)benzoic acid (0.85 mmol, 211 mg, 1.5 equiv), Na_2CO_3 (2.84 mmol, 301 mg, 5.0 equiv) and $\text{PdCl}_2(\text{dppf})$ (0.06 mmol, 42 mg, 10 mol%) in anhydrous THF (8 mL) was stirred at 84°C for 20 h. Additional purification was carried out by flash chromatography on silica gel with hexane/ethyl acetate/acetic acid (10:10:0.1) as eluent. To the resulting solid was added heptane (10 mL) and removed under reduced pressure (3 times) to remove residual acetic acid. The title compound, **19b** (0.06 mmol, 17 mg, 10%) was obtained as a white solid. $T_m = 216-220^\circ\text{C}$. $^1\text{H NMR}$ (400 MHz, methanol- d_4) δ 8.16 (s, 1H), 7.90 (d, $J = 7.7$ Hz, 1H), 7.75 (d, $J = 7.8$ Hz, 1H), 7.56 (d, $J = 8.1$ Hz, 2H), 7.49-7.36 (m, 3H), 4.21 (s, 2H), 2.78 (s, 3H). $^{13}\text{C NMR}$ (101 MHz, methanol- d_4) δ 170.1, 142.2, 140.8, 139.0, 133.1, 132.2, 130.1, 129.6, 129.6, 129.0, 128.2, 47.4, 40.6. HRMS (ESI): Calcd. for $\text{C}_{15}\text{H}_{14}\text{O}_4\text{NS}$ [M-H] $^-$ 304.0649; found 304.0646. UHPLC: purity = 96.4 %

3'-(2-methylsulfonamidoethyl)biphenyl-3-carboxylic acid, **20**:



Synthesis of *N*-(3-bromophenethyl)methanesulfonamide: To a solution of methanesulfonyl chloride (1.60 mmol, 0.12 mL, 1.0 equiv) in ethanol (3 mL), 2-(3-bromophenyl)ethan-1-amine (3.20 mmol, 639 mg, 2.0 equiv) was added and the mixture was stirred at room temperature. The reaction was monitored by TLC. After completion the solvent was removed under reduced pressure and the remaining solid dissolved in a small amount of water. The solution was applied to a C18 precolumn before purification on a 60 g C18 column with a gradient of acetonitrile in water (10–80%). The title compound (1.07 mmol, 295 mg, 66%) was obtained as a white solid. $^1\text{H NMR}$ (400 MHz, CDCl_3): δ 7.41-7.36 (m, 2H), 7.19 (t, $J = 7.6$ Hz, 1H), 7.15 (m, 1H), 3.38 (t, $J = 6.9$ Hz, 2H), 2.86 (s, 3H), 2.85 (t, $J = 7.6$ Hz,

2H). ^{13}C NMR (101 MHz, CDCl_3): δ 140.3, 132.0, 130.5, 130.2, 127.7, 123.0, 44.2, 40.6, 36.3. HRMS (ESI): Calcd. for $\text{C}_9\text{H}_{13}\text{O}_2\text{NBrS}$ $[\text{M}+\text{H}]^+$ 277.9850; found 277.9674.

Synthesis of 3'-(2-methylsulfonylamidoethyl)biphenyl-3-carboxylic acid, **20**: The compound was prepared according to general procedure B. *N*-(3-bromophenethyl)methanesulfonamide (0.72 mmol, 200 mg, 1.5 equiv), 3-(4,4,5,5-tetramethyl-1,3,2-dioxaborolan-2-yl)benzoic acid (0.48 mmol, 119 mg, 1.0 equiv), Na_2CO_3 (2.40 mmol, 254 mg, 5.0 equiv) and $\text{PdCl}_2(\text{dppf})$ (0.05 mmol, 35 mg, 10 mol%) in anhydrous THF (8 mL) was stirred at 85 °C for 20h. The aqueous mixture was washed with hexane (3 x 30 mL) instead of ethyl acetate. After purification the title compound, **20** (0.11 mmol, 35 mg, 11%) was obtained as a white solid. $T_m = 130^\circ\text{C}$. ^1H NMR (400 MHz, methanol- d_4) δ 8.24 (t, $J = 1.8$ Hz, 1H), 7.93 (dt, $J = 7.7, 1.4$ Hz, 1H), 7.67 (s, 1H), 7.57 (s, 1H), 7.53 (d, $J = 7.8$ Hz, 1H), 7.41 (m, 2H), 7.24 (d, $J = 7.7$ Hz, 1H), 3.40-3.34 (m, 2H), 2.92 (t, $J = 7.4$ Hz, 2H), 2.82 (s, 3H). ^{13}C NMR (101 MHz, methanol- d_4) δ 175.3, 142.6, 141.8, 140.8, 139.7, 130.1, 129.7, 129.3, 129.2, 129.0, 128.9, 128.7, 126.2, 45.7, 39.9, 37.8. HRMS (ESI): Calcd. $\text{C}_{16}\text{H}_{16}\text{O}_4\text{NS}$ $[\text{M}-\text{H}]^-$ 318.0806; found 318.0797. UHPLC: purity = 99.0 %

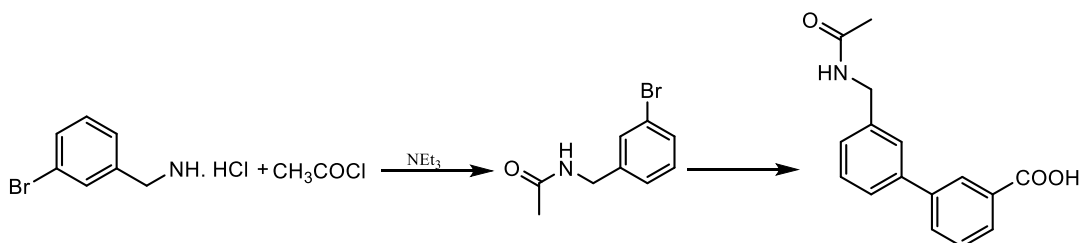
3'-acetamidobiphenyl-3-carboxylic acid, **21a**:

According to procedure A, 3-bromobenzoic acid (1.24 mmol, 250 mg, 1 equiv), 3-acetamidophenylboronic acid (1.86 mmol, 333 mg, 1.5 equiv), potassium phosphate (6.20 mmol, 1.32 g, 5 equiv) and $\text{PdCl}_2(\text{PPh}_3)_2$ (0.124 mmol, 87 mg, 10 mol%) gave **21a** (1.21 mmol, 310 mg, 98 %) as white solid. $T_m = 294^\circ\text{C}$. ^1H NMR (400 MHz, $\text{DMSO}-d_6$) δ 10.30 (s, 1H), 8.15 (t, $J = 1.7$ Hz, 1H), 7.91 (t, $J = 1.9$ Hz, 1H), 7.84 (dt, $J = 7.6, 1.3$ Hz, 1H), 7.64 (d, $J = 9.0$ Hz, 1H), 7.52-4.49 (m, 1H), 7.40-7.27 (m, 3H), 2.08 (s, 3H). ^{13}C NMR (101 MHz, $\text{DMSO}-d_6$) δ 169.0168.9, 142.6, 141.7, 140.4, 139.2, 129.6, 128.7, 128.1, 127.7, 126.8, 121.6, 118.1, 117.7, 24.5. HRMS (ESI): Calcd. for $\text{C}_{15}\text{H}_{12}\text{NO}_3$ $[\text{M}-\text{H}]^-$ 254.0823; found 254.0828. UHPLC: purity = 97.4 %

4'-acetamidobiphenyl-3-carboxylic acid, **21b**:

According to procedure A, 3-bromobenzoic acid (1.24 mmol, 250 mg, 1.0 equiv), 4-acetamidophenylboronic acid (1.86 mmol, 307 mg, 1.5 equiv), potassium phosphate (6.20 mmol, 1.32 g, 5.0 equiv) and $\text{PdCl}_2(\text{PPh}_3)_2$ (0.124 mmol, 87 mg, 10 mol%) gave **21b** (1.20 mmol, 290 mg, 97 %) as white solid. $T_m = 295-296^\circ\text{C}$. ^1H NMR (400 MHz, $\text{DMSO}-d_6$) δ 10.29 (s, 1H), 8.13 (s, 1H), 7.80 (d, $J = 7.4$ Hz, 1H), 7.71 (d, $J = 8.3$ Hz, 2H), 7.58 (d, $J = 8.3$ Hz, 2H), 7.53 (d, $J = 7.6$ Hz, 1H), 7.31 (t, $J = 7.5$ Hz, 1H), 2.08 (s, 3H). ^{13}C NMR (101 MHz, $\text{DMSO}-d_6$) δ 168.9, 168.9, 142.7, 139.1, 138.9, 135.8, 128.1, 128.0, 127.3, 127.1, 126.4, 119.8, 24.50. HRMS (ESI): Calcd. for $\text{C}_{15}\text{H}_{12}\text{NO}_3$ $[\text{M}-\text{H}]^-$ 254.0823; found 254.0818. UHPLC: purity = 99.1 %

3'-(acetamidomethyl)biphenyl-3-carboxylic acid, **22**:

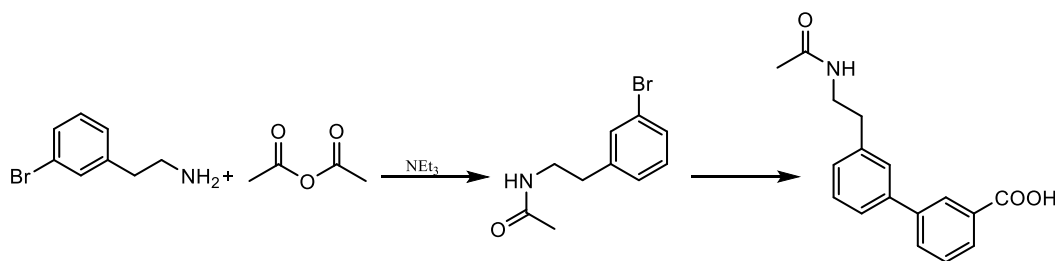


Synthesis of *N*-(3-bromobenzyl)acetamide: A solution of 3-bromobenzylamine hydrochloride (1.75 mmol, 389 mg, 1.0 equiv) and Et_3N (17.5 mmol, 2.44 mL, 10.0 equiv) in CH_2Cl_2 (3.5 mL) was cooled to 0 °C. Acetyl chloride (2.28 mmol, 0.16 mL, 1.3 equiv) was added and the mixture was stirred for 3 h at 30 °C. The solvent was removed under reduced pressure and the resulting solid dissolved in CH_2Cl_2 (40 mL). The organic phase was washed with 1N HCl (1 x) and water (3 x 30 mL). It was dried over Na_2SO_4 ,

filtered and the solvent removed under reduced pressure. The title compound (373 mg, 93%) was obtained as a yellowish solid and used without further purification for the next step. ^1H NMR (400 MHz, CDCl_3): δ 7.43-7.38 (m, 2H), 7.22-7.18 (m, 2H), 4.41 (m, 2H), 2.03 (s, 3H). ^{13}C NMR (101 MHz, CDCl_3): δ 170.1, 140.8, 130.8, 130.7, 130.4, 126.5, 122.8, 43.2, 23.4. HRMS (ESI): Calcd. for $\text{C}_9\text{H}_{11}\text{ONBr}$ $[\text{M}+\text{H}]^+$ 228.0019; found, 228.0018; $[\text{M} + \text{Na}]^+$, calcd for $\text{C}_9\text{H}_{10}\text{ONBrNa}$, 249.9838; found, 249.9837.

Synthesis of 3'-(acetamidomethyl)biphenyl-3-carboxylic acid, **22**: According to general procedure B, *N*-(3-bromobenzyl)acetamide (0.66 mmol, 150 mg, 1.0 equiv), 3-(4,4,5,5-tetramethyl-1,3,2-dioxaborolan-2-yl)benzoic acid (0.99 mmol, 245 mg, 1.5 equiv), potassium phosphate (2.63 mmol, 558 mg, 4.0 equiv) and XPhos-Pd G2 (6.6×10^{-3} mmol, 5.2 mg, 1 mol%) in anhydrous THF (4 mL) was stirred at 85 °C for 16.5 h. The aqueous mixture was washed with hexane (3 x 30 mL). After purification the title compound, **22** (0.57 mmol, 155 mg, 87%) was obtained as a white solid. $T_m = 129^\circ\text{C}$. ^1H NMR (400 MHz, methanol- d_4) δ 8.23 (s, 1H), 7.93 (d, $J = 9.0$ Hz, 1H), 7.66 (d, $J = 6.2$ Hz, 1H), 7.62-7.51 (m, 2H), 7.38-7.45 (m, 2H), 7.27 (d, $J = 7.5$ Hz, 1H), 4.43 (s, 2H), 2.01 (s, 3H). ^{13}C NMR (101 MHz, methanol- d_4) δ 175.3, 173.1, 142.7, 141.7, 140.5, 139.8, 130.1, 129.7, 129.3, 129.3, 128.9, 127.6, 127.3, 126.9, 44.3, 25.0. HRMS (ESI): Calcd. for $\text{C}_{16}\text{H}_{14}\text{NO}_3$ $[\text{M}-\text{H}]^-$ 268.0979; found 268.0977. UHPLC: purity = 82.6 %

3'-(2-acetamidoethyl)biphenyl-3-carboxylic acid, **23a**:

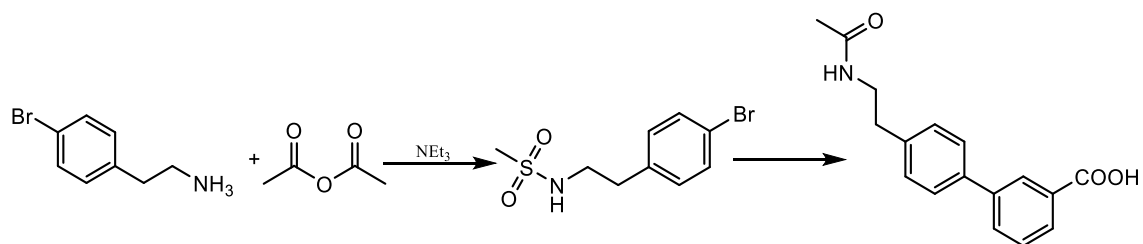


Synthesis of *N*-(3-bromophenethyl)acetamide: To a solution of 2-(3-bromophenyl)ethan-1-amine (1.65 mmol, 0.24 mL, 1.0 equiv) in CH_2Cl_2 (3.5 mL), Et_3N (1.82 mmol, 0.25 mL, 1.1 equiv) and acetic anhydride (1.98 mmol, 0.19 mL, 1.2 equiv) were added. The reaction mixture was stirred at rt and monitored by TLC. After 1.5 h the solvent was removed under reduced pressure and the resulting yellow oil diluted with CH_2Cl_2 . The organic phase was washed with water (3 x 20 mL), dried over Na_2SO_4 , filtered and the solvent removed under reduced pressure. The title compound (400 mg, 100%) was obtained as a yellowish oil. ^1H NMR (400 MHz, CDCl_3): δ 7.38-7.32 (m, 2H), 7.17 (m, 1H), 7.11 (m, 1H), 5.64 (1H, s), 3.48 (m, 2H), 2.78 (t, $J = 7.0$ Hz, 2H), 1.94 (3H, s). ^{13}C NMR (101 MHz, CDCl_3): δ 170.3, 141.4, 131.9, 130.3, 129.8, 127.5, 122.8, 40.6, 35.4, 23.4. HRMS (ESI): Calcd. for $\text{C}_{10}\text{H}_{13}\text{ONBr}$ $[\text{M}+\text{H}]^+$ 242.0175; found 242.0174.

Synthesis of 3'-(2-acetamidoethyl)biphenyl-3-carboxylic acid, **23a**: The compound was prepared according to general procedure B. *N*-(3-bromophenethyl)acetamide (0.62 mmol, 150 mg, 1.0 equiv), 3-(4,4,5,5-tetramethyl-1,3,2-dioxaborolan-2-yl)benzoic acid (0.93 mmol, 231 mg, 1.5 equiv), Na_2CO_3 (3.10, 328 mg, 5.0 equiv) and $\text{PdCl}_2(\text{dppf})$ (0.06 mmol, 45 mg, 10 mol%) in anhydrous THF (8 mL) was stirred at 85 °C for 19 h. After RP chromatography, the compound was further purified by flash chromatography on silica gel using a mixture of an acidic stock solution (acetic acid/ H_2O /MeOH/ethyl acetate, 3:2:3:3) and ethyl acetate (1:25) as eluent. To the resulting solid heptane (10 mL x 3) was added and removed under reduced pressure to remove residual acetic acid. Compound **23a** (0.29 mmol, 80 mg, 46%) was obtained as a slightly yellow solid. $T_m = 54-56^\circ\text{C}$. ^1H NMR (400 MHz, methanol- d_4) δ 8.25 (s, 1H), 7.99 (d, $J = 7.7$ Hz, 1H), 7.81 (d, $J = 8.7$ Hz, 1H), 7.57-7.45 (m, 3H), 7.38 (t, $J = 7.6$ Hz, 1H), 7.23 (d, $J = 7.5$ Hz, 1H), 3.44 (t, $J = 7.3$ Hz, 2H), 2.87 (t, $J = 7.3$ Hz, 2H), 1.92 (s, 3H). ^{13}C NMR (101 MHz, methanol- d_4) δ 174.7, 171.9, 144.0, 143.1, 142.7, 133.5, 131.5, 131.3, 130.8, 130.6, 130.5, 129.9,

127.5, 43.4, 37.9, 23.9. HRMS (ESI): Calcd. for $C_{17}H_{16}NO_3$ $[M-H]^-$ 282.1136; found 282.1129. UHPLC: purity = 97.9 %

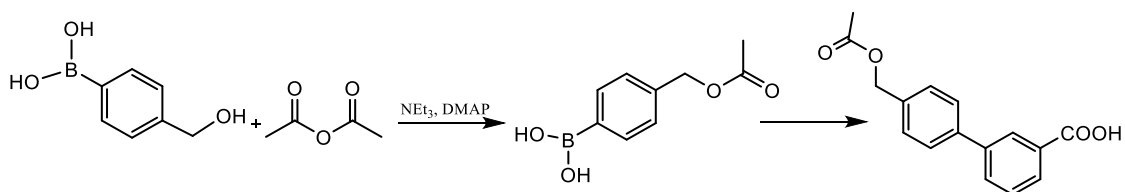
4'-(2-acetamidoethyl)biphenyl-3-carboxylic acid, **23b**:



Synthesis of N-(3'-bromobiphenyl-3-yl)methylacetamide: The compound was prepared according to the procedure described for starting material of **23a**. The title compound (399 mg, 100%) was obtained as a white solid. 1H NMR (400 MHz, $CDCl_3$): δ 7.42 (m, 2H), 7.06 (m, 2H), 5.54 (s, 1H), 3.47 (m, 2H), 2.77 (t, J = 7.0 Hz, 2H), 1.93 (s, 3H). ^{13}C NMR (101 MHz, $CDCl_3$): δ 170.2, 138.0, 131.8, 130.6, 120.5, 40.6, 35.2, 23.4. HRMS (ESI): Calcd. for $C_{10}H_{13}ONBr$ $[M+H]^+$ 242.0175; found 242.0177.

Synthesis of 4'-(2-acetamidoethyl)biphenyl-3-carboxylic acid, **23b**. The compound was prepared according to general procedure B. N-(3'-bromobiphenyl-3-yl)methylacetamide (0.62 mmol, 150 mg, 1.0 equiv), 3-(4,4,5,5-tetramethyl-1,3,2-dioxaborolan-2-yl)benzoic acid (0.93 mmol, 231 mg, 1.5 equiv), Na_2CO_3 (3.10 mmol, 328 mg, 5.0 equiv) and $PdCl_2(dppf)$ (0.06 mmol, 45 mg, 10 mol%) in anhydrous THF (8 mL) was stirred at 85 °C for 18.5 h. After RP chromatography, the compound was further purified by flash chromatography on silica gel using a mixture of an acidic stock solution (acetic acid/ H_2O /MeOH/ethyl acetate, 3:2:3:3) and ethyl acetate (1:59) and then acidic stock solution/ethyl acetate (1:9) as eluent. To the resulting solid heptane (10 mL x 3) was added and removed under reduced pressure to remove residual acetic acid. Compound **23b** (0.21 mmol, 60 mg, 34%) was obtained as a white solid. T_m = 204-205°C. 1H NMR (400 MHz, methanol- d_4) δ 8.24 (s, 1H), 7.98 (d, J = 7.7 Hz, 1H), 7.82 (d, J = 7.7 Hz, 1H), 7.62-7.47 (m, 3H), 7.32 (d, J = 8.2 Hz, 2H), 3.43 (t, J = 7.3 Hz, 2H), 2.84 (t, J = 7.3 Hz, 2H), 1.92 (s, 3H). ^{13}C NMR (101 MHz, methanol- d_4) δ 211.4, 174.7, 171.3, 143.9, 141.7, 140.9, 134.0, 133.7, 131.9, 131.4, 130.8, 130.3, 129.5, 129.4, 43.4, 37.5, 23.9. HRMS (ESI): Calcd. for $C_{17}H_{16}NO_3$ $[M-H]^-$ 282.1136; found 282.1129. UHPLC: purity = 99.2%

3-(acetoxymethylphenyl)boronic acid, **24**:



Synthesis of 3-(acetoxymethylphenyl)boronic acid: To a stirred mixture of 3-(hydroxymethylphenyl)boronic acid (1.03 mmol, 157 mg, 1.0 equiv), DMAP (0.11 mmol, 14 mg, 11 mol%) and Et_3N (3.09 mmol, 0.43 mL, 3.0 equiv) in CH_2Cl_2 /anhydrous THF (7.2 mL, 5:1) and acetic anhydride (3.09 mmol, 0.29 mL, 3.0 equiv) was added. The solution was stirred at rt and monitored by TLC. After 5h the reaction mixture was washed with 1N HCl (3 x 20 mL) and $NaHCO_3$ solution (3 x 20 mL). The organic phase was dried over Na_2SO_4 , filtered and the solvent removed under reduced pressure. The crude product was purified with flash chromatography on silica gel with 5% MeOH in CH_2Cl_2 as eluent. The title compound (0.86 mmol, 166 mg, 86%) was obtained as a white solid. 1H NMR (400 MHz, methanol- d_4): δ 7.73-7.44 (m, 2H), 7.37-7.20 (m, 2H), 5.03 (2H, s), 2.00 (s, 3H). ^{13}C NMR (101 MHz, methanol- d_4): δ 172.7, 134.7,

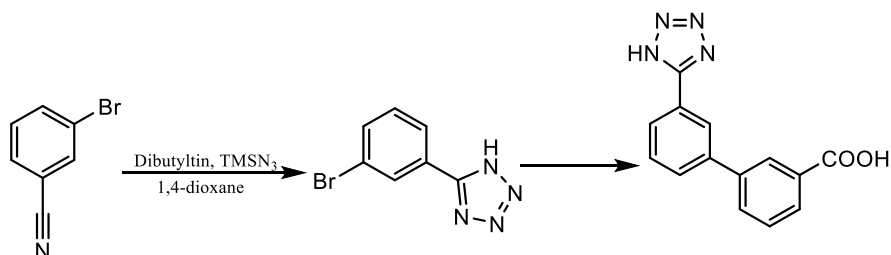
134.4, 131.1, 130.6, 128.7, 67.5, 20.8. HRMS (ESI): Calcd. for $C_9H_{10}O_4B$ $[M-H]^-$ 193.0678; found 193.0680.

Synthesis of 3'-acetoxymethyl-biphenyl-3-carboxylic acid **24**: According general procedure B, 3-(acetoxymethyl)phenylboronic acid, **7** (0.39 mmol, 75 mg, 1.5 equiv), potassium phosphate (1.03 mmol, 219 mg, 4.0 equiv), XPhos Pd G2 (2.58×10^{-3} mmol, 2.0 mg, 1 mol%), in anhydrous THF (6 mL) was stirred at 88 °C for 20 h. The crude product was purified by flash chromatography on silica gel with hexane/ethyl acetate/acetic acid (9:1:1%) as eluent gave **24** (0.13 mmol, 35 mg, 34%) as a brownish solid. $T_m = 80^\circ C$. 1H NMR (400 MHz, methanol- d_4) δ 8.26 (s, 1H), 8.01 (d, $J = 7.7$ Hz, 1H), 7.85 (d, $J = 7.7$ Hz, 1H), 7.68-7.51 (m, 3H), 7.47 (t, $J = 7.6$ Hz, 1H), 7.38 (d, $J = 7.7$ Hz, 1H), 5.18 (s, 2H), 2.10 (s, 3H). ^{13}C NMR (101 MHz, Methanol- d_4) δ 172.7, 169.8, 142.4, 141.8, 138.5, 132.7, 132.5, 130.3, 130.1, 129.7, 129.1, 128.6, 127.9, 67.2, 20.8. HRMS (ESI): Calcd. for $C_{16}H_{13}O_4$ $[M-H]^-$ 269.0819; found 269.0817. UHPLC: purity = 95.7%

3-(2-(1H-imidazol-1-yl)pyrimidin-5-yl)benzoic acid, **25**:

According to general procedure A, 5-bromo-2-(1H-imidazol-1-yl)pyrimidine (0.39 mmol, 100 mg, 1.0 equiv), 3-carboxyphenylboronic acid pinacol ester (0.39 mmol, 97 mg, 1.0 equiv), potassium phosphate (1.95 mmol, 413 mg, 5.0 equiv) and $PdCl_2(PPh_3)_2$ (0.04 mmol, 27 mg, 10 mol%) after purification gave **25** (0.28 mmol, 75 mg, 72%) was obtained as a white solid. $T_m = 297^\circ C$. 1H NMR (400 MHz, deuterium oxide) δ 8.78 (s, 2H), 8.37 (s, 1H), 7.95 (s, 1H), 7.82-7.72 (m, 1H), 7.68 (s, 1H), 7.56 (d, $J = 7.6$ Hz, 1H), 7.46-7.35 (m, 1H), 7.11 (s, 1H), 7.04 (s, 1H). ^{13}C NMR (101 MHz, deuterium oxide) δ 174.2, 156.4, 152.3, 137.2, 136.2, 131.9, 131.3, 129.4, 129.3, 129.2, 128.6, 126.6, 121.7, 117.0. HRMS (ESI): Calcd. for $C_{14}H_9N_4O_2$ $[M-H]^-$ 265.0731; found 265.0731. UHPLC: purity = 95.2%

3'-(1H-tetrazol-5-yl)-biphenyl-3-carboxylic acid, **26a**:

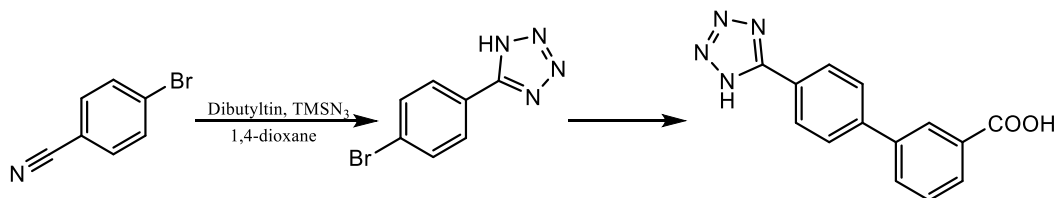


Synthesis of 5-(3-bromophenyl)-1H-tetrazole: Dibutyltin oxide (0.33 mmol, 82 mg, 0.2 equiv), and trimethylsilyl azide (3.33 mmol, 383 mg, 2 equiv) were added to a solution of 3-bromobenzonitrile (300 mg, 1.67 mmol, 1 equiv) in anhydrous 1,4-dioxane (2 mL/mmol). The reaction mixture was subjected to microwave irradiation in a tightly sealed microwave vessel for 50 min at $150^\circ C$, then cooled to room temperature. The solvent was removed under reduced pressure. The residue was dissolved in diethyl ether (10 mL) and extracted with 2 M aq. NaOH (3 x 10 mL). The aqueous layer was acidified with 4 M aq. HCl to pH 1 and extracted with ethyl acetate (4 x 10 mL). The organic extract was washed with brine (10 mL), dried over $MgSO_4$, and evaporated under reduced pressure to give the intermediate tetrazole (1.45 mmol, 326 mg, 86%) as a white solid. 1H NMR (400 MHz, methanol- d_4) δ 8.22-8.21 (m, 1H), 8.01 (d, $J = 7.9$ Hz, 1H), 7.74 (d, $J = 7.9$ Hz, 1H), 7.50 (t, $J = 7.9$ Hz, 1H). ^{13}C NMR (101 MHz, methanol- d_4) δ 157.3, 135.3, 132.3, 131.0, 128.0, 126.9, 124.2.

According to general procedure A, 5-(3-bromophenyl)-1H-tetrazole (0.73 mmol, 163 mg, 1.2 equiv), 3-carboxyphenylboronic acid pinacol ester (0.60 mmol, 150 mg, 1.0 equiv), potassium phosphate (3.00 mmol, 636 mg, 5.0 equiv) and $PdCl_2(PPh_3)_2$ (0.06 mmol, 42 mg, 10 mol%) after purification gave **26a** (0.58 mmol, 159 mg, 99%) as a white solid. $T_m = 295-297^\circ C$. 1H NMR (400 MHz, methanol- d_4) δ 8.41 (s, 1H), 8.35 (s, 1H), 8.04 (d, $J = 8.1$ Hz, 1H), 7.98 (d, $J = 8.1$ Hz, 1H), 7.82 (d, $J = 8.0$ Hz, 1H), 7.74 (d, $J = 7.9$

Hz, 1H), 7.56 (t, $J = 7.8$ Hz, 1H), 7.50 (t, $J = 7.6$ Hz, 1H). ^{13}C NMR (101 MHz, methanol- d_4) δ 175.3, 162.9, 142.8, 141.6, 139.8, 131.9, 130.2, 129.8, 129.3, 128.9, 126.6, 126.3, 128.3. HRMS (ESI): Calcd. $\text{C}_{14}\text{H}_9\text{N}_4\text{O}_2$ [M-H] $^-$ 265.0731; found 265.0728. UHPLC: purity = 96.7%

4'-(1H-Tetrazol-5-yl)biphenyl-3-carboxylic acid, **26b**:



Synthesis of 5-(4-bromophenyl)-1H-tetrazole: Dibutyltin oxide (0.33 mmol, 82 mg, 0.2 equiv), and trimethylsilyl azide (3.33 mmol, 383 mg, 2 equiv) were added to a solution of 4-bromobenzonitrile (300 mg, 1.67 mmol, 1 equiv) in anhydrous 1,4-dioxane (2 mL/mmol). The reaction mixture was subjected to microwave irradiation in a tightly sealed vessel for 50 min at 150 °C, then cooled to room temperature. The solvent was removed under reduced pressure. The residue was dissolved in diethyl ether (10 mL) and extracted with 2 M aq. NaOH (3 x 10 mL). The aqueous layer was acidified with 4 M aq. HCl to pH 1 and extracted with ethyl acetate (4 x 10 mL). The organic extract was washed with brine (10 mL), dried over MgSO_4 , and evaporated under reduced pressure to give the intermediate tetrazole (1.36 mmol, 307 mg, 82%) as a white solid. ^1H NMR (400 MHz, $\text{DMSO}-d_6$) δ 8.07-7.92 (m, 2H), 7.91-7.76 (m, 2H). ^{13}C NMR (101 MHz, $\text{DMSO}-d_6$) δ 155.6, 132.9, 129.3, 125.0, 124.3.

According to general procedure A, 5-(4-bromophenyl)-1H-tetrazole (0.58 mmol, 130 mg, 1.2 equiv), 3-carboxyphenylboronic acid pinacol ester (0.48 mmol, 120 mg, 1.0 equiv), potassium phosphate (2.93 mmol, 614 mg, 5.0 equiv) and $\text{PdCl}_2(\text{PPh}_3)_2$ (0.05 mmol, 34 mg, 10 mol%) after purification gave the title compound, **26b** (0.44 mmol, 119 mg, 93%) as a white solid. $T_m = 301^\circ\text{C}$. ^1H NMR (400 MHz, methanol- d_4) δ 8.32 (s, 1H), 8.15 (d, $J = 8.3$ Hz, 2H), 7.97 (d, $J = 7.6$ Hz, 1H), 7.83-7.72 (m, 3H), 7.48 (t, $J = 7.7$ Hz, 1H). ^{13}C NMR (101 MHz, methanol- d_4) δ 175.2, 162.7, 142.6, 141.4, 139.8, 130.4, 129.7, 129.4, 128.8, 128.3, 128.2. HRMS (ESI): Calcd. for $\text{C}_{14}\text{H}_9\text{N}_4\text{O}_2$ [M-H] $^-$ 265.0731; found 265.0722. UHPLC: purity = 98.3%

3-(Naphthalen-2-yl)benzoic acid, **27**:

According to general procedure A, 2-bromonaphthalene (1.20 mmol, 250 mg, 1.0 equiv), 3-(4,4,5,5-tetramethyl-1,3,2-dioxaborolan-2-yl)benzoic acid (1.81 mmol, 448 mg, 1.5 equiv), potassium phosphate (6.02 mmol, 1.28 g, 5.0 equiv) and $\text{PdCl}_2(\text{PPh}_3)_2$ (0.124 mmol, 85 mg, 10 mol%) after purification gave **27** (0.81 mmol, 200 mg, 67%) as a white solid. $T_m = 263-266^\circ\text{C}$. ^1H NMR (400 MHz, deuterium oxide) δ 8.04 (t, $J = 1.8$ Hz, 1H), 7.74 (m, 1H), 7.35 (s, 0H), 7.23-7.08 (m, 4H), 7.03 (t, $J = 7.7$ Hz, 1H), 6.99-6.87 (m, 2H). ^{13}C NMR (101 MHz, deuterium oxide) δ 175.0, 139.8, 136.9, 136.7, 132.9, 132.0, 129.3, 128.6, 128.2, 127.8, 127.8, 127.4, 127.2, 126.0, 125.7, 125.0, 124.7. HRMS (ESI): Calcd. for $\text{C}_{17}\text{H}_{11}\text{O}_2$ [M-H] $^-$ 247.0765; found 247.0759. UHPLC: purity = 98.6%

3-(Quinolin-7-yl)benzoic acid, **28**:

The compound was prepared according to general procedure A. 6-Bromoquinoline (1.20 mmol, 250 mg, 1.0 equiv), 3-(4,4,5,5-tetramethyl-1,3,2-dioxaborolan-2-yl) benzoic acid (1.80 mmol, 447 mg, 1.5 equiv), potassium phosphate (6.00 mmol, 1.28 g, 5.0 equiv) and $\text{PdCl}_2(\text{PPh}_3)_2$ (0.12 mmol, 84 mg, 10 mol%) gave **28** (1.04 mmol, 260 mg, 87%) as a white solid. $T_m = 295-298^\circ\text{C}$. ^1H NMR (400 MHz, methanol- d_4) δ 8.86 (dd, $J = 4.4, 1.7$ Hz, 1H), 8.47 (dd, $J = 8.3, 1.7$ Hz, 1H), 8.43 (t, $J = 1.8$ Hz, 1H), 8.25 (d, $J = 1.9$ Hz, 1H), 8.20-8.10 (m, 2H), 8.03 (d, $J = 7.7$ Hz, 1H), 7.87 (dt, $J = 7.8, 1.5$ Hz, 1H), 7.63-7.42 (m, 2H). ^{13}C NMR (101 MHz, ethanol- d_4) δ 175.0, 151.1, 148.1, 140.9, 140.6, 140.0,

138.7, 130.7, 130.2, 130.1, 129.8, 129.6, 129.6, 129.3, 126.7, 122.9. HRMS (ESI): Calcd. for $C_{16}H_{10}NO_2$ [M-H]⁻ 248.0717; found 248.0714. UHPLC: purity = 96.2 %

3-(6-Aminopyridin-3-yl)benzoic acid, **29**:

According to general procedure A, 5-bromopyridin-2-amine (0.87 mmol, 150 mg, 1.0 equiv), 3-(4,4,5,5-tetramethyl-1,3,2-dioxaborolan-2-yl)benzoic acid (1.30 mmol, 323 mg, 1.5 equiv), potassium phosphate (4.34 mmol, 920 mg, 5.0 equiv) and $PdCl_2(PPh_3)_2$ (0.09 mmol, 61 mg, 10 mol%) gave **29** (0.26 mmol, 56 mg, 36%) as an orange solid. $T_m = 277^\circ C$. 1H NMR (400 MHz, methanol- d_4) δ 8.21 (s, 1H), 8.14 (t, $J = 1.8$ Hz, 1H), 7.88 (dt, $J = 7.7, 1.4$ Hz, 1H), 7.80 (dd, $J = 8.7, 2.5$ Hz, 1H), 7.60-7.50 (m, 1H), 7.41 (t, $J = 7.7$ Hz, 1H), 6.82-6.55 (m, 1H). ^{13}C NMR (101 MHz, methanol- d_4) δ 175.3, 160.1, 145.9, 139.8, 138.9, 138.0, 129.4, 128.7, 128.6, 127.8, 127.4, 110.3. HRMS (ESI): Calcd. for $C_{12}H_9N_2O_2$ [M-H]⁻ 213.0670; found 213.0669. UHPLC: purity = 96.3 %

3-(Pyrimidin-5-yl)benzoic acid, **30**:

According to general procedure A, 5-bromopyrimidine (1.57 mmol, 250 mg, 1.0 equiv), 3-(4,4,5,5-tetramethyl-1,3,2-dioxaborolan-2-yl)benzoic acid (2.36 mmol, 585 mg, 1.5 equiv), potassium phosphate (7.86 mmol, 1.67 g, 5.0 equiv), $PdCl_2(PPh_3)_2$ (0.16 mmol, 110 mg, 10 mol%), gave **30** (0.70 mmol, 140 mg, 45%) as a light brown solid. $T_m = T_m = 289^\circ C$ decomposes. 1H NMR (400 MHz, deuterium oxide) δ 9.00 (s, 1H), 8.88 (s, 2H), 7.99 (t, $J = 1.8$ Hz, 1H), 7.86 (m, 1H), 7.67-7.61 (m, 1H), 7.50 (t, $J = 7.7$ Hz, 1H). ^{13}C NMR (101 MHz, deuterium oxide) δ 174.5, 155.7, 154.6, 137.3, 133.7, 132.8, 129.5, 129.3, 129.2, 127.0. HRMS (ESI): Calcd. for $C_{11}H_7N_2O_2$ [M-H]⁻ 199.0513 found 199.0511. UHPLC: purity = 99.4 %

3-(2-Aminopyrimidin-4-yl)benzoic acid, **31**:

According to general procedure A, 5-bromo-4-methylpyrimidin-2-amine (0.80 mmol, 150 mg, 1.0 equiv), 3-(4,4,5,5-tetramethyl-1,3,2-dioxaborolan-2-yl) benzoic acid (1.20 mmol, 298 mg, 1.5 equiv), potassium phosphate (4.01 mmol, 851 mg, 5.0 equiv) and $PdCl_2(PPh_3)_2$ (0.08 mmol, 56 mg, 10 mol%) gave **31** (0.53 mmol, 122 mg, 67%) as a yellow solid. $T_m = 330^\circ C$ (decomposes). 1H NMR (400 MHz, methanol- d_4) δ 8.12 (s, 1H), 8.03-7.92 (m, 1H), 7.89 (s, 1H), 7.50 (t, $J = 7.7$ Hz, 1H), 7.44-7.33 (m, 1H). ^{13}C NMR (101 MHz, methanol- d_4) δ 175.0, 167.4, 162.8, 158.7, 139.1, 136.9, 132.2, 131.0, 129.4, 129.3, 126.0, 22.6. HRMS (ESI): Calcd. for $C_{12}H_{10}N_3O_2$ [M-H]⁻ 228.0778; found 228.0776. UHPLC: purity = 99.0 %

3-(1-Methyl-1H-pyrrol-2-yl)benzoic acid, **32**:

The compound was prepared according to general procedure A. 3-bromobenzoic acid (1.24 mmol, 250 mg, 1.0 equiv), 1-methyl-2-(4,4,5,5-tetramethyl-1,3,2-dioxaborolan-2-yl)-1H-pyrrole (1.87 mmol, 386 mg, 1.5 equiv), potassium phosphate (6.22 mmol, 1.32 g, 5.0 equiv) and $PdCl_2(PPh_3)_2$ (0.12 mmol, 81 mg, 10 mol%) after purification by flash chromatography on silica gel using 2% methanol in CH_2Cl_2 as eluent afforded **32** (0.03 mmol, 15 mg, 6%) as a white solid. $T_m = 162-165^\circ C$. 1H NMR (400 MHz, methanol- d_4) δ 7.94 (s, 1H), 7.83 (d, $J = 7.7$ Hz, 1H), 7.52 (d, $J = 6.2$ Hz, 1H), 7.39 (t, $J = 7.8$ Hz, 2H), 6.65 (s, 1H), 6.18-5.82 (m, 5H), 3.56 (s, 3H). ^{13}C NMR (101 MHz, methanol- d_4) δ 169.8, 135.3, 134.5, 133.7, 132.2, 130.3, 129.6, 128.7, 125.5, 110.0, 108.8, 35.3. HRMS (ESI): Calcd. for $C_{12}H_{10}NO_2$ [M-H]⁻ 200.0717; found 200.0715. UHPLC: purity = 95.5 %

3-(Thiazol-5-yl)benzoic acid, **33**:

The compound was prepared according to general procedure A. 5-bromothiazole (1.52 mmol, 250 mg, 1.0 equiv), 3-(4,4,5,5-tetramethyl-1,3,2-dioxaborolan-2-yl)benzoic acid (2.29 mmol, 567 mg, 1.5 equiv), potassium phosphate (7.62 mmol, 1.62 g, 5.0 equiv) and $PdCl_2(PPh_3)_2$ (0.15 mmol, 107 mg, 10

mol%), gave **33** (0.37 mmol, 76 mg, 24%) as a brownish solid. $T_m = 208^\circ\text{C}$ (decomposes). ^1H NMR (400 MHz, deuterium oxide) δ 8.21 (t, $J = 1.8$ Hz, 1H), 7.93-7.83 (m, 2H), 7.77 (d, $J = 3.3$ Hz, 1H), 7.52 (d, $J = 3.3$ Hz, 1H), 7.47 (t, $J = 7.7$ Hz, 1H). ^{13}C NMR (101 MHz, deuterium oxide) δ 174.5, 168.9, 142.8, 137.2, 132.4, 130.6, 129.2, 128.7, 126.8, 120.6. HRMS (ESI): Calcd. for $\text{C}_{10}\text{H}_6\text{O}_2\text{NS}$ $[\text{M}-\text{H}]^-$ 204.0125; found 204.0120. UHPLC: purity = 96.0 %

3-(1H-Indol-5-yl)benzoic acid, **34**:

According to general procedure A, 5-bromo-1H-indole (1.28 mmol, 250 mg, 1 equiv), 3-(4,4,5,5-tetramethyl-1,3,2-dioxaborolan-2-yl)benzoic acid (1.91 mmol, 475 mg, 1.5 equiv), potassium phosphate (6.38 mmol, 1.35 g, 5.0 equiv) and $\text{PdCl}_2(\text{PPh}_3)_2$ (0.13 mmol, 90 mg, 10 mol%) after purification by flash chromatography on silica gel using hexane/ethyl acetate/acetic acid (9:1:0.01) as eluent gave **34** (0.25 mmol, 60 mg, 20 %) as a yellowish solid. $T_m = 190\text{-}192^\circ\text{C}$ ^1H NMR (400 MHz, methanol- d_4) δ 8.30 (s, 1H), 7.94 (d, $J = 7.7$ Hz, 1H), 7.87 (d, $J = 7.8$ Hz, 1H), 7.82 (s, 1H), 7.57-7.35 (m, 3H), 7.27 (d, $J = 3.1$ Hz, 1H), 6.52 (d, $J = 3.3$ Hz, 1H). ^{13}C NMR (101 MHz, methanol- d_4) δ 170.2, 144.5, 137.5, 132.6, 132.6, 132.3, 130.1, 129.8, 129.2, 128.3, 126.5, 121.7, 119.7, 112.6, 102.9. HRMS (ESI): Calcd. for $\text{C}_{15}\text{H}_{10}\text{O}_2\text{N}$ $[\text{M}-\text{H}]^-$ 236.0717; found 236.0716. UHPLC: purity = 95.8 %

3-(Pyridin-2-yl)benzoic acid, **35**:

According to general procedure A, 3-bromobenzoic acid (1.24 mmol, 250 mg, 1.0 equiv), 2-Pyridineboronic acid N-phenyldiethanolamine ester (1.86 mmol, 499 mg, 1.5 equiv), potassium phosphate (6.20 mmol, 1.31 g, 5.0 equiv) and $\text{PdCl}_2(\text{PPh}_3)_2$ (0.12 mmol, 87 mg, 10 mol%) gave **35** (1.13 mmol, 224 mg, 91%) as white solid. $T_m = 101\text{-}103^\circ\text{C}$. ^1H NMR (400 MHz, methanol- d_4) δ 8.64 (d, $J = 5.0$ Hz, 1H), 8.56 (s, 1H), 8.08 (t, $J = 7.6$ Hz, 2H), 8.03-7.89 (m, 2H), 7.57-7.50 (m, 1H), 7.47-7.30 (m, 2H). ^{13}C NMR (101 MHz, methanol- d_4) δ 173.6, 158.7, 150.3, 140.2, 138.9, 138.2, 132.1, 131.1, 130.5, 129.5, 129.1, 128.9, 123.8, 122.6. HRMS (ESI): Calcd. for $\text{C}_{12}\text{H}_8\text{O}_2\text{N}$ $[\text{M}-\text{H}]^-$ 198.0561; found 198.0552. UHPLC: purity = 98.6 %

1.3 Screening of catalysts

General procedure:

3-Bromo-5-iodobenzoic acid (0.03–0.06 mmol, 1.0 equiv.) was dissolved in the indicated solvent (0.5–1 mL/0.01 mmol substrate). The boronic acid or ester (1.5 equiv.) and base (5.0 equiv.) were added. The solution was degassed by vacuum/Ar cycles (10 times) before addition of the palladium catalyst and further degassed (5 times). The resulting mixture was stirred at the indicated temperature under an inert atmosphere for the indicated reaction time. The crude reaction mixture was analysed by HRMS to determine the ratio of **int-39** : disubstituted **38** : starting material. The reaction mixture was filtered through Celite bed and diluted with water (approx. 30 mL) before washing with chloroform (3 x 30 mL). The aqueous phase was concentrated under reduced pressure and applied to a C18 precolumn before purification on a 60 g C18 column with a gradient of acetonitrile in water (0–5% over 15 min) to yield the product.

Table S11: Screening of reaction conditions for the coupling of 3-bromo-5-iodobenzoic acid

| Entry | Catalyst [mol% in Pd] | Base | Temp [°C] / Time [h] | Solvent | Ratio (int-39:38:sm) | Isol. yield [%] |
|-------|---|--------------------------------|----------------------|---------------------|----------------------|-----------------|
| 1 | RuPhos-Pd G3 (10) | K ₃ PO ₄ | 60 / 24 | dioxane/water (1:1) | 8 : 10 : 10 | nd |
| 2 | RuPhos-Pd G3 (5) | K ₃ PO ₄ | 60 / 24 | toluene/water (1:1) | 10 : 6 : 0.3 | nd |
| 3 | XantPhos-Pd G3 (5) | K ₃ PO ₄ | 40 / 48 | dioxane/water (1:1) | 10 : 1 : 0 | nd |
| 4 | XantPhos-Pd G3 (5) | K ₃ PO ₄ | 40 / 24 | toluene/water (1:1) | 10 : 1 : 3 | 70 |
| 5 | Pd(dppf)Cl ₂ (5) | K ₃ PO ₄ | 60 / 24 | dioxane/water (1:1) | 10 : 1 : 3 | 80 |
| 6 | XPhos-Pd G2 (1) | K ₃ PO ₄ | 60 / 24 | dioxane/water (1:1) | 10 : 7 : 1 | nd |
| 7 | SPhos-Pd G3 (5) | K ₃ PO ₄ | 60 / 24 | dioxane/water (1:1) | 10 : 2 : 0 | 40 |
| 8 | Pd ₂ (dba) ₃ •CHCl ₃ /SPhos 1:1 (10) | K ₃ PO ₄ | 60 / 24 | dioxane/water (1:1) | 10 : 1 : 0.4 | 55 |
| 9 | Pd ₂ (dba) ₃ •CHCl ₃ /SPhos 1:1 (10) | K ₃ PO ₄ | 80 / 24 | dioxane/water (1:1) | 10 : 1 : 0.3 | 55 |
| 8 | Pd ₂ (dba) ₃ •CHCl ₃ /SPhos 1:1 (10) | K ₃ PO ₄ | 40 / 24 | <i>tert</i> -BuOH | 10 : 4 : 4 | nd |
| 9 | Pd ₂ (dba) ₃ •CHCl ₃ /SPhos 1:1 (10) | K ₃ PO ₄ | 40 / 20 | toluene/water (1:1) | 10 : 1 : 3 | 65 |
| 10 | Pd ₂ (dba) ₃ •CHCl ₃ /SPhos 1:1 (10) | K ₃ PO ₄ | 60 / 10 | dioxane:water (1:1) | 5 : 4 : 10 | nd |
| 11 | Pd ₂ (dba) ₃ •CHCl ₃ /SPhos 1:1 (10) | K ₃ PO ₄ | 60 / 48 | dioxane:water (1:1) | 10 : 4 : 1 | nd |
| 12 | Pd ₂ (dba) ₃ •CHCl ₃ /SPhos 1:2 (5) | K ₃ PO ₄ | 60 / 24 | dioxane/water (1:1) | 10 : 0.7 : 0 | 40 |

1.4 Synthesis of symmetrical 3,5-disubstituted benzoic acid derivatives

3,5-Di(3-acetamidophenyl)benzoic acid **36**:

3-Bromo-5-iodobenzoic acid (0.30 mmol, 100 mg, 1.0 equiv), 3-acetamidophenylboronic acid (0.45 mmol, 816 mg, 1.5 equiv), potassium phosphate (1.5 mmol, 324 mg, 5.0 equiv) were dissolved in a mixture of water/dioxane (1:1). The solution was degassed by vacuum/Ar cycles (10 times) before addition of Pd₂(dba)₃•CHCl₃ (15 mg, 5 mol%), and XPhos (7.2 mg, 5 mol%) and further degassed (5 times). The resulting mixture was stirred at 60 °C for 20–24 hours. The reaction mixture was filtered through Celite bed and diluted with water (approx. 30 mL) before washing with chloroform (3 x 30 mL). The aqueous phase was concentrated under reduced pressure and applied to a C18 precolumn before purification on a 60 g C18 column with a gradient of acetonitrile in water (0–5% over 15 min) to provide **36** (60 mg, 54%) as white powder. T_m = 211–212 °C. ¹H NMR (400 MHz, methanol-*d*₄) δ 8.21 (s, 1H), 7.90 (t, *J* = 1.7 Hz, 1H), 7.81 (t, *J* = 1.7 Hz, 2H), 7.68 (d, *J* = 8 Hz, 2H), 7.43 (s, 1H), 7.49–7.46 (m, 2H), 7.43–7.39 (m, 2H), 2.16 (s, 6H). ¹³C NMR (101 MHz, methanol-*d*₄) δ 175.0, 171.8, 142.9, 142.3, 140.5, 132.2, 130.4, 128.2, 128.1, 123.9, 120.3, 119.7, 24.0. HRMS (ESI): Calcd. for C₂₃H₁₉N₂O₄ [M-H]⁻ 387.1350; found 387.1342. UHPLC: purity = 97.5 %

3,5-di(4-acetamidophenyl)benzoic acid **37**:

3,5-Dibromobenzoic acid (1.01 mmol, 300 mg, 1.0 equiv), 3-acetamidophenylboronic acid (0.81 mmol, 178 mg, 0.75 equiv), potassium phosphate (3.76 mmol, 0.80 g, 3.5 equiv) and PdCl₂(PPh₃)₂ (0.11 mmol, 77 mg, 10 mol%) were stirred in a mixture of water/dioxane (1:1) for 24 hours at 95 °C under argon atmosphere. The crude reaction mixture was filtered through Celite and diluted with water (approx. 30 mL) before washing with chloroform (3 x 30 mL). The aqueous phase was concentrated under reduced pressure and applied to a C18 precolumn before purification on a 60 g C18 column with a gradient of acetonitrile in water (0–100 % over 12 minutes). The fractions were analysed by MS and fractions containing **37** were combined. The product was purified by reverse-phase automated flash chromatography before being subjected to purification by HPLC, to yield **37** (0.09 mmol, 34 mg, 11%) as a white solid. T_m = 245–247 °C. ¹H NMR (400 MHz, methanol-*d*₄) δ 8.24 (s, 2H), 7.98 (d, *J* = 7.8 Hz, 2H),

7.85 (d, $J = 7.9$ Hz, 2H), 7.68-7.66 (m, 2H), 7.63-7.60 (m, 2H), 7.57-7.53 (m, 1H), 2.16 (s, 6H). ^{13}C NMR (101 MHz, methanol- d_4) δ 175.2, 171.7, 142.0, 140.2, 139.4, 137.9, 131.7, 128.4, 128.2, 127.6, 127.4, 123.3, 121.4, 116.2, 23.9. HRMS (ESI): Calcd. for $\text{C}_{23}\text{H}_{19}\text{N}_2\text{O}_4$ $[\text{M}-\text{H}]^-$ 387.1350; found 387.1340. UHPLC: purity = 100 %

3,5-diquinolin-6-ylbenzoic acid **38**:

3,5-Dibromobenzoic acid (0.11 mmol, 33 mg, 1.0 equiv), 6-quinolinylboronic acid pinacol ester (0.23 mmol, 60 mg, 2.0 equiv), potassium phosphate (0.58 mmol, 125 mg, 5.0 equiv) were dissolved in tert-butanol. The solution was degassed by vacuum/Ar cycles (10 times) before addition of XPhos-Pd G2 (5 mol%, 5 mg) and further degassed (5 times). The resulting mixture was stirred at 60 °C for 20–24 hours. The reaction mixture was filtered through Celite bed and diluted with water (approx. 30 mL) before washing with chloroform (3 x 30 mL). The aqueous phase was concentrated under reduced pressure and applied to a C18 precolumn before purification by C18 RP flash chromatography with a gradient of acetonitrile in water (0–5% over 15 min) to yield **38** (0.08 mmol, 29 mg, 65%) as white powder. $T_m = 291\text{--}292^\circ\text{C}$. ^1H NMR (400 MHz, methanol- d_4) δ 8.87-8.86 (m, 2H), 8.52-8.50 (m, 2H), 8.46 (m, 2H), 8.38 (m, 2H), 8.29-8.26 (m, 3H), 8.18 (s, 1H), 8.16 (s, 1H), 7.61-7.58 (dd, $J = 8.3, 4.2$ Hz, 2H). ^{13}C NMR (101 MHz, methanol- d_4) δ 174.4, 151.1, 148.0, 141.5, 140.5, 138.6, 130.6, 130.1, 129.5, 128.7, 126.9, 122.8. HRMS (ESI): Calcd. for $\text{C}_{25}\text{H}_{15}\text{N}_2\text{O}_2$ $[\text{M}-\text{H}]^-$ 375.1139; found 375.1133. UHPLC: purity = 99.1 %

1.5 Synthesis of unsymmetrical 3,5-disubstituted benzoic acid derivatives

3-(3'-Acetamidophenyl)-5-pyridin-4-ylbenzoic acid **39**: attempted synthesis from 3,5-dibromobenzoic acid

3,5-Dibromobenzoic acid (1.01 mmol, 300 mg, 1.0 equiv), 3-acetamidophenylboronic acid (0.81 mmol, 178 mg, 0.75 equiv), potassium phosphate (3.76 mmol, 0.80 g, 3.5 equiv) and $\text{PdCl}_2(\text{PPh}_3)_2$ (0.11 mmol, 77 mg, 10 mol%) were stirred in a mixture of water/dioxane (1:1) for 24 hours at 95 °C under argon atmosphere. The crude reaction mixture was filtered through Celite and diluted with water (approx. 30 mL) before washing with chloroform (3 x 30 mL). The aqueous phase was concentrated under reduced pressure and applied to a C18 precolumn before purification by C18 RP flash chromatography with a gradient of acetonitrile in water (10–100 % over 12 minutes). The fractions were analysed by MS and fractions containing **int-39** were combined and reacted with pyridin-4-ylboronic acid (0.97 mmol, 119 mg, 1.2 equiv), potassium phosphate (4.05 mmol, 0.86 g, 5.0 equiv) and $\text{PdCl}_2(\text{PPh}_3)_2$ (0.08 mmol, 56 mg, 10 mol%). The product was purified by reverse-phase automated flash chromatography before being subjected to purification by HPLC, to yield **39** (0.12 mmol, 39 mg, 15%) as a white solid. $T_m = 244^\circ\text{C}$. ^1H NMR (400 MHz, methanol- d_4) δ 8.22 (s, 1H), 7.92 (d, $J = 7.6$ Hz, 1H), 7.76 (s, 2H), 7.68-7.60 (m, 3H), 7.46-7.33 (m, 4H), 2.14 (s, 3H). ^{13}C NMR (101 MHz, methanol- d_4) δ 175.3, 171.7, 143.0, 141.5, 140.4, 139.8, 130.3, 129.7, 129.3, 129.3, 128.9, 123.7, 120.1, 119.6, 23.9. UHPLC: purity = 97.9%

3-Bromo-5-(quinolin-6-yl) benzoic acid **int-40**:

3-Bromo-5-iodobenzoic acid (0.15 mmol, 50 mg, 1.0 equiv), 6-quinolinylboronic acid pinacol ester (0.22 mmol, 58 mg, 1.5 equiv) and potassium phosphate (0.76 mmol, 162 mg, 5.0 equiv) were dissolved in a mixture of water/dioxane (1:1). The solution was degassed by vacuum/Ar cycles (10 times) before addition of $\text{Pd}_2(\text{dba})_3 \cdot \text{CHCl}_3$ (5 mol%, 7.5 mg), and SPhos (5 mol%, 3.1 mg) and further degassed (5 times). The resulting mixture was stirred at 60 °C for 20–24 hours. The reaction mixture was filtered through a Celite bed and diluted with water (approx. 30 mL) before washing with chloroform (3 x 30 mL). The aqueous phase was concentrated under reduced pressure and applied to a C18 precolumn before purification on a 60 g C18 column with a gradient of acetonitrile in water (0–5% over 20 min). Product **int-40** (0.07 mmol, 23 mg, 45%) was obtained as a white powder. $T_m = 288^\circ\text{C}$. ^1H NMR (400

MHz, methanol- d_4) δ 8.92-8.91 (m, 1H), 8.49-8.46 (m, 1H), 8.35 (s, 1H), 8.28 (s, 2H), 8.10 (s, 2H), 8.02-8.01 (m, 1H), 7.97-7.96 (m, 1H), 7.59-7.56 (dd, $J = 8.3, 4.2$ Hz, 1H). ^{13}C NMR (101 MHz, DMSO- d_6) δ 166.6, 150.8, 147.2, 143.6, 140.6, 136.8, 136.5, 131.7, 131.1, 129.6, 128.5, 128.2, 127.4, 126.5, 125.8, 121.9, 121.7; HRMS (ESI): Calcd. for $\text{C}_{16}\text{H}_9^{79}\text{BrNO}_2$ $[\text{M}-\text{H}]^-$ 325.9822; found 325.9822.

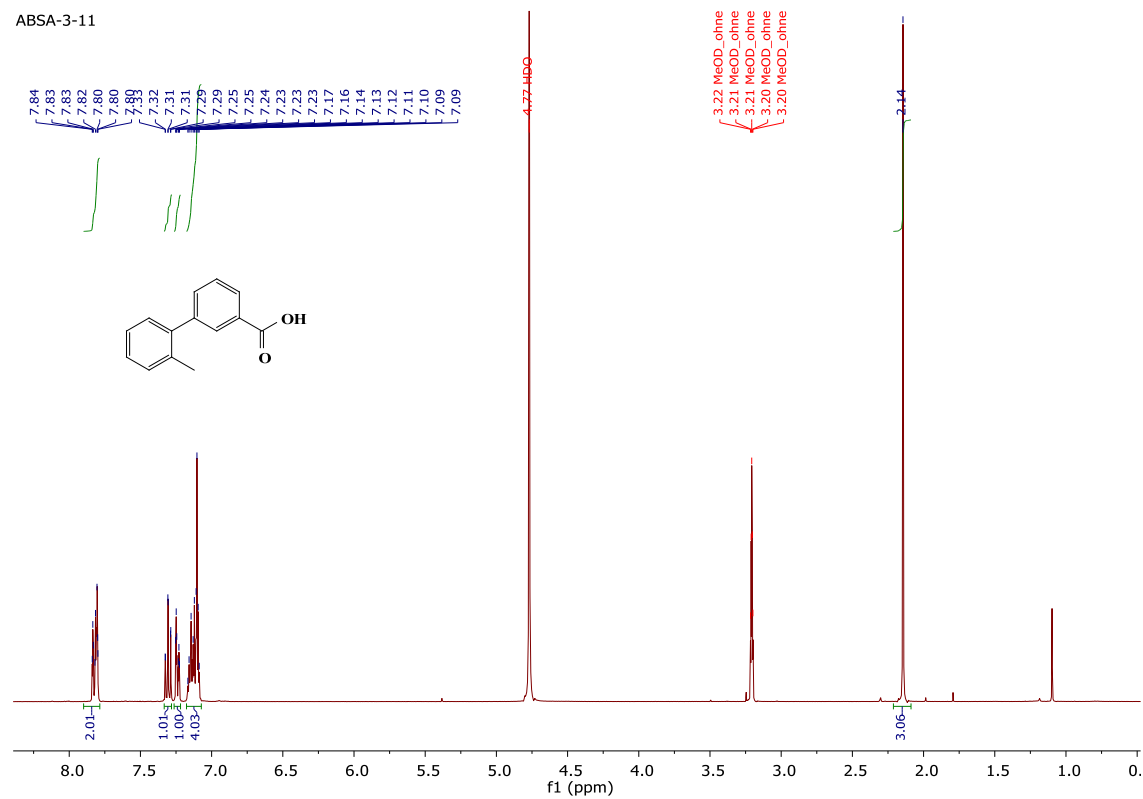
3-(3'-Acetamidophenyl)-5-quinolin-6-ylbenzoic acid **40**:

3-Bromo-5-(quinolin-6-yl) benzoic acid **int-40** (0.039 mmol, 13 mg, 1.0 equiv), 3-acetamidophenylboronic acid (0.55 mmol, 10 mg, 1.5 equiv) and potassium phosphate (0.20 mmol, 0.42 g, 5.0 equiv) were dissolved in tert-butanol. The solution was degassed by vacuum/Ar cycles (10 times) before addition of Xphos-Pd G2 (5 mol%, 1.5 mg) and further degassed (5 times). The resulting mixture was stirred at 60 °C for 20–24 hours. The reaction mixture was filtered through Celite bed and diluted with water (approx. 30 mL) before washing with chloroform (3 x 30 mL). The aqueous phase was concentrated under reduced pressure and applied to a C18 precolumn before purification on a 60 g C18 column with a gradient of acetonitrile in water (0–5% over 20 min). Product **40** (0.023 mmol, 9 mg, 90%) was obtained as white powder. $T_m = 261\text{--}264^\circ\text{C}$. ^1H NMR (400 MHz, methanol- d_4) δ 8.87-8.83 (m, 1H), 8.56-8.45 (m, 1H), 8.41-8.39 (m, 1H), 8.35-8.20 (m, 3H), 8.18-8.11 (m, 1H), 8.08 (t, $J = 1.8$ Hz, 1H), 7.87-7.86 (m, 1H), 7.72-7.68 (m, 1H), 7.62-7.56 (m, 1H), 7.56-7.49 (m, 1H), 7.46-7.42 (m, 1H), 2.17 (s, 3H). ^{13}C NMR (101 MHz, DMSO- d_6) δ 174.7, 171.8, 151.2, 148.2, 142.8, 142.5, 141.4, 140.8, 140.7, 140.5, 138.8, 130.8, 130.4, 130.3, 129.7, 128.6, 128.5, 128.5, 127.0, 123.9, 123.0, 120.3, 119.7, 23.9. HRMS (ESI): Calcd. for $\text{C}_{24}\text{H}_{18}\text{N}_2\text{O}_3$ $[\text{M}-\text{H}]^-$ 381.1245; found 381.1243. UHPLC: purity = 96.4 %.

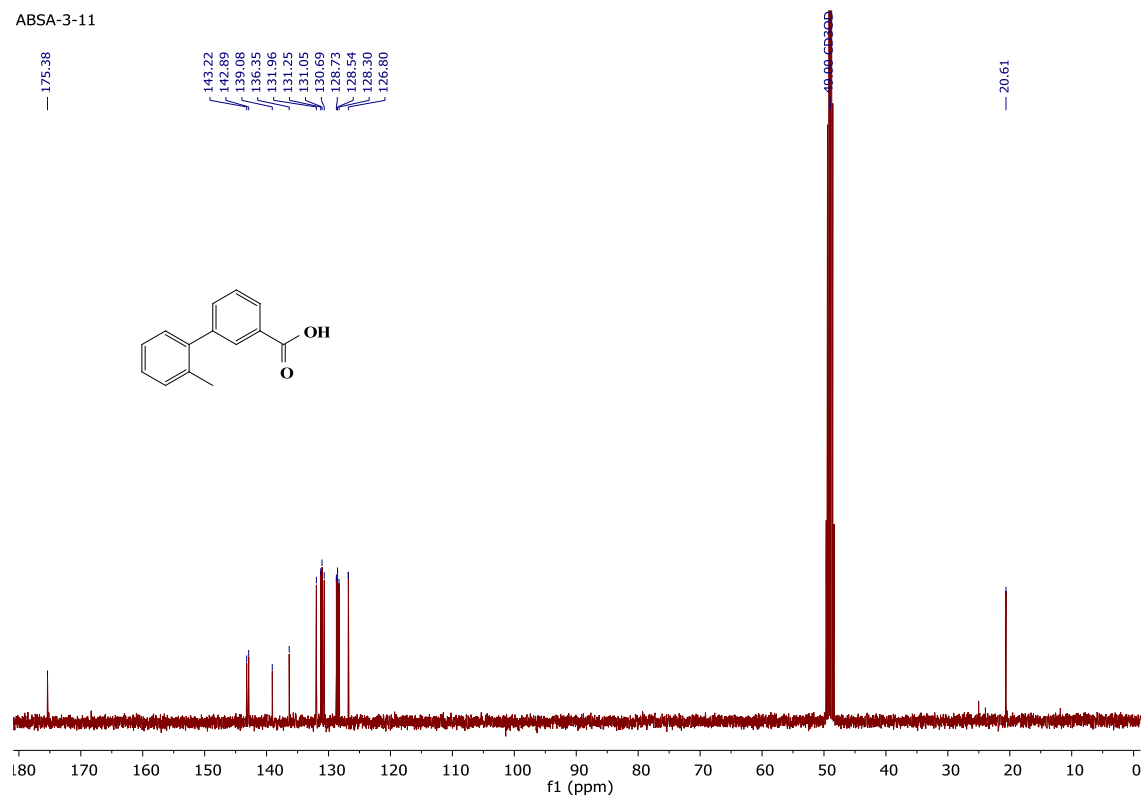
2 NMR spectra of compounds 3–40:

2.1 2'-methylbiphenyl-3-carboxylic acid, 3a:

2.1.1 ¹H NMR of 3a



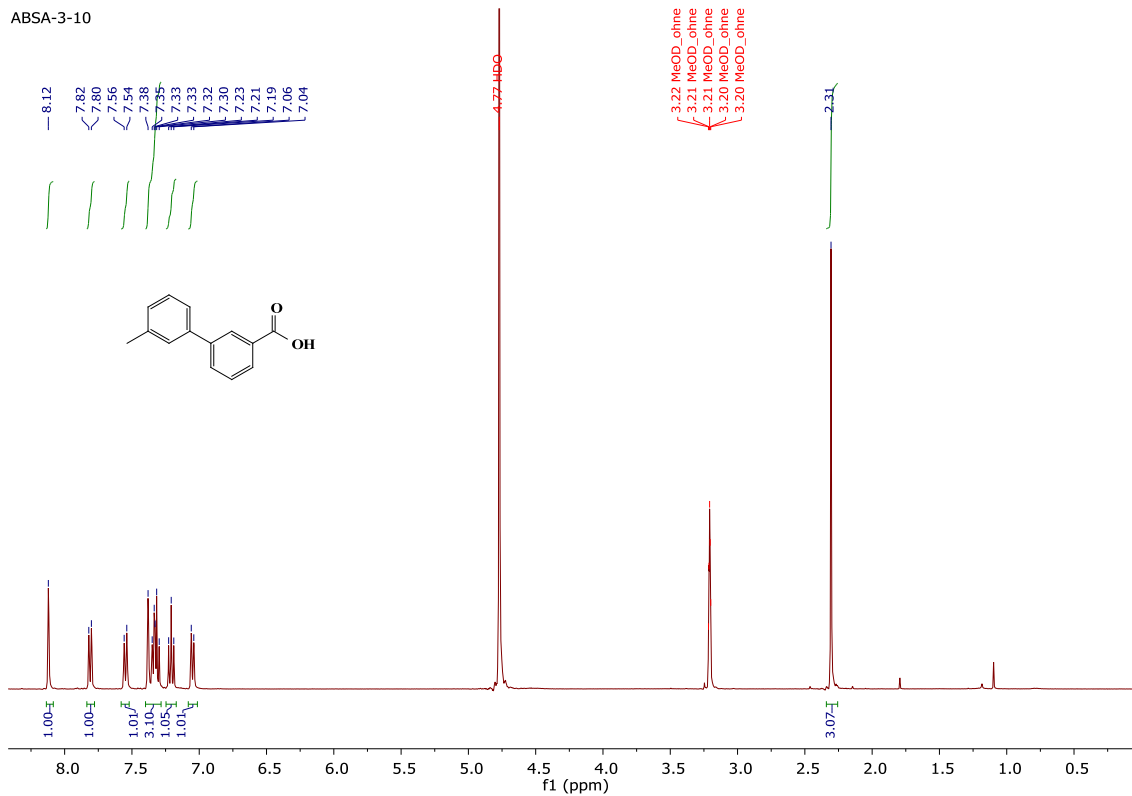
2.1.2 ¹³C NMR of 3a



2.2 3'-methylbiphenyl-3-carboxylic acid, **3b**:

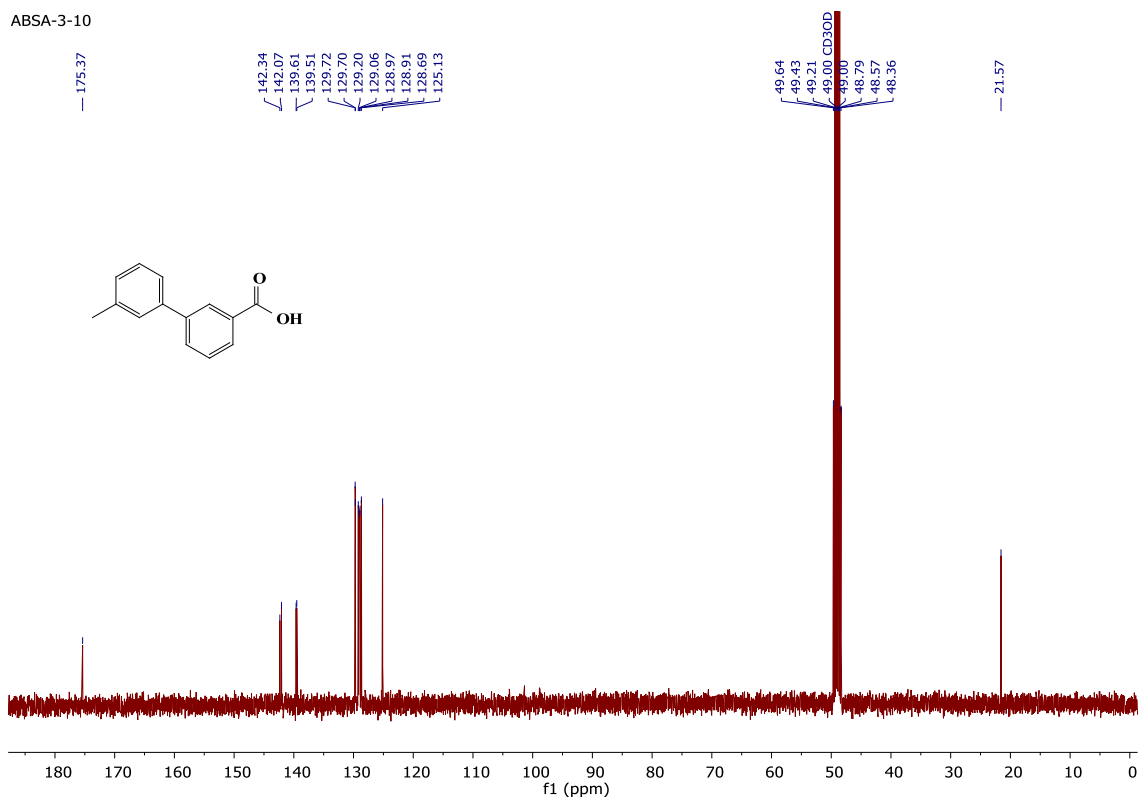
2.2.1 ^1H NMR of **3b**

ABSA-3-10



2.2.2 ^{13}C NMR of **3b**

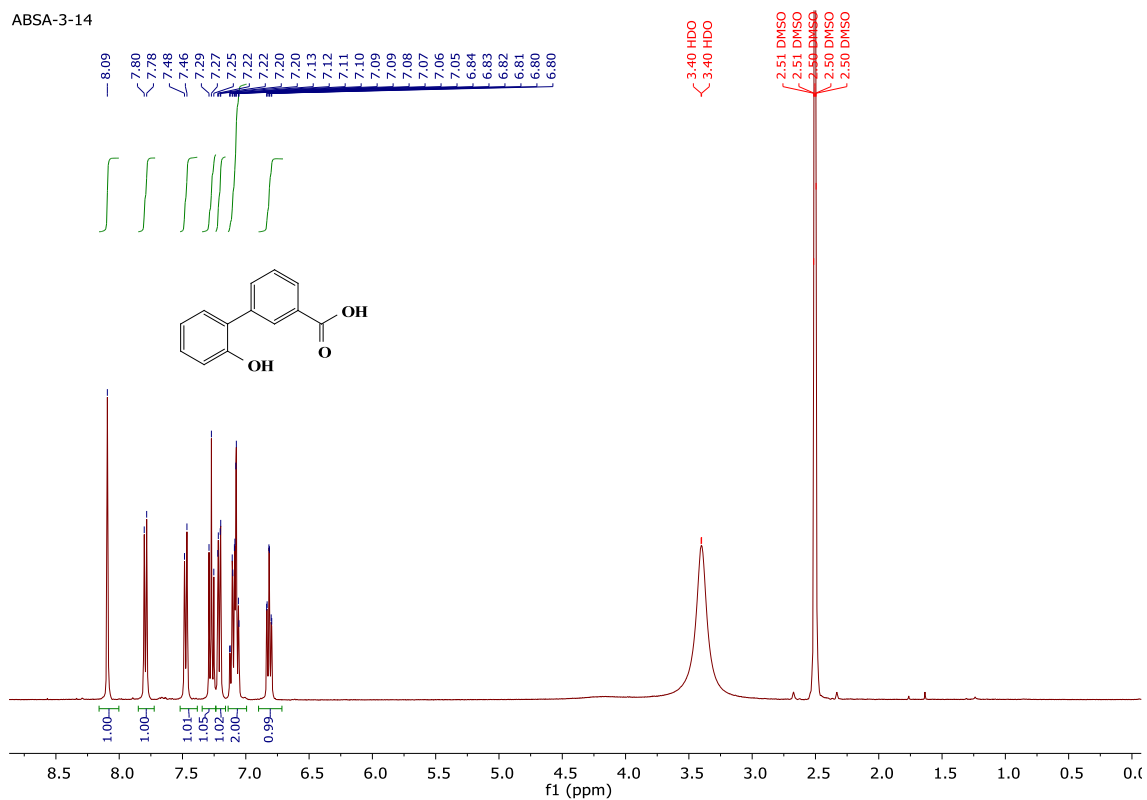
ABSA-3-10



2.3 2'-hydroxybiphenyl-3-carboxylic acid 4a:

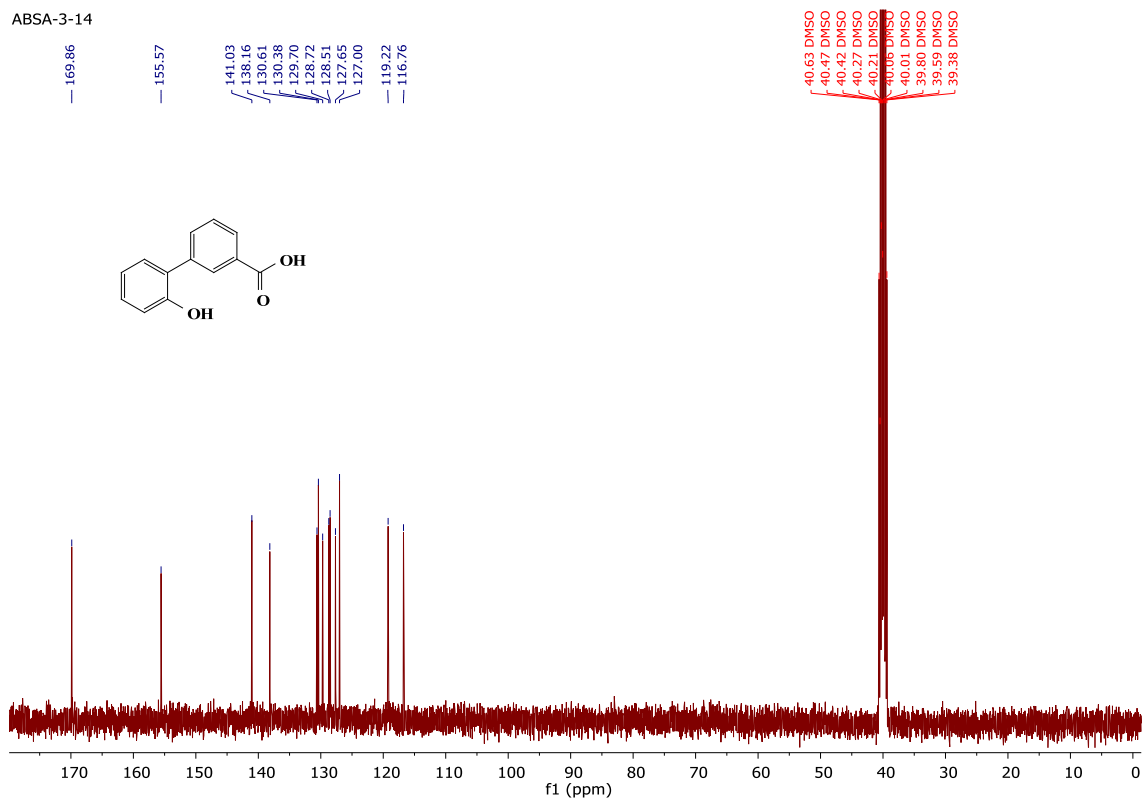
2.3.1 ¹H NMR of 4a

ABSA-3-14



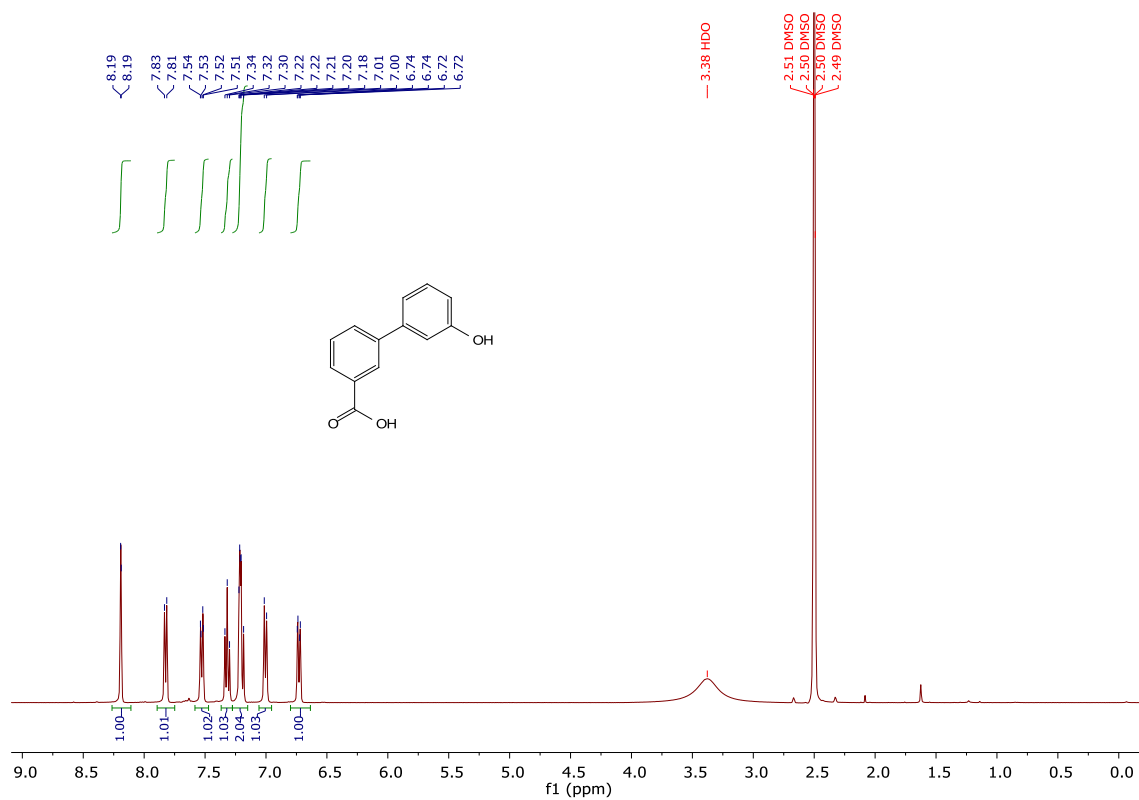
2.3.2 ¹³C NMR of 4a

ABSA-3-14

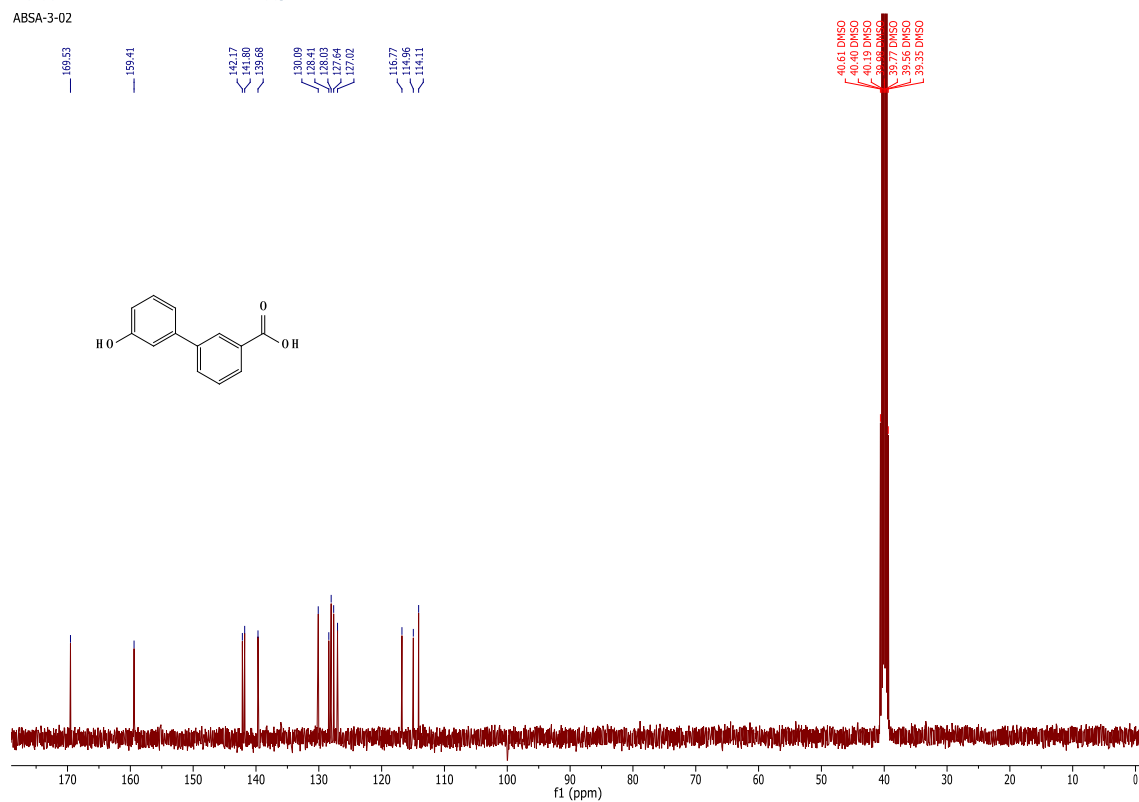


2.4 3'-hydroxybiphenyl-3-carboxylic acid, **4b**:

2.4.1 ^1H NMR of **4b**

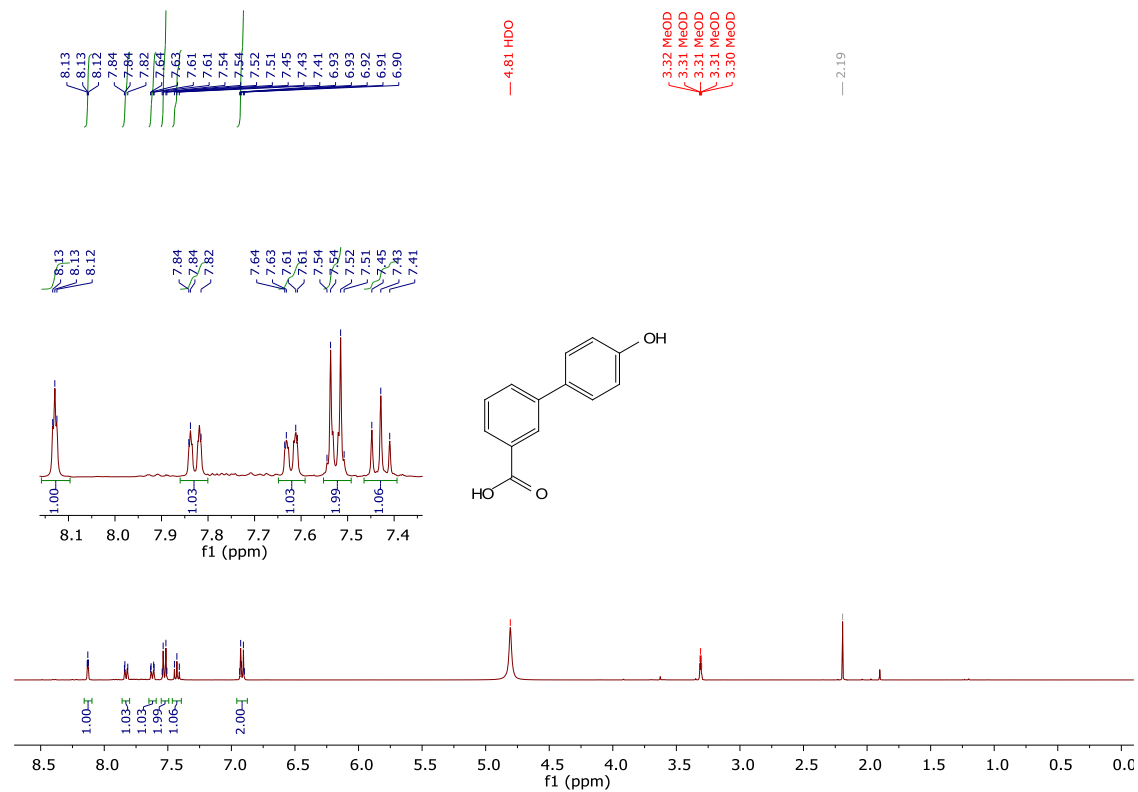


2.4.2 ^{13}C NMR of **4b**

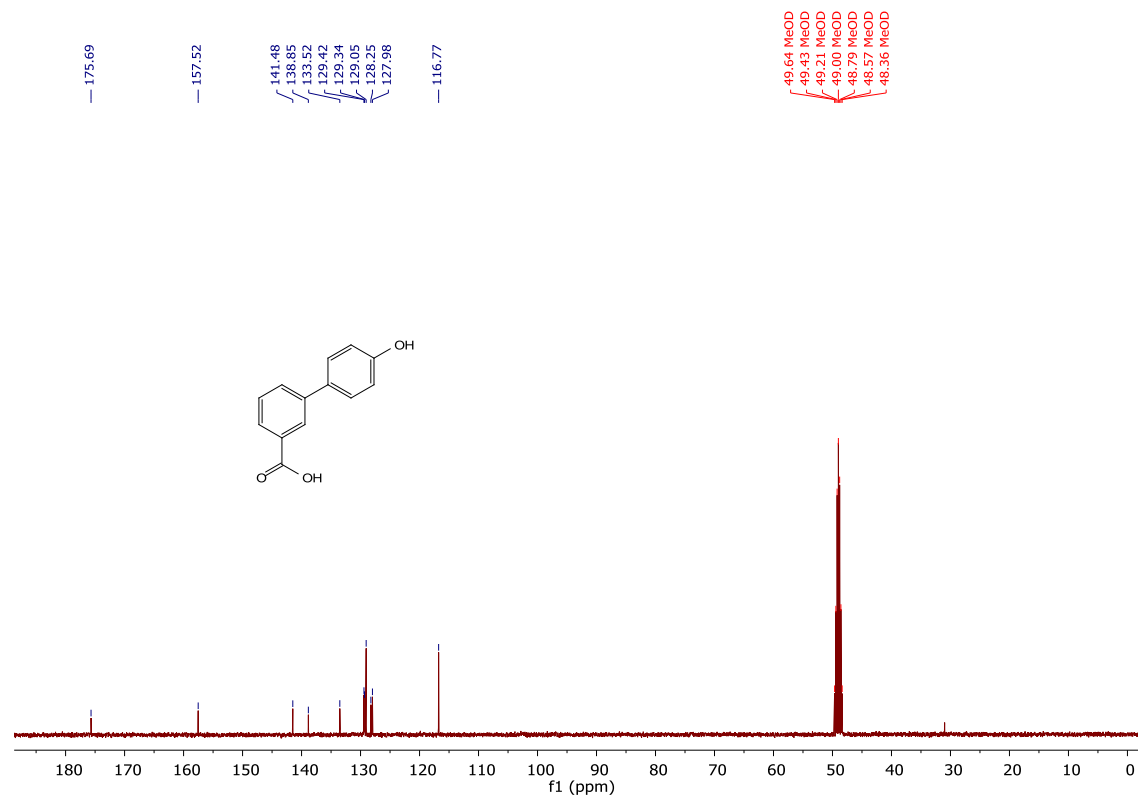


2.5 4'-hydroxybiphenyl-3-carboxylic acid, **4c**:

2.5.1 ¹H NMR of **4c**

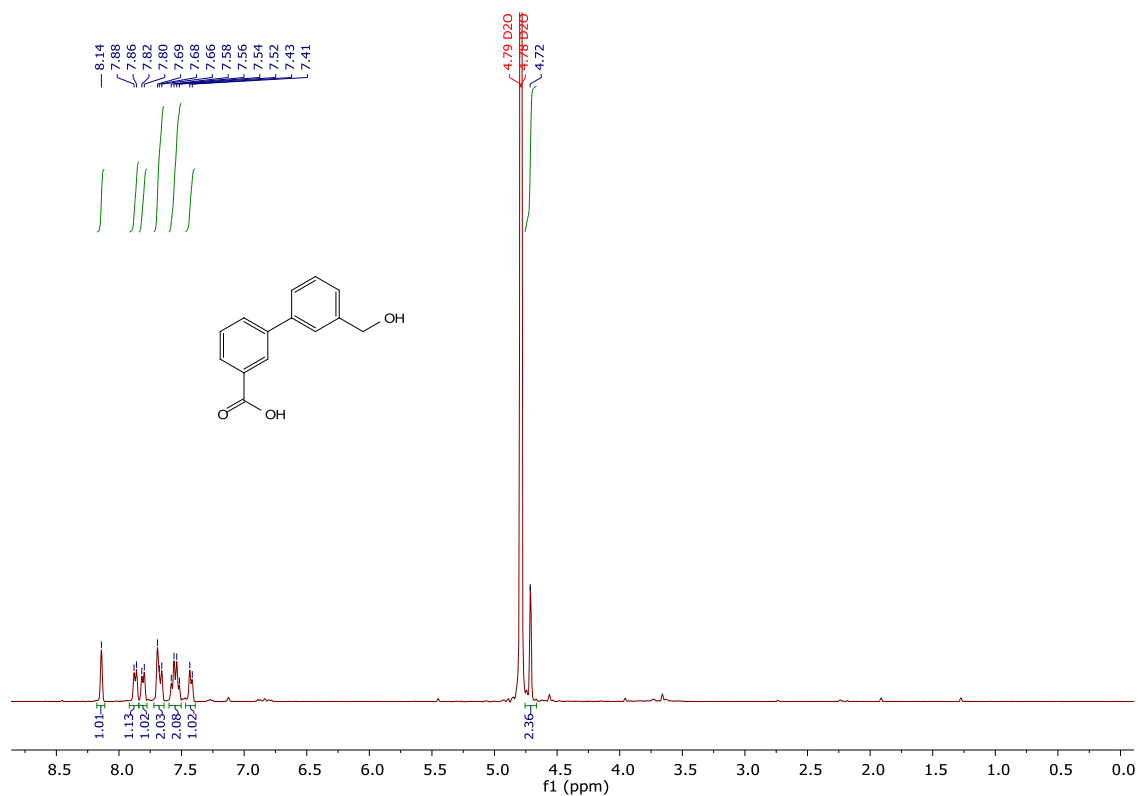


2.5.2 ¹³C NMR of **4c**

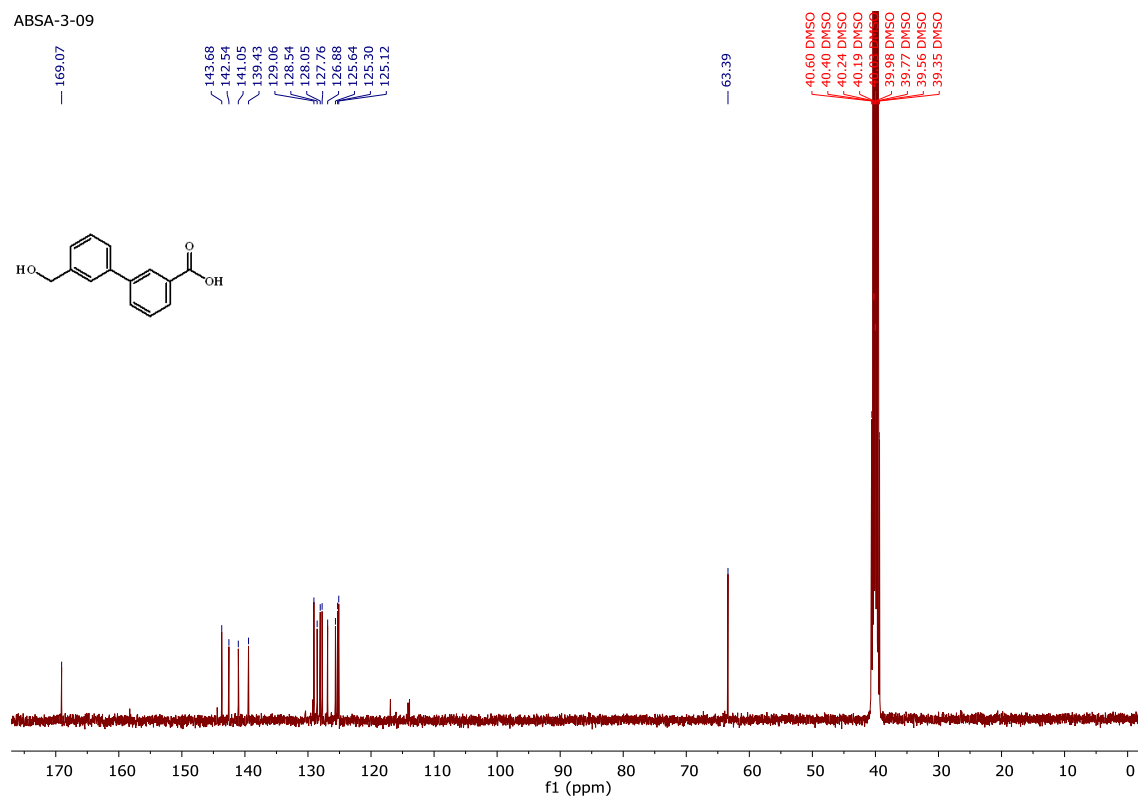


2.6 3'-(hydroxymethyl)biphenyl-3-carboxylic acid 5:

2.6.1 ^1H NMR of 5



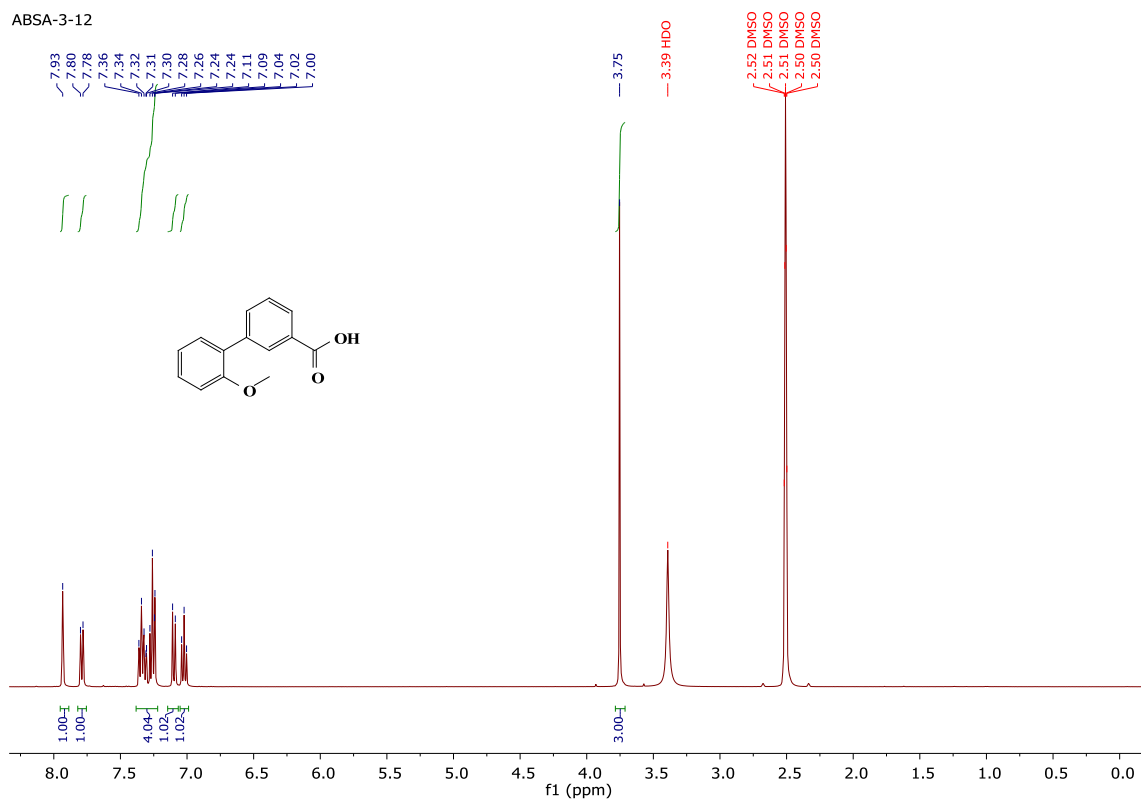
2.6.2 ^{13}C NMR of 5



2.7 2'-methoxybiphenyl-3-carboxylic acid, **6a**:

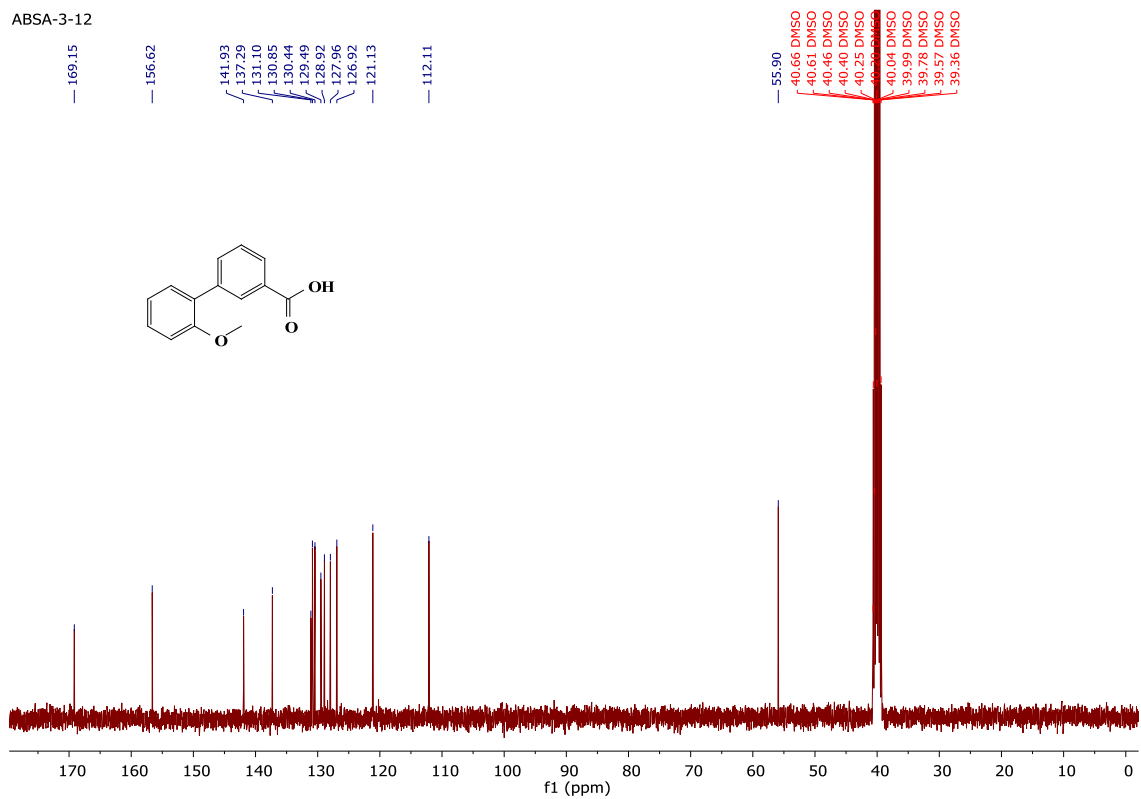
2.7.1 ^1H NMR of **6a**

ABSA-3-12



2.7.2 ^{13}C NMR of **6a**

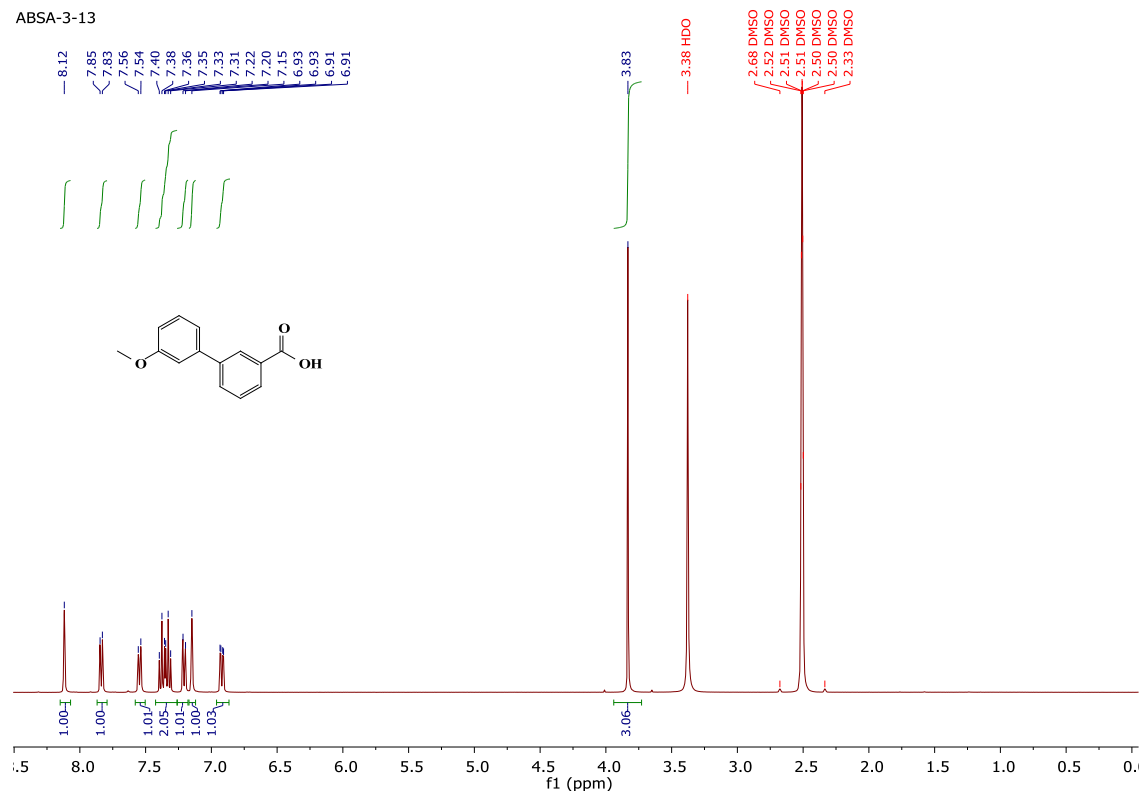
ABSA-3-12



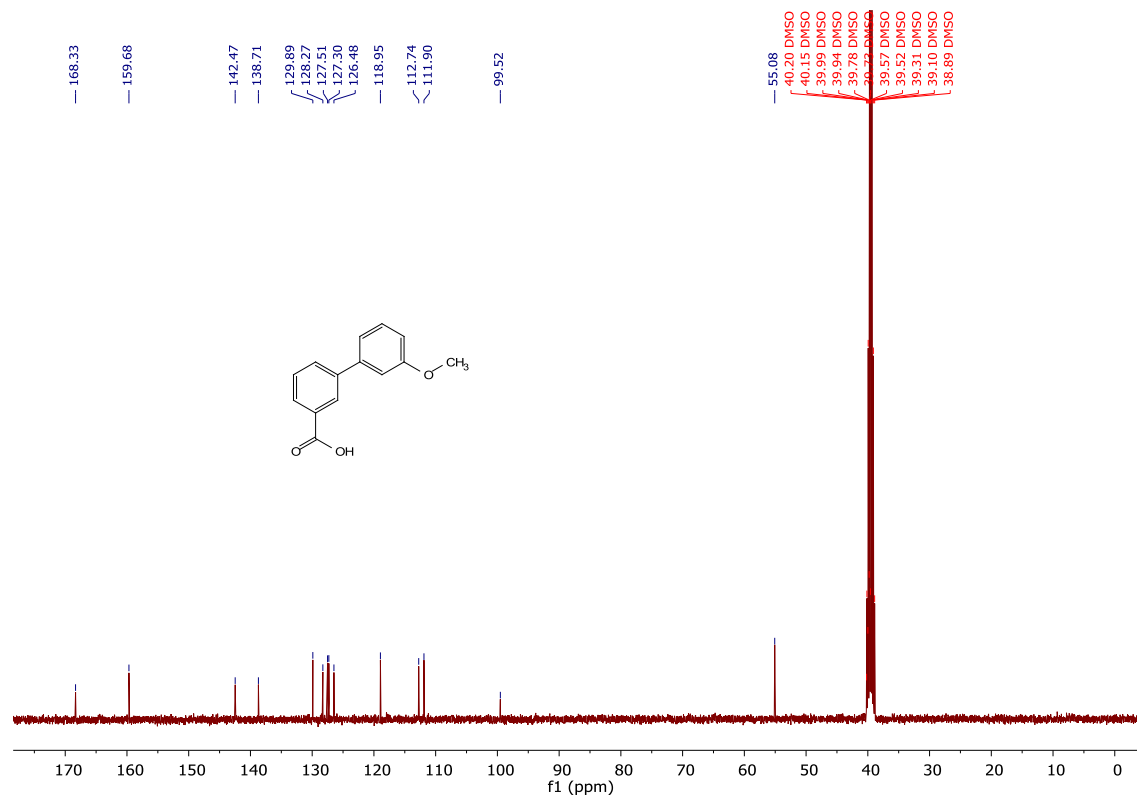
2.8 3'-methoxybiphenyl-3-carboxylic acid, **6b**:

2.8.1 ^1H NMR of **6b**

ABSA-3-13



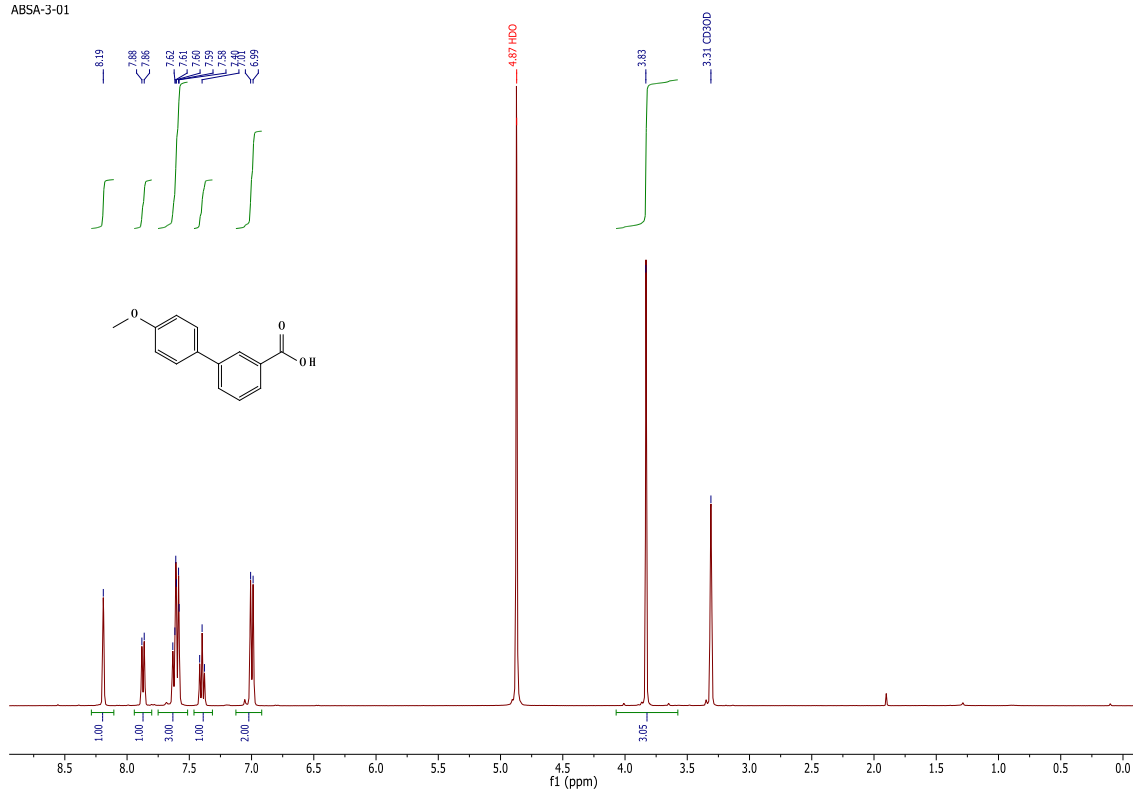
2.8.2 ^{13}C NMR of **6b**:



2.9 4'-methoxybiphenyl-3-carboxylic acid **6c**:

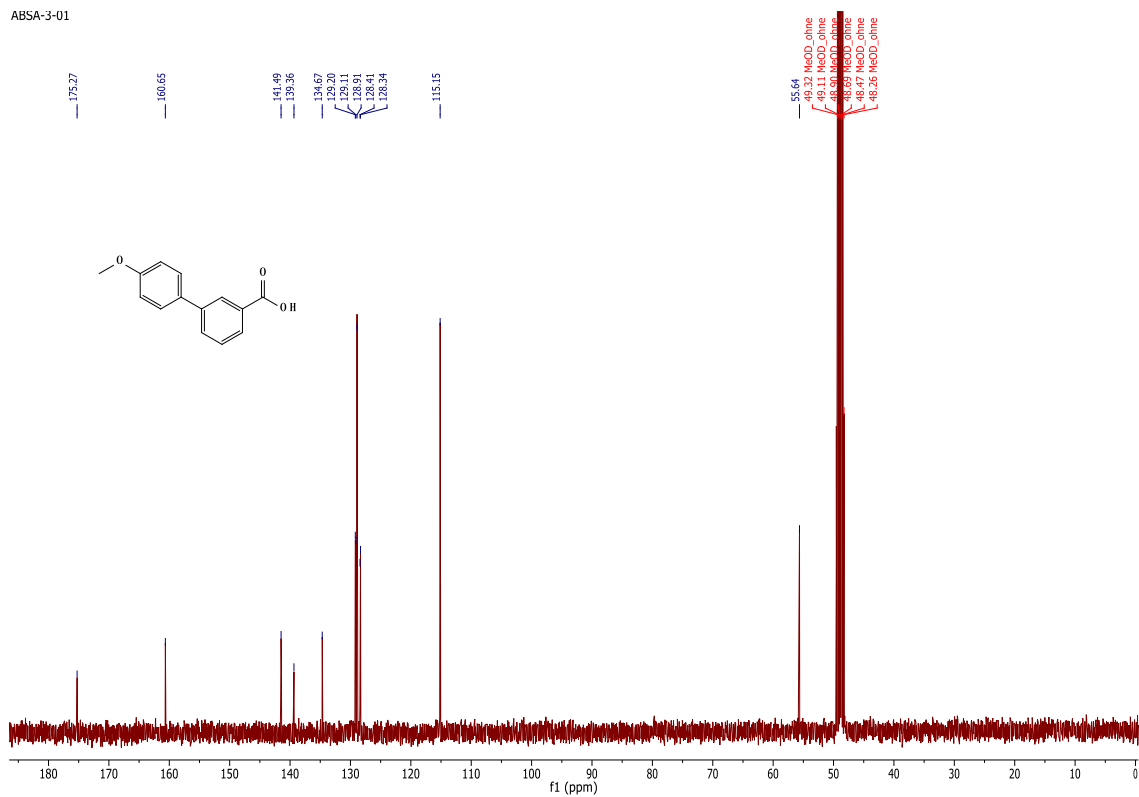
2.9.1 ^1H NMR of **6c**

ABSA-3-01



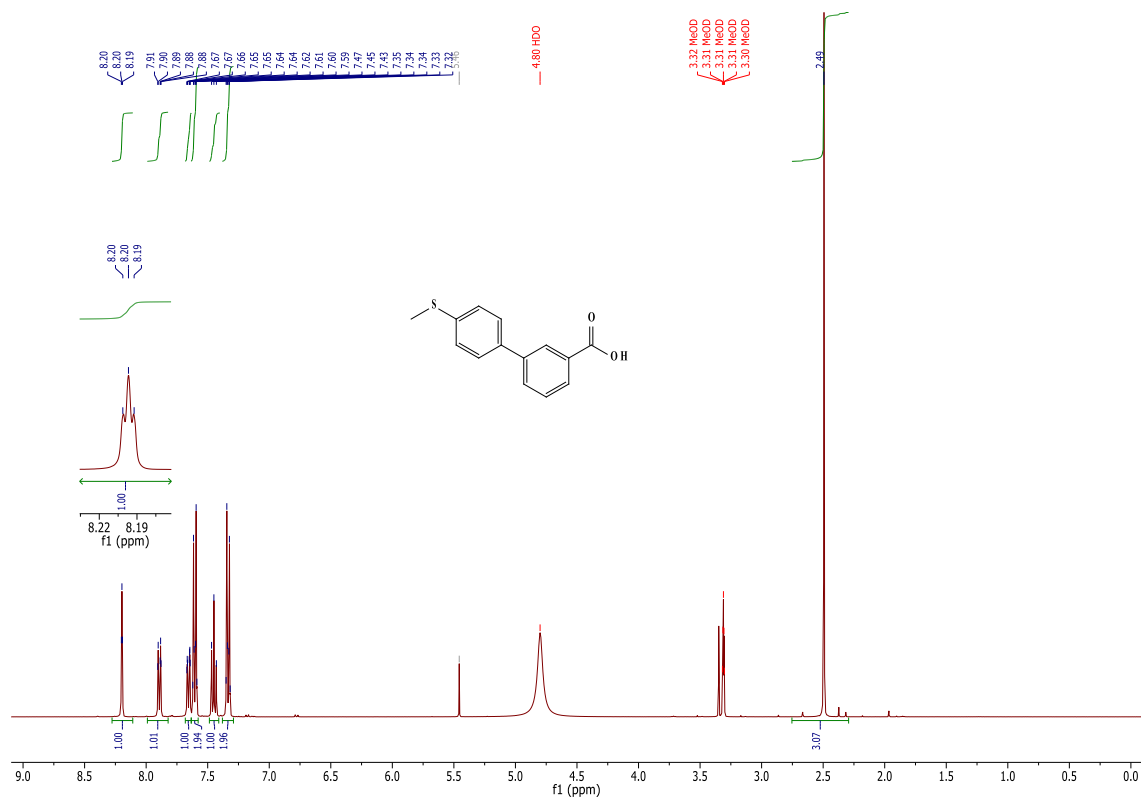
2.9.2 ^{13}C NMR of **6c**

ABSA-3-01

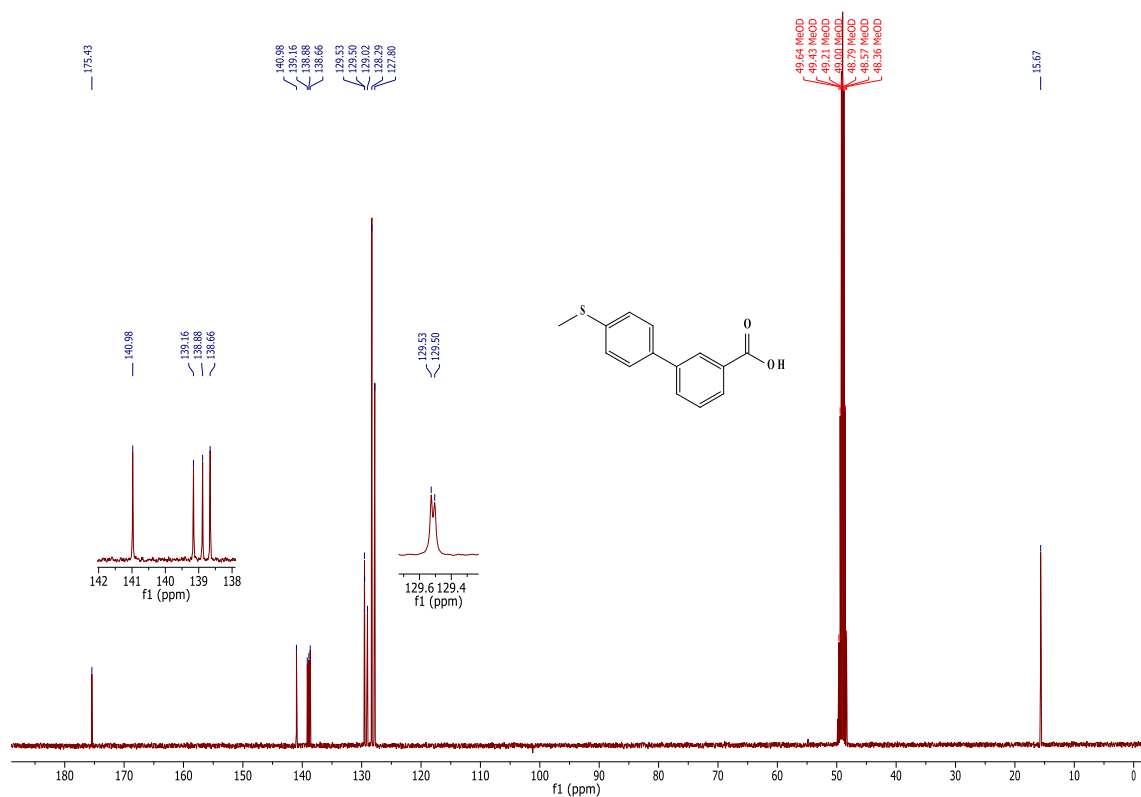


2.10 4'-methylthiobiphenyl]-3-carboxylic acid, 7:

2.10.1 ¹H NMR of 7



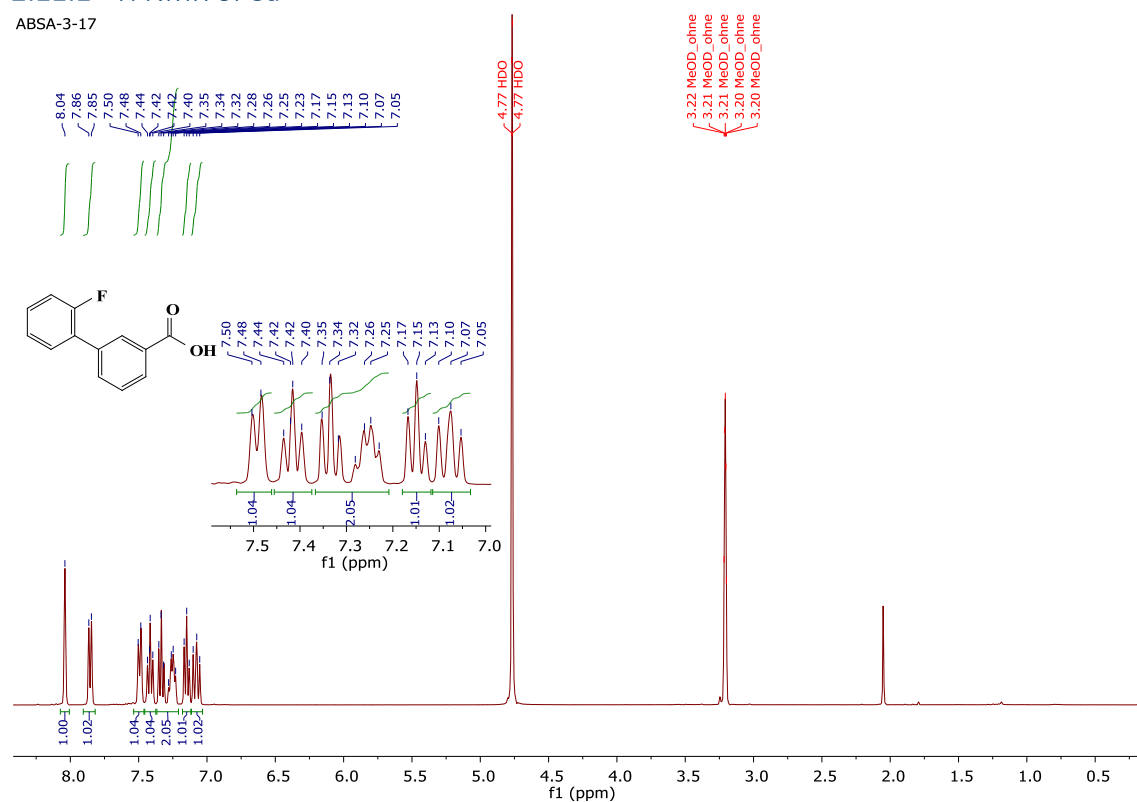
2.10.2 ¹³C NMR of 7



2.11 2'-fluorobiphenyl-3-carboxylic acid, **8a**:

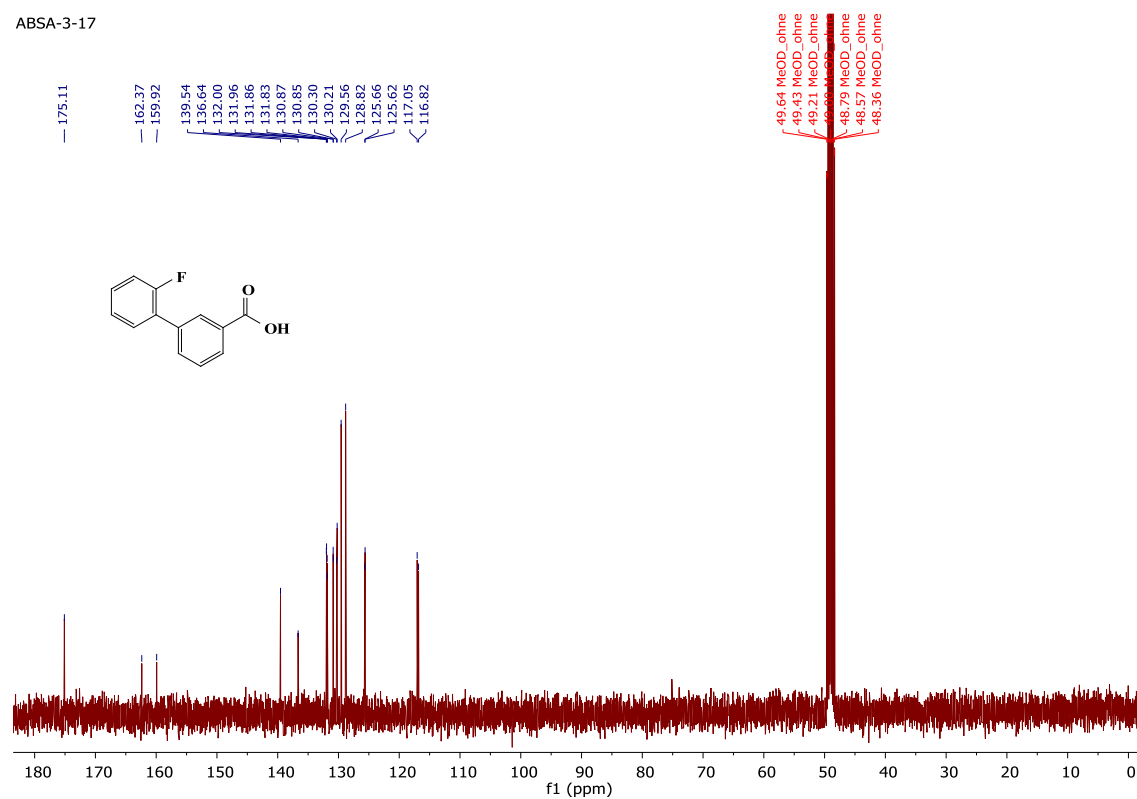
2.11.1 ¹H NMR of **8a**

ABSA-3-17



2.11.2 ¹³C NMR of **8a**

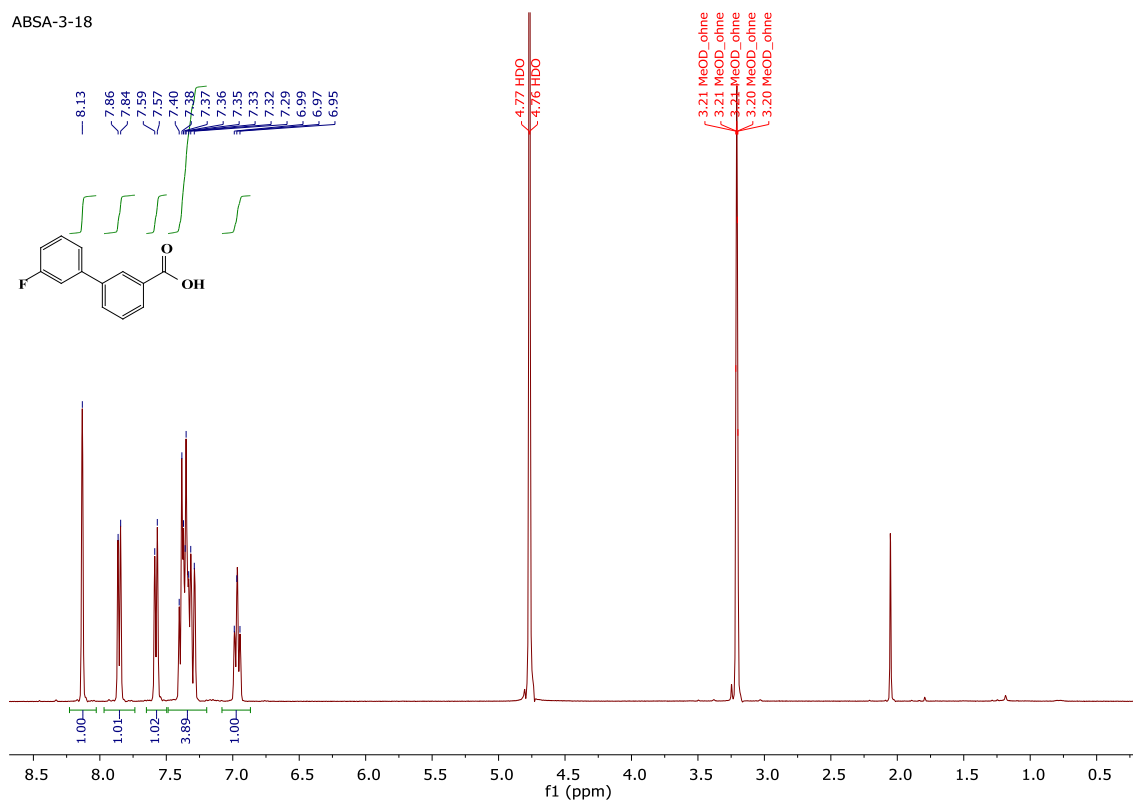
ABSA-3-17



2.12 3'-fluorobiphenyl-3-carboxylic acid **8b**:

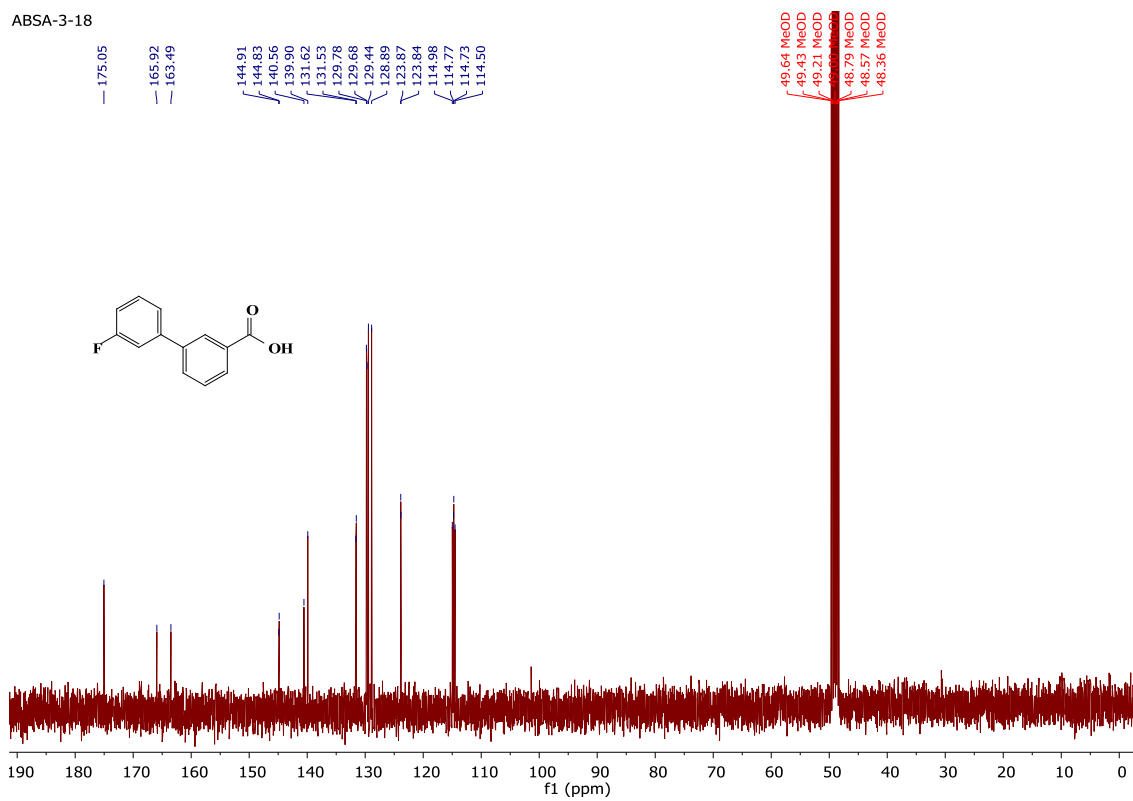
2.12.1 ^1H NMR of **8b**

ABSA-3-18



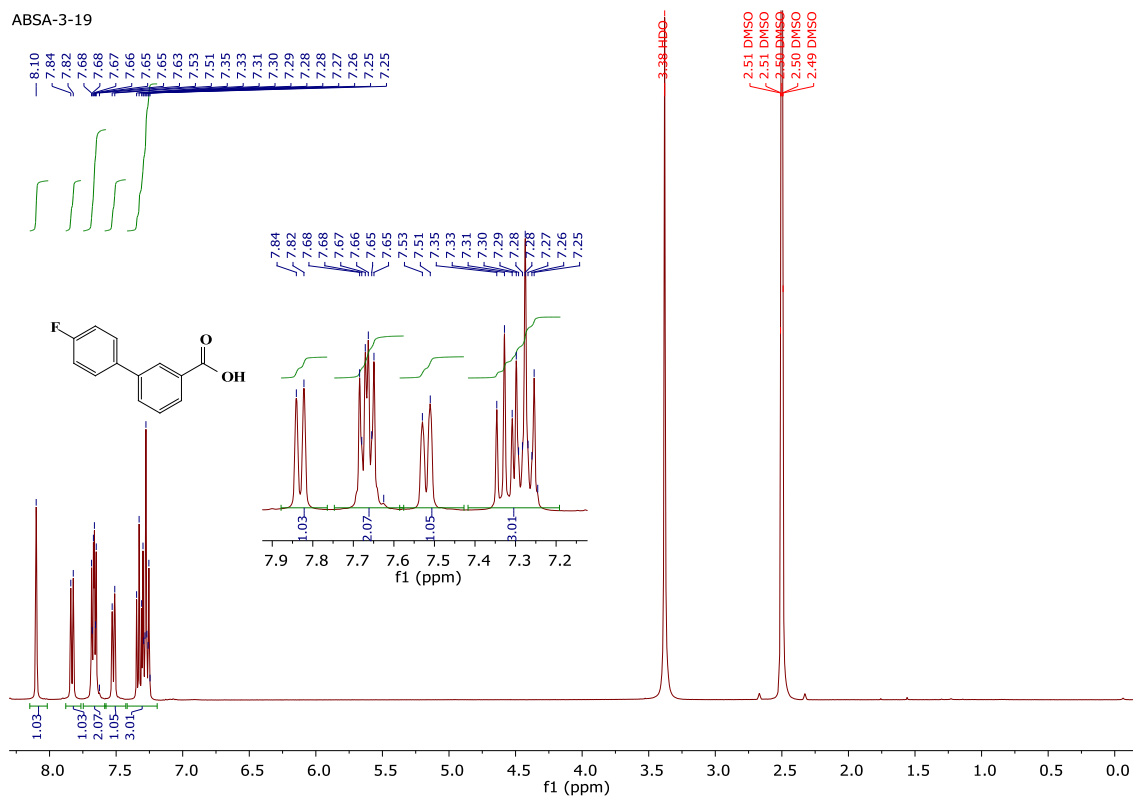
2.12.2 ^{13}C NMR of **8b**

ABSA-3-18

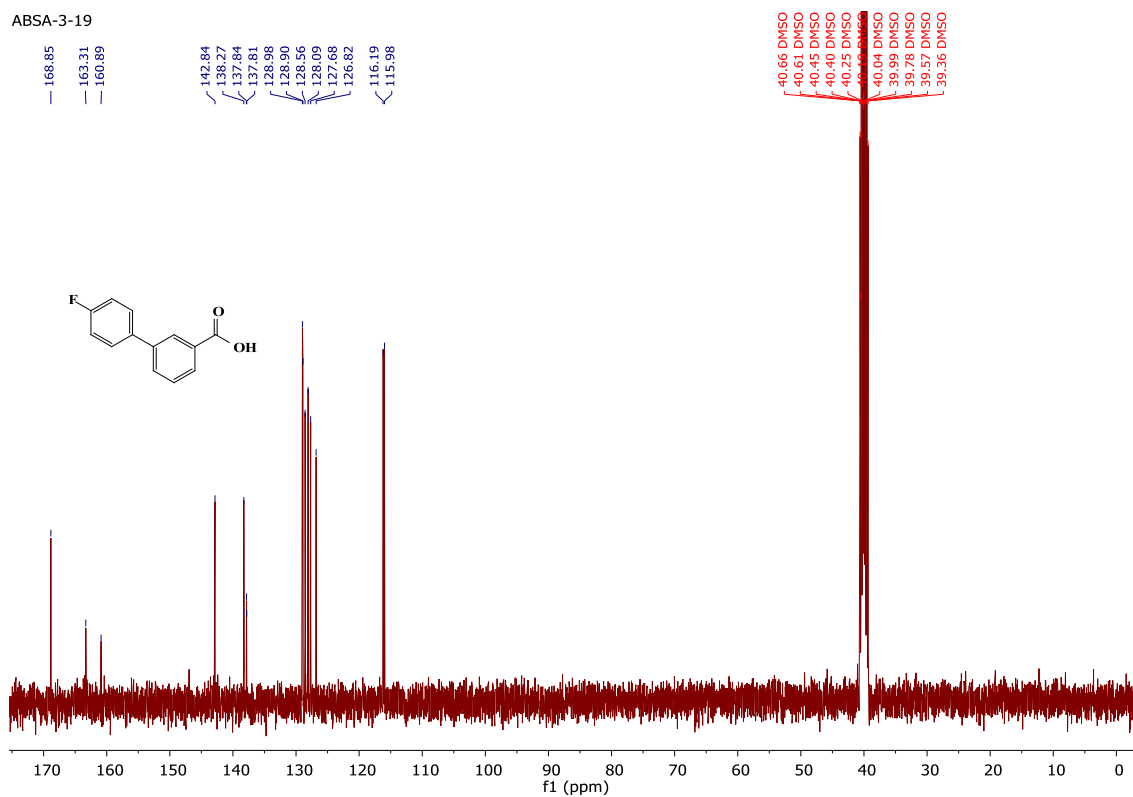


2.13 4'-fluorobiphenyl-3-carboxylic acid, **8c**:

2.13.1 ^1H NMR of **8c**

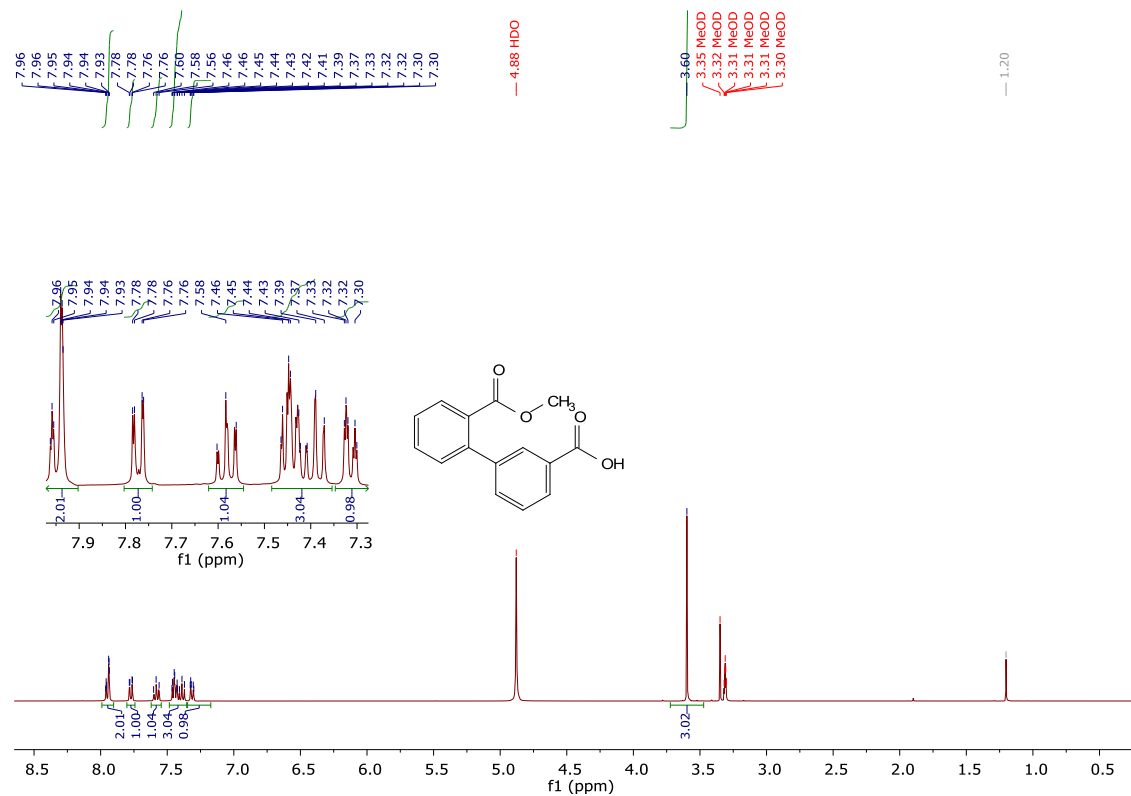


2.13.2 ^{13}C NMR of **8c**

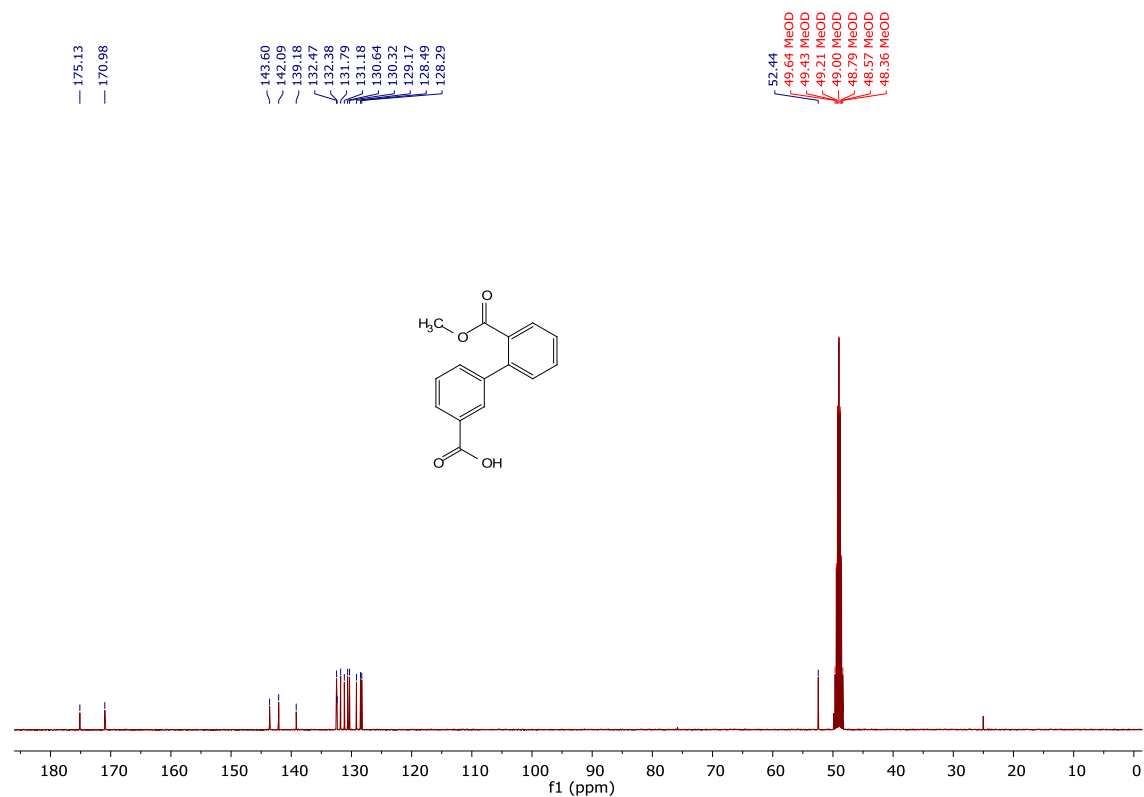


2.14 2'-(methoxycarbonyl)biphenyl-3-carboxylic acid, **9a**:

2.14.1 ^1H NMR of **9a**



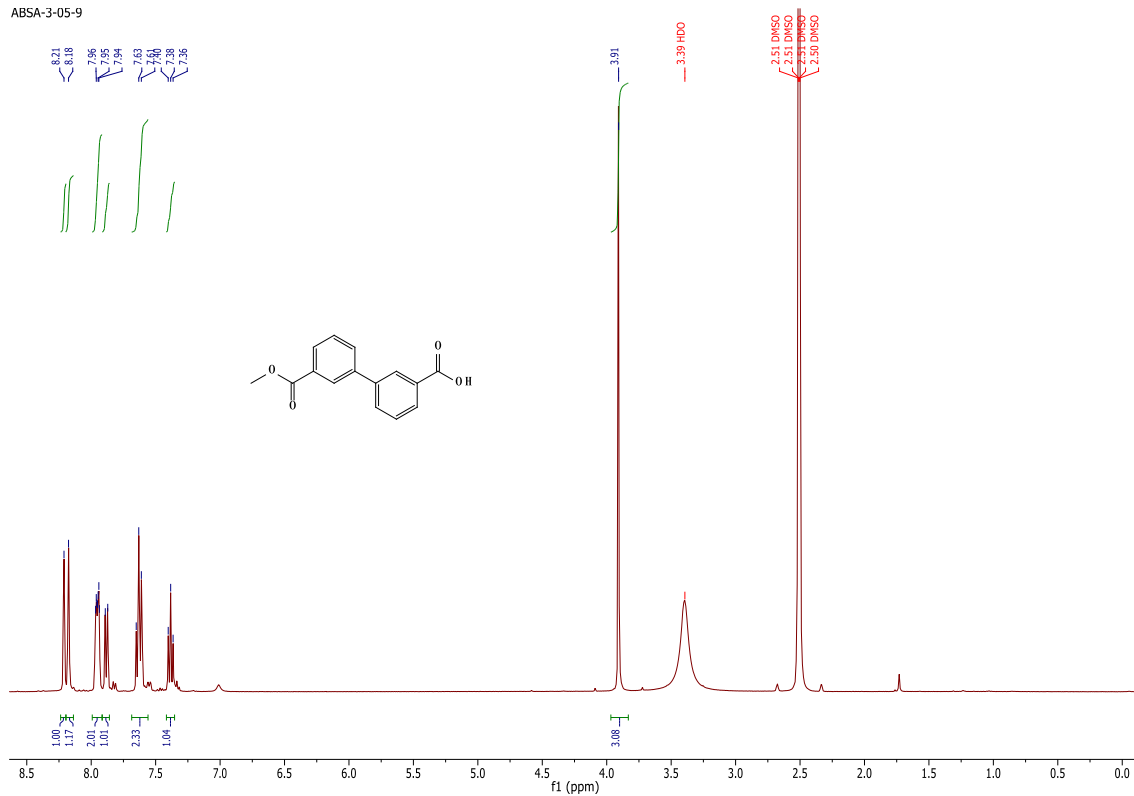
2.14.2 ^{13}C NMR of **9a**



2.15 3'-(methoxycarbony)biphenyl-3-carboxylic acid, **9b**:

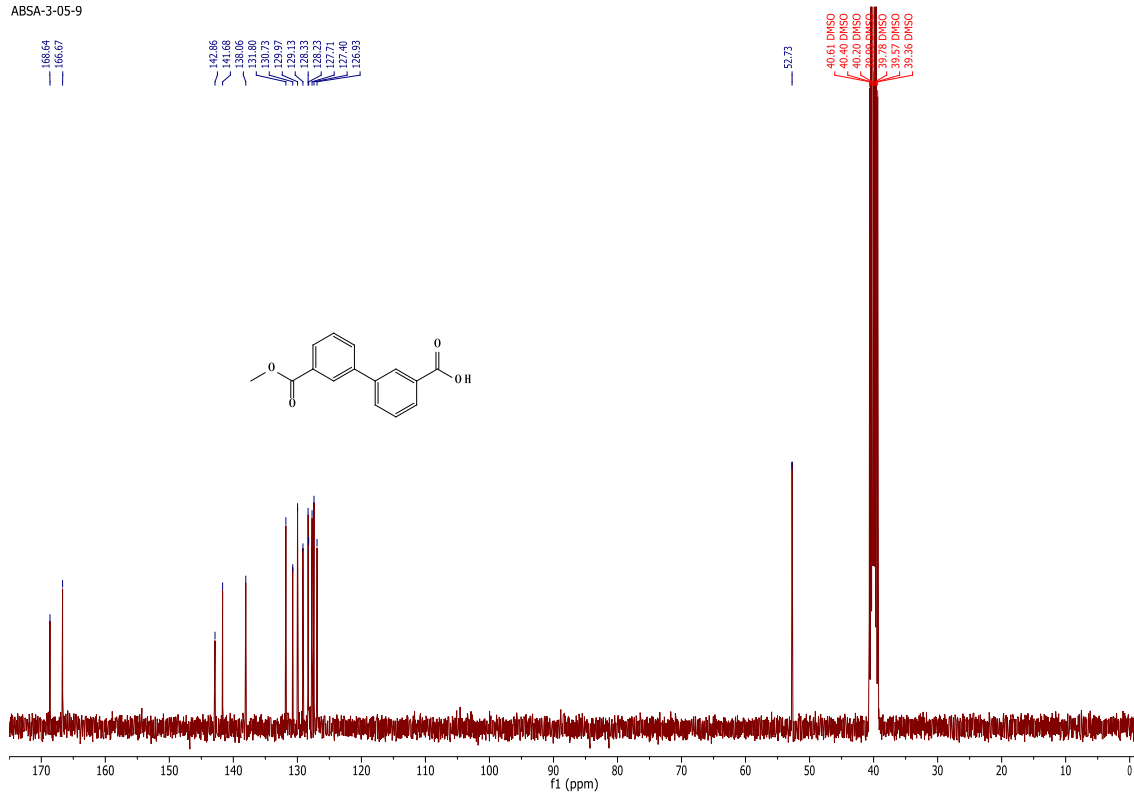
2.15.1 ^1H NMR of **9b**

ABSA-3-05-9



2.15.2 ^{13}C NMR of **9b**

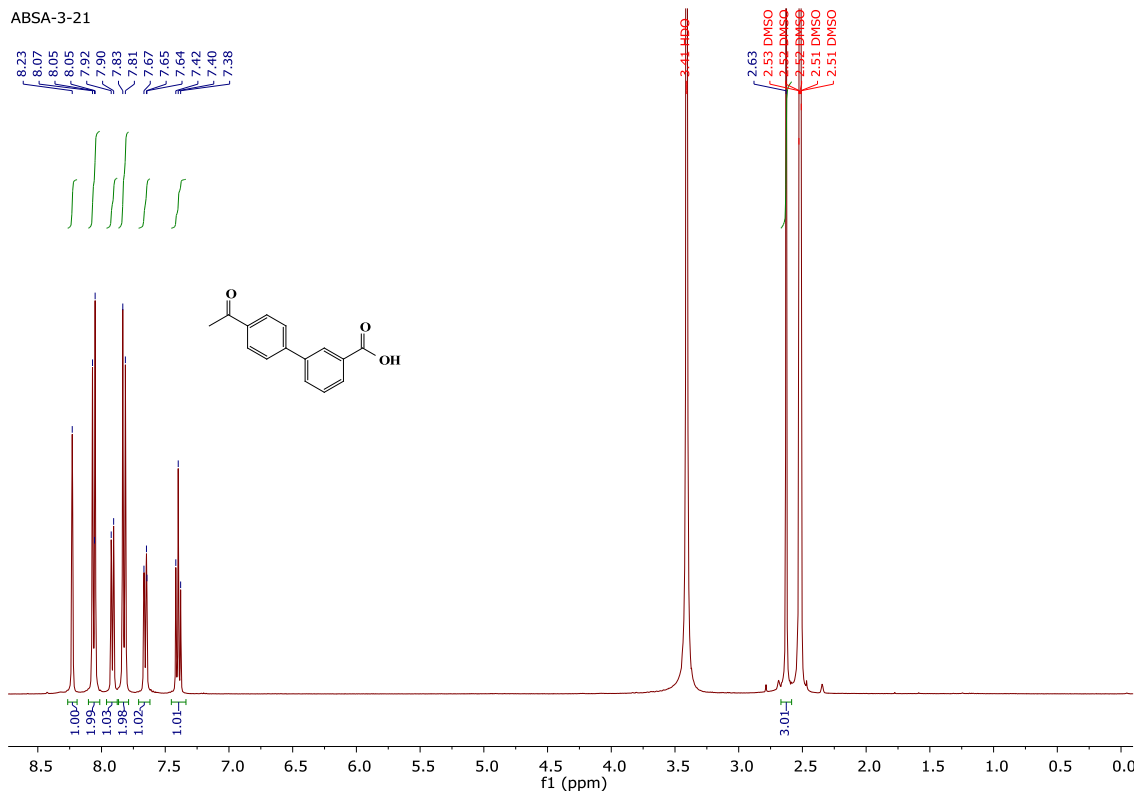
ABSA-3-05-9



2.16 4'-acetylbiphenyl-3-carboxylic acid **10**:

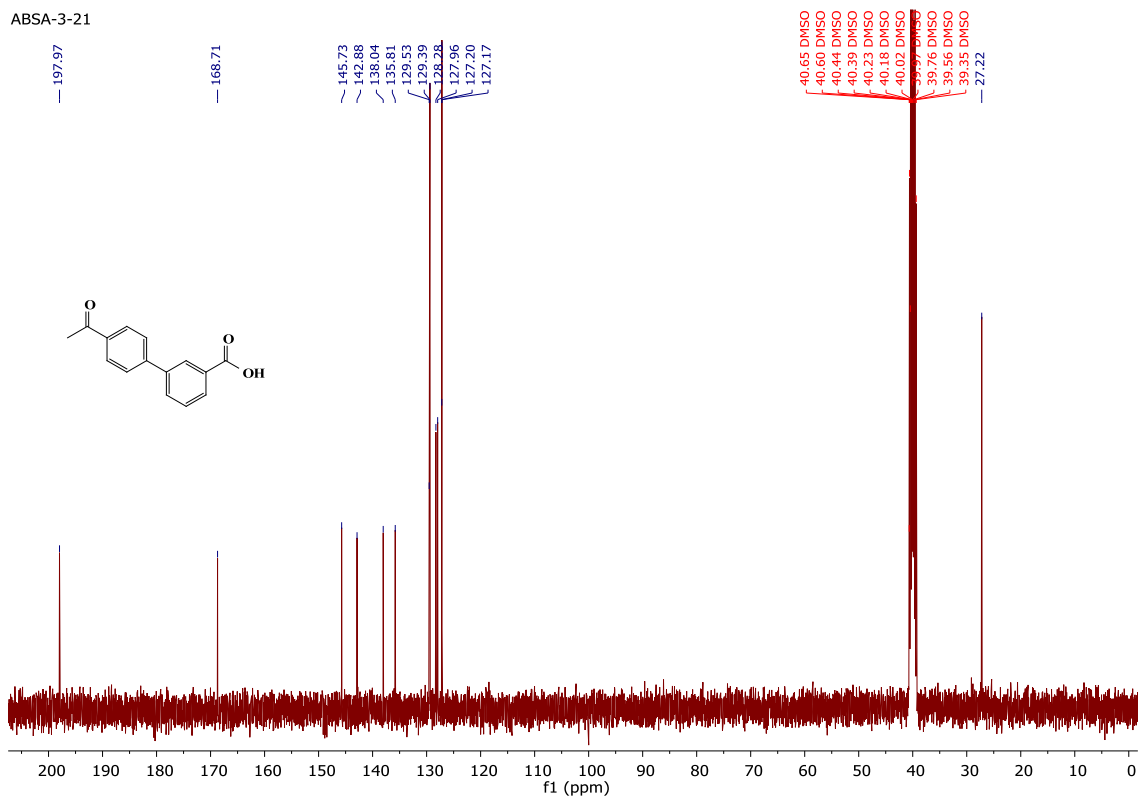
2.16.1 ¹H NMR of **10**

ABSA-3-21



2.16.2 ¹³C NMR of **10**

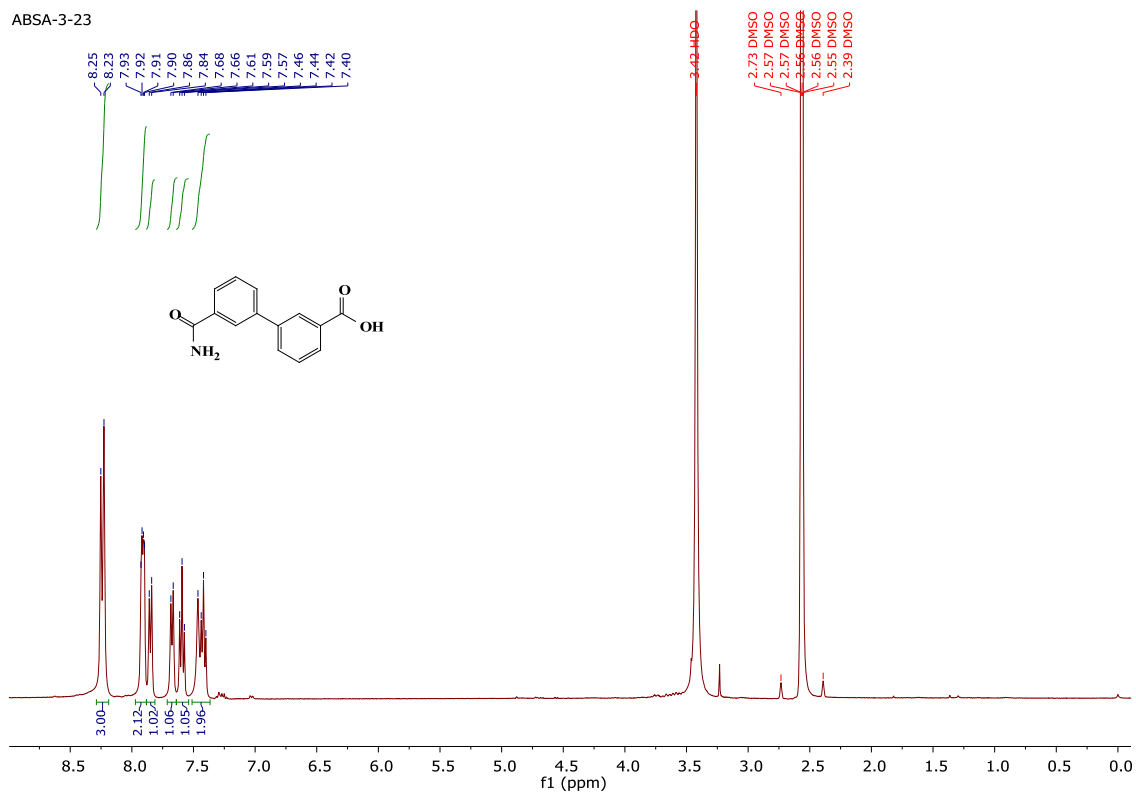
ABSA-3-21



2.17 3'-carbamoylbiphenyl-3-carboxylic acid, **11a**:

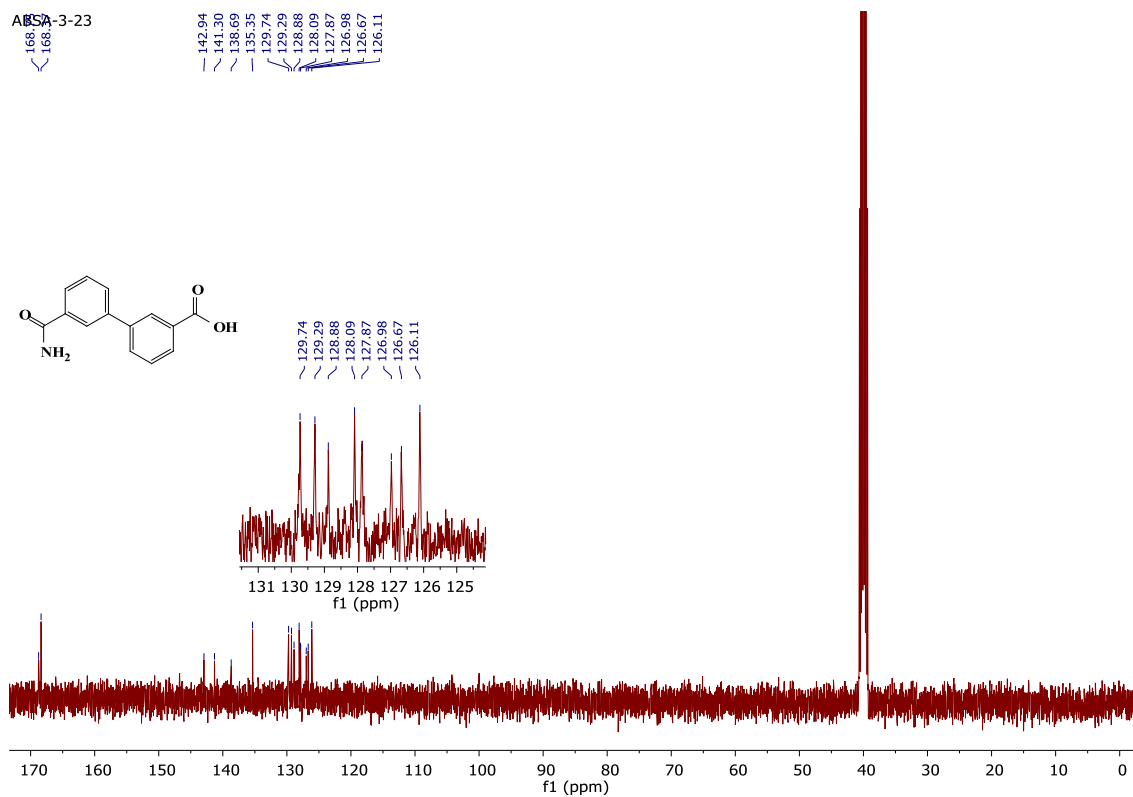
2.17.1 ^1H NMR of **11a**

ABSA-3-23



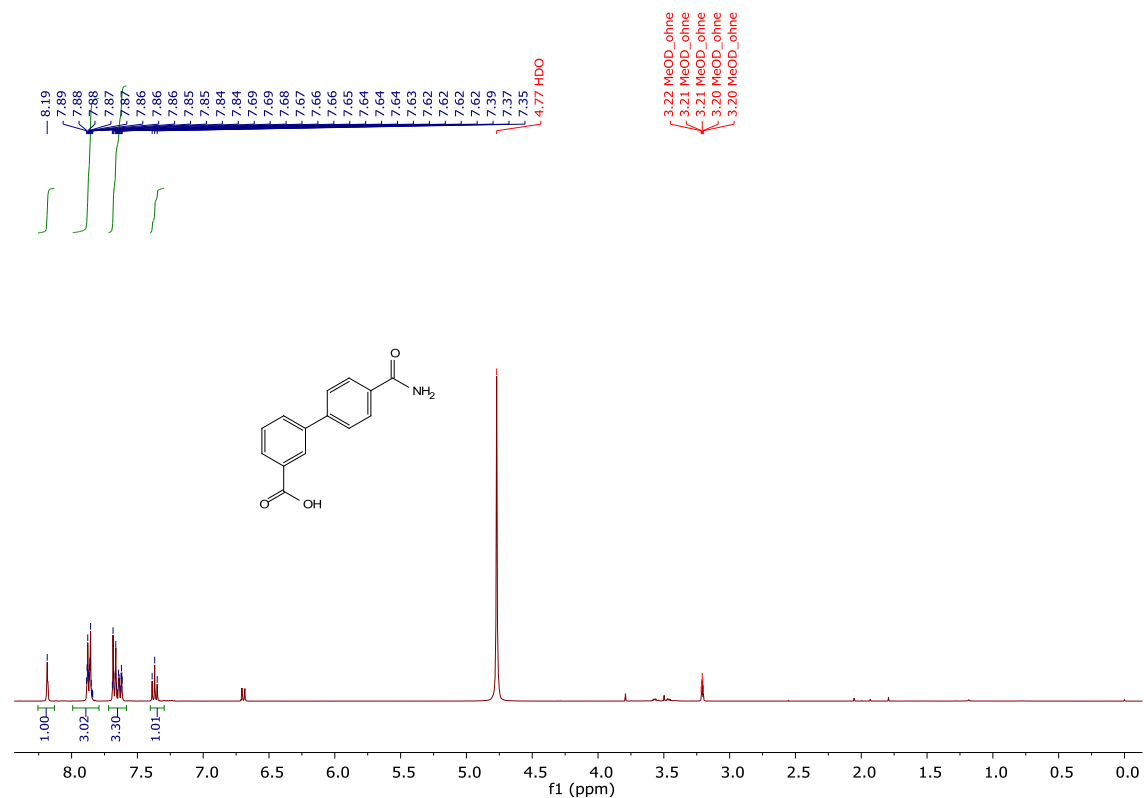
2.17.2 ^{13}C NMR of **11a**

ABSA-3-23

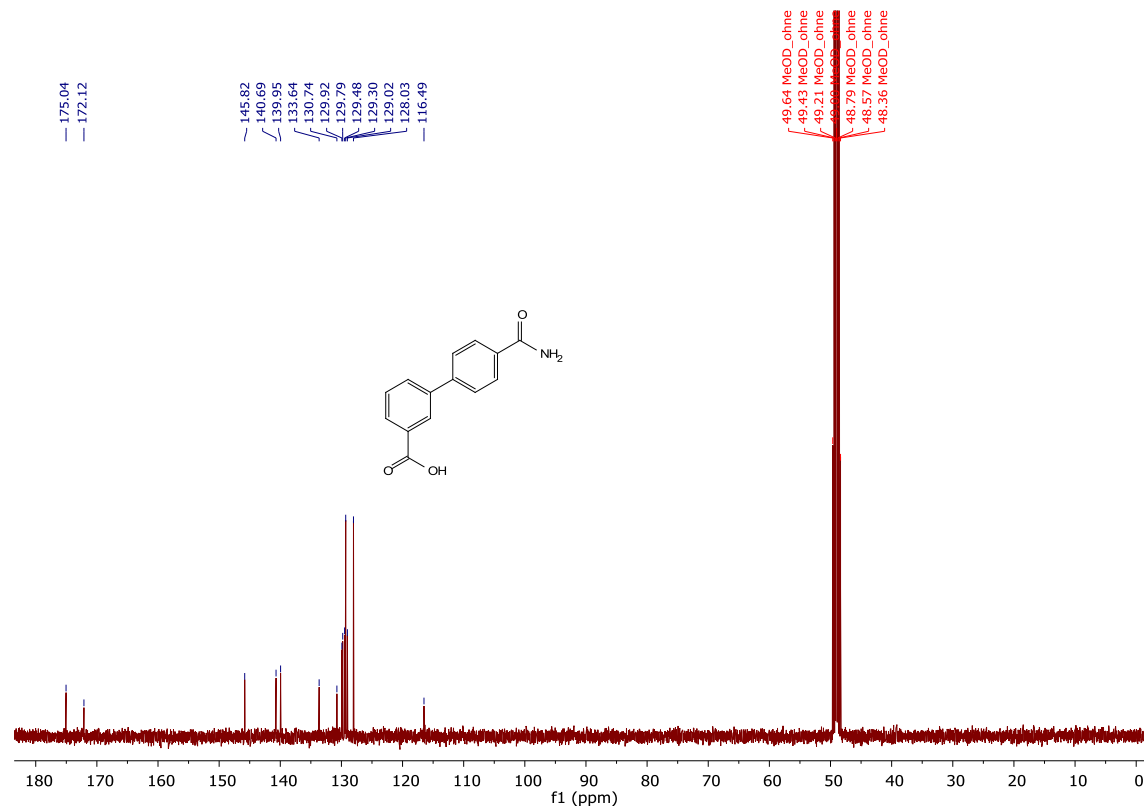


2.18 4'-carbamoylbiphenyl-3-carboxylic acid, **11b**:

2.18.1 ^1H NMR of **11b**



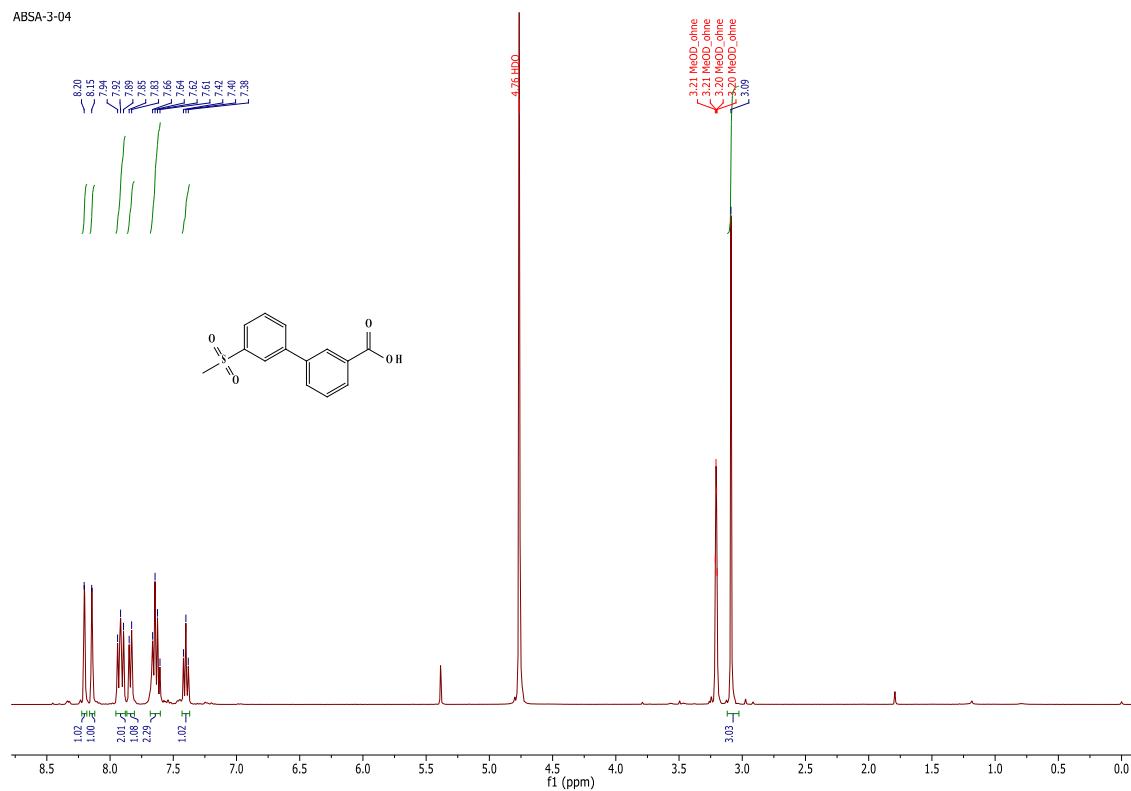
2.18.2 ^{13}C NMR of **11b**



2.19 3'-(methylsulfonyl)biphenyl-3-carboxylic acid, 12a:

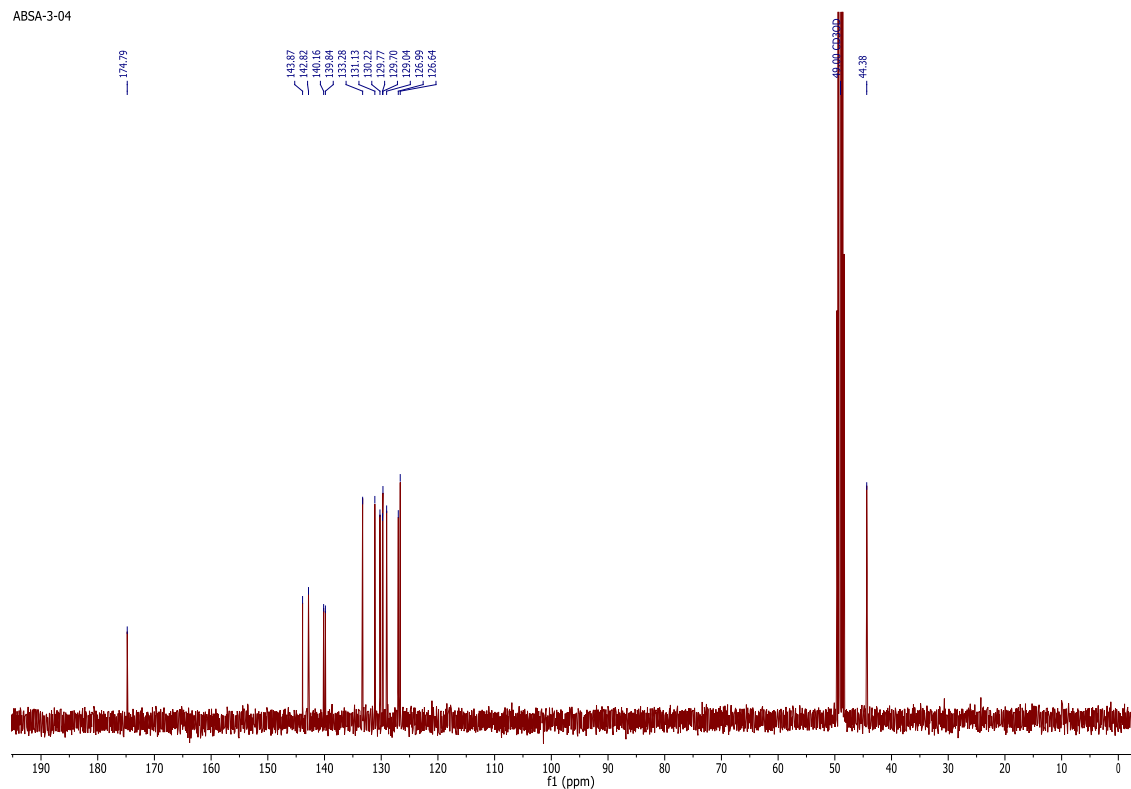
2.19.1 ¹H NMR of 12a

ABSA-3-04



2.19.2 ¹³C NMR of 12a

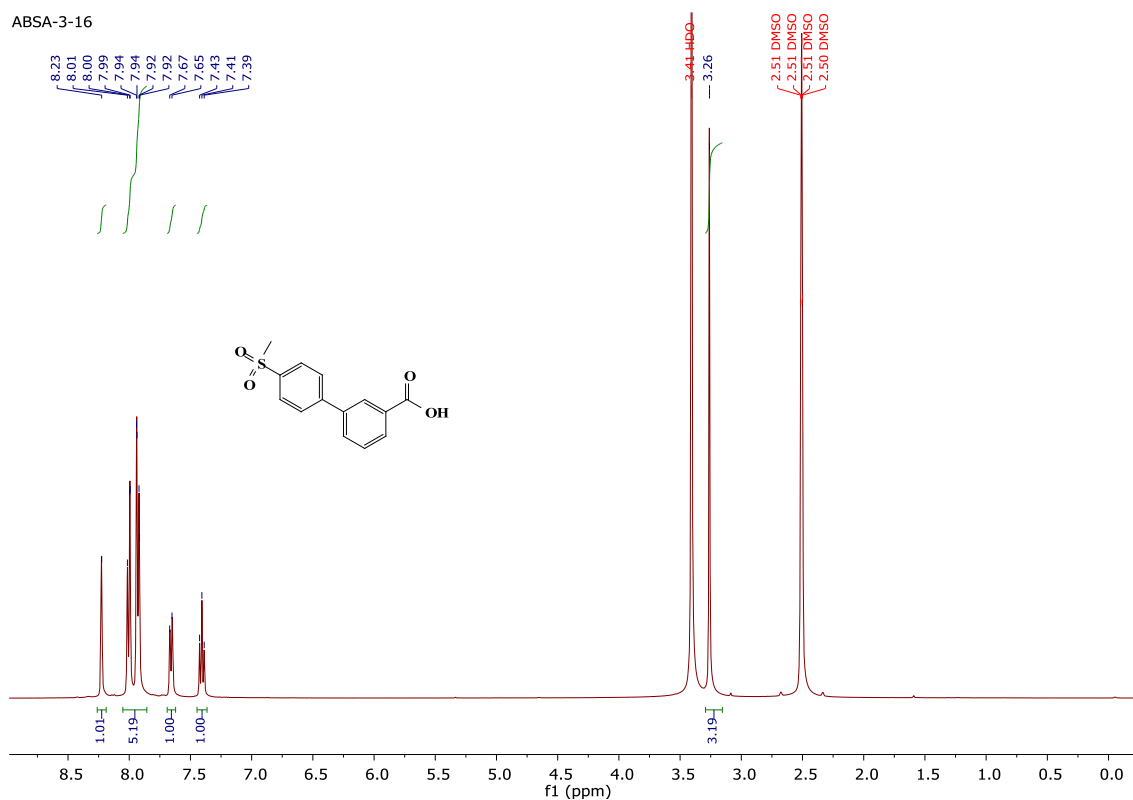
ABSA-3-04



2.20 4'-(methylsulfonyl)biphenyl-3-carboxylic acid, 12b:

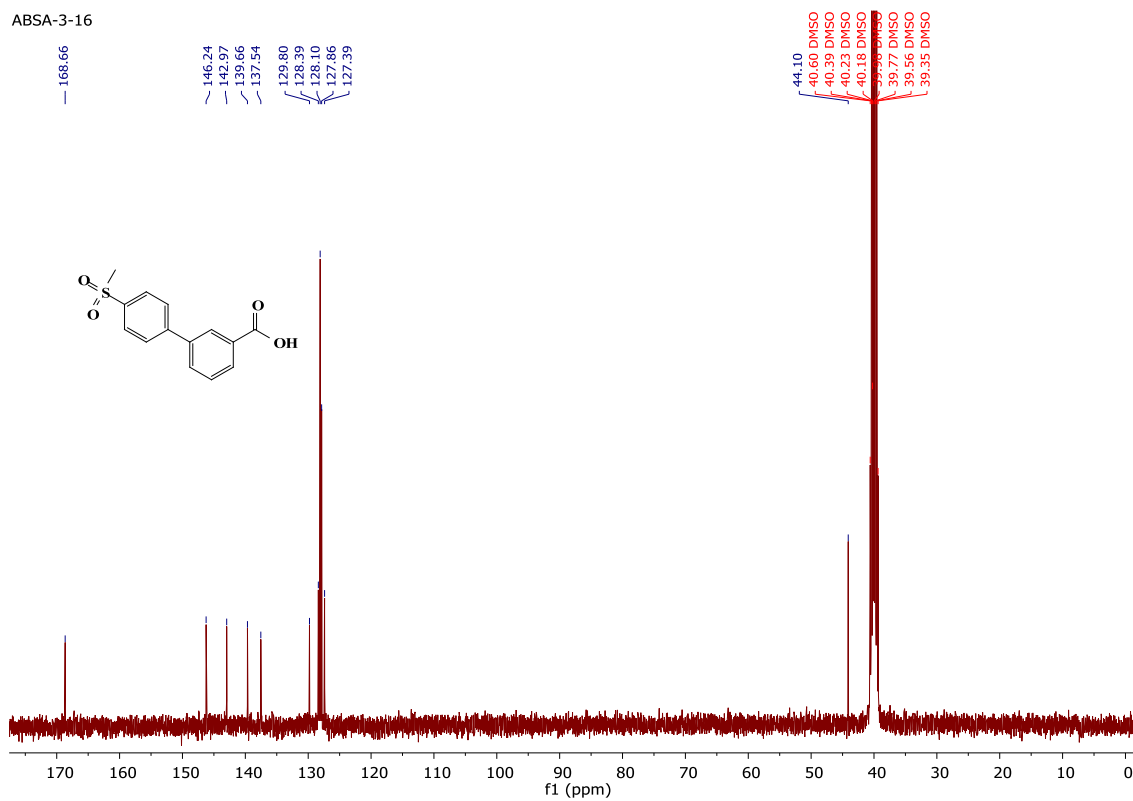
2.20.1 ^1H NMR of 12b

ABSA-3-16



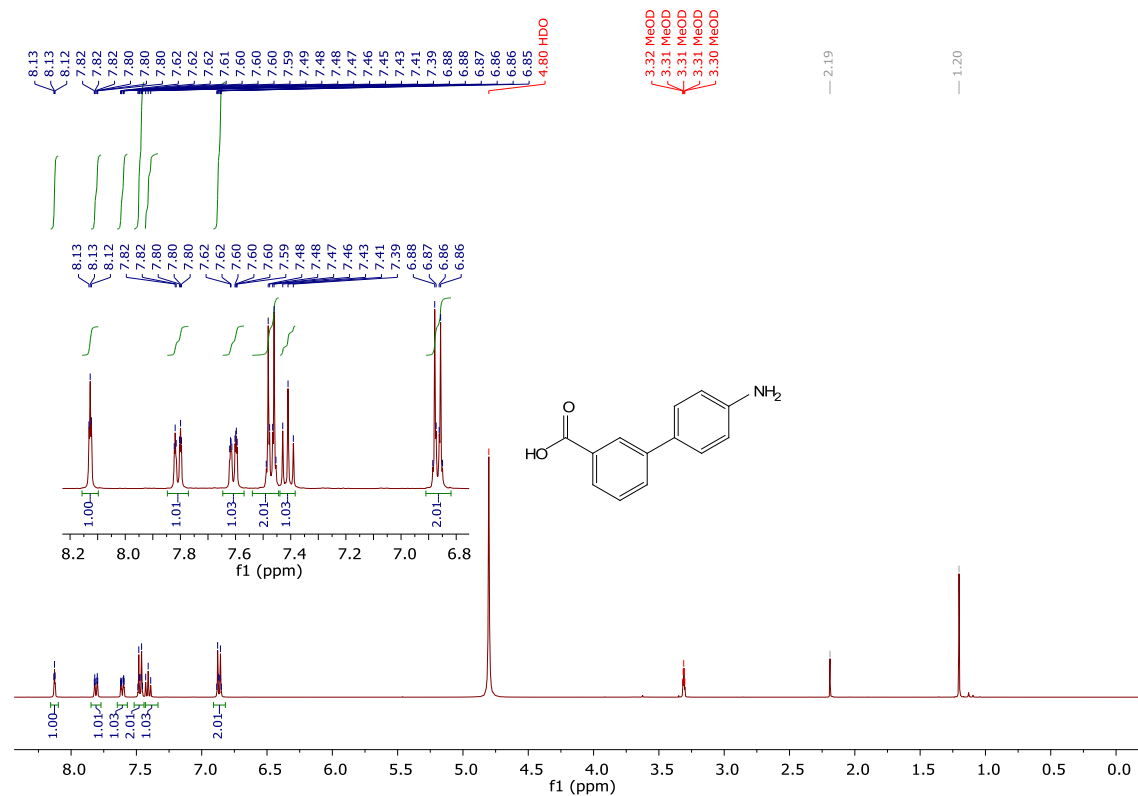
2.20.2 ^{13}C NMR of 12b

ABSA-3-16



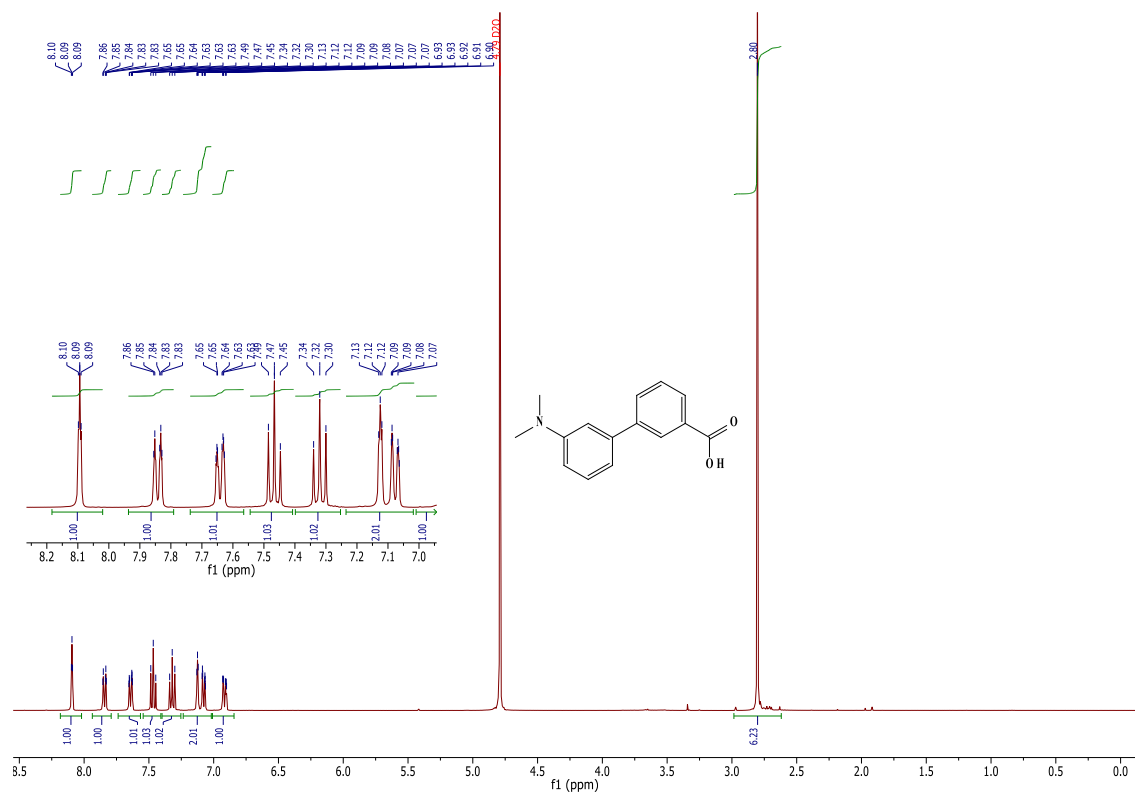
2.21 4'-aminobiphenyl-3-carboxylic acid, **13**:

2.21.1 ¹H NMR of **13**

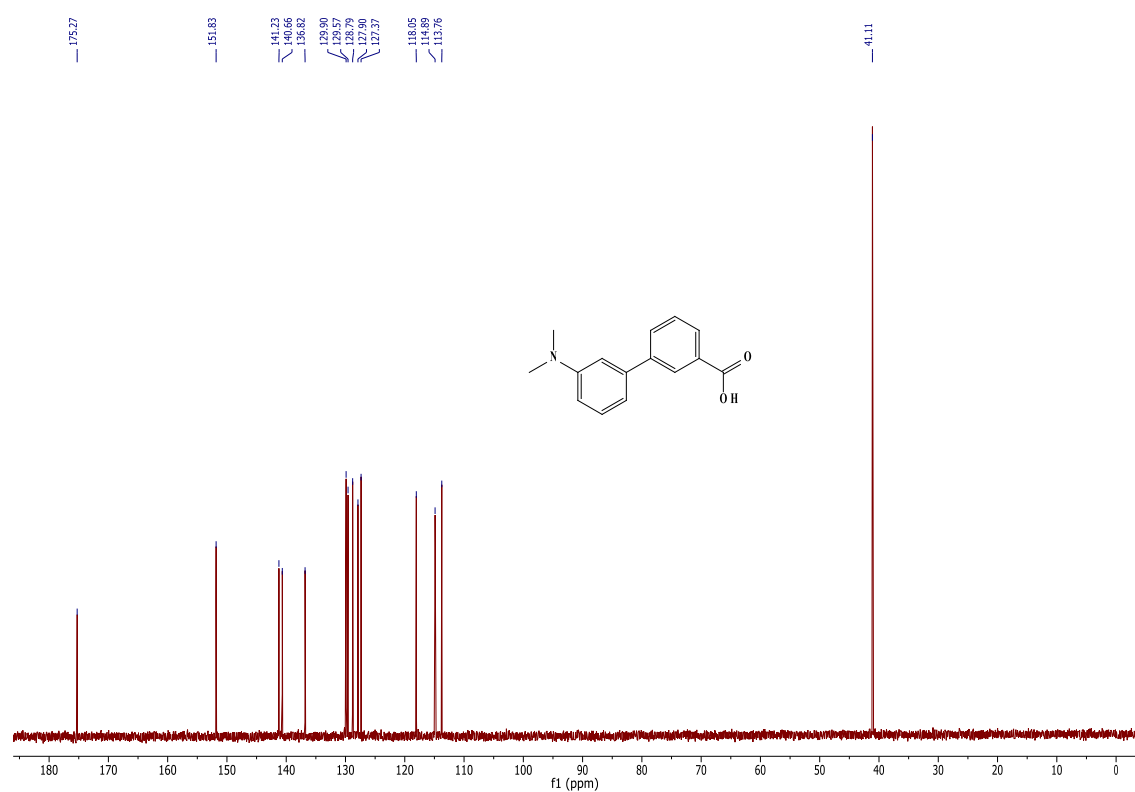


2.22 4'-dimethylaminobiphenyl-3-carboxylic acid, **14**:

2.22.1 ^1H NMR of **14**

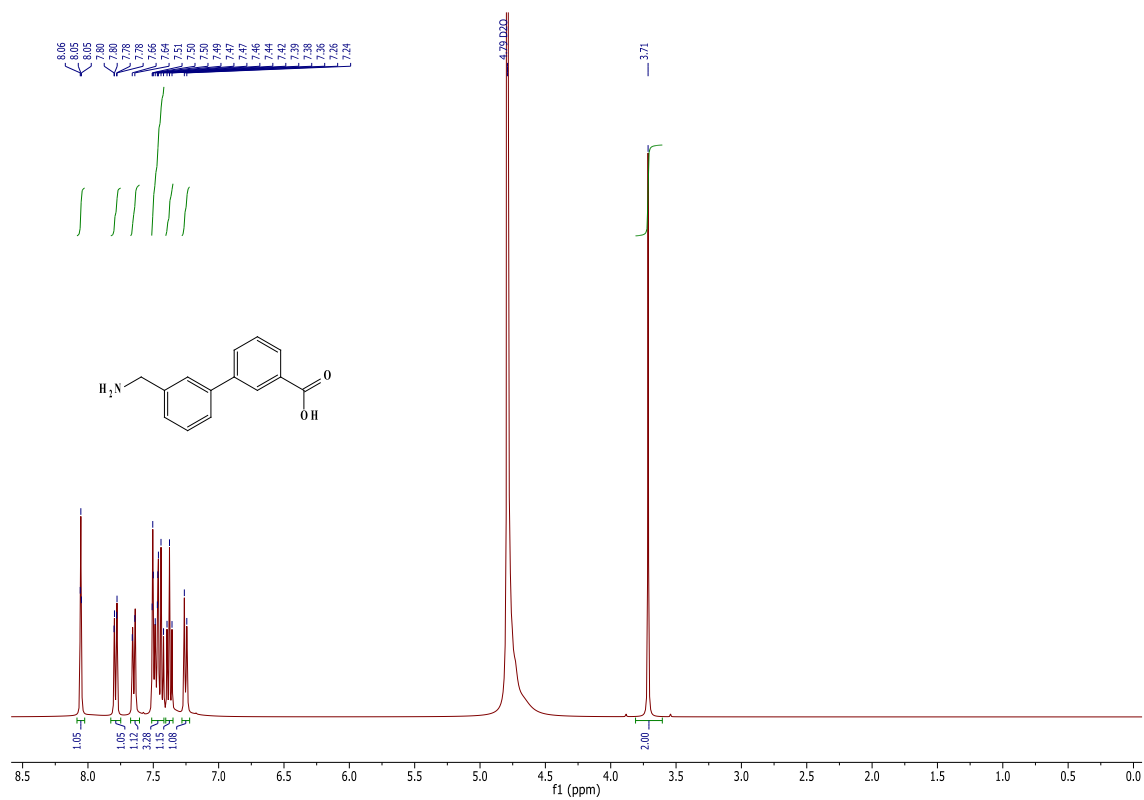


2.22.2 ^{13}C NMR of **14**

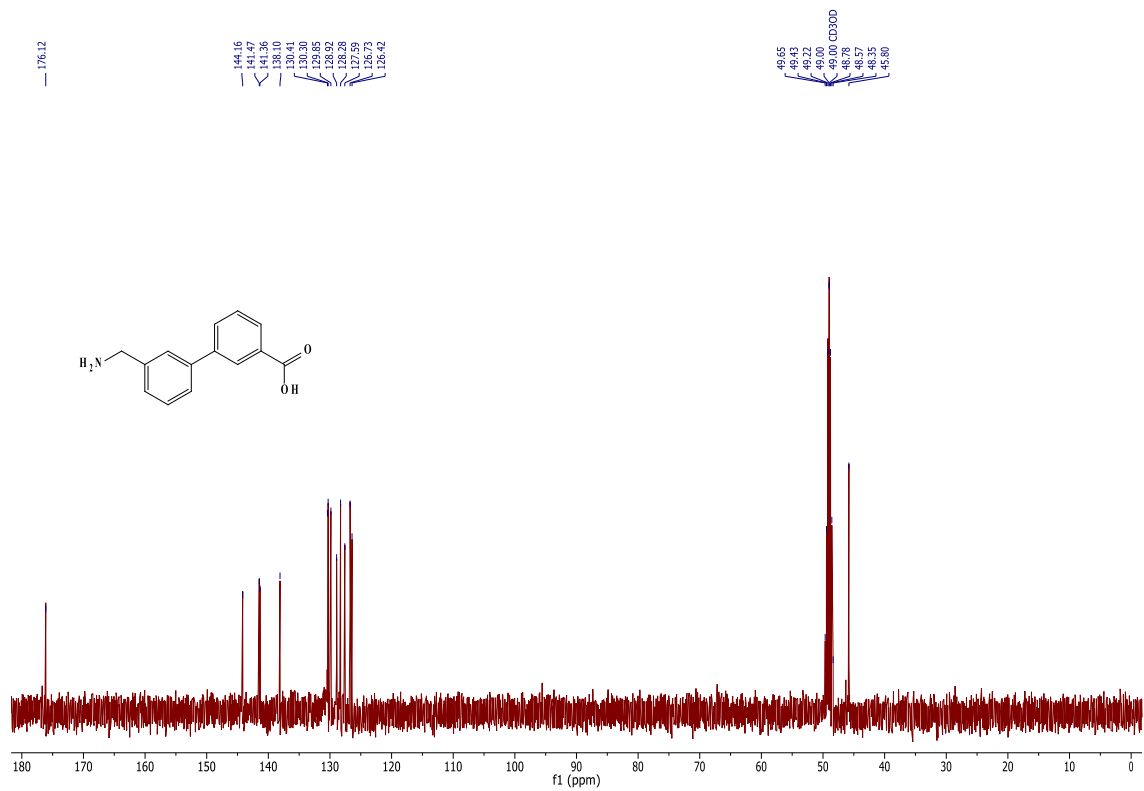


2.23 3'-aminomethylbiphenyl-3-carboxylic acid, **15a**:

2.23.1 ^1H NMR of **15a**

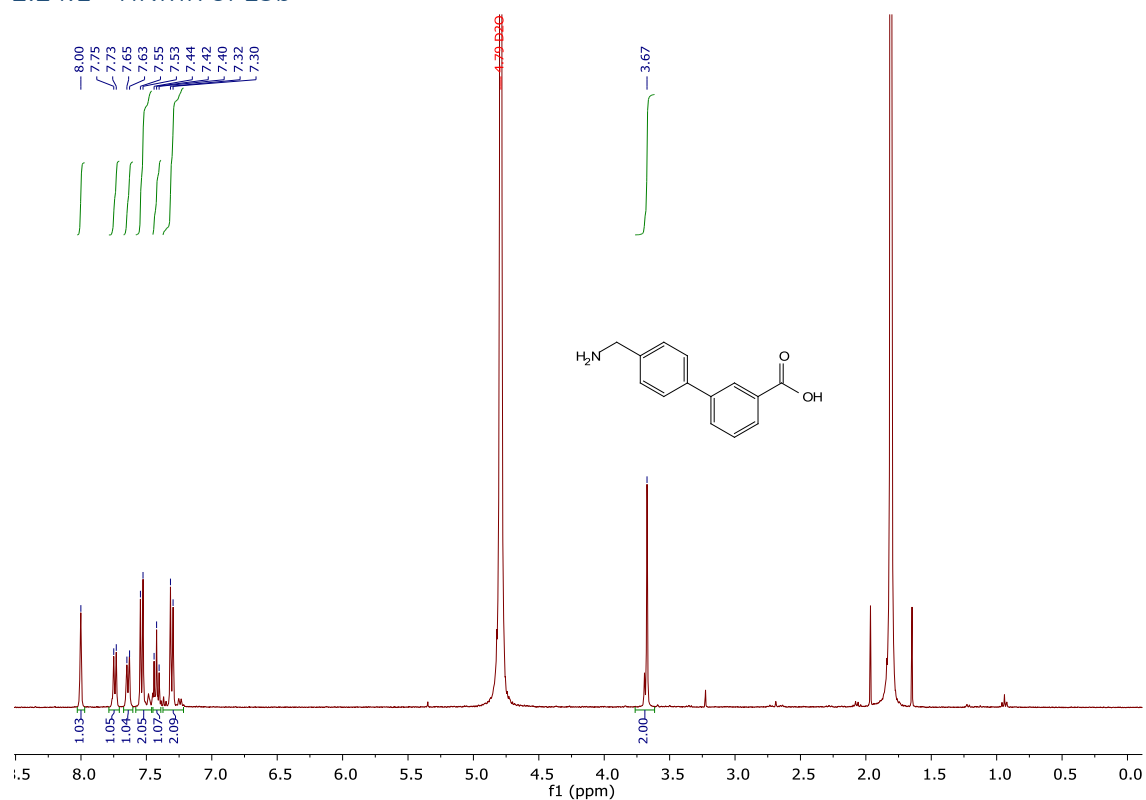


2.23.2 ^{13}C NMR of **15a**

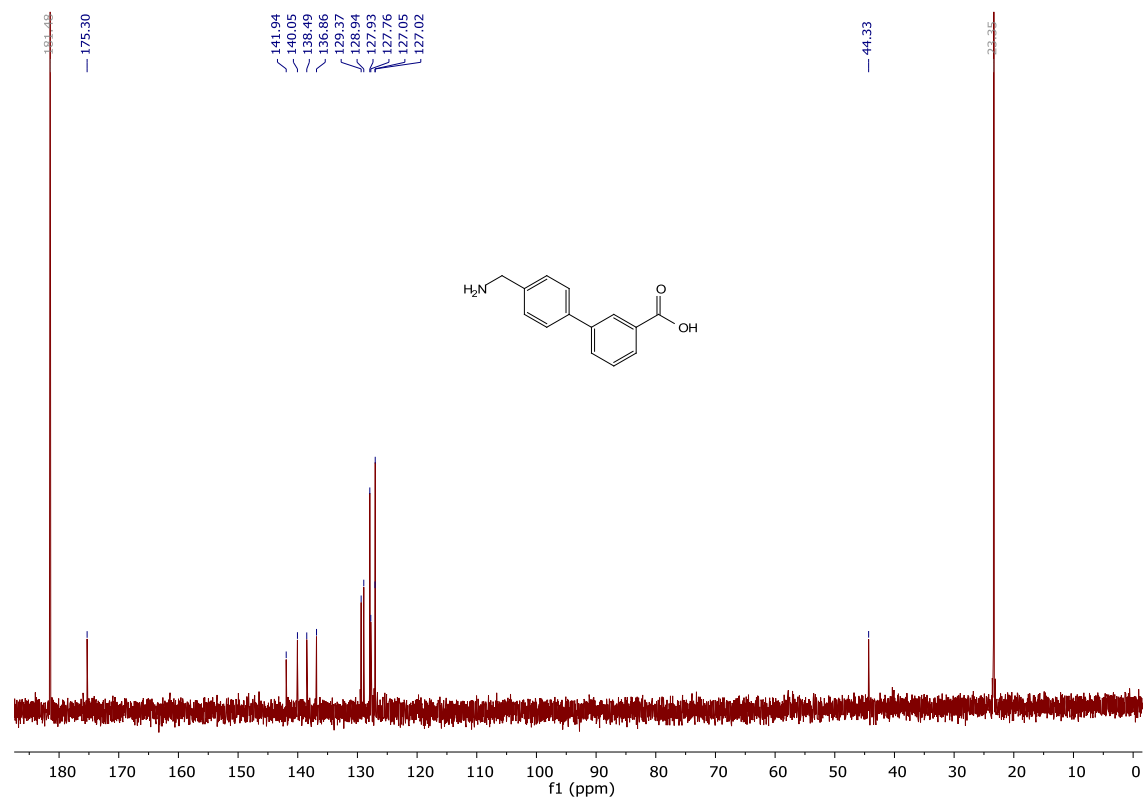


2.24 4'-(aminomethyl)biphenyl-3-carboxylic acid, **15b**:

2.24.1 ^1H NMR of **15b**

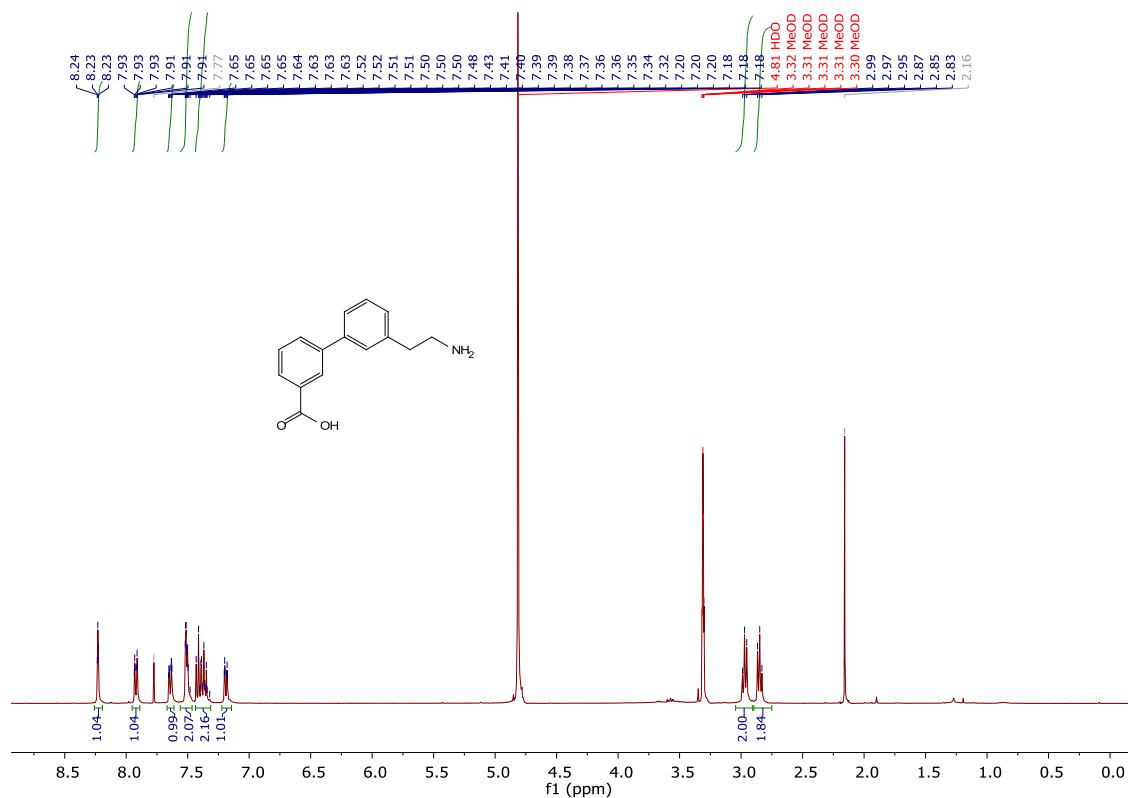


2.24.2 ^{13}C NMR of **15b**

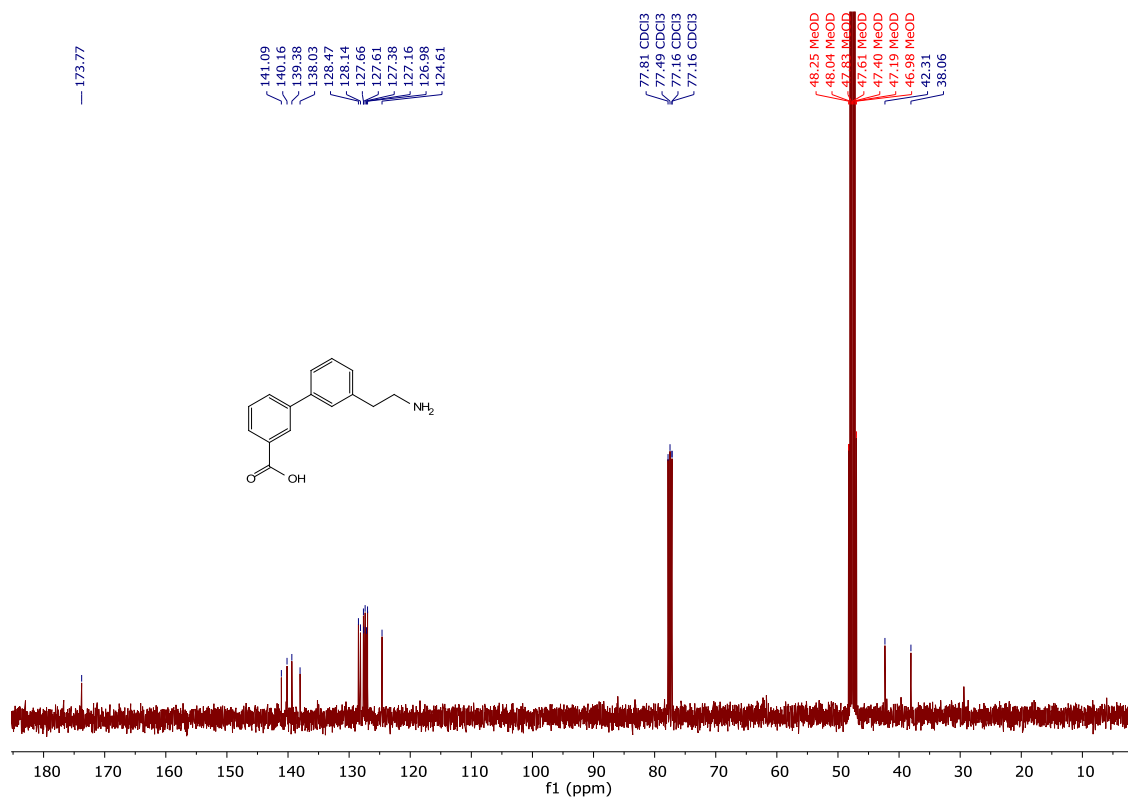


2.25 3'-(2-aminoethyl)biphenyl-3-carboxylic acid, **16a**:

2.25.1 ¹H NMR of **16a**

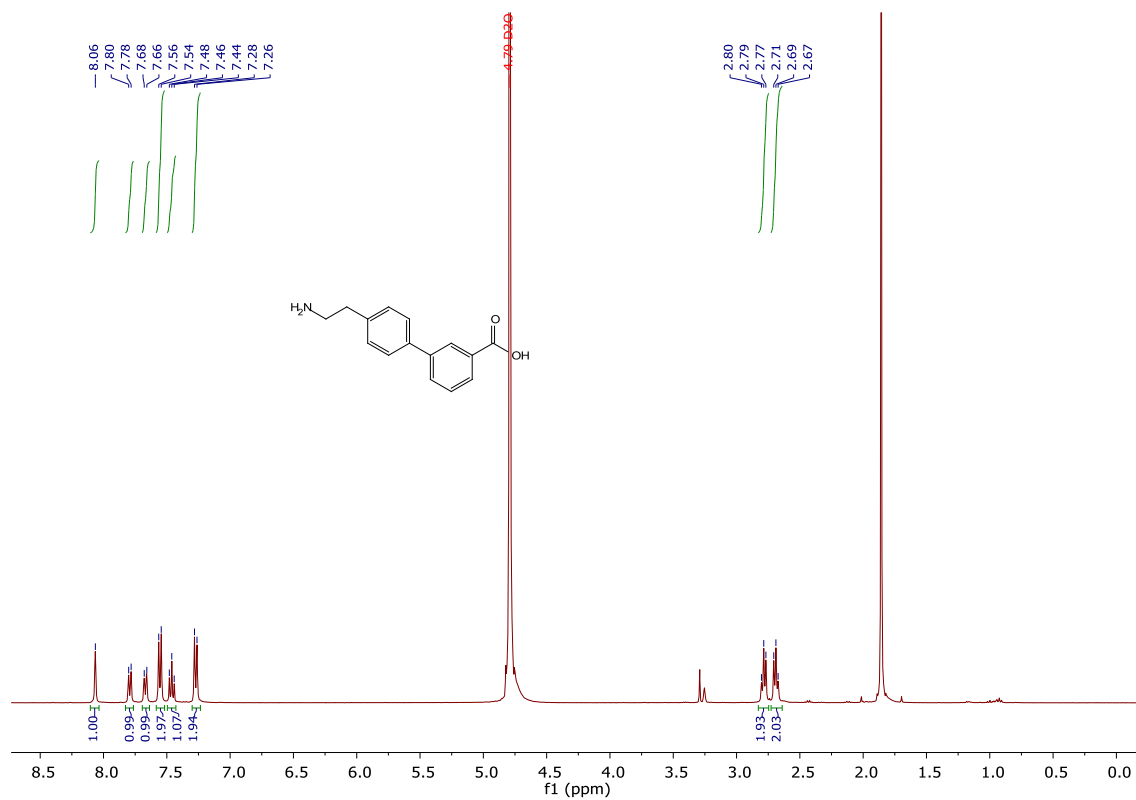


2.25.2 ¹³C NMR of **16a**

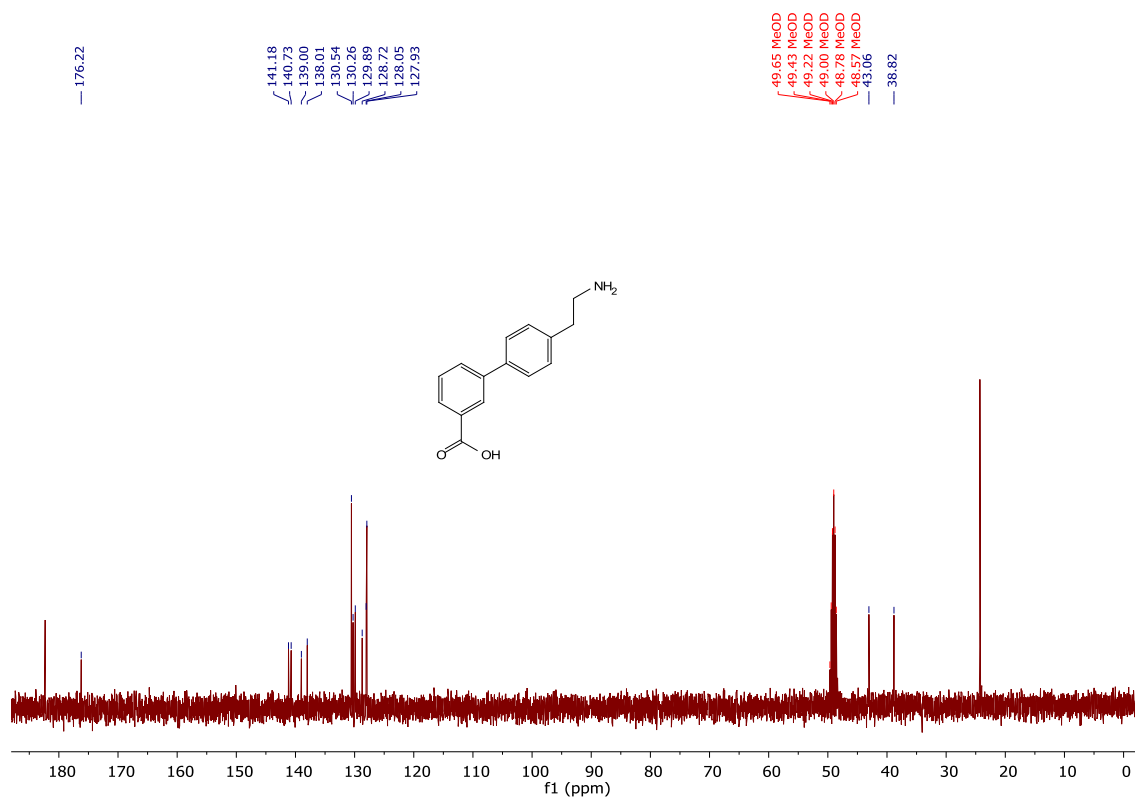


2.26 4'-(2-aminoethyl)biphenyl-3-carboxylic acid, **16b**:

2.26.1 ¹H NMR of **16b**

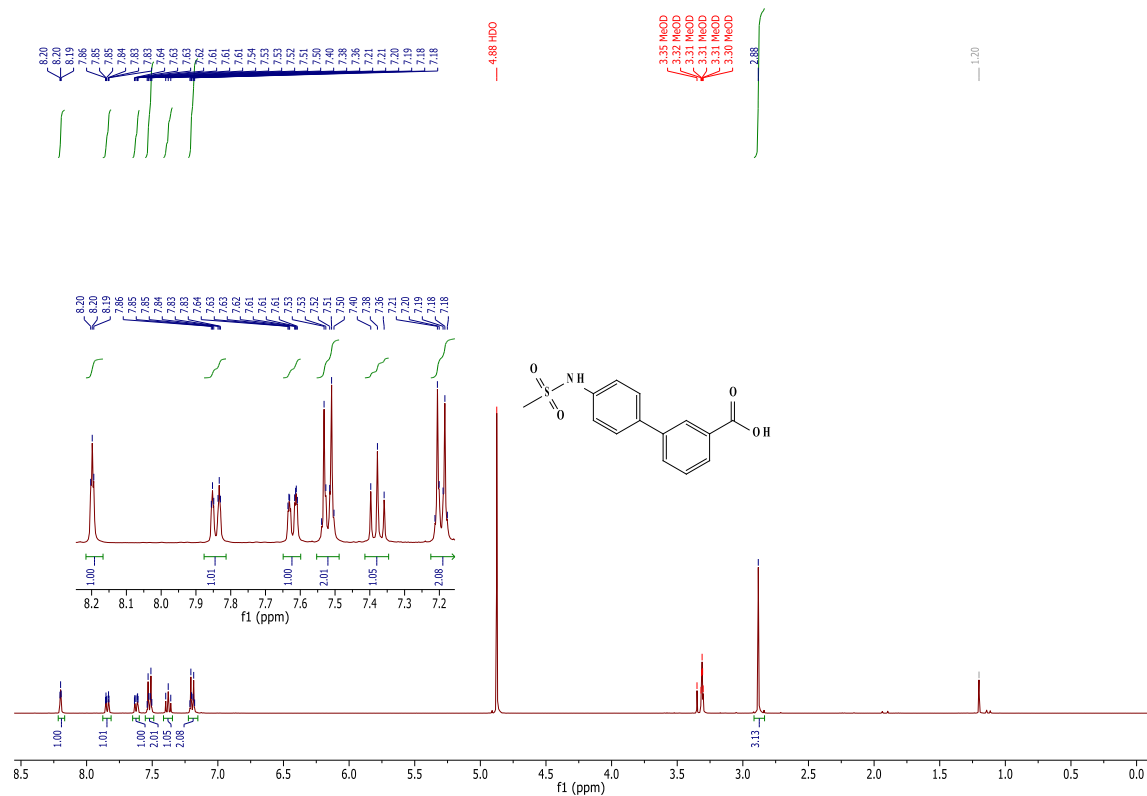


2.26.2 ¹³C NMR of **16b**

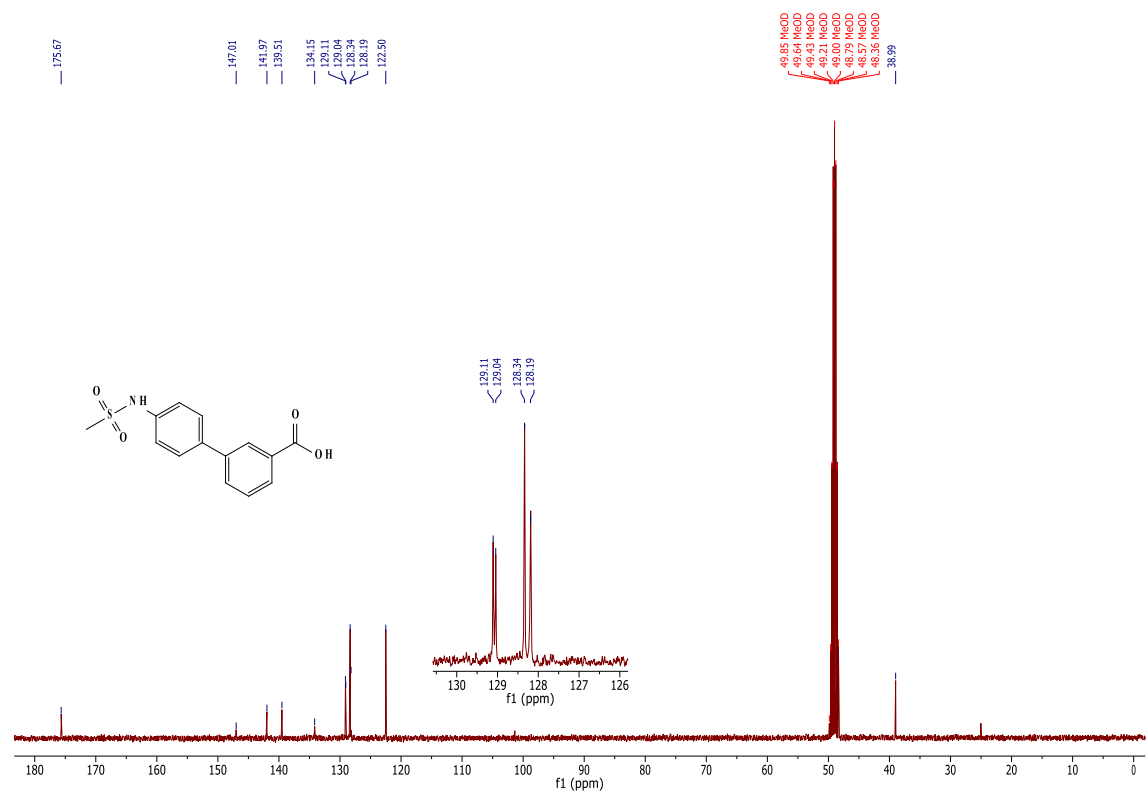


2.27 4'-(methylsulfonylamino)biphenyl-3-carboxylic acid, 17:

2.27.1 ¹H NMR of 17

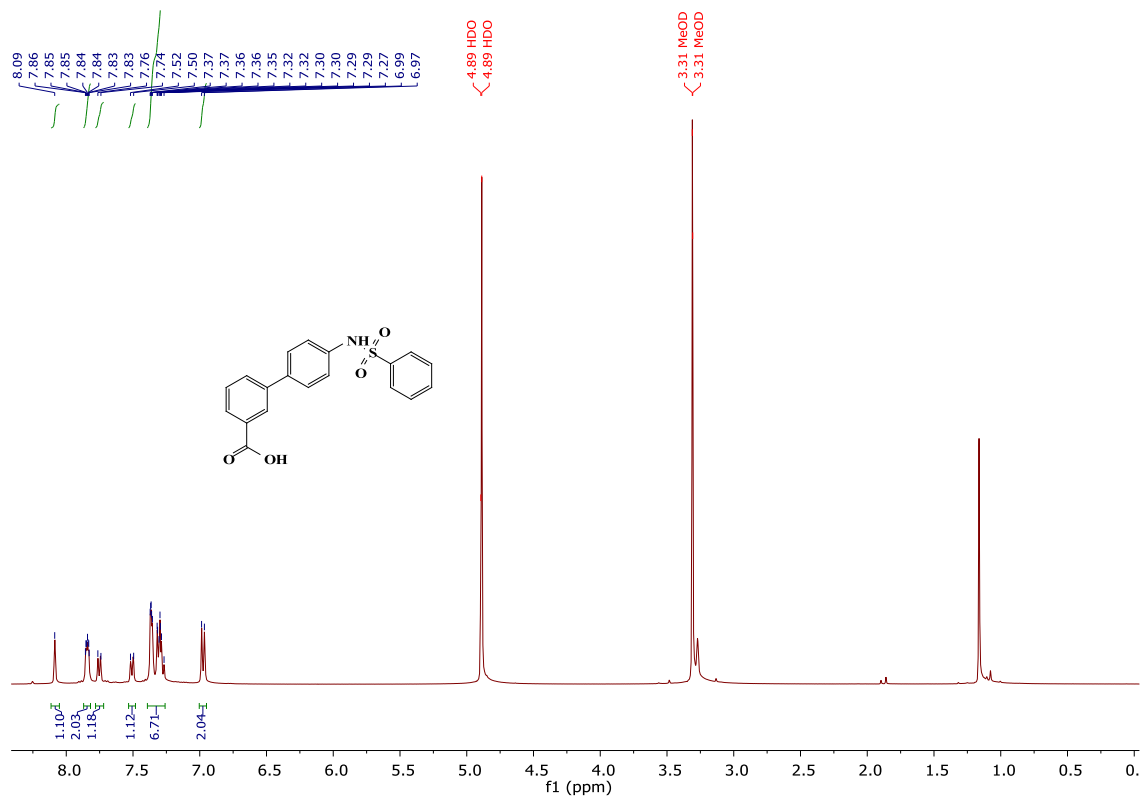


2.27.2 ¹³C NMR of 17

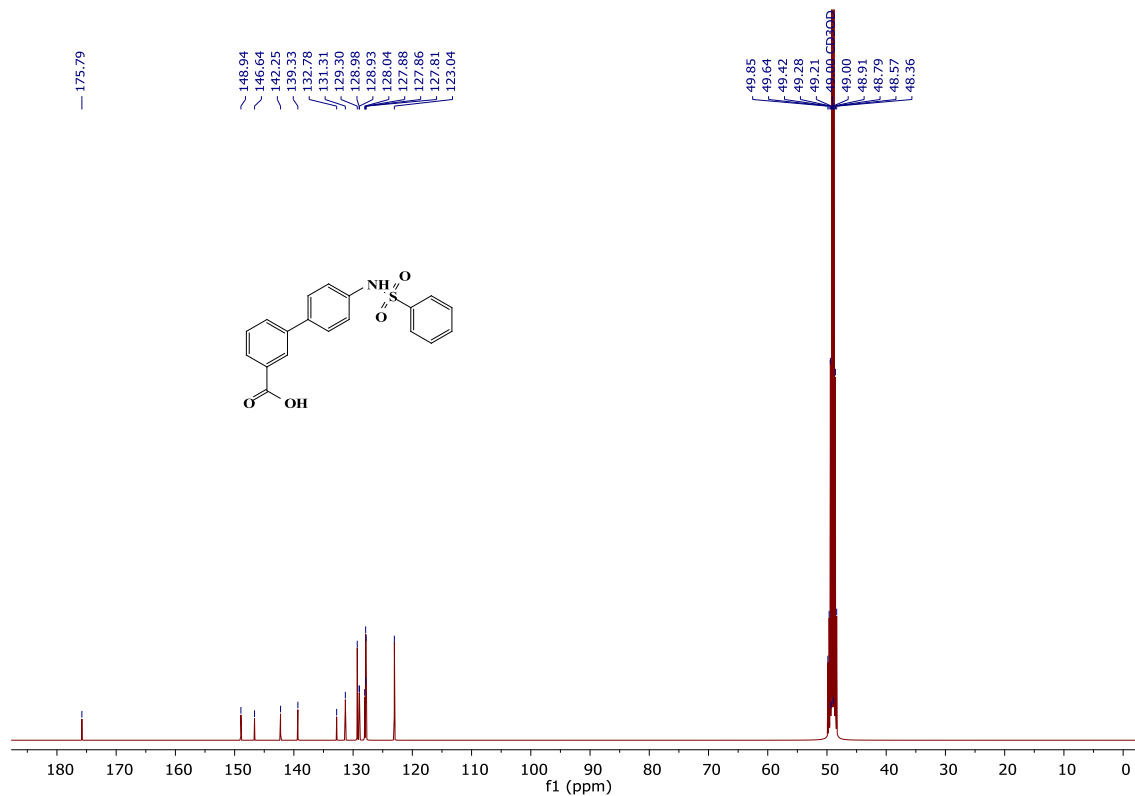


2.28 4'-(phenylsulfonamido)biphenyl-3-carboxylic acid, **18**:

2.28.1 ^1H NMR of **18**

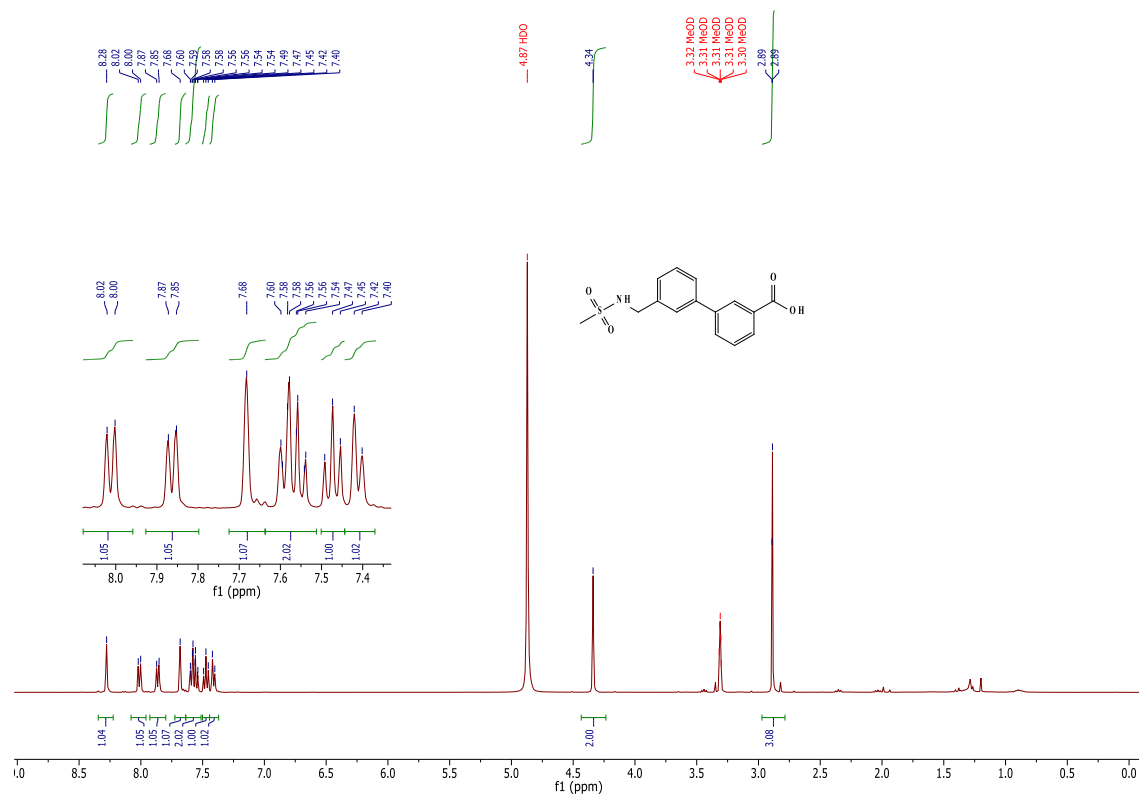


2.28.2 ^{13}C NMR of **18**

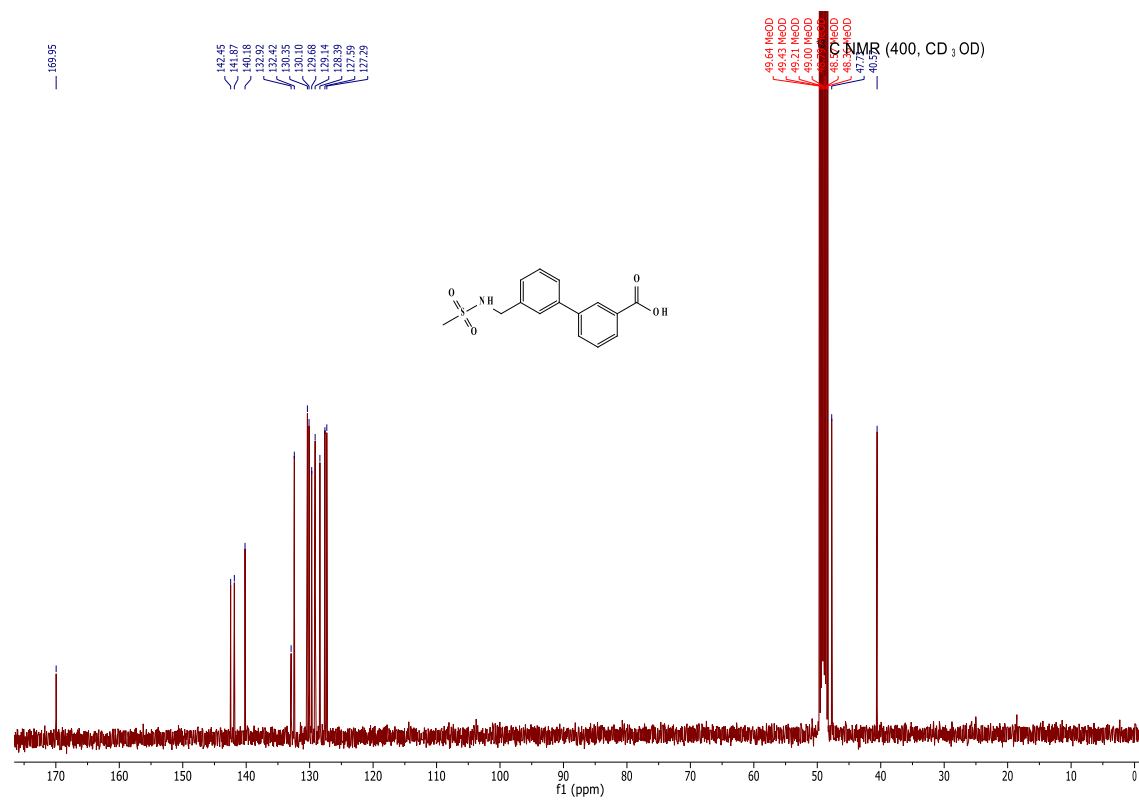


2.29 3'-(methylsulfonamidomethyl)biphenyl-3-carboxylic acid, **19a**:

2.29.1 ¹H NMR of **19a**

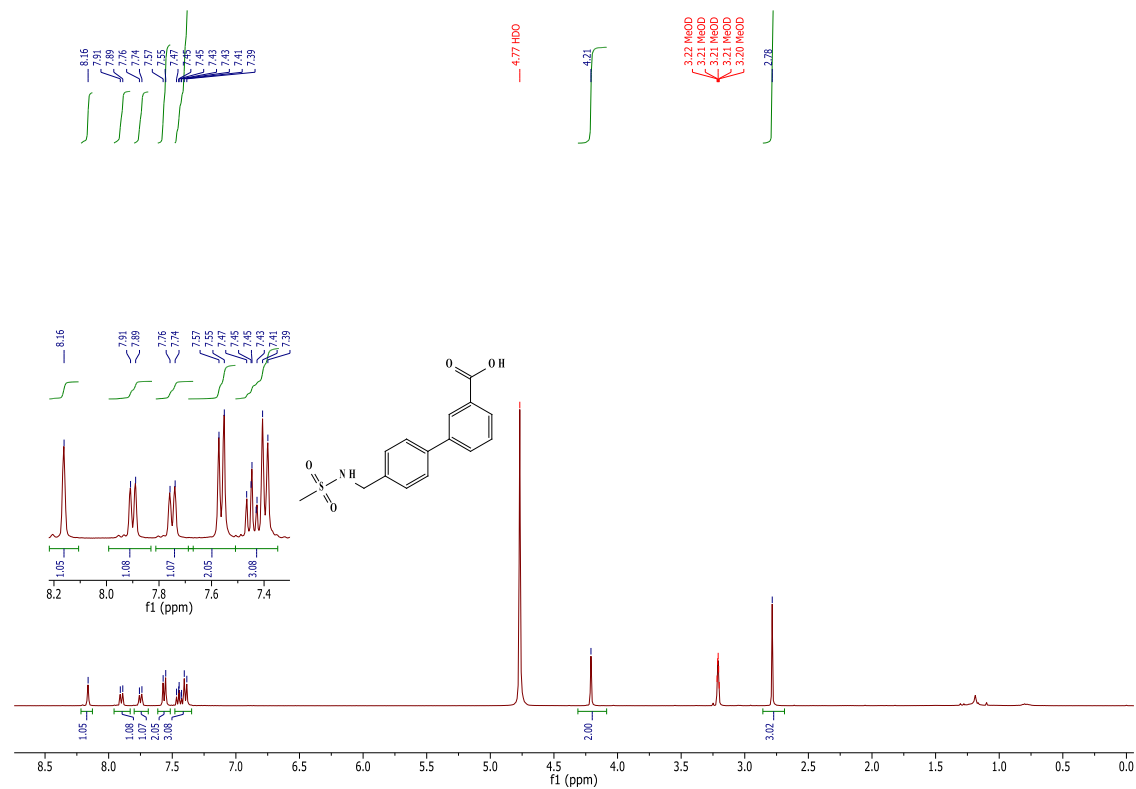


2.29.2 ¹³C NMR of **19a**

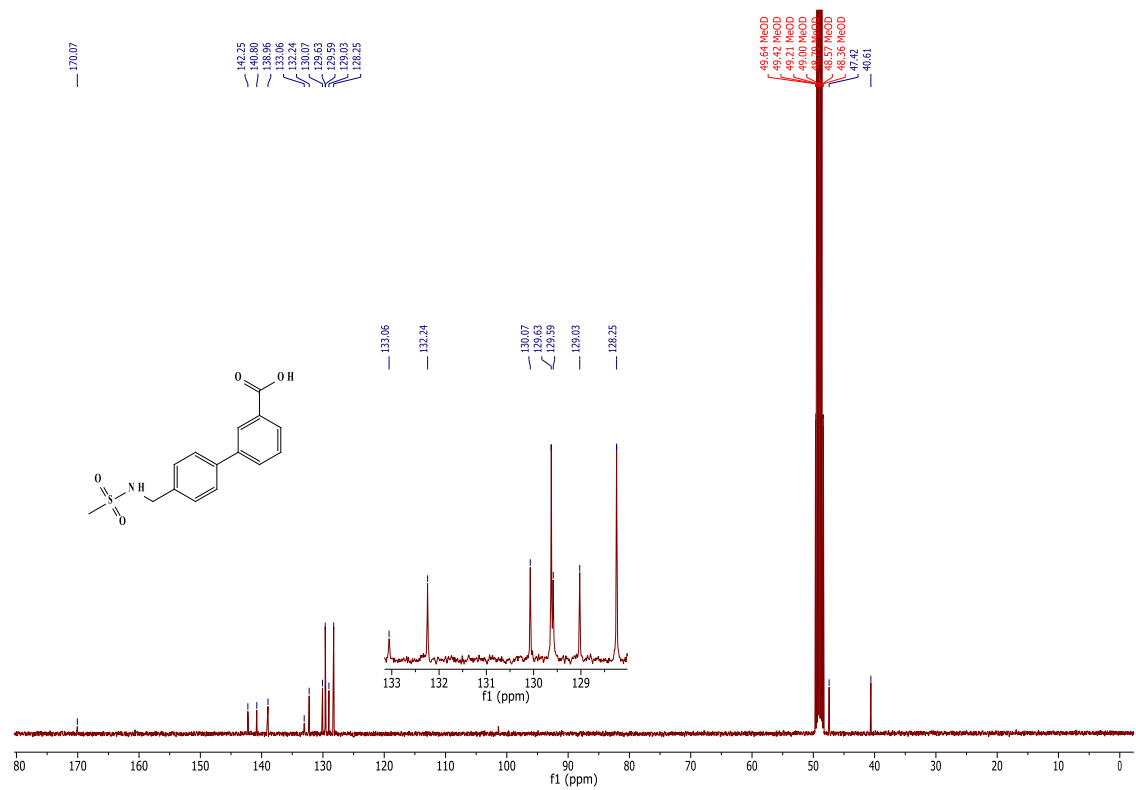


2.30 4'-(methylsulfonamidomethyl)biphenyl-3-carboxylic acid, **19b**:

2.30.1 ^1H NMR of **19b**

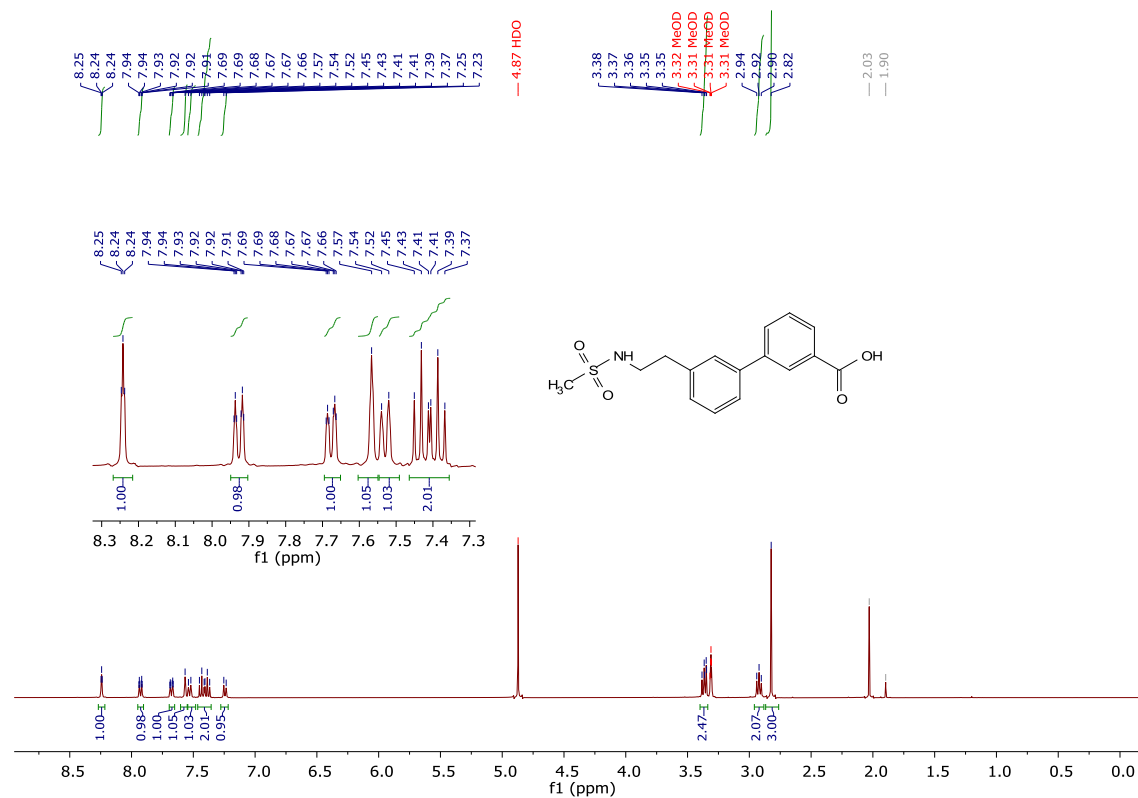


2.30.2 ^{13}C NMR of **19b**

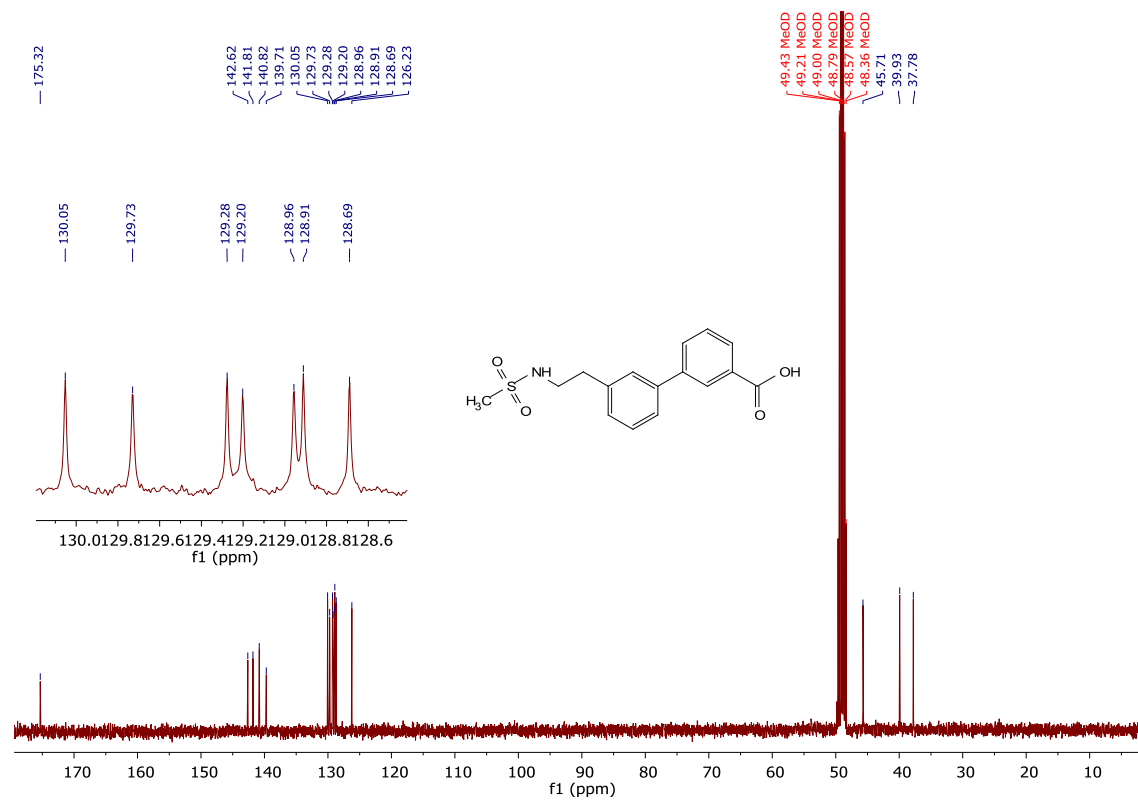


2.31 3'-(2-methylsulfonamidoethyl)biphenyl-3-carboxylic acid, 20:

2.31.1 ¹H NMR of 20

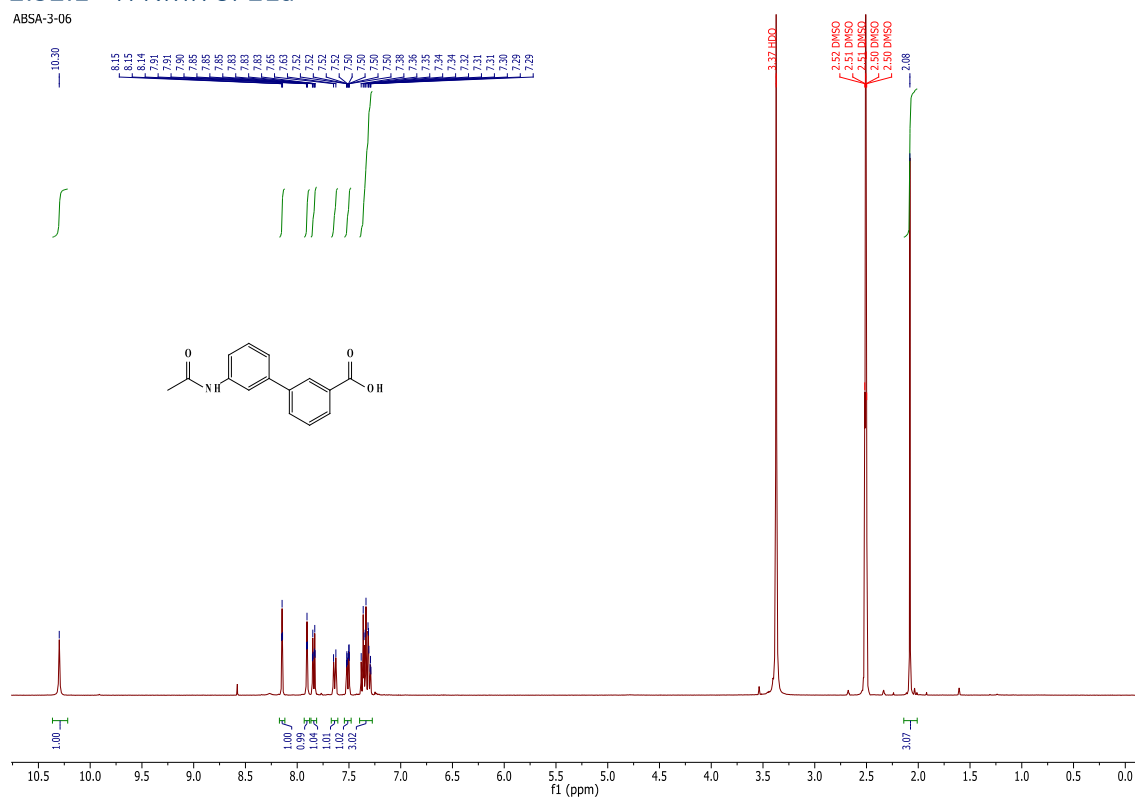


2.31.2 ¹³C NMR of 20

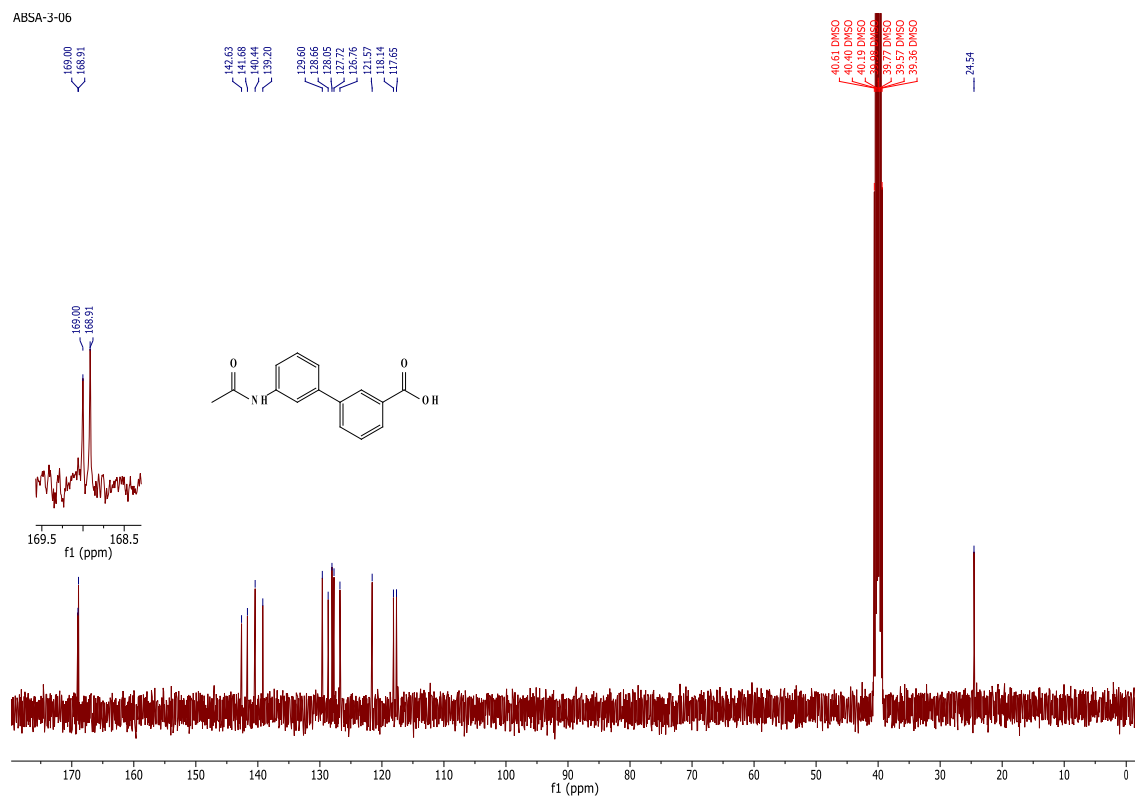


2.32 3'-acetamidobiphenyl-3-carboxylic acid, **21a**:

2.32.1 ^1H NMR of **21a**



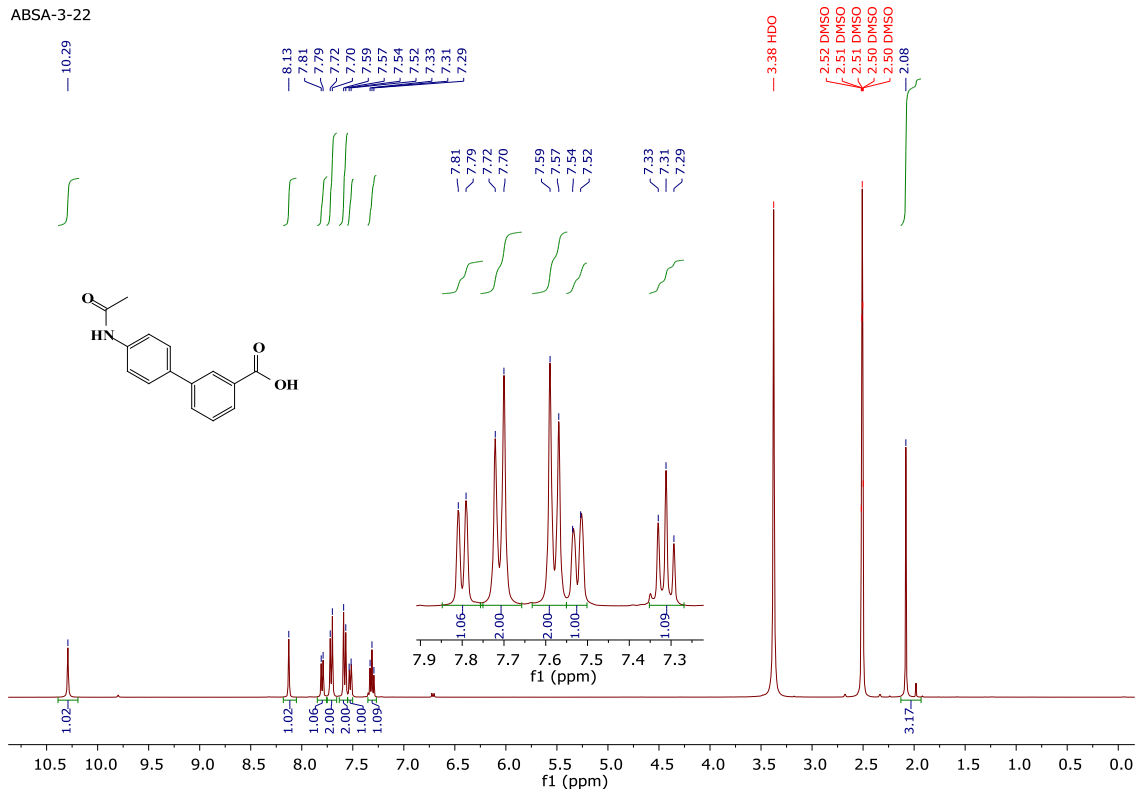
2.32.2 ^{13}C NMR of **21a**



2.33 4'acetamidobiphenyl-3-carboxylic acid, 21b:

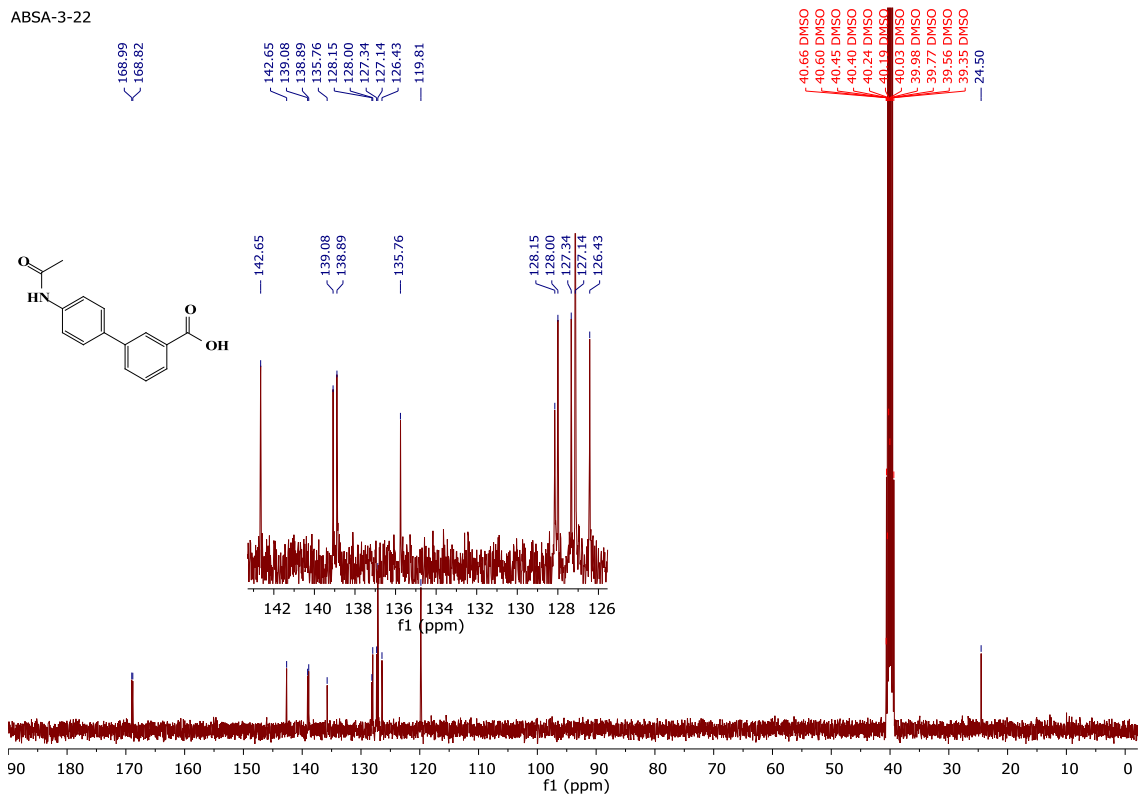
2.33.1 ¹H NMR of 21b

ABSA-3-22



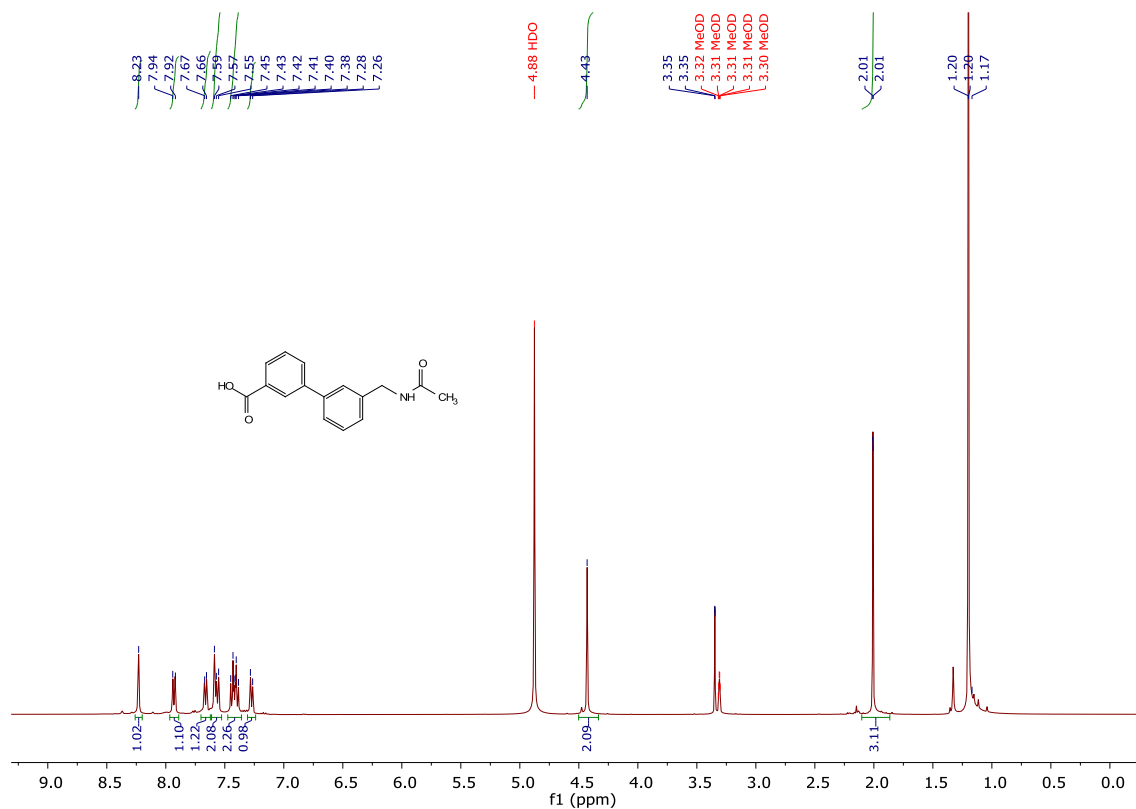
2.33.2 ¹³C NMR of 21b

ABSA-3-22

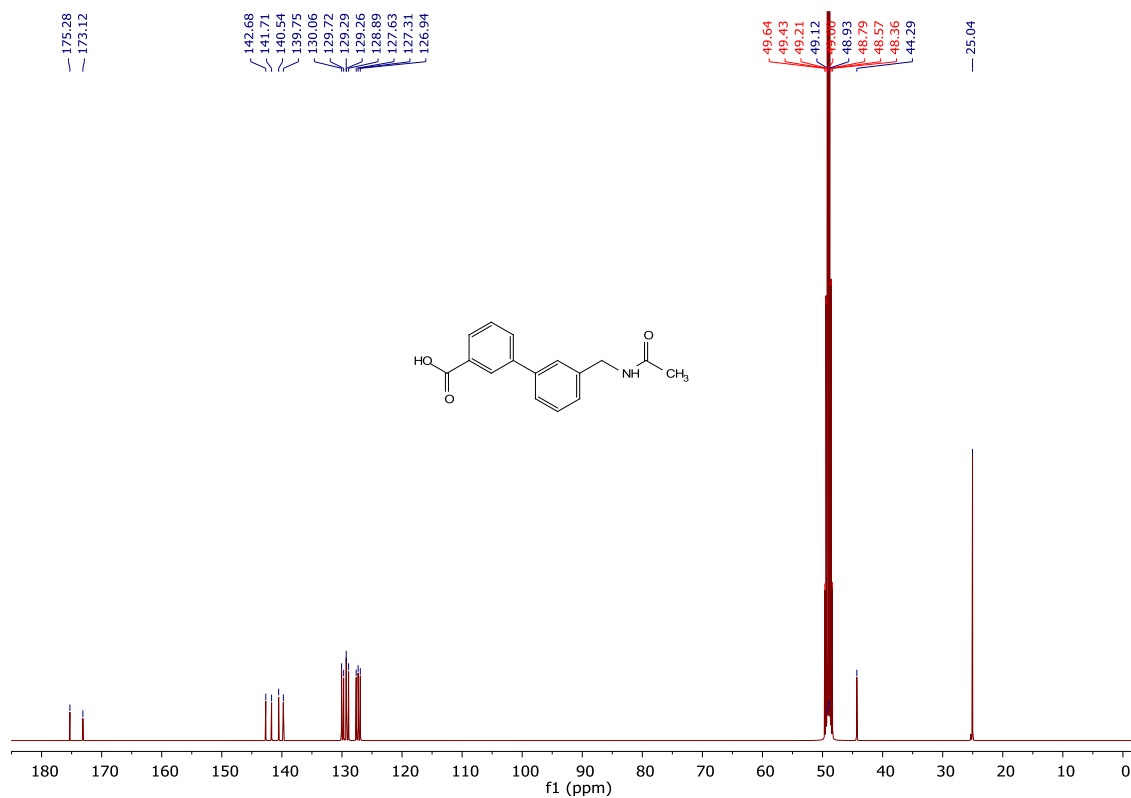


2.34 3'-(acetamidomethyl)biphenyl]-3-carboxylic acid, **22**:

2.34.1 ^1H NMR of **22**

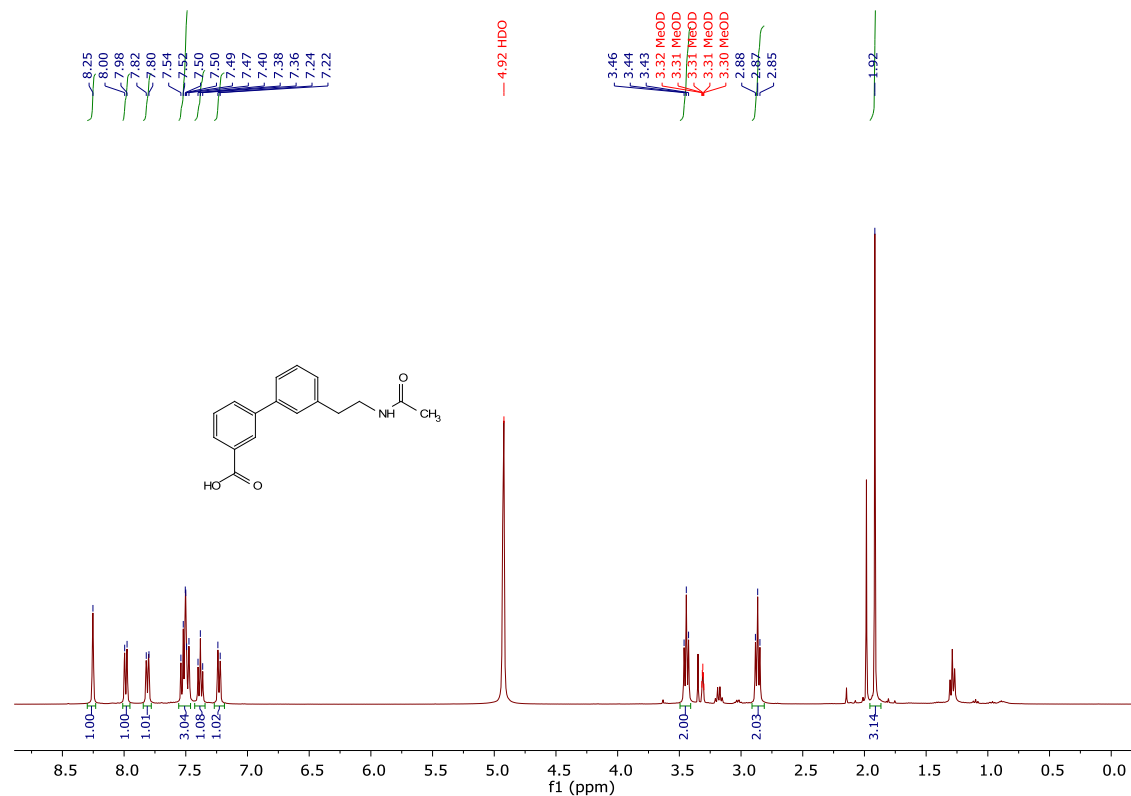


2.34.2 ^{13}C NMR of **22**

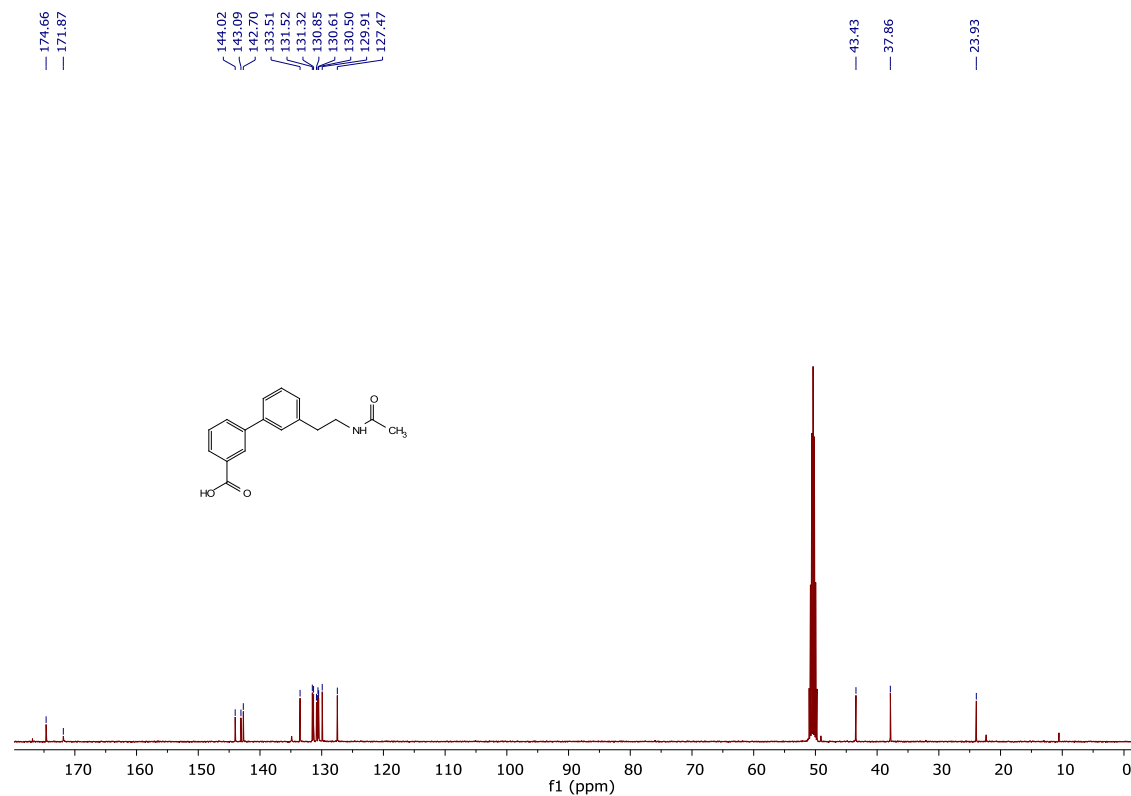


2.35 3'-(2-acetamidoethyl)biphenyl]-3-carboxylic acid, **23a**:

2.35.1 ^1H NMR of **23a**

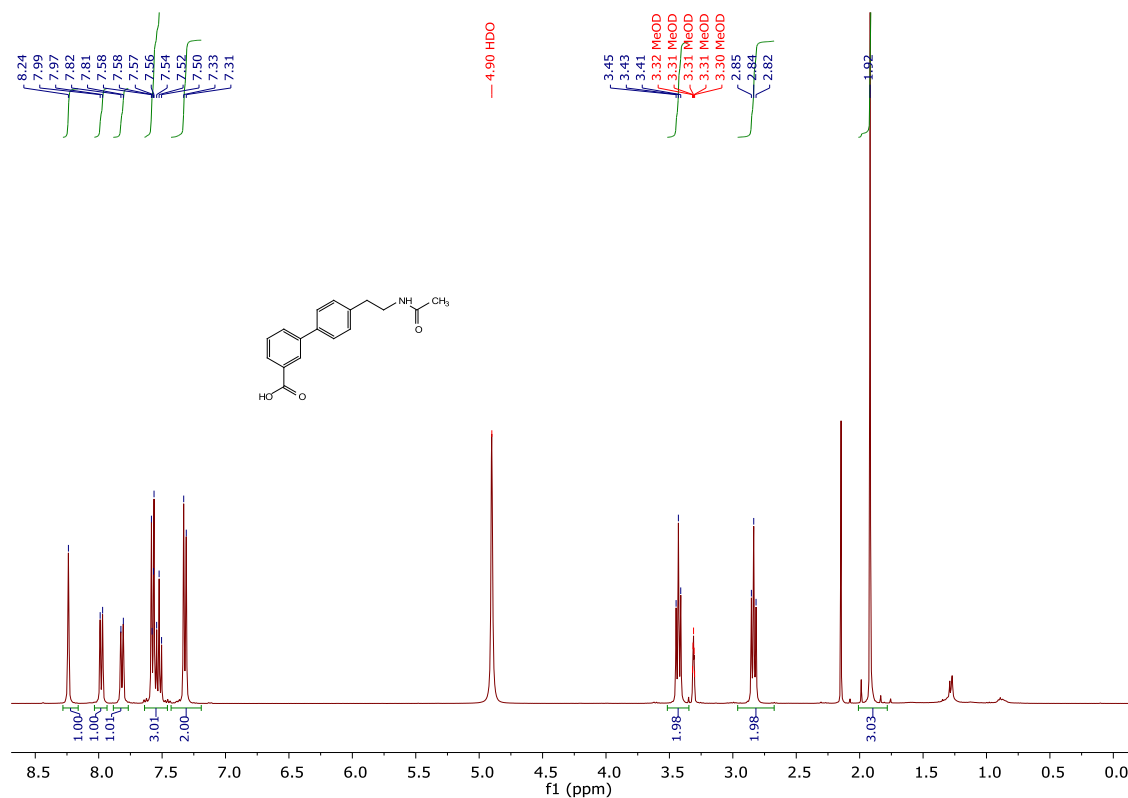


2.35.2 ^{13}C NMR of **23a**

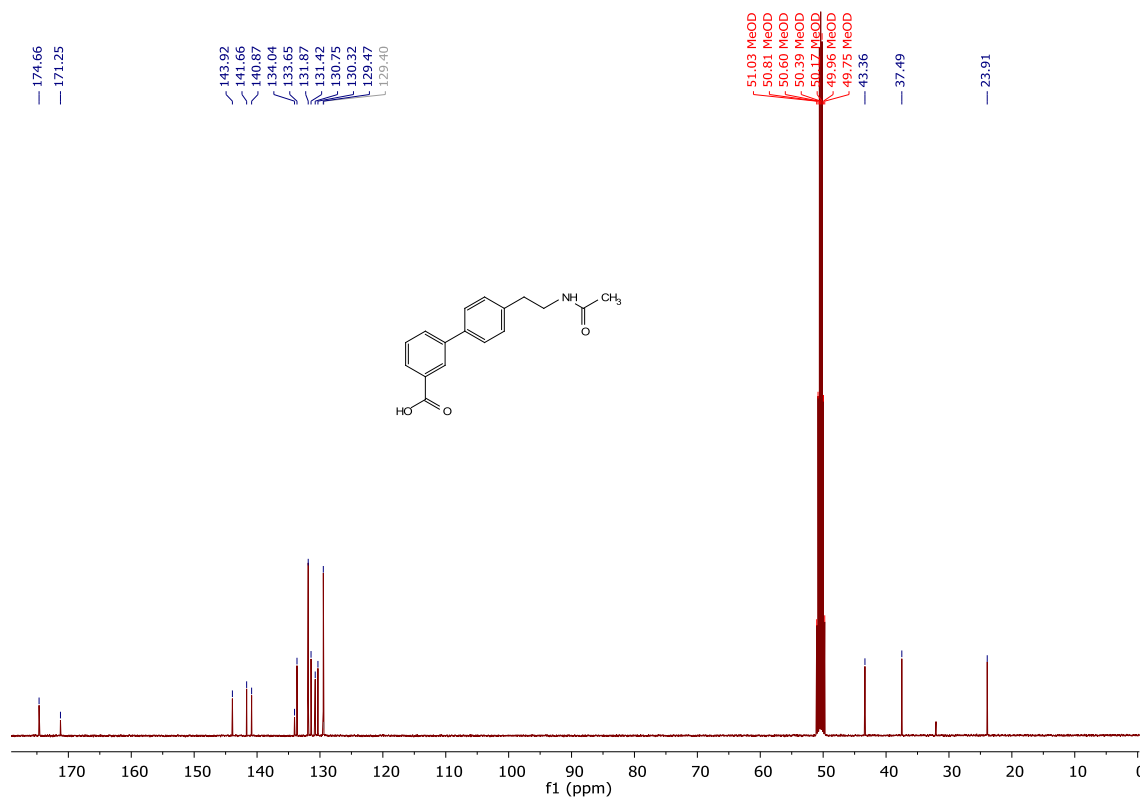


2.36 4'-(2-acetamidoethyl)biphenyl]-3-carboxylic acid, 23b:

2.36.1 ^1H NMR of 23b

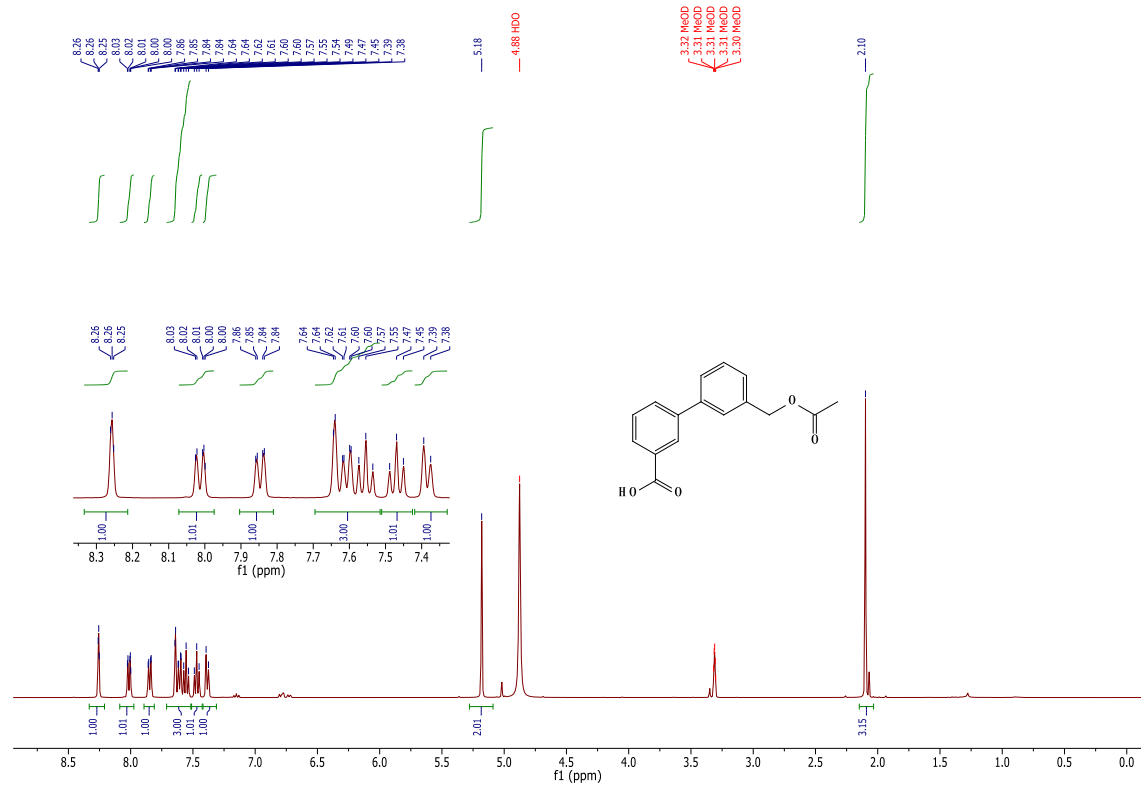


2.36.2 ^{13}C NMR of 23b

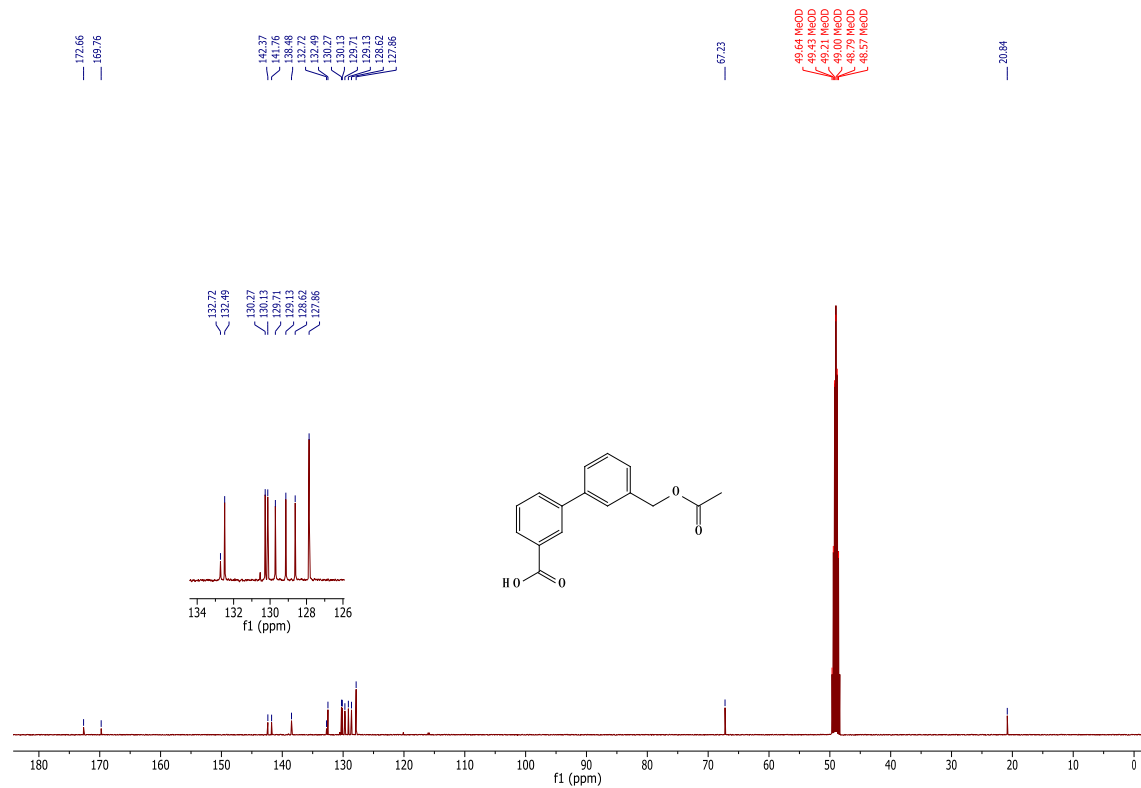


2.37 3'-acetoxymethylbiphenyl-3-carboxylic acid, **24**:

2.37.1 ^1H NMR of **24**



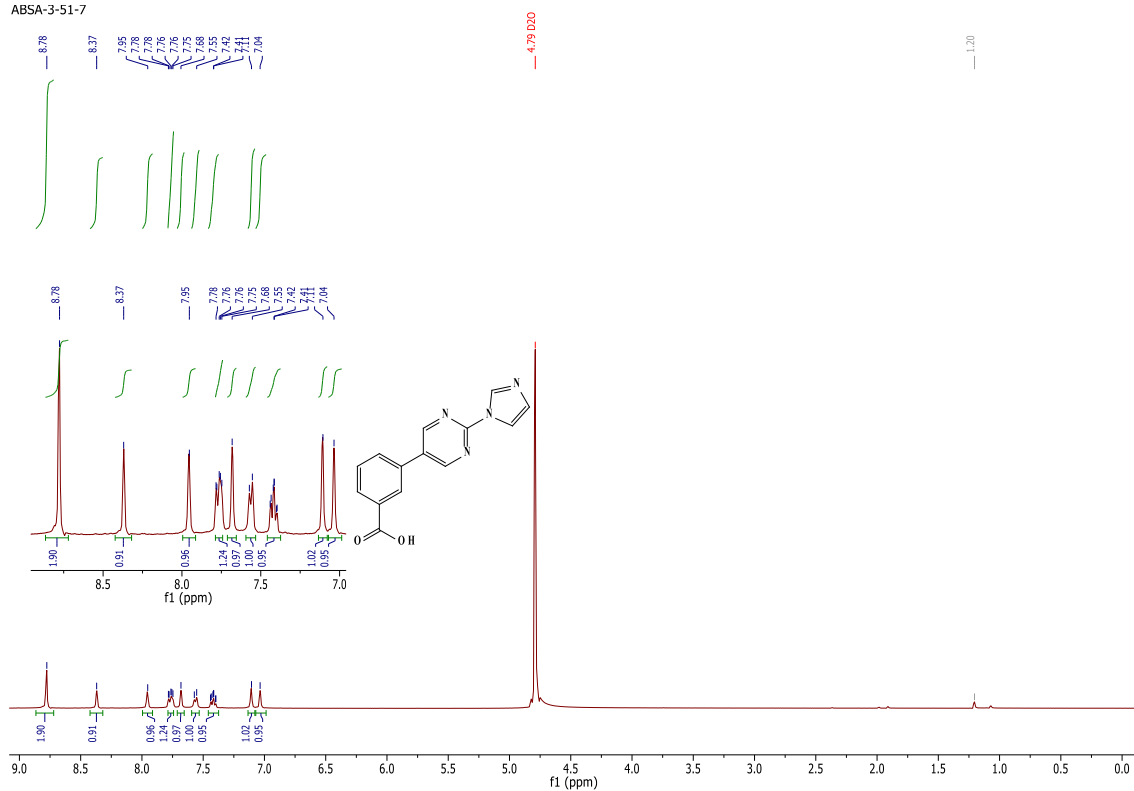
2.37.2 ^{13}C NMR of **24**



2.38 4'-(1H-imidazol-1-yl)biphenyl-3-carboxylic acid, 25:

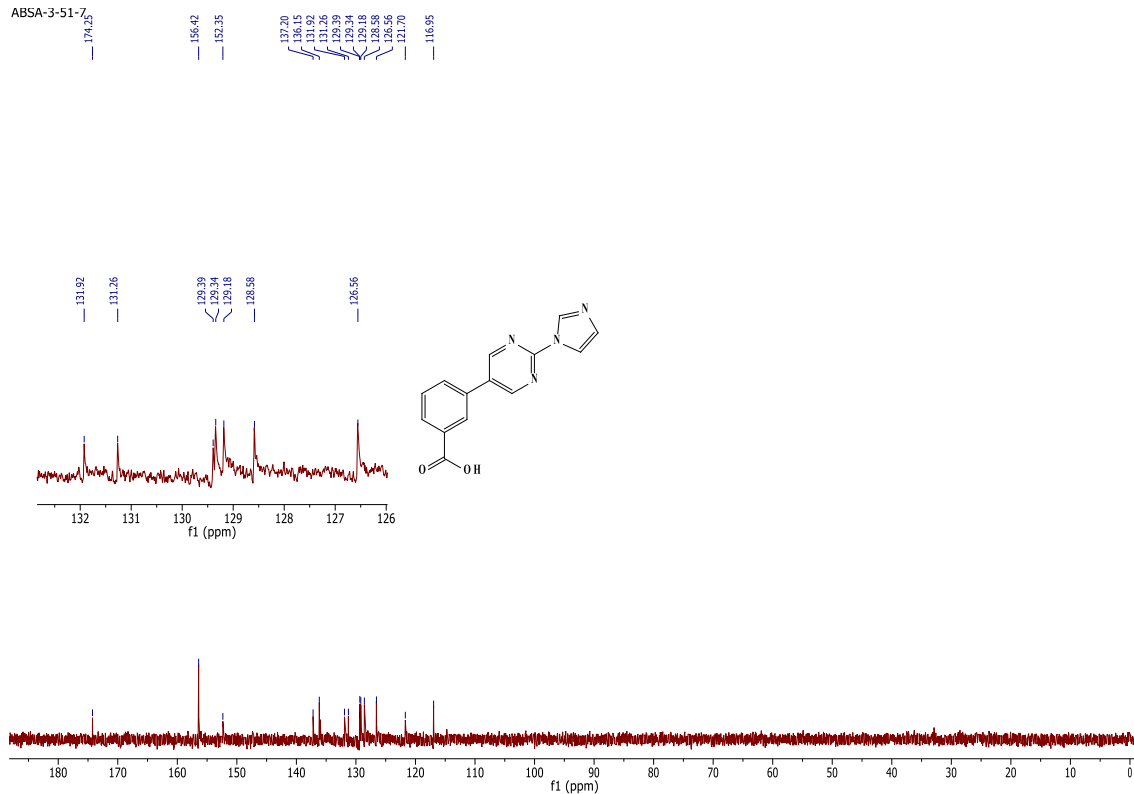
2.38.1 ¹H NMR of 25

ABSA-3-51-7



2.38.2 ¹³C NMR of 25

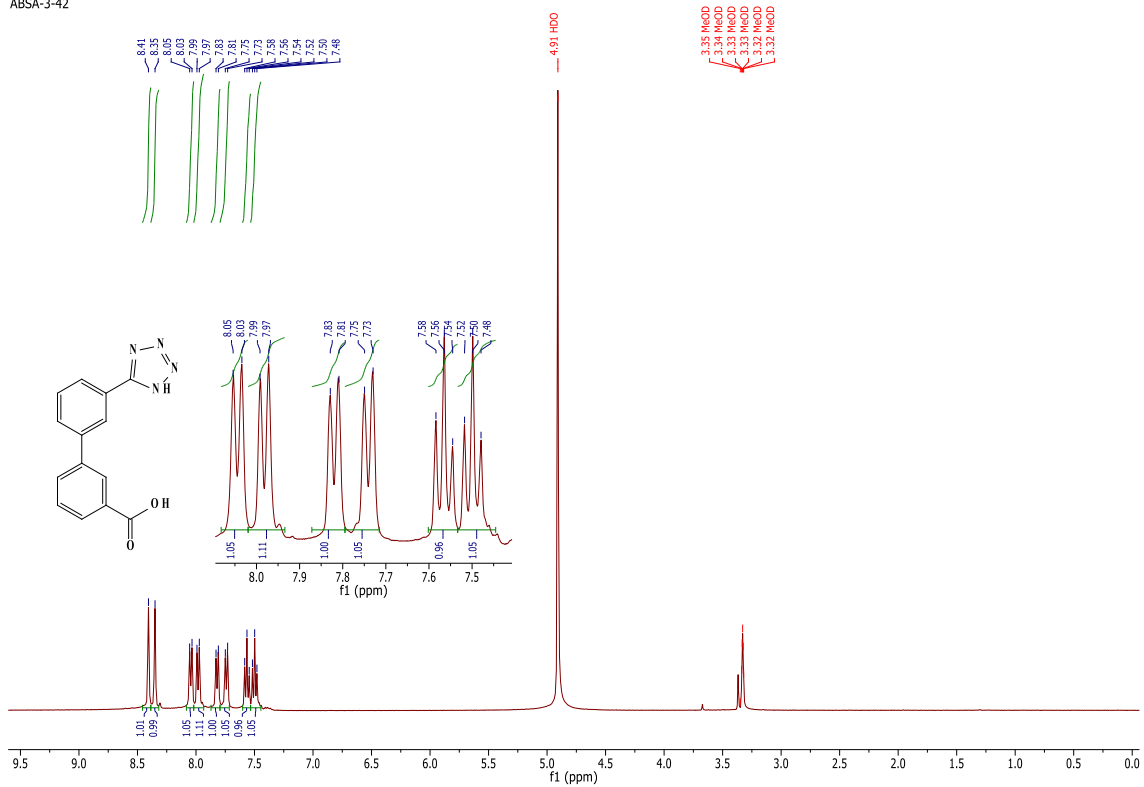
ABSA-3-51-7



2.39 3'-(1H-tetrazol-5-yl)biphenyl-3-carboxylic acid, 26a:

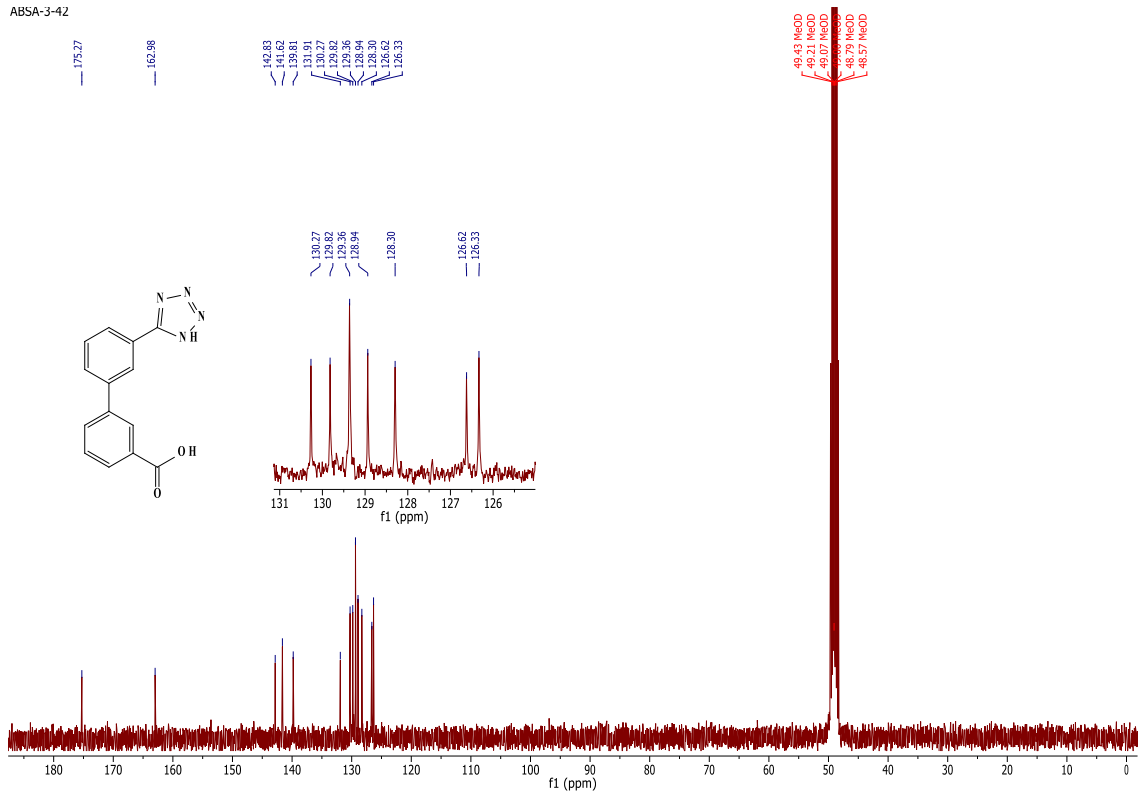
2.39.1 ¹H NMR of 26a

ABSA-3-42



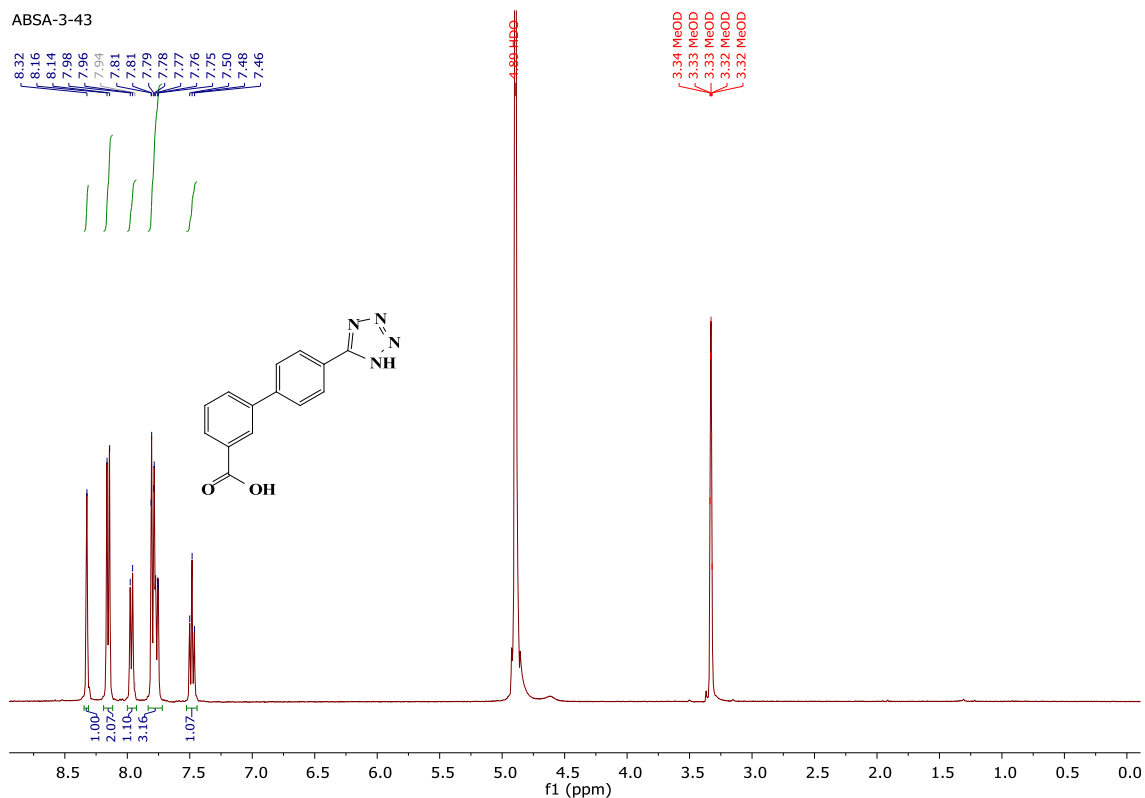
2.39.2 ¹³C NMR of 26a

ABSA-3-42

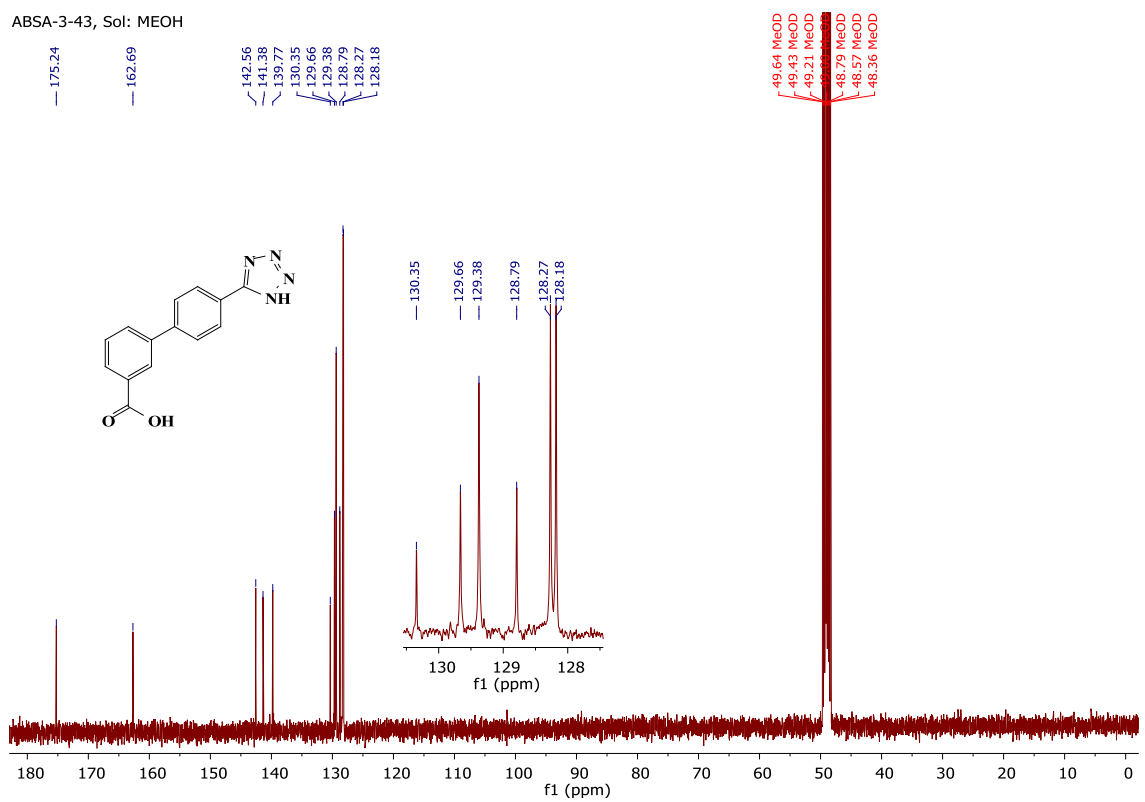


2.40 4'-(1H-tetrazol-5-yl)biphenyl-3-carboxylic acid, **26b**:

2.40.1 ^1H NMR of **26b**

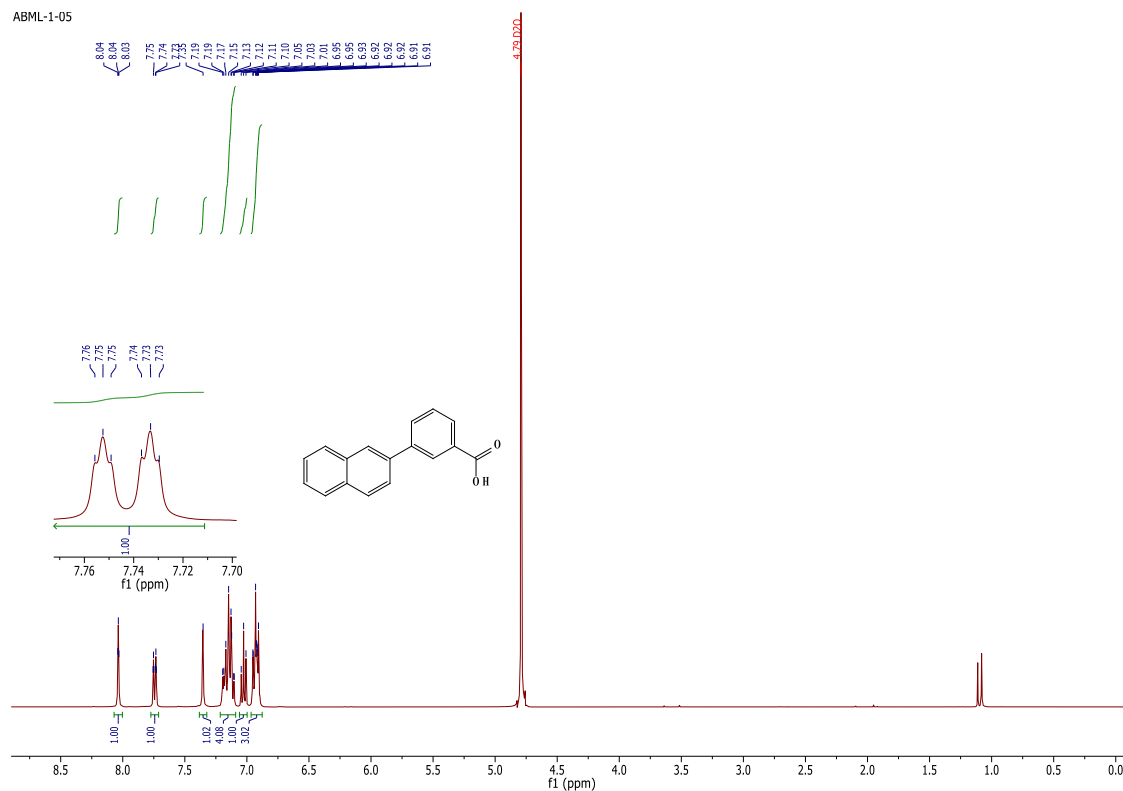


2.40.2 ^{13}C NMR of **26b**

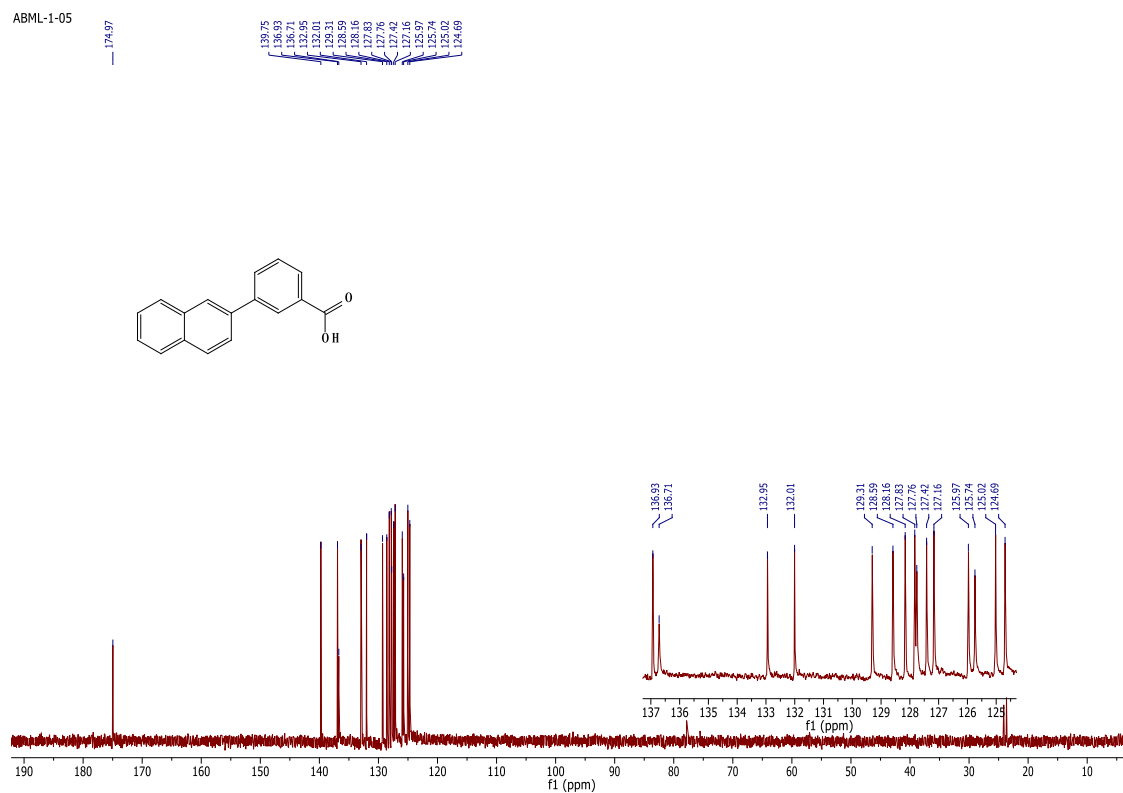


2.41 3-(naphthalen-2-yl)benzoic acid, 27:

2.41.1 ^1H NMR of 27

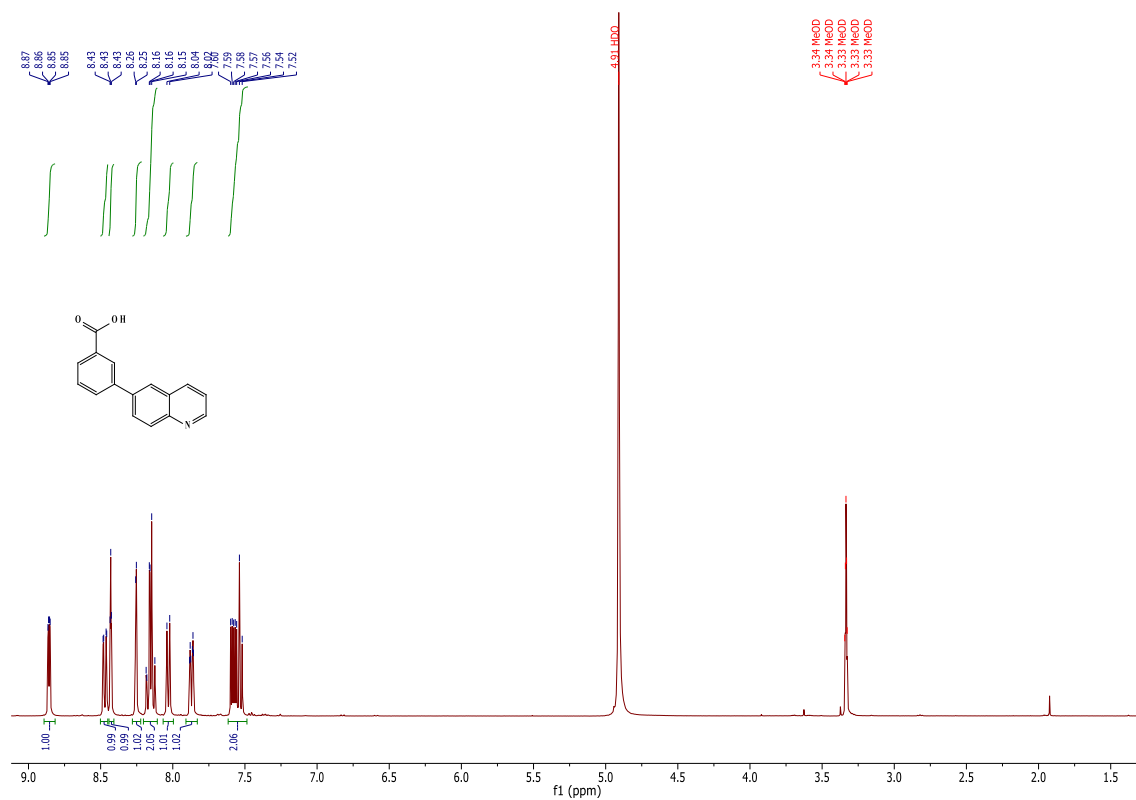


2.41.2 ^{13}C NMR of 27

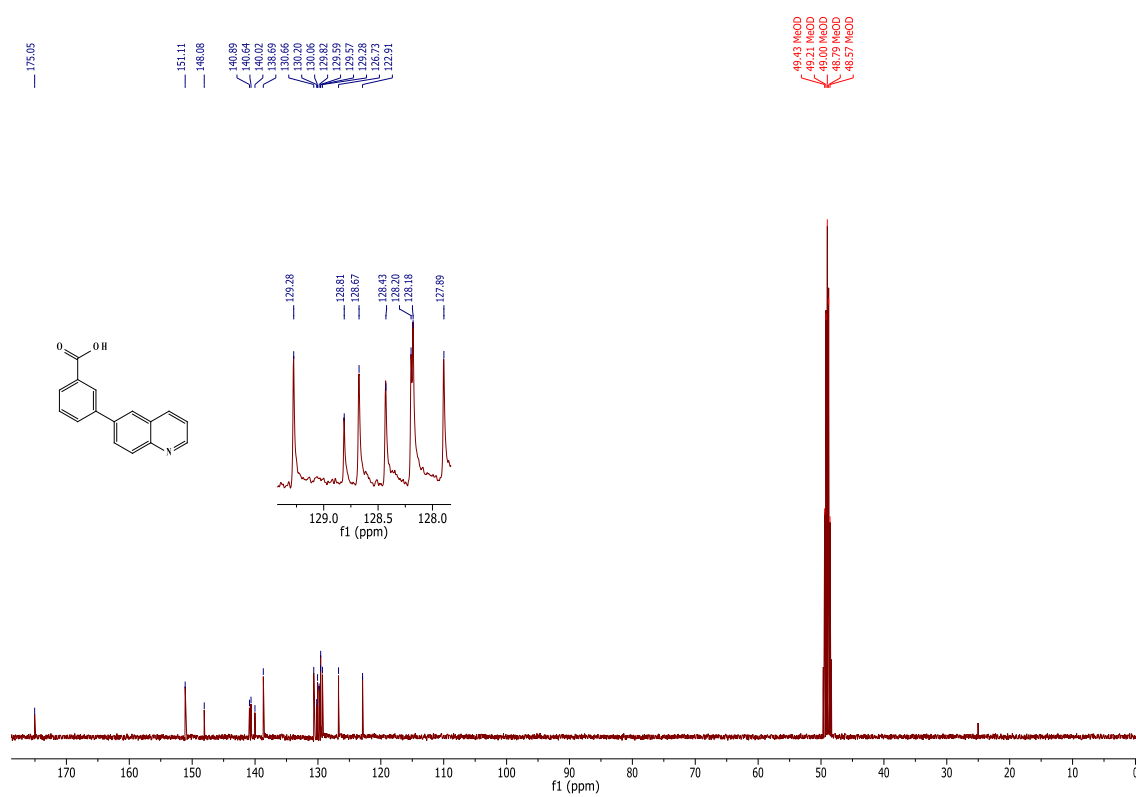


2.42 3-(quinolin-7-yl)benzoic acid, 28:

2.42.1 ¹H NMR of 28

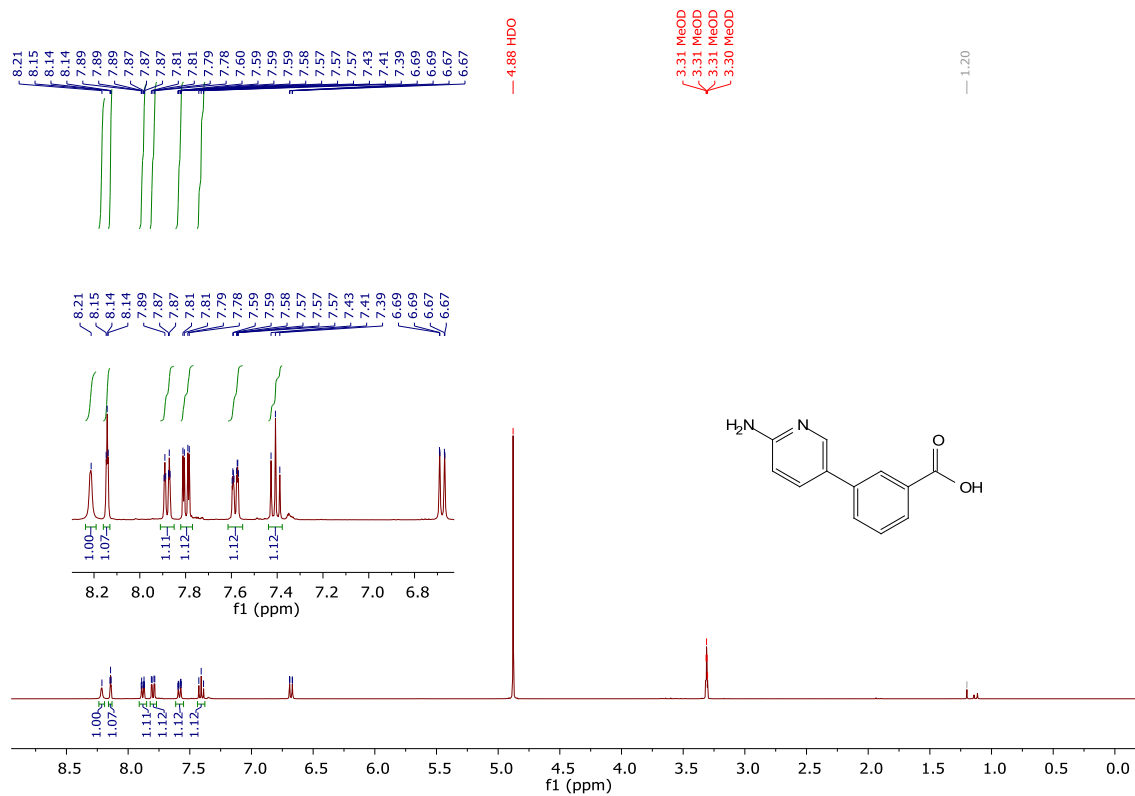


2.42.2 ¹³C NMR of 28

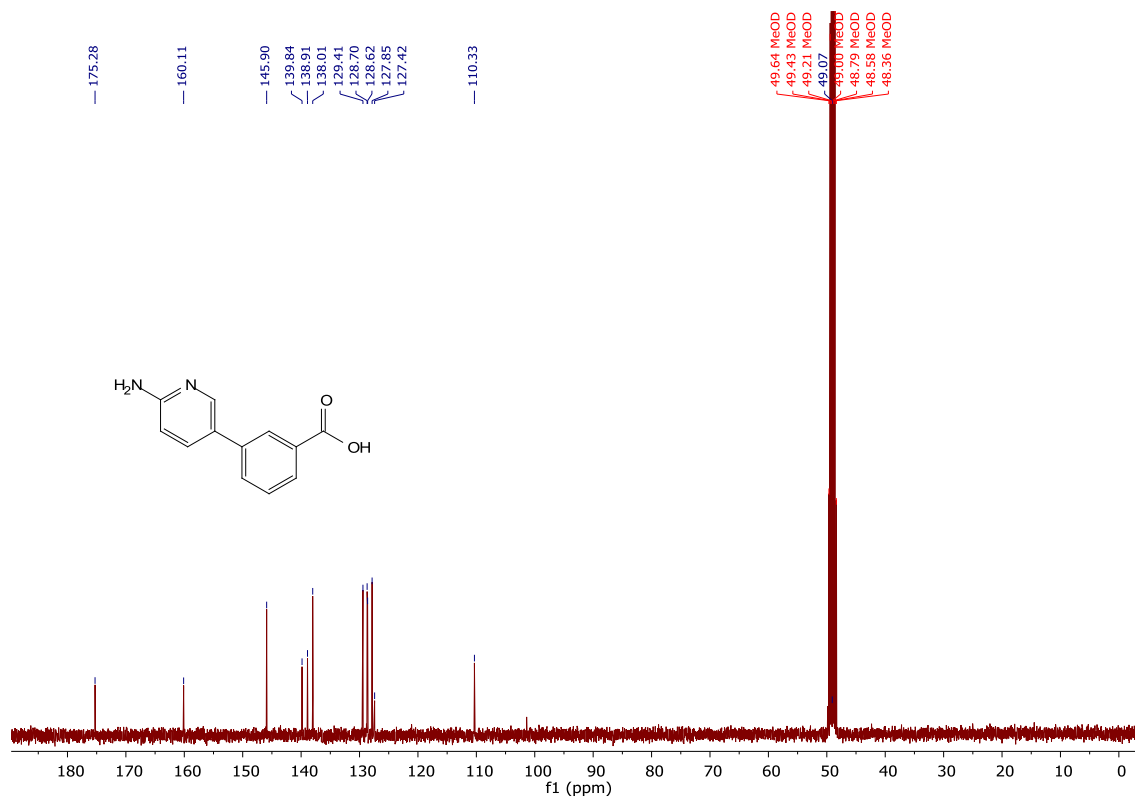


2.43 3-(6-aminopyridin-3-yl)benzoic acid, 29:

2.43.1 ^1H NMR of 29

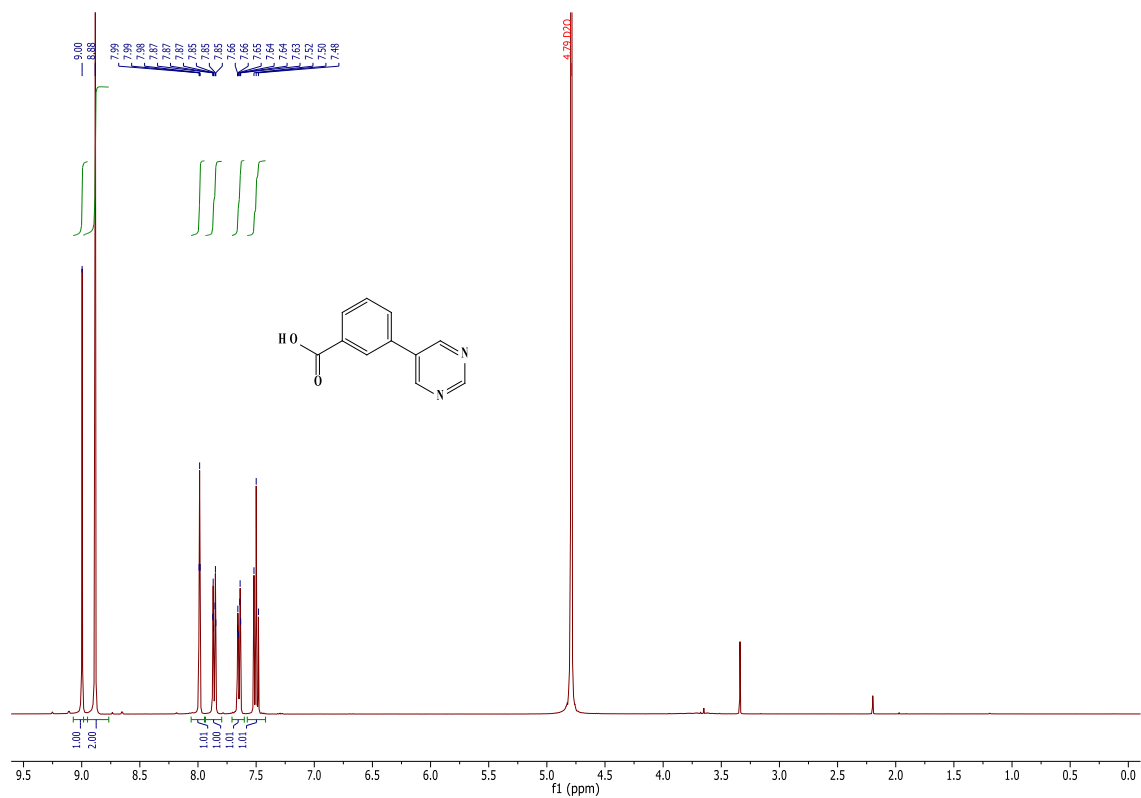


2.43.2 ^{13}C NMR of 29

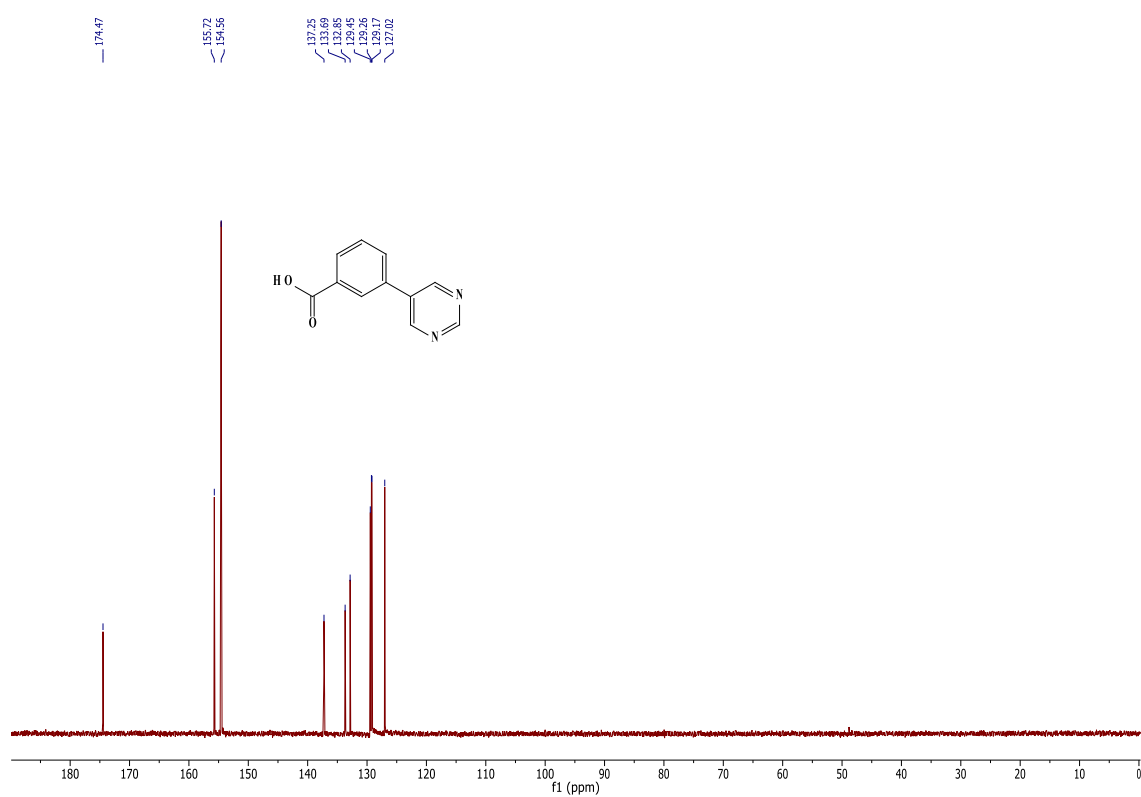


2.44 3-(pyrimidin-5-yl)benzoic acid, 30:

2.44.1 ¹H NMR of 30

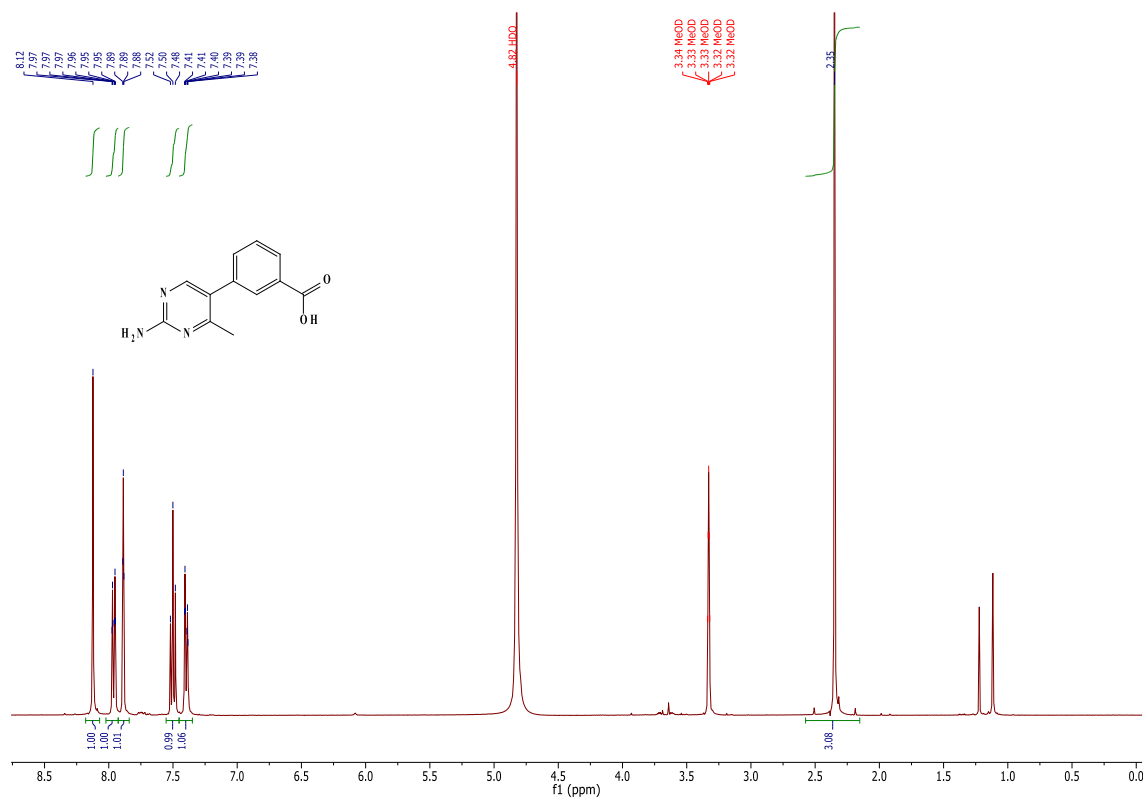


2.44.2 ¹³C NMR of 30

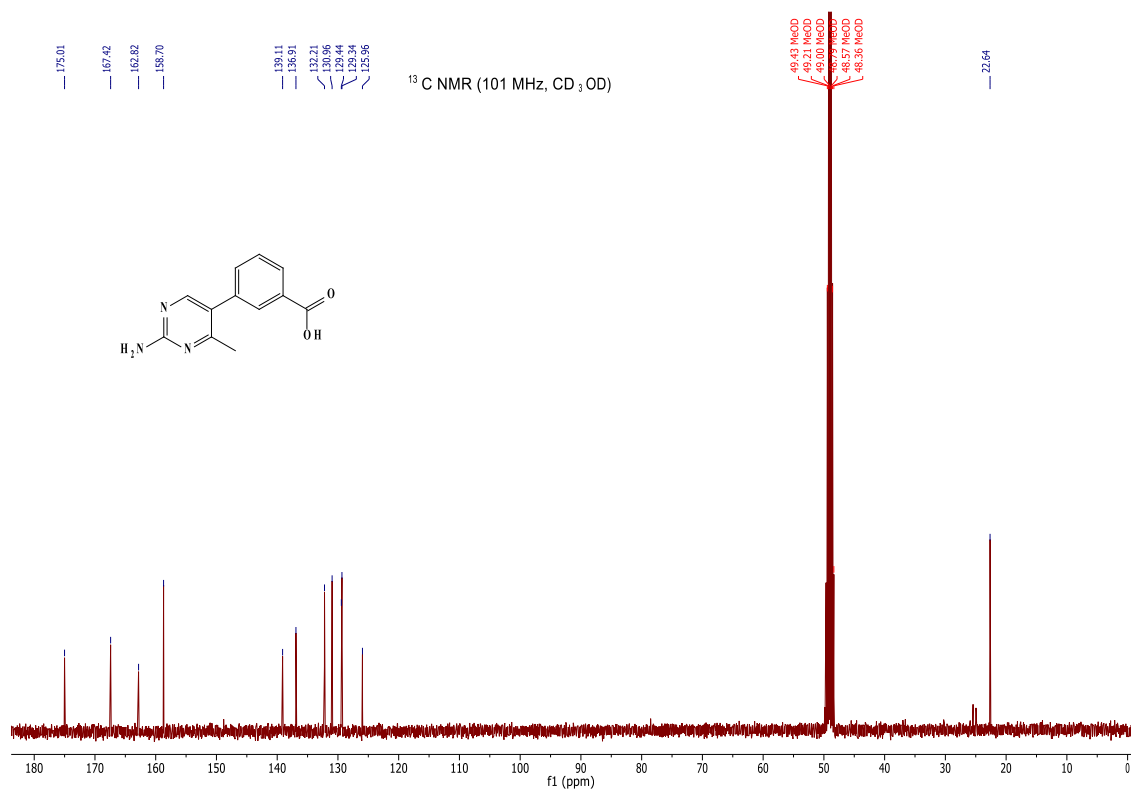


2.45 3-(2-aminopyrimidin-4-yl)benzoic acid, **31**:

2.45.1 ^1H NMR of **31**



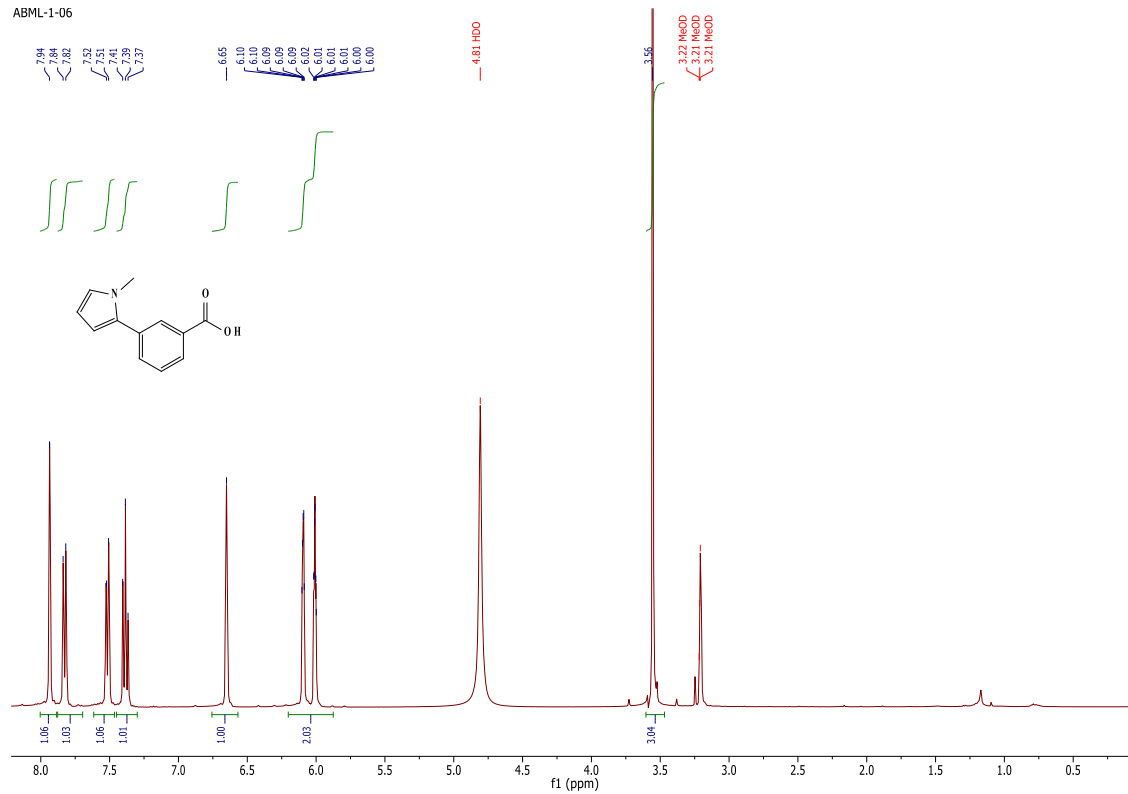
2.45.2 ^{13}C NMR of **31**



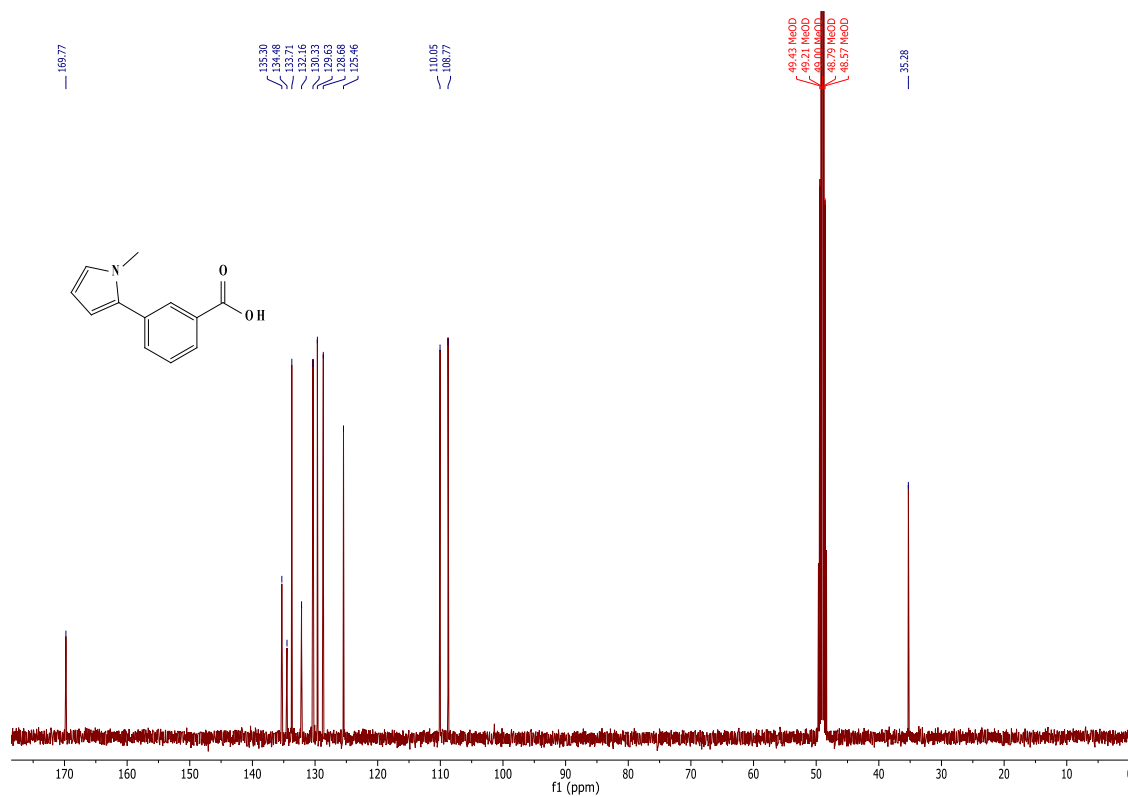
2.46 3-(1-methyl-1H-pyrrol-2-yl)benzoic acid, **32**:

2.46.1 ^1H NMR of **32**

ABML-1-06

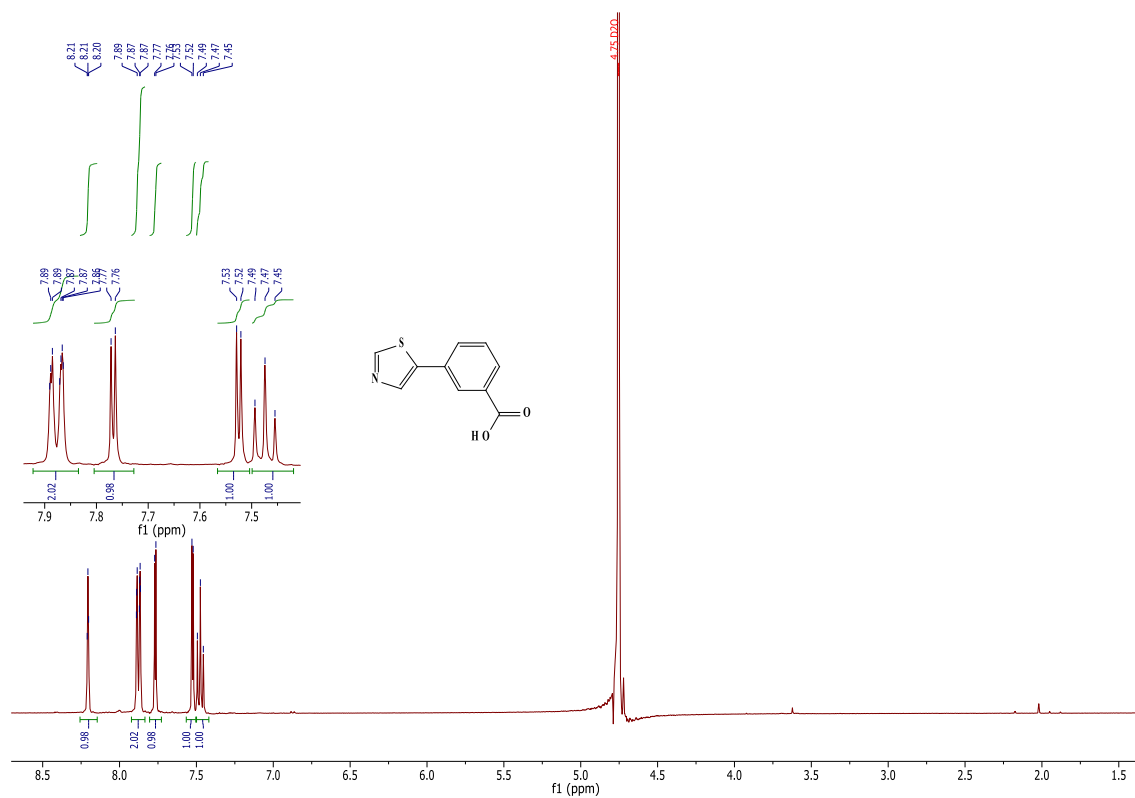


2.46.2 ^{13}C NMR of **32**

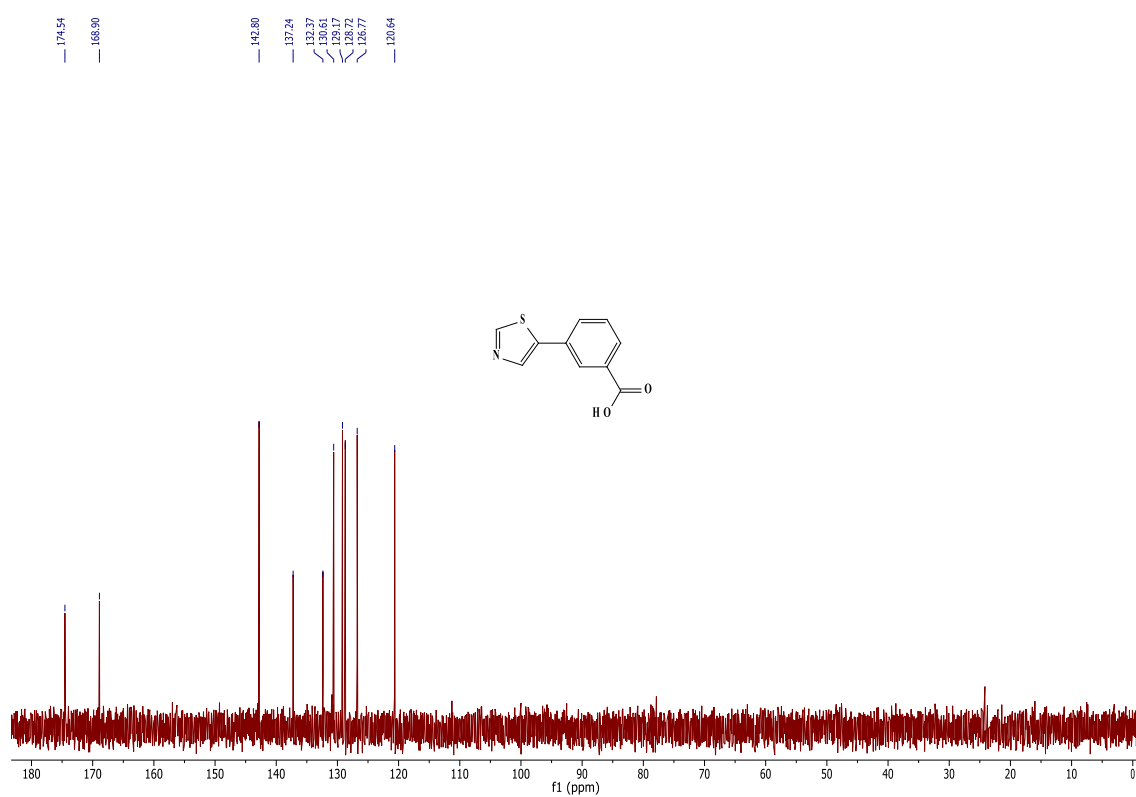


2.47 3-(thiazol-5-yl)benzoic acid, **33**:

2.47.1 ^1H NMR of **33**

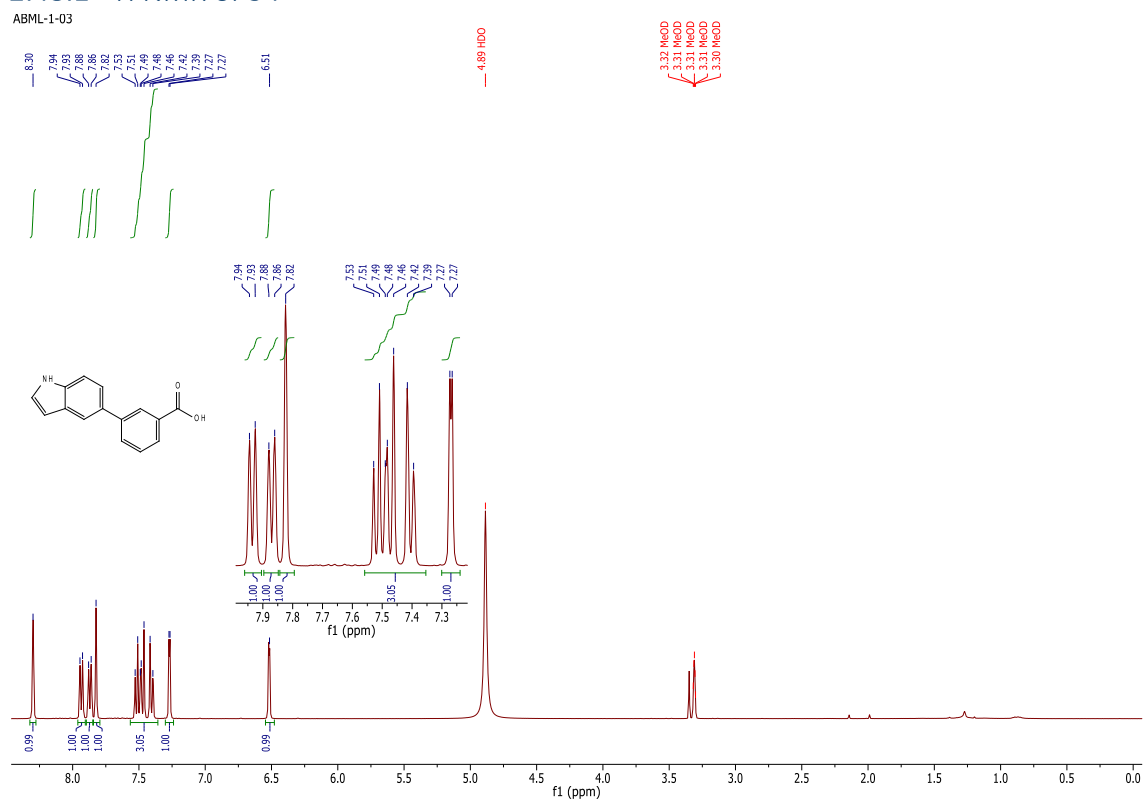


2.47.2 ^{13}C NMR of **33**

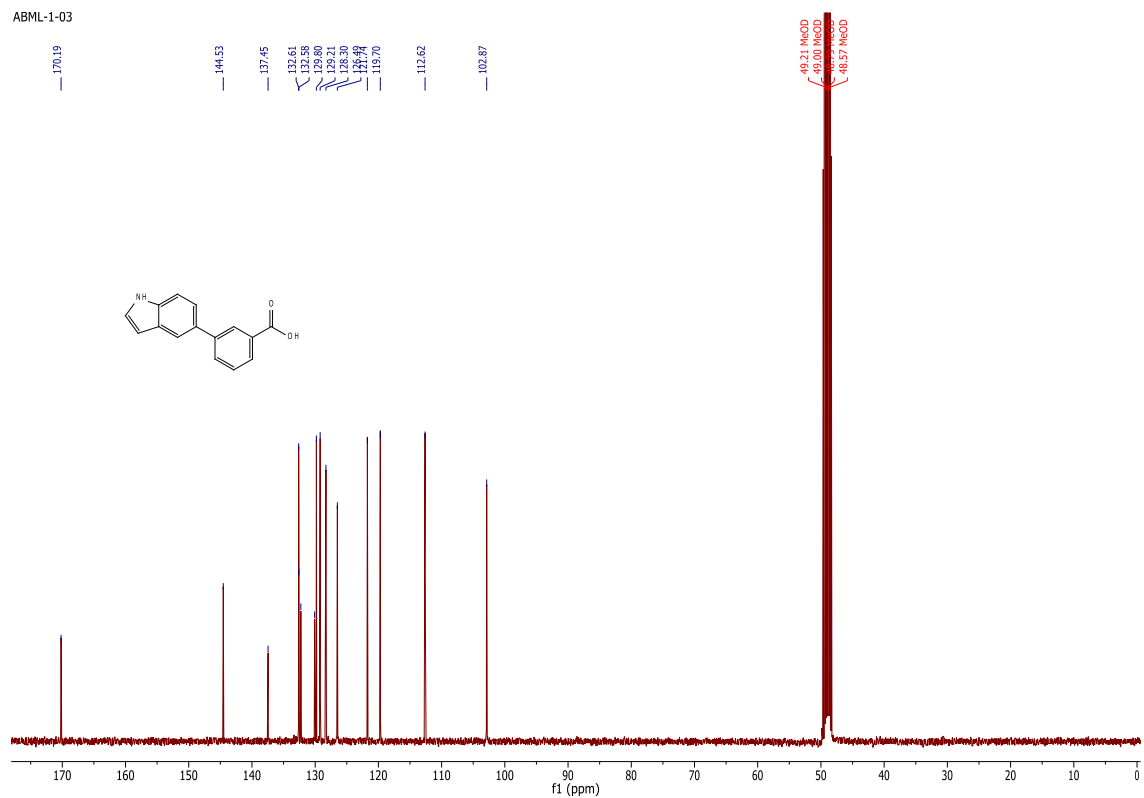


2.48 3-(1H-indol-5-yl)benzoic acid, **34**:

2.48.1 ¹H NMR of **34**



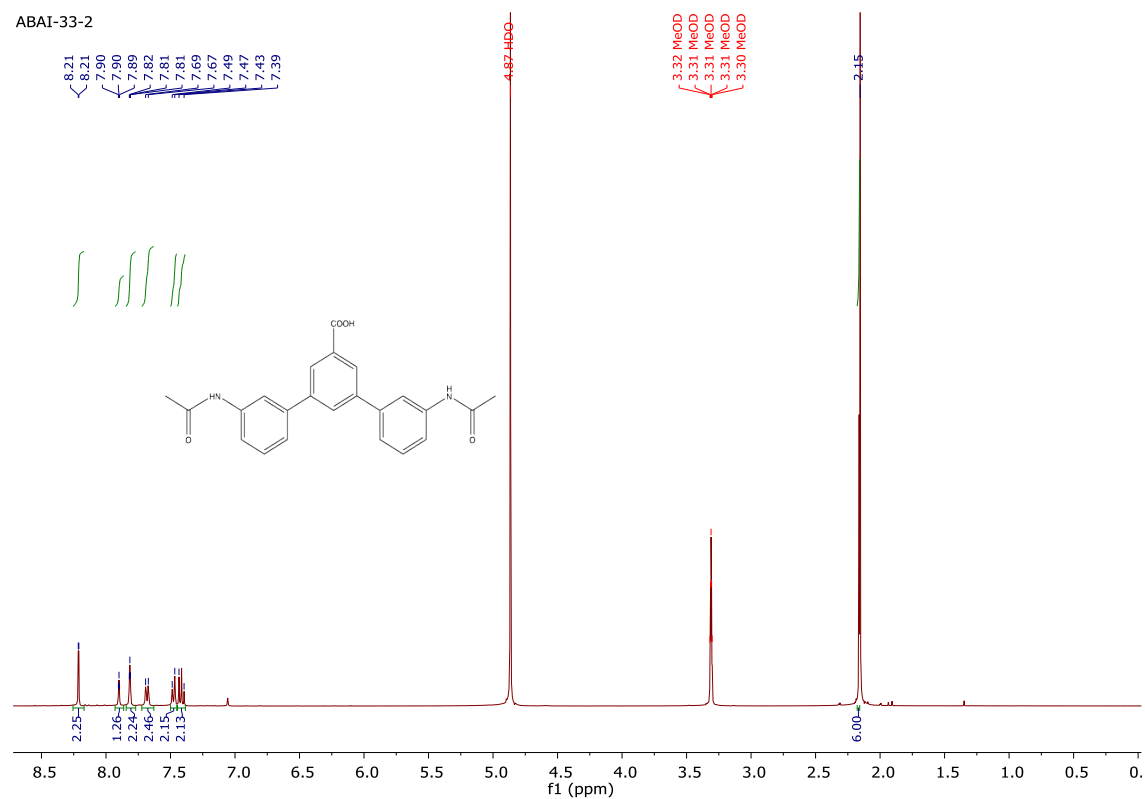
2.48.2 ¹³C NMR of **34**



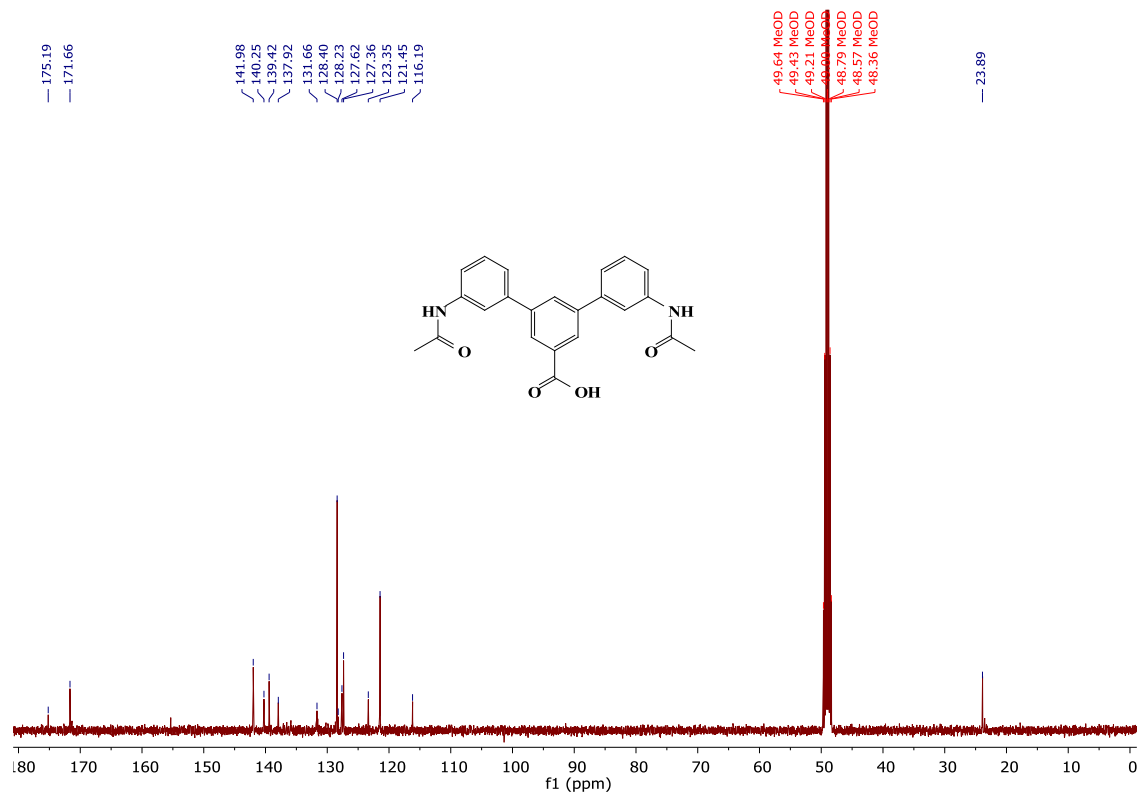
2.50 symmetrical 3,5-disubstituted benzoic acid derivatives

2.51 3,5-Di(3-acetamidophenyl)benzoic acid 36:

2.51.1 ¹H NMR of 36

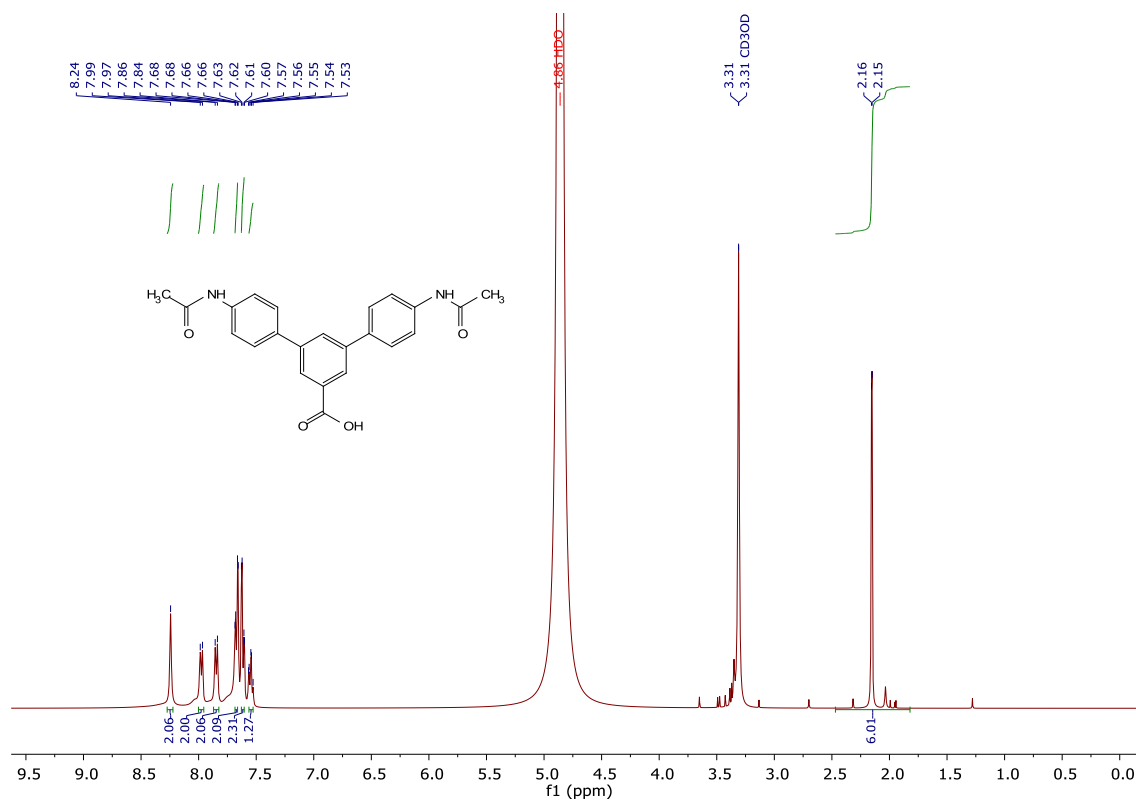


2.51.2 ¹³C NMR of 36

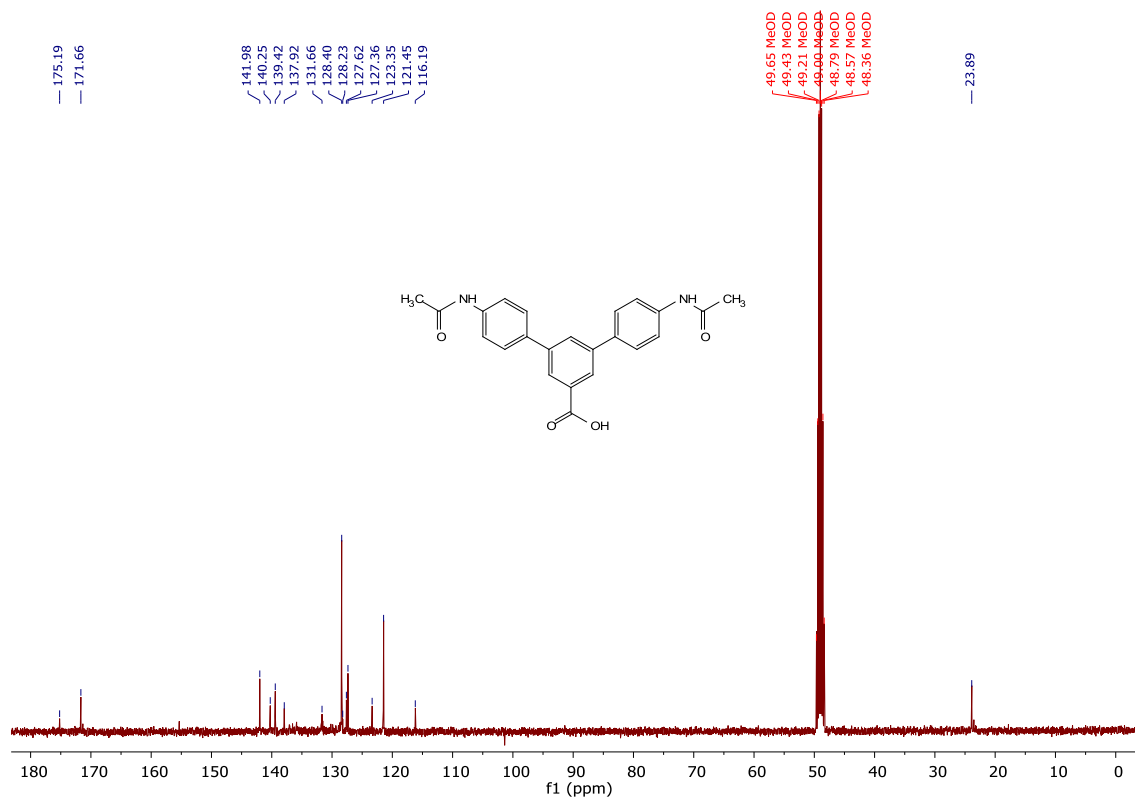


2.52 3,5-di(4-acetamidophenyl)benzoic acid 37:

2.52.1 ¹H NMR of 37

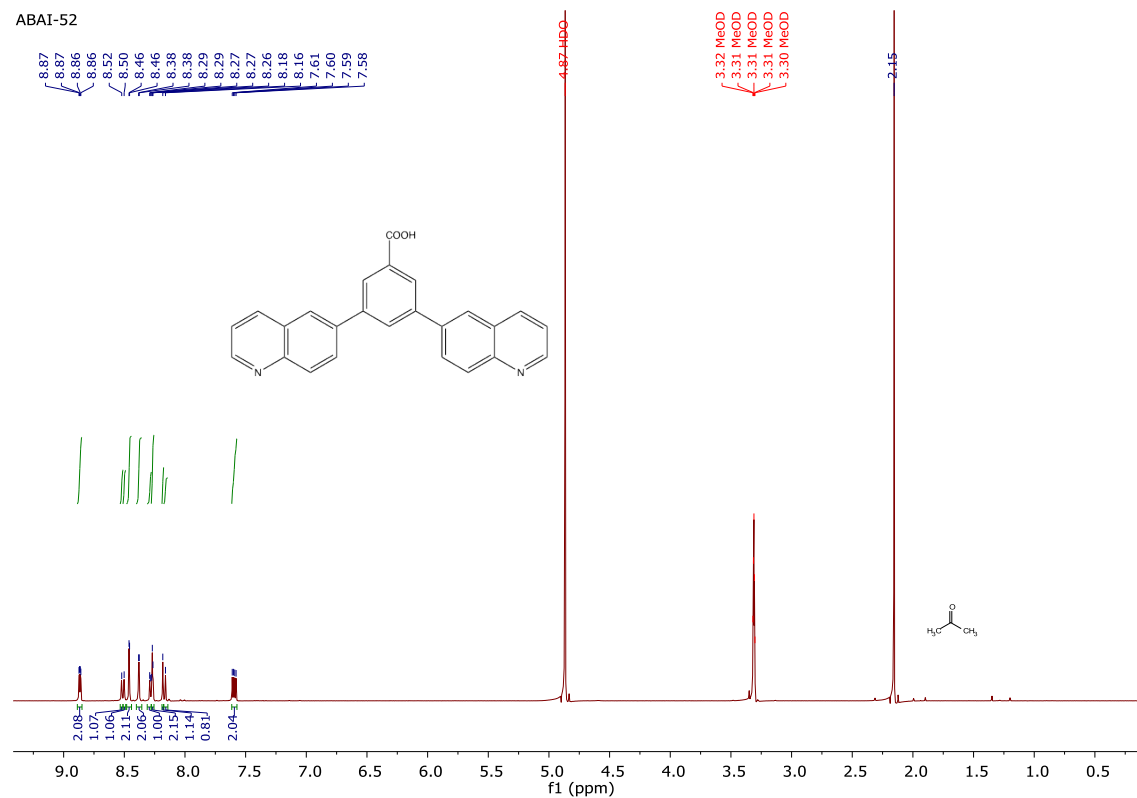


2.52.2 ¹³C NMR of 37

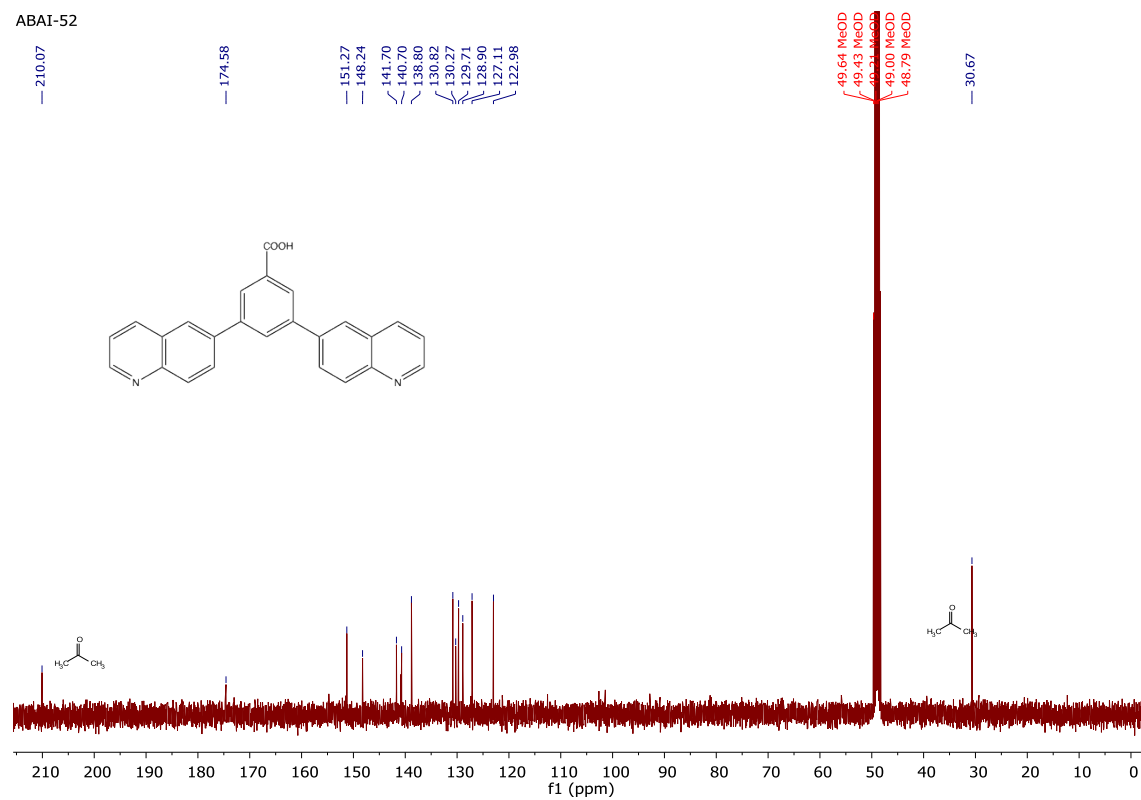


2.53 3,5-diquinolin-6-ylbenzoic acid **38**:

2.53.1 ¹H NMR of **38**



2.53.2 ¹³C NMR of **38**

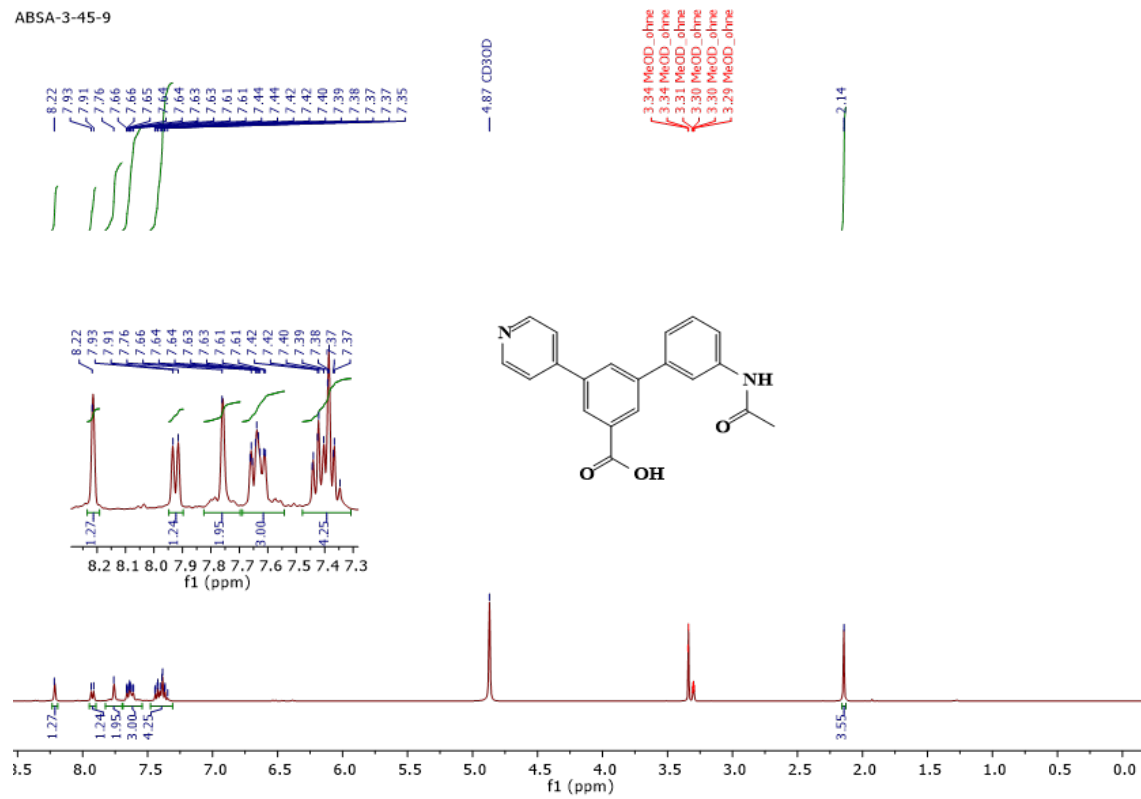


2.54 unsymmetrical 3,5-disubstituted benzoic acid derivatives

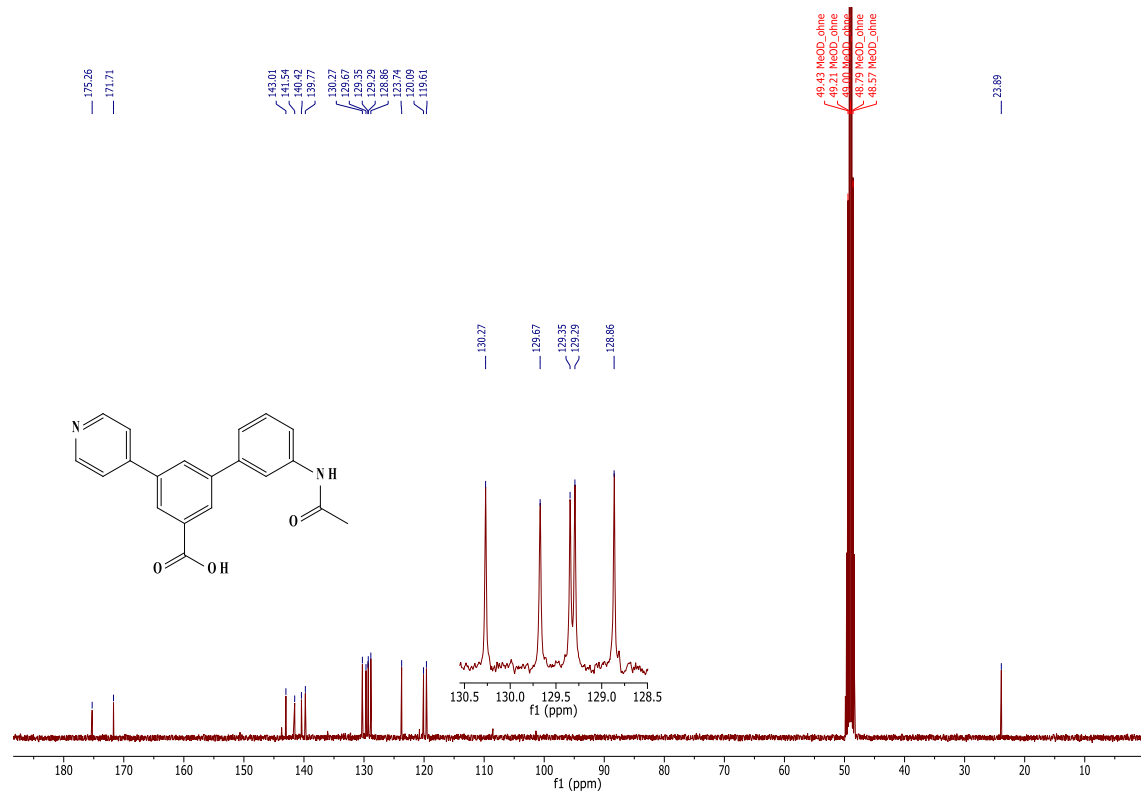
2.55 3-(3'-Acetamidophenyl)-5-pyridin-4-ylbenzoic acid 39:

2.55.1 ¹H NMR of 39

ABSA-3-45-9



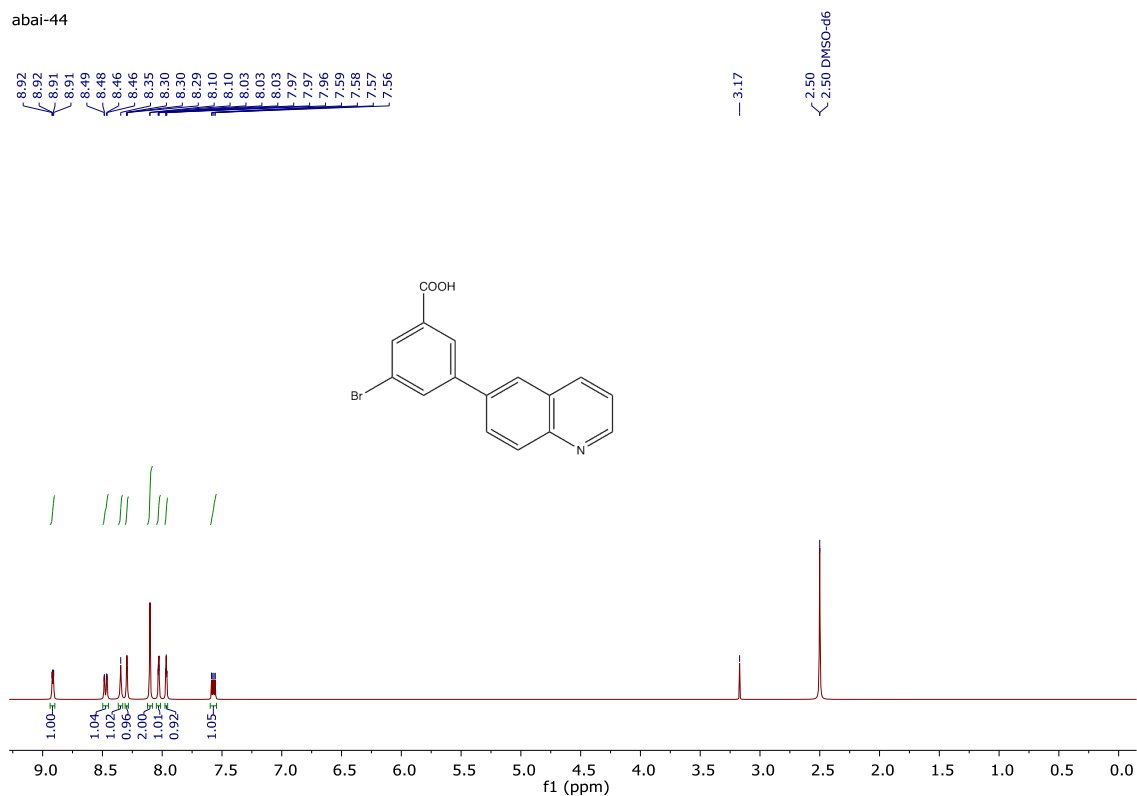
2.55.2 ¹³C NMR of 39



2.56 3-Bromo-5-(quinolin-6-yl) benzoic acid int-40:

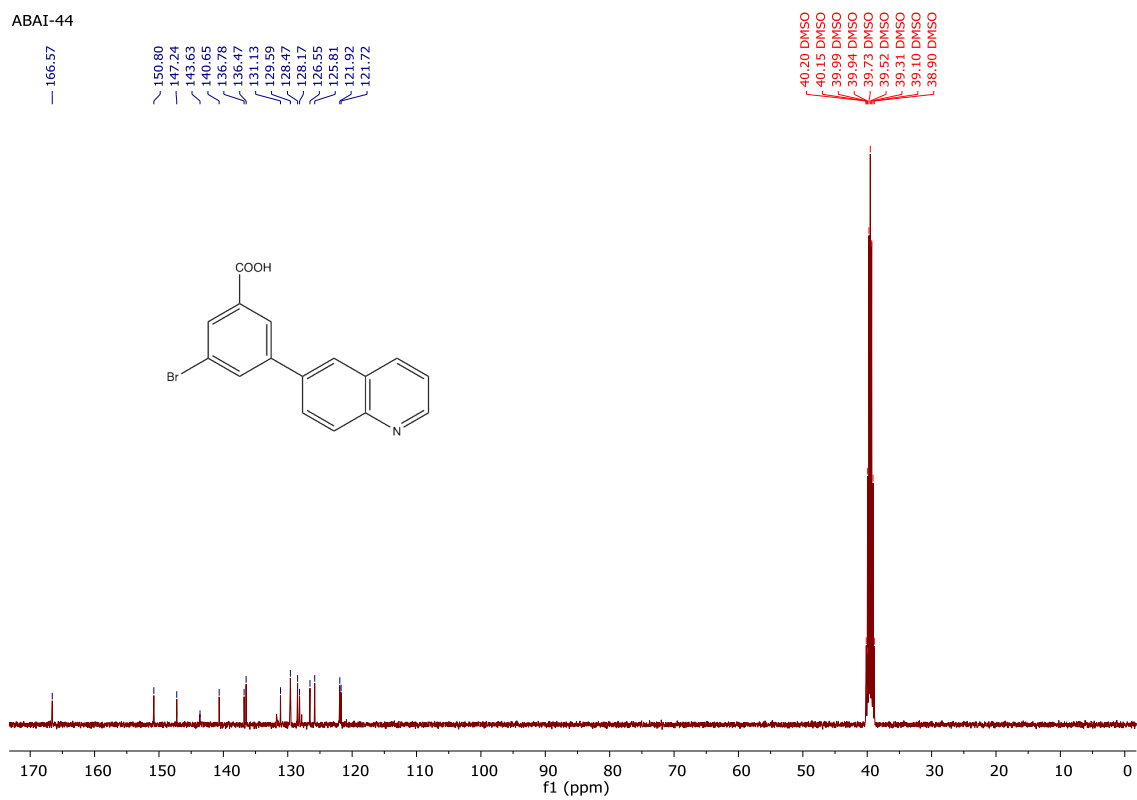
2.56.1 ¹H NMR of int-40

abai-44



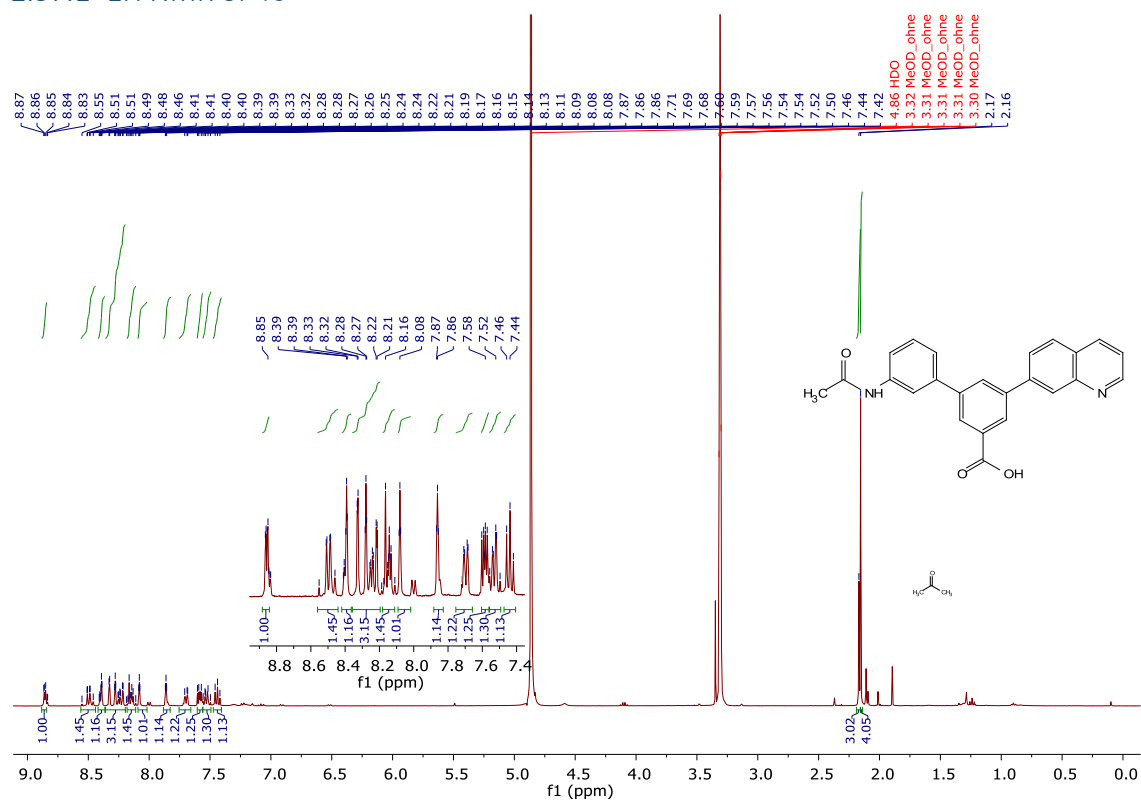
2.56.2 ¹³C NMR of int-40

ABAI-44

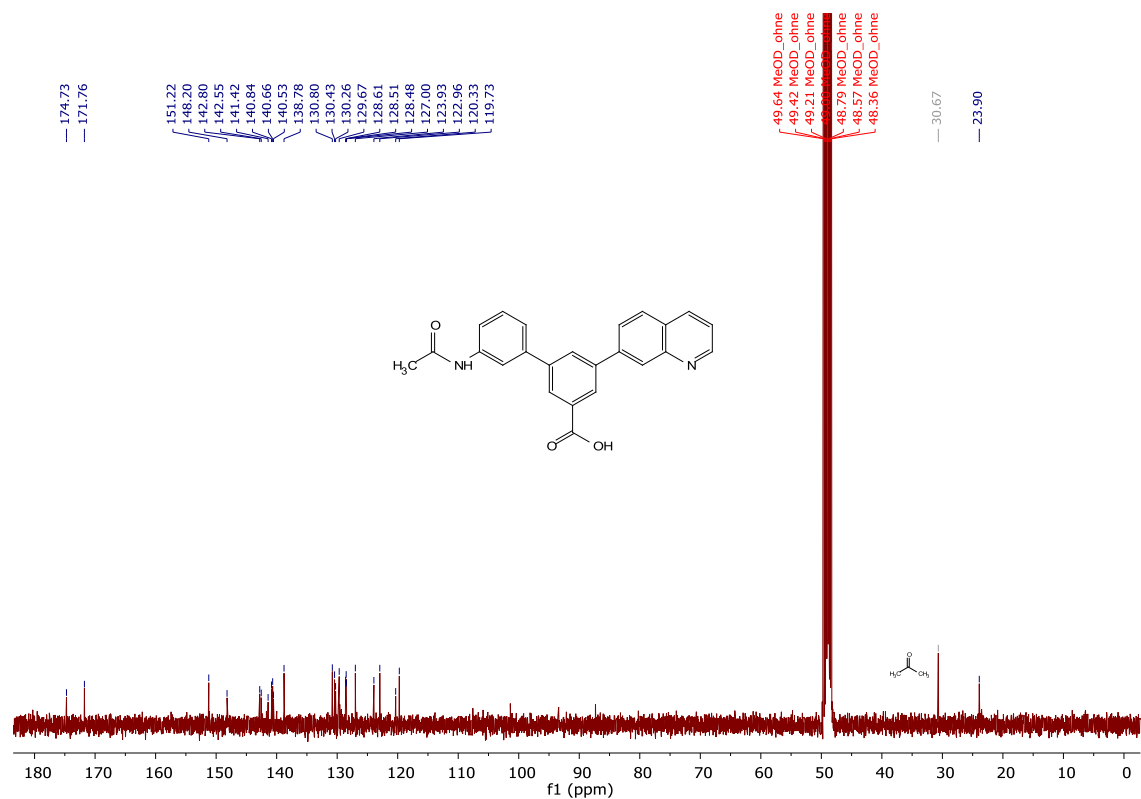


2.57 3-(3'-Acetamidophenyl)-5-quinolin-6-ylbenzoic acid **40**:

2.57.1 ¹H NMR of **40**



2.57.2 ¹³C NMR of **40**



Paper II

Carbonylative Suzuki–Miyaura couplings of sterically hindered aryl halides: synthesis of 2-arylbenzoate derivatives

Aya Ismael, Troels Skrydstrup, and Annette Bayer.

Org. Biomol. Chem., 2020, 18, 175. DOI: [10.1039/d0ob00044b](https://doi.org/10.1039/d0ob00044b).

PAPER



Cite this: *Org. Biomol. Chem.*, 2020, **18**, 1754

Received 8th January 2020,
Accepted 3rd February 2020

DOI: 10.1039/d0ob00044b

rsc.li/obc

Carbonylative Suzuki–Miyaura couplings of sterically hindered aryl halides: synthesis of 2-aryloxybenzoate derivatives†

Aya Ismael,^a Troels Skrydstrup^b and Annette Bayer^{a*}

We have developed a carbonylative approach to the synthesis of diversely substituted 2-aryloxybenzoate esters featuring a new protocol for the carbonylative coupling of aryl bromides with boronic acids and a new strategy to favour carbonylative over non-carbonylative reactions. Two different synthetic pathways – (i) the alkoxycarbonylation of 2-bromo benzophenones and (ii) the carbonylative Suzuki–Miyaura coupling of 2-bromobenzoate esters – were evaluated. The latter approach provided a broader substrate tolerance, and thus was the preferred pathway. We observed that 2-substituted aryl bromides were challenging substrates for carbonylative chemistry favouring the non-carbonylative pathway. However, we found that carbonylative Suzuki–Miyaura couplings can be improved by slow addition of the boronic acid, suppressing the unwanted direct Suzuki coupling and, thus increasing the yield of the carbonylative reaction.

Introduction

Through our program on fragment-based design of metallo-β-lactamase inhibitors, we became interested in the development of efficient strategies for the synthesis of functionalized 2-aryloxybenzoic acids **1** (Scheme 1).¹ Among other, 2-aryloxybenzoic acids have gained keen interest as synthetic intermediates for accessing bioactive compounds,^{2–7} as subunits of natural products and pharmaceuticals *e.g.* (–)-balanol⁸ and pitfenone, and as fragment-sized inhibitors of the human aldo-keto reductase AKR1C3⁹ and the hepatitis C virus NS3 protease.¹⁰ Most commonly, 2-aryloxybenzoic acids are prepared from phthalic anhydride by treatment with organometallic reagents^{2,7,11} or by a Friedel–Crafts acylation^{3,5,12} with aromatic nucleophiles. However, these methods are incompatible with many functional groups, requiring excess Lewis acid and harsh reaction conditions, and often provide poor regioselective control. On the other hand, the biaryl ketone sub-scaffold of 2-aryloxybenzoic acids has been synthesized by transition metal-catalyzed carbonylative cross-couplings of organometallic reagents and aryl electrophiles,^{13–15} or the non-decar-

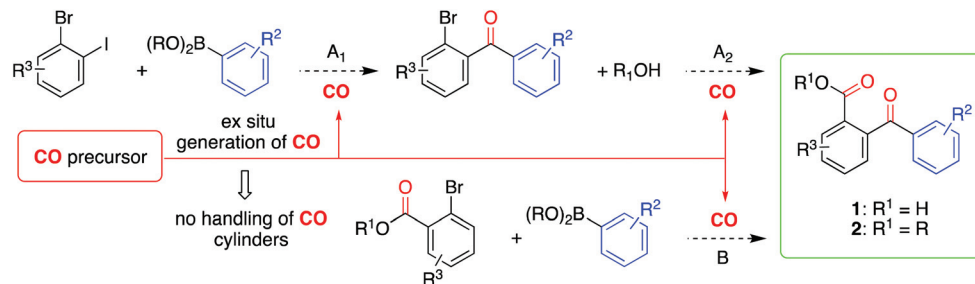
bonylative coupling of acyl electrophiles, *e.g.* carboxylic acids,^{16–18} esters^{19–21} or amides.^{19,22} Despite the advances in the synthesis of biaryl ketones, only few methods have been demonstrated to be applicable for the formation of 2-aryloxybenzoic acid derivatives. Such methods comprise of the Pd-catalyzed *ortho*-C–H activation of benzoic acids followed by decarboxylative coupling with α-oxocarboxylic acids,²³ Pd-catalyzed *ortho*-C–H activation of aryl amides followed by coupling with aryl aldehydes,²⁴ and the Pd-catalyzed coupling of 2-iodobenzoates with aldehydes.²⁵ However, the available protocols have limited regiocontrol and/or substrate scope especially with regard to electron-deficient aryl groups.

In this study, we investigated two alternative routes towards 2-aryloxybenzoate esters **2** featuring carbonylative couplings using safe and easy to handle *ex situ* generated CO as a key step (Scheme 1). In the first approach (route A), we examined the Pd-catalyzed alkoxycarbonylation of 2-bromo functionalized biaryl ketones, which in turn could be prepared by carbonylative Suzuki–Miyaura couplings of 2-bromiodobenzene. In the second approach (route B), we investigated the carbonylative Suzuki–Miyaura coupling of 2-bromo substituted benzoate esters. A new protocol for the carbonylative coupling of aryl bromides and simple boronic acids preventing the use of iodide salts as additives or high-pressure CO gas was developed. Moreover, we demonstrate that slow addition of the nucleophilic coupling reagent is an uninvestigated strategy to enhance formation of the carbonylative product over the non-carbonylative side-product. The latter discovery was essential for sterically-demanding *ortho*-substituted aryl bromides in order to provide useful yields of the carbonylative coupling products.

^aDepartment of Chemistry, Faculty of Science and Technology, UiT The Arctic University of Norway, N-9037 Tromsø, Norway.
E-mail: annette.bayer@uit.no

^bCarbon Dioxide Activation Center (CADIA), Interdisciplinary Nanoscience Center (iNANO) and Department of Chemistry, Aarhus University, Gustav Wieds Vej 14, 8000 Aarhus C, Denmark

† Electronic supplementary information (ESI) available. See DOI: 10.1039/d0ob00044b

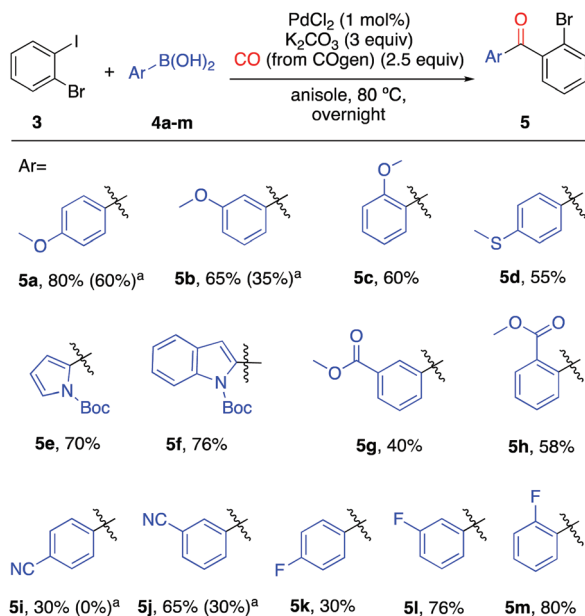


Scheme 1 Routes towards 2-arylbenzoic acid derivatives explored in this work.

Results and discussion

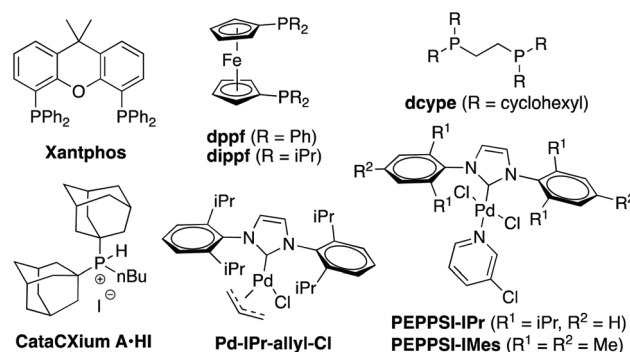
Carbonylative Suzuki–Miyaura of 2-bromiodobenzene (step A₁)

Initially, we focused on the Pd-catalyzed carbonylative Suzuki–Miyaura coupling of 2-bromiodobenzene **3** with aryl boronic acids **4** in order to prepare substituted 2-bromobenzophenone derivatives **5** as starting materials for further alkoxy-carbonylation reactions (Scheme 2). A range of catalysts derived from a variety of Pd sources including Pd(OAc)₂,²⁶ Pd(dba)₂,²⁷ Pd(PPh₃)₂Cl₂,²⁸ PdCl₂, PEPPSI-IPr²⁹ were evaluated for the carbonylative coupling of the aryl iodide in presence of a bromide using 2-bromiodobenzene **3** and 4-methoxyphenyl boronic acid **4a** (Table ESI-1†). The yields varied from 10% to 65% of the furnished benzophenone (Table ESI-1,† entries 1–5), and



Scheme 2 Carbonylative Suzuki–Miyaura coupling of 2-bromiodobenzene with boronic acids. Reaction conditions: Chamber A: **3** (0.18 mmol), PdCl₂ (1 mol%) and K₂CO₃ (0.55 mmol) in anisole (3 ml). Chamber B: COgen (0.45 mmol), Pd(dba)₂ (5 mol%) and TTBP-HBF₄ (5 mol%) in anisole (3 ml). DIPEA (3 equiv.) was added to chamber B to start CO formation, before **4** (1.2 equiv.) in anisole (3 ml) was added slowly to chamber A (general procedure A, ESI†).^a Yield obtained when **4** (1.2 equiv.) was added to chamber A before CO release (general procedure B, ESI†).

competitive formation of the direct coupling product (biphenyl) was a major limitation. The most promising catalytic system identified from the screening used PdCl₂ as catalyst precursor, K₂CO₃ as base, and anisole as solvent (Table ESI-1,† entry 5).



In addition, several methods for the *ex situ* generation of carbon monoxide from formic acid,³⁰ oxalyl chloride,³¹ COgen,³² and electrochemical reduction of CO₂ to CO³³ were screened to prevent the risk of handling toxic carbon monoxide from a cylinder (Table ESI-2†). The most promising and convenient CO source turned out to be 9-methylfluorene-9-carbonyl chloride (COgen) (Table ESI-2,† entry 3). Oxalyl chloride as CO source provided comparable results if the CO gas was generated outside the reaction chamber making the handling more inconvenient (Table ESI-2,† entry 5), while both formic acid and electrochemical reduction of CO₂ resulted in substantially reduced yields (Table ESI-2,† entries 1 and 7).

The catalytic system employing PdCl₂ as precatalyst was further optimized with regard to different reaction times, temperatures, and slow addition of the boronic acid. Yields up to 65% of the carbonylated product were obtained with PdCl₂ (3 mol%) at 80 °C for 20 h (Table ESI-1,† entry 5). Reduction of the catalyst loading to 1 mol% led to a slight decrease in yield to 60% (Table ESI-1,† entry 6) and 1 mol% of precatalyst was used in the following reactions. A lower reaction temperature led to incomplete conversion and lower yields (Table ESI-1,† entries 7 and 8). Addition of KI to favour carbonylative over direct coupling²⁸ did not improve the yield (Table ESI-1,† entry 11). However, when the aryl boronic acid was added slowly over 2 h, direct coupling was suppressed and the yield

improved up to 80% (Table ESI-1,† entry 13). Similarly, the yield of the carbonylated product was improved from 30% to 60% by slow addition of the aryl boronic acid for reactions with PEPPSI-IPr as the precatalyst (Table ESI-1,† entries 4 and 15).

Then, we explored the scope of the Pd-catalyzed reaction using PdCl₂ with respect to different aryl and heteroaromatic boronic acids **4** (Scheme 2). In all cases, slow addition of the aryl boronic acid increased the yield by 20–35 percentage points. Both electron-rich and electron-deficient aryl boronic acids (**4a–c**, **e**, **f**, **j**, **l**, **m**) gave moderate to high yields (60–80%) of the products. However, some electron-deficient boronic acids **4g**, **i** and **k** provided lower yields in the range of 30–40%. *ortho*-Substituents on the boronic acid (**4c**, **h** and **m**) and some electron-rich heterocycles (**4e** and **f**) were well tolerated to the reaction conditions. However, hydroxy and *N*-acyl substituted aryl boronic acids and 2-furyl boronic acid only provided products from the direct coupling instead of carbonylative coupling.

Hydroxy- or alkoxy-carbonylation of 2-bromo-substituted biaryl ketones (step A₂)

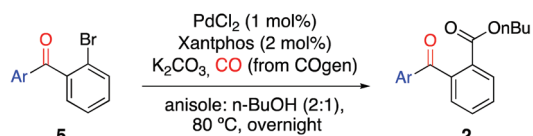
With a set of 2-bromobenzophenone derivatives **5a–m** in hand, we investigated the Pd-catalyzed hydroxy- and alkoxy-carbonylation to transform the aryl bromide into the carboxylic acid or ester, respectively.³⁴ Previous reports on Pd-catalyzed hydroxycarbonylation^{30,34–36} or alkoxy-carbonylation^{26,34,37,38} have had little focus on *ortho*-substituted aryl bromides. Unfortunately, all attempts to transform 2-bromo-4'-methoxybenzophenone **5a** directly to 2-(4-methoxybenzoyl)benzoic acid *via* a hydroxycarbonylation using MePh₂SiCO₂H³⁵ were unsuccessful (Table ESI-3†).

Next, we turned our attention to the alkoxy-carbonylation of 2-bromobenzophenones **5** (Scheme 3).³⁷ Using **5a** as the test substrate, a range of precatalysts and ligands (Pd(OAc)₂, PdCl₂ or Pd(dba)₂ with Xantphos, dppf or PPh₃, Pd(PPh₃)₂Cl₂/IMes,³⁹ dppf(PdCl₂), PEPPSI-IPr or PEPPSIIMes), nucleophiles (MeOH, *i*PrOH, *n*-BuOH, *t*-BuONa, EtONa), bases and solvents

were screened (Table ESI-4†). Only few systems were able to provide the corresponding alkyl 2-(4-methoxybenzoyl)benzoate **2**. Comparison of the catalyst performance for 2-bromo-substituted **5a** and the corresponding 4-bromo-substituted analog showed that the yields were highly influenced by the substitution pattern. For example, for catalyst systems based on dppf (PdCl₂) or Pd(OAc)₂/Xantphos, the yields dropped from >95% for the 4-bromo-substituted analog to an 11% yield for 2-bromo-substituted **5a** under otherwise identical conditions (Table ESI-5†). The best results for the latter were obtained with PdCl₂ and Xantphos as catalytic system, *n*-butanol as the nucleophile, K₂CO₃ as the base and anisole as solvent furnishing the ester **2a** in acceptable yield (65%) (Table ESI-4,† entry 12). We applied these conditions to our library of 2-bromobenzophenone derivatives **5a–m** (Scheme 2). While the substrates **5a**, **b**, **k** and **m** gave alkoxy-carbonylation products **2a–d** in acceptable yields (65%, 60%, 63% and 55%, respectively), compounds **5c–h** and **5l** gave low yields to no product. Over all, we conclude that while the carbonylative Suzuki–Miyaura coupling was tolerant to a variety of aryl boronic acids, the alkoxy-carbonylation of 2-bromo-biaryl ketones displayed a high dependence on the substrate structure rendering the approach unsuitable for the synthesis of a larger library of compounds.

Carbonylative Suzuki–Miyaura coupling with 2-bromobenzoates (route B₁)

Due to the limited substrate scope of the alkoxy-carbonylation of 2-bromobenzophenone derivatives, we decided to study the carbonylative Suzuki–Miyaura coupling of methyl 2-bromobenzoates **6** (Table 1). Few examples of carbonylative couplings with aryl bromides^{28,40–43} have been reported and those rely on the use of iodide salts as additives (3 equiv.),²⁸ high pressure of CO gas (5 bar)^{41–43} or the use of less accessible boronate esters⁴⁰ like DABO boronates⁴⁴ or aryl trihydroxyborates⁴⁵ instead of boronic acids. Only two examples of successful



Scheme 3 Palladium-catalyzed alkoxy-carbonylation of 2-bromo biaryl ketones. Reaction conditions: Chamber A: **5** (1.0 equiv., 0.18 mmol), PdCl₂ (2 mol%), Xantphos (3 mol%), K₂CO₃ (3 equiv., 0.55 mmol) in anisole : *n*-BuOH (2 : 1, 3 ml). Chamber B: COgen (107 mg, 2.5 equiv., 0.45 mmol), Pd(dba)₂ (12 mg, 5 mol%) and TTBP·HBF₄ (6.3 mg, 5 mol%) in anisole (3 ml). DIPEA (240 mg, 3 equiv.) was added to chamber B to start CO release.

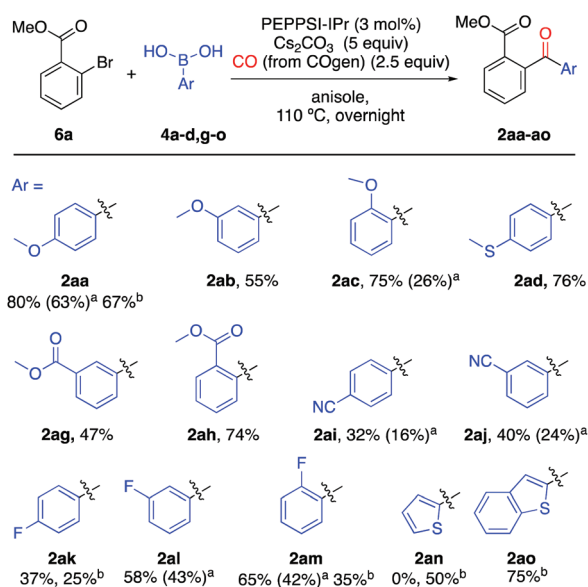
Table 1 Boronate derivatives in carbonylative Suzuki–Miyaura couplings

| Boronic acid derivatives | Catalyst system | Yield |
|--------------------------|---------------------------------------|-------|
| | Pd(acac) ₂ /cataXCium A·HI | 67% |
| | Pd(acac) ₂ /cataXCium A·HI | 65% |
| | Pd(acac) ₂ /CataXCium A·HI | 30% |
| | PEPPSI-IPr | 63% |
| | PEPPSI-IPr/slow addition of 4a | 80% |

couplings with *ortho*-substituted substrates were reported.⁴¹ While carbonylative couplings of sterically hindered, electron-rich aryl iodides have been achieved with PEPPSI-IPr as the precatalyst,²⁹ electron-poor aryl bromides like **6** have been shown to be challenging substrates favouring non-carbonylative direct couplings providing biaryl derivatives.^{28,41} In this perspective, general methods for carbonylative Suzuki–Miyaura couplings of aryl bromides with boronic acids are still needed.

With methyl 2-bromobenzoate **6a** as the test substrate, the protocol reported by Skrydstrup and Molander⁴⁰ using Pd(acac)₂/CataCXium A·HI (5/10 mol%) afforded acceptable yields of **2aa** with 65–67% when the DABO boronate⁴⁴ **7a** or aryl trihydroxyborate⁴⁵ **8** were used as the nucleophilic coupling reagent (Table 1). However, the yield decreased to 30% with the boronic acid **4a**. Attempts to increase the yield by slow addition of the DABO boronate **6** or the trihydroxyborate **7** were not successful due to low solubility of these boronic acid derivatives in the reaction medium (toluene/water). The use of other solvent systems dramatically reduced the yields (Table ESI-6,† entries 4–8).

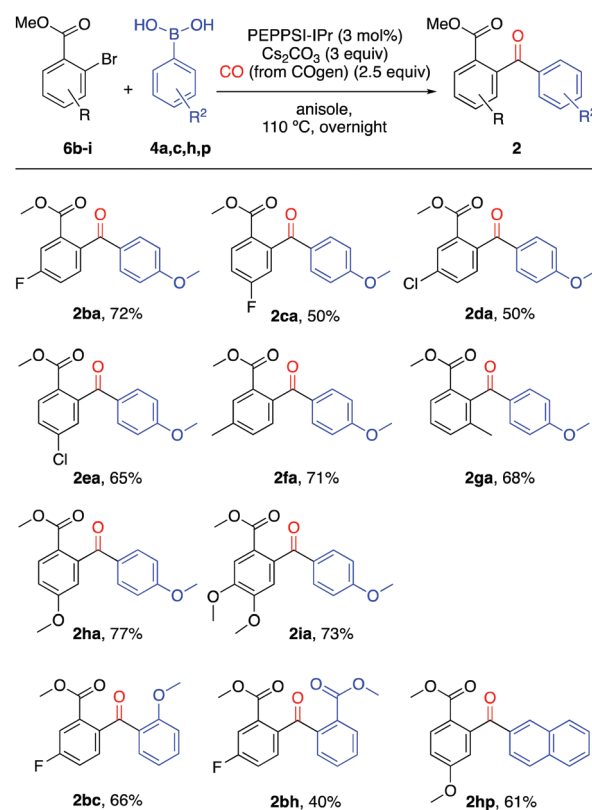
Therefore, we proceeded to identify reaction conditions for the coupling of 2-bromobenzoate **6a** with aryl boronic acids **4a** using COgen as the carbon monoxide source. A range of experimental conditions including different palladium sources and ligands (Pd(acac)₂ or Pd(OAc)₂/CataCXium A or A·HI,⁴⁰



Scheme 4 Suzuki–Miyaura coupling of methyl 2-bromobenzoate **6a** with boronic acids **4**. Reaction conditions: Chamber A: **6a** (1.0 equiv., 0.47 mmol), PEPPSI-IPr (3 mol%) and Cs₂CO₃ (3 equiv., 1.4 mmol) in anisole (3 ml). Chamber B: COgen (282 mg, 2.5 equiv., 1.2 mmol), Pd(dba)₂ (30 mg, 5 mol%) and TTBP·HBF₄ (10 mg, 5 mol%) in anisole (3 ml). DIPEA (450 mg, 3 equiv.) was added to chamber B, before **4** (1.5 equiv.) was added slowly to chamber A (general procedure C, ESI†).^aYield obtained when **4** (1.5 equiv.) was added to chamber A before CO release (general procedure D, ESI†).^bYield obtained by reaction with DABO boronate **7** (1.5 equiv.) using Pd(acac)₂/2 CataCXium A·HI (5 mol%) as catalyst (general procedure E, ESI†).

Pd(OAc)₂ or PdCl₂/Xantphos, Xantphos-G2, PEPPSI-IPr, [Pd(IPr)(allyl)Cl], Pd(PPh₃)₂Cl₂^{28,43} and Ni(COD)/dcype) and solvents were screened (Table ESI-6,† entries 9–20). In most of the systems, the undesired non-carbonylative coupling was the dominant reaction pathway (Table ESI-6,† entries 9–15). Only the Pd(IPr)-based catalytic systems were able to accomplish the carbonylative Suzuki–Miyaura coupling (Table ESI-6,† entries 16–19). The best system using PEPPSI-IPr (3 mol%) as catalyst precursor, Cs₂CO₃ as base in chlorobenzene or anisole as solvent provided the product **2aa** in 63% yield (Table 1 and Table ESI-6,† entry 16). The yield could be further increased to 80% by slow addition of the boronic acid (Table 1 and Table ESI-6,† entry 17).

A range of aryl boronic acids **4** were tested to examine the scope of the reaction as depicted in Scheme 4. Most of the electron rich boronic acids (**4a**, **c** and **d**) provided good yields (**2aa**: 80%; **2ac**: 75%; **2ad**: 76%), while electron-deficient boronic acids (**4g**, **i**, **j**, **k** and **l**) generally led to lower yields (**2ag**: 47%; **2ai**: 32%; **2aj**: 40%; **2ak**: 37%; **2al**: 58%). Yields obtained with slow addition of the aryl boronic acid were consistently higher (**2aa**: 80%; **2ac**: 75%; **2ai**: 32%; **2aj**: 40%; **2al**:



Scheme 5 Substrate scope of carbonylative Suzuki–Miyaura coupling of methyl 2-bromobenzoate derivatives **6** with boronic acids **4**. Reaction conditions: Chamber A: **6** (1.0 equiv., 0.47 mmol), PEPPSI-IPr (3 mol%) and Cs₂CO₃ (3 equiv., 1.4 mmol) in anisole (3 ml). Chamber B: COgen (282 mg, 2.5 equiv., 1.2 mmol), Pd(dba)₂ (30 mg, 5 mol%) and TTBP·HBF₄ (10 mg, 5 mol%) in anisole (3 ml). DIPEA (450 mg, 3 equiv.) was added to chamber B, before **4** (1.5 equiv.) was added slowly to chamber A (general procedure C, ESI†).

58%; **2am**: 65%), when compared with yields obtained by instantaneous addition (**2aa**: 63%; **2ac**: 26%; **2ai**: 16%; **2aj**: 24%; **2al**: 43%; **2am**: 42%). Slow addition of the boronic acid under reaction conditions seems to favour the CO insertion step by slowing down the faster transmetalation^{28,41} due to limited access to the organometallic nucleophile.

Aryl boronic acids containing acidic protons and the heteroaromatic boronic acid **4n** only underwent direct coupling instead of carbonylative coupling using PEPPSI-IPr. Couplings with heteroaromatic organometallic reagents could be achieved using the corresponding DABO boronates providing **2an** and **2ao** with Pd(acac)₂/CataCXium A-HI as the catalytic system.

We further investigated the scope of the reaction with regard to a range of substituted methyl 2-bromobenzoates **6b-i** (Scheme 5). Aryl bromide **6** with both electron-withdrawing **6b-e** and donating substituents **6f-i** gave acceptable yields (50–72%). Surprisingly, also the coupling of *ortho* disubstituted **6g** provided good yields (**2ga**: 68%). The lowest yield (**2bh**: 40%) was obtained for the coupling of the electron-deficient **6b** with the electron-deficient boronic acid **4p**.

Conclusions

In summary, two routes for accessing 2-aryloxybenzoate esters have been evaluated. In the first strategy, the key step was the alkoxyacylation of 2-bromo-diarylketones, which unfortunately appeared sensitive to the substitution pattern of the aryl bromide. The second strategy employed a carbonylative Suzuki–Miyaura coupling of 2-bromobenzoate esters, which was more robust with regard to the structure of aryl bromide and the aryl boronic acid. The latter approach was exploited to prepare a range of diversely substituted 2-aryloxybenzoate esters.

Moreover, we found that slow addition of the boronic acid is a strategy to favour carbonylative over non-carbonylative processes in Suzuki–Miyaura couplings – a finding that should be of general value.

Conflicts of interest

The authors declare the following competing financial interest (s): T.S. is co-owner of SyTracks A/S, which commercializes the two-chamber system (COWare) and COgen.

Acknowledgements

This work has been performed with support from NordForsk (Grant No. 85378) and the Danish National Research Foundation (Grant No. DNR118).

Notes and references

- 1 T. Christopheit, T. J. Carlsen, R. Helland and H. K. Leiros, *J. Med. Chem.*, 2015, **58**, 8671–8682.
- 2 C. J. Lim, S. H. Kim, B. H. Lee, K. S. Oh and K. Y. Yi, *Bioorg. Med. Chem. Lett.*, 2012, **22**, 427.
- 3 A. F. Watson, J. F. Liu, K. Bennaceur, C. J. Drummond, J. A. Endicott, B. T. Golding, R. J. Griffin, K. Haggerty, X. H. Lu, J. M. McDonnell, D. R. Newell, M. E. M. Noble, C. H. Revill, C. Riedinger, Q. Xu, Y. Zhao, J. Lunec and I. R. Hardcastle, *Bioorg. Med. Chem. Lett.*, 2011, **21**, 5916.
- 4 J. P. Cueva, A. Gallardo-Godoy, J. I. Juncosa, P. A. Vidi, M. A. Lill, V. J. Watts and D. E. Nichols, *J. Med. Chem.*, 2011, **54**, 5508–5521.
- 5 T. Ukita, Y. Nakamura, A. Kubo, Y. Yamamoto, Y. Moritani, K. Saruta, T. Higashijima, J. Kotera, M. Takagi, K. Kikkawa and K. Omori, *J. Med. Chem.*, 2001, **44**, 2204–2218.
- 6 M. Van der Mey, A. Hatzelmann, I. J. Van der Laan, G. J. Sterk, U. Thibaut and H. Timmerman, *J. Med. Chem.*, 2001, **44**, 2511.
- 7 P. Aeberli, P. Eden, J. H. Gogerty, W. J. Houlihan and C. Penberthy, *J. Med. Chem.*, 1975, **18**, 177–182.
- 8 J. W. Lampe, P. F. Hughes, C. K. Biggers, S. H. Smith and H. Hu, *J. Org. Chem.*, 1996, **61**, 4572–4581.
- 9 S. Gobec, P. Brozic and T. L. Rizner, *Bioorg. Med. Chem. Lett.*, 2005, **15**, 5170–5175.
- 10 D. F. Wyss, A. Arasappan, M. M. Senior, Y. S. Wang, B. M. Beyer, F. G. Njoroge and M. A. McCoy, *J. Med. Chem.*, 2004, **47**, 2486.
- 11 S. Seo, M. Slater and M. F. Greaney, *Org. Lett.*, 2012, **14**, 2650.
- 12 N. O. Calloway, *Chem. Rev.*, 1935, **17**, 327–392.
- 13 J.-B. Peng, F.-P. Wu and X.-F. Wu, *Chem. Rev.*, 2019, **119**, 2090–2127.
- 14 X.-F. Wu, *RSC Adv.*, 2016, **6**, 83831–83837.
- 15 M. Beller and X.-F. Wu, Carbonylative Coupling Reactions with Organometallic Reagents, in *Transition Metal Catalyzed Carbonylation Reactions: Carbonylative Activation of C–X Bonds*, Springer, Berlin, Heidelberg, 2013, pp. 65–94.
- 16 S. Panja, P. Maity and B. C. Ranu, *J. Org. Chem.*, 2018, **83**, 12609–12618.
- 17 P. M. Garcia-Barrantes, K. McGowan, S. W. Ingram and C. W. Lindsley, *Tetrahedron Lett.*, 2017, **58**, 898–901.
- 18 S. Si, C. Wang, N. Zhang and G. Zou, *J. Org. Chem.*, 2016, **81**, 4364–4370.
- 19 S. Shi, S. P. Nolan and M. Szostak, *Acc. Chem. Res.*, 2018, **51**, 2589–2599.
- 20 T. Ben Halima, W. Zhang, I. Yalaoui, X. Hong, Y. F. Yang, K. N. Houk and S. G. Newman, *J. Am. Chem. Soc.*, 2017, **139**, 1311–1318.
- 21 S. Shi, P. Lei and M. Szostak, *Organometallics*, 2017, **36**, 3784–3789.
- 22 N. A. Weires, E. L. Baker and N. K. Garg, *Nat. Chem.*, 2016, **8**, 75–79.
- 23 J. Miao and H. Ge, *Org. Lett.*, 2013, **15**, 2930–2933.
- 24 N. Zhang, Q. Yu, R. Chen, J. Huang, Y. Xia and K. Zhao, *Chem. Commun.*, 2013, **49**, 9464–9466.
- 25 B. Suchand and G. Satyanarayana, *J. Org. Chem.*, 2016, **81**, 6409–6423.
- 26 P. Sharma, S. Rohilla and N. Jain, *J. Org. Chem.*, 2017, **82**, 1105–1113.

- 27 H. Li, M. Yang, Y. Qi and J. Xue, *Eur. J. Org. Chem.*, 2011, 2662–2667.
- 28 T. Ishiyama, H. Kizaki, T. Hayashi, A. Suzuki and N. Miyaoura, *J. Org. Chem.*, 1998, **63**, 4726–4731.
- 29 B. M. O’Keefe, N. Simmons and S. F. Martin, *Org. Lett.*, 2008, **10**, 5301–5304.
- 30 F. P. Wu, J. B. Peng, X. Qi and X. F. Wu, *J. Org. Chem.*, 2017, **82**, 9710–9714.
- 31 S. V. Hansen and T. Ulven, *Org. Lett.*, 2015, **17**, 2832–2835.
- 32 P. Hermange, A. T. Lindhardt, R. H. Taaning, K. Bjerglund, D. Lupp and T. Skrydstrup, *J. Am. Chem. Soc.*, 2011, **133**, 6061–6071.
- 33 D. U. Nielsen, X.-M. Hu, K. Daasbjerg and T. Skrydstrup, *Nat. Catal.*, 2018, **1**, 244–254.
- 34 M. Beller and X.-F. Wu, Hydroxy-, Alkoxy- and Aminocarbonylations of C–X Bonds. In *Carbonylative Coupling Reactions with Organometallic Reagents*, in *Transition Metal Catalyzed Carbonylation Reactions: Carbonylative Activation of C–X Bonds*, Springer, Berlin, Heidelberg, 2013, pp. 13–52.
- 35 S. D. Friis, T. L. Andersen and T. Skrydstrup, *Org. Lett.*, 2013, **15**, 1378–1381.
- 36 S. Korsager, R. H. Taaning and T. Skrydstrup, *J. Am. Chem. Soc.*, 2013, **135**, 2891–2894.
- 37 Z. Xin, T. M. Gogsig, A. T. Lindhardt and T. Skrydstrup, *Org. Lett.*, 2012, **14**, 284–287.
- 38 H. Neumann, A. Brennführer, P. Groß, T. Riermeier, J. Almena and M. Beller, *Adv. Synth. Catal.*, 2006, **348**, 1255–1261.
- 39 B. T. Sargent and E. J. Alexanian, *J. Am. Chem. Soc.*, 2016, **138**, 7520–7523.
- 40 K. M. Bjerglund, T. Skrydstrup and G. A. Molander, *Org. Lett.*, 2014, **16**, 1888–1891.
- 41 H. Neumann, A. Brennführer and M. Beller, *Chem. – Eur. J.*, 2008, **14**, 3645–3652.
- 42 L. Kaganovsky, D. Gelman and K. Rueck-Braun, *J. Organomet. Chem.*, 2010, **695**, 260–266.
- 43 S. Couve-Bonnaire, J.-F. Carpentier, A. Mortreux and Y. Castanet, *Tetrahedron Lett.*, 2001, **42**, 3689–3691.
- 44 M. K. Reilly and S. D. Rychnovsky, *Synlett*, 2011, 2392–2396.
- 45 A. N. Cammidge, V. H. Goddard, H. Gopee, N. L. Harrison, D. L. Hughes, C. J. Schubert, B. M. Sutton, G. L. Watts and A. J. Whitehead, *Org. Lett.*, 2006, **8**, 4071–4074.

Supporting information for
Carbonylative Suzuki-Miyaura couplings of sterically hindered aryl halides:
Synthesis of 2-arylbenzoate derivatives.

Aya Ismael,¹ Troels A. Skrydstrup,² and Annette Bayer^{1*}

¹ Department of Chemistry, Faculty of Science and Technology, UiT The Arctic University of Norway, N-9037 Tromsø, Norway.

² Carbon Dioxide Activation Center (CADIAC), Interdisciplinary Nanoscience Center (iNANO) and Department of Chemistry, Aarhus University, Gustav Wieds Vej 14, 8000 Aarhus C, Denmark

Table of content:

| | | |
|--|--|----|
| 1 | Experimental procedures..... | 2 |
| 1.1 | General | 2 |
| 1.2 | General procedures | 2 |
| 1.3 | Preparation and characterization of 2-bromobenzophenone derivatives 5. | 3 |
| 1.4 | Preparation and characterization of 2-benzoylbenzoate esters 2 from 2-bromobenzophenones 5 by alkoxy carbonylation..... | 5 |
| 1.5 | Preparation and characterization of 2-benzoylbenzoate esters 2 from 2-bromobenzoates 6 by Suzuki-Miyaura couplings. | 6 |
| 2 | Additional experimental information..... | 10 |
| 2.1 | Two-chamber set-up: | 10 |
| 2.2 | Screening of catalysts and conditions for the Suzuki- Miyaura coupling of 2-bromoiodobenzene 3 with 4-methoxyphenyl boronic acid 4a..... | 10 |
| Table ESI-1. Carbonylative Suzuki-Miyaura coupling of 2-bromoiodobenzene 3 with 4-methoxyphenyl boronic acid 4a | | 11 |
| 2.3 | Screening of precursors for ex-situ generation of CO. | 11 |
| Table ESI-2. Screening of CO precursors. | | 12 |
| 2.4 | Attempts to hydroxycarbonylate 2-bromoiodobenzene 3 or 2-bromobenzophenone 5a..... | 12 |
| Table ESI-3. Screening of catalyst and conditions for hydroxycarbonylation of 3 or 5a. | | 13 |
| 2.5 | Screening for catalysts and conditions for the alkoxy carbonylation of 2-bromobenzophenone 5a | 13 |
| Table ESI-4. Screening for conditions for alkoxy carbonylation on the 2-bromobenzophenone..... | | 14 |
| Table ESI-5. Control experiments for alkoxy carbonylation with 4-bromobenzophenone..... | | 14 |
| 2.6 | Screening for catalysts and conditions for the carbonylative Suzuki-Miyaura coupling of methyl 2-bromobenzoate 6a..... | 15 |
| Table ESI-6. Optimization of reaction conditions for the palladium catalyzed carbonylative Suzuki-Miyaura coupling of methyl-2-bromobenzoate 6a..... | | 15 |
| 3 | References | 16 |
| 4 | Spectra..... | 17 |
| 4.1 | Spectra for diaryl ketones 5..... | 17 |
| 4.2 | Spectra for butyl 2-benzoylbenzoate esters 2..... | 39 |
| 4.3 | Spectra for methyl 2-benzoylbenzoate esters 2..... | 45 |
| 4.4 | Spectra for products from control experiments for hydroxycarbonylations (section 1.4)..... | 82 |

1 Experimental procedures

1.1 General

Unless otherwise noted, purchased chemicals were used as received without further purification. Solvents were dried according to standard procedures on molecular sieves 4A.¹ MePh₂SiCO₂H (silaCOgen) was prepared as reported previously.² DABO boronates **7a** and sodium trihydroxy(4-methoxyphenyl)borate **8a** were prepared according to the previously reported protocol.³ Flash chromatography was carried out on silica gel 60 (230–400 mesh). NMR spectra were obtained on a 400 MHz NMR spectrometer. The chemical shifts are reported in ppm relative to the solvent residual peak. Data are represented as follows: chemical shift, multiplicity (s = singlet, d = doublet, t = triplet, q = quartet, dt = double triplet, m = multiplet), coupling constant (J, Hz) and integration. Chemical shifts (δ) are reported in ppm relative to the residual solvent peak (CDCl₃: δ H 7.26 and δ C 77.16; Methanol-d₄: δ H 3.31 and δ C 49.00; deuterium oxide: δ H 4.79; DMSO-d₆ δ H 2.51 and δ C 39.52). Positive ion electrospray ionization mass spectrometry was conducted on a Thermo Electron LTQ Orbitrap XL spectrometer. The reactions were performed in the previously reported two-chamber system² under an argon atmosphere, and a glovebox was employed for weighing out the reagents.

1.2 General procedures

General procedure A: Carbonylative Suzuki Miyaura coupling of 2-bromoiodobenzene **3** with slow addition.

Chamber A: 2-Bromoiodobenzene **3** (50 mg, 1.0 equiv, 0.18 mmol), PdCl₂ (0.3 mg, 1 mol%), K₂CO₃ (70 mg, 3 equiv, 0.55 mmol) were dissolved in anisole (1 ml). Chamber B: COgen (107 mg, 2.5 equiv, 0.45 mmol), Pd(dba)₂ (12 mg, 5 mol%), tri-*tert*-butylphosphonium tetrafluoroborate (TTBP•HBF₄) (6.3 mg, 5 mol%) and DIPEA (240 mg, 3 equiv) were dissolved in anisole (3 ml). Chamber B was stirred and heated to 80 °C to release CO until gas evolution stops. After release of the CO, both chambers were stirred and heated to 80 °C and a solution of aryl boronic acid **4** (1.2 equiv) in anisole (2 ml) was added slowly (1-2 h) to the reaction mixture in chamber A. The two-chamber system was then placed in an oil bath and stirred at 80 °C for 20 hours. The reaction mixture was filtered through celite and concentrated on a rotavapor. The crude was purified by column chromatography with pentane: EtOAc (8:2) as eluent.

General procedure B: Carbonylative Suzuki Miura coupling of 2-bromoiodobenzene **3** with instantaneous addition.

Chamber A: 2-Bromoiodobenzene **3** (50 mg, 1.0 equiv, 0.18 mmol), PdCl₂ (0.3 mg, 1 mol%), K₂CO₃ (70 mg, 3 equiv, 0.55 mmol) and aryl boronic acid **4** (1.2 equiv) were dissolved in anisole (3 ml). Chamber B: COgen (107 mg, 2.5 equiv, 0.45 mmol), Pd(dba)₂ (12 mg, 5 mol%), TTBP•HBF₄ (6.3 mg, 5 mol%) were added together and dissolved in anisole (3 ml) before DIPEA (240 mg, 3 equiv) was added. Both chambers were stirred and heated at 80°C under tightly closed system for 20 hours. The reaction mixture was filtered through celite and concentrated on a rotavapor. The crude was purified by column chromatography with pentane: EtOAc (8:2) as eluent.

General procedure C: Carbonylative Suzuki-Miyaura coupling of methyl 2-bromobenzoate **6** with slow addition.

Chamber A: Methyl 2-bromobenzoate **6** (100 mg, 1.0 equiv, 0.47 mmol), PEPPSI-IPr (9.4 mg, 3 mol%), Cs₂CO₃ (450 mg, 3 equiv, 1.4 mmol) were dissolved in anisole (1 ml). Chamber B: COgen (282 mg, 2.5 equiv, 1.2 mmol), Pd(dba)₂ (30 mg, 5 mol%), TTBP•HBF₄ (10 mg, 5 mol%) and DIPEA (240 mg, 3 equiv) were dissolved in anisole (3 ml). The reaction mixture in Chamber B was stirred and heated to 80

ESI : Carbonylative Suzuki-Miyaura couplings of sterically hindered aryl halides.

°C to release CO until gas evolution stops. After release of the CO, both chambers were stirred and heated to 110 °C and a solution of aryl boronic acid **4** (1.5 equiv) in anisole (2 ml) was added slowly (1-2 h) to the reaction mixture in chamber A. The two-chamber system was then placed in an oil bath and stirred at 110 °C for 20 hours. The reaction mixture was filtered through celite and concentrated on a rotavapor. The crude was purified by column chromatography with pentane: EtOAc (7:3) as eluent.

General procedure D: Carbonylative Suzuki-Miyaura coupling of methyl 2-bromobenzoate **6.**

Chamber A: Methyl 2-bromobenzoate **6** (1.0 equiv, 0.47 mmol), aryl boronic acid **4** (1.5 equiv), PEPPSI-IPr (3 mol%), Cs₂CO₃ (3 equiv, 1.4 mmol) were dissolved in anisole (3 ml). Chamber B: COgen (282 mg, 2.5 equiv, 1.2 mmol), Pd(dba)₂ (30 mg, 5 mol%), TTBP•HBF₄ (10 mg, 5 mol%) were dissolved in anisole (3 ml) before DIPEA (450 mg, 3 equiv) was added. The two-chamber system was then placed in an oil bath and stirred at 110 °C for 20 hours. The reaction mixture was filtered through celite and concentrated on a rotavapor. The crude was purified by column chromatography with pentane:EtOAc (7:3) as eluent.

General procedure E: Carbonylative Suzuki Miura coupling of methyl 2-bromobenzoate with DABO boronates or sodium borate salt.

Chamber A: Methyl 2-bromobenzoate **6** (50 mg, 1.0 equiv, 0.23 mmol), Pd(acac)₂ (3.5 mg, 5 mol%), CataCXium A•HI (11 mg, 10 mol%), and the DABO boronate **7** or sodium borate salt **8** (1.5 equiv) were dissolved in toluene: H₂O (1:1; 3 ml). Chamber B: COgen (140 mg, 2.5 equiv, 0.58 mmol), Pd(dba)₂ (26 mg, 5 mol%), TTBP•HBF₄ (13 mg, 5 mol%) were dissolved in anisole (3 ml) before DIPEA (241 mg, 3 equiv) was added. The two-chamber system was then placed in an oil bath and stirred at 110 °C for 20 hours. The reaction mixture was filtered through celite and concentrated on a rotavapor. The crude was purified by column chromatography with pentane:EtOAc (7:3) as eluent.

General procedure F: Alkoxy carbonylation of 2-bromobenzophenone derivatives **5 with *n*-BuOH.**

Chamber A: 2-bromobenzophenone **5** (1 equiv), PdCl₂ (2 mol%), Xantphos (4 mol%), K₂CO₃ (3 equiv) were dissolved in anisole: *n*-BuOH (1:1; 3 ml). Chamber B: COgen (2.5 equiv), Pd(dba)₂ (5 mol%), TTBP•HBF₄ (5 mg, 5 mol%) were dissolved in anisole (3 ml) before DIPEA (3 equiv) was added. The two-chamber system was then placed in an oil bath and stirred under heating for 20 hours. The reaction mixture was filtered through celite and concentrated on a rotavapor. The crude was purified by column chromatography with pentane: EtOAc (7:3).

1.3 Preparation and characterization of 2-bromobenzophenone derivatives **5.**

2-Bromophenyl 4-methoxyphenyl methanone (5a). 2-Bromoiodobenzene **3** (50 mg) was reacted with 4-methoxyphenyl boronic acid **4a** (35 mg, 0.21 mmol, 1.2 equiv). Reactions were performed both by the general procedure A or B to provide **5a** (procedure A: 41 mg, 80%; procedure B: 31 mg, 60%) as a colourless solid. Mp 91-93 °C. NMR: δH (400 MHz; CDCl₃) 7.79 (2H, d, *J* 8.8), 7.64 (1H, d, *J* 7.9), 7.40 (1H, d, *J* 7.9), 7.33 (2H, t, *J* 7.5), 6.94 (2H, d, *J* 8.8), 3.88 (3H, s). δC (101 MHz, CDCl₃) 194.9, 164.6, 141.6, 133.5, 133.1, 131.3, 129.6, 129.2, 127.6, 119.9, 114.4, 56.0. HRMS (ESI): Calcd. for C₁₄H₁₁O₂⁷⁹BrNa [M+H]⁺ 312.9840; found 312.9827. The spectroscopic data is corresponding to the previously reported in literature.⁴

2-Bromophenyl 3-methoxyphenyl methanone (5b). 2-Bromoiodobenzene **3** (50 mg) was reacted with 3-methoxyphenyl boronic acid **4b** (35 mg, 0.21 mmol, 1.2 equiv). Reactions were performed both by the general procedure A or B to provide **5b** (procedure A: 35 mg, 65%; procedure B: 18 mg, 35%) as a white solid. Mp 85-87 °C. NMR: δH (400 MHz, CDCl₃) 7.56 (1H, d, *J* 7.7), 7.36 (1H, s), 7.32 (1H, d, *J* 7.7), 7.26 (3H, t, *J* 7.6), 7.21-7.15 (1H, m), 7.08-7.05 (1H, m), 3.77 (3H, s). δC (101 MHz, CDCl₃) 195.8,

ESI : Carbonylative Suzuki-Miyaura couplings of sterically hindered aryl halides.

160.0, 140.8, 137.6, 133.3, 131.3, 129.7, 129.0, 127.3, 123.6, 120.6, 119.6, 113.8, 55.6. HRMS (ESI): Calcd. for $C_{14}H_{11}O_2^{79}BrNa [M+H]^+$ 312.9840; found 312.9827. The spectroscopic data is corresponding to the previously reported in literature.⁵

2-Bromophenyl 2-methoxyphenyl methanone (5c). 2-Bromiodobenzene **3** (50 mg) was reacted with (2-methoxyphenyl) boronic acid (35 mg, 0.21 mmol, 1.2 equiv) according to the general procedure A to provide **5c** (31 mg, 60%) as a white solid. Mp 66.3-68 °C. NMR: δH (400 MHz, $CDCl_3$) 7.56-7.52 (1H, m), 7.48-7.44 (1H, m), 7.39 (1H, t, J 7.6), 7.27-7.23 (2H, m), 7.19-7.12 (1H, m), 6.91 (1H, t, J 7.6), 6.82-6.80 (1H, m), 3.53 (s, 3H). δC (101 MHz, $CDCl_3$) 195.3, 159.5, 142.8, 134.5, 133.1, 131.9, 131.0, 129.4, 127.3, 127.1, 120.8, 119.6, 112.1, 55.9. HRMS (ESI): Calcd. for $C_{14}H_{11}O_2^{79}BrNa [M+H]^+$ 312.9840; found 312.9827. The spectroscopic data is corresponding to the previously reported in literature.⁵

2-Bromophenyl 4-(methylthio)phenyl methanone (5d). 2-Bromiodobenzene **3** (50 mg) was reacted with (4-(methylthio) phenyl) boronic acid (45 mg, 0.27mmol, 1.5 equiv) according to the general procedure A to provide **5d** (30 mg, 55%) as a white solid. NMR: δH (400 MHz, $CDCl_3$) 7.70 (2H, d, J 8.4), 7.63 (1H, d, J 7.6), 7.40 (1H, d, J 7.6), 7.37-7.27 (2H, m), 7.27-7.20 (2H, m), 2.51 (3H, s). δC (101 MHz, $CDCl_3$) 195.0, 147.3, 140.9, 140.5, 133.3, 132.5, 131.2, 130.7, 129.0, 128.2, 127.4, 125.0, 119.6, 14.8. HRMS (ESI): Calcd. for $C_{14}H_{11}^{81}BrOS [M+H]^+$ 308.9727; found 308.9756

tert-Butyl 2-(2-bromobenzoyl)-1H-pyrrole-1-carboxylate (5e). 2-Bromiodobenzene **3** (50 mg) was reacted with (1-(tert-butoxycarbonyl)-1H-pyrrol-2-yl)boronic acid **4e** (45 mg, 0.21 mmol, 1.2 equiv) according to the general procedure A to provide **5e** (43 mg, 70%) as a yellow oil. NMR: δH (400 MHz, $CDCl_3$) 7.63 (1H, d, J 7.7), 7.48-7.46 (2H, m), 7.38 (2H, t, J 7.5), 7.33 (2H, t, J 7.5), 6.53-6.52 (1H, m), 6.18 (1H, t, J 3.3), 1.56 (9H, s). δC (101 MHz, $CDCl_3$) 184.6, 149.2, 140.9, 134.0, 133.7, 132.1, 130.6, 129.6, 127.5, 125.3, 121.0, 110.9, 85.6, 77.8, 77.7, 77.5, 77.2, 28.0. HRMS (ESI): Calcd. for $C_{16}H_{16}^{81}BrNNaO_3 [M+H]^+$ 374.0278; found 374.0177.

tert-Butyl 2-(2-bromobenzoyl)-1H-indole-1-carboxylate (5f). 2-Bromiodobenzene **3** (50 mg) was reacted with (1-(tert-butoxycarbonyl)-1H-indol-2-yl)boronic acid **4f** (55 mg, 0.21 mmol, 1.5 equiv) according to the general procedure A to provide **5f** (53 mg, 76%) as a yellow oil. NMR: δH (400 MHz, $CDCl_3$) 8.14 (1H, d, J 9.2), 7.69-7.67 (1H, m), 7.58-7.56 (2H, m), 7.49-7.45 (1H, m), 7.44-7.36 (2H, m), 7.28 – 7.24 (1H, m), 6.84 (1H, s), 1.58 (9H, s). δC NMR (101 MHz, $CDCl_3$) 186.0, 149.5, 139.7, 139.2, 137.8, 134.0, 132.4, 131.0, 127.9, 127.4, 127.3, 123.5, 122.9, 121.1, 118.7, 115.0, 84.9, 27.9. HRMS (ESI): Calcd. for $C_{20}H_{18}^{79}BrNNaO_3 [M+H]^+$ 422.0368; found 422.0353.

Methyl 3-(2-bromobenzoyl)benzoate (5g). 2-Bromiodobenzene **3** (50 mg) was reacted with 3-(methoxycarbonyl)phenyl boronic acid **4g** (38 mg, 0.21 mmol, 1.2 equiv) according to the general procedure A to provide **5g** (22 mg, 40 %) as a colorless oil. NMR: δH (400 MHz, $CDCl_3$) 8.43 (1H, s), 8.27 (1H, d, J 7.8), 8.01 (1H, d, J 7.8), 7.67 (1H, d, J 7.8), 7.57(1H, t, J 7.8), 7.47-7.43 (1H, m), 7.41 – 7.36 (2H, m), 3.93 (3H, s). δC (101 MHz, $CDCl_3$) 195.2, 166.3, 140.2, 136.7, 134.5, 134.3, 133.5, 131.7, 131.3, 131.0, 129.3, 129.1, 127.6, 119.7, 52.7. HRMS (ESI): Calcd. for $C_{15}H_{11}O_3^{79}BrNa [M+H]^+$; 340.9789 found 340.9757.

Methyl 2-(2-bromobenzoyl)benzoate (5h). 2-Bromiodobenzene **3** (50 mg) was reacted with 2-(methoxycarbonyl) phenyl boronic acid **4h** (35 mg, 0.21 mmol, 1.2 equiv) according to the general procedure A to provide **5h** (33 mg, 58%) as a viscous colourless oil. NMR: δH (400 MHz, $CDCl_3$) 7.88-7.86 (1H, m), 7.70-7.68 (1H, m), 7.60-7.57 (2H, m), 7.50-7.48 (1H, m), 7.39-7.36 (1H, m), 7.33-7.31 (2H, m), 3.69 (3H, s). δC (101 MHz, $CDCl_3$) 195.49, 167.58, 140.09, 138.43, 134.68, 132.64, 131.78, 131.27, 131.15, 129.94, 129.57, 127.16, 121.55, 77.48, 77.16, 76.84, 52.72. HRMS (ESI): Calcd. for $C_{15}H_{11}O_3^{81}BrNa [M+H]^+$; 342.9769 found 342.9757. The spectroscopic data is corresponding to the previously reported in literature.⁶

4-(2-Bromobenzoyl)benzonitrile (5i). 2-Bromiodobenzene **3** (50 mg) was reacted with (4-cyanophenyl) boronic acid **4i** (31 mg, 0.21 mmol, 1.2 equiv). Reactions were performed both by the general procedure A or B to provide **5i** (procedure A: 15 mg, 30%; procedure B: 0 mg, 0%) as a white solid. Mp 113-115

ESI : Carbonylative Suzuki-Miyaura couplings of sterically hindered aryl halides.

$^{\circ}\text{C}$. NMR: δH (400 MHz, CDCl_3) 7.90 (2H, d, J 8.2), 7.77 (2H, d, J 8.2), 7.67 (1H, d, J 7.8), 87.49 – 7.39 (1H, m), 7.38-7.36 (1H, m). δC (101 MHz, CDCl_3) 194.6, 139.6, 139.4, 133.6, 132.6, 132.1, 130.5, 129.4, 127.7, 119.7, 118.0, 116.9. HRMS (ESI): Calcd. for C_{14}H_8 $^{79}\text{BrNNaO}$ $[\text{M}+\text{H}]^+$ 307.9687; found 307.9672. The spectroscopic data is corresponding to the previously reported in literature.⁷

3-(2-Bromobenzoyl)benzotrile (5j). 2-Bromiodobenzene **3** (50 mg) was reacted with (3-cyanophenyl) boronic acid **4j** (31 mg, 0.21 mmol, 1.2 equiv). Reactions were performed following the general procedure A or B to provide **5j** (procedure A: 33 mg, 65%; procedure B: 15 mg, 30%) as a colorless oil. NMR: δH (400 MHz, CDCl_3) 8.06 (1H, d, J 8.2), 8.03 (1H, s), 7.87 (1H, d, J 7.7), 7.68 (1H, d, J 7.7), 7.62 (1H, t, J 7.8), 7.49-7.40 (2H, m), 7.37-7.35 (1H, m). δC (101 MHz, CDCl_3) 194.0, 139.4, 137.2, 136.6, 133.9, 133.8, 133.6, 132.1, 129.9, 129.3, 127.8, 119.6, 117.9, 113.4. HRMS (ESI): Calcd. for C_{14}H_8 $^{81}\text{BrNNaO}$ $[\text{M}+\text{H}]^+$ 309.9666; found 309.9653.

2-Bromophenyl 4-fluorophenyl methanone (5k). 2-Bromiodobenzene **3** (50 mg) was reacted with (4-fluorophenyl) boronic acid **4k** (30 mg, 0.13mmol, 1.2 equiv), according to the general procedure A to provide **5k** (15 mg, 30%) as a white solid. Mp 51-53 $^{\circ}\text{C}$. NMR: δH (400 MHz, CDCl_3) 7.84 (2H, m), 7.65 (1H, d, J 7.8), 7.45-7.41 (1H, m), 7.40-7.30 (2H, m), 7.14 (2H, t, J 8.5). δC (101 MHz, CDCl_3) 194.5, 166.3 (d, J 256.5), 140.6, 133.4, 133.0 (d, J 10.1), 132.7 (d, J 2.9), 131.4, 129.0, 127.5, 119.6, 116.0 (d, J 22.2). HRMS (ESI): Calcd. for C_{13}H_8 $^{79}\text{BrFNaO}$ $[\text{M}+\text{H}]^+$ 300.9640; found 300.9630. The spectroscopic data is corresponding to the previously reported in literature.⁸

2-Bromophenyl 3-fluorophenyl methanone (5l). 2-Bromiodobenzene **3** (50 mg) was reacted with 3-fluorophenyl boronic acid **4l** (30 mg, 0.13 mmol, 1.2 equiv), according to the general procedure A to provide **5l** (37 mg, 76%) as a white solid. NMR: δH (400 MHz, CDCl_3) 7.66 (1H, d, J 7.8), 7.54 (2H, t, J 9.7), 7.47-7.42 (2H, m), 7.40-7.34 (2H, m), 7.33-7.28 (1H, m). δC (101 MHz, CDCl_3) 194.7, 162.9 (d, J 249.5), 140.2, 138.4 (d, J 6.1), 133.5, 131.6, 130.5 (d, J 8.1), 129.1, 127.5, 126.3 (d, J 3.0), 120.9 (d, J 22.2), 119.6, 116.7 (d, J 22.2). HRMS (ESI): Calcd. for C_{13}H_8 $^{79}\text{BrFNaO}$ $[\text{M}+\text{H}]^+$ 300.9640; found 300.9630.

2-Bromophenyl 2-fluorophenyl methanone (5m). 2-Bromiodobenzene **3** (50 mg) was reacted with 2-fluorophenyl boronic acid **4m** (30 mg, 0.13 mmol, 1.2 equiv) according to the general procedure A to provide **5m** (39 mg, 80%) as a white solid. NMR: δH (400 MHz, CDCl_3) 7.61 (1H, t, J 7.5), 7.47 (1H, d, J 7.8), 7.44-7.38 (1H, m), 7.26-7.25 (2H, m), 7.23-7.17 (1H, m), 7.10 (1H, t, J 7.6), 6.97-6.92 (1H, m). δC (101 MHz, CDCl_3) 192.90, 161.8 (d, J 259.6), 141.7, 135.23 (d, J 8.1), 133.5, 131.8, 129.4, 127.5, 125.9 (d, J 10.1), 124.5 (d, J 3.0), 119.5, 116.8 (d, J 22.2). HRMS (ESI): Calcd. for C_{13}H_8 $^{81}\text{BrFNaO}$ $[\text{M}+\text{H}]^+$ 302.9620; found 302.9608.

1.4 Preparation and characterization of 2-benzoylbenzoate esters **2** from 2-bromobenzophenones **5** by alkoxyacylation.

Butyl 2-(4-methoxybenzoyl)benzoate (2a). (2-Bromophenyl)(4-methoxyphenyl)methanone **5a** (40 mg, 0.14 mmol) was transformed to **2a** (28 mg, 65%) according to the general procedure F. NMR: δH (400 MHz, CDCl_3) 8.05 (1H, d, J 8.8), 7.73 (2H, d, J 8.9), 7.63-7.59 (1H, m), 7.56-7.52 (1H, m), 7.36 (1H, d, J 8.8), 6.90 (2H, d, J 8.9), 4.05 (2H, t, J 6.6), 3.85 (3H, s), 1.46-1.39 (2H, m), 1.27-1.18 (3H, m), 0.82 (3H, t, J 7.4). δC (101 MHz, CDCl_3) 195.82, 166.24, 163.69, 142.06, 132.32, 131.92, 130.41, 130.32, 129.41, 129.38, 127.67, 113.83, 77.48, 77.16, 76.84, 65.53, 55.62, 30.40, 19.21, 13.78. HRMS (ESI): Calcd. for $\text{C}_{19}\text{H}_{20}\text{NaO}_4$ $[\text{M}+\text{H}]^+$ 335.1259; found 335.1260.

Butyl 2-(3-methoxybenzoyl)benzoate (2b). (2-Bromophenyl)(3-methoxyphenyl)methanone **5b** (30 mg, 0.1 mmol) was transformed to **2b** (19 mg, 60%) according to the general procedure F. NMR: δH (400 MHz, CDCl_3) 8.06 (1H, d, J 7.6), 7.63 (1H, t, J 7.5), 7.56 (1H, t, J 7.5), 7.44-7.43 (1H, m), 7.39-7.37 (1H, m), 7.30 (1H, t, J 7.9), 7.21-7.18 (1H, m), 7.11-7.09 (1H, m), 4.05 (2H, t, J 6.6), 3.84 (3H, s), 1.48 – 1.41 (2H, m), 1.28-1.15 (2H, m), 0.83 (3H, t, J 7.4). δC (101 MHz, CDCl_3) 196.9, 166.1, 159.9, 141.8,

ESI : Carbonylative Suzuki-Miyaura couplings of sterically hindered aryl halides.

138.6, 132.4, 130.3, 129.7, 129.6, 129.6, 127.8, 122.9, 120.0, 113.1, 77.5, 77.2, 76.8, 65.6, 55.6, 30.4, 19.2, 13.8. HRMS (ESI): Calcd. for $C_{19}H_{20}NaO_4$ $[M+H]^+$ 335.1259; found 335.1260.

Butyl 2-(4-fluorobenzoyl)benzoate (2c). (2-Bromophenyl)(4-fluorophenyl)methanone **5k** (15mg, 0.054 mmol), was transformed to **2c** (10 mg, 63%) according to the general procedure F. δ H (400 MHz, $CDCl_3$) 8.07 (1H, d, J 8.6), 7.81-7.77 (2H, m), 7.66-7.62 (1H, m), 7.59-7.55 (1H, m), 7.37 (1H, d, J 8.6), 7.10 (2H, t, J 8.6), 4.06 (2H, t, J 6.6), 1.49-1.41 (2H, m), 1.27-1.21 (3H, m), 0.84 (3H, t, J 7.4). δ C (101 MHz, $CDCl_3$) 195.6, 166.0, 165.9 (d, J 255.5), 141.6, 133.8, 132.5, 132.2, 132.2 (d, J 10.1), 132.1, 130.4, 129.8, 129.4, 127.6, 115.9, 115.7, 77.5, 77.2, 76.8, 65.6, 30.4, 19.2, 13.9, 13.8. HRMS (ESI): Calcd. for $C_{18}H_{17}FNaO_3$ $[M+H]^+$ 323.1059; found 323.1059.

Butyl 2-(2-fluorobenzoyl)benzoate (2d). (2-Bromophenyl)(4-methoxyphenyl)methanone **5m** (40 mg, 0.47 mmol) was transformed to **2d** (22 mg, 50%) according to the general procedure F. NMR: δ H (400 MHz, $CDCl_3$) 8.53 (1H, d, J 7.6), 8.38-8.33 (1H, m), 8.12-8.10 (1H, m), 8.07-8.05 (1H, m), 7.89-7.87 (2H, m), 7.77-7.75 (1H, m), 7.69-7.61 (1H, m), 7.60-7.55 (1H, m), 4.62 (2H, t, J 6.6), 2.03-1.99 (2H, m), 1.84-1.71 (3H, m), 1.36 (3H, t, J 7.4). δ C (101 MHz, $CDCl_3$) 193.7, 166.3, 163.2, 161.9 (d, J 258.6), 160.7, 143.5, 134.99, 135.0 (d, J 9.1), 134.6, 132.3, 131.5, 130.1, 129.7, 127.0, 125.9, 124.3 (d, J 4.0), 124.3, 117.0, 116.9 (d, J 23.2), 116.8, 65.6, 30.5, 19.2, 13.8. HRMS (ESI): Calcd. for $C_{18}H_{17}FNaO_3$ $[M+H]^+$ 323.1059; found 323.1059.

1.5 Preparation and characterization of 2-benzoylbenzoate esters **2** from 2-bromobenzoates **6** by Suzuki-Miyaura couplings.

Methyl 2-(4-methoxybenzoyl)benzoate (2aa). Methyl 2-bromobenzoate **6a** (100 mg for procedure C and D; 50 mg for procedure E) was reacted with 4-methoxyphenyl boronic acid **4a** (105 mg, 1.5 equiv, 0.66 mmol), DABO boronate 2-(4-methoxyphenyl)-1,3,6,2-dioxazaboroane **7a** (82 mg, 1.5 equiv, 0.37 mmol) or sodium trihydroxy(4-methoxyphenyl)borate **8a** (72 mg, 1.5 equiv, 0.37 mmol). Reactions were performed following general procedure C, D or E to provide **2aa** as a colorless oil. Procedure C with **4a**: 100 mg, 80%; procedure D with **4a**: 80 mg, 63%; procedure E with **7a**: 45 mg, 67%; procedure E with **8a**: 44 mg, 65%. NMR: δ H (400 MHz, $CDCl_3$) 8.02 (1H, d, J 7.6), 7.71 (2H, d, J 8.8), 7.61 (1H, t, J 7.5), 7.53 (1H, t, J 7.5), 7.37 (1H, d, J 7.6), 6.89 (2H, d, J 8.8), 3.83 (3H, s), 3.63 (3H, s). δ C (101 MHz, $CDCl_3$) 195.9, 166.5, 163.6, 142.1, 132.4, 132.3, 131.7, 130.3, 130.2, 129.4, 129.2, 127.8, 113.8, 55.6, 52.3. HRMS (ESI): Calcd. for $C_{16}H_{14}NaO_4$ $[M+H]^+$ 293.0790; found 293.0784. The spectroscopic data is corresponding to the previously reported in literature.⁶

Methyl 2-(3-methoxybenzoyl) benzoate (2ab). Methyl 2-bromobenzoate **6a** (100 mg) was reacted with 3-methoxyphenyl boronic acid **4b** (105 mg, 1.5 equiv, 0.66 mmol) according to the general procedure C to provide **2ab** (65 mg, 52%) as a colorless oil. NMR: δ H (400 MHz, $CDCl_3$) 7.90 (1H, d, J 8.7), 7.61-7.46 (1H, m), 7.46-7.33 (1H, m), 7.28 (2H, s), 7.21-7.08 (1H, m), 7.05 (1H, d, J 7.7), 6.96 (1H, dd, J 8.7, 3.2), 3.70 (3H, s), 3.50 (3H, s). δ C (101 MHz, $CDCl_3$) 196.9, 166.5, 159.9, 141.8, 138.6, 132.5, 132.0, 131.2, 130.1, 130.0, 129.7, 129.6, 129.3, 129.0, 127.8, 122.5, 119.8, 113.0, 55.5, 55.3, 52.7, 52.3. HRMS (ESI): Calcd. for $C_{16}H_{14}NaO_4$ $[M+H]^+$ 293.0790; found 293.0784.

Methyl 2-(2-methoxybenzoyl)benzoate (2ac). Methyl 2-bromobenzoate **6a** (100 mg) was reacted with 2-methoxyphenyl boronic acid **4c** (105 mg, 1.5 equiv, 0.66 mmol) according to the general procedure C to provide **2ac** (93 mg, 74%) as a white solid, Mp 100-103 °C. NMR: δ H (400 MHz, $CDCl_3$) 7.87 (1H, d, J 8.7), 7.74-7.67 (1H, m), 7.53 (1H, t, J 7.5), 7.50-7.42 (2H, m), 7.36 (1H, d, J 8.7), 6.99 (1H, t, J 7.9), 6.90 (1H, d, J 8.3), 3.59 (3H, s), 3.57 (3H, s). δ C (101 MHz, $CDCl_3$) 195.7, 167.3, 159.0, 143.8, 134.2, 131.7, 131.6, 129.5, 129.3, 127.5, 127.0, 120.5, 112.2, 77.4, 55.7, 52.1. HRMS (ESI): Calcd. for $C_{16}H_{14}NaO_4$ $[M+H]^+$ 293.0790; found 293.0784.

Methyl 2-(4-(methylthio)benzoyl) benzoate (2ad). Methyl 2-bromobenzoate **6a** (100 mg) was reacted with 4-(methylthio) phenyl boronic acid (110 mg, 1.5 equiv, 0.65 mmol) according to the general procedure C to provide (101 mg, 76%) as a white solid, Mp 84-87 °C. 1H NMR (400 MHz, $CDCl_3$) δ

ESI : Carbonylative Suzuki-Miyaura couplings of sterically hindered aryl halides.

8.02 (1H, d, *J* 8.6), 7.64 (2H, d, *J* 8.5), 7.61-7.59 (1H, m), 7.53-7.51 (1H, m), 7.36 (2H, d, *J* 8.6), 7.21 (2H, d, *J* 8.5), 3.62 (3H, s), 2.47 (3H, s). δ C NMR (101 MHz, CDCl₃) 196.1, 166.4, 146.1, 141.8, 133.5, 132.4, 130.1, 129.7, 129.5, 129.1, 127.7, 124.9, 52.3, 14.7. HRMS (ESI): Calcd. for C₁₆H₁₄ NaO₃S [M+H]⁺ 309.0561; found 309.0559.

Methyl 2-(3-(methoxycarbonyl)benzoyl)benzoate (2ag). Methyl 2-bromobenzoate **6a** (100 mg) was reacted with 3-(methoxycarbonyl)phenyl boronic acid **4g** (125 mg, 1.5 equiv, 0.70 mmol) according to the general procedure C to provide **2ag** (65 mg, 47%) as a colorless oil. NMR: δ H (400 MHz, CDCl₃) 8.37 (1H, s), 8.23-8.21 (1H, m), 8.07 (1H, d, *J* 8.6), 7.96-7.95 (1H, m), 7.70-7.63 (1H, m), 7.63-7.56 (1H, m), 7.53 (1H, t, *J* 7.8), 7.40 (1H, d, *J* 8.6), 3.90 (3H, s), 3.64 (3H, s). δ C (101 MHz, CDCl₃) 196.4, 166.4, 141.4, 137.7, 134.0, 133.4, 132.8, 130.8, 130.5, 130.4, 130.0, 129.2, 128.9, 127.8, 52.5, 52.4. HRMS (ESI): Calcd. for C₁₇H₁₄ NaO₅ [M+H]⁺ 321.0739; found 321.0730

Dimethyl 2,2'-carbonyldibenzoate (2ah). Methyl 2-bromobenzoate **6a** (100 mg) was reacted with 2-(methoxycarbonyl)phenyl boronic acid **4h** (125 mg, 1.5 equiv, 0.70 mmol). Reactions were performed both by the general procedure C and D to provide **2ah** as a white solid, Mp 205-207 °C. Procedure C: 103 mg, 75%; procedure D: 36 mg, 26%. NMR: δ H (400 MHz, CDCl₃) 7.78 (2H, d, *J* 8.6), 7.58-7.56 (2H, m), 7.53-7.48 (2H, m), 7.40 (2H, d, *J* 8.6), 3.73 (6H, s). δ C (101 MHz, CDCl₃) 195.7, 168.3, 138.5, 132.0, 131.4, 131.2, 129.7, 129.4, 128.9, 77.4, 52.6. HRMS (ESI): Calcd. for C₁₇H₁₄ NaO₅ [M+H]⁺ 321.0739; found 321.0730.

Methyl 2-(4-cyanobenzoyl) benzoate (2ai). Methyl 2-bromobenzoate **6a** (100 mg) was reacted with 4-cyanophenyl boronic acid **4i** (102 mg, 1.5 equiv, 0.7 mmol). Reactions were performed following general procedure C or D to provide **2ai** as a colourless oil. Procedure C: 40 mg, 32%; procedure D: 20 mg, 16%. NMR: δ H (400 MHz, CDCl₃) 8.08 (1H, d, *J* 8.6), 7.83 (2H, d, *J* 8.6), 7.73 (2H, d, *J* 8.6), 7.69-7.67 (1H, m), 7.64 – 7.60 (1H, m), 7.40 (1H, d, *J* 8.6), 3.67 (3H, s). δ C (101 MHz, CDCl₃) 195.4, 165.8, 140.6, 140.2, 132.7, 132.2, 130.1, 130.0, 129.2, 128.8, 127.4, 117.8, 116.0, 52.3. HRMS (ESI): Calcd. for C₁₆H₁₁NNaO₃ [M+H]⁺ 288.0637; found 288.0630.

Methyl 2-(3-cyanobenzoyl) benzoate (2aj). Methyl 2-bromobenzoate **6a** (100 mg) was reacted with (3-cyanophenyl) boronic acid **4j** (102 mg, 1.5 equiv, 0.7 mmol). Reactions were performed following general procedure C or D to provide **2aj** as a colourless oil. Procedure C: 48 mg, 40%; procedure D: 32 mg, 26%. NMR: δ H (400 MHz, CDCl₃) 8.10 (1H, d, *J* 8.6), 8.03-7.01 (1H, m), 7.96 (1H, s), 7.83-7.81 (1H, m), 7.70 (1H, t, *J* 7.5), 7.66 – 7.59 (1H, m), 7.58-7.56 (1H, m), 7.38 (1H, d, *J* 8.6), 3.70 (3H, s). δ C NMR (101 MHz, CDCl₃) 195.5, 166.4, 141.1, 138.6, 136.3, 133.4, 133.3, 133.2, 130.9, 130.6, 130.1, 129.3, 127.9, 118.4, 113.5, 52.9. Calcd. for C₁₆H₁₁NNaO₃ [M+H]⁺ 288.0637; found 288.0630.

Methyl 2-(4-fluorobenzoyl) benzoate (2ak). Methyl 2-bromobenzoate **6a** (100 mg for procedure C; 50 mg for procedure E) was reacted with 4-fluorophenyl boronic acid **4k** (100 mg, 1.5 equiv, 0.7 mmol) or 2-(4-fluorophenyl)-1,3,6,2-dioxazaborocane **7k** (73 mg, 1.5 equiv, 0.35 mmol) according to the general procedure C or E to provide **2ak** as a colourless oil. Procedure C: 45 mg, 37%; procedure E: 15 mg, 25%. NMR: δ H (400 MHz, CDCl₃) 8.05 (1H, d, *J* 8.7), 7.79-7.75 (2H, m), 7.66-7.62 (1H, m), 7.59-7.55 (1H, m), 7.38 (1H, d, *J* 8.7), 7.12-7.07 (2H, m), 3.65 (3H, s). δ C (101 MHz, CDCl₃) 195.5, 166.4, 165.8 (d, *J* 256.5), 164.4, 141.5, 133.8 (d, *J* 3.0), 132.5, 132.0 (d, *J* 9.1), 130.3, 129.8, 129.2, 127.6, 115.8 (d, *J* 20.2), 52.3. HRMS (ESI): Calcd. for C₁₅H₁₁ FNaO₃ [M+H]⁺ 281.0590; found 281.0584. The spectroscopic data is corresponding to the previously reported in literature.⁶

Methyl 2-(3-fluorobenzoyl) benzoate (2al). Methyl 2-bromobenzoate **6a** (100 mg) was reacted with (3-fluorophenyl) boronic acid **4l** (100 mg, 1.5 equiv, 0.7 mmol). Reactions were performed following general procedure C or D to provide **2al** as a colorless oil. Procedure C: 70 mg, 58%; procedure D: 51 mg, 43%. NMR: δ H (400 MHz, CDCl₃) 8.06 (1H, d, *J* 8.7), 7.67-7.63 (1H, m), 7.60-7.56 (1H, m), 7.50-7.44 (2H, m), 7.41-7.35 (2H, m), 7.29-7.21 (1H, m), 3.66 (3H, s). δ C (101 MHz, CDCl₃) 196.2, 166.6, 163.2 (d, *J* 249.5), 141.8, 139.7 (d, *J* 7.1), 133.0, 130.7, 130.6, 130.3, 129.5, 128.1, 125.5 (d, *J* 3.0), 120.6 (d, *J* 21.6), 116.1 (d, *J* 23.2), 52.7. HRMS (ESI): Calcd. for C₁₅H₁₁ FNaO₃ [M+H]⁺ 281.0590; found 281.0584.

ESI : Carbonylative Suzuki-Miyaura couplings of sterically hindered aryl halides.

Methyl 2-(2-fluorobenzoyl) benzoate (2am). Methyl 2-bromobenzoate **6a** (100 mg for procedure C and D; 50 mg for procedure E) was reacted with 2-fluorophenyl boronic acid **4m** (100 mg, 1.5 equiv, 0.7 mmol) or 2-(2-fluorophenyl)-1,3,6,2-dioxazaborocane **7m** (73 mg, 1.5 equiv, 0.35 mmol). Reactions were performed following general procedure C, D or E to provide **2am** as a white solid, Mp 56-59 °C. Procedure C: 78 mg, 65%; procedure D: 50 mg, 42%; procedure E: 21 mg, 35%. NMR: δ H (400 MHz, CDCl₃) 8.02 (1H, d, *J* 8.8), 7.85-7.81 (1H, m), 7.67-7.63 (1H, m), 7.61-7.52 (2H, m), 7.44-7.42 (1H, m), 7.31-7.24 (1H, m), 7.12-7.07 (1H, m), 3.72 (3H, s). δ C (101 MHz, CDCl₃) 193.8, 166.8, 161.7 (d, *J* 258.6), 134.8 (d, *J* 9.1), 132.5, 131.3, 130.00 (d, *J* 19.2), 128.9, 127.2, 125.9 (d, *J* 10.0), 124.3 (d, *J* 4.0), 116.87 (d, *J* 22.2), 52.4. HRMS (ESI): Calcd. for C₁₅H₁₁FNao₃ [M+H]⁺ 281.0590; found 281.0584.

Methyl 2-(thiophene-2-carbonyl) benzoate (2an). Methyl 2-bromobenzoate **6a** (50 mg), was reacted with 2-(thiophen-2-yl)-1,3,6,2-dioxazaborocane **7n** (69 mg, 1.5 equiv, 0.35 mmol) according to the general procedure E to provide **2an** (29 mg, 50%) as a colourless oil. NMR: δ H (400 MHz, CDCl₃) 8.02 (1H, d, *J* 7.6), 7.65-7.61 (2H, m), 7.58-7.54 (2H, m), 7.45 (1H, d, *J* 7.6), 7.35-7.33 (1H, m), 3.67 (3H, s). δ C (101 MHz, CDCl₃) 190.7, 166.7, 142.8, 142.2, 133.9, 132.4, 130.3, 129.9, 129.3, 127.8, 127.4, 126.8, 52.4. The spectroscopic data is corresponding to the previously reported in literature.⁹

Methyl 2-(benzo[b]thiophene-2-carbonyl) benzoate (2ao). Methyl 2-bromobenzoate **6a** (50 mg), was reacted with 2-(benzo[b]thiophen-2-yl)-1,3,6,2-dioxazaborocane **7o** (86 mg, 1.5 equiv, 0.35 mmol) according to the general procedure E to provide **2ao** (55 mg, 75%) as a yellow solid. Mp 78-80 °C. NMR: δ H (400 MHz, CDCl₃) 7.89 (1H, d, *J* 7.5), 7.68 (1H, d, *J* 8.0), 7.57 (1H, d, *J* 8.0), 7.48-7.45 (2H, m), 7.42 – 7.39 (1H, m), 7.33(1H, d, *J* 7.5), 7.25-7.22 (1H, m), 7.17-7.14 (1H, m), 3.48 (3H, s). δ C (101 MHz, CDCl₃) 190.7, 166.3, 144.1, 142.8, 140.8, 138.9, 132.4, 131.6, 130.3, 130.1, 129.2, 127.7, 127.5, 126.1, 125.0, 123.0, 52.4. HRMS (ESI): Calcd. for C₁₇H₁₂NaO₃S [M+H]⁺ 319.0405; found 319.0407.

Methyl 5-fluoro-2-(4-methoxybenzoyl)benzoate (2ba). Methyl 2-bromo-5-fluorobenzoate **6b** (50 mg, 0.21 mmol), was reacted with (4-methoxyphenyl) boronic acid **4a** (48 mg, 1.5 equiv, 0.32 mmol) according to the general procedure E to provide **2ba** (44 mg, 72%) as a colourless oil. NMR: δ H (400 MHz, CDCl₃) 7.72-7.68 (3H, m), 7.44-7.37 (1H, m), 7.33-7.28 (1H, m), 6.92-6.90 (2H, m), 3.85 (3H, s), 3.64 (3H, s). δ C (101 MHz, CDCl₃) 194.8, 165.5 (d, *J* 3.0), 163.8, 162.8 (d, *J* 251.5), 138.1 (d, *J* 3.0), 131.7, 130.2, 130.0 (d, *J* 8.1), 119.4 (d, *J* 22.2), 117.2 (d, *J* 23.2), 113.9, 77.4, 55.6, 52.6. HRMS (ESI): Calcd. for C₁₆H₁₃FNao₄ [M+H]⁺ 311.0696; found 311.0695.

Methyl 4-fluoro-2-(4-methoxybenzoyl)benzoate (2ca). Methyl 2-bromo-4-fluorobenzoate **6c** (57 mg, 0.24 mmol), was reacted with (4-methoxyphenyl) boronic acid **4a** (48 mg, 1.5 equiv, 0.32 mmol) according to the general procedure E to provide **2ca** (35 mg, 50%) as a colourless oil. NMR: δ H (400 MHz, CDCl₃) 8.08 (1H, dd, *J* 8.7, 5.4), 7.72 (2H, d, *J* 9.0), 7.24-7.19 (1H, m), 7.07 (1H, dd, *J* 8.3, 2.6), 6.92 (2H, d, *J* 9.0), 3.86 (3H, s), 3.64 (3H, s). δ C (101 MHz, CDCl₃) 194.2, 165.5, 164.9 (d, *J* 257.5), 163.9, 145.1 (d, *J* 7.1), 133.1 (d, *J* 10.1), 131.8, 129.7, 125.2 (d, *J* 3.0), 116.5 (d, *J* 21.2), 115.2 (d, *J* 24.2), 114.0, 55.7, 52.4. HRMS (ESI): Calcd. for C₁₆H₁₃FNao₄ [M+H]⁺ 311.0696; found 311.0695.

Methyl 5-chloro-2-(4-methoxybenzoyl)benzoate (2da). Methyl 2-bromo-5-chlorobenzoate **6d** (50 mg, 0.20 mmol), was reacted with (4-methoxyphenyl) boronic acid **4a** (45 mg, 1.5 equiv, 0.30 mmol) according to the general procedure E to provide **2da** (30 mg, 50%) as a colourless oil. NMR: δ H (400 MHz, CDCl₃) 8.01 (1H, d, *J* 2.1), 7.71 (2H, d, *J* 9.0), 7.59 (1H, dd, *J* 8.1, 2.1), 7.33 (1H, d, *J* 8.1), 6.91 (2H, d, *J* 9.0), 3.86 (3H, s), 3.65 (3H, s). δ C (101 MHz, CDCl₃) 194.8, 165.5, 163.9, 140.4, 135.7, 132.4, 131.8, 131.0, 130.3, 130.1, 129.3, 114.0, 55.6, 52.7. HRMS (ESI): Calcd. for C₁₆H₁₃ClNaO₄ [M+H]⁺ 327.0400; found 327.0401.

Methyl 4-chloro-2-(4-methoxybenzoyl)benzoate (2ea). Methyl 2-bromo-4-chlorobenzoate **6e** (50 mg, 0.20 mmol), was reacted with (4-methoxyphenyl) boronic acid **4a** (46 mg, 1.5 equiv, 0.30 mmol) according to the general procedure E to provide **2ea** (40 mg, 65%) as a colourless oil. NMR: δ H (400 MHz, CDCl₃) 7.99 (1H, d, *J* 8.4), 7.72 (2H, d, *J* 9.0), 7.51 (1H, dd, *J* 8.4, 2.0), 7.36 (2H, d, *J* 2.0), 6.92 (2H, d, *J* 9.0), 3.86 (3H, s), 3.65 (3H, s). δ C (101 MHz, CDCl₃) 194.2, 165.7, 163.9, 143.8, 139.1, 131.8,

ESI : Carbonylative Suzuki-Miyaura couplings of sterically hindered aryl halides.

131.8, 129.8, 129.6, 127.9, 127.4, 114.0, 55.7, 52.5. HRMS (ESI): Calcd. for C₁₆H₁₃ClNaO₄ [M+H]⁺ 327.0400; found 327.0402.

Methyl 2-(4-methoxybenzoyl)-5-methylbenzoate (2fa). Methyl 2-bromo-5-methylbenzoate **6f** (57 mg, 0.19 mmol), was reacted with (4-methoxyphenyl) boronic acid **4a** (49 mg, 1.5 equiv, 0.32 mmol) according to the general procedure E to provide **2fa** (50 mg, 71%) as a colourless oil. NMR: δH (400 MHz, CDCl₃) 7.82 (1H, s), 7.72 (2H, d, *J* 9.0), 7.41 (1H, d, *J* 8.4), 7.28 (1H, d, *J* 7.7), 6.89 (2H, d, *J* 9.0), 3.84 (3H, s), 3.60 (3H, s), 2.45 (3H, s). δC (101 MHz, CDCl₃) 196.0, 166.9, 163.5, 139.8, 139.2, 132.9, 131.7, 130.6, 129.4, 128.0, 113.8, 77.4, 55.6, 52.2, 21.3. HRMS (ESI): Calcd. for C₁₇H₁₆NaO₄ [M+H]⁺ 307.0900; found 307.0947.

Methyl 2-(4-methoxybenzoyl)-3-methylbenzoate (2ga). Methyl 2-bromo-3-methylbenzoate **6g** (59 mg, 0.26 mmol), was reacted with (4-methoxyphenyl) boronic acid **4a** (49 mg, 1.5 equiv, 0.32 mmol) according to the general procedure E to provide **2ga** (50 mg, 68%) as a colourless oil. NMR: δH (400 MHz, CDCl₃) 7.92 (1H, d, *J* 8.5), 7.73-7.71 (2H, m), 7.45-7.40 (2H, m), 6.90 (2H, d, *J* 9.1), 3.84 (3H, s), 3.67 (3H, s), 2.17 (3H, s). δC (101 MHz, CDCl₃) 197.0, 166.4, 163.7, 141.9, 135.6, 135.0, 131.1, 130.7, 128.6, 128.3, 127.9, 114.0, 77.4, 19.3. HRMS (ESI): Calcd. for C₁₇H₁₆NaO₄ [M+H]⁺ 307.0946; found 307.0945.

Methyl 4-methoxy-2-(4-methoxybenzoyl) benzoate (2ha). Methyl 2-bromo-4-methoxybenzoate **6h** (50 mg, 0.20 mmol), was reacted with (4-methoxyphenyl) boronic acid **4a** (46 mg, 1.5 equiv, 0.30 mmol) according to the general procedure E to provide **2ha** (47 mg, 77%) as a colourless oil. NMR: δH (400 MHz, CDCl₃) 8.01 (1H, d, *J* 8.8), 7.73 (2H, d, *J* 9.0), 7.00 (1H, dd, *J* 8.8, 2.6), 6.89 (2H, d, *J* 9.0), 6.83 (1H, d, *J* 2.6), 3.85 (3H, s), 3.84 (3H, s), 3.61 (3H, s). δC (101 MHz, CDCl₃) 195.6, 166.0, 163.6, 162.9, 144.6, 132.4, 131.7, 130.2, 120.9, 114.8, 113.9, 112.7, 77.4, 55.8, 55.6, 52.0. HRMS (ESI): Calcd. for C₁₇H₁₆NaO₅ [M+H]⁺ 323.0895; found 323.0894.

Methyl 2-(4-methoxybenzoyl)-5-methylbenzoate (2ia). Methyl 2-bromo-4,5-dimethoxybenzoate **6i** (50 mg, 0.18 mmol), was reacted with (4-methoxyphenyl) boronic acid **4a** (40 mg, 1.5 equiv, 0.26 mmol) according to the general procedure E to provide **2ia** (44 mg, 73%) as a white solid, Mp 151-153 °C. NMR: δH (400 MHz, CDCl₃) 7.70 (2H, d, *J* 9.0), 7.50 (1H, s), 6.89 (2H, d, *J* 9.0), 6.84 (1H, s), 3.97 (3H, s), 3.90 (3H, s), 3.84 (3H, s), 3.55 (3H, s). δC (101 MHz, CDCl₃) 195.6, 166.2, 163.5, 152.3, 149.3, 136.0, 131.5, 130.7, 121.5, 113.8, 112.2, 110.3, 56.3, 55.6, 52.1. HRMS (ESI): Calcd. for C₁₈H₁₈NaO₆ [M+H]⁺ 353.1001; found 353.1001. The spectroscopic data is corresponding to the previously reported in literature.¹⁰

Methyl 5-fluoro-2-(2-methoxybenzoyl)benzoate (2bc). Methyl 2-bromo-5-fluorobenzoate **6b** (50 mg, 0.24 mmol), was reacted with (2-methoxyphenyl) boronic acid **4c** (49 mg, 1.5 equiv, 0.32 mmol) according to the general procedure E to provide **2bc** (40 mg, 66%) as a colourless oil. NMR: δH (400 MHz, CDCl₃) 7.72 (1H, dd, *J* 7.7, 1.8), 7.54 (1H, dd, *J* 8.9, 2.6), 7.51-7.44 (1H, m), 7.42-7.38 (1H, m), 7.25-7.20 (1H, m), 7.02 (1H, t, *J* 7.5), 6.92 (1H, d, *J* 8.4), 3.61 (3H, s), 3.60 (3H, s). δC (101 MHz, CDCl₃) 194.6, 166.5, 166.4 (d, *J* 2.0), 162.9 (d, *J* 252.5), 158.9, 139.7 (d, *J* 4.0), 134.4, 132.3 (d, *J* 7.1), 131.5, 130.2 (d, *J* 8.1), 127.0, 120.7, 118.6 (d, *J* 22.2), 116.4 (d, *J* 24.2), 112.2, 55.7, 52.5. HRMS (ESI): Calcd. for C₁₆H₁₃FNao₄ [M+H]⁺ 311.0696; found 311.0693.

Methyl 5-fluoro-2-(2-(methoxycarbonyl)benzoyl)benzoate (2bh). Methyl 2-bromo-5-fluorobenzoate **6b** (50 mg, 0.24 mmol), was reacted with 2-(methoxycarbonyl)phenylboronic acid **4h** (58 mg, 1.5 equiv, 0.32 mmol) according to the general procedure E to provide **2bh** (30 mg, 40%) as a colorless oil. NMR: δH (400 MHz, CDCl₃) 7.85 (1H, d, *J* 8.8), 7.61-7.53 (2H, m), 7.44 (1H, dd, *J* 5.9, 2.6), 7.42-7.41 (1H, m), 7.40 (1H, s), 3.78 (3H, s), 3.74 (3H, s). δC (101 MHz, CDCl₃) 194.5, 167.9, 167.5 (d, *J* 2.0), 164.1 (d, *J* 255.5), 138.9, 135.2 (d, *J* 8.1), 134.3 (d, *J* 4.0), 132.6 (d, *J* 9.1), 131.5, 131.4 (d, *J* 27.3), 129.5 (d, *J* 37.4), 117.9, 117.8 (d, *J* 22.2), 116.7 (d, *J* 24.2), 77.4, 53.0, 52.7. HRMS (ESI): Calcd. for C₁₇H₁₃FNao₅ [M+H]⁺ 339.0645; found 339.0640.

ESI : Carbonylative Suzuki-Miyaura couplings of sterically hindered aryl halides.

Methyl 2-(2-naphthoyl)-4-methoxybenzoate (2hp). Methyl 2-bromo-4-methoxybenzoate **6h** (50 mg, 0.20 mmol), was reacted with 2-naphthylboronic acid **4p** (52 mg, 1.5 equiv, 0.30 mmol) according to the general procedure E to provide **2hp** (57 mg, 61%) as a colourless oil. NMR: δ H (400 MHz, CDCl₃) 8.09-8.07 (2H, m), 8.02 (1H, dd, *J* 8.6, 1.7), 7.93-7.88 (1H, m), 7.86-7.83 (2H, m), 7.60-7.56 (1H, m), 7.53-7.48 (1H, m), 7.08 (1H, dd, *J* 8.8, 2.6), 6.93 (1H, d, *J* 2.6), 3.89 (3H, s), 3.57 (3H, s). δ C (101 MHz, CDCl₃) 197.0, 166.0, 163.0, 144.4, 135.8, 134.7, 132.6, 132.5, 131.6, 129.8, 128.7, 127.9, 126.8, 124.4, 121.1, 115.1, 112.9, 77.4, 55.8, 52.1. HRMS (ESI): Calcd. for C₁₉H₁₄NaO₄ [M+H]⁺ 329.0790; found 329.0790.

2 Additional experimental information

2.1 Two-chamber set-up:

The reactions were performed in the previously reported two-chamber system (Fig 1) under an argon atmosphere.

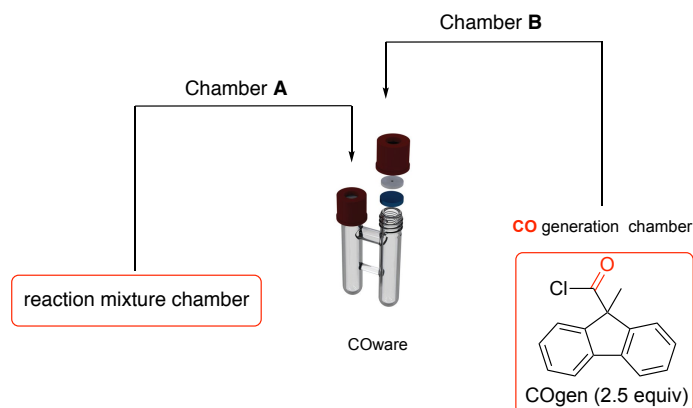
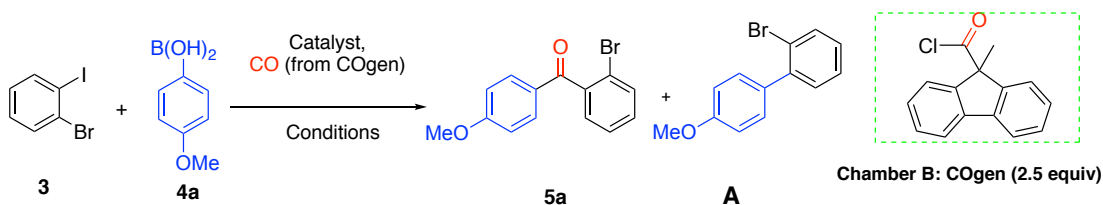


Fig 1. The two-chamber system used in the reactions, and the CO generator (COgen)

2.2 Screening of catalysts and conditions for the Suzuki-Miyaura coupling of 2-bromiodobenzene **3** with 4-methoxyphenyl boronic acid **4a**.



Procedure:

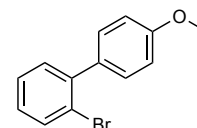
Chamber A: 2-Bromiodobenzene **3** (50 mg, 1.0 equiv, 0.18 mmol), aryl boronic acid **4a** (1.2 equiv), catalyst and base were dissolved in a solvent (3 ml).

Chamber B: COgen (107 mg, 2.5 equiv, 0.45 mmol), Pd(dba)₂ (12 mg, 5 mol%), tri-*tert*-butylphosphonium tetrafluoroborate (TTBP•HBF₄) (6.3 mg, 5 mol%) were dissolved in anisole (3 ml).

DIPEA (240 mg, 3 equiv) was added to chamber B to release CO. The mixture was stirred at 80 °C in a tightly closed system for 20 hours. The reaction mixture was filtered through celite and concentrated on a rotavapor. The crude was purified by column chromatography with pentane: EtOAc (8:2) as eluent. The ratio (5a: A) has been evaluated based on the crude ¹³C NMR spectra. The experimental data and the NMR spectra of the byproduct A is shown later.

Characterization of 2-bromo-4'-methoxy-1,1'-biphenyl A (from direct coupling).

The title compound was isolated as a side product from reactions towards **5a**. NMR: δ H (400 MHz, CDCl₃) 7.66 (1H, d, *J* 7.8), 7.40-7.31 (4H, m), 7.22-7.13 (1H, m), 6.97



ESI : Carbonylative Suzuki-Miyaura couplings of sterically hindered aryl halides.

(2H, d, *J* 8.7), 3.87 (3H, s). δ C (101 MHz, CDCl₃) 159.2, 142.3, 133.7, 133.2, 131.5, 130.7, 128.5, 127.9, 127.5, 123.0, 114.3, 113.5, 77.5, 77.2, 76.8, 55.5, 55.4.

Table ESI-1. Carbonylative Suzuki-Miyaura coupling of 2-bromoiodobenzene **3** with 4-methoxyphenyl boronic acid **4a**.

| Entry | Catalyst (mol%) | base | Rxn. time (h) | T (°C) | Solvent | Addition | Approx. ratio ^c 5a : A | Isol. yield (%) |
|-------|--|---|---------------|--------|---------------|-------------------|-----------------------------------|-----------------|
| 1 | Pd(PPh ₃) ₂ Cl ₂ (3) | K ₂ CO ₃ | 20 | 80 | Anisole | normal | 0.7 : 1 | 50 |
| 2 | Pd(OAc) ₂ (2) | K ₂ CO ₃ | 20 | 80 | Anisole | normal | 0.1 : 1 | 10 |
| 3 | Pd(dba) ₂ (3) | K ₂ CO ₃ | 20 | 80 | Anisole | normal | 0.5 : 1 | 35 |
| 4 | PEPPSI-IPr (3) | CS ₂ CO ₃ | 20 | 80 | Chlorobenzene | normal | 0.7 : 1 | 30 |
| 5 | PdCl ₂ (3) | K ₂ CO ₃ | 20 | 80 | Anisole | normal | 0.7 : 1 | 65 |
| 6 | PdCl ₂ (1) | K ₂ CO ₃ | 20 | 80 | Anisole | normal | 0.7 : 1 | 60 |
| 7 | PdCl ₂ (1) | K ₂ CO ₃ | 20 | 50 | Anisole | normal | 0.2 : 1 | 30 |
| 8 | PdCl ₂ (1) | K ₂ CO ₃ | 20 | 60 | Anisole | normal | 0.3 : 1 | 35 |
| 9 | PdCl ₂ (1) | K ₂ CO ₃ | 40 | 80 | Anisole | normal | 1 : 1 | 65 |
| 10 | PdCl ₂ ^b (1) | K ₂ CO ₃ ^b | 20 | 80 | Anisole | normal | 1 : 0.9 | 55 |
| 11 | PdCl ₂ (1) | K ₂ CO ₃ /KI | 20 | 80 | Anisole | normal | 0.6 : 1 | 55 |
| 12 | PdCl ₂ (1) | CS ₂ CO ₃ | 20 | 80 | Anisole | normal | 1 : 1 | 60 |
| 13 | PdCl ₂ (1) | K ₂ CO ₃ | 20 | 80 | Anisole | slow ^a | 1 : 0.1 | 80 |
| 14 | PdCl ₂ (1) | K ₂ CO ₃ | 20 | 100 | Anisole | slow ^a | 1 : 0.1 | 80 |
| 15 | PEPPSI- IPr (3) | CS ₂ CO ₃ | 20 | 80 | Chlorobenzene | slow ^a | 1 : 1 | 60 |
| 16 | PEPPSI- IPr (3) | CS ₂ CO ₃ | 20 | 120 | Chlorobenzene | slow ^a | 1 : 1 | 65 |

^a Instead of dissolving **4a** in chamber A before CO release, a solution of aryl boronic acid **4a** (1.2 equiv) in anisole (2 ml) was added slowly (1-2 h) to the reaction mixture in chamber A after CO release. See General procedure A. ^b PdCl₂ and K₂CO₃ were used as a premix with ratio 1:300. ^c The ratio (5a : A) is approximately determined using ¹³C NMR of the crude product mixture.

2.3 Screening of precursors for ex-situ generation of CO.

Procedures:

Chamber A: 2-Bromoiodobenzene **3** (50 mg, 1.0 equiv, 0.18 mmol), PdCl₂ (0.3 mg, 1 mol%), K₂CO₃ (70 mg, 3 equiv, 0.55 mmol) were dissolved in a solvent (3 ml). In case of normal addition, the aryl boronic acid **4a** (1.2 equiv) was added to the mixture before CO generation was started. In case of slow addition, the aryl boronic acid **4a** (1.2 equiv) was dissolved in anisole (2 ml) and added after CO generation over a period of 1-2 hours.

Chamber B for entry 1 and 2: Fe-tetraphenylporphyrin (6 mg), TBABF₄ (1.1g), DMF (30 ml), and tetrafluoroethylene (2 ml) were introduced to chamber B. Electrodes were mounted and the COware was sealed tightly with the screw caps fitted with teflon-coated silicon seals.

The reaction mixture in chamber A was bubbled through with CO₂ for 10-15 min until saturation. The ElectroWare⁴ was set up using galvanostatic configuration. The electrodes were connected and the electrolysis began, while both reaction chambers were stirring. Chamber B kept stirring at room temperature, while the other chamber A was placed in a preheated hotplate at 80 °C for 18 h. The reaction mixture was filtered through celite and concentrated on a rotavapor. The crude was purified by column chromatography with pentane: EtOAc (8:2) as eluent.¹¹

ESI : Carbonylative Suzuki-Miyaura couplings of sterically hindered aryl halides.

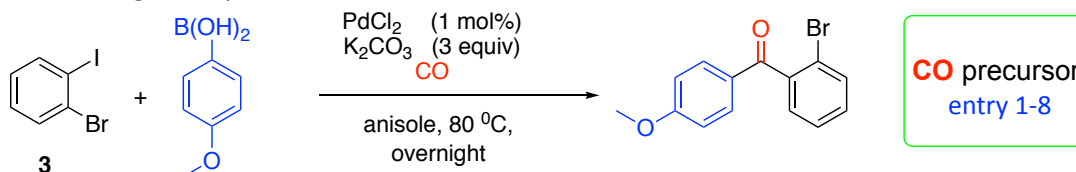
Chamber B for entry 3 and 4: COgen (107 mg, 2.5 equiv, 0.45 mmol), Pd(dba)₂ (12 mg, 5 mol%), tri-*tert*-butylphosphonium tetrafluoroborate (TTBP•HBF₄) (6.3 mg, 5 mol%) and DIPEA (240 mg, 3 equiv) were dissolved in anisole (3 ml).

The mixture was stirred at 80 °C in a tightly closed system for 20 hours. The reaction mixture was filtered through celite and concentrated on a rotavapor. The crude was purified by column chromatography with pentane: EtOAc (8:2) as eluent.

For entry 5 and 6: To a two necked round bottomed flask degassed and charged with aqueous solution of NaOH (2 M, 20 ml), a balloon was fitted via 5 ml syringe cylinder at one neck. The syringe cylinder was filled with CaCl₂ as a drying agent, that was kept in place by cotton wool pads at both sides. Through the other neck oxalyl chloride was added slowly with a syringe to the basic solution. The evolved gas was collected in the balloon. The CO balloon was transferred to the reaction mixture vial (chamber A). The mixture was stirred at 80 °C in a tightly closed system for 20 hours. The reaction mixture was filtered through celite and concentrated on a rotavapor. The crude was purified by column chromatography with pentane: EtOAc (8:2) as eluent.¹²

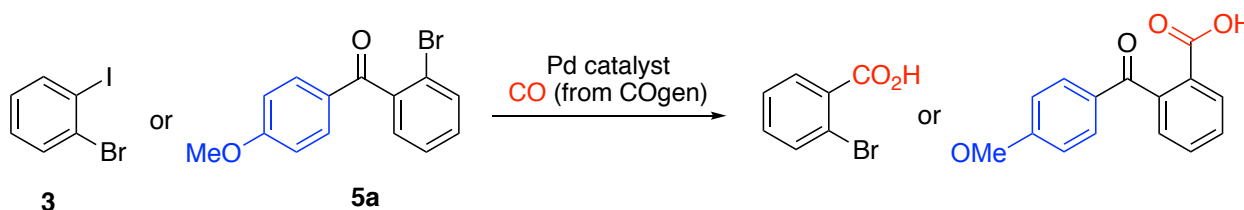
Chamber B for entry 7 and 8: Sulfuric acid (1.5 mmol) was introduced before the two-chamber system was tightened and heated at 80 °C. Then formic acid was added slowly to chamber B. The reaction mixture was allowed to stir at 80 °C for 18h.¹³

Table ESI-2. Screening of CO precursors.



| no | CO source | Addition of boronic acid | Isolated yield (%) |
|----|--|--------------------------|--------------------|
| 1 | CO ₂ reduction | Normal | 29 |
| 2 | CO ₂ reduction | Slow addition | 30 |
| 3 | COgen | Normal | 60 |
| 4 | COgen | Slow addition | 80 |
| 5 | Oxalyl chloride+ NaOH (aq) | Normal (ballon) | 60 |
| 6 | Oxalyl chloride + NaOH (aq) | Slow addition (ballon) | 60 |
| 7 | Formic acid+ H ₂ SO ₄ (1.2 mmol) | Normal (ballon) | 10 |
| 8 | Formic acid+ H ₂ SO ₄ (1.2 mmol) | In situ | 0 |

2.4 Attempts to hydroxycarbonylate 2-bromoiodobenzene 3 or 2-bromobenzophenone 5a



Procedures:

In a dry and clean 8 ml vial equipped with a stirring bar, the aryl halide (1 equiv.), MePh₂SiCOOH (64 mg, 1.5 equiv), base (2-3 equiv.), palladium precursor and ligand were dissolved in 3 ml dioxane. The vial was tightly sealed with a screw cap. The reaction was allowed to stir for overnight at 40 °C. The crude mixture was then poured into water (30 ml) and diluted with DCM before pH was adjusted to 10.

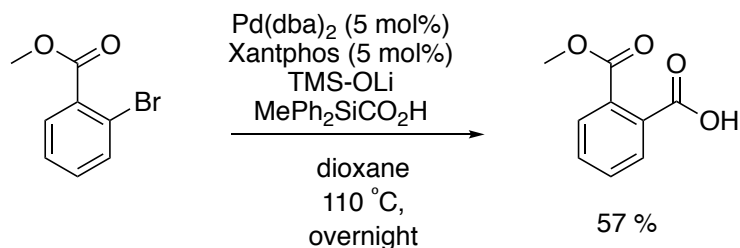
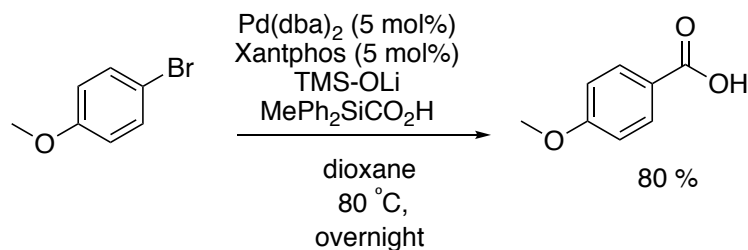
ESI : Carbonylative Suzuki-Miyaura couplings of sterically hindered aryl halides.

The aqueous phase was washed with DCM several times. The combined aqueous phase was acidified to pH 2-3 using HCl (4M) and then washed with DCM for several times. The combined organic phase was then dried over MgSO₄, filtered by suction and concentrated *in vacuo* to leave the product as colorless solid.

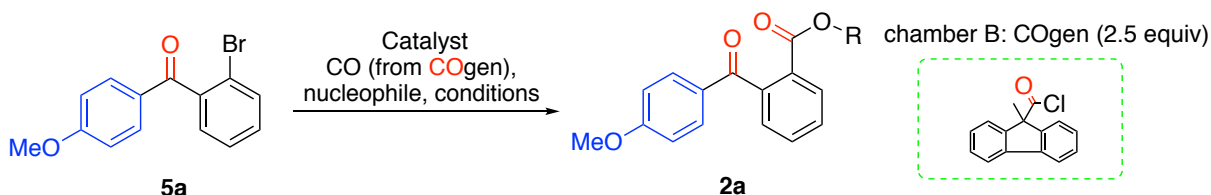
Table ESI-3. Screening of catalyst and conditions for hydroxycarbonylation of **3** or **5a**.

| Entry | Subst. | Pd source (mol%) | Ligand (mol%) | Base | Carboxylate source | Solvent | eq. CO | T (°C) | Isol. yield % |
|-------|--------|--------------------------|-----------------------|--------|---------------------------------------|---------|--------|--------|---------------|
| 4 | 3 | Pd(dba) ₂ (5) | - | TMSOLi | MePh ₂ SiCO ₂ H | dioxane | 2.5 | 110 | - |
| 6 | 3 | Pd(dba) ₂ (5) | Xantphos (5) | TMSOK | MePh ₂ SiCO ₂ H | toluene | 1.5 | 60 | traces |
| 7 | 3 | Pd(dba) ₂ (5) | Xantphos (5) | TMSOK | MePh ₂ SiCO ₂ H | dioxane | 1.5 | 60 | 60 |
| 8 | 5a | Pd(dba) ₂ (5) | Xantphos (5) | TMSOLi | MePh ₂ SiCO ₂ H | dioxane | 1.5 | 80 | - |
| 9 | 5a | Pd(dba) ₂ (5) | Xantphos (5) | TMSOLi | MePh ₂ SiCO ₂ H | dioxane | 1.5 | 115 | - |
| 10 | 5a | Pd(dba) ₂ (5) | PPh ₃ (10) | TMSOLi | MePh ₂ SiCO ₂ H | dioxane | 2.5 | 110 | - |

The following control experiments were performed to establish that the procedure gives the wanted carboxylation product for standard substrates.



2.5 Screening for catalysts and conditions for the alkoxy carbonylation of 2-bromobenzophenone **5a**



Procedure:

ESI : Carbonylative Suzuki-Miyaura couplings of sterically hindered aryl halides.

Chamber A: 2-Bromophenyl-4-methoxyphenylmethanone **5a** (1.0 equiv, 0.47 mmol), Pd precursor and base (3 equiv) were dissolved in solvent (2 ml). The nucleophile (2 equiv) was added to the reaction mixture.

Chamber B: COgen (2.5 equiv), Pd(dba)₂ (5 mol%), TTBP•HBF₄ (5 mol%) were dissolved in anisole (3 ml) before DIPEA (3 equiv) was added. The mixture was stirred with heating in a tightly closed system for 20-24 hours.

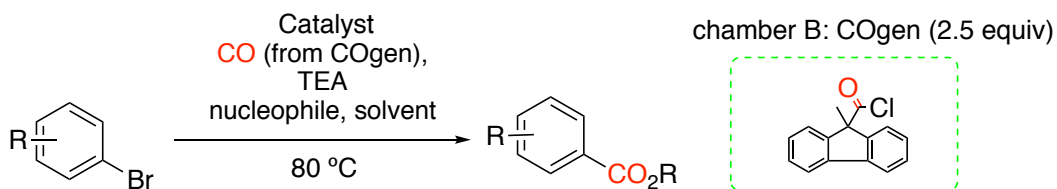
The reaction mixture in chamber A was filtered through celite and concentrated on a rotavapor. The crude was purified by column chromatography with pentane : EtOAc (7:3) as eluent.

Table ESI-4. Screening for conditions for alkoxyacylation on the 2-bromobenzophenone.

| Entry | Pd source (mol%) | Ligand (mol%) | Nucl. | Base | Solvent | T (°C) | Isol. yield (%) |
|-------|--|---------------|------------------|---------------------------------|-----------------------------|--------|-----------------|
| 1 | dppf(PdCl ₂) (10) | | H ₂ O | TEA | H ₂ O: THF (1:4) | 120 | -* |
| 2 | dppf(PdCl ₂) (10) | Dppf (20) | iPrOH | TEA | DMF | 80 | 11 |
| 3 | dppf(PdCl ₂) (10) | Dppf (20) | nBuOH | TEA | DMF | 80 | -* |
| 4 | Pd(OAc) ₂ (2) | Xantphos (4) | iPrOH | TEA | TEA | 80 | 15 |
| 5 | Pd(OAc) ₂ (2) | Xantphos (4) | nBuOH | TEA | TEA | 80 | 11 |
| 6 | Pd(OAc) ₂ (2) | Xantphos (4) | MeOH | TEA | Dioxane | 110 | 5 |
| 7 | dppf(PdCl ₂) (10) | Dppf (20) | MeOH | TEA | DMF | 80 | -* |
| 8 | Pd(dba) ₂ (5) | Dippf (5) | EtONa | - | THF | 80 | -* |
| 9 | PEPPSI-IPr (3) | | nBuOH | Cs ₂ CO ₃ | Chlorobenzene | 80 | -* |
| 10 | PEPPSI (5) | IMes (10) | nBuOH | Cs ₂ CO ₃ | Chlorobenzene | 110 | -* |
| 11 | Pd(PPh ₃) ₂ Cl ₂ (5) | IMes (10) | nBuOH | Cs ₂ CO ₃ | Heptane | 120 | -* |
| 12 | PdCl ₂ (2) | Xantphos (2) | nBuOH | K ₂ CO ₃ | Anisole | 110 | 65 |

* Only starting material or the corresponding biphenyl were detected.

Table ESI-5. Control experiments for alkoxyacylation with 4-bromobenzophenone.

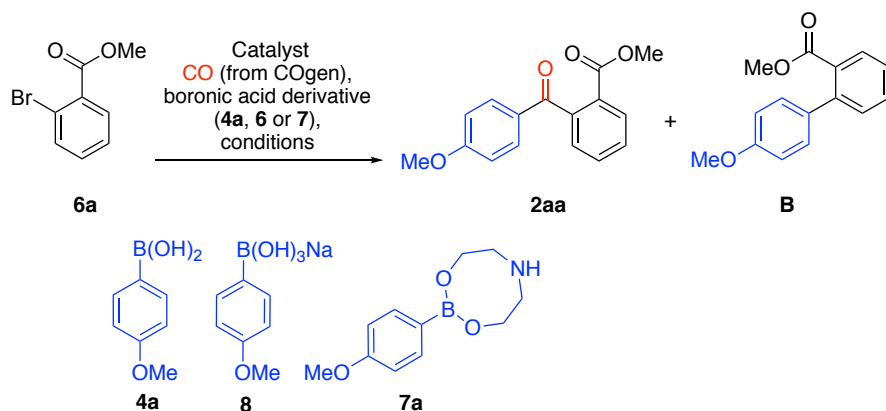


| Entry | Substrate | Pd source (mol%) | Ligand (mol%) | Nucl. | Base | Solvent | Isol. yield (%) |
|-------|-----------|----------------------------|---------------|--------|------|---------|-----------------|
| 1 | | Pd(OAc) ₂ (2) | Xantphos (4) | nBuOH | TEA | TEA | 99 |
| 2 | | dppfPdCl ₂ (10) | Dppf (20) | iPrOH | TEA | DMF | 97 |
| 3 | | Pd(OAc) ₂ (2) | Xantphos (4) | nBuOH | TEA | TEA | 11 |
| 4 | | dppfPdCl ₂ (10) | Dppf (20) | iPrOH | TEA | DMF | 11 |
| 5 | | Pd(dba) ₂ (5) | Dippf (5) | tBuONa | - | THF | 60 |

ESI : Carbonylative Suzuki-Miyaura couplings of sterically hindered aryl halides.

2.6 Screening for catalysts and conditions for the carbonylative Suzuki-Miyaura coupling of methyl 2-bromobenzoate **6a**

Table ESI-6. Optimization of reaction conditions for the palladium catalyzed carbonylative Suzuki-Miyaura coupling of methyl-2-bromobenzoate **6a**.

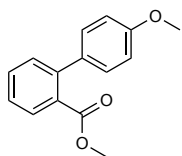


| Entry | Pd-source (mol%) | Ligand (mol%) | Nuc. | base | solvent | T (°C) | addition | Ratio ^d 2aa: B | Isol. yield (%) |
|-----------------|---|---------------------|-----------|---------------------------------|---|--------|----------|---------------------------|---------------------|
| 1 ^a | Pd(acac) ₂ (5) | CataCXium A•HI (10) | 8 | - | Toluene: H ₂ O (10:1) | 80 | normal | 1 : 0.45 | 65 ^a |
| 2 ^a | Pd(acac) ₂ (5) | CataCXium A•HI (10) | 7a | - | Toluene: H ₂ O (10:1) | 95 | normal | 1 : 0.3 | 67 ^a |
| 3 | Pd(acac) ₂ (5) | CataCXium A (10) | 4a | K ₂ CO ₃ | Toluene: H ₂ O (10:1) | 100 | normal | - | 30 |
| 4 ^a | Pd(acac) ₂ (5) | CataCXium A•HI (10) | 7a | - | DMSO | 90 | normal | - | traces ^a |
| 5 ^a | Pd(acac) ₂ (5) | CataCXium A•HI (10) | 7a | - | DMF: H ₂ O (10:1) | 90 | normal | - | -. ^a |
| 6 | Pd(acac) ₂ (5) | CataCXium A•HI (10) | 7a | - | Toluene: H ₂ O: MeOH (10:1:1) | 90 | slow | - | traces |
| 7 | Pd(acac) ₂ (5) | CataCXium A•HI (10) | 7a | - | Toluene: H ₂ O: TBAB (1:1:0.5) | 95 | slow | - | traces |
| 8 ^a | Pd(acac) ₂ (5) | CataCXium A•HI (10) | 7a | - | Dioxane: H ₂ O (10:1) | 95 | normal | - | -. ^a |
| 9 ^b | PdCl ₂ (1) | | 4a | K ₂ CO ₃ | Anisole | 110 | normal | - | -. ^b |
| 10 ^b | Pd(OAc) ₂ (5) | CataCXium A (10) | 4a | K ₂ CO ₃ | Toluene: H ₂ O (10:1) | 110 | normal | - | -. ^b |
| 11 ^b | Pd(PPh) ₃ Cl ₂ (10) | | 4a | K ₂ CO ₃ | Anisole | 110 | normal | 0.2 : 1 | 20 ^b |
| 12 ^b | Pd(OAc) ₂ (5) | Xantphos (5) | 4a | Cs ₂ CO ₃ | Toluene | 80 | normal | 0.3 : 1 | 20 ^b |
| 13 ^c | Xantphos G2 (5) | | 4a | K ₂ CO ₃ | Anisole | 100 | slow | - | traces ^c |
| 14 ^b | Pd(OAc) ₂ (5) | CataCXium A (10) | 4a | K ₂ CO ₃ | Dioxane | 100 | normal | - | traces ^b |
| 15 ^b | PdCl ₂ (2) | Xantphos (4) | 4a | K ₂ CO ₃ | Toluene | 100 | normal | - | -. ^b |
| 16 ^b | PEPPSI-IPr (3) | | 4a | Cs ₂ CO ₃ | Chlorobenzene | 80 | normal | 1 : 0.5 | 60 ^b |
| 17 ^c | PEPPSI-IPr (3) | | 4a | Cs ₂ CO ₃ | Chlorobenzene | 110 | slow | 1 : 0.15 | 80 ^c |

| | | | | | | | | |
|-----------------|----------------------|-----------|---------------------------------|---------------------------------|-----|--------|----------|-----------------|
| 18 ^c | PEPPSI-IPr (3) | 4a | Cs ₂ CO ₃ | Anisole | 110 | slow | 1 : 0.15 | 80 ^c |
| 19 ^b | PEPPSI-Allyl (3) | 4a | Cs ₂ CO ₃ | Anisole | 110 | normal | 1: 0.6 | 50 ^b |
| 20 ^b | Ni(COD) ₂ | dcype | 4a | Cs ₂ CO ₃ | 110 | normal | - | -.*,b |

a Following general procedure E. b Following general procedure D. c Following general procedure C. d The ratio (2aa : B) was determined using ¹³C NMR of the crudes. *Only starting material or the corresponding biphenyl B were detected.

Characterization of methyl 4'-methoxy-[1,1'-biphenyl]-2-carboxylate **B**.



The title compound was isolated as a side product from reactions towards **2aa**. NMR: δ H (400 MHz, CDCl₃) 7.70 (1H, d, *J* 8.2), 7.41 (1H, t, *J* 8.3), 7.29 (2H, d, *J* 7.3), 7.16 (2H, d, *J* 8.8), 6.85 (2H, d, *J* 8.8), 3.75 (3H, s), 3.58 (3H, s). δ C (101 MHz, CDCl₃) 169.5, 159.1, 142.1, 133.7, 131.3, 131.0, 130.8, 129.8, 129.6, 126.9, 113.7, 77.5, 77.2, 76.8, 55.4, 52.1.

3 References

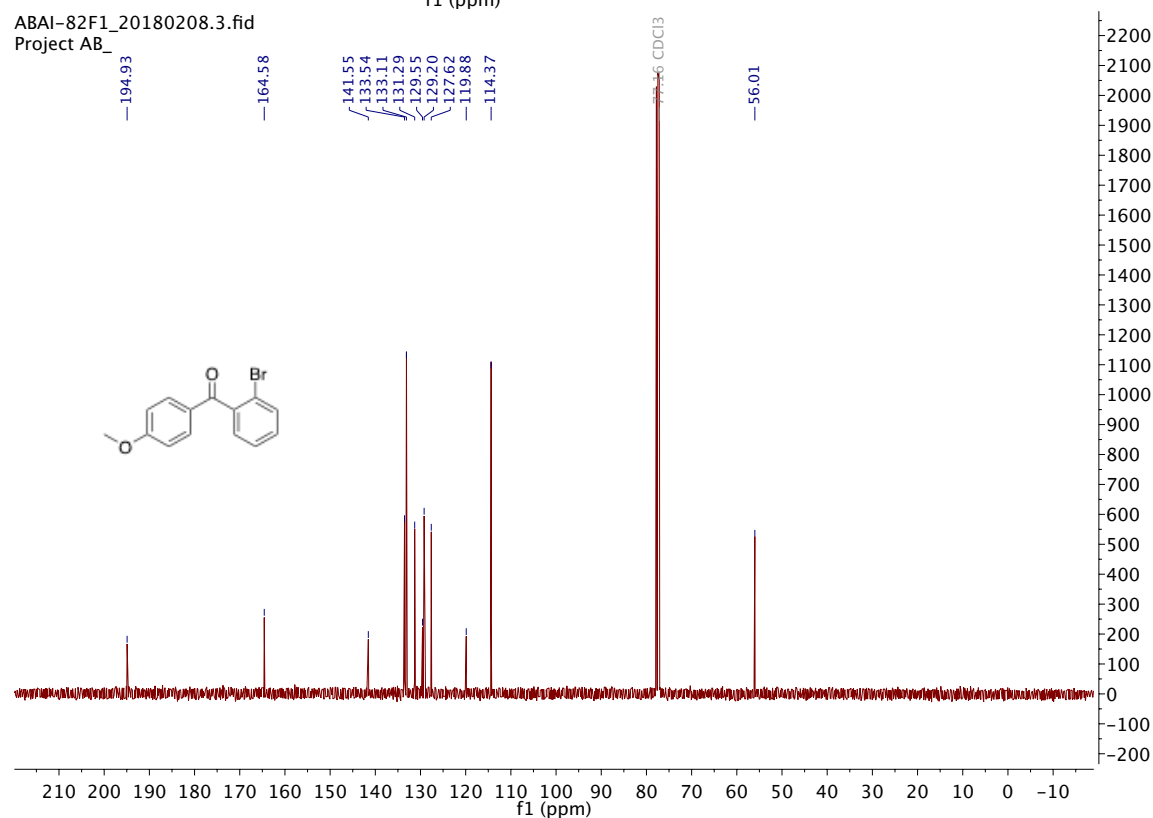
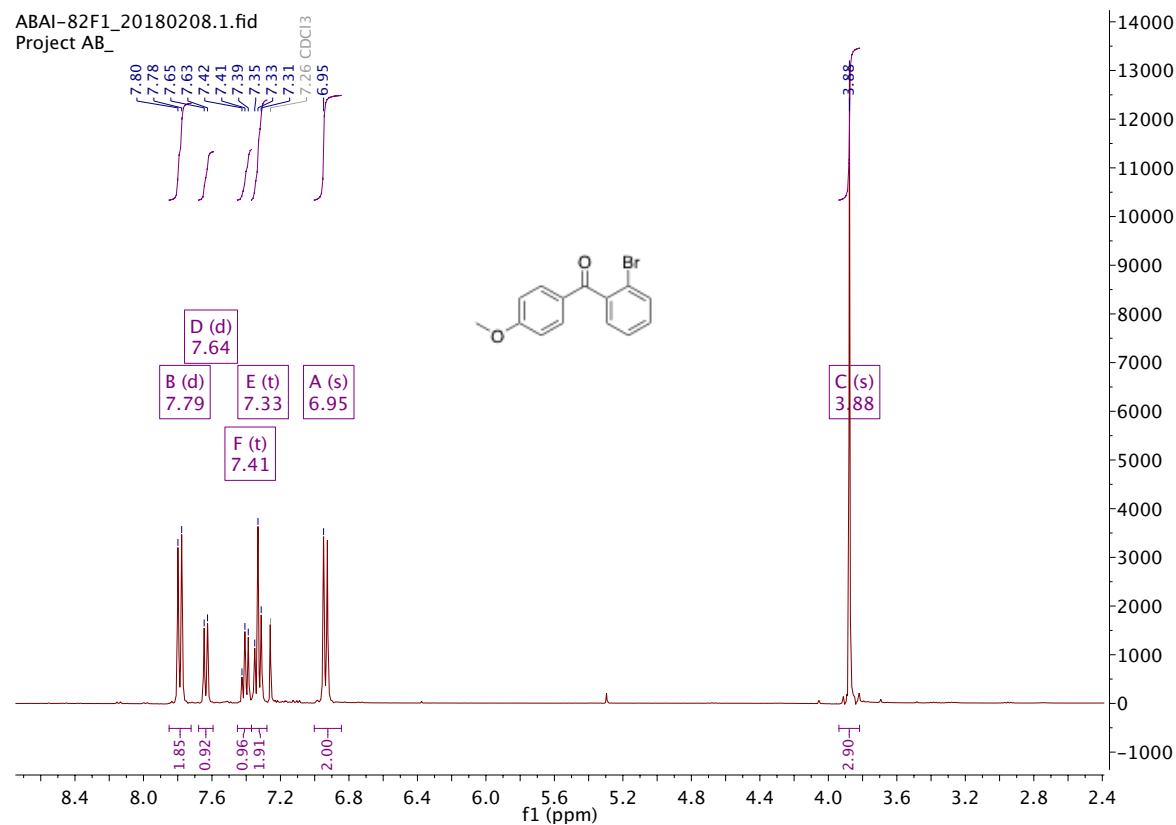
- W. L. F. Armarego and C. L. L. Chai, in *Purification of Laboratory Chemicals*, eds. W. L. F. Armarego and C. L. L. Chai, Butterworth-Heinemann, Oxford, 6th edn., 2009, DOI: <https://doi.org/10.1016/B978-1-85617-567-8.50012-3>, pp. 88-444.
- A. Ahlburg, A. T. Lindhardt, R. H. Taaning, A. E. Modvig and T. Skrydstrup, *J. Org. Chem.*, 2013, **78**, 10310-10318.
- J. J. Dunsford, E. R. Clark and M. J. Ingleson, *Dalton Trans.*, 2015, **44**, 20577-20583.
- S. S. Mochalov, A. N. Fedotov, E. V. Trofimova and N. S. Zefirov, *Russ. J. Org. Chem.*, 2018, **54**, 403-413.
- P. Wójcik, M. Mart, S. Ulukanli and A. M. Trzeciak, *RSC Adv.*, 2016, **6**, 36491-36499.
- B. Suchand and G. Satyanarayana, *J. Org. Chem.*, 2016, **81**, 6409-6423.
- J. W. Lockner, D. D. Dixon, R. Risgaard and P. S. Baran, *Org. Lett.*, 2011, **13**, 5628-5631.
- T. J. Hu, G. Zhang, Y. H. Chen, C. G. Feng and G. Q. Lin, *J. Am. Chem. Soc.*, 2016, **138**, 2897-2900.
- M. M. M. Raposo, A. M. B. A. Sampaio and G. Kirsch, *J. Heterocycl. Chem.*, 2005, **42**, 1245-1251.
- N. A. R. Hatam and D. A. Whiting, *J. Chem. Soc. C*, 1969, 1921-1932
- M. T. Jensen, M. H. Rønne, A. K. Ravn, R. W. Juhl, D. U. Nielsen, X.-M. Yu, S. U. Pedersen, K. Daasbjerg and T. Skrydstrup, *Nat. Commun.*, 2017, **8**, 489.
- S. V. F. Hansen and T. Ulven, *Org. Lett.*, 2015, **17**, 2832-2835.
- C. Brancour, T. Fukuyama, Y. Mukai, T. Skrydstrup, I. Ryu, *Org. Lett.* 2013, **15**, 2794-2797.

ESI : Carbonylative Suzuki-Miyaura couplings of sterically hindered aryl halides.

4 Spectra

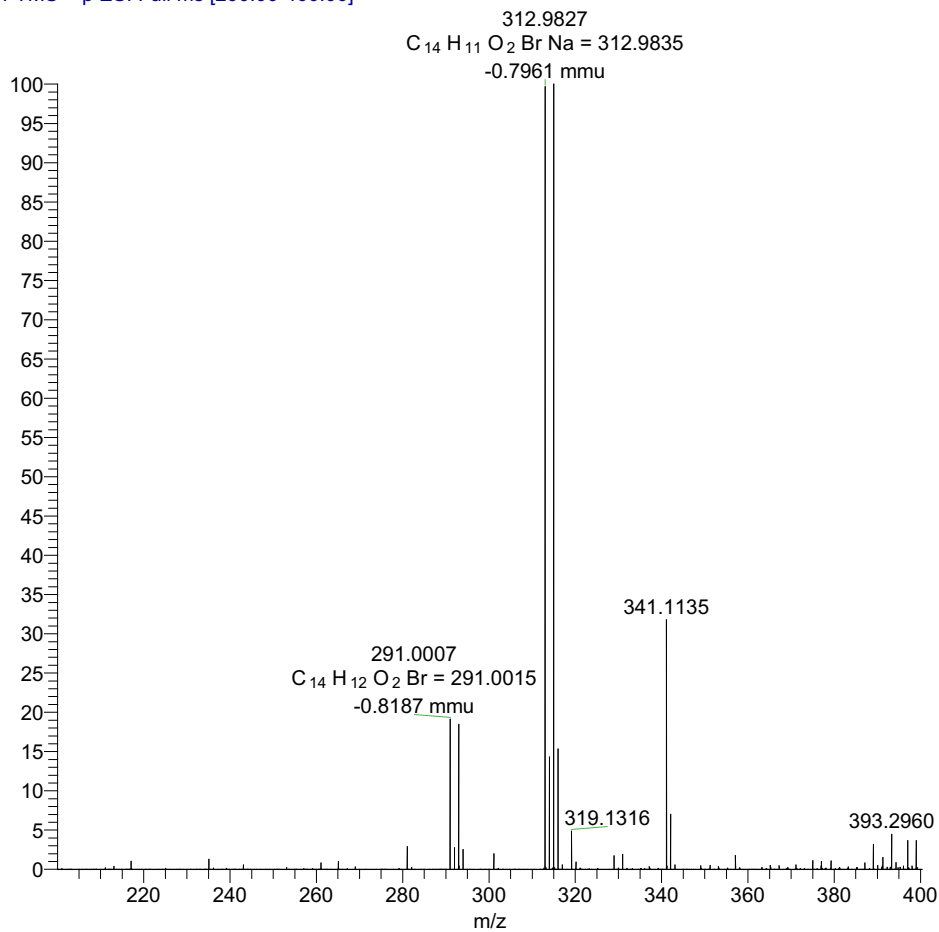
4.1 Spectra for diaryl ketones 5

2-Bromophenyl 4-methoxyphenyl methanone 5a.



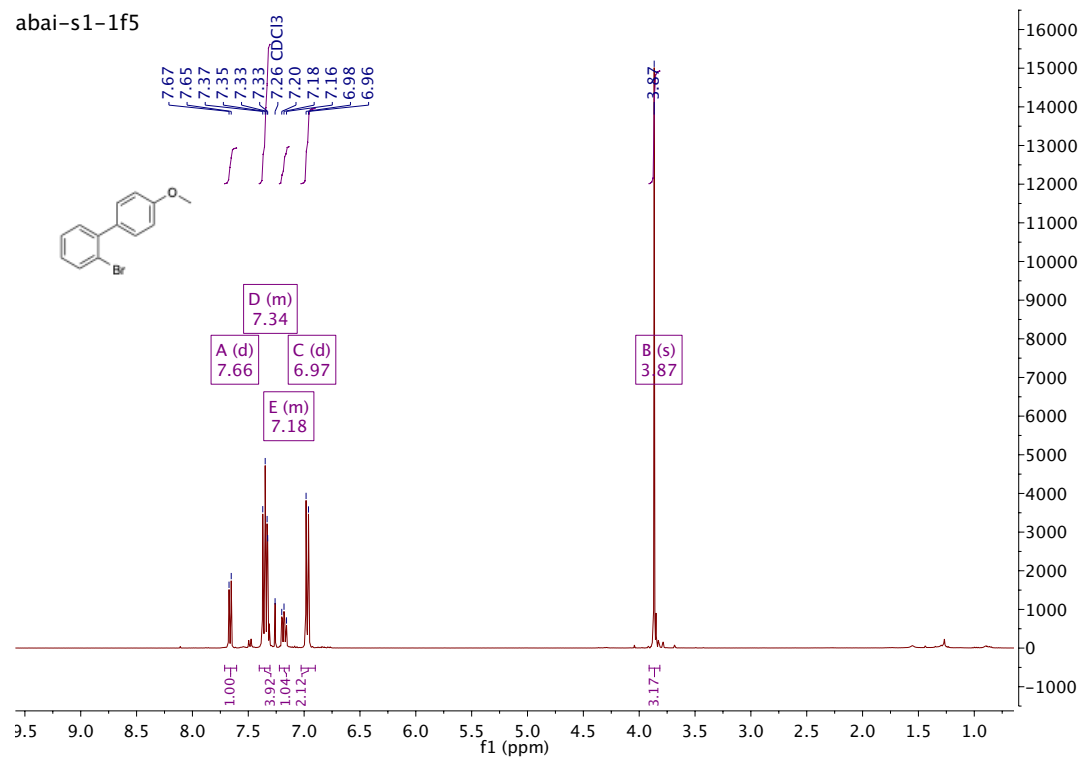
ESI : Carbonylative Suzuki-Miyaura couplings of sterically hindered aryl halides.

abai-85-1_180618144811 #1-4 RT: 0.00-0.09 AV: 4 NL: 2.58
T: FTMS + p ESI Full ms [200.00-400.00]



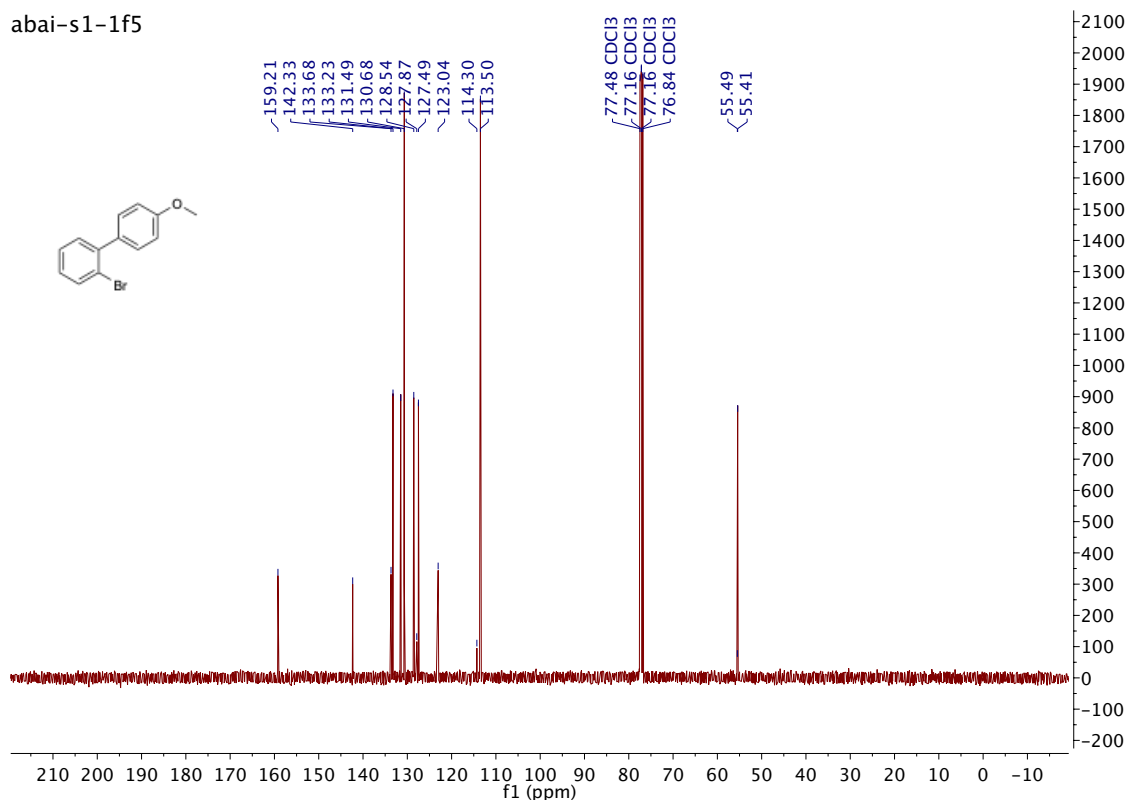
2-bromo-4'-methoxy-1,1'-biphenyl A (from direct coupling)

abai-s1-1f5



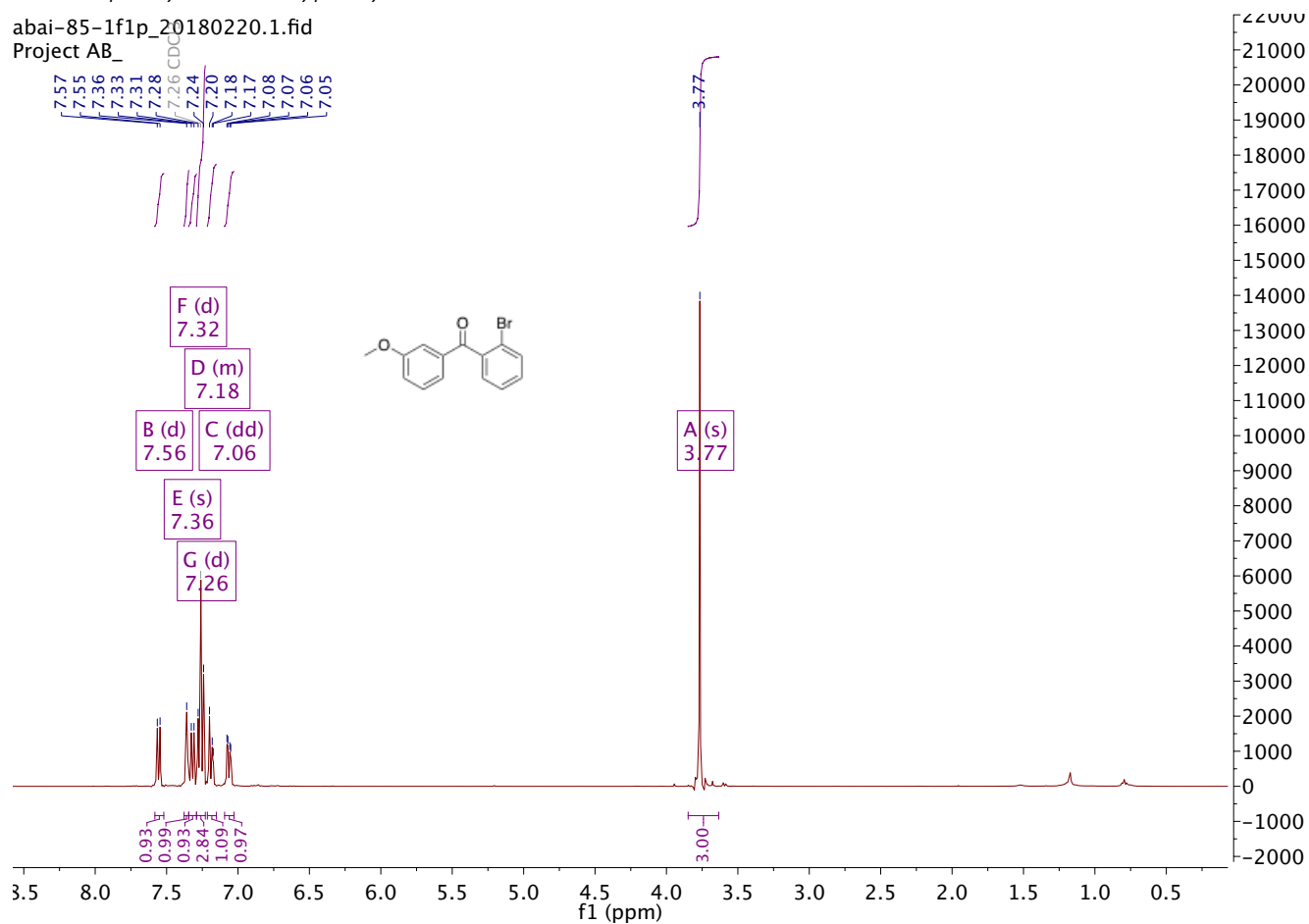
ESI : Carbonylative Suzuki-Miyaura couplings of sterically hindered aryl halides.

abai-s1-1f5



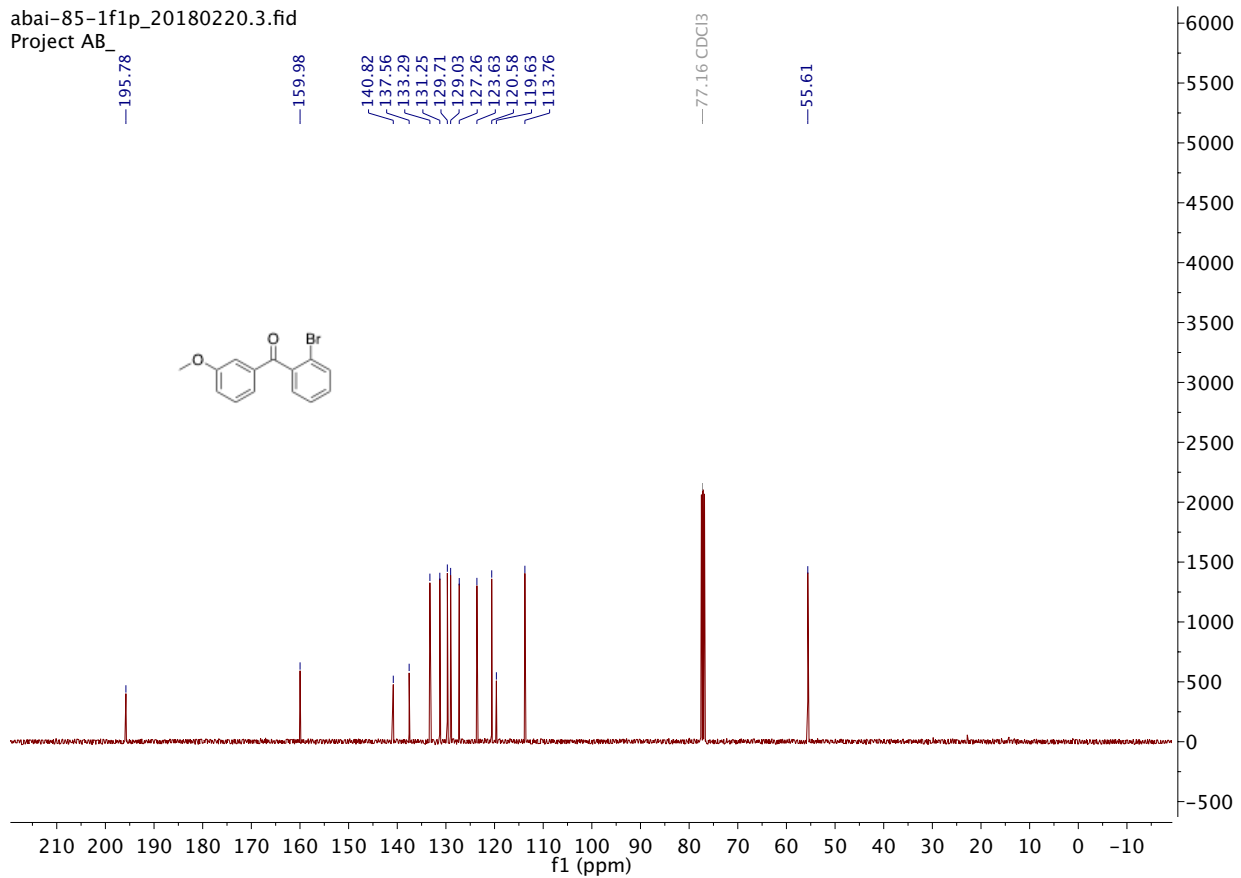
2-Bromophenyl 3-methoxyphenyl methanone **5b**

abai-85-1f1p_20180220.1.fid
Project AB_

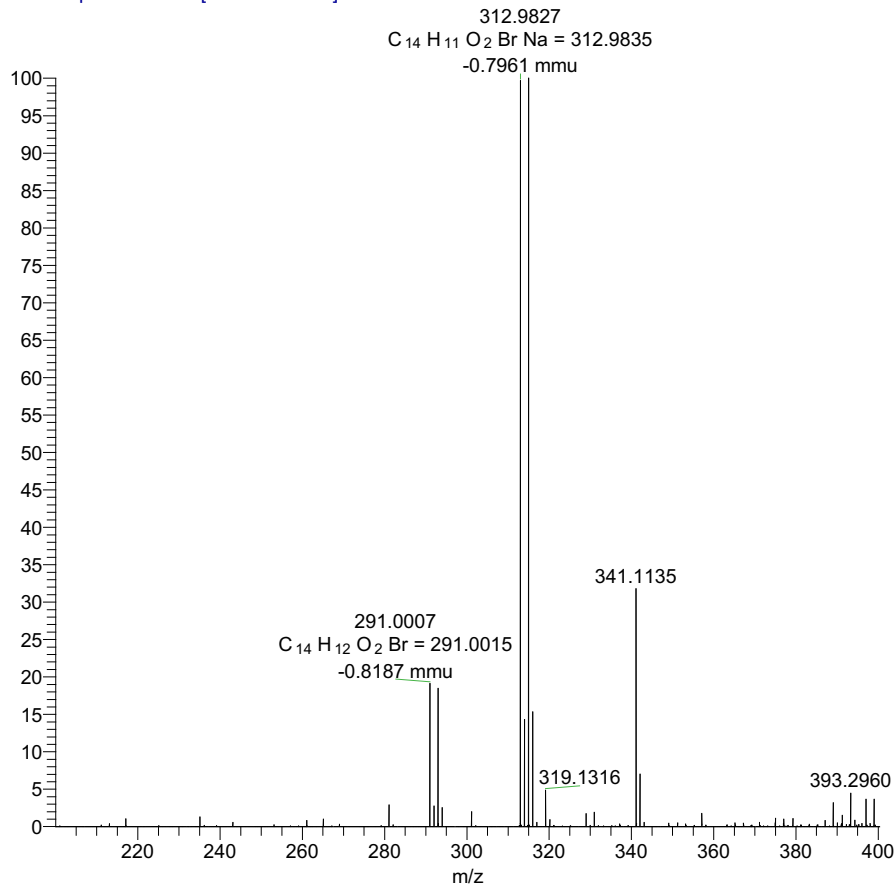


ESI : Carbonylative Suzuki-Miyaura couplings of sterically hindered aryl halides.

abai-85-1f1p_20180220.3.fid
Project AB_

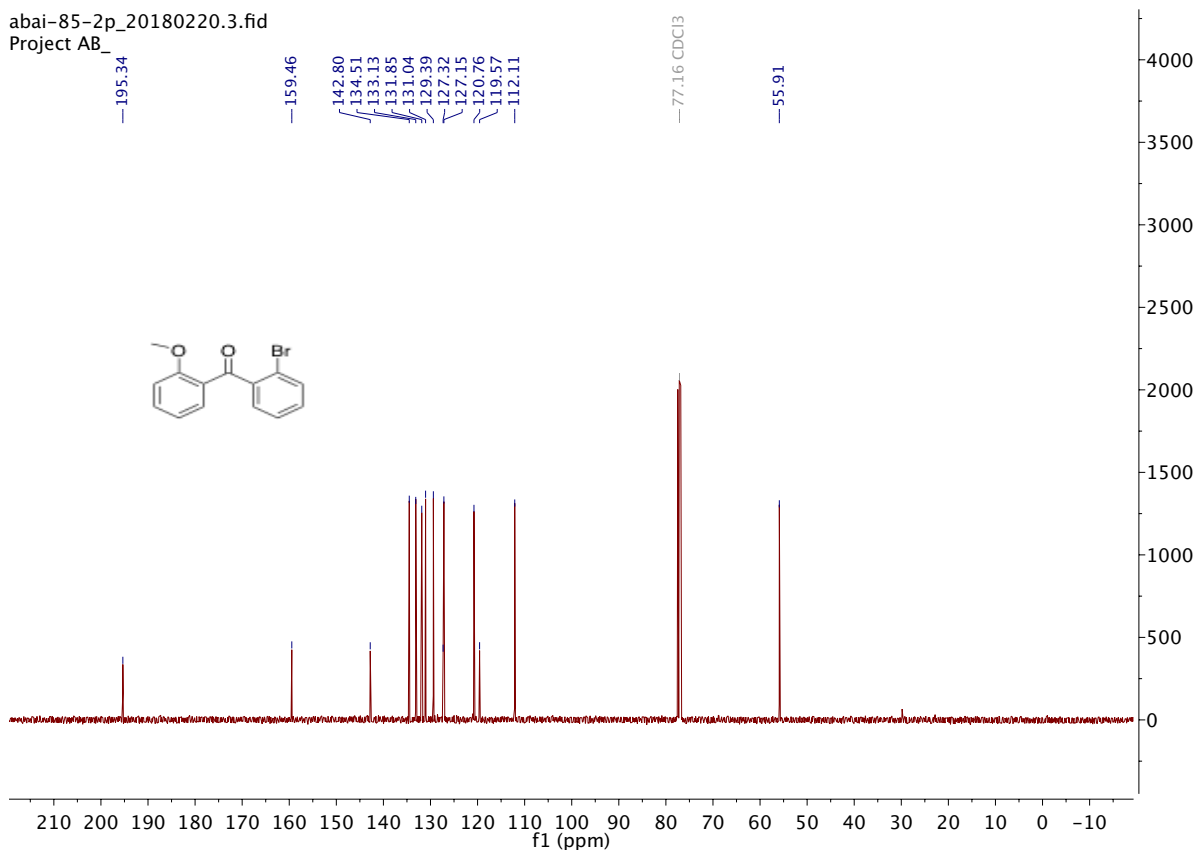
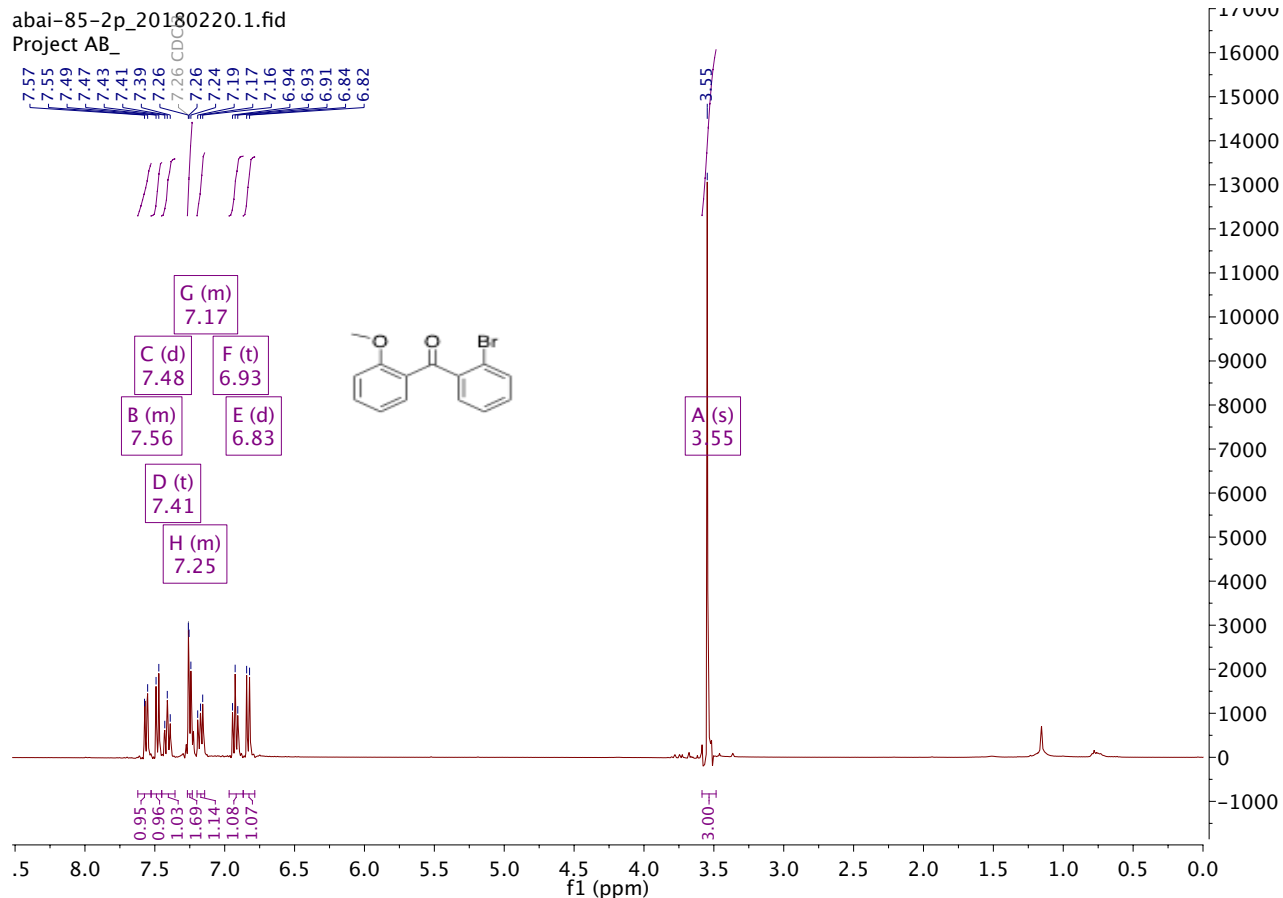


abai-85-1_180618144811 #1-4 RT: 0.00-0.09 AV: 4 NL: 2.58
T: FTMS + p ESI Full ms [200.00-400.00]



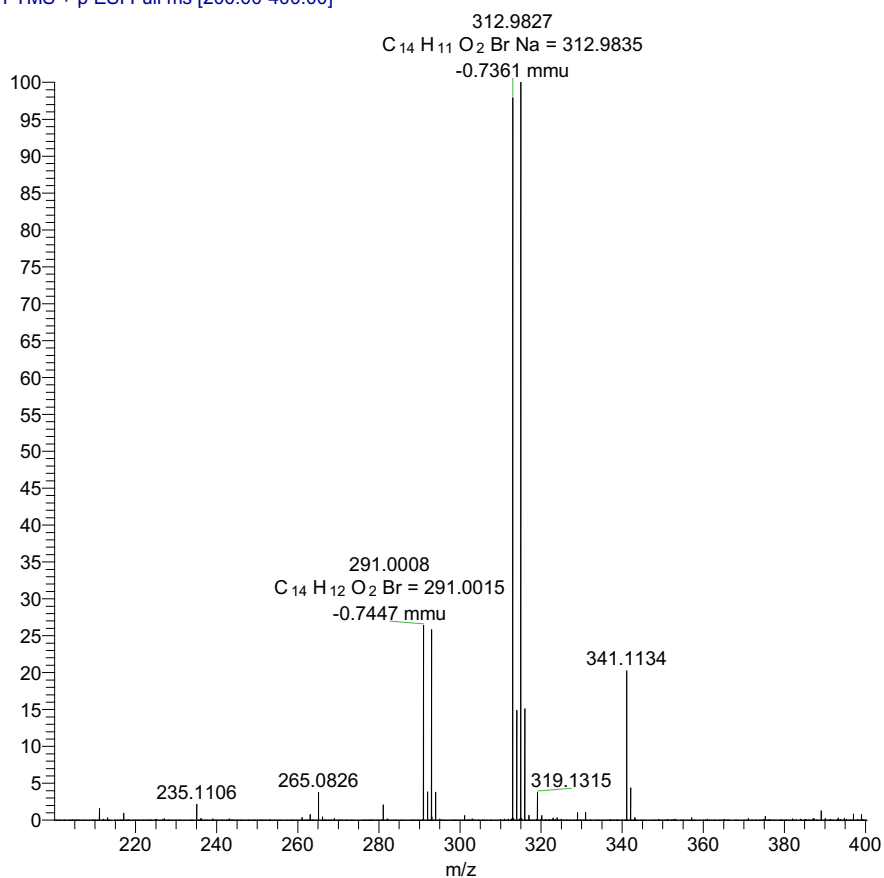
ESI : Carbonylative Suzuki-Miyaura couplings of sterically hindered aryl halides.

2-Bromophenyl 2-methoxyphenyl methanone 5c

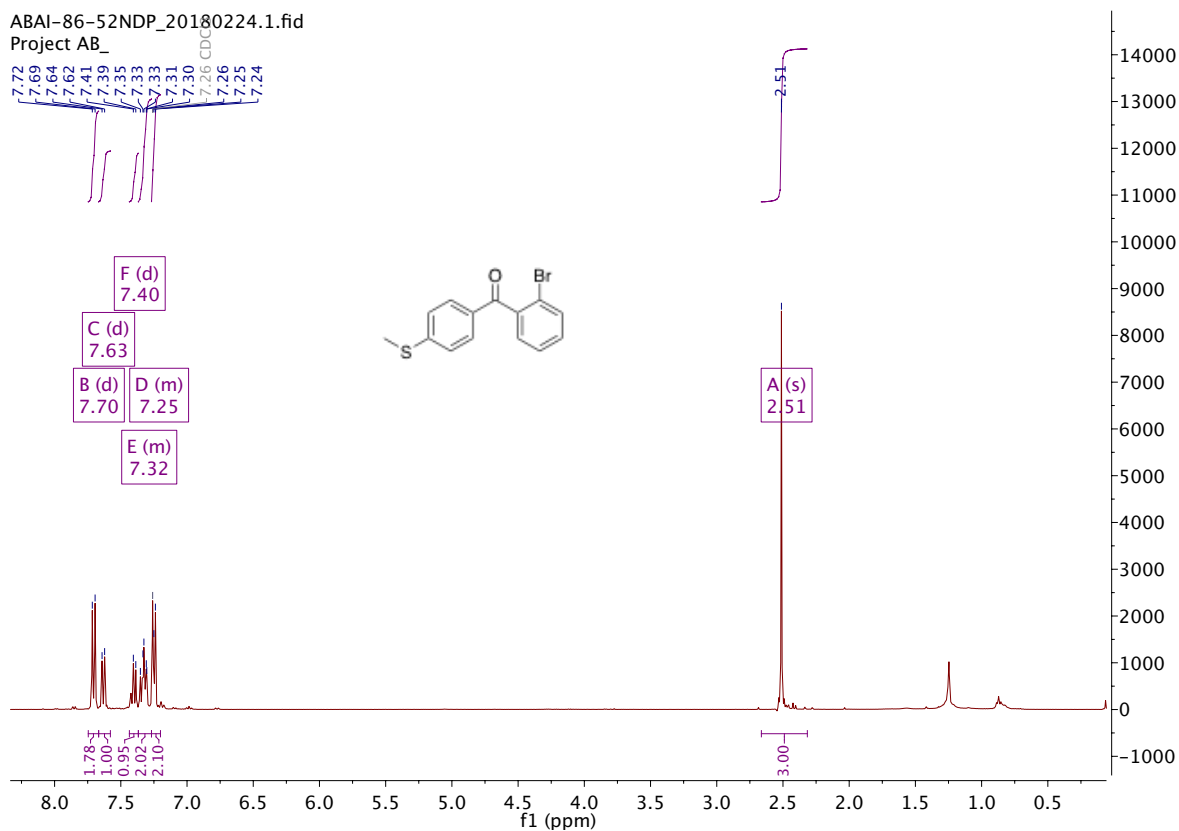


ESI : Carbonylative Suzuki-Miyaura couplings of sterically hindered aryl halides.

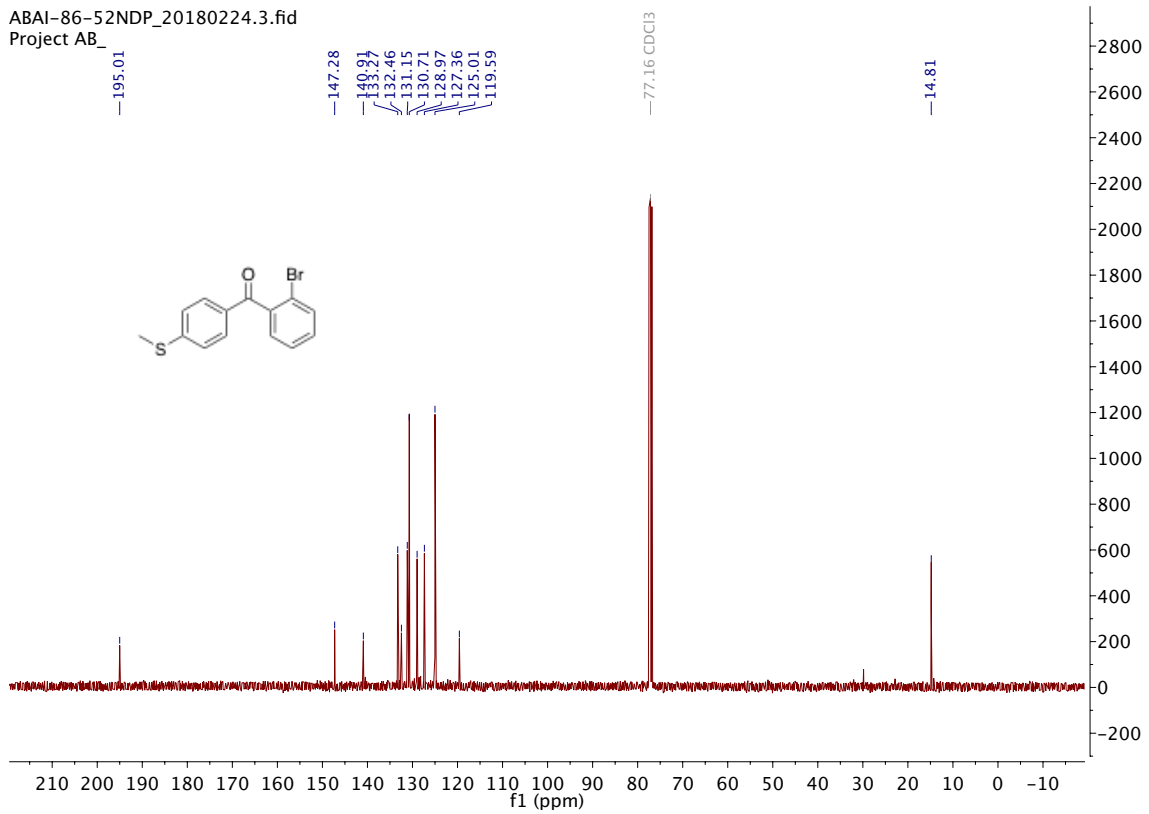
abai-85-2_180618145336 #1-5 RT: 0.00-0.11 AV: 5 NL: 2.85
T: FTMS + p ESI Full ms [200.00-400.00]



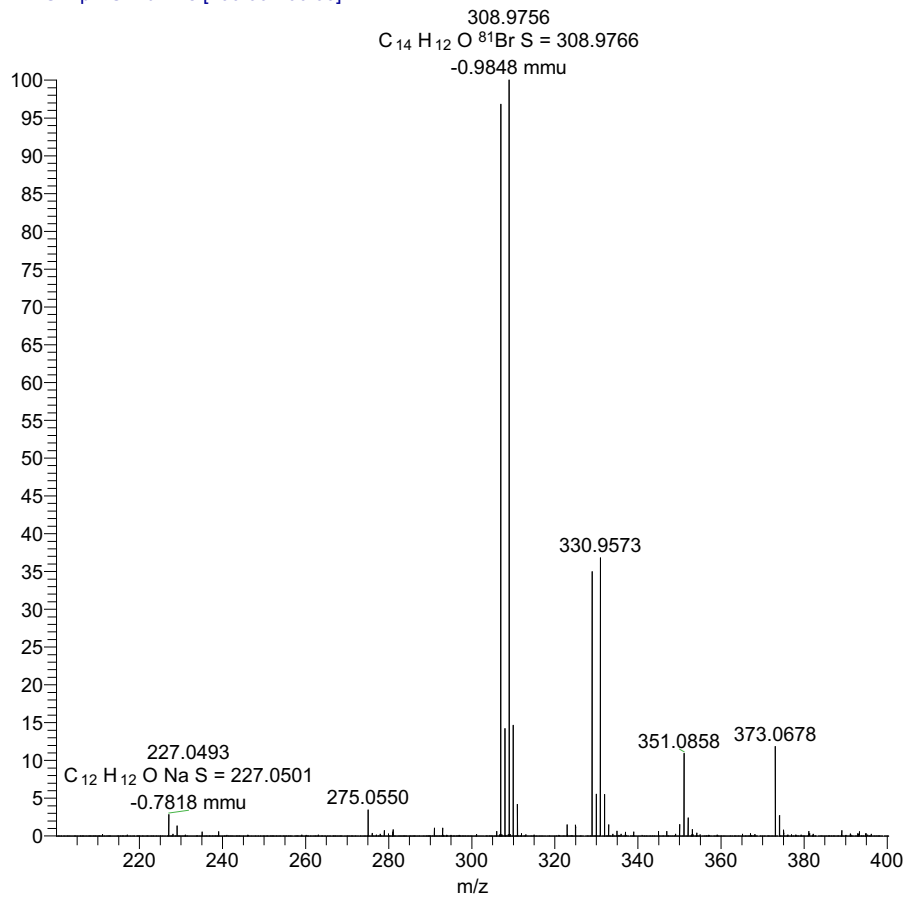
2-Bromophenyl 4-(methylthio)phenyl methanone **5d**



ESI : Carbonylative Suzuki-Miyaura couplings of sterically hindered aryl halides.



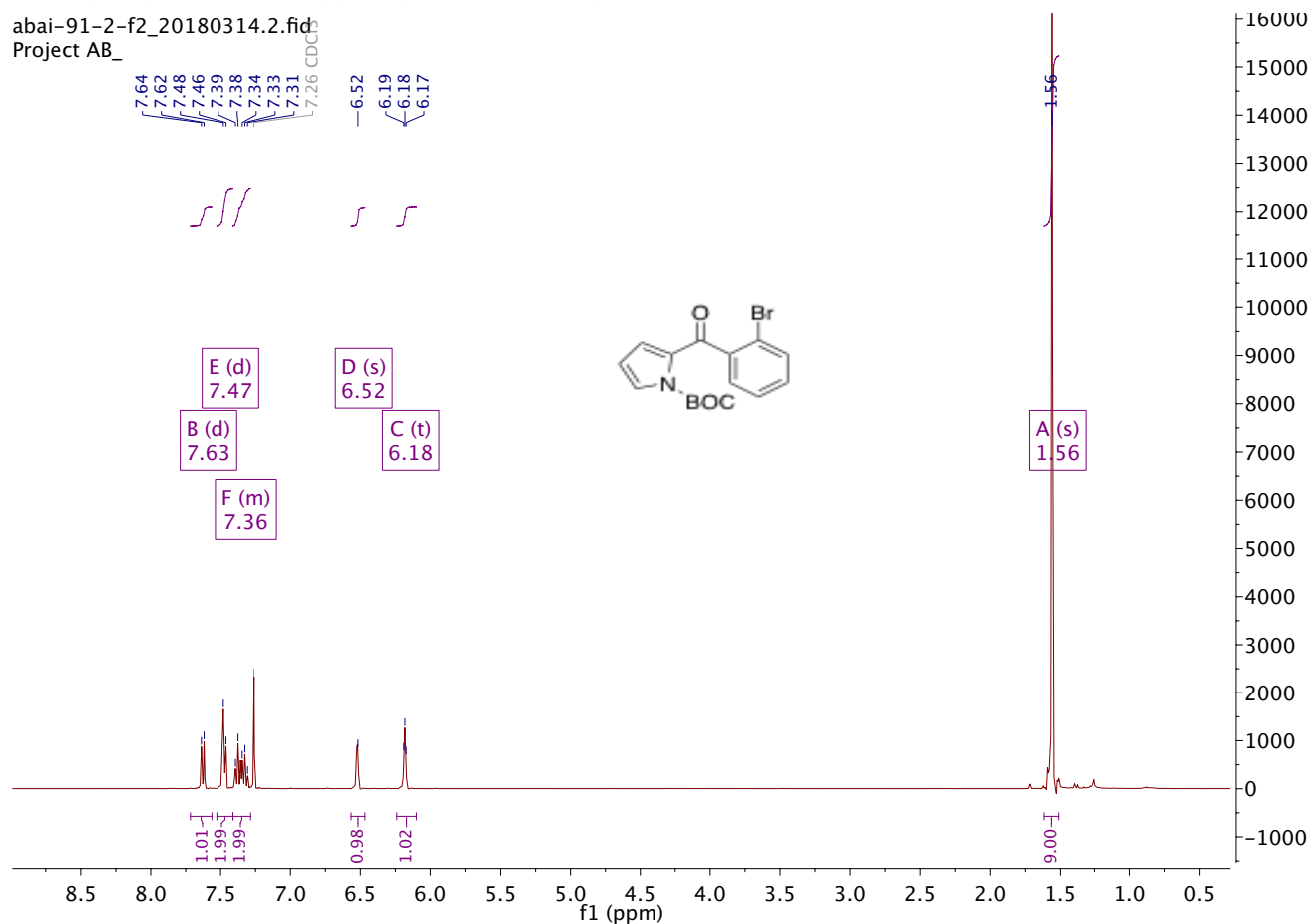
abai-86-5_180618152120 #1-5 RT: 0.01-0.12 AV: 5 NL: 2.15
T: FTMS + p ESI Full ms [200.00-400.00]



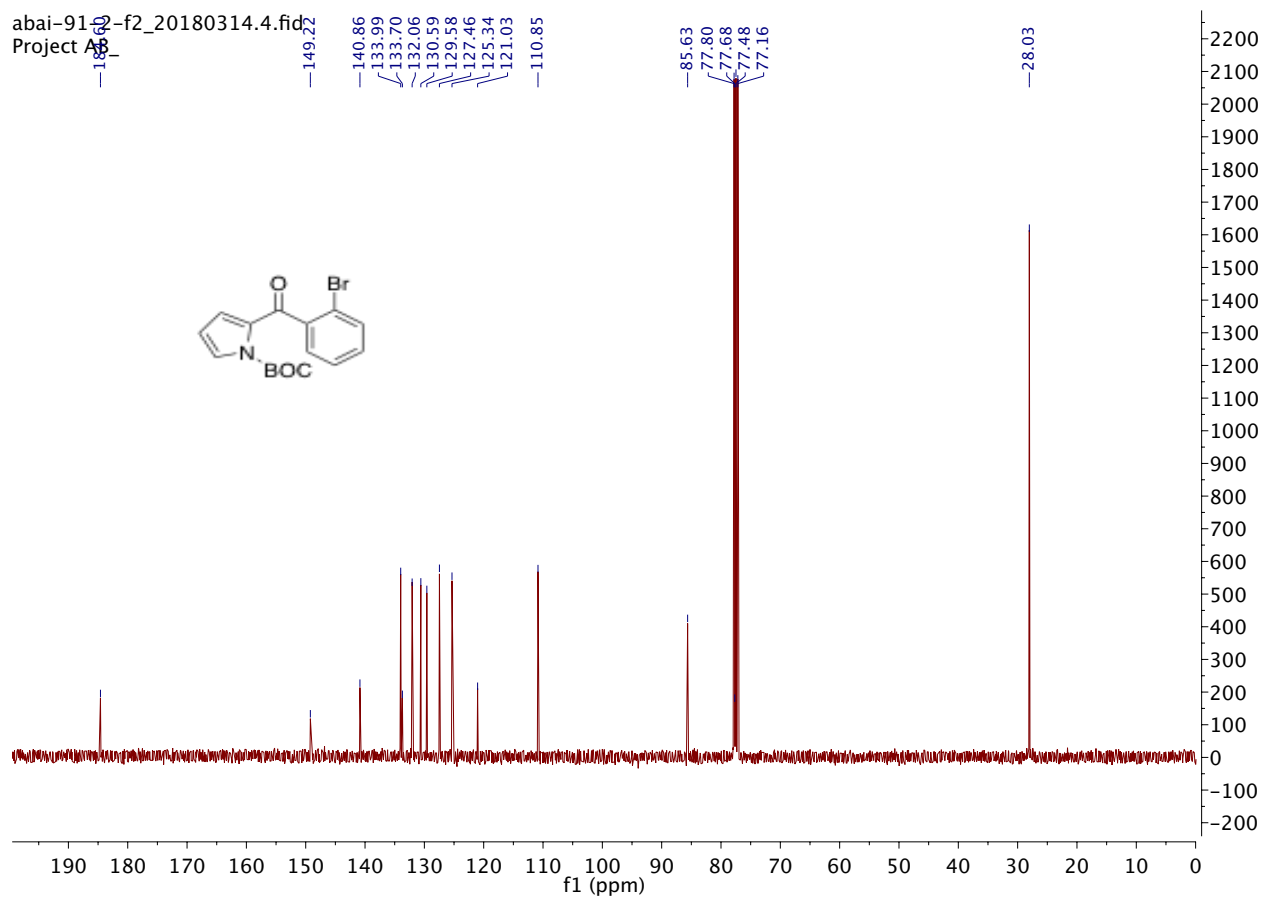
ESI : Carbonylative Suzuki-Miyaura couplings of sterically hindered aryl halides.

tert-Butyl 2-(2-bromobenzoyl)-1H-pyrrole-1-carboxylate **5e**

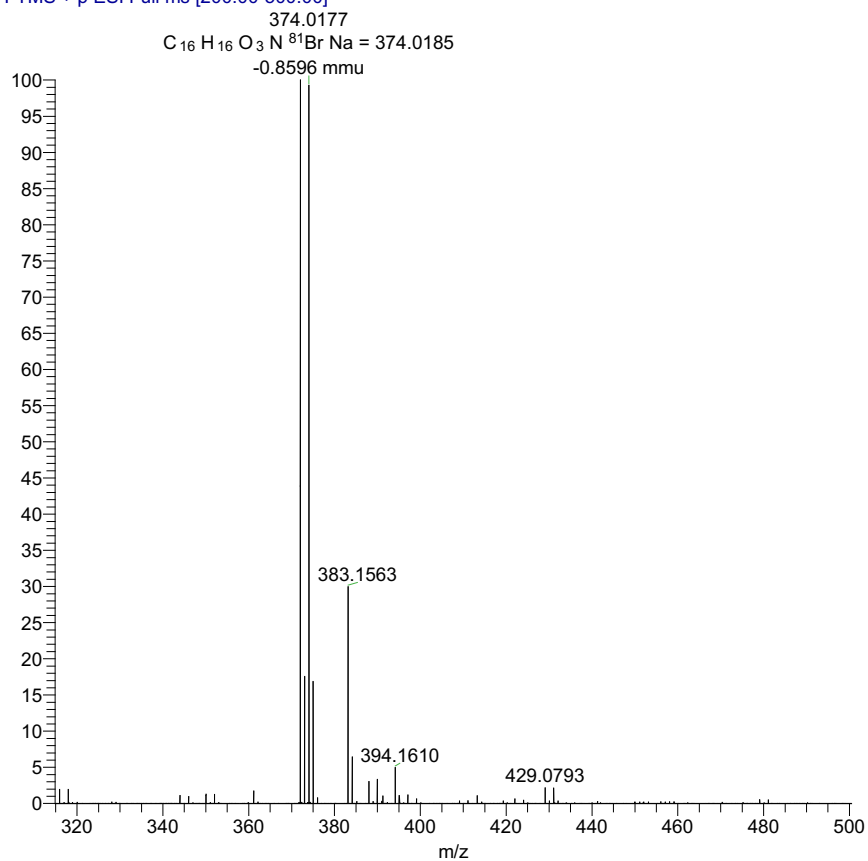
abai-91-2-f2_20180314.2.fid
Project AB_



ESI : Carbonylative Suzuki-Miyaura couplings of sterically hindered aryl halides.



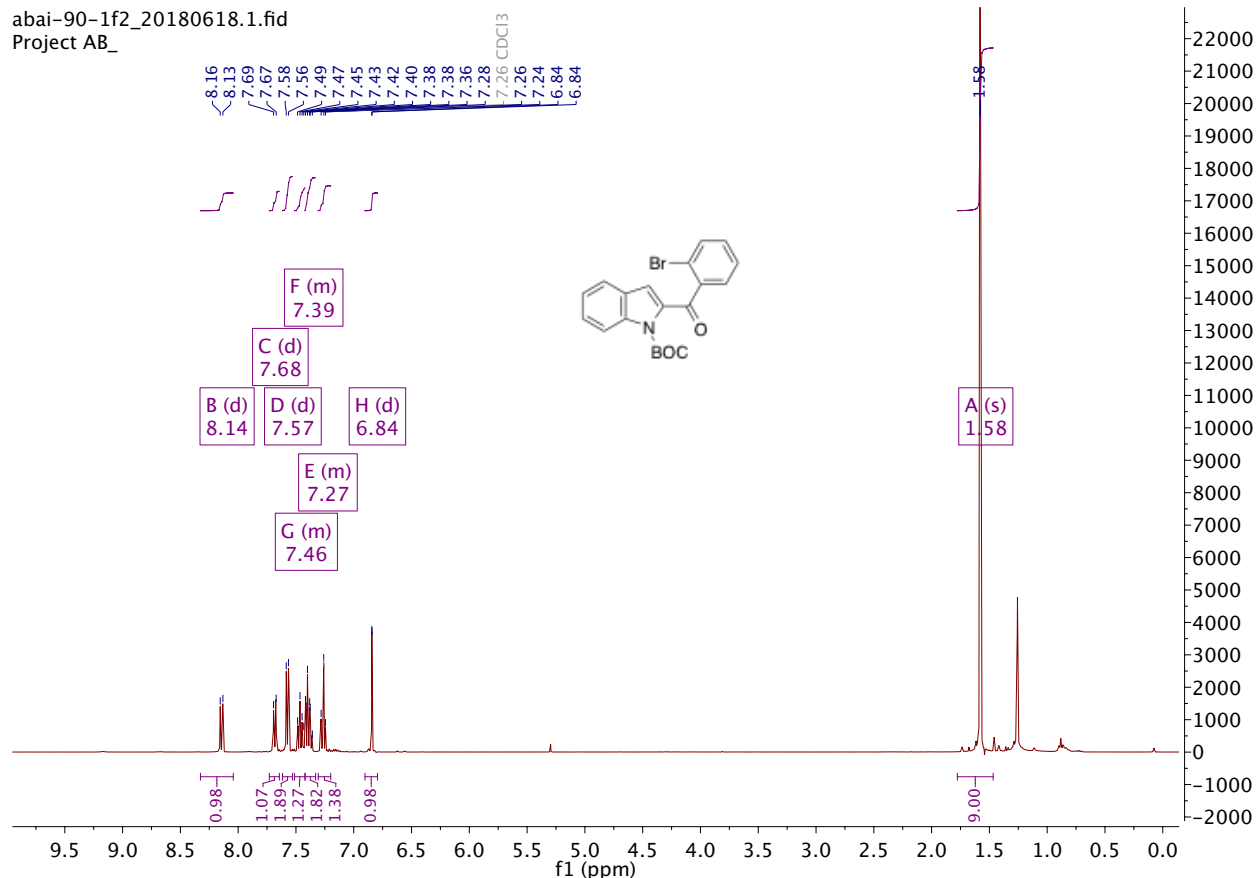
abai-91-2f2_180618163441 #1-5 RT: 0.02-0.13 AV: 5 NL: 1.1
T: FTMS + p ESI Full ms [200.00-500.00]



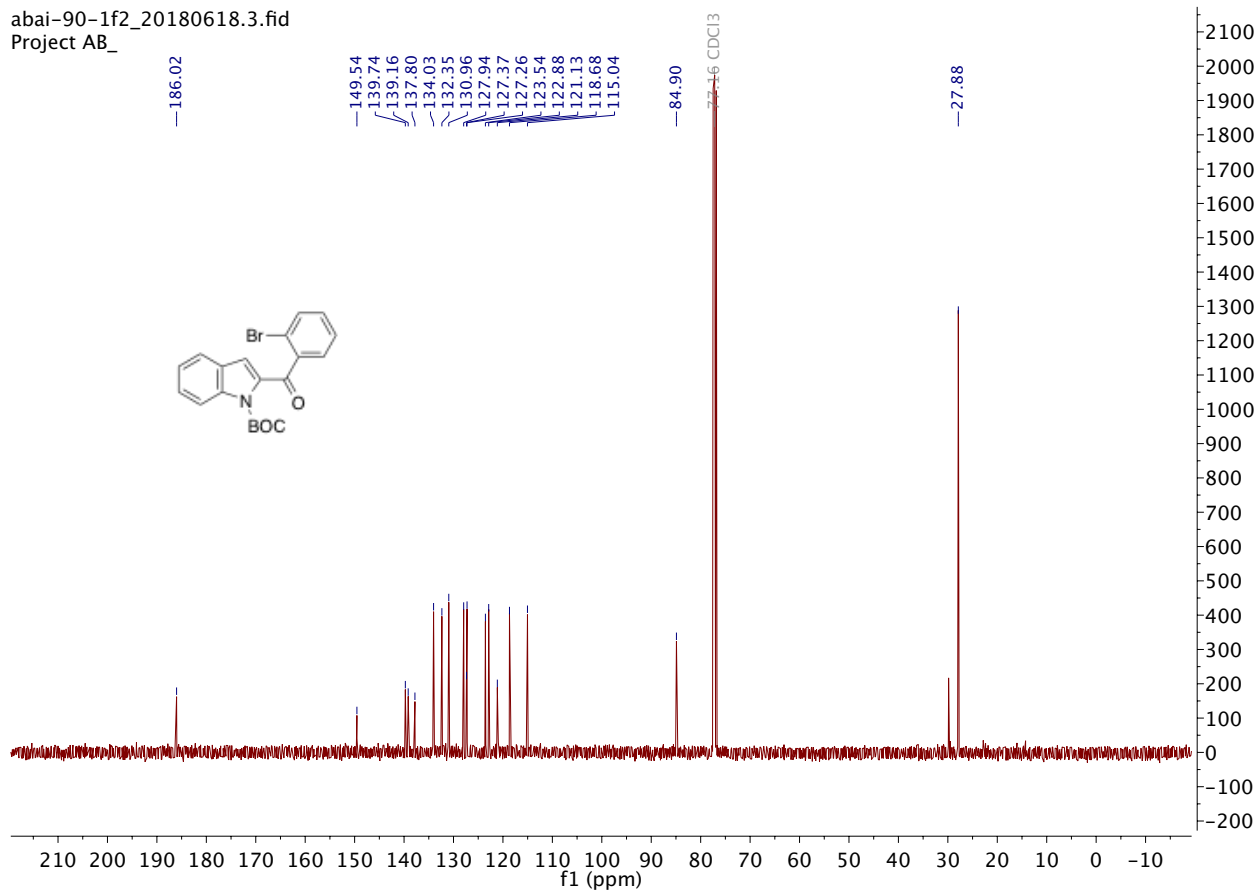
ESI : Carbonylative Suzuki-Miyaura couplings of sterically hindered aryl halides.

tert-butyl 2-(2-bromobenzoyl)-1H-indole-1-carboxylate **5f**

abai-90-1f2_20180618.1.fid
Project AB_

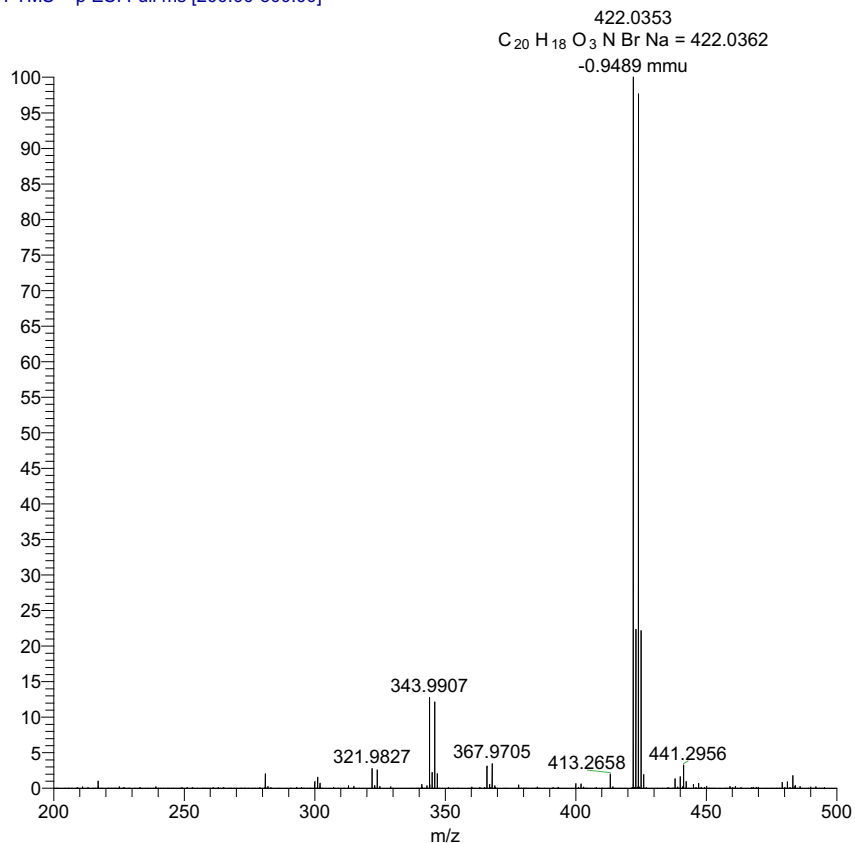


abai-90-1f2_20180618.3.fid
Project AB_



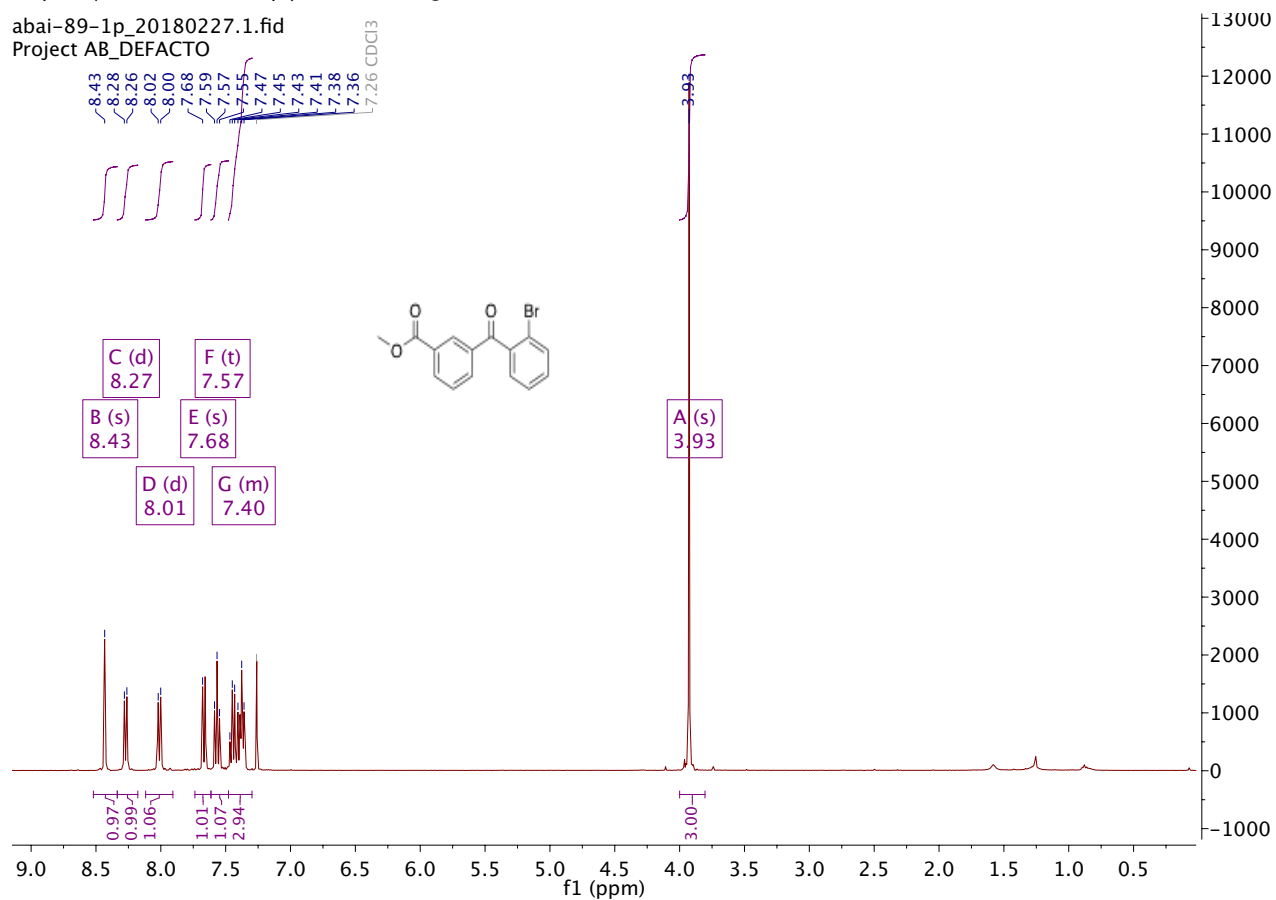
ESI : Carbonylative Suzuki-Miyaura couplings of sterically hindered aryl halides.

abai-90-1_180618162022 #4 RT: 0.09 AV: 1 NL: 6.40E7
T: FTMS + p ESI Full ms [200.00-500.00]



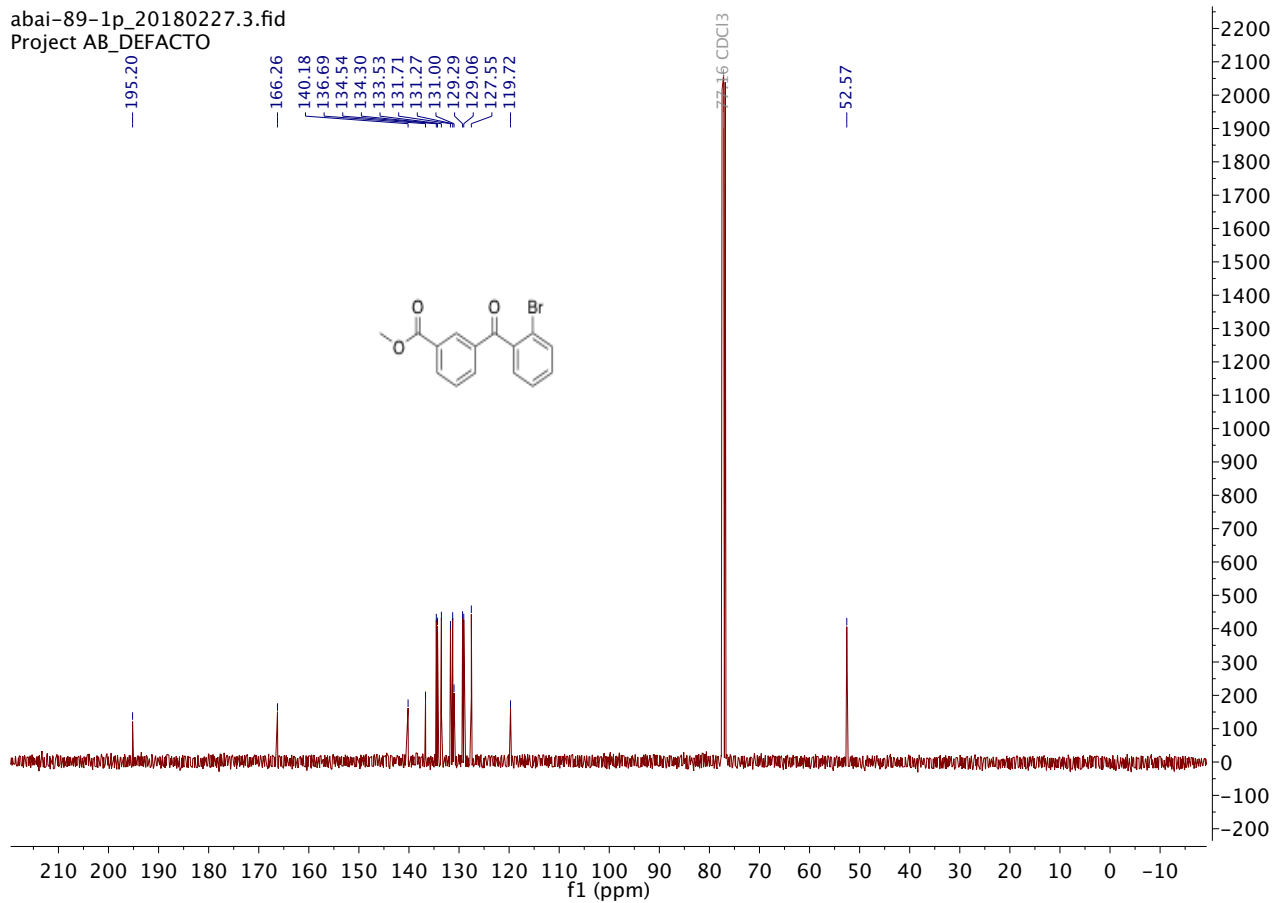
Methyl 3-(2-bromobenzoyl)benzoate **5g**

abai-89-1p_20180227.1.fid
Project AB_DEFACTO

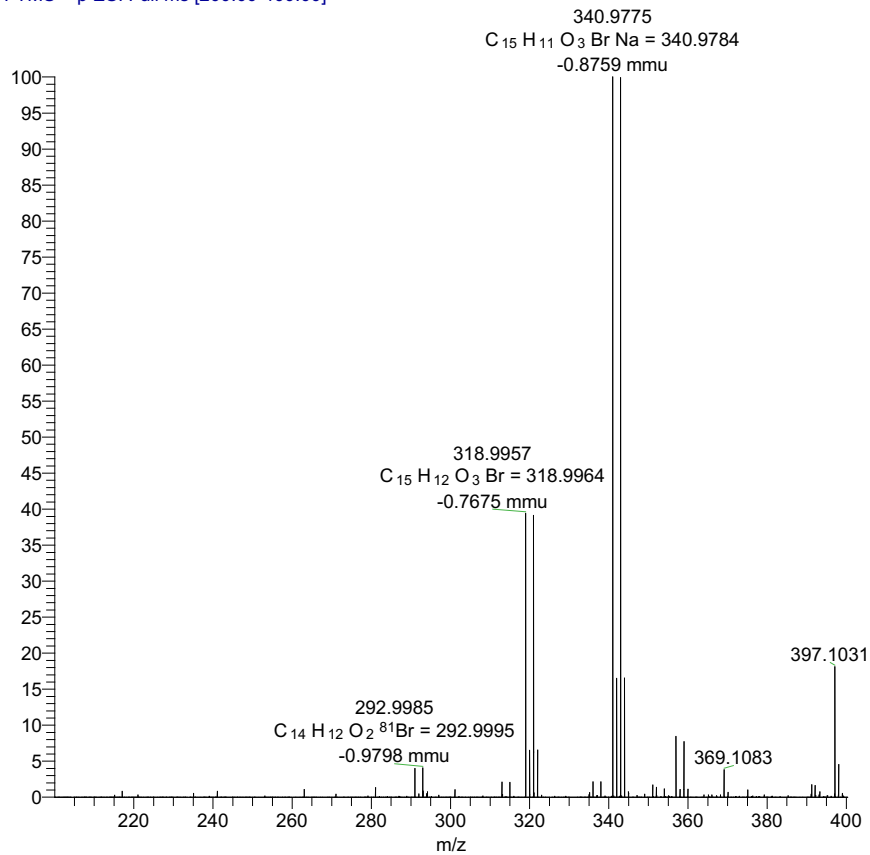


ESI : Carbonylative Suzuki-Miyaura couplings of sterically hindered aryl halides.

abai-89-1p_20180227.3.fid
Project AB_DEFACTO



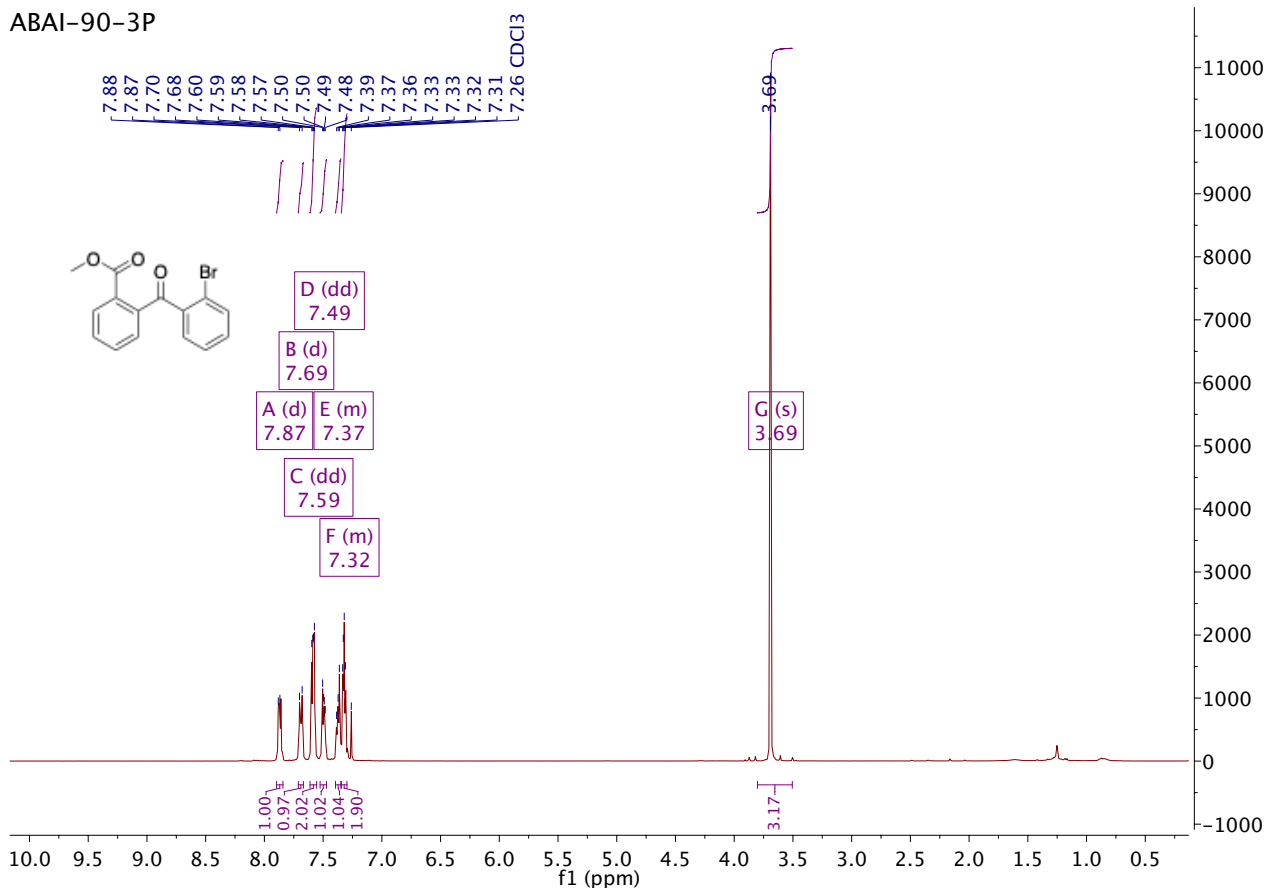
abai-89-1_180618154346 #1-5 RT: 0.02-0.13 AV: 5 NL: 1.39
T: FTMS + p ESI Full ms [200.00-400.00]



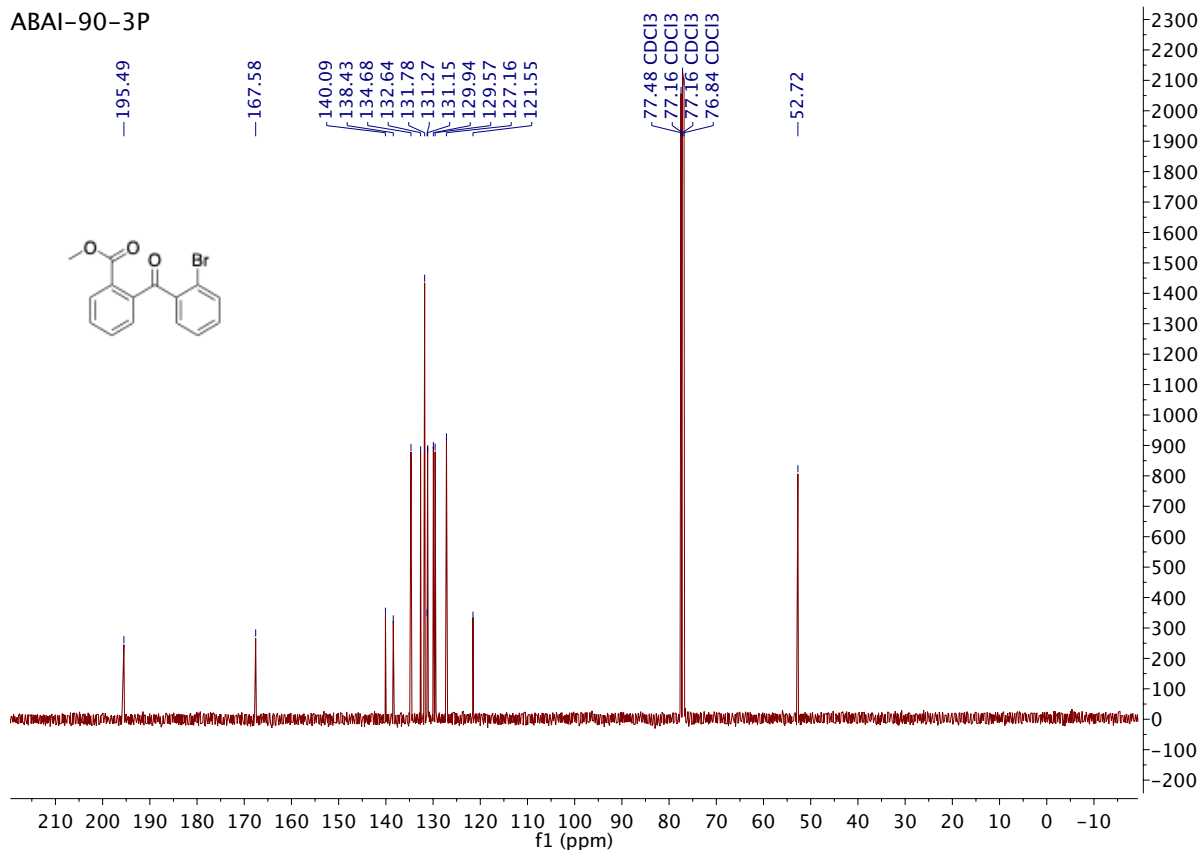
ESI : Carbonylative Suzuki-Miyaura couplings of sterically hindered aryl halides.

Methyl 2-(2-bromobenzoyl)benzoate **5h**

ABAI-90-3P

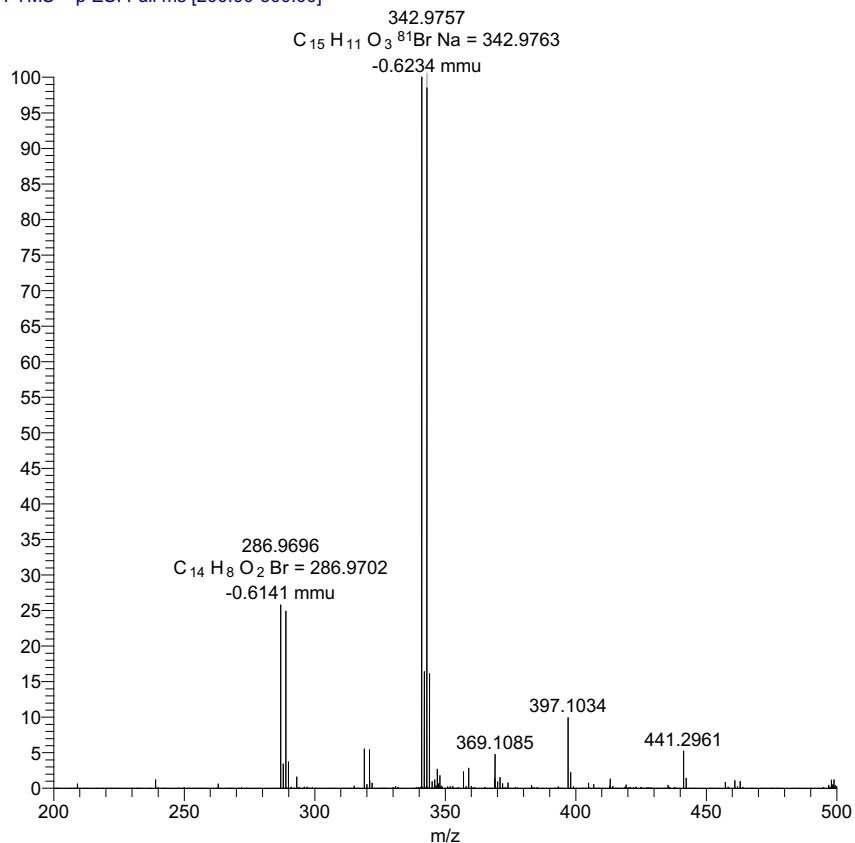


ABAI-90-3P



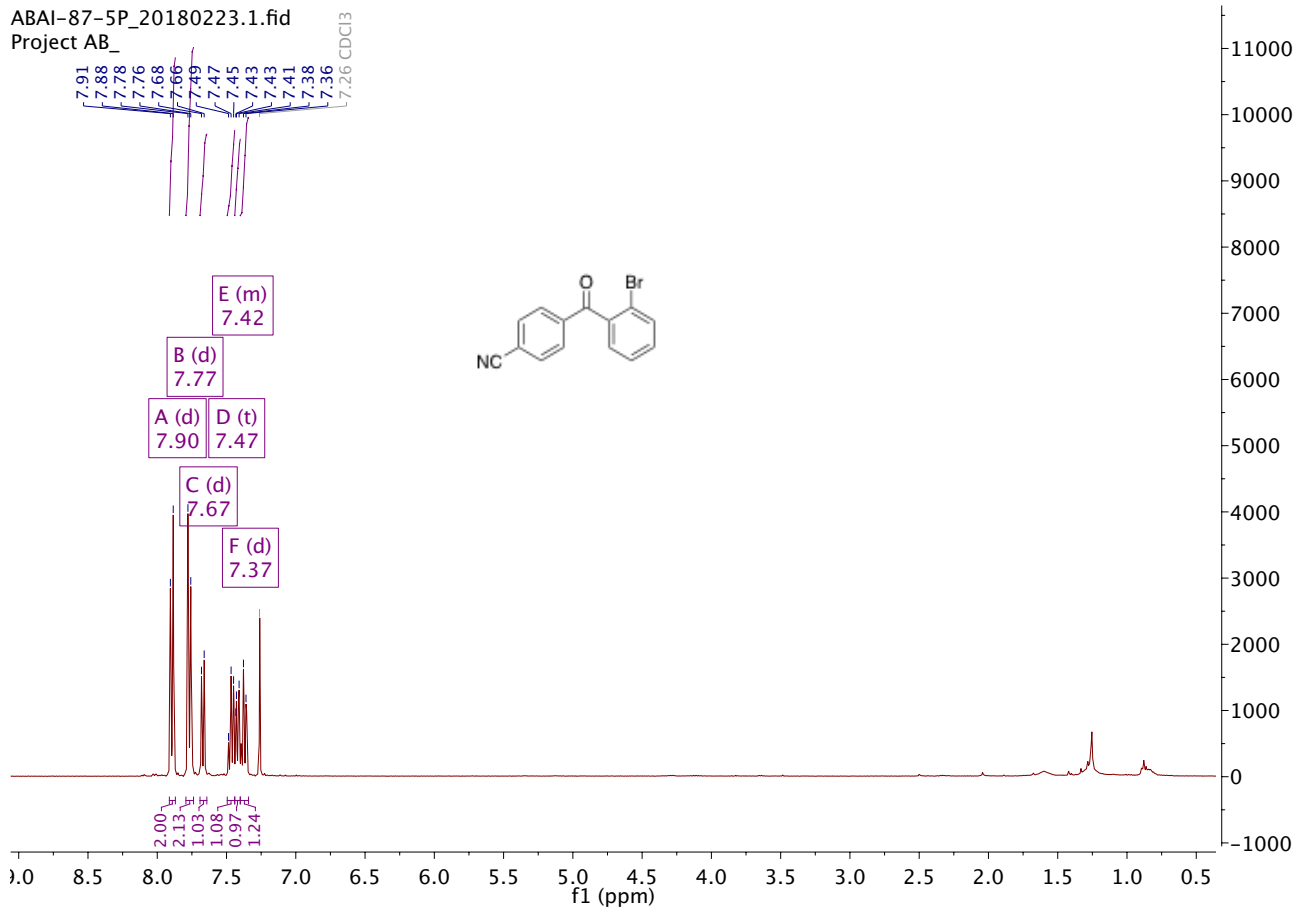
ESI : Carbonylative Suzuki-Miyaura couplings of sterically hindered aryl halides.

abai-90-3p_180618164331 #3 RT: 0.07 AV: 1 NL: 3.32E7
T: FTMS + p ESI Full ms [200.00-500.00]

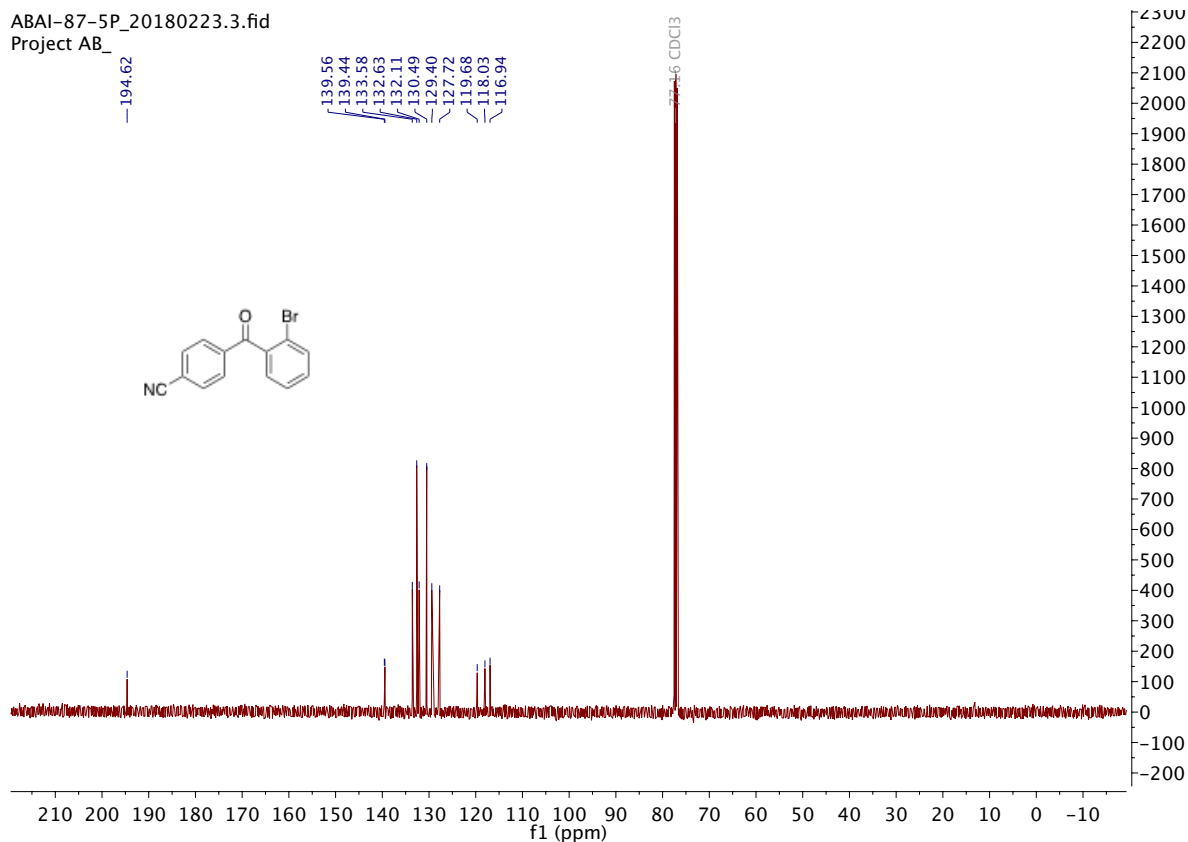


4-(2-Bromobenzoyl)benzonitrile **5i**

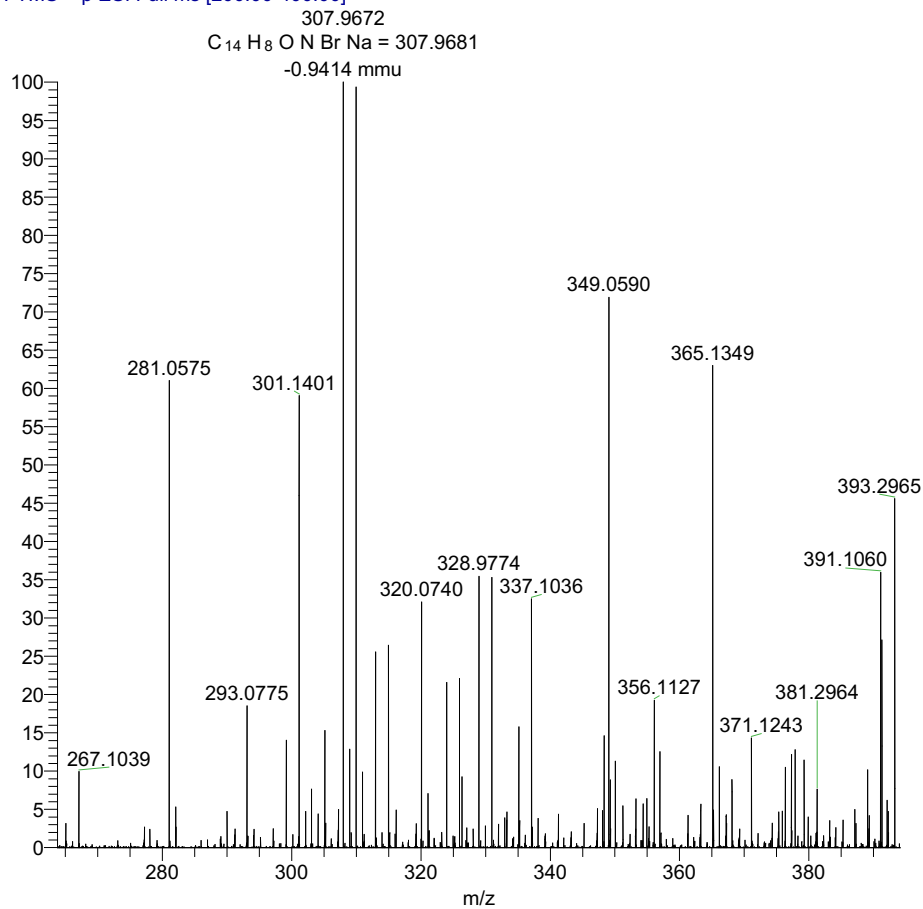
ABAI-87-5P_20180223.1.fid
Project AB_



ESI : Carbonylative Suzuki-Miyaura couplings of sterically hindered aryl halides.

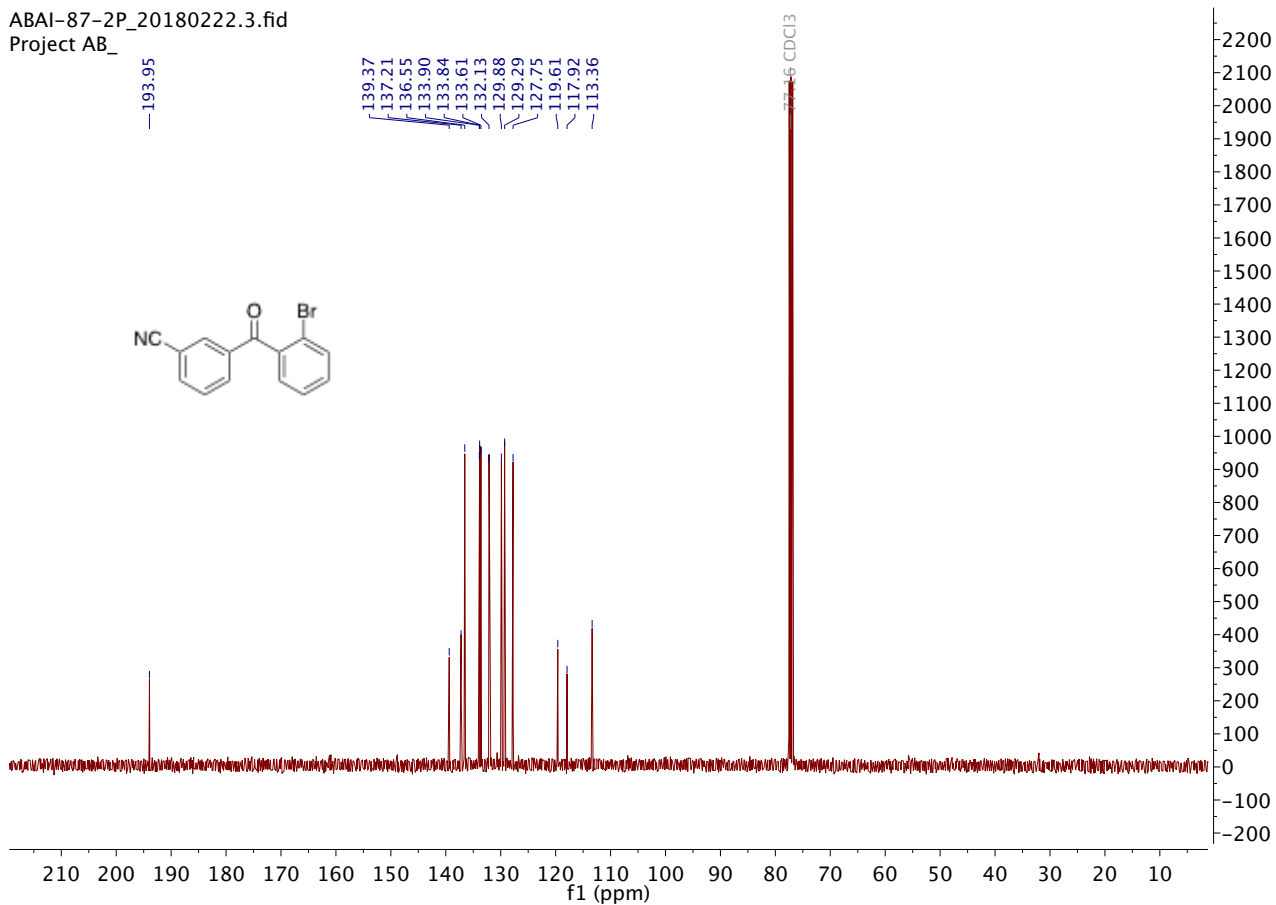
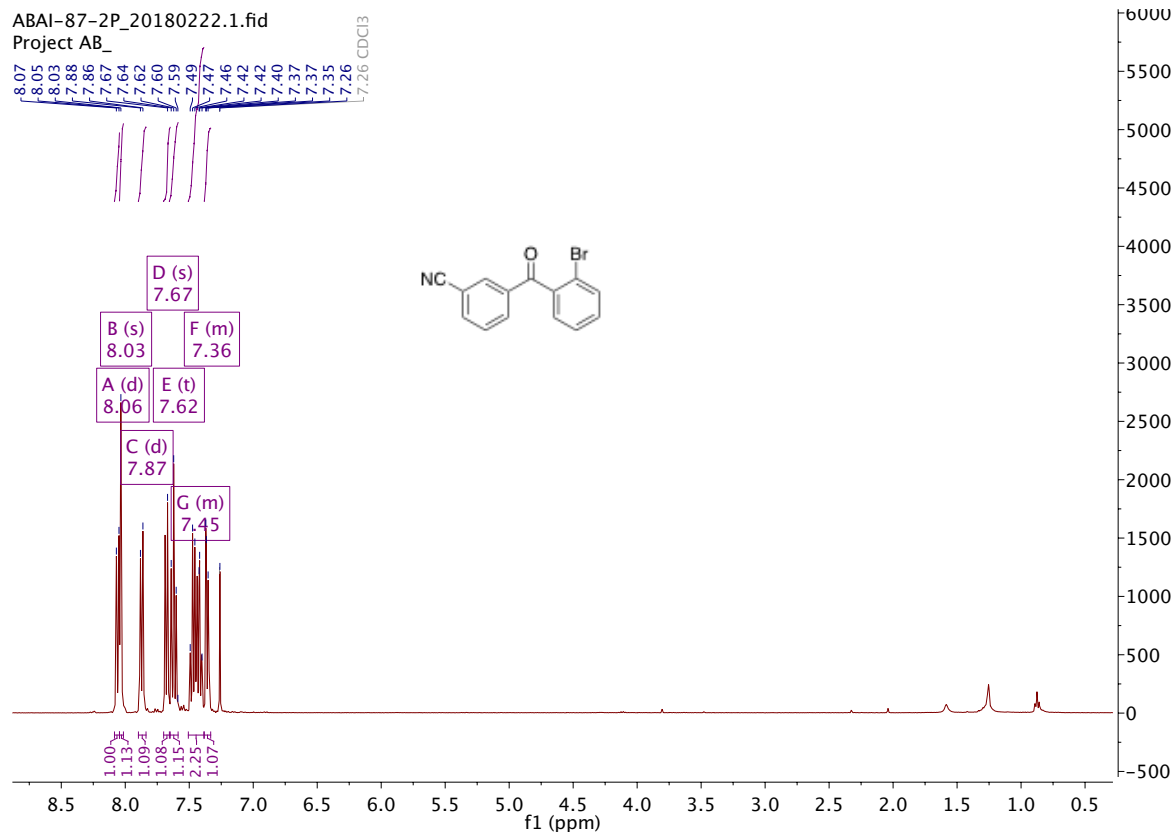


abai-87-5_180618154346 #1-5 RT: 0.02-0.13 AV: 5 NL: 1.76
T: FTMS + p ESI Full ms [200.00-400.00]



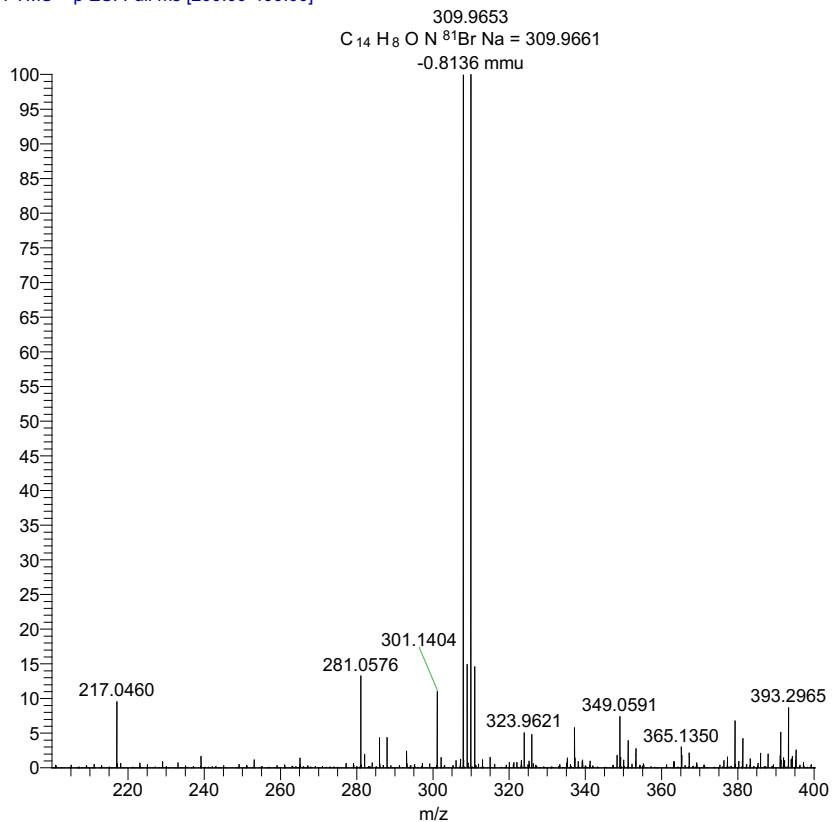
ESI : Carbonylative Suzuki-Miyaura couplings of sterically hindered aryl halides.

3-(2-Bromobenzoyl)benzonitrile **5j**



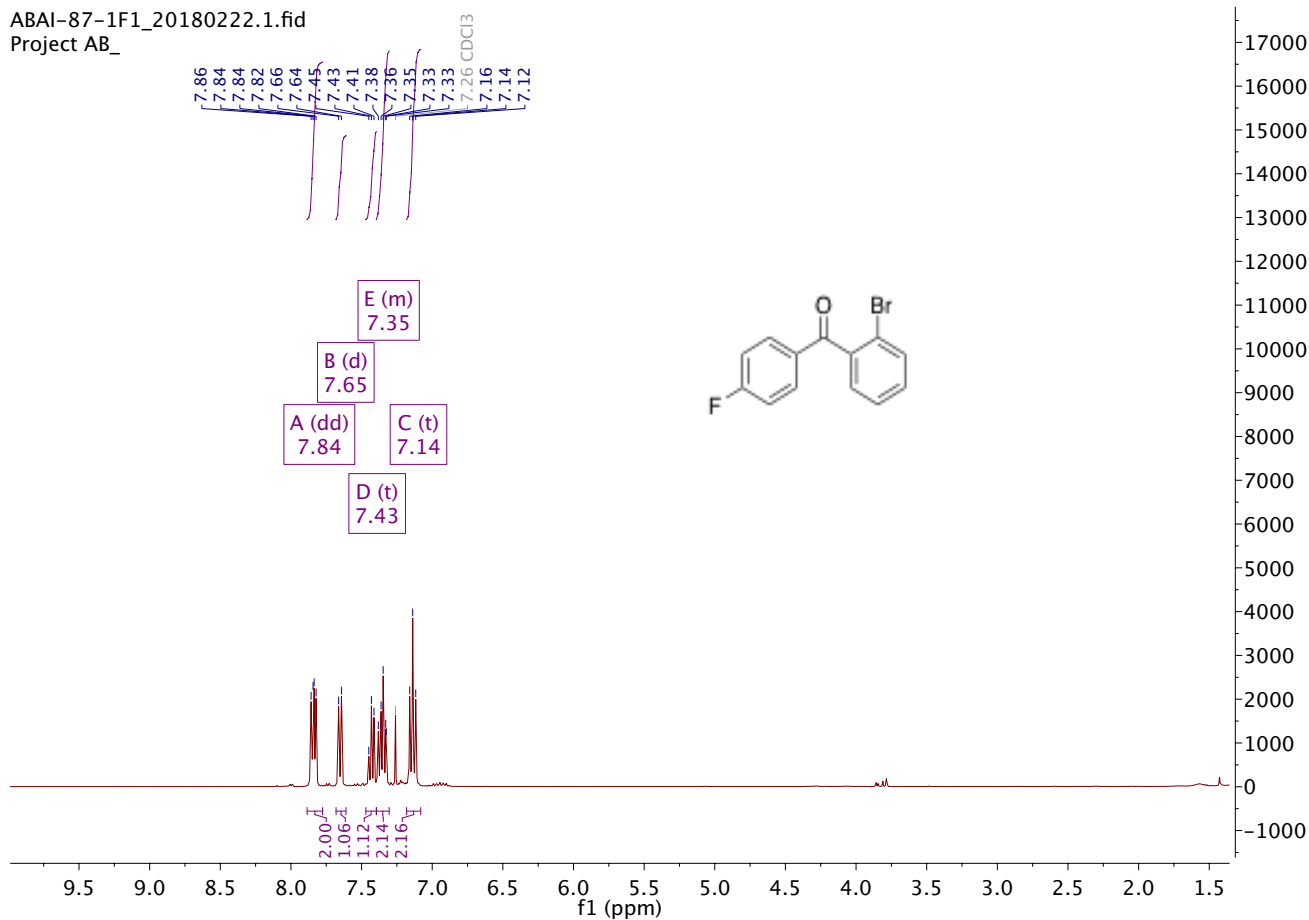
ESI : Carbonylative Suzuki-Miyaura couplings of sterically hindered aryl halides.

abai-87-2p_180618154346 #1-5 RT: 0.00-0.11 AV: 5 NL: 7.4
 T: FTMS + p ESI Full ms [200.00-400.00]



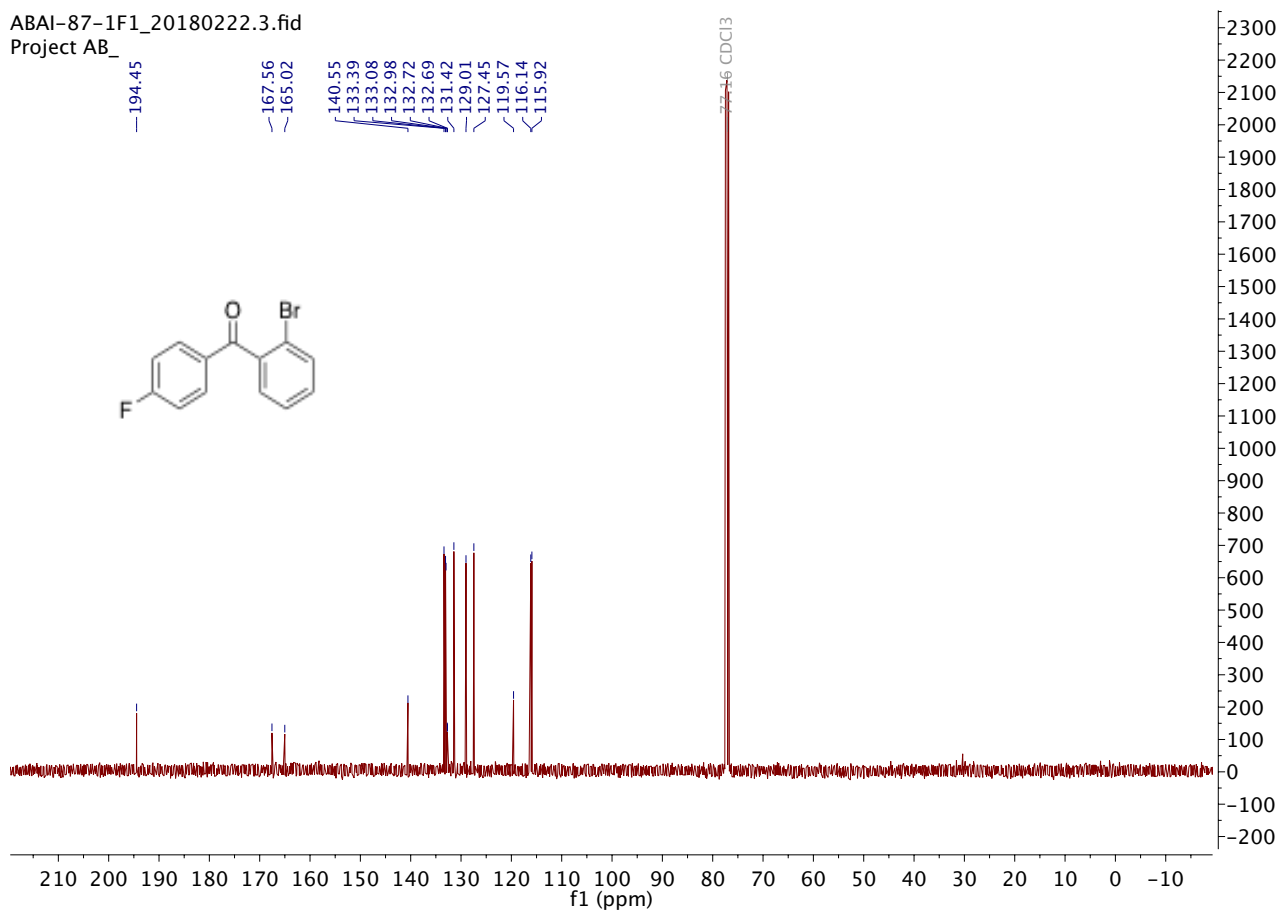
2-Bromophenyl 4-fluorophenyl methanone 5k

ABAI-87-1F1_20180222.1.fid
 Project AB_



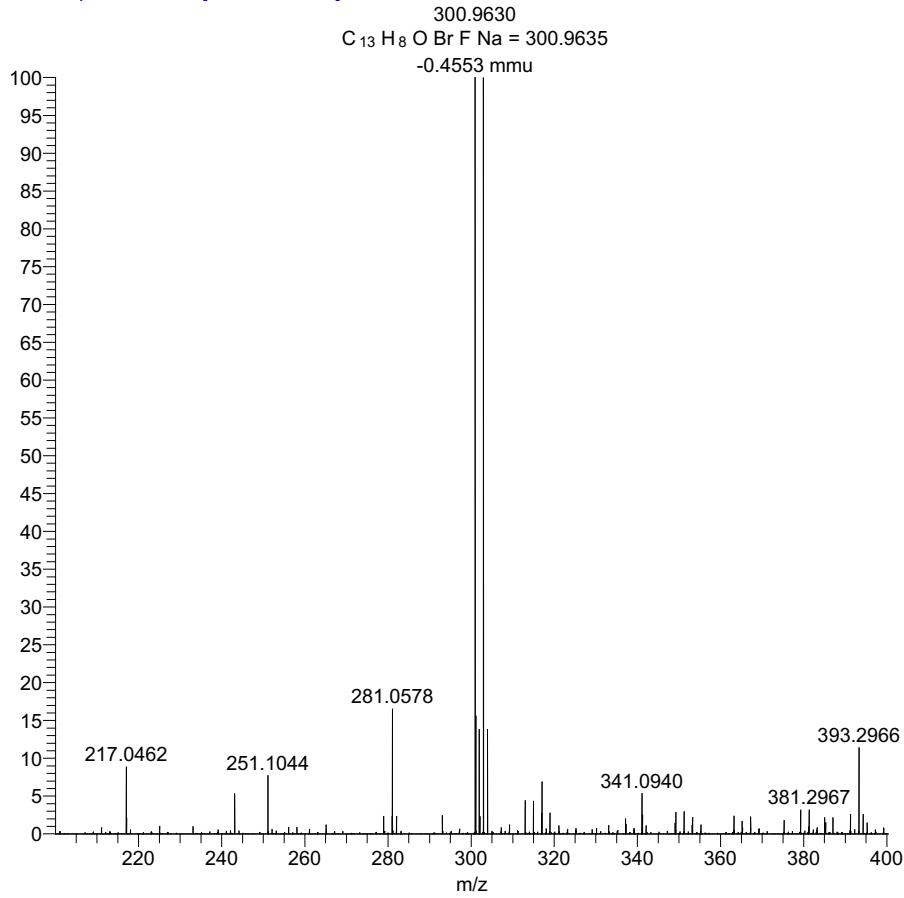
ESI : Carbonylative Suzuki-Miyaura couplings of sterically hindered aryl halides.

ABAI-87-1F1_20180222.3.fid
Project AB_

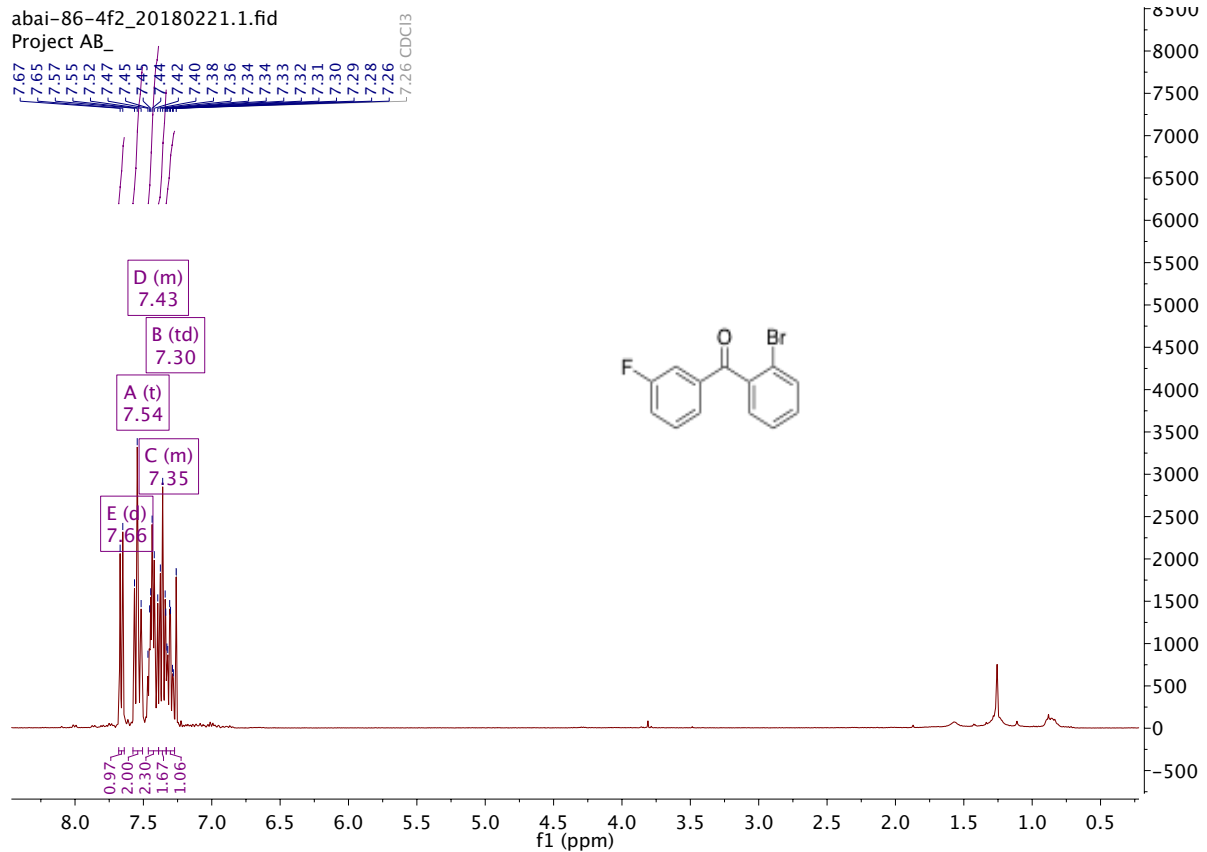


ESI : Carbonylative Suzuki-Miyaura couplings of sterically hindered aryl halides.

abai-86-4-f1_180618150932 #1-4 RT: 0.02-0.10 AV: 4 NL: 1.
T: FTMS + p ESI Full ms [200.00-400.00]

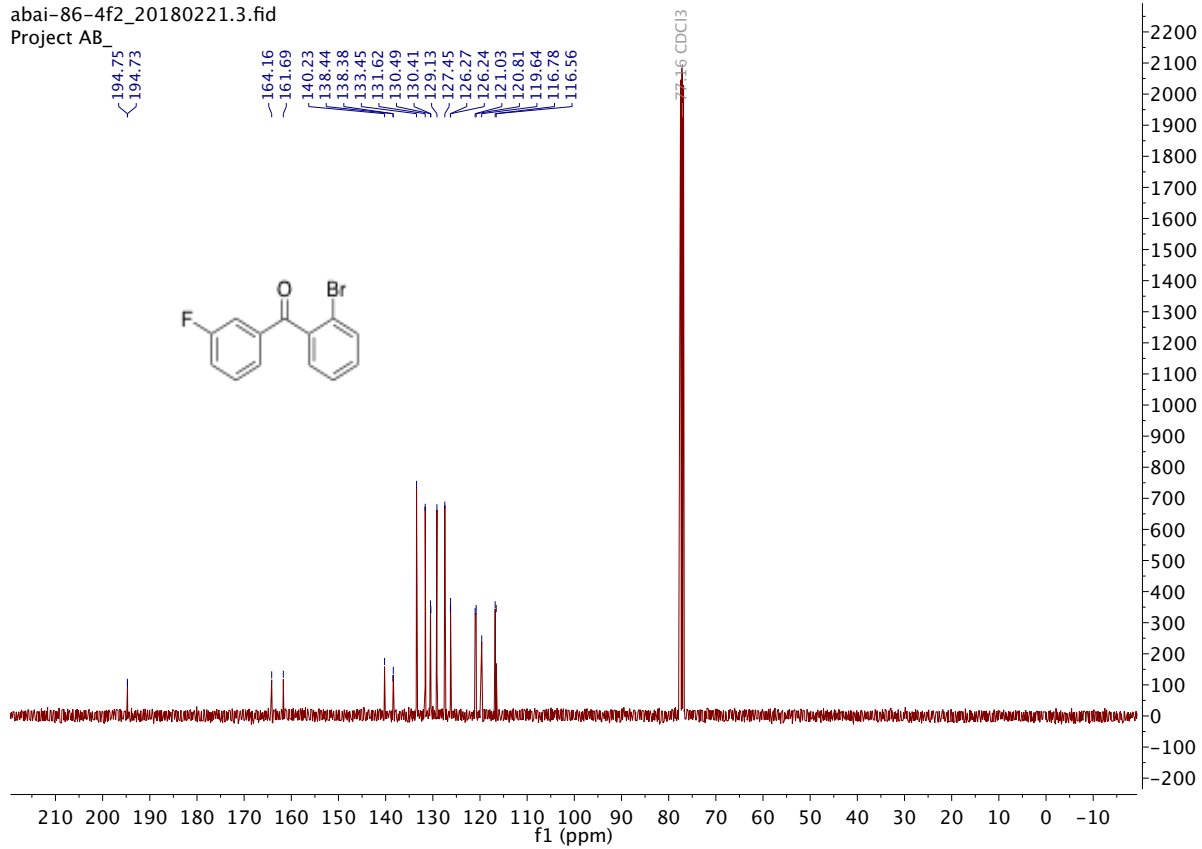


2-bromophenyl 3-fluorophenyl methanone 5I

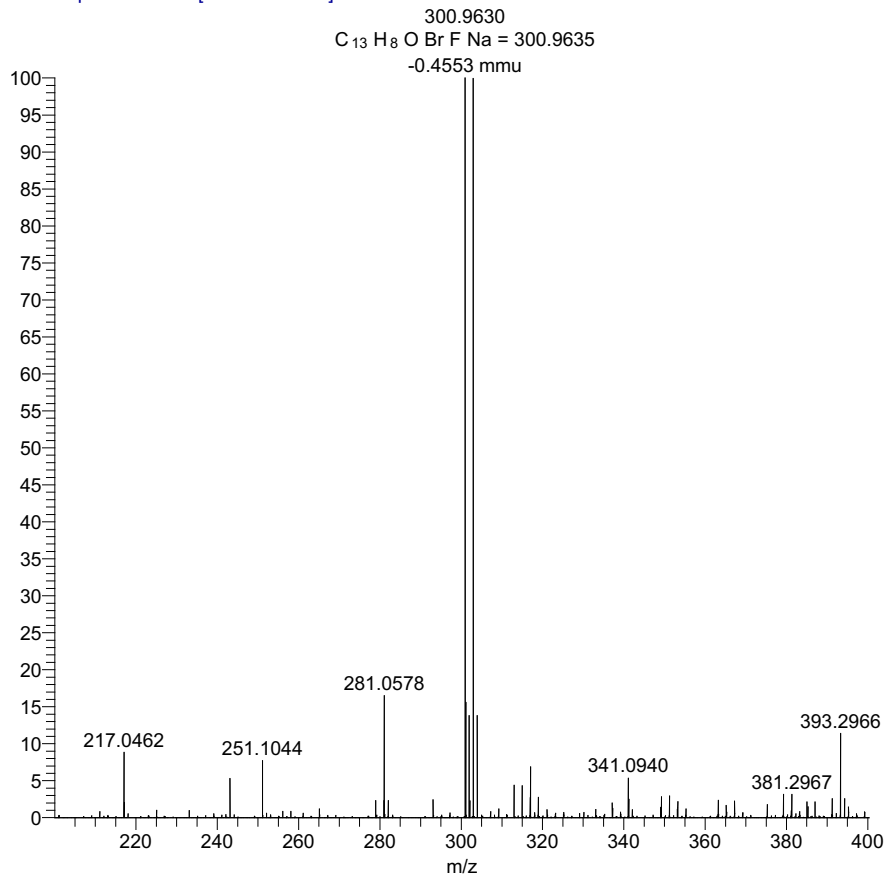


ESI : Carbonylative Suzuki-Miyaura couplings of sterically hindered aryl halides.

abai-86-4f2_20180221.3.fid
Project AB



abai-86-4-f1_180618150932 #1-4 RT: 0.02-0.10 AV: 4 NL: 1
T: FTMS + p ESI Full ms [200.00-400.00]

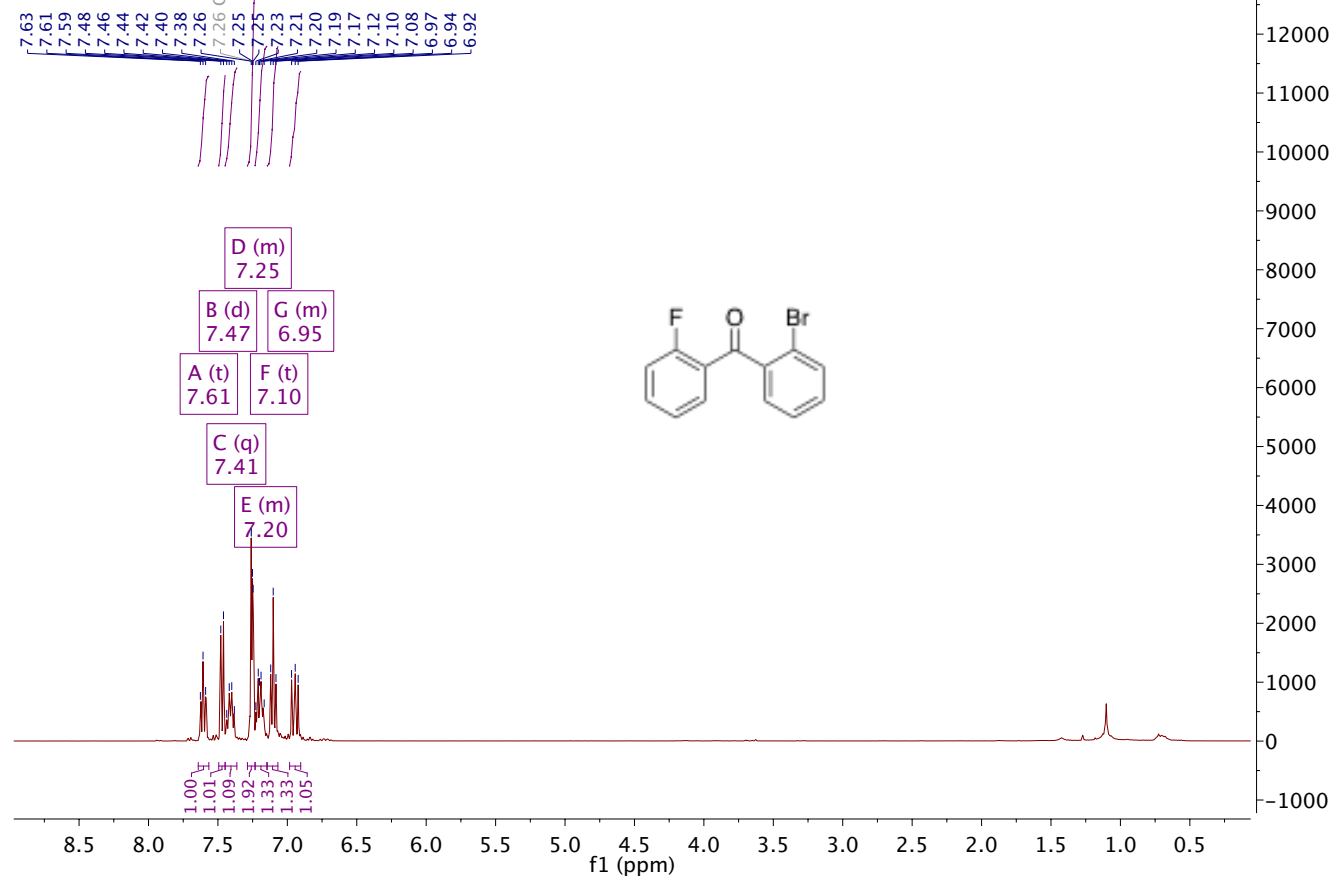


ESI : Carbonylative Suzuki-Miyaura couplings of sterically hindered aryl halides.

2-Bromophenyl 2-fluorophenyl methanone **5m**

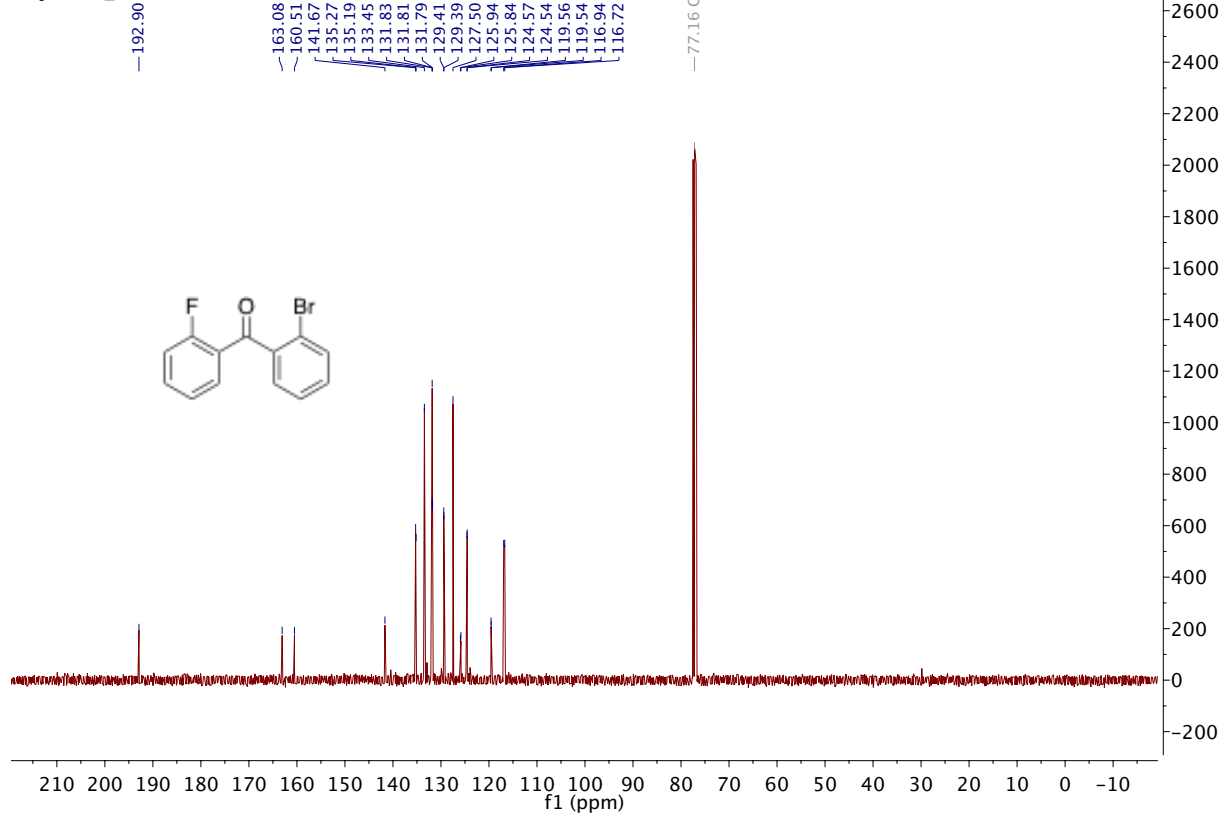
abai-86-3_20180221.1.fid

Project AB_



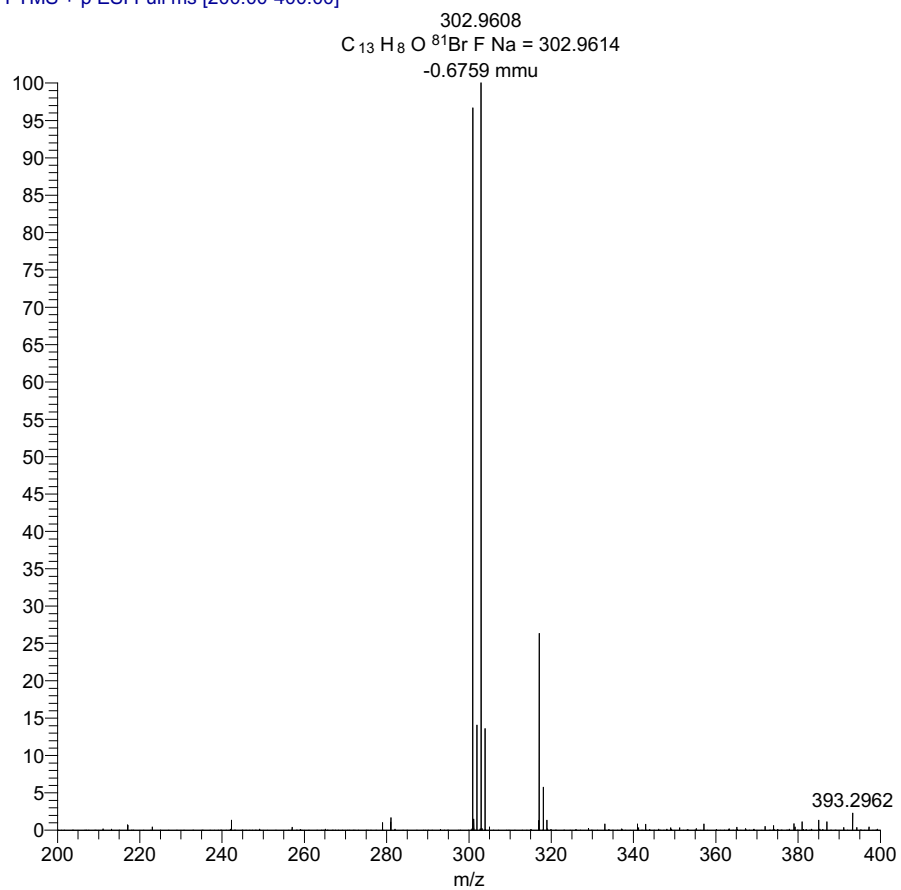
abai-86-3_20180221.3.fid

Project AB_



ESI : Carbonylative Suzuki-Miyaura couplings of sterically hindered aryl halides.

abai-86-3_180618173109 #1 RT: 0.01 AV: 1 NL: 3.90E7
T: FTMS + p ESI Full ms [200.00-400.00]

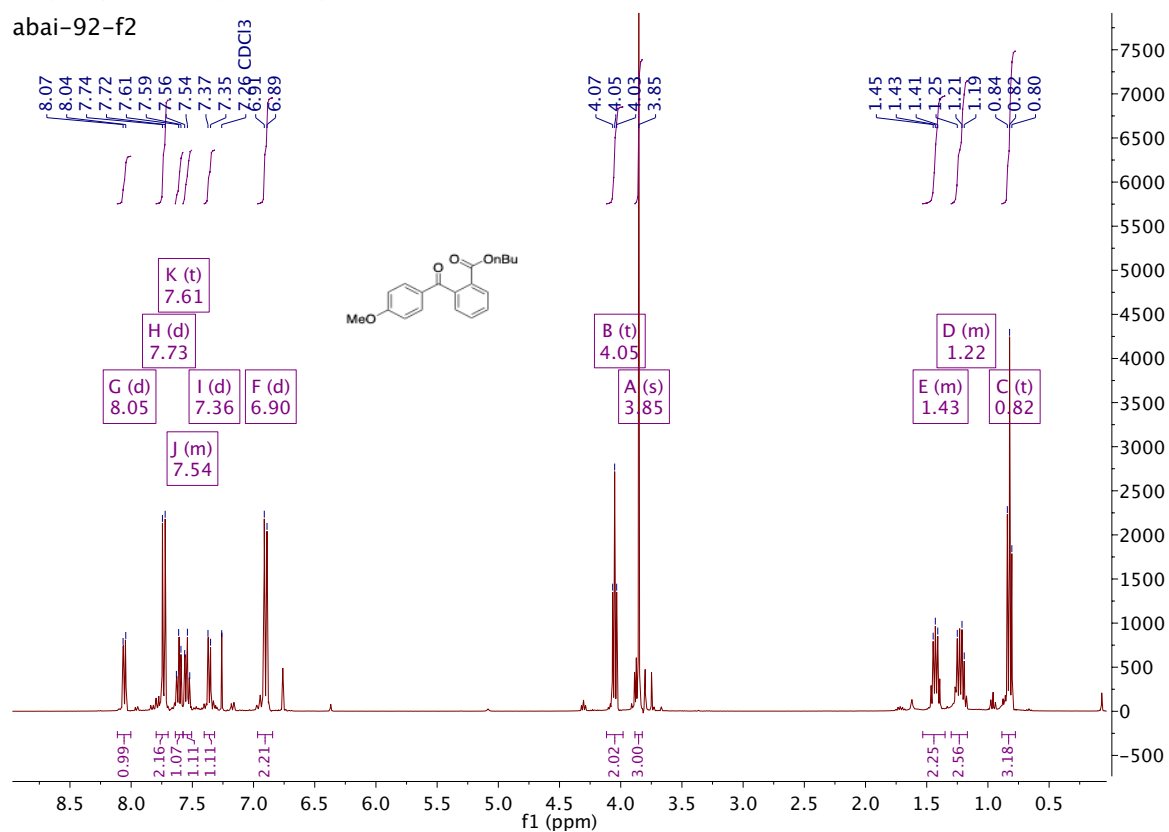


ESI : Carbonylative Suzuki-Miyaura couplings of sterically hindered aryl halides.

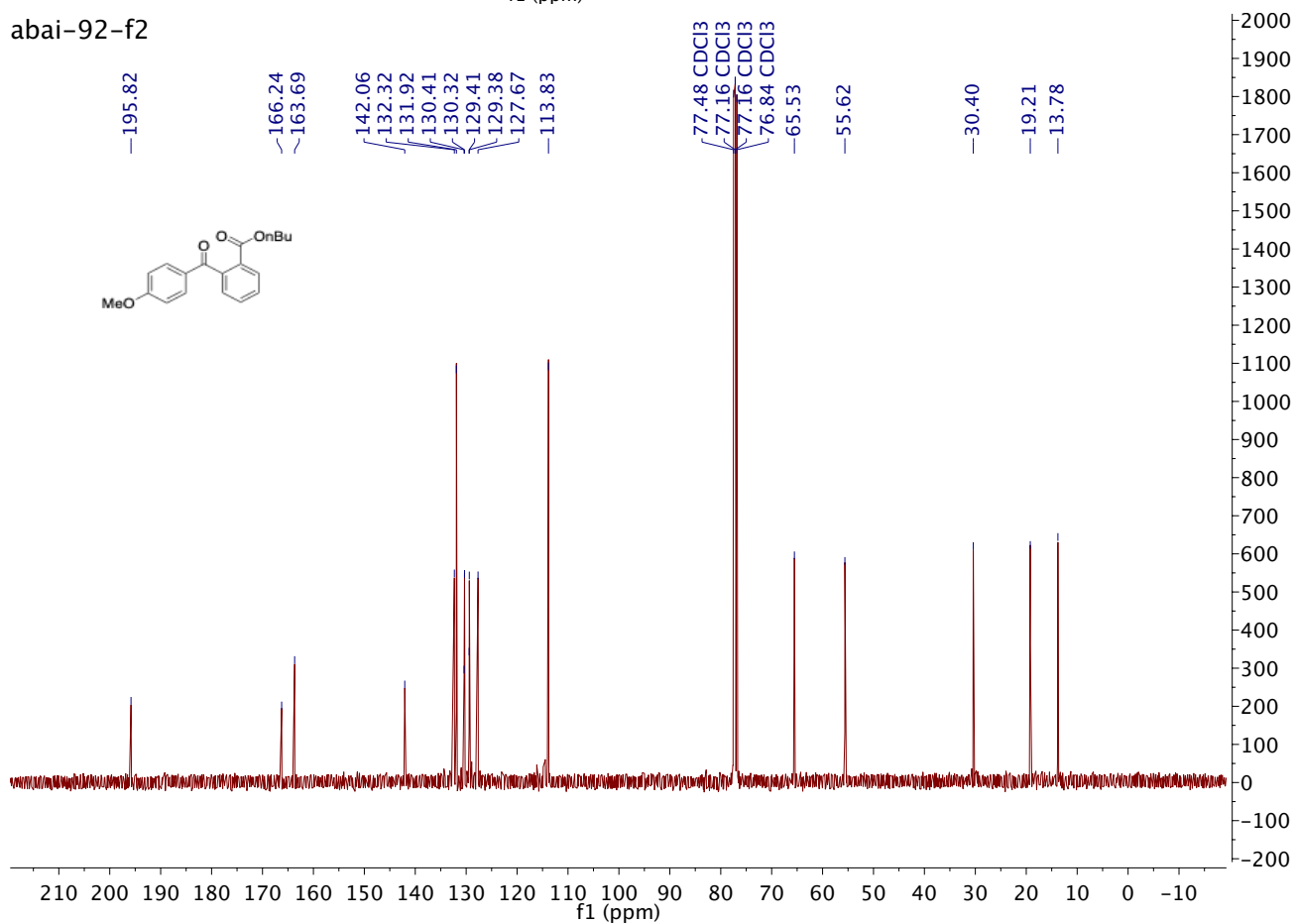
4.2 Spectra for butyl 2-benzoylbenzoate esters 2

Butyl 2-(4-methoxybenzoyl)benzoate **2a**

abai-92-f2

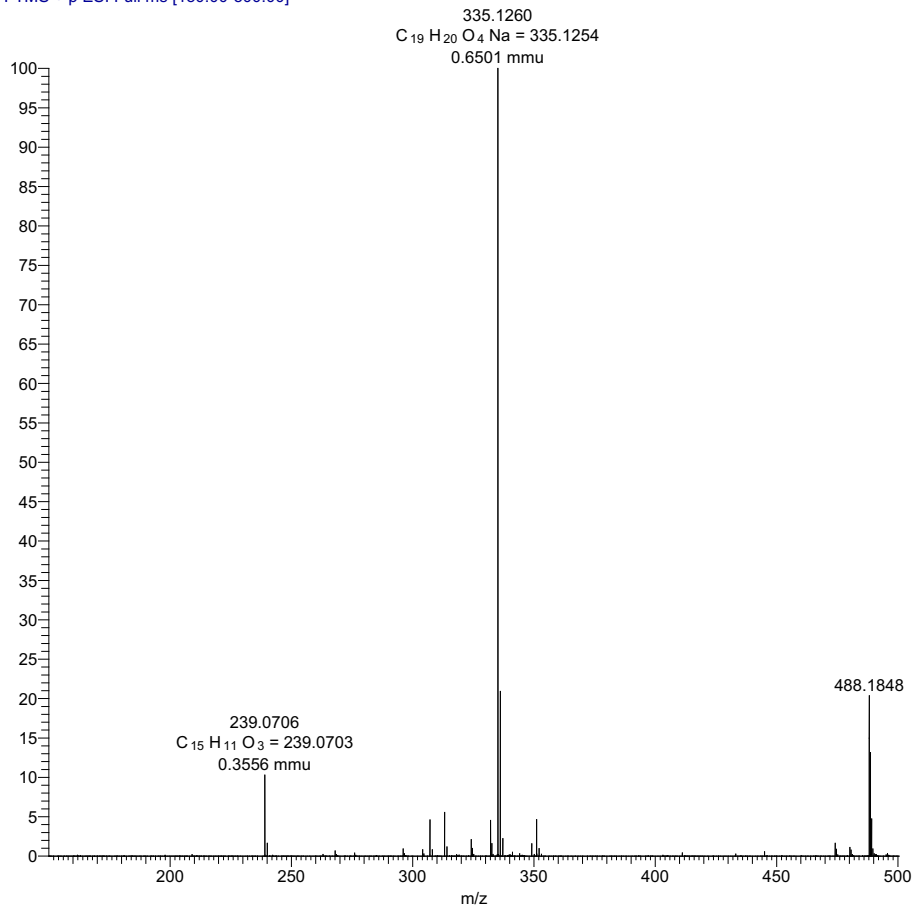


abai-92-f2



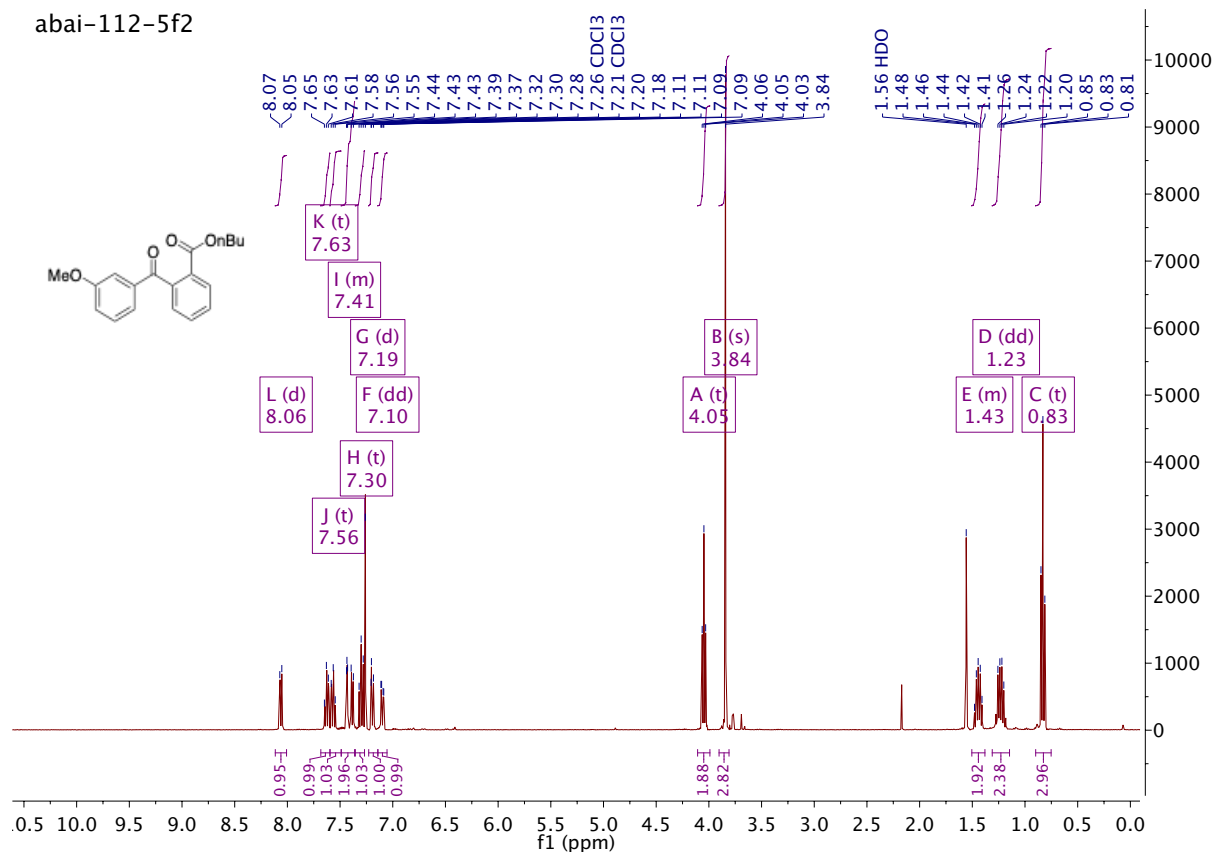
ESI : Carbonylative Suzuki-Miyaura couplings of sterically hindered aryl halides.

abai-112-6f3_190627172410 #1-4 RT: 0.01-0.10 AV: 4 NL: 5.01E7
 T: FTMS + p ESI Full ms [150.00-500.00]



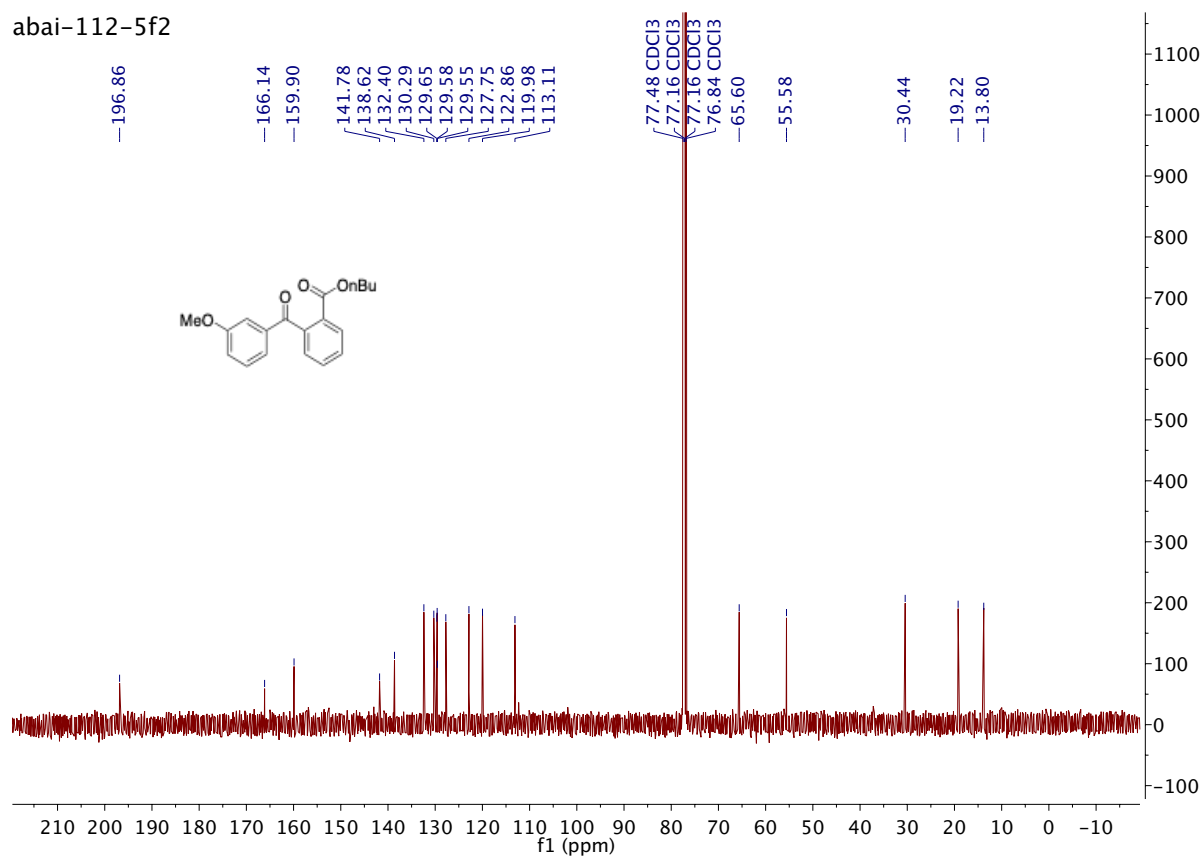
Butyl 2-(3-methoxybenzoyl)benzoate **2b**

abai-112-5f2

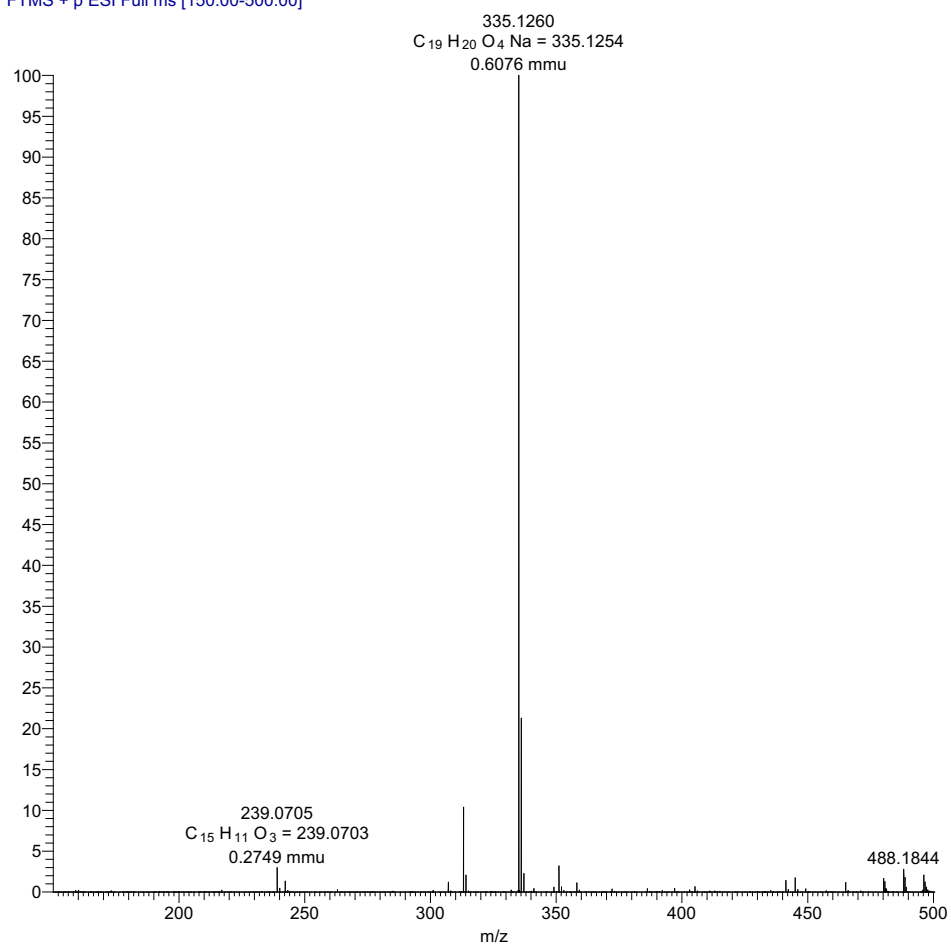


ESI : Carbonylative Suzuki-Miyaura couplings of sterically hindered aryl halides.

abai-112-5f2



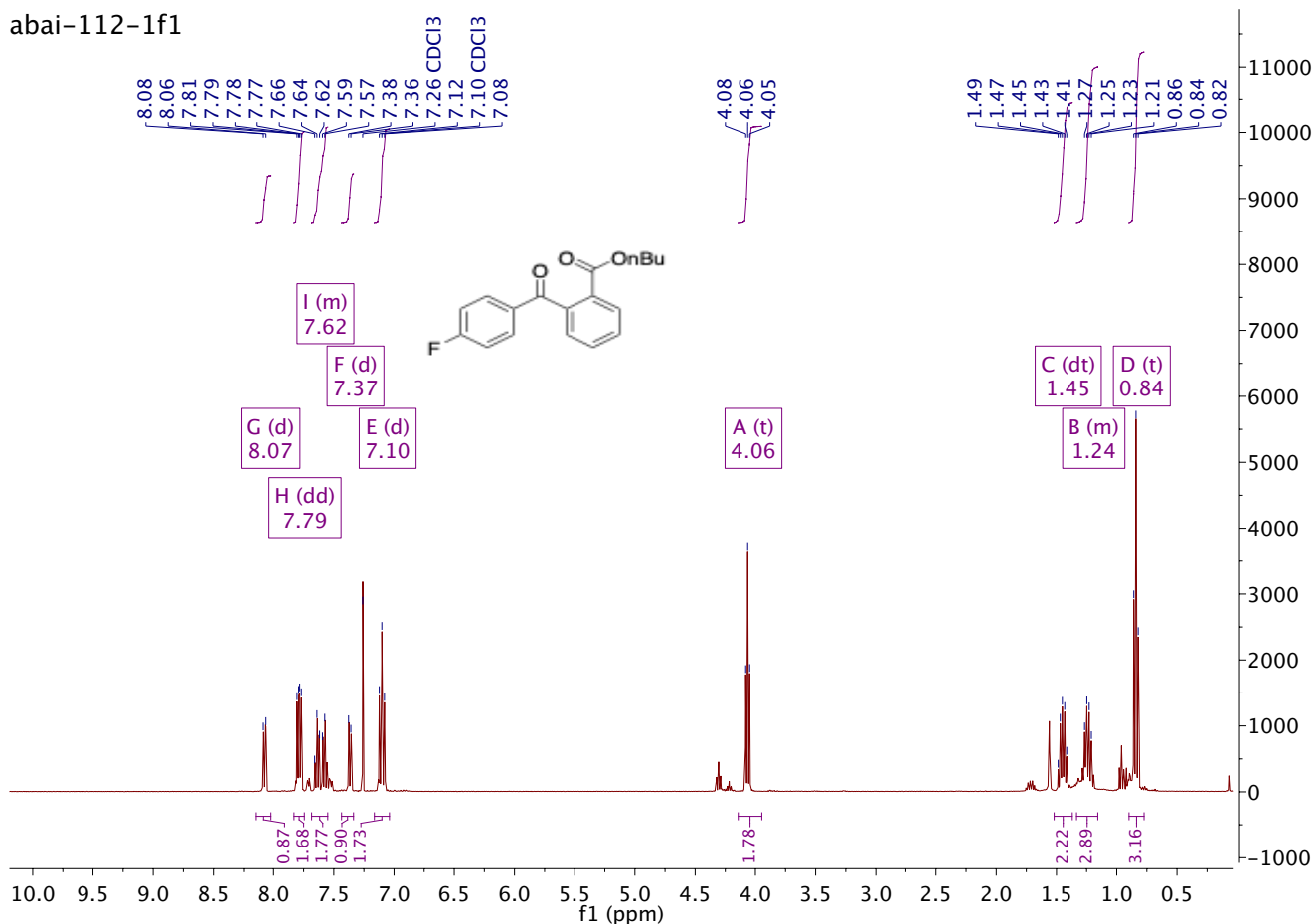
abai-112-5f2_190627172410 #1-5 RT: 0.00-0.11 AV: 5 NL: 4.27E7
T: FTMS + p ESI Full ms [150.00-500.00]



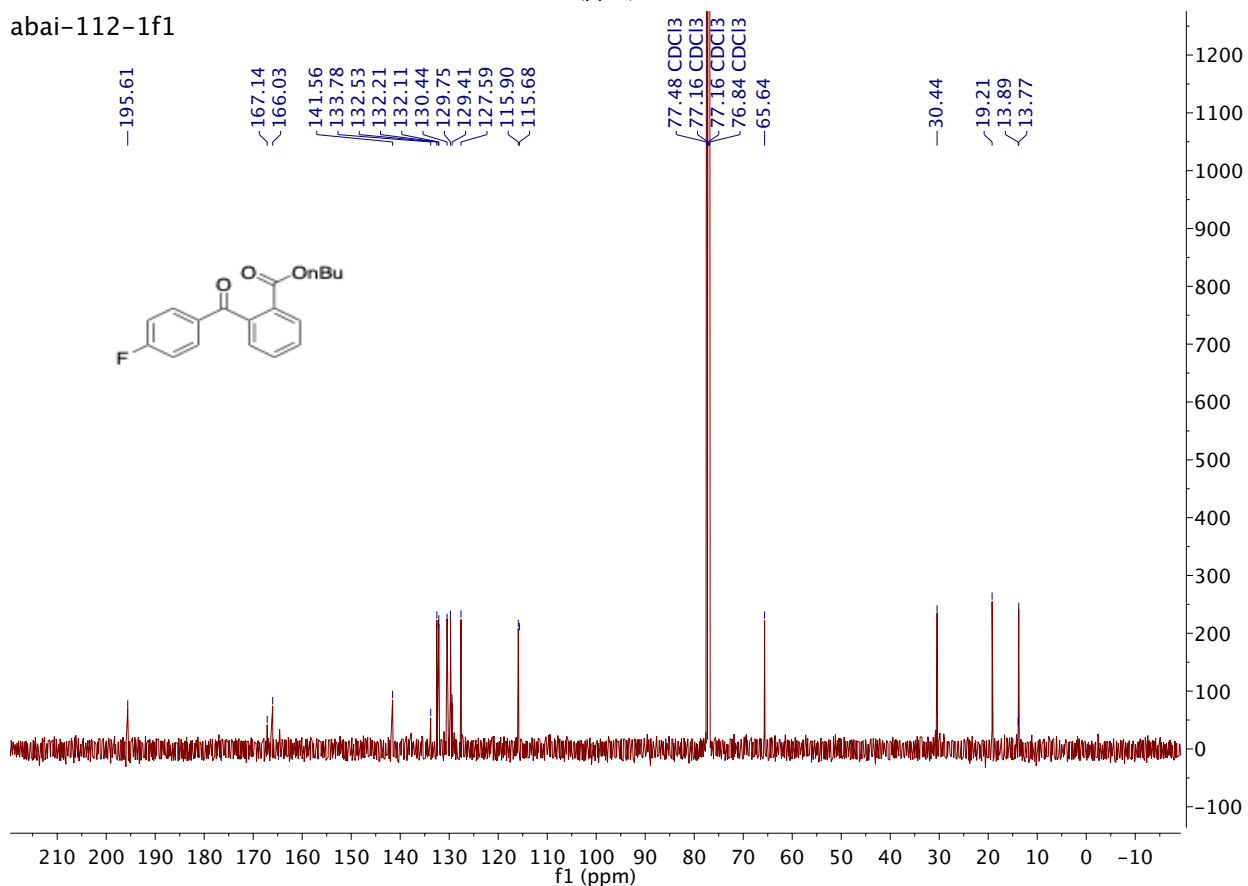
ESI : Carbonylative Suzuki-Miyaura couplings of sterically hindered aryl halides.

Butyl 2-(4-fluorobenzoyl)benzoate **2c**

abai-112-1f1

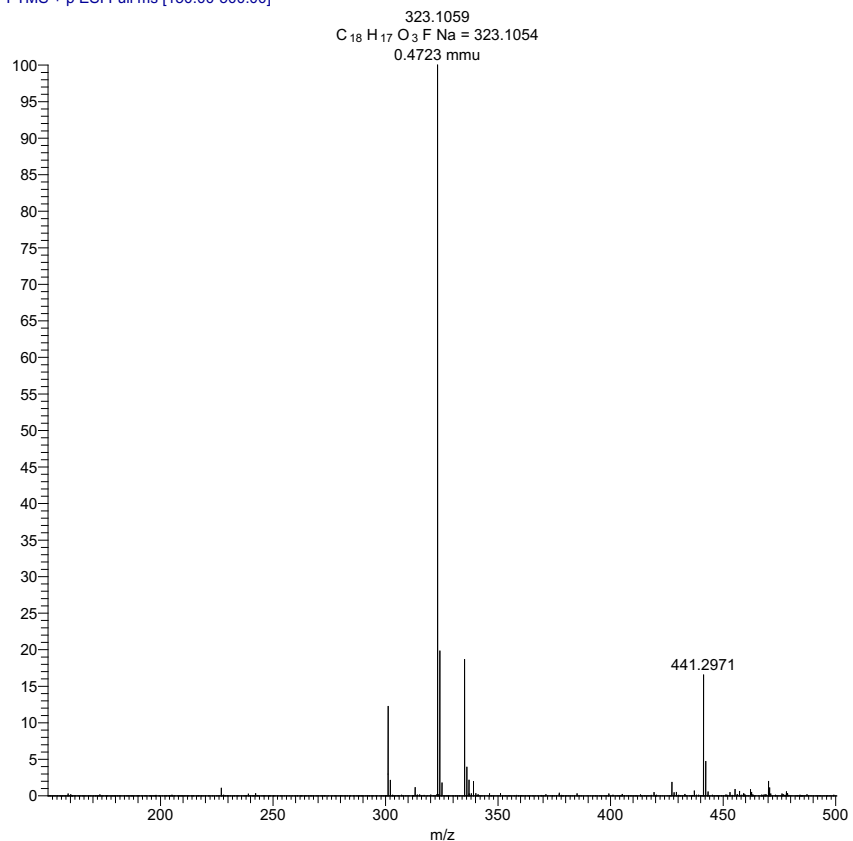


abai-112-1f1



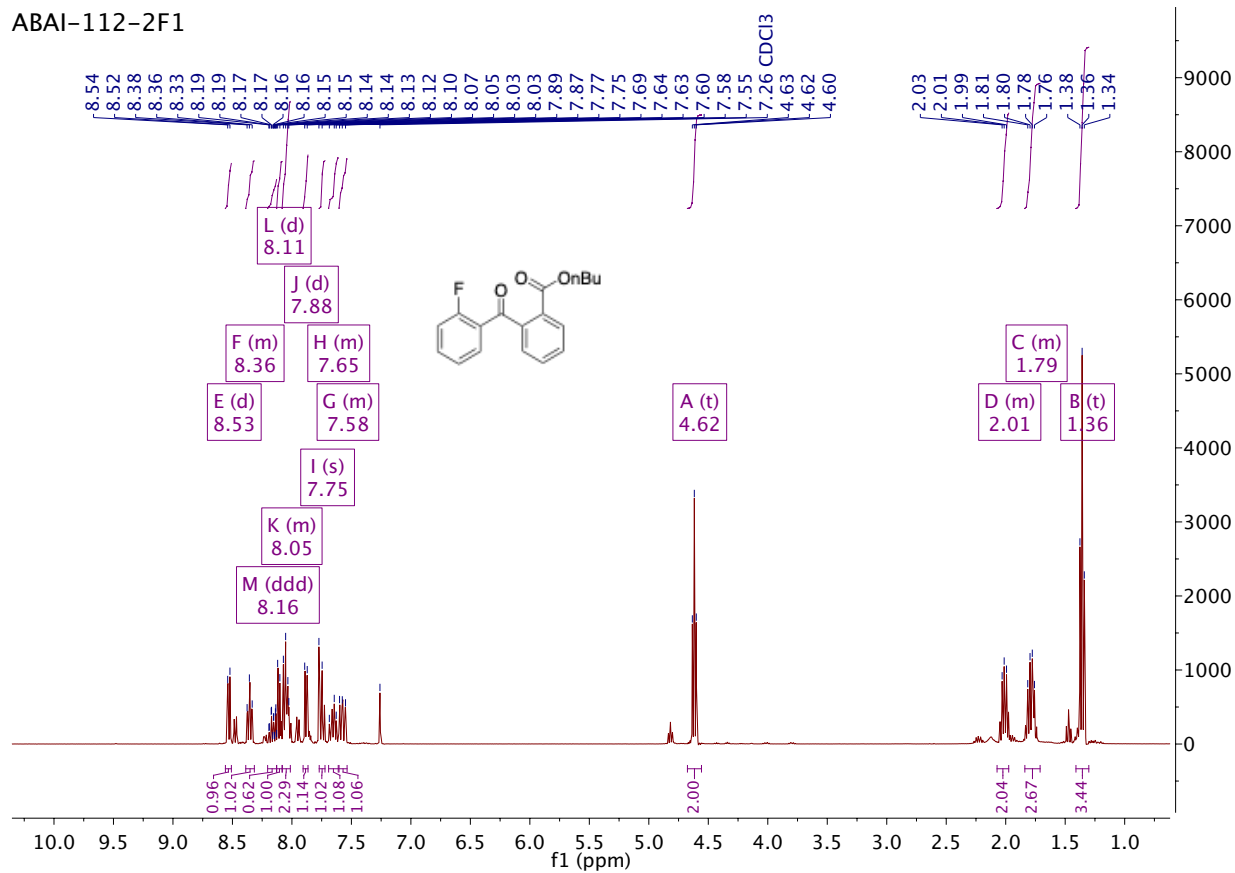
ESI : Carbonylative Suzuki-Miyaura couplings of sterically hindered aryl halides.

abai-112-1f1_190627172410 #1-5 RT: 0.01-0.12 AV: 5 NL: 6.71E7
 T: FTMS + p ESI Full ms [150.00-500.00]



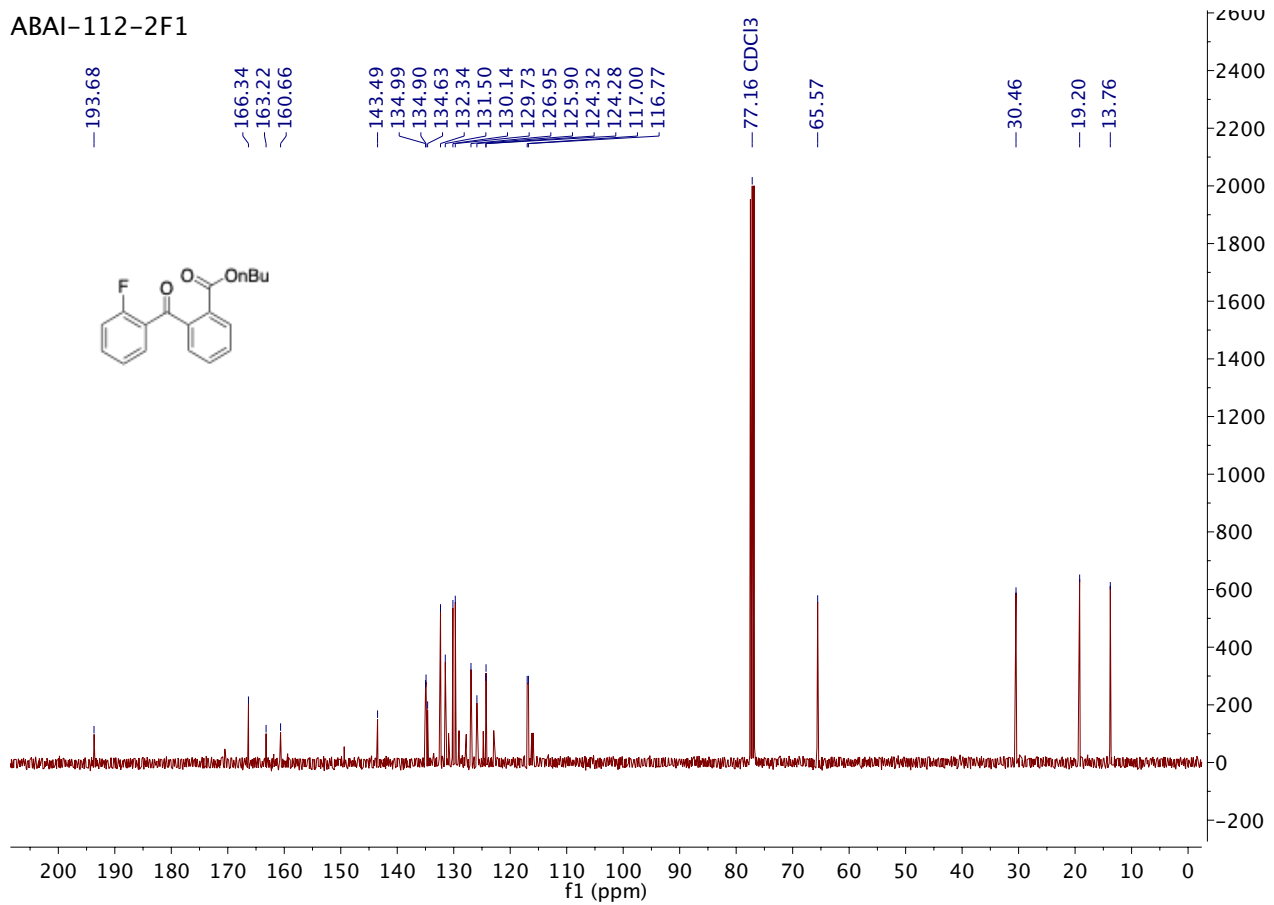
Butyl 2-(2-fluorobenzoyl)benzoate **2d**

ABAI-112-2F1

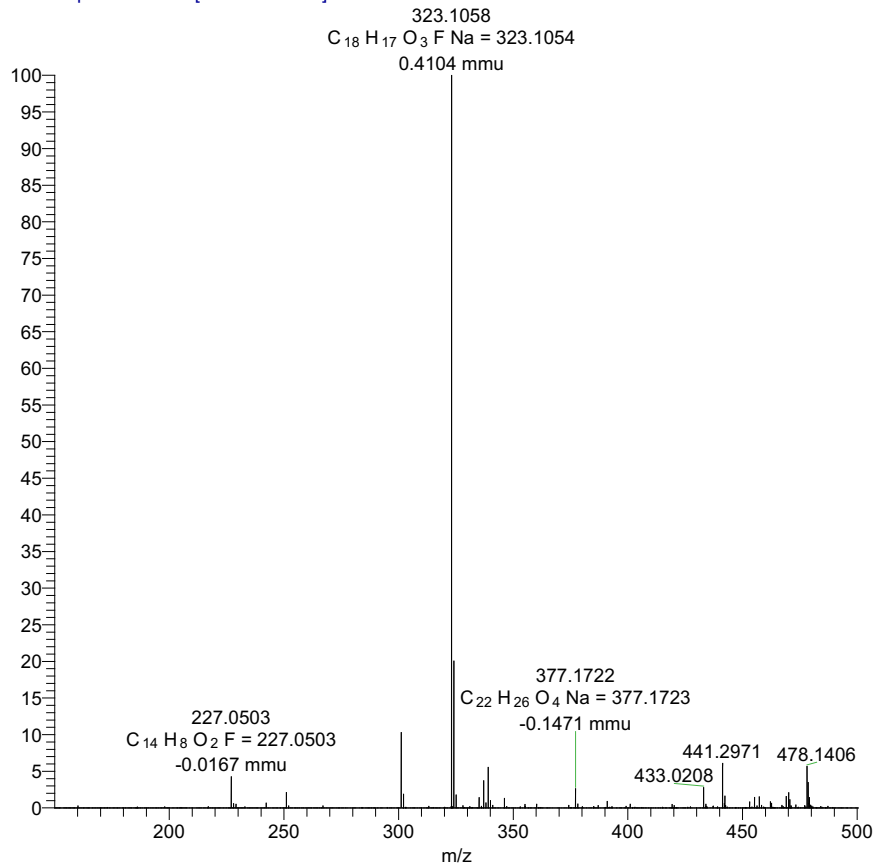


ESI : Carbonylative Suzuki-Miyaura couplings of sterically hindered aryl halides.

ABAI-112-2F1



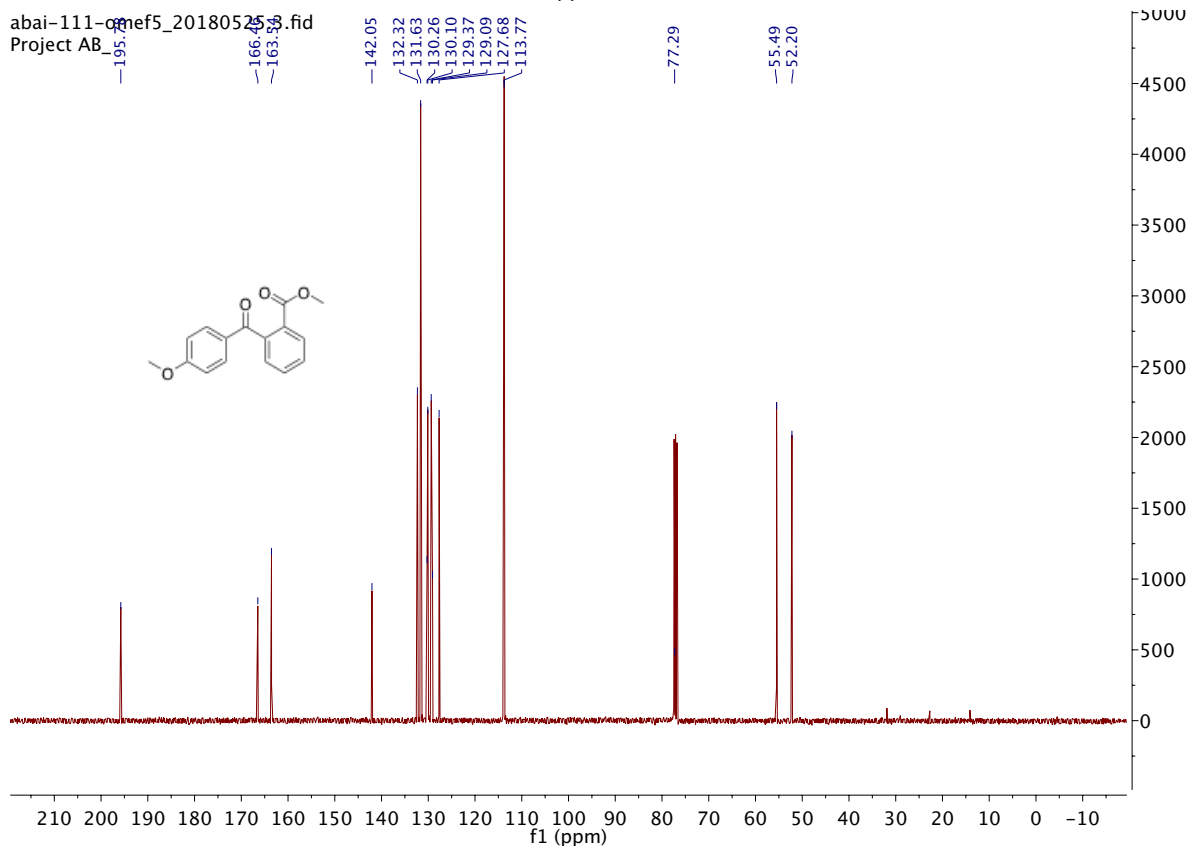
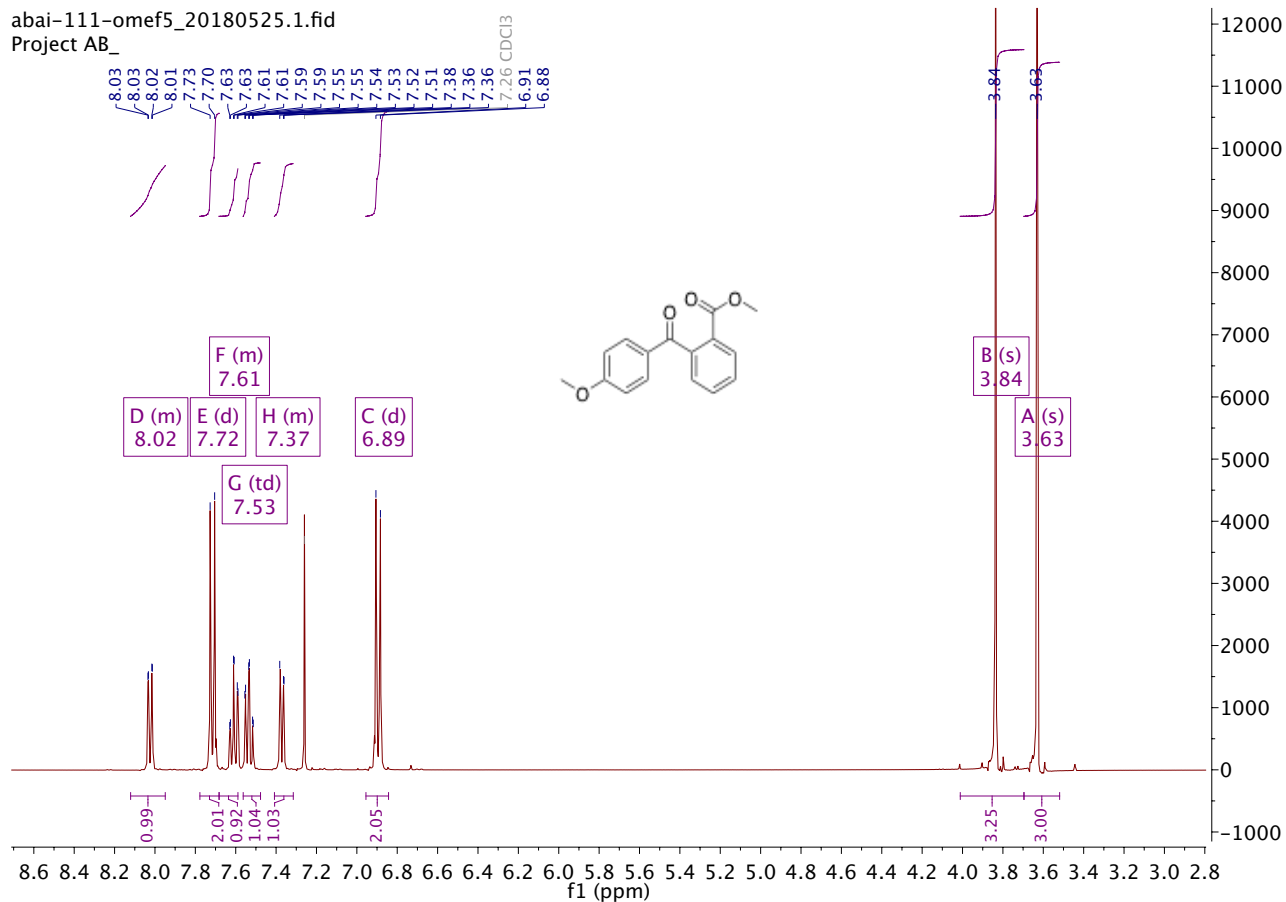
abai-112-2f1_190627172410 #1-5 RT: 0.01-0.12 AV: 5 NL: 3
T: FTMS + p ESI Full ms [150.00-500.00]



4.3 Spectra for methyl 2-benzoylbenzoate esters 2

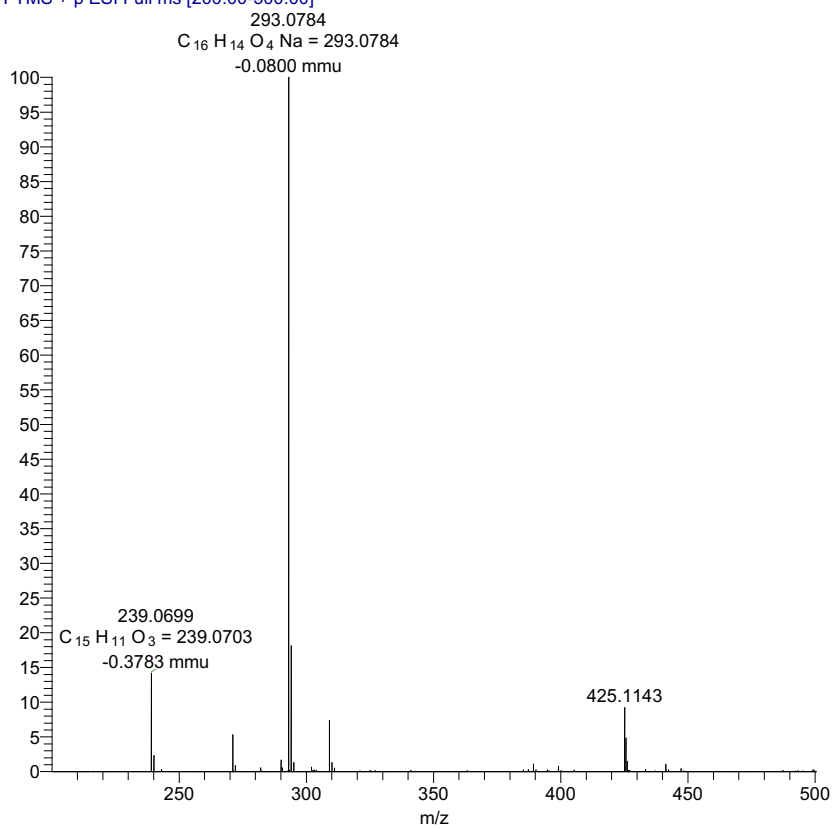
Methyl 2-(4-methoxybenzoyl)benzoate **2aa**

abai-111-omef5_20180525.1.fid
Project AB_



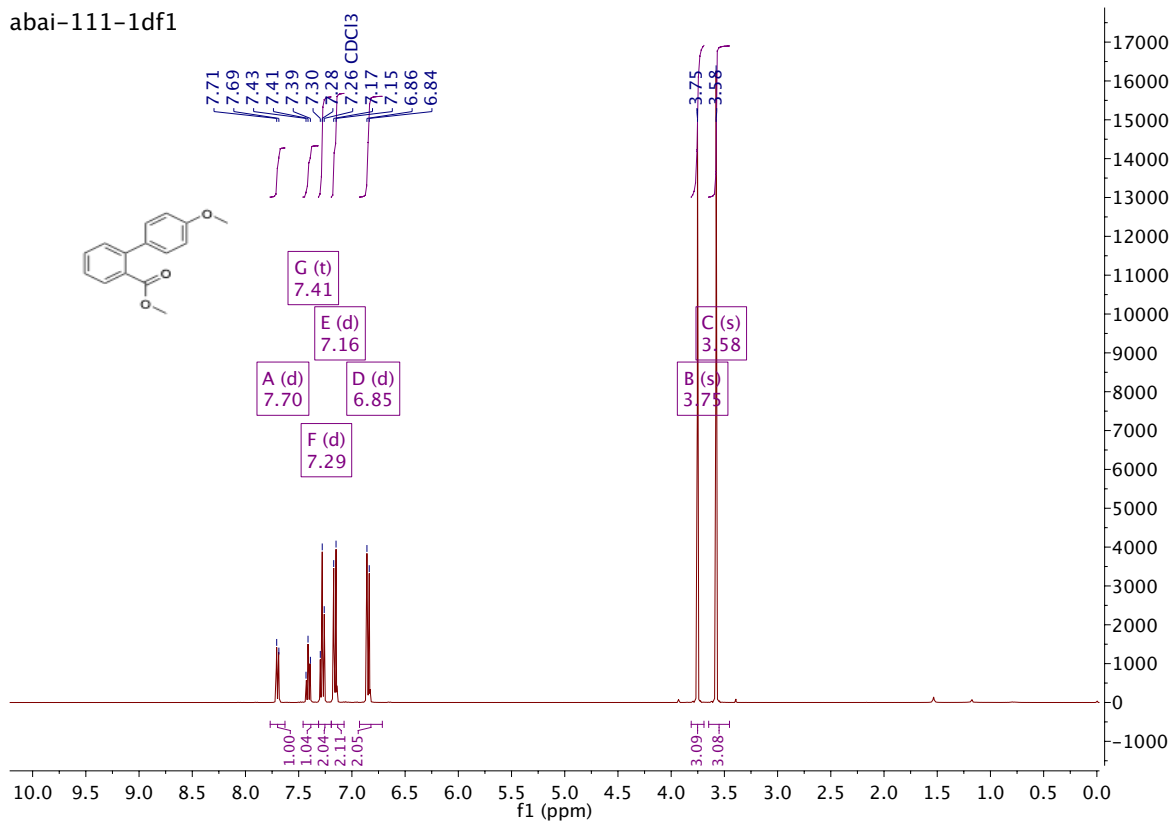
ESI : Carbonylative Suzuki-Miyaura couplings of sterically hindered aryl halides.

ABAI-111-1DF2_180618105745 #1-5 RT: 0.01-0.12 AV: 5 NI 7
 T: FTMS + p ESI Full ms [200.00-500.00]



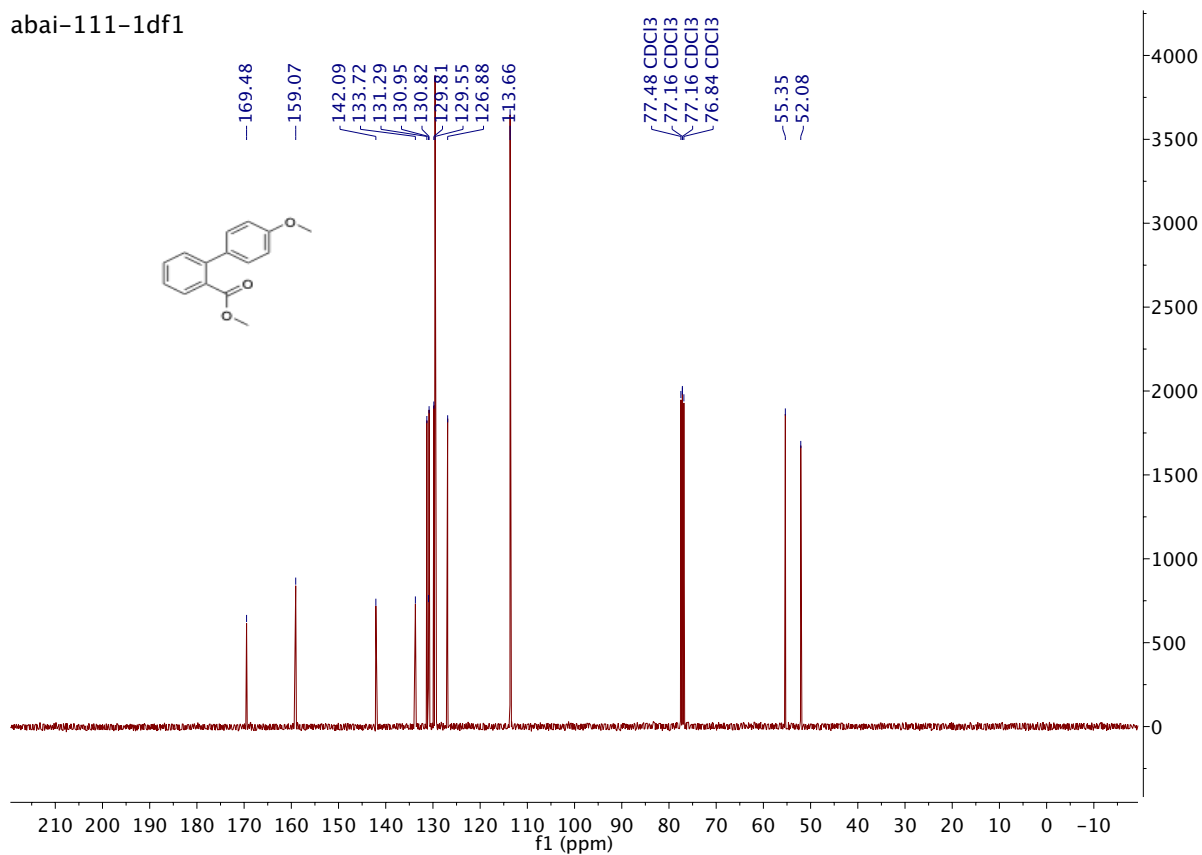
methyl 4'-methoxy-[1,1'-biphenyl]-2-carboxylate **B** (from direct coupling).

abai-111-1df1



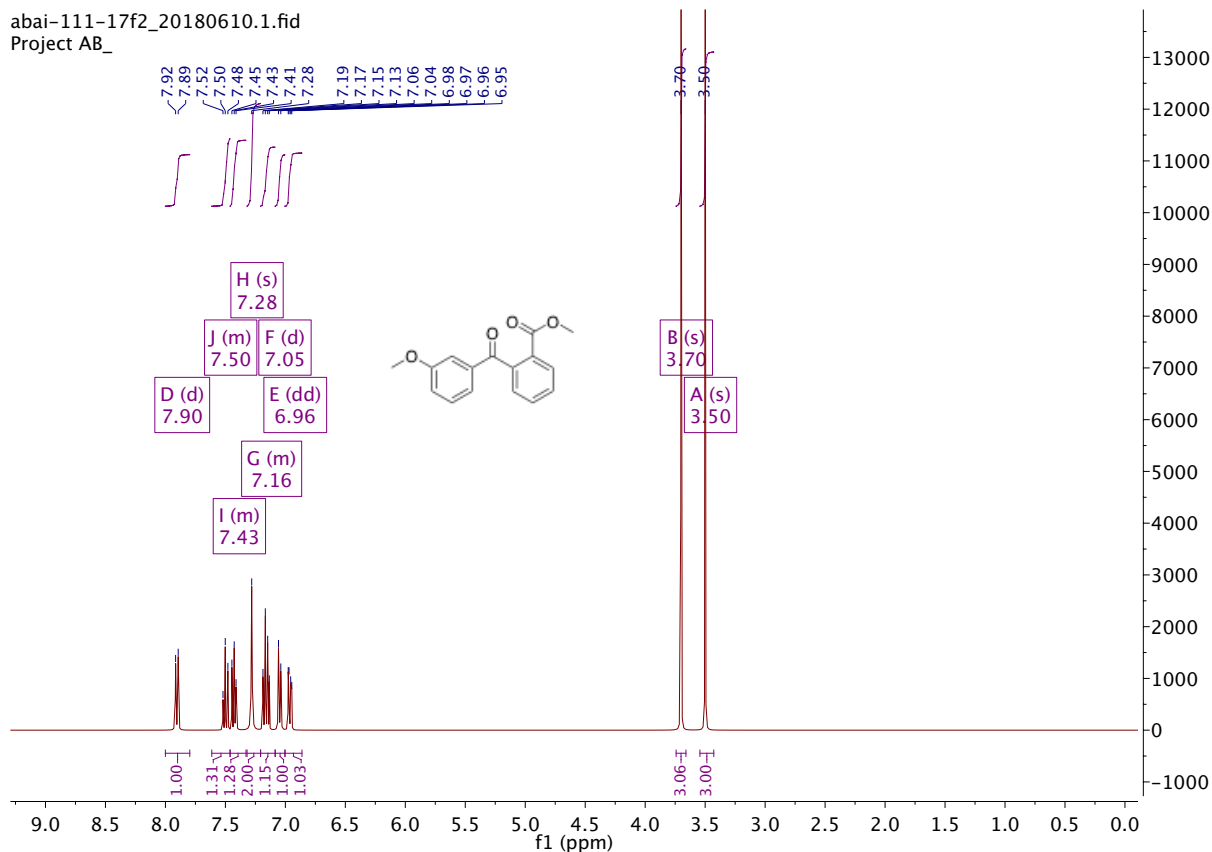
ESI : Carbonylative Suzuki-Miyaura couplings of sterically hindered aryl halides.

abai-111-1df1



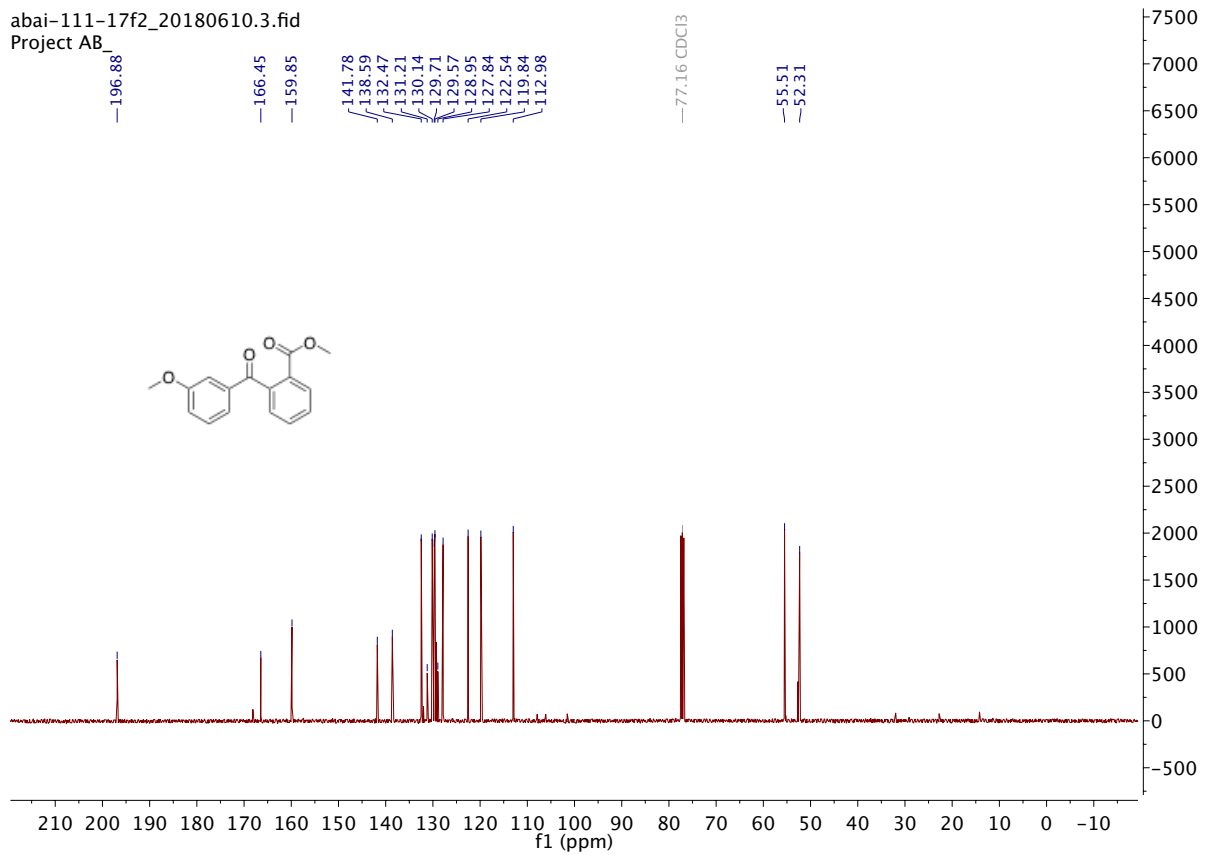
Methyl 2-(3-methoxybenzoyl) benzoate **2ab**

abai-111-17f2_20180610.1.fid
Project AB_

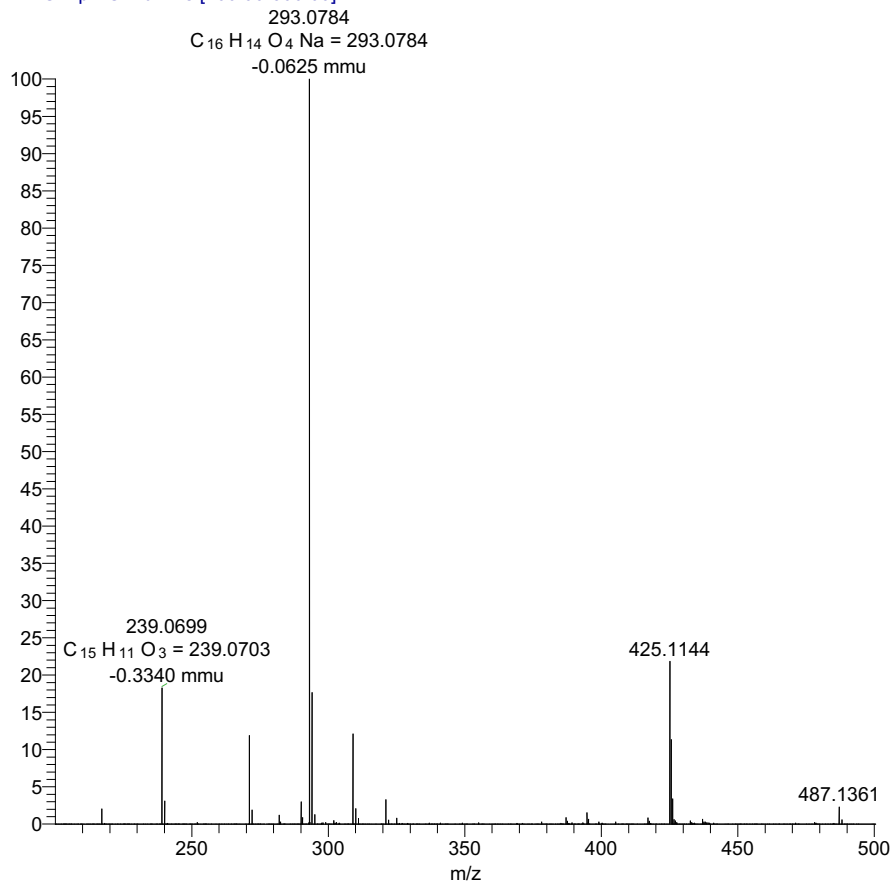


ESI : Carbonylative Suzuki-Miyaura couplings of sterically hindered aryl halides.

abai-111-17f2_20180610.3.fid
Project AB



ABAI-111-17-F2 #1-4 RT: 0.02-0.11 AV: 4 NL: 6.66E7
T: FTMS + p ESI Full ms [200.00-500.00]

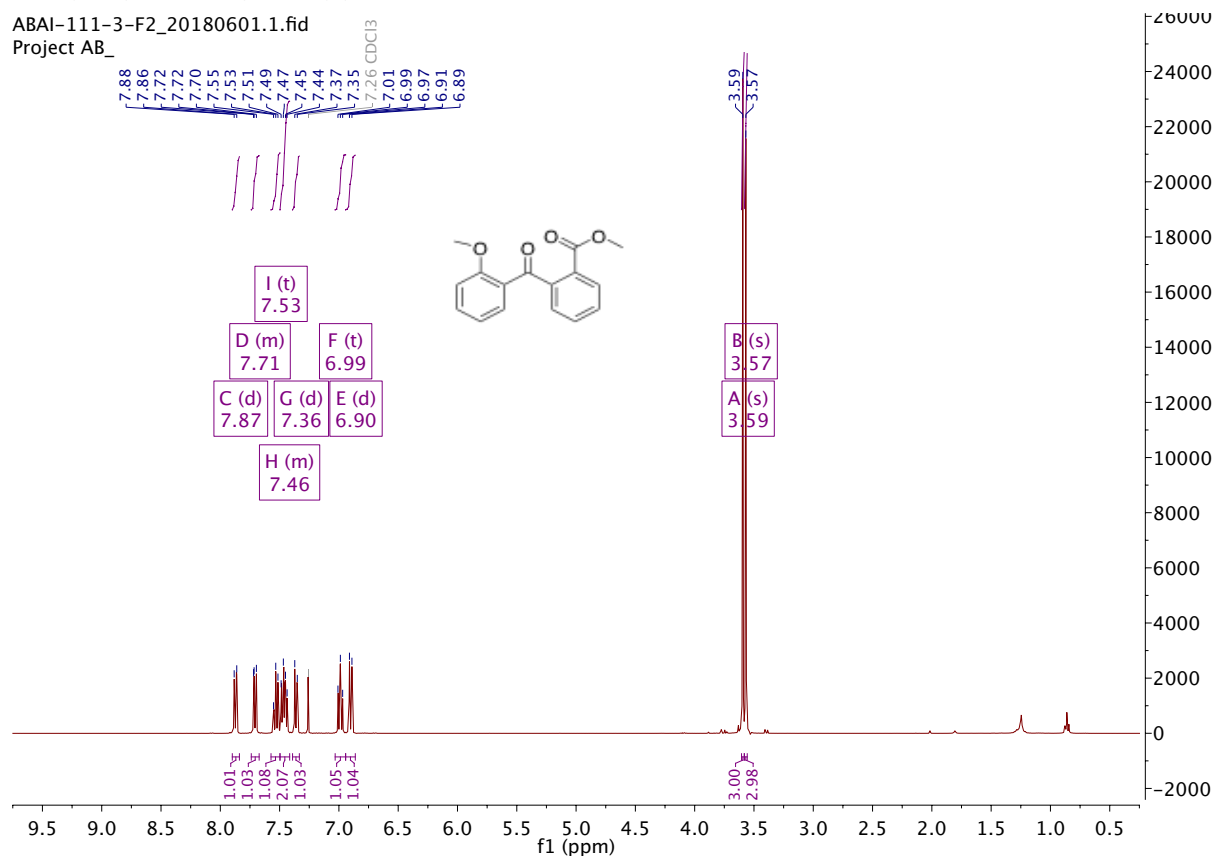


ESI : Carbonylative Suzuki-Miyaura couplings of sterically hindered aryl halides.

Methyl 2-(2-methoxybenzoyl)benzoate **2ac**

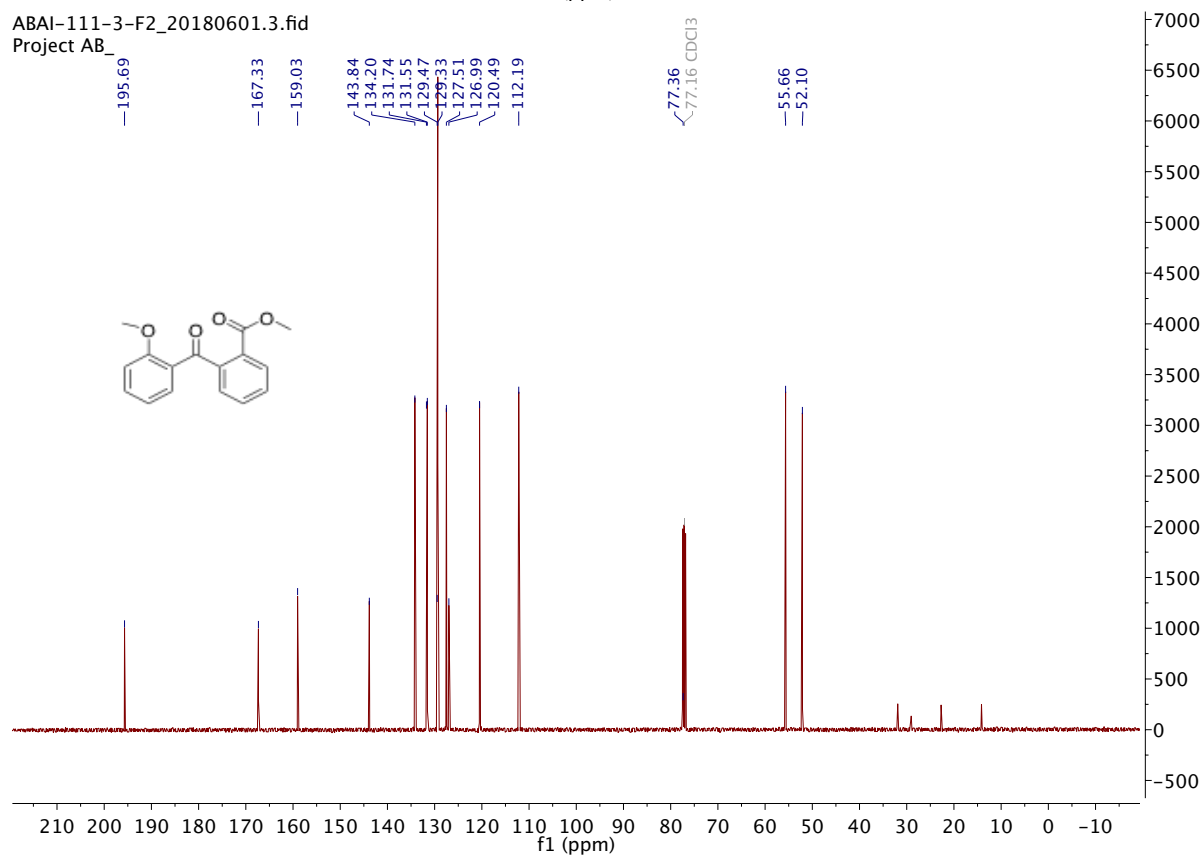
ABAI-111-3-F2_20180601.1.fid

Project AB_



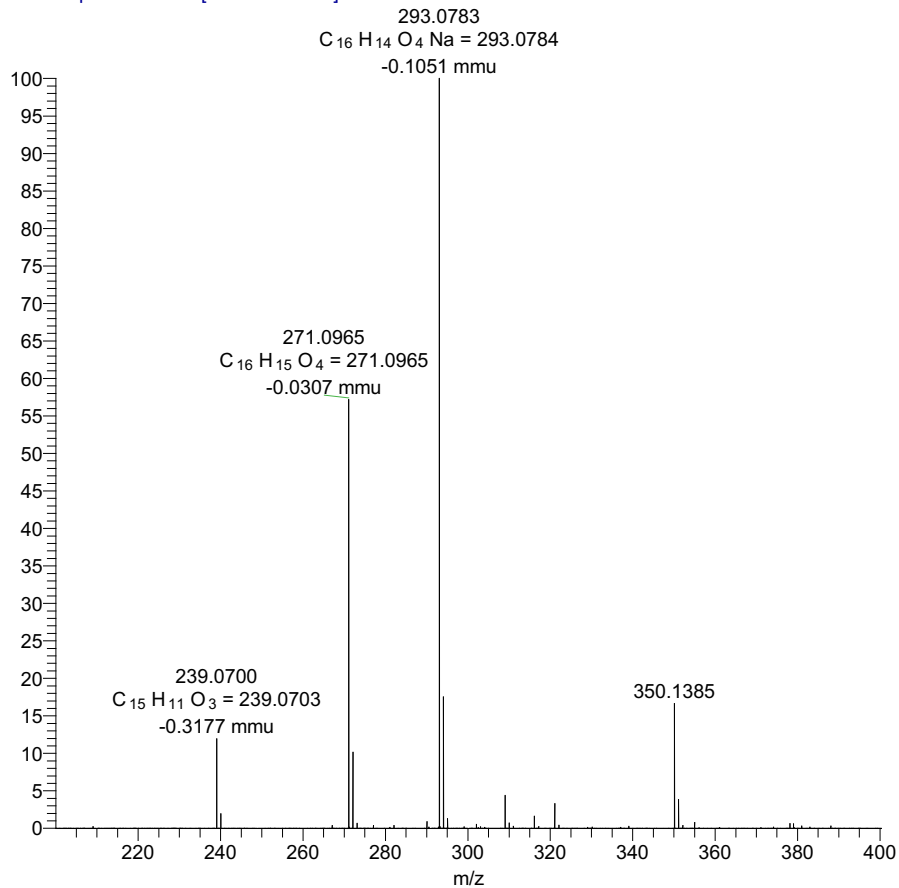
ABAI-111-3-F2_20180601.3.fid

Project AB_



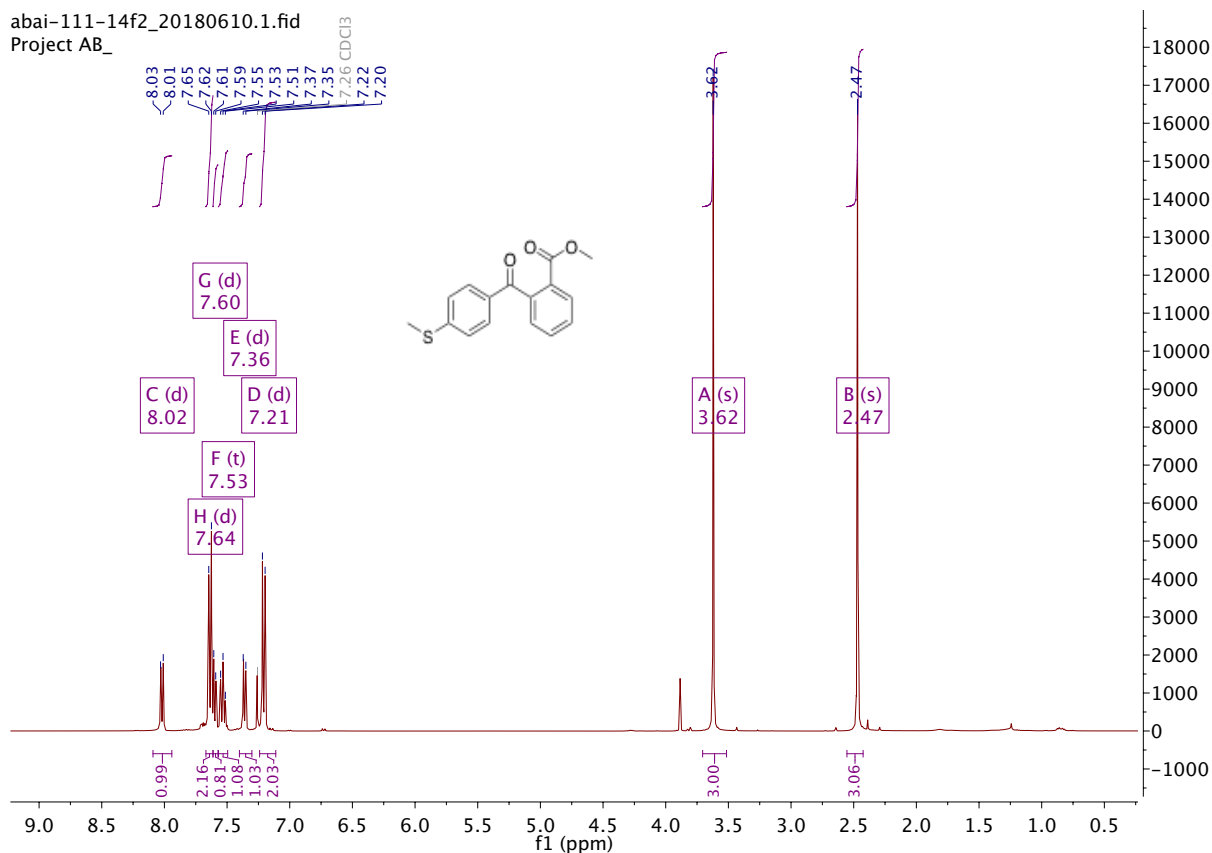
ESI : Carbonylative Suzuki-Miyaura couplings of sterically hindered aryl halides.

ABAI-111-3-F2_180618115027 #1-4 RT: 0.02-0.11 AV: 4 NL
 T: FTMS + p ESI Full ms [200.00-400.00]



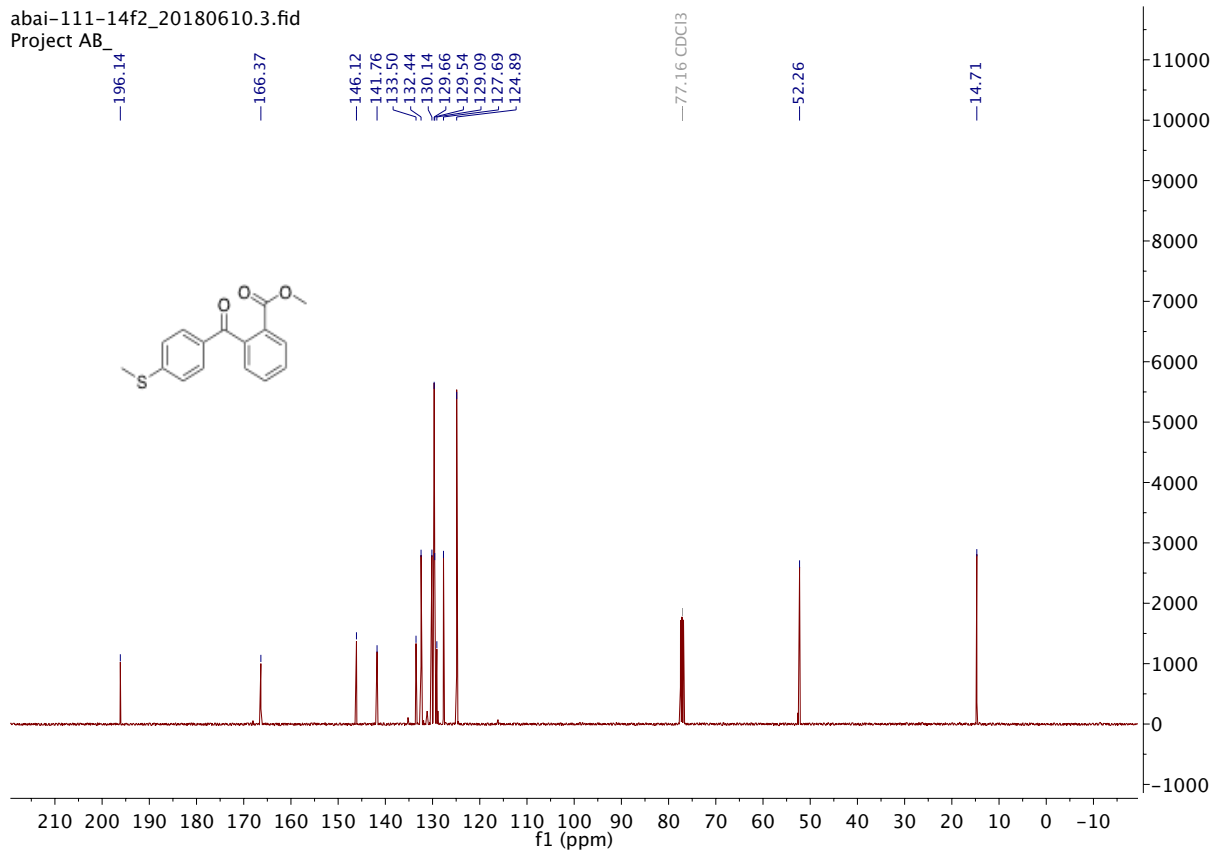
Methyl 2-(4-(methylthio)benzoyl) benzoate **2ad**

abai-111-14f2_20180610.1.fid
 Project AB_

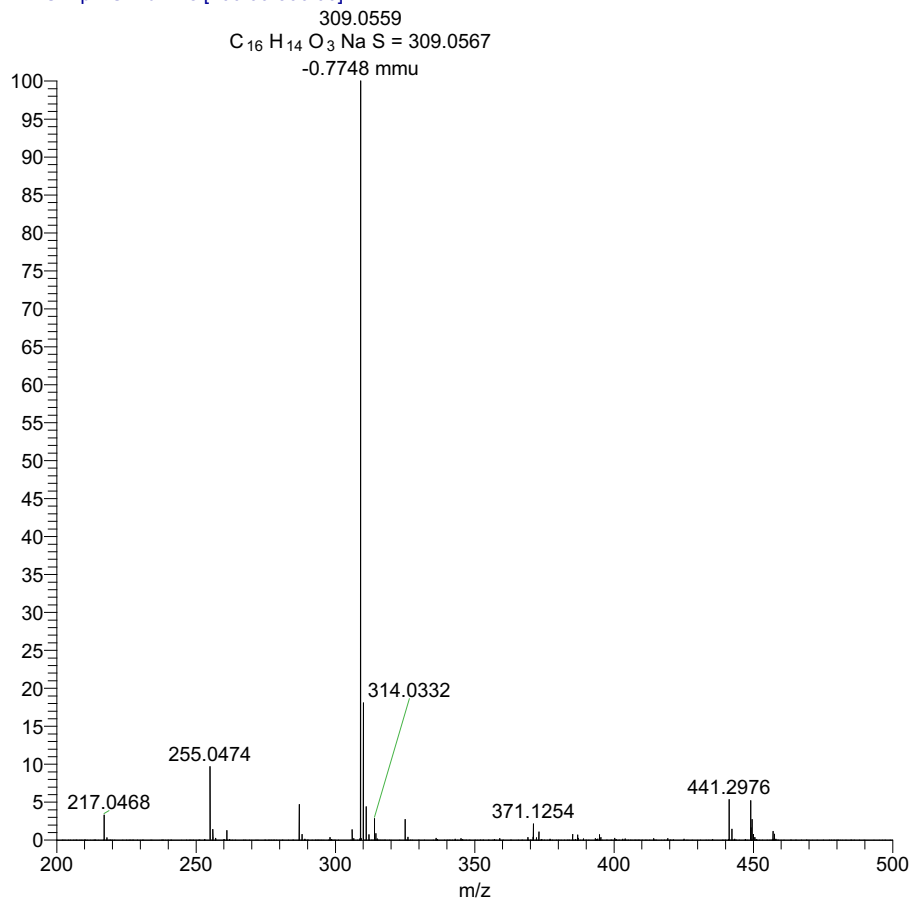


ESI : Carbonylative Suzuki-Miyaura couplings of sterically hindered aryl halides.

abai-111-14f2_20180610.3.fid
Project AB_



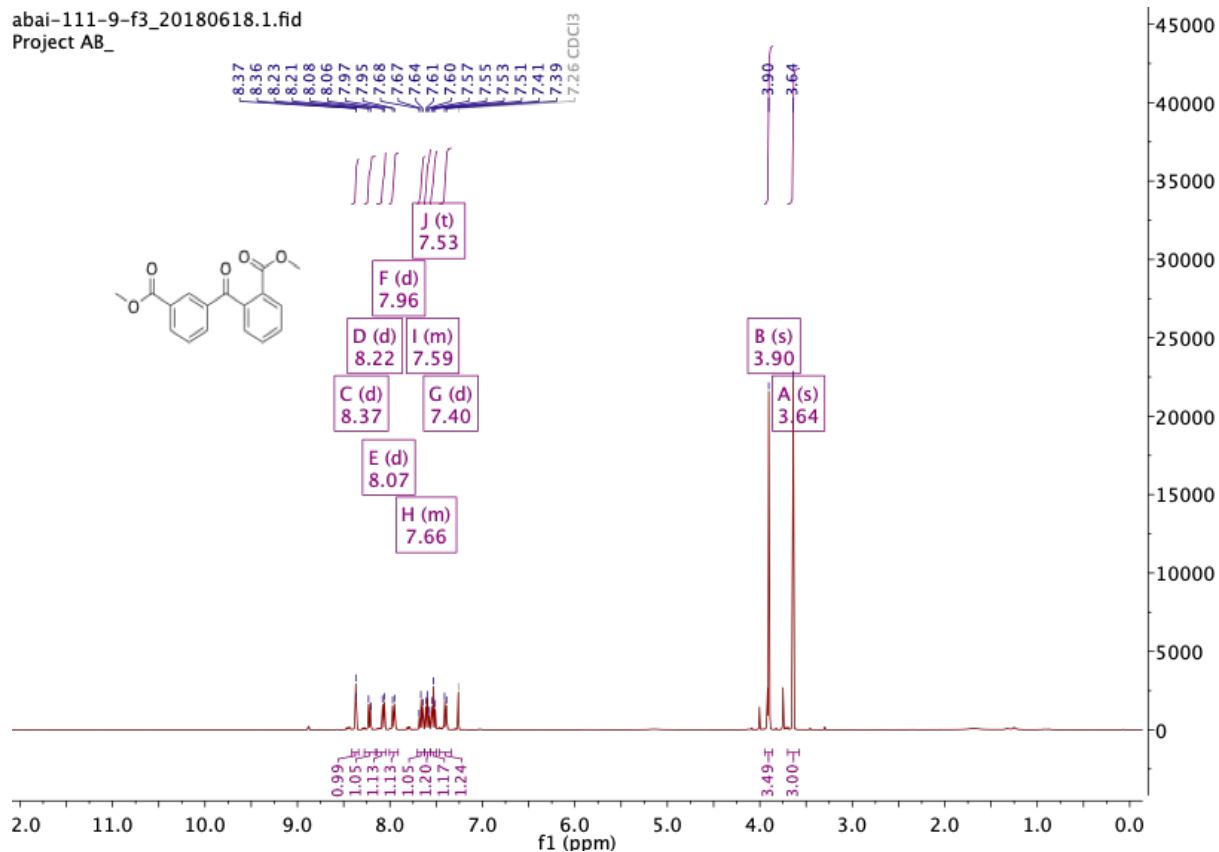
ABAI-111-14F2 #4 RT: 0.11 AV: 1 NL: 6.49E7
T: FTMS + p ESI Full ms [200.00-500.00]



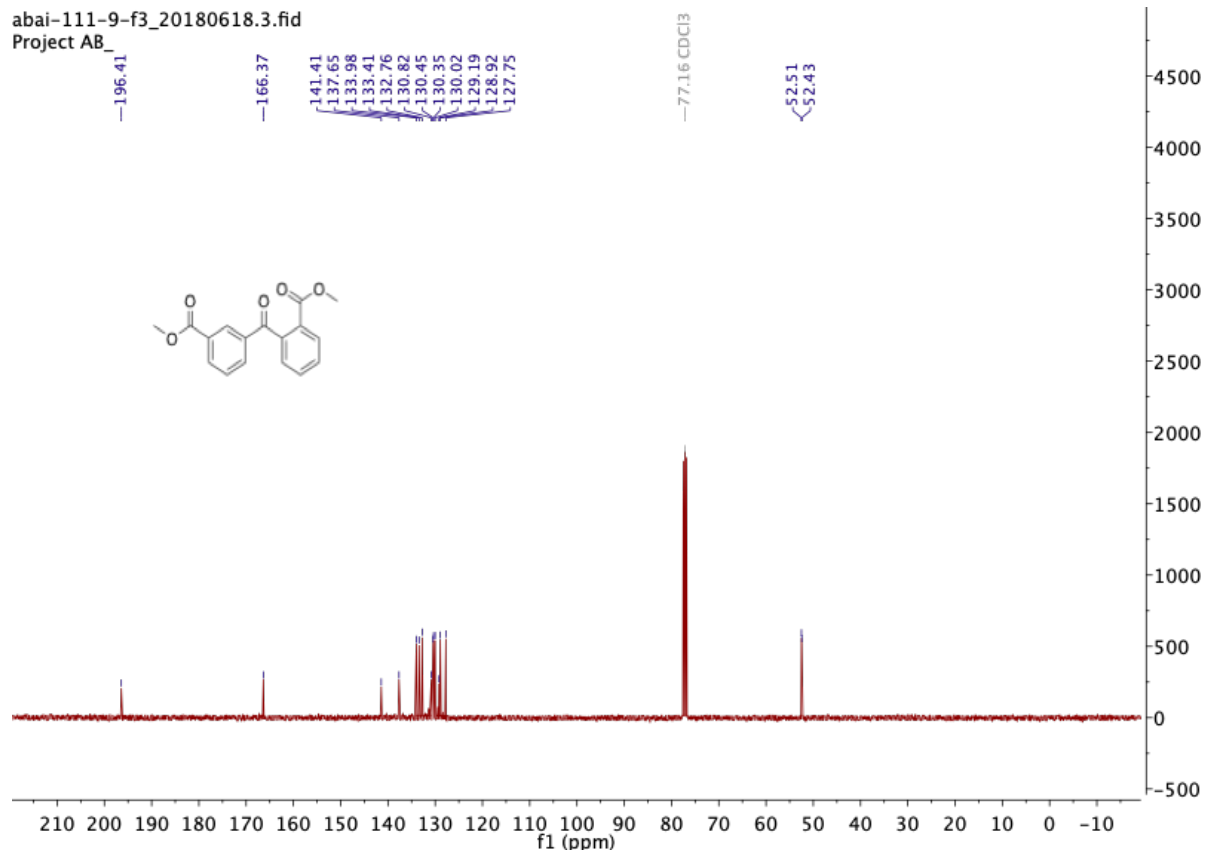
ESI : Carbonylative Suzuki-Miyaura couplings of sterically hindered aryl halides.

Methyl 2-(3-(methoxycarbonyl)benzoyl)benzoate **2ag**

abai-111-9-f3_20180618.1.fid
Project AB_

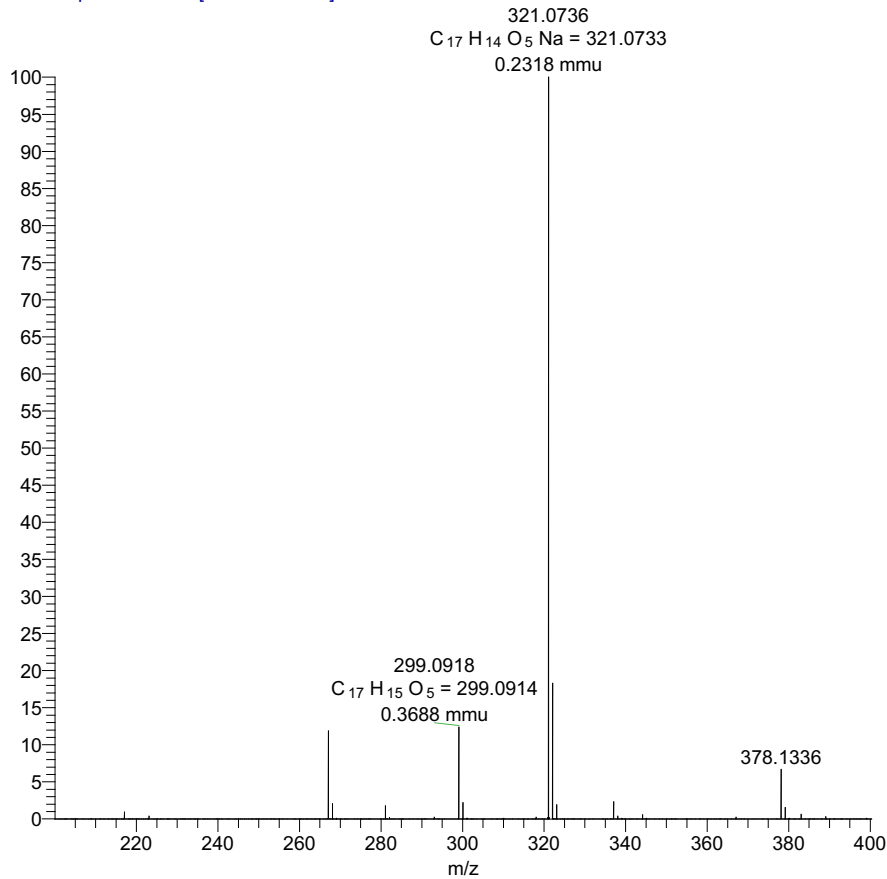


abai-111-9-f3_20180618.3.fid
Project AB_



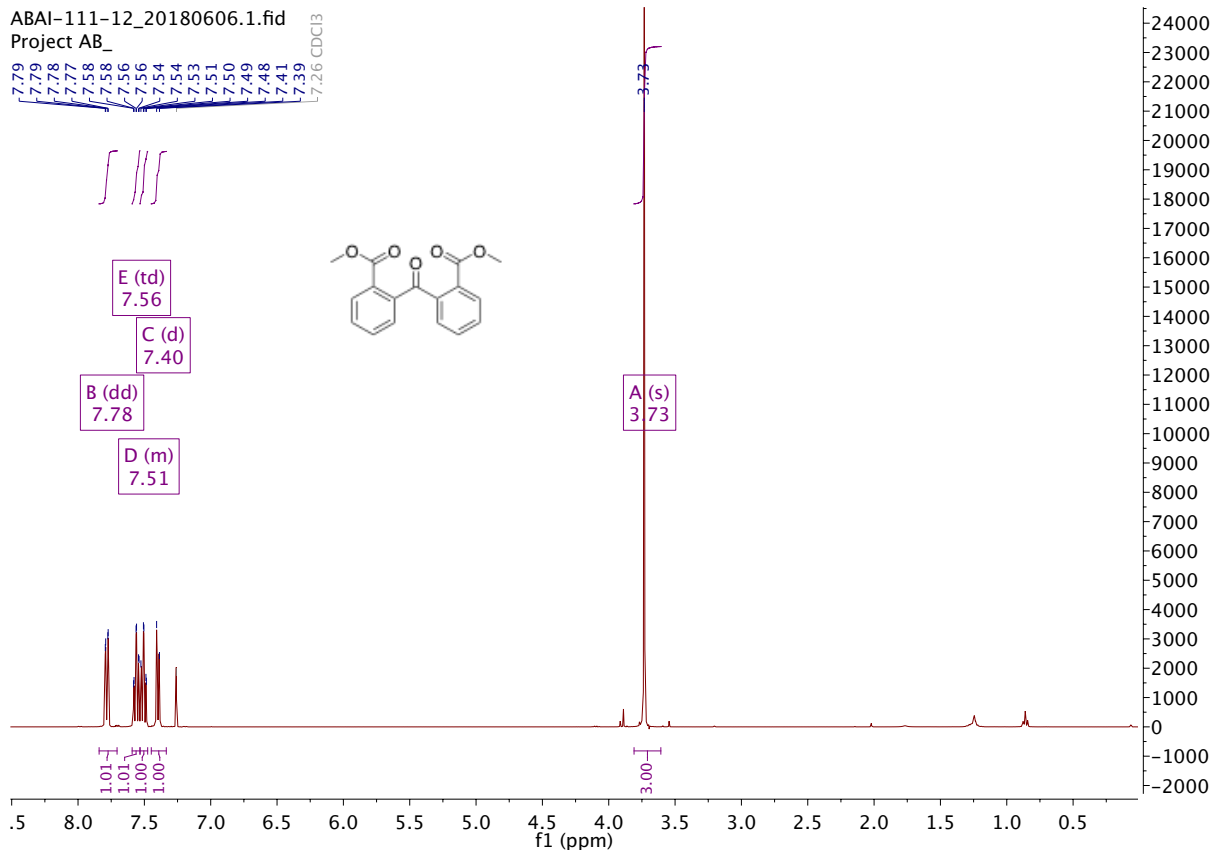
ESI : Carbonylative Suzuki-Miyaura couplings of sterically hindered aryl halides.

ABAI-111-9_180618122059 #1-5 RT: 0.01-0.13 AV: 5 NL: 3;
T: FTMS + p ESI Full ms [200.00-400.00]



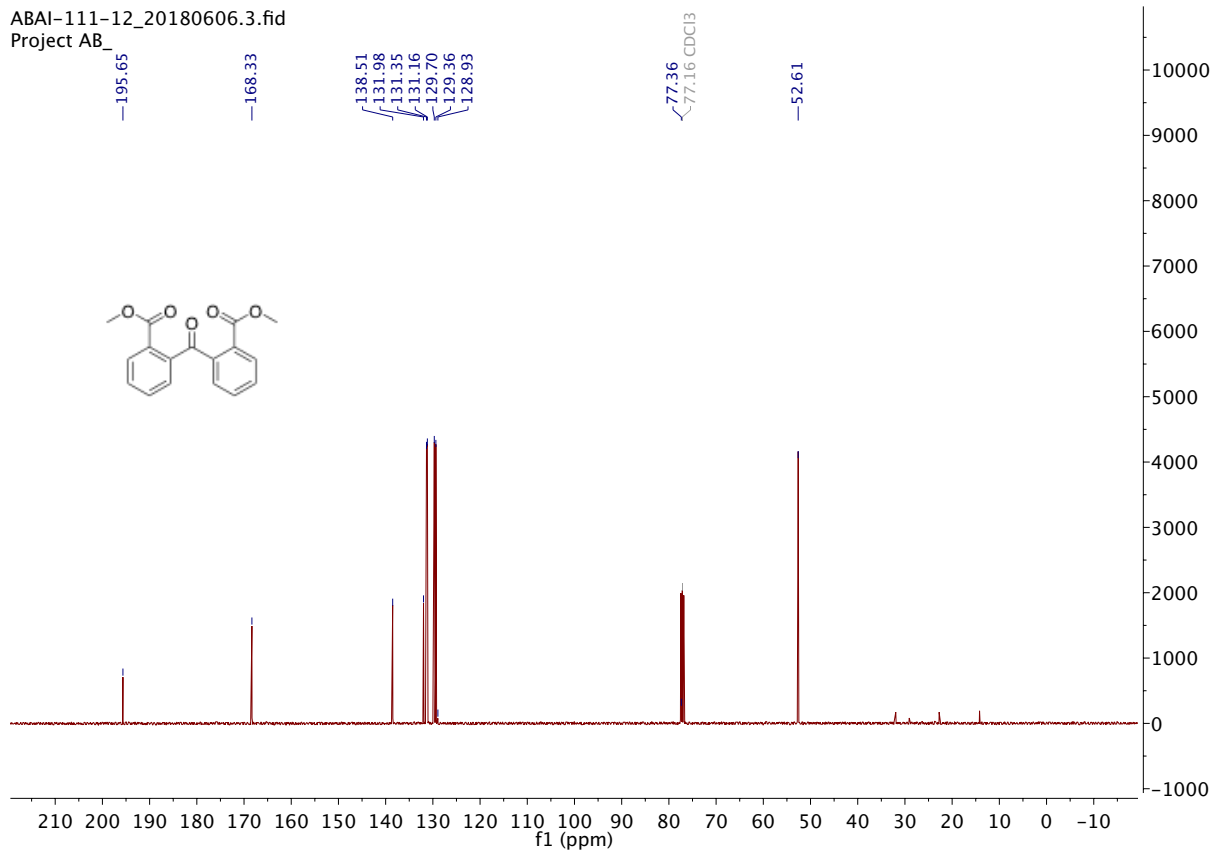
Dimethyl 2,2'-carbonyldibenzoate **2ah**

ABAI-111-12_20180606.1.fid
Project AB_

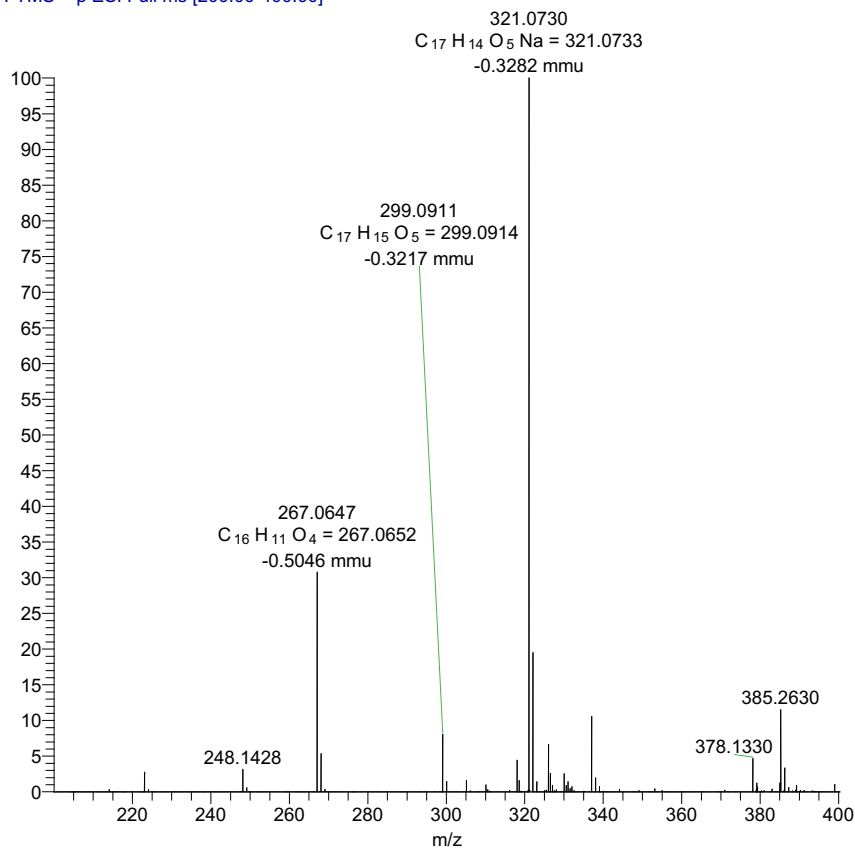


ESI : Carbonylative Suzuki-Miyaura couplings of sterically hindered aryl halides.

ABAI-111-12_20180606.3.fid
Project AB

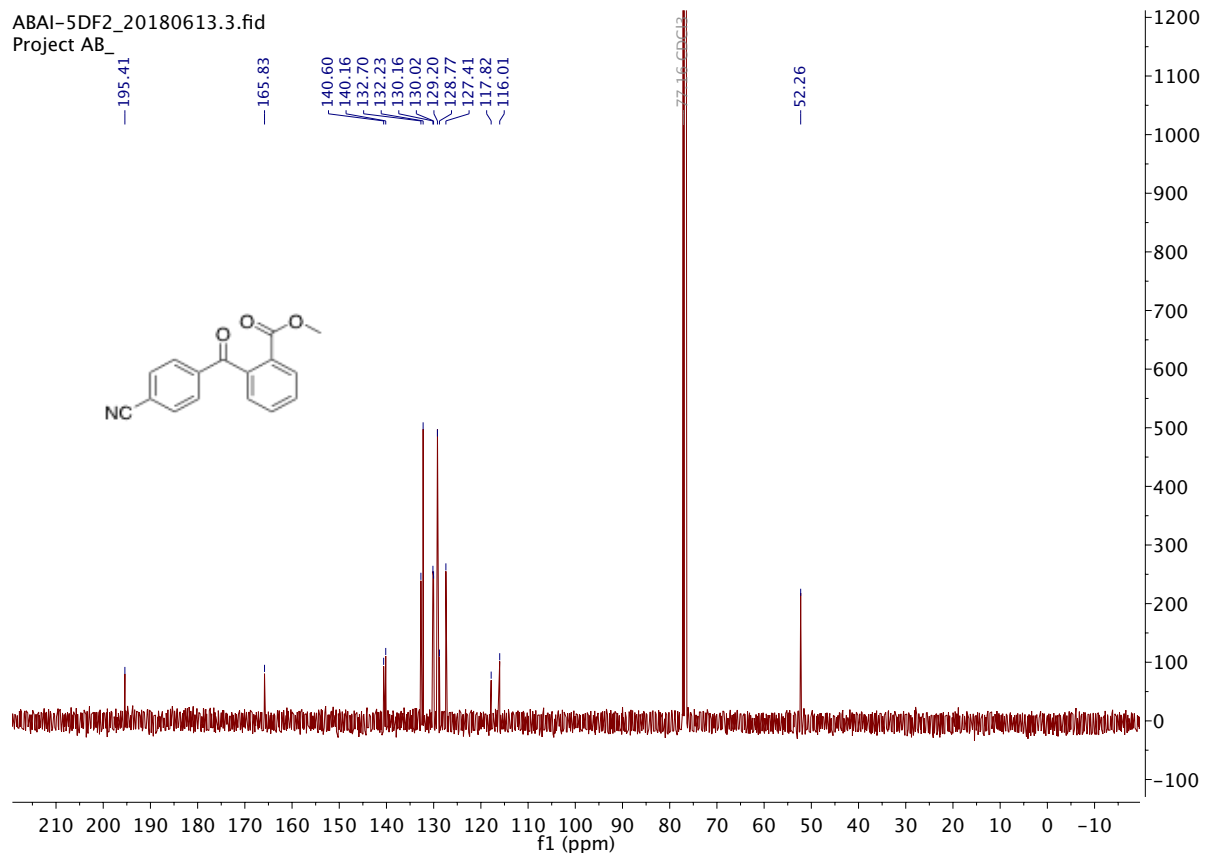
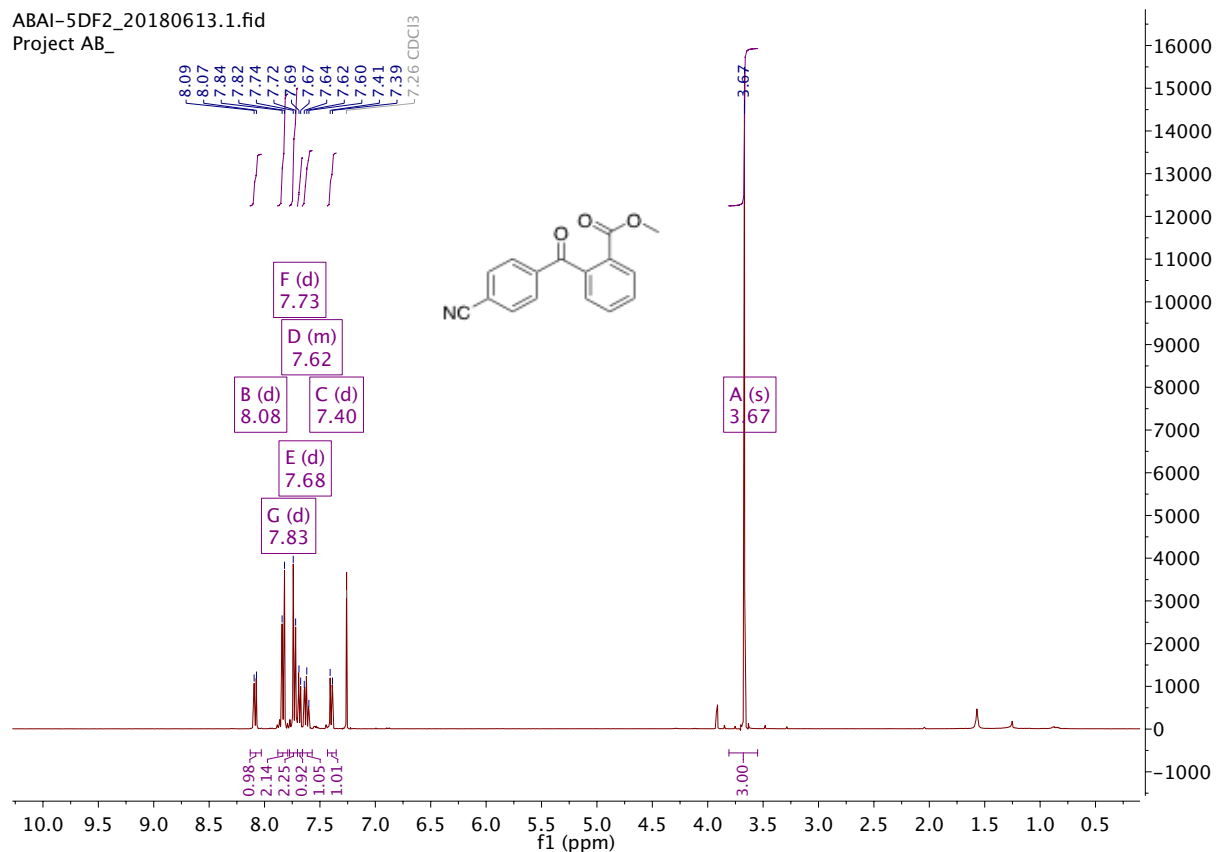


ABAI-111-7D-F2_180618115027 #1-4 RT: 0.02-0.11 AV: 4 N E7
T: FTMS + p ESI Full ms [200.00-400.00]



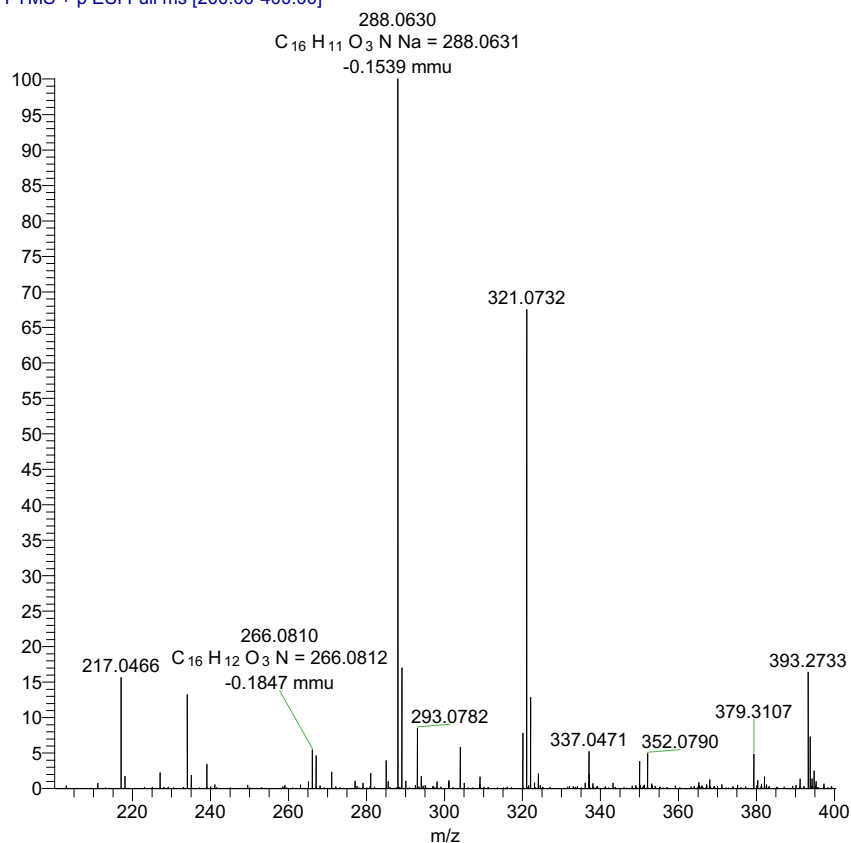
ESI : Carbonylative Suzuki-Miyaura couplings of sterically hindered aryl halides.

Methyl 2-(4-cyanobenzoyl) benzoate **2ai**



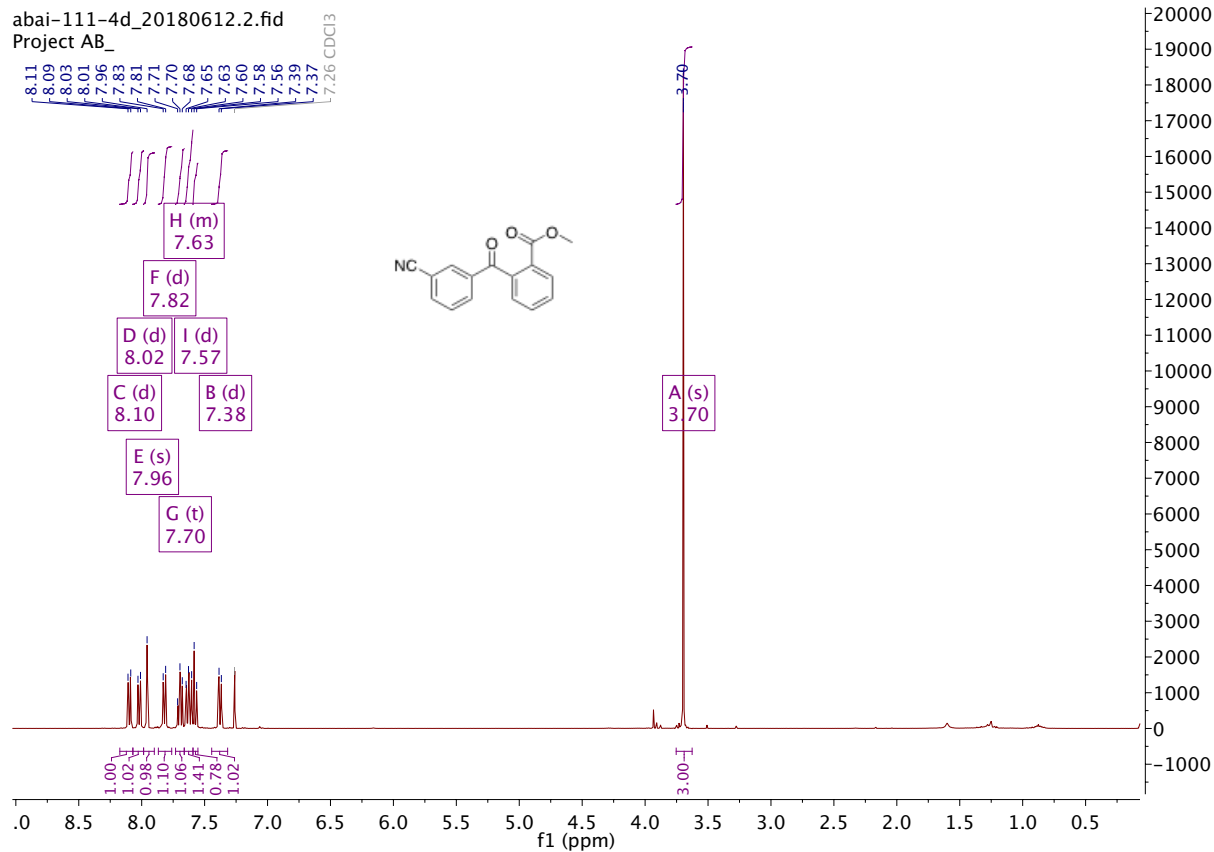
ESI : Carbonylative Suzuki-Miyaura couplings of sterically hindered aryl halides.

ABAI-111-5DF2_180618113446 #1-4 RT: 0.01-0.09 AV: 4 NI 6
 T: FTMS + p ESI Full ms [200.00-400.00]



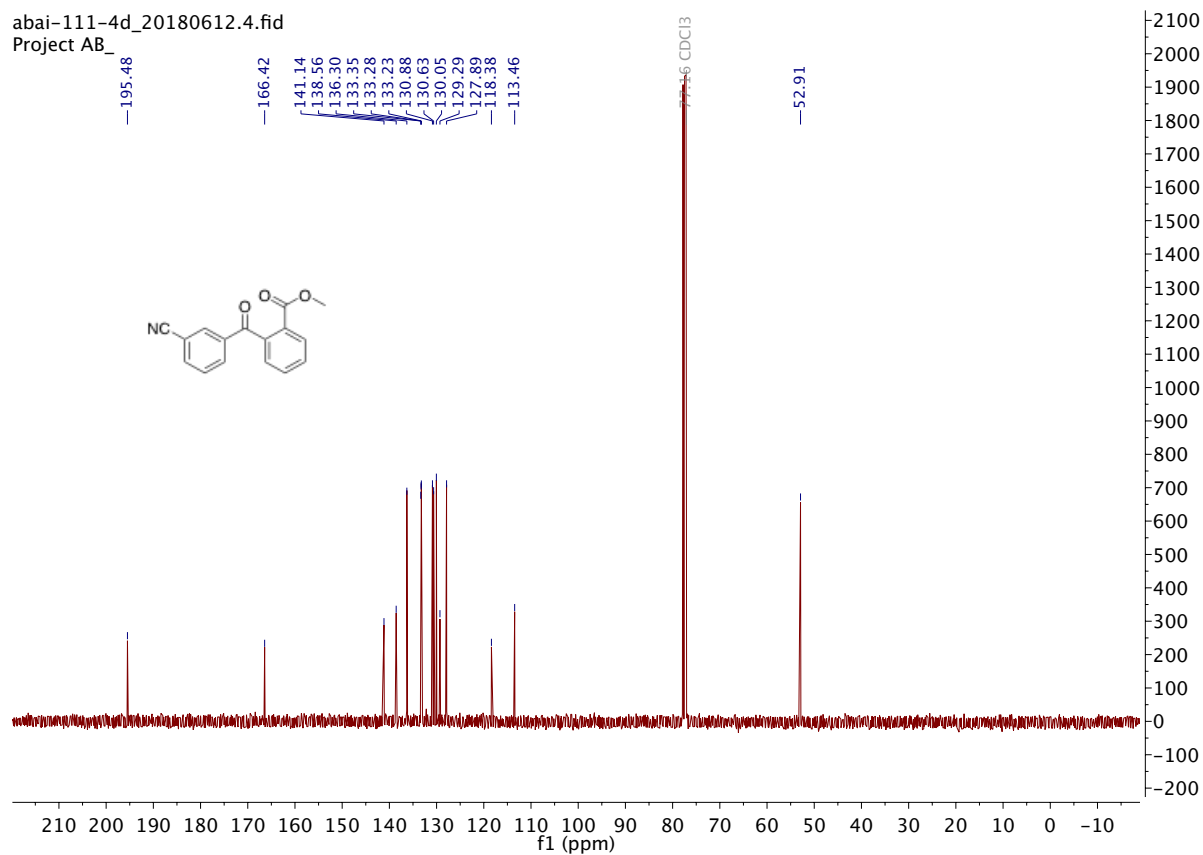
Methyl 2-(3-cyanobenzoyl) benzoate **2aj**

abai-111-4d_20180612.2.fid
 Project AB_

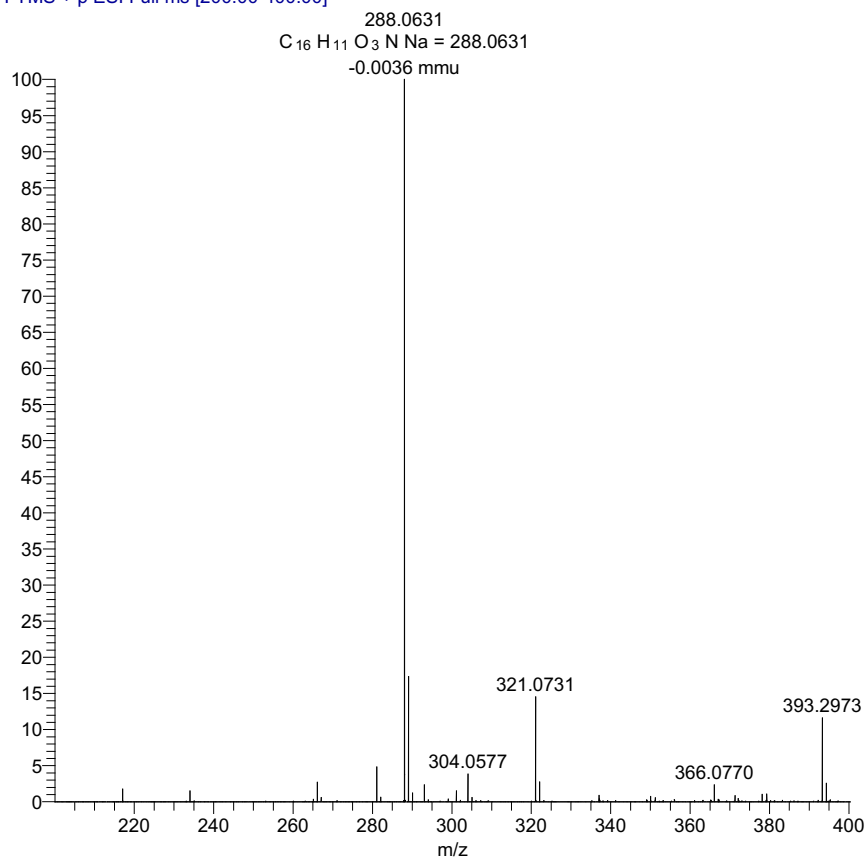


ESI : Carbonylative Suzuki-Miyaura couplings of sterically hindered aryl halides.

abai-111-4d_20180612.4.fid
Project AB_



ABAI-111-4D-F2_180618113446 #1-4 RT: 0.02-0.10 AV: 4 N E7
T: FTMS + p ESI Full ms [200.00-400.00]

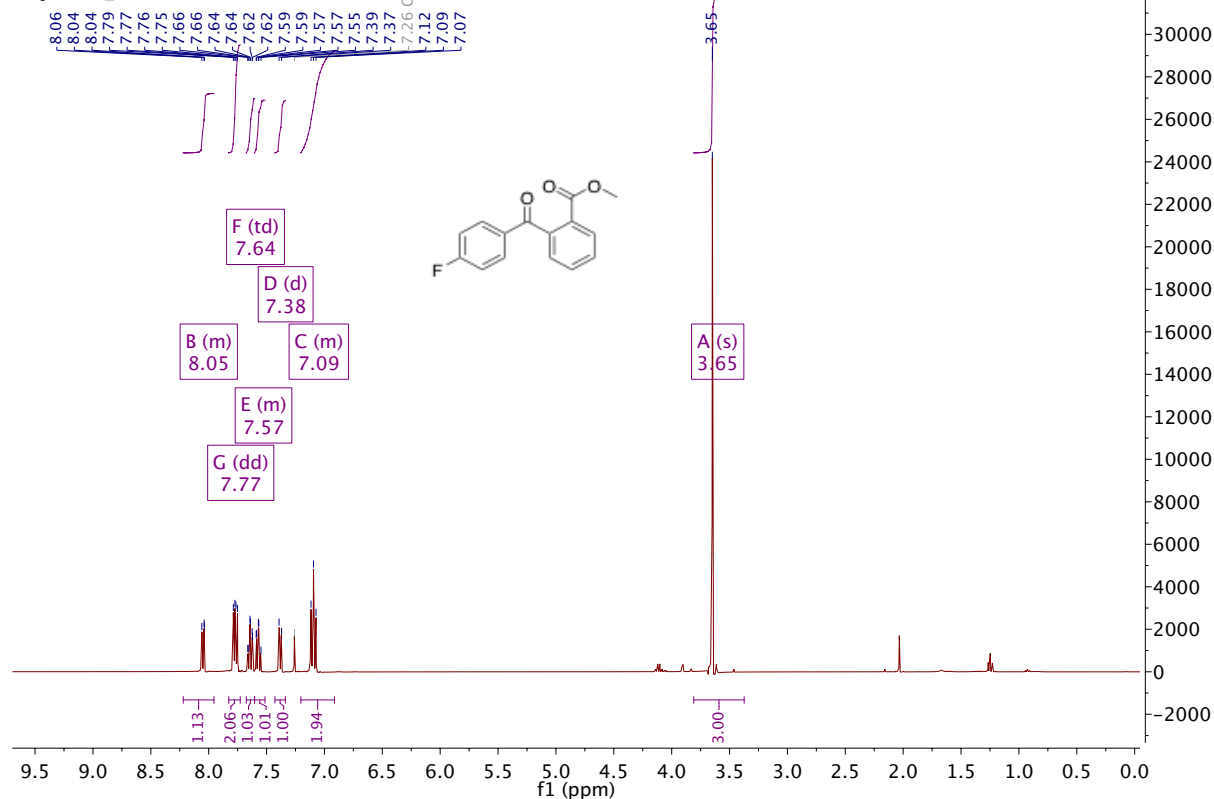


ESI : Carbonylative Suzuki-Miyaura couplings of sterically hindered aryl halides.

Methyl 2-(4-fluorobenzoyl) benzoate **2ak**

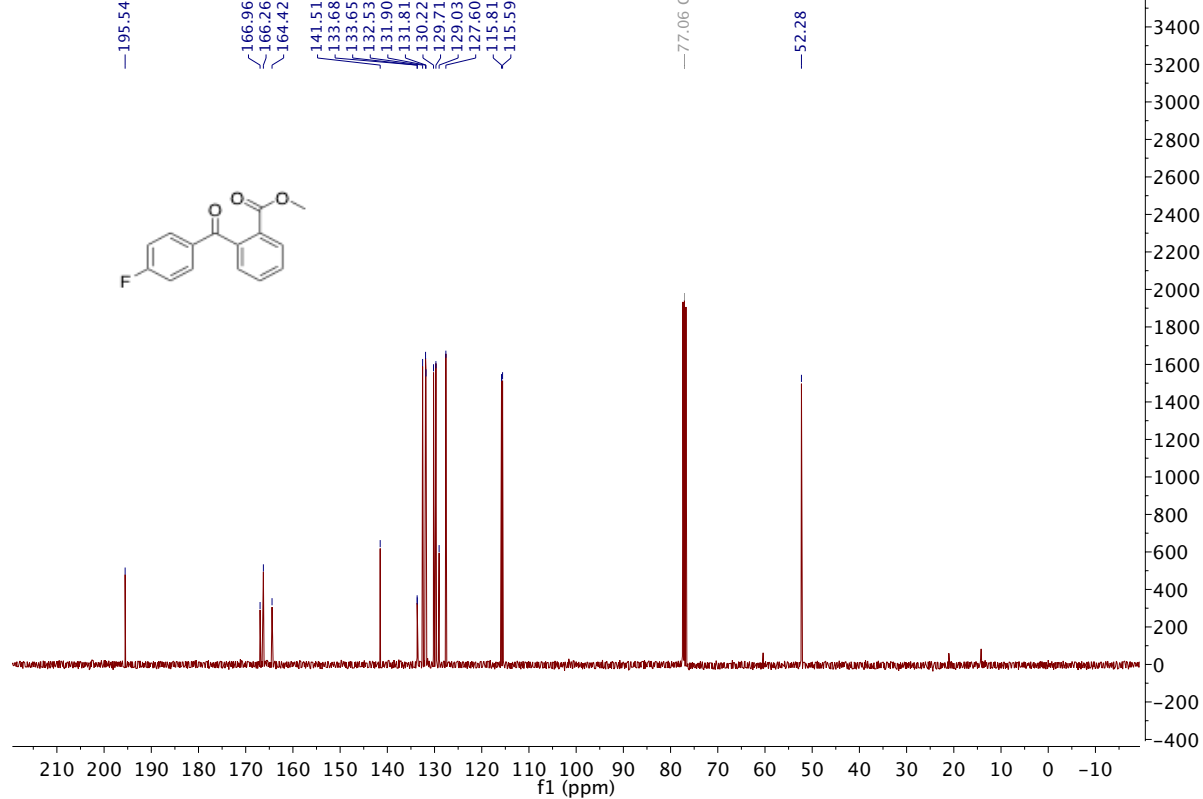
abai-111-6d_20180612.2.fid

Project AB_



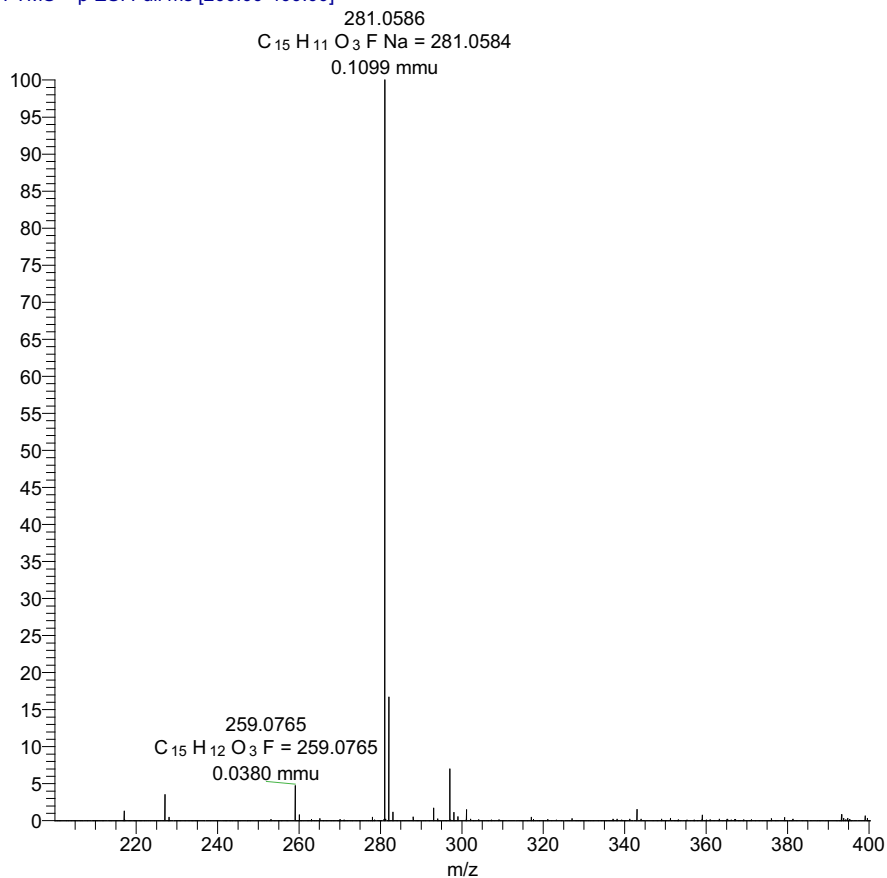
abai-111-6d_20180612.4.fid

Project AB_



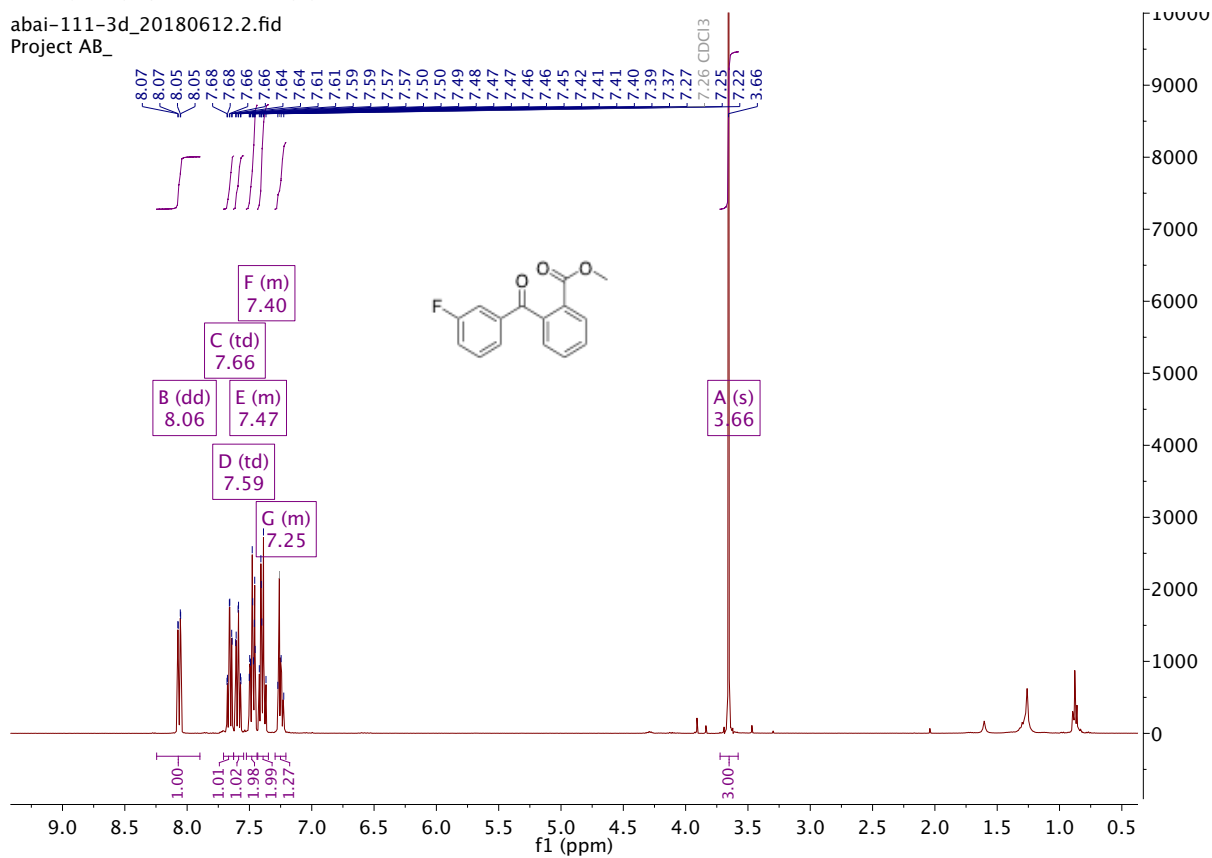
ESI : Carbonylative Suzuki-Miyaura couplings of sterically hindered aryl halides.

ABAI-111-6D-F2_180618113446 #1-4 RT: 0.02-0.11 AV: 4 N E7
T: FTMS + p ESI Full ms [200.00-400.00]



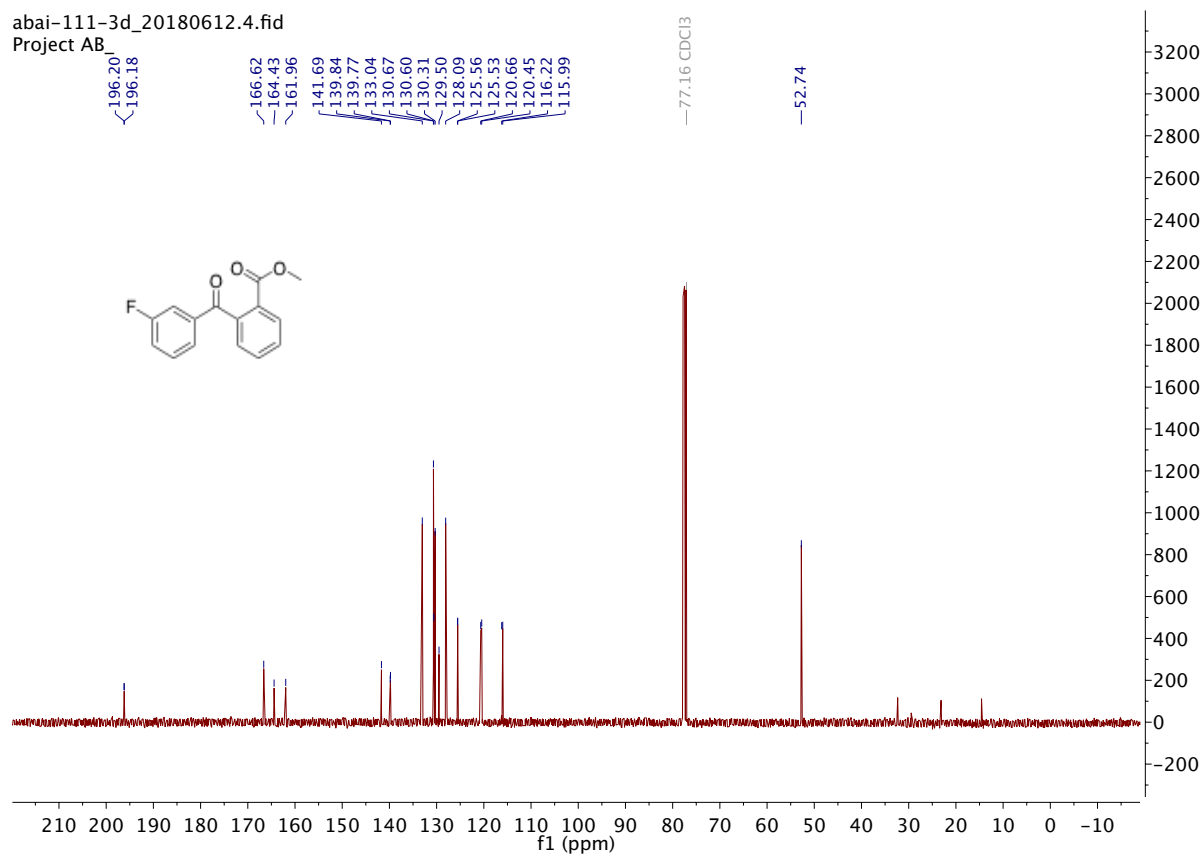
Methyl 2-(3-fluorobenzoyl) benzoate **2a**

abai-111-3d_20180612.2.fid
Project AB_

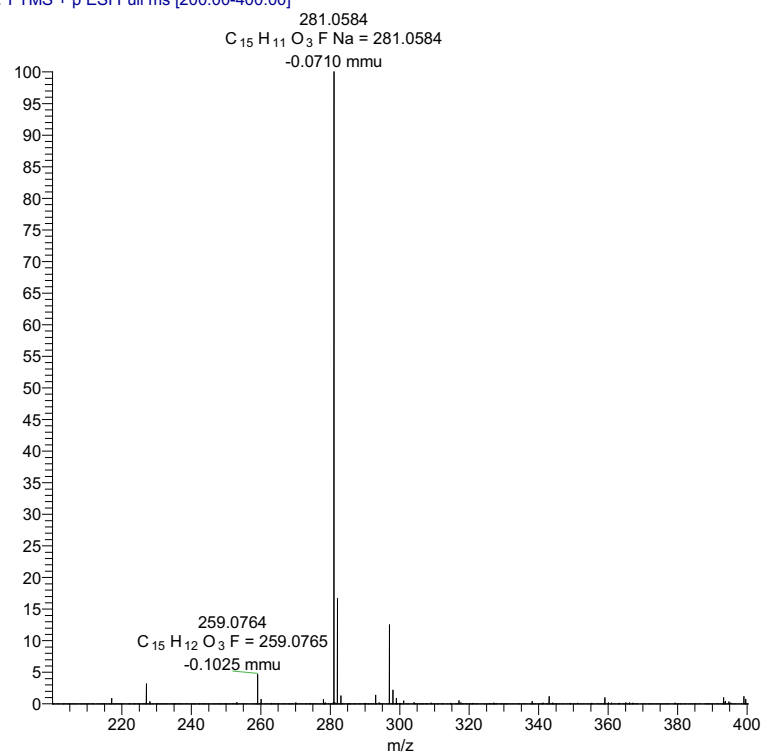


ESI : Carbonylative Suzuki-Miyaura couplings of sterically hindered aryl halides.

abai-111-3d_20180612.4.fid
Project AB



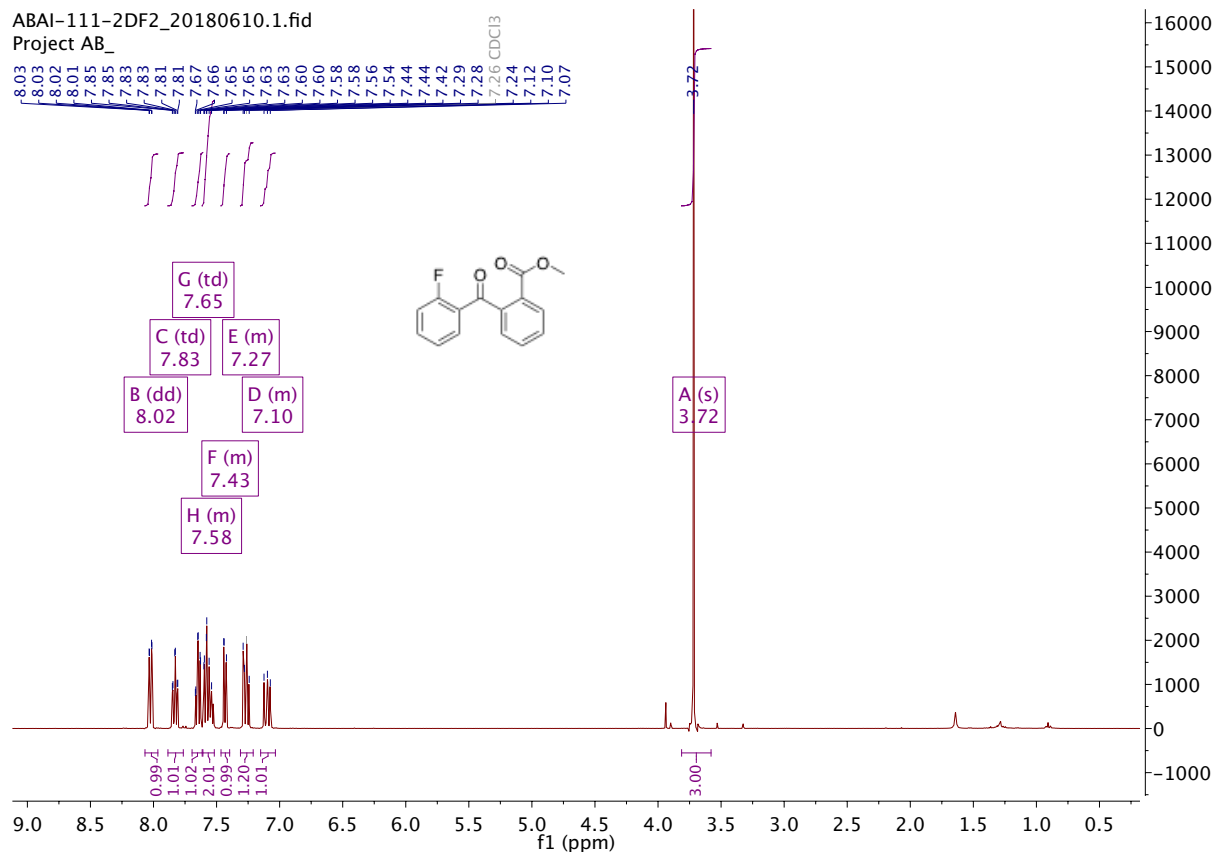
ABAI-111-3D_180618113446 #1-5 RT: 0.01-0.13 AV: 5 NL: 1
T: FTMS + p ESI Full ms [200.00-400.00]



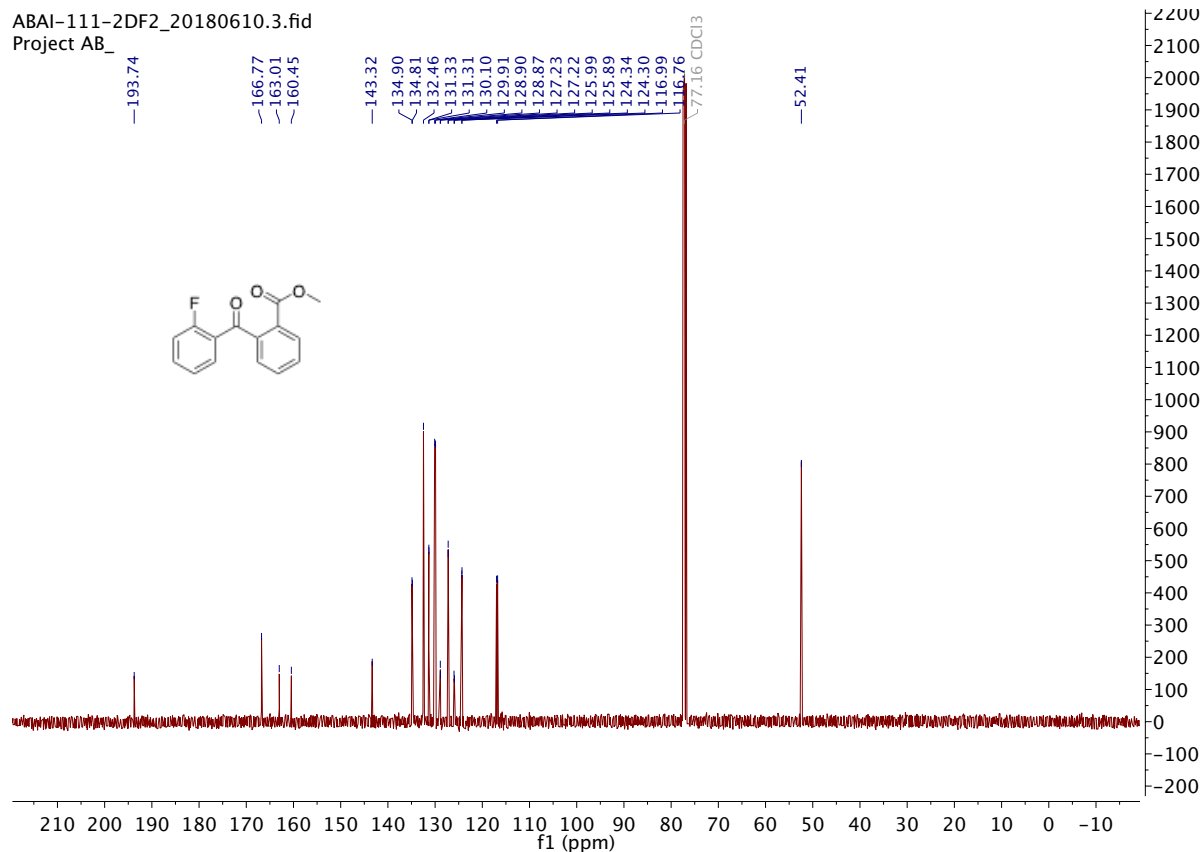
ESI : Carbonylative Suzuki-Miyaura couplings of sterically hindered aryl halides.

Methyl 2-(2-fluorobenzoyl) benzoate **2am**

ABAI-111-2DF2_20180610.1.fid
Project AB_

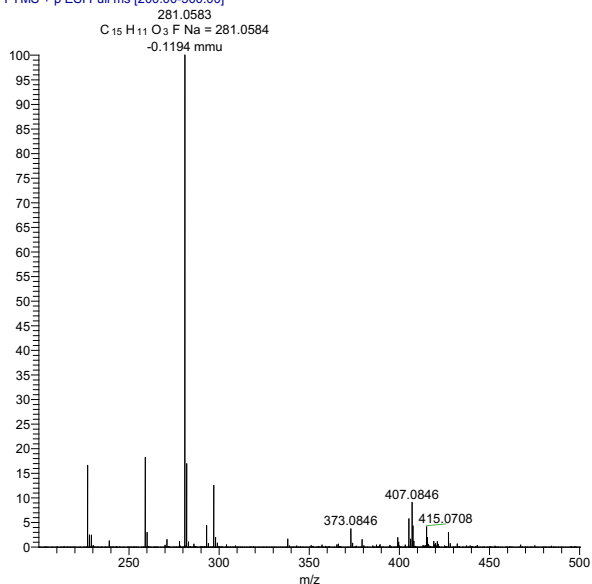


ABAI-111-2DF2_20180610.3.fid
Project AB_



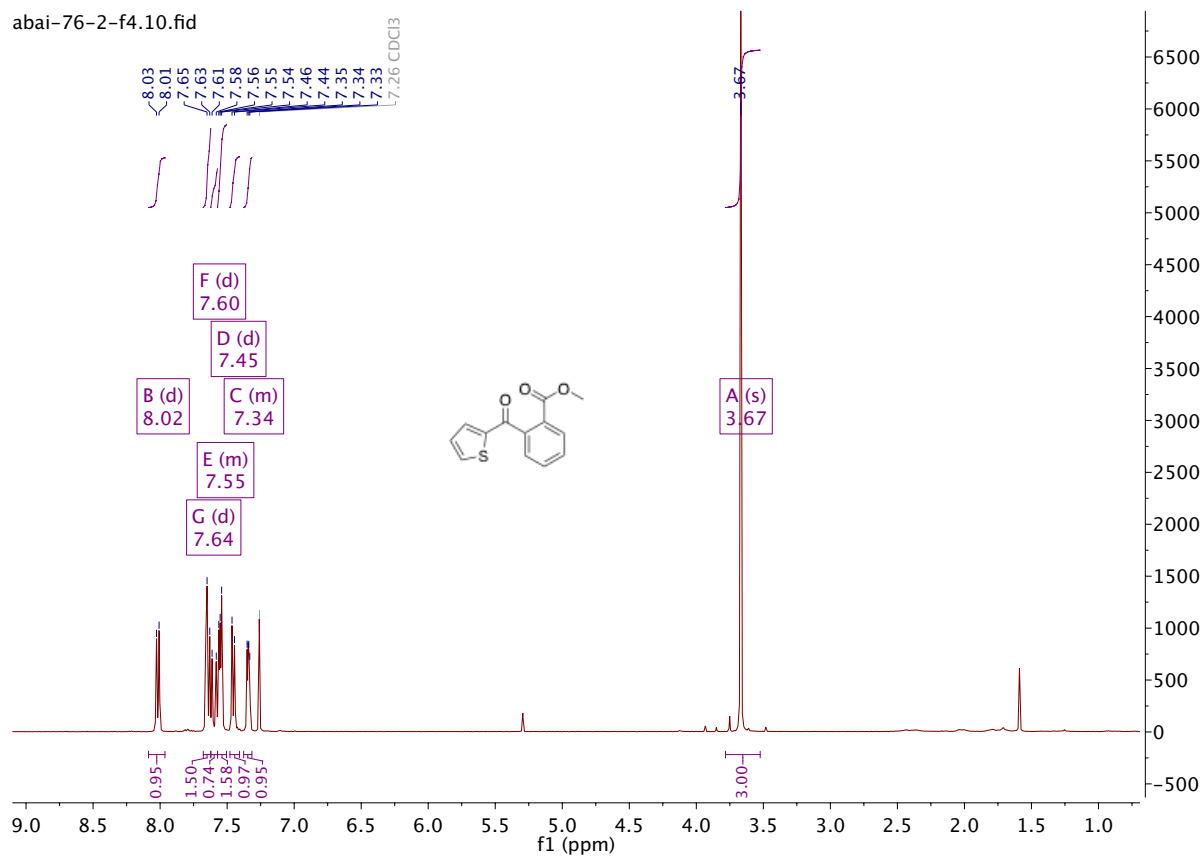
ESI : Carbonylative Suzuki-Miyaura couplings of sterically hindered aryl halides.

ABAI-111-2DF2 #1-4 RT: 0.01-0.10 AV: 4 NL: 3.70E7
T: FTMS + p ESI Full ms [200.00-500.00]



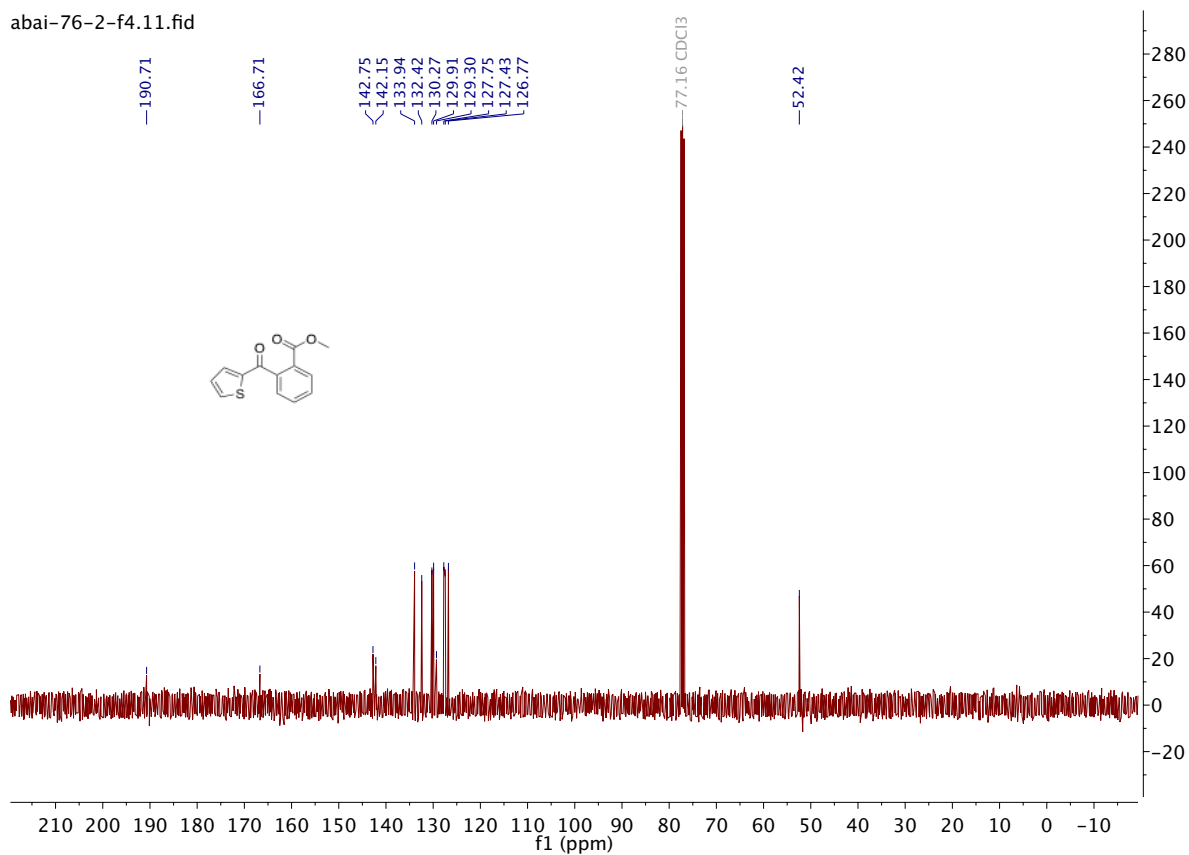
Methyl 2-(thiophene-2-carbonyl) benzoate **2an**

abai-76-2-f4.10.fid



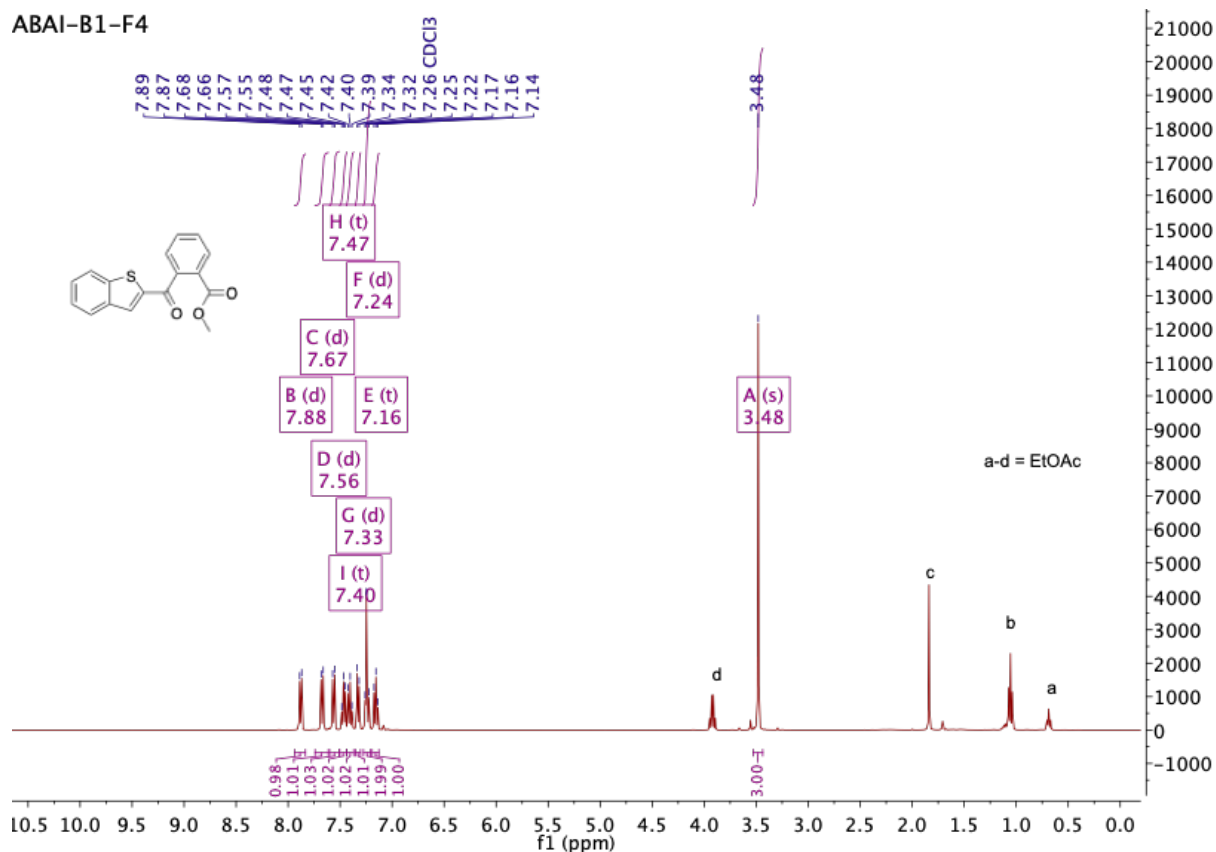
ESI : Carbonylative Suzuki-Miyaura couplings of sterically hindered aryl halides.

abai-76-2-f4.11.fid



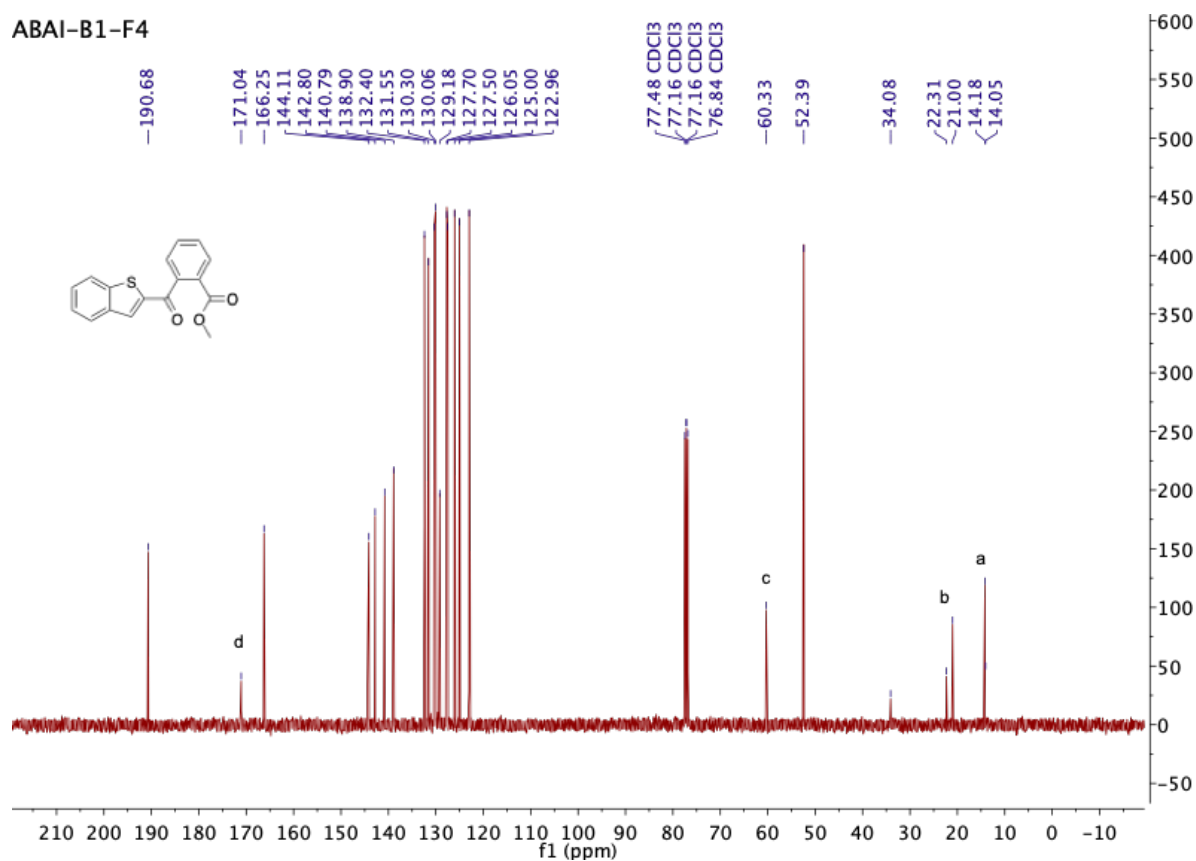
Methyl 2-(benzo[b]thiophene-2-carbonyl) benzoate **2ao**

ABAI-B1-F4



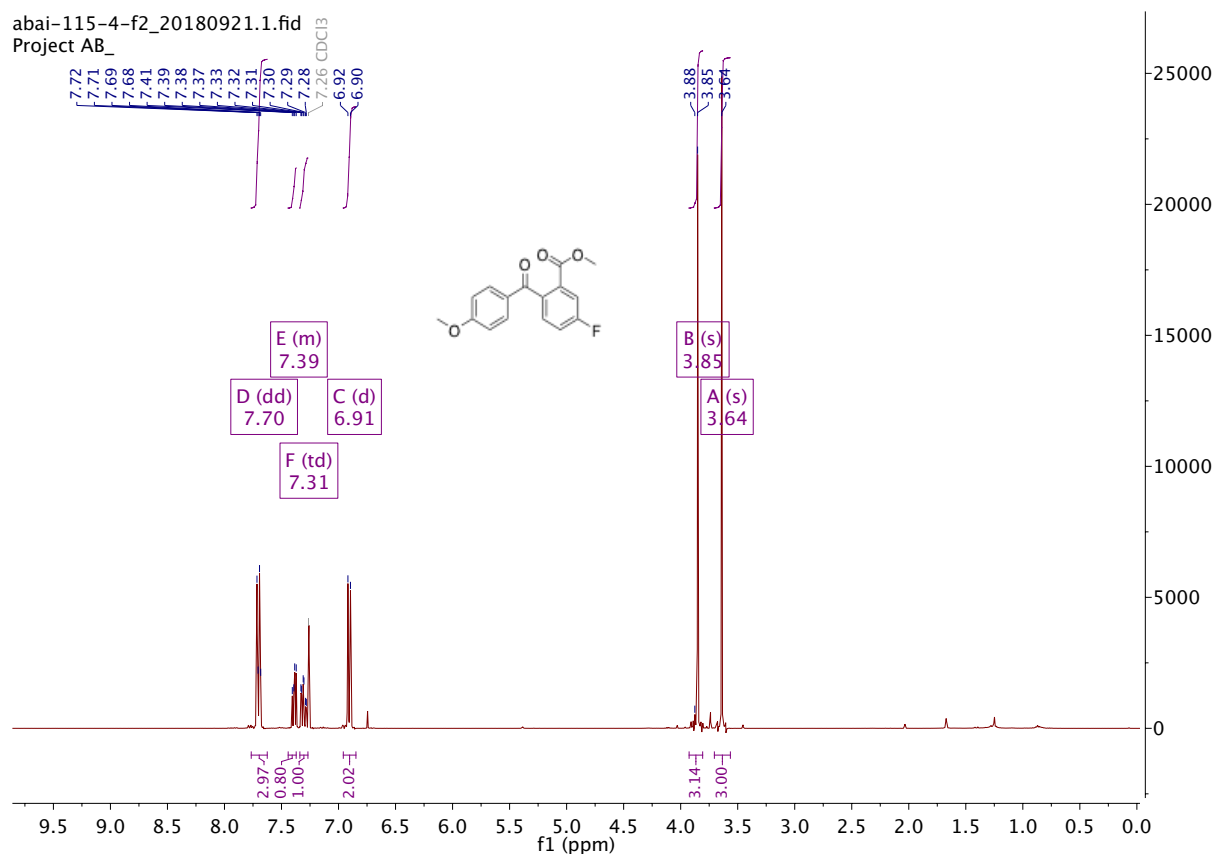
ESI : Carbonylative Suzuki-Miyaura couplings of sterically hindered aryl halides.

ABAI-B1-F4



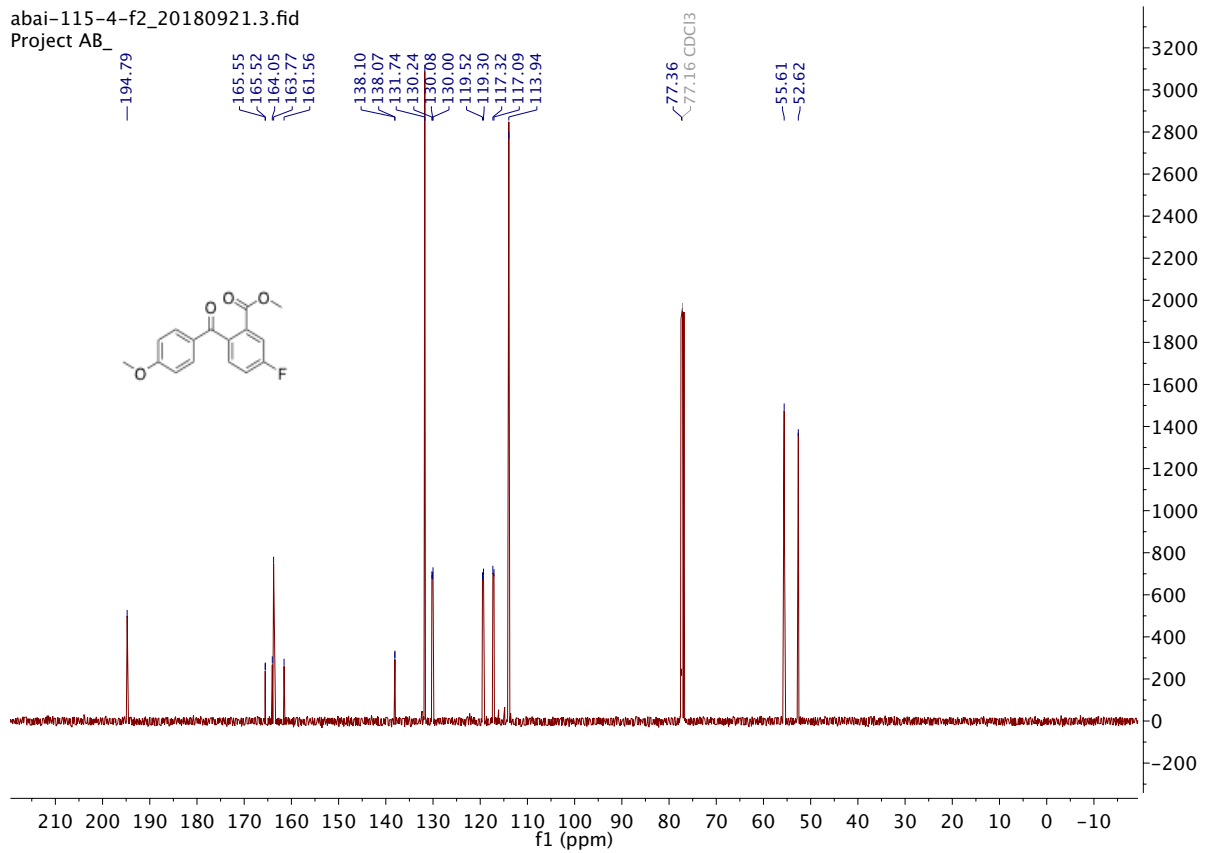
Methyl 5-fluoro-2-(4-methoxybenzoyl)benzoate **2ba**

abai-115-4-f2_20180921.1.fid
Project AB_

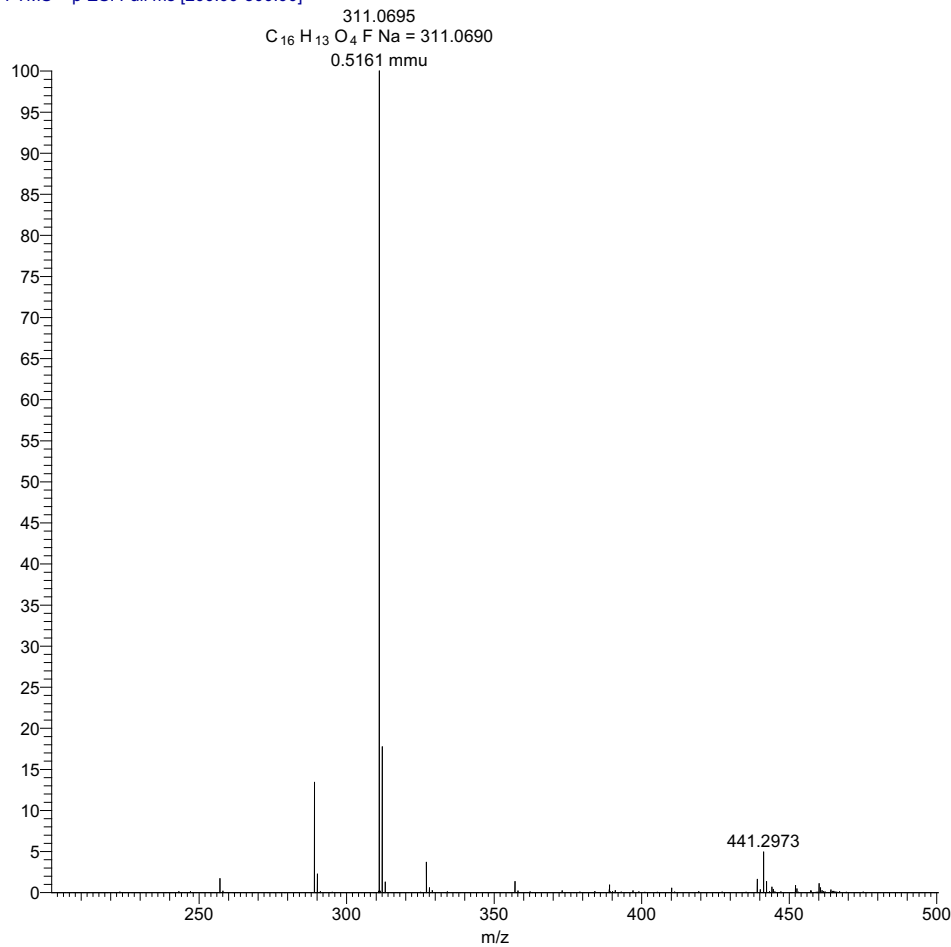


ESI : Carbonylative Suzuki-Miyaura couplings of sterically hindered aryl halides.

abai-115-4-f2_20180921.3.fid
Project AB_



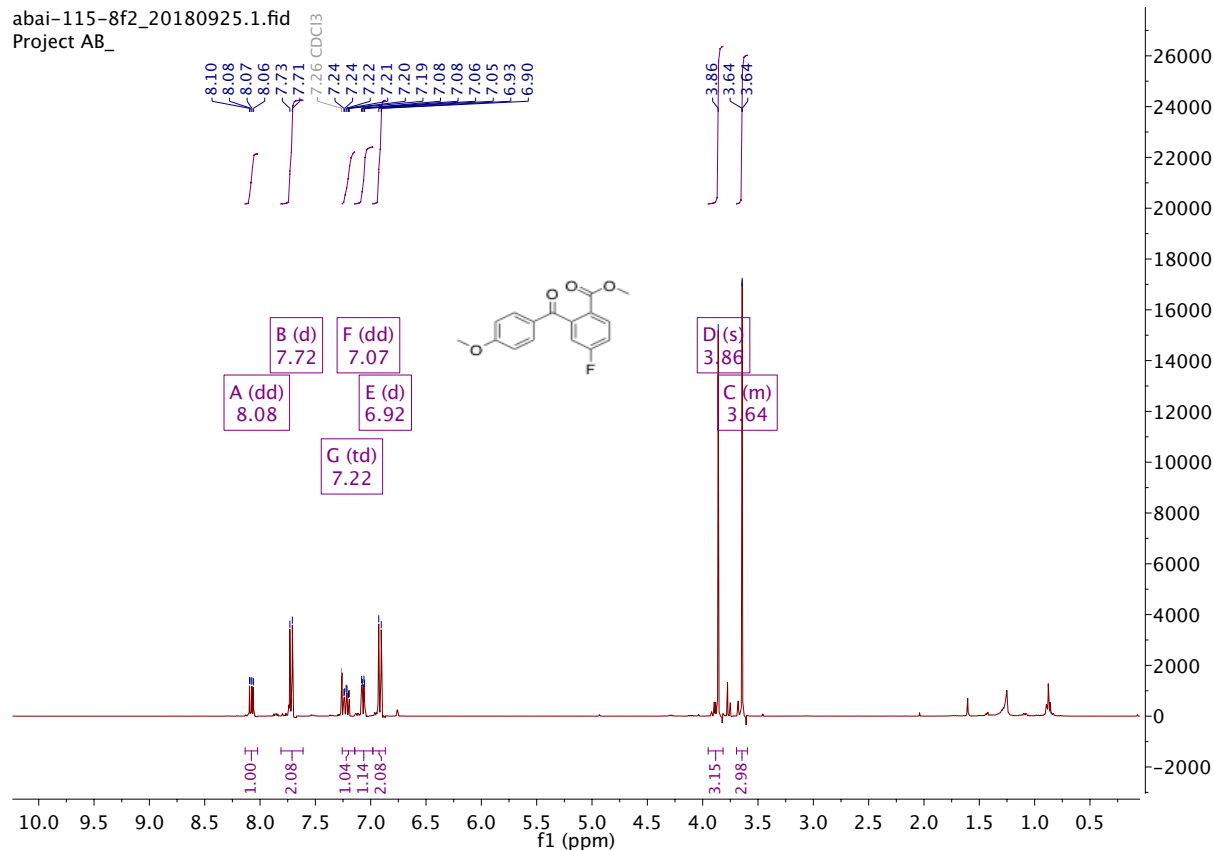
abai-115-4f2_181005104518 #1-5 RT: 0.01-0.12 AV: 5 NL: 6.61E7
T: FTMS + p ESI Full ms [200.00-500.00]



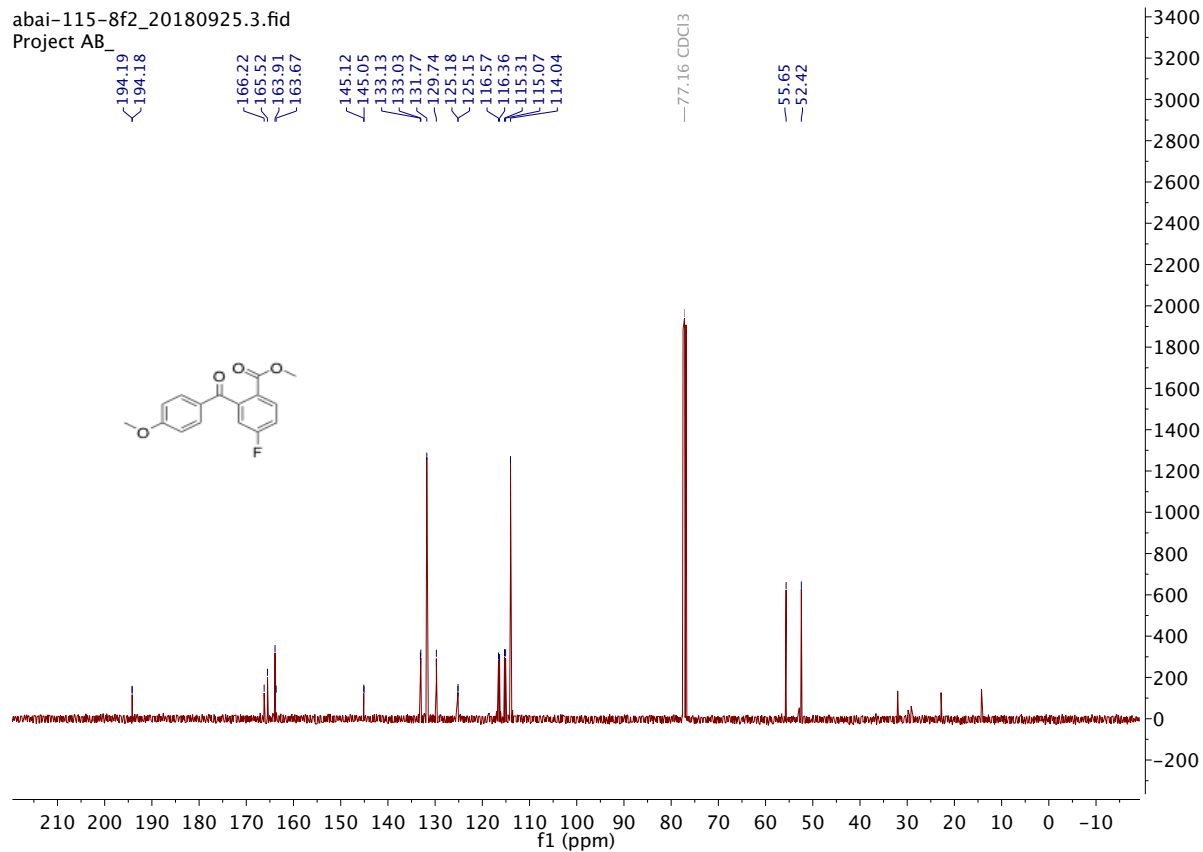
ESI : Carbonylative Suzuki-Miyaura couplings of sterically hindered aryl halides.

Methyl 4-fluoro-2-(4-methoxybenzoyl)benzoate **2ca**

abai-115-8f2_20180925.1.fid
Project AB_

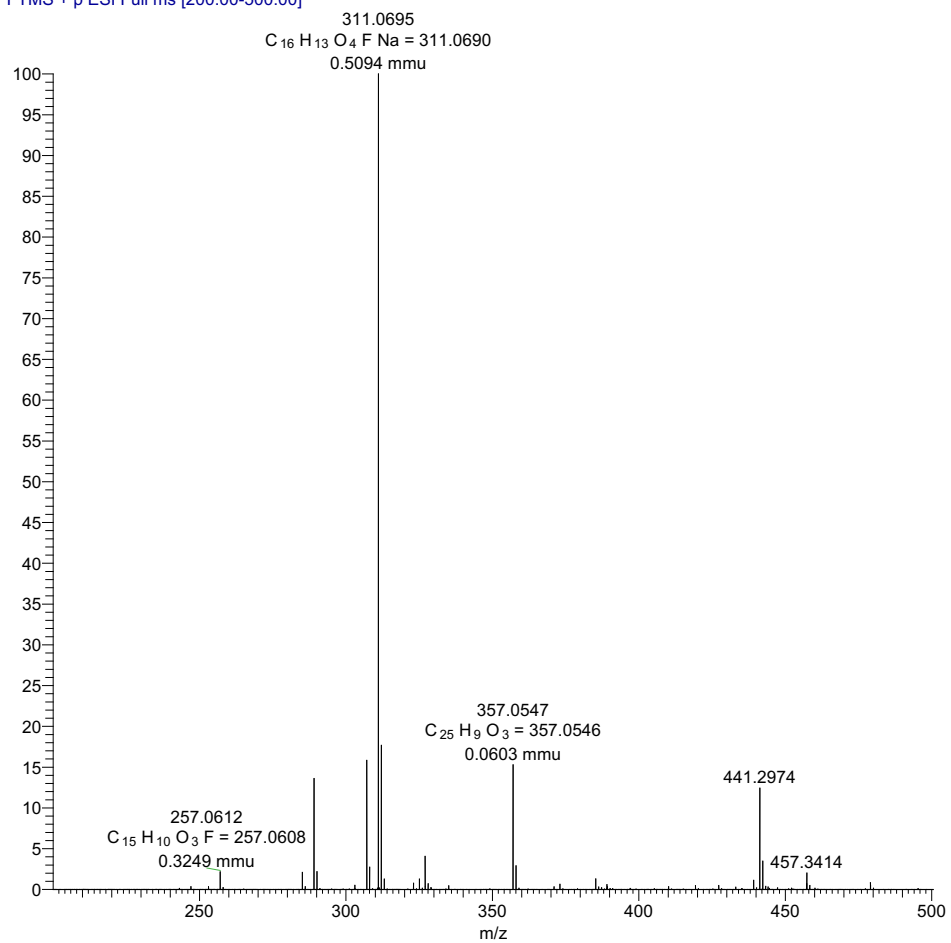


abai-115-8f2_20180925.3.fid
Project AB_



ESI : Carbonylative Suzuki-Miyaura couplings of sterically hindered aryl halides.

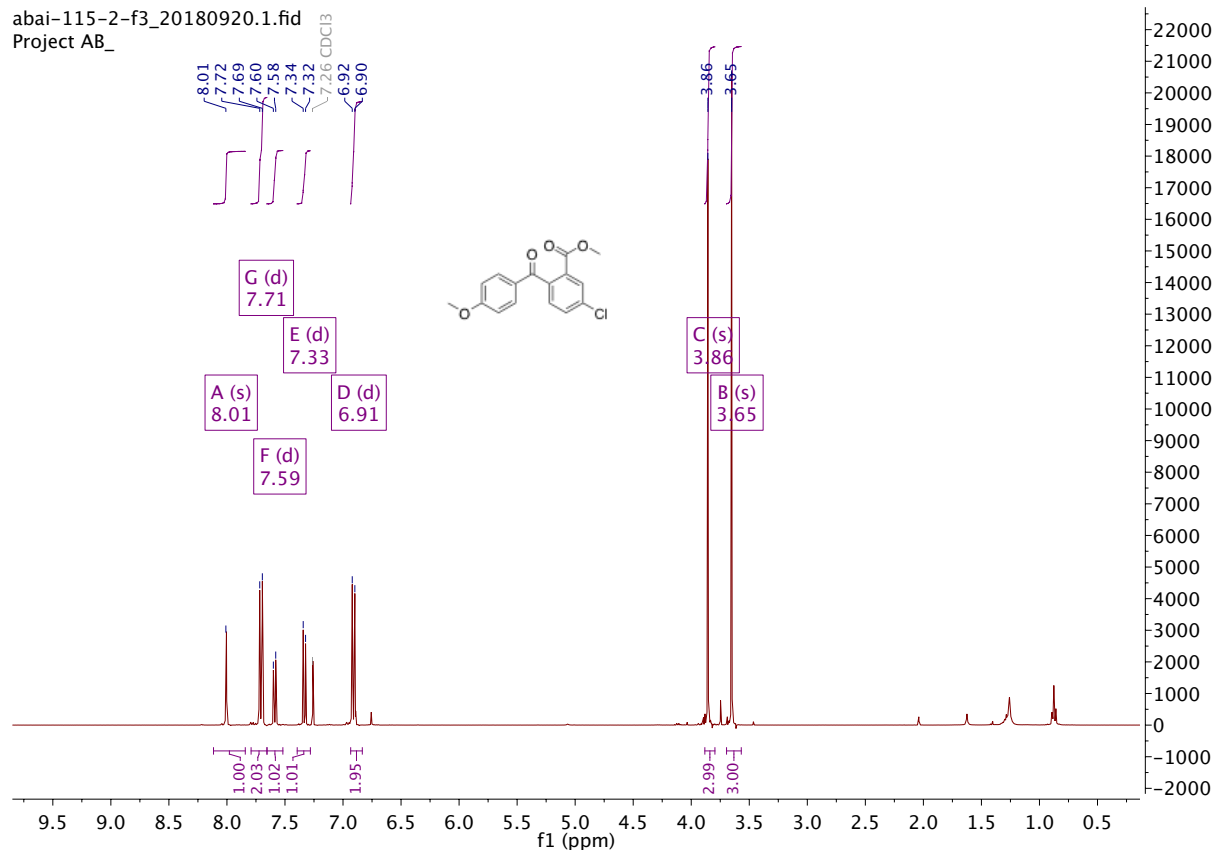
abai-115-8f2_181005161140 #1-5 RT: 0.01-0.12 AV: 5 NL: 5.13E7
T: FTMS + p ESI Full ms [200.00-500.00]



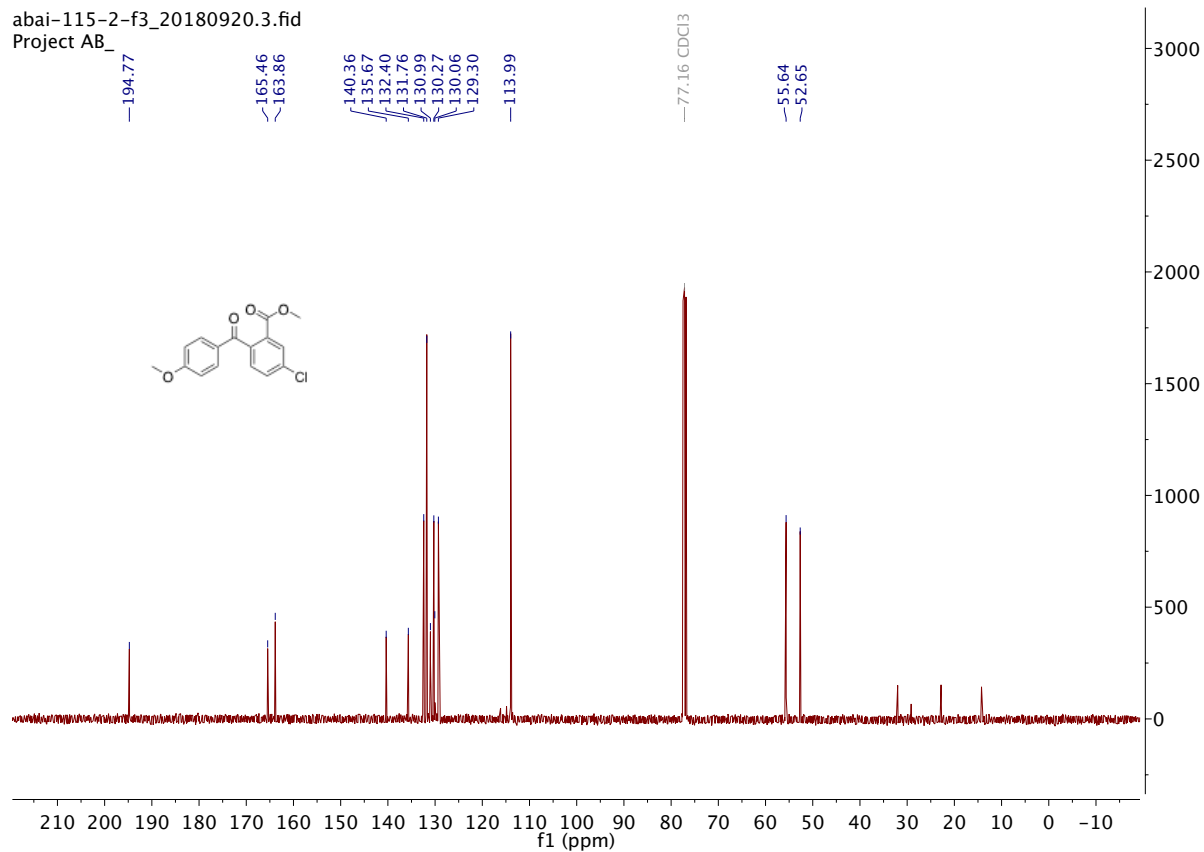
ESI : Carbonylative Suzuki-Miyaura couplings of sterically hindered aryl halides.

Methyl 5-chloro-2-(4-methoxybenzoyl)benzoate **2da**

abai-115-2-f3_20180920.1.fid
Project AB_

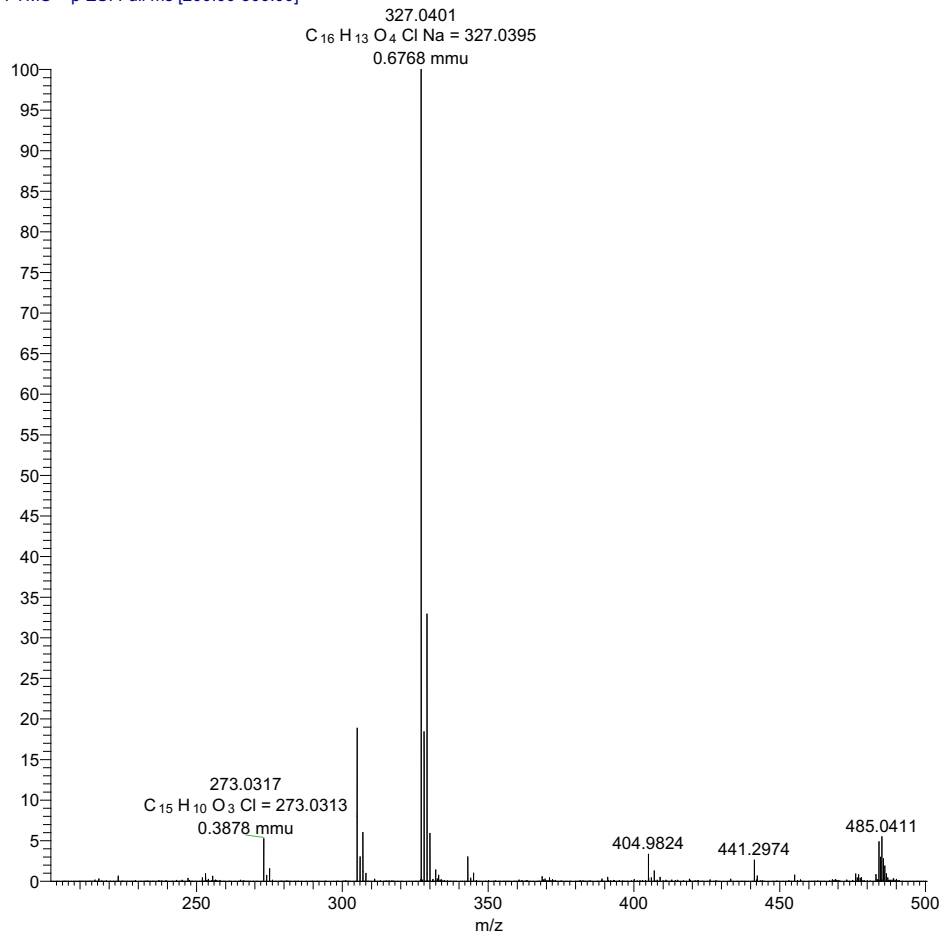


abai-115-2-f3_20180920.3.fid
Project AB_



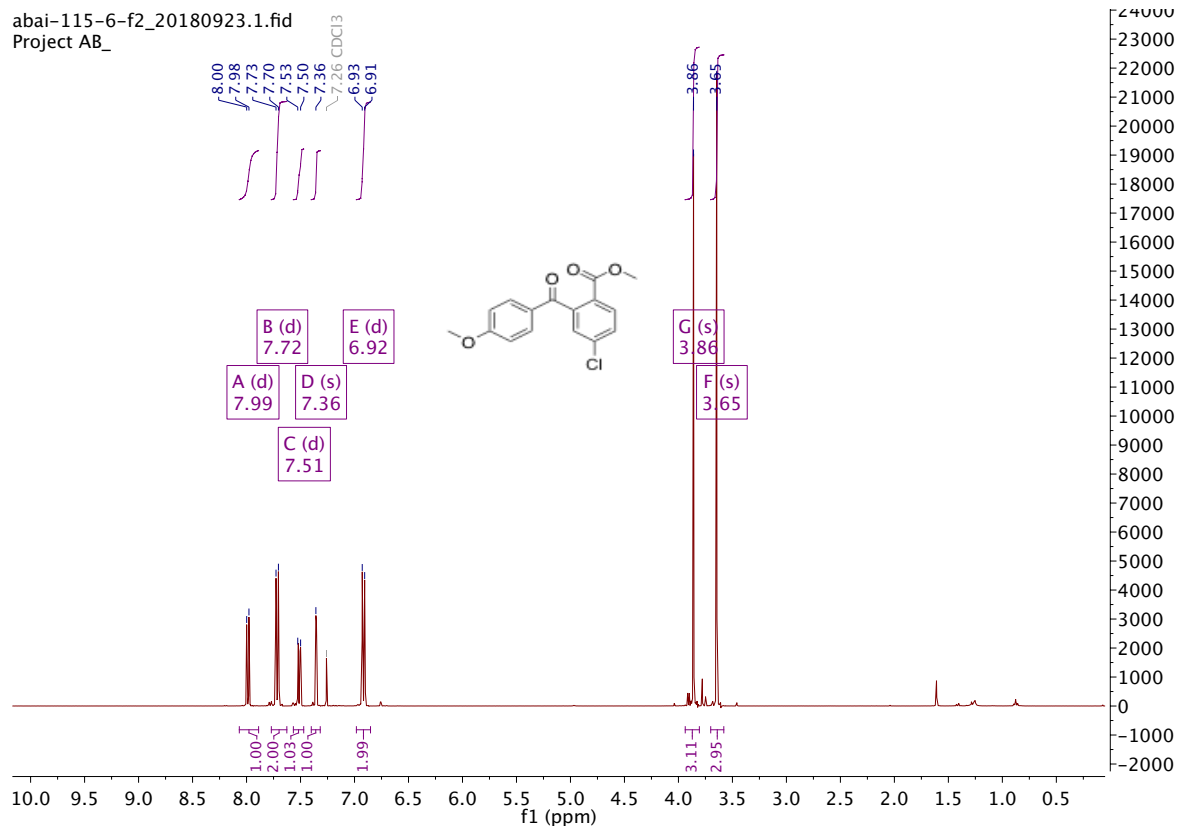
ESI : Carbonylative Suzuki-Miyaura couplings of sterically hindered aryl halides.

abai-115-2f3_181005104518 #1-5 RT: 0.02-0.13 AV: 5 NL: 3.24E7
 T: FTMS + p ESI Full ms [200.00-500.00]



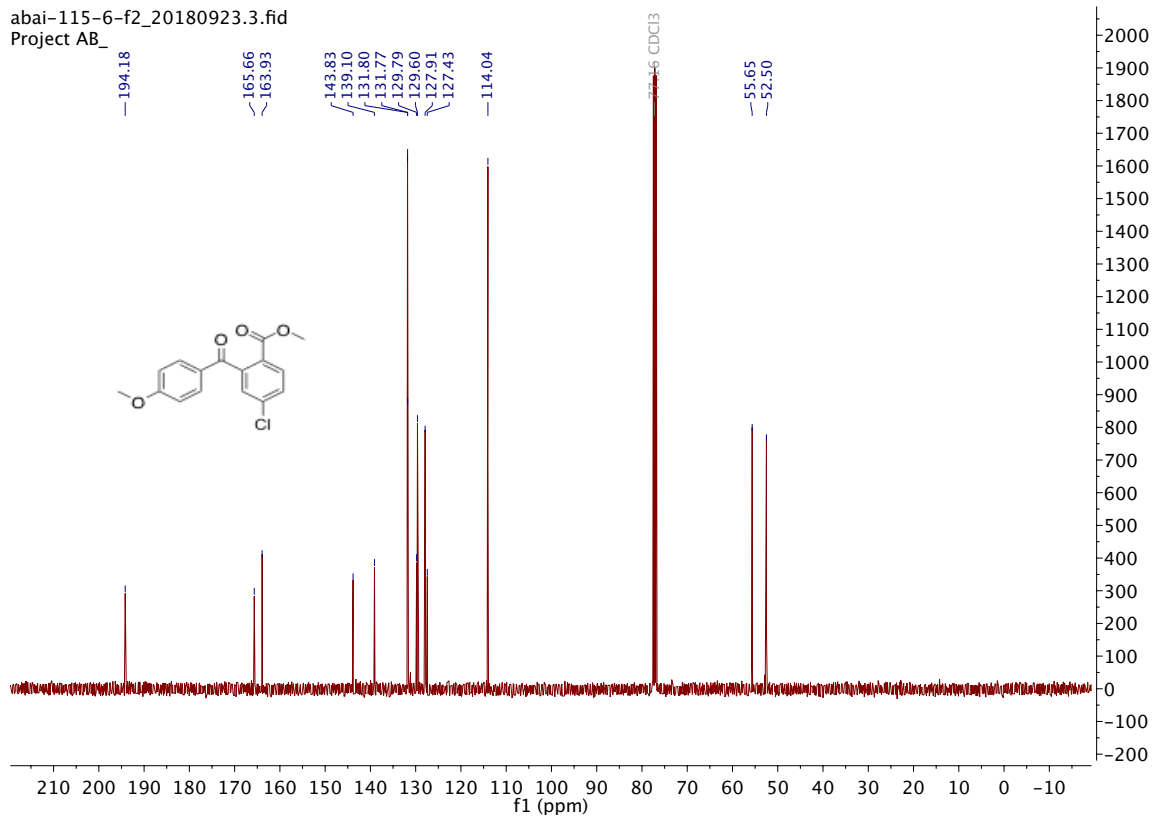
Methyl 4-chloro-2-(4-methoxybenzoyl)benzoate **2ea**

abai-115-6-f2_20180923.1.fid
 Project AB_

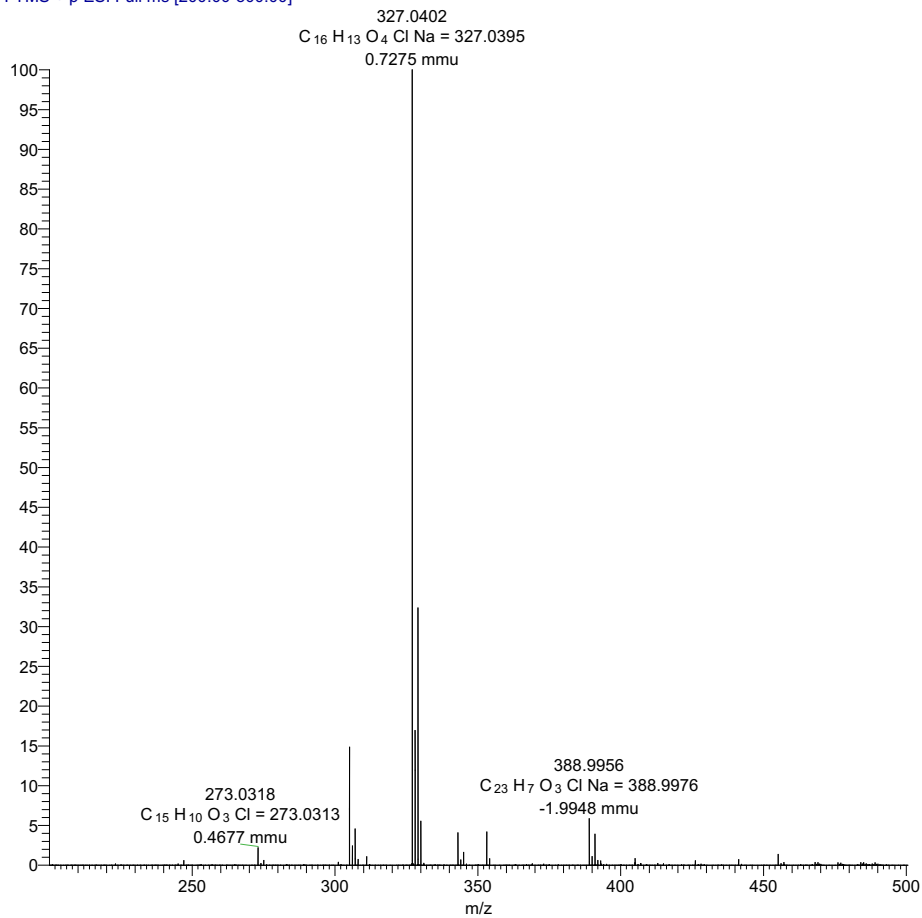


ESI : Carbonylative Suzuki-Miyaura couplings of sterically hindered aryl halides.

abai-115-6-f2_20180923.3.fid
Project AB_



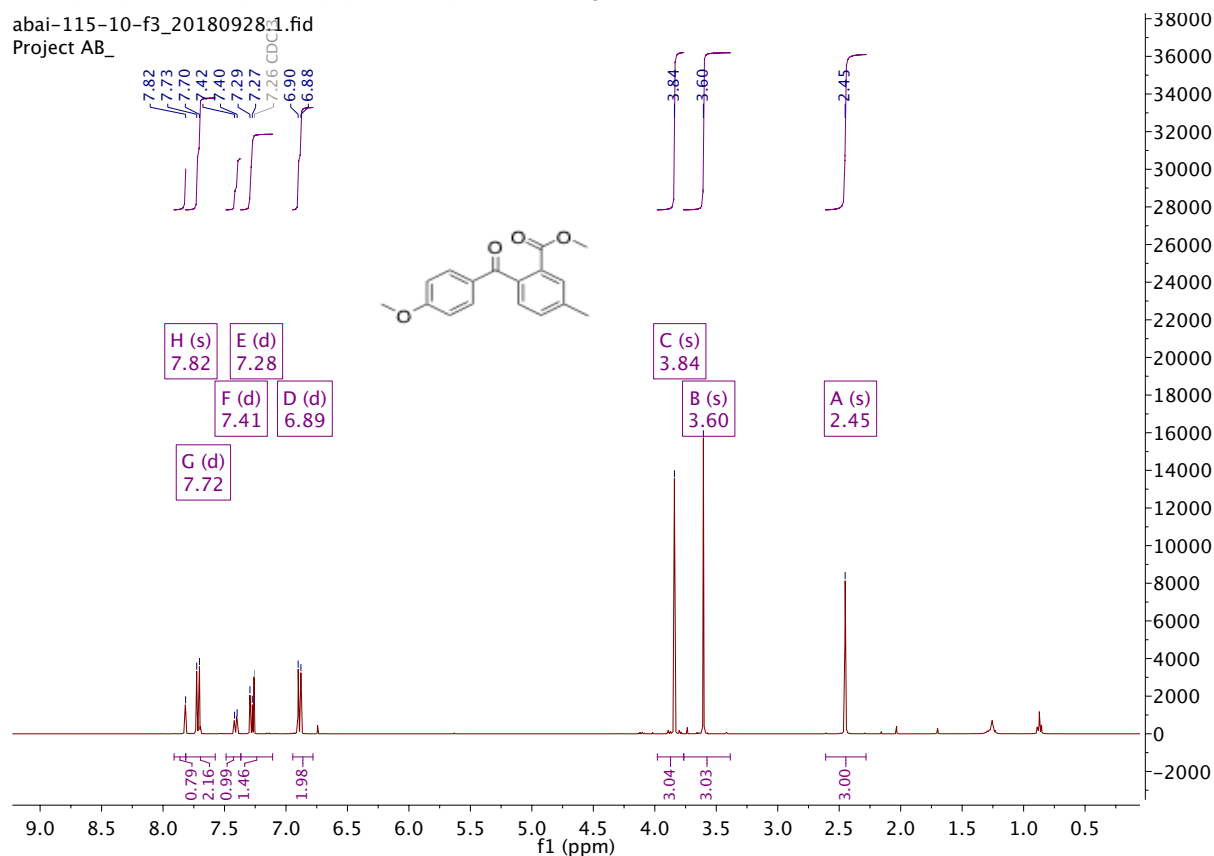
abai-115-6f2_181005161140 #1-4 RT: 0.02-0.10 AV: 4 NL: 2.18E7
T: FTMS + p ESI Full ms [200.00-500.00]



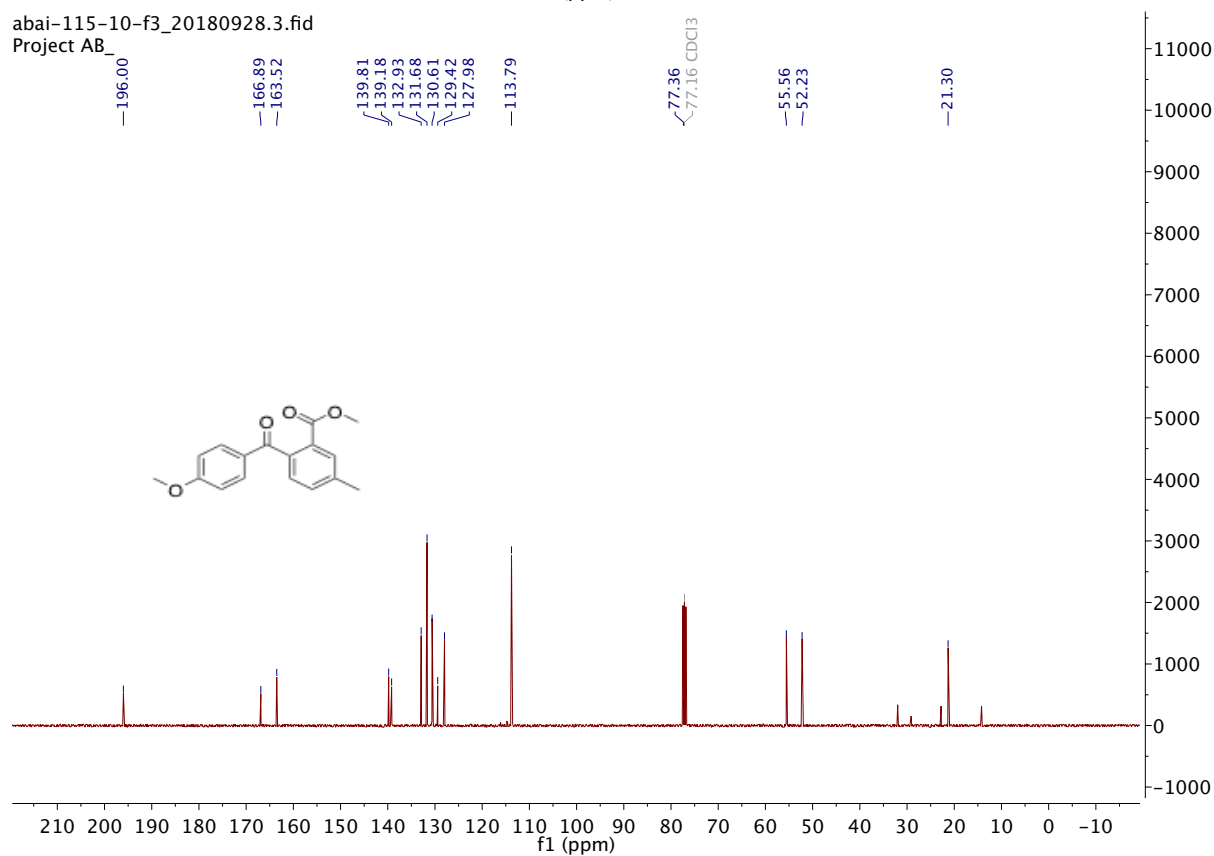
ESI : Carbonylative Suzuki-Miyaura couplings of sterically hindered aryl halides.

Methyl 2-(4-methoxybenzoyl)-5-methylbenzoate **2fa**

abai-115-10-f3_20180928:1.fid
Project AB_

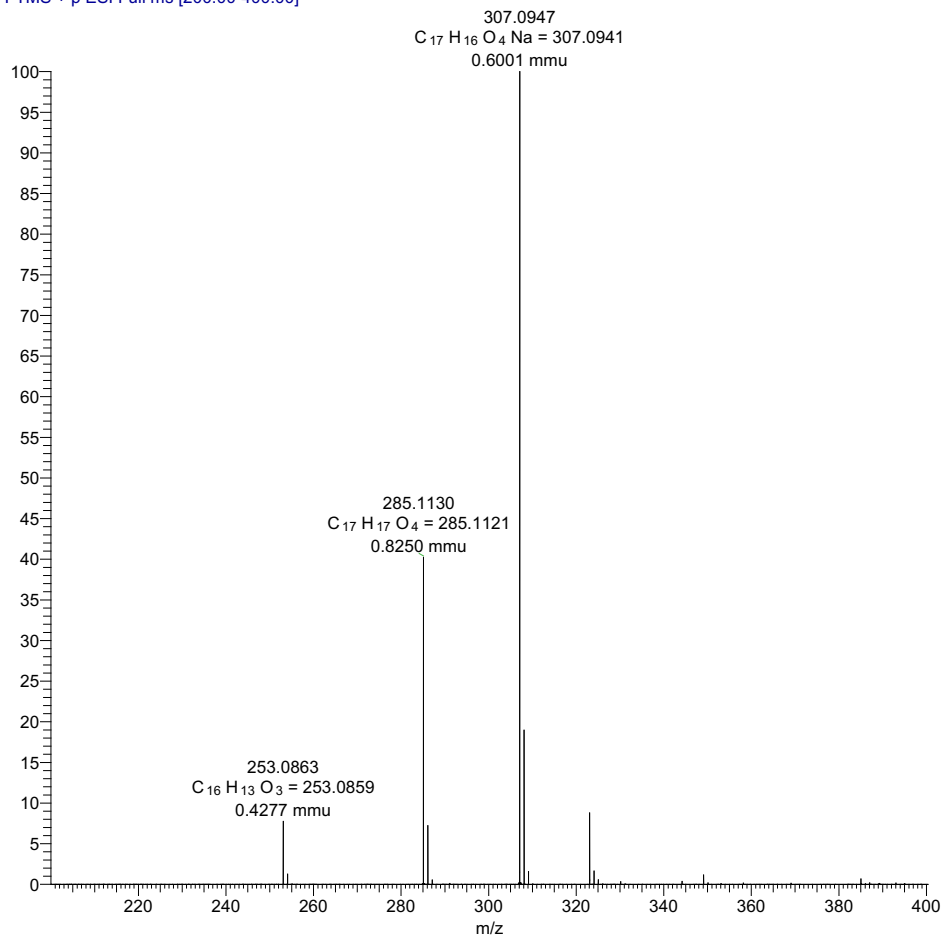


abai-115-10-f3_20180928:3.fid
Project AB_



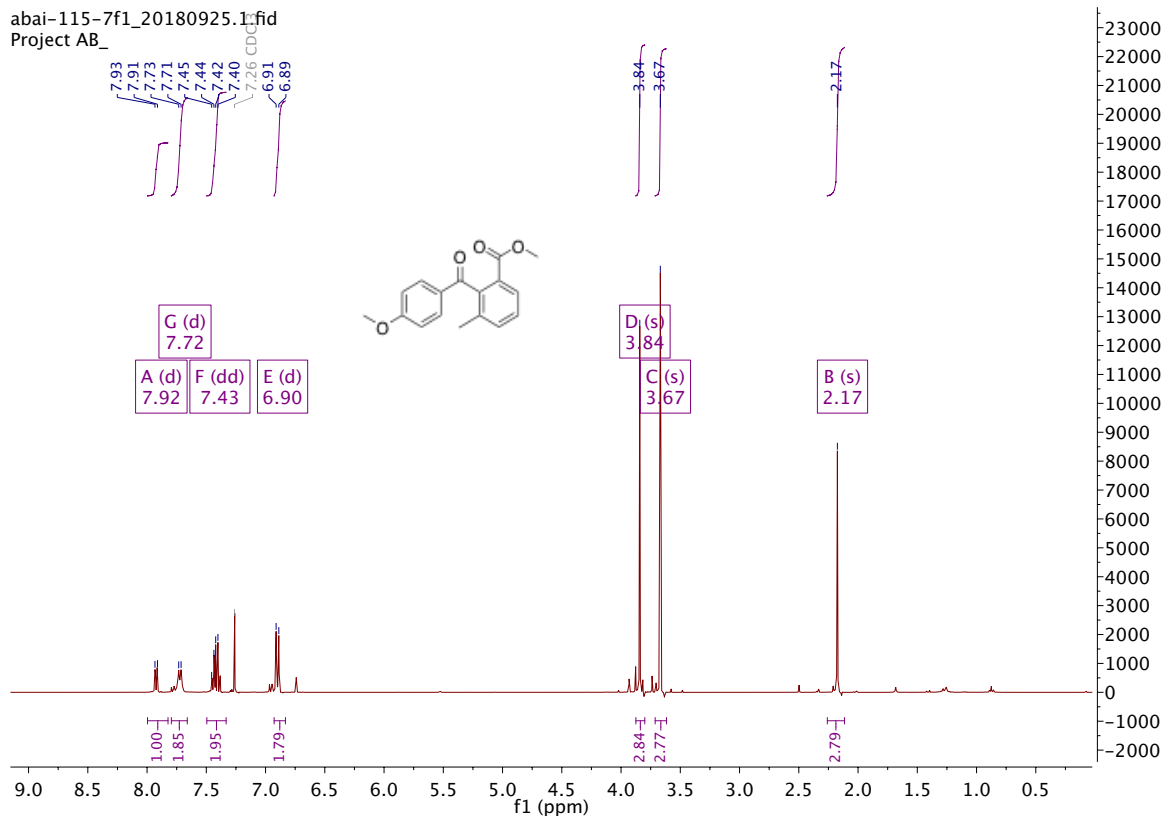
ESI : Carbonylative Suzuki-Miyaura couplings of sterically hindered aryl halides.

abai-115-10-f3_181005163548 #1-4 RT: 0.01-0.10 AV: 4 NL: 5.33E7
 T: FTMS + p ESI Full ms [200.00-400.00]



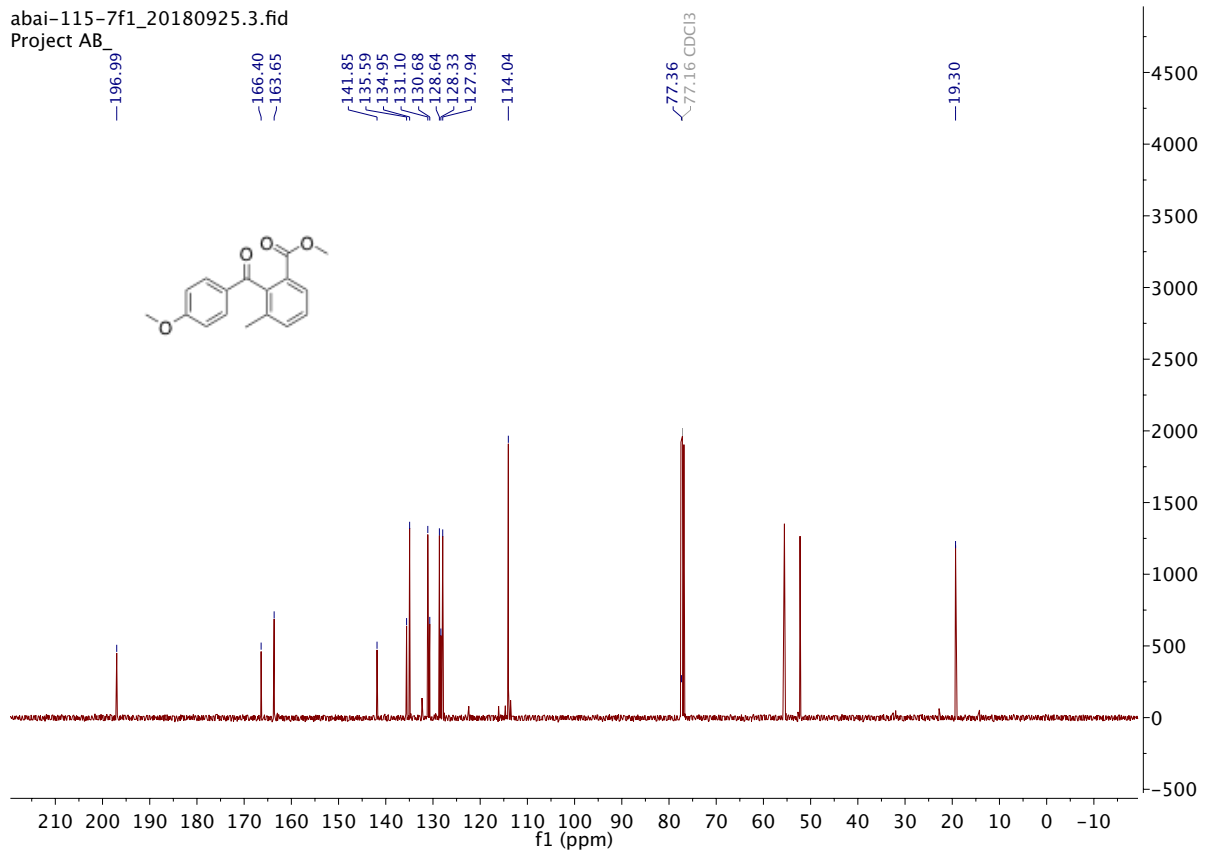
Methyl 2-(4-methoxybenzoyl)-3-methylbenzoate **2ga**

abai-115-7f1_20180925.1.fid
 Project AB_

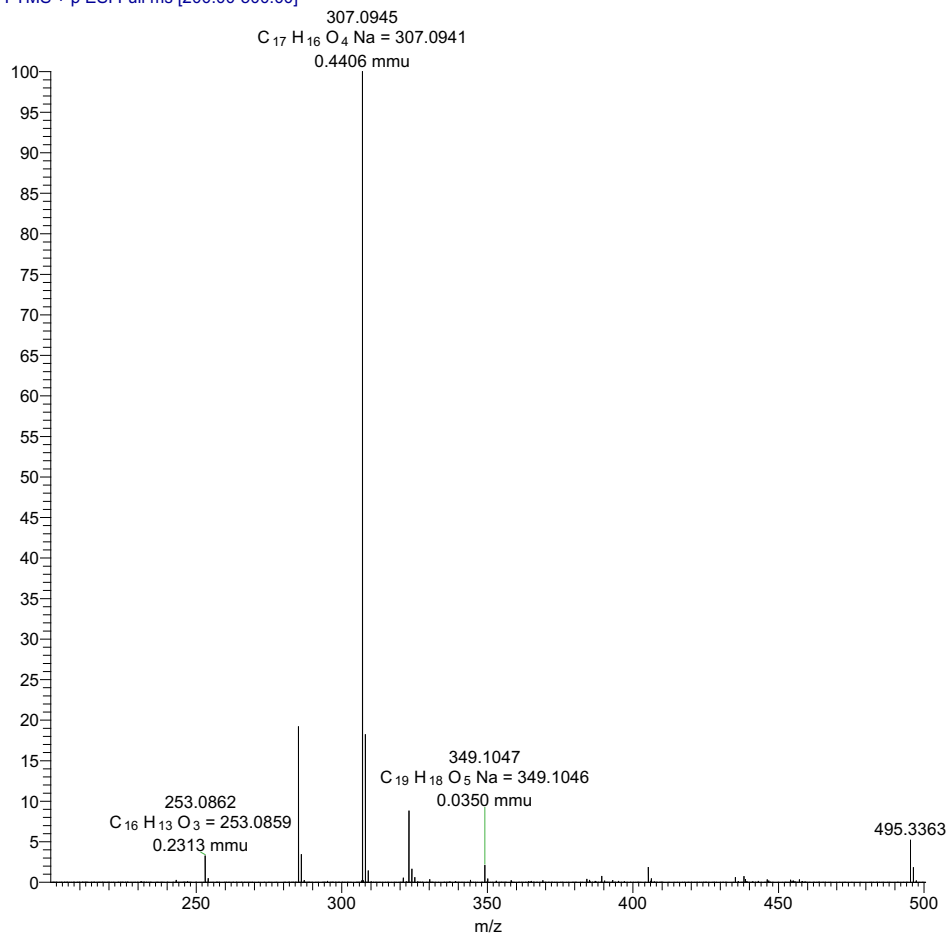


ESI : Carbonylative Suzuki-Miyaura couplings of sterically hindered aryl halides.

abai-115-7f1_20180925.3.fid
Project AB



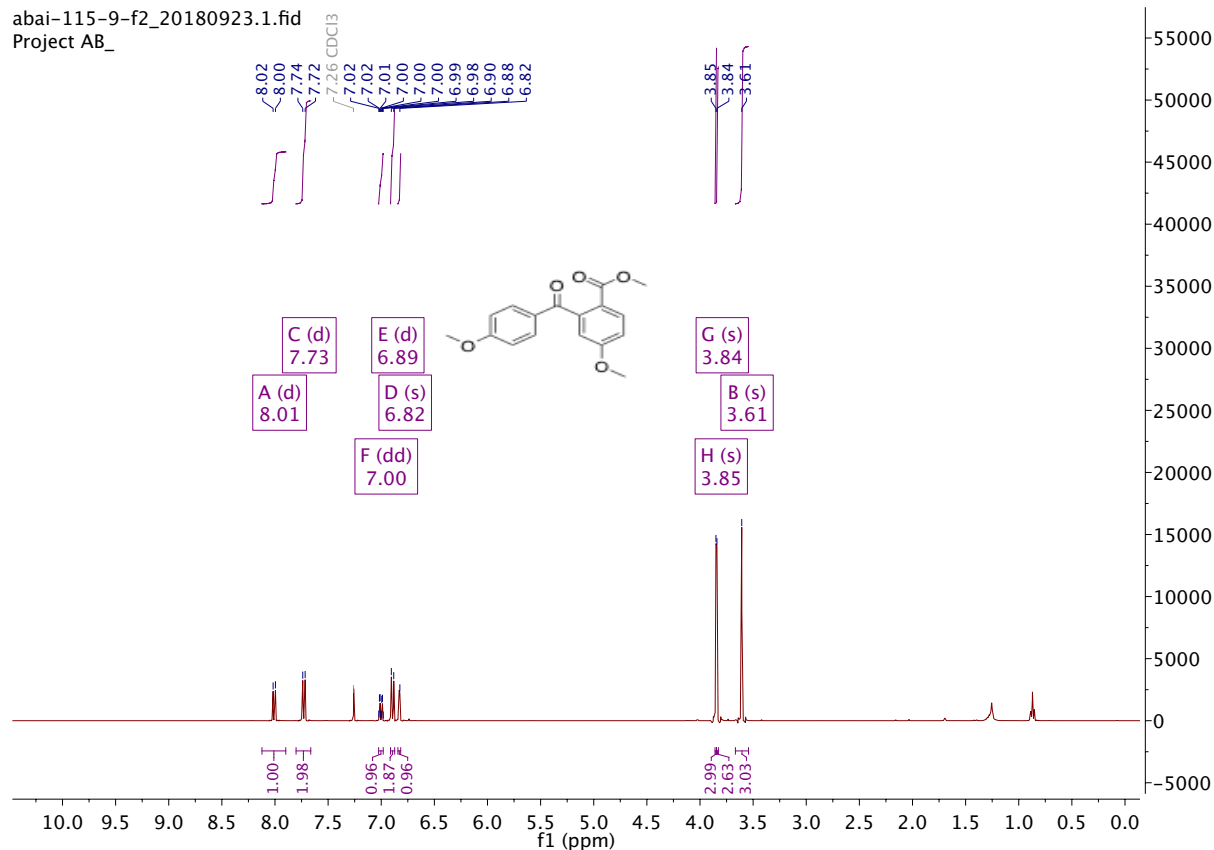
abai-115-7f1_181005161140 #1-5 RT: 0.01-0.12 AV: 5 NL: 6.95E7
T: FTMS + p ESI Full ms [200.00-500.00]



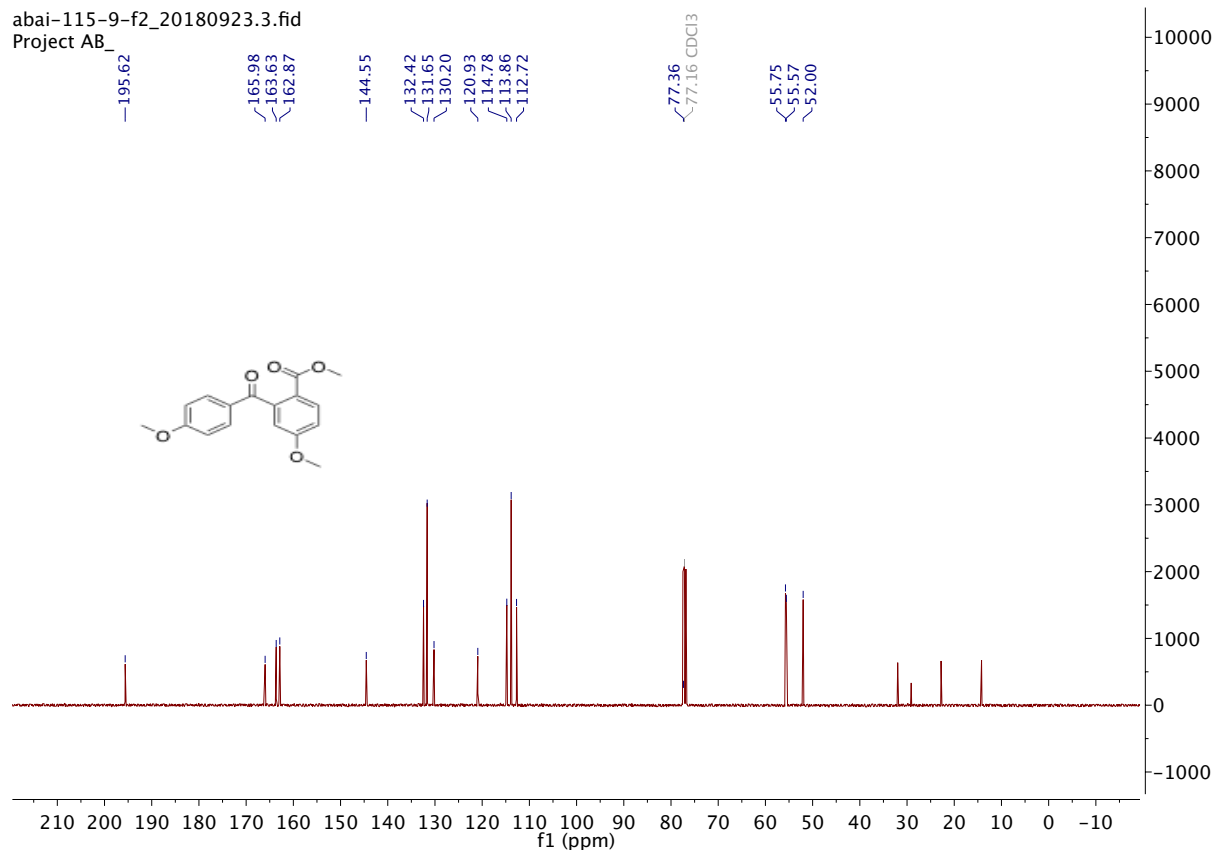
ESI : Carbonylative Suzuki-Miyaura couplings of sterically hindered aryl halides.

Methyl 4-methoxy-2-(4-methoxybenzoyl) benzoate **2ha**

abai-115-9-f2_20180923.1.fid
Project AB_

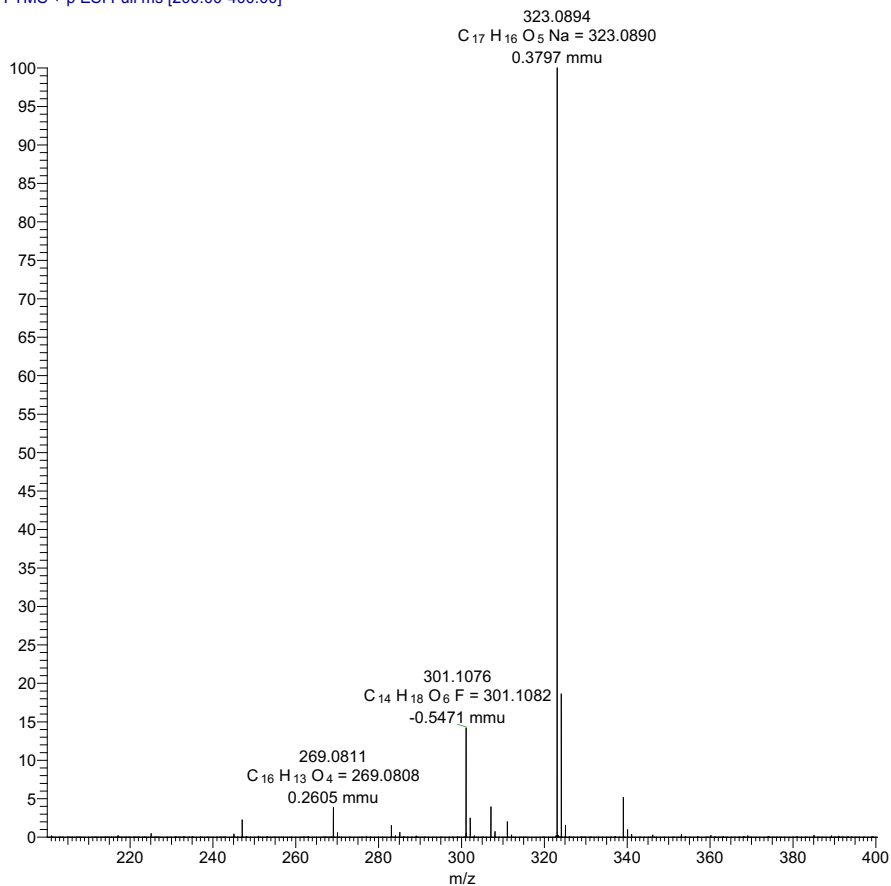


abai-115-9-f2_20180923.3.fid
Project AB_



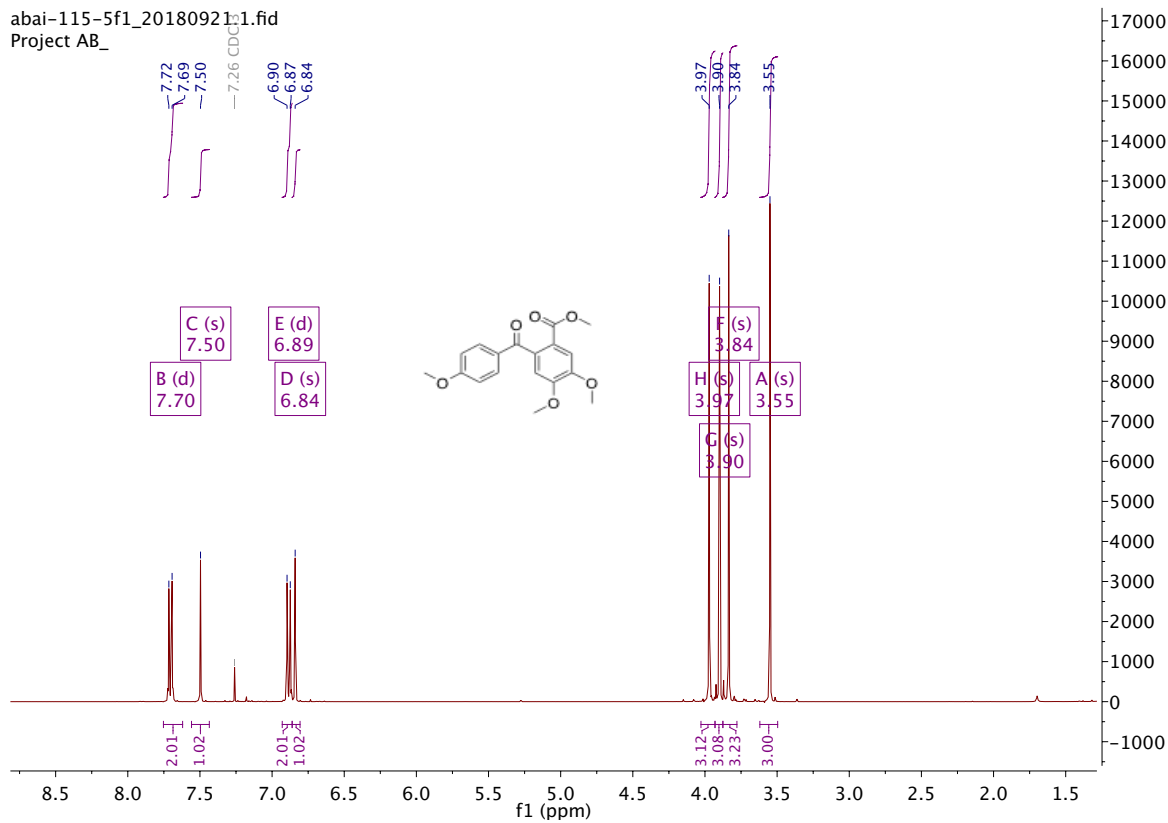
ESI : Carbonylative Suzuki-Miyaura couplings of sterically hindered aryl halides.

abai-115-9f2_181005163548 #1-4 RT: 0.02-0.11 AV: 4 NL: 1.01E7
T: FTMS + p ESI Full ms [200.00-400.00]



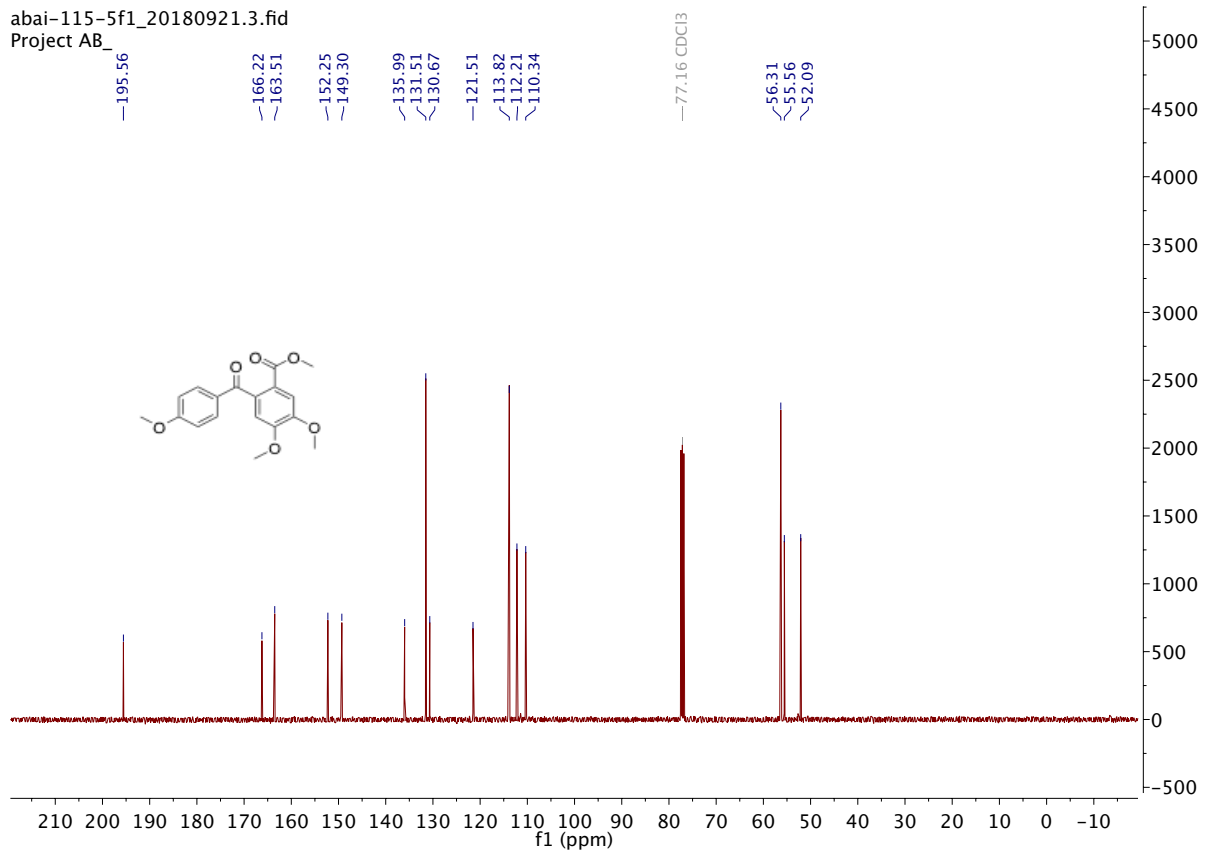
Methyl 2-(4-methoxybenzoyl)-5-methylbenzoate **2ia**

abai-115-5f1_201809211.fid
Project AB_

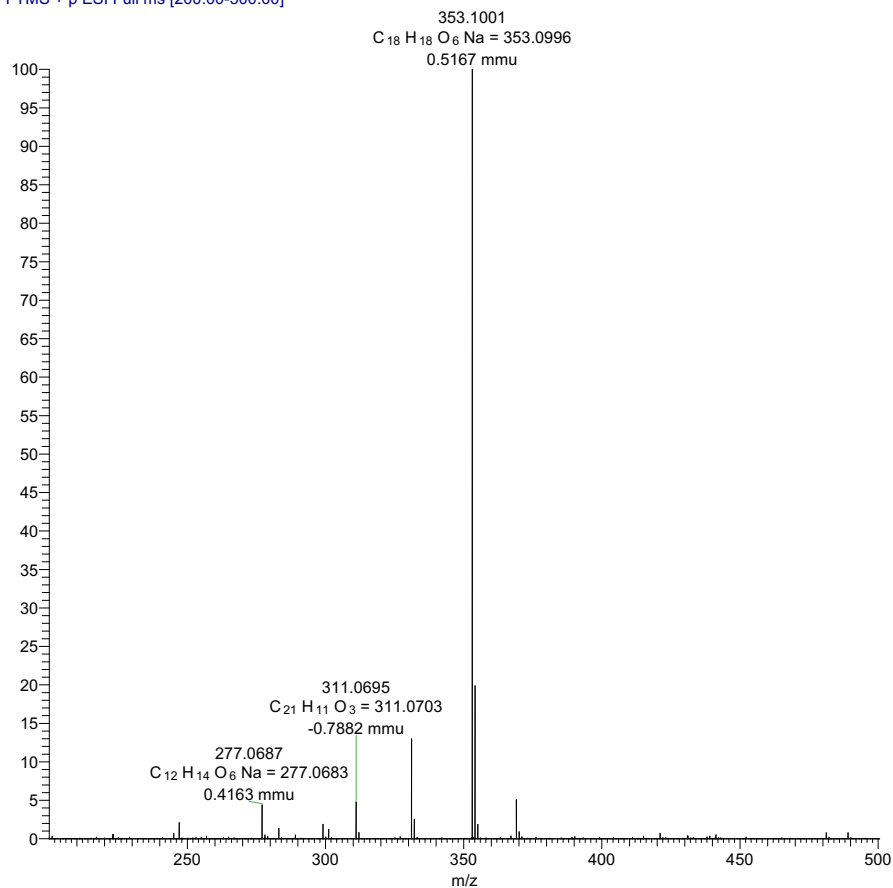


ESI : Carbonylative Suzuki-Miyaura couplings of sterically hindered aryl halides.

abai-115-5f1_20180921.3.fid
Project AB_



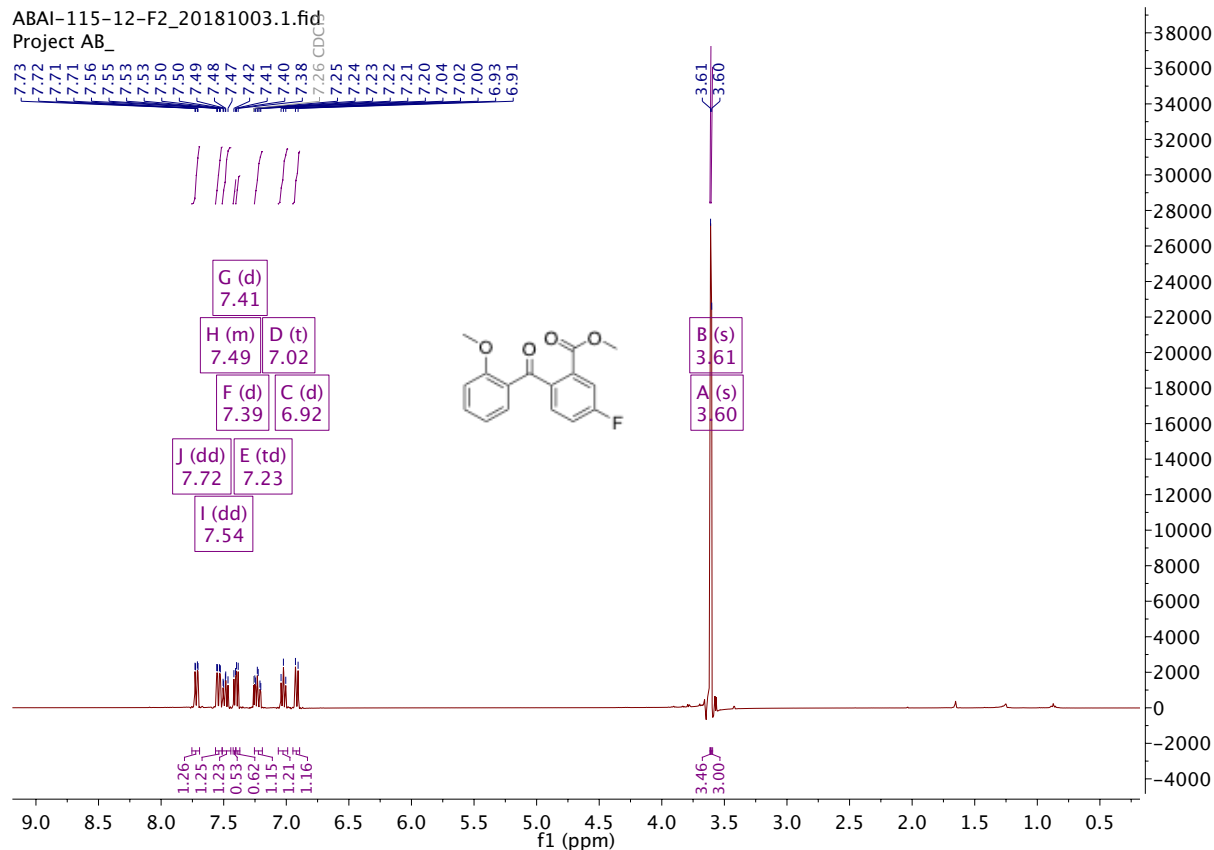
abai-115-5f1_181005161140 #1-5 RT: 0.02-0.13 AV: 5 NL: 1.10E7
T: FTMS + p ESI Full ms [200.00-500.00]



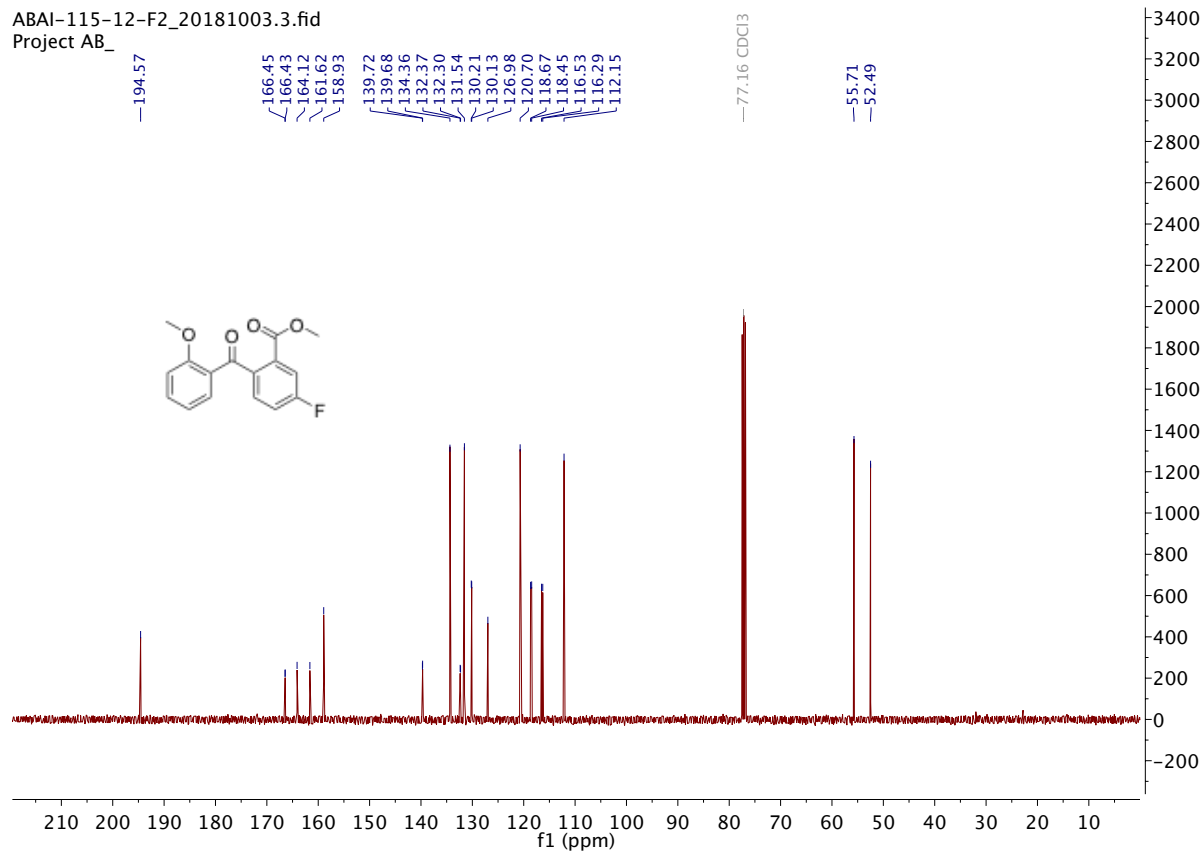
ESI : Carbonylative Suzuki-Miyaura couplings of sterically hindered aryl halides.

Methyl 5-fluoro-2-(2-methoxybenzoyl)benzoate **2bc**

ABAI-115-12-F2_20181003.1.fid
Project AB_

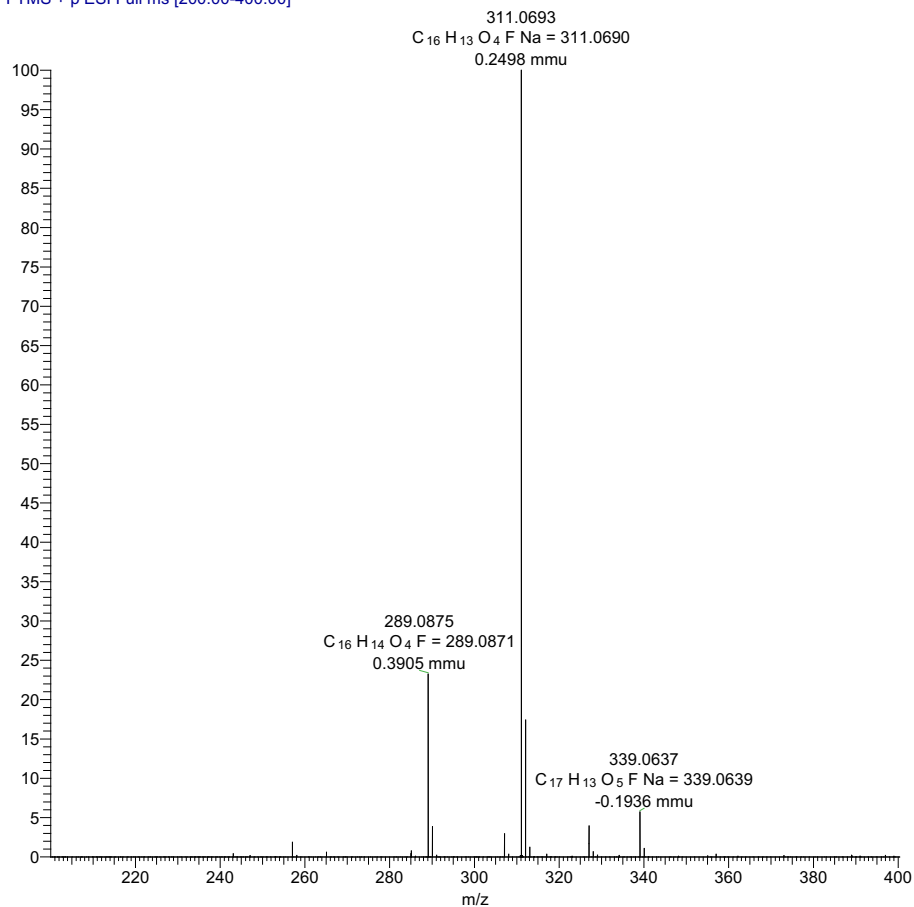


ABAI-115-12-F2_20181003.3.fid
Project AB_



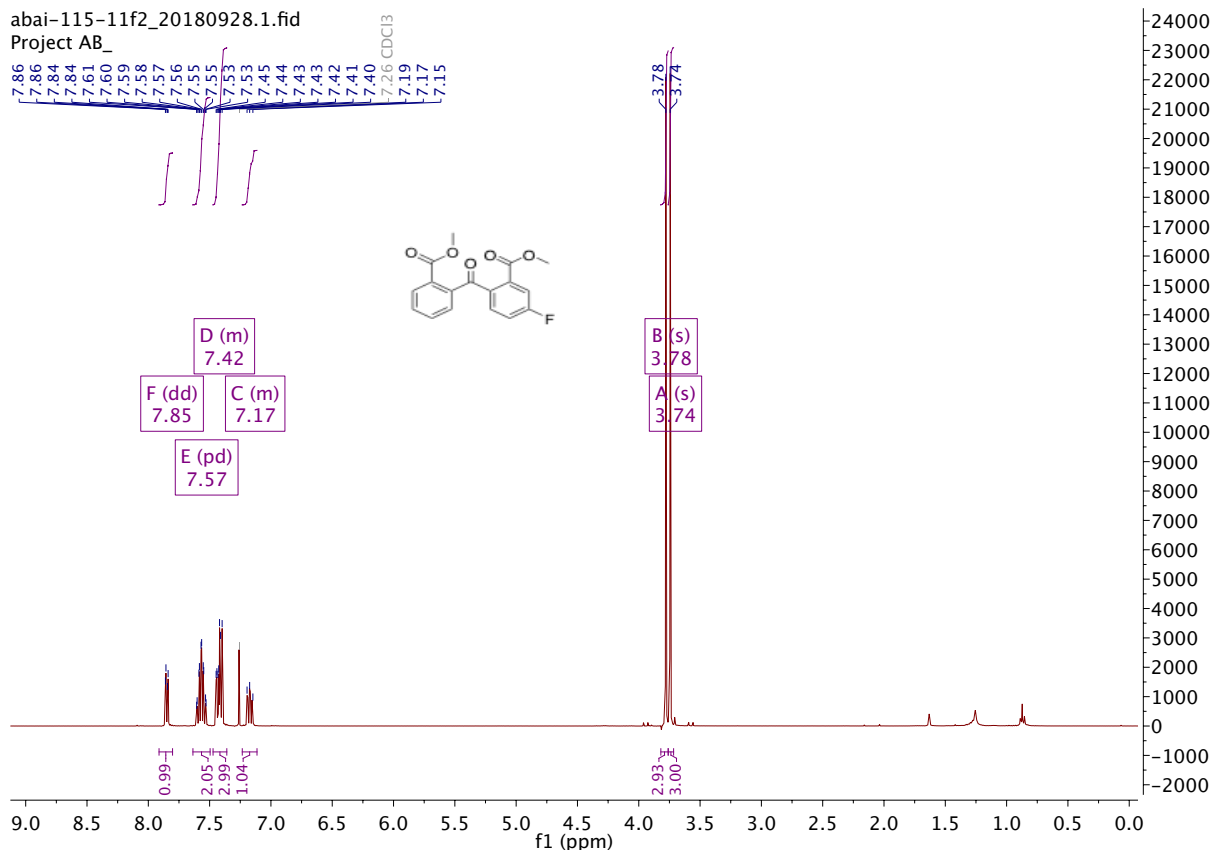
ESI : Carbonylative Suzuki-Miyaura couplings of sterically hindered aryl halides.

abai-115-12-f2_181005163548 #1-4 RT: 0.01-0.10 AV: 4 NL: 4.68E7
 T: FTMS + p ESI Full ms [200.00-400.00]



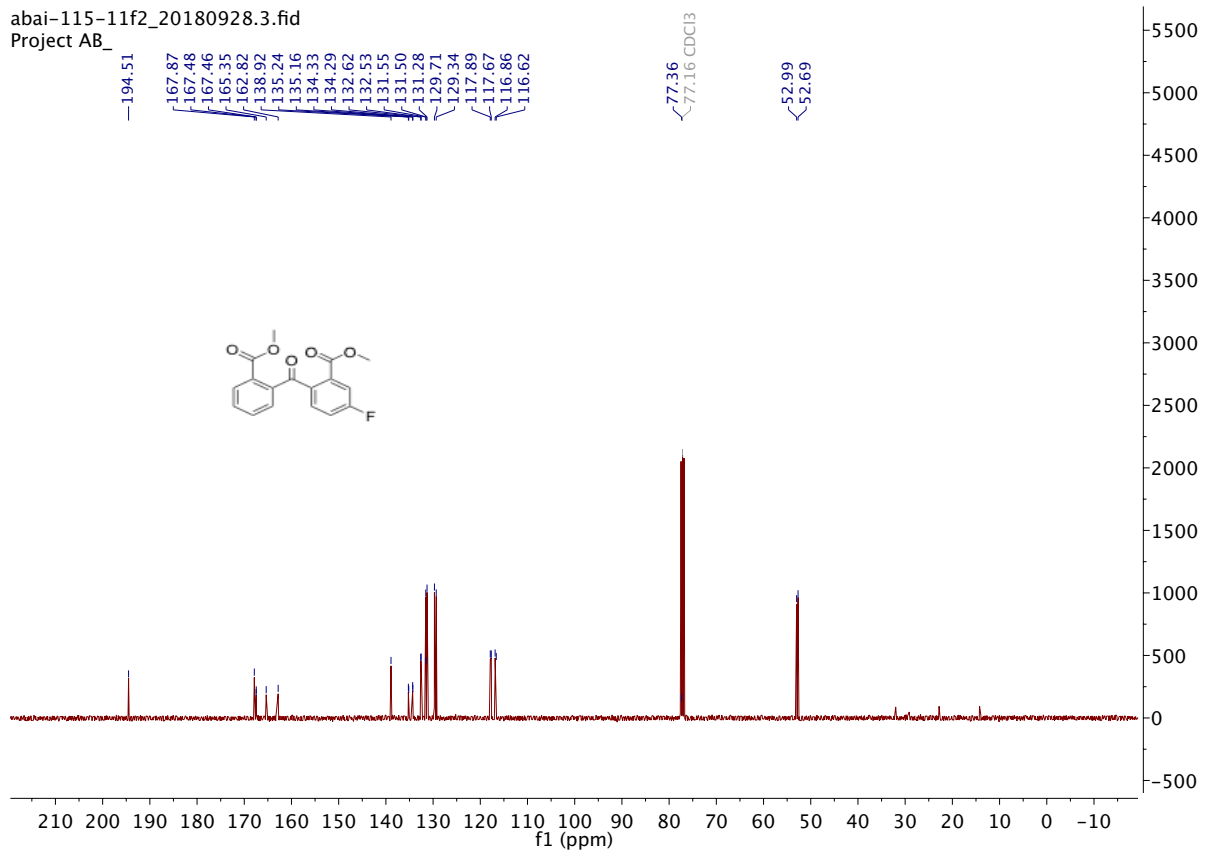
Methyl 5-fluoro-2-(2-(methoxycarbonyl)benzoyl)benzoate **2bh**

abai-115-11f2_20180928.1.fid
 Project AB_

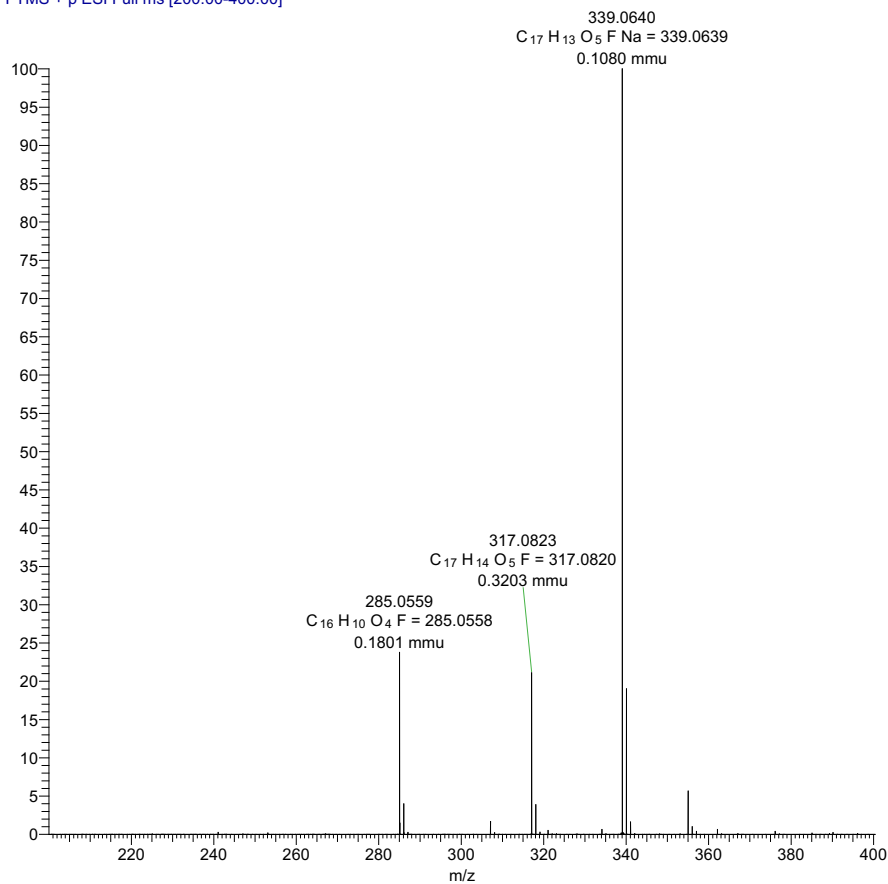


ESI : Carbonylative Suzuki-Miyaura couplings of sterically hindered aryl halides.

abai-115-11f2_20180928.3.fid
Project AB_

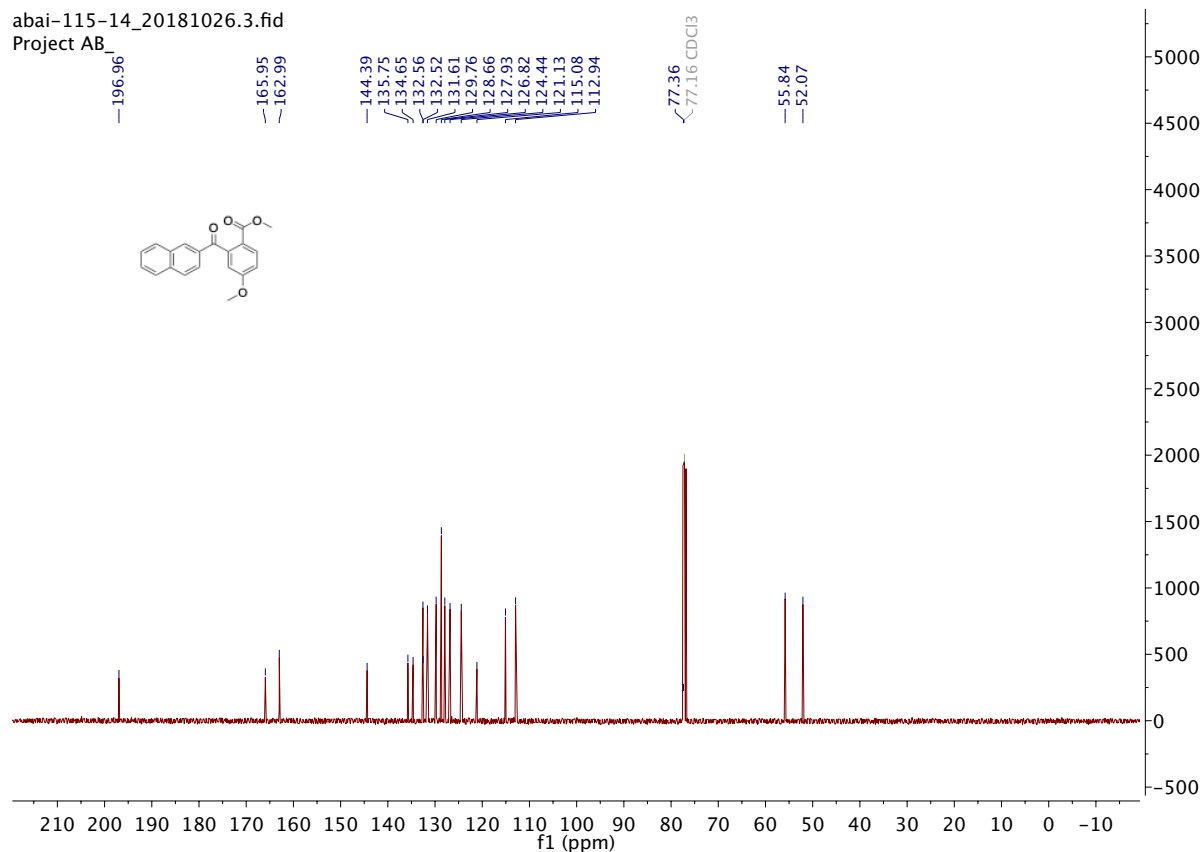
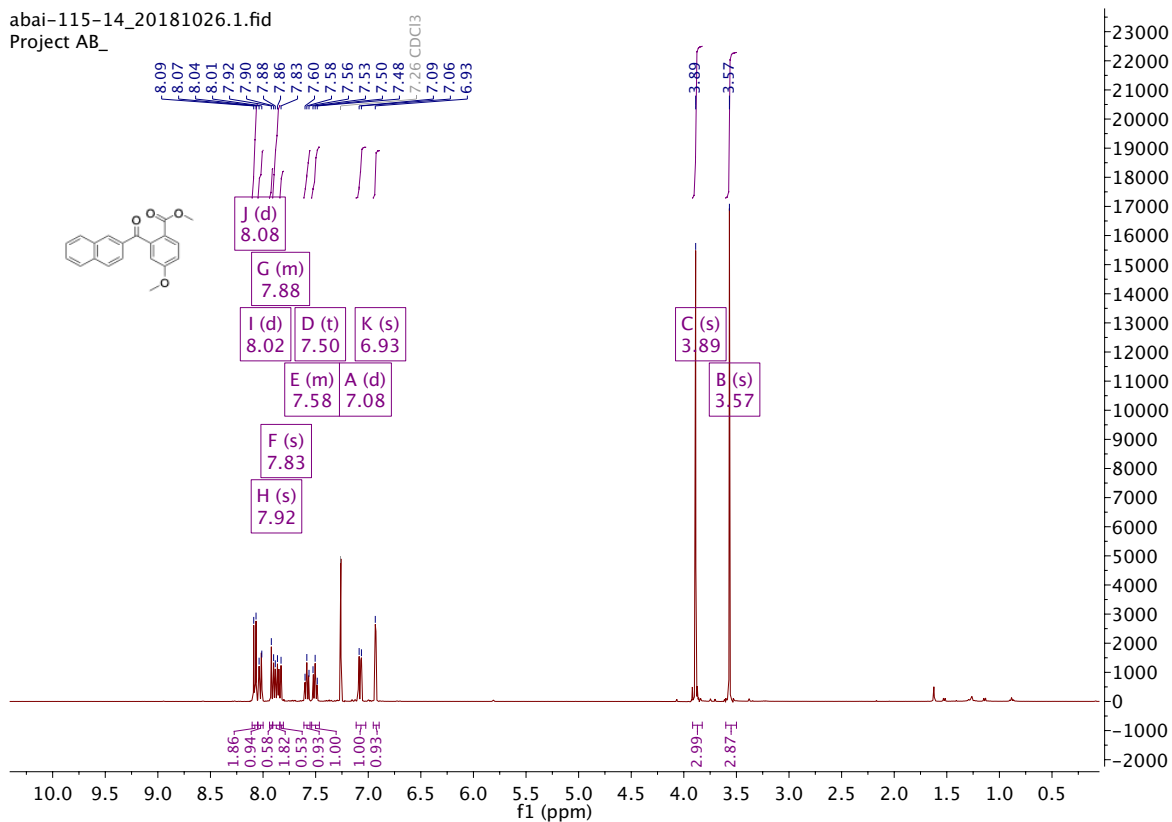


abai-115-11_181005163548 #1-4 RT: 0.02-0.11 AV: 4 NL: 3.76E7
T: FTMS + p ESI Full ms [200.00-400.00]



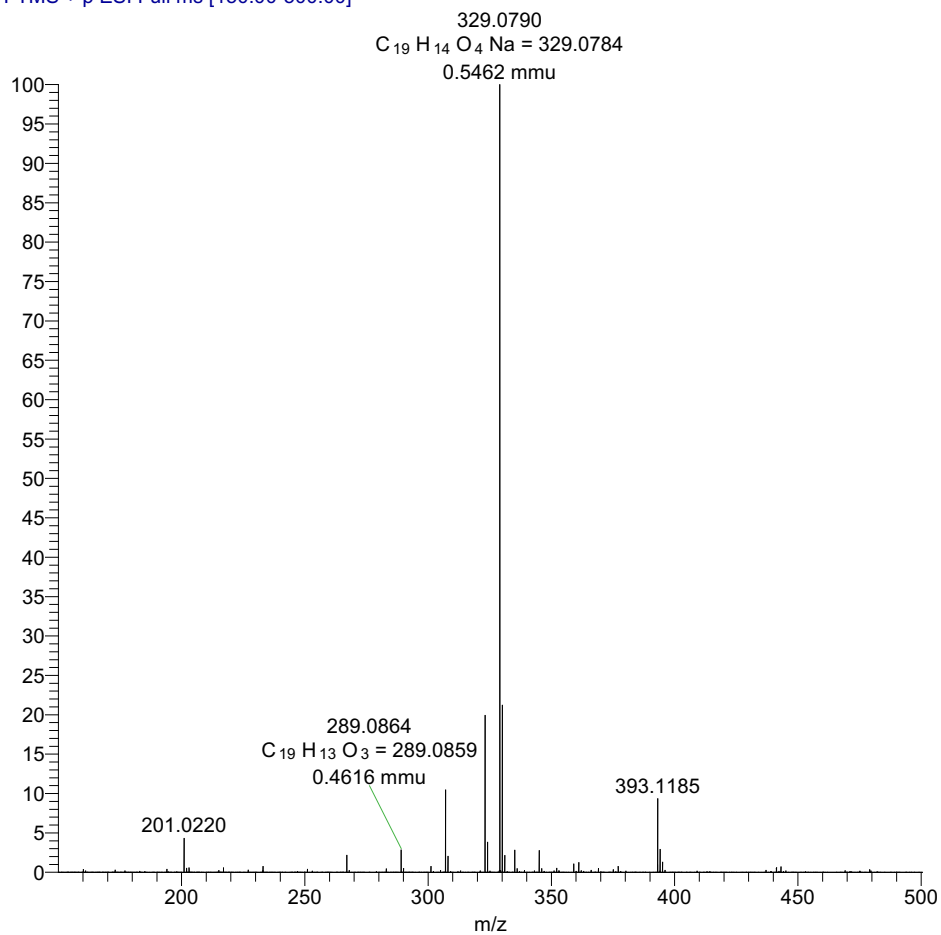
ESI : Carbonylative Suzuki-Miyaura couplings of sterically hindered aryl halides.

Methyl 2-(2-naphthoyl)-4-methoxybenzoate **2hp**



ESI : Carbonylative Suzuki-Miyaura couplings of sterically hindered aryl halides.

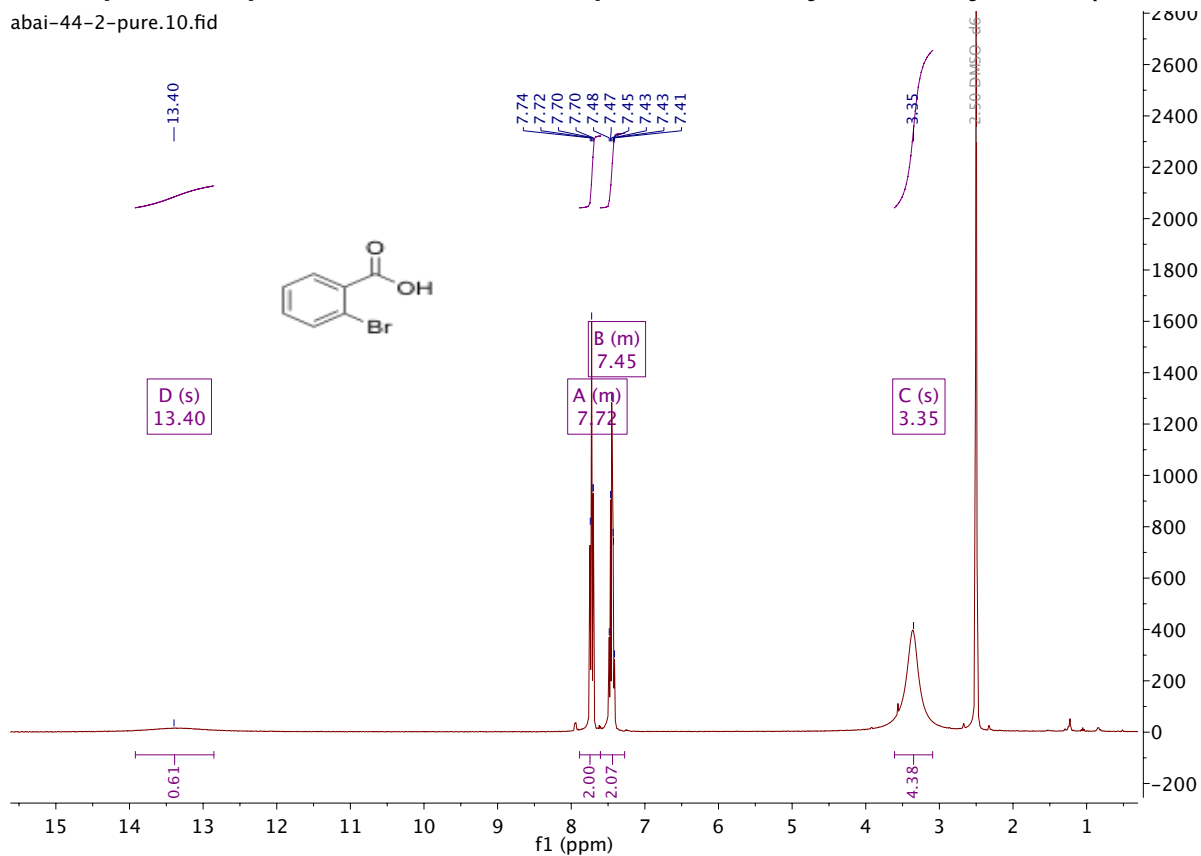
abai-115-4h_190627172410 #1-5 RT: 0.00-0.11 AV: 5 NL: 5
T: FTMS + p ESI Full ms [150.00-500.00]



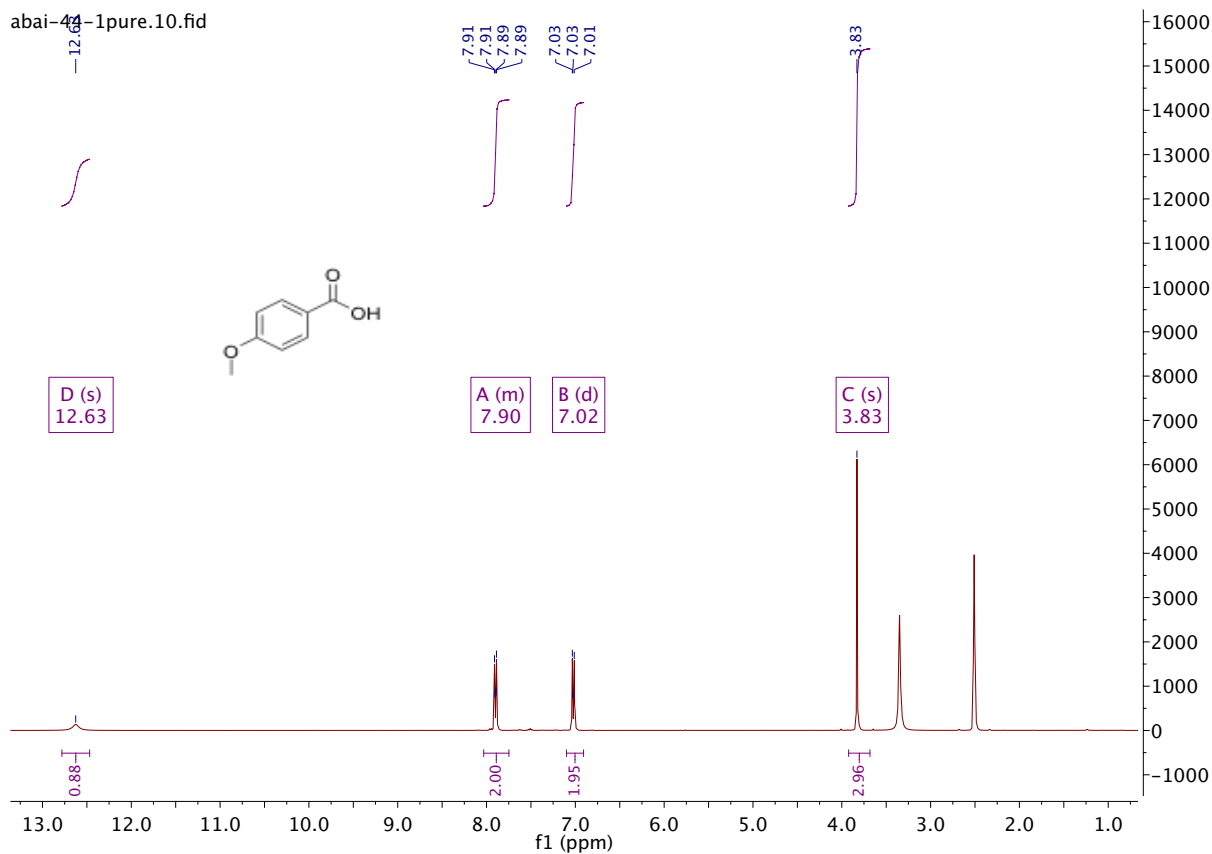
ESI : Carbonylative Suzuki-Miyaura couplings of sterically hindered aryl halides.

4.4 Spectra for products from control experiments for hydrocarbonylations (section 1.4).

abai-44-2-pure.10.fid

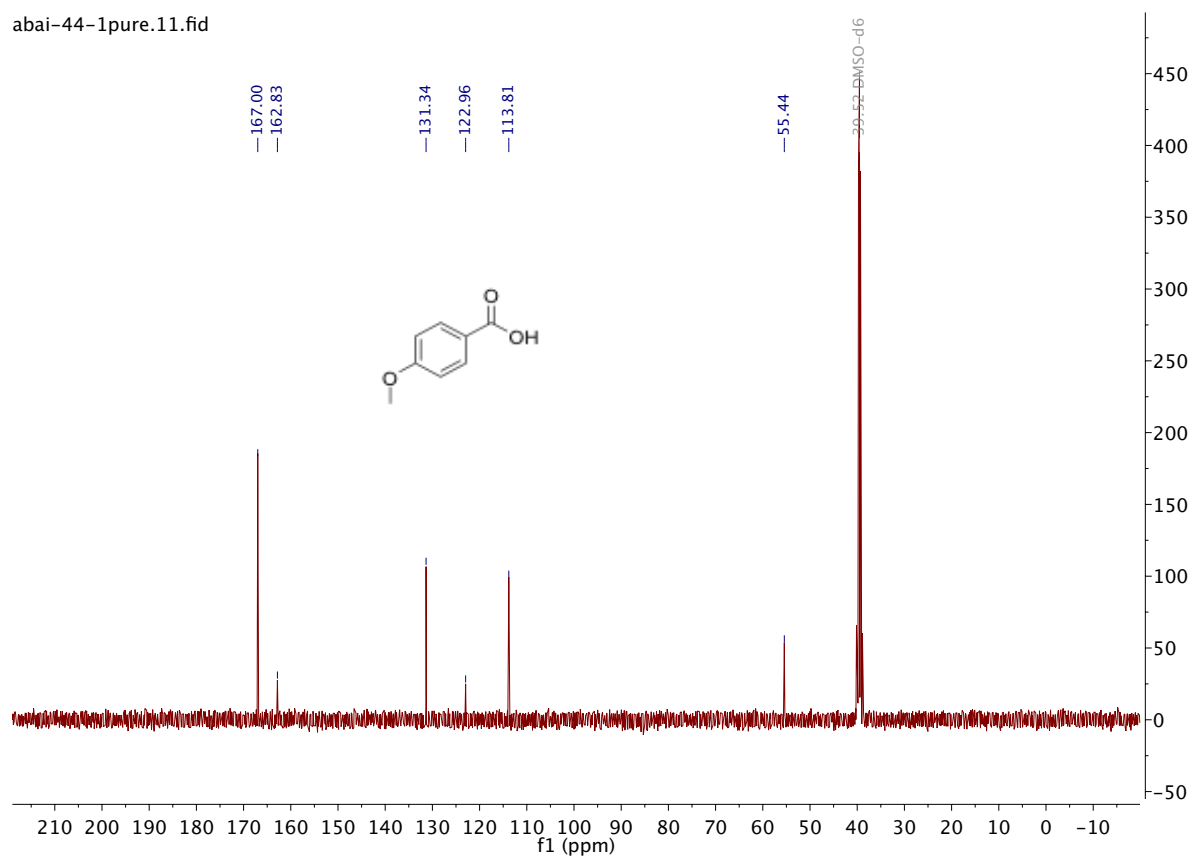


abai-44-1pure.10.fid

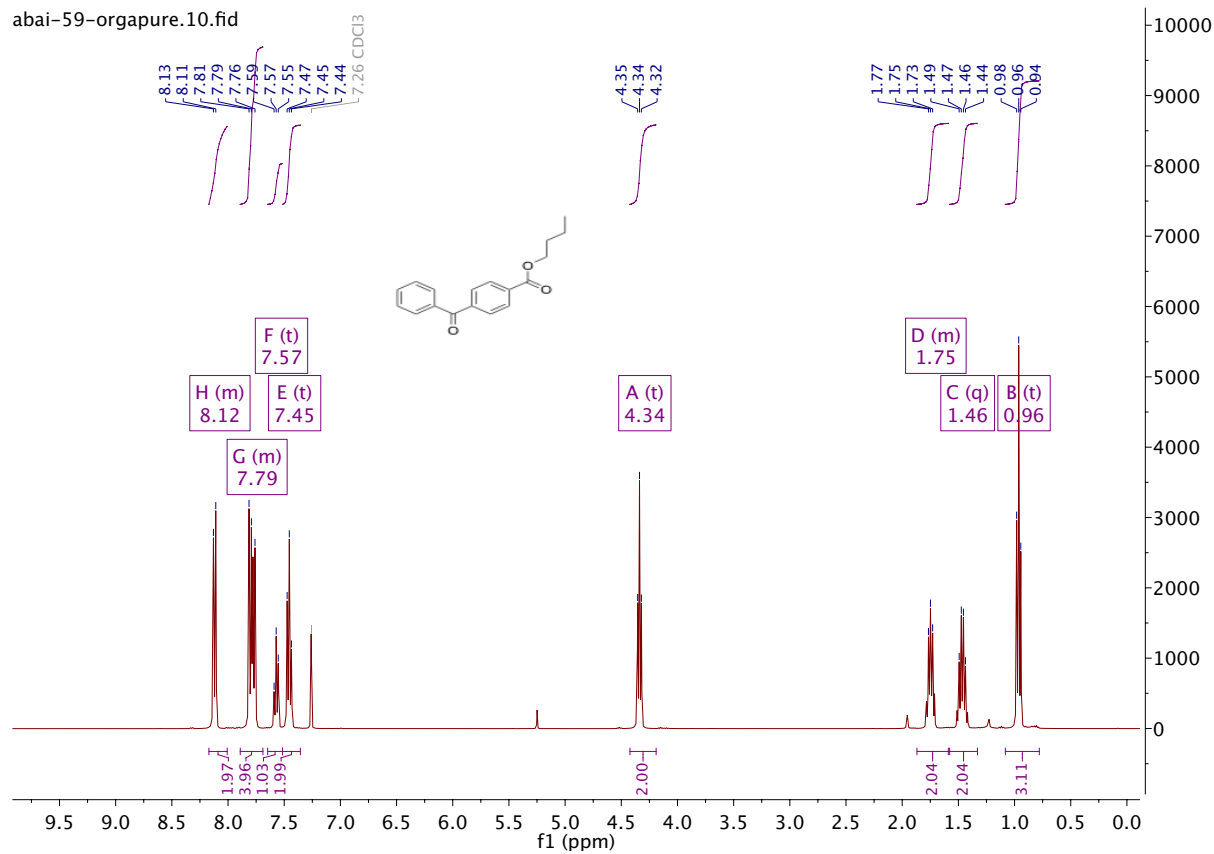


ESI : Carbonylative Suzuki-Miyaura couplings of sterically hindered aryl halides.

abai-44-1pure.11.fid

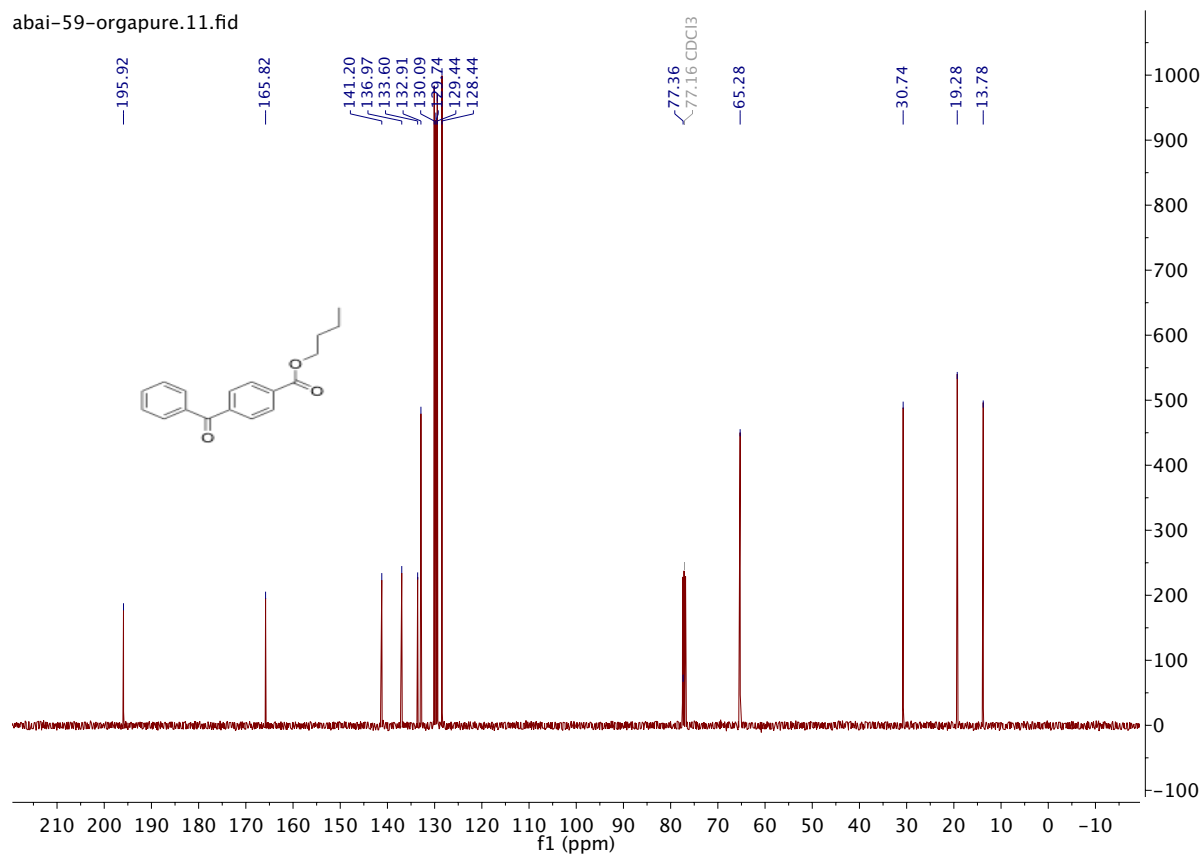


abai-59-orgapure.10.fid



ESI : Carbonylative Suzuki-Miyaura couplings of sterically hindered aryl halides.

abai-59-orgapure.11.fid



Paper III

Renewable Solvents for Pd-Catalyzed Carbonylations

Aya Ismael, Ashot Gevorgyan, Troels Skrydstrup, and Annette Bayer

Manuscript is submitted

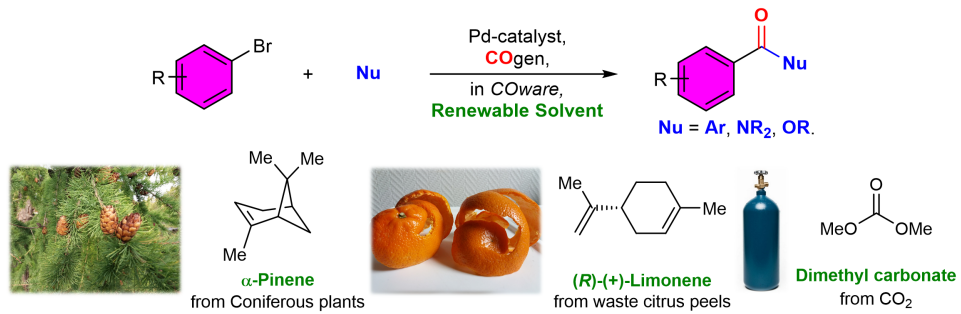
Organic Process Research & Development

Renewable Solvents for Palladium-Catalyzed Carbonylation Reactions

*Aya Ismael,^a Ashot Gevorgyan,^a Troels Skrydstrup,^b and Annette Bayer^{*a}*

a. Department of Chemistry, Faculty of Science and Technology, UiT The Arctic University of Norway, N-9037 Tromsø, Norway; b. Carbon Dioxide Activation Center (CADIAC), Interdisciplinary Nanoscience Center (iNANO) and Department of Chemistry, Aarhus University, Gustav Wieds Vej 14, 8000 Aarhus C, Denmark.

TOC GRAPHIC:



ABSTRACT: Solvents constitute the largest component for many chemical processes and substitution of non-renewable solvents is a long-standing goal for green chemistry. Here we show that Pd-catalyzed carbonylative couplings, such as carbonylative cross couplings, aminocarbonylations and alkoxycarbonylations, can be successfully realized using renewable solvents. The present research covers not only well-established renewable solvents, such as 2-methyltetrahydrofuran, limonene and dimethyl carbonate, but also recently introduced biomass-derived 1,1-diethoxyethane, isosorbide dimethyl ether, eucalyptol, rose oxide, γ -terpinene and α -pinene. The carbonylative coupling of boronic acids and aryl bromides works well in limonene. Aminocarbonylation gave excellent results in dimethyl carbonate, α -pinene and limonene, while alkoxycarbonylation was successful in 2-methyltetrahydrofuran, α -pinene, γ -terpinene and dimethyl carbonate. The developed renewable methodologies can be used for the synthesis of commercial drug Trimetozine and an analogue of Itopride.

KEYWORDS: renewable solvents, carbonylative C-C coupling, aminocarbonylation, alkoxycarbonylation, palladium catalysis, carbon monoxide.

INTRODUCTION

According to the development plan of the United Nations General Assembly "*Transforming Our World: The 2030 Agenda for Sustainable Development*" initiated in 2015, considerable efforts are needed over the coming decade to build a better and more sustainable future.¹ The realization of most of the aspects of "*The 2030 Agenda for Sustainable Development*" can be directly conditioned by sustainable innovations in chemical research.

Today, most of the industrial processes and particularly the pharmaceutical industry are largely based on the application of non-renewable solvents, which usually constitute over 80% of

materials needed for the production of the final ingredients.² As a result, yearly manufacture of non-renewable and hazardous common organic solvents exceeds 20 million metric tons.^{2d} A recent survey on the solvents used in the pharmaceutical industry for the period 1997 - 2012 revealed that the top 10 most frequently used solvents are dichloromethane, hexane, diisopropyl ether, 1,2-dimethoxyethane, 1,4-dioxane, 1,2-dichloroethane, diethyl ether, chloroform, diglyme and chlorobenzene.³ This unsustainable practice can be addressed by the development and popularization of renewable and safe solvent candidates.

Liquids or low melting chemicals available from the valorization of biomass^{4,5} as well as chemicals derived from the reduction of CO₂^{6,7} have enormous potential to replace the common non-renewable solvents utilized in organic synthesis.³ The most frequently used solvents available from biomass are polar protic ethanol, glycerol and its derivatives, and choline chloride-based deep eutectic solvents, polar aprotic 2-methyltetrahydrofuran (2MeTHF), cyrene and γ -valerolactone (GVL), as well as nonpolar limonene and *p*-cymene (Fig. 1).^{4,5} Among CO₂-derived chemicals carbonates and ethers like dimethoxymethane (methylal) have attracted attention as solvents (Fig. 1).^{6,7} Recently, we have shown that biomass-derived solvents such as nonpolar ethers (1,1-diethoxyethane (acetal), dimethyl isosorbide, eucalyptol, rose oxide) and terpenes (γ -terpinene and α -pinene) can be successfully used in Cu-catalyzed carboxylation reactions (Fig. 1).⁵¹

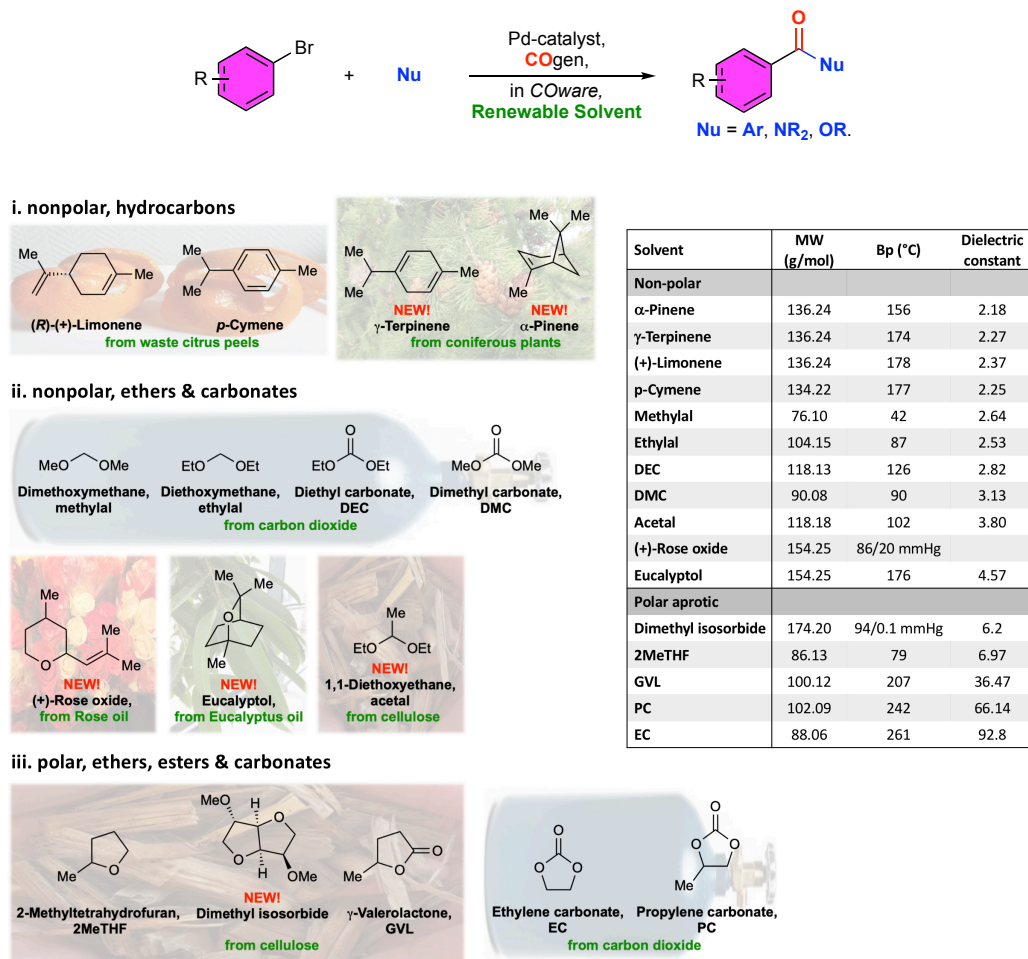


Figure 1. Overview of present work and renewable solvents used in the work (pictures taken by AG).

A complete life cycle assessment (LCA) of the latter solvents is not available, but most of them are significantly less toxic compared to common organic solvents.⁸ Low toxicity is particularly inherent to naturally occurring dimethyl isosorbide, GVL and eucalyptol, ethanol-derived diethoxyethane (acetal), as well as CO₂-derived diethyl carbonate (DEC), dimethyl carbonate (DMC) and methylal. Among others, these solvents are used in large quantities in the pharmaceutical and food industries as additives, antiseptic and flavoring agents.⁹ There is no need to continue increasing the consumption of non-renewable solvents for processes where renewable solvents provide comparable outcome.

Renewable solvents have proven to be suitable for a variety of transformations including classical condensation reactions and transition-metal (TM)-catalyzed cross-couplings.⁴⁻⁶ However, the use of renewable solvents as reaction media for carbonylative couplings with CO remain largely unexplored.^{10,11} The fact that the Pd-catalyzed carbonylations have found numerous applications in modern drug discovery and isotopic labeling of pharmaceuticals^{10d,e,g} makes the development of renewable methodologies for carbonylations a task of great significance. This work describe the use of newly introduced biomass-derived solvents (acetal, dimethyl isosorbide, γ -terpinene, α -pinene, eucalyptol, and rose oxide, Fig. 1), and previously studied renewable solvents (2MeTHF, GVL, limonene, *p*-cymene, DMC, DEC, ethylene carbonate (EC), propylene carbonate (PC), methylal and diethoxymethane (ethylal) Fig. 1) for Pd-catalyzed carbonylations.

RESULTS AND DISCUSSION

A range of renewable solvents were studied for carbonylative couplings of aryl bromides with arylboronic acids,¹² amines (aminocarbonylation)¹³ and alcohols (alkoxycarbonylation) (Fig. 1).¹⁴ We decided to focus on Pd-based catalytic systems that have proven to be versatile catalysts for carbonylative couplings.^{11k,12-14} For safety reasons the reactions were conducted in two chamber reactors (COware) developed in the group of Skrydstrup, using stoichiometric quantities of CO generated *ex situ* from COgen (9-methyl-9*H*-fluorene-9-carbonyl chloride).^{10e} The solvent's polarity was approximated as nonpolar and polar based on their dielectric constant; a solvent was classified as polar if the dielectric constant was over 5 (Fig. 1, Table S1).

Carbonylative C-C couplings of aryl bromides and arylboronic acids

As a starting point, we analyzed the carbonylative coupling of 3-bromoanisole with *m*-tolylboronic acid (Chart 1). We focused on the catalytic system based on Pd(acac)₂ as catalyst precursor, and di(1-adamantyl)-*n*-butylphosphine hydroiodide (cataCXium AHI) as ligand,

originally developed in the group of Skrydstrup.^{12g} The original protocol relied on cyclic diethanolamine esters of boronic acids (DABO boronates) or aryl trihydroxyborates as successful starting materials and used toluene/H₂O (10:1) or toluene as solvent.^{12g} We initiated our work by developing a simplified protocol where the aryl trihydroxyborates was generated *in situ* from simple boronic acids by addition of 1M aqueous NaOH, thus preventing the external, up-front preparation of the organoboronate (see ESI, Table S1, entry 3).

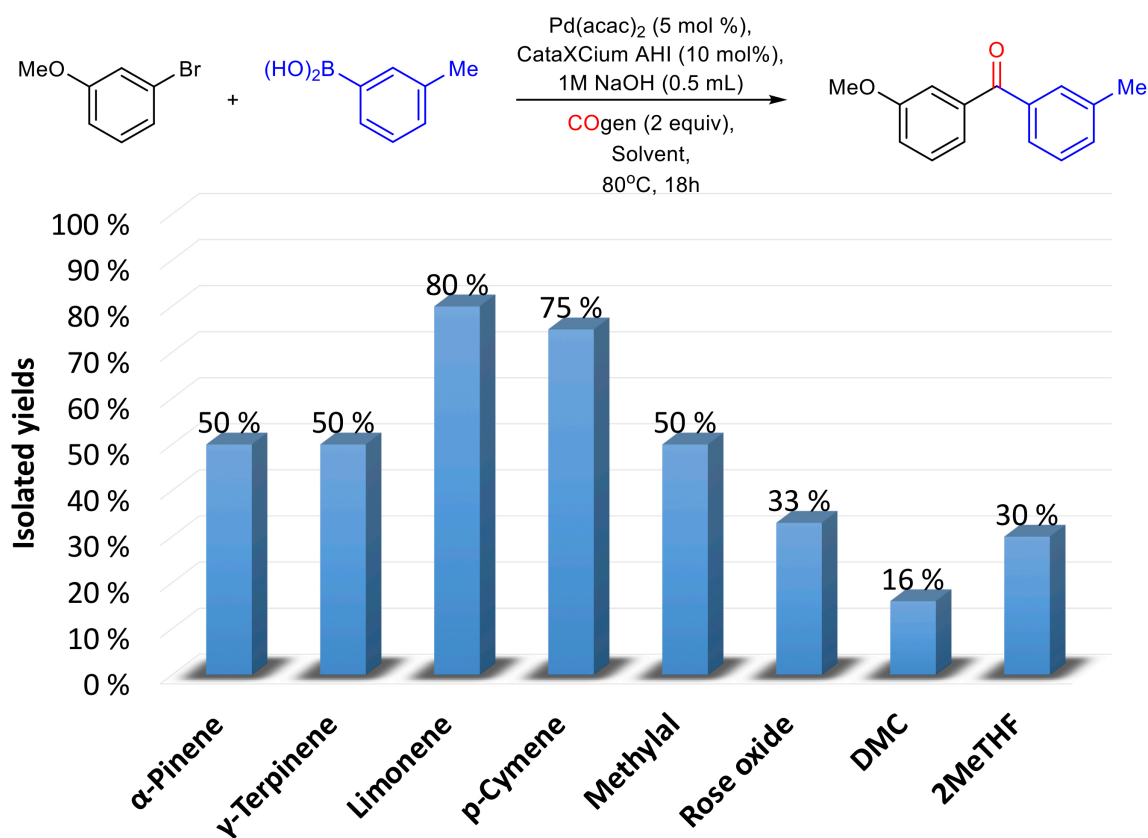
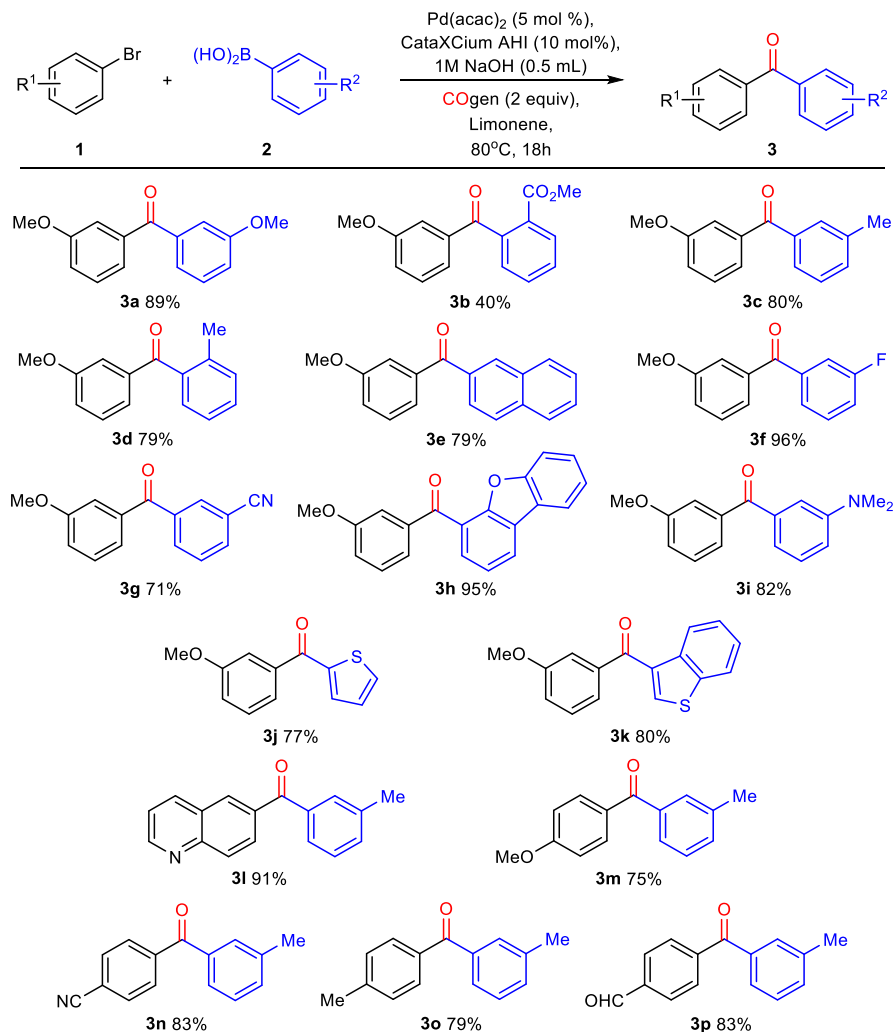


Chart 1. Screening of renewable solvents for carbonylative coupling of *m*-tolylboronic acid and 3-bromoanisole.

Using the modified protocol, we investigated the efficiency of various renewable solvents in the Pd-catalyzed carbonylative coupling of *m*-tolylboronic acid and 3-bromoanisole (Chart 1, see also Table S1 for a correlation of solvent polarity and yields). It has to be noted that the final reaction

media contained approx. 15% (v/v) of water in all cases due to the addition of aqueous NaOH. Our studies revealed that nonpolar ethers and carbonates (rose oxide, methylal, DMC) and polar ether 2MeTHF provide the carbonylation product in low to moderate yields (16-50%). In contrast, biomass-derived nonpolar hydrocarbons (limonene, *p*-cymene, γ -terpinene, α -pinene) gave consistently better yields with *p*-cymene and limonene being the best solvents (75% and 80% isolated yield, respectively); an observation that correlates well with the use of toluene or toluene/water as solvent in previous studies providing the corresponding product in 90% yield.^{12g} Despite the fact that limonene possesses a terminal and an internal double bond, the Heck-type arylation of the solvent was not observed under the reaction conditions. Neither were related side products noted for reactions in rose oxide, γ -terpinene and α -pinene.

We proceeded to analyze the generality of the Pd-catalyzed carbonylative couplings in limonene as solvent (Scheme 1). Examination of a variety of aromatic boronic acids and aryl bromides indicated a good substrate scope. The yields varied from 71-95% for electron-rich (**3a**, **3c**, **3d**, **3e**, **3h**, **3i**), electron-deficient aryl (**3f**, **3g**) and heterocyclic boronic acids (**3j**, **3k**). The broad applicability of boronic acids is particularly interesting as the use of *in situ* generated aryl trihydroxyborates extended the substrate scope beyond the limitations associated with isolation of unstable trihydroxyborate salts.^{12g} Similarly, both electron-rich (**3m**, 75%; **3o**, 79%) and electron-deficient (**3n**, 83%; **3p**, 83%) aryl bromides as well as heteroaryl bromides (**3l**, 91%) were successful in the carbonylative couplings. We observed a low yield only for 2-methoxycarbonylphenylboronic acid (**3b**, 40%), which may be due to steric hindrance or side reactions such as hydrolysis of the ester. Overall, the observed yields were at the same level as previously reported protocols using toluene as solvent,^{12e,g} indicating that limonene is a renewable alternative for carbonylative couplings of boronic acids and aryl bromides.



Scheme 1. Scope of carbonylative coupling of boronic acids and aryl bromides using the sustainable solvent limonene.

Aminocarbonylation of aryl bromides

Next, we examined the Pd-catalyzed aminocarbonylation reaction of aryl bromides. Here, we focused on the catalytic system developed in the group of Buchwald using $\text{Pd}(\text{OAc})_2$ as Pd source, 4,5-bis(diphenylphosphino)-9,9-dimethylxanthene as ligand (XantPhos) and toluene as solvent.^{14c} The Pd-catalyst was tested in renewable solvents on the model reaction of *N*-methylaniline with 4-bromobenzonitrile (Chart 2).

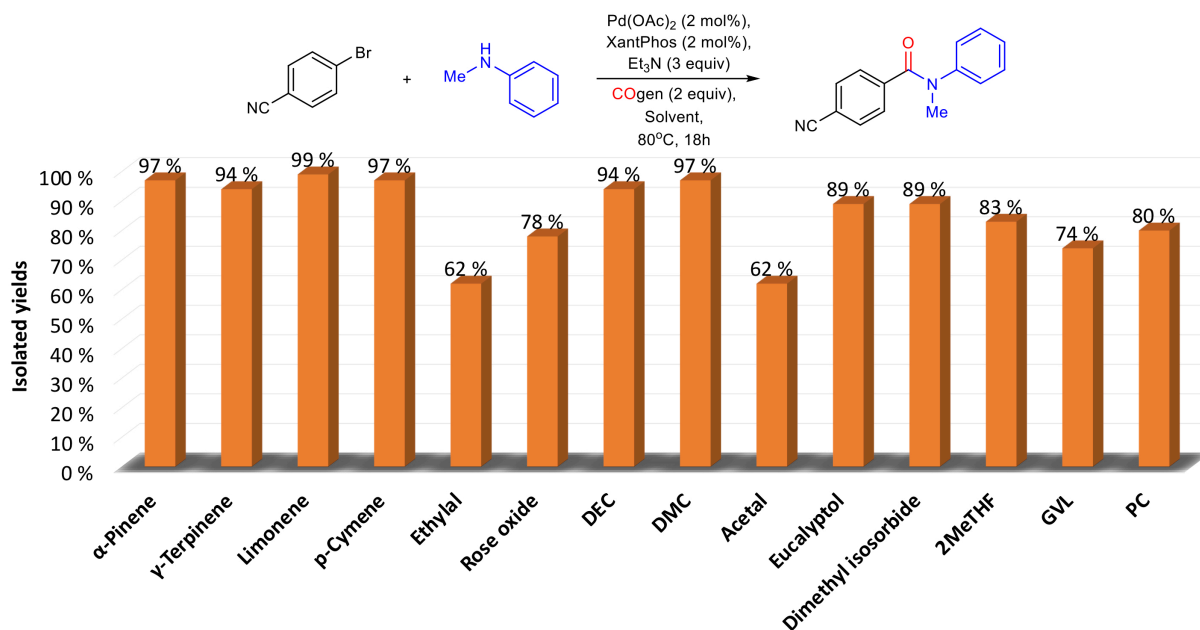
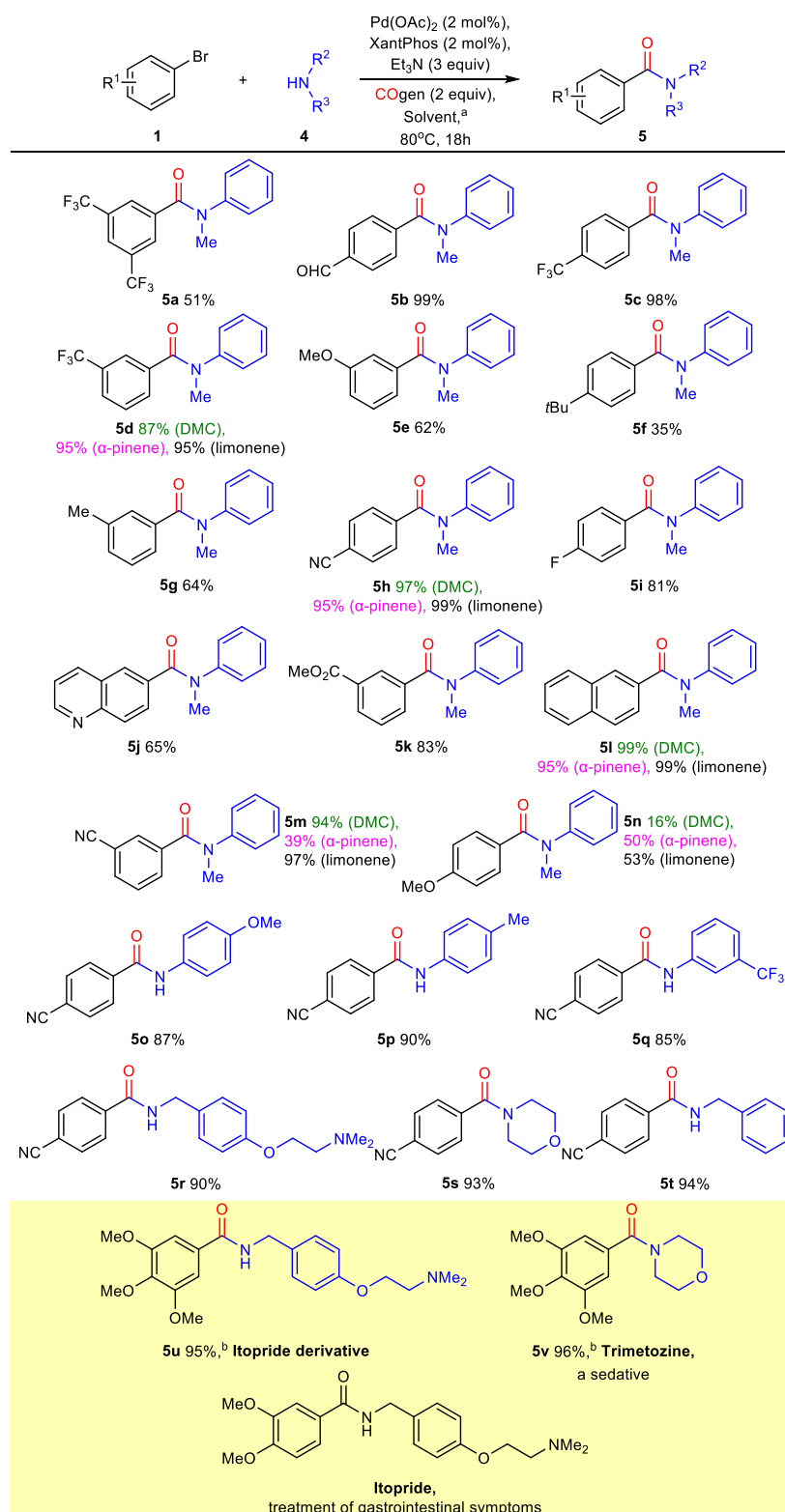


Chart 2. Screening of renewable solvents for aminocarbonylation with resulting isolated yields.

Our studies demonstrated that for this aminocarbonylation exceptional results can be obtained in most of the renewable solvents (Chart 2). As a general trend, all reactions in nonpolar hydrocarbons provided excellent yield (limonene, 99%; *p*-cymene, 97%; γ -terpinene, 94%; α -pinene; 97%); in good correlation with previous work being performed in toluene as solvent providing the product in 97% yield.^{14c} Excellent yields were also obtained in nonpolar carbonates (DMC, 97%; DEC, 94%). Other solvents like polar carbonate PC and lactone GVL, and nonpolar and polar ethers (ethylal, acetal, rose oxide, eucalyptol, dimethyl isosorbide, 2MeTHF) were less efficient with yields ranging between 62-89%.

Noteworthy, under the conditions used for aminocarbonylation we did not observe side reactions like hydroamination or Mizoroki-Heck coupling for solvents possessing double bonds.

As several renewable solvents provided good yields, we screened the top three best solvents (DMC, α -pinene, limonene) for several aminocarbonylations (Scheme 2). These studies revealed that except for the products **5m** and **5n**, the best solvents DMC, α -pinene and limonene gave



Scheme 2. Scope of aminocarbonylation of aryl bromides. ^a Unless otherwise mentioned, the reaction was performed in DMC. ^b XantPhos Pd G3 was used instead of Pd(OAc)₂/XantPhos.

comparable results for several aminocarbonylations (**5d**, **5h**, **5l**). For the product **5m**, α -pinene (39%) turned out far less effective than other solvents, while for the product **5n**, DMC provided low yield (16%) (Scheme 2). For an extended analysis of the substrate scope, we therefore decided to focus on the use of DMC, as it is considerably less toxic and less expensive than the two other solvents.¹⁵

Reactions with variously substituted aryl bromides illustrated that many functional groups (CHO, CN, CO₂Me) were well tolerated. In general, aryl bromides with electron-withdrawing substituents provided corresponding aminocarbonylation products in good to quantitative yields (**5b**, 99%; **5c**, 98%; **5d**, 87%; **5h**, 97%; **5i**, 81%; **5k**, 83%; **5m** 94%), except for **5a** (51% yield). Electron-rich aryl bromides were less effective producing the corresponding amides from low to acceptable yields (**5e**, 62%; **5f**, 35%; **5g**, 64%; **5n**, 16%). However, the aminocarbonylation of electron-rich 3,4,5-trimethoxyphenyl bromide, using XantPhos Pd G3 as catalyst, provided the commercial drug Trimetozine (**5v**, 96% yield, a sedative) and an analogue of Itopride (**5u**, 95% yield, Itopride is used for treatment of gastrointestinal symptoms) in excellent yields.^{13b} The reaction worked well also with fused systems like naphthalene (**5l**, 99%) and heterocycles (**5j**, 65%) (Scheme 2). Changes in the amine structure were tolerated well and both anilines with electron-donating and -withdrawing substituents, and primary and secondary aliphatic amines were successfully coupled with 4-bromobenzonitrile and CO (Scheme 2, **5o**, 87%; **5p**, 90%; **5q**, 85%; **5r**, 90%; **5s**, 93%; **5t**, 94%). Overall, the observed trends were in agreement with reports of aminocarbonylations performed in non-renewable solvents.^{13,14c} The good yields and substrate scope indicate that renewable solvents like DMC, α -pinene and limonene can effectively replace 1,4-dioxane, toluene and THF frequently used in Pd-catalyzed aminocarbonylation reactions.^{10b,13,14c}

Alkoxy carbonylation of aryl bromides

Finally, we analyzed the potential adaptation of renewable solvents for Pd-catalyzed alkoxy carbonylation.¹⁴ For the initial studies, we examined the alkoxy carbonylation of 2-bromonaphthalene with sodium *tert*-butoxide and CO using the catalytic system based on Pd(dba)₂ as catalyst precursor and 1,1'-bis(diisopropylphosphino)ferrocene (dippf) as ligand first reported by Skrydstrup and coworkers for alkoxy carbonylations in THF (Chart 3).^{14f} The screening of renewable solvents showed that excellent results can be achieved also for the Pd-catalyzed alkoxy carbonylations (Chart 3).

Not surprisingly, the polar ether 2MeTHF (91% yield) was among the best solvents, as previous studies were performed in THF (88% yield).^{14f} Interestingly, excellent yields of 93% were also obtained in some nonpolar hydrocarbons (γ -terpinene, α -pinene), while other nonpolar hydrocarbons (limonene, 56%), ethers (methylal, 45%; ethylal, 64%; acetal, 55%; rose oxide, 36%; eucalyptol, 82%), and carbonates (DEC, 45%) provided low to moderate yields. In nonpolar carbonate DMC, instead of *tert*-butoxycarbonylation, the product of methoxycarbonylation was isolated in 93% yield (Chart 3, Scheme 4). This was the only observation where the solvent was chemically transformed in the reaction. Similar transesterifications were not observed for the other carbonates (DEC, PC, EC). Polar solvents (dimethyl isosorbide, 30%; GVL, 64%; PC, 60%; EC, 30% yield) were less efficient.

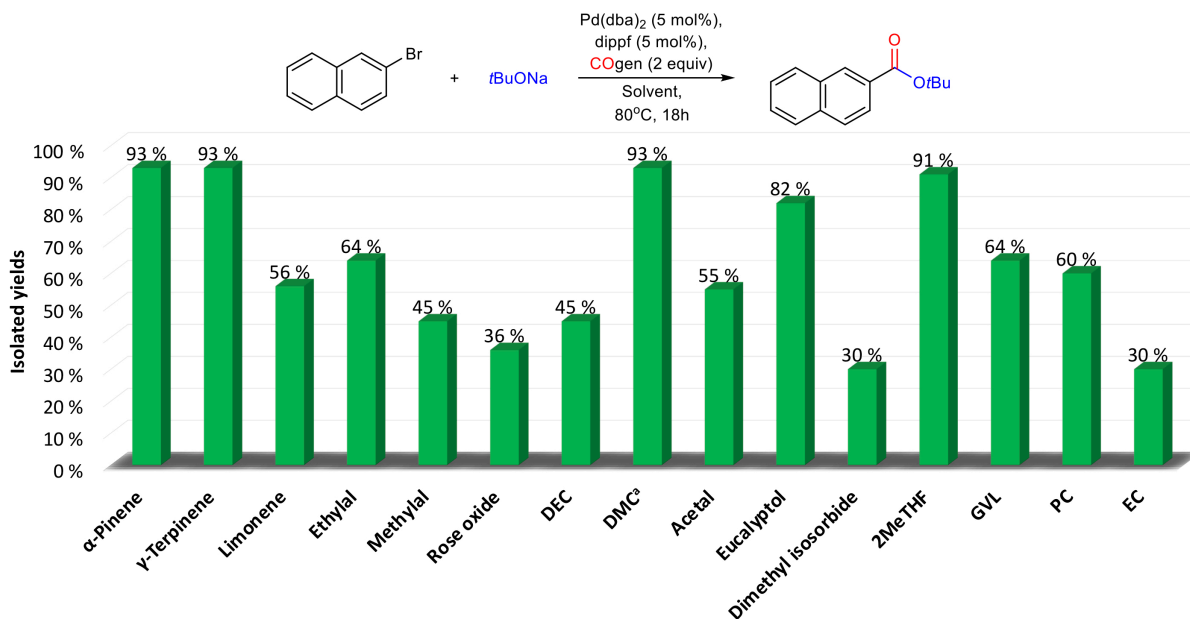
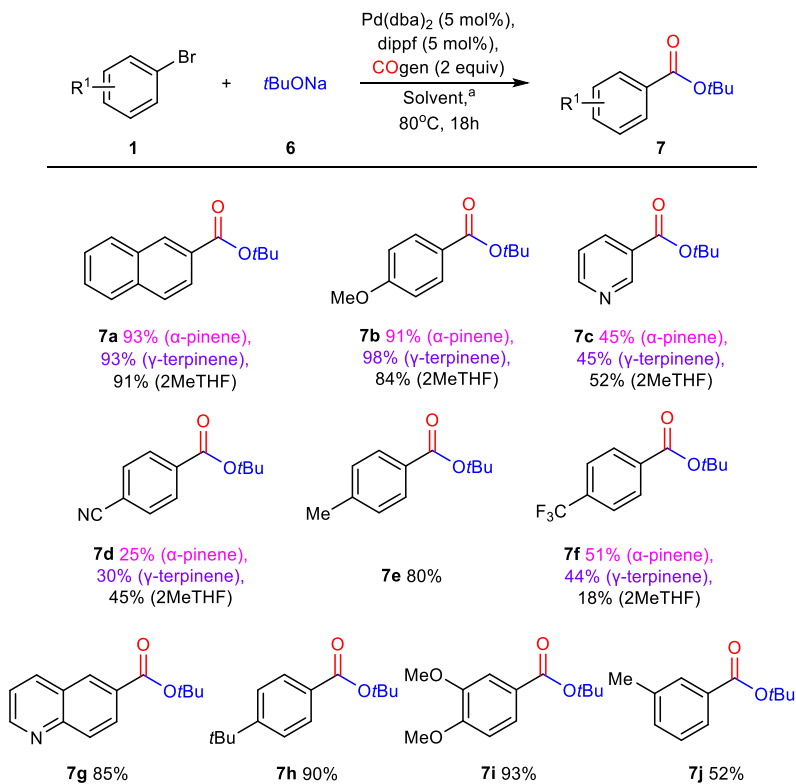


Chart 3. Screening of renewable solvents for alkoxy-carbonylation with resulting isolated yields.

^a In DMC, methoxycarbonylation was observed.

As for aminocarbonylation, we screened the top three best solvents (2MeTHF, α -pinene and γ -terpinene) for alkoxy-carbonylations of several substrates (Chart 3, Scheme 3). These studies revealed that the choice of solvent is dependent on the substrate. 2MeTHF was the best solvent for the products **7c** (52%) and **7d** (45%). The best yields of **7b** were seen in γ -terpinene (98%), whereas γ -terpinene was not a good reaction media for the product **7f** (44%). α -Pinene appeared to be the best solvent for the products **7a** (93%) and **7f** (51%) and in general showed good performance for most of the substrates.



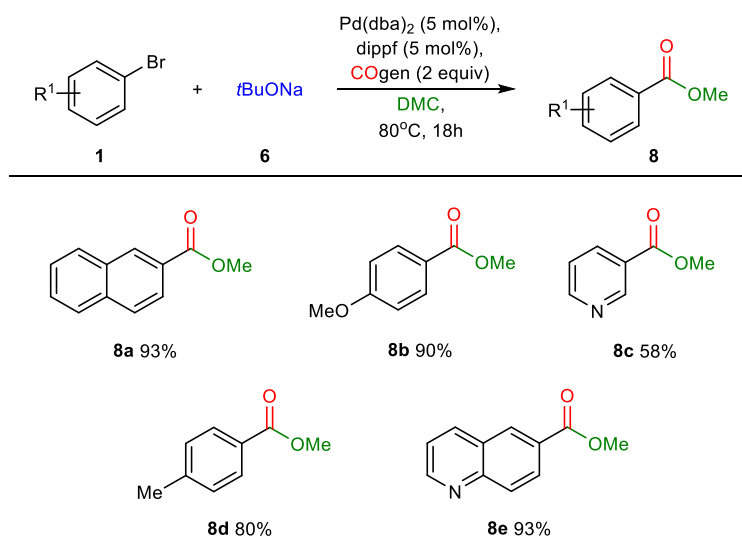
Scheme 3. Scope of *tert*-butoxycarbonylation of aryl bromides. ^a Unless otherwise mentioned, the reaction was performed in α -pinene.

The following investigation of the scope of *tert*-butoxycarbonylation in α -pinene as solvent showed that both electron-rich and -deficient aryl bromides can be effectively transformed into the corresponding products in moderate to good yields (Scheme 3). The best yields were observed for *tert*-butoxycarbonylation of electron-rich aryl bromides (**7a**, 93%; **7b**, 91%; **7e**, 80%; **7g**, 85%; **7h**, 90%; **7i**, 93%). It should be noted that aryl bromides possessing electron-withdrawing groups and electron-deficient 3-bromopyridine were less effective and gave products in moderate yields (**7c**, 45%; **7d**, 25%; **7f**, 51%). Similar observations were reported by Skrydstrup et al. for alkoxycarbonylations performed in THF.^{14f} Overall, our studies indicate that for alkoxycarbonylations renewable solvent perform on the same level, and in some cases even better, than previously reported non-renewable solvents.^{10,14} Renewable solvents such as 2MeTHF,

DMC, α -pinene and γ -terpinene can be useful alternatives for trimethylamine, hexafluoroisopropanol, THF, toluene and dimethyl sulfoxide frequently used for alkoxy carbonylation reactions.¹⁴

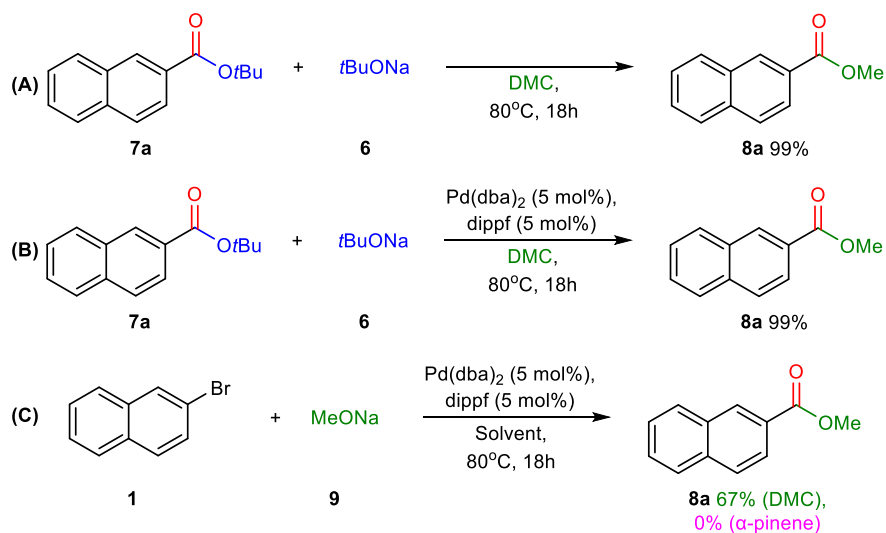
Studies on the alkoxy carbonylation in DMC.

In general, alkoxy carbonylation reactions rely on the use of bulky alcohols, phenols or corresponding alkoxides.¹⁴ Alcohols possessing α -hydrogens have found limited applications due to the side processes associated with β -hydride elimination.^{14b,d} Therefore, we had a closer look at the methoxy carbonylations observed in DMC. The scope of the reaction was briefly studied on a range of substituted aryl bromides (Scheme 4). The reaction gave good yields for electron-rich 4-bromoanisole (**8b** 90%) and 4-bromotoluene (**8d**, 80%), as well as for 2-bromonaphthalene (**8a**, 93%) and 6-bromoquinoline (**8e**, 93%). Moderate yields were observed for electron-deficient aryl bromides (**8c**, 58%). For most of the products in Scheme 4, traces of *tert*-butoxy carbonylation were seen along with the main methoxy carbonylation product.



Scheme 4. Scope of methoxy carbonylation of aryl bromides.

To gain a better understanding of the mechanism of the observed methoxycarbonylation, we performed a set of control experiments (Scheme 5). The *tert*-butyl ester **7a** was transformed into corresponding methyl ester **8a** in quantitative yield when treated with NaOtBu in DMC. The transesterification took place in presence and absence of the Pd-catalyst (Scheme 5, A, B). In addition, the Pd-catalyzed methoxycarbonylation of 2-bromonaphthalene with sodium methoxide in DMC provided the methoxycarbonylated product in 67% yield, while an equivalent experiment in α -pinene did not lead to methoxycarbonylation (Scheme 5, C). These findings indicate that two different reaction pathways may contribute to the formation of methoxycarbonylated products: (i) the Pd-catalyzed alkoxycarbonylation with *tert*-butoxide followed by a transesterification with sodium methoxide generated *in situ* from the reaction of excess sodium *tert*-butoxide with DMC; and (ii) the Pd-catalyzed methoxycarbonylation with *in-situ* generated sodium methoxide.



Scheme 5. Control experiments to elucidate the formation of methoxycarbonylated products.

CONCLUSIONS

We have shown that Pd-catalyzed carbonylative transformations can be conducted in biomass- and CO₂-derived solvents with exceptionally high efficiency. A vast array of renewable solvents was

analyzed for this purpose, including both well-established (2MeTHF, GVL, limonene, *p*-cymene, DMC, DEC, PC, EC) and recently introduced solvent candidates (acetal, dimethyl isosorbide, γ -terpinene, α -pinene, eucalyptol, rose oxide, methylal and ethylal). The work covered Pd-catalyzed carbonylative coupling of boronic acids and aryl bromides, aminocarbonylation and alkoxy carbonylation. For each of these transformations we have found several renewable solvents, which can successfully substitute traditional non-renewable solvents. For carbonylative coupling of boronic acids and aryl bromides the best results were observed in limonene and *p*-cymene. Aminocarbonylation worked well in DMC, α -pinene and limonene, whereas the best solvents for alkoxy carbonylation turned out to be 2MeTHF, α -pinene, γ -terpinene and DMC. Most of the known methodologies on alkoxy carbonylation are limited to bulky alkoxides and alcohols. We could show that this drawback can be overcome by the use of DMC, which lead to methoxycarbonylated products. Finally, yet importantly, aminocarbonylation in renewable solvents can be used for the production of commercial drug Trimetozine and an analogue of Itopride.

EXPERIMENTAL METHODS

General considerations.

Solvents used in the work are purchased from Sigma Aldrich if not otherwise stated. 2MeTHF (anhydrous, $\geq 99\%$, inhibitor-free, 673277-1L), methylal (absolute, over molecular sieve, $\geq 99.0\%$, 47676-250ML), ethylal (absolute, over molecular sieve, $\geq 99.0\%$, 47675-500ML-F), DMC (anhydrous, $\geq 99\%$, 517127-1L), DEC (anhydrous, $\geq 99\%$, 517135-1L), PC (anhydrous, 99.7%, 310328-1L) and EC (anhydrous, 99%, 676802-1L) were bought as anhydrous solvents equipped with a septa. Other renewable solvents were reagent grade; they were degassed, kept over activated molecular sieves (4 Å) at least a week before use and stored under Ar atmosphere. The purity of

the solvents used in the work were as follows: acetal (99%, inhibitor-free, A902-500ML); dimethyl isosorbide (98%, inhibitor-free, 247898-100G); GVL (99%, V403-500G); γ -terpinene (97%, 223190-100ML); α -pinene (98%, 147524-250ML); limonene (97%, 183164-100ML); *p*-cymene (99%, C121452-1L); eucalyptol (99%, inhibitor-free, C80601-500ML); rose oxide (97%, inhibitor-free, TCI, M2363-25G).

2MeTHF, acetal, dimethyl isosorbide, eucalyptol, rose oxide, methylal and ethylal are ethers and may form peroxides when stored under air. However, peroxide tests (test strips for peroxide, MQuant[®], Supelco[®], VWR/Merck 1.10081.0001) of freshly bought solvents did not show any noticeable levels of peroxides. Acetal, methylal and ethylal can be hydrolyzed in the presence of strong acids when heated. Under basic conditions, which are frequently used for the reactions involving organometallics, acetal, methylal and ethylal are stable. GVL, DMC, DEC, PC and EC can be hydrolyzed in the presence of strongly basic water solutions; under anhydrous conditions, they are stable. γ -Terpinene, limonene and eucalyptol can be converted to *p*-cymene when heated above 220°C.^{4b} Overall, the examined renewable solvents appeared to be stable under the conditions used in this work. We have not observed the formation of side-products e.g. originating from hydrolysis of the carbonate, ethers and esters used as solvents in this work (an exception was alkoxycarbonylation in DMC). It should be noted that the oxidation products of terpenes can be allergens.⁹

The reactions were performed in the previously reported two-chamber system (COware with total volume 20 mL, ESI Fig. S1) under an argon atmosphere, and a glovebox was employed for weighing out the reagents.

Warning! Most of the reactions were performed in specialized glassware under pressure. The glassware should always be examined for damages before any manipulation. All laboratory safety

procedures must be followed strictly and the work with pressure tubes must be conducted behind a shield.

General procedure for Pd-catalyzed carbonylative coupling of boronic acids and aryl bromides (Scheme 1).

Chamber A was sequentially charged with aryl bromide (50 mg, 1.0 equiv), boronic acid (1.2 equiv), Pd(acac)₂ (5 mol%), cataCXium AHI (10 mol%), 1M NaOH (500 μl) and dry solvent (3 mL). The reaction mixtures consisted of an organic and an aqueous layer. Precipitation of palladium was not observed.

Chamber B was sequentially charged with COgen (2 equiv), Pd(dba)₂ (5 mol%), tri-*tert*-butylphosphonium tetrafluoroborate (TTBP•HBF₄) (5 mol%), DIPEA (3 equiv) and 1,4-dioxane (3 mL). The two-chamber system was closed tightly with suitable caps and **Chamber B** was stirred at 80 °C until the release of CO was stopped. This was followed by stirring of both chambers at 80 °C for 18 hours. The resulting mixture of **Chamber A** was filtered through celite and concentrated using a rotary evaporator. The crude was purified by column chromatography with heptane: EtOAc (9:1) eluent.

General procedure for Pd-catalyzed aminocarbonylation (Scheme 2).

Chamber A was sequentially charged with aryl bromide (50 mg, 1.0 equiv), corresponding amine (1.5 equiv), Pd(OAc)₂ (2 mol%), XantPhos (2 mol%), triethylamine (3 equiv) and dry solvent (3 mL). At the onset of the reaction, the mixture was homogeneous, while precipitation of palladium species (Pd-black) was observed during the course of the reaction both in conventional and renewable solvents.

Chamber B was sequentially charged with COgen (2 equiv), Pd(dba)₂ (5 mol%), tri-*tert*-butylphosphonium tetrafluoroborate (TTBP•HBF₄) (5 mol%), 1,4-dioxane (3 mL) and DIPEA (3

equiv). Addition of DIPEA initialize the release of CO. The two-chamber system was closed tightly with suitable caps and stirred at 80 °C for 18 hours. The resulting mixture of **Chamber A** was filtered through celite and concentrated using a rotary evaporator. The crude was purified by column chromatography with heptane : EtOAc (9:2) eluent.

General procedure for Pd-catalyzed alkoxycarbonylation (Scheme 3, 4).

Chamber A was sequentially charged with aryl bromide (50 mg, 1.0 equiv), *t*BuONa (1.5 equiv), Pd(dba)₂ (5 mol%), 1,1'-bis(diisopropylphosphino)ferrocene (dippf) (5 mol%) and corresponding dry solvent (3 mL). At the onset of the reaction, the mixture was homogeneous, while precipitation of palladium species was observed during the course of the reactions both in conventional and renewable solvents.

Chamber B was sequentially charged with COgen (2 equiv), Pd(dba)₂ (5 mol%), tri-*tert*-butylphosphonium tetrafluoroborate (TTBP•HBF₄) (5 mol%), 1,4-dioxane (3 mL) and DIPEA (3 equiv). Addition of DIPEA initialize the release of CO. The two-chamber system was closed tightly with suitable caps and stirred at 80 °C for 18 hours. The resulting mixture of **Chamber A** was filtered through celite and concentrated using a rotary evaporator. The crude was purified by column chromatography with heptane : EtOAc (9:1) eluent.

ASSOCIATED CONTENT

Supporting Information.

The following files are available free of charge.

Detailed description of experiments and results, analytical and spectroscopic data (PDF)

AUTHOR INFORMATION

Corresponding Author

* Corresponding author: Annette Bayer; e-mail: annette.bayer@uit.no

Author Contributions

The manuscript was written through contributions of all authors. All authors have given approval to the final version of the manuscript.

Notes

The authors declare the following competing financial interest(s): T.S. is co-owner of SyTracks A/S, which commercializes the two-chamber system (COware) and COgen.

ACKNOWLEDGMENT

We gratefully acknowledge financial support from NordForsk (Grant No. 85378) and the Tromsø Research Foundation (Grant No. TFS2016KHH).

ABBREVIATIONS

2MeTHF = 2-methyltetrahydrofuran; acetal = 1,1-diethoxyethane; COgen = 9-methyl-9H-fluorene-9-carbonyl chloride; COware = two chamber reactor; cataCXium AHI = di(1-adamantyl)-*n*-butylphosphine hydride; DMC = dimethyl carbonate; DEC = diethyl carbonate; DIPEA = N,N-diisopropylethylamine; dippf = 1,1'-bis(diisopropylphosphino)ferrocene; EtOAc = ethyl acetate; EC = ethylene carbonate; GVL = γ -valerolactone; LCA = life-cycle assessment; PC = propylene carbonate; Pd(acac)₂ = palladium(II) acetylacetonate; Pd(OAc)₂ = palladium(II) acetate; Pd(dba)₂ = bis(dibenzylideneacetone)palladium(0); TTBP•HBF₄ = tri-*tert*-butylphosphonium tetrafluoroborate; XantPhos = 4,5-bis(diphenylphosphino)-9,9-dimethylxanthene; XantPhos Pd G3 = [(4,5-bis(diphenylphosphino)-9,9-dimethylxanthene)-2-(2'-amino-1,1'-biphenyl)]palladium(II) methanesulfonate.

REFERENCES

1. United Nations General Assembly, *Transforming Our World: The 2030 Agenda for Sustainable Development*, **2015**.
2. For a general discussion on perspectives of solvent use in the industry, see: (a) Sheldon, R. A. Green solvents for sustainable organic synthesis: state of the art. *Green Chem.* **2005**, *7*, 267-278. (b) Constable, D. J. C.; Jimenez-Gonzalez, C.; Henderson, R. K. Perspective on Solvent Use in the Pharmaceutical Industry. *Org. Process Res. Dev.* **2007**, *11*, 133-137. (c) Jimenez-Gonzalez, C.; Ponder, C. S.; Broxterman, Q. B.; Manley, J. B. Using the Right Green Yardstick: Why Process Mass Intensity Is Used in the Pharmaceutical Industry To Drive More Sustainable Processes. *Org. Process Res. Dev.* **2011**, *15*, 912-917. (d) Clark, J. H.; Farmer, T. J.; Hunt, A. J.; Sherwood, J. Opportunities for Bio-Based Solvents Created as Petrochemical and Fuel Products Transition towards Renewable Resources. *Int. J. Mol. Sci.* **2015**, *16*, 17101-17159.
3. For a survey on the most frequently used solvents, see: Ashcroft, C. P.; Dunn, P. J.; Hayler, J. D.; Wells, A. S. Survey of Solvent Usage in Papers Published in Organic Process Research & Development 1997-2012. *Org. Process Res. Dev.* **2015**, *19*, 740-747.
4. For recent reviews on applications of biomass-derived solvents, see: (a) Pace, V.; Hoyos, P.; Castoldi, L.; de Mara, P. D.; Alcantara, A. R. 2-Methyltetrahydrofuran (2-MeTHF): A Biomass-Derived Solvent with Broad Application in Organic Chemistry. *ChemSusChem* **2012**, *5*, 1369-1379. (b) Gu, Y.; Jerome, F. Bio-based solvents: an emerging generation of fluids for the design of eco-efficient processes in catalysis and organic chemistry. *Chem. Soc. Rev.* **2013**, *42*, 9550-9570. (c) Hulsbosch, J.; Vos, D. E. D.; Binnemans, K.; Ameloot, R.

- Biobased Ionic Liquids: Solvents for a Green Processing Industry? *ACS Sustainable Chem. Eng.* **2016**, *4*, 2917-2931. (d) Santoro, S.; Ferlin, F.; Luciani, L.; Ackermann, L.; Vaccaro, L. Biomass-derived solvents as effective media for cross-coupling reactions and C-H functionalization processes. *Green Chem.* **2017**, *19*, 1601-1612. (e) Santoro, S.; Marrocchi, A.; Lanari, D.; Ackermann, L.; Vaccaro, L. Towards Sustainable C-H Functionalization Reactions: The Emerging Role of Bio-Based Reaction Media. *Chem. Eur. J.* **2018**, *24*, 13383-13390. (f) Clarke, C. J.; Tu, W.-C.; Levers, O.; Brohl, A.; Hallett, J. P. Green and Sustainable Solvents in Chemical Processes. *Chem. Rev.* **2018**, *118*, 747-800. (g) Gandeepan, P.; Kaplaneris, N.; Santoro, S.; Vaccaro, L.; Ackermann, L. Biomass-Derived Solvents for Sustainable Transition Metal-Catalyzed C-H Activation. *ACS Sustainable Chem. Eng.* **2019**, *7*, 8023-8040.
5. For recent applications of biomass-derived solvents, see: (a) Xu, J.; Huang, W.; Bai, R.; Queneau, Y.; Jerome, F.; Gu, Y. Utilization of bio-based glycolaldehyde aqueous solution in organic synthesis: application to the synthesis of 2,3-dihydrofurans. *Green Chem.* **2019**, *21*, 2061-2069. (b) He, B.; Zheng, L.-S.; Phansavath, P.; Ratovelomanana-Vidal, V. RhIII-Catalyzed Asymmetric Transfer Hydrogenation of α -Methoxy β -Ketoesters through DKR in Water: Toward a Greener Procedure. *ChemSusChem* **2019**, *12*, 3032-3036. (c) Xu, Y.-T.; Li, C.-Y.; Huang, X.-B.; Gao, W.-X.; Zhou, Y.-B.; Liu, M.-C.; Wu, H.-Y. Photoinduced hydroxylation of arylboronic acids with molecular oxygen under photocatalyst-free conditions. *Green Chem.* **2019**, *21*, 4971-4975. (d) Wu, C.; Xiao, H.-J.; Wang, S.-W.; Tang, M.-S.; Tang, Z.-L.; Xia, W.; Li, W.-F.; Cao, Z.; He, W.-M. Natural Deep Eutectic Solvent-Catalyzed Selenocyanation of Activated Alkynes via an Intermolecular H-Bonding Activation Process. *ACS Sustainable Chem. Eng.* **2019**, *7*, 2169-2175. (e) Planer, S.; Jana, A.; Grela, K.

- Ethyl Lactate: A Green Solvent for Olefin Metathesis. *ChemSusChem* **2019**, *12*, 4655-4661.
- (f) Yao, J.; Liu, N.; Yin, L.; Xing, J.; Lu, T.; Dou, X. Catalytic asymmetric synthesis of chiral phenols in ethanol with recyclable rhodium catalyst. *Green Chem.* **2019**, *21*, 4946-4950. (g) Nejrotti, S.; Iannicelli, M.; Jamil, S. S.; Arnodo, D.; Blangetti, M.; Prandi, C. Natural deep eutectic solvents as an efficient and reusable active system for the Nazarov cyclization. *Green Chem.* **2020**, *22*, 110-117. (h) Mukherjee, S.; Pramanik, A. Catalyst-Free One-Pot Three-Component Synthesis of 4-Hydroxy-3-pyrazolylcoumarins in Ethanol at Room Temperature: Enolisable Aroylhydrazones as Efficient Ambident Nucleophile. *ACS Sustainable Chem. Eng.* **2020**, *8*, 403-414. (i) Bodachivskyi, I.; Kuzhiumparambil, U.; Williams, D. B. G. Catalytic Valorization of Native Biomass in a Deep Eutectic Solvent: A Systematic Approach toward High-Yielding Reactions of Polysaccharides. *ACS Sustainable Chem. Eng.* **2020**, *8*, 678-685. (j) Chen, L.; Shi, Y.; Gao, B.; Zhao, Y.; Jiang, Y.; Zha, Z.; Xue, W.; Gong, L. Lignin Nanoparticles: Green Synthesis in a γ -Valerolactone/Water Binary Solvent and Application to Enhance Antimicrobial Activity of Essential Oils. *ACS Sustainable Chem. Eng.* **2020**, *8*, 714-722. (k) Baby, J. N.; Sriram, B.; Wang, S.-F.; George, M. Effect of Various Deep Eutectic Solvents on the Sustainable Synthesis of MgFe₂O₄ Nanoparticles for Simultaneous Electrochemical Determination of Nitrofurantoin and 4-Nitrophenol. *ACS Sustainable Chem. Eng.* **2020**, *8*, 1479-1486. (l) Gevorgyan, A.; Hopmann, K. H.; Bayer, A. Exploration of New Biomass-Derived Solvents: Application to Carboxylation Reactions. *ChemSusChem* **2020**, *13*, 2080-2088.
6. For selected reviews on CO₂-derived solvents, see: (a) Schaffner, B.; Schaffner, F.; Verevkin, S. P.; Borner, A. Organic Carbonates as Solvents in Synthesis and Catalysis. *Chem. Rev.* **2010**, *110*, 4554-4581. (b) Fiorani, G.; Perosa, A.; Selva, M. Dimethyl carbonate: a versatile reagent

- for a sustainable valorization of renewables. *Green Chem.* **2018**, *20*, 288-322. (c) Sun, R.; Delidovich, I.; Palkovits, R. Dimethoxymethane as a Cleaner Synthetic Fuel: Synthetic Methods, Catalysts, and Reaction Mechanism. *ACS Catal.* **2019**, *9*, 1298-1318.
7. For recent applications of CO₂-derived solvents, see: (a) Choluj, A.; Krzesinski, P.; Ruszczyńska, A.; Bulska, E.; Kajetanowicz, A.; Grela, K. Noncovalent Immobilization of Cationic Ruthenium Complex in a Metal-Organic Framework by Ion Exchange Leading to a Heterogeneous Olefin Metathesis Catalyst for Use in Green Solvents. *Organometallics* **2019**, *38*, 3397-3405. (b) Selva, M.; Perosa, A.; Rodriguez-Padron, D.; Luque, R. Applications of Dimethyl Carbonate for the Chemical Upgrading of Biosourced Platform Chemicals. *ACS Sustainable Chem. Eng.* **2019**, *7*, 6471-6479. (c) Gadde, K.; Daelemans, J.; Maes, B. U. W.; Tehrani, K. A. Lewis acidic FeCl₃ promoted 2-aza-Cope rearrangement to afford α -substituted homoallylamines in dimethyl carbonate. *RSC Adv.* **2019**, *9*, 18013-18017. (d) Meng, D.; Li, D.; Ollevier, T. Recyclable iron(ii) caffeine-derived ionic salt catalyst in the Diels-Alder reaction of cyclopentadiene and α,β -unsaturated N-acyl-oxazolidinones in dimethyl carbonate. *RSC Adv.* **2019**, *9*, 21956-21963. (e) Carreras, V.; Besnard, C.; Gandon, V.; Ollevier, T. Asymmetric CuI-Catalyzed Insertion Reaction of 1-Aryl-2,2,2-trifluoro-1-diazoethanes into Si-H Bonds. *Org. Lett.* **2019**, *21*, 9094-9098. (f) Jordan, A.; Denton, R. M.; Sneddon, H. F. Development of a More Sustainable Appel Reaction. *ACS Sustainable Chem. Eng.* **2020**, *8*, 2300-2309. (g) Gevorgyan, A.; Hopmann, K. H.; Bayer, A. Formal C-H Carboxylation of Unactivated Arenes. *Chem. Eur. J.* **2020**, *26*, 6064-6069.
8. There are some studies on LCA for 2MeTHF, α -pinene, *p*-cymene, limonene, DMC and DEC, see: (a) Majeau-Bettez, G.; Hawkins, T. R.; Stromman, A. H. Life Cycle Environmental Assessment of Lithium-Ion and Nickel Metal Hydride Batteries for Plug-In Hybrid and

Battery Electric Vehicles. *Environ. Sci. Technol.* **2011**, *45*, 4548-4554. (b) Pourbafrani, M.; McKechnie, J.; MacLean, H. L.; Saville, B. A. Life cycle greenhouse gas impacts of ethanol, biomethane and limonene production from citrus waste. *Environ. Res. Lett.* **2013**, *8*, 015007. (c) Khoo, H. H.; Wong, L. L.; Tan, J.; Isoni, V.; Sharratt, P. Synthesis of 2-methyl tetrahydrofuran from various lignocellulosic feedstocks: Sustainability assessment via LCA. *Resour. Conserv. Recycl.* **2015**, *95*, 174-182. (d) Isoni, V.; Wong, L. L.; Khoo, H. H.; Halim, I.; Sharratt, P. Q-SAVESS: a methodology to help solvent selection for pharmaceutical manufacture at the early process development stage. *Green Chem.* **2016**, *18*, 6564-6572. (e) Garcia-Herrero, I.; Cuellar-Franca, R. M.; Enriquez-Gutierrez, V. M.; Alvarez-Guerra, M.; Irabien, A.; Azapagic, A. Environmental Assessment of Dimethyl Carbonate Production: Comparison of a Novel Electrosynthesis Route Utilizing CO₂ with a Commercial Oxidative Carbonylation Process. *ACS Sustainable Chem. Eng.* **2016**, *4*, 2088-2097. (f) Helmdach, D.; Yaseneva, P.; Heer, P. K.; Schweidtmann, A. M.; Lapkin, A. A. A Multiobjective Optimization Including Results of Life Cycle Assessment in Developing Biorenewables-Based Processes. *ChemSusChem* **2017**, *10*, 3632-3643. (g) Cadena, E.; Adani, F.; Font, X.; Artola, A. Including an Odor Impact Potential in Life Cycle Assessment of waste treatment plants. *Int. J. Environ. Sci. Technol.* **2018**, *15*, 2193-2202. (h) Thonemann, N.; Pizzol, M. Consequential life cycle assessment of carbon capture and utilization technologies within the chemical industry. *Energy Environ. Sci.* **2019**, *12*, 2253-2263.

9. The oxidation products of terpenes can be allergens. For general overview of flavors and fragrances, see: (a) *Handbook of Flavors and Fragrances*, Ash, M.; Ash, I., Synapse Information Resources, New York, **2006**, ISBN-13: 978-1890595876. (b) *Flavours and Fragrances: Chemistry, Bioprocessing and Sustainability*, Berger, R. G. (Ed.), Springer,

Berlin, **2007**, ISBN: 978-3-540-49338-9. (c) *Martindale: The Complete Drug Reference*, Brayfield, A. (Ed.), 39th ed., Pharmaceutical Press, **2017**, ISBN: 978-0-85711-309-2.

10. For selected reviews on carbonylative couplings, see: (a) Wu, X.-F.; Neumann, H.; Beller, M. Palladium-catalyzed carbonylative coupling reactions between Ar-X and carbon nucleophiles. *Chem. Soc. Rev.* **2011**, *40*, 4986-5009. (b) Roy, S.; Roy, S.; Gribble, G. W. Metal-catalyzed amidation. *Tetrahedron* **2012**, *68*, 9867-9923. (c) Fang, W.; Zhu, H.; Deng, Q.; Liu, S.; Liu, X.; Shen, Y.; Tu, T. Design and Development of Ligands for Palladium-Catalyzed Carbonylation Reactions. *Synthesis* **2014**, *46*, 1689-1708. (d) Rahman, O. [¹¹C]Carbon monoxide in labeling chemistry and positron emission tomography tracer development: scope and limitations. *J. Label Compd. Radiopharm* **2015**, *58*, 86-98. (e) Friis, S. D.; Lindhardt, A. T.; Skrydstrup, T. The Development and Application of Two-Chamber Reactors and Carbon Monoxide Precursors for Safe Carbonylation Reactions. *Acc. Chem. Res.* **2016**, *49*, 594-605. (f) Bai, Y.; Davis, D. C.; Dai, M. Natural Product Synthesis via Palladium-Catalyzed Carbonylation. *J. Org. Chem.* **2017**, *82*, 2319-2328. (g) Taddei, C.; Gee, A. D. Recent progress in [¹¹C]carbon dioxide ([¹¹C]CO₂) and [¹¹C]carbon monoxide ([¹¹C]CO) chemistry. *J. Label Compd. Radiopharm* **2018**, *61*, 237-25. (h) Peng, J.-B.; Wu, X.-F. Ligand- and Solvent-Controlled Regio- and Chemodivergent Carbonylative Reactions. *Angew. Chem. Int. Ed.* **2018**, *57*, 1152-1160. (i) Akerbladh, L.; Odell, L. R.; Larhed, M. Palladium-Catalyzed Molybdenum Hexacarbonyl-Mediated Gas-Free Carbonylative Reactions. *Synlett* **2019**, *30*, 141-155. (j) Peng, J.-B.; Wu, F.-P.; Wu, X.-F. First-Row Transition-Metal-Catalyzed Carbonylative Transformations of Carbon Electrophiles. *Chem. Rev.* **2019**, *119*, 2090-2127.
11. For recent applications of carbonylative couplings, see: (a) Le, Z.; Ying, J.; Wu, X.-F. More than a CO source: palladium-catalyzed carbonylative synthesis of butenolides from propargyl

alcohols and TFBen. *Org. Chem. Front.* **2019**, *6*, 3158-3161. (b) Qi, X.; Lai, M.; Zhu, M.-J.; Peng, J.-B.; Ying, J.; Wu, X.-F. 1-Arylvinyloxy formats: A New CO Source and Ketone Source in Carbonylative Synthesis of Chalcone Derivatives. *ChemCatChem* **2019**, *11*, 5252-5255. (c) Peng, J.-B.; Li, D.; Geng, H.-Q.; Wu, X.-F. Palladium-Catalyzed Amide Synthesis via Aminocarbonylation of Arylboronic Acids with Nitroarenes. *Org. Lett.* **2019**, *21*, 4878-4881. (d) Wu, F.-P.; Li, D.; Peng, J.-B.; Wu, X.-F. Carbonylative Transformation of Allylarenes with CO Surrogates: Tunable Synthesis of 4-Arylbutanoic Acids, 2-Arylbutanoic Acids, and 4-Arylbutanals. *Org. Lett.* **2019**, *21*, 5699-5703. (e) Xu, J.-X.; Wu, X.-F. Cobalt-Catalyzed Alkoxy carbonylation of Epoxides to β -Hydroxyesters. *J. Org. Chem.* **2019**, *84*, 9907-9912. (f) Lu, B.; Cheng, Y.; Chen, L.-Y.; Chen, J.-R.; Xiao, W.-J. Photoinduced Copper-Catalyzed Radical Aminocarbonylation of Cycloketone Oxime Esters. *ACS Catal.* **2019**, *9*, 8159-8164. (g) Lopatka, P.; Markovic, M.; Koos, P.; Ley, S. V.; Gracza, T. Continuous Pd-Catalyzed Carbonylative Cyclization Using Iron Pentacarbonyl as a CO Source. *J. Org. Chem.* **2019**, *84*, 14394-14406. (h) Sardana, M.; Bergman, J.; Ericsson, C.; Kingston, L. P.; Schou, M.; Dugave, C.; Audisio, D.; Elmore, C. S. Visible-Light-Enabled Aminocarbonylation of Unactivated Alkyl Iodides with Stoichiometric Carbon Monoxide for Application on Late-Stage Carbon Isotope Labeling. *J. Org. Chem.* **2019**, *84*, 16076-16085. (i) Cheng, R.; Zhao, H.-Y.; Zhang, S.; Zhang, X. Nickel-Catalyzed Carbonylation of Secondary Trifluoromethylated, Difluoromethylated, and Nonfluorinated Aliphatic Electrophiles with Arylboronic Acids under 1 atm of CO. *ACS Catal.* **2020**, *10*, 36-42. (j) Ying, J.; Le, Z.; Wu, X.-F. Benzene-1,3,5-triyl Triflate (TFBen)-Promoted Palladium-Catalyzed Carbonylative Synthesis of 2-Oxo-2,5-dihydropyrroles from Propargyl Amines. *Org. Lett.* **2020**, *22*, 194-198. (k) Ismael, A.;

Skrydstrup, T.; Bayer, A. Carbonylative Suzuki-Miyaura couplings of sterically hindered aryl halides: synthesis of 2-arylbenzoate derivatives. *Org. Biomol. Chem.* **2020**, *18*, 1754-1759.

12. For selected works on carbonylative coupling of boronic acids and aryl halides, see: (a) Maerten, E.; Hassouna, F.; Couve-Bonnaire, S.; Mortreux, A.; Carpentier, J.-F.; Castanet, Y. Direct Synthesis of Benzoylpyridines from Chloropyridines via a Palladium-Carbene Catalyzed Carbonylative Suzuki Cross-Coupling Reaction. *Synlett* **2003**, *12*, 1874-1876. (b) Maerten, E.; Sauthier, M.; Mortreux, A.; Castanet, Y. Palladium-N-heterocyclic carbene an efficient catalytic system for the carbonylative cross-coupling of pyridine halides with boronic acids. *Tetrahedron* **2007**, *63*, 682-689. (c) O'Keefe, B. M.; Simmons, N.; Martin, S. F. Carbonylative Cross-Coupling of ortho-Disubstituted Aryl Iodides. Convenient Synthesis of Sterically Hindered Aryl Ketones. *Org. Lett.* **2008**, *10*, 5301-5304. (d) Neumann, H.; Brennfuhrer, A.; Beller, M. An Efficient and Practical Sequential One-Pot Synthesis of Suprofen, Ketoprofen and Other 2-Arylpropionic Acids. *Adv. Synth. Catal.* **2008**, *350*, 2437-2442. (e) Neumann, H.; Brennfuhrer, A.; Beller, M. A General Synthesis of Diarylketones by Means of a Three-Component Cross-Coupling of Aryl and Heteroaryl Bromides, Carbon Monoxide, and Boronic acids. *Chem. Eur. J.* **2008**, *14*, 3645-3652. (f) Ahlburg, A.; Lindhardt, A. T.; Taaning, R. H.; Modvig, A. E.; Skrydstrup, T. An Air-Tolerant Approach to the Carbonylative Suzuki-Miyaura Coupling: Applications in Isotope Labeling. *J. Org. Chem.* **2013**, *78*, 10310-10318. (g) Bjerglund, K. M.; Skrydstrup, T.; Molander, G. A. Carbonylative Suzuki Couplings of Aryl Bromides with Boronic Acid Derivatives under Base-Free Conditions. *Org. Lett.* **2014**, *16*, 1888-1891. (h) Gautam, P.; Dhiman, M.; Polshettiwar, V.; Bhanage, B. M. KCC-1 supported palladium nanoparticles as an efficient and sustainable

nanocatalyst for carbonylative Suzuki-Miyaura cross-coupling. *Green Chem.* **2016**, *18*, 5890-5899.

13. For selected works on aminocarbonylation, see: (a) Lagerlund, O.; Larhed, M. Microwave-Promoted Aminocarbonylations of Aryl Chlorides Using Mo(CO)₆ as a Solid Carbon Monoxide Source. *J. Comb. Chem.* **2006**, *8*, 4-6. (b) Appukkuttan, P.; Axelsson, L.; Eycken, E. V. d.; Larhed, M. Microwave-assisted, Mo(CO)₆-mediated, palladium-catalyzed aminocarbonylation of aryl halides using allylamine: from exploration to scale-up. *Tetrahedron Lett.* **2008**, *49*, 5625-5628. (c) Odell, L. R.; Savmarker, J.; Larhed, M. Microwave-promoted aminocarbonylation of aryl triflates using Mo(CO)₆ as a solid CO source. *Tetrahedron Lett.* **2008**, *49*, 6115-6118. (d) Nielsen, D. U.; Taaning, R. H.; Lindhardt, A. T.; Gogsig, T. M.; Skrydstrup, T. Palladium-Catalyzed Approach to Primary Amides Using Nongaseous Precursors. *Org. Lett.* **2011**, *13*, 4454-4457. (e) Lindhardt, A. T.; Simonssen, R.; Taaning, R. H.; Gogsig, T. M.; Nilsson, G. N.; Stenhagen, G.; Elmore, C. S.; Skrydstrup, T. ¹⁴Carbon monoxide made simple - novel approach to the generation, utilization, and scrubbing of ¹⁴carbon monoxide. *J. Label Compd. Radiopharm* **2012**, *55*, 411-418. (f) Nordeman, P.; Odell, L. R.; Larhed, M. Aminocarbonylations Employing Mo(CO)₆ and a Bridged Two-Vial System: Allowing the Use of Nitro Group Substituted Aryl Iodides and Aryl Bromides. *J. Org. Chem.* **2012**, *77*, 11393-11398. (g) Andersen, T. L.; Caneschi, W.; Ayoub, A.; Lindhardt, A. T.; Couri, M. R. C.; Skrydstrup, T. 1,2,4- and 1,3,4-Oxadiazole Synthesis by Palladium-Catalyzed Carbonylative Assembly of Aryl Bromides with Amidoximes or Hydrazides. *Adv. Synth. Catal.* **2014**, *356*, 3074-3082. (h) Friis, S. D.; Skrydstrup, T.; Buchwald, S. L. Mild Pd-Catalyzed Aminocarbonylation of (Hetero)Aryl Bromides with a Palladacycle Precatalyst. *Org. Lett.* **2014**, *16*, 4296-4299. (i) Liu, S.; Wang, H.; Daia, X.; Shi, F. Organic ligand-free

carbonylation reactions with unsupported bulk Pd as catalyst. *Green Chem.* **2018**, *20*, 3457-3462. (j) Collin, H. P.; Reis, W. J.; Nielsen, D. U.; Lindhardt, A. T.; Valle, M. S.; Freitas, R. P.; Skrydstrup, T. COtab: Expedient and Safe Setup for Pd-Catalyzed Carbonylation Chemistry. *Org. Lett.* **2019**, *21*, 5775-5778.

14. For selected works on alkoxy carbonylation, see: (a) Lou, R.; VanAlstine, M.; Sun, X.; Wentland, M. P. Preparation of N-hydroxysuccinimido esters via palladium-catalyzed carbonylation of aryl triflates and halides. *Tetrahedron Lett.* **2003**, *44*, 2477-2480. (b) Kormos, C. M.; Leadbeater, N. E. Alkoxy carbonylation of aryl iodides using gaseous carbon monoxide and pre-pressurized reaction vessels in conjunction with microwave heating. *Org. Biomol. Chem.* **2007**, *5*, 65-68. (c) Martinelli, J. R.; Watson, D. A.; Freckmann, D. M. M.; Barder, T. E.; Buchwald, S. L. Palladium-Catalyzed Carbonylation Reactions of Aryl Bromides at Atmospheric Pressure: A General System Based on Xantphos. *J. Org. Chem.* **2008**, *73*, 7102-7107. (d) Yamamoto, Y. The First General and Selective Palladium(II)-Catalyzed Alkoxy carbonylation of Arylboronates: Interplay among Benzoquinone-Ligated Palladium(0) Complex, Organoboron, and Alcohol Solvent. *Adv. Synth. Catal.* **2010**, *352*, 478-492. (e) Friis, S. D.; Taaning, R. H.; Lindhardt, A. T.; Skrydstrup, T. Silacarboxylic Acids as Efficient Carbon Monoxide Releasing Molecules: Synthesis and Application in Palladium-Catalyzed Carbonylation Reactions. *J. Am. Chem. Soc.* **2011**, *133*, 18114-18117. (f) Xin, Z.; Gogsig, T. M.; Lindhardt, A. T.; Skrydstrup, T. An Efficient Method for the Preparation of Tertiary Esters by Palladium-Catalyzed Alkoxy carbonylation of Aryl Bromides. *Org. Lett.* **2012**, *14*, 284-287. (g) Almeida, A. M. d.; Andersen, T. L.; Lindhardt, A. T.; Almeida, M. V. d.; Skrydstrup, T. General Method for the Preparation of Active Esters by Palladium-Catalyzed Alkoxy carbonylation of Aryl Bromides. *J. Org. Chem.* **2015**, *80*, 1920-1928. (h) Solano, M.

V.; Miera, G. G.; Pascanu, V.; Inge, A. K.; Martin-Matute, B. Versatile Heterogeneous Palladium Catalysts for Diverse Carbonylation Reactions under Atmospheric Carbon Monoxide Pressure. *ChemCatChem*, **2018**, *10*, 1089-1095.

15. For safety data sheets of DMC and limonene, see: (a)

<https://www.sigmaaldrich.com/MSDS/MSDS/DisplayMSDSPage.do?country=NO&language=EN->

[generic&productNumber=D152927&brand=SIAL&PageToGoToURL=https%3A%2F%2Fwww.sigmaaldrich.com%2Fcatalog%2Fproduct%2Fsial%2Fd152927%3Flang%3Den](https://www.sigmaaldrich.com/MSDS/MSDS/DisplayMSDSPage.do?country=NO&language=EN-generic&productNumber=D152927&brand=SIAL&PageToGoToURL=https%3A%2F%2Fwww.sigmaaldrich.com%2Fcatalog%2Fproduct%2Fsial%2Fd152927%3Flang%3Den). (b)

<https://www.sigmaaldrich.com/MSDS/MSDS/DisplayMSDSPage.do?country=NO&language=EN->

[generic&productNumber=183164&brand=SIGMA&PageToGoToURL=https%3A%2F%2Fwww.sigmaaldrich.com%2Fcatalog%2Fproduct%2Fsigma%2F183164%3Flang%3Den](https://www.sigmaaldrich.com/MSDS/MSDS/DisplayMSDSPage.do?country=NO&language=EN-generic&productNumber=183164&brand=SIGMA&PageToGoToURL=https%3A%2F%2Fwww.sigmaaldrich.com%2Fcatalog%2Fproduct%2Fsigma%2F183164%3Flang%3Den).

Supplementary Information

Renewable Solvents for Palladium-Catalyzed Carbonylation Reactions

Aya Ismael,^a Ashot Gevorgyan,^a Troels Skrydstrup^b and Annette Bayer^{*a}

^a Department of Chemistry, Faculty of Science and Technology, UiT The Arctic University of Norway, N-9037 Tromsø, Norway.

^b Carbon Dioxide Activation Center (CADIAC), Interdisciplinary Nanoscience Center (iNANO) and Department of Chemistry, Aarhus University, Gustav Wieds Vej 14, 8000 Aarhus C, Denmark.

E-mail: annette.bayer@uit.no

Table of Contents

| | | |
|------------|--|-----------|
| 1. | General considerations | 2 |
| 2. | The two-chamber system used in the work | 3 |
| 3. | Overview of solvents used in the study and their properties | 4 |
| 4. | Optimization of carbonylative Suzuki-Miyaura coupling with boronic acids | 5 |
| 5. | Screening of solvents | 5 |
| 5.1 | Screening of solvents for carbonylative coupling of boronic acids and aryl halides | 5 |
| 5.2 | Screening of solvents for the aminocarbonylation | 6 |
| 5.3 | Screening of solvents for the alkoxy carbonylation | 6 |
| 6. | General procedures | 6 |
| 6.1 | General procedure A: Carbonylative coupling of boronic acids and aryl halides | 6 |
| 6.2 | General procedure B: Aminocarbonylation | 7 |
| 6.3 | General procedure C: Alkoxy carbonylation | 7 |
| 7. | Control experiments on methoxycarbonylation | 7 |
| 8. | Characterisation of products | 8 |
| 9. | References | 19 |
| 10. | Copies of spectra | 21 |

1. General considerations

All chemicals and solvents were purchased from Sigma Aldrich and VWR and were used as received without further purification. Solvents were dried according to standard procedures on molecular sieves 4 Å.¹ Flash chromatography was carried out on silica gel 60 (230–400 mesh). NMR spectra were obtained on a Bruker Avance 400 MHz at 20°C. Data are represented as follows: chemical shift, multiplicity (s = singlet, d = doublet, t = triplet, q = quartet, dt = double triplet, m = multiplet), coupling constant (*J*, Hz) and integration. Chemical shifts (δ) are reported in ppm relative to the residual solvent peak (CDCl₃: δ H 7.26 and δ C 77.16; Methanol-d₄: δ H 3.31 and δ C 49.00; Deuteriumoxid: δ H 4.79; DMSO-d₆: δ H 2.51 and δ C 39.52). The raw data was analyzed with MestReNova (Version 10.0.2-15465). Positive ion electrospray ionization mass spectrometry was conducted on a Thermo electron LTQ Orbitrap XL spectrometer. The data was analyzed with Thermo Scientific Xcalibur software. Melting points were measured using Stuart SMP50 automatic melting point detector. Infrared spectra were recorded on a Agilent Cary 630 FT-IR spectrometer and absorptions are reported in wavenumber (cm⁻¹); s = strong, m = medium, w = weak.

Solvents used in the work were purchased from Sigma Aldrich if not otherwise stated. 2MeTHF (anhydrous, \geq 99%, inhibitor-free, [673277-1L](#)), methylal (absolute, over molecular sieve, \geq 99.0%, [47676-250ML](#)), ethylal (absolute, over molecular sieve, \geq 99.0%, [47675-500ML-F](#)), dimethylcarbonate (anhydrous, \geq 99%, [517127-1L](#)), diethylcarbonate (anhydrous, \geq 99%, [517135-1L](#)), propylene carbonate (anhydrous, 99.7%, [310328-1L](#)) and ethylene carbonate (anhydrous, 99%, [676802-1L](#)) were bought as anhydrous solvents equipped with a septa. Other renewable solvents were reagent grade; they were degassed, kept over activated molecular sieves (4 Å) at least for a week before use and stored under Ar atmosphere. The purity of the solvents used in the work were as follows: diethoxyethane (99%, inhibitor-free, [A902-500ML](#)); dimethyl isosorbide (98%, inhibitor-free, [247898-100G](#)); GVL (99%, [V403-500G](#)); γ -terpinene (97%, [223190-100ML](#)); α -pinene (98%, [147524-250ML](#)); (*R*)-(+)-limonene (97%, [183164-100ML](#)); *p*-cymene (99%, [C121452-1L](#)); eucalyptol (99%, inhibitor-free, [C80601-500ML](#)); (+)-rose oxide (97%, inhibitor-free, Chemtronica/TCI [M2363-25G](#)).

2MeTHF, acetal, dimethyl isosorbide, eucalyptol, rose oxide, methylal and ethylal are ethers and may form peroxides when stored under air; however, peroxide tests (Test strips for peroxide, MQuant[®], Supelco[®], VWR/Merck [1.10081.0001](#)) of freshly bought solvents did not show any noticeable levels of peroxides. Acetal, methylal and ethylal can be hydrolyzed in the presence of strong acids when heated. Under basic conditions, which are frequently used for the reactions involving organometallics, acetal, methylal and ethylal are stable. GVL, DMC, DEC, PC and EC can be hydrolyzed in the presence of strongly basic water solutions; under anhydrous conditions, they are stable. γ -Terpinene, limonene and eucalyptol can be converted to *p*-cymene when heated above 220°C. Overall, the examined renewable solvents appeared to be stable under the conditions used in this work. It should be noted that the oxidation products of terpenes can be allergens.

The reactions were performed in the previously reported two-chamber system (COware with total volume of 20 mL, Fig. S1) under an argon atmosphere, and a glovebox was employed for weighing out the reagents.

Warning! Most of the reactions were performed in specialized glassware under pressure. The glassware should always be examined for damages before any manipulation. All laboratory safety procedures must be followed strictly and the work with pressure tubes must be conducted behind a shield.

2. The two-chamber system used in the work

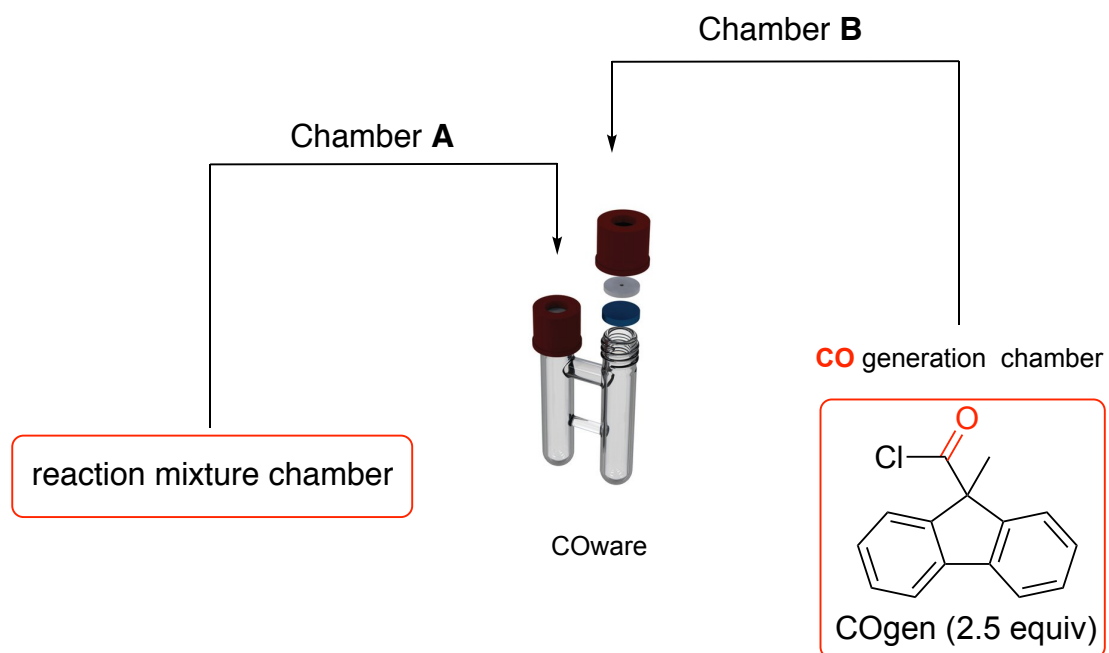


Fig. S1. The two-chamber system used in the work, and the CO generator (COgen).

3. Overview of solvents used in the study and their properties

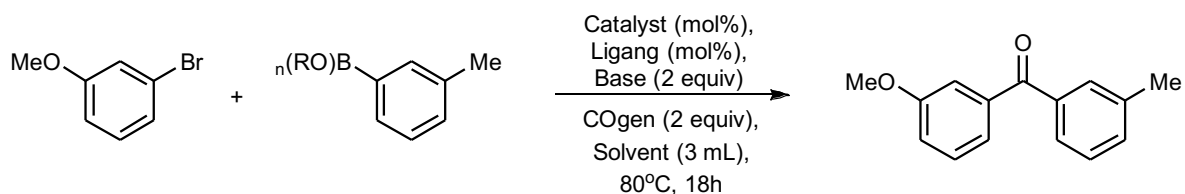
Table S1. Overview of solvent properties and isolated yield from solvent screens. Solvents are organized by increasing dielectric constant.

| Solvent | MW (g/mol) | Bp (°C) | Dielectric constant ¹ | Compound class | C-C yield (%) | C-N yield (%) | C-O yield (%) |
|----------------------------------|------------|-------------|----------------------------------|--------------------|------------------------|------------------------|------------------------|
| non-polar | | | | | | | |
| α -Pinene | 136.24 | 156 | 2.18 | hydrocarbon | 50 | 97 | 93 |
| γ -Terpinene | 136.24 | 174 | 2.27 ² | hydrocarbon | 50 | 94 | 93 |
| (+)-Limonene | 136.24 | 178 | 2.37 | hydrocarbon | 80 | 99 | 56 |
| <i>p</i> -Cymene | 134.22 | 177 | 2.25 ³ | hydrocarbon | 75 | 97 | |
| Toluene | 92.14 | 111 | 2.38 | hydrocarbon | 90¹⁰ | 97¹¹ | |
| Diethoxymethane (ethylal) | 104.15 | 87 | 2.53 ⁴ | ether | | 62 | 64 |
| Dimethoxymethane (methylal) | 76.10 | 42 | 2.64 | ether | 50 | | 45 |
| Diethylcarbonate (DEC) | 118.13 | 126 | 2.82 | carbonate | | 94 | 45 |
| Dimethylcarbonate (DMC) | 90.08 | 90 | 3.13 ⁵ | carbonate | 16 | 97 | 93* |
| 1,1-Diethoxyethane (acetal) | 118.18 | 102 | 3.80 | ether | | 62 | 55 |
| (+)-Rose oxide | 154.25 | 86/20 mmHg | | ether | 33 | 78 | 36 |
| Eucalyptol | 154.25 | 176 | 4.57 | ether | | 89 | 82 |
| polar aprotic | | | | | | | |
| Dimethyl isosorbide (DMI) | 174.20 | 94/0.1 mmHg | 6.2 ⁶ | ether | | 89 | 30 |
| 2-Methyltetrahydrofuran (2MeTHF) | 86.13 | 79 | 6.97 ⁷ | ether | 30 | 83 | 91 |
| Tetrahydrofuran (THF) | 72.11 | 65 | 7.52 | ether | | | 88¹² |
| γ -Valerolactone (GVL) | 100.12 | 207 | 36.47 ⁸ | ester | | 74 | 64 |
| Propylenecarbonate (PC) | 102.09 | 242 | 66.14 | carbonate | | 80 | 60 |
| Ethylenecarbonate (EC) | 88.06 | 261 | 92.8 ⁹ | carbonate | | | 30 |

* Yield of product corresponding to an overall methoxycarbonylation. ¹ Values obtained from CRC Handbook of Chemistry and Physics (85th ed.) unless specified otherwise. T = 15 to 30 °C. ² Value obtained from: Thomas, G. A.; Hawkins, J. E. *J. Am. Chem. Soc.* **1954**, *76* (19), 4856-4858. ³ Value obtained from: Altshuller, A. P., *J. Phys. Chem.* **1954**, *58* (5), 392-395. ⁴ Value obtained from: Philippe, R.; Plette, A. M., *Bull. Soc. Chim. Belg.* **1955**, *64*, 600-27. ⁵ Value obtained from: Rivas, M. A.; Pereira, S. M.; Banerji, N.; Iglesias, T. P., *J. Chem. Thermodyn.* **2004**, *36* (3), 183-191. ⁶ Value obtained from: Zia, H.; Ma, J. K. H.; O'Donnell, J. P.; Luzzi, L. A. *Pharm. Res.* **1991**, *8* (4), 502-504. ⁷ Value obtained from: Aycock, D. F. *Org. Process Res. Dev.* **2007**, *11* (1), 156-159. ⁸ Value obtained from: Aparicio, S.; Alcalde, R. *Phys. Chem. Chem. Phys.* **2009**, *11* (30), 6455-6467. ⁹ Value obtained from: Ding, M. S. *J. Electrochem. Soc.* **2003**, *150* (4), A455. ¹⁰ Bjerglund, K. M.; Skrydstrup, T.; Molander, G. A. *Org. Lett.* **2014**, *16*, 1888-1891. ¹¹ Martinelli, J. R.; Watson, D. A.; Freckmann, D. M. M.; Barder, T. E.; Buchwald, S. L. *J. Org. Chem.* **2008**, *73*, 7102-7107. ¹² Xin, Z.; Gogsig, T. M.; Lindhardt, A. T.; Skrydstrup, T. *Org. Lett.* **2012**, *14*, 284-287.

4. Optimization of carbonylative Suzuki-Miyaura coupling with boronic acids

Table S2. Catalyst screening for the carbonylative coupling of boronic acids and 3-bromoanisole.



| Entry | Boronic acid derivative | Catalyst (mol%) | Ligand (mol%) | Base | Solvent | Isol. Yield (%) |
|----------------|-------------------------|---------------------------|--------------------|---------------------------------|---------------------------------|-----------------|
| 1 | | Pd(OAc) ₂ (3) | IMes (4) | Cs ₂ CO ₃ | 1,4-Dioxane | 40 |
| 2 ^d | | Pd(acac) ₂ (5) | CataXCiumA.HI (10) | - | Toluene | 83 |
| 3 ^d | | Pd(acac) ₂ (5) | CataXCiumA.HI (10) | - | Toluene:H ₂ O (10:1) | 45 |
| 4 | | Pd(acac) ₂ (5) | CataXCiumA.HI (10) | 1M aq. NaOH | Toluene | 82 |

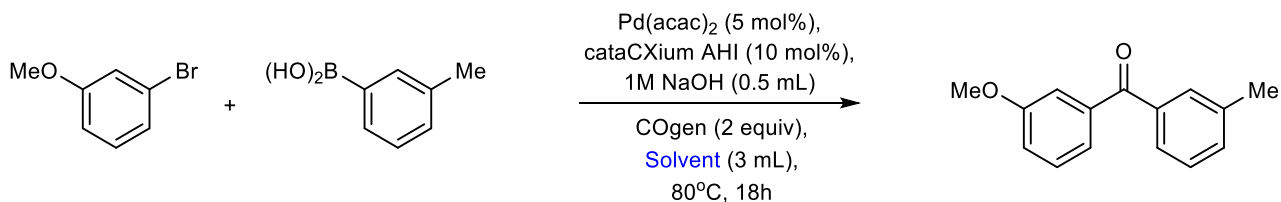
The reagents were weighed in the glove box!

Chamber A was sequentially charged with 3-methoxybromobenzene (50 mg, 1.0 equiv), corresponding organoboronate (1.2 equiv), Pd-catalyst (3-5 mol%), ligand (4-10 mol%), base (0-2 equiv) and corresponding solvent (3 mL).

Chamber B was sequentially charged with COgen (2 equiv), Pd(dba)₂ (5 mol%), tri-*tert*-butylphosphonium tetrafluoroborate (TTBP•HBF₄) (5 mol%), 1,4-dioxane (3 mL) and DIPEA (3 equiv). Addition of DIPEA initialize the release of CO. The two-chamber system was closed tightly with suitable caps and stirred at 80°C for 18 hours. The resulting mixture of **Chamber A** was filtered through celite and concentrated using a rotary evaporator. The crude was purified by column chromatography with heptane : EtOAc (9:2) eluent.

5. Screening of solvents

5.1 Screening of solvents for carbonylative coupling of boronic acids and aryl halides.



The reagents were weighed in the glove box!

Chamber A was sequentially charged with 3-methoxybromobenzene (50 mg, 1.0 equiv), *m*-tolylboronic acid (1.2 equiv), Pd(acac)₂ (5 mol%), cataCXium AHI (10 mol%), 1M NaOH (500 μl) and corresponding dry solvent (3 mL).

Chamber B was sequentially charged with COgen (2 equiv), Pd(dba)₂ (5 mol%), tri-*tert*-butylphosphonium tetrafluoroborate (TTBP•HBF₄) (5 mol%), 1,4-dioxane (3 mL) and DIPEA (3 equiv). Addition of DIPEA initialize the release of CO. The two-chamber system was closed tightly with suitable caps and stirred at 80°C for 18 hours. The resulting mixture of **Chamber A** was filtered through celite and concentrated using a rotary evaporator. The crude was purified by column chromatography with heptane : EtOAc (9:2) eluent.

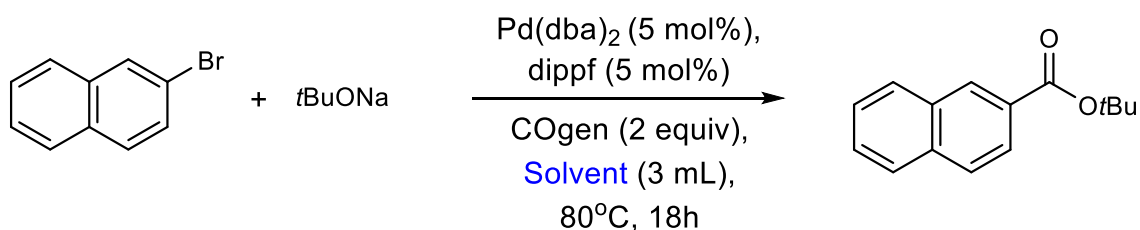
5.2 Screening of solvents for the aminocarbonylation.



Chamber A was sequentially charged with 4-bromobenzonitrile (50 mg, 1.0 equiv), *N*-methylaniline (1.5 equiv), Pd(OAc)₂ (2 mol%), XantPhos (2 mol%), triethylamine (3 equiv) and corresponding dry solvent (3 mL).

Chamber B was sequentially charged with COgen (2 equiv), Pd(dba)₂ (5 mol%), tri-*tert*-butylphosphonium tetrafluoroborate (TTBP•HBF₄) (5 mol%), 1,4-dioxane (3 mL) and DIPEA (3 equiv). Addition of DIPEA initialize the release of CO. The two-chamber system was closed tightly with suitable caps and stirred at 80°C for 18 hours. The resulting mixture of **Chamber A** was filtered through celite and concentrated using a rotary evaporator. The crude was purified by column chromatography with heptane : EtOAc (9:2) eluent.

5.3 Screening of solvents for the alkoxy carbonylation.



Chamber A was sequentially charged with 2-bromonaphthalene (50 mg, 1.0 equiv), *t*BuONa (1.5 equiv), Pd(dba)₂ (5 mol%), 1,1'-bis(diisopropylphosphino)ferrocene (dippf) (5 mol%) and corresponding dry solvent (3 mL).

Chamber B was sequentially charged with COgen (2 equiv), Pd(dba)₂ (5 mol%), tri-*tert*-butylphosphonium tetrafluoroborate (TTBP•HBF₄) (5 mol%), 1,4-dioxane (3 mL) and DIPEA (3 equiv). Addition of DIPEA initialize the release of CO. The two-chamber system was closed tightly with suitable caps and stirred at 80°C for 18 hours. The resulting mixture of **Chamber A** was filtered through celite and concentrated using a rotary evaporator. The crude was purified by column chromatography with heptane : EtOAc (9:1) eluent.

6. General procedures

The reagents were weighed in the glove box!

6.1 General procedure A: Carbonylative coupling of boronic acids and aryl halides.

Chamber A was sequentially charged with aryl bromide (50 mg, 1.0 equiv), boronic acid (1.2 equiv), Pd(acac)₂ (5 mol%), cataCXium AHI (10 mol%), 1M NaOH (500 μl) and dry solvent (3 mL).

Chamber B was sequentially charged with COgen (2 equiv), Pd(dba)₂ (5 mol%), tri-*tert*-butylphosphonium tetrafluoroborate (TTBP•HBF₄) (5 mol%), DIPEA (3 equiv) and 1,4-dioxane (3 mL). The two-chamber system was closed tightly with suitable caps and **Chamber B** was stirred at 80°C until the release of CO was stopped. This was followed by stirring of both chambers at 80°C for 18 hours. The resulting mixture of **Chamber A** was

filtered through celite and concentrated using a rotary evaporator. The crude was purified by column chromatography with heptane : EtOAc (9:1) eluent.

6.2 General procedure B: Aminocarbonylation.

Chamber A was sequentially charged with aryl bromide (50 mg, 1.0 equiv), corresponding amine (1.5 equiv), Pd(OAc)₂ (2 mol%), XantPhos (2 mol%), (in the case of **5u** and **5v** Pd(OAc)₂/XantPhos system was replaced by XantPhos Pd G3 (2 mol%)), triethylamine (3 equiv) and corresponding dry solvent (3 mL).

Chamber B was sequentially charged with COgen (2 equiv), Pd(dba)₂ (5 mol%), tri-*tert*-butylphosphonium tetrafluoroborate (TTBP•HBF₄) (5 mol%), 1,4-dioxane (3 mL) and DIPEA (3 equiv). Addition of DIPEA initialize the release of CO. The two-chamber system was closed tightly with suitable caps and stirred at 80°C for 18 hours. The resulting mixture of **Chamber A** was filtered through celite and concentrated using a rotary evaporator. The crude was purified by column chromatography with heptane : EtOAc (9:2) eluent.

6.3 General procedure C: Alkoxy carbonylation.

Chamber A was sequentially charged with aryl bromide (50 mg, 1.0 equiv), *t*BuONa (1.5 equiv), Pd(dba)₂ (5 mol%), 1,1'-bis(diisopropylphosphino)ferrocene (dippf) (5 mol%) and corresponding dry solvent (3 mL).

Chamber B was sequentially charged with COgen (2 equiv), Pd(dba)₂ (5 mol%), tri-*tert*-butylphosphonium tetrafluoroborate (TTBP•HBF₄) (5 mol%), 1,4-dioxane (3 mL) and DIPEA (3 equiv). Addition of DIPEA initialize the release of CO. The two-chamber system was closed tightly with suitable caps and stirred at 80°C for 18 hours. The resulting mixture of **Chamber A** was filtered through celite and concentrated using a rotary evaporator. The crude was purified by column chromatography with heptane : EtOAc (9:1) eluent.

7. Control experiments on methoxycarbonylation.

Transesterification in the absence of Pd-catalyst

10 mL pressure vial was sequentially charged with *tert*-butyl 2-naphthoate (26 mg, 1.0 equiv), *t*BuONa (1.5 equiv) and dry DMC (3 mL). The pressure vial was closed tightly with suitable cap and stirred at 80°C for 18 hours. The resulting mixture was filtered through celite and concentrated using a rotary evaporator. The crude was purified by column chromatography with heptane : EtOAc (9:1) eluent.

Transesterification in the presence of Pd-catalyst

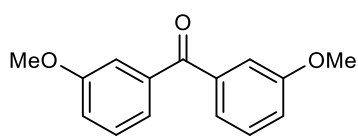
10 mL pressure vial was sequentially charged with *tert*-butyl 2-naphthoate (26 mg, 1.0 equiv), *t*BuONa (1.5 equiv), Pd(dba)₂ (5 mol%), 1,1'-bis(diisopropylphosphino)ferrocene (dippf) (5 mol%) and dry DMC (3 mL). The pressure vial was closed tightly with suitable cap and stirred at 80°C for 18 hours. The resulting mixture was filtered through celite and concentrated using a rotary evaporator. The crude was purified by column chromatography with heptane : EtOAc (9:1) eluent.

Pd-catalyzed methoxycarbonylation with sodium methoxide

Chamber A was sequentially charged with 2-bromonaphthalene (50 mg, 1.0 equiv), MeONa (1.5 equiv), Pd(dba)₂ (5 mol%), 1,1'-bis(diisopropylphosphino)ferrocene (dippf) (5 mol%) and dry DMC (3 mL).

Chamber B was sequentially charged with COgen (2 equiv), Pd(dba)₂ (5 mol%), tri-*tert*-butylphosphonium tetrafluoroborate (TTBP•HBF₄) (5 mol%), 1,4-dioxane (3 mL) and DIPEA (3 equiv). Addition of DIPEA initialize the release of CO. The two-chamber system was closed tightly with suitable caps and stirred at 80°C for 18 hours. The resulting mixture of **Chamber A** was filtered through celite and concentrated using a rotary evaporator. The crude was purified by column chromatography with heptane : EtOAc (9:1) eluent.

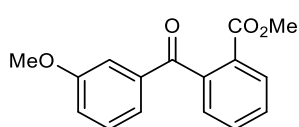
8. Characterisation of products



Bis(3-methoxyphenyl)methanone, 3a.² 1-Bromo-3-methoxybenzene (50 mg, 0.26 mmol) was reacted with (3-methoxyphenyl)boronic acid (48 mg, 0.32 mmol) according to the general procedure A to provide the product (57 mg, 89%) as red oil. ¹H NMR (400 MHz, CDCl₃): δ = 7.24-7.20 (m, 6H), 7.00-6.99

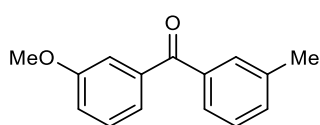
(m, 2H), 3.72 (s, 6H). ¹³C NMR (101 MHz, CDCl₃): δ = 196.6, 159.9, 139.3, 129.6, 123.2, 119.2, 114.7, 55.8.

HRMS (ESI): Calcd. for C₁₅H₁₄O₃Na [M+Na]⁺ 265.0835; found 265.0837.



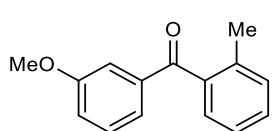
Methyl 2-(3-methoxybenzoyl)benzoate, 3b.³ 1-Bromo-3-methoxybenzene (50 mg, 0.26 mmol) was reacted with (2-(methoxycarbonyl)phenyl)boronic acid (57 mg, 0.32 mmol) according to the general procedure A to provide the product (25

mg, 40%) as yellow oil. ¹H NMR (400 MHz, CDCl₃): δ = 7.90 (d, *J* = 8.7 Hz, 1H), 7.61-7.46 (m, 1H), 7.46-7.33 (m, 1H), 7.28 (s, 2H), 7.21-7.08 (m, 1H), 7.05 (d, *J* = 7.7 Hz, 1H), 6.96 (dd, *J* = 8.7, 3.2 Hz, 1H), 3.70 (s, 3H), 3.50 (s, 3H). ¹³C NMR (101 MHz, CDCl₃): δ = 196.9, 166.5, 159.9, 141.8, 138.6, 132.5, 131.2, 130.1, 129.7, 129.6, 129.0, 127.8, 122.5, 119.8, 113.0, 55.5, 52.3. **HRMS (ESI):** Calcd. for C₁₆H₁₄O₄Na [M+Na]⁺ 293.0784; found 293.0787.



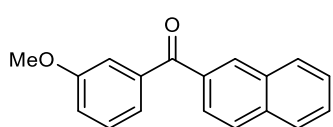
(3-Methoxyphenyl)(m-tolyl)methanone, 3c.⁴ 1-Bromo-3-methoxybenzene (50 mg, 0.26 mmol) was reacted with *m*-tolylboronic acid (44 mg, 0.32 mmol) according to the general procedure A to provide the product (48 mg, 80%) as

yellow oil. ¹H NMR (400 MHz, CDCl₃): δ = 7.63 (s, 1H), 7.58 (d, *J* = 7.3 Hz, 1H), 7.43-7.29 (m, 5H), 7.14-7.11 (m, 1H), 3.85 (s, 3H), 2.41 (s, 3H). ¹³C NMR (101 MHz, CDCl₃): δ = 196.8, 159.6, 139.1, 138.2, 137.7, 133.3, 130.5, 129.2, 128.1, 127.4, 122.9, 118.8, 114.4, 55.5, 21.4. **HRMS (ESI):** Calcd. for C₁₅H₁₄O₂Na [M+Na]⁺ 249.0886; found 249.0886.



(3-Methoxyphenyl)(o-tolyl)methanone, 3d.⁵ 1-Bromo-3-methoxybenzene (50 mg, 0.26 mmol) was reacted with *o*-tolylboronic acid (44 mg, 0.32 mmol) according to the general procedure A to provide the product (57 mg, 79%) as brown oil. ¹H NMR

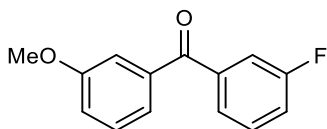
(400 MHz, CDCl₃): δ = 7.47-7.46 (m, 1H), 7.45-7.40 (m, 1H), 7.38-7.36 (m, 1H), 7.35-7.33 (m, 1H), 7.32-7.31 (m, 2H), 7.30-7.28 (m, 1H), 7.18-7.15 (m, 1H), 3.88 (s, 3H), 2.38 (s, 3H). ¹³C NMR (101 MHz, CDCl₃): δ = 198.5, 159.8, 139.2, 138.7, 136.8, 131.1, 130.3, 129.5, 128.5, 125.3, 123.4, 119.9, 113.9, 55.5. **HRMS (ESI):** Calcd. for C₁₅H₁₄O₂Na [M+Na]⁺ 249.0886; found 249.0886.



(3-Methoxyphenyl)(naphthalen-2-yl)methanone, 3e.⁶ 1-Bromo-3-methoxybenzene (50 mg, 0.26 mmol) was reacted with naphthalen-2-ylboronic acid (55 mg, 0.32 mmol) according to the general procedure A to provide the

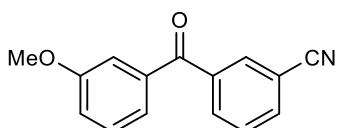
product (53 mg, 79%) as yellow oil. ¹H NMR (400 MHz, CDCl₃): δ = 8.29 (s, 1H), 7.94-7.5 (m, 2H), 7.94-7.88

(m, 2H), 7.61 (t, $J = 7.5$ Hz, 1H), 7.55 (t, $J = 7.5$ Hz, 1H), 7.43-7.40 (m, 3H), 7.22-7.10 (m, 1H), 3.87 (s, 3H). ^{13}C NMR (101 MHz, CDCl_3): $\delta = 196.6, 159.7, 139.3, 135.4, 134.9, 132.3, 131.9, 129.5, 129.4, 128.4, 128.4, 127.9, 126.9, 125.9, 123.0, 118.9, 114.5, 55.6$. HRMS (ESI): Calcd. for $\text{C}_{18}\text{H}_{14}\text{O}_2\text{Na}$ $[\text{M}+\text{Na}]^+$ 285.0886; found 285.0889.



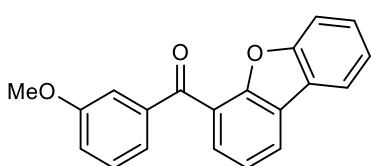
(3-Fluorophenyl)(3-methoxyphenyl)methanone, 3f.⁷ 1-Bromo-3-methoxybenzene (50 mg, 0.26 mmol) was reacted with (3-fluorophenyl)boronic acid (44 mg, 0.32 mmol) according to the general procedure A to provide the product (59 mg, 96%) as yellow oil. ^1H NMR (400

MHz, CDCl_3): $\delta = 7.58$ (d, $J = 7.7$ Hz, 1H), 7.51-7.49 (m 1H), 7.48-7.43 (m, 1H), 7.41-7.37 (m, 1H), 7.35 (s, 1H), 7.33 (s, 1H), 7.32-7.27 (m, 1H), 7.15 (dd, $J = 8.1, 3.7$ Hz, 1H), 3.86 (s, 3H). ^{13}C NMR (101 MHz, CDCl_3): $\delta = 195.2$ (d, $J = 2.3$ Hz), 162.6 (d, $J = 248.2$ Hz), 159.8, 139.8 (d, $J = 6.4$ Hz), 138.5, 130.1 (d, $J = 7.7$ Hz), 129.5, 125.9 (d, $J = 3.2$ Hz), 122.9, 119.6 (d, $J = 21.3$ Hz), 119.3, 116.9 (d, $J = 22.6$ Hz), 114.4, 55.6. HRMS (ESI): Calcd. for $\text{C}_{14}\text{H}_{11}\text{O}_2\text{FNa}$ $[\text{M}+\text{Na}]^+$ 253.0635; found 253.0637.



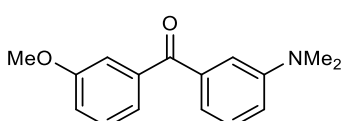
3-(3-Methoxybenzoyl)benzonitrile, 3g.⁸ 1-Bromo-3-methoxybenzene (50 mg, 0.26 mmol) was reacted with (3-cyanophenyl)boronic acid (47 mg, 0.32 mmol) according to the general procedure A to provide the product (45 mg, 71%) as yellow oil. ^1H NMR (400 MHz, CDCl_3): $\delta = 8.06$ (s, 1H), 8.02 (d, $J = 7.9$ Hz, 1H),

7.85 (d, $J = 7.9$ Hz, 1H), 7.62 (t, $J = 7.8$ Hz, 1H), 7.40 (t, $J = 7.8$ Hz, 1H), 7.32 (s, 1H), 7.28-7.25 (m, 1H), 7.18-7.15 (m, 1H), 3.86 (s, 3H). ^{13}C NMR (101 MHz, CDCl_3): $\delta = 194.3, 159.9, 138.8, 137.7, 135.4, 133.9, 133.5, 129.7, 129.5, 122.8, 119.7, 118.0, 114.4, 112.9, 55.6$. HRMS (ESI): Calcd. for $\text{C}_{15}\text{H}_{12}\text{NO}_2$ $[\text{M}+\text{H}]^+$ 238.0863; found 238.0882.



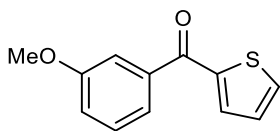
Dibenzob[d]furan-4-yl(3-methoxyphenyl)methanone, 3h. 1-Bromo-3-methoxybenzene (50 mg, 0.26 mmol) was reacted with dibenzob[d]furan-4-ylboronic acid (68 mg, 0.32 mmol) according to the general procedure A to provide the product (76 mg, 95%) as orange oil. ^1H NMR (400 MHz,

CDCl_3): $\delta = 8.15$ (d, $J = 8.8$ Hz, 1H), 8.00 (d, $J = 8.2$ Hz, 1H), 7.70 (d, $J = 8.8$ Hz, 1H), 7.56 (d, $J = 8.2$ Hz, 1H), 7.52-7.51 (m, 1H), 7.49-7.45 (m, 1H), 7.44-7.43 (m, 1H), 7.42-7.41 (m, 1H), 7.40-7.35 (m, 2H), 7.18-7.16 (m, 1H), 3.86 (s, 3H). ^{13}C NMR (101 MHz, CDCl_3): $\delta = 193.8, 159.8, 156.5, 154.0, 139.1, 129.4, 128.7, 127.9, 125.7, 124.2, 123.5, 123.4, 123.3, 122.5, 120.8, 119.9, 114.2, 112.3, 55.6$. IR (ATR, cm^{-1}) $\nu = 2959$ (s), 2929 (s), 1873 (m), 1719 (s), 1614 (w), 1462 (w), 1369 (s), 1294 (s), 1261 (s), 1171 (s), 1123 (s), 780 (s). HRMS (ESI): Calcd. for $\text{C}_{20}\text{H}_{14}\text{O}_3\text{Na}$ $[\text{M}+\text{Na}]^+$ 325.0835; found 325.0840.



3-(Dimethylamino)phenyl(3-methoxyphenyl)methanone, 3i. 1-Bromo-3-methoxybenzene (50 mg, 0.26 mmol) was reacted with 3-((dimethylamino)phenyl)boronic acid (53 mg, 0.32 mmol) according to the

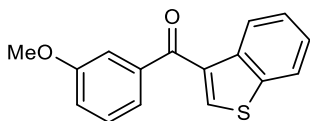
general procedure A to provide the product (56 mg, 82%) as yellow oil. $^1\text{H NMR}$ (400 MHz, CDCl_3): δ = 7.30-7.27 (m, 3H), 7.24-7.14 (m, 1H), 7.09-7.08 (m, 1H), 7.04-6.99 (m, 1H), 6.97 (d, J = 7.6 Hz, 1H), 6.85-7.83 (m, 1H), 3.76 (s, 3H), 2.90 (s, 6H). $^{13}\text{C NMR}$ (101 MHz, CDCl_3): δ = 197.6, 159.7, 150.8, 139.7, 138.7, 129.5, 129.1, 123.3, 119.1, 119.1, 116.8, 114.8, 113.6, 55.9, 40.9. **HRMS (ESI)**: Calcd. for $\text{C}_{16}\text{H}_{17}\text{O}_2\text{NNa}$ [$\text{M}+\text{Na}$] $^+$ 278.1151; found 278.1156.



(3-Methoxyphenyl)(thiophen-3-yl)methanone, 3j.⁹ 1-Bromo-3-methoxybenzene

(50 mg, 0.26 mmol) was reacted with thiophen-2-ylboronic acid (41 mg, 0.32 mmol) according to the general procedure A to provide the product (45 mg, 77%) as orange oil. $^1\text{H NMR}$ (400 MHz, CDCl_3): δ = 7.72 (d, J = 6.1 Hz, 1H), 7.67 (d, J = 4.9 Hz,

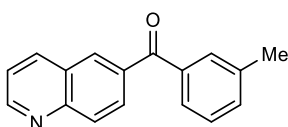
1H), 7.47-7.41 (m, 1H), 7.40-7.38 (m, 2H), 7.17-7.15 (m, 1H), 7.14-7.12 (m, 1H), 3.87 (s, 3H). $^{13}\text{C NMR}$ (101 MHz, CDCl_3): δ = 188.1, 159.7, 143.7, 139.6, 135.0, 134.4, 129.5, 128.1, 121.9, 118.8, 113.9, 55.6. **HRMS (ESI)**: Calcd. for $\text{C}_{12}\text{H}_{10}\text{O}_2\text{NaS}$ [$\text{M}+\text{Na}$] $^+$ 241.0294; found 241.0295.



Benzo[b]thiophen-3-yl(3-methoxyphenyl)methanone, 3k. 1-Bromo-3-

methoxybenzene (50 mg, 0.26 mmol) was reacted with benzo[b]thiophen-3-ylboronic acid (57 mg, 0.32 mmol) according to the general procedure A to provide the product (47 mg, 80%) as orange oil. $^1\text{H NMR}$ (400 MHz, CDCl_3): δ 8.58

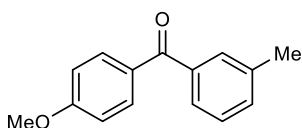
(d, J = 8.2 Hz, 1H), 8.02 (s, 1H), 7.90 (d, J = 8.2 Hz, 1H), 7.52 (t, J = 8.2 Hz, 1H), 7.47-7.43 (m, 1H), 7.40-7.42 (m, 2H), 7.17-7.15 (m, 1H), 7.14-7.12 (m, 1H), 3.87 (s, 3H). $^{13}\text{C NMR}$ (101 MHz, CDCl_3): δ = 190.6, 159.8, 140.7, 140.1, 138.4, 137.5, 134.8, 129.5, 125.8, 125.7, 125.3, 122.4, 122.3, 118.8, 114.0, 55.6. **HRMS (ESI)**: Calcd. for $\text{C}_{16}\text{H}_{12}\text{O}_2\text{NaS}$ [$\text{M}+\text{Na}$] $^+$ 291.0450; found 291.0453.



Quinolin-6-yl(m-tolyl)methanone, 3l. 6-Bromoquinoline (50 mg, 0.24 mmol) was

reacted with *m*-tolylboronic acid (39 mg, 0.29 mmol) according to the general procedure A to provide the product (54 mg, 91%) as yellow oil. $^1\text{H NMR}$ (400 MHz,

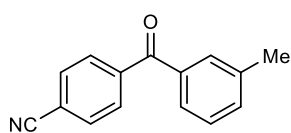
CDCl_3): δ = 9.02 (d, J = 5.9 Hz, 1H), 8.25 (s, 1H), 8.22-8.21 (m, 1H), 8.19 (s, 1H), 8.15-8.13 (m, 1H), 7.67 (s, 1H), 7.61 (d, J = 7.4 Hz, 1H), 7.48 (dd, J = 8.3, 4.2 Hz, 1H), 7.41 (dt, J = 14.9, 7.6 Hz, 2H), 2.43 (s, 3H). $^{13}\text{C NMR}$ (101 MHz, CDCl_3): δ = 196.4, 152.6, 149.9, 138.5, 137.6, 137.5, 135.8, 133.6, 131.4, 130.6, 129.9, 129.7, 128.4, 127.5, 127.4, 122.1, 21.5. **HRMS (ESI)**: Calcd. for $\text{C}_{17}\text{H}_{13}\text{ONNa}$ [$\text{M}+\text{Na}$] $^+$ 270.0889; found 270.0893.



(4-Methoxyphenyl)(m-tolyl)methanone, 3m.⁴ 1-Bromo-4-methoxybenzene (50

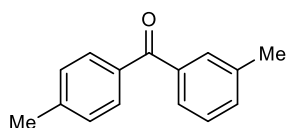
mg, 0.28 mmol) was reacted with *m*-tolylboronic acid (44 mg, 0.32 mmol) according to the general procedure A to provide the product (45 mg, 75%) as

yellow oil. $^1\text{H NMR}$ (400 MHz, CDCl_3): δ = 7.83 (d, J = 8.9 Hz, 2H), 7.58 (s, 1H), 7.53 (d, J = 7.0 Hz, 1H), 7.39-7.33 (m, 2H), 6.96 (d, J = 8.9 Hz, 2H), 3.89 (s, 3H), 2.42 (s, 3H). $^{13}\text{C NMR}$ (101 MHz, CDCl_3): δ = 195.9, 163.3, 138.5, 138.2, 132.8, 132.7, 130.4, 130.3, 128.1, 127.1, 113.6, 55.6, 21.5. **HRMS (ESI)**: Calcd. for $\text{C}_{15}\text{H}_{14}\text{O}_2\text{Na}$ [$\text{M}+\text{Na}$] $^+$ 249.0886; found 249.0890.



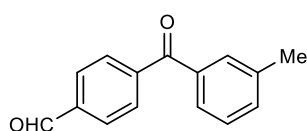
4-(3-Methylbenzoyl)benzonitrile, 3n.¹⁰ 4-Bromobenzonitrile (50 mg, 0.27 mmol) was reacted with *m*-tolylboronic acid (45 mg, 0.33 mmol) according to the general procedure A to provide the product (50 mg, 83%) as white solid. Mp 118-121 °C.

¹H NMR (400 MHz, CDCl₃): δ = 7.86 (d, *J* = 8.5 Hz, 2H), 7.78 (d, *J* = 8.5 Hz, 2H), 7.60 (s, 1H), 7.54 (d, *J* = 7.5 Hz, 1H), 7.45 (d, *J* = 7.5 Hz, 1H), 7.40-7.37 (m, 1H), 2.43 (s, 3H). **¹³C NMR (101 MHz, CDCl₃):** δ = 195.4, 141.5, 138.7, 136.5, 134.2, 132.3, 130.3, 128.6, 127.5, 118.2, 115.7, 21.5. **HRMS (ESI):** Calcd. for C₁₅H₁₂ON [M+H]⁺ 222.0913; found 222.0914.



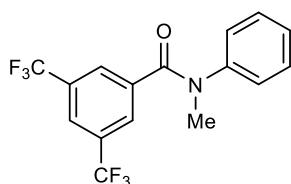
***m*-Tolyl(*p*-tolyl)methanone, 3o.**¹¹ 1-Bromo-4-methylbenzene (50 mg, 0.29 mmol) was reacted with *m*-tolylboronic acid (48 mg, 0.35 mmol) according to the general procedure A to provide the product (48 mg, 79%) as yellow oil. **¹H NMR (400 MHz, CDCl₃):** δ = 7.65 (d, *J* = 8.0 Hz, 2H), 7.54 (s, 1H), 7.50-7.48 (m, 1H), 7.34-7.28 (m, 2H), 7.21 (d, *J* = 8.0 Hz, 2H), 2.37 (s, 3H), 2.35 (s, 3H).

¹³C NMR (101 MHz, CDCl₃): δ = 196.8, 143.2, 138.1, 138.1, 135.1, 133.0, 130.4, 130.4, 129.0, 128.1, 127.3, 21.7, 21.5. **HRMS (ESI):** Calcd. for C₁₅H₁₄ONa [M+Na]⁺ 233.0937; found 233.0938.



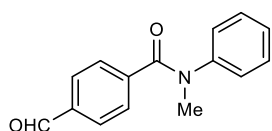
4-(3-Methylbenzoyl)benzaldehyde, 3p. 4-Bromobenzaldehyde (50 mg, 0.27 mmol) was reacted with *m*-tolylboronic acid (44 mg, 0.32 mmol) according to the general procedure A to provide the product (50 mg, 83%) as white solid. Mp 79-82 °C.

¹H NMR (400 MHz, CDCl₃): δ = 10.12 (s, 1H), 7.99 (d, *J* = 8.2 Hz, 2H), 7.90 (d, *J* = 8.2 Hz, 2H), 7.62 (s, 1H), 7.56 (d, *J* = 7.5 Hz, 1H), 7.43 (d, *J* = 7.5 Hz, 1H), 7.39-7.35 (m, 1H), 2.42 (s, 3H). **¹³C NMR (101 MHz, CDCl₃):** δ = 196.1, 191.7, 142.8, 138.6, 136.9, 134.0, 130.4, 129.6, 128.4, 127.5, 21.5. **HRMS (ESI):** Calcd. for C₁₅H₁₃O₂ [M+H]⁺ 225.0910; found 225.0907.



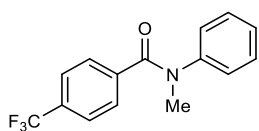
***N*-Methyl-*N*-phenyl-3,5-bis(trifluoromethyl)benzamide, 5a.** 1-Bromo-3,5-bis(trifluoromethyl)benzene (50 mg, 29.5 μl, 0.17 mmol) was reacted with *N*-methyl aniline (28 μl, 0.26 mmol) according to the general procedure B to provide the product (30 mg, 51%) as white solid. Mp 85-88 °C.

¹H NMR (400 MHz, CDCl₃): δ = 7.73 (s, 3H), 7.30-7.27 (m, 2H), 7.24-7.20 (m, 1H), 7.04 (d, *J* = 7.4 Hz, 2H), 3.54 (s, 3H). **¹³C NMR (101 MHz, CDCl₃):** δ = 167.3, 143.9, 137.9, 131.3 (q, *J* = 33.6 Hz), 130.8, 129.9, 129.3, 127.8, 127.1, 124.3, 123.7-122.8 (m), 121.6, 118.9, 38.6. **HRMS (ESI):** Calcd. for C₁₆H₁₁ONF₆Na [M+Na]⁺ 370.0637; found 370.0641.



4-Formyl-*N*-methyl-*N*-phenylbenzamide, 5b.¹² 4-Bromobenzaldehyde (50 mg, 0.27 mmol) was reacted with *N*-methyl aniline (43 μl, 0.43 mmol) according to the general procedure B to provide the product (66 mg, 99%) as colourless oil.

¹H NMR (400 MHz, CDCl₃): δ = 9.90 (s, 1H), 7.66 (d, *J* = 8.2 Hz, 2H), 7.42 (d, *J* = 8.2 Hz, 2H), 7.22-7.18 (m, 2H), 7.15-7.12 (m, 1H), 7.02-7.00 (d, *J* = 7.5 Hz, 2H), 3.49 (s, 3H). **¹³C NMR (101 MHz, CDCl₃):** δ = 191.6, 169.4, 144.2, 141.8, 136.5, 129.4, 129.2, 129.1, 127.1, 127.0, 38.3. **HRMS (ESI):** Calcd. for C₁₅H₁₄O₂N [M+H]⁺ 240.1019; found 240.1023.

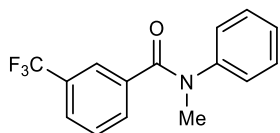


***N*-Methyl-*N*-phenyl-4-(trifluoromethyl)benzamide, 5c.**¹³ 4-Bromobenzotrifluoride

(50 mg, 31.1 μ l, 0.22 mmol) was reacted with *N*-methyl aniline (36 μ l, 0.33 mmol)

according to the general procedure B to provide the product (61 mg, 98%) as white

solid. Mp 80-83 °C. **¹H NMR (400 MHz, CDCl₃):** δ = 7.43-7.38 (m, 4H), 7.25-7.21 (m, 2H), 7.18-7.14 (m, 1H), 7.02 (d, J = 7.5 Hz, 2H), 3.50 (s, 3H). **¹³C NMR (101 MHz, CDCl₃):** δ = 169.2, 144.3, 139.6, 131.4 (q, J = 32.6 Hz), 129.5, 129.1, 127.8, 127.1, 127.0, 125.1, 124.9 (q, J = 3.8 Hz), 122.4, 119.7, 38.5. **HRMS (ESI):** Calcd. for C₁₅H₁₃ONF₃ [M+H]⁺ 280.0944; found 280.0948.

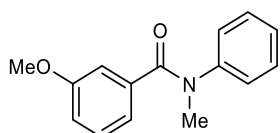


***N*-Methyl-*N*-phenyl-3-(trifluoromethyl)benzamide, 5d.**¹⁴ 3-Bromobenzotrifluoride

(50 mg, 36 μ l, 0.22 mmol) was reacted with *N*-methyl aniline (36 μ l, 0.33 mmol)

according to the general procedure B to provide the product (54 mg, 87%) as yellow

oil. **¹H NMR (400 MHz, CDCl₃):** δ = 7.53 (s, 1H), 7.43 (t, J = 6.6 Hz, 2H), 7.24-7.22 (m, 1H), 7.20 (d, J = 7.6 Hz, 2H), 7.15-7.12 (m, 1H), 7.00 (d, J = 7.6 Hz, 2H), 3.48 (s, 3H). **¹³C NMR (101 MHz, CDCl₃):** δ = 169.4, 144.4, 136.7, 132.0, 130.3 (q, J = 32.7 Hz), 129.8, 129.5, 128.4, 127.1, 127.0, 126.3 (q, J = 3.8 Hz), 125.9 (q, J = 3.8 Hz), 125.0, 122.3, 38.5. **HRMS (ESI):** Calcd. for C₁₅H₁₃ONF₃ [M+H]⁺ 280.0944; found 280.0948.

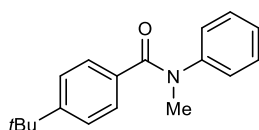


3-Methoxy-*N*-methyl-*N*-phenylbenzamide, 5e.¹⁵ 1-Bromo-3-methoxybenzene (50

mg, 33.8 μ l, 0.27 mmol) was reacted with *N*-methyl aniline (44 μ l, 0.43 mmol)

according to the general procedure B to provide the product (40 mg, 62%) as yellow

oil. **¹H NMR (400 MHz, CDCl₃):** δ = 7.24-7.20 (m, 2H), 7.15-7.11 (m, 1H), 7.06-7.02 (m, 3H), 6.86 (s, 1H), 6.84-6.82 (m, 1H), 6.77-6.75 (m, 1H), 3.64 (s, 3H), 3.48 (s, 3H). **¹³C NMR (101 MHz, CDCl₃):** δ = 170.5, 159.0, 145.0, 137.2, 129.2, 128.8, 126.9, 126.6, 121.3, 116.1, 113.8, 55.3, 38.5. **HRMS (ESI):** Calcd. for C₁₅H₁₅O₂NNa [M+Na]⁺ 264.0995; found 264.0997.

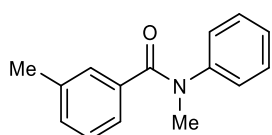


4-(*tert*-Butyl)-*N*-methyl-*N*-phenylbenzamide, 5f.¹⁶ 1-Bromo-4-(*tert*-butyl)benzene

(50 mg, 40.7 μ l, 0.23 mmol) was reacted with *N*-methyl aniline (38 μ l, 0.35 mmol)

according to the general procedure B to provide the product (22 mg, 35%) as white

solid. Mp 100-103 °C. **¹H NMR (400 MHz, CDCl₃):** δ = 7.25-7.22 (m, 4H), 7.18 (s, 1H), 7.17-7.12 (m, 2H), 7.05 (d, J = 7.3 Hz, 2H), 3.49 (s, 3H), 1.22 (s, 9H). **¹³C NMR (101 MHz, CDCl₃):** δ = 170.7, 153.0, 145.3, 132.9, 129.2, 128.8, 127.0, 126.5, 124.7, 38.7, 34.8, 31.4, 31.2. **HRMS (ESI):** Calcd. for C₁₈H₂₁ONNa [M+Na]⁺ 290.1515; found 290.1526.

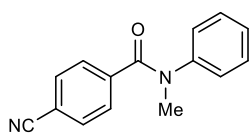


***N*,3-Dimethyl-*N*-phenylbenzamide, 5g.**¹⁷ 1-Bromo-3-methylbenzene (50 mg, 35.6 μ l,

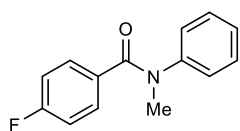
0.29 mmol) was reacted with *N*-methyl aniline (47 μ l, 0.43 mmol) according to the

general procedure B to provide the product (42 mg, 64%) as yellow oil. **¹H NMR (400**

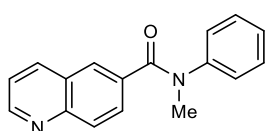
MHz, CDCl₃): δ = 7.24-7.20 (m, 3H), 7.14-7.11 (m, 1H), 7.04-7.02 (m, 3H), 7.00-6.99 (m, 2H), 3.48 (s, 3H), 2.21 (s, 3H). **¹³C NMR (101 MHz, CDCl₃):** δ = 170.9, 145.1, 137.6, 135.9, 130.4, 129.5, 129.2, 127.5, 127.0, 126.5, 125.8, 38.5, 21.3. **HRMS (ESI):** Calcd. for C₁₅H₁₅ONNa [M+Na]⁺ 248.1046; found 248.1050.



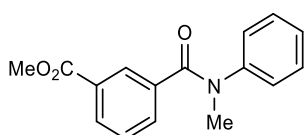
4-Cyano-N-methyl-N-phenylbenzamide, 5h.¹⁸ 4-Bromobenzonitrile (50 mg, 0.27 mmol) was reacted with *N*-methyl aniline (45 μ l, 0.43 mmol) according to the general procedure B to provide the product (63 mg, 97%) as colourless oil. **¹H NMR (400 MHz, CDCl₃):** δ = 7.43 (d, *J* = 8.4 Hz, 2H), 7.35 (d, *J* = 8.4 Hz, 2H), 7.24-7.20 (m, 2H), 7.17-7.13 (m, 1H), 7.00-6.98 (d, *J* = 7.5 Hz, 2H), 3.47 (s, 3H). **¹³C NMR (101 MHz, CDCl₃):** δ = 168.3, 143.6, 140.0, 131.3, 129.2, 128.9, 126.9, 126.6, 117.8, 112.8, 38.0. **HRMS (ESI):** Calcd. for C₁₅H₁₃ON₂ [M+H]⁺ 237.1022; found 237.1033.



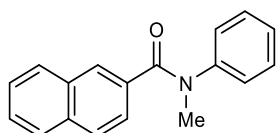
4-Fluoro-N-methyl-N-phenylbenzamide, 5i.¹⁵ 1-Bromo-4-fluorobenzene (50 mg, 32 μ l, 0.28 mmol) was reacted with *N*-methyl aniline (46.4 μ l, 0.43 mmol) according to the general procedure B to provide the product (53 mg, 81%) as orange oil. **¹H NMR (400 MHz, CDCl₃):** δ = 7.32-7.30 (m, 2H), 7.28-7.22 (m, 2H), 7.18-7.15 (m, 1H), 7.03-7.02 (m, 2H), 6.84 (t, *J* = 8.7 Hz, 2H), 3.49 (s, 3H). **¹³C NMR (101 MHz, CDCl₃):** δ = 169.7, 163.3 (d, *J* = 250.2 Hz), 145.0, 132.0, 132.0, 131.2 (d, *J* = 8.6 Hz), 129.4, 127.0, 126.8, 114.9 (d, *J* = 21.8 Hz), 38.6. **HRMS (ESI):** Calcd. for C₁₄H₁₂ONFNa [M+Na]⁺ 252.0795; found 252.0798.



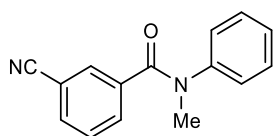
N-Methyl-N-phenylquinoline-6-carboxamide, 5j.¹⁹ 6-Bromo-quinoline (50 mg, 32.5 μ l, 0.24 mmol) was reacted with *N*-methyl aniline (39 μ l, 0.35 mmol) according to the general procedure B to provide the product (41mg, 65%) as colourless oil. **¹H NMR (400 MHz, CDCl₃):** δ = 8.88 (d, *J* = 5.9 Hz, 1H), 8.03 (d, *J* = 9.0 Hz, 1H), 7.88 (s, 1H), 7.84 (d, *J* = 8.8 Hz, 1H), 7.53 (d, *J* = 8.8 Hz, 1H), 7.36 (dd, *J* = 8.3, 4.2 Hz, 1H), 7.22-7.18 (m, 2H), 7.13-7.12 (m, 1H), 7.08-7.06 (m, 2H), 3.56 (s, 3H). **¹³C NMR (101 MHz, CDCl₃):** δ = 169.9, 151.6, 148.3, 144.7, 136.8, 134.3, 129.5, 129.3, 129.3, 128.9, 127.5, 127.1, 126.9, 121.7, 38.7. **HRMS (ESI):** Calcd. for C₁₇H₁₄ON₂Na [M+Na]⁺ 285.0998; found 285.1004.



Methyl 3-(methyl(phenyl)carbamoyl)benzoate, 5k. Methyl 3-bromobenzoate (50 mg, 0.23 mmol) was reacted with *N*-methyl aniline (38 μ l, 0.35 mmol) according to the general procedure B to provide the product (52 mg, 83%) as colourless oil. **¹H NMR (400 MHz, CDCl₃):** δ = 8.00 (s, 1H), 7.89 (d, *J* = 7.8 Hz, 1H), 7.43 (d, *J* = 7.8 Hz, 1H), 7.22-7.18 (m, 2H), 7.15-7.11 (m, 2H), 7.03 (d, *J* = 7.4 Hz, 2H), 3.83 (s, 3H), 3.49 (s, 3H). **¹³C NMR (101 MHz, CDCl₃):** δ = 169.7, 166.3, 144.6, 136.4, 132.9, 130.7, 130.1, 129.9, 129.4, 128.0, 127.1, 126.9, 52.3, 38.5. **HRMS (ESI):** Calcd. for C₁₆H₁₅O₃NNa [M+Na]⁺ 292.0944; found 292.0949.

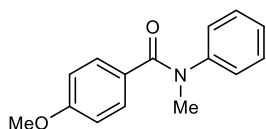


N-Methyl-N-phenyl-2-naphthamide, 5l.¹⁷ 2-Bromonaphthalene (50 mg, 0.24 mmol) was reacted with *N*-methyl aniline (40 μ l, 0.40 mmol) according to the general procedure B to provide the product (64 mg, 99%) as colourless oil. **¹H NMR (400 MHz, CDCl₃):** δ = 7.91 (s, 1H), 7.71 (d, *J* = 7.8 Hz, 2H), 7.59 (d, *J* = 8.6 Hz, 1H), 7.47-7.40 (m, 2H), 7.33 (d, *J* = 8.5 Hz, 1H), 7.21-7.17 (m, 2H), 7.12-7.07 (m, 3H), 3.56 (s, 3H). **¹³C NMR (101 MHz, CDCl₃):** δ = 170.3, 144.7, 133.3, 133.0, 132.1, 129.2, 129.0, 128.4, 127.3, 127.0, 126.9, 126.6, 126.2, 126.0, 125.2, 38.3. **HRMS (ESI):** Calcd. for C₁₈H₁₅ONNa [M+Na]⁺ 284.1046; found 284.1051.



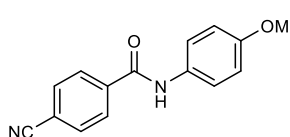
3-Cyano-N-methyl-N-phenylbenzamide, 5m. 3-Bromobenzonitrile (50 mg, 0.27 mmol) was reacted with *N*-methyl aniline (45 μ l, 0.43 mmol) according to the general procedure B to provide the product (61 mg, 94%) as white solid. Mp 72-75

$^1\text{H NMR}$ (400 MHz, CDCl_3): δ = 7.54 (s, 1H), 7.48-7.45 (m, 2H), 7.24-7.20 (m, 3H), 7.17-7.15 (m, 1H), 6.99 (d, J = 7.6 Hz, 2H), 3.46 (s, 3H). $^{13}\text{C NMR}$ (101 MHz, CDCl_3): δ = 168.2, 144.0, 137.3, 133.0, 132.9, 132.4, 129.6, 128.8, 127.4, 127.0, 118.1, 112.2, 38.5. **HRMS (ESI):** Calcd. for $\text{C}_{15}\text{H}_{13}\text{ON}_2$ $[\text{M}+\text{H}]^+$ 237.1022; found 237.1033.



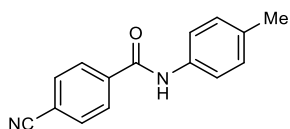
4-Methoxy-N-methyl-N-phenylbenzamide, 5n.¹³ 1-Bromo-4-methoxybenzene (50 mg, 33.5 μ l, 0.27 mmol) was reacted with *N*-methyl aniline (44 μ l, 0.43 mmol) according to the general procedure B to provide the product (10 mg, 16%) as yellow

oil. $^1\text{H NMR}$ (400 MHz, CDCl_3): δ = 7.27-7.23 (m, 2H), 7.21 (d, J = 7.9 Hz, 2H), 7.13 (t, J = 7.4 Hz, 1H), 7.02 (d, J = 8.2 Hz, 2H), 6.64 (d, J = 8.9 Hz, 2H), 3.72 (s, 3H), 3.47 (s, 3H). $^{13}\text{C NMR}$ (101 MHz, CDCl_3): δ = 170.4, 160.7, 145.6, 131.0, 129.3, 128.1, 127.0, 126.4, 113.1, 55.3, 38.8. **HRMS (ESI):** Calcd. for $\text{C}_{15}\text{H}_{15}\text{O}_2\text{NNa}$ $[\text{M}+\text{Na}]^+$ 264.0995; found 264.0997.



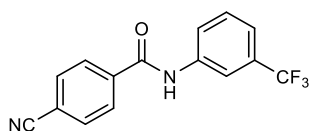
4-Cyano-N-(4-methoxyphenyl)benzamide, 5o.²⁰ 4-Bromobenzonitrile (50 mg, 0.27 mmol) was reacted with *p*-anisidine (50 mg, 0.41 mmol) according to the general procedure B to provide the product (60 mg, 87%) as white solid. Mp 157-

160 $^{\circ}\text{C}$. $^1\text{H NMR}$ (400 MHz, CDCl_3): δ = 7.96 (d, J = 8.4 Hz, 2H), 7.78-7.76 (m, 3H), 7.52 (d, J = 8.4 Hz, 2H), 6.92 (d, J = 8.9 Hz, 2H), 3.82 (s, 3H). $^{13}\text{C NMR}$ (101 MHz, CDCl_3): δ = 163.9, 157.2, 139.1, 132.7, 130.4, 127.9, 122.4, 118.1, 114.5, 55.7. **HRMS (ESI):** Calcd. for $\text{C}_{15}\text{H}_{12}\text{O}_2\text{N}_2\text{Na}$ $[\text{M}+\text{Na}]^+$ 275.0791; found 275.0795.



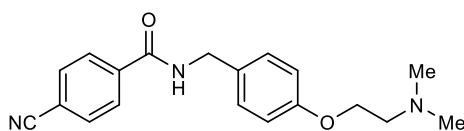
4-Cyano-N-(*p*-tolyl)benzamide, 5p.²¹ 4-Bromobenzonitrile (50 mg, 0.27 mmol) was reacted with *p*-toluidine (44 mg, 0.41 mmol) according to the general procedure B to provide the product (60 mg, 90%) as white solid. Mp 178-180 $^{\circ}\text{C}$. $^1\text{H NMR}$ (400

MHz, CDCl_3): δ = 7.96 (d, J = 8.2 Hz, 2H), 7.81 (bs, 1H), 7.77 (d, J = 8.3 Hz, 2H), 7.50 (d, J = 8.2 Hz, 2H), 7.19 (d, J = 8.3 Hz, 2H), 2.35 (s, 3H). $^{13}\text{C NMR}$ (101 MHz, CDCl_3): δ = 162.3, 139.1, 135.2, 134.8, 132.7, 129.9, 127.9, 120.6, 118.1, 115.5, 21.1. **HRMS (ESI):** Calcd. for $\text{C}_{15}\text{H}_{12}\text{ON}_2$ $[\text{M}+\text{Na}]^+$ 237.1022; found 237.1024.



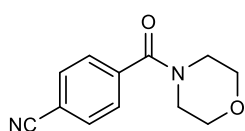
4-Cyano-N-(3-(trifluoromethyl)phenyl)benzamide, 5q. 4-Bromobenzonitrile (50 mg, 0.27 mmol) was reacted with 3-(trifluoromethyl)aniline (51.4 μ l, 0.41 mmol) according to the general procedure B to provide the product (68 mg, 85%) as

white solid. Mp 166-168 $^{\circ}\text{C}$. $^1\text{H NMR}$ (400 MHz, CDCl_3): δ = 8.01 (m, 3H), 7.93 (s, 1H), 7.86 (d, J = 8.1 Hz, 1H), 7.80 (d, J = 8.3 Hz, 2H), 7.52 (t, J = 7.9 Hz, 1H), 7.47-7.44 (m, 1H). $^{13}\text{C NMR}$ (101 MHz, CDCl_3): δ = 164.2, 138.4, 137.9, 132.9, 131.8 (d, J = 32.7 Hz), 130.0, 127.9, 123.6, 121.9 (d, J = 3.7 Hz), 117.9, 117.3 (d, J = 4.0 Hz), 115.9. **HRMS (ESI):** Calcd. for $\text{C}_{15}\text{H}_8\text{OF}_3\text{N}_2$ $[\text{M}-\text{H}]^-$ 289.0594; found 289.0587.



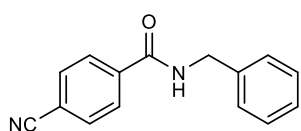
4-Cyano-N-(4-(2-(dimethylamino)ethoxy)benzyl)benzamide, 5r.

4-Bromobenzonitrile (50 mg, 0.27 mmol) was reacted with 2-(4-(aminomethyl)phenoxy)-*N,N*-dimethylethan-1-amine (80 mg, 0.41 mmol) according to the general procedure B to provide the product (80 mg, 90%) as white solid. Mp 109-112 °C. **¹H NMR (400 MHz, CDCl₃):** δ = 7.87 (d, *J* = 8.5 Hz, 2H), 7.72-7.25 (d, *J* = 8.5 Hz, 2H), 7.25 (m, 2H), 6.90 (d, *J* = 8.7 Hz, 2H), 6.45 (bs, 1H), 4.57 (d, *J* = 5.5 Hz, 2H), 4.08 (t, *J* = 5.6 Hz, 2H), 2.78 (t, *J* = 5.6 Hz, 2H), 2.38 (s, 6H). **¹³C NMR (101 MHz, CDCl₃):** δ = 165.6, 158.6, 138.5, 132.6, 129.9, 129.5, 127.8, 118.1, 115.3, 115.1, 66.0, 58.2, 45.9, 44.1. **HRMS (ESI):** Calcd. for C₁₉H₂₂O₂N₃ [M+H]⁺ 324.1707; found 324.1714.



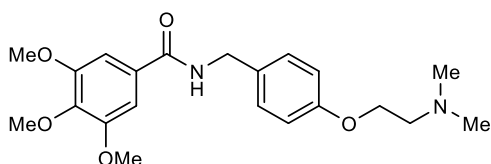
4-(Morpholine-4-carbonyl)benzonitrile, 5s.²²

4-Bromobenzonitrile (50 mg, 0.27 mmol) was reacted with morpholine (36 μl, 0.41 mmol) according to the general procedure B to provide the product (55 mg, 93%) as white solid. Mp 143-145.6 °C. **¹H NMR (400 MHz, CDCl₃):** δ = 7.70 (d, *J* = 8.4 Hz, 2H), 7.49 (d, *J* = 8.4 Hz, 2H), 3.75-3.60 (m, 6H), 3.41-3.35 (m, 2H). **¹³C NMR (101 MHz, CDCl₃):** δ = 165.8, 138.3, 137.7, 132.5, 128.9, 127.9, 127.9, 127.8, 118.1, 115.1, 44.3. **HRMS (ESI):** Calcd. for C₁₂H₁₂O₂N₂Na [M+Na]⁺ 239.0791; found 239.0809.



N-Benzyl-4-cyanobenzamide, 5t.²³

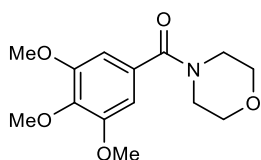
4-Bromobenzonitrile (50 mg, 0.27 mmol) was reacted with phenylmethanamine (45 μl, 0.41 mmol) according to the general procedure B to provide the product (61 mg, 94%) as white solid. Mp 148-150 °C. **¹H NMR (400 MHz, CDCl₃):** δ = 7.85 (d, *J* = 8.5 Hz, 2H), 7.65 (d, *J* = 8.5 Hz, 2H), 7.36-7.27 (m, 5H), 6.93 (bs, 1H), 4.59 (d, *J* = 5.7 Hz, 2H). **¹³C NMR (101 MHz, CDCl₃):** δ = 165.8, 138.3, 137.7, 132.5, 128.9, 127.9, 127.9, 127.8, 118.1, 115.1, 44.3. **HRMS (ESI):** Calcd. for C₁₅H₁₂ON₂Na [M+Na]⁺ 259.0842; found 259.0841.



N-(4-(2-(Dimethylamino)ethoxy)benzyl)-3,4,5-

trimethoxybenzamide, 5u.

5-Bromo-1,2,3-trimethoxybenzene (50 mg, 0.20 mmol) was reacted with 2-(4-(aminomethyl)phenoxy)-*N,N*-dimethylethan-1-amine (78 mg, 0.40 mmol) and XantPhos Pd G3 (38 mg, 2 mol%) according to the general procedure B to provide the product (75 mg, 95%) as white solid. Mp 105-108 °C. **¹H NMR (400 MHz, CDCl₃):** δ = 7.22 (d, *J* = 8.6 Hz, 2H), 7.04 (s, 2H), 6.89 (bs, 1H), 6.82 (d, *J* = 8.6 Hz, 2H), 4.49 (d, *J* = 5.7 Hz, 2H), 4.07 (t, *J* = 5.5 Hz, 2H), 3.82 (s, 9H), 2.82 (t, *J* = 5.5 Hz, 2H), 2.39 (s, 6H). **¹³C NMR (101 MHz, CDCl₃):** δ = 167.0, 158.0, 153.1, 140.8, 130.9, 129.9, 129.3, 114.7, 104.6, 65.4, 60.9, 58.0, 56.6, 45.5, 43.6. **HRMS (ESI):** Calcd. for C₂₁H₂₉O₅N₂ [M+H]⁺ 389.2071; found 389.2080.



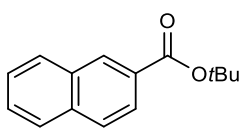
Morpholino(3,4,5-trimethoxyphenyl)methanone,

5v.²⁴

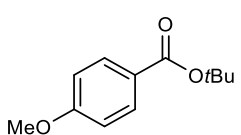
5-Bromo-1,2,3-

trimethoxybenzene (50 mg, 0.20 mmol) was reacted with morpholine (36 μl, 0.40 mmol) and XantPhos Pd G3 (38 mg, 2 mol%) according to the general procedure B to provide the product (55 mg, 96%) as white solid. Mp 116-118 °C. **¹H NMR (400 MHz,**

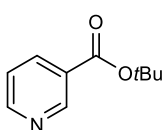
CDCl₃): δ = 6.59 (s, 2H), 3.84-3.82 (m, 10H), 3.65 (bs, 7H). **¹³C NMR (101 MHz, CDCl₃)**: δ = 170.5, 153.7, 139.7, 131.0, 104.7, 67.3, 61.3, 56.6. **HRMS (ESI)**: Calcd. for C₁₄H₁₉O₅NNa [M+Na]⁺ 304.1155; found 304.1165.



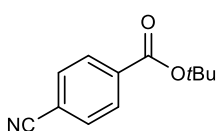
tert-Butyl 2-naphthoate, 7a.²⁵ 2-Bromonaphthalen (50 mg, 0.24 mmol) was reacted with tBuONa (34 mg, 0.35 mmol) according to the general procedure C to provide the product (51 mg, 93%) as yellow oil. **¹H NMR (400 MHz, CDCl₃)**: δ = 8.56 (s, 1H), 8.06-8.03 (m, 1H), 7.95 (d, J = 7.9 Hz, 1H), 7.87-7.85 (m, 2H), 7.62-7.47 (m, 2H), 1.67 (s, 9H). **¹³C NMR (101 MHz, CDCl₃)**: δ = 166.0, 135.4, 132.6, 130.8, 129.4, 128.0, 128.0, 127.8, 126.6, 125.5, 81.2, 28.4. **HRMS (ESI)**: Calcd. for C₁₅H₁₆O₂Na [M+Na]⁺ 251.1043; found 251.1044.



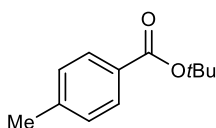
tert-Butyl 4-methoxybenzoate, 7b.²⁵ 1-Bromo-4-methoxybenzene (50 mg, 33.5 μ l, 0.27 mmol) was reacted with tBuONa (39 mg, 0.36 mmol) according to the general procedure C to provide the product (54 mg, 98%) as colourless oil. **¹H NMR (400 MHz, CDCl₃)**: δ = 7.94 (d, J = 8.8 Hz, 2H), 6.89 (d, J = 8.8 Hz, 2H), 3.84 (s, 3H), 1.58 (s, 9H). **¹³C NMR (101 MHz, CDCl₃)**: δ = 165.7, 163.1, 131.5, 124.6, 113.5, 80.6, 55.5, 28.4. **HRMS (ESI)**: Calcd. for C₁₂H₁₆O₃Na [M+Na]⁺ 231.0992; found 231.0988.



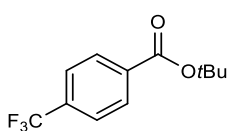
tert-Butyl nicotinate, 7c.²⁵ 3-Bromopyridine (50mg, 30.5 μ l, 0.32 mmol) was reacted with tBuONa (46 mg, 0.48 mmol) according to the general procedure C to provide the product (29 mg, 52%) as yellow oil. **¹H NMR (400 MHz, CDCl₃)**: δ = 9.15 (s, 1H), 8.73-8.72 (m, 1H), 8.22 (d, J = 7.9 Hz, 1H), 7.45-7.30 (m, 1H), 1.59 (s, 9H). **¹³C NMR (101 MHz, CDCl₃)**: δ = 164.5, 153.0, 151.0, 137.0, 127.9, 123.3, 82.2, 28.3. **HRMS (ESI)**: Calcd. for C₁₀H₁₄O₂N [M+H]⁺ 180.1019; found 180.1014.



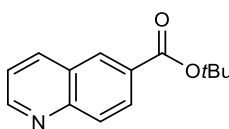
tert-Butyl 4-cyanobenzoate, 7d.²⁵ 1-Bromo-4-benzonitrile (50mg, 0.27 mmol) was reacted with tBuONa (40 mg, 0.48 mmol) according to the general procedure C to provide the product (25 mg, 45%) as colourless oil. **¹H NMR (400 MHz, CDCl₃)**: δ = 8.07 (d, J = 8.5 Hz, 2H), 7.71 (d, J = 8.5 Hz, 2H), 1.60 (s, 9H). **¹³C NMR (101 MHz, CDCl₃)**: δ = 164.4, 136.3, 132.5, 130.4, 118.6, 116.3, 82.8, 28.5. **HRMS (ESI)**: Calcd. for C₁₂H₁₃O₂NNa [M+Na]⁺ 226.0838; found 226.0855.



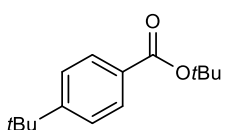
tert-Butyl 4-methylbenzoate, 7e.²⁶ 1-Bromo-4-methylbenzene (50mg, 0.27 mmol) was reacted with tBuONa (42 mg, 0.43 mmol) according to the general procedure C to provide the product (50 mg, 80%) as yellow oil. **¹H NMR (101 MHz, CDCl₃)**: δ = 7.88 (d, J = 8.0 Hz, 2H), 7.21 (d, J = 8.0 Hz, 2H), 2.39 (s, 3H), 1.59 (s, 9H). **¹³C NMR (101 MHz, CDCl₃)**: δ = 166.3, 143.3, 129.9, 129.3, 81.1, 28.7, 22.0. **HRMS (ESI)**: Calcd. for C₁₂H₁₆O₂Na [M+Na]⁺ 215.1043; found 215.1038.



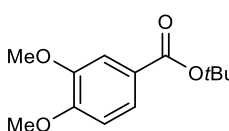
tert-butyl 4-(trifluoromethyl)benzoate, 7f.²⁵ 4-Bromobenzotrifluoride (50 mg, 31.1 μ l, 0.22 mmol) was reacted with tBuONa (40 mg, 0.48 mmol) according to the general procedure C to provide the product (28 mg, 51%) as yellow oil. ¹H NMR (101 MHz, CDCl₃): δ 8.10 (d, J = 8.2 Hz, 2H), 7.68 (d, J = 8.2 Hz, 2H), 1.61 (s, 9H). ¹³C NMR (101 MHz, CDCl₃): δ 164.6, 135.4, 134.1 (d, J = 32.5 Hz), 129.9, 125.8 – 124.5 (m), 82.1, 28.3. HRMS (ESI): Calcd. for C₁₂H₁₃F₃O₂Na [M+Na]⁺ 269.0760; found 269.0756.



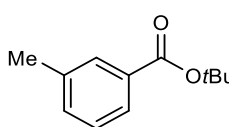
tert-Butyl quinoline-6-carboxylate, 7g. 6-Bromoquinoline (50 mg, 0.24 mmol) was reacted with tBuONa (34 mg, 0.34 mmol) according to the general procedure C to provide the product (47 mg, 85%) as yellow oil. ¹H NMR (400 MHz, CDCl₃): δ = 8.97-8.96 (m, 1H), 8.50 (s, 1H), 8.33-8.16 (m, 2H), 8.10 (d, J = 8.8 Hz, 1H), 7.43 (dd, J = 8.3, 4.2 Hz, 1H), 1.63 (s, 9H). ¹³C NMR (101 MHz, CDCl₃): δ = 165.3, 152.3, 150.0, 137.4, 130.7, 130.1, 129.6, 129.2, 127.5, 121.8, 81.7, 28.3. HRMS (ESI): Calcd. for C₁₄H₁₅O₂N [M+Na]⁺ 230.1176; found 230.1195.



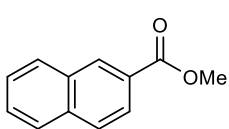
tert-Butyl 4-(tert-butyl)benzoate, 7h.²⁵ 1-Bromo-4-(tert-butyl)benzene (50 mg, 0.23 mmol) was reacted with tBuONa (33 mg, 0.34 mmol) according to the general procedure C to provide the product (50 mg, 90%) as colourless oil. ¹H NMR (400 MHz, CDCl₃): δ = 7.94 (d, J = 8.6 Hz, 2H), 7.44 (d, J = 8.6 Hz, 2H), 1.60 (s, 9H), 1.34 (s, 9H). ¹³C NMR (101 MHz, CDCl₃): δ = 165.6, 155.8, 129.1, 124.9, 80.4, 34.8, 31.0, 28.0. HRMS (ESI): Calcd. for C₁₅H₂₂O₂Na [M+Na]⁺ 257.1512; found 257.1537.



tert-Butyl 3,4-dimethoxybenzoate, 7i.²⁵ 4-Bromo-1,2-dimethoxybenzene (50 mg, 0.23 mmol) was reacted with tBuONa (33 mg, 0.34 mmol) according to the general procedure C to provide the product (51 mg, 93%) as yellow oil. ¹H NMR (400 MHz, CDCl₃): δ = 7.62-7.60 (m, 1H), 7.51-7.50 (m, 1H), 6.85 (d, J = 8.4 Hz, 1H), 3.92 (s, 6H), 1.58 (s, 9H). ¹³C NMR (101 MHz, CDCl₃): δ = 165.8, 152.7, 148.6, 124.7, 123.4, 112.0, 110.2, 80.8, 56.1, 28.4. HRMS (ESI): Calcd. for C₁₃H₁₈O₄Na [M+Na]⁺ 261.1097; found 261.1095.

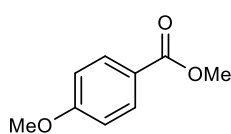


tert-Butyl 3-methylbenzoate, 7j.²⁷ 1-Bromo-3-methylbenzene (50 mg, 35.6 μ l, 0.27 mmol) was reacted with tBuONa (42 mg, 0.43 mmol) according to the general procedure C to provide the product (32 mg, 52%) as orange oil. ¹H NMR (400 MHz, CDCl₃): δ = 7.80-7.78 (m, 2H), 7.34-7.28 (m, 2H), 2.39 (s, 3H), 1.60 (s, 9H). ¹³C NMR (101 MHz, CDCl₃): δ = 166.1, 138.0, 133.3, 132.1, 130.1, 128.2, 126.7, 28.4, 21.4. HRMS (ESI): Calcd. for C₁₂H₁₆O₂Na [M+Na]⁺ 215.1043; found 215.1037.



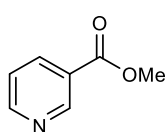
Methyl 2-naphthoate, 8a. 1-Bromo-4-methoxybenzene (50 mg, 33.5 μ l, 0.27 mmol) was reacted with tBuONa (39 mg, 0.36 mmol) in dimethyl carbonate according to the general procedure C to provide the product (49 mg, 93%) as yellow oil. ¹H NMR (400 MHz, CDCl₃): δ = 8.62 (s, 1H), 8.07 (d, J = 10.2 Hz, 1H), 7.95 (d, J = 8.0 Hz, 1H), 7.88 (d, J = 8.8 Hz, 2H), 7.69-7.46 (m,

2H), 3.99 (s, 3H). $^{13}\text{C NMR}$ (101 MHz, CDCl_3): δ = 167.3, 135.6, 132.6, 131.2, 129.4, 128.3, 128.2, 127.9, 127.5, 126.7, 125.3, 52.3. **HRMS (ESI)**: Calcd. for $\text{C}_{12}\text{H}_{10}\text{O}_2\text{Na}$ $[\text{M}+\text{Na}]^+$ 209.0573; found 209.0566.



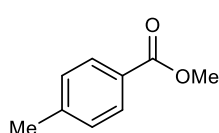
Methyl 4-methoxybenzoate, 8b.²⁸ 1-Bromo-4-methoxybenzene (50 mg, 33.5 μl , 0.27 mmol) was reacted with *t*BuONa (39 mg, 0.36 mmol) in dimethyl carbonate according to the general procedure C to provide the product (40 mg, 90%) as yellow oil. $^1\text{H NMR}$

(400 MHz, CDCl_3): δ = 7.99 (d, J = 8.9 Hz, 2H), 6.91 (d, J = 8.9 Hz, 2H), 3.87 (s, 3H), 3.84 (s, 3H). $^{13}\text{C NMR}$ (101 MHz, CDCl_3): δ = 167.0, 163.4, 131.7, 122.7, 113.7, 55.5, 52.0. **HRMS (ESI)**: Calcd. for $\text{C}_9\text{H}_{10}\text{O}_3\text{Na}$ $[\text{M}+\text{H}]^+$ 167.0705; found 167.0717.



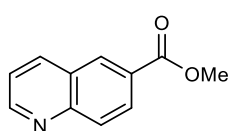
Methyl nicotinate, 8c.²⁹ 3-Bromopyridine (50 mg, 30.5 μl , 0.32 mmol) was reacted with *t*BuONa (46 mg, 0.48 mmol) in dimethyl carbonate according to the general procedure C to provide the product (25 mg, 58%) as orange oil. $^1\text{H NMR}$ (400 MHz, CDCl_3): δ = 9.21 (s, 1H),

8.76 (s, 1H), 8.28 (d, J = 7.9 Hz, 1H), 7.38 (dd, J = 7.7, 4.9 Hz, 1H), 3.94 (s, 3H). $^{13}\text{C NMR}$ (101 MHz, CDCl_3): δ = 165.9, 153.5, 151.0, 137.1, 126.1, 123.4, 52.5. **HRMS (ESI)**: Calcd. for $\text{C}_7\text{H}_8\text{O}_2\text{N}$ $[\text{M}+\text{H}]^+$ 138.0550; found 138.0545.



Methyl 4-methylbenzoate, 8d.³⁰ 1-Bromo-4-methylbenzene (50mg, 0.27 mmol) was reacted with *t*BuONa (42 mg, 0.43 mmol) in dimethyl carbonate according to the general procedure C to provide (35 mg, 80%) as colourless oil. $^1\text{H NMR}$ (400 MHz, CDCl_3): δ = 7.93

(d, J = 8.2 Hz, 2H), 7.23 (d, J = 8.2 Hz, 2H), 3.89 (s, 3H), 2.40 (s, 3H). $^{13}\text{C NMR}$ (101 MHz, CDCl_3): δ = 167.3, 143.7, 129.7, 129.2, 127.5, 52.0, 21.8. **HRMS (ESI)**: Calcd. for $\text{C}_9\text{H}_{10}\text{O}_2\text{Na}$ $[\text{M}+\text{H}]^+$ 151.0754; found 151.0757.



Methyl quinoline-6-carboxylate, 8e.³¹ 6-Bromoquinoline (50 mg, 0.24 mmol) was reacted with *t*BuONa (34 mg, 0.34 mmol) in dimethyl carbonate according to the general procedure C to provide the product (42 mg, 93%) as white solid. Mp 80-82 $^\circ\text{C}$. $^1\text{H NMR}$

(400 MHz, CDCl_3): δ = 8.95-8.94 (m, 1H), 8.51 (s, 1H), 8.25-7.23 (m, 1H), 8.18 (d, J = 7.8 Hz, 1H), 8.10-8.08 (m, 1H), 7.40 (dd, J = 8.3, 4.2 Hz, 1H), 3.94 (s, 3H). $^{13}\text{C NMR}$ (101 MHz, CDCl_3): δ = 166.6, 152.5, 150.1, 137.3, 131.0, 129.8, 128.9, 128.1, 127.4, 121.9, 52.5. **HRMS (ESI)**: Calcd. for $\text{C}_{11}\text{H}_{10}\text{NO}_2$ $[\text{M}+\text{H}]^+$ 188.0706; found 188.0717.

9. References

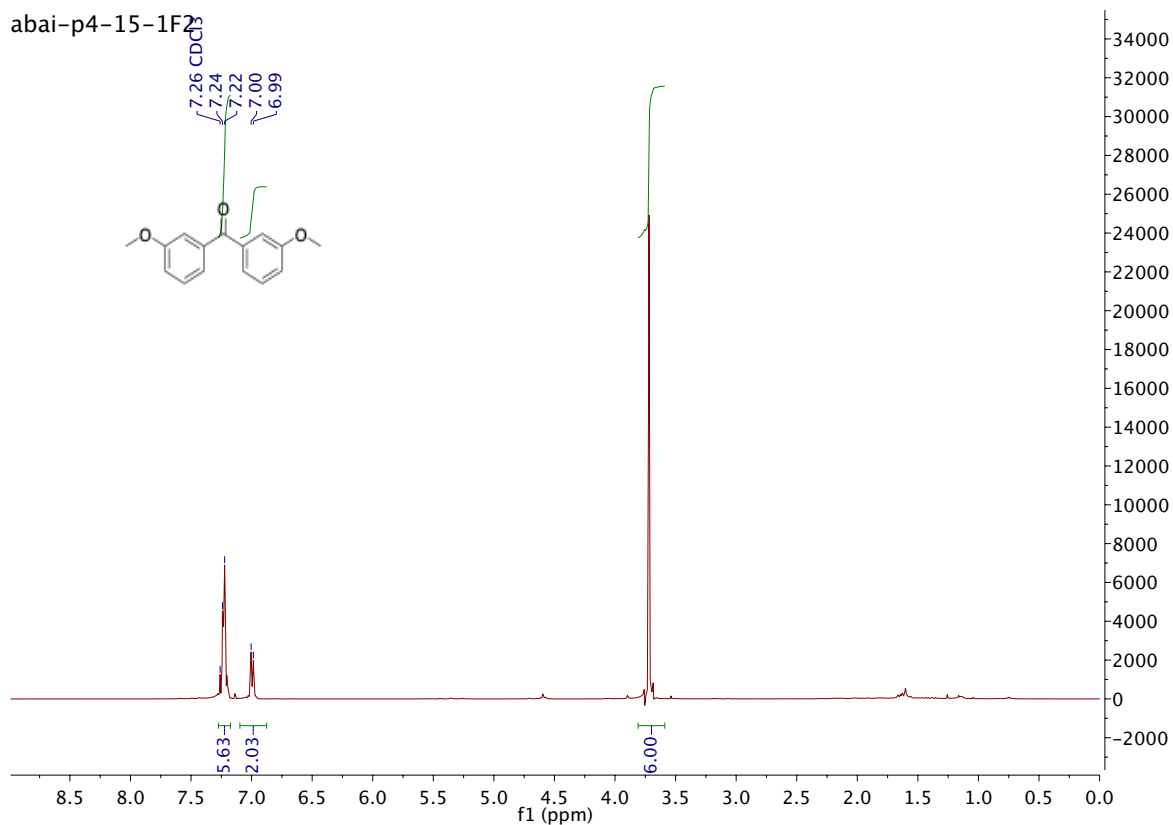
- (1) Armarego, W. L. F.; Chai, C. L. L. *Purification of Laboratory Chemicals*; Butterworth-Heinemann, 2003.
- (2) Rérat, A.; Michon, C.; Agbossou-Niedercorn, F.; Gosmini, C. Synthesis of Symmetrical Diaryl Ketones by Cobalt-Catalyzed Reaction of Arylzinc Reagents with Ethyl Chloroformate. *Eur. J. Org. Chem.* **2016**, 4554–4560.
- (3) Suchand, B.; Satyanarayana, G. Palladium-Catalyzed Direct Acylation: One-Pot Relay Synthesis of Anthraquinones. *Synthesis* **2019**, *51*, 769–779.
- (4) Bjerglund, K. M.; Skrydstrup, T.; Molander, G. A. Carbonylative Suzuki Couplings of Aryl Bromides with Boronic Acid Derivatives under Base-Free Conditions. *Org. Lett.* **2014**, *16*, 1888–1891.
- (5) Chen, J.; Chen, C.; Ji, C.; Lu, Z. Cobalt-Catalyzed Asymmetric Hydrogenation of 1,1-Diarylethenes. *Org. Lett.* **2016**, *18*, 1594–1597.
- (6) Sharma, P.; Rohilla, S.; Jain, N. Palladium Catalyzed Carbonylative Coupling for Synthesis of Arylketones and Arylesters Using Chloroform as the Carbon Monoxide Source. *J. Org. Chem.* **2017**, *82* (2), 1105–1113.
- (7) Chen, C.; Liu, P.; Luo, M.; Zeng, X. Kumada Arylation of Secondary Amides Enabled by Chromium Catalysis for Unsymmetric Ketone Synthesis under Mild Conditions. *ACS Catal.* **2018**, *8*, 5864–5868.
- (8) Inamoto, K.; Saito, T.; Katsuno, M.; Sakamoto, T.; Hiroya, K. Palladium-Catalyzed C-H Activation/Intramolecular Amination Reaction: A New Route to 3-Aryl/Alkylindazoles. *Org. Lett.* **2007**, *9*, 2931–2934.
- (9) Keumi, T.; Yoshimura, K.; Shimada, M.; Kitajima, H. 2-(Trifluoromethylsulfonyloxy)Pyridine as a Reagent for the Ketone Synthesis from Carboxylic Acids and Aromatic Hydrocarbons. *Bull. Chem. Soc. Jpn.* **1988**, *61*, 455–459.
- (10) Gautam, P.; Dhiman, M.; Polshettiwar, V.; Bhanage, B. M. KCC-1 Supported Palladium Nanoparticles as an Efficient and Sustainable Nanocatalyst for Carbonylative Suzuki-Miyaura Cross-Coupling. *Green Chem.* **2016**, *18*, 5890–5899.
- (11) Yu, D.; Xu, F.; Li, D.; Han, W. Transition-Metal-Free Carbonylative Suzuki-Miyaura Reactions of Aryl Iodides with Arylboronic Acids Using *N*-Formylsaccharin as CO Surrogate. *Adv. Synth. Catal.* **2019**, *361*, 3102–3107.
- (12) Xiao, P.; Tang, Z.; Wang, K.; Chen, H.; Guo, Q.; Chu, Y.; Gao, L.; Song, Z. Chemoselective Reduction of Sterically Demanding *N,N*-Diisopropylamides to Aldehydes. *J. Org. Chem.* **2018**, *83*, 1687–1700.
- (13) Mishra, A.; Chauhan, S.; Verma, P.; Singh, S.; Srivastava, V. TBHP-Initiated Transamidation of Secondary Amides via C–N Bond Activation: A Metal-Free Approach. *Asian J. Org. Chem.* **2019**, *8*, 853–857.
- (14) Panini, P.; Chopra, D. Experimental and Computational Insights into the Nature of Weak Intermolecular Interactions in Trifluoromethyl-Substituted Isomeric Crystalline *N*-Methyl-*N*-Phenylbenzamide. *New J. Chem.* **2015**, *39*, 8720–8738.
- (15) Pan, Y.; Luo, Z.; Xu, X.; Zhao, H.; Han, J.; Xu, L.; Fan, Q.; Xiao, J. Ru-Catalyzed Deoxygenative Transfer Hydrogenation of Amides to Amines with Formic Acid/Triethylamine. *Adv. Synth. Catal.* **2019**, *361*, 3800–3806.
- (16) Mai, W. P.; Song, G.; Yuan, J. W.; Yang, L. R.; Sun, G. C.; Xiao, Y. M.; Mao, P.; Qu, L. B. NBu_4NI -Catalyzed Unexpected Amide Bond Formation between Aldehydes and Aromatic Tertiary Amines.

RSC Adv. **2013**, *3*, 3869–3872.

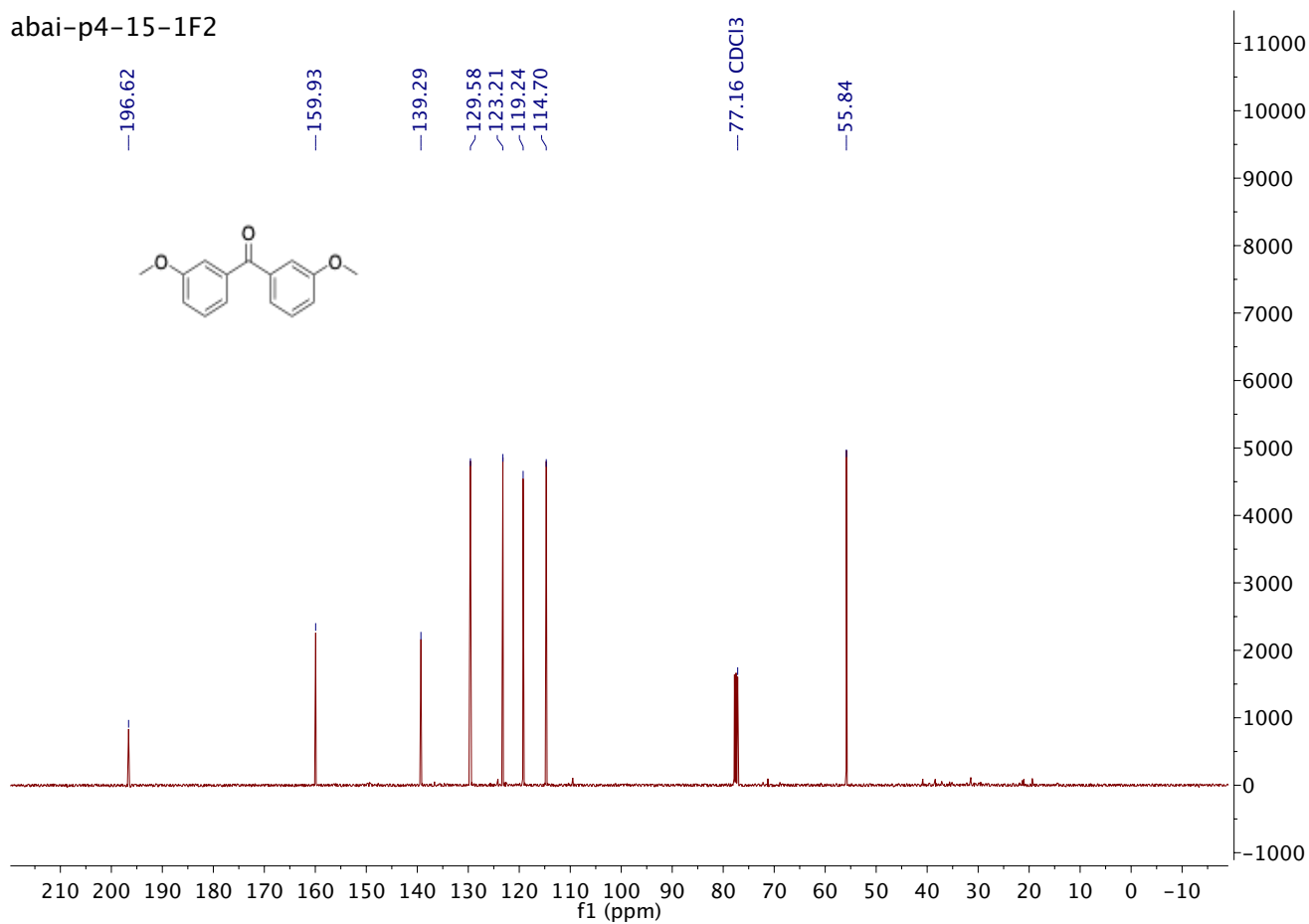
- (17) Zhang, Z.; Liu, Y. H.; Zhang, X.; Wang, X. C. KMnO_4 -Mediated Oxidative C–N Bond Cleavage of Tertiary Amines: Synthesis of Amides and Sulfonamides. *Tetrahedron* **2019**, *75*, 2763–2770.
- (18) Martinelli, J. R.; Watson, D. A.; Freckmann, D. M. M.; Barder, T. E.; Buchwald, S. L. Palladium-Catalyzed Carbonylation Reactions of Aryl Bromides at Atmospheric Pressure: A General System Based on Xantphos. *J. Org. Chem.* **2008**, *73*, 7102–7107.
- (19) Baroudi, A.; Alicea, J.; Flack, P.; Kirincich, J.; Alabugin, I. V. Radical O→C Transposition: A Metal-Free Process for Conversion of Phenols into Benzoates and Benzamides. *J. Org. Chem.* **2011**, *76*, 1521–1537.
- (20) Sahay, I. I.; Ghalsasi, P. S.; Singh, M.; Begum, R. Revisiting Aryl Amidine Synthesis Using Metal Amide and/or Ammonia Gas: Novel Molecules and Their Biological Evaluation. *Synth. Commun.* **2017**, *47*, 1400–1408.
- (21) Gao, J.; Wang, G. W. Direct Oxidative Amidation of Aldehydes with Anilines under Mechanical Milling Conditions. *J. Org. Chem.* **2008**, *73*, 2955–2958.
- (22) Liu, S.; Wang, H.; Dai, X.; Shi, F. Organic Ligand-Free Carbonylation Reactions with Unsupported Bulk Pd as Catalyst. *Green Chem.* **2018**, *20* (15), 3457–3462.
- (23) Vico Solano, M.; González Miera, G.; Pascanu, V.; Inge, A. K.; Martín-Matute, B. Versatile Heterogeneous Palladium Catalysts for Diverse Carbonylation Reactions under Atmospheric Carbon Monoxide Pressure. *ChemCatChem* **2018**, *10*, 1089–1095.
- (24) Hosni, Z.; Rajoub, N.; Houson, I.; Nordon, A.; Benyahia, B.; Florence, A. Autonomous Control and Dynamics Simulation of a 3-Stages Countercurrent Liquid-Liquid Extraction: Trimetozine Purification as a Case Study. *ChemRxiv* **2019**. <https://doi.org/10.26434/CHEMRXIV.9542378.V1>
- (25) Xin, Z.; Gøgsig, T. M.; Lindhardt, A. T.; Skrydstrup, T. An Efficient Method for the Preparation of Tertiary Esters by Palladium-Catalyzed Alkoxy carbonylation of Aryl Bromides. *Org. Lett.* **2012**, *14*, 284–287.
- (26) Wang, S. M.; S Alharbi, N.; Qin, H. L. Construction of Esters through Sulfuryl Fluoride (SO_2F_2) Mediated Dehydrative Coupling of Carboxylic Acids with Alcohols at Room Temperature. *Synthesis*. **2019**, *51*, 3901–3907.
- (27) Roslin, S.; Odell, L. R. Visible-Light Photocatalysis as an Enabling Tool for the Functionalization of Unactivated $\text{C}(\text{sp}^3)$ -Substrates. *Eur. J. Org. Chem.* **2017**, 1993–2007.
- (28) Tang, S.; Yuan, J.; Liu, C.; Lei, A. Direct Oxidative Esterification of Alcohols. *Dalton Transactions*. **2014**, *43*, 13460–13470.
- (29) Verma, K. K.; Singh, U. K.; Jain, J. Design, Synthesis and Biological Activity of some 4, 5-Disubstituted-2, 4-Dihydro-3H-1, 2, 4-Triazole-3-Thione Derivatives. *Cent. Nerv. Syst. Agents Med. Chem.* **2019**, *19*, 197–205.
- (30) Liu, H.; Li, Z.; Wang, J.; Lu, S.; Wang, M.; Liu, Y.; Li, C. Carboxylation of Toluene with CO_2 -Derived Dimethyl Carbonate over Amorphous Ti–Zr Mixed-Metal Oxide Catalysts. *ChemCatChem* **2020**, *12*, 95–99.
- (31) Liao, C.; Li, X.; Yao, K.; Yuan, Z.; Chi, Q.; Zhang, Z. Efficient Oxidative Dehydrogenation of N-Heterocycles over Nitrogen-Doped Carbon-Supported Cobalt Nanoparticles. *ACS Sustain. Chem. Eng.* **2019**, *7*, 13646–13654.

10. Copies of spectra

Compound 3a

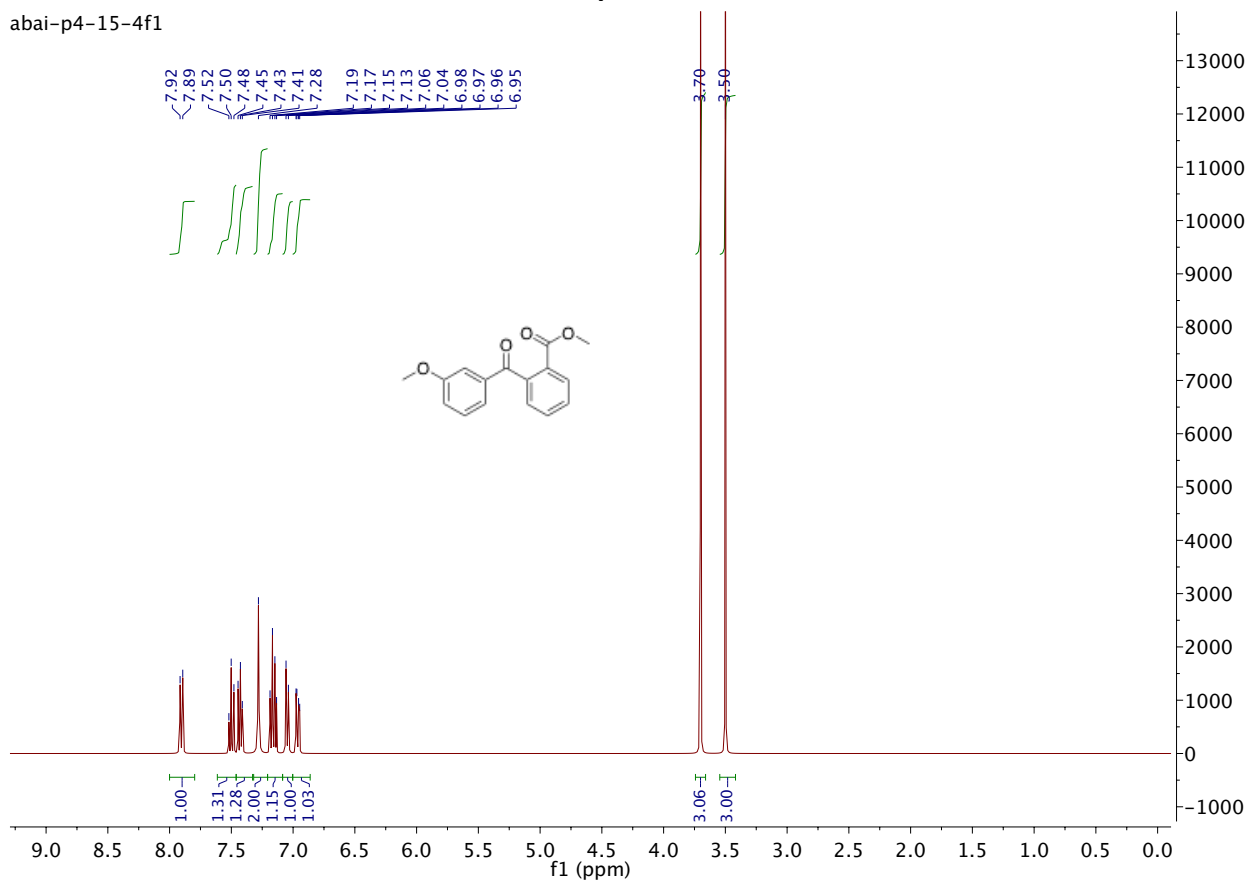


abai-p4-15-1F2

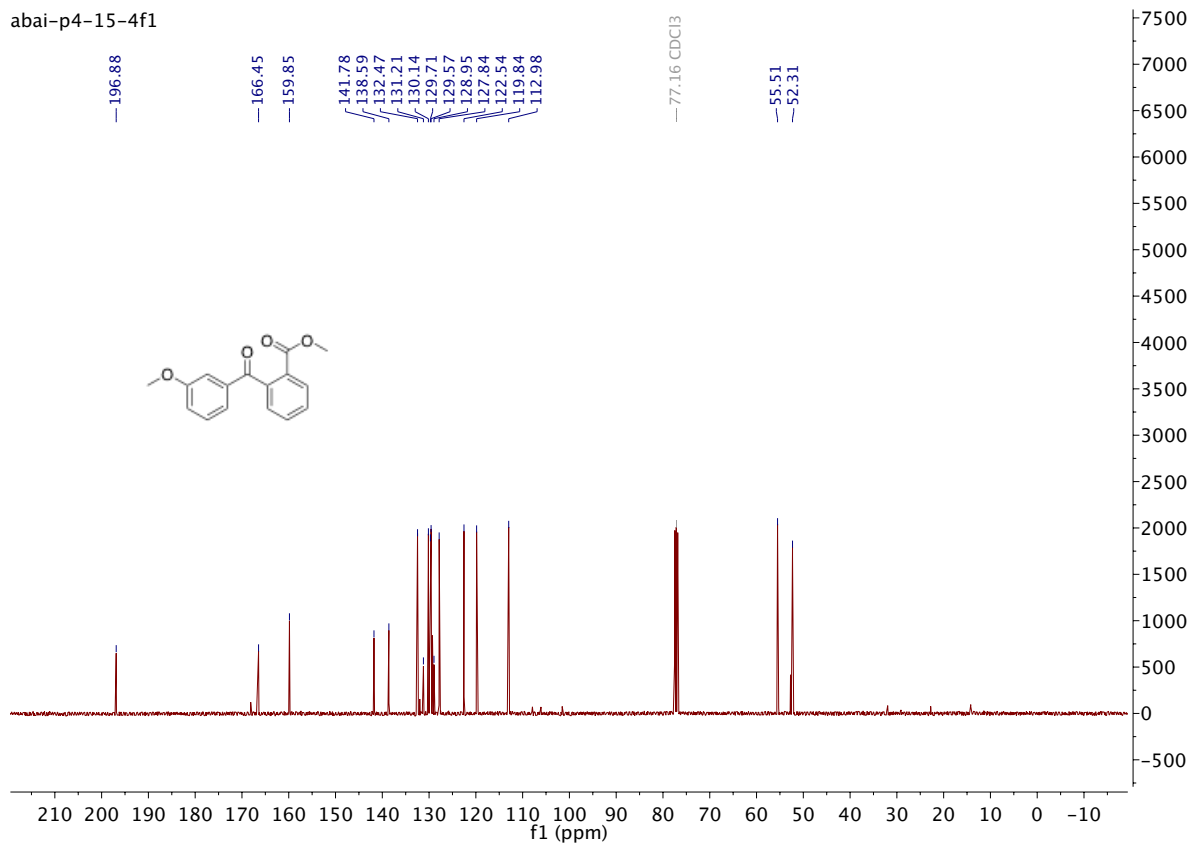


Compound 3b

abai-p4-15-4f1

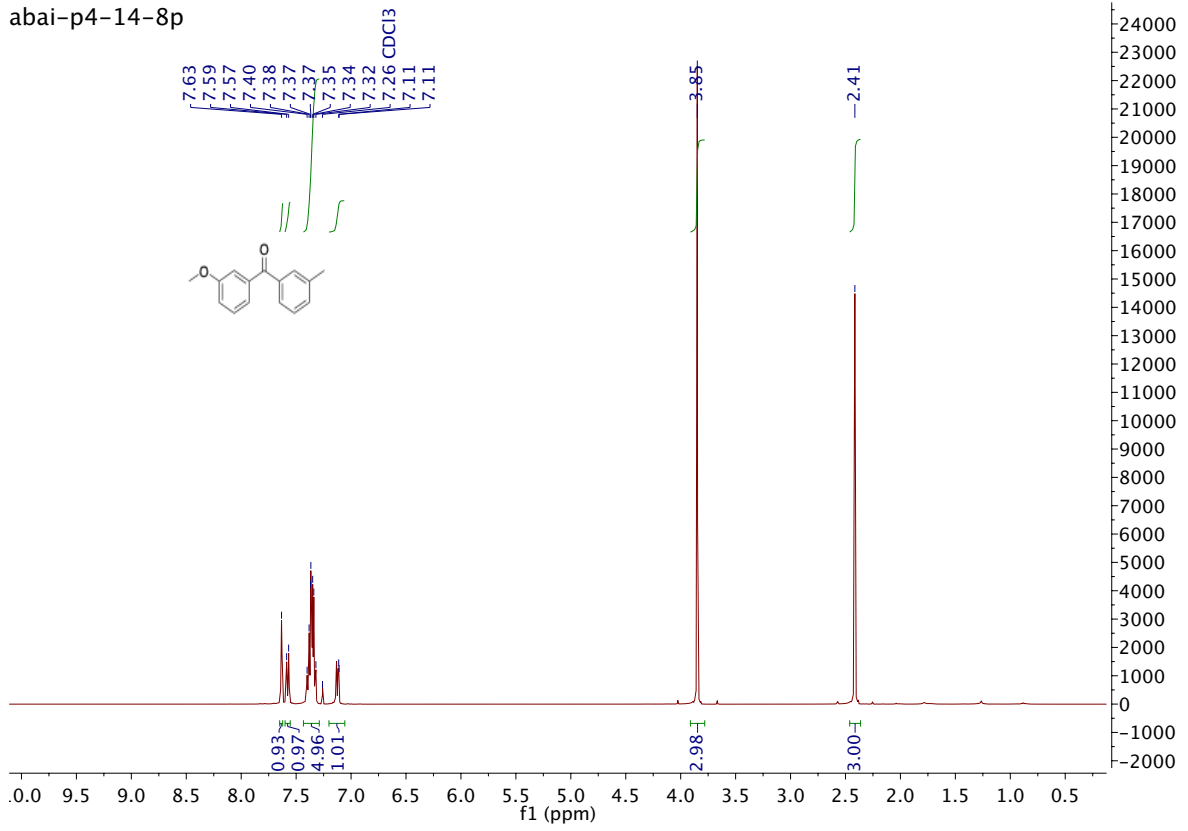


abai-p4-15-4f1

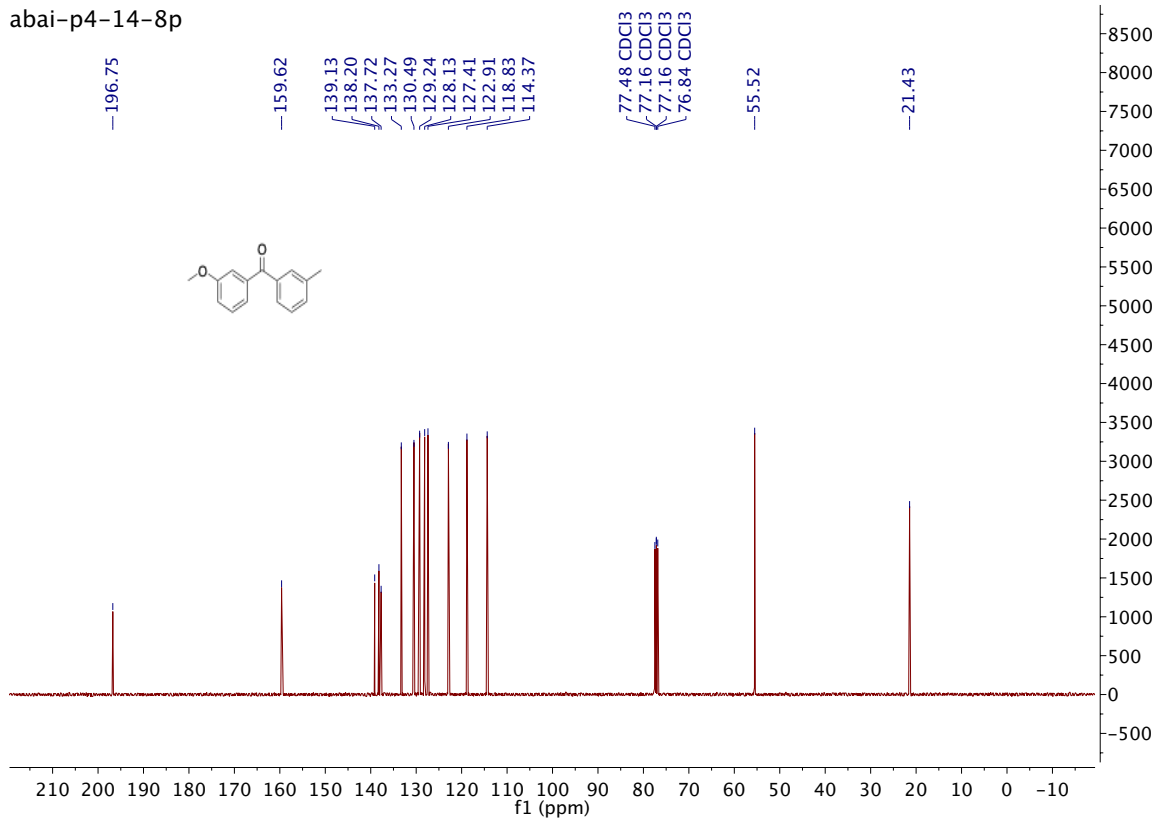


Compound 3c

abai-p4-14-8p

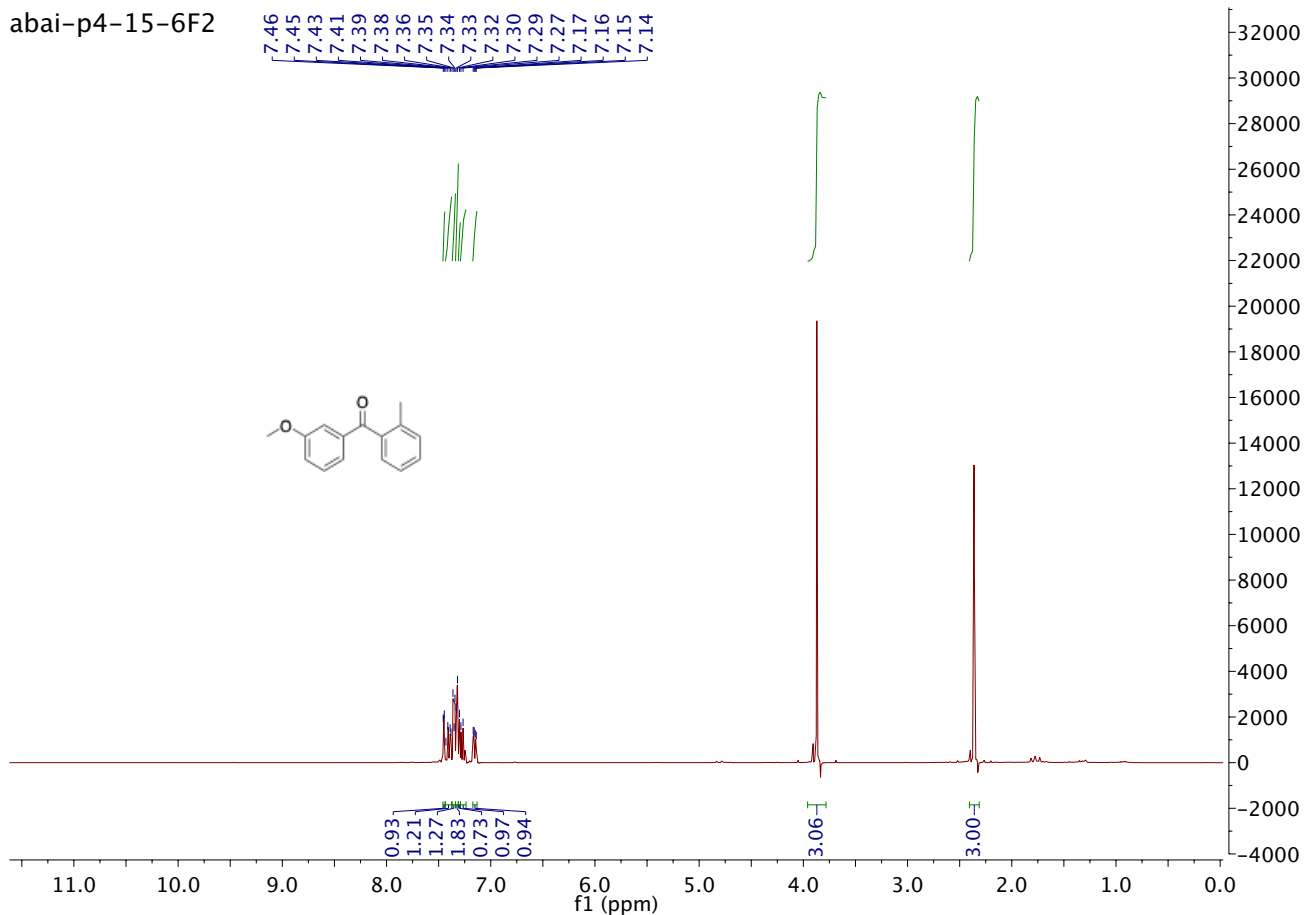


abai-p4-14-8p

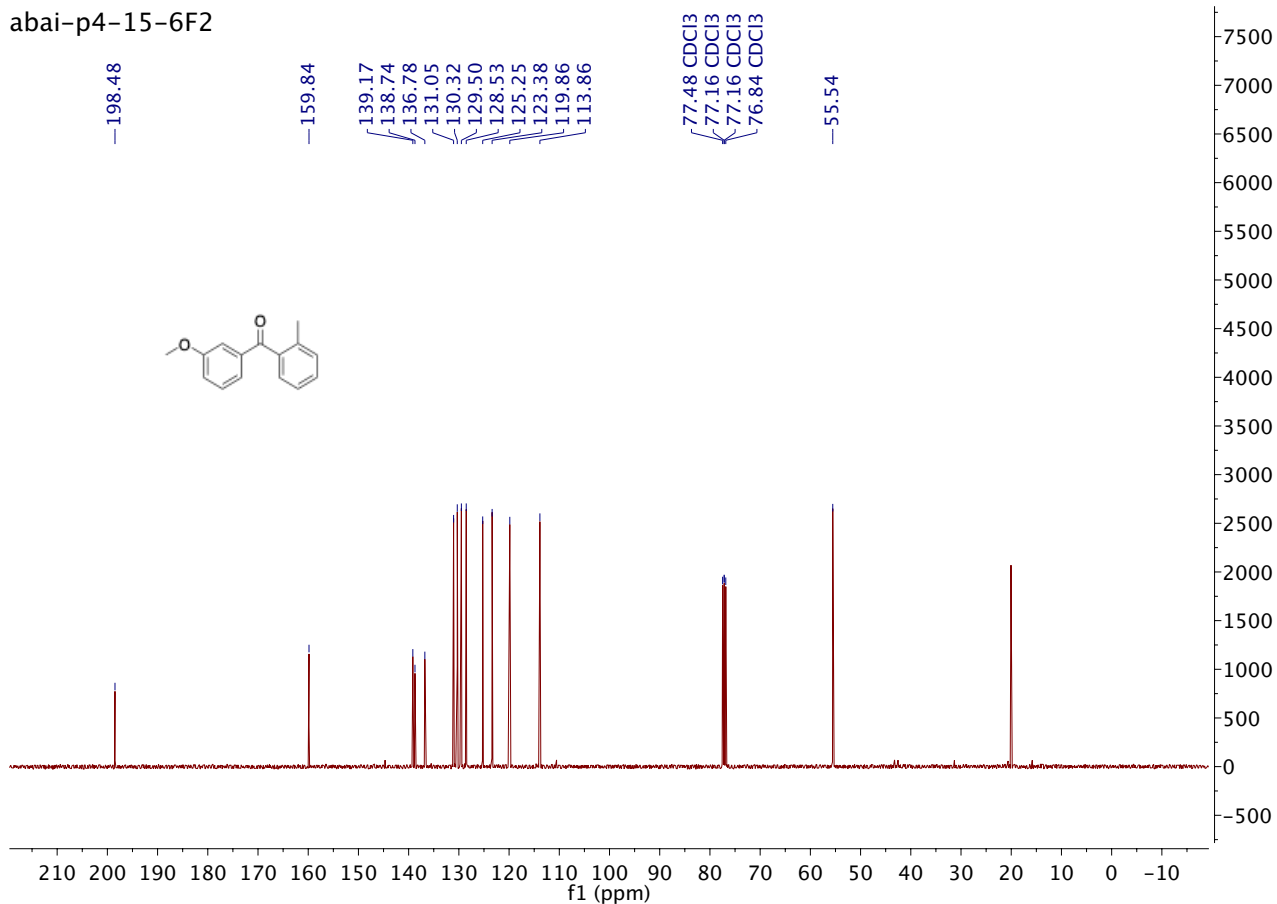


Compound 3d

abai-p4-15-6F2

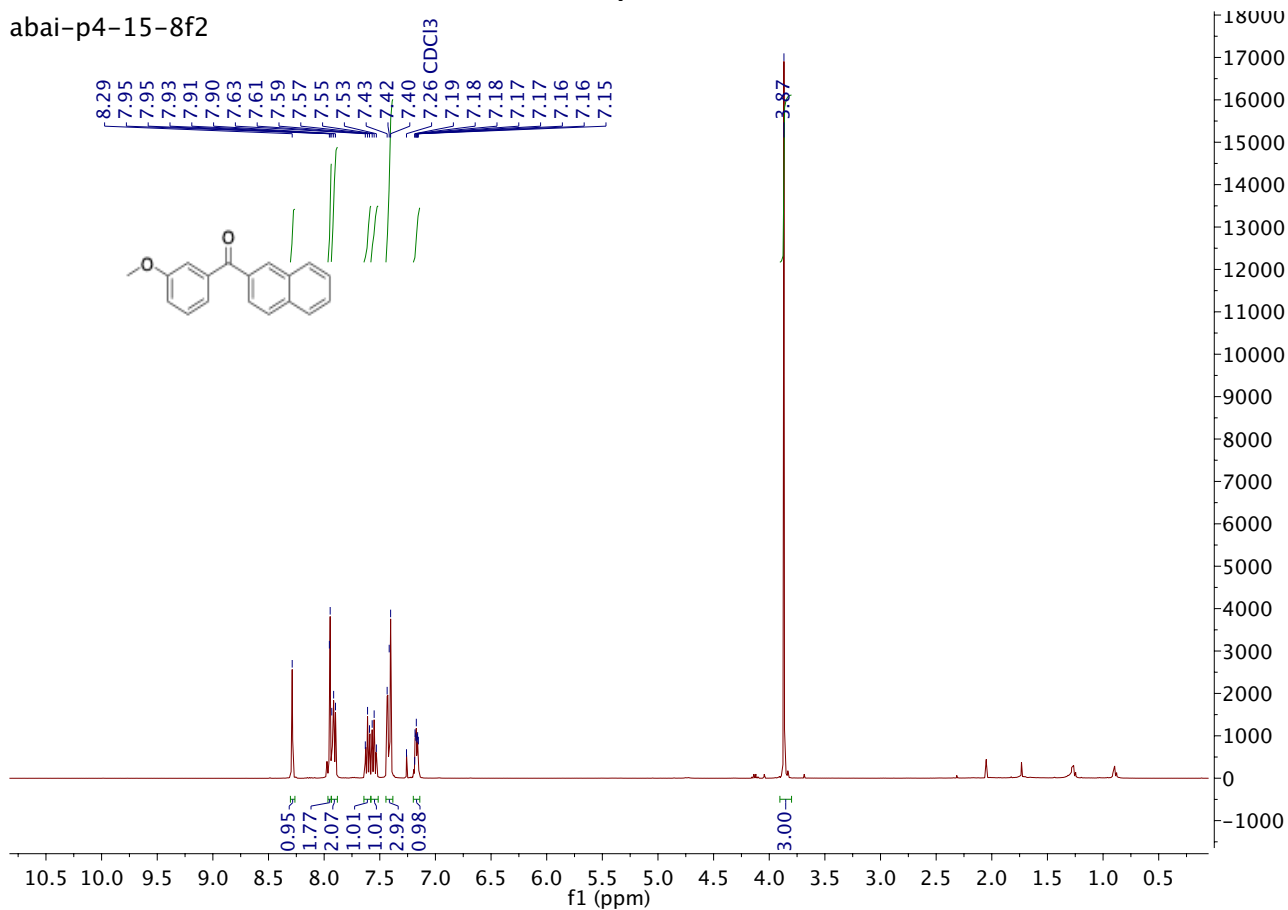


abai-p4-15-6F2

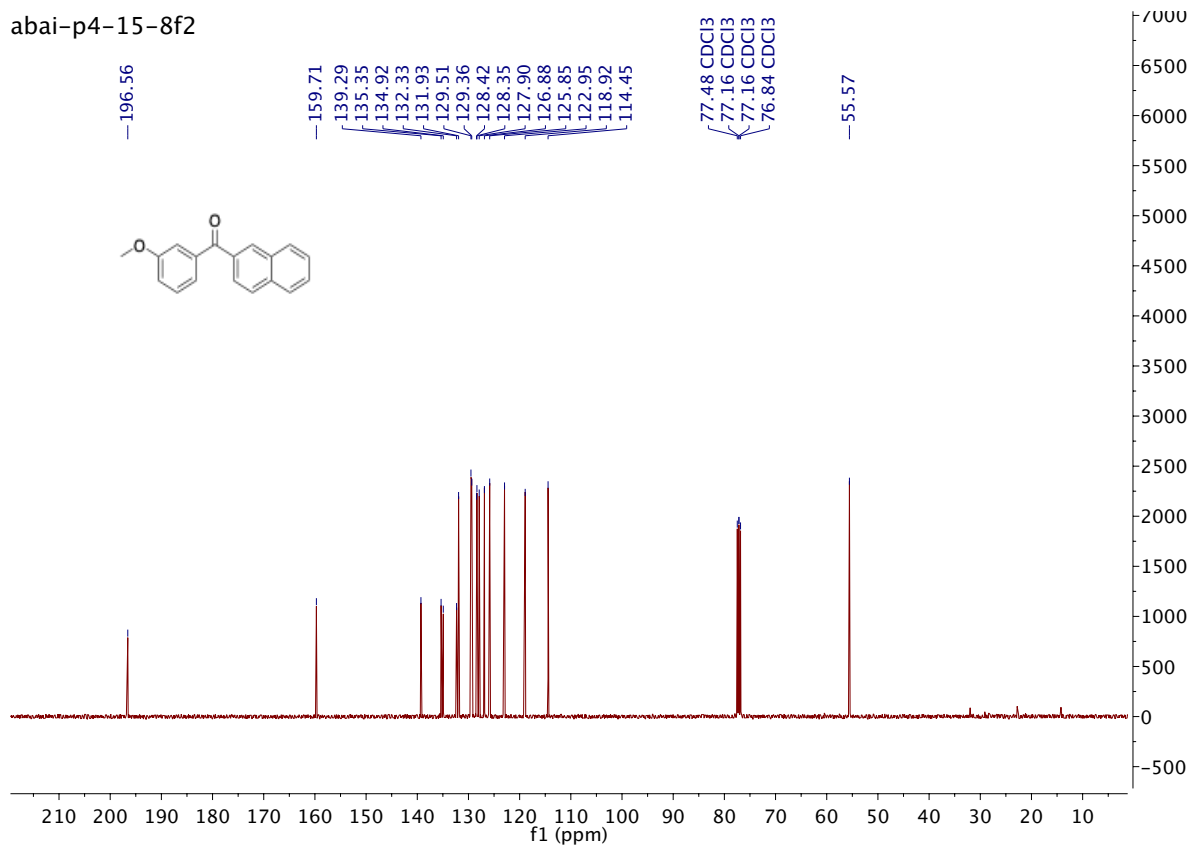


Compound 3e

abai-p4-15-8f2

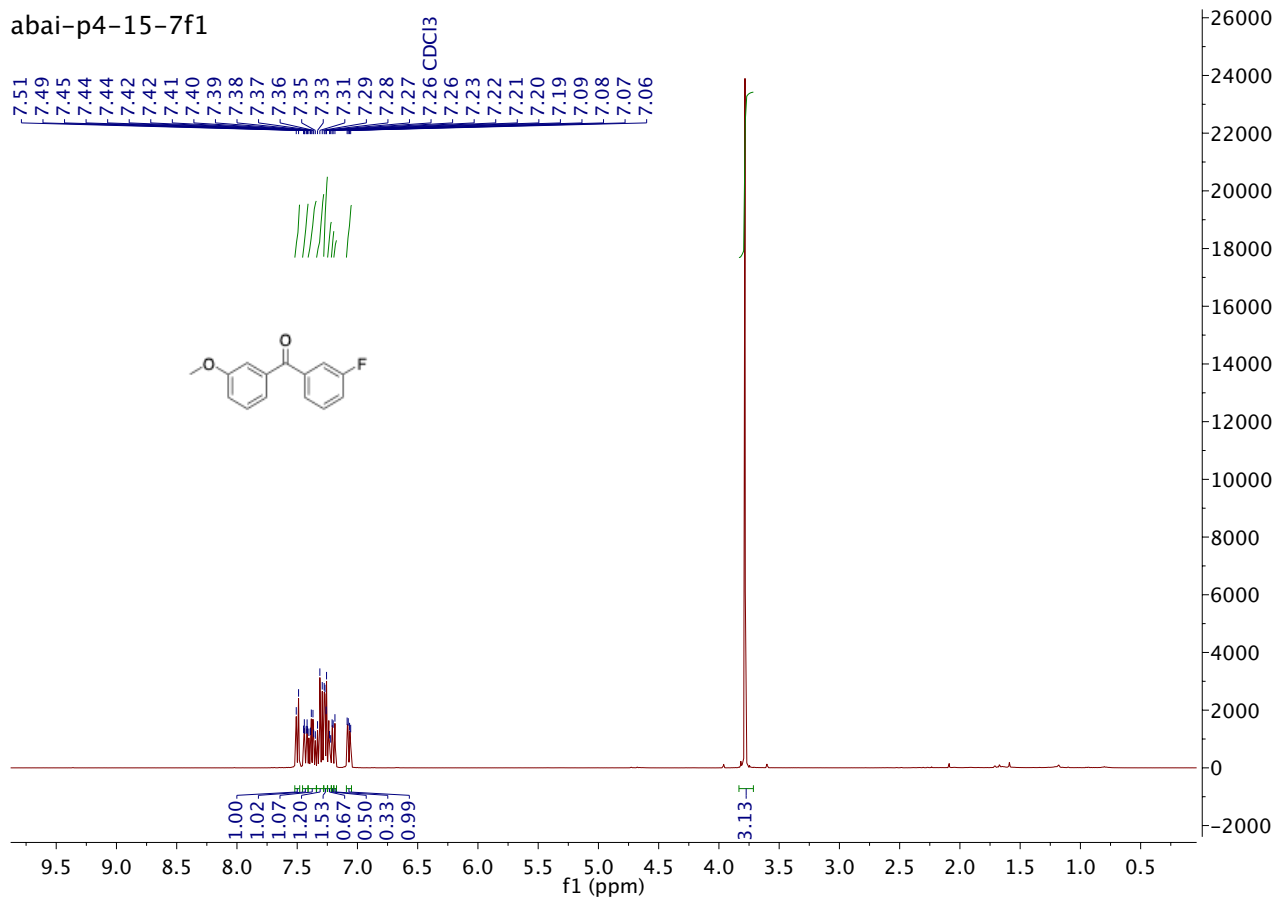


abai-p4-15-8f2

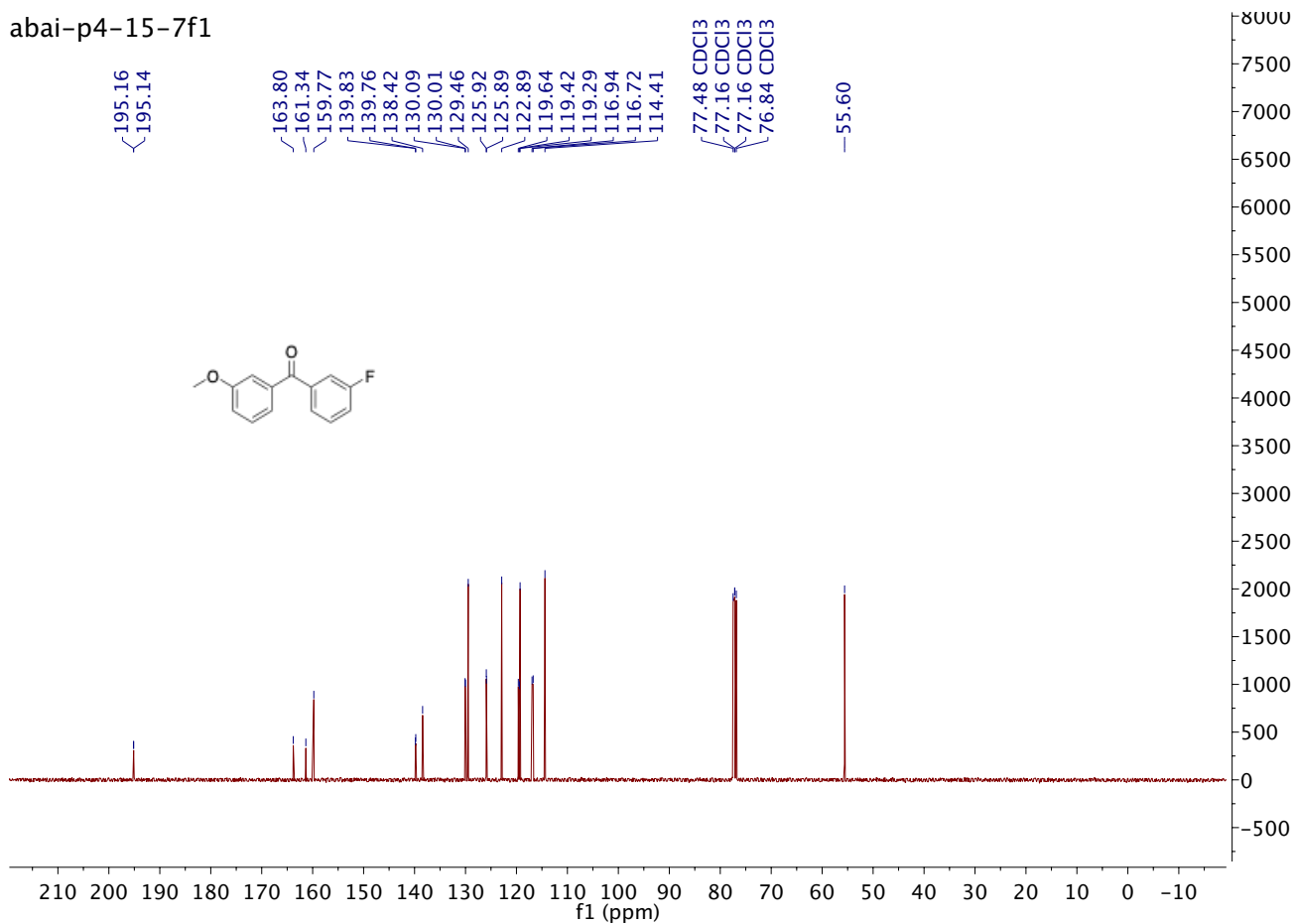


Compound 3f

abai-p4-15-7f1

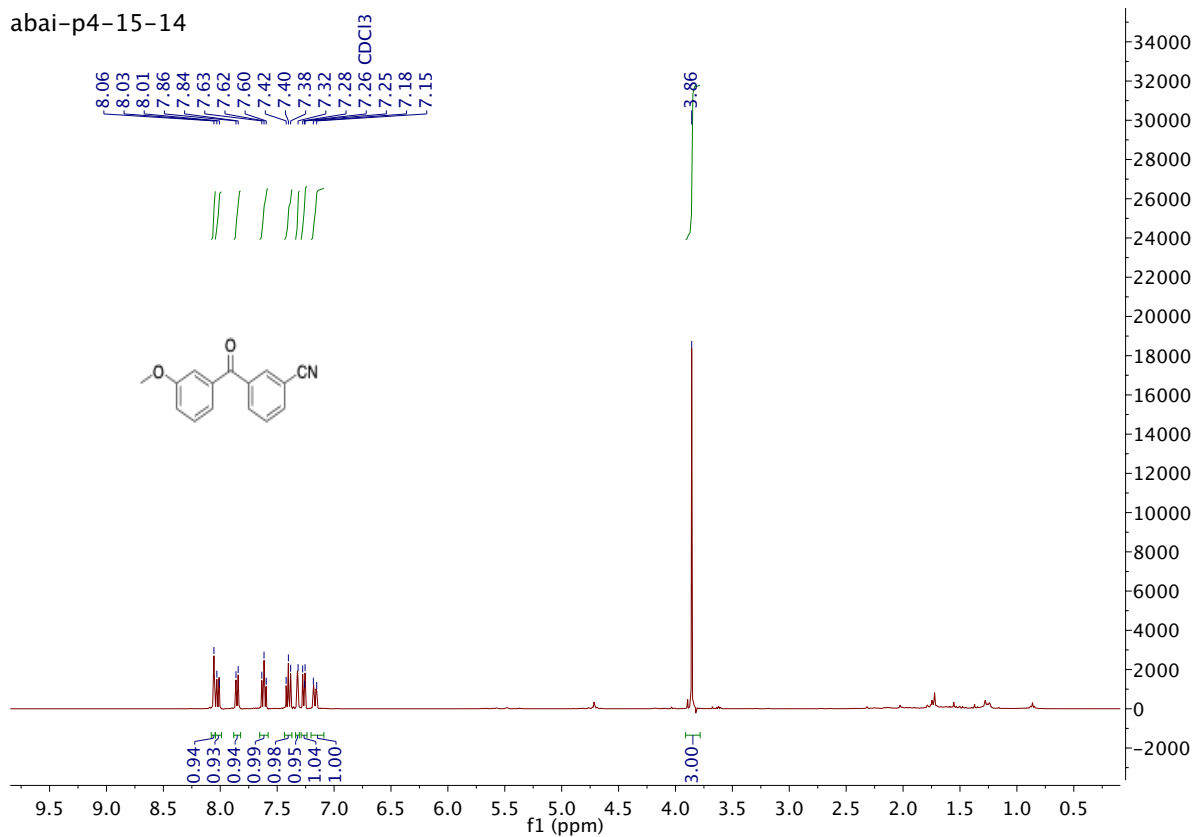


abai-p4-15-7f1

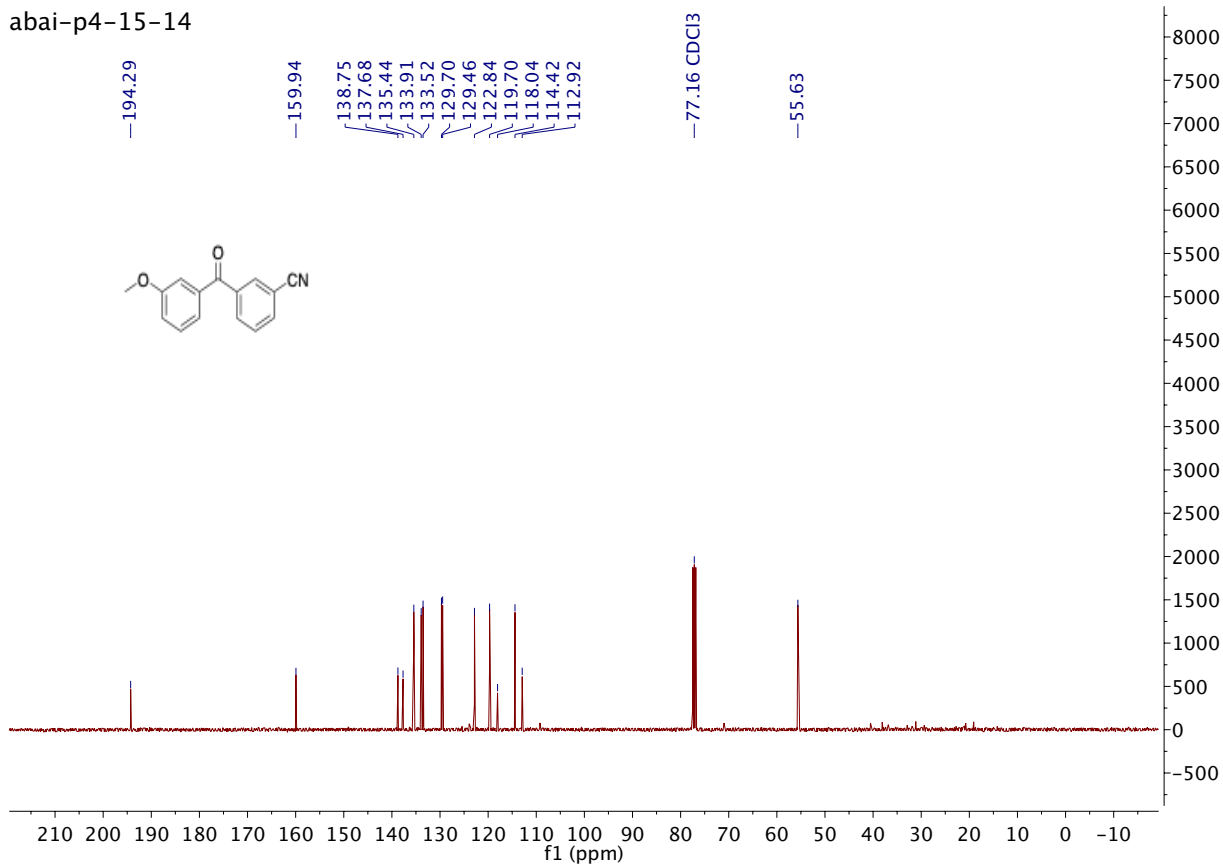


Compound 3g

abai-p4-15-14

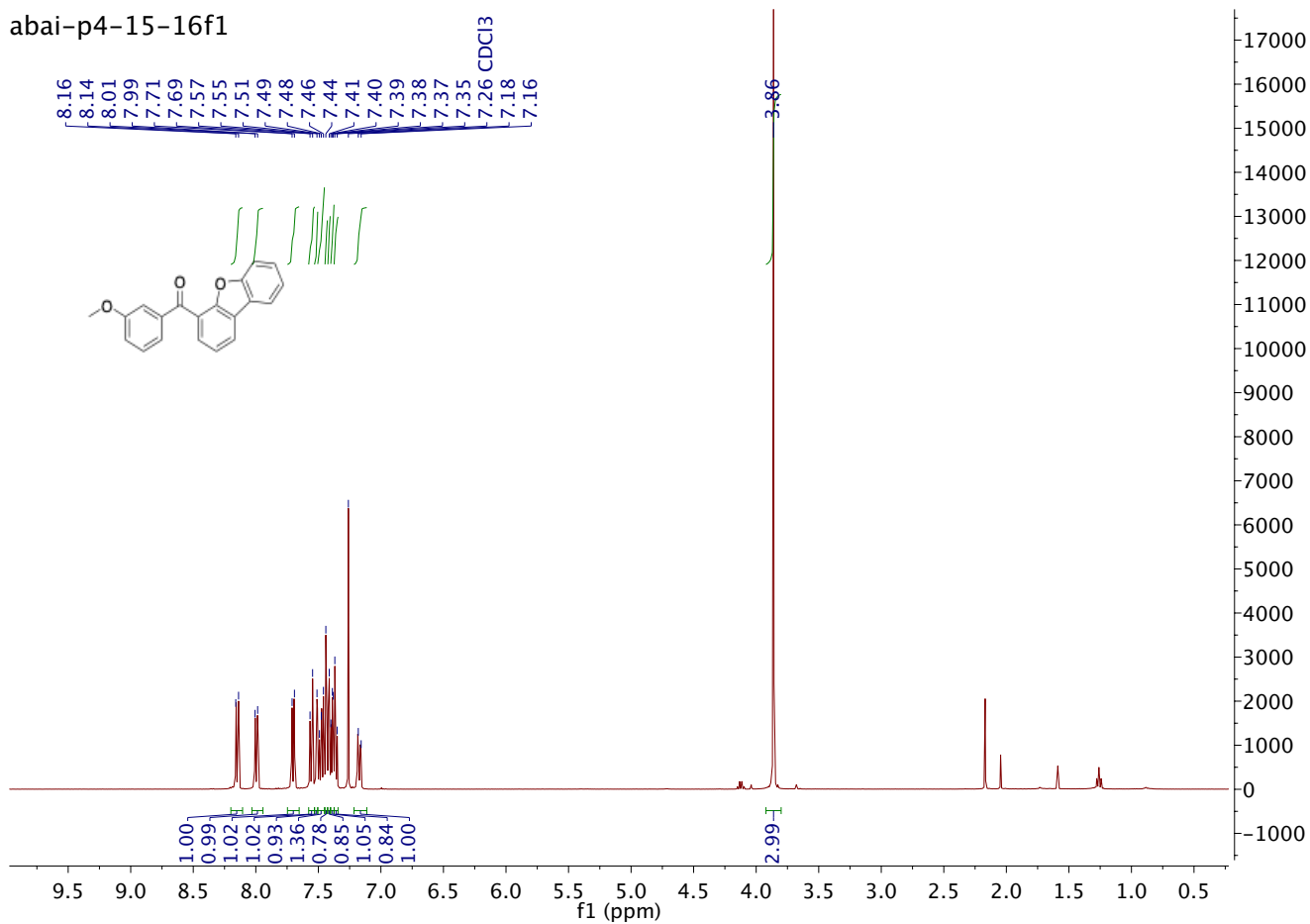


abai-p4-15-14

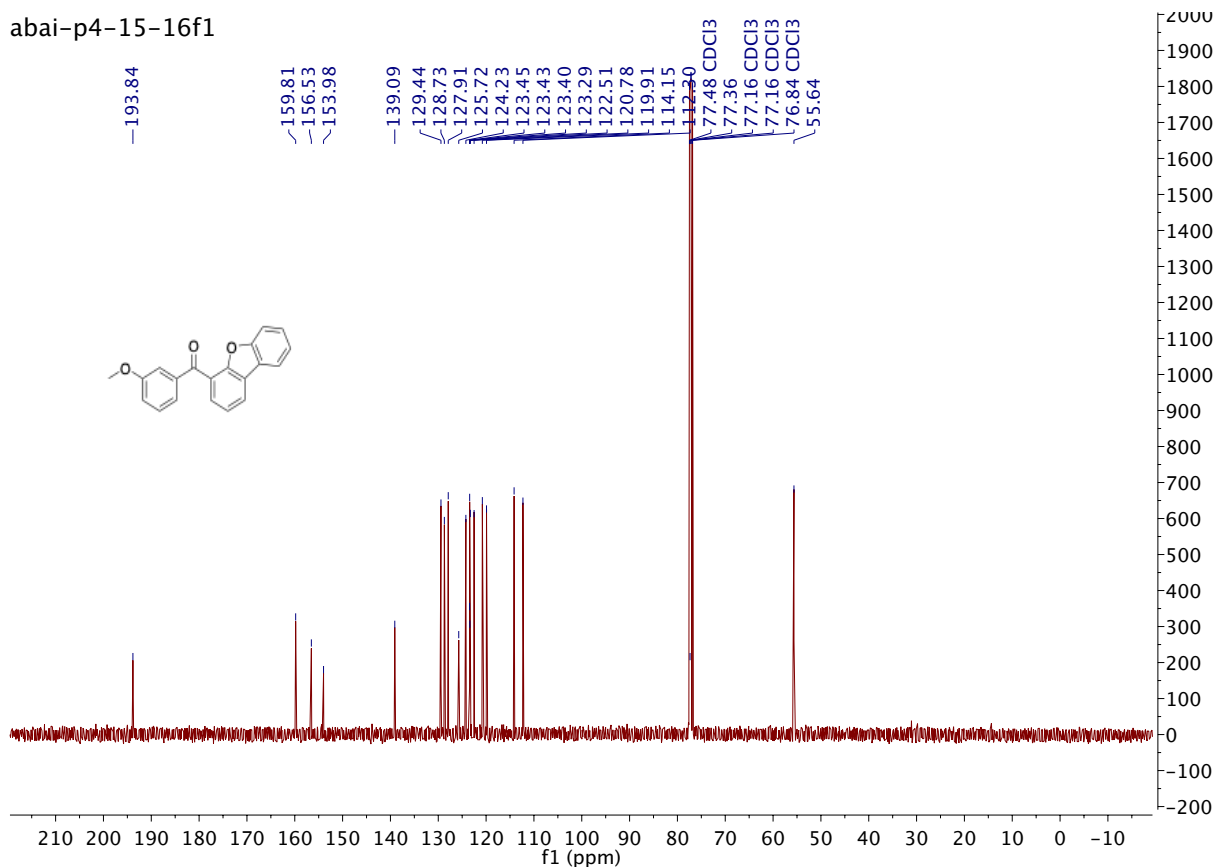


Compound 3h

abai-p4-15-16f1

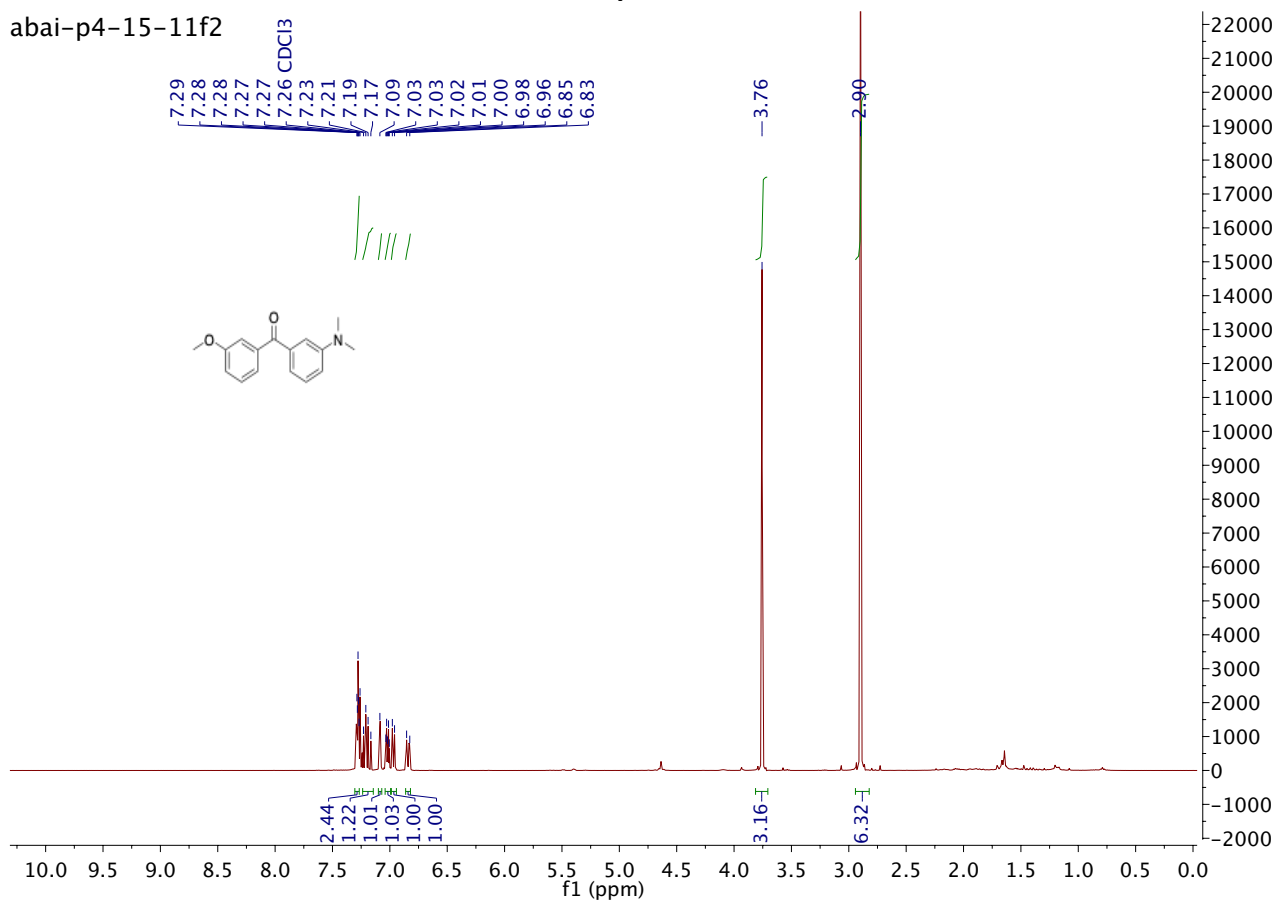


abai-p4-15-16f1

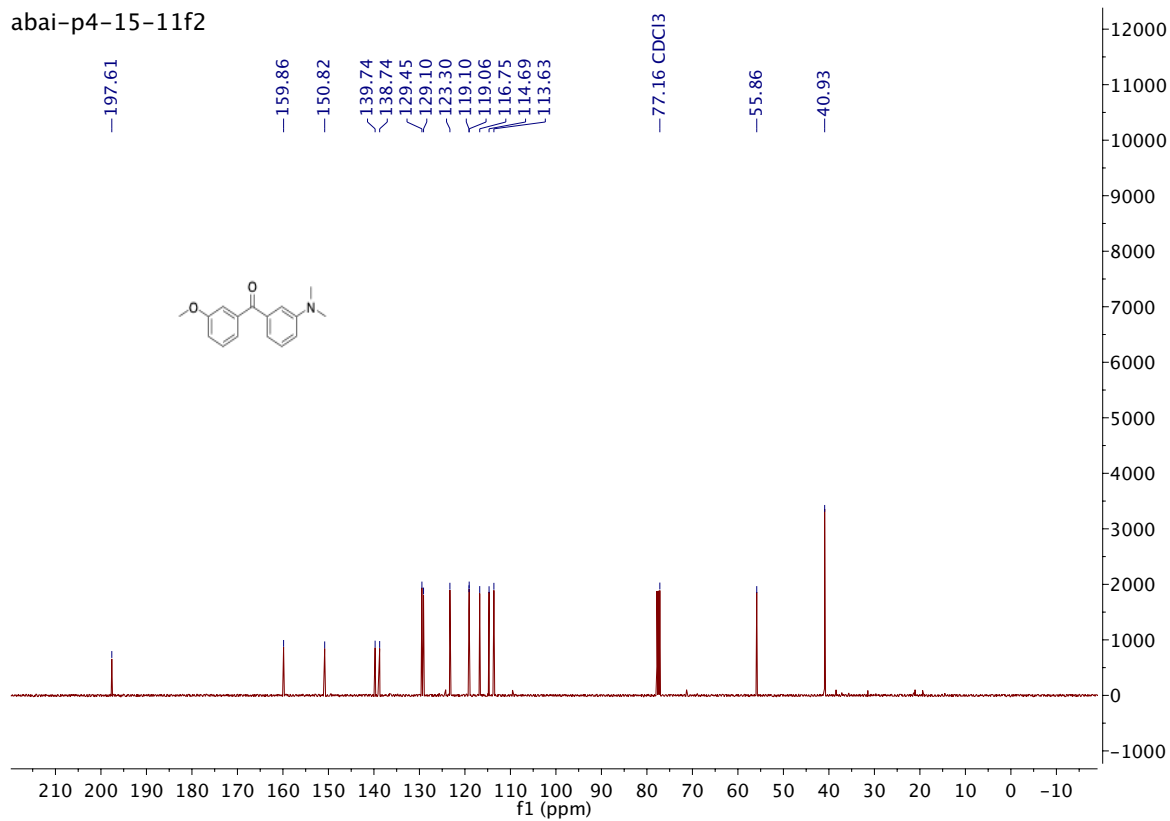


Compound 3i

abai-p4-15-11f2

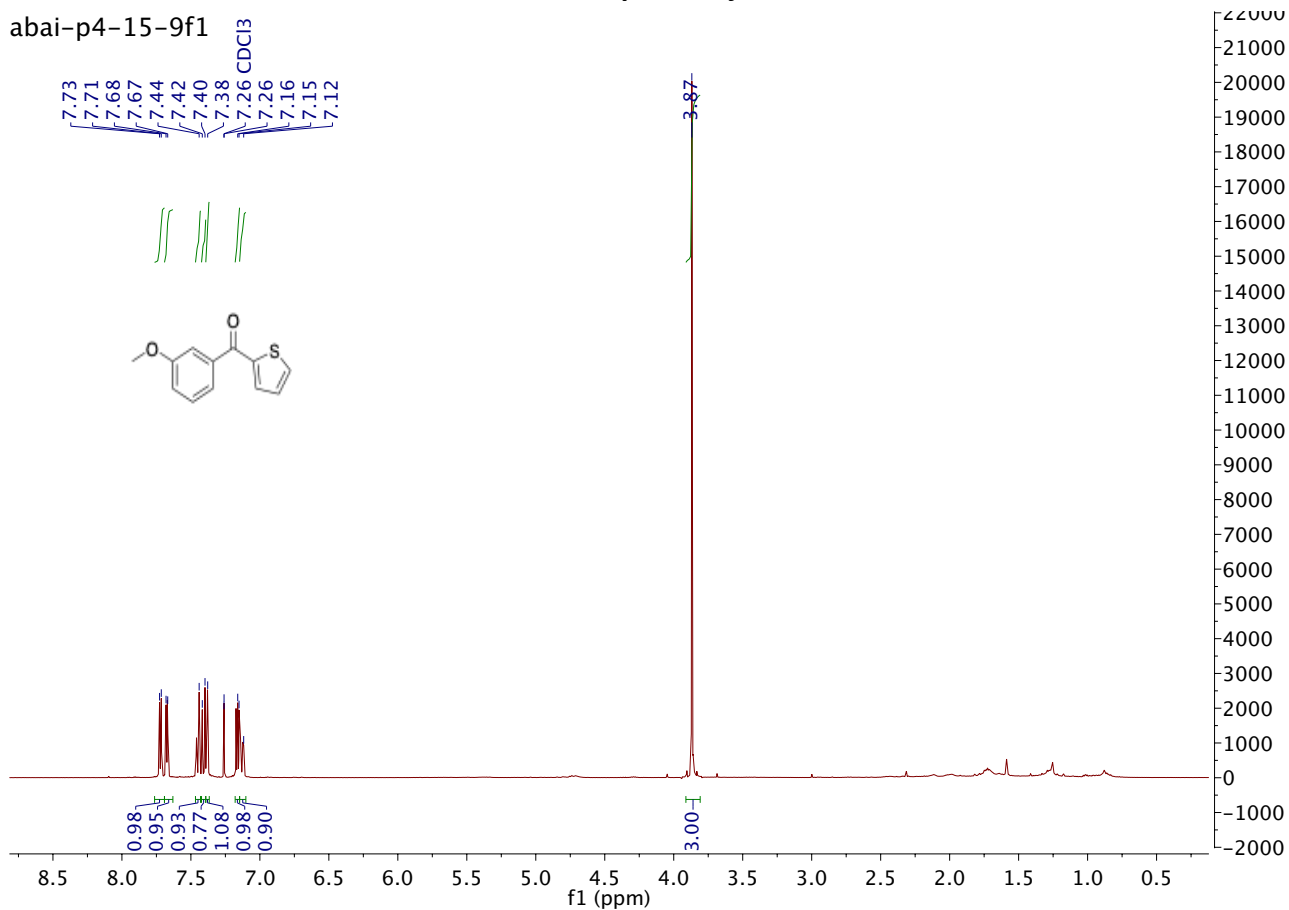


abai-p4-15-11f2

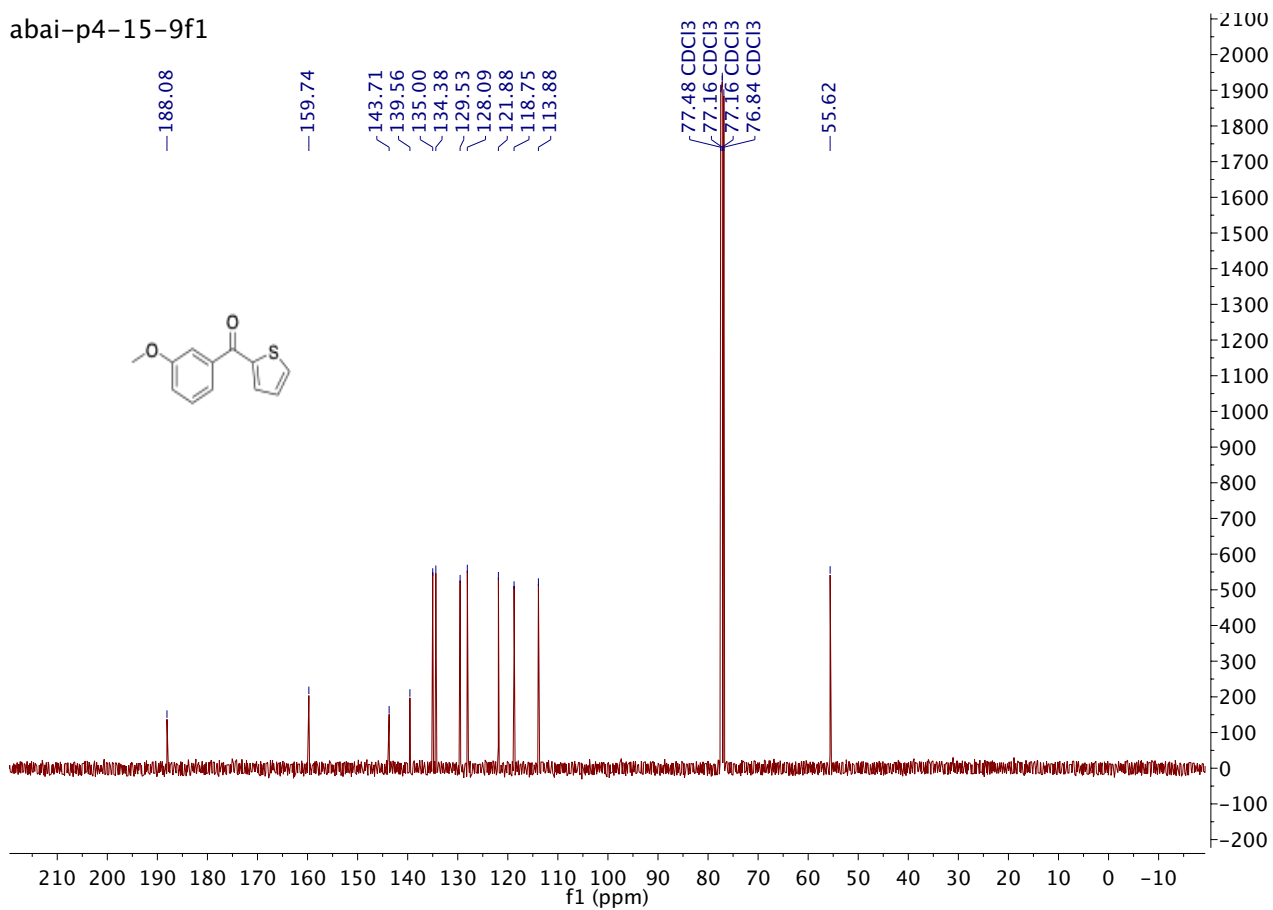


Compound 3j

abai-p4-15-9f1

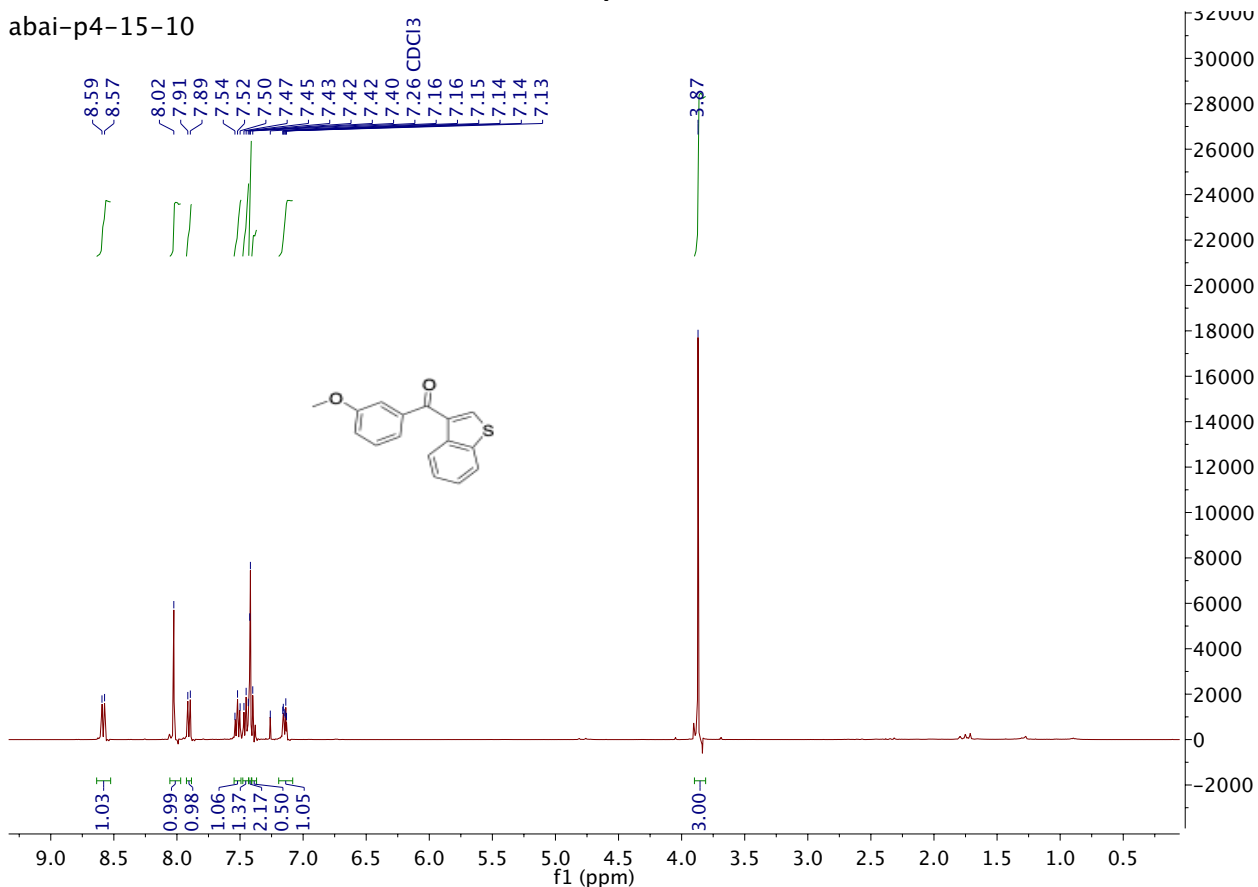


abai-p4-15-9f1

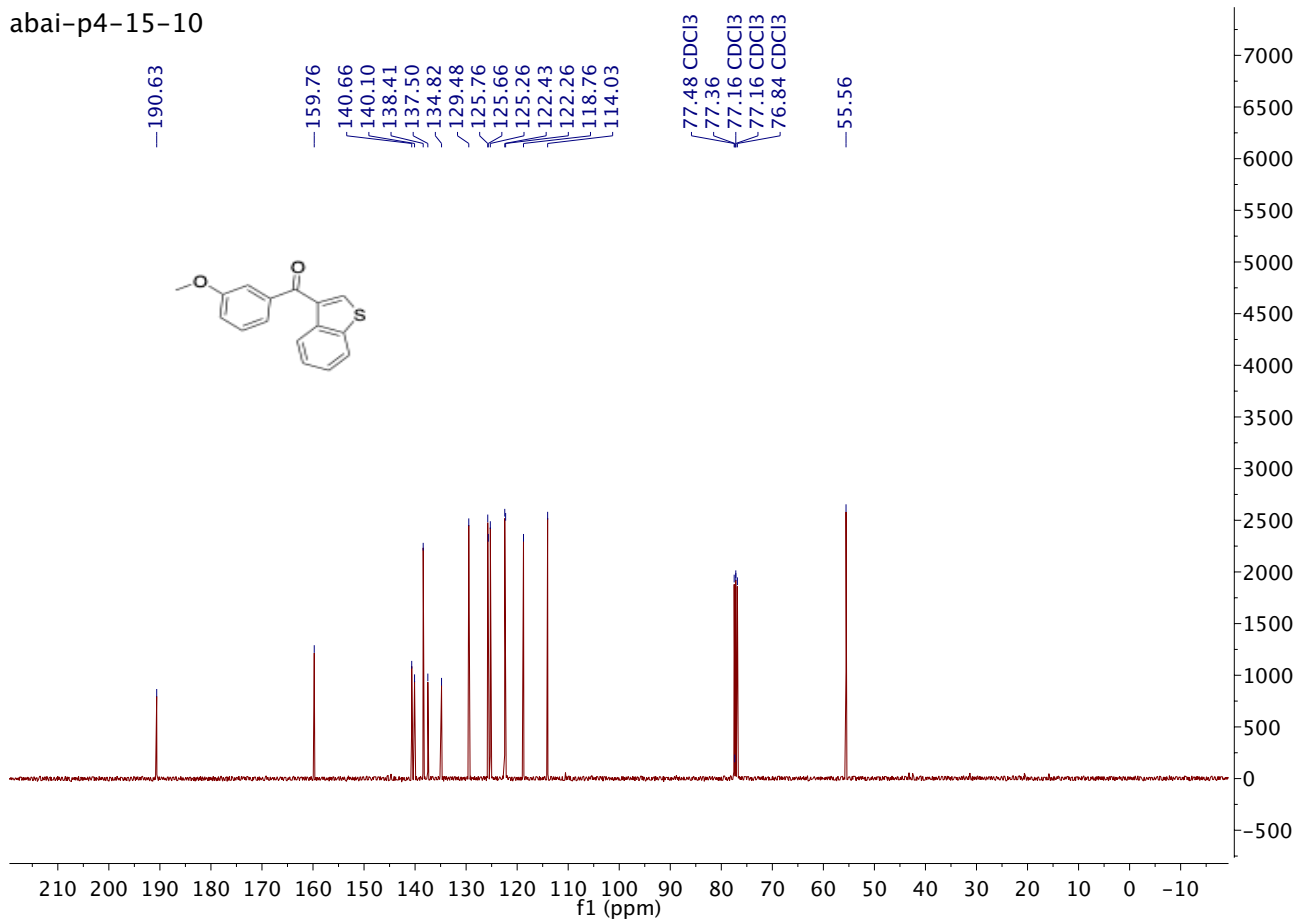


Compound 3k

abai-p4-15-10

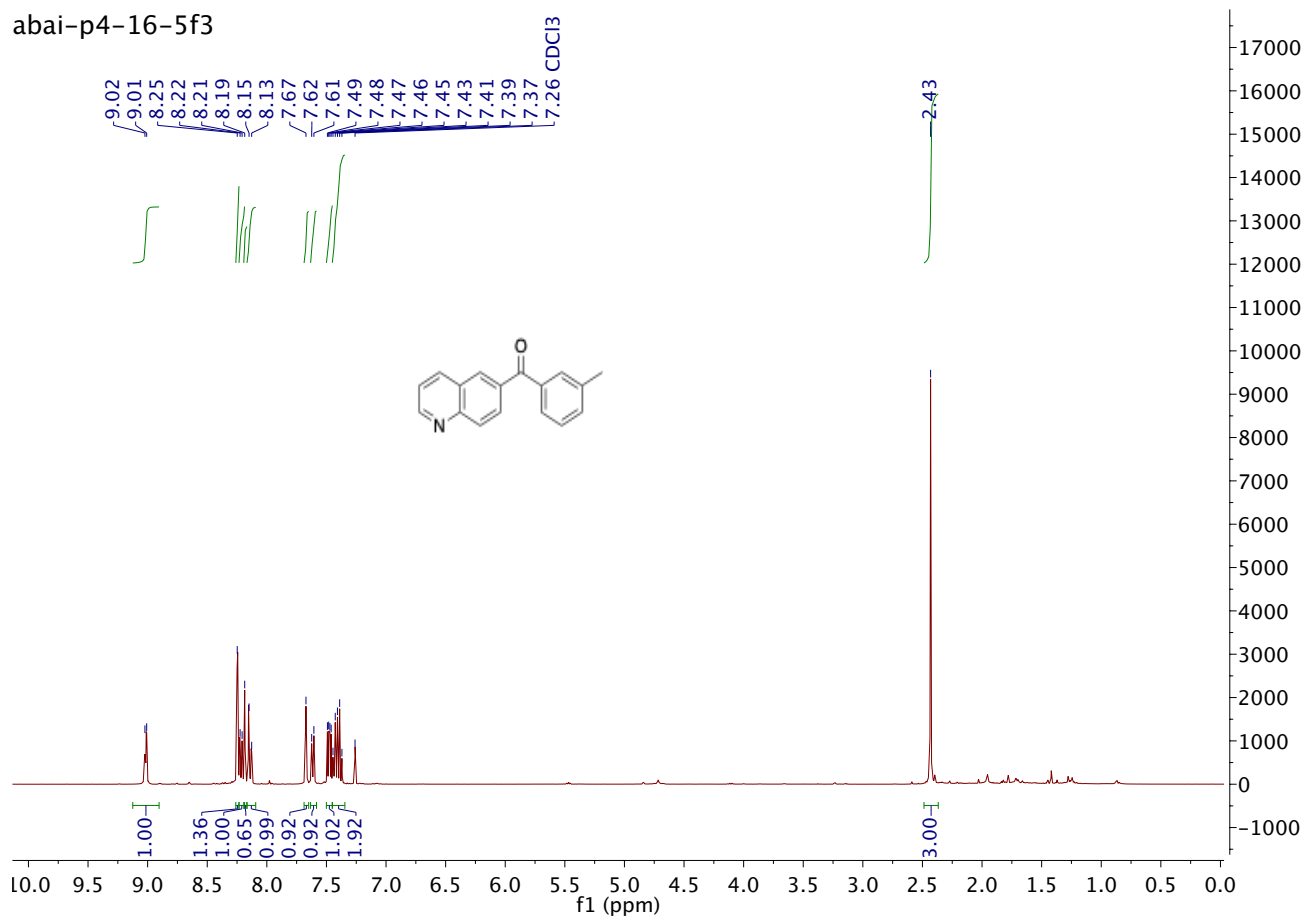


abai-p4-15-10

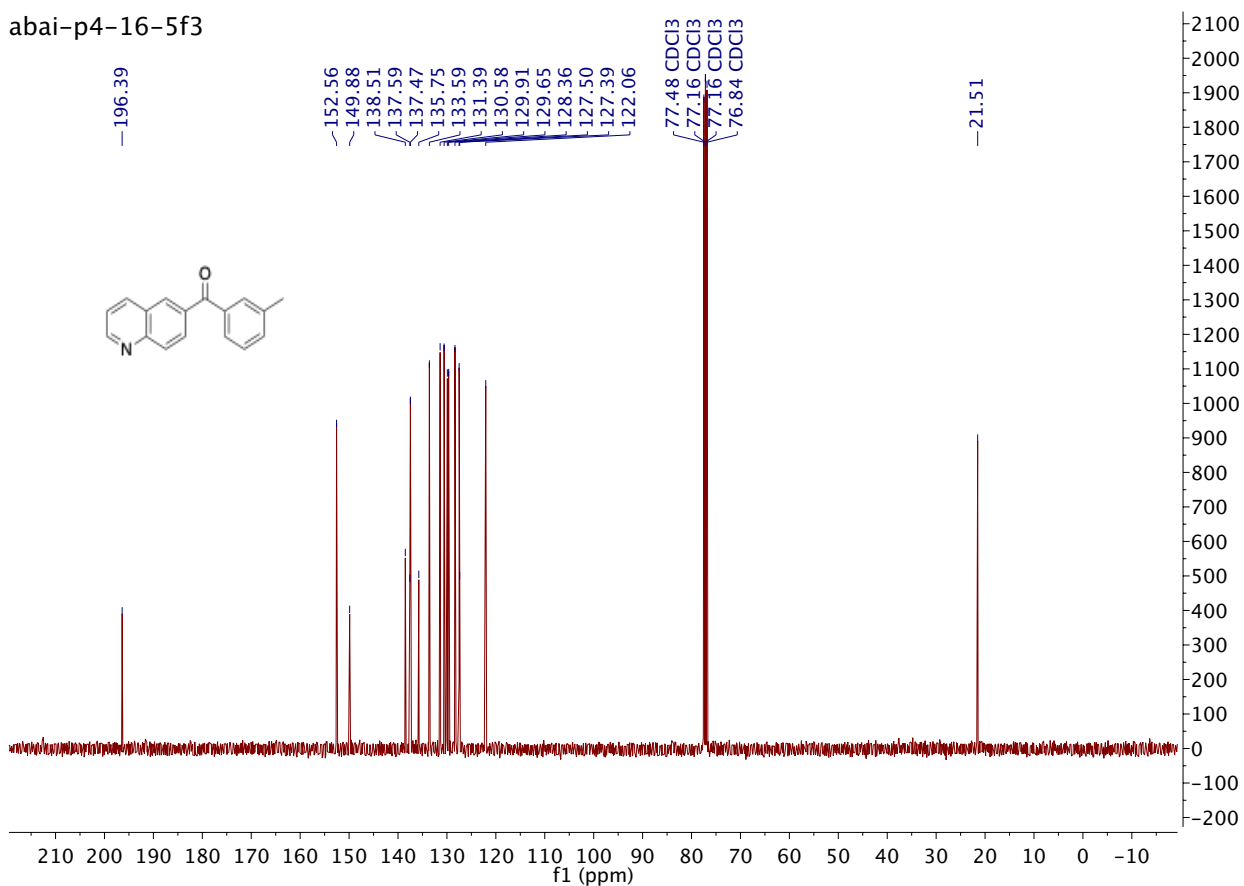


Compound 3I

abai-p4-16-5f3

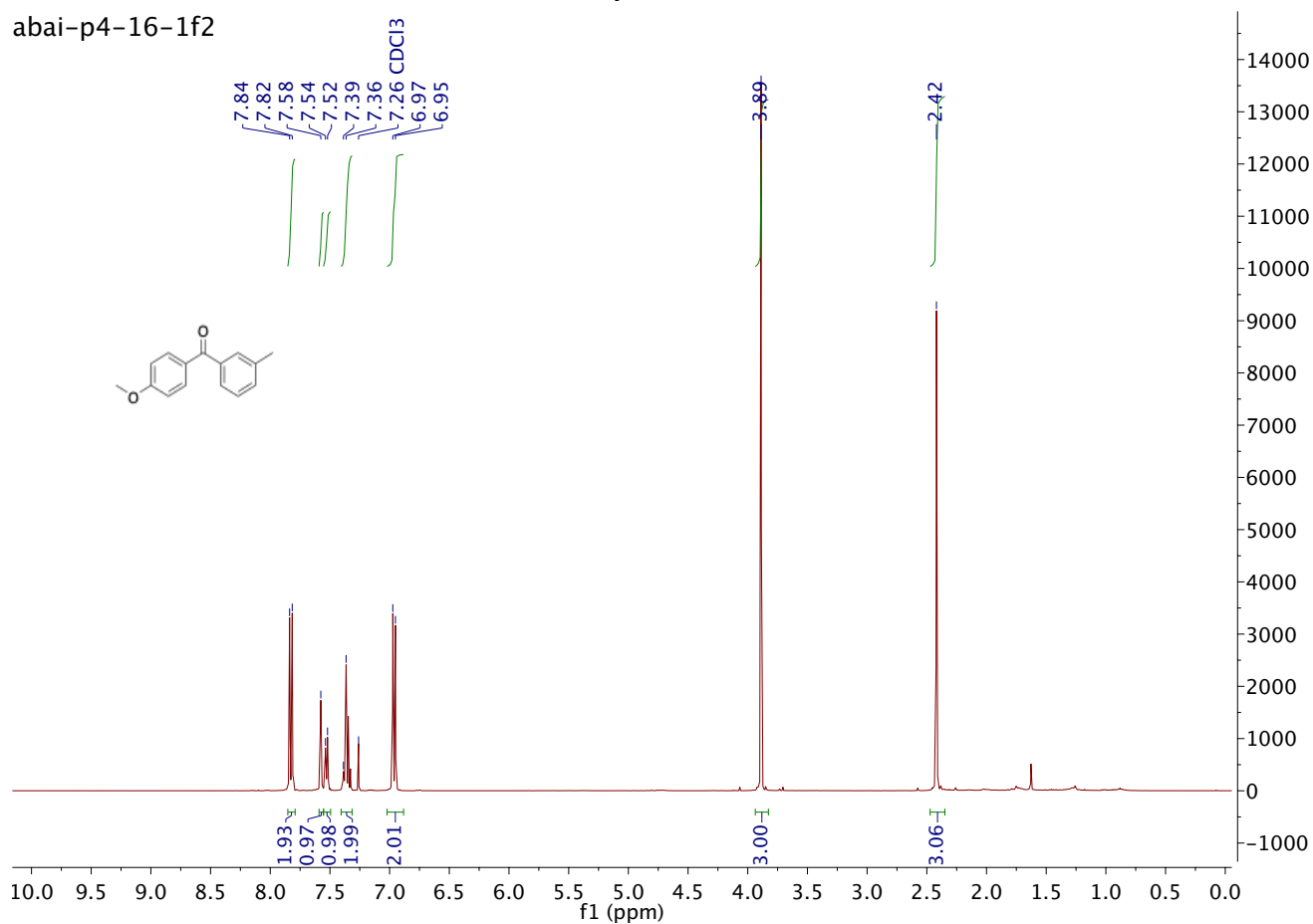


abai-p4-16-5f3

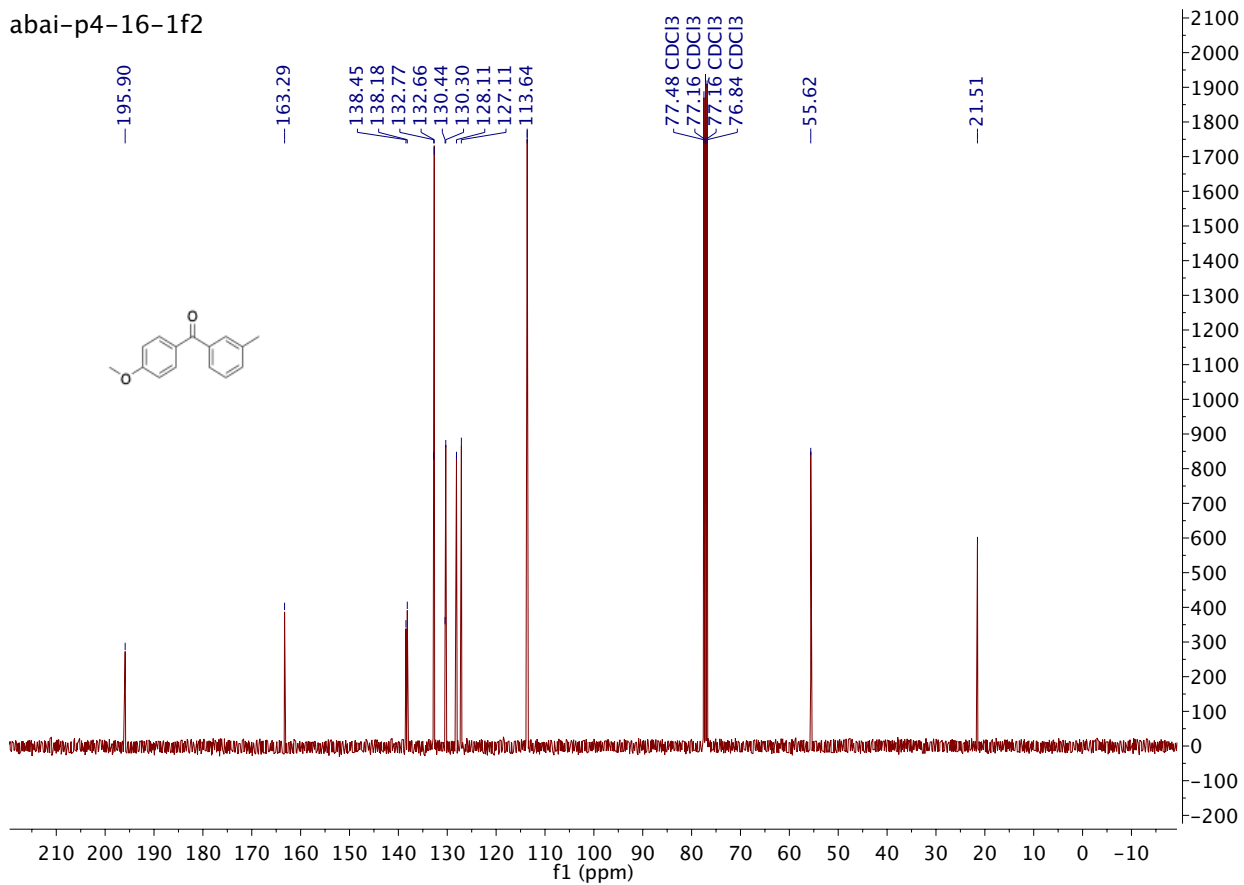


Compound 3m

abai-p4-16-1f2

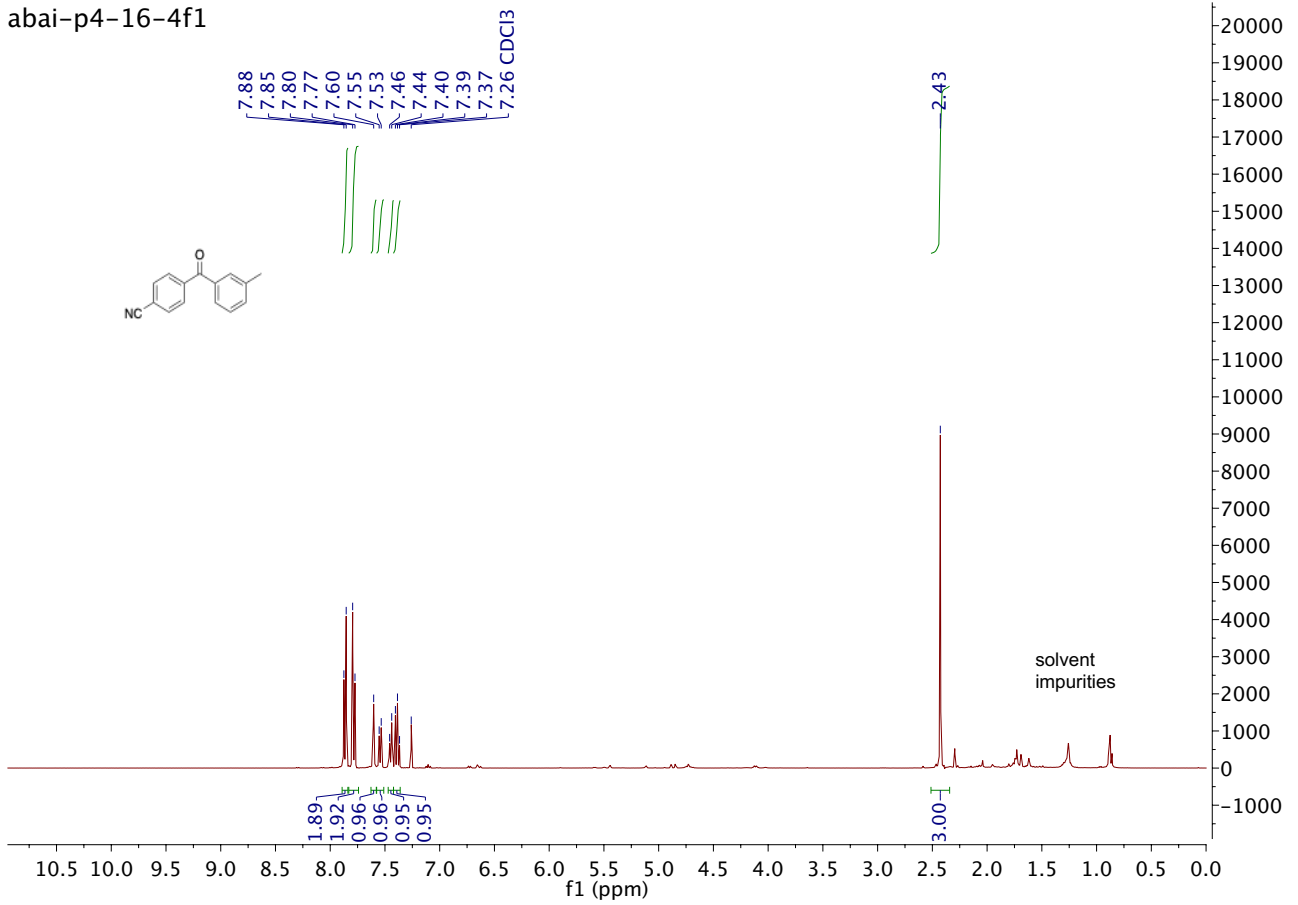


abai-p4-16-1f2

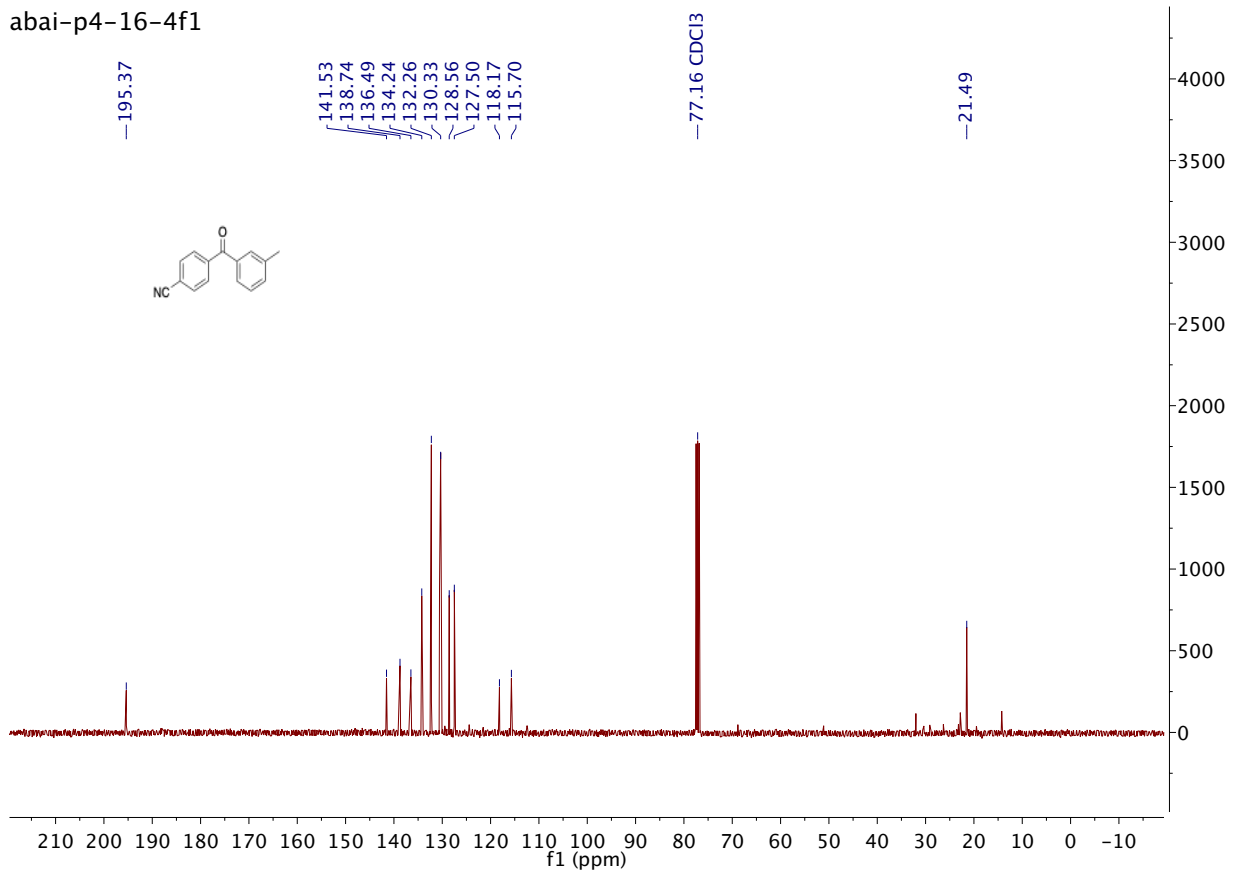


Compound 3n

abai-p4-16-4f1

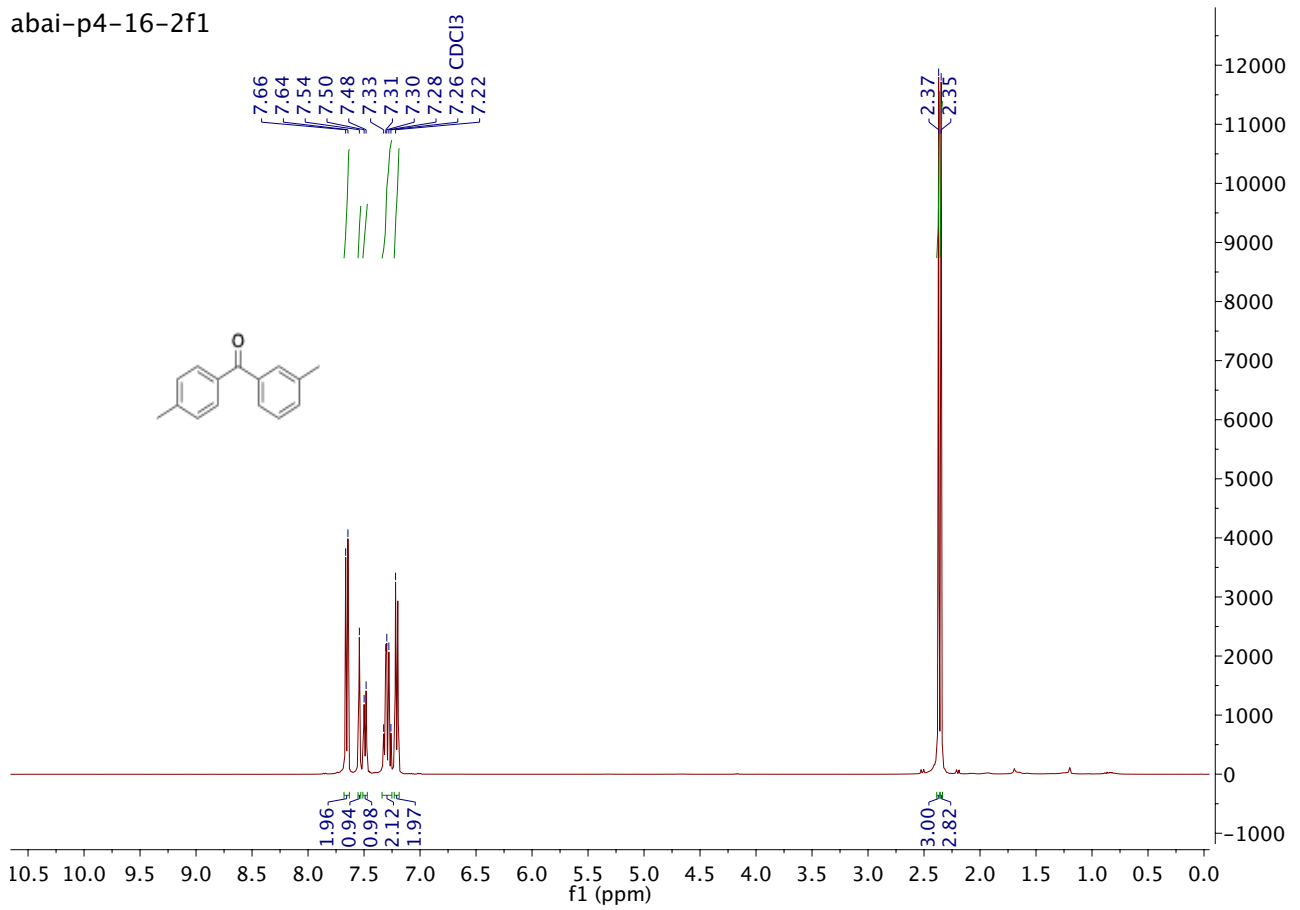


abai-p4-16-4f1

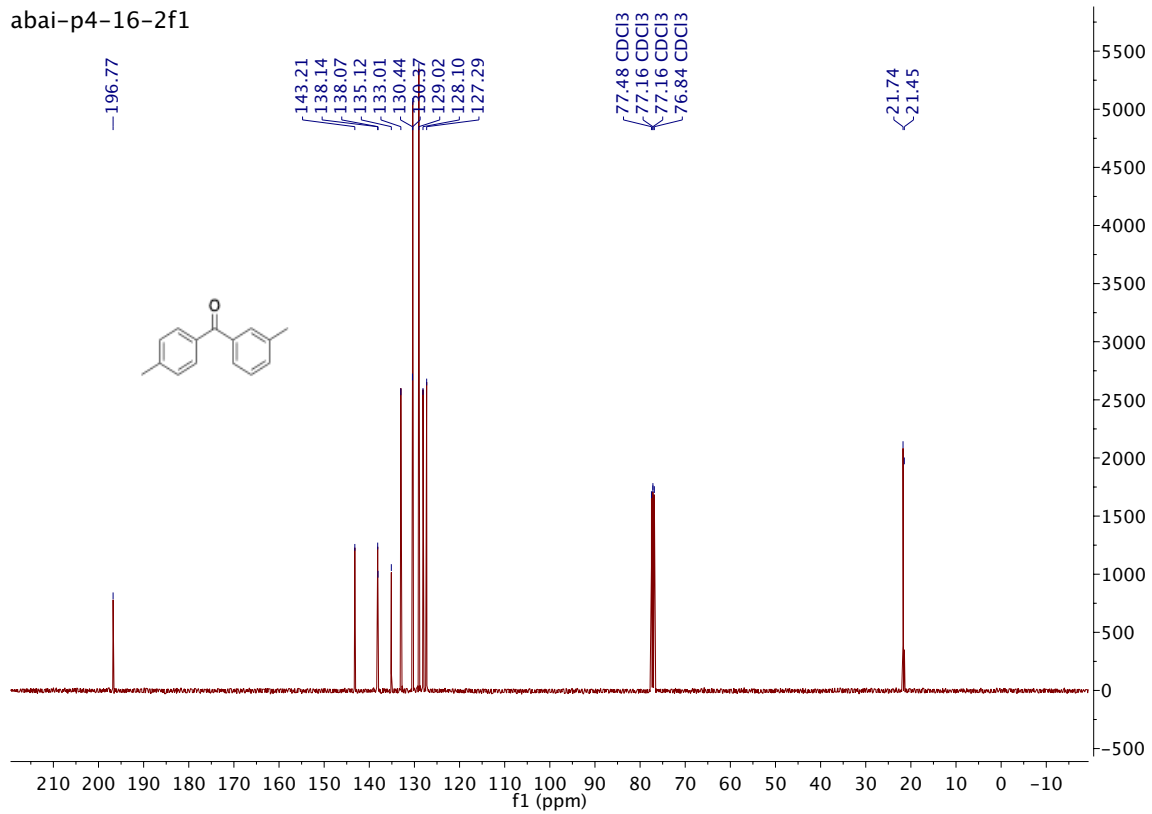


Compound 3o

abai-p4-16-2f1

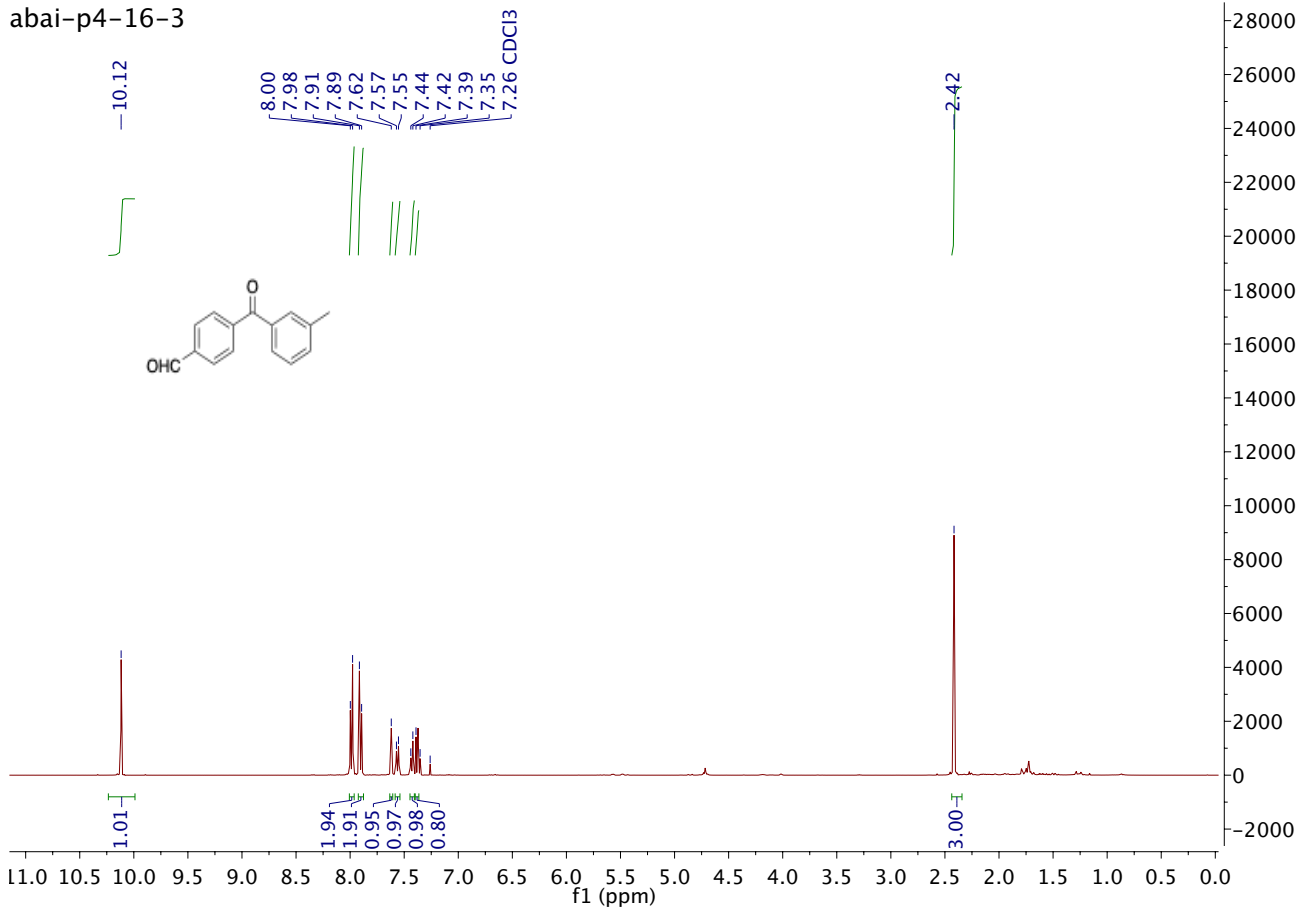


abai-p4-16-2f1

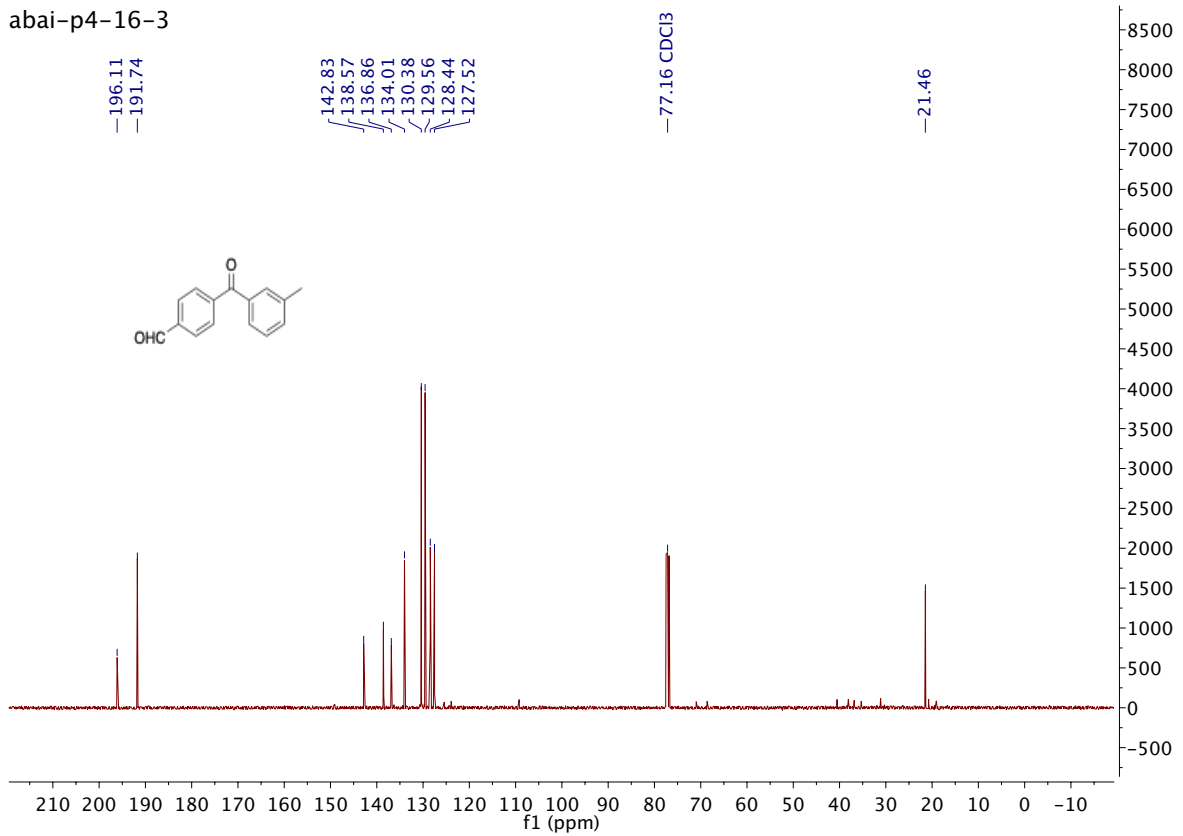


Compound 3p

abai-p4-16-3

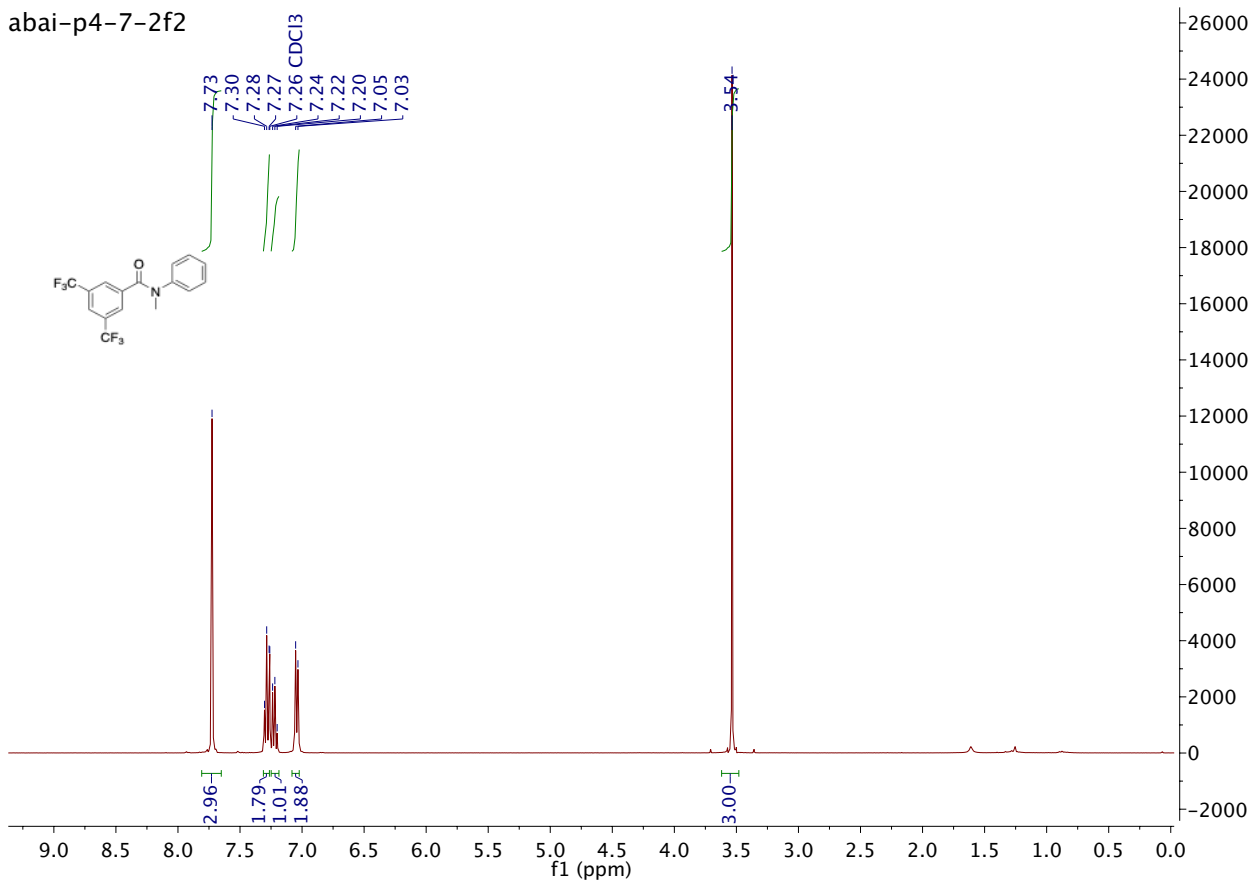


abai-p4-16-3

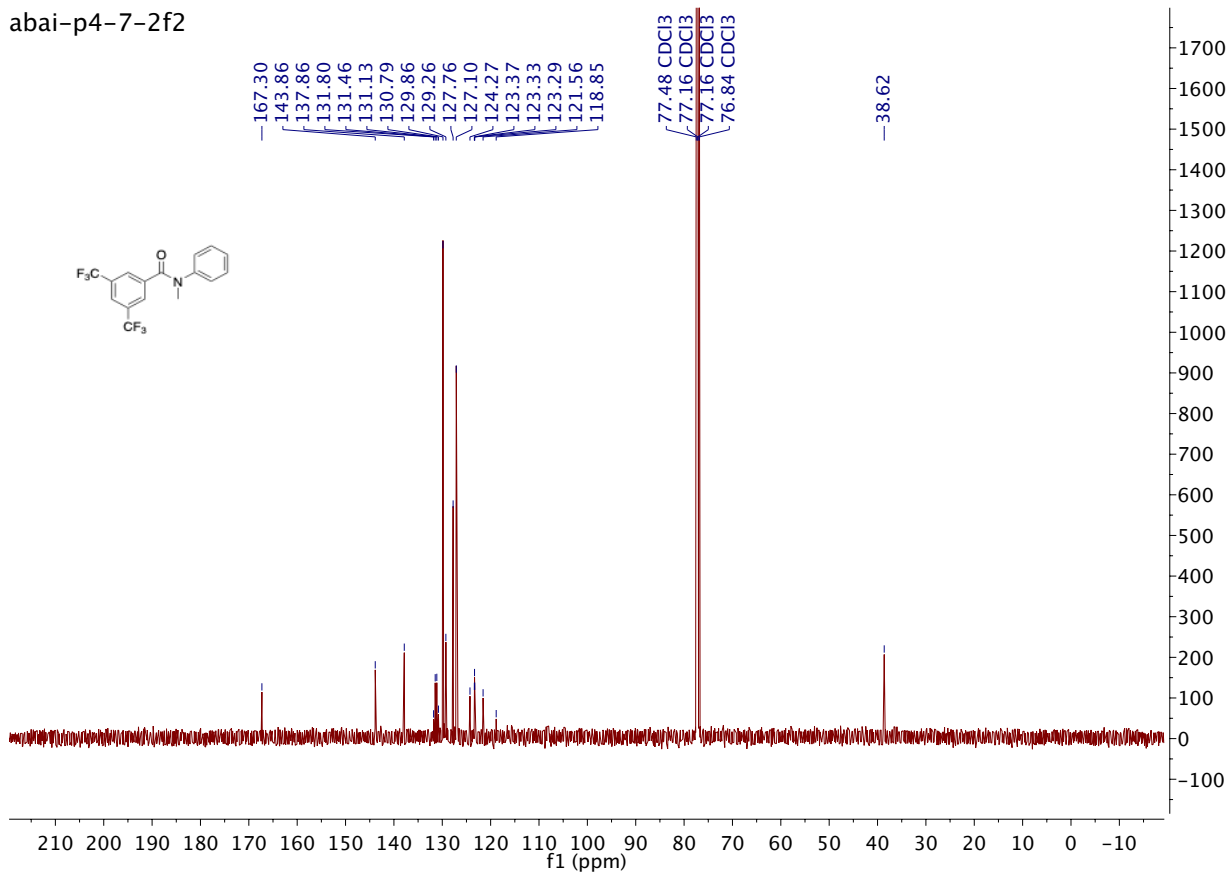


Compound 5a

abai-p4-7-2f2

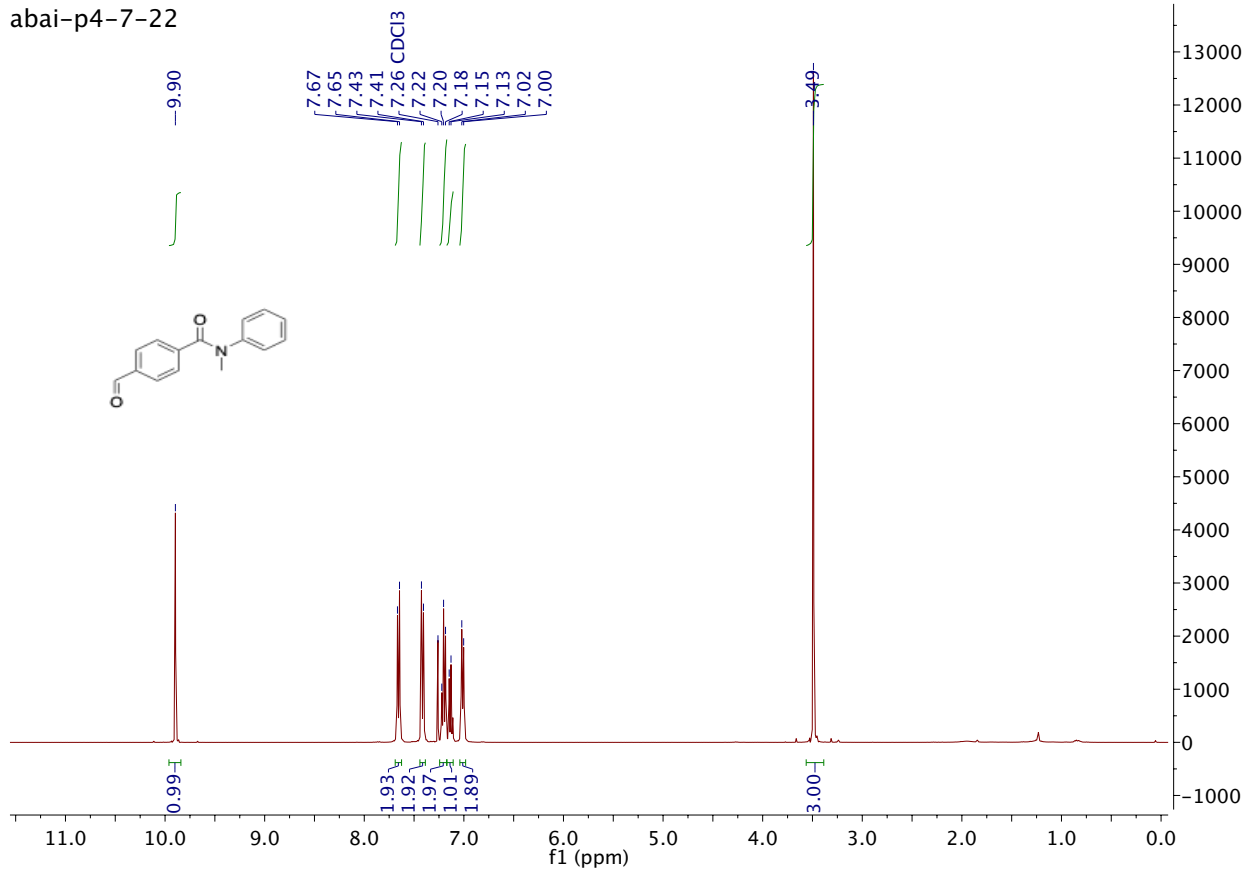


abai-p4-7-2f2

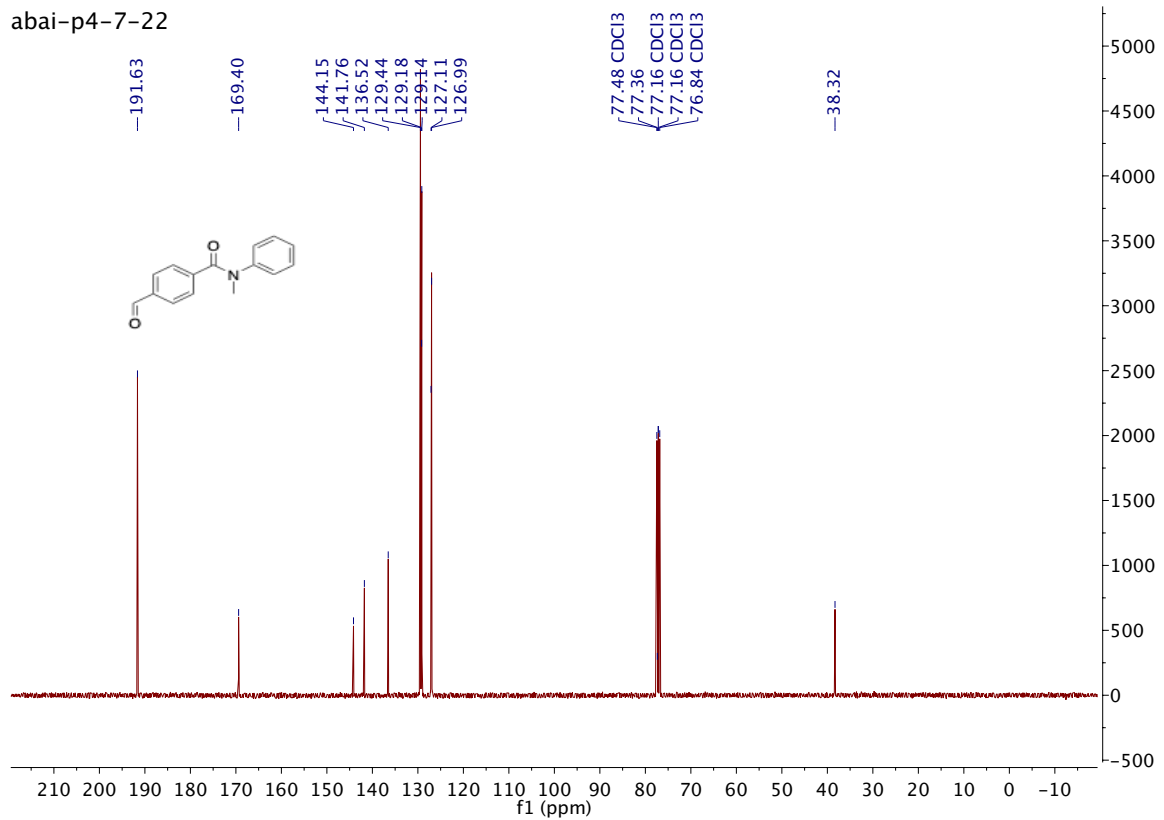


Compound 5b

abai-p4-7-22

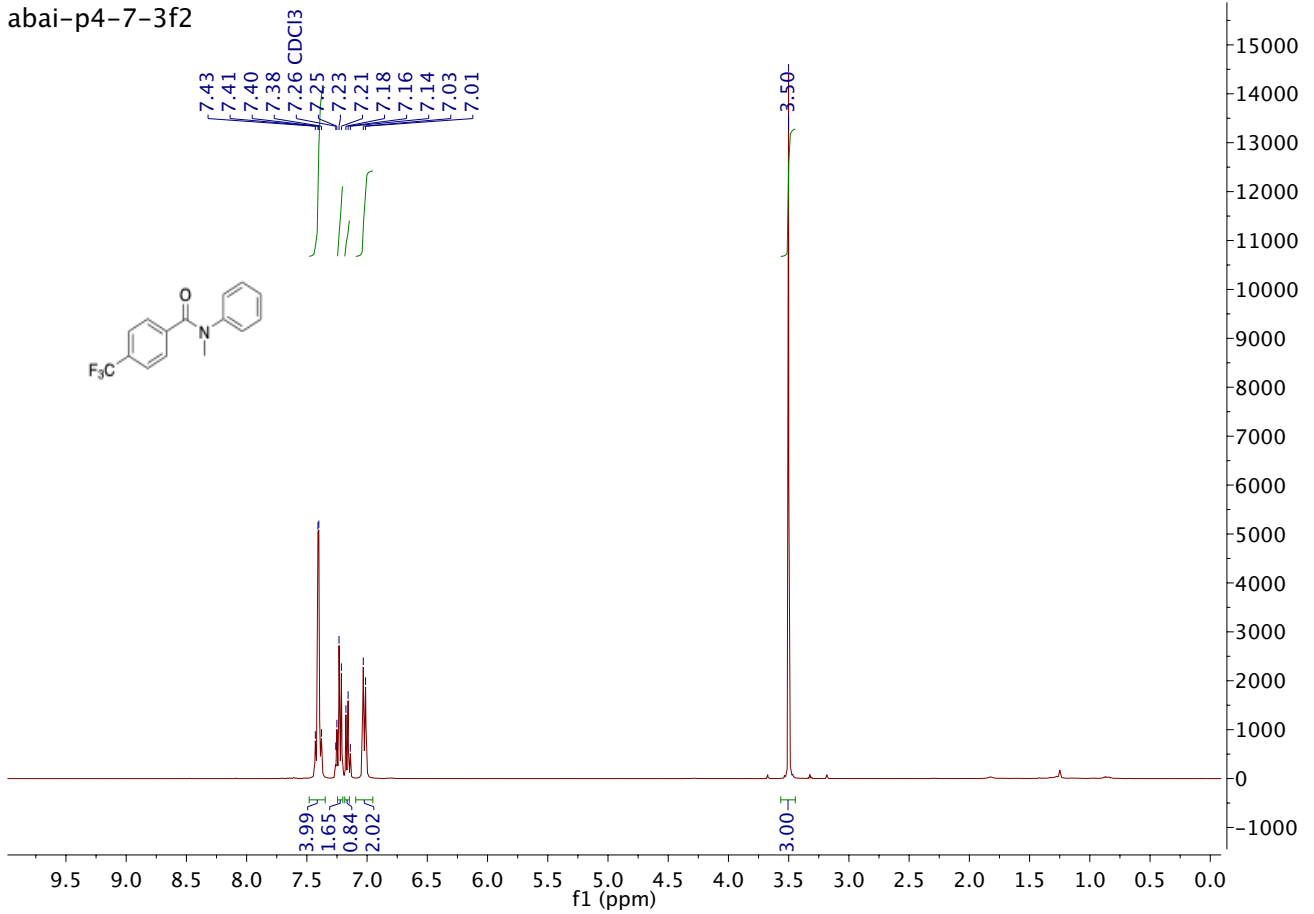


abai-p4-7-22

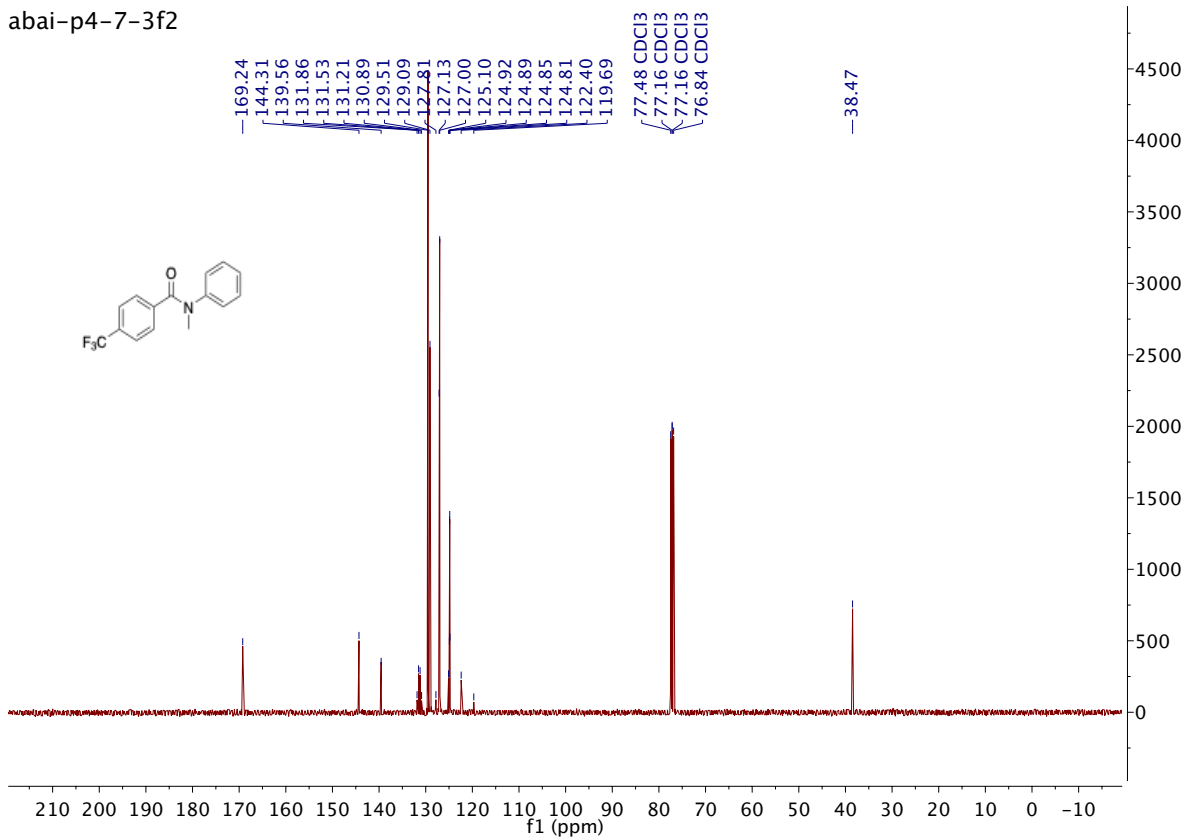


Compound 5c

abai-p4-7-3f2

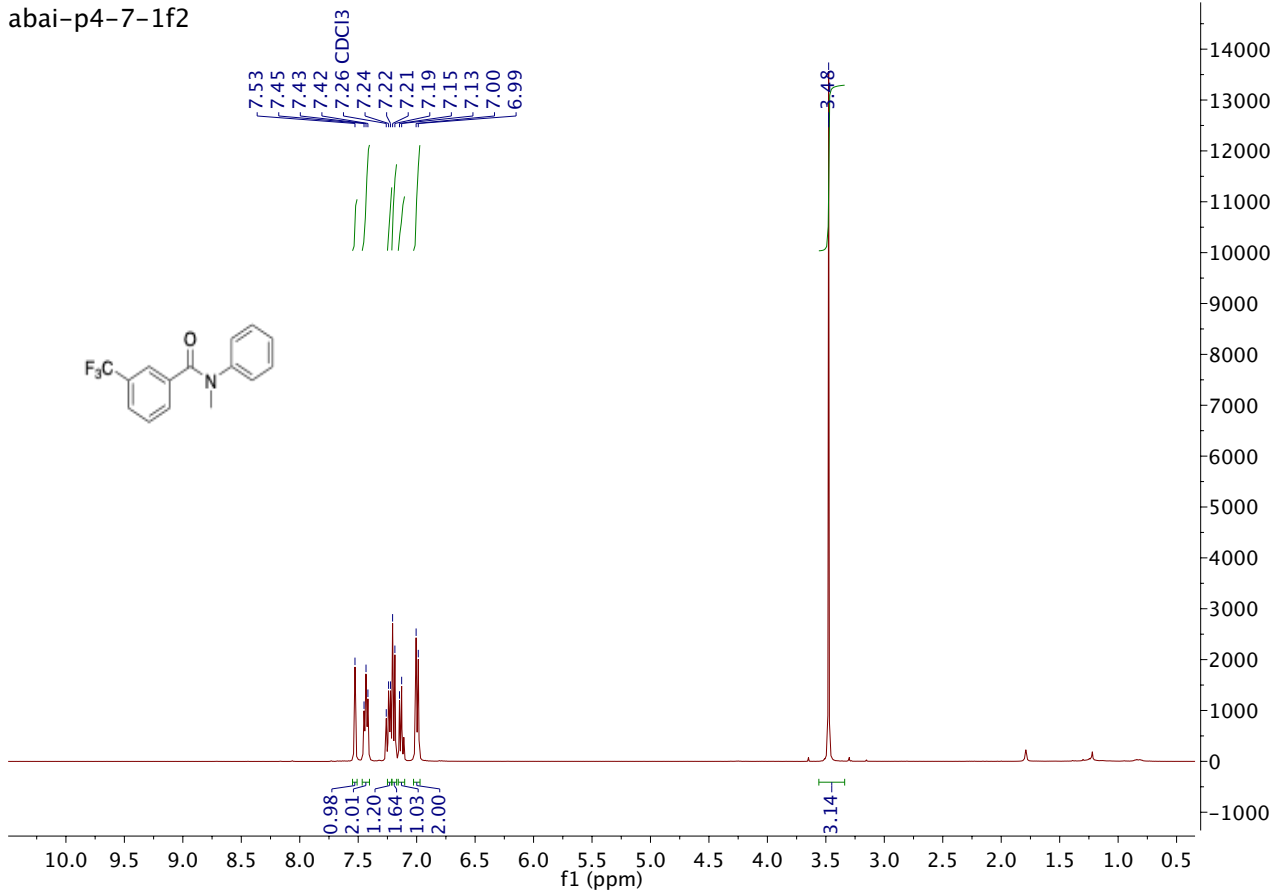


abai-p4-7-3f2

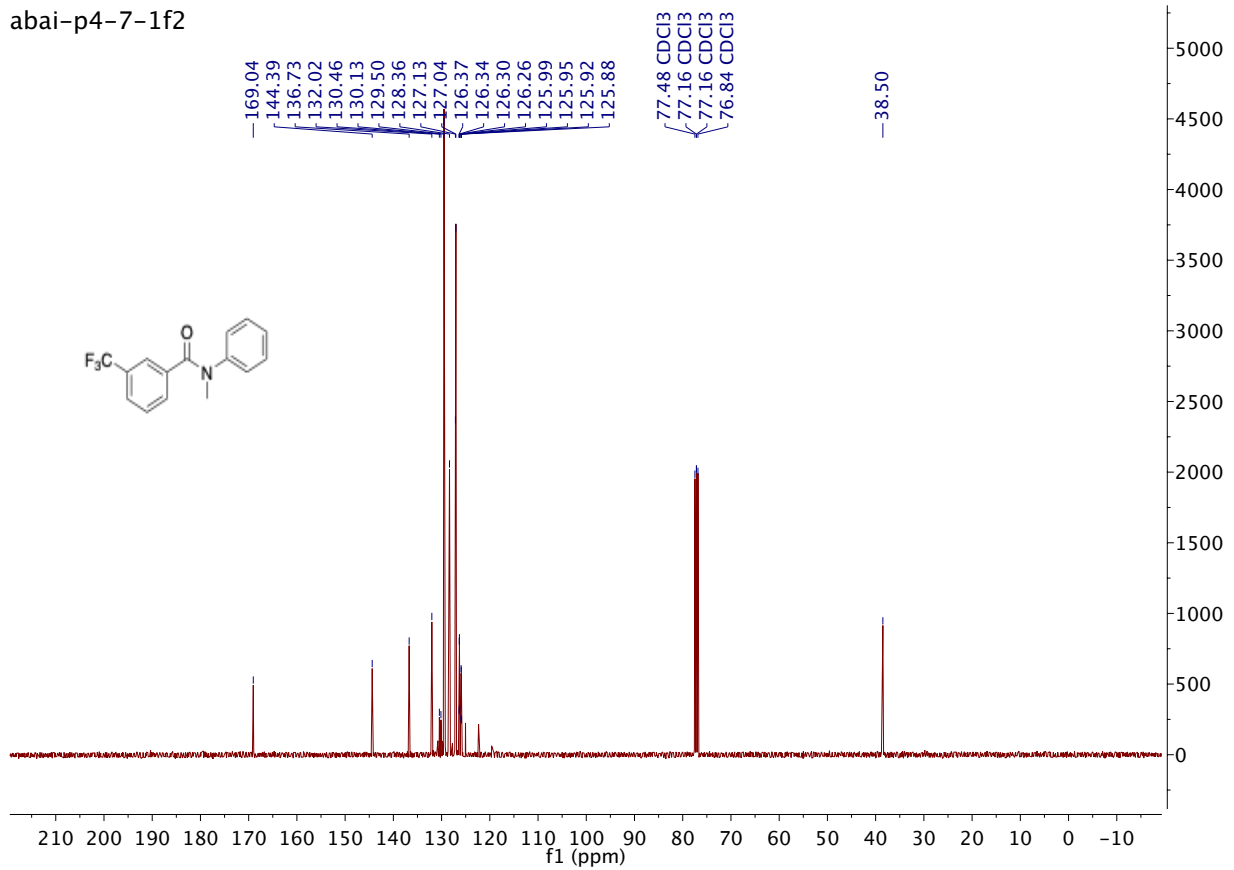


Compound 5d

abai-p4-7-1f2

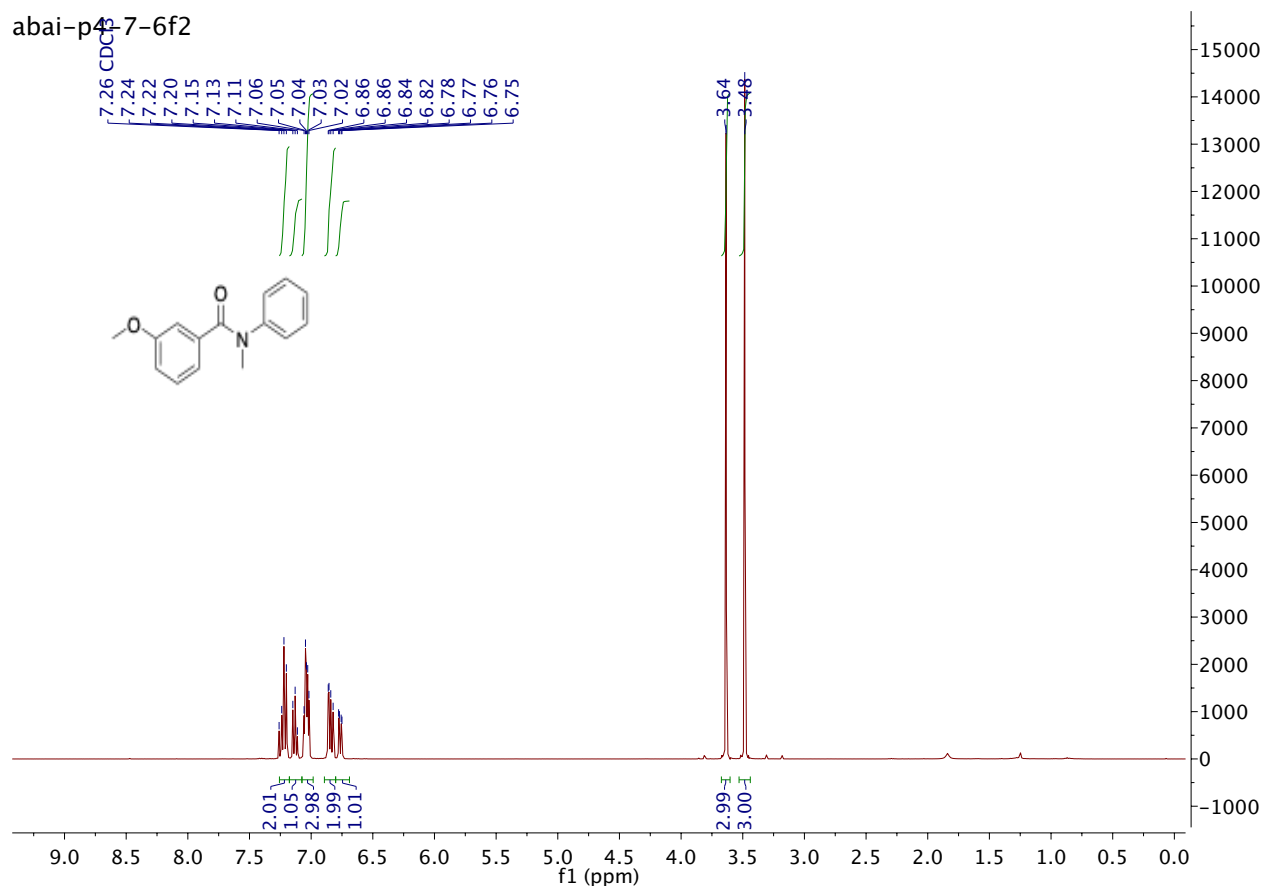


abai-p4-7-1f2

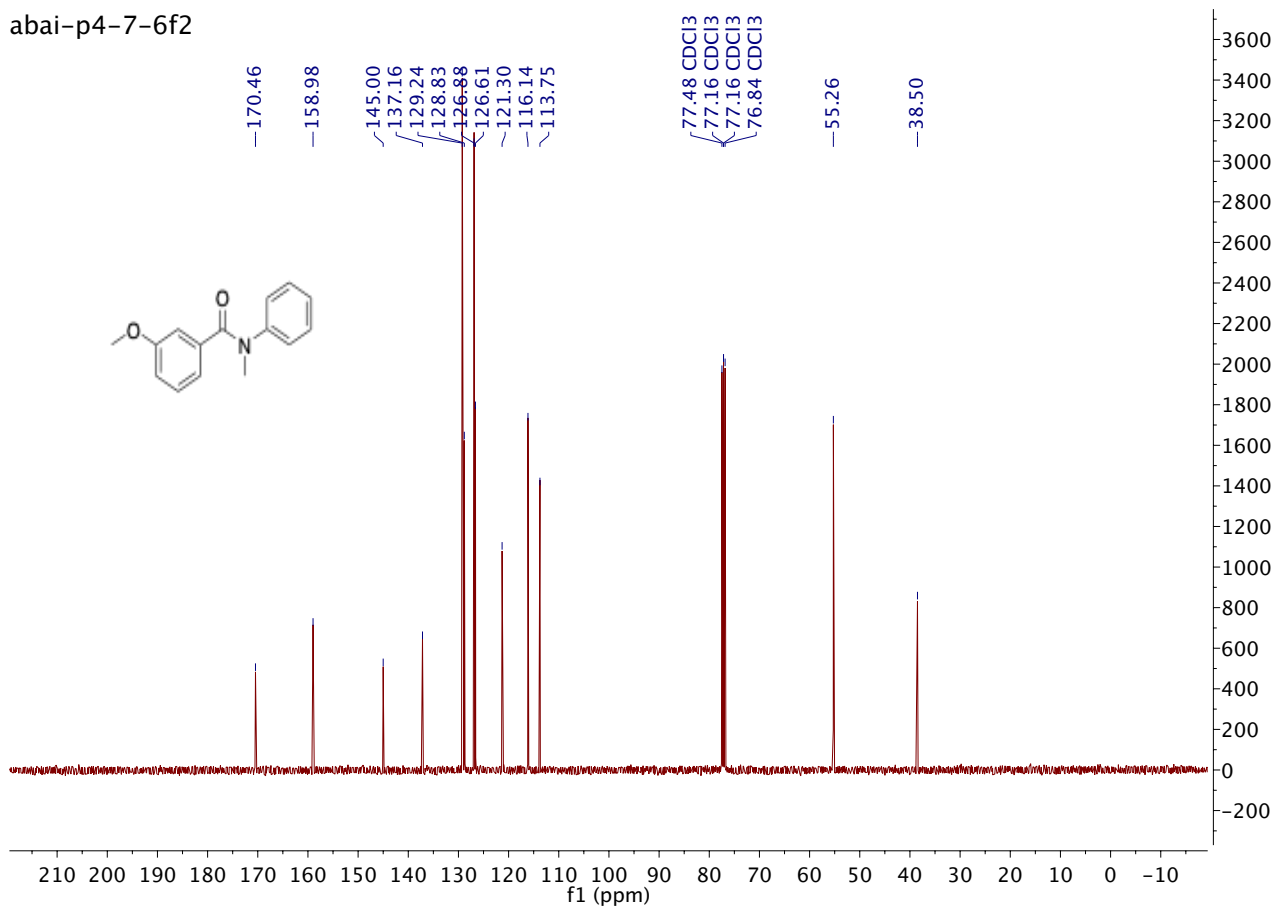


Compound 5e

abai-p4-7-6f2

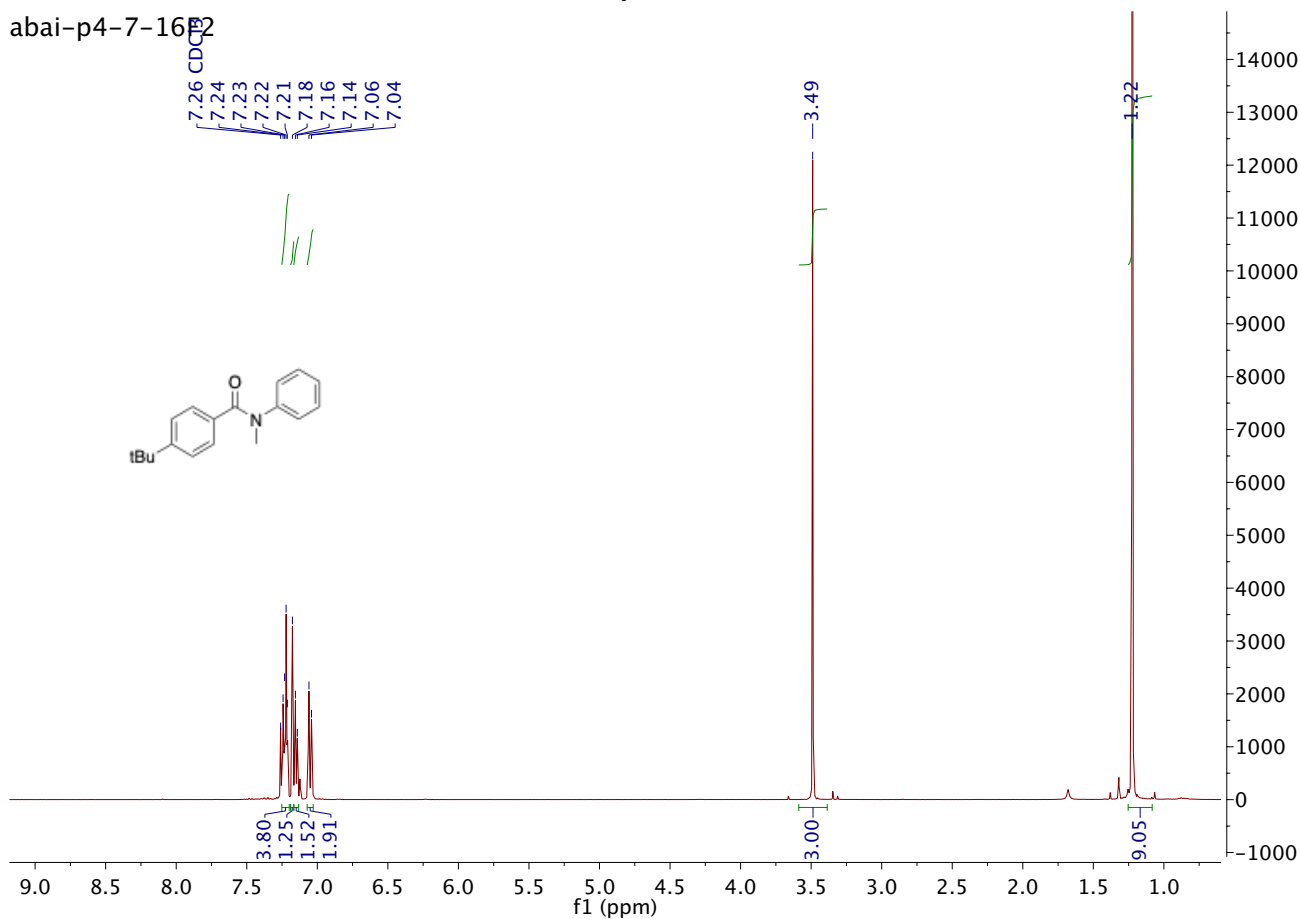


abai-p4-7-6f2

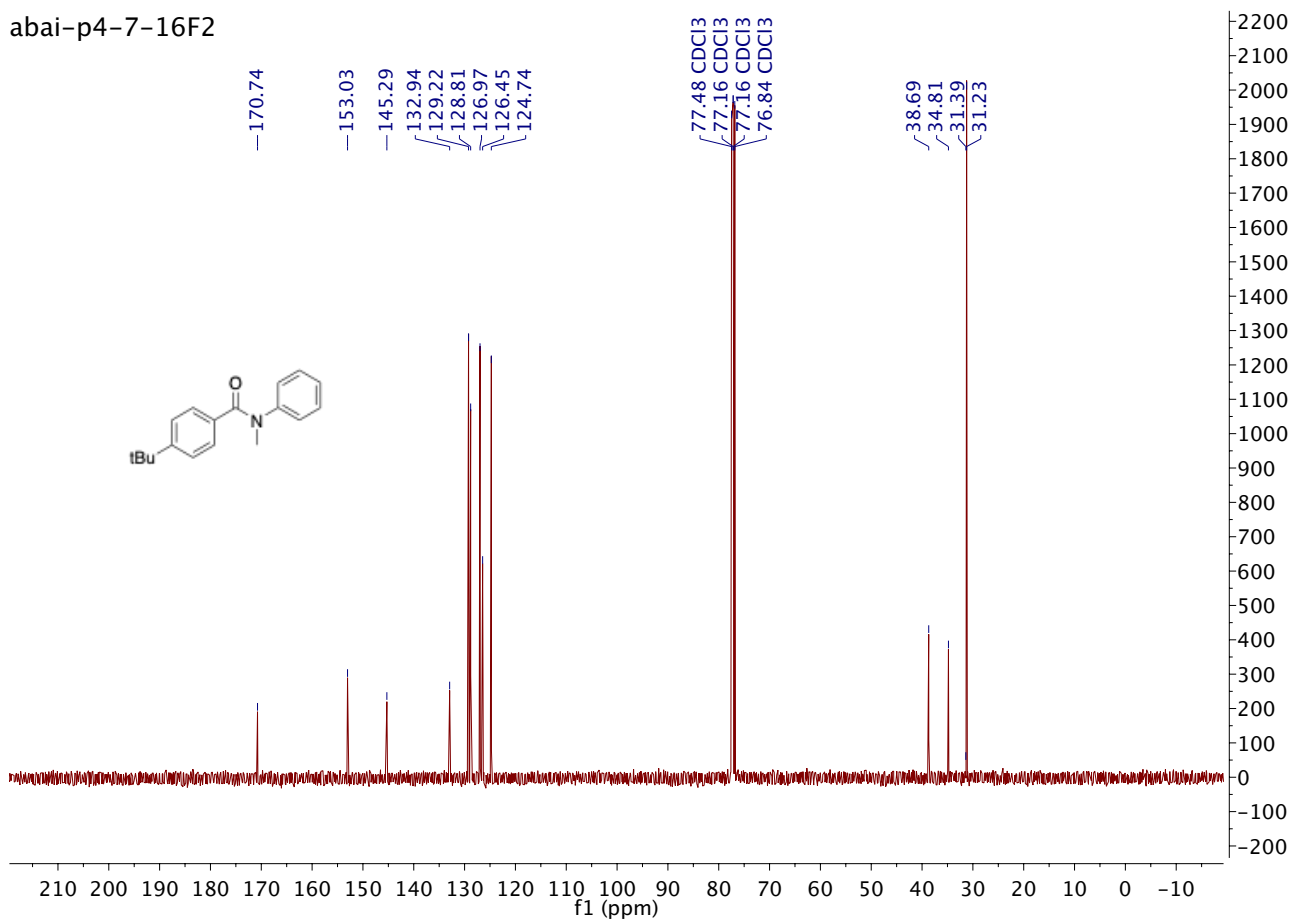


Compound 5f

abai-p4-7-16F2

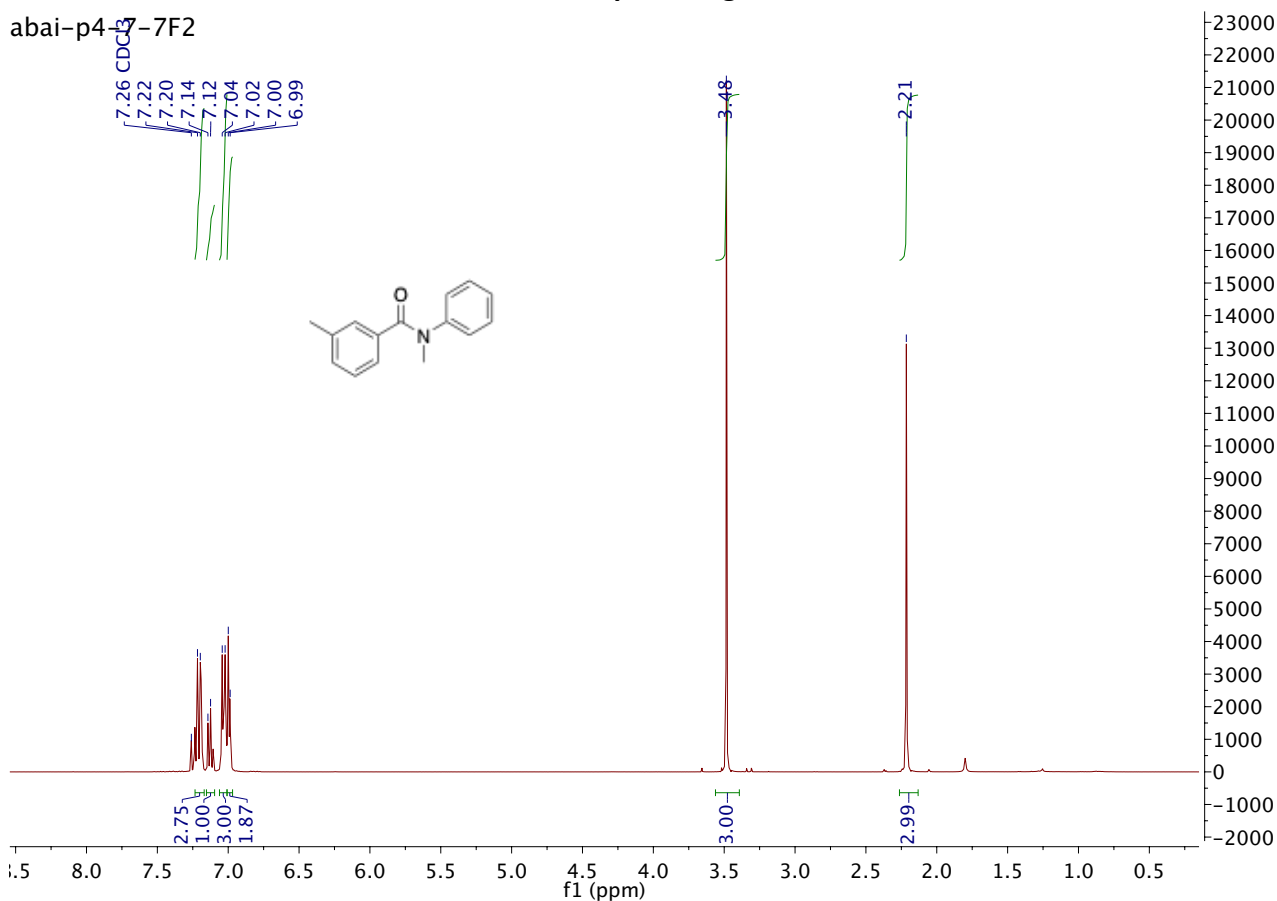


abai-p4-7-16F2

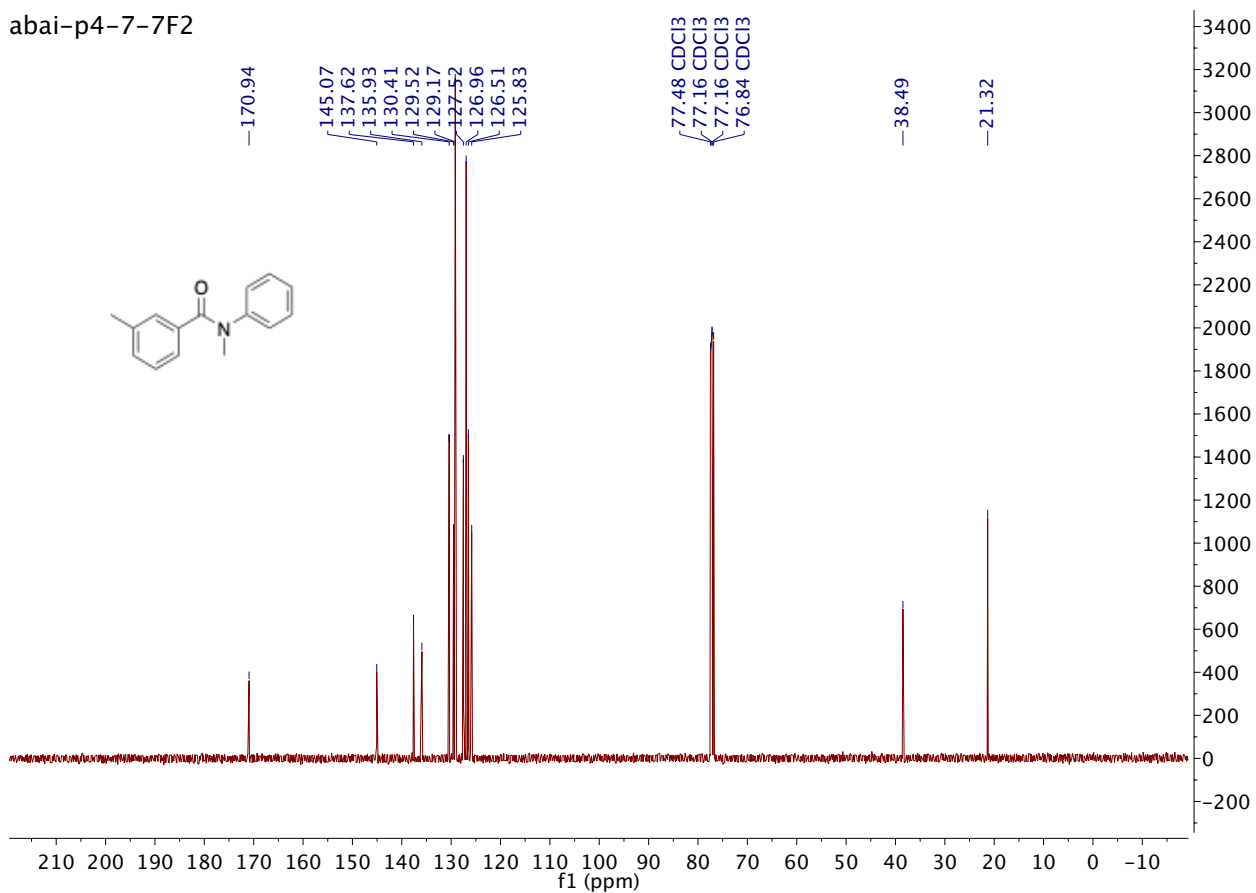


Compound 5g

abai-p4-7-7F2

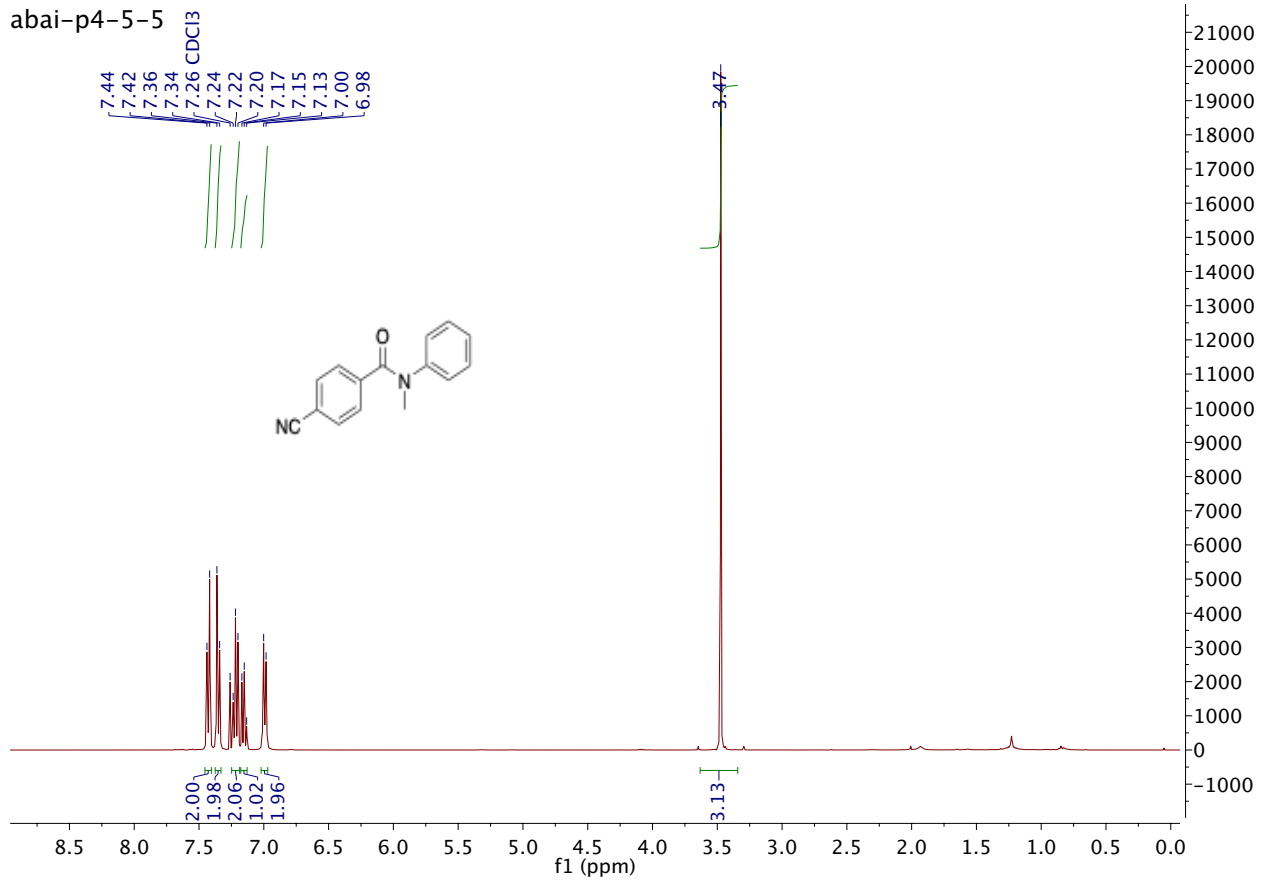


abai-p4-7-7F2

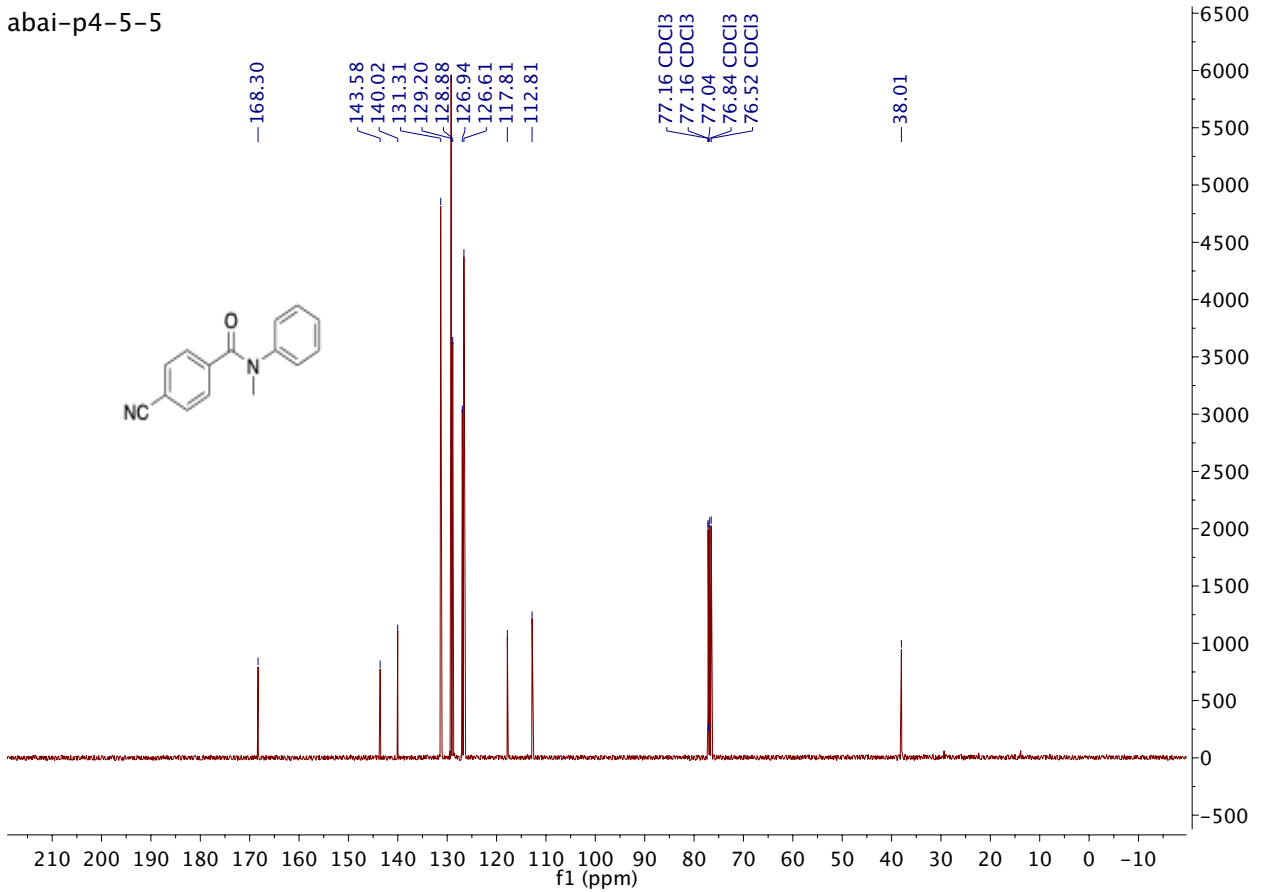


Compound 5h

abai-p4-5-5

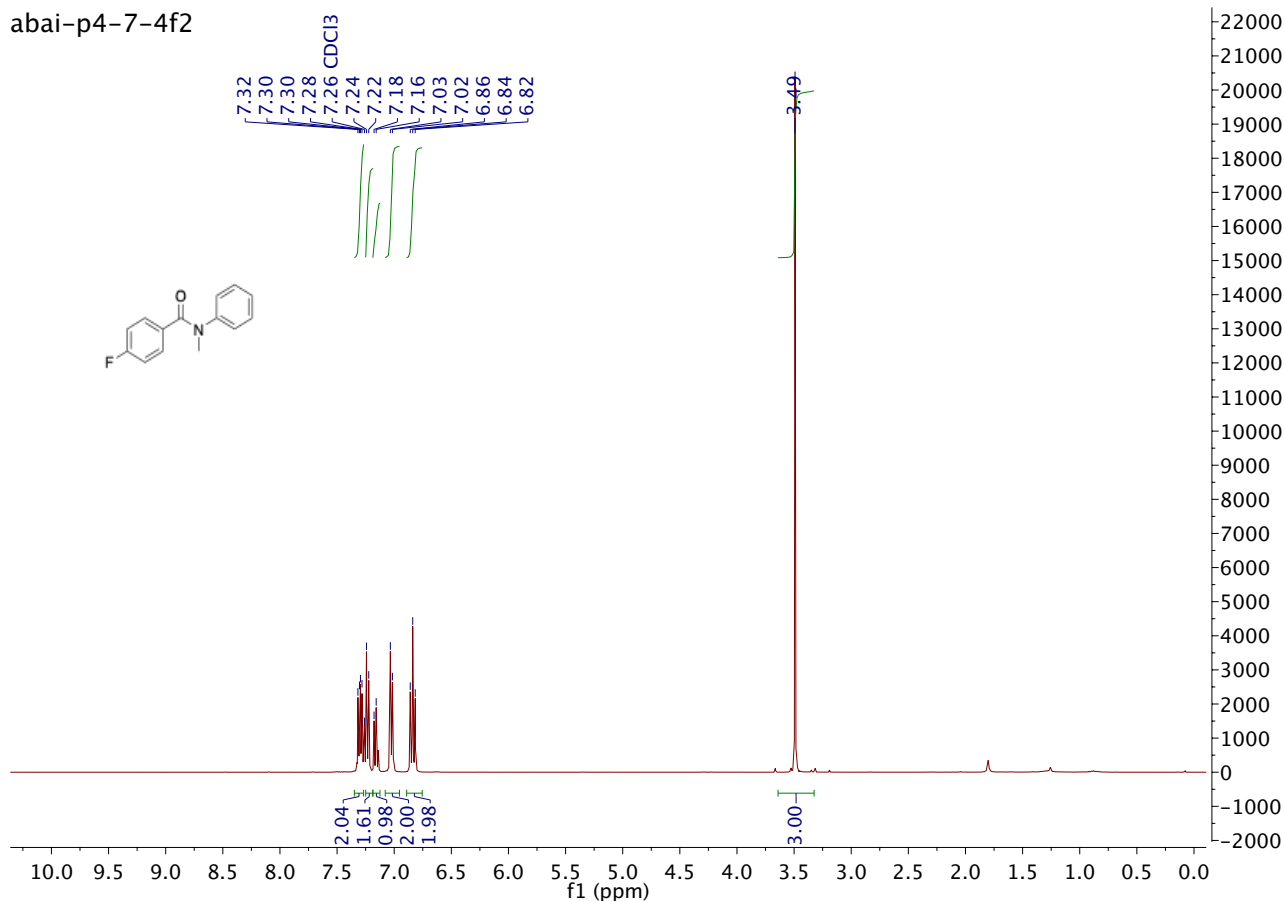


abai-p4-5-5

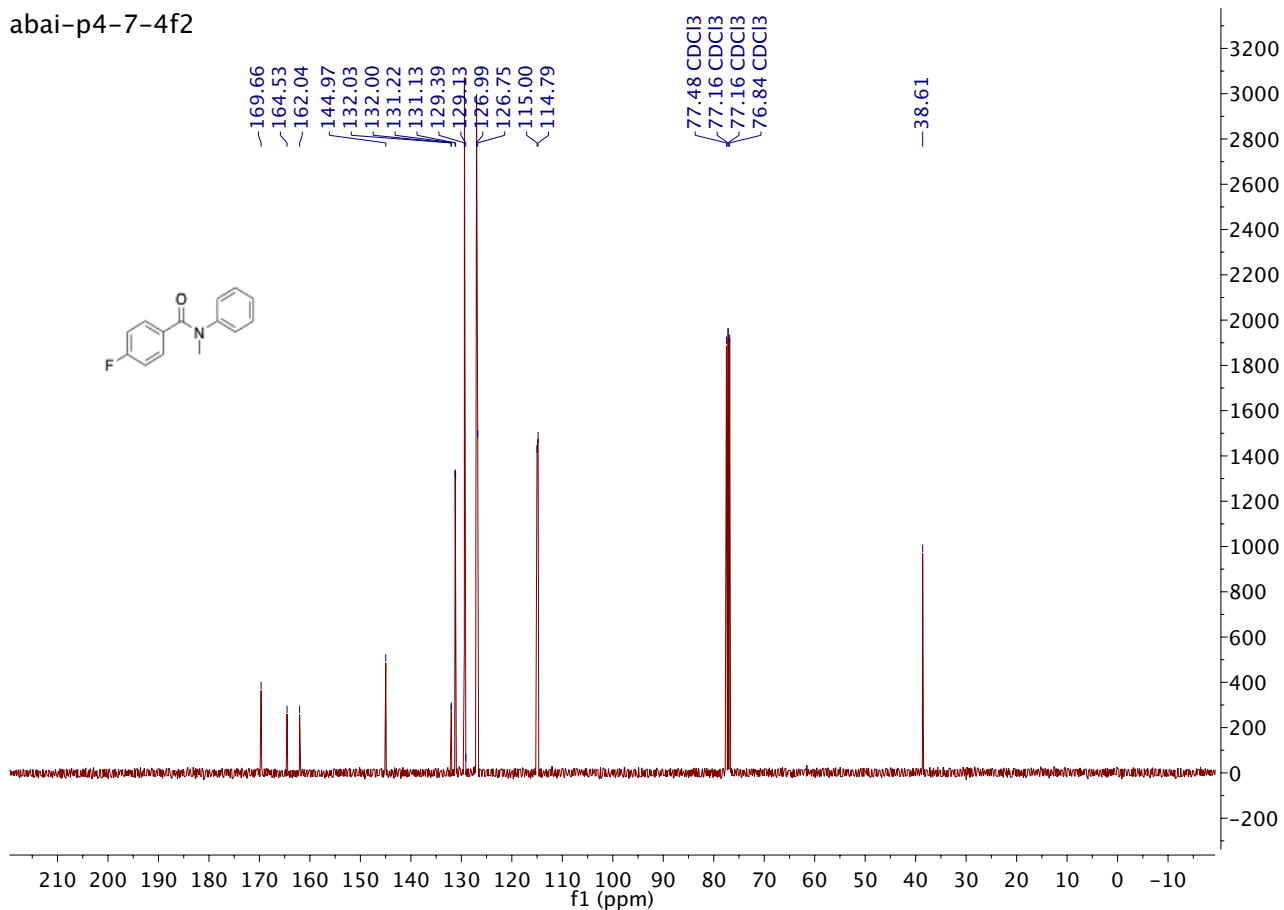


Compound 5i

abai-p4-7-4f2

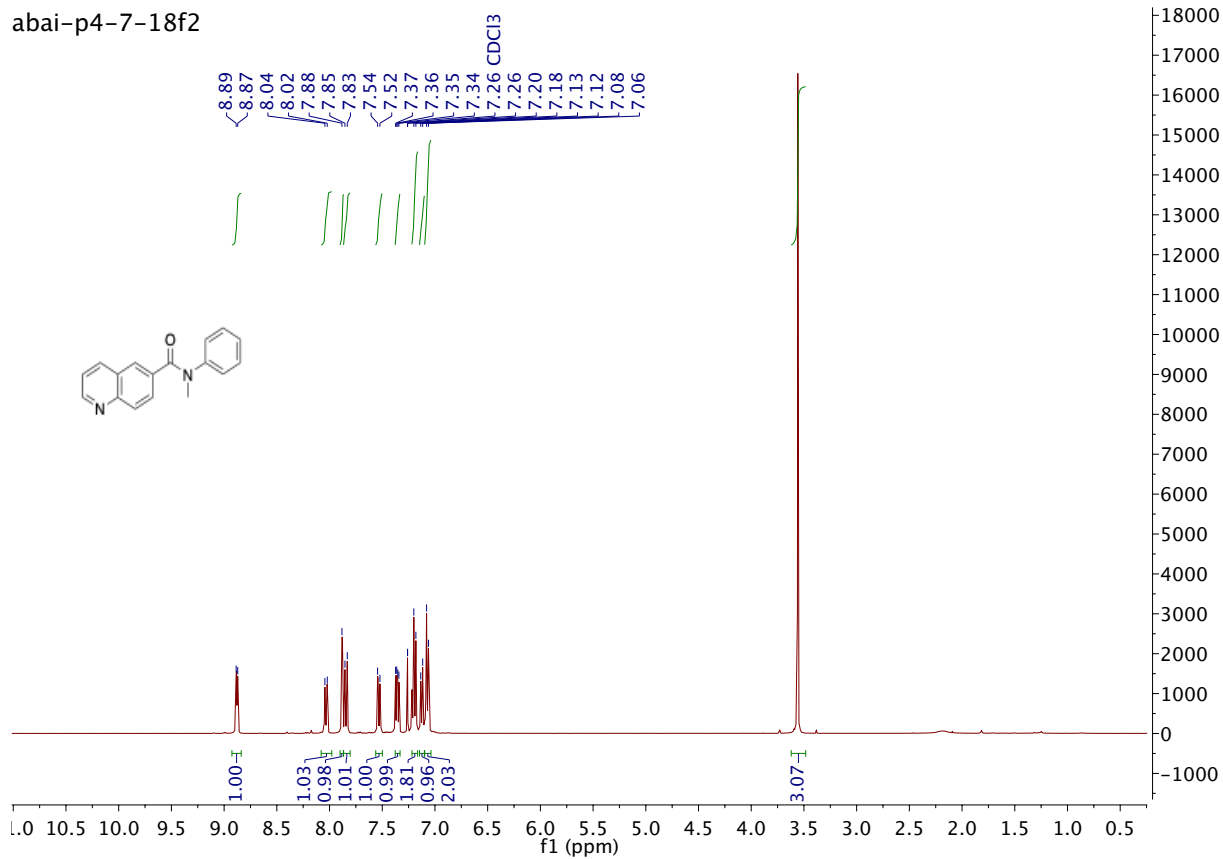


abai-p4-7-4f2

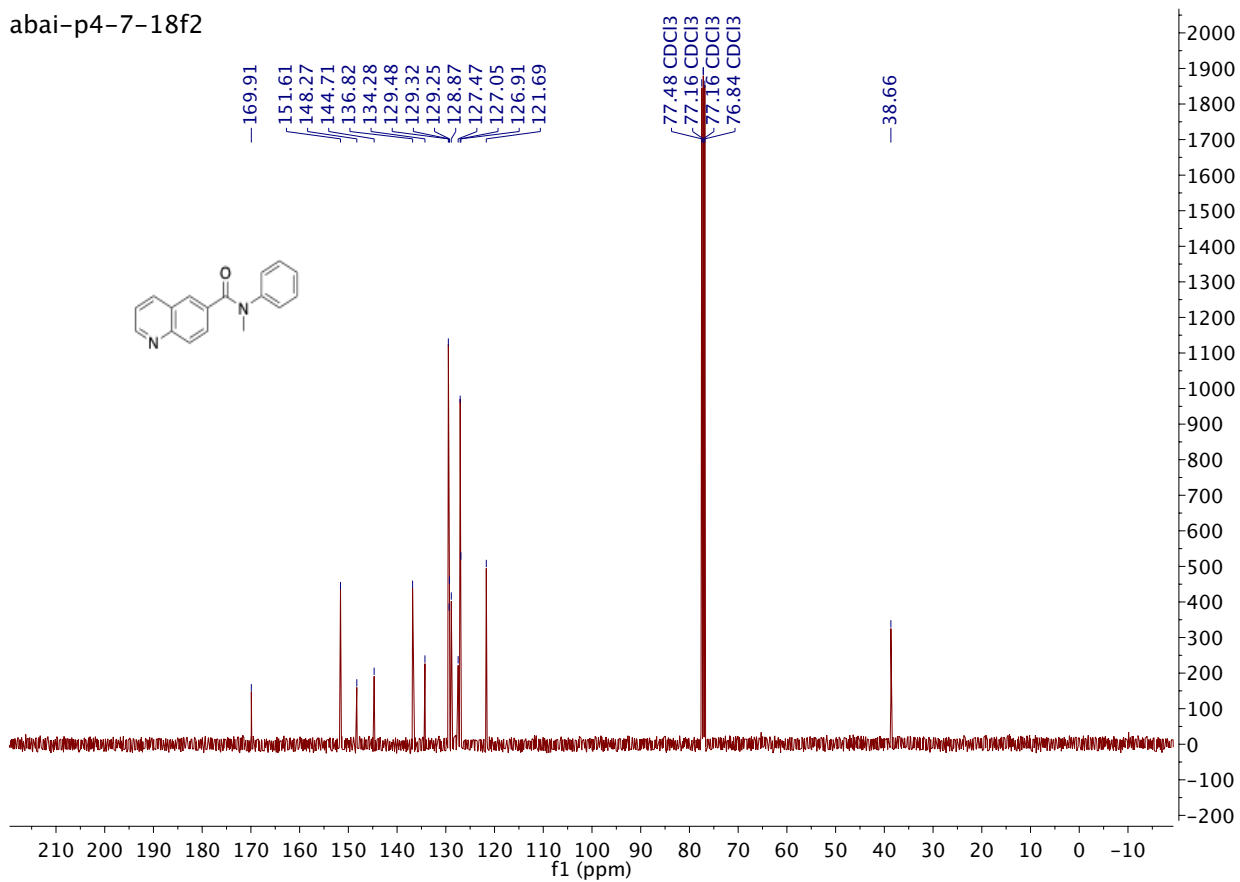


Compound 5j

abai-p4-7-18f2

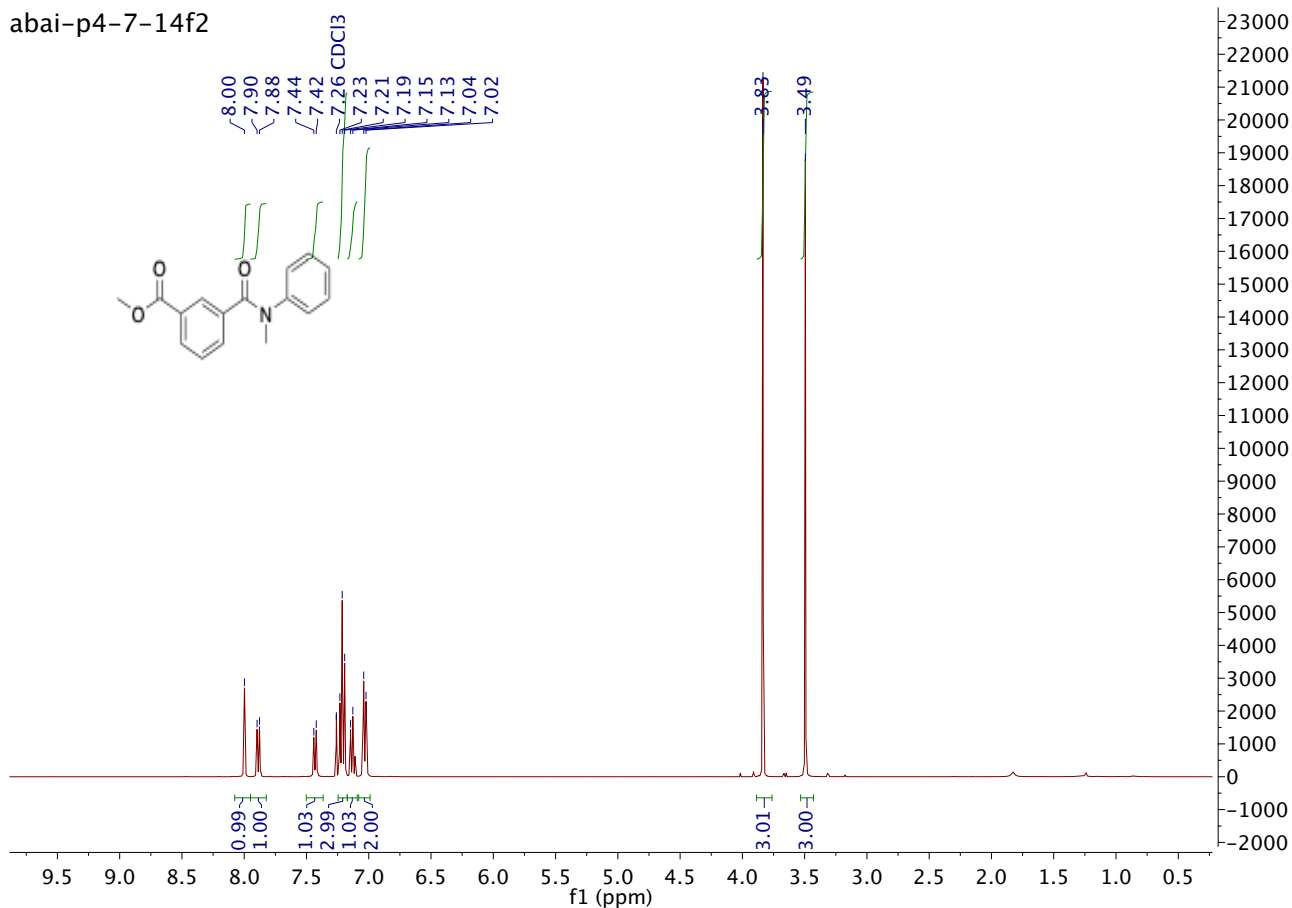


abai-p4-7-18f2

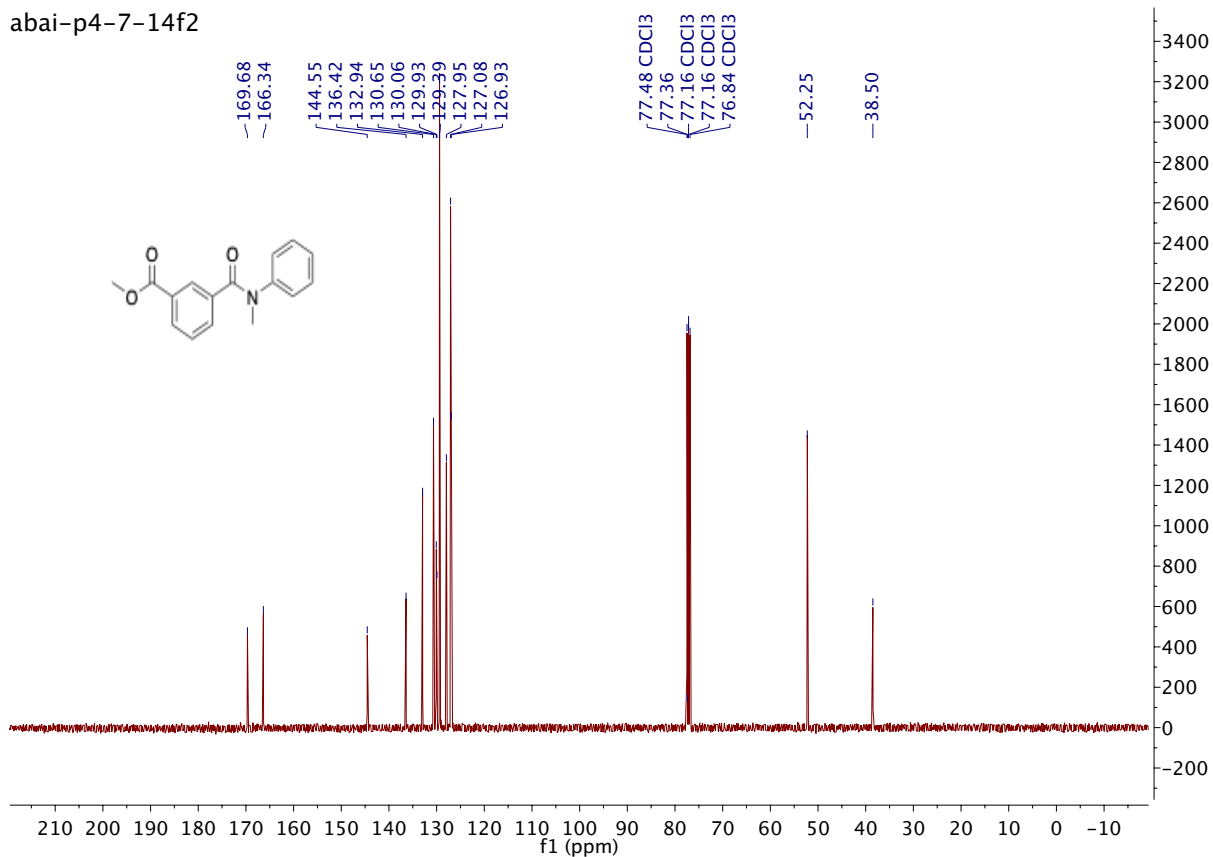


Compound 5k

abai-p4-7-14f2

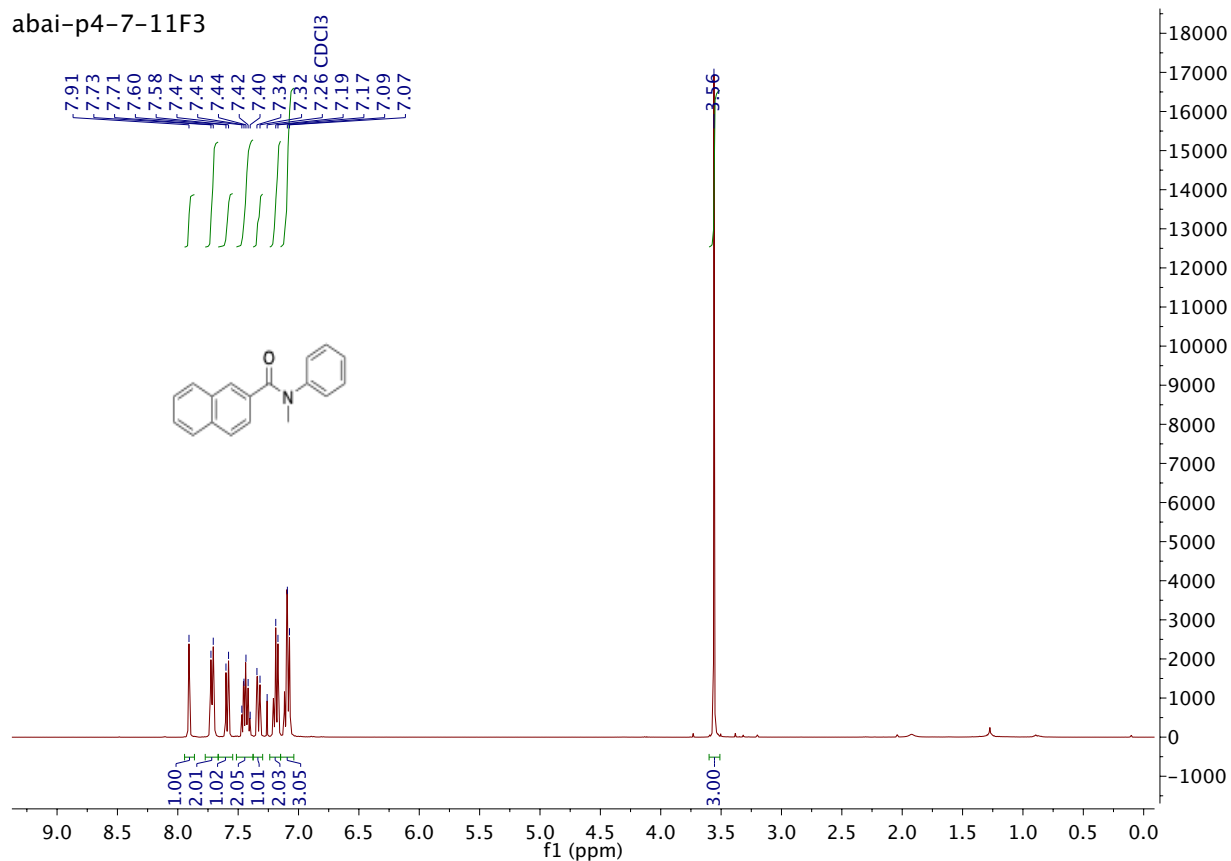


abai-p4-7-14f2

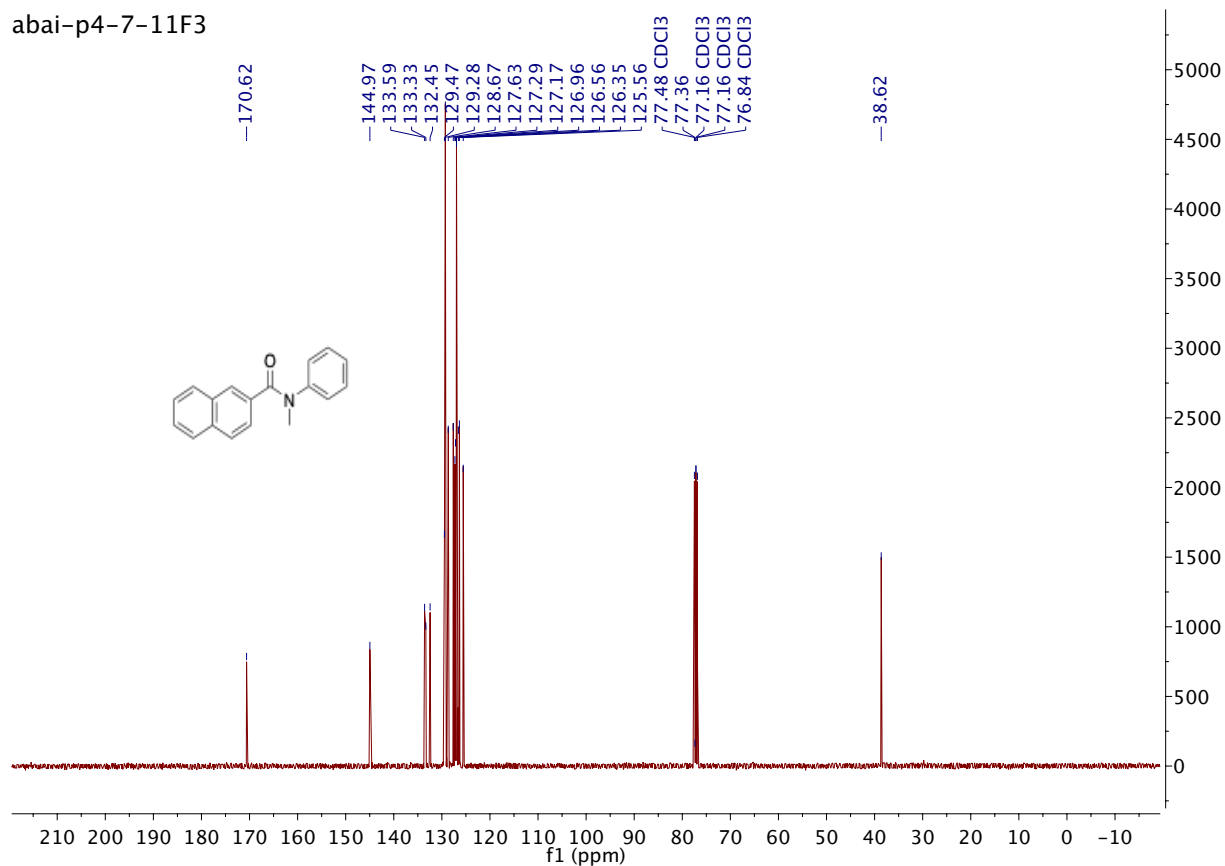


Compound 5I

abai-p4-7-11F3

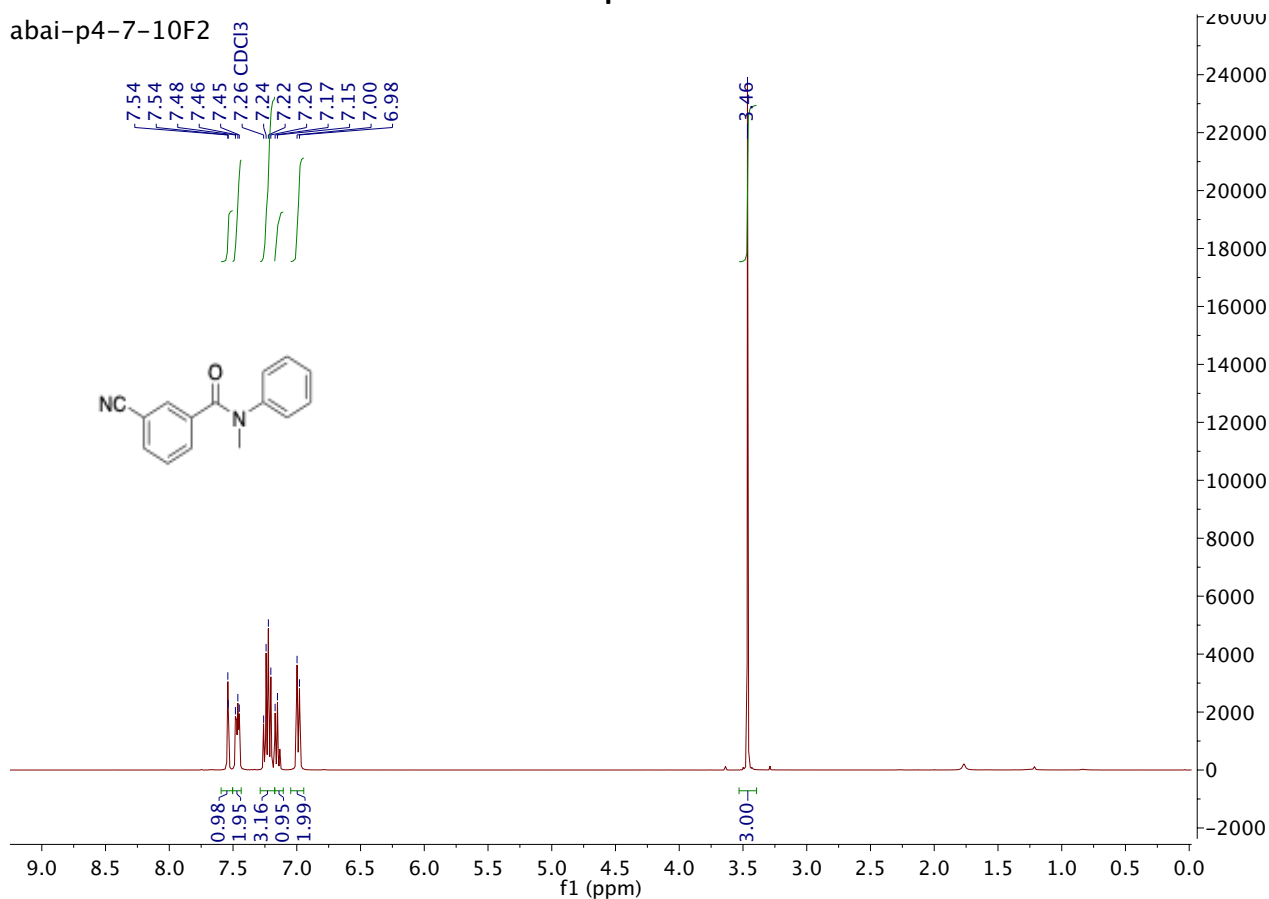


abai-p4-7-11F3

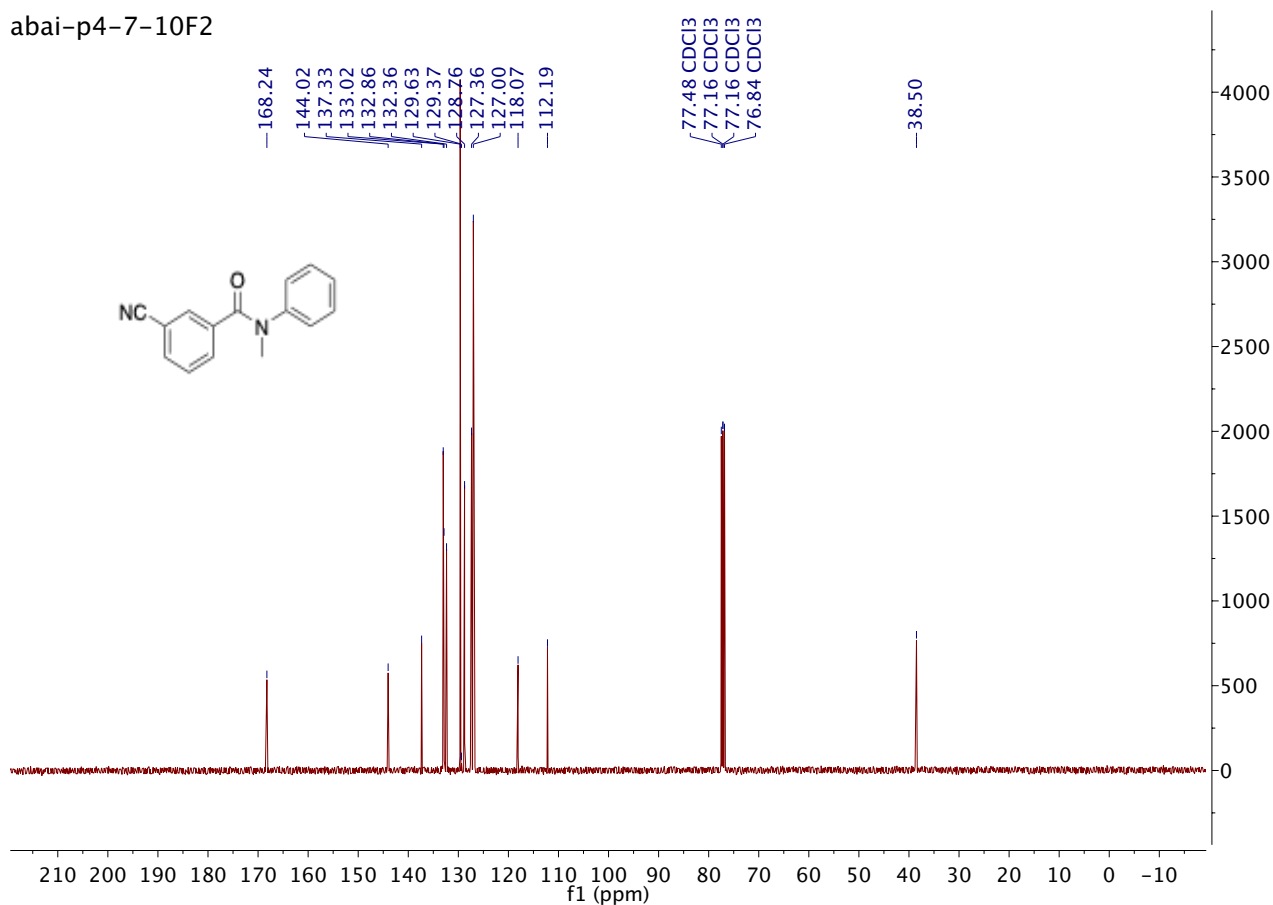


Compound 5m

abai-p4-7-10F2

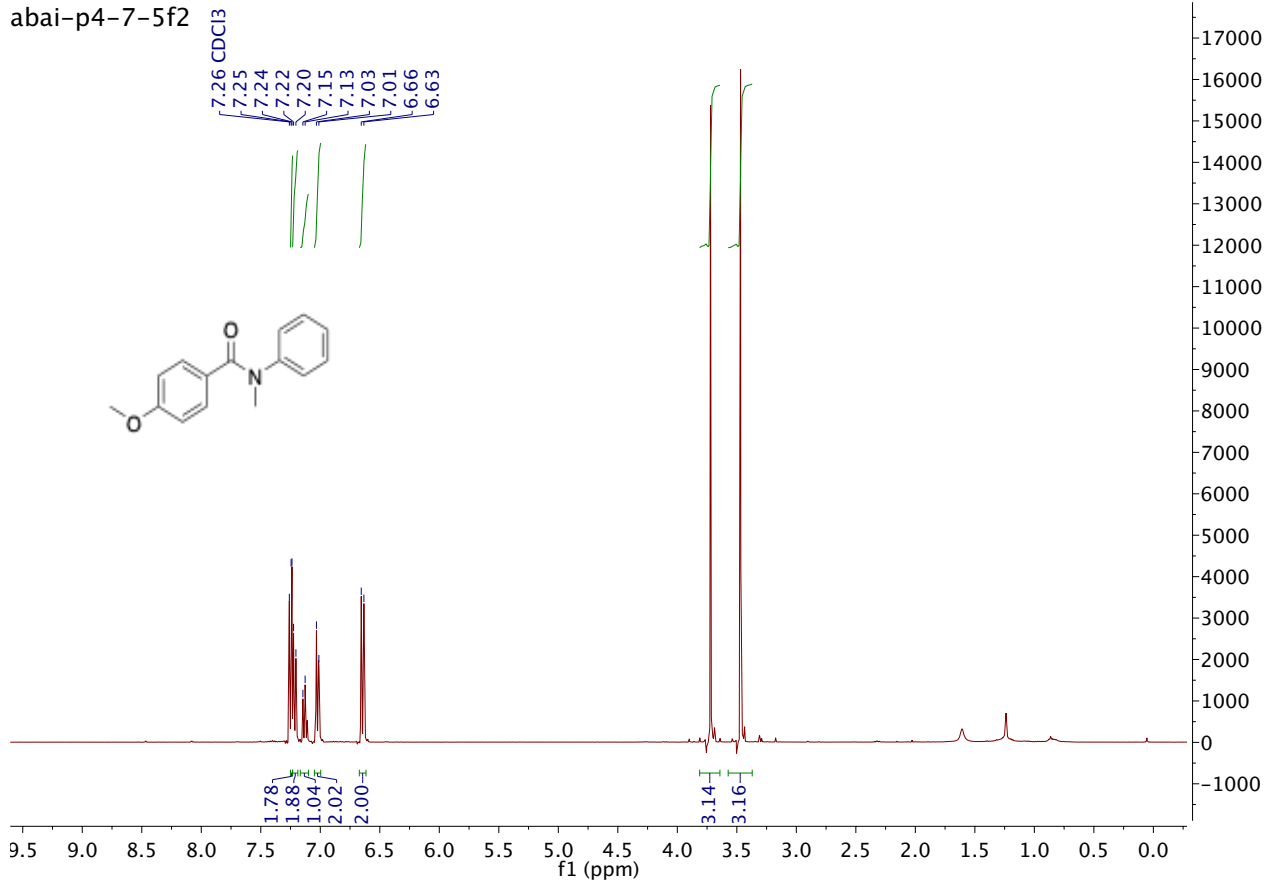


abai-p4-7-10F2

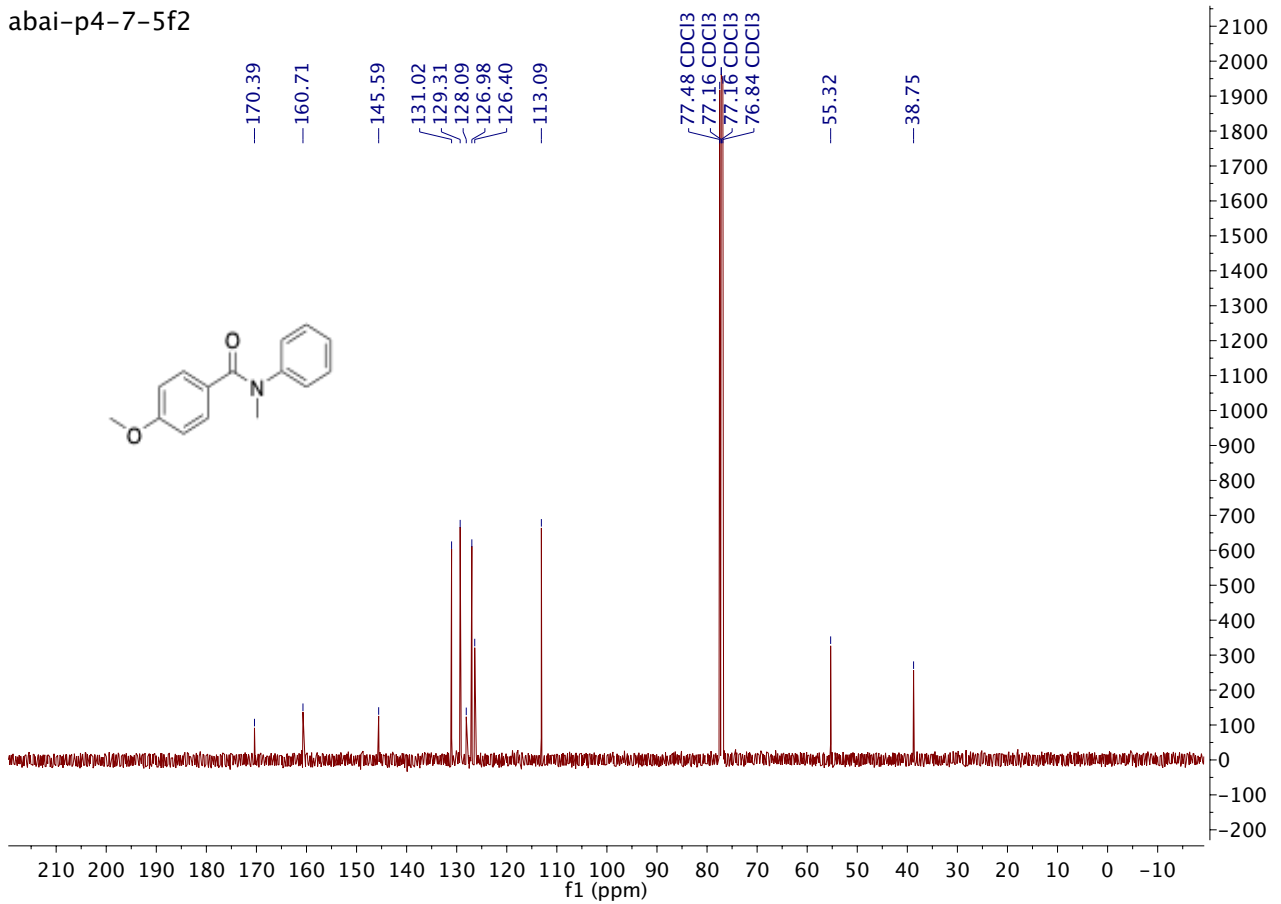


Compound 5n

abai-p4-7-5f2

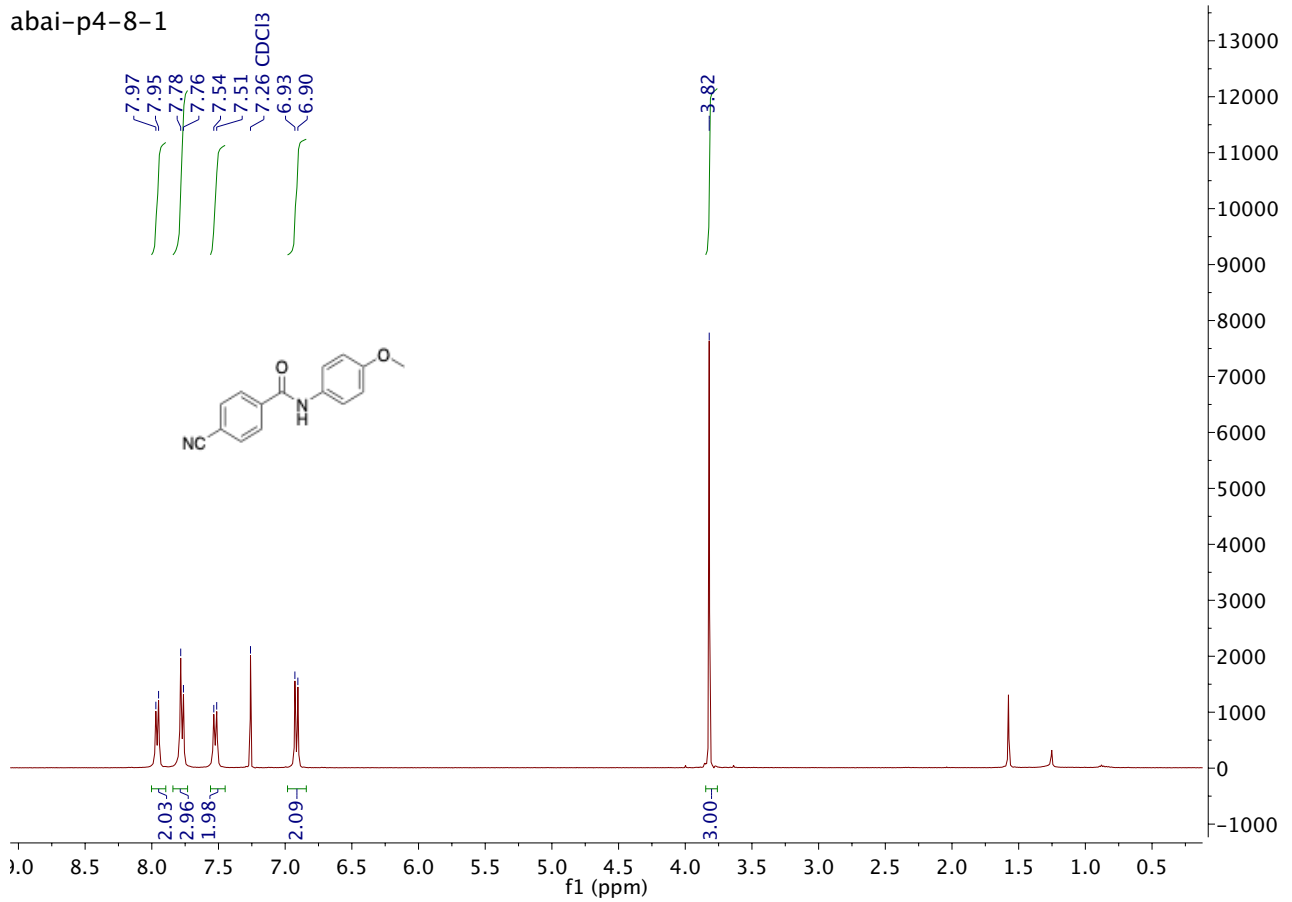


abai-p4-7-5f2

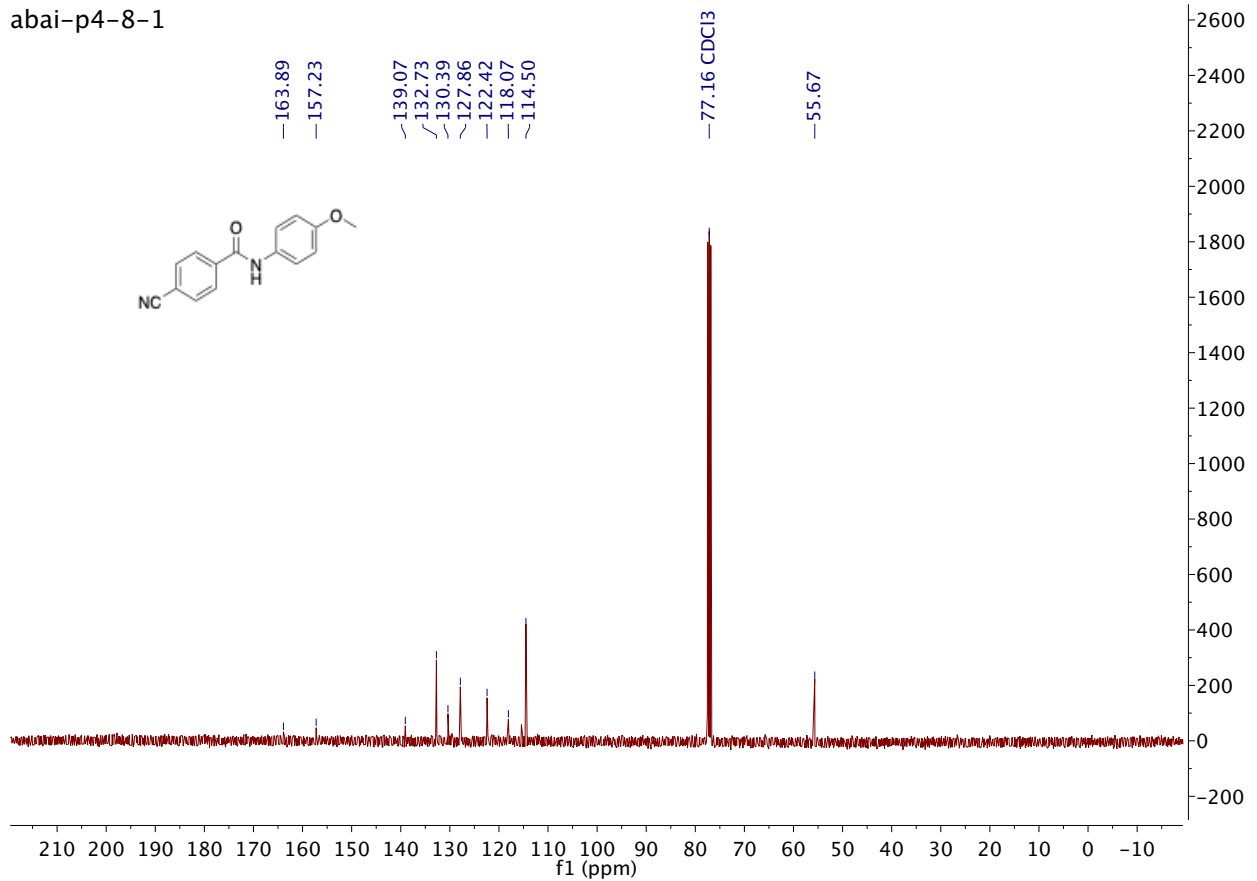


Compound 5o

abai-p4-8-1

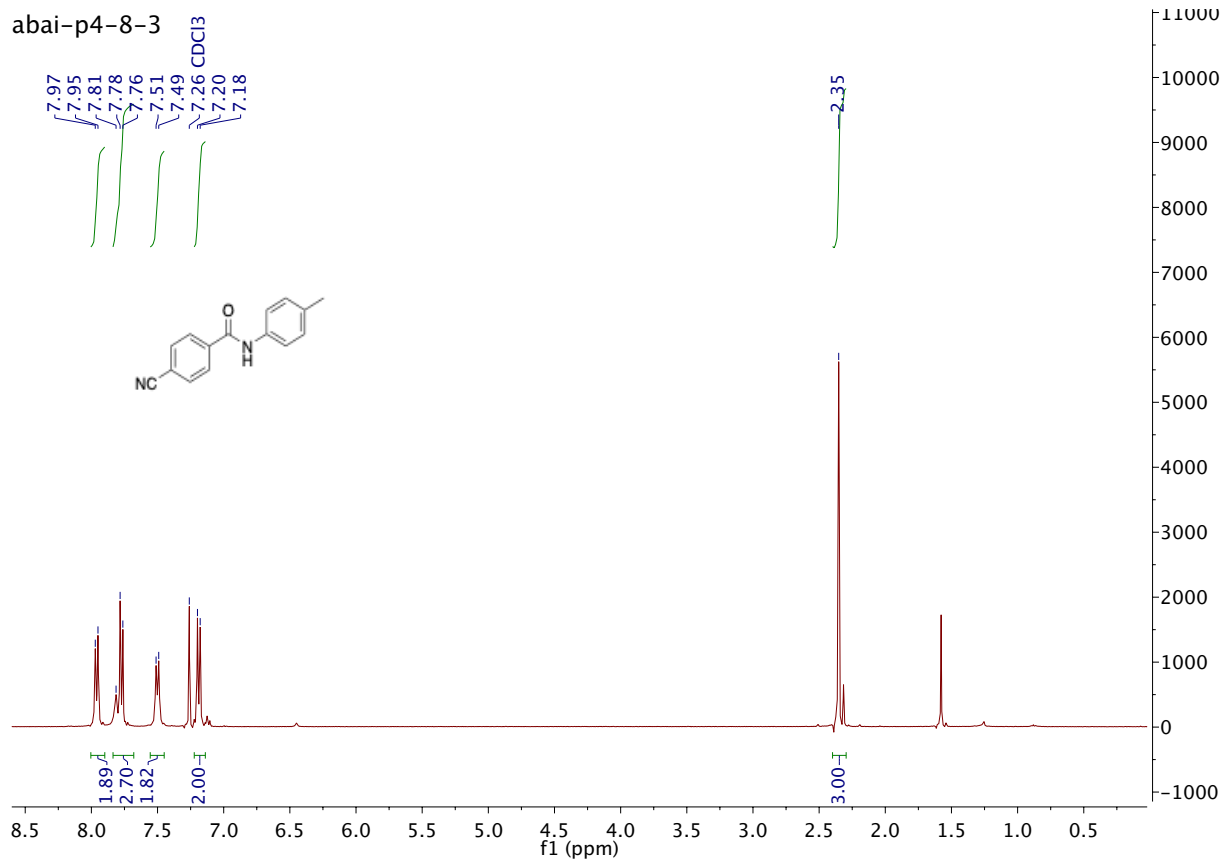


abai-p4-8-1

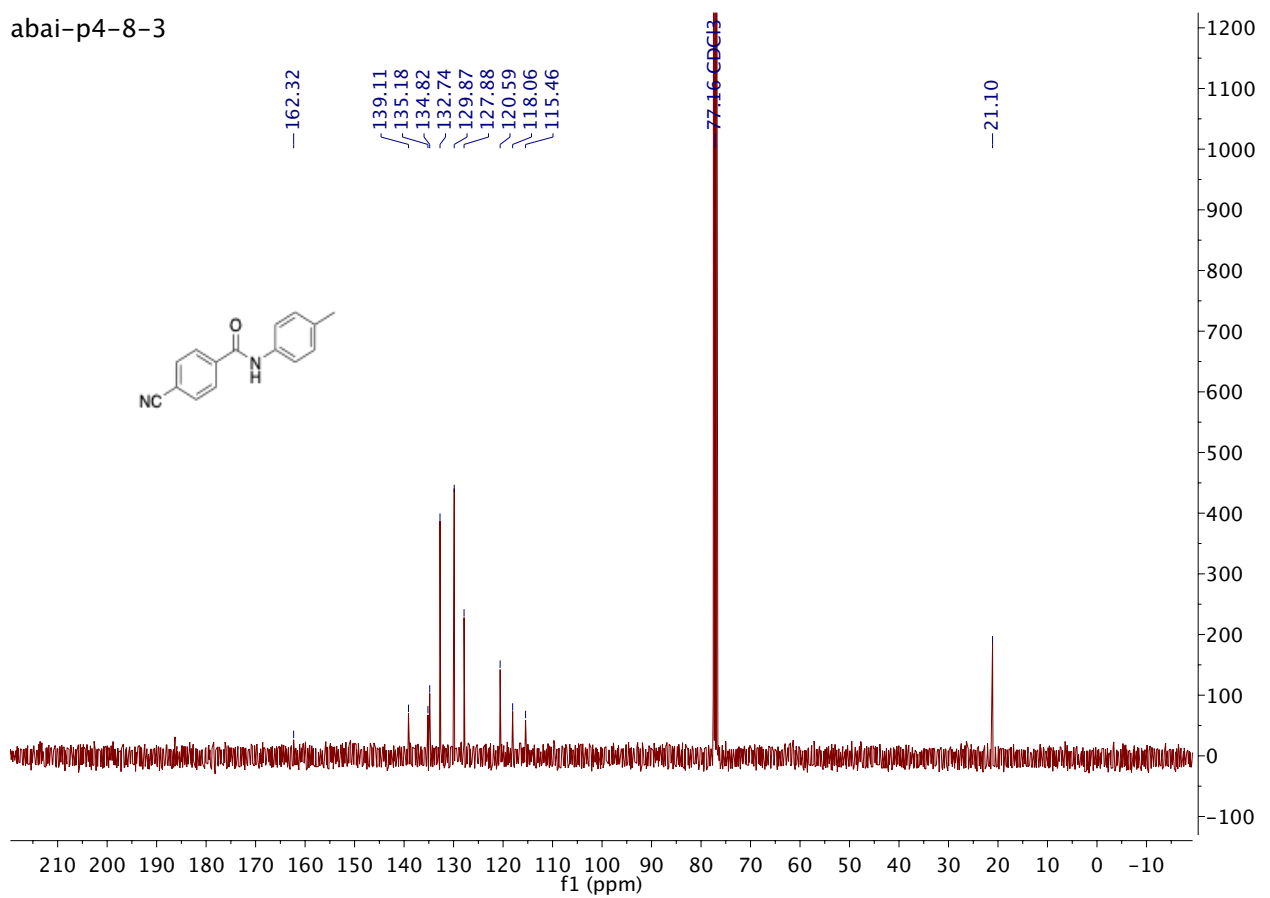


Compound 5p

abai-p4-8-3

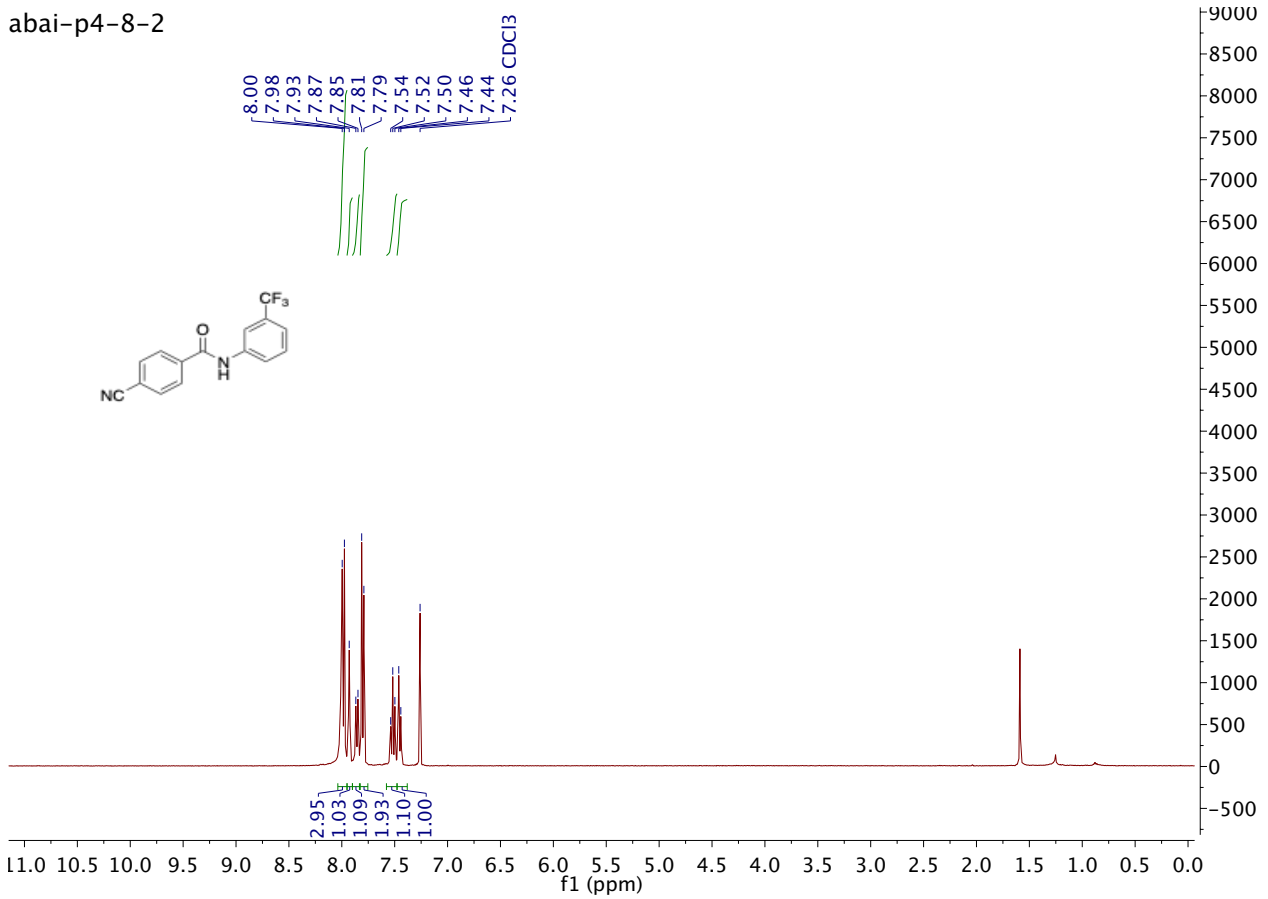


abai-p4-8-3

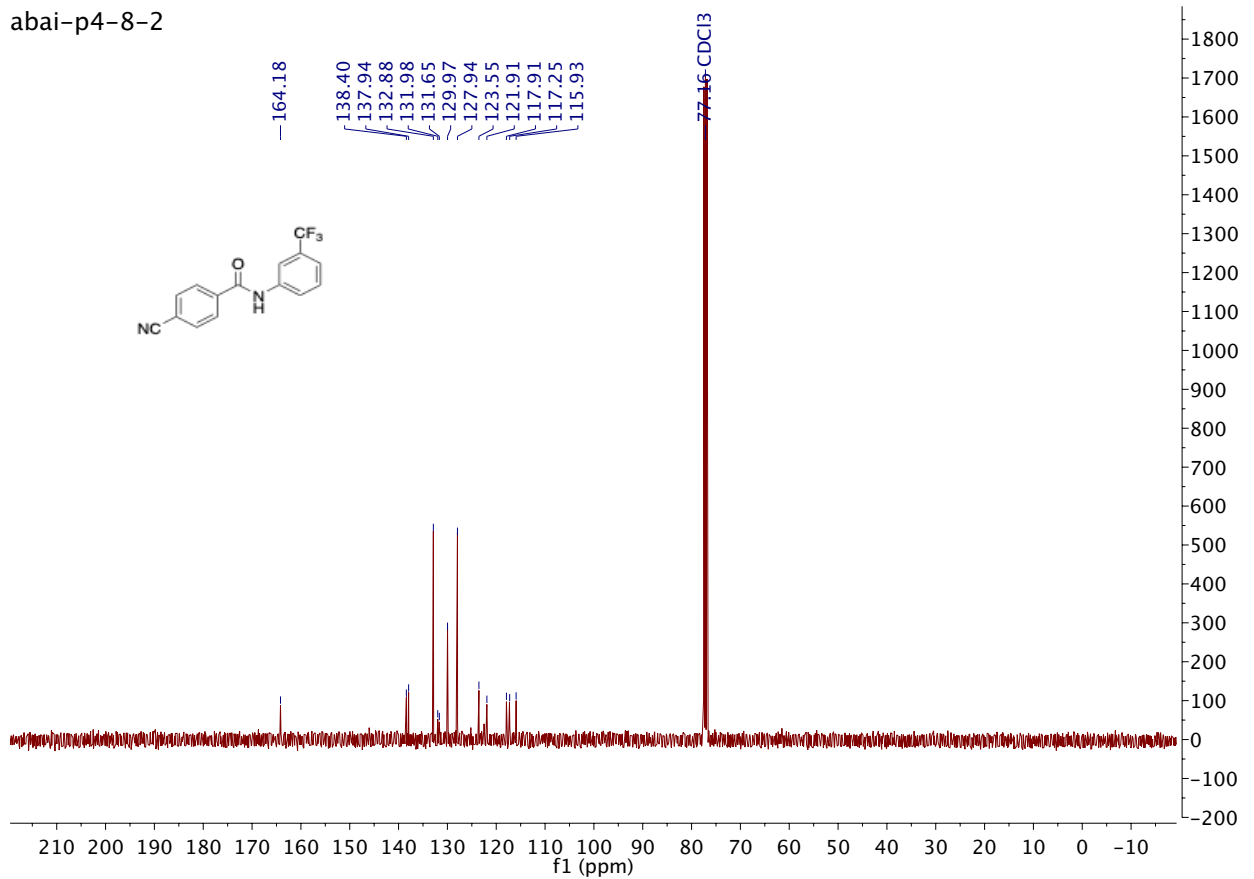


Compound 5q

abai-p4-8-2

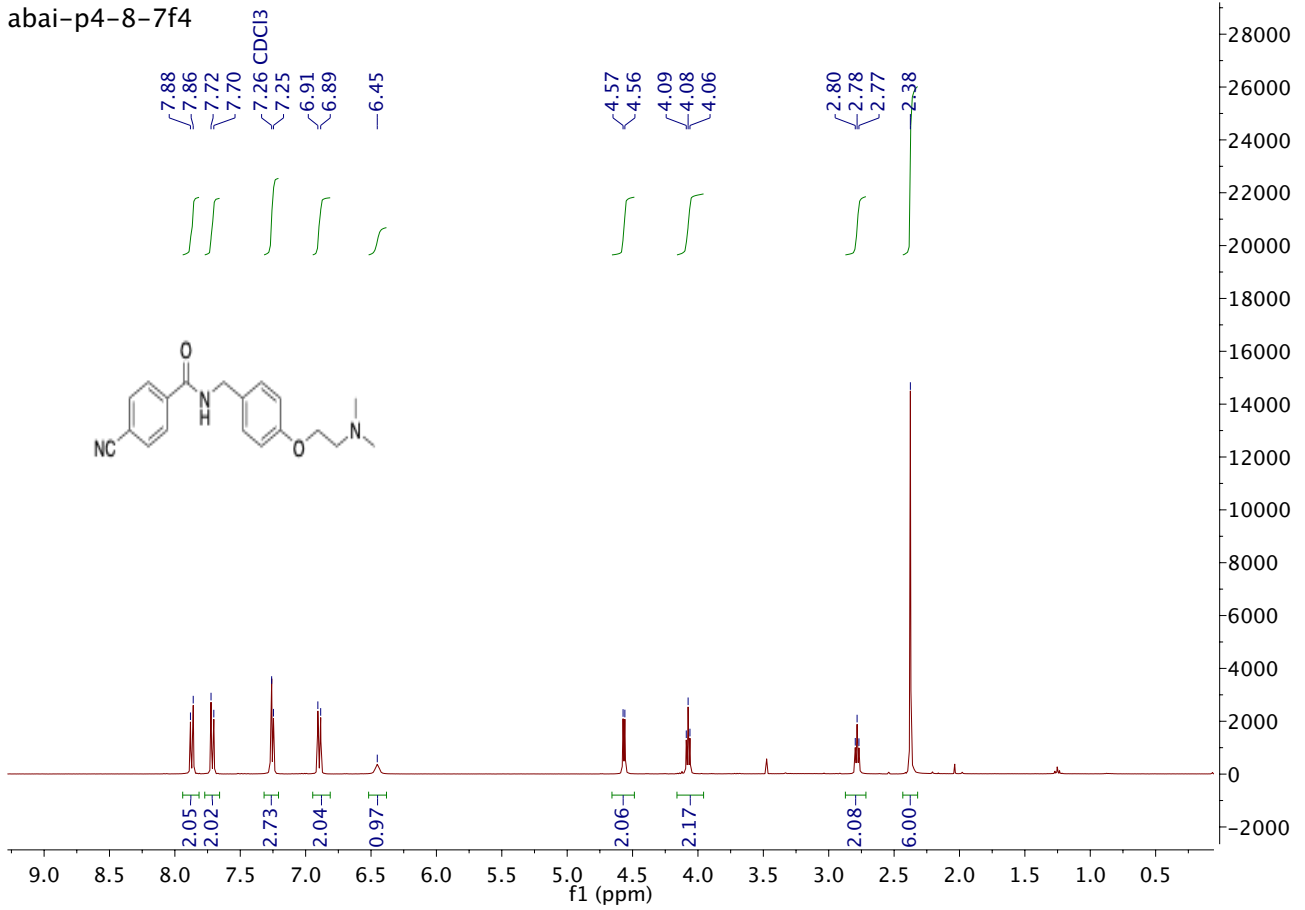


abai-p4-8-2

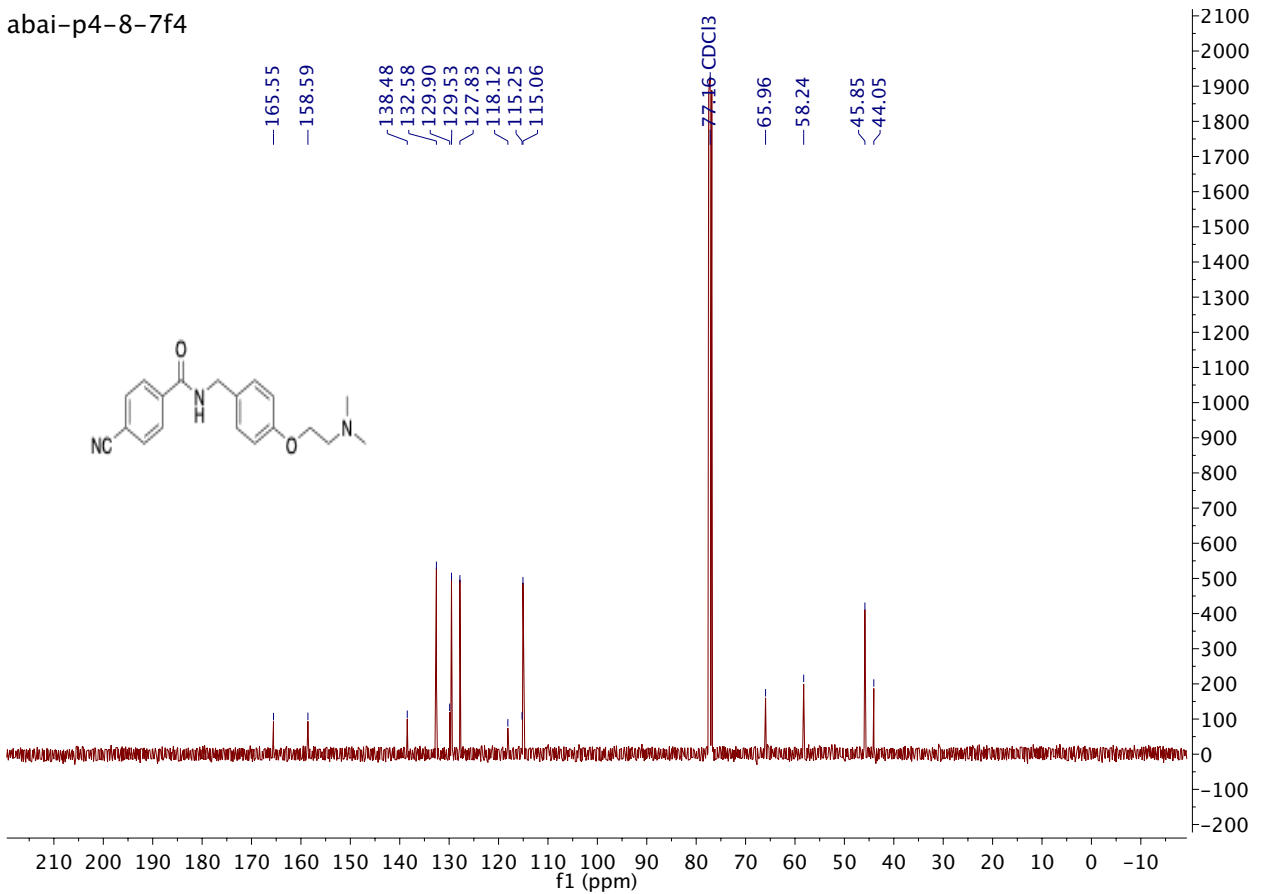


Compound 5r

abai-p4-8-7f4

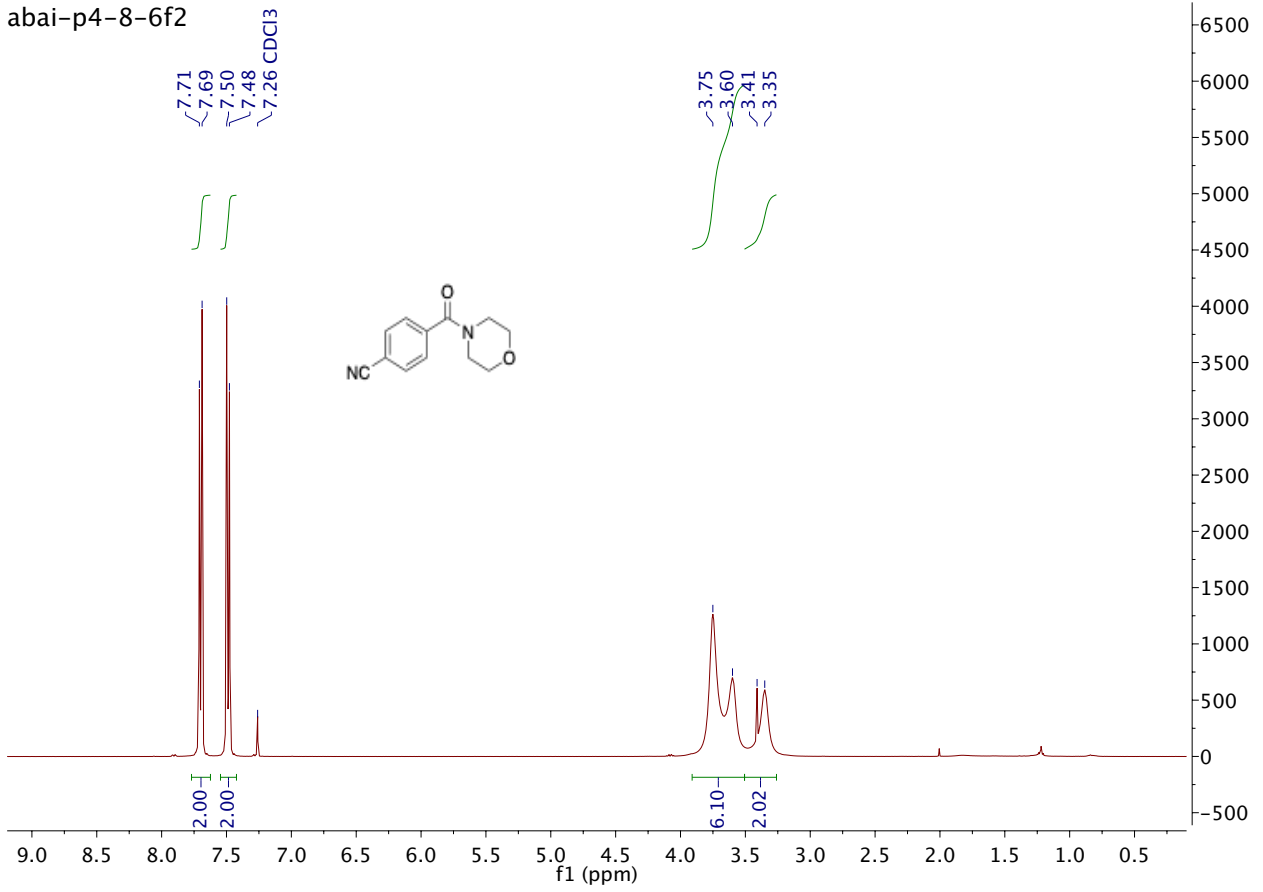


abai-p4-8-7f4

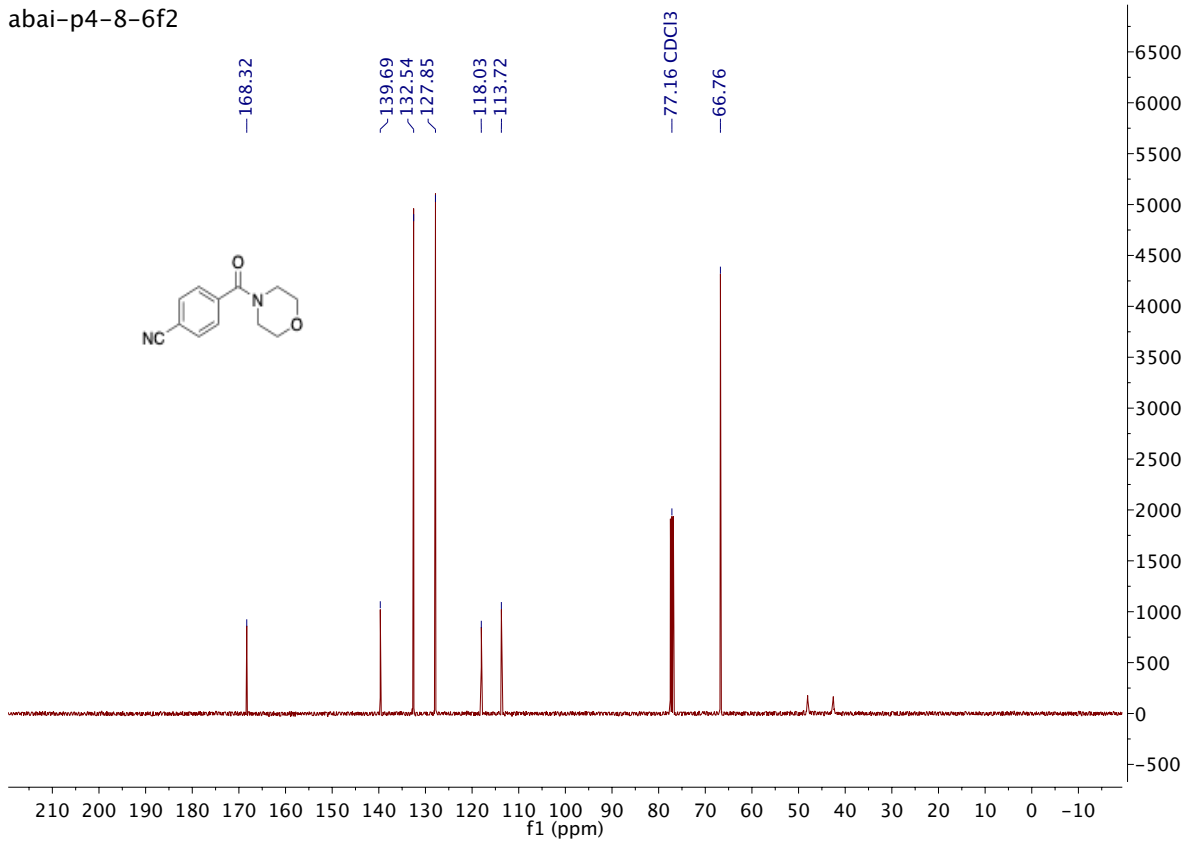


Compound 5s

abai-p4-8-6f2

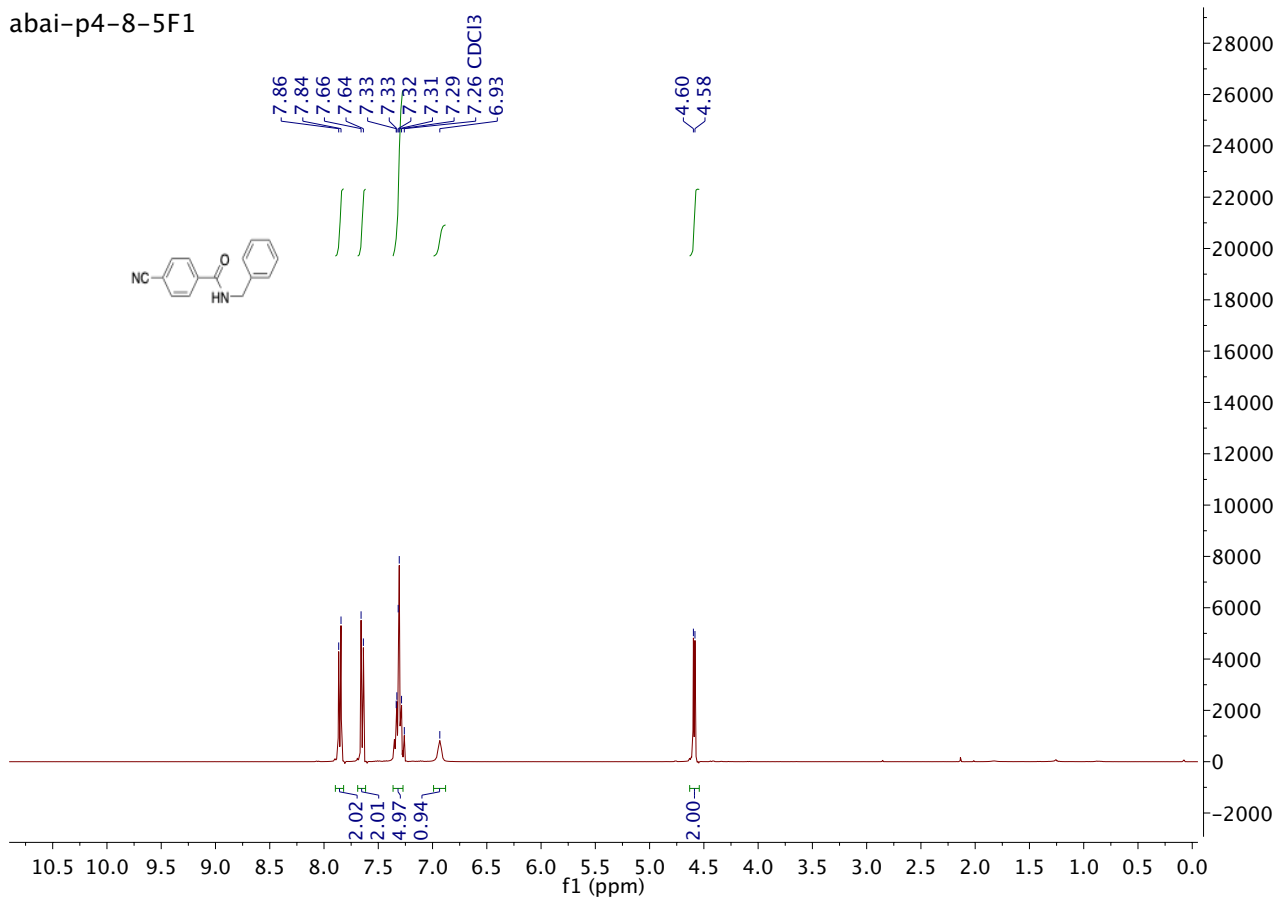


abai-p4-8-6f2

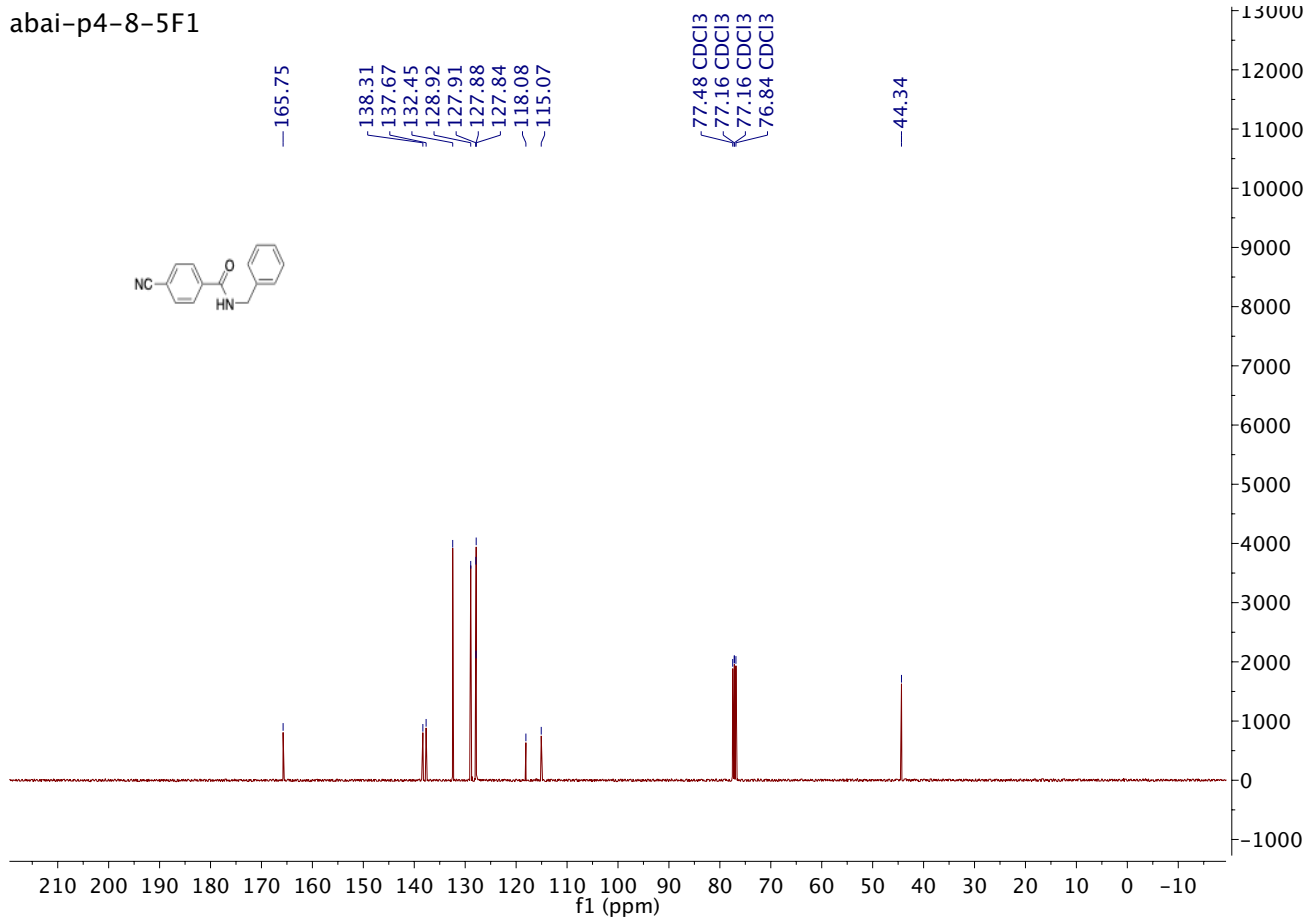


Compound 5t

abai-p4-8-5F1



abai-p4-8-5F1



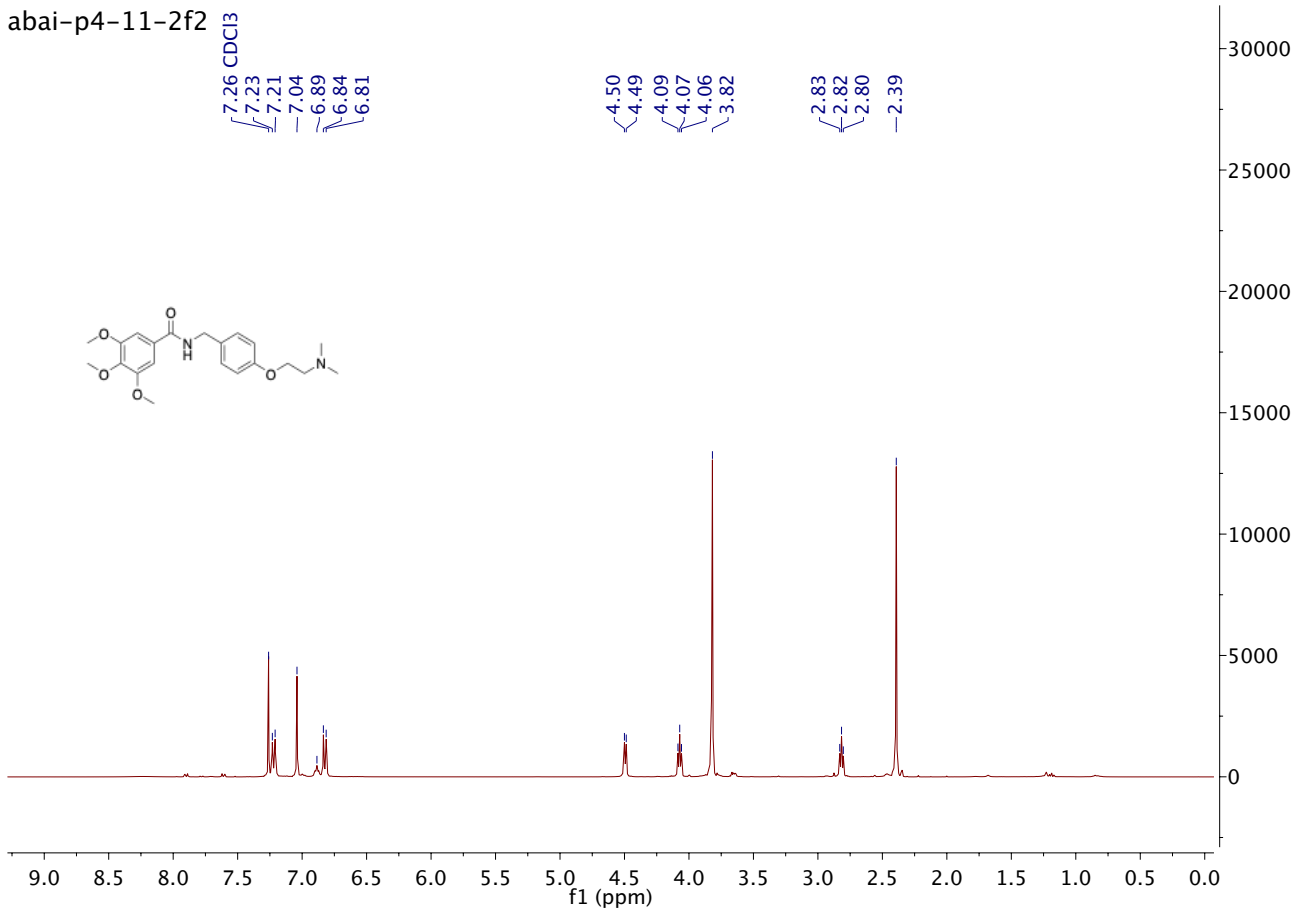
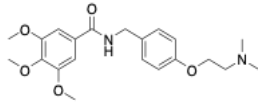
Compound 5u

abai-p4-11-2f2

7.26 CDCl₃
7.23
7.21
7.04
6.89
6.84
6.81

4.50
4.49
4.09
4.07
4.06
3.82

2.83
2.82
2.80
2.39



abai-p4-11-2f2

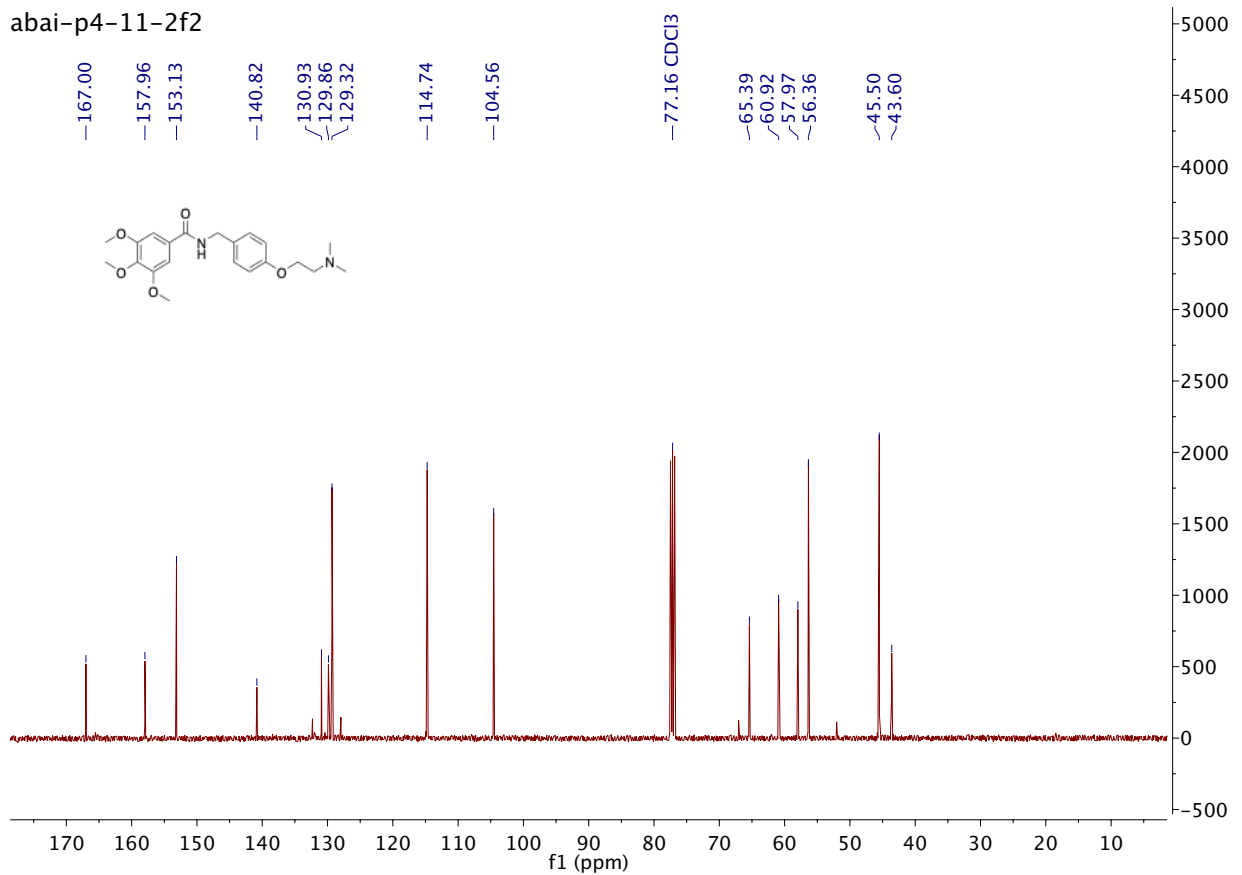
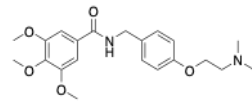
167.00
157.96
153.13

140.82
130.93
129.86
129.32

114.74
104.56

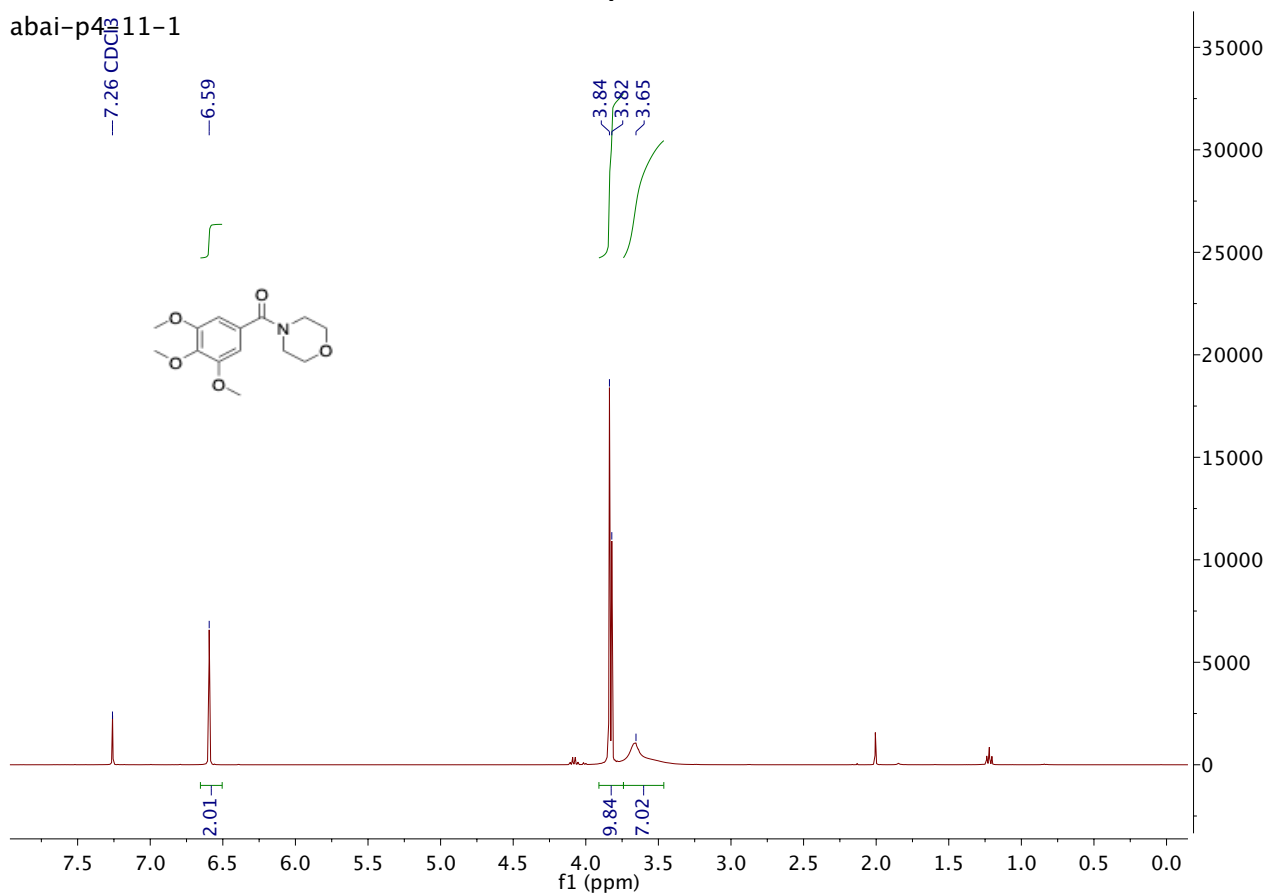
77.16 CDCl₃

65.39
60.92
57.97
56.36
45.50
43.60

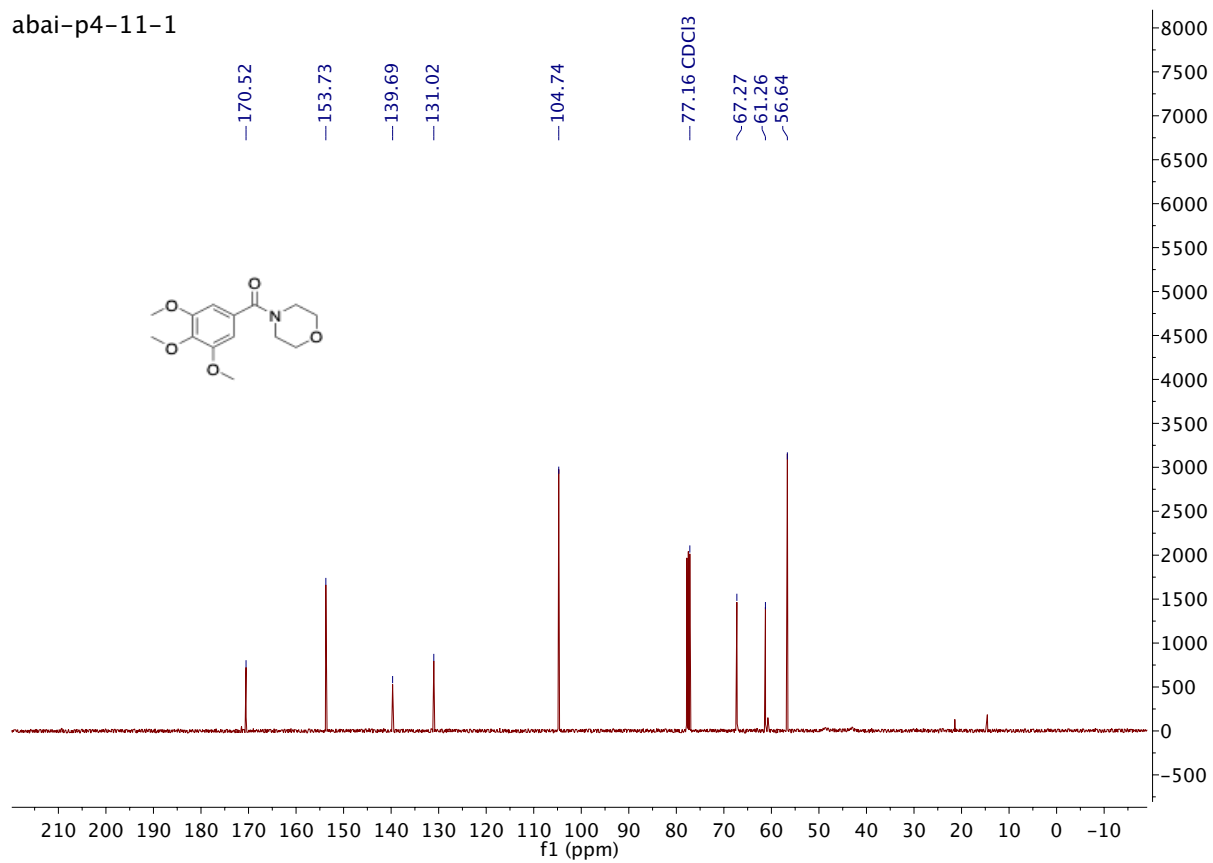


Compound 5v

abai-p4-11-1

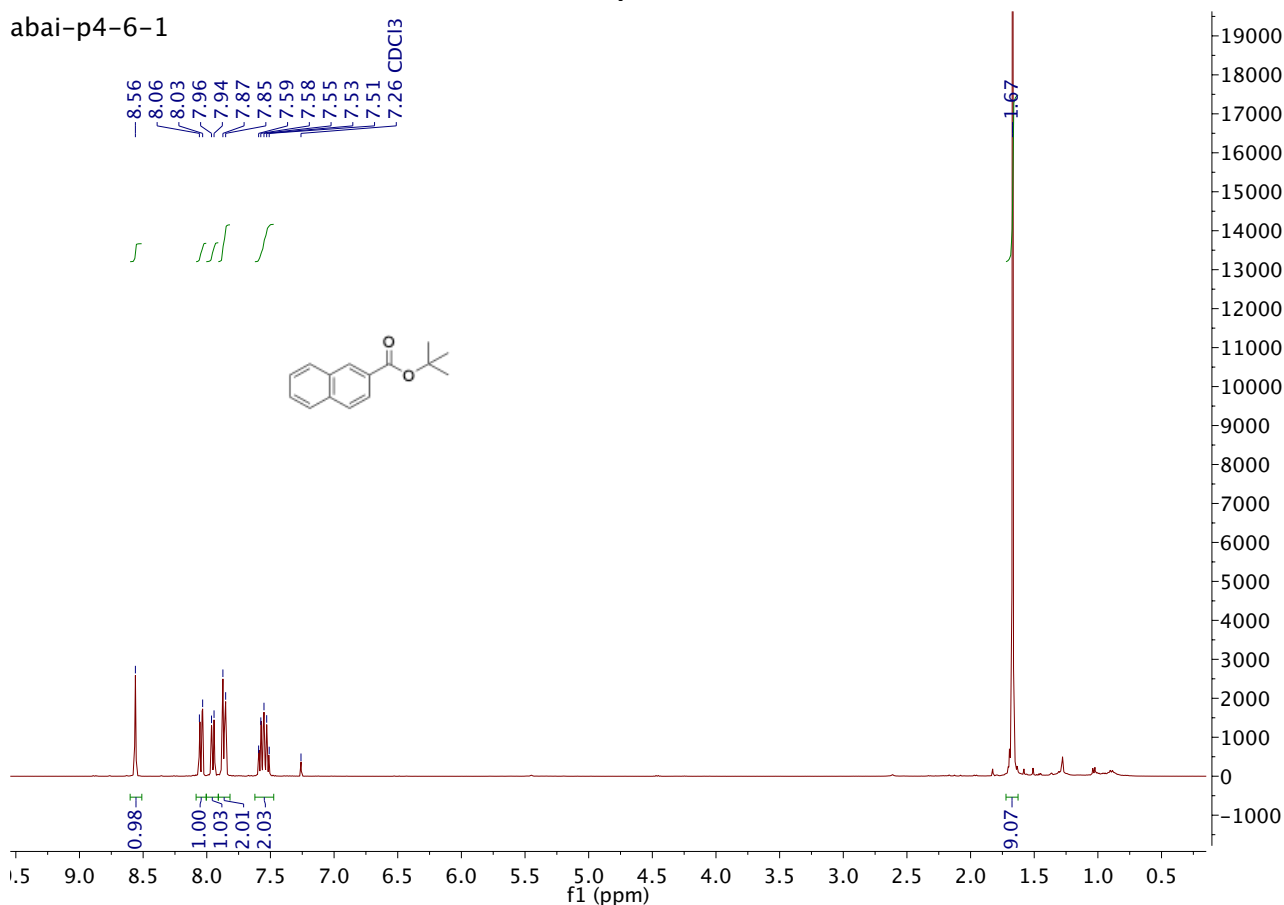


abai-p4-11-1

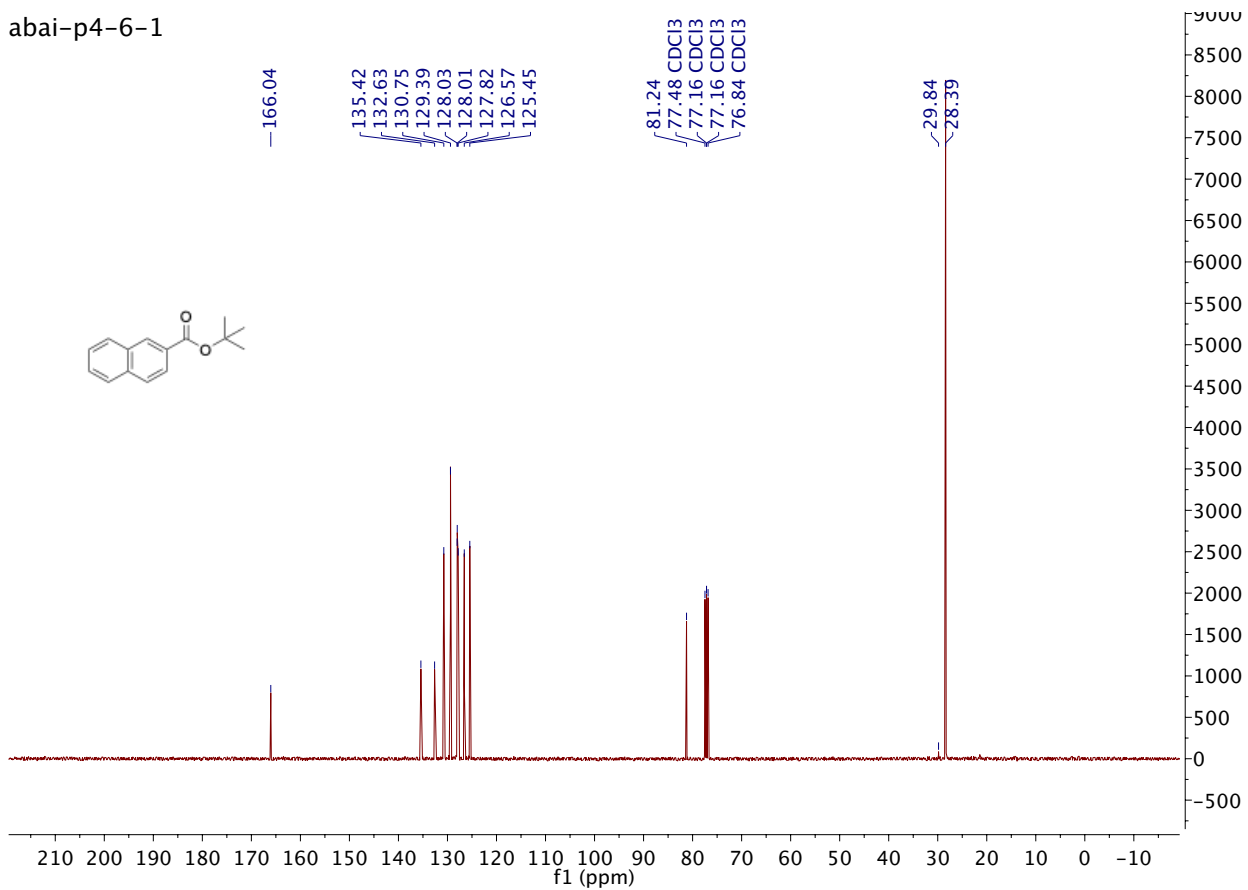


Compound 7a

abai-p4-6-1

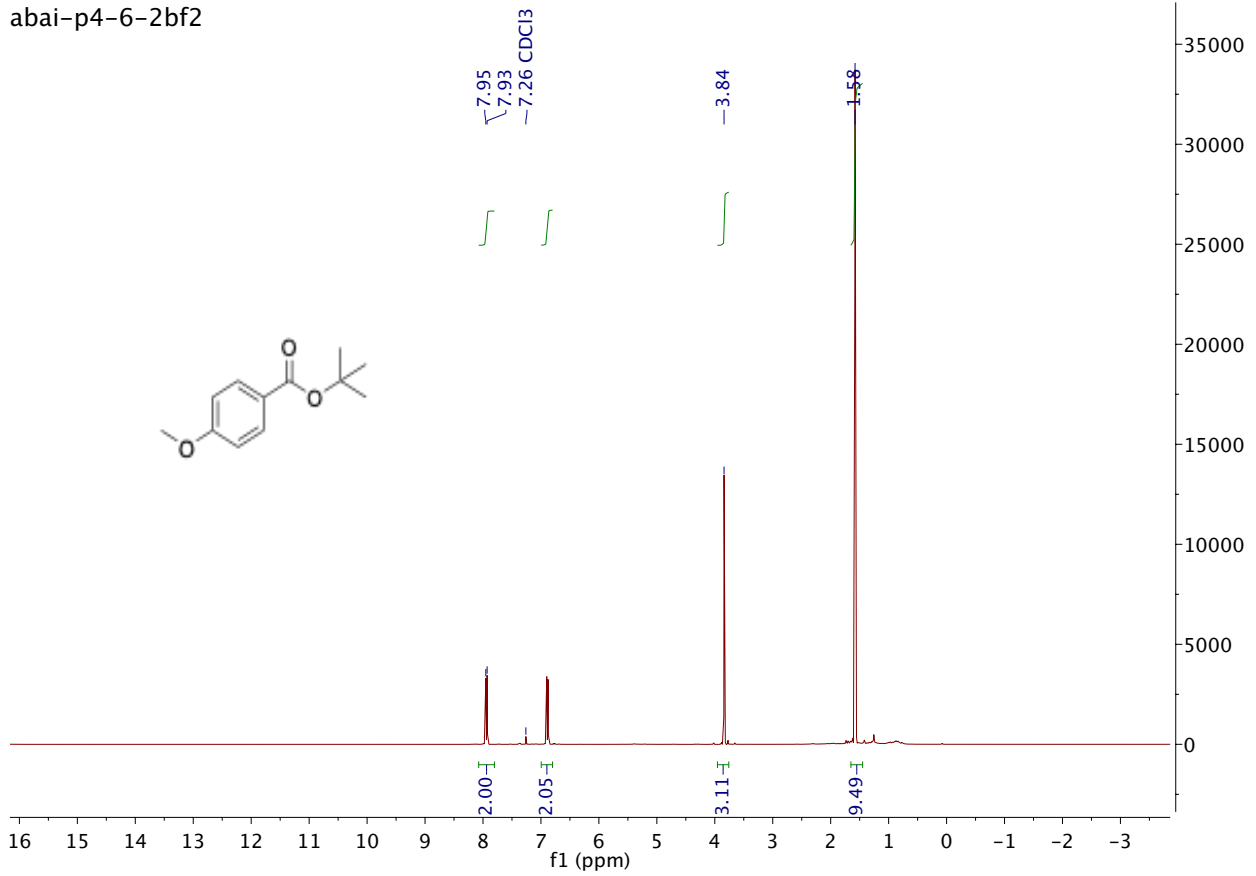


abai-p4-6-1

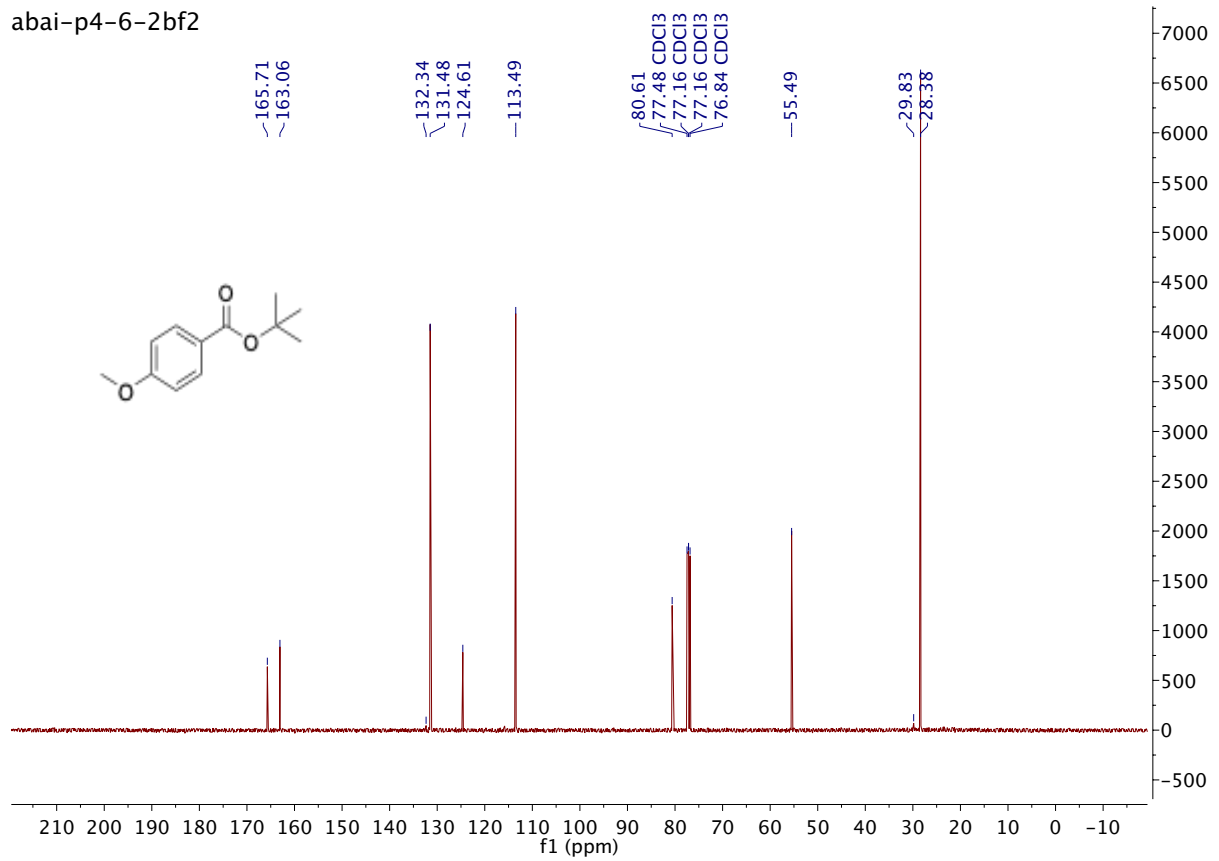


Compound 7b

abai-p4-6-2bf2

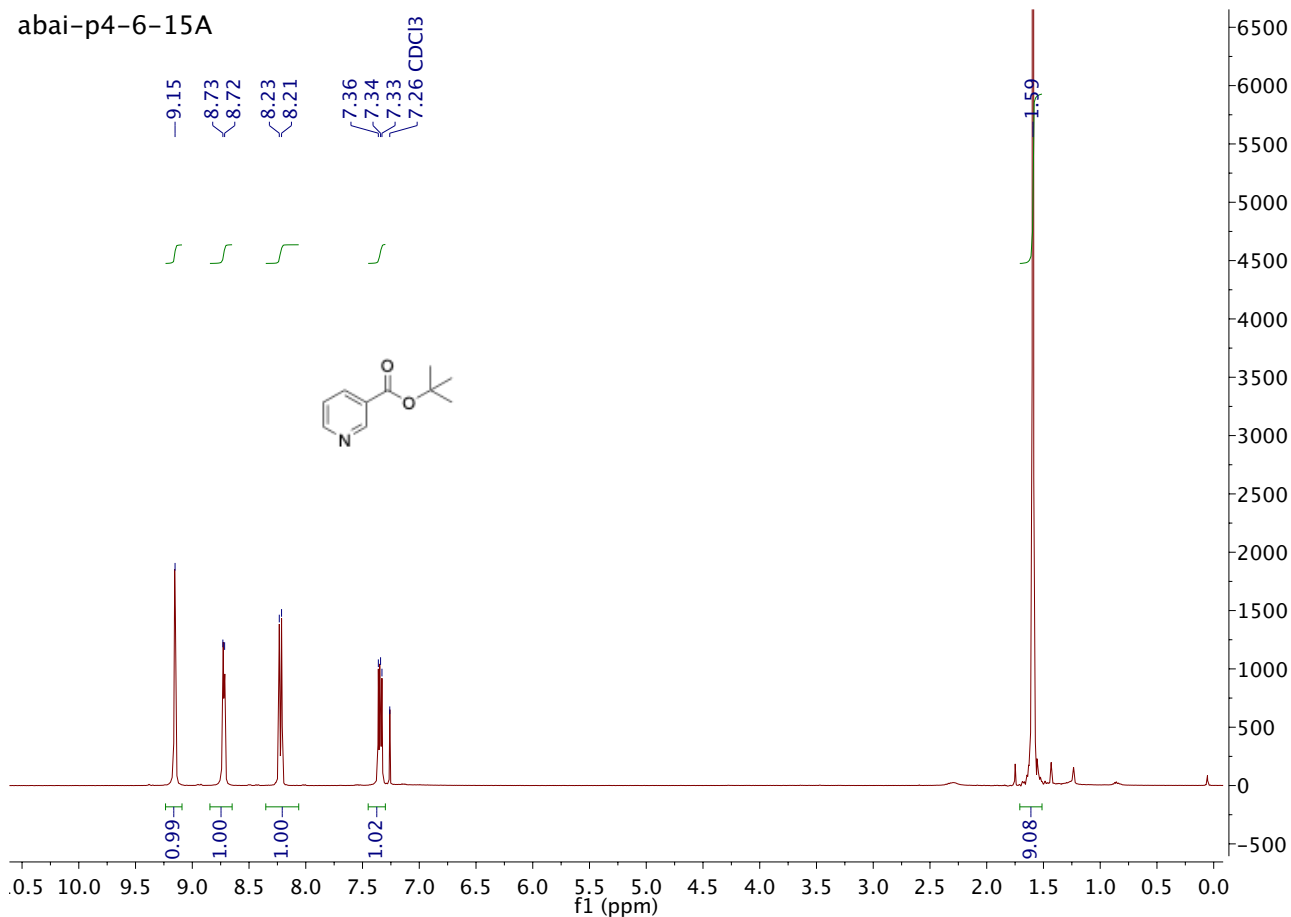


abai-p4-6-2bf2

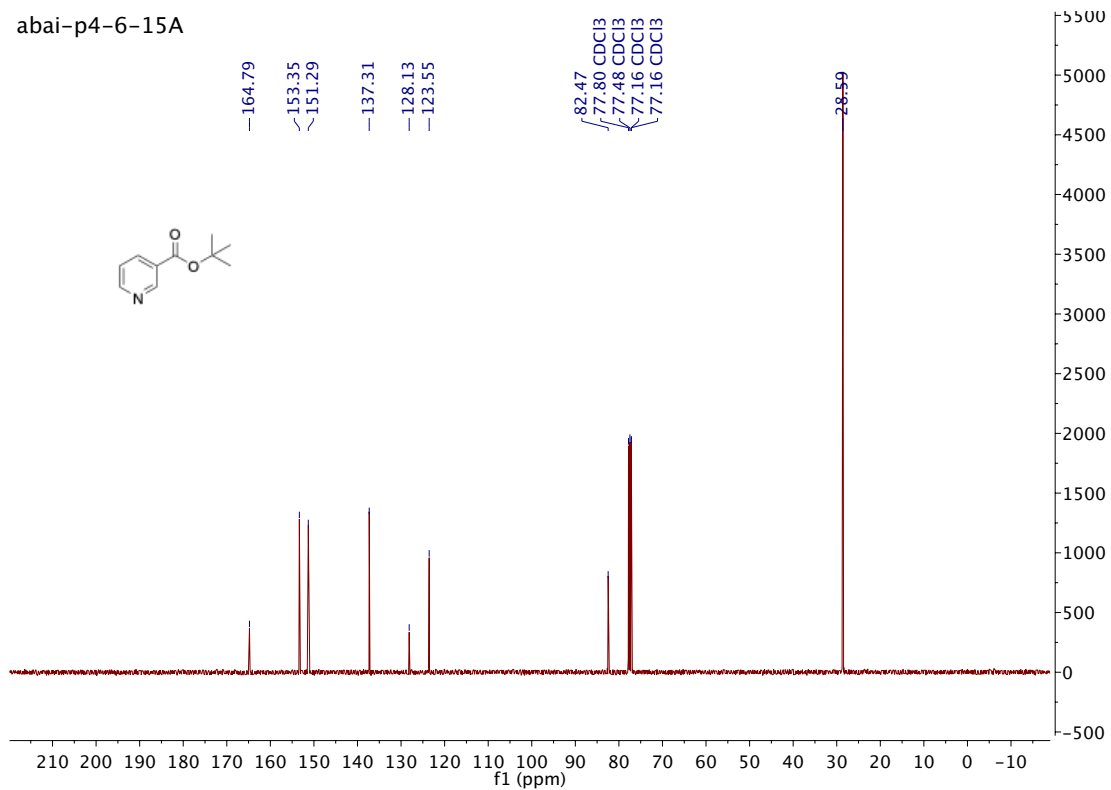


Compound 7c

abai-p4-6-15A

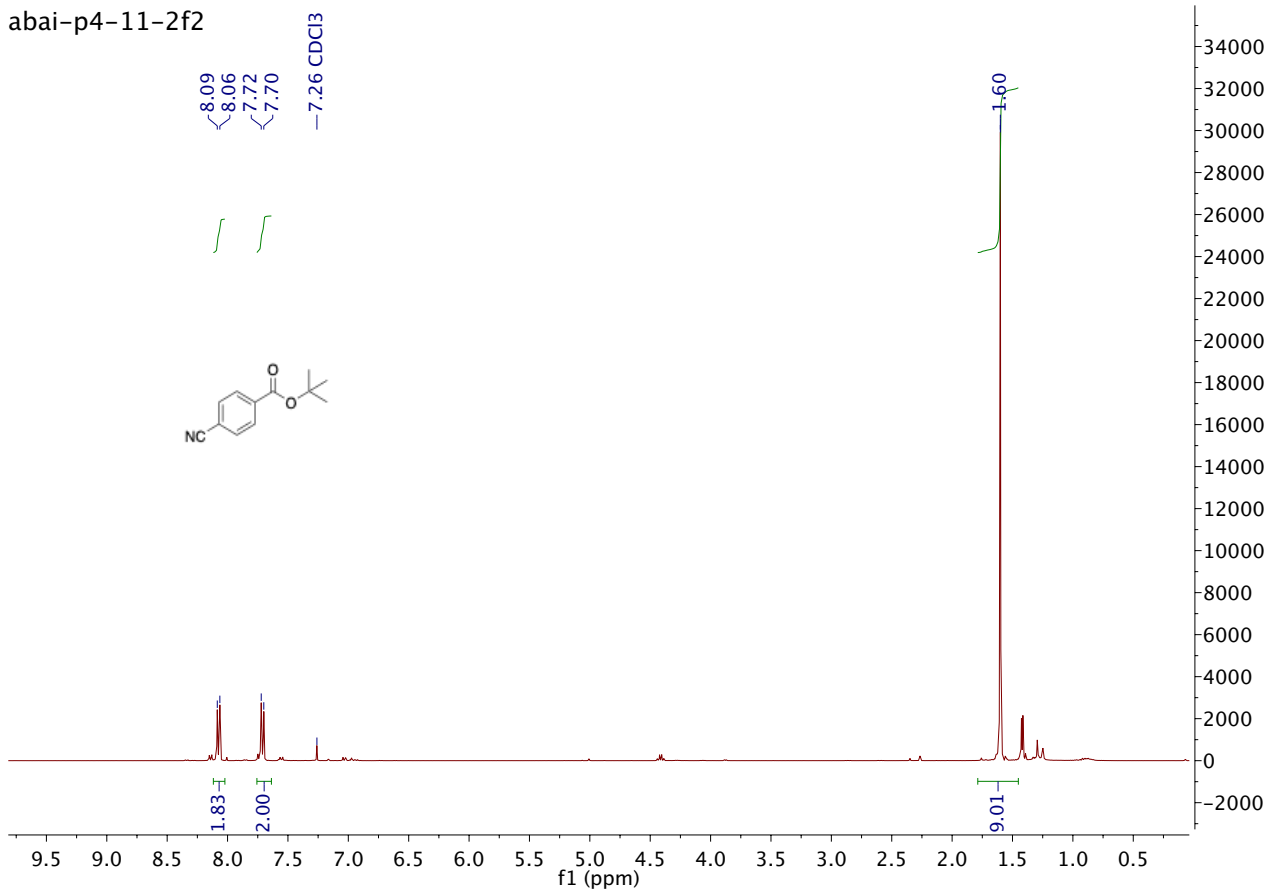


abai-p4-6-15A

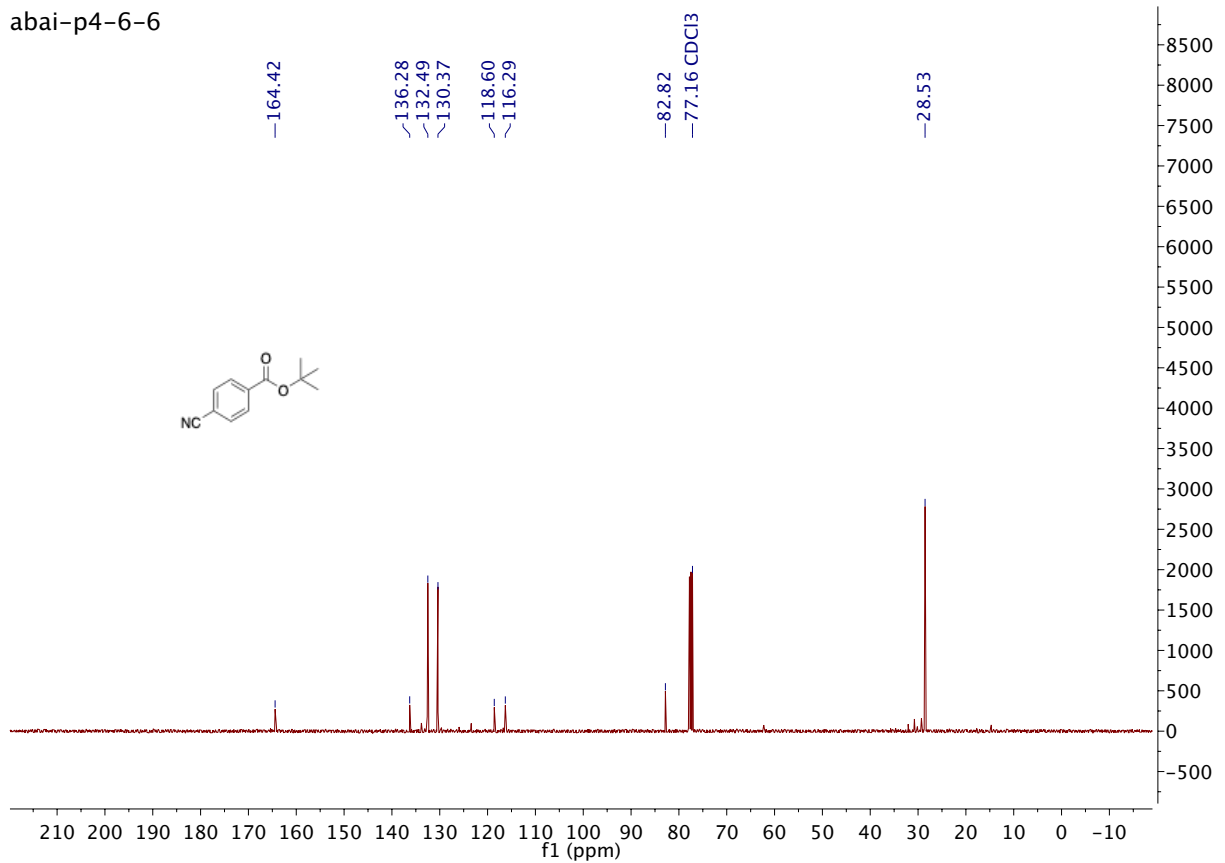


Compound 7d

abai-p4-11-2f2

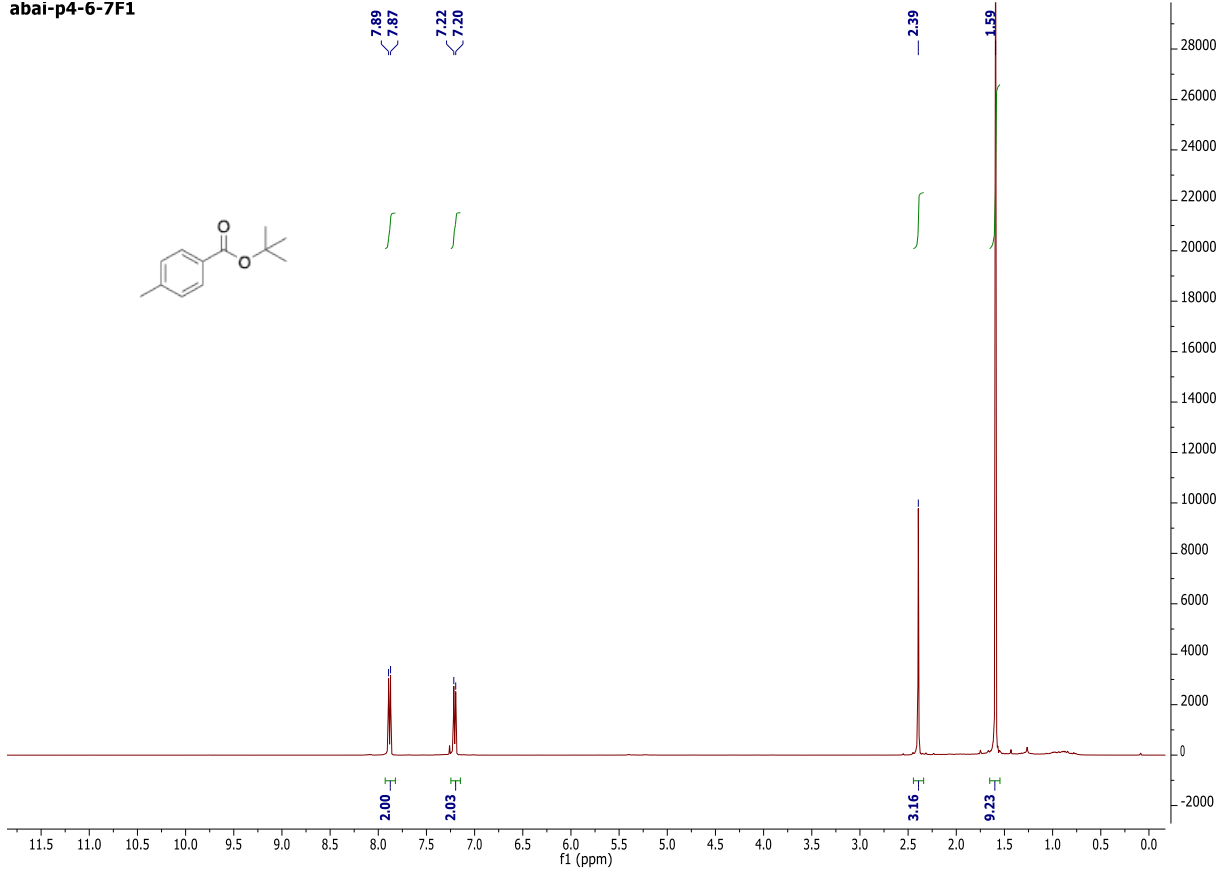


abai-p4-6-6

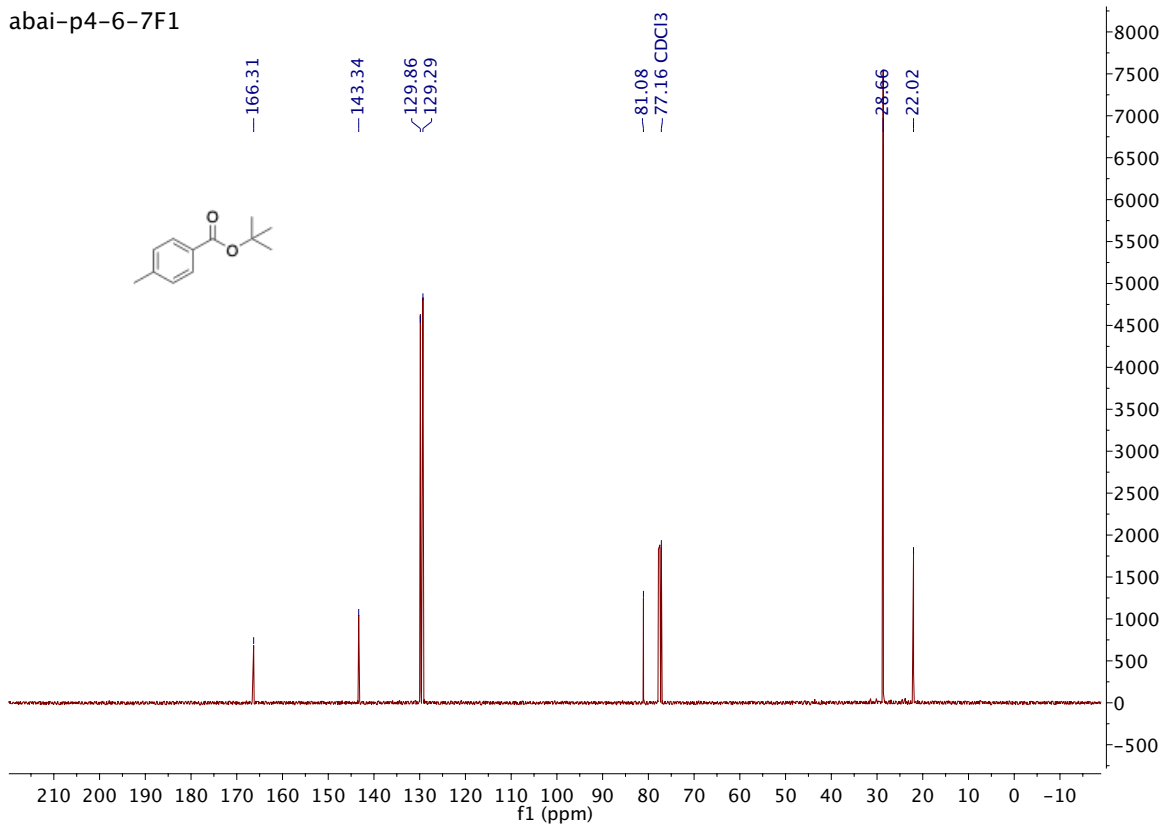


Compound 7e

abai-p4-6-7F1

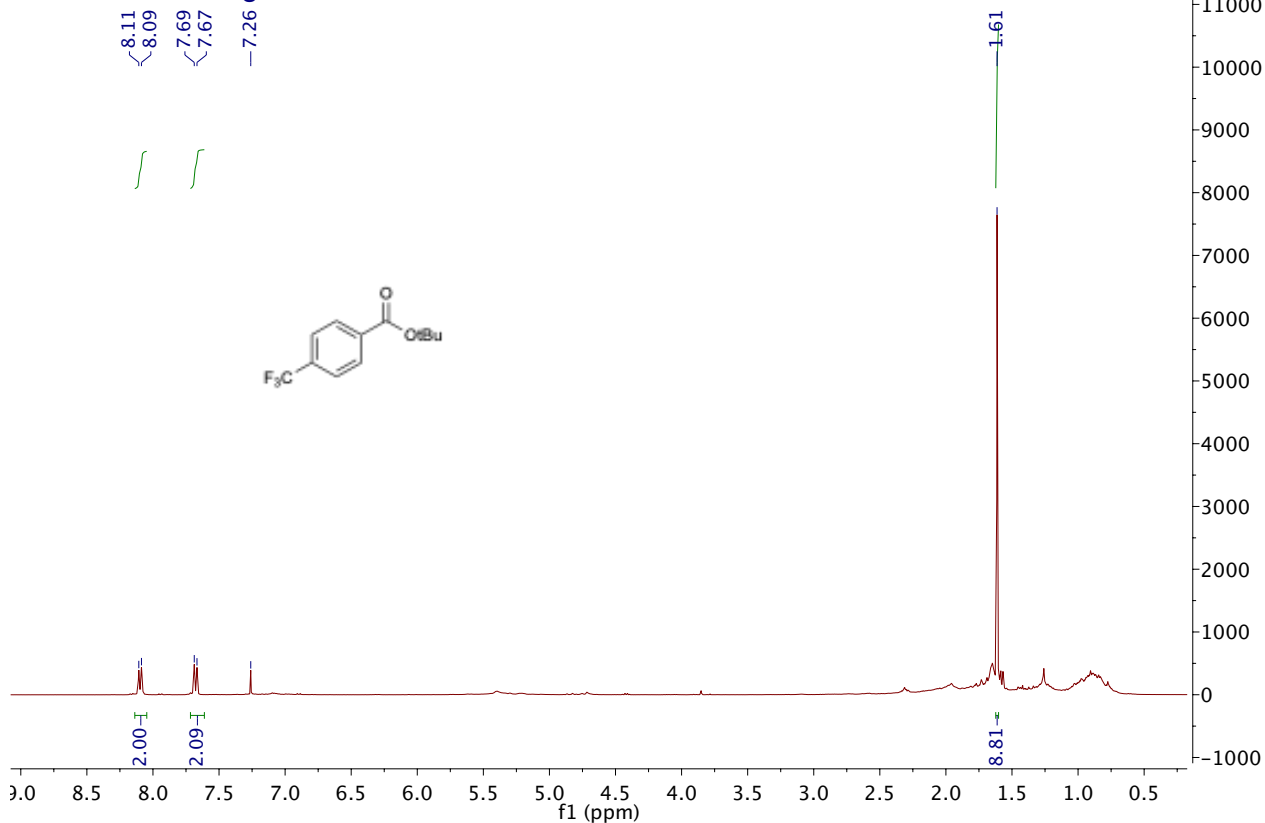


abai-p4-6-7F1

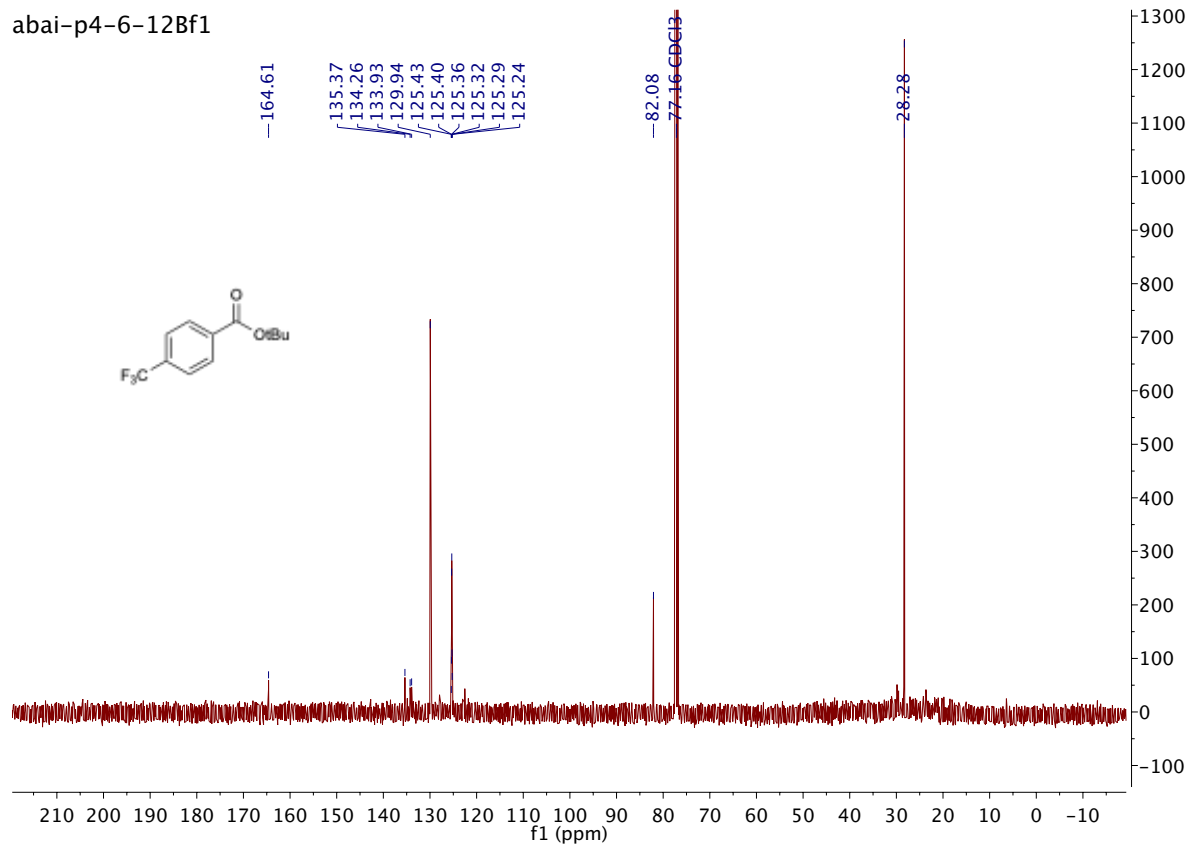


Compound 7f

abai-p4-6-12Bf1

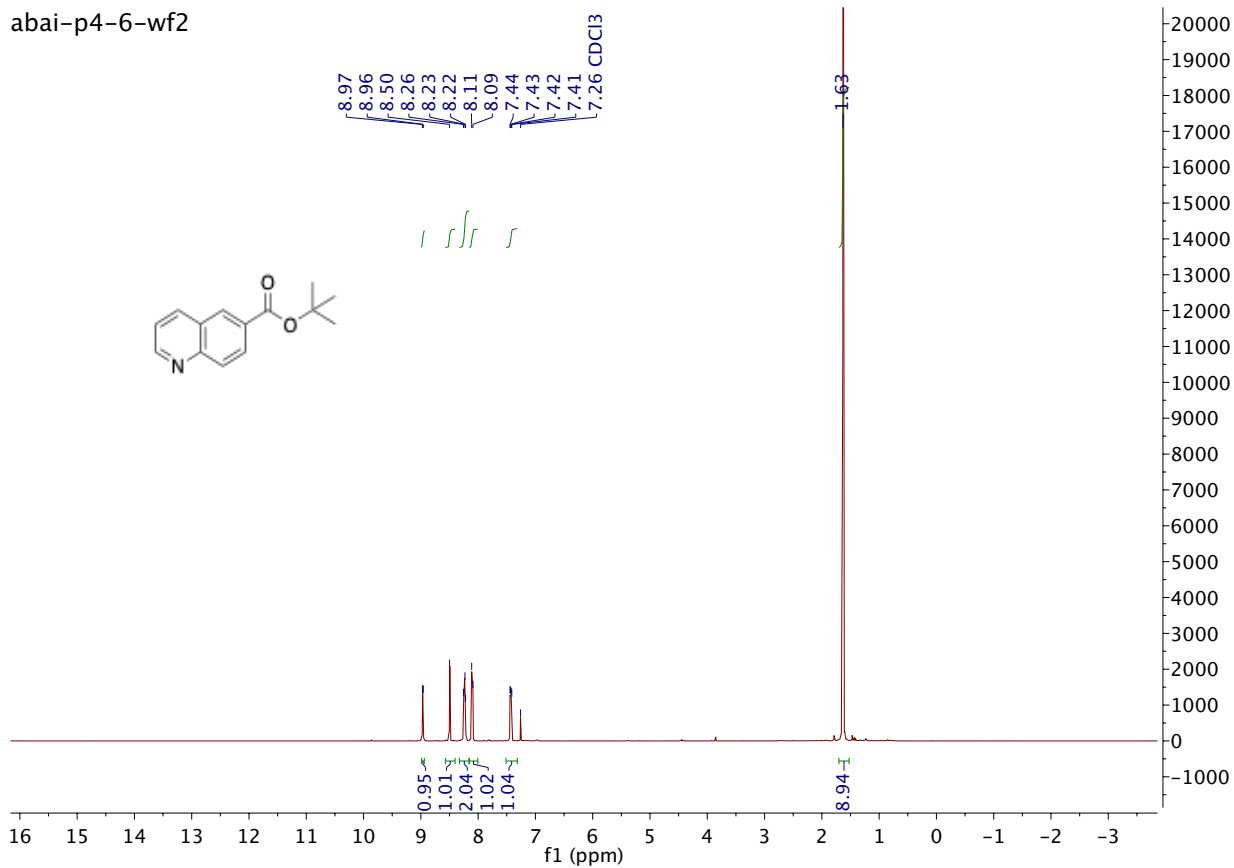


abai-p4-6-12Bf1

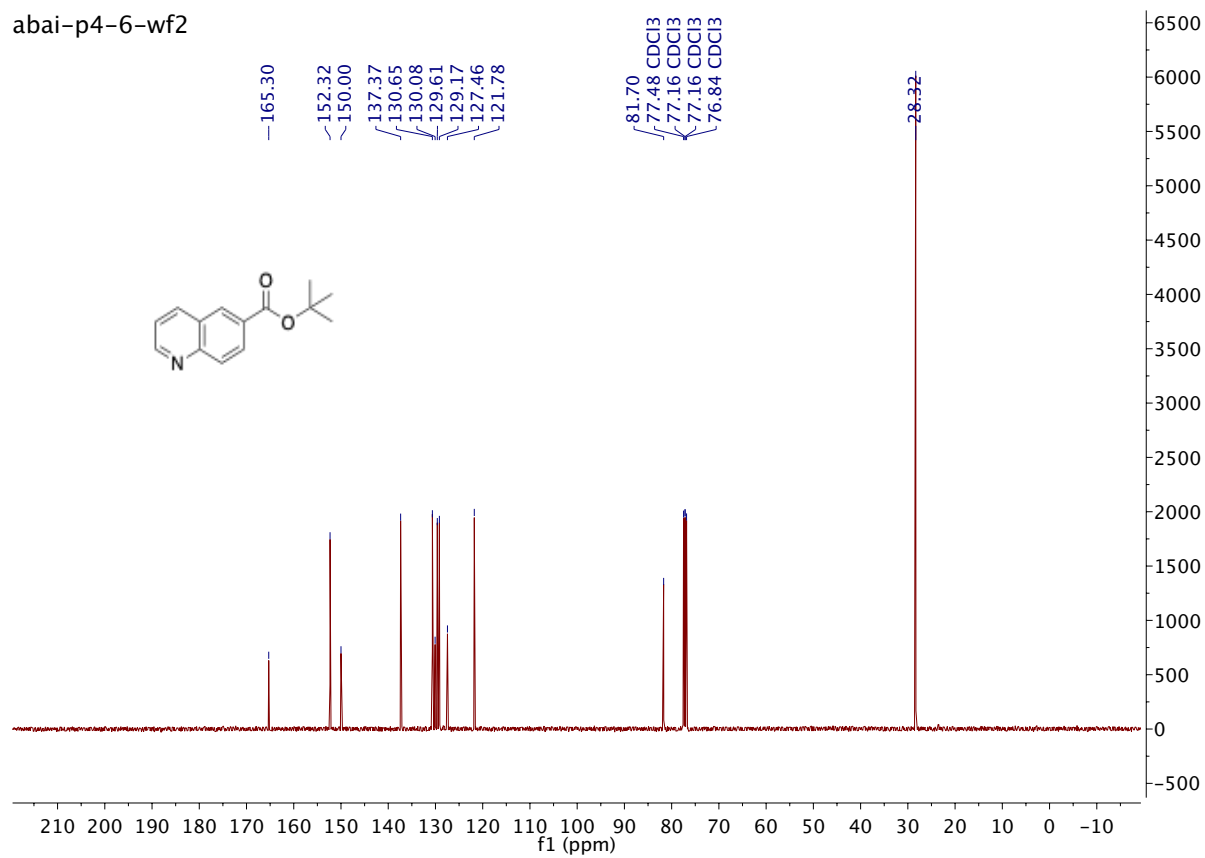


Compound 7g

abai-p4-6-wf2

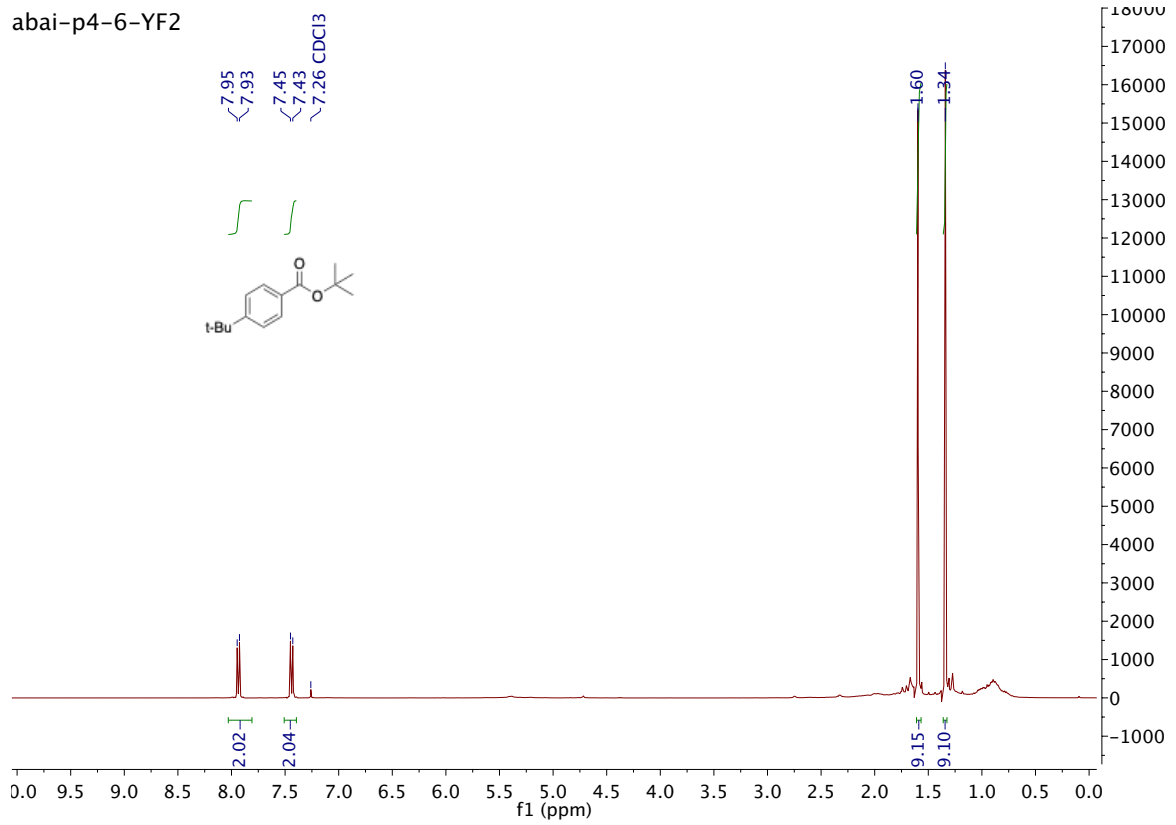


abai-p4-6-wf2

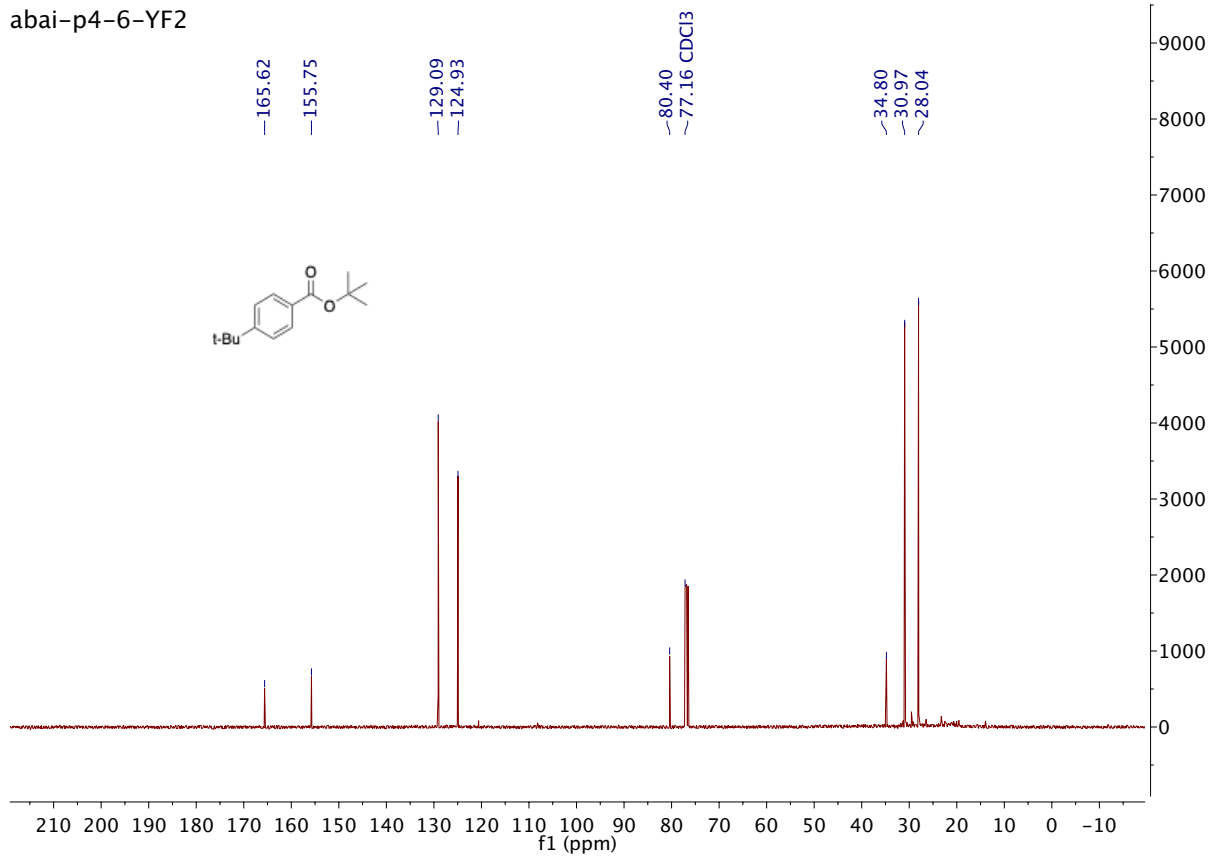


Compound 7h

abai-p4-6-YF2

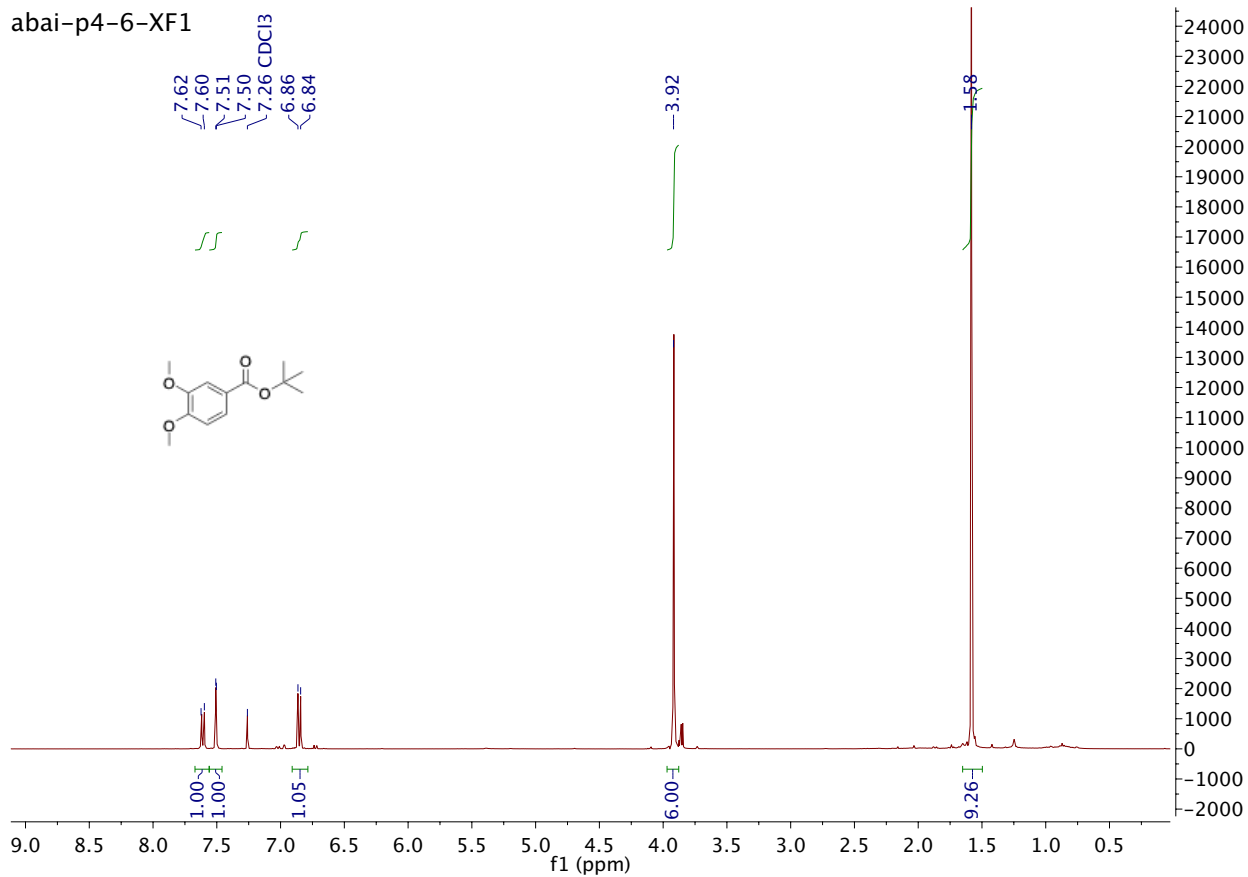


abai-p4-6-YF2

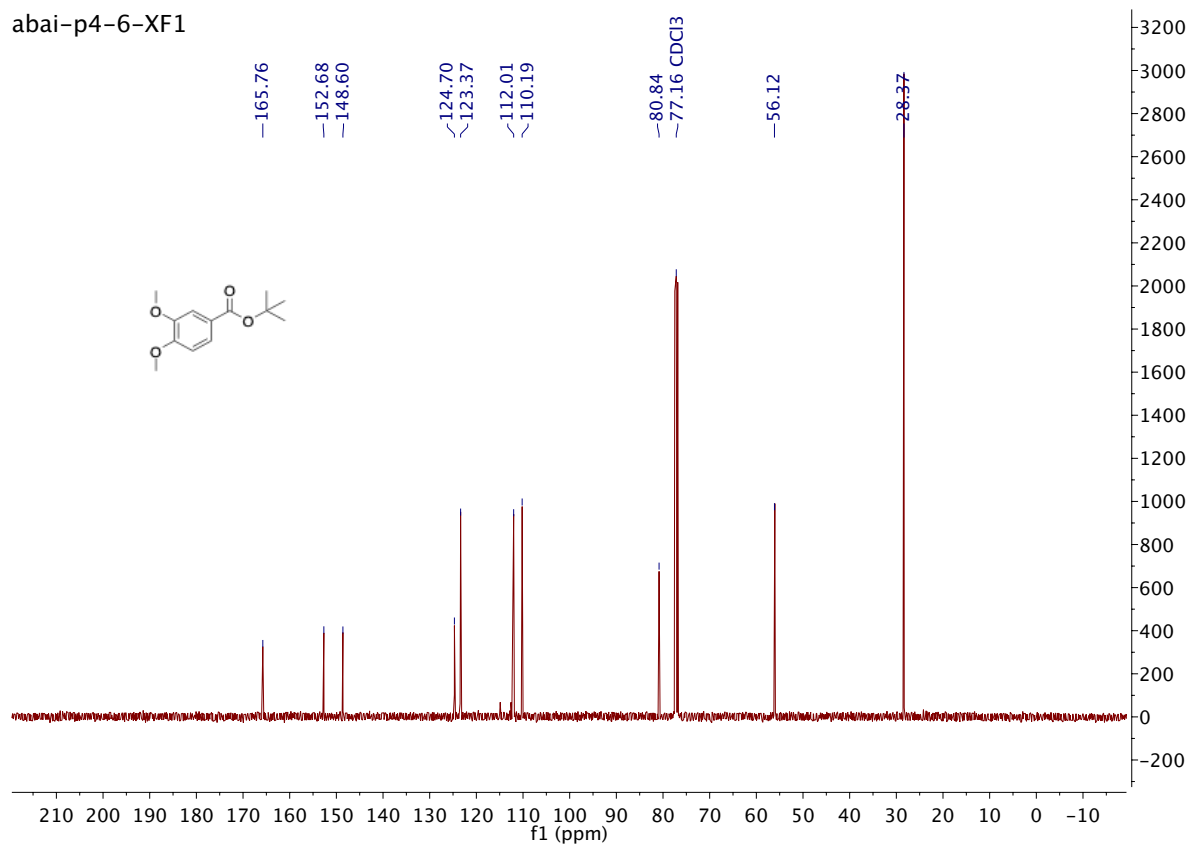


Compound 7i

abai-p4-6-XF1

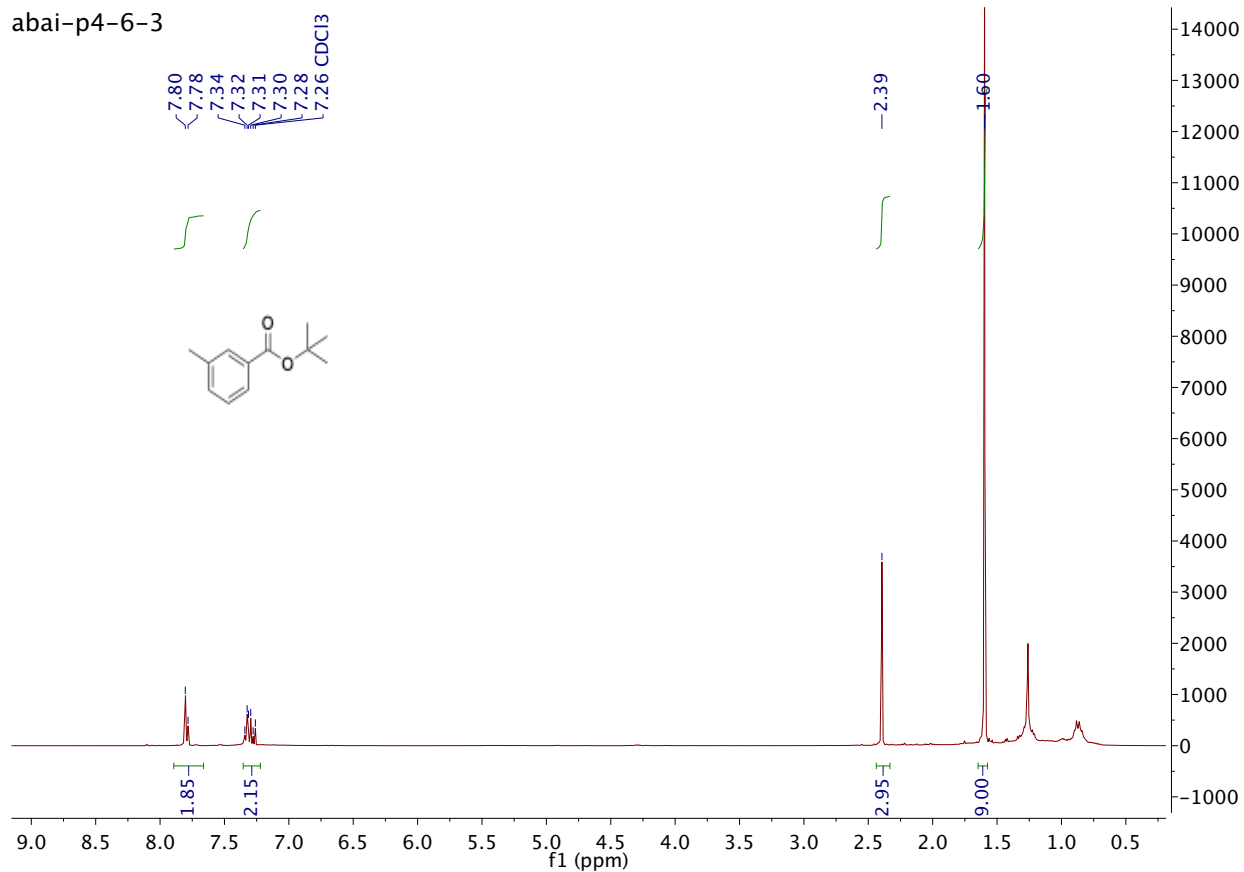


abai-p4-6-XF1

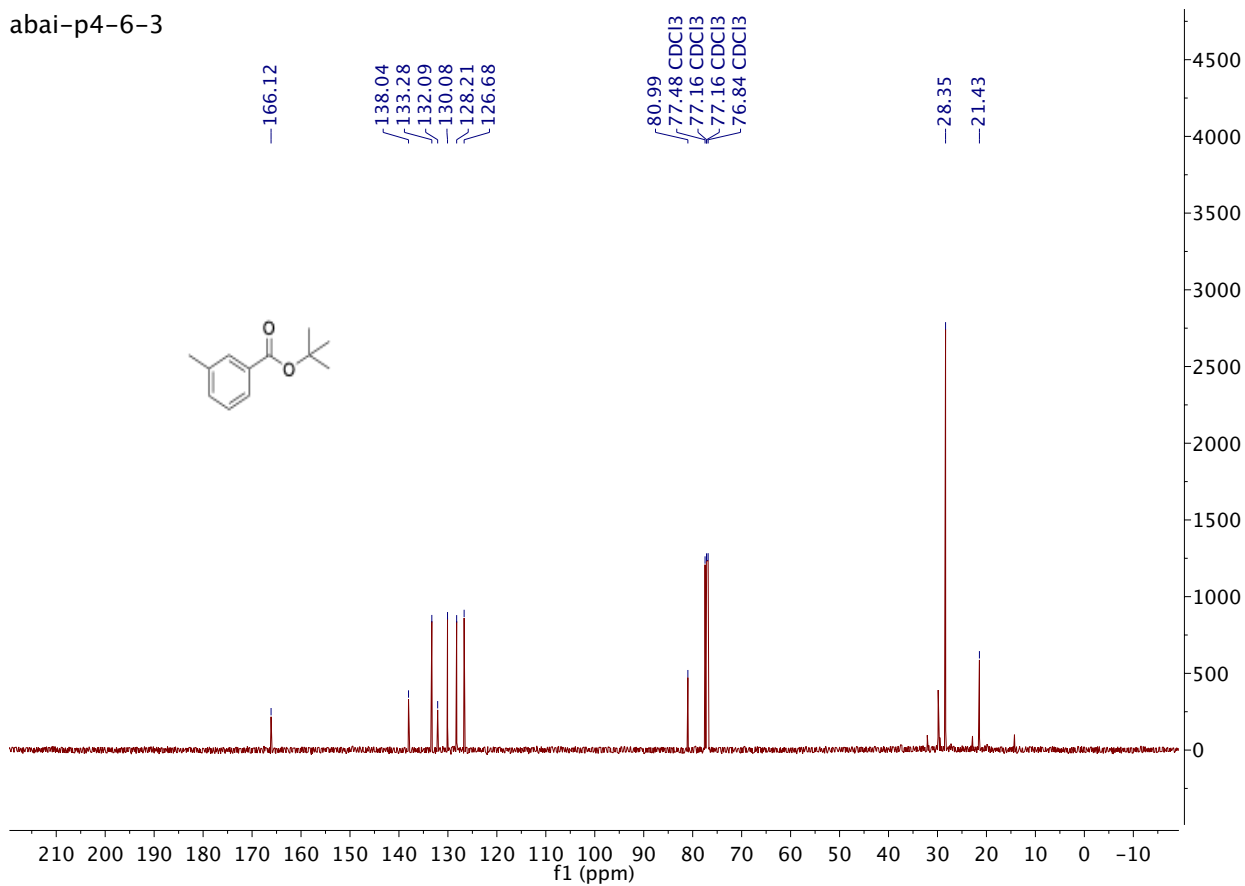


Compound 7j

abai-p4-6-3

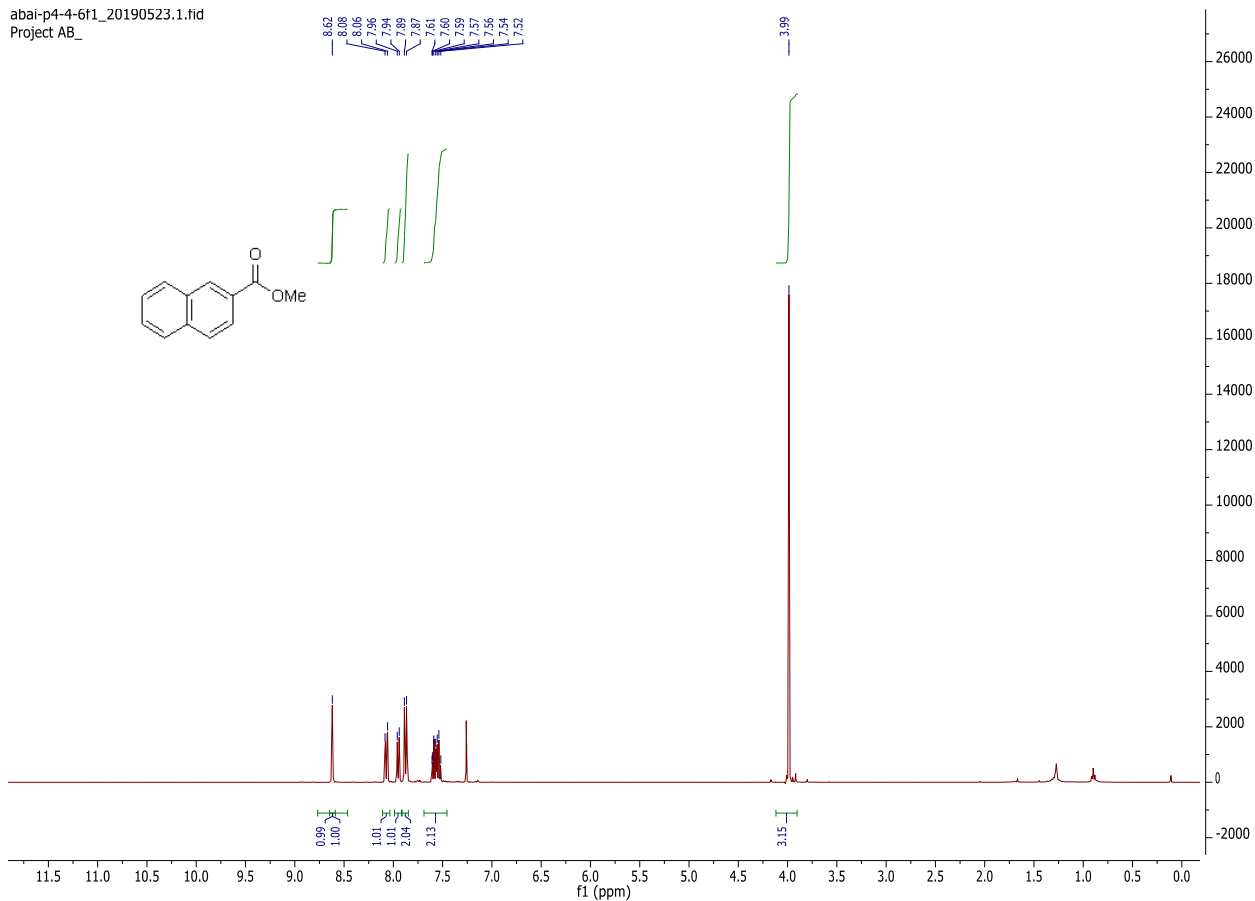


abai-p4-6-3

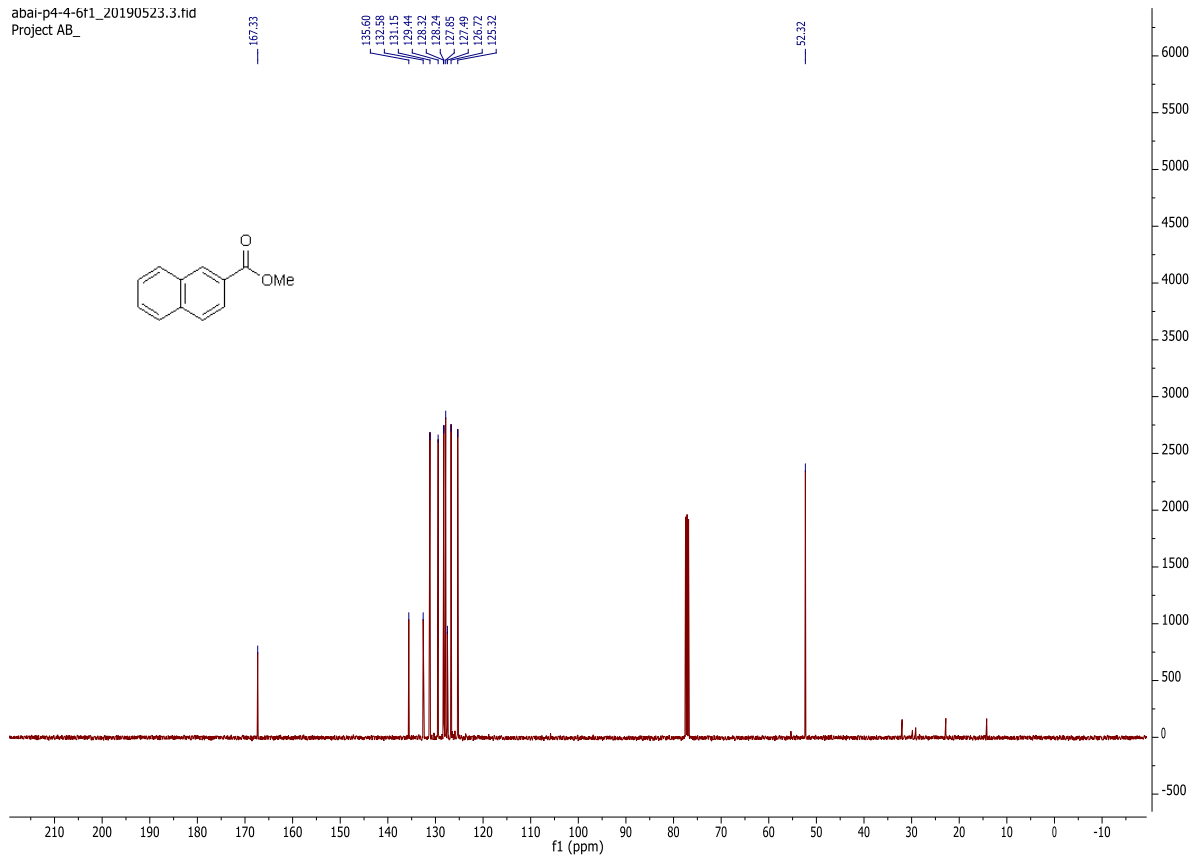


Compound 8a

abai-p4-4-6f1_20190523.1.fid
Project AB_

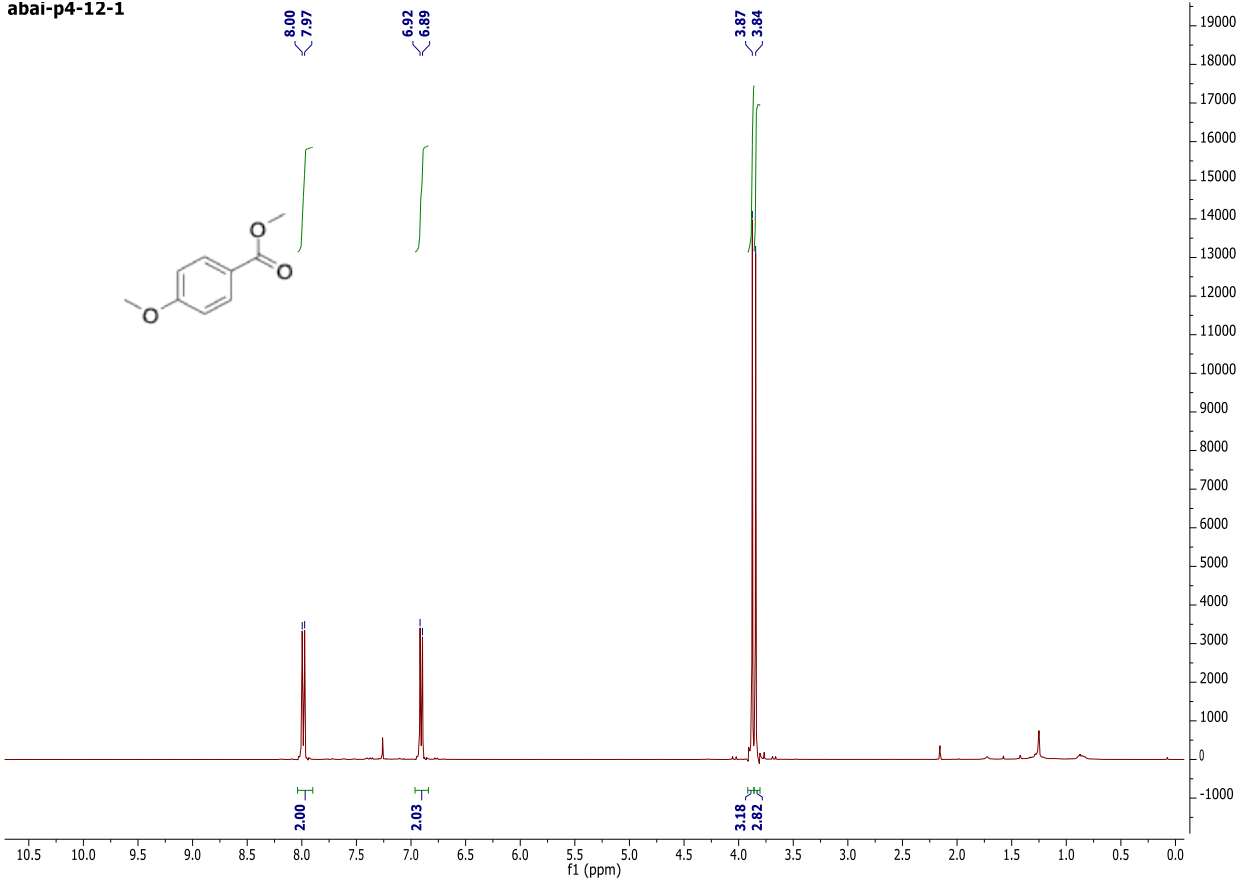


abai-p4-4-6f1_20190523.3.fid
Project AB_

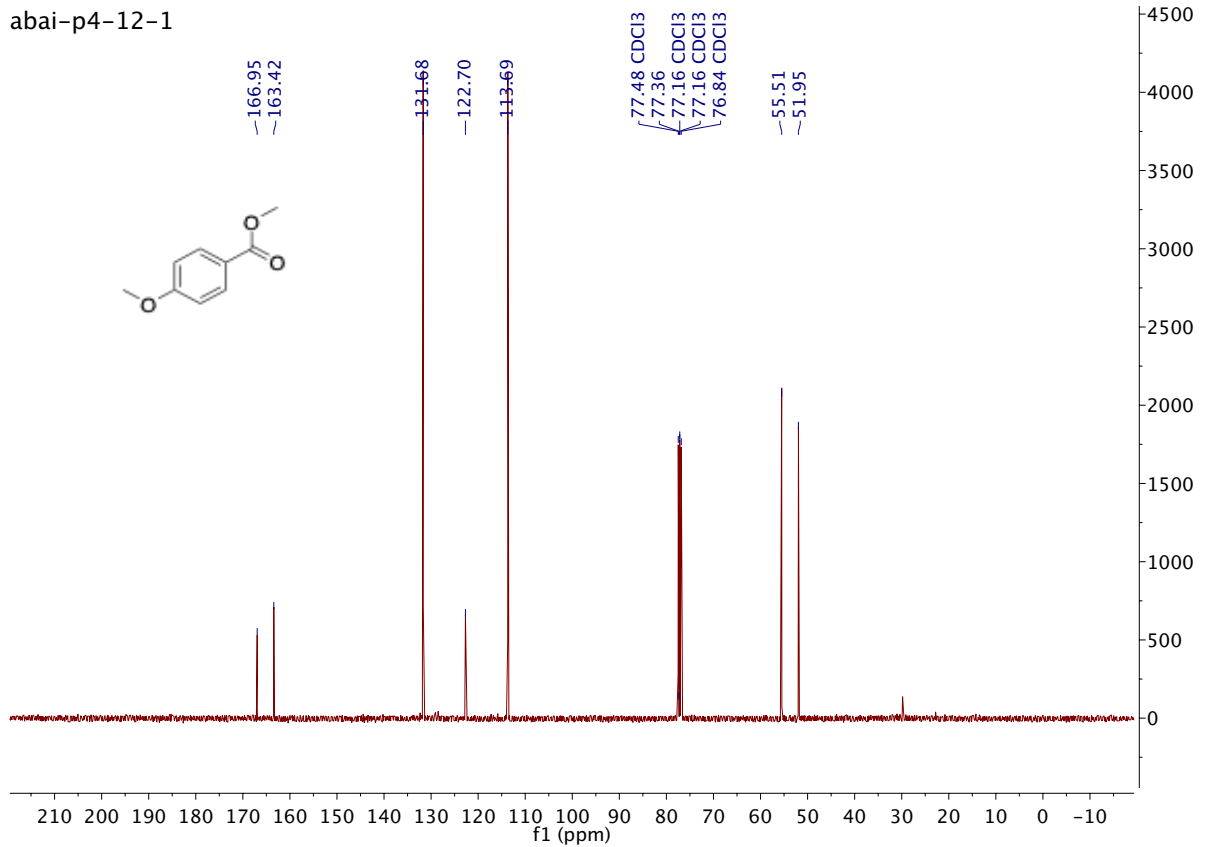


Compound 8b

abai-p4-12-1

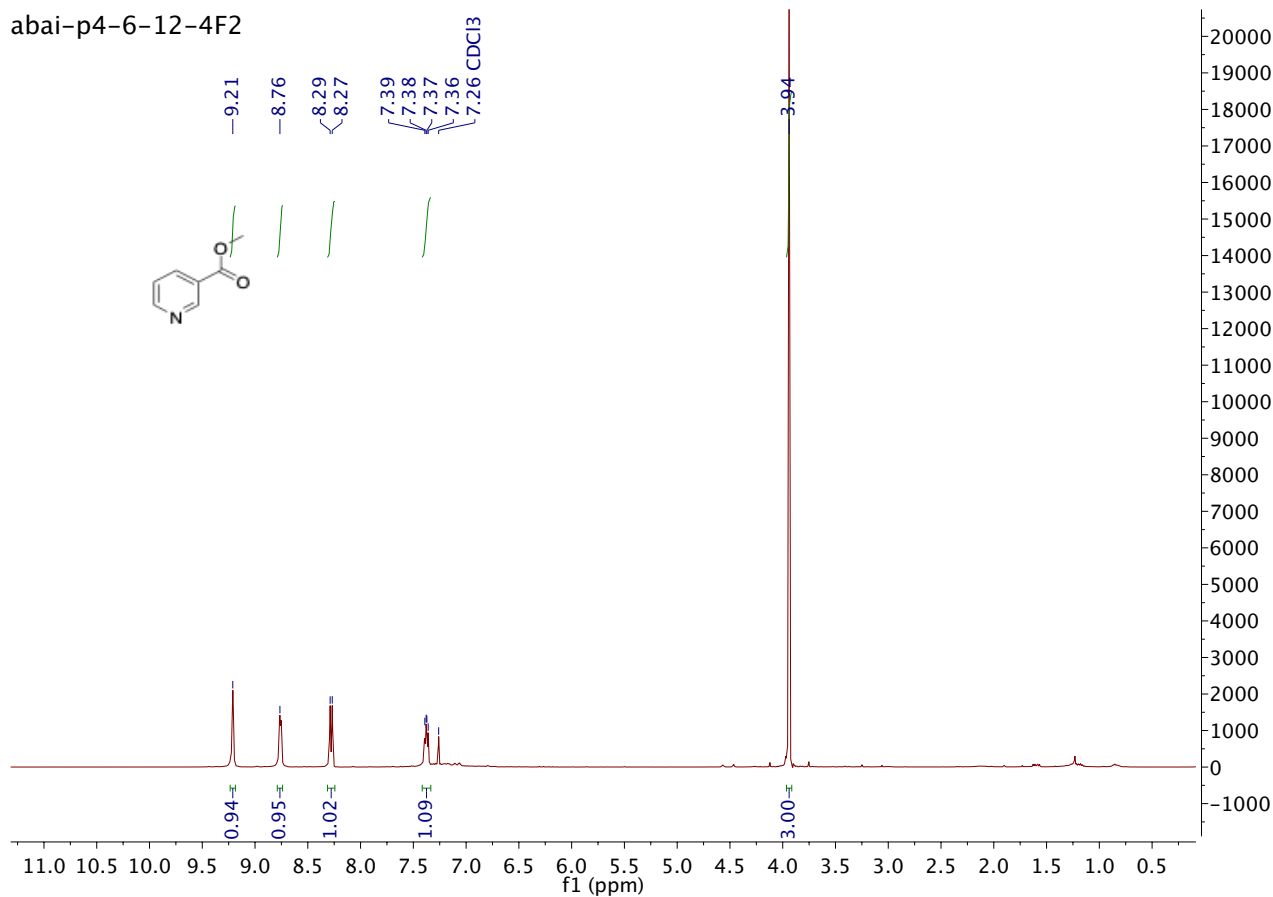


abai-p4-12-1

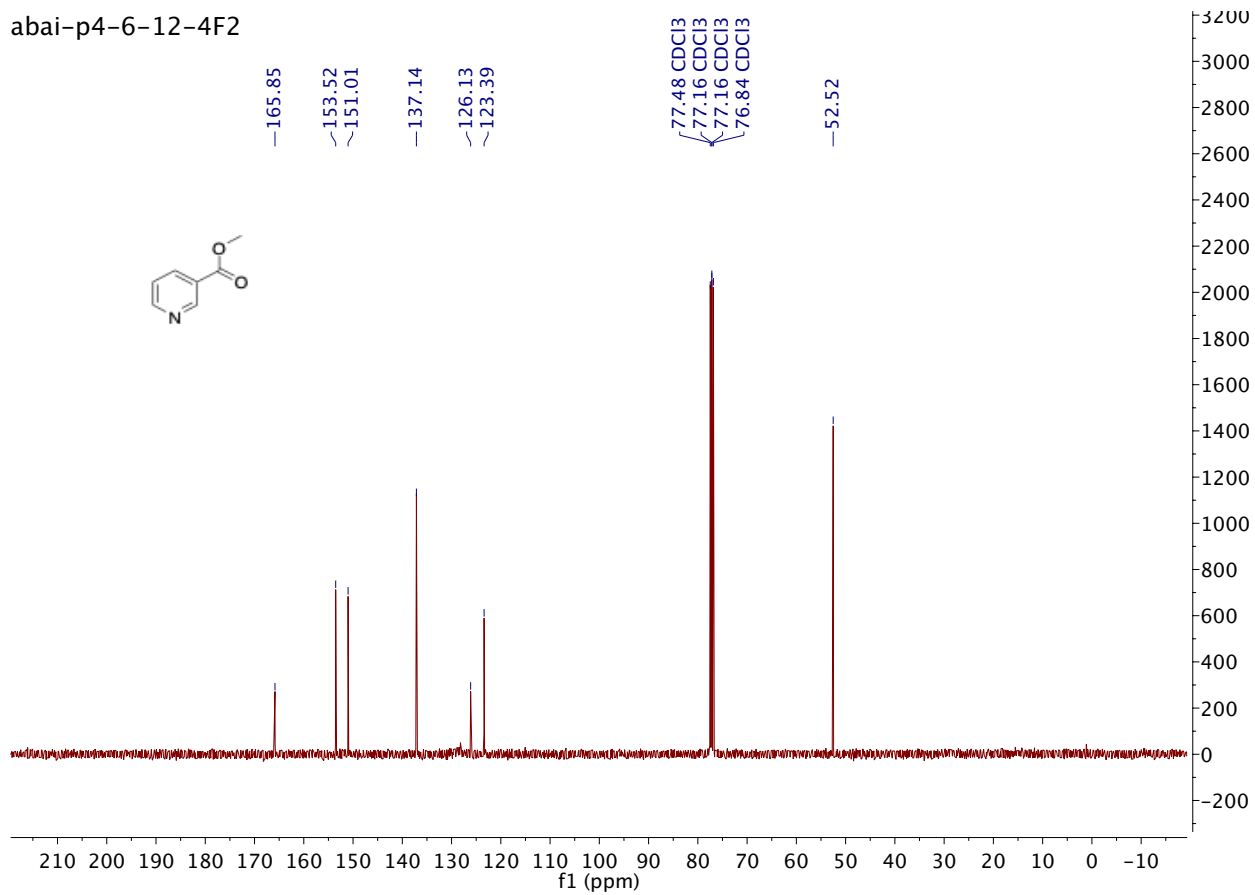


Compound 8c

abai-p4-6-12-4F2

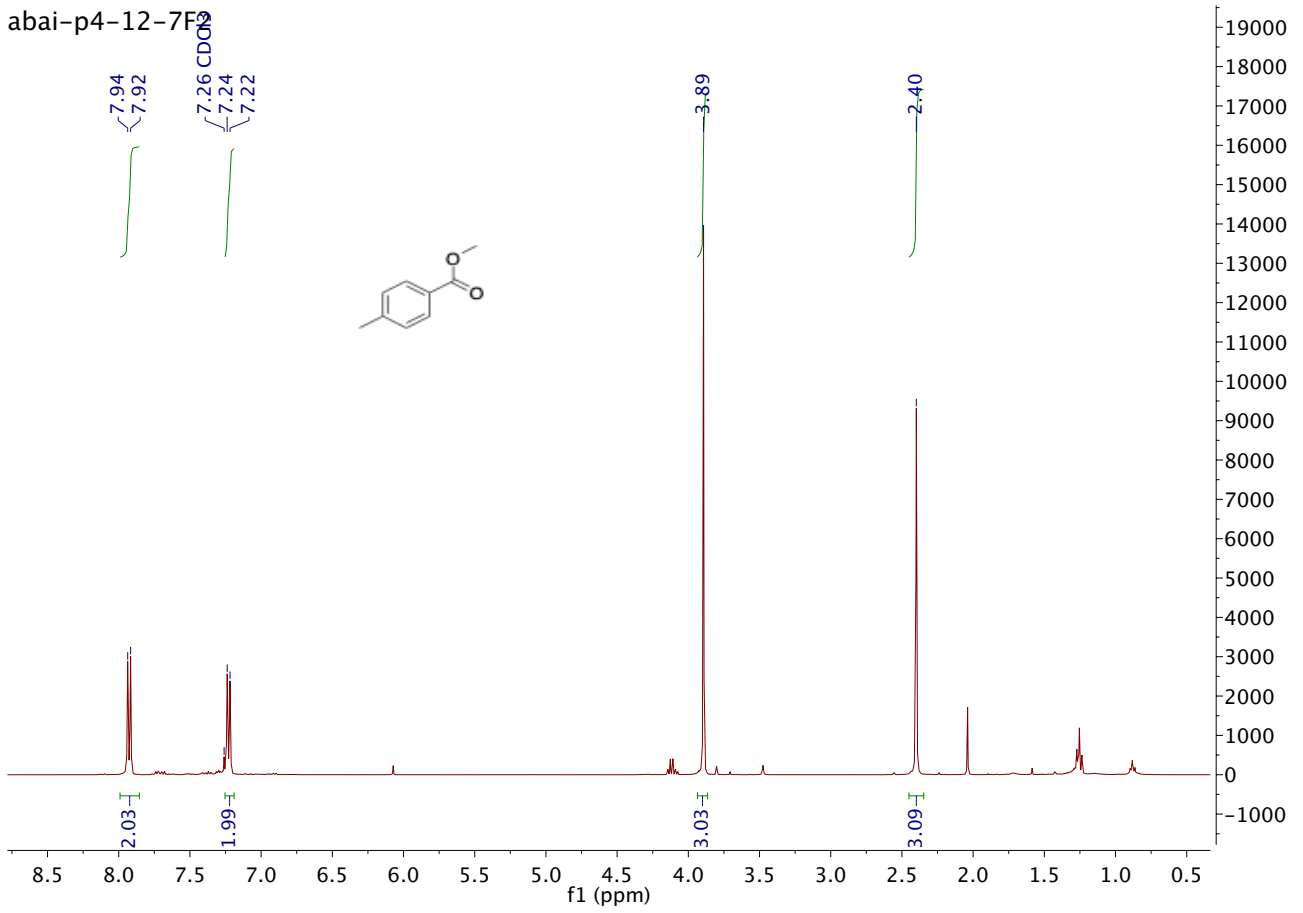


abai-p4-6-12-4F2

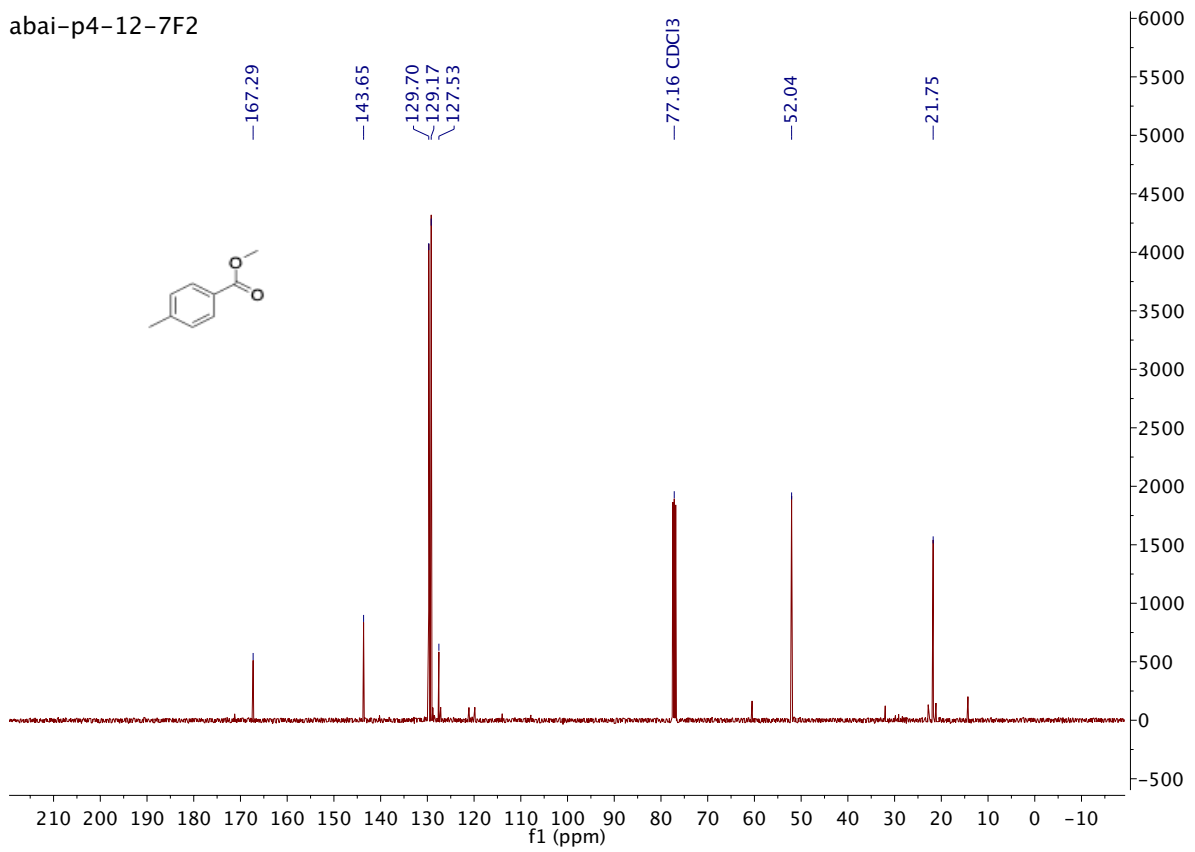


Compound 8d

abai-p4-12-7F9

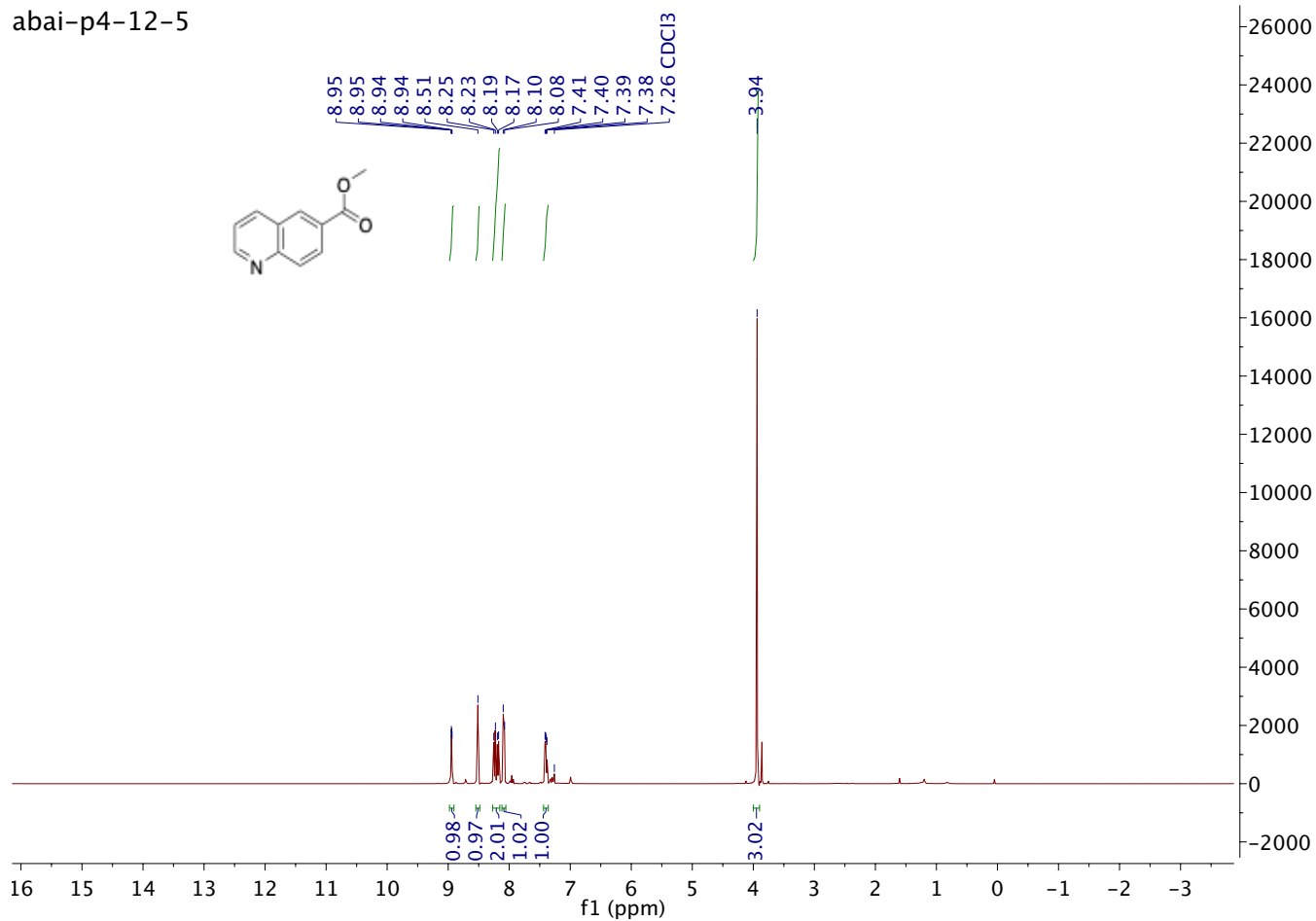


abai-p4-12-7F2



Compound 8e

abai-p4-12-5



abai-p4-12-5

